School of Civil and Environmental Engineering

University of Technology, Sydney

Sydney, Australia

EXPERIMENTAL AND NUMERICAL STUDY OF TIME-DEPENDENT BEHAVIOUR OF REINFORCED SELF-COMPACTING CONCRETE SLABS

By

Farhad Aslani

BSc (Civil), MSc (Structure)

A thesis submitted in partial fulfilment of

the requirements for the degree of

Doctor of Philosophy

February 2014

CERTIFICATE OF ORIGINAL AUTHORSHIP

I certify that the work in this thesis has not previously been submitted for a degree nor has it been submitted as part of requirements for a degree except as fully acknowledged within the text.

I also certify that the thesis has been written by me. Any help that I have received in my research work and the preparation of the thesis itself has been acknowledged. In addition, I certify that all information sources and literature used are indicated in the thesis.

Farhad Aslani

February 2014

To My Family

ACKNOWLEDGEMENTS

The research presented in this PhD thesis was undertaken in the Centre for Built Infrastructure Research (CBIR), School of Civil and Environmental Engineering, Faculty of Engineering and Information Technology (FEIT) at the University of Technology, Sydney (UTS).

I wish to express my sincerest gratitude to my principal supervisor, Dr. Shami Nejadi for his patience, outstanding guidance, knowledge, motivation, wisdom and caring support provided throughout my thesis. It was an honour and a pleasure to be his student. His exceptional personality and positive attitude became a source of inspiration and a role model for my professional and personal development. Utmost gratitude is also forwarded to my co-supervisor, Professor Bijan Samali for his guidance, motivation and support throughout my study. I am heartily thankful to Dr. Hamid Valipour for his encouragement, guidance and unfailing assistance throughout this study. It was possible to fulfil my dream of completing PhD due to their invaluable advice, kind response to my interest and support given from beginning of my study.

I also gratefully acknowledge the financial assistance provided by FEIT, UTS provided as International Research Scholarship, Boral, BOSFA, and Concrite companies. The assistance from the staff in Concrete, Structures and Material Testing Laboratories at UTS has been very important in completing the tests included in the thesis. I would like to thank all working staff in those laboratories. Working in the lab would never have been easy without the assistance provided by all these people.

I would like to express my deepest gratitude to my family for their love, support and encouragement while I was thousands of miles away from home. My special thanks also go to my friends for their support and motivation. I offer my regards and blessings to all of those who supported me in any respect during the completion of this study.

Farhad Aslani

December 2013

LIST OF PUBLICATIONS

Journal papers:

Aslani, F. & Nejadi, S. 2013, 'Creep and Shrinkage of Self-Compacting Concrete with and without Fibers,' *Journal of Advanced Concrete Technology*, vol.11, no.10, pp. 251-265.

Aslani, F. & Nejadi, S. 2013, 'Mechanical Characteristics of Self-Compacting Concrete with and without Fibers,' *Magazine of Concrete Research*, vol.65, no.10, pp. 608–622.

Aslani, F. & Nejadi, S. 2012, 'Mechanical properties of conventional and self-compacting concrete: An analytical study,' *Construction and Building Materials*, vol.36, pp.330-347.

Aslani, F. & Nejadi, S. 2012, 'Bond Behavior of Reinforcement in Conventional and Self-Compacting Concrete,' *Advances in Structural Engineering -An International Journal-*, vol.15, no.12, 2033–2051.

Aslani, F. & Nejadi, S. 2012, 'Bond characteristics of steel fibre reinforced self-compacting concrete,' *Canadian Journal of Civil Engineering*, vol.39, no.7, pp. 834-848.

Aslani, F. & Nejadi, S. 2012, 'Shrinkage Behavior of Self-Compacting Concrete,' *Journal of Zhejiang University SCIENCE A*, vol.13, no.6, pp.407-419.

Aslani, F. & Nejadi, S. 2012, 'Bond characteristics of steel fiber and deformed reinforcing steel bar embedded in steel fiber reinforced self-compacting concrete (SFRSCC),' *Central European Journal of Engineering*, vol.2, no.3, pp. 445-470.

Aslani, F. & Nejadi, S. 2012, 'Bond Characteristics of Reinforcing Steel Bars Embedded in Self-Compacting Concrete,' *Australian Journal of Structural Engineering*, vol.13, no.3, pp.279-295.

Aslani, F., Nejadi, S. & Samali, B. 2013, 'Short Term Flexural Cracking Control of Reinforced Self-Compacting Concrete One Way Slabs with and without Fibres,' *Construction and Building Materials*, under review.

Aslani, F., Nejadi, S. & Samali, B. 2013, 'Long Term Flexural Cracking Control of Reinforced Self-Compacting Concrete One Way Slabs with and without Fibres,' *Construction and Building Materials*, under review.

Conference papers:

Aslani, F., Nejadi, S. & Samali, B. 2013, 'Energy dissipation in self-compacting concrete with or without fibers in compression,' *Fifth North American Conference on the Design and Use of Self-Consolidating Concrete*, May 12–15, 2013, Chicago, IL, USA, pp. 1-10.

Aslani, F. & Nejadi, S. 2012, 'Comparison of the Analytical Models to Determine Modulus of Rupture of Self-Compacting Concrete and Conventional Concrete,' *Australasian Conference on the Mechanics of Structures and Materials, 22nd ACMSM: 'Materials to Structures: Advancement through Innovation'* Sydney, Australia, pp. 1105-1112.

Nejadi, S. & Aslani, F. 2012, 'Bond Constitutive Relationship for Steel Fiber Reinforced Self-Compacting,' *Bond in Concrete 2012, Bond, Anchorage, Detailing - Fourth International Symposium*, 17th-20th June 2012, Brescia, Italy, pp.931-939.

Aslani, F. & Nejadi, S. 2012, 'Bond Characteristics of Deformed Reinforcing Steel Bars Embedded in Steel Fibre Reinforced Self-Compacting Concrete,' *Bond in Concrete 2012, Bond, Anchorage, Detailing - Fourth International Symposium*, 17th-20th June 2012, Brescia, Italy, pp.757-764.

Aslani, F. & Nejadi, S. 2011, 'A comparison of the bond characteristics in conventional and self-compacting concrete, Part I: experimental results,' *The 9th*

Symposium on High Performance Concrete, edKhrapko, M; Wallevik, O, 9th-12th August 2011, Rotorua, New Zealand, pp.435-442.

Aslani, F. & Nejadi, S. 2011, 'A comparison of the bond characteristics in conventional and self-compacting concrete, Part II: code provisions and empirical equations,' *The 9th Symposium on High Performance Concrete*, edKhrapko, M; Wallevik, O, 9th-12th August 2011, Rotorua, New Zealand, pp.443-450.

Aslani, F. & Nejadi, S. 2011, 'Comparison of creep prediction models for self-compacting and conventional concrete,' *The 9th Symposium on High Performance Concrete*, edKhrapko, M; Wallevik, O, 9th-12th August 2011, Rotorua, New Zealand, pp.1-10.

Aslani, F. & Nejadi, S. 2011, 'Comparison of shrinkage prediction models for self-compacting and conventional concrete,' *The 9th Symposium on High Performance Concrete,* edKhrapko, M; Wallevik, O, 9th-12th August 2011, Rotorua, New Zealand, pp.1-10.

Aslani, F. & Nejadi, S. 2011, 'Evaluation and comparison of analytical models to determine the bond characteristics of steel fiber reinforced self-compacting concrete,' *The 9th Symposium on High Performance Concrete*, edKhrapko, M; Wallevik, O, 9th-12th August 2011, Rotorua, New Zealand, pp.1-8.

Nejadi, S. & Aslani, F. 2011, 'Evaluation and Comparison of the Compressive Stress-Strain relationships of Self-Compacting Concrete and Conventional Concrete,' *Concrete 2011-Building a Sustainable Future*, 12th-14th October 2011, Perth, Western Australia, pp.1-10.

Aslani, F. & Nejadi, S. 2011, 'Comparison of the Analytical Models to Determine Modulus of Elasticity of Self-Compacting Concrete and Conventional Concrete,' *Structural Engineering World Congress (SEWC)*, 4th-6th April 2011, Como, Italy, pp. 1-10.

Aslani, F. & Nejadi, S. 2011, 'Evaluation and Comparison of Experimental Results to Determine the Bond Characteristics of Steel Fiber Reinforced Self-Compacting Concrete,' *Structural Engineering World Congress (SEWC)*, 4th-6th April 2011, Como, Italy, pp. 1-8.

Aslani, F. & Nejadi, S. 2011, 'Evaluation and Comparison of the Analytical Models to Determine Tensile Strength of Self-Compacting Concrete and Conventional Concrete,' *Structural Engineering World Congress (SEWC)*, 4th-6th April 2011, Como, Italy, pp. 1-9.

Aslani, F. & Nejadi, S. 2011, 'Evaluation and Comparison of the Analytical Models to Predict Creep and Shrinkage Behavior of Self-Compacting Concrete,' *Structural Engineering World Congress (SEWC)*, 4th-6th April 2011, Como, Italy, pp. 1-10.

LIST OF NOTATIONS

Chapter 3

γ	unit weight of concrete
ϕ	fibre inclination angle
λ, μ	coefficients of linear equation of the stress-strain curve
λ_f, μ_f	coefficients of linear equation of the SFRSCC stress-strain curve
κ_1	first proposed constant value for MOE prediction
κ_2	second proposed constant value for MOE prediction
η_1	first proposed constant value for TS prediction
η_2	second proposed constant value for TS prediction
μ_i	initial coefficient of friction
μ_{ss}	steady state value of the coefficient of friction attained at large pullout distances
σ_c	concrete stress
σ_{cf}	SFRSCC compressive stress
σ_{ctf}	SFRSCC tensile stress
ε	concrete strain
ε'_c	strain corresponding with the maximum stress f'_c
ε'_{cf}	strain at peak stress of SFRSCC
ε^*	corresponding strain to the 0.85 f_{ctf}
ε_{ct}	tensile concrete strain
ε_f	SFRSCC strain
τ_{max}	maximum bond strength
$\tau_{max(app)}$	maximum apparent bond shear strength
$\tau_{f(app)}$	fibre apparent bond shear strength
τ_f	fibre bond shear strength
τ_u	ultimate bond strength
a	radius of fibre
c	concrete cover

c (fibre)	a constant that governs the rate at which the coefficient of friction decays with increase in pullout distance
d_b	diameter of the steel bar
d_f	diameter of fibre
E_c	modulus of elasticity of concrete
E_{cf}	modulus of elasticity of SFRSCC
E_{sec}	secant modulus of elasticity
E_{secf}	secant modulus of elasticity of SFRSCC
f	snubbing friction coefficient
f'_c	maximum compressive strength of concrete
f'_{cf}	compressive strength of SFRSCC
f'_{cy}	maximum compressive strength of cylinder concrete specimens
f'_{cu}	maximum compressive strength of cube concrete specimens
f_{cr}	modulus of rupture of concrete
f_{ct}	tensile strength of concrete
f_{ctf}	tensile strength of SFRSCC
k	spalling coefficient and ϕ is in radians
l_d	embedded length of the steel bar
l_f	length of fibre
l_f/d_f	aspect ratio
n	material parameter that depends on the shape of the stress-strain curve
n_f	SFRSCC parameter that depends on the shape of the stress-strain curve
n_1	modified material parameter at the ascending branch
n_{1f}	modified SFRSCC parameter at the ascending branch
n_2	modified material parameter at the descending branch
n_{2f}	modified SFRSCC parameter at the descending branch
p_{d1} and p_{d2}	fibre pullout distances
$P_{p_{d1}}$ and $P_{p_{d2}}$	fibre pullout loads corresponding to pullout distances p_{d1} and p_{d2}
P_m	measured fibre pullout load
R.I.	fibre reinforcing index
s, s_1, s_2, s_3	slip related to pullout bond test

$U_{peak}(\phi)$	peak slip displacement corresponding to the peak load with the inclination angle ϕ
V_f	fibre volume fraction
W_p	work of fibre pullout
Chapter 4	
α	coefficient representing the influence of the cement type
β	represents time dependency of drying shrinkage
γ	coefficient representing the influence of the cement and admixtures type
η	constant related to compressive strength and water content
κ	conventional scalar damage index
μ, λ and α	parameters to be obtained from a least square minimization procedure
β_{sc}	coefficient which depends on the type of cement
σ'_{cp}	creep stress unit
ε'_{sh}	final value of shrinkage strain
$\varepsilon'_{ds\rho}$	the final value of drying shrinkage strain
$\varepsilon'_{ds\infty}$	final value of drying shrinkage
$\varepsilon'_{as\infty}$	final value of autogenous shrinkage strain
ε'_{cr}	final value of creep strain per unit stress
ε'_{bc}	final value of basic creep strain per unit stress
ε'_{dc}	final value of drying creep strain per unit stress
$(\varepsilon_{sh})_u$	ultimate shrinkage strain
$\varepsilon_e(t)$	instantaneous strain
$\varepsilon'_{cs}(t,t_0)$	shrinkage strain of concrete from age to t
$\varepsilon'_{ds}(t,t_0)$	drying shrinkage strain of concrete from age to t
$\varepsilon'_{as}(t,t_0)$	autogenous shrinkage strain of concrete from age to t
$\varepsilon'_{sc}(t,t_0)$	shrinkage strain of concrete from age of t_0 to t
$\varepsilon'_{as}(t,t_0)$	autogenous shrinkage strain of concrete from the start of setting to age t
$\varepsilon'_{cc}(t, t', t_0)$	creep strain
Δt_i	number of days where the temperature T prevails
$T(\Delta t_i)$	temperature (°C) during the time period Δt_i
c	cement

c/p	cement to powder ratio
f'_c	compressive strength
$f'_{c,28d}$	compressive strength at the age of 28 days
f_{cm}	mean compressive strength of concrete at the age of 28 day
f_{cmo}	10 MPa
$f_{cm}(t)$	mean value of compressive strength at time t
f	constant based on the duration of curing
h_0	100 mm
h	notional size of member (mm)
RH_0	100%
RH	relative humidity (%)
s' and n	parameters that have to be specifically calibrated for each SCC concrete mix by using experimental results
t_1	1 day
t_0	effective age (days) of concrete at the beginning of drying
t'	effective age (days) of concrete at the beginning of loading
t	effective age (days) of concrete during loading respectively
T_0	1 °C
v/s	volume to surface ratio
w	water
w/c	water to cement ratio

Chapter 5

α and β	empirical constants related to compressive strength model
η and μ	empirical constants related to modulus of elasticity
γ and λ	empirical constants related to tensile strength
ψ and ϕ	empirical constants related to modulus of rupture
ω and ρ	empirical constants related to energy dissipated under compression
χ, ξ	coefficients of linear equation of stress-strain curve
σ_c	concrete stress
ε	concrete strain
ε'_c	strain corresponding with the maximum stress f'_c

ε_u	ultimate deformation
E_c	modulus of elasticity
E_{cN}	N-SCC mix modulus of elasticity
E_{cfD}	D-SCC mix modulus of elasticity
E_{cfS}	S-SCC mix modulus of elasticity
E_{cfDS}	DS-SCC mix modulus of elasticity
E_{sec}	secant modulus of elasticity
f'_c	maximum compressive strength of concrete
f'_{cN}	N-SCC mix compressive strength
f'_{cfD}	D-SCC mix compressive strength
f'_{cfS}	S-SCC mix compressive strength
f'_{cfDS}	DS-SCC mix compressive strength
f_{ctN}	N-SCC mix tensile strength
f_{ctfD}	D-SCC mix tensile strength
f'_{ctfS}	S-SCC mix tensile strength
f'_{ctfDS}	DS-SCC mix tensile strength
f_{crN}	N-SCC mix modulus of rupture
f_{crfD}	D-SCC mix modulus of rupture
f_{crfS}	S-SCC mix modulus of rupture
f_{crfDS}	DS-SCC mix modulus of rupture
G_c	energy dissipated under compression
G_{cN}	N-SCC mix energy dissipated under compression
G_{cfD}	D-SCC mix energy dissipated under compression
G_{cfS}	S-SCC mix energy dissipated under compression
G_{cfDS}	DS-SCC mix energy dissipated under compression
n	material parameter that depends on the shape of the stress-strain curve
n_1	modified material parameter at the ascending branch
n_2	modified material parameter at the descending branch

Chapter 6

τ_b	bond shear stress
M_s	in-service bending moment

M_{cr}	cracking moment
kd	compression chord of depth
b	width
A_{st}	tensile reinforcement of area
A_{ct}	area of tensile concrete
d	depth
I_{cr}	second moment of area about the centroidal axis
σ_{ct}	uniform tensile stress of concrete
b^*	width of the section at the level of the centroid of the tensile steel
ρ	tensile reinforcement ratio
n	modular ratio
M	applied moment
f_y	steel yield stress
f_{ct}	direct tensile strength of the concrete
λ_1	load duration factor
λ_2	reduction in bond stress as the steel stress σ_{st1} factor
λ_3	significant increase in bond stress factor
ρ_{tc}	reinforcement ratio of the tension chord
d_b	reinforcing bar diameter
s_{min}	minimum crack spacing
s_{max}	maximum crack spacing
$(w_i)_{tc}$	instantaneous crack width
k_{cover}	a term to account for the dependence of crack width on the clear concrete cover
w_{max}	maximum crack width
l_{es}	transfer length
ε_{sm}	mean steel strain
ε_{cm}	mean concrete strain
σ_{cf}	stress in the fibre reinforced concrete
$\sigma^{i}_{cf,cr}$	imaginary cracking stress of the fibre reinforced concrete
τ_{sm}	average bond stress over load transmission length

E_s	modulus of elasticity of reinforcing bar
ρ_s	reinforcing ratio of steel reinforcement
α_b	shape coefficient of strain courses
α_E	ratio of the modulus of elasticity of steel to the modulus of elasticity of concrete
f_R	relative rib area of the rebars
σ_s	stress in the reinforcing bar at a crack
F	applied load
A_s	cross-sectional area of the steel bars
G_f	fracture energy of the concrete matrix
σ_{cf0}	maximum post-cracking stress
w_0	crack width corresponding to maximum post-cracking stress
σ_{cf0}	maximum post-cracking stress
η	coefficient of fibre orientation
g	coefficient of fibre efficiency
ρ_f	volume fraction of fibres
l_f	fibre length
d_f	fibre diameter
τ_{fm}	mean fibre-matrix bond stress
f_{ctm}	mean tensile strength of the plain concrete matrix
E_f	modulus of elasticity of the fibres
$\sigma^j_{cf,cr}$	maximum stress of the ascending fibre phase

Chapter 7

α_b	shape coefficient of strain courses
$\alpha_{E,s}$	ratio of the modulus of elasticity of steel to the modulus of elasticity of concrete
$\alpha_{E,f}$	ratio of the modulus of elasticity of fibre to the modulus of elasticity of concrete
η	fibre orientation coefficient
$\varepsilon_{f,shr}$	shrinkage shortening of the fibres
ρ_s	reinforcing ratio of steel reinforcement

ρ_f	fibre content
ρ_{tc}	reinforcement ratio of the tension chord
σ_{cf}	stress in the fibre reinforced concrete
τ_b	bond shear stress
τ_{sm}	average bond stress over load transmission length
A_{st}	tensile reinforcement of area
A_{ct}	area of tensile concrete
b	width
d_b	reinforcing bar diameter
E_s	modulus of elasticity of reinforcing bar
kd	compression chord of depth
M_{cr}	cracking moment
M_s	in-service bending moment
s^*	final maximum crack spacing

Chapter 8

α_e	modular ratio = E_s / E_c
α_b	shape coefficient of strain courses
α_E	ratio of the modulus of elasticity of steel to the modulus of elasticity of concrete
β	empirical coefficient to assess the mean strain over $l_{s,max}$
β_{ac}	ratio of the distances from the neutral axis to the extreme tension fibre
β_{ec}	coefficient relating the average crack width to the design value
β_{mc}	empirical coefficient to assess the average strain within $l_{s,max}$
ϕ	diameter of the steel fibre
ρ	relaxation coefficient
ρ_{ef}	effective steel ratio
φ	creep coefficient
σ_s	steel stress
σ_{sr}	maximum steel stress in a crack in the crack formation stage
σ_{cti}	uniform average tensile stress
τ_{bi}	short-term bond stress

τ_{bm}	mean bond strength
τ_{sm}	average bond stress over load transmission length
ε_{cm}	mean strain in the concrete between the cracks
ε_{s2}	maximum steel strain at the crack
ε_{sr2}	steel strain at the crack
ε_{cs}	free shrinkage strain of concrete
ε_{sm}	mean strain in the reinforcement at the design loads
η_r	coefficient taking account of shrinkage contribution
A_{ct}	cross-sectional area of concrete in the tensile zone
$A_{c,eff}$	effective area of the tensile concrete surrounding the tensile reinforcement of depth
A_e	effective tension area of concrete surrounding the flexural tension reinforcement
$A_{s,min}$	minimum tensile reinforcement area
A_{st}	cross-sectional area of tensile steel reinforcement
c	clear cover to the longitudinal reinforcement
d	depth to the tensile reinforcement
d_b	bar diameter
d_c	distance from centre of bar to extreme tension fibre
d_n	depth of compression zone in a fully cracked section
D	overall depth of a cross-section
E_s	steel modulus of elasticity
f_{ct}	concrete matrix tensile strength
$f_{ct,eff}$	mean value of the axial tensile strength of concrete at the time cracking
f_{ctm}	mean value of axial tensile strength
F_{cr}	cracking force
f_{Fts}	steel fibre tensile strength
f_s	maximum stress permitted in the reinforcement immediately after crack formation
f_y	steel bar yield stress
k_t	factor that depends on the duration of load

k_1	coefficient depending upon bond quality
k_2	coefficient depending upon the shape of the strain diagram
l_{es}	transfer length
$l_{s,max}$	length over which slip between steel and concrete occurs
L	length of the steel fibre
M_{cr}	cracking moment
M_{max}	maximum moment
n_b	number of reinforcing bar
s	bar spacing
s_{rm}	average crack spacing
$s_{r,max}$	maximum crack spacing
w_k	maximum crack width
w_m	average crack width
w_{max}	maximum crack width

LIST OF ACRONYMS

AEA	air-entraining admixtures
CA	coarse aggregate
CC	conventional concrete
CD	casting direction
CRI	concrete research institute
CRC	conventional reinforced concrete
CS	compressive strength
CSSC	compressive stress-strain curve
c/p	cement to powder ratio
EFA	Eraring Fly Ash
FA	fine aggregate
FCL	first crack load
FCD	first crack deflection
FEM	finite element method
FRC	fibre-reinforced concrete
FRSCC	fibre-reinforced self-compacting concrete
FTS	flexural tensile strength
H	horizontal casting direction
HMR	high moment region
HRWR	high range water reducer
GGBFS	ground granulated blast furnace slag
LVDT	linear variable displacement transducer
MOE	modulus of elasticity
MOR	modulus of rupture
RH	relative humidity
RC	reinforced concrete
RVE	representative volume element
SC	slag cement

SCC	self-compacting concrete
SFC	super flowable concrete
SFRC	steel fibre-reinforced concrete
SFRSCC	steel fibre reinforced self-compacting concrete
SHCC	strain hardening cementitious composites
SLC	shrinkage limited cement
SP	superplaticizers
SUCST	specimen utilized in the compressive strength test
TS	tensile strength
UHPFRC	high and ultrahigh performance fibre reinforced concrete
V-D	vertical down casting direction
V-U	vertical up casting direction
w/c	water-cement ratio
w/cm	water-cementitious materials ratio
VMA	viscosity modifying admixture
WHS	workplace health and safety
WR	water reducer

TABLE OF CONTENTS

LIST OF FIGURES

LIST OF TABLES

ABSTRACT

Developments in concrete technology provide engineers, designers, suppliers and contractors with new methods of approaching engineering problems. Many of these developments are engineered solutions to technical and commercial problems, by either improving the current practices or overcoming limitations in the existing technology. One of the developments is Self-Compacting Concrete (SCC). SCC refers to a 'highly flow-able, non-segregating concrete that can be spread into place, fill the formwork, and encapsulate the reinforcement without the aid of any mechanical consolidation' as defined by the American Concrete Institute (ACI). SCC is regarded as one of the most promising developments in concrete technology due to significant advantages over Conventional Concrete (CC). Many different factors can influence a decision to adopt SCC over CC ranging from structural performance to associated costs. These decisions should be well informed and based on a sound understanding of such factors.

In addition, Fibre Reinforced Self-Compacting Concrete (FRSCC) is a relatively new composite material which congregates the benefits of the SCC technology with the profits derived from the fibre addition to a brittle cementitious matrix. Fibres improve many of the properties of SCC elements including tensile strength, ductility, toughness, energy absorption capacity, fracture toughness and cracking.

For a structure (made by CC, SCC and FRSCC) to remain serviceable, crack widths must be small enough to be acceptable from an aesthetic point of view, to avoid waterproofing and deterioration problems by preventing the ingress of water and harmful substances. Crack control is therefore an important aspect of the design of reinforced concrete structures at the serviceability limit state. Limited researches have been undertaken to understand cracking and crack control of SCC and FRSCC members. Since, the time-dependent mechanisms of SCC and FRSCC are still not completely understood; a reliable and universally accepted design procedure for cracking and crack control of SCC and FRSCC members has not been developed yet. There exists a need for both theoretical and experimental research to study the critical factors which affect the time-dependent cracking of SCC and FRSCC members.

In this study cracking caused by external loads in reinforced SCC and FRSCC slabs is examined experimentally and analytically. The mechanisms associated with the flexural cracking due to the combined effects of constant sustained service loads and shrinkage are observed. One of the primary objectives of this study is to develop analytical models that accurately predict the hardened mechanical properties of SCC and FRSCC. Subsequently, these models have been successfully applied to simulate time-dependent cracking of SCC and FRSCC one-way slabs.

Series of tests on eight prismatic, singly reinforced concrete one-way slabs subjected to monotonically increasing loads or to constant sustained service loads for up to 240 days, were conducted. An analytical model is presented to simulate instantaneous and time-dependent flexural cracking of SCC and FRSCC members. It should be emphasized that any analytical model developed for calculation of crack width and crack spacing of reinforced SCC and FRSCC slabs must be calibrated by experimental data and verified by utilizing Finite Element Method (FEM). The analytical predictions of crack width and crack spacing for the SCC and FRSCC one-way slabs are in reasonably good agreement with the experimental observations.

CHAPTER 1

INTRODUCTION

CHAPTER 1

INTRODUCTION

1.1 BACKGROUND

Self-Compacting Concrete (SCC) can be placed under its own weight without compaction. In addition, it is cohesive enough to be handled without segregation and bleeding. Modification of the mix design of SCC can have a significant influence on the material's mechanical properties. Therefore, it is important to investigate whether all of the current design assumptions about Conventional Concrete (CC) structures are also valid for SCC structures.

Unlike Japan, USA, and Europe, there has been a reluctance to employ SCC technologies in the Australian construction industry. The Australian construction industry, like the UK industry, has developed a culture of being particularly slow to adopt and resistant to accept change. This culture has hindered the commercialisation of technologies such as SCC, discouraging interest outside academic institutions. SCC in Australia has been considered as an improvement over current applications of Super Flowable Concrete (SFC). It exceeds the current limitations of CC and SFC in providing superior material properties, namely passing ability through dense reinforcement, segregation resistance, bleeding and drying shrinkage. It maintains a higher degree of homogeneity in the concrete mix and allows for improved batch consistency over SFC, resulting in less material defects and increasing durability. SCC is considered a viable option in Australia where limitations of CC in relation to achieving full and consistent coverage of reinforcement in intricate designs and the Workplace Health and Safety (WHS) issues related to working in confined spaces to vibrate CC are present.

Compared to CC, SCC achieves higher quality in the construction process by relying far less on the skill of workers for adequate compaction. In overcoming the need for external mechanical compaction of freshly placed concrete, the potential for durability

defects resulting from inadequate compaction are significantly reduced. The material allows for improved compaction over CC, achieving a more uniform, dense and consistent concrete structure and ultimately resulting in a more durable product. When designed and placed correctly, SCC offers advantages in the areas of sustainability, material properties, product quality, financial costs, project programming and associated labour. Relevant advantages for the adoption of SCC within the context of this report include those related to WHS and quality issues. The aforementioned advantages are a direct result of the properties of SCC, namely the flowing ability, passing ability and resistance to segregation. For instance, the flowing ability of SCC removes the need for external compaction, therefore provides additional advantages associated with WHS such as all those associated with noise pollution. It also allows for an increase in productivity in the construction process, which may lead to significant economic savings. SCC has also been beneficial in addressing the issue of the shortage of skilled labourers in the workforce, as the application of the product is independent of workmanship. The passing ability of SCC is beneficial in intricate designs, congested reinforcement as well as perfectly suited for precast construction due to productivity and quality factors. The resistance to segregation significantly reduces surface defects, air voids and encases all reinforcement without the need for vibration, which ultimately creates a superior product and ensures a higher quality finish in comparison to CC.

Just like all types of concrete, SCC has limitations. SCC has substantial differences in production in comparison to CC due to the sensitivity to variations in quality and consistency of mix constituents (Goodier, 2003). SCC's sensitivity to variation requires a high degree of accuracy in batching which subsequently relies on comprehensive testing to ensure the batching is consistent. The batching itself may need additional additives when it is compared to CC such as superplasticisers, Viscosity Modifying Admixtures (VMAs) and higher powder contents. As SCC requires higher powder contents, lower water to cement ratio and additional chemical admixtures compared to CC, the raw material cost of the SCC increase making it more expensive. This additional cost as well as the necessary testing has limited its use to only specialised applications but CC will not provide the specified level of quality.

Generally, the incorporation of fibres improves engineering performance of structural and non-structural concrete. The use of Fibre-Reinforced Concrete (FRC) is also of special interest for retrofit and seismic design. The incorporation of metallic fibres can be problematic on some situations, especially when the fibre volume is high and the FRC is cast in sections with a moderate to high degree of reinforcement. The fibre content, length, aspect ratio, and shape play an important role in controlling workability of FRC. Such concrete presents greater difficulty in handling and requires more deliberate planning and workmanship than established concrete construction procedures. The additional compaction effort is required for such concrete which contributes to the increase in construction cost. In order to provide sufficient compaction, improve fibre dispersion, and reduce the risk of entrapping voids, the FRC is often proportioned to be fluid enough to reduce the need for vibration consolidation and facilitate placement. An extension of this approach can involve the use of SCC to eliminate or greatly reduce the need for vibration and facilitates placement. A truly Fibre-Reinforced Self-Compacting Concrete (FRSCC) should spread into place under its own weight and achieve consolidation without internal or external vibration, ensure proper dispersion of fibres, and undergo minimum entrapment of air voids and loss of homogeneity until hardening. Lack of proper self-compaction or intentional vibration and compaction can result in macro- and micro-structural defects that can affect mechanical performance and durability (Khayat and Roussel, 2000).

The use of FRSCC probably, will swiftly increase in the next few years, since this composite material introduces several superior advantages on the concrete technology. In fact, the partial or total replacement of the conventional steel bar reinforcement by discrete fibres optimizes the construction process. The assembly of the reinforcement bars in the construction of concrete structures has a significant economical impact on the cost of this type of constructions, due to the man-labour costs that it requires. In the developed countries, the cost of man-labour is significant, and diminishing the man-labour will decrease the construction costs. For this reason, FRSCC is a very promising construction material with high potential of application, mainly in the cases where fibres can replace conventional reinforcement. At the present time, however, the FRSCC technology is not yet fully developed. Moreover, the mechanical behaviour of FRSCC material is still not clearly

understood. The energy absorption capacity and the impact strength of cement based materials are the properties most benefited by the addition of fibres to concrete.

1.2 STATE OF THE PROBLEM

Generally, strength and serviceability are the two main criteria to be satisfied in the design of reinforced concrete structures. Strength is the ability of the structure to carry the design ultimate loads without collapsing. The strength of a structure may usually be determined with reasonable accuracy because reinforced concrete structures are commonly designed to provide ductile failure, i.e., yielding of the reinforcement before failure of the concrete. Serviceability refers to the behaviour of structures at working loads, with particular reference to cracking and deflection. Both cracking and deflection are primarily dependent on the properties and behaviour of the concrete but are more difficult to predict because of the non-linear, inelastic and time-dependent nature of the concrete. If structural designers do not adequately account for this non-linear behaviour, serviceability problems may result. Therefore, crack control is an important aspect of the design of reinforced concrete structures at the serviceability limit state (Nejadi, 2005). Because concrete is low in tensile strength, cracks are inevitable in reinforced concrete structures. Therefore, studying the cracking behaviour and controlling the width of cracks in reinforced concrete members are absolutely necessary.

For a structure that is made by SCC and FRSCC (e.g. bridges and tall buildings) to remain serviceable, crack widths must be small enough to be acceptable from an aesthetic point of view, small enough to avoid waterproofing problems and to prevent the ingress of water that may lead to corrosion of the reinforcement. Despite its importance, building code provisions for crack control mostly have been developed from laboratory observations of the instantaneous behaviour of reinforced SCC and FRSCC members under load and fail to account adequately for the time-dependent development of cracking. In this study cracking caused by external loads in reinforced SCC and FRSCC elements is examined experimentally and numerically.

Limited researches have been undertaken to understand cracking and crack control for SCC and FRSCC members. Also, the time-dependent mechanisms and interactions are still not completely understood. In addition, a reliable and universally accepted design procedure has not been developed. There exists a need for both theoretical and experimental research of the critical factors which affect time-dependent cracking of SCC and FRSCC. One of the primary objectives in this study is to develop analytical models that accurately predict hardened mechanical properties of SCC and FRSCC. Then, these mechanical models have been successfully applied to simulate time-dependent cracking of SCC and FRSCC one-way slabs. It should be emphasized that any analytical model developed for predicting long-term behaviour of reinforced SCC and FRSCC structures and for calculation of crack width and crack spacing must be verified by experimental data by using Finite Element Method (FEM) and calibrated by experimental data. However, experimental information on the long-term behaviour and crack width under sustained loads is very limited. Therefore, laboratory controlled test data for the long-term development of cracking is also required.

1.3 OBJECTIVES AND SCOPE OF THE THESIS

The objectives of this research are as follows:

- To investigate the hardened properties of SCC and FRSCC, including the mechanical properties, bond characteristics, shrinkage, and creep, to compare with those of CC and FRC and proposing new models to accurately prediction of the hardened properties of SCC and FRSCC.

- To implement these proposed models for hardened properties of SCC and FRSCC by utilizing ATENA software to simulate the time-dependent cracking of SCC and FRSCC one-way slabs.

- To study the mechanisms associated with flexural cracking of reinforced SCC and FRSCC one-way slabs and the influence of the many factors that affect the width and spacing of flexural cracks under sustained service loads.

- To obtain laboratory controlled data to calibrate, validate, and extend analytical models that are being developed concurrently with the experimental program.

- To develop a new analytical model that simulates flexural cracking and design oriented procedures to calculate crack widths and crack spacing of reinforced SCC and FRSCC one-way slabs.

- To accurately measure the material properties, including the creep and shrinkage characteristics of the concrete used in the reinforced SCC and FRSCC elements.

- To investigate of the effects of various parameters on time-dependent cracking of reinforced SCC and FRSCC structures by running a series of FEM parametric studies on slab specimens.

To achieve these objectives, the work has been subdivided into a number of discrete tasks which are summarized as follows:

1. A test program was carried out to develop information about the mechanical properties of SCC and FRSCC. For this purpose, four different mixes including - plain SCC, steel, polypropylene, and hybrid FRSCC - were considered in the test program. The mechanical properties including the compressive and splitting tensile strengths, modulus of elasticity, modulus of rupture, and compressive stress-strain curve were monitored and recorded. These properties were tested and monitored at 3, 7, 14, 28, 56, and 91 days.

2. Eight prismatic, singly reinforced concrete one-way slabs were cast and moist cured for a period of 28 days, and then tested under third point loading over a simply supported span of 3.5 m. The distribution and extent of both primary and secondary cracking were recorded at all stages of loading. The results were subsequently used in the development and calibration of an analytical model to simulate flexural cracking in reinforced SCC and FRSCC slabs.

3. An experimental program including eight slab specimens for the long-term tests was carried out. These specimens were monitored under sustained loads for up to 240 days to measure the cracking and deformations due to service loads and to quantify the effects of steel area, steel stress, and concrete shrinkage. The gradual development of cracking and the gradual increase in crack width with time were carefully monitored and recorded during the test.

4. Tests were also conducted to obtain the creep and shrinkage characteristics of the SCC and FRSCC to provide accurate data for analysing the specimens.

5. An analytical model was developed to model flexural cracking in reinforced SCC and FRSCC one-way slabs in bending. In the proposed model, the tension chord model (Marti et al, 1998) was modified and used to simulate and study the tension zone of a flexural member and the time-dependent effects of creep and shrinkage.

6. In this study, the effective tension area of concrete A_{ct}, is assumed to be constant after cracking and independent of time. New analytical models for calculating the effective tension area for SCC and FRSCC slab specimens were proposed and calibrated according to the test results.

7. Using the analytical models presented in task 5, analysis of the test specimens were undertaken with crack width and crack spacing being of particular interest. The accuracy of each model is assessed by comparison with the measured experimental values. Despite cracking being a random phenomenon and the measured crack widths and crack spacing in structural members showing large scatter, good agreement was obtained between the measured experimental and predicted values, both for instantaneous and time-dependent behaviour.

8. The crack width and crack spacing calculation procedures outlined in six international concrete codes, namely Eurocode 2 (1991), CEB-FIP (1990), ACI318-89 and ACI318-99 (1999), Eurocode 2 (2004), ACI 318-08 (2008), and fib-Model Code (2010) are presented and the code predictions are compared with the analytical model proposed in task 5 above and the measured experimental values. A comparison between the experimental results, analytical model, and international

codes was also presented diagrammatically for SCC and FRSCC slab specimens for both instantaneous and time-dependent behaviour.

9. Investigation of the effects of various parameters on time-dependent cracking of reinforced SCC and FRSCC elements was carried out by running a series of numerical parametric studies on slab specimens.

1.4 LAYOUT OF THE THESIS

This thesis is presented in ten Chapters and five appendices. Chapter 2 of this thesis provides a review of previous SCC studies related to history and development, advantages and limitations, fresh properties, mechanical properties, bond characteristics, shrinkage and creep, and available full-scale time-dependent SCC.

Chapter 3 is a state-of-the-art review on the hardened SCC properties and available equations. Also, in Chapter 3 for each hardened SCC property, new models for precise prediction of the mechanical properties are proposed.

Chapter 4 is a state-of-the-art review on the time-dependent behaviour of hardened SCC and available equations. Also, in Chapter 4 new empirical equations for precise prediction of shrinkage and creep are proposed.

Chapter 5 describes the experimental program for materials properties of proposed SCC and FRSCC mixtures.

Chapters 6 and 7 describe the experimental program for SCC and FRSCC short-term and long-term flexural cracking, respectively. Detailed test results of the crack width, crack history and crack pattern for each specimen are included in both Chapters. The results are summarised and discussed at the end of each Chapter.

The analytical model for flexural cracking developed for short-term and time-dependent behaviour, is presented in Chapter 8. An evaluation of the crack width and crack spacing calculation procedures in accordance with six international codes is also presented and the results are discussed and compared diagrammatically at the end of this Chapter.

Chapter 9 evaluates the finite element models described in the ATENA software. Also, developed models in the previous Chapters about the SCC and FRSCC mechanical properties, bond characteristics, shrinkage and creep, crack width and crack spacing are used in the ATENA software. At end of this Chapter a parametric investigation using the proposed models to study time-dependent cracking has been done and the results are summarised and discussed.

Finally, Chapter 10 summarizes the conclusions drawn from the investigation of this study and recommendations for future research are made. Additional information is provided in the Appendices.

Appendix A describes the entire fibre pullout process.

Appendix B shows some fresh property tests.

Appendix C presents flexural toughness methods and specifications.

Appendix D presents short-term concrete surface strains at steel level and steel strains.

Appendix E presents long-term concrete surface strains at steel level and steel strains.

Appendix F presents creep and shrinkage testing procedure.

Appendix G shows typical FEM analysis results.

CHAPTER 2

LITERATURE REVIEW

CHAPTER 2

LITERATURE REVIEW

2.1 BACKGROUND AND DEVELOPMENT OF SCC

2.1.1 History

Initially referred to as high performance concrete, Self-Compacting Concrete (SCC) prototype mixes first emerged in Japan in 1988 as a result of efforts to achieve more durable concrete structures. Pioneered by Kazumaza Ozawa and Koichi Maekawa at the University of Tokyo (Ozawa et al., 1989) and in collaboration with leading construction companies and concrete suppliers, SCC was developed to address concerns with concrete durability experienced in Japan in the early 1980's due to a decreasing skilled labour market and pressure from clients for a higher quality finished product. The development of SCC was an extension of existing concrete technologies in highly workable and underwater concretes that at the time were developed from a need for improved cohesiveness with fine aggregates.

The extensive development of SCC technologies and success in ready-mixed concrete markets experienced in Japan, led to European interest in the late 1990's and numerous research projects including the RILEM conference. From the success of the Conference, a technical committee was established with the clear objective to gather, analyse and present a literature review based on the technologies evolving from SCC. The committee also aimed at finding a unified view on testing and evaluation of material properties, which at the time was a pressing issue as many researches were unsure of the consistency with the properties of the SCC in comparison to CC.

The success of cast in-situ applications eventually led to the introduction of SCC technology into the pre-cast concrete market. Although the same quality issues were not prevalent in the pre-cast industry, adoption of the technology was embraced due to the potential for a superior finish with fewer defects and increased productivity. Initially, SCC

was better suited to pre-cast markets due to the higher degree of control available in pre-cast construction, allowing for the batching accuracy and consistency required. Accuracy in batching is critical in ensuring the final product is successful due to the heightened sensitivity to variation in quality and consistency in SCC mix constituents. Experience gained from commercial application has increased accuracy and consistency in batching, making SCC more applicable to the cast in-situ markets.

2.1.2 Development

Since its initial development in Japan, extensive research and development of SCC technology was driven by large construction companies and academic institutions within Japan and eventually spread internationally to countries across Europe and North America. Academic institutions in Japan, Germany and the Scandinavian countries have led the way in research and testing of SCC material properties. Large construction companies, ready mix concrete suppliers and pre-cast manufacturers in Japan, France and Holland have driven product development due to the material's increasing acceptance and application within industry. National bodies and groups across Europe and North America have developed and continue to develop guidelines and standards related to the SCC's materials design, application and performance. National bodies and groups across Europe and North America have addressed the need for established guidelines and standards related to the SCC's materials design, application and testing. European committees have developed material testing methods and placement practices related to the commercial application of the technology.

Research, development and application of SCC was limited to and concentrated in Japan and Europe initially with the technology later spreading through North and South America and eventually to Australia. Major developments and applications of SCC in Japan and Europe have been outlined below, followed by the adoption of the technology in the Australian construction industry.

- *Japan – Late 1980's*

Beginning in 1989, research papers on concrete mixes with properties similar to those now identified with SCC were increasingly published with reference to mix design and fresh properties. Case studies on early applications of SCC technology were first published in the early 1990's and commercial research and development quickly followed, leading to commercial applications as early as June of 1990 in Japan (Okamura and Ouchi, 2003). The first significant international workshop dedicated to SCC was held at the University of Tokyo in October 1998 focussing on the development of SCC outside of Japan. A committee established by the Japanese Society of Civil Engineers (JSCE) in 1997 published the first recommendations for the practical application of SCC in 1999 and research by academic institutions, national committees and large construction companies continue into areas such as composite structures (Goodier, 2003). The first commercial application of SCC in Japan was in the construction of a building in June 1990 and soon after was incorporated in the construction of the towers for the Shin-kiba Ohashi pre-stressed cable stay bridge in 1991. Lightweight applications of SCC emerged as early as 1992 in the main girder of a cable-stayed bridge and further use has gradually increased. Despite this significant development, SCC is still considered a 'specialty concrete' as opposed to 'standard concrete' in Japan (Okamura and Ouchi, 2003).

- *Europe –1990's*

As research and development continued in Japan primarily by the large commercial construction companies, interest and eventual application of SCC technologies spread to parts of Europe in the 1900's, initially in the Scandinavian countries, followed by France and the Netherlands, and eventually by others including Germany and the United Kingdom. Sweden was the forerunner in Europe with further development and research associated with SCC. The Concrete Research Institute (CRI) initiated a seminar in Sweden in 1993, which led to a project dealing with the incorporation of SCC in housing construction. The findings and results from this project led to the first European based project entitled Brite-EuRam which began in 1997. The aim of the project was to reduce the cost, program and increase quality of in-situ cast concrete construction by utilising a vibrationless product.

The project was broken up into two sections: 'the development of SCC with or without steel fibres and full-scale experiments in civil engineering and housing' (Goodier 2003).

In conjunction with this project the CRI also collaborated with the Swedish National Roads Authority (SNRA) to use SCC in casting of bridge construction, consequently resulting in the first of three bridges to be solely constructed by using SCC outside of Japan (Goodier, 2003). The total cost of the bridge was also reduced by 5-15% by selecting SCC over CC. In addition, energy consumption and greenhouse emission was reduced by 20-30% (Goodier, 2003). In this project it has been also noted that the hardened properties of SCC were superior in comparison to CC particularly in the area of 'compressive strength, frost resistance, permeability and reinforcement bond strength,' however a major adversity at the time was lack of testing methods that could analyse the passing ability, filling ability and resistance to segregation (Goodier, 2003).

The positive testing and application that occurred from the Brite-EuRam project has seen the expansion of SCC being utilised in pre-cast and in-situ applications in Scandinavia, France, Netherlands, Germany and the United Kingdom. However a major adversity at the time was a lack of testing methods. In order to address this issue, the European Union granted further researches which resulted in the adoption of appropriate testing methods and standardised provisions.

- *Australian Application*

Unlike Japan and some of European countries, there has been a reluctance to employ SCC technologies in the Australian construction industry (Ravindrarajah et al., 2003). The Australian construction industry, much like the UK industry, has developed a culture of being particularly slow to adopt and resistant to accept change. This culture has hindered the commercialisation of technologies such as SCC, discouraging interest outside of academic institutions. SCC in Australia has been considered an improvement of current applications of SFC (Madrio and Chirgwin, 2011). It exceeds the current limitations of CC and SFC in providing superior material properties, namely passing ability through reinforcement, segregation resistance, bleeding and drying shrinkage. It maintains a higher degree of homogeneity in the concrete mix and allows for improved batch consistency over

SFC, resulting in less material defects and increased durability. SCC is considered a viable option in Australia where limitations of CC in relation to achieving full and consistent coverage of reinforcement in intricate designs and the Workplace Health and Safety (WHS) issues related to working in confined to CC spaces are present.

The research and development undertaken in Australia has been limited to academic institutions and recently to government authorities, with commercial applications limited to only the largest concrete suppliers. Consequently, development with local materials has been relatively slow and its use has been limited to highly specialised applications which hinders economies of scale and discourages industry adoption further.

2.2 ADVANTAGES OF SCC

Compared to CC, SCC achieves higher quality in the construction process by relying far less on the skill of workers for adequate compaction. In overcoming the need for external mechanical compaction of freshly placed concrete, the potential for durability defects resulting from inadequate compaction are significantly reduced. The material allows for improved compaction over CC independent of workmanship, achieving a more uniform, dense and consistent concrete structure and ultimately resulting in a more durable product. When designed and placed correctly, SCC offers advantages in the areas of material properties, product quality, financial costs, project programming and associated labour. Relevant advantages for the adoption of SCC within the context of this report include those related to WHS and quality issues.

Naik et al. (2012) describes other advantages of SCC over CC as follows:

- Saving of costs on machinery, energy, and labour related to consolidation of concrete by eliminating it during concreting placement operations.
- High-level of quality control due to more sensitivity of moisture content of ingredients and compatibility of chemical admixtures.
- High-quality finish, which is critical in architectural concrete, precast construction, as well as for cast-in-place concrete construction.

- Reduces the need for surface defects remedy (patching).
- Increase of the service life of the moulds/formwork.
- Promotes the development of a more rational concrete production.
- Industrialized production of concrete.
- Ensuring better quality of cover for reinforcement bars.
- Reduction in the construction time.
- Improves the quality, durability, and reliability of concrete structures due to better compaction and homogeneity of concrete.
- Easily placed in thin-walled elements or elements with limited access.
- Ease of placement results in cost savings through reduced equipment and labour requirement.
- Improves working environment at construction sites by reducing noise pollution.
- Eliminate noises due to vibration; effective especially at precast concrete products plants.
- Eliminates the need for hearing protection.
- Improves working conditions and productivity in construction industry.
- It can enable the concrete supplier to provide better consistency in delivering concrete, thus reduces the need for interventions at the plants or at the job sites.
- Provides opportunity for using high-volume of by-product materials such as fly ash, quarry fines, blast furnace slag, limestone dust, and other similar fine mineral materials.
- Reduces the workers compensation premium due to the reduction in chances of accidents.

The aforementioned advantages are a direct result of the properties of SCC, namely the flowing ability, passing ability and resistance to segregation. For instance, the flowing ability of SCC removes the need for external compaction, therefore provides additional advantages associated with WHS such as all those associated with noise pollution. It also allows for an increase in productivity in the construction process, which may lead to significant economic savings. SCC has also been beneficial in addressing the issue of the shortage of skilled labourers in the workforce, as the application of the product is independent of workmanship. The passing ability of SCC is beneficial in intricate designs, congested reinforcement as well as being perfectly suited for precast construction due to productivity and quality factors. The resistance to segregation significantly reduces surface defects, air voids and encases all reinforcement without the need for vibration, which ultimately creates a superior product and ensures a higher quality finish in comparison to CC.

2.3 LIMITATIONS OF SCC

Just like all types of concrete, SCC has limitations. SCC has substantial differences in production in comparison to CC due to the sensitivity to variations in quality and consistency of mix constituents (Goodier, 2003). SCC's sensitivity to variation requires a high degree of accuracy in batching which subsequently relies on comprehensive testing to ensure the batching is consistent. The batching itself may need additional additives when it is compared to CC such as superplasticisers, Viscosity Modifying Admixtures (VMAs) and higher powder contents. As SCC requires higher powder contents, lower water to cement ratio and additional chemical admixtures compared to CC, increase in the raw material cost of the concrete makes it more expensive. This additional cost as well as the necessary testing has limited use of SCC to only specialised applications where CC will not provide the specified level of quality.

Unfortunately there is minimal research that addresses the comparative costs between unskilled labourers applying the product and engineers testing the batching and design. Although there are cost savings associated with a decrease in labour on site, there is an increase in labour required for testing purposes. Moreover, lack of evidence and knowledge

of the long-term behaviour and durability of SCC due to the nature of new technology. There is also a reluctance to utilise SCC in commercial application due to the current perception that this type of technology is a specialised (niche) product. For instance, Goodier (2003) purports that in the UK market, consultants were hesitant to adopt SCC as there was a lack of guidance, principles and effective test methods, not to mention a positive longstanding reputation of CC.

As the mix design used in SCC is highly sensitive to variation, it is crucial that selections of materials are rigorously tested and precise measurements and monitoring of each batch is methodically assessed. CC can cope with variations by adjusting the amount of mechanical compaction whereas SCC requires alterations to the proportions of fine aggregates, coarse aggregates, cement, powder, water and admixtures. Furthermore, the mix must undergo additional fresh property testing both on-site and in the laboratory (Goodier, 2003). Although there are limitations with SCC, they are by far outweighed by its many advantages and the progression with the technologies associated with SCC that has enabled the limitations to be gradually reduced. It is envisioned that most, if not all limitations will be overcome with continual advances and this will ultimately lead to the transition from it being a 'specialist' concrete to a standard concrete.

2.4 KEY DRIVERS OF DEVELOPMENT OF SCC

The fact that many of the advantages of SCC are achieved independent of workmanship assists in adding validity to the adoption of SCC. SCC addressed the problem faced in Japan with the shortage of skilled labour in 1980s but it also has considerable benefits that are social, economic and environmental when compared to CC. SCC has drastically reduced overall construction time, which is evident in a number of case studies. For instance, Goodier (2003) suggested a case study in France by the Lafarge Group where two identical apartment blocks, one using CC and the other SCC, were constructed. The case study found that the apartment block using SCC was completed two and half months ahead of schedule with a financial saving of 21.4%. In addition to economic benefits, SCC has a high quality finish which is superior to CC. The flowing and passing ability has made intricate architectural designs possible which would have been avoided in the past due to

their high congestion of reinforcement. The elimination of compaction is one of the significant advantages that separate SCC from CC. The elimination of compaction has removed noise pollution in the environment, reduced WHS issues and allowed work to continue past restricted hours which directly speeds up the construction period.

Although it is considered that SCC will never completely replace CC, its steady growth in the concrete industry is a direct result of clients searching for a higher quality finished product. Overall, SCC can provide a superior product which is more durable and better quality than CC yet has considerable advantages making it evolve into a product that was initially perceived as being a 'special concrete' but has proven to be a standard concrete worthy of consideration in both precast and cast in-situ markets.

2.5 FRESH PROPERTIES OF SCC

Literature has reported that SCC possesses similar fresh property characteristics as CC but with improved qualities in regards to flow (Madrio and Chirgwin, 2011). Key fresh flow properties that characterise a concrete mix as self-compacting include;

i) Filling/flowing ability/fluidity – the ability to flow into and fill all areas of the formwork under its own weight (i.e. without the need for external vibration/consolidation)

ii) Passing ability – the ability to pass through congested reinforcement whilst resisting segregation, separation or blocking

iii) Stability/resistance to segregation – the ability to remain homogeneous in composition

The superior flowability achieved in SCC overcomes the limitations experienced in CC and is the primary reason for its adoption over CC in instances of intricate or congested reinforcement. This removes the need for external compaction or consolidation and therefore reduces the chance of defects associated with poor compaction. Improved passing ability and resistance to segregation over CC and particularly SFC are advantages that address the shortcomings of high fluidity from inclusion of superplasticisers alone. Although mixes of SFC can achieve the flowability observed in SCC, SFC lacks the ability to self-compact under its own weight and pass congested reinforcement without segregation

of SCC. The high fluidity in SFC may be achieved by the addition of superplasticisers or excess water alone. The addition of VMA's and/or powders in SCC reduces segregation and the effects of bleeding, drying shrinkage and assists in maintaining homogeneity of the concrete caused by excess water in the concrete mix.

These properties are generally achieved by the addition of chemical admixtures, namely superplasticisers and VMA's. The flowabilty is achieved by adding superplasticisers (as opposed to water in SFC) and the stability is achieved by adding VMA's and/or increasing the amount of powdered materials. The purpose of VMA's and powdered materials is to increase the viscosity of the mix, resisting segregation and providing stability in the mix. There have been considerable advances in superplasticiser technologies that have enabled SCC to be produced with sufficient viscosity by addition of superplasticiser alone, reducing the reliance on VMA's and additional powdered constituents.

2.5.1 Testing of Fresh Properties

In order to understand the degree of self compactability of an SCC mix, specialised testing methods have been developed to test the fresh properties unique to SCC. Quantifying the filling ability, passing ability and resistance to segregation of a SCC mix is essential to providing quality in the form of consistent supply and properties. It has been acknowledged that no single test can measure all three properties (Madrio and Chirgwin, 2011). Common testing methods such as the Slump Flow, J-ring, L-box, V-Flow, and U-Flow tests are described below. The purpose of these tests is to determine whether a mix is in fact self-compactable and to evaluate the degree of deformability and viscosity of the SCC mix.

- *Slump Flow Test*

Similar to the CC slump test, a standard Abram's standard slump cone is filled but in inverted direction with the SCC mix but not compacted. Once the cone is lifted, the average diameter across two perpendicular directions is taken as the slump flow value. Nagataki and Fujiwara (1995) consider a slump-flow between 500 and 700 mm as sufficient to qualify a mix as self-compacting. Concrete mixes with slump-flows greater than 700 mm are expected to segregate and slump-flows less than 500 mm are considered to have

insufficient passing ability. The slump-flow test is used to evaluate flowability quality of SCC. The slump-flow test measures the capability of the mix to deform under its own weight in isolation and determines the consistency and cohesiveness of the concrete. An example of a slump-flow test and apparatus is illustrated in the Figure 2.1.

- *J-ring Test*

Similar to the slump-flow test, an Abram's standard slump cone filled with concrete and surrounded by reinforcing bars (see Figure 2.2) is lifted. The concrete flows through and past the reinforcing bars. The average diameter across two perpendicular directions is taken as the slump flow value. Based on the results of the j-ring test, the passing ability of the mix is assessed (Naik et al., 2012).

- *L-Box Test*

The L-Box test consists of filling the vertical portion of the L-Box apparatus (see Figure 2.3) and allowing any segregation or bleeding to occur. The time for concrete to flow past nominated distances and the height of concrete at each end are measured. The L-Box test measures filling, passing and resistance to segregation properties (Sonebi et al., 2012).

- *V-Flow Test*

The V-Flow test involves measuring the time taken for a completely filled V-Flow funnel test apparatus (see Figure 2.4) to empty once opened. Concrete is generally considered to be self-compacting with a V-Flow time (Ferraris et al., 2000) of 6 seconds or less (Naik et al., 2012). The V-Flow test evaluates the flowabiility of a concrete mix.

- *U-Flow Test*

The U-Flow test involves filling a single chamber of a U-Flow device (see Figure 2.5) then measuring the height to which the concrete rises through the reinforcing bars into the opposing chamber when opened. Concrete is generally considered self-compacting if it achieves a filling height of at least 70% of the maximum possible height. The U-Flow test measures filling, passing and resistance to segregation properties (Naik et al., 2012).

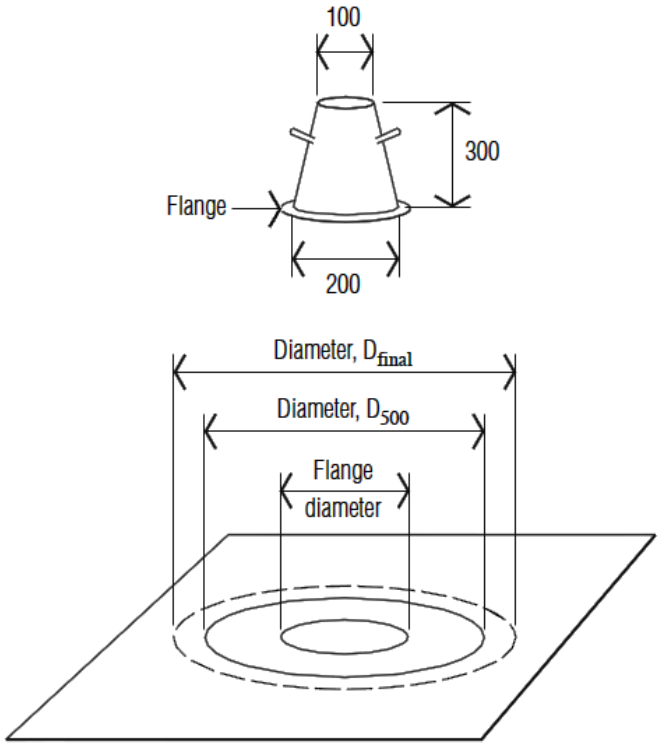

Figure 2.1 Slump Flow Apparatus

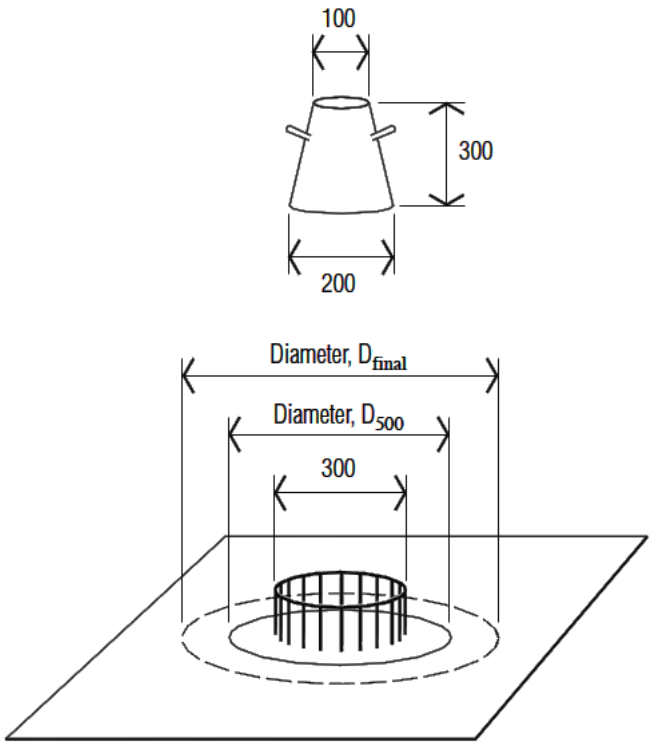

Figure 2.2 J-Ring Apparatus

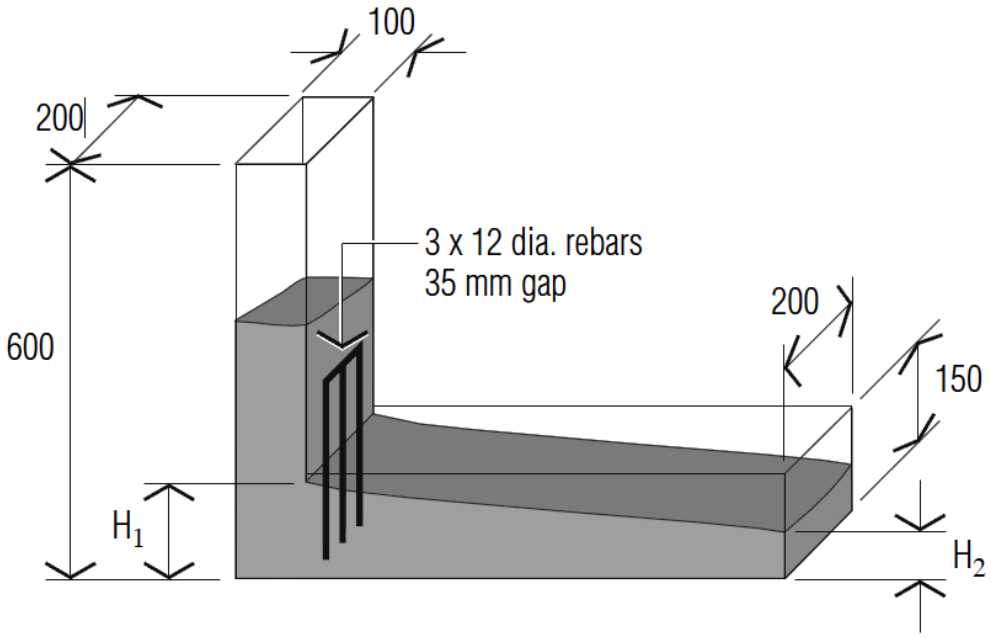

Figure 2.3 L-Box Apparatus

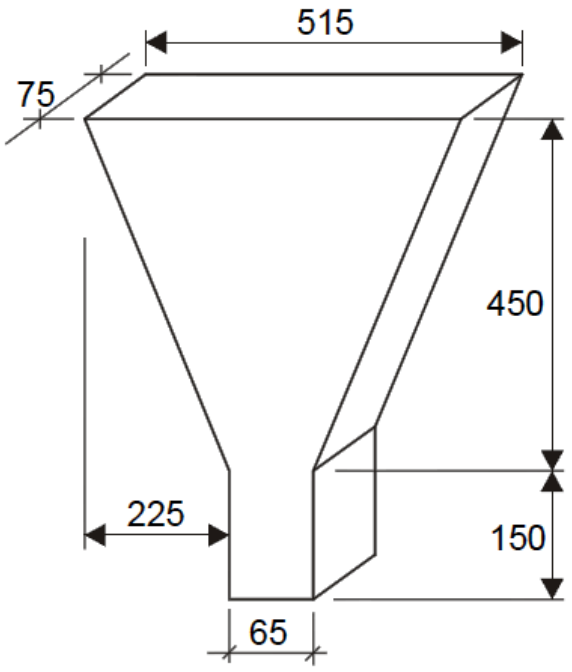

Figure 2.4 V-Flow Apparatus

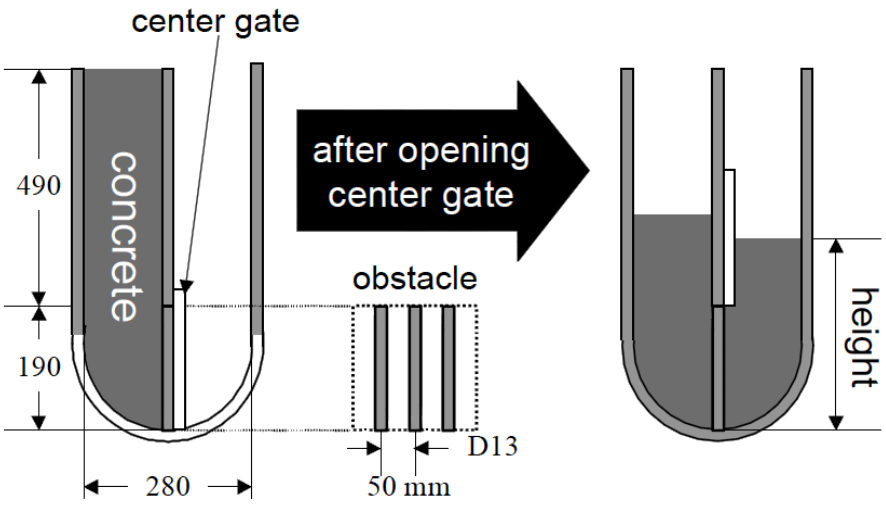

Figure 2.5 U-Flow Apparatus

2.6 MECHANICAL PROPERTIES OF SCC

Fresh properties of SCC could potentially influence the mechanical properties of SCC. These mechanical properties are crucial to the design and performance of Reinforced Concrete (RC) structures. Modulus of Elasticity (MOE) represents the stress-strain relationship in the elastic range and is used in the prediction of deflection and camber of concrete members. Modulus of Rupture (MOR) and Tensile Strength (TS) are measurements of the tensile strength of concrete and are used to predict and limit the allowable stresses in critical tension regions in concrete members. These properties are used to predict the elastic behaviour and flexural capacity of structural members in design standards. In this study, test results are used to evaluate the impact of SCC mixture proportions on mechanical properties and then compared these properties with those of CC. The applicability of the available prediction equations are evaluated in Chapter 3. Other available prediction equations are also assessed to determine if they can reasonably predict the mechanical properties of SCC. When necessary, new prediction equations are proposed for SCC in this study.

2.6.1 Compressive Strength (CS)

Compressive strength (CS) is the representative value of mechanical properties. This value should be evaluated to predict the behaviour of structural components because this value is highly correlated to elastic behaviour, tensile strength, flexural strength, and bond strength. CS is dependent on the age of the concrete, the gradation of the aggregate, curing conditions, type of admixtures, water-cement ratio, curing, temperature, and testing parameters such as size of equipment and loading conditions (Mehta and Monterio 2005).

According to a comprehensive survey on SCC by Kim (2008), the compressive strength of SCC is controlled mainly by the composition of the powder -this is generally the water-cementitious materials ratio (w/cm). Water-powder ratio typically includes limestone dust, etc.- rather than the water to powder ratios as is typical with conventional concrete (Domone, 2006). The w/cm dominantly affects the compressive strength rather than the total paste volume (Pineaud et al., 2005). SCC has higher compressive strength than CC (D'Ambrosia et al., 2005; Hamilton and Labonte, 2005; Issa et al., 2005; Naito et al., 2006), whereas coarse and fine aggregate ratio did not affect the early and later compressive strength in a range between 38 MPa and 66 MPa. VMAs can also influence the rate of hydration of cement at low water-cement ratios because they limit the available water for hydration and also alter the air void system. Therefore, reduced compressive strength has been observed in SCC when using VMAs at low water-cement ratios (Girgis and Tuan, 2004; Khayat, 1996; Khayat, 1998). However, over dosage of VMAs did not influence the hardened properties of SCC (MacDonanld and Lukkarila, 2002).

In general, development of compressive strength and the impact of mixture proportions on strength are not fully understood for application of the SCC mixtures in precast, prestressed structural members because the proportions and compositions are highly advanced (Kim, 2008). Furthermore, there was insufficient research about hardened properties of SCC mixtures considering the crucial design criterion of the plants, high concrete compressive strength at release. Compressive strength is directly used in predicting other mechanical properties, bond characteristics, and overall structural performance.

2.6.2 Modulus of Elasticity (MOE)

Generally, MOE is used to determine deflection of structures for serviceability requirements and in seismic analysis for deformation and drift calculations. MOE is also used in prestressed concrete for calculating the elastic shortening of concrete and creep loss. Current models of CC may not take into consideration the complexity of SCC, and thus may predict the MOE of SCC inaccurately. Kim (2008) mentioned that many researchers have recognized aggregate characteristics as an important parameter in predicting MOE of concrete (ACI Committee 363, 1992; Aitcin and Mehta, 1990; Carrasquillo et al., 1981). CEB-FIP (1990) and AASHTO LRFD Bridge Design Specifications (2006) consider the aggregate as an important parameter in predicting MOE along with compressive strength. Stiffness of concrete mostly depends on the stiffness of both paste and aggregate, and when the aggregate stiffness is significant, the volume of coarse aggregate could also influence the MOE of the concrete. MOE of high-strength concrete depends primarily on the stiffness of the cement paste rather than on the aggregate compared to normal compressive strength concrete (Cetin and Carrasquillo, 1998). Both MOE and strength of concrete also depend on the aggregate characteristics. The MOE of SCC is typically lower than that of CC with the same strength due to the lower volume of coarse aggregate in SCC mixtures (Bonen and Shah, 2004; Dehn et al., 2000; Felekoglu et al., 2007; Ma and Dietz, 2002; Naito et al., 2006; Walraven, 2005; Zia et al., 2005). In addition, the coarse to fine aggregate ratio does not affect MOE (Schindler et al., 2007), while the total paste volume affects the MOE of SCC mixtures (Pineaud et al., 2005). However, the impact of SCC mixture proportions on MOE has not been fully understood for application of SCC in precast, prestressed structural members associated with prestress losses, camber, and deflection. According to several existing equations, MOE is estimated using the concrete compressive strength and unit weight.

2.6.3 Tensile Strength (TS)

Another essential mechanical parameter is the TS of concrete. The TS of concrete is important for predicting the initiation of cracking of a concrete member when subjected to external loads (Walraven, 2005) and restrained shrinkage effect (Nejadi, 2005). Several factors influence the TS of concrete, including the strength of the paste and the bond

between the aggregate and paste. Additionally, Domone (2007) reported that the type of aggregate affects the tensile strength of concrete. Since SCC mixtures typically have different proportions compared to CC mixtures, SCC mixtures have potentially different TS due to the complexity of the strength of components. Kim (2008) mentioned that most of the published articles show that for a certain compressive strength, SCC tends to have slightly higher TS than CC does (Köning et al., 2001; Hauke, 2001; Fava et al., 2003). Nearly, all previously conducted SCC researches include active additions to provide necessary fines for this type of concrete and hence to improve their mechanical properties compared to CC. For example, Köning et al. (2001) and Hauke (2001) recorded a tensile strength increase of 13.5% and 9.1%, respectively, in SCCs made with fly ash. According to Fava et al. (2003), in SCCs made with granulated blast furnace slag, this increase is 10.5%. On the other hand, when limestone filler is used, Fava et al. (2003) and Daoud et al. (2003) reported a tensile strength in SCC that was 11.15% and 7.9% respectively lower than in CC.

2.6.4 Modulus of Rupture (MOR)

Many design codes use the flexural tensile strength or MOR as the cracking strength. Concrete flexural tensile strength is generally considered as a negligible characteristic in reinforced concrete applications. This is because the flexural tensile strength has little effect, and is generally ignored in determining the flexural resistance of reinforced concrete members. For durability reasons, however, it is desirable to prevent RC structures from cracking under permanent loadings and to control cracking in reinforced concrete elements. In addition, minimum flexural reinforcement is usually determined so that the flexural strength is greater than the cracking moment to ensure some level of safety. For serviceability limit states, TS and MOR are often more important parameters than compressive strength. Serviceability criteria are gaining importance as owners are increasingly interested in durability as well as safety because it affects total long-term cost and cost-effectiveness of structures during their service life. Hence, there is a vital need predict the SCC flexural tensile strength accurately.

The flexural and tensile strengths of SCC are typically improved relative to CC due to the improved microstructure of the paste, particularly the improved interfacial transition

zone and the denser bulk paste (Klug and Holschemacher, 2003). Turcry et al. (2002) found that the flexural strength was slightly higher for SCC than a CC of comparable compressive strength. Kim (2008) found that MOR of SCC mixtures containing river gravel was higher than that of the limestone SCC mixtures. Also, SCC mixtures exhibit lower MOR values when compared with the CC mixtures. Das and Chatterjee (2012) revealed that flexural tensile strength of SCC was distinctly higher than that of CC, by around 7.4%.

2.7 BOND CHARACTERISTICS OF SCC

Highly flowable concrete mixtures such as SCC have a potential risk of segregation of aggregate and paste, resulting in reduced bond due to bleeding. Section R 12.2.4 (ACI Committee 318, 2005) indicates the reduced bond capacity of horizontal reinforcement near the top surface resulting from bleeding as the top-bar effect. Available pull-out tests in the literature that were performed to evaluate the relative bond resistance for SCC and CC mixtures containing both top and bottom bars are considered in this study. Also, this study determined whether the top bar factor in the available Specifications was applicable to the SCC mixtures evaluated in this study. Moreover, bond characteristics of FRSCC are compared and discussed in this study. The applicability of the available bond prediction equations are presented in Chapter 3.

2.7.1 Bond Characteristics of Reinforcing Steel Bars Embedded in CC and SCC

It is important to ensure that all of the assumptions and test results upon which the structural design models are based for CC structures are also valid for SCC structures. One of the important properties of hardened concrete is its bond strength with reinforced steel. The bond strength between reinforcement and concrete is a basic phenomenon that allows reinforced concrete to behave as a composite structural material. Generally, in composite materials, forces are transferred between two materials through two types of actions: physicochemical (adhesion) and mechanical (friction and bearing action). These actions are activated by various states of stress. The relative importance of these actions depends on the surface texture and geometry of the bars (Valcuende and Parra, 2009). In addition, there are other factors that can influence the bond behaviour of the reinforcement, including

those that influence the quality of the concrete. As a result, changing the mix design can lead to changes in the mechanical properties of the material, including the steel-to-concrete bond.

Bond has been the subject of different studies on SCC, but the conclusions are very contradictory. Some researchers indicate that bond strengths of reinforcing bars in SCC are higher than those measured for CC. Other researchers see no differences or even lower bond strength. Most studies agree that the bond strength of rebars in SCC is larger than in CC, even if the values obtained are somewhat variable. Gibbs and Zhu (1999) found 32% differences CC and SCC, whereas for Sonebi and Bartos (1999) they are about 16-40%, for Zhu et al. (2004) 31-44%, for Valcuende and Parra (2009) 1-17% and for Collepardi et al. (2005) as much as 7%. Nevertheless, some authors like Schiessl and Zilch (2001), and Dehn et al. (2000) found that CC performed better and may achieve a 15% greater ultimate bond strength. The above mentioned percentages are based on a direct comparison of the measured bond strengths regardless of the concrete compressive strengths of the mixes (which can differ significantly for CC compared to SCC). In most cases the values obtained for SCC are above those for CC. Moreover, a trend is noticed with respect to the bar diameter. From that point on the normalized ultimate bond strength is decreasing for increasing diameters although some measurements are out of line.

Powder type SCC was also used in the study of Sonebi and Bartos (1999). The compressive strength in this case varied between 38 MPa and 80 MPa for a water-to-cement ratio of 0.37-0.38. The pull-out specimens (prisms 100 × 100 × 150 mm) with bond lengths of 6 or 10 times of bar diameter (12 or 20 mm), all failed in splitting. Bond strengths were 16 to 40% higher than those recorded for the CC mixtures. A reduction in bond strength was noticed when the bar diameter was increased from 12 mm to 20 mm.

Dehn et al. (2000) performed tests on powder-type SCC with a water to cement ratio of 0.41 and a compressive strength of approximately 55 MPa. The bond strength was evaluated after 1, 3, 7 and 28 days. It seemed that all specimens failed in pull-out and no cracks were observed at the surface of the concrete specimens. No direct tests on CC were done, but a comparison was made based on the bond law of Konig for CC. The tested SCC showed higher bond strength than the predicted values at all ages. Domone (2007) collected

a large amount of the bond strength to compressive strength data. Domone claims, based on these results, that the bond strength of steel to SCC is certainly not lower than to the equivalent CC. In some cases it may be even higher. However, Domone advises to run a number of tests with any particular mix and bar geometry to substantiate any increased bond capacity, and this because of the inherent scatter in data and the range of properties that can be expected for SCC.

A comparison of the mean and ultimate bond strength of conventional vibrated concrete and self-compacting concrete was done by Valcuende and Parra (2009). By using pull-out specimens (failing in pull-out) made of concretes with a compressive strength of 30 to 65 MPa, they showed that the mean bond strength for SCC was 10% to 30% higher than for CC. However, when the ultimate bond strength was compared, the differences were only 1% to 17%. A possible explanation, according to the researchers, can be found in the fact that bleeding has less influence on the failure load than on the service load and that the tested CC mixes had higher tensile strengths.

Three different bar diameters (8, 12 and 16 mm) were studied in the research project of Boel et al. (2010). Pull-out specimens were used with a bond length of 3.5 of bar diameter. They reported that during the tests, the load was applied progressively up to failure by performing displacement controlled experiments at a speed of 0.02 mm/s. The results showed small differences in the slip (corresponding to the ultimate bond strength) between SCC and CC specimens. The bond strength of SCC was higher than that of CC for each bar diameter. All mixes showed an increase in bond strength for an increasing reinforcement bar diameter. This increase was up to 55% for one of the SCC mixes when the diameter increased from 8 mm to 16 mm.

2.7.2 Bond Characteristics of Steel Fibre Reinforced SCC

In the fresh state, SFRSCC homogeneously spreads due to its own weight, without any additional compaction energy, due to filling and passing ability, as well as segregation resistance. In the hardened state, the addition of fibres to a brittle cementitious matrix mostly contributes to the improvement of the impact resistance and the energy absorption

capacity (ACI Committee 544, 2008), because the fibres that bridge the cracks will allow stress transfer between the cracked planes and then retard the crack opening propagation.

Steel Fibre-Reinforced Concrete (SFRC) resists tensile forces through a composite action of the matrix and the fibres. A part of the tensile force is resisted by the matrix, while the other part is resisted by the fibres. Each of these resistances is determined by the stress transfer at the fibre–matrix interface, which is achieved by the bond defined as the shear stress acting at the interface. Before any cracking takes place, elastic stress transfer is dominant. At more advanced stages of loading, debonding across the interface usually takes place, and frictional slip governs the stress transfer at the interface. Therefore, the mechanical properties of SFRC, especially its tensile strength, tensile stress–strain curve, and toughness, are influenced by the bond characteristics at the fibre–matrix interface (Mandel et al., 1987, Stang and Shah, 1986, Armelin and Banthia, 1997, Li et al., 2002). Accordingly, it is necessary to study the bond properties between the matrix and fibre prior to examining the various mechanical properties of SFRC (Lee et al., 2010). The bond characteristics depend on several factors including the orientation of the fibres relative to the direction of the applied load, the embedded length of the fibres, the shape of the fibres, and strength of the matrix. Many researches concerning bond properties have been conducted to reveal the effects of the parameters related to fibre geometry or strength of the matrix (Chanvillard and Aïtcin, 1996, Sujivorakul et al. 2000, Ezeldin and Balaguru, 1989, Shannag et al. 1996, 1997, Orange et al., 1999, Morton and Groves, 1974, Bartos, 1981, Li et al. 1990). Several models to predict the pullout behaviour of fibres have been proposed (Wang et al., 1988, Stang et al. 1995, Lin et al. 1999, Nammur and Naaman, 1991, Naaman et al. 1991) so far. However, the inclination angle of a fibre in a cementitious matrix has a strong influence on the pullout resistance. Although several researchers have performed experiments to investigate the effect of the fibre inclination angle, the focus was mostly on the peak pullout load. Thus, fibre inclination effect is still disputable (Armelin and Banthia, 1997, Morton and Groves, 1974, Bartos, 1981, Li et al. 1990). It is generally agreed that the effect of fibre inclination angle on the pullout load and pullout energy depends on the fibre aspect ratio (ratio of fibre length to equivalent fibre diameter), fibre shape (straight, hooked, corrugated etc.), and material properties such as yield strength whether the fibre material is metallic or synthetic (Lee et al., 2010). Based on the choice of criterion which is used for

the fibre-matrix interfacial debonding, the theoretical analysis of the fibre pullout problem can be classified into two distinct approaches: strength-based and fracture mechanics-based approaches. Theoretical models based on the former approach use maximum interfacial shear stress as the interfacial debonding criterion. Therefore, when the interfacial shear stress exceeds the interfacial bond strength, debonding is supposed to occur. On the other hand, in the theoretical models based on the concepts of fracture mechanics, the debonded zone is considered as an interfacial crack, and the extension of the crack depends on the energy criterion that should be satisfied (Dubey, 1999).

2.8 SHRINKAGE AND CREEP OF SCC

High paste volumes, e.g. SCC mixtures, may lead to increased shrinkage and creep, which increases concrete deformation strain in RC structures. The objective of this portion of this study is to measure and compare available shrinkage and creep experimental results for SCC and CC mixtures. The applicability of the available prediction equations is evaluated. Other available prediction equations are also assessed to determine if they can reasonably predict shrinkage and creep in SCC in Chapter 4.

2.8.1 Shrinkage of SCC

In comparison with CC, SCC contains larger quantities of mineral fillers such as finely crushed limestone or fly ash, higher quantities of high-range water-reducing admixtures, and smaller maximum size of the coarse aggregate. These modifications in the composition of the mixture affect the behaviour of the concrete in its hardened state, including the creep and the shrinkage deformations.

The overall shrinkage of concrete corresponds to a combination of several shrinkages, that is, plastic shrinkage, autogenous shrinkage, drying shrinkage, thermal shrinkage, and carbonation shrinkage. In designing the CC, shrinkage is taken as drying shrinkage, which is the strain associated with the loss of moisture from the concrete under drying conditions. The CC with a relatively high w/cm (higher than 0.40) exhibits a relatively low autogenous shrinkage, with values less than 100 μstrain (Davis, 1940). In contrast, the SCC used in precast, prestressed applications has typically a low w/c ratio (0.32 to 0.40). Lower w/c

values, coupled with a high content of binder, lead to greater autogenous shrinkage. Such shrinkage increases with the use of finely ground supplementary cementitious materials and fillers employed in the SCC. Therefore, both drying and autogenous shrinkage deformations have to be accounted for in the structural detailing of the reinforced concrete and the prestressed concrete members (Khayat and Long, 2010). Kim (2008) indicated that because the SCC has a higher paste volume (or higher sand to aggregate ratio) to achieve high workability and high early strength, several researchers have claimed larger shrinkage and creep of the SCC for concrete (Issa et al., 2005; Naito et al., 2006; Suksawang et al., 2006; Schindler et al., 2007). Although mechanical properties of the SCC are superior to those of the CC, shrinkage of SCC is significantly high (Issa et al., 2005). Naito et al. (2006) also found that the SCC exhibits higher shrinkage than the CC, which is due to the higher fine aggregate volume in the SCC, and that the shrinkage of the SCC and the CC was 40% and 6% higher than that of the ACI 209R (1997) prediction model, respectively.

2.8.2 Creep of SCC

Different methodologies are followed in different countries to obtain the SCC creep (Ouchi et al., 2003), and few studies are available concerning its long-term behaviour (Persson, 2001; 2005; Poppe and De Shutter, 2001; Seng and Shima, 2005; Mazzotti et al., 2006). It is not clear in the available studies if current international standards apply successfully for the SCC (Klug and Holschemaker, 2003; Vidal et al., 2005; Landsberger and Fernandez-Gomez, 2007). Moreover, it is not assessed if the long-term properties can be predicted with reference to the conventional mechanical and physical parameters only (such as strength, w/c), or the adoption of parameters concerning the mix design is needed.

Naito et al. (2006) found that the creep coefficient of the SCC and the CC was 40 and 6 precent higher than the ACI 209 (1992) prediction model, respectively. Different methodology followed to obtain SCC in different countries (Ouchi et al., 2003) and limited number of studies are available concerning its long-term behaviour (Persson 2001, 2005; Poppe and De Shutter 2001; Seng and Shima, 2005; Mazzotti et al., 2006). It is not clear in the available studies if current international standards apply successfully for the SCC (Klug and Holschemaker, 2003; Vidal et al., 2005; Landsberger and F.-Gomez, 2007). Moreover, it is not assessed if long-term properties can be predicted with reference to conventional

mechanical and physical parameters only (like strength, water-cement ratio (w/c), etc) or the adoption of parameters concerning the mix design is needed.

2.9 FULL-SCALE TIME-DEPENDENT SCC AND FRSCC STUDIES FROM THE LITERATURE

In this section a summary of the available research studies about long-term behaviour of reinforced SCC members is presented. The concrete properties, test methods, specimens dimensions, and conclusions of each study are presented.

2.9.1 Buratti et al. (2010) – "Long-Term Behaviour of Fibre-Reinforced Self-Compacting Concrete Beams"

This study describes the results of an experimental campaign aimed at investigating the long-term behaviour of beams cast using FRSCCs containing either steel or synthetic fibres in comparison with that of plain SCC beams with standard reinforcement. The flexural behaviour of six different beams was investigated in a long-term four point bending test under constant loading. All the beams were pre-cracked before the long-term test. The tests showed that fibres have an important role in controlling the increase of crack opening over time. The greatest reduction in the delayed crack opening was obtained using a mixture of steel and macro synthetic fibres.

Six 300 × 120 × 2000 mm (width × height × length) beams were considered in the present study, as summarized in Table 2.1. The geometry of the beams was defined in order to be representative of a strip of concrete floor. The first beam, named REBAR in the following, was cast using plain SCC concrete and contained conventional steel reinforcing bars (ϕ8/10 cm, i.e. three steel bars in total). All the other beams were cast using FRSCC and did not contain any reinforcing bars. Three different FRSCCs were used; two containing different dosages, 25 kg/m^3 and 35 kg/m^3 respectively, of steel fibres and one containing a combination of steel and synthetic fibres (see Tables 2.1 and 2.2). Two beams were cast for each of the first two FRSCCs (named SF25a, SF25b, SF35a, and SF35b in the following). Only one beam was cast with the concrete containing the combination of fibres

(named MIX in the following). The synthetic fibres used in this last beam are usually employed to reduce shrinkage induced cracking in industrial pavements. The compressive strength of the hardened concrete was also measured at 7 and 28 days, obtaining the results given in Table 2.3. Prior to the long-term tests, the beams have been pre-cracked up to a CMOD of 0.2 mm. This value has been assumed as representative of the crack width of concrete floors at the serviceability limit state. In order to better control the position of the crack, all beams have been notched at mid-span (notch 10 mm deep).

Table 2.1 Summary of the beams considered. The fibre dosage is given both as mass per volume unit and as volume percentage (Buratti et al., 2010)

Beam	Fibre type	Fibre dosage	Rebar
MIX	Steel A & B + Synthetic	17 kg/m3 – 0.21% (St. A) + 3 kg/m3 – 0.04% (St. B) + 0.3 kg/m3 – 0.003% (Synth.)	-
SF25a	Steel A	25 kg/m3 – 0.32%	-
SF25b	Steel A	25 kg/m3 – 0.32%	-
SF35a	Steel A	35 kg/m3 – 0.45%	-
SF35b	Steel A	35 kg/m3 – 0.45%	-
REBAR	-	-	ϕ8/10”

Table 2.2 Geometry of the fibres used (Buratti et al., 2010)

Fibre type	D (mm)	L (mm)
Steel A	0.75	50
Steel B	0.6	33
Synthetic	18×10^{-3}	6

Table 2.3 Cube compressive strength of the concrete for the different casts (Buratti et al., 2010)

Cast	f'_c (7 days) MPa	f'_c (28 days) MPa
MIX	27.3	33.4
SF25a	31.5	40.1
SF25b	34.2	42.2
SF35a	31.0	39.9
SF35b	32.6	40.1
REBAR	31.4	42.0

In this phase, a three-point bending scheme was adopted, and the tests were run under mid-span deflection control. The same machine used for the 150×150×550 mm specimens (which was adapted to the beam size) was employed in this phase and a distance between the supports of 80 cm was set (see Figure 2.6a). After the cracking phase, the long-term tests were performed using a four-point bending scheme.

Figures 2.6b-d show the experimental setup. Each beam is sustained by two steel systems at the intermediate supports, thus creating a central span of 750 mm, where the bending moment is constant and the shear is null. The dead loads were applied at the beams extremities at a distance of 525 mm from the inner supports, by using concrete blocks; they were supported by a steel system composed of a base plate connected by two threaded rods to transverse hollow rods placed on the top of the beam (Figure 2.6d). The load values, calculated following the criterion described at the end of the previous section, are reported in Table 2.4.

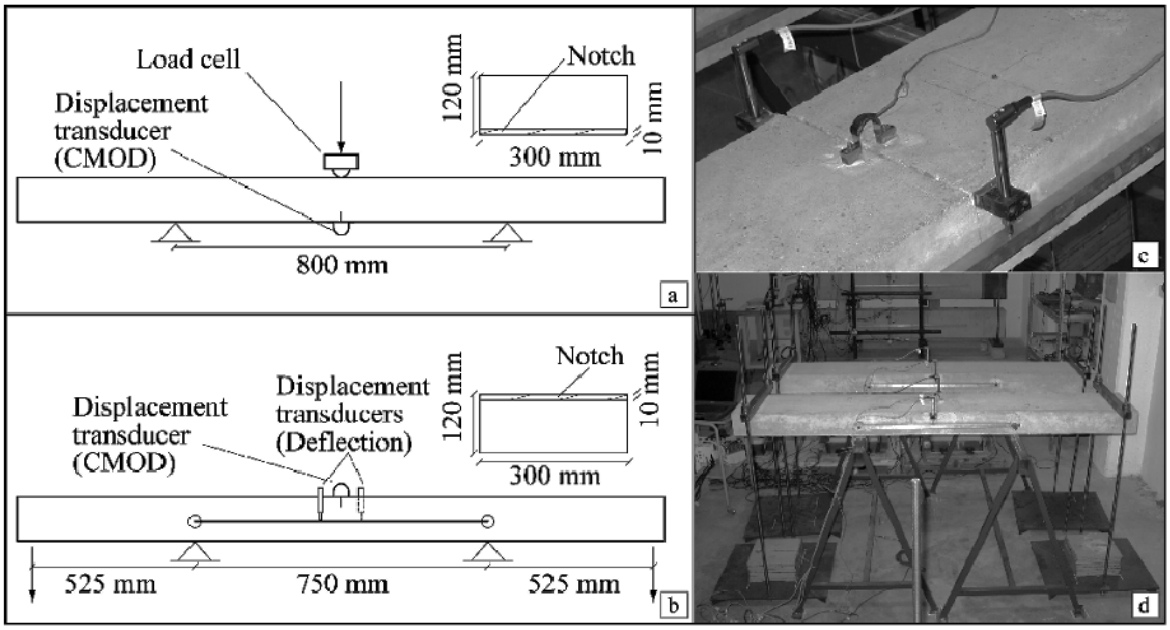

Figure 2.6 (a) Test set-up for pre-cracking the beams; (b) test set-up for the long-term tests; (c) detail of the transducers used in the long-term tests; (d) two beams during the long-term test (Buratti et al., 2010)

Table 2.4 Loads applied on each end of the beams during the long-term test (Buratti et al., 2010)

Beam	Load (kN)
MIX	2.50
SF25a	2.53
SF25b	2.51
SF35a	2.14
SF35b	3.36
REBAR	2.56

Conclusions of this study: The tests performed showed that the magnitude of the delayed deformation can be high, up to 150% of the instantaneous counterpart. The rate of delayed deformation increased at lower rates for the FRSCC beams than for the plain SCC beam containing standard reinforcing bars. In particular, the lowest long-term damage was obtained for the specimen containing a combination of steel fibres of different sizes and of synthetic fibres usually employed to reduce shrinkage.

2.9.2 Mazzotti and Savoia (2009) – "Long-Term Deflection of Reinforced Self-Consolidating Concrete Beams"

In this study the long-term behaviour of reinforced SCC beams has been investigated. Tests on concrete cylindrical specimens made with a specific SCC mixture have been performed first, showing that shrinkage and creep deformations are greater than predicted by European Model Code 1990 provisions. Long-term tests on reinforced SCC beams have also been performed according to the four-point bending scheme. The maximum stress on concrete in compression was approximately 35% of strength at the time of loading (37 days). The time evolution of mid-span deflection as well as the strains at the compressive and tensile sides has been recorded. The beam deflection has been compared with the predictions by existing analytical models. The creep strength interaction has been also investigated by performing failure tests on control beams before and after long-term tests, and comparing them with tests on beams subjected to long-term loading. A small flexural strength increase with age at testing has been observed from the comparison of failure tests. It is related on a small compressive strength increase due to concrete aging, whereas the damage due to long-term

loading previously applied was not significant. A medium-high-strength SCC mixture, mainly used in the precast industry, was adopted for this study; to achieve self-consolidation without increasing the compressive strength, a nonreactive filler was used (locally available limestone filler). Six reinforced SCC beams were cast, with dimensions of 15 × 25 × 320 cm. The mean yielding stress of the steel reinforcement is f_{ym} = 540 MPa. The rheological properties of the SCC mixture have been preliminarily investigated by performing long-term tests on 10 × 20 cm cylinders, cored from a thick concrete slab (120 × 40 × 30 cm) to obtain cylindrical concrete specimens with homogeneous distribution of aggregates. The slab and all beams were cast together from the same concrete batch. The main results of the experimental long-term tests on SCC cylinders are described in the following section. After demolding of beams and coring of cylinders, all specimens were cured at 20 °C and RH = 98% for 14 days and then stored at 20 °C and RH = 60% until 1 day before testing.

The six SCC beams subjected to testing had the cross-section and steel reinforcement shown in Figure 2.7. To obtain a remarkable portion of concrete under long-term compression, large steel reinforcement at the traction side (3ϕ20) and smaller bars on the compressive side (2ϕ10) were adopted. All beams were tested according to the four-point bending scheme reported in Figure 2.7. Two beams (T1, T2) were loaded up to failure before long-term testing (37 days after casting) to obtain the short-term flexural strength at the initial time of creep tests. Two beams (T3, T4) were subjected to long-term loading for 404 days. At the end of the tests, they were loaded up to failure together with two other control beams (T5, T6) that were never loaded before.

As for the long-term tests, a mechanical system was designed to apply two constant forces to a couple of beams simultaneously, according to the four-point bending scheme (Figure 2.8). At the beam extremities, the load is applied by means of two pairs of steel tendons, equipped with large diameter steel springs. The springs are used to ensure a small variation of the applied force due to the beam long-term deflection. When necessary, the applied load is adjusted to its nominal value by acting on bolts, placed between the tendons and the spring system. Two load cells are placed on the intermediate supports between the beams to measure the variation of the applied load with time.

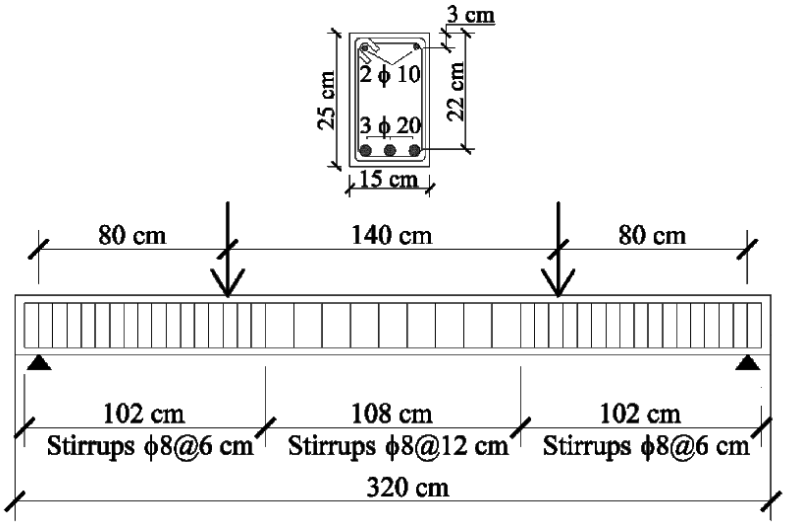

Figure 2.7 (a) Cross section and (b) side view of reinforced concrete beams (Mazzotti and Savoia, 2009)

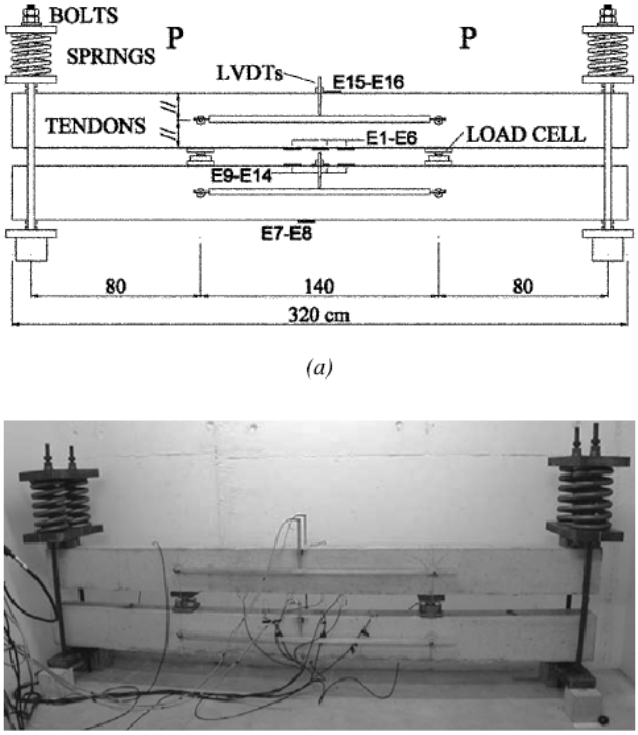

Figure 2.8 Experimental setup for long-term tests on SCC beams: (a) loading scheme and instrumentation; and (b) picture of experimental setup (Mazzotti and Savoia, 2009)

Conclusions of this study: (a) The long-term behaviour of SCC is qualitatively similar to the case of CC, both in terms of total shrinkage and total creep; the creep strain attains an almost constant increase rate (in the time log scale) after approximately 2 months from casting. Nevertheless, creep and shrinkage are much greater for the specific SCC evaluated in this study than in the case of CC. Cylinders subjected to the long-term load show a 10 to 15% strength increase with respect to the cylinder never loaded, due to the positive effect of a moderate pressure on the development with time of the CSH gel and on the reduction of the porosity, also called compaction phenomena. (b) Similarly, the long-term deflection rate of beams under flexure is almost constant (in the time log scale) after the same period of time. On the contrary, the tensile strain rate in concrete close to the transverse cracks reduces after a few months from loading, suggesting crack opening stabilization. Most of the irreversible deflection and tensile strain are due to the shrinkage effect during the test. (c) Crack widths increase only very slightly under the long-term loading, and their contribution to the long-term beam deflection is negligible.

2.9.3 Xiao-jie et al. (2008) – "Long term behaviour of self-compacting reinforced concrete beams"

In this research, tests were carried out on 8 SCC beams and 4 CC beams. The effects of mode of consolidation, load level, reinforcing ratio and structural type on long-term behaviour of SCC were investigated. Under the same environmental conditions, the shrinkage-time curve of a SCC beam is very similar to that of the normal concrete beam. For both self-compacting reinforced concrete beams and normal reinforced concrete beams, the rate of shrinkage at early stages is higher, the shrinkage strain at 2 months is about 60% of the maximum value at one year. The shrinkage strain of the self-compacting reinforced concrete beam after one year is about 450×10^{-6}. Creep deflection of the self-compacting reinforced concrete beam decreases as the tensile reinforcing ratio increases. The deflection creep coefficient of the self-compacting reinforced concrete beam after one and a half year is about 1.6, which is very close to that of normal reinforced concrete beams cast with vibration. Extra cautions considering shrinkage and creep behaviour are not needed for the use of SCC in engineering practices.

Among the 12 tested beams, 3 beams were used for contrastive shrinkage beams, and the remaining 9 beams were used for creep testing under long term loading. Parameters of beam specimens for long term test are listed in Table 2.5. Concrete blocks with dimensions of 200 mm×200 mm×550 mm were cast at the same time, which were used to simulate the sustained concentrated loads. The mechanical properties of concrete are shown in Table 2.6. The elastic modulus tests were carried out at 28 days.

Details of specimens and instrument of configuration are shown in Figures 2.9-2.12. The deflection at the midpoint and the support of the tested beams were measured by dial gauge with a precision of 0.01 mm and the concrete strain at the same level of reinforcement was measured by dial gauge with a higher precision of 0.001 mm. The experiment was carried out in the Building Material Laboratory of Central South University and the humidity was kept constant by a dehumidifying machine. The test was started on 26th, Jan. 2005 and lasted for 540 days. The test setup is shown in Figure 2.13.

Table 2.5 Parameters of beam specimens for long term test (Xiao-jie et al., 2008)

Series	Beam specimen	Mode of consolidation	Reinforcement	Load/kN	Remark
1	c-1a	Vibrating	4 d 12 mm	2.2	
	c-1b				
2	c-2	Vibrating	4 d 12 mm	1.65	
3	c-3	Vibrating	4 d 12 mm	0	Shrinkage beam
4	sc-1a	Self-compacting	4 d 12 mm	2.2	
	sc-1b				
5	sc-2	Self-compacting	2 d 12 mm 2 d 16 mm	2.2	
6	sc-3	Self-compacting	4 d 12 mm	1.65	
7	sc-4	Self-compacting	4 d 12 mm	0	Shrinkage beam
8	sc-5	Self-compacting	2 d 12 mm	0	Shrinkage beam
			2 d 16 mm		
9	sc-6a	Self-compacting	4 d 12 mm	2.2	Continuous beam
	sc-6b				

Table 2.6 Mechanical properties of concrete (Xiao-jie et al., 2008)

Mode of consolidation	Compressive strength (MPa)			MOE (GPa)
	3 days	7 days	28 days	
Vibrating	23	42	53	35.3
Self-compacting	16	35	41	32.0

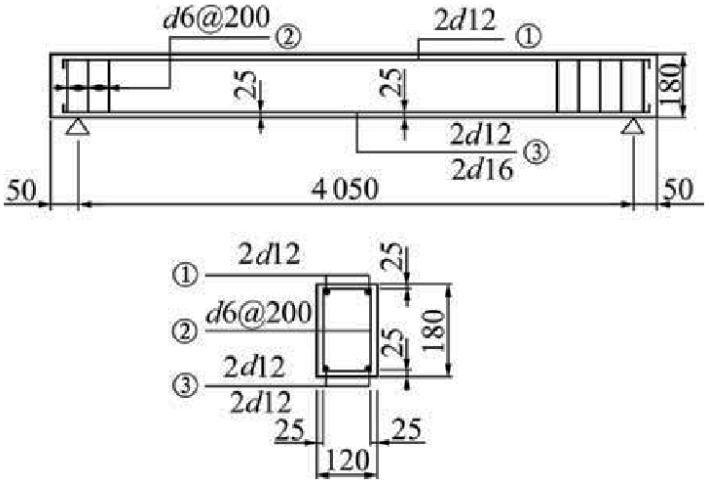

Figure 2.9 Reinforcement details of simple beam (unit: mm) (Xiao-jie et al., 2008)

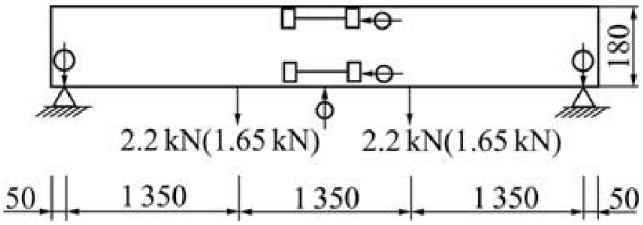

Figure 2.10 Layout of measuring points of simple beam (unit: mm) (Xiao-jie et al., 2008)

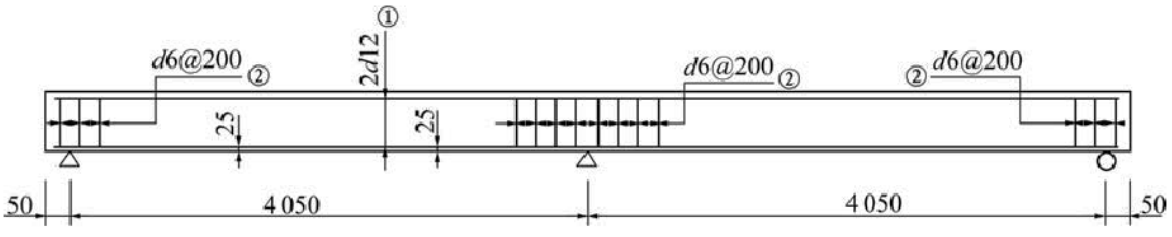

Figure 2.11 Reinforcement details of two-span continuous beam (unit: mm) (Xiao-jie et al., 2008)

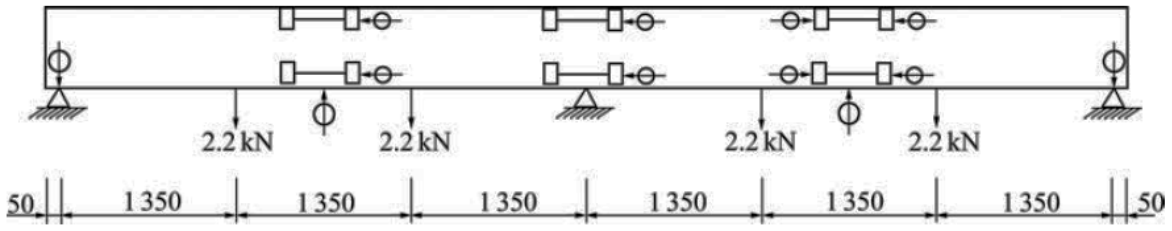

Figure 2.12 Layout of measuring points of two-span continuous beam (unit: mm) (Xiao-jie et al., 2008)

Figure 2.13 Test setup of long term experiment: (a) Shrinkage beam; (b) Simple beam; (c) Continuous beam (Xiao-jie et al., 2008)

Conclusions of this study: (a) An increase in reinforcing ratio can reduce shrinkage deformation. The shrinkage strain of SCC increases as the age increases. The shrinkage strain curves converge after 6 months. (b) Under the same environmental conditions, the shrinkage-time curve of self-compacting concrete is very similar to that of normal concrete. The shrinkage strain of self-compacting concrete after one year is about 450×10^{-6}. (c) The deflection creep coefficient of self-compacting reinforced concrete beams after 18 months is about 1.6, which is very close to normal reinforced concrete beams cast with vibration. Extra cautions considering shrinkage and creep behaviour are not needed for the use of SCC in engineering practices.

2.10 SUMMARY

According to the several research studies and recommendations, SCC mixtures typically have a high paste volume and low coarse aggregate to minimize the friction of particles and maximize stability. Therefore, many researchers are concerned that SCC mixture proportions could affect adversely hardened properties such as less aggregate interlock resulting in low shear capacity and high shrinkage and creep. Low elastic modulus could also increase the gap between actual and predicted behaviours (i.e., deflection, camber). Several researchers around the world have conducted research to develop SCC mixture proportions, evaluate mechanical and time-dependent properties, and validate with full-scale tests. Many researchers have noted several advantages of SCC such as ease of placement, reduction of casting time, and better finishing when used in concrete structural members. However, some researchers had difficulties in field application due to a lack of robustness of SCC resulting in some segregation, poor workability, poor surface quality, and/or low mechanical or bond strength (Burgueño and Haq, 2007; Erkmen et al., 2007; Ozyildrim, 2007).

Time-dependent SCC and FRSCC full-scale tests are also performed to evaluate field application, structural behaviour, cracking behaviour, and deflection calculations. In general, when the quality of fresh SCC is satisfactory, the overall performance of SCC is comparable to that of CC. However, information to characterize the hardened properties of SCC for concrete members is still limited. The applicability of international codes of the time-dependent behaviour, which is based on CC and FRC, has not been fully evaluated for use in designing SCC and FRSCC members. In this study comprehensive test results will be provided and the applicability of the mechanical properties and the mechanisms associated with flexural cracking of reinforced SCC and FRSCC elements and the influence of the many factors that affect the width and spacing of flexural cracks under sustained service loads will also be discussed.

CHAPTER 3

HARDENED CONCRETE PROPERTIES

CHAPTER 3

HARDENED CONCRETE PROPERTIES

3.1 INTRODUCTION

The behaviour of hardened concrete can be characterized in terms of its short-term (essentially instantaneous) and long-term properties. Short-term properties include strength in compression, tension, bond, modulus of elasticity, and modulus of rupture. The long-term properties include creep, shrinkage, fatigue, and durability characteristics such as porosity, permeability, freeze-thaw, and abrasion resistance. In this section the short-term hardened properties of SCC and FRSCC, including the mechanical properties, and bond characteristics, are compared and discussed with CC and FRC experimentally and numerically.

SCC consists of the same components as CC (cement, water, aggregates, admixtures, and mineral additions), but the final composition of the mixture and its fresh characteristics are different. Compared to CC, SCC contains larger quantities of mineral fillers such as finely crushed limestone or fly ash as well as higher quantities of high-range water-reducing admixtures, and the maximum size of the coarse aggregate is smaller. These modifications in the composition of the mixture affect the behaviour of the concrete in its hardened state. Therefore, precise understanding of behaviour and performance of the SCC is becoming more important as use of this type of concrete mix grows more common. Using SCC can result in enormous labour and cost savings. It is important to estimate accurately the crucial mechanical properties of this structural material, including modulus of elasticity (MOE), tensile strength (TS), modulus of rupture (MOR), compressive stress-strain (σ-ε) curve (CSSC) and bond characteristics to achieve at a safe and economic analysis and design.

3.2 MODULUS OF ELASTICITY (MOE)

3.2.1 Experimental and Analytical Database for MOE

Using experimental results from published investigations as a database is an effective tool for studying the applicability of the various MOE for both SCC and CC. To apply the models to a particular concrete mixture accurately, it is necessary to use only the investigations that are adequately consistent with the applied testing methodology. The experimental results included in the database have been carried on mainly from papers presented at conferences and published articles on SCC. The database includes information regarding the composition of the mixtures, fresh properties of SCC, testing methodology, and conditions. However, the mechanical characteristics have not been investigated as much as other aspects of SCC, and the available published experimental data in the literature are still not very extensive. Using experimental results from different sources can be problematic because: 1) there is often insufficient information regarding the exact composition of the concrete mixtures; 2) the size of the specimen, curing condition, and testing methodology vary between different investigations and, in some cases, this information is not fully indicated; and 3) in many cases, it is difficult to extract the relevant experimental values because the published results are incomplete or are presented in graphic form and the data values have to be extrapolated from the graphs.

Tables 3.1 and 3.2 are a general summary of the MOE of the concrete mixtures included in the database. Tables 3.1 and 3.2 also include information regarding the curing age, type of curing, type of the cement, type of the filler, and type of Fine Aggregate (FA) and Coarse Aggregate (CA). Dominant properties of the available mixes in the database are that the curing age is 28 days, type of curing is moist, type of cement is ordinary Portland cement, types of filler are fly ash and limestone, and type of aggregate for FA is natural sand and for CA is natural river gravel, crushed granite and limestone. In the literature, several analytical and numerical models try to represent the MOE for both SCC and CC mixtures. Tables 3.3 and 3.4 show some of these proposed models for calculating the MOE of SCC and CC. These models vary in complexity and precision in the calculations.

From the recently published paper of Aslani and Nejadi (2011a) of the MOE databases (Tables 3.1 to 3.4), the following conclusions can be drawn: a) the two ACI 318 (2005) and Dinakar et al. (2008) CC models predict MOE reasonably well for both SCC and CC mixtures; and b) the two Leemann and Hoffmann (2005) and Kim (2008) SCC models predict MOE reasonably well for SCC mixtures only. In this section, the proposed MOE models for CC and SCC are based on regression analyses of the existing experimental data; the base of the proposed models is ACI 318 (2005).

3.2.2 Proposed MOE Model

The proposed MOE models cover SCC with different types of aggregate (river gravel, crushed granite, and limestone) and fillers (fly ash and limestone) in the mixture. Also, general MOE model are considered for CC, SCC, and SCC-CC.

The proposed model for MOE is presented by Eq. (3.1).

$$E_c = \kappa_1 \left(f'_c\right)^{\kappa_2} \tag{3.1}$$

where:

Mixing Properties	κ_1	κ_2
CC	4835	0.490
SCC	4150	0.525
SCC with River Gravel, Crushed Granite Aggregate	3995	0.533
SCC with Limestone Aggregate	6847	0.410
SCC with Fly Ash Filler	3655	0.548
SCC with Limestone Filler	9455	0.345
General Model for both SCC and CC	3202	0.587

3.2.3 Comparison of the MOE Analytical Models

Figure 3.1 shows the MOE versus compressive strength for the CC mixtures listed in the database (Tables 3.1 and 3.2) and comparison of the proposed ACI 318 (2008) and Dinakar et al. (2008) models. Figures 3.2 and 3.3 show the comparison of the experimental results versus calculated values from the proposed ACI 318 (2008) and Dinakar et al. (2008) models for the MOE in CC mixtures. Figures 3.4 and 3.5 show the MOE versus compressive strength for the SCC mixtures in the database and the proposed ACI 318

(2008), Dinakar et al. (2008), Leemann and Hoffmann (2005), and Kim (2008) models. Figures 3.6 and 3.7 show the comparison of the experimental results versus calculated values for proposed, Leemann and Hoffmann (2005) and Kim (2008) models for MOE of the SCC mixtures.

Figure 3.8 shows the MOE versus compressive strength for the SCC mixtures listed in the database (Tables 3.1 and 3.2) and comparison of the proposed MOE models that covered SCC with different types of aggregates (river gravel, crushed granite, and limestone), fillers (fly ash and limestone) in the mix design, and general SCC-CC model.

As shown in Table 3.5 for CC mixtures, the proposed model provides a better prediction of MOE with a coefficient of correlation factor (R^2) of 0.86 compared to 0.75 for the ACI 318 (2008) and 0.72 for the Dinakar et al. (2008) models (Figures 3.1 to 3.3). In addition, from Table 3.5 for SCC mixtures, the proposed model provides a better prediction of MOE with a coefficient of correlation factor (R^2) of 0.87 compared to 0.74 for the ACI 318 (2008), 0.71 for the Dinakar et al. (2008), 0.69 for the Leemann and Hoffmann (2005), and 0.79 for the Kim (2008) models (Figures 3.4 to 3.7).

Furthermore, proposed MOE models (Eq.3.1) for SCC mixtures without considering different type of aggregates and fillers show that there are small differences between proposed SCC models with CC, but when the types of aggregates and fillers are changed, the amount of the difference is larger. The amount of MOE predicted by the CC model for concrete with 60 MPa compressive strength, 0.75%, is greater than for the overall SCC model, but this amount for the SCC model with river gravel and crushed granite aggregate is 1.5% and for the SCC model with fly ash filler is 3% greater. Also, the amount of MOE predicted by the CC model, 1.5%, is less than for the SCC model with limestone aggregate and close to 7% less than for the SCC model with limestone filler.

These differences are changeable with compressive strength (i.e. for high compressive strength concrete more than 80 MPa is low, but for normal compressive strength concrete, more than 45 MPa is large). To overcome these differences between SCC and CC, a general model is proposed as shown in Eq. (3.1). This MOE model is suitable for both SCC and CC and can be used as a major model in design.

Table 3.1 MOE experimental database

Reference	No. of mixtures		Curing age (days)	Type of curing	Type of cement
	SCC	CC			
Kim et al. (1998)	5	3	28 and 90	Moist	Ordinary Portland cement
Persson (2001)	4	4	28	Drying and Sealed	Ordinary Portland cement
Vieira and Bettencourt (2003)	1	1	3, 28 and 180	Free and Sealed	CEM I 42.5 R
Leemann and Hoffmann (2005)	9	4	28	Moist	CEM I 42.5 N
Bílek and Schmid (2005)	6	3	28, 90, 180 and 365	Moist	CEM I 52.5 R and CEM I 42.5 R
Felekoğlu et al. (2007)	5	0	28	Moist	CEM I 42.5 N
Dinakar et al. (2008)	8	5	28	Moist	CEM I 42.5 N
Kim (2008)	14	4	28	Moist	CEM III
Therán (2008)	40	4	28	Moist	Ordinary Portland cement
Topçu and Uygunoğlu (2010)	5	0	28	Moist	CEM I 42.5 R
Liu (2010)	6	0	7, 28, 60, 90, 120, 150 and 180	Moist	CEM I 42.5 N
Almeida Filho et al. (2010)	3	0	28	Moist	Ordinary Portland cement
Parra et al. (2011)	4	4	7, 28 and 90	Moist	CEM II/B-M (V-LL) 32.5N and CEM II/B-M (V-LL) 42.5R
Total of 142 mixtures	110	32			

Table 3.2 MOE experimental database (continued)

Reference	Type of filler	Type of Aggregate	
		FA	CA
Kim et al. (1998)	Fly ash	Sea sand	Crushed stone
Persson (2001)	Silica fume	Quartzite sandstone	
Vieira and Bettencourt (2003)	Fly ash and Limestone	Natural siliceous sand	Limestone
Leemann and Hoffmann (2005)	Fly ash	Natural sand	Natural gravel
Bílek and Schmid (2005)	GGBFS, Fly ash, Slag, Limestone and Ground stone	Sand 0/4 mm	Crush, aggr. 8/16 mm
Felekoğlu et al. (2007)	Limestone	Crushed 0–5mm limestone	Crushed limestone 15mm maximum size
Dinakar et al. (2008)	Fly ash	Well-graded river sand	Maximum grain size of 12 mm
Kim (2008)	Fly ash	Fordyce murphy and TXI (Austin) natural sand	Fordyce murphy river gravel, Hanson aggregate limestone
Therán (2008)	Fly ash, Silica fume and Blast furnace slag	Manufactured sand	Maximum grain size of 12 mm
Topçu and Uygunoğlu (2010)	Fly ash and Limestone	Natural river sand	Pumice, volcanic tuff and diatomite with a maximum size of 16 mm
Liu (2010)	Fly ash	Sand 0/4 mm	4/10 mm and 10/20 mm gravel
Almeida Filho et al. (2010)	Limestone	0-2 mm and 0–5 mm sands	5–12 mm and 12–18 mm gravels
Parra et al. (2011)	Limestone	Fine sand 0/2	Coarse sand 0/4

Table 3.3 MOE models for CC

Reference	Models of E_c for CC (SI units, MPa)
Jobse and Moustfa (1984)	$E_c = 0.103\ \lambda^{1.5} \left(\sqrt{f_c'}\right)^{0.5}$ γ: unit weight of concrete (kg/m^3)
Ahmad and Shah (1985)	$E_c = 3.38\times10^{-5} \times \lambda^{2.5} \left(\sqrt{f_c'}\right)^{0.65}$ γ: unit weight of concrete (kg/m^3)
Cook (1989)	$E_c = 3.22\times10^{-5} \times \lambda^{2.5} \left(f_c'\right)^{0.315}$ γ: unit weight of concrete (kg/m^3)
CEB (1993)	$E_c = 10000\left(f_c' + 8\right)^{1/3}$
CEB-FIP (1990)	$E_c = 21500\alpha \left(f_c'/10\right)^{1/3}$ α = 1.2 for basalt, dense limestone aggregates; 1.0 for quartzite aggregates; 0.9 for limestone aggregates; 0.7 for sandstone aggregates.
Gardner and Zao (1991)	$E_c = 9\sqrt[3]{f_c'} \quad for \quad f_c' > 27\ MPa$
ACI 363R (1992)	$E_c = 3320\left(f_c'\right)^{0.5} + 6890$
NS 3473 (1992)	$E_c = 9500\left(f_c'\right)^{0.3}$
Guitierrez and Canovas (1995)	$E_c = 8340\sqrt[3]{f_c'}$
EHE (1998)	$E_c = 10000\sqrt[3]{f_c'}$
NBR 6118 (2003)	$E_c = 5600\sqrt{f_c'}$
Leemann and Hoffmann (2005)	$E_c = 5480\left(f_c'\right)^{0.5}$
ACI 318 (2005)	$E_c = 4730\left(f_c'\right)^{0.5}$
AASHTO (2006)	$E_c = 0.043K_1\ \lambda^{1.5} \left(f_c'\right)^{0.5}$ K_1: Correction factor for source of aggregate. No specific value is recommended, and should be taken as 1.00 unless determined by physical test.
Dinakar et al. (2008)	$E_c = 4550\left(f_c'\right)^{0.5}$

Table 3.4 MOE models for SCC

Reference	Models of E_c for SCC (SI units, MPa)
Persson (2001)	$E_c = 3750\left(f_c'\right)^{0.5}$
Leemann and Hoffmann (2005)	$E_c = 4740\left(f_c'\right)^{0.5}$
Felekoğlu et al. (2007)	$E_c = 1570\left(f_c'\right)^{0.8}$
Dinakar et al. (2008)	$E_c = 4180\left(f_c'\right)^{0.5}$
Kim (2008)	$E_c = 10153\left(f_c'\right)^{0.343} \left(\frac{\gamma}{2400}\right)^{3.3}$

Table 3.5 Coefficient of correlation factor (R^2) for MOE

Reference	CC		SCC	
	Predicted/Experimental MOE	R^2	Predicted/Experimental MOE	R^2
ACI 318 (2008)	1.203	0.75	1.069	0.74
Dinakar et al. (2008)	1.157	0.72	1.028	0.71
Leemann and Hoffmann (2005)	-	-	1.071	0.69
Kim (2008)	-	-	1.100	0.79
Proposed Model	1.185	0.86	1.033	0.87

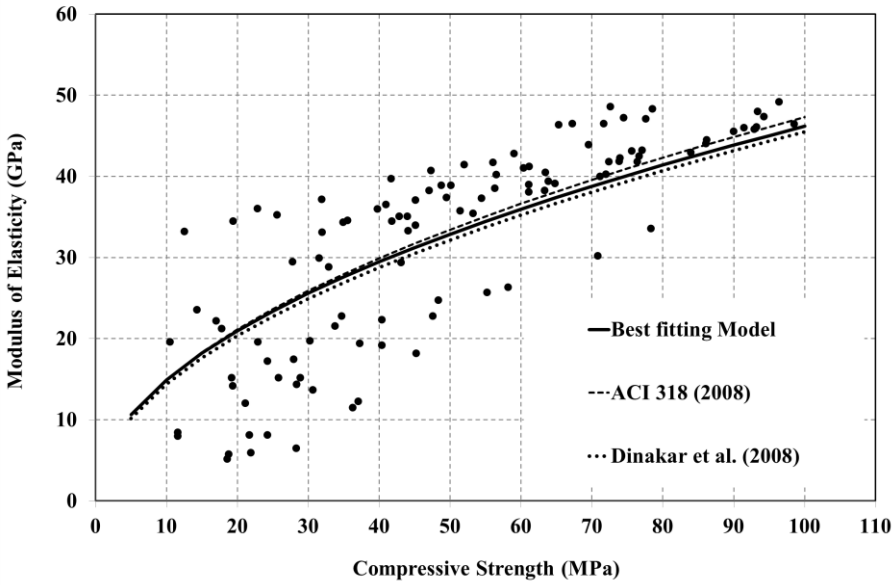

Figure 3.1 Comparison of the MOE CC proposed model, ACI 318 (2008) model and Dinakar et al. (2008) model versus CC experimental database

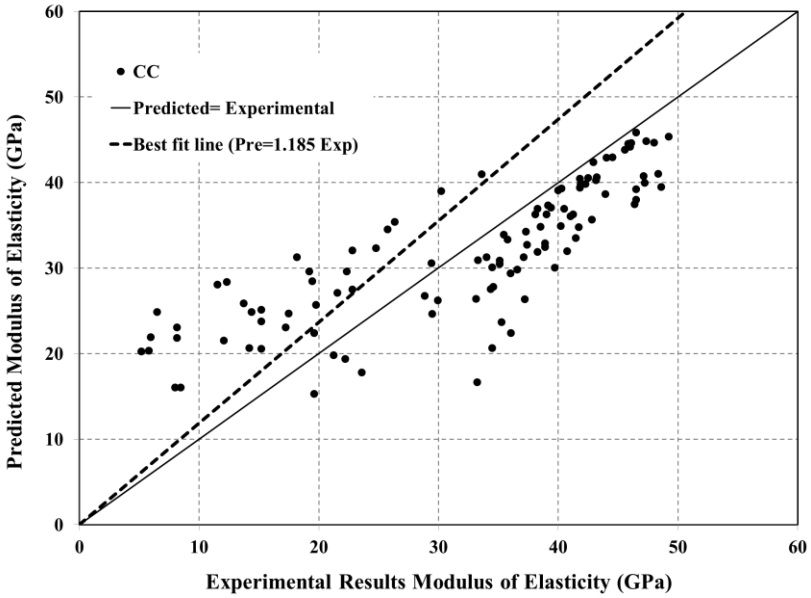

Figure 3.2 Comparison of the experimental results versus calculated values from the proposed model for MOE in the CC mixtures

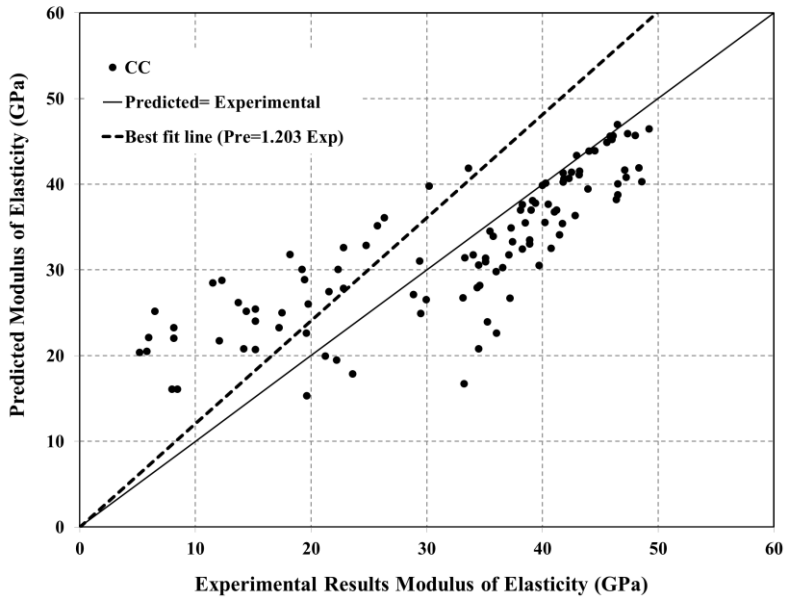

(a)

Figure 3.3(a) Comparison of the experimental results versus calculated values from (a) ACI 318 (2008) models for MOE in the CC mixtures

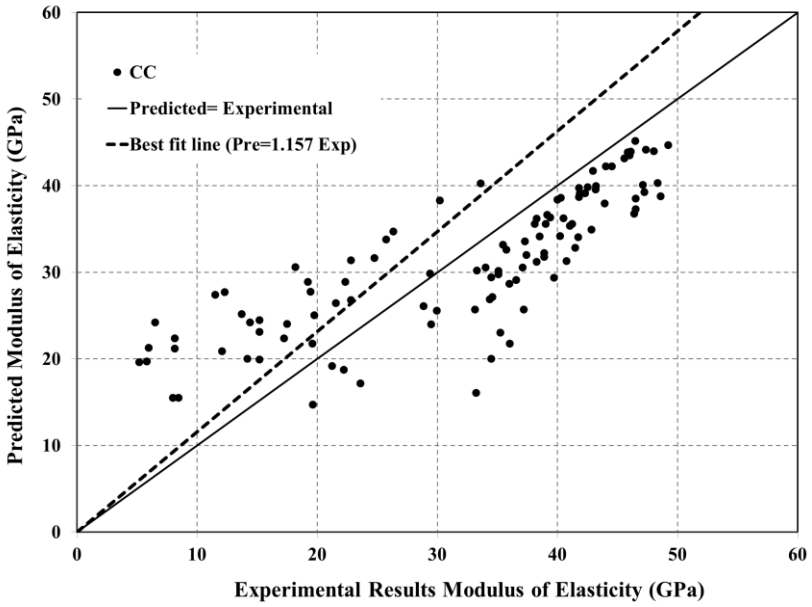

(b)

Figure 3.3(b) Comparison of the experimental results versus calculated values from Dinakar et al. (2008) models for MOE in the CC mixtures

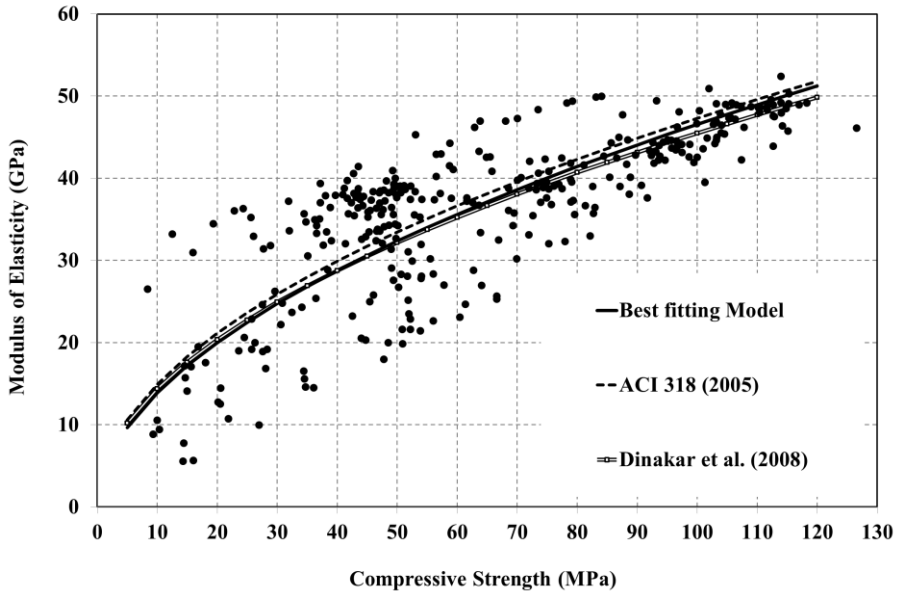

Figure 3.4 Comparison of the MOE CC proposed model, ACI 318 (2008) model and Dinakar et al. (2008) model versus SCC experimental database

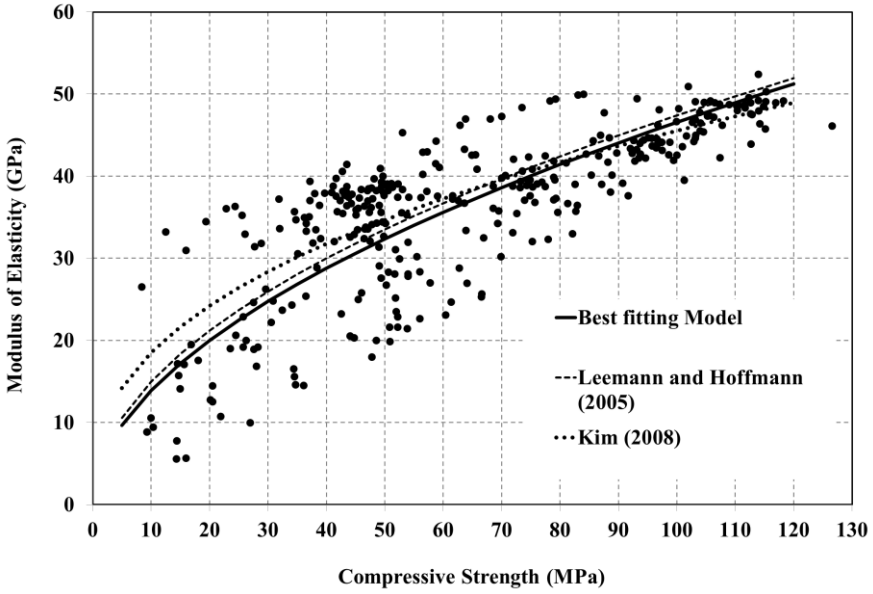

Figure 3.5 Comparison of the MOE SCC proposed model, Leemann and Hoffmann (2005) model and Kim (2008) model versus SCC experimental database

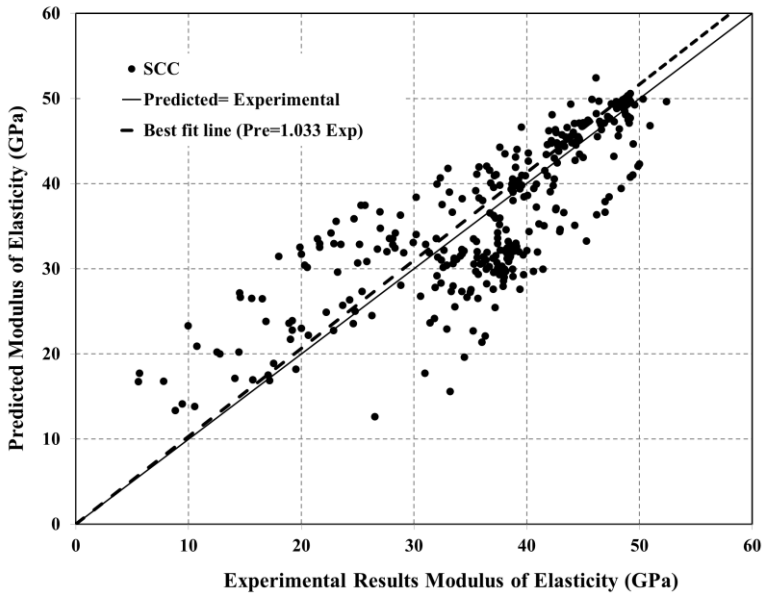

Figure 3.6 Comparison of the experimental results versus calculated values from the proposed model for MOE in the SCC mixtures

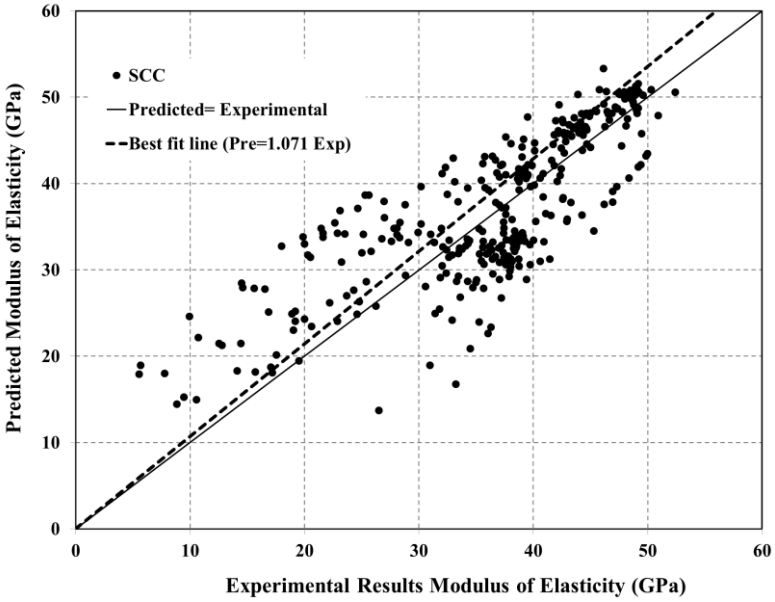

(a)

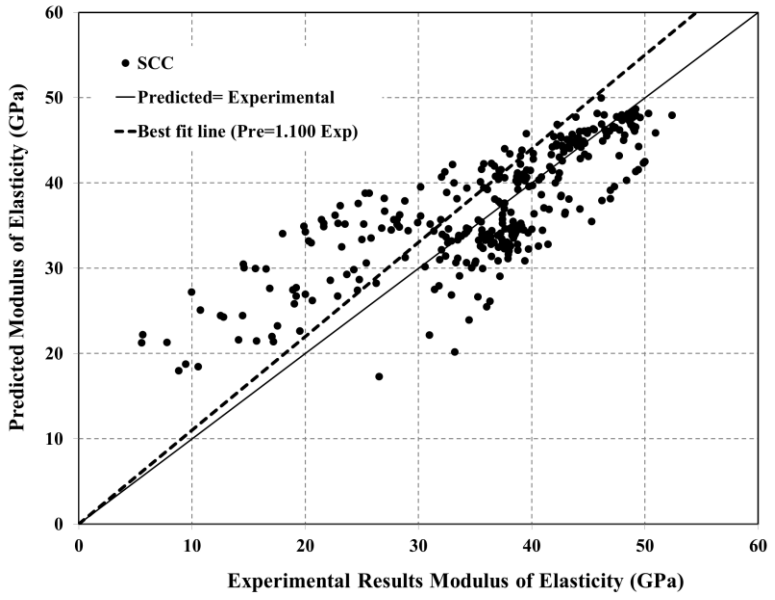

(b)

Figure 3.7 Comparison of the experimental results versus calculated values from the (a) Leemann and Hoffmann (2005) and (b) Kim (2008) models for MOE in the SCC mixtures

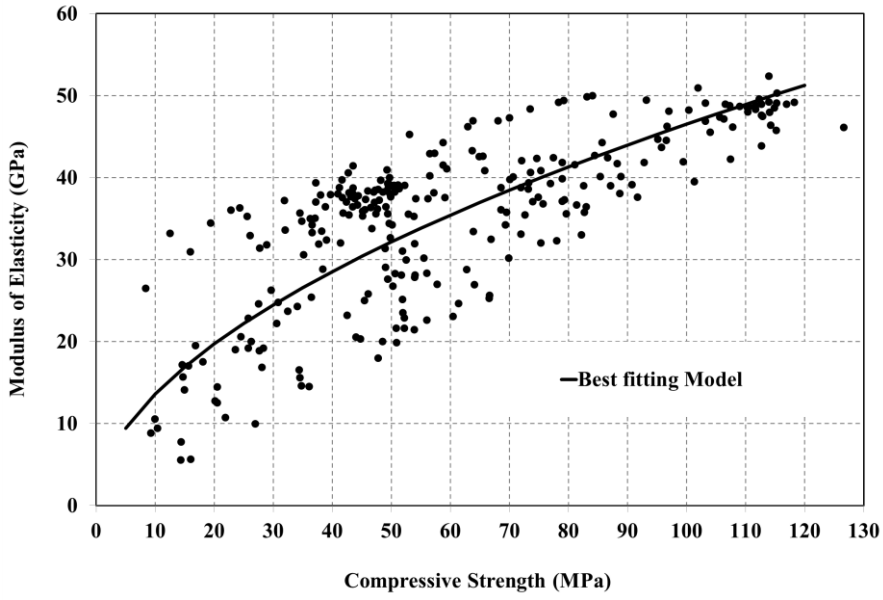

(a)

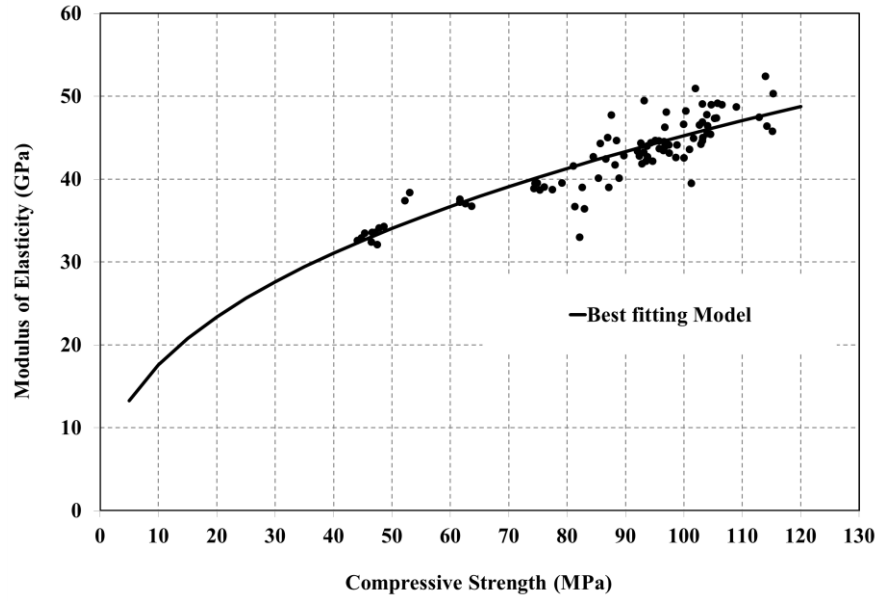

(b)

Figure 3.8(a,b) MOE versus compressive strength for the proposed models of SCC mixtures included in the database (a) with river gravel aggregate, (b) limestone aggregate

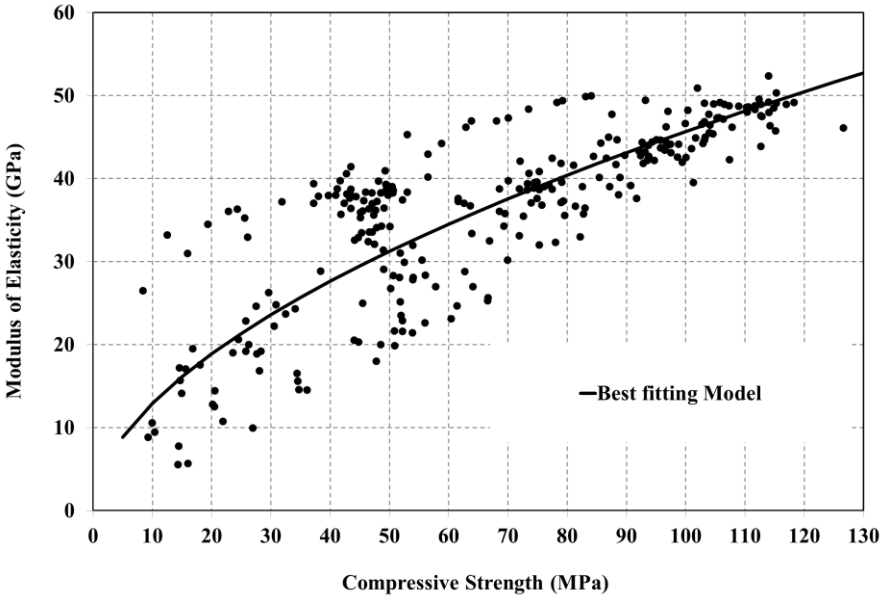

(c)

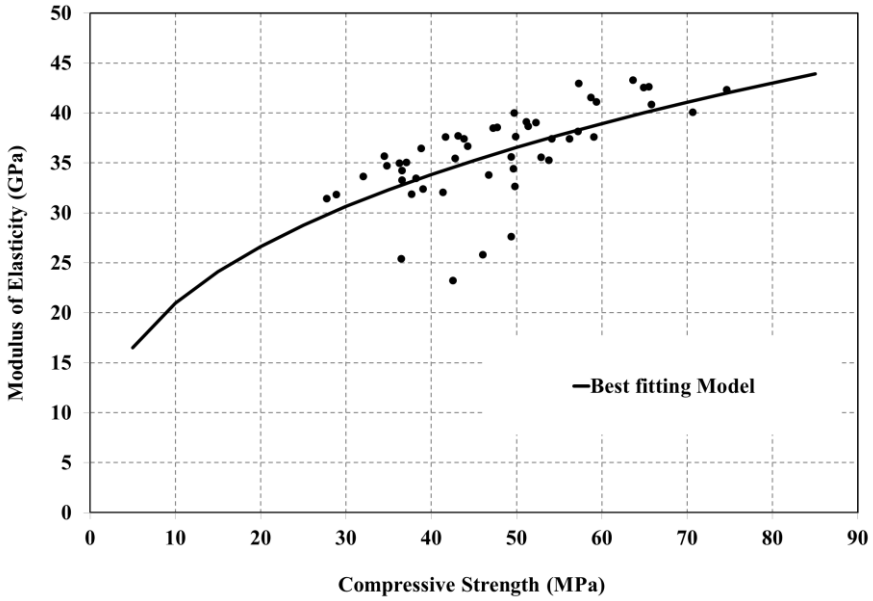

(d)

Figure 3.8(c,d) MOE versus compressive strength for the proposed models of SCC mixtures included in the database (c) fly ash filler, (d) limestone filler

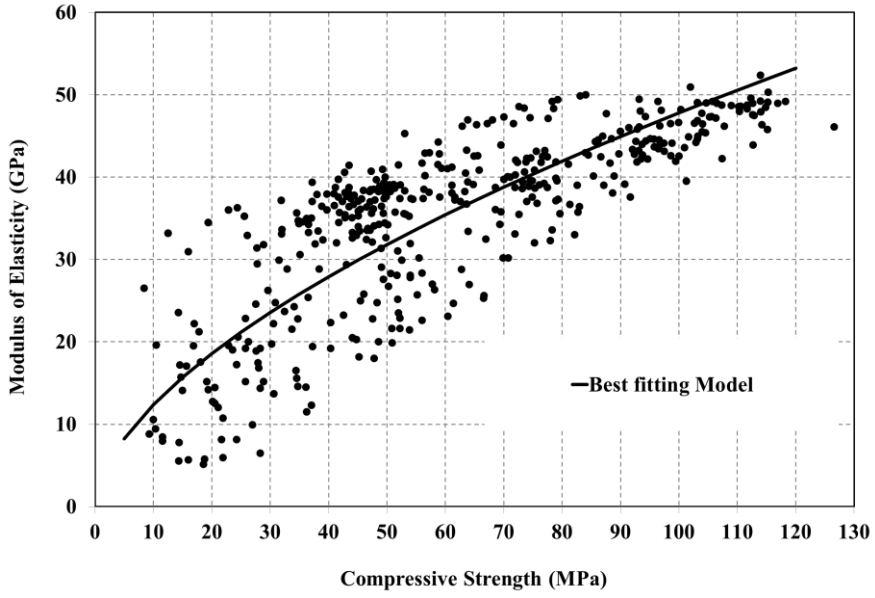

(e)

Figure 3.8(e) MOE versus compressive strength for the proposed models of SCC mixtures included in the database (e) general model for both SCC and CC

3.3 TENSILE STRENGTH (TS)

3.3.1 Experimental and Analytical Database for TS

Tables 3.6 and 3.7 are a general summary of the TS of the concrete mixtures included in the database. Tables 3.6 and 3.7 also include information regarding the curing age, type of curing, type of the cement, type of the filler, and type of Fine Aggregate (FA) and Coarse Aggregate (CA). Dominant properties of the available mixes in the database are as follows: the curing age is 28 days, type of curing is moist, type of cement is ordinary Portland cement, types of filler are fly ash and limestone, and type of aggregate which for FA is natural sand and for CA is natural river gravel, crushed granite and limestone. In the literature, several analytical and numerical models try to represent the TS for both SCC and CC mixtures. Tables 3.8 and 3.9 show some of these models that they vary in complexity and precision in the calculations.

From an investigation conducted by Aslani and Nejadi (2011b) in the TS database (Tables 3.6 to 3.8), the following conclusions can be made: a) the Carino and Lew (1982),

Raphael (1984), CEB-FIP (1990) and Gardner (1990) CC models predict TS more accurately for SCC and CC mixtures; and b) the two Parra et al. (2011) and Topçu and Uygunoğlu (2010) SCC models predict TS mostly conservative for SCC mixtures. In this section, the proposed TS models for CC and SCC are based on regression analyses on the existing experimental data, and the base of the proposed models is ACI 318 (2005).

3.3.2 Proposed TS Models

The proposed TS models covered SCC with different types of aggregates (river gravel, crushed granite, and limestone) and fillers (fly ash and limestone) in the mixture. Also, general TS model is considered for CC, SCC, and SCC-CC. The TS proposed models are presented in Eq. (3.2).

$$f_{ct} = \eta_1 \left(f_c'\right)^{\eta_2} \tag{3.2}$$

where:

Mixing Properties	η_1	η_2
CC	0.190	0.780
SCC	0.115	0.893
SCC with River Gravel, Crushed Granite Aggregate	0.115	0.912
SCC with Limestone Aggregate	0.472	0.551
SCC with Fly Ash Filler	0.251	0.712
SCC with Limestone Filler	0.082	0.965
General Model for both SCC and CC	0.134	0.587

3.3.3 Comparison of the TS Analytical Models

Figure 3.9 shows the TS versus compressive strength for the CC mixtures included in the database (Tables 3.6 and 3.7) and the proposed, Carino and Lew (1982), Raphael (1984), CEB-FIP (1990) and Gardner (1990) CC models. Figures 3.10 and 3.11 show the comparison of TS for the experimental results versus calculated values of the proposed, Carino and Lew (1982), Raphael (1984), CEB-FIP (1990) and Gardner (1990) models in CC mixtures. Figures 3.12 and 3.13 show the TS versus compressive strength for the SCC mixtures included in the database and the proposed Carino and Lew (1982), Raphael (1984), CEB-FIP (1990), Gardner (1990), Parra et al. (2011), and Topçu and Uygunoğlu

(2010) models. Figures 3.14 and 3.15 show the comparison of TS for the experimental results versus calculated values for the proposed Parra et al. (2011) and Topçu and Uygunoğlu (2010) models in SCC mixtures. Figure 3.16 shows the TS versus compressive strength for the SCC mixtures included in the database (Tables 3.6 and 3.7) and comparison of the proposed TS models that cover SCC with different types of aggregates (river gravel, crushed granite and limestone), fillers (fly ash and limestone) in the mixture, and general SCC-CC model.

From Table 3.10, the proposed model in this section provides a better prediction of TS values, with a coefficient of correlation factor (R^2) of 0.83 compared to 0.61 for the Carino and Lew (1982), 0.66 for the Raphael (1984), 0.60 for the CEB-FIP (1990), and 0.66 for the Gardner (1990) models (Figures 3.9 to 3.11) in CC mixtures. Moreover, as shown in Table 3.10, the proposed model provides a better prediction of TS values with a coefficient of correlation factor (R^2) of 0.87 compared to 0.61 for the Carino and Lew (1982), 0.66 for the Raphael (1984), 0.60 for the CEB-FIP (1990), 0.66 for the Gardner (1990), 0.81 for the Parra et al. (2011), and 0.72 for the Topçu and Uygunoğlu (2010) models (Figures 3.11 to 3.15) in SCC mixtures. Moreover, proposed TS models (Eq.3.2) for SCC mixtures without considering different type of aggregates and fillers showed that there is little difference between proposed SCC models with CC, but when the types of aggregates and fillers are changed, the difference is larger.

The value of TS predicted by the CC model for concrete with 60 MPa compressive strength, 3.8%, is greater than the overall SCC model, but this amount for the SCC model with limestone aggregate is 2.5%, and for SCC model with fly ash filler is 0.05% greater. But, the amount of TS predicted by CC model, 4%, is less than SCC model with the river gravel and crushed granite aggregate and nearly 7.5% less than the SCC model with limestone filler. These differences are unstable with compressive strength (i.e. for high compressive strength concrete more than 80 MPa the difference is low, but for normal compressive strength concrete, more than 45 MPa the difference is high). To overcome these differences between SCC and CC, a general TS model is proposed as shown in Eq. (3.2). This TS model is appropriate for both SCC and CC and can be used as a principal model in design.

Table 3.6 TS experimental database

Reference	No. of SCC mixtures	No. of CC mixtures	Curing age (days)	Type of cement
Kim et al. (1998)	5	3	28 and 90	Ordinary Portland cement
Druta (2004)	5	5	28	Ordinary Portland cement
Brouwers and Radix (2005)	3	0	28	CEM III/B 42.5 N LH/HS
Felekoğlu et al. (2007)	5	0	28	CEM I 42.5 N
Dinakar et al. (2008)	8	5	28	CEM I 42.5 N
Sekhar and Rao (2008)	8	0	28,90 and 180	Ordinary Portland cement
Sukumar et al. (2008)	10	5	28	Ordinary Portland cement
Kim (2008)	14	4	28	CEM III
Liu (2010)	6	0	7, 28, 60, 90, 120, 150 and 180	CEM I 42.5 N
Topçu and Uygunoğlu (2010)	5	0	28	CEM I 42.5 R
Almeida Filho et al. (2010)	3	0	28	Ordinary Portland cement
Parra et al. (2011)	4	4	7, 28 and 90	CEM II/B-M (V-LL) 32.5N and CEM II/B-M (V-LL) 42.5R
Siddique (2011)	5	0	7, 28, 90 and 365	Ordinary Portland cement
Total of 107 mixtures	81	26		

Table 3.7 TS experimental database (continued)

Reference	Type of filler	Type of Aggregate	
		FA	CA
Kim et al. (1998)	Fly ash	Sea sand	Crushed stone
Druta (2004)	Fly Ash, Silica Fume and Blast Furnace Slag	Natural sand with maximum size of 1 mm	River gravel with maximum size of 19.5 mm
Brouwers and Radix (2005)	Fly ash and Limestone	Sand 0 – 1 mm	Rhine gravel 4 – 16 mm
Felekoğlu et al. (2007)	Limestone	Crushed 0–5mm limestone	Crushed limestone 15mm maximum size
Dinakar et al. (2008)	Fly ash	Well-graded river sand	Maximum grain size of 12 mm
Sekhar and Rao (2008)	Fly ash	River sand	Crushed angular granite metal of 10 mm size
Sukumar et al. (2008)	Fly ash	River sand	Crushed granite of 12 mm
Kim (2008)	Fly ash	Fordyce murphy and TXI (Austin) natural sand	Fordyce murphy river gravel, Hanson aggregate limestone
Liu (2010)	Fly ash	Sand 0/4 mm	4/10 mm and 10/20 mm gravel
Topçu and Uygunoğlu (2010)	Fly ash and Limestone	Natural river sand	Pumice, volcanic tuff and diatomite with a maximum size of 16 mm
Almeida Filho et al. (2010)	Limestone	0-2 mm and 0–5 mm sands	5–12 mm and 12–18 mm gravels
Parra et al. (2011)	Limestone	Fine sand 0/2	Coarse sand 0/4
Siddique (2011)	Fly ash	Natural sand with 4.75 mm maximum size	Crushed stone with 16 mm maximum size

Table 3.8 TS models for CC

Reference	Models of Splitting tensile strength for CC (SI units, MPa)
Akazawa (1953)	$f_{ct} = 0.209(f_c')^{0.73}$
Carneiro and Barcellor (1953)	$f_{ct} = 0.185(f_c')^{0.735}$
Vinayaka (1959)	$f_{ct} = 0.88(f_c')^{0.716}$
Sen and Desayi (1962)	$f_{ct} = 0.682(f_c')^{0.73}$
Carino and Lew (1982)	$f_{ct} = 0.272(f_c')^{0.71}$
Raphael (1984)	$f_{ct} = 0.313(f_c')^{0.667}$
Ahmad and Shah (1985)	$f_{ct} = 0.46(f_c')^{0.55}$
CEB-FIP (1990)	$f_{ct} = 1.56\left[\frac{f_c' - 8}{10}\right]^{2/3}$
Gardner (1990)	$f_{ct} = 0.313(f_c')^{0.667}$
Oluokun (1991)	$f_{ct} = 0.206(f_c')^{0.69}$
Burg and Ost (1992)	$f_{ct} = 7.3(f_c')^{0.5}$
ACI 363 (1992)	$f_{ct} = 0.56(f_c')^{0.5}$
NEN 6722 (2000)	$f_{ct} = 1 + 0.05 f_c'$
Hueste et al. (2004)	$f_{ct} = 0.55\sqrt{f_c'}$
ACI 318 (2005)	$f_{ct} = 0.56(f_c')^{0.5}$
AASHTO (2006)	$f_{ct} = 0.59(f_c')^{0.5}$
Dinakar et al. (2008)	$f_{ct} = 0.65(f_c')^{0.5}$

Table 3.9 TS models for SCC

Reference	Models of Splitting tensile strength for SCC (SI units, MPa)
Felekoğlu et al. (2007)	$f_{ct} = 0.43(f_c')^{0.6}$
Dinakar et al. (2008)	$f_{ct} = 0.82(f_c')^{0.5}$
Sukumar et al. (2008)	$f_{ct} = 0.0843 f_c' + 0.818$
Kim (2008)	1. Lower Bound $f_{ct} = 0.52(f_c')^{0.5}$ 2. Mean $f_{ct} = 0.68(f_c')^{0.5}$ 3. Upper Bound $f_{ct} = 0.85(f_c')^{0.5}$
Topçu and Uygunoğlu (2010)	$f_{ct} = 0.0602 f_c' + 0.2009$
Parra et al. (2011)	$f_{ct} = 0.28(f_c')^{2/3}$

Table 3.10 Coefficient of correlation factor (R^2) for TS

Reference	CC		SCC	
	Predicted/Experimental TS	R^2	Predicted/Experimental TS	R^2
Carino and Lew (1982)	1.096	0.61	1.240	0.79
Raphael (1984)	1.060	0.66	1.222	0.78
CEB-FIP (1990)	1.010	0.60	1.043	0.79
Gardner (1990)	1.060	0.66	1.222	0.78
Parra et al. (2011)	-	-	1.092	0.81
Topçu and Uygunoğlu (2010)	-	-	0.883	0.72
Proposed Model	1.016	0.83	1.027	0.87

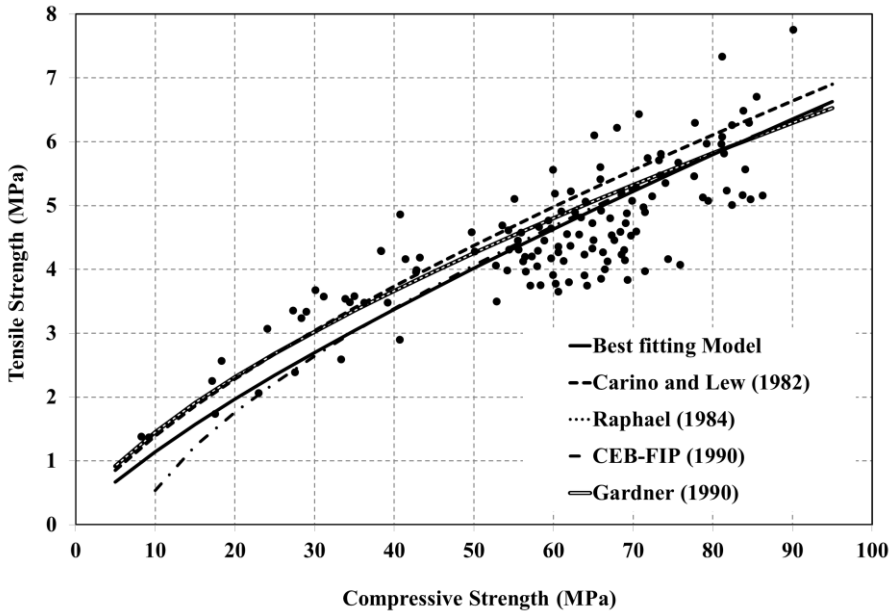

Figure 3.9 Comparison of the TS CC proposed model, Carino and Lew (1982), Raphael (1984), CEB-FIP (1990) and Gardner (1990) models versus CC experimental database

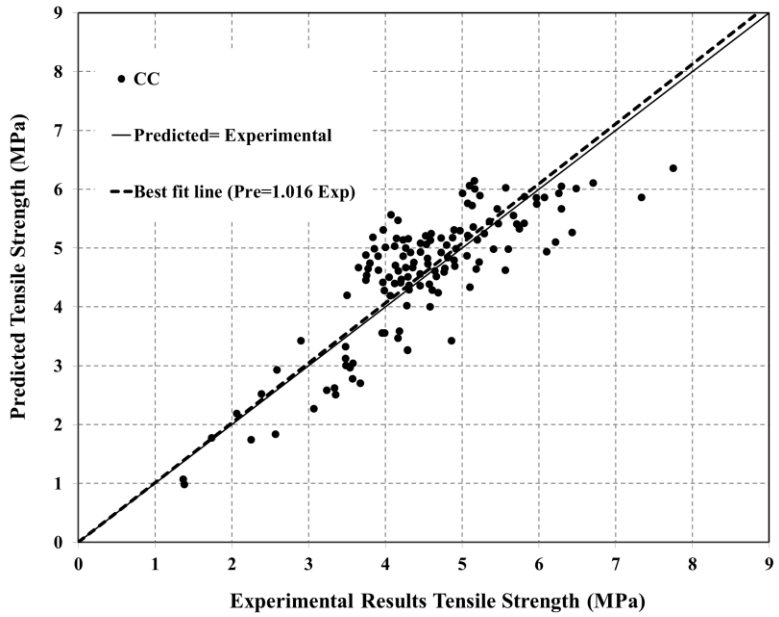

Figure 3.10 Comparison of the experimental results versus calculated values from the proposed model for TS in the CC mixtures

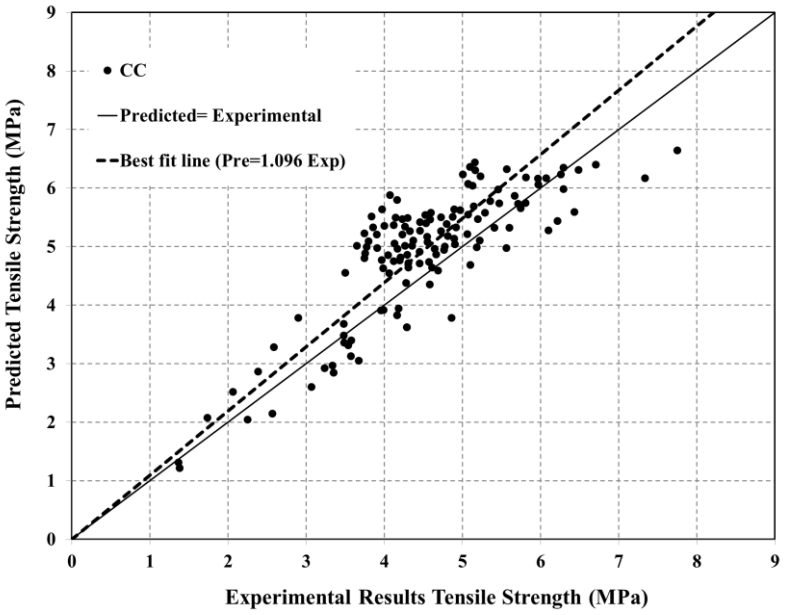

(a)

Figure 3.11(a) Comparison of the experimental results versus calculated values from (a) Carino and Lew (1982) model for TS in the CC mixtures

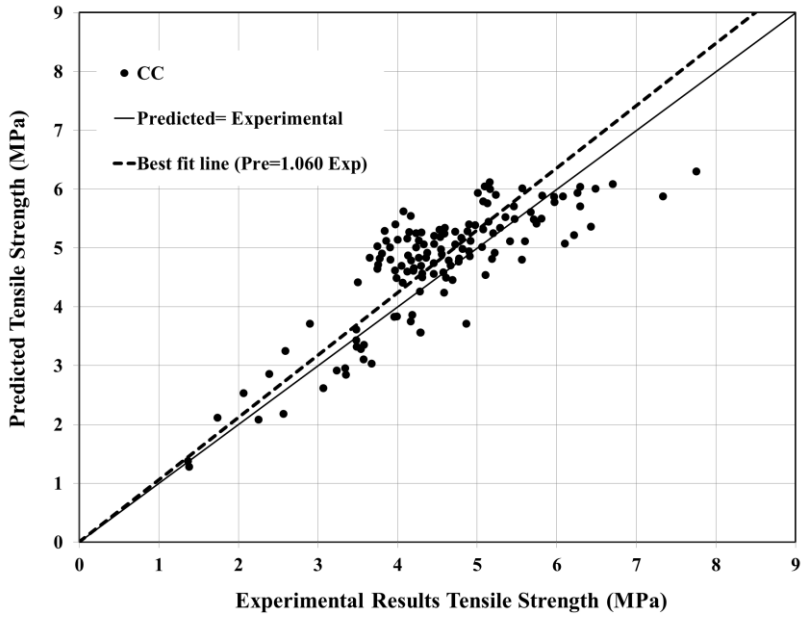

(b)

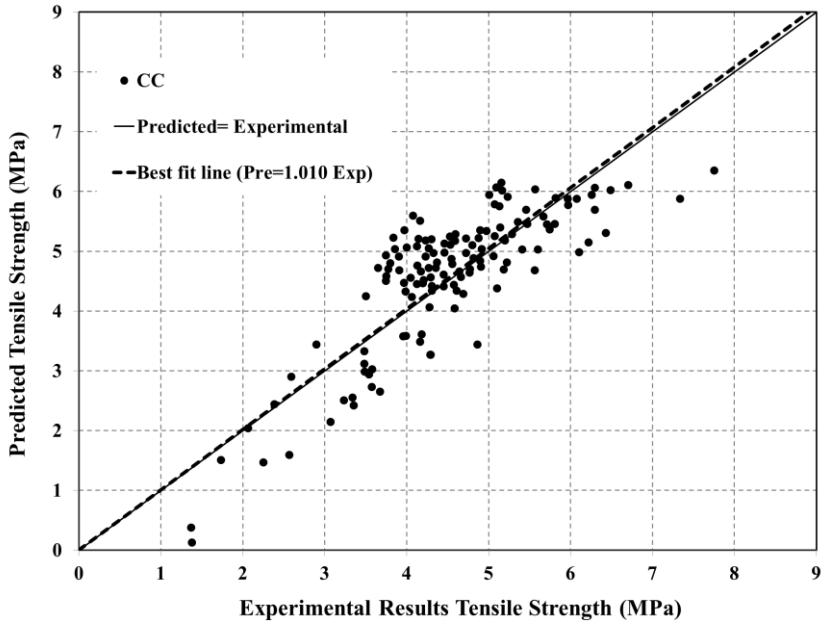

(c)

Figure 3.11(b,c) Comparison of the experimental results versus calculated values from (b) Raphael (1984) and (c) CEB-FIP (1990) models for TS in the CC mixtures

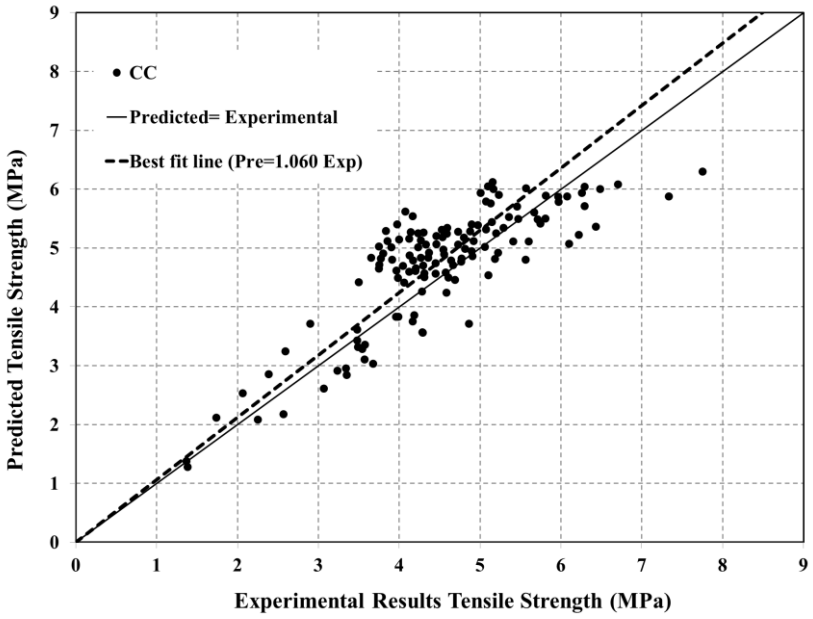

(d)

Figure 3.11(d) Comparison of the experimental results versus calculated values from (d) Gardner (1990) model for TS in the CC mixtures

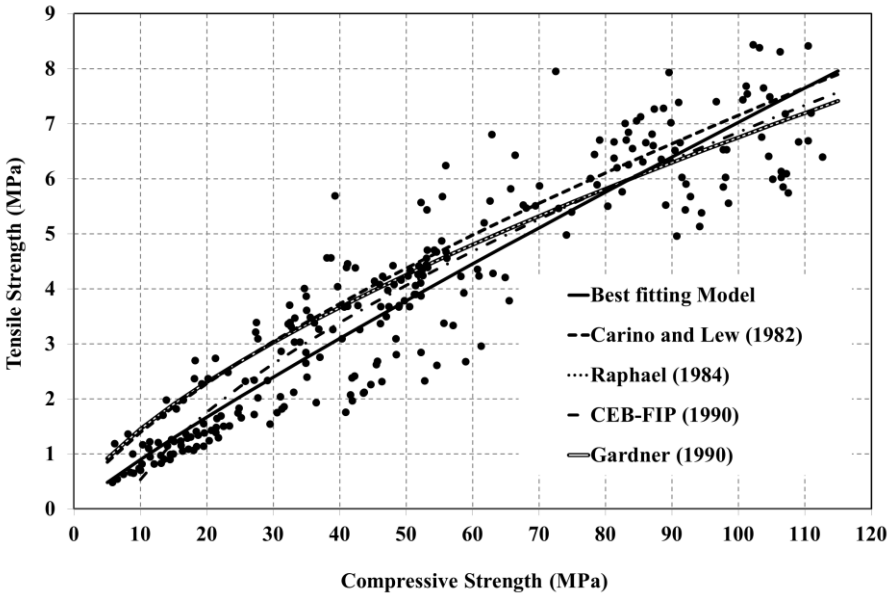

Figure 3.12 Comparison of the TS CC proposed model, Carino and Lew (1982), Raphael (1984), CEB-FIP (1990) and Gardner (1990) models versus SCC experimental database

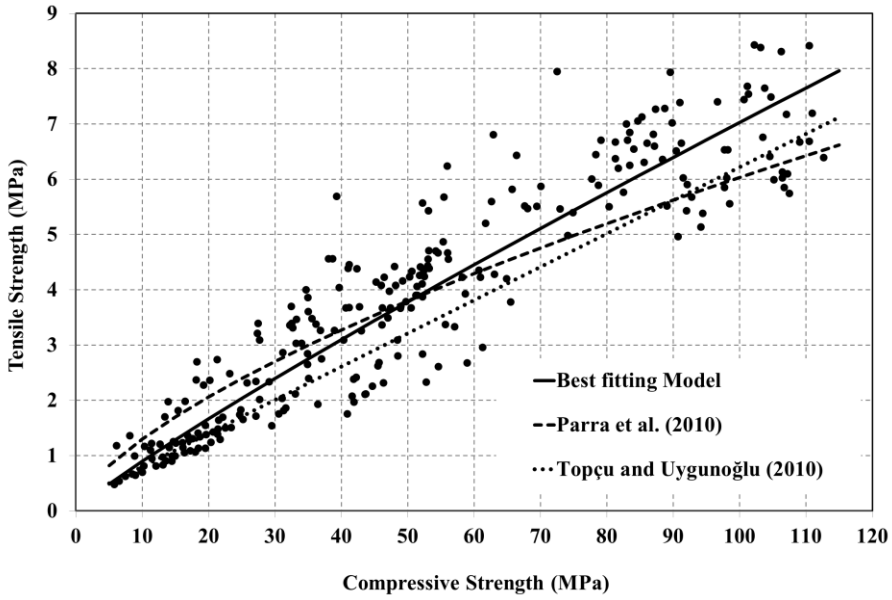

Figure 3.13 Comparison of the TS CC proposed model, Parra et al. (2011) and Topçu and Uygunoğlu (2010) models versus SCC experimental database

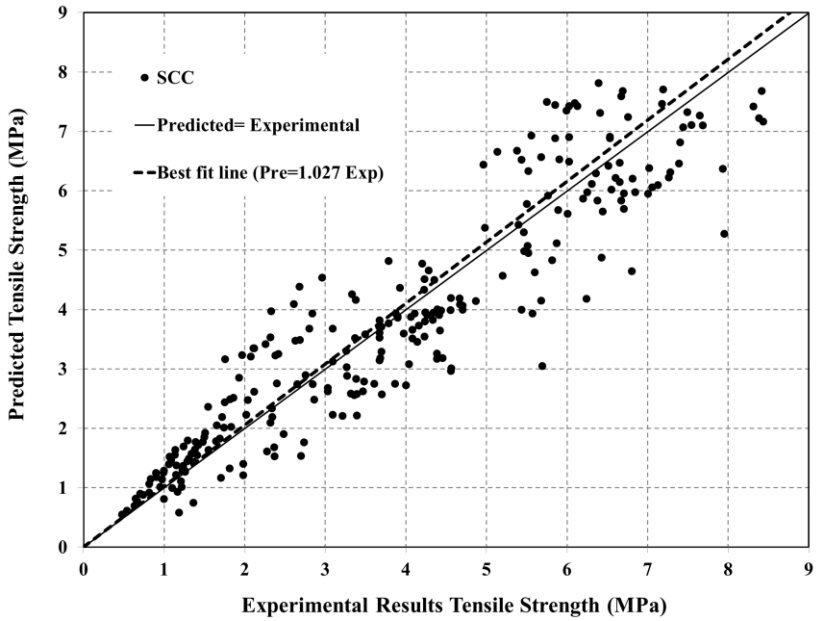

Figure 3.14 Comparison of the experimental results versus calculated values from proposed model for TS in the SCC mixtures

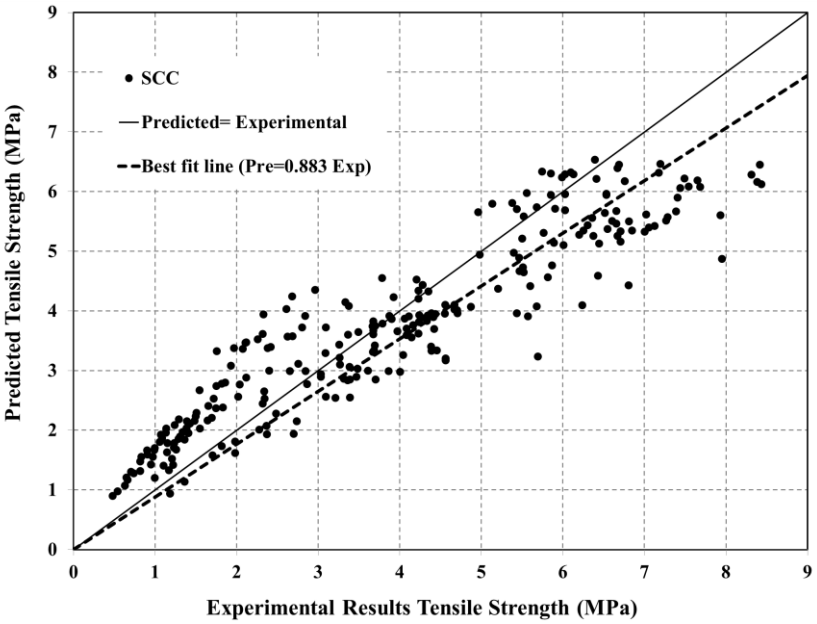

(a)

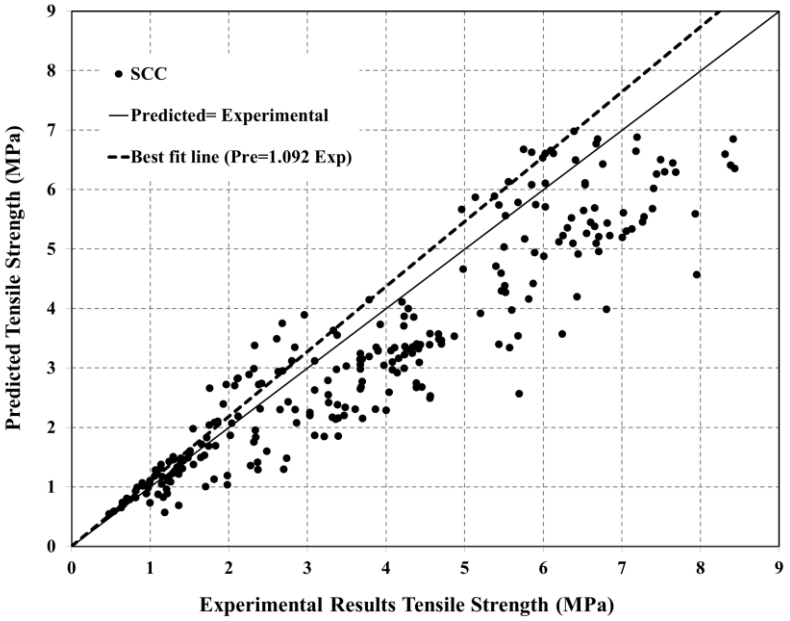

(b)

Figure 3.15 Comparison of the experimental results versus calculated values from (a) Parra et al. (2011) and (b) Topçu and Uygunoğlu (2010) model for TS in the SCC mixtures

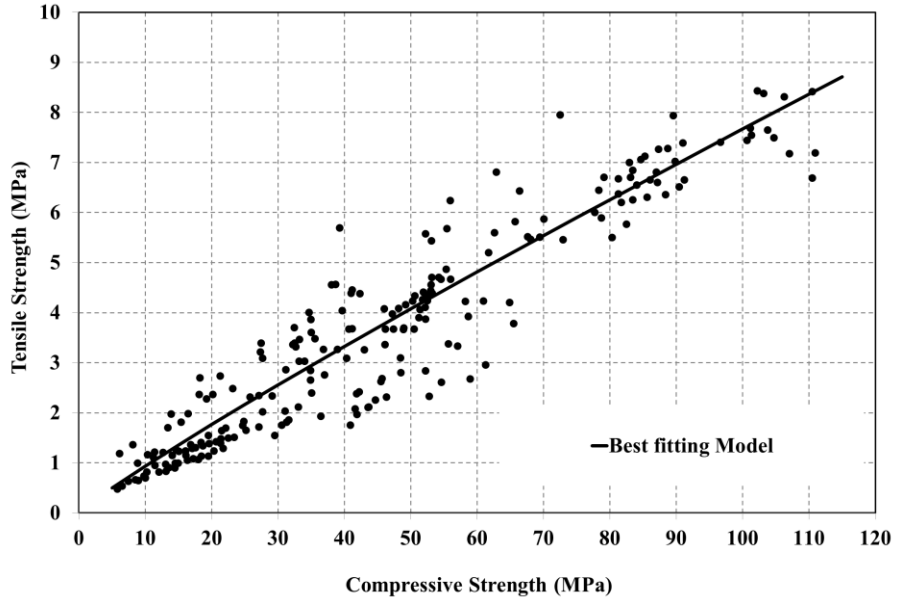

(a)

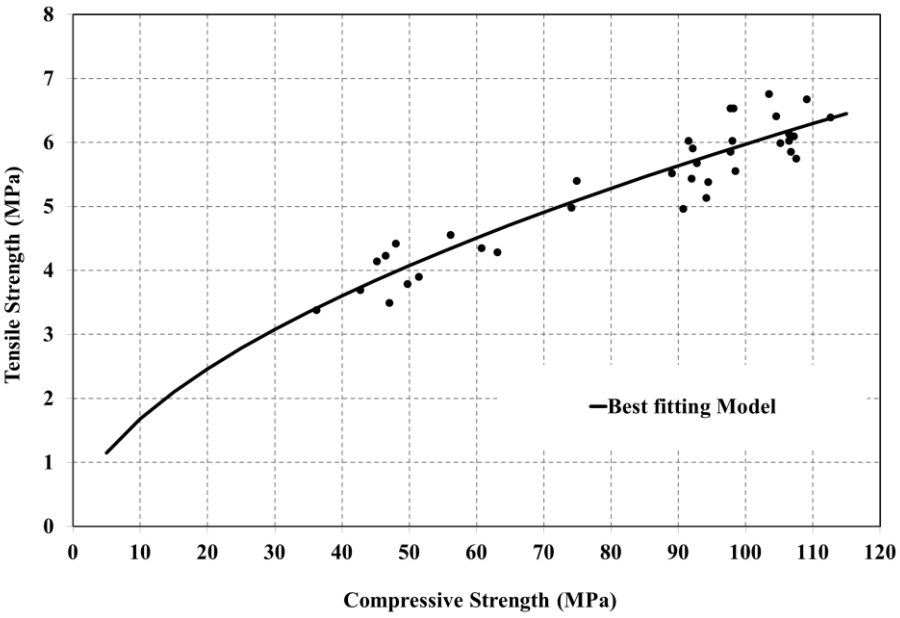

(b)

Figure 3.16(a, b) TS versus compressive strength for the proposed models of SCC mixtures included in the database (a) with river gravel aggregate and (b) limestone aggregate

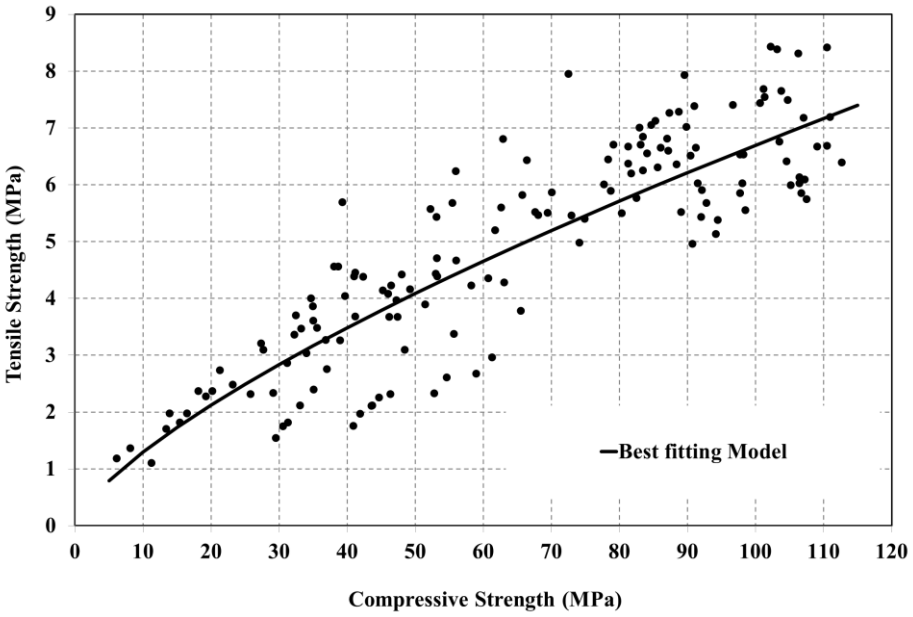

(c)

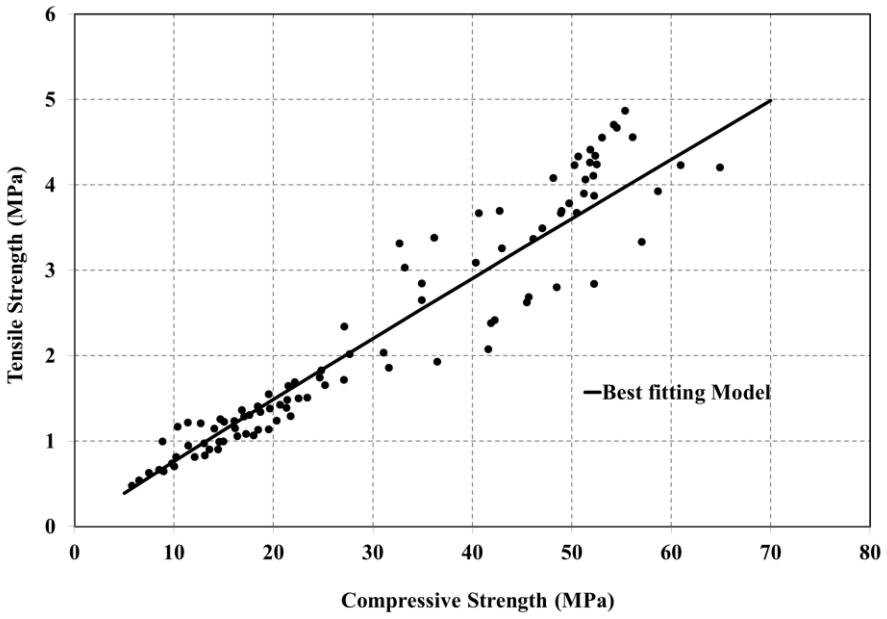

(d)

Figure 3.16(c, d) TS versus compressive strength for the proposed models of SCC mixtures included in the database (c) fly ash filler, (d) limestone filler

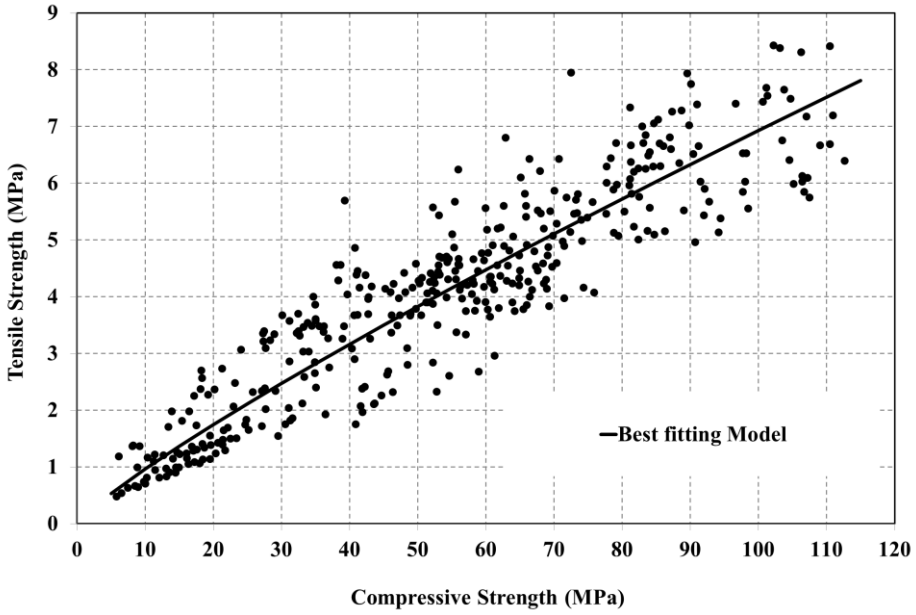

(e)

Figure 3.16(e) TS versus compressive strength for the proposed models of SCC mixtures included in the database (e) general model for both SCC and CC

3.4 MODULUS OF RUPTURE (MOR)

3.4.1 Experimental and Analytical Database for MOR

Tables 3.11 and 3.12 are a general summary of the concrete mixtures included in the database. The database includes test results from eleven different investigations, with a total of 175 different SCC mixtures. Tables 3.11 and 3.12 also include information regarding the fine and coarse aggregate type, cement type, filler type, and type of Specimen Utilized in the Compressive Strength Test (SUCST). Dominant properties of the available mixes in the database are that the curing age is 28 days, type of cement is Ordinary Portland Cement (OPC), types of filler are fly ash and limestone, type of fine aggregate is natural sand, types of coarse aggregate are natural and crushed gravels, and types of SUCST are cylinders (100 mm × 200 mm) and cubes (100 mm).

In the literature, several analytical and numerical models have been proposed to represent the MOR for both SCC and CC mixtures. Tables 3.13 and 3.14 are shown ten

MOR models for CC and five MOR models for SCC. Table 3.13 include MOR models for CC of Carasquillo et al. (1981), Ahmad and Shah (1985), CEB-FIP (1990), ACI 363 (1992), Légeron and Paultre (2000), Canadian Code (CSA A23.3, 2004), Leemann and Hoffmann (2005), New Zealand Code (NZS 3101, 2006), AASHTO (2006), and ACI Code (2008). Also, Leemann and Hoffmann (2005), Kim (2008), Dehwah (2012), Das and Chatterjee (2012), and Mohammadhassani et al. (2012) MOR models for SCC are included in Table 3.14.

3.4.2 Comparison of Proposed MOR Model with Available MOR Models

Figure 3.17.(a to j) shows comparison of the MOR experimental results versus calculated values from the CC mixture models listed in Table 3.13. Furthermore, Figure 3.18 shows the MOR results versus compressive strength for the SCC mixtures listed in the database (Tables 3.11 and 3.12) and comparison of the models in Table 3.13. Also, in Table 3.15, MOR predicted/experimental values for CC, coefficients of correlation factor (R^2), and percentages of CC prediction models errors are included. As shown in Table 3.15 for the CC models, the Carasquillo et al. (1981), ACI 363 (1992), AASHTO (2006) provide a better prediction of MOR with a coefficient of correlation factor (R^2) of 0.80 compared to 0.70 for Ahmad and Shah (1985) and Légeron and Paultre (2000), 0.68 for CEB-FIP (1990) and Leemann and Hoffmann (2005), 0.62 for New Zealand Code (NZS 3101, 2006), 0.54 for ACI Code (2008), and 0.49 for Canadian Code (CSA A23.3, 2004). Also, these three prediction models are overestimated with 2.74% for the Carasquillo et al. (1981) model, 5.75 % for the ACI 363 (1992) and AASHTO (2006) models. As shown in Figure 3.18, Carasquillo et al. (1981), Ahmad and Shah (1985), ACI 363 (1992), and AASHTO (2006) provide better prediction.

However, the other CC prediction models properties are summarized in Table 3.15. Figure 3.19.(a to e) shows comparison of the MOR experimental results versus calculated values from the SCC mixture models in Table 3.14 and proposed model (Eq.3.3). Furthermore, Figure 3.20 shows the MOR results versus compressive strength for the SCC mixtures listed in the database (Tables 3.11 and 3.12) and comparison of the models in Table 3.14 and proposed model. Also, in Table 3.16, MOR predicted/experimental values

for SCC, coefficients of correlation factor (R^2), and over or under estimate percentage of SCC prediction models are included. The MOR proposed models are presented in Eq. (3.3).

$$f_{cr} = 0.771\left(f_c'\right)^{0.5378} \tag{3.3}$$

As shown in Table 3.16 for the SCC models, Leemann and Hoffmann (2005) provide better prediction of MOR with a coefficient of correlation factor (R^2) of 0.76 compared to 0.69 for Das and Chatterjee (2012), 0.63 for Dehwah (2012), 0.43 for Mohammadhassani et al. (2012), and 0.41 for Kim (2008). Also, Leemann and Hoffmann (2005) model prediction is overestimated by 4.02%. The other SCC models prediction properties are summarized in Table 3.16. As shown in Figure 3.20, for the MOR results versus compressive strength, none of the MOR models for SCC has a good prediction. The proposed MOR model for SCC mixture has 0.85 coefficient of correlation factor (R^2) and model prediction is overestimated by 3.02%.

Table 3.11 MOR experimental results database

Reference	No. of SCC mixtures	Fine aggregate	Coarse aggregate
Fava et al. (2003)	2	Natural Sand	Natural Gravel
Leemann and Hoffmann (2005)	9	Natural Sand	Natural Gravel
Koehler and Fowler (2007)	85	Limestone, Dolomitic Limestone, Dolomite, Granite, Traprock, River Sand	Limestone, River Gravel, Dolomite
Kim (2008)	14	Natural Sand	River gravel and limestone
Türkel and Kandemir (2010)	4	Crushed limestone, and olivine basalt	Limestone and olivine basalt
Corinaldesi and Moriconi (2011)	1	Quartz sand	Natural Gravel
Khaeel et al. (2011)	12	Natural sand	Uncrushed gravel, crushed gravel, crushed limestone
Vilanova et al. (2009)	34	Various	Various
Mohammadhassani et al. (2012)	8	Natural Sand, River Sand	Crushed granite
Dehwah (2012)	5	Dune sand	Crushed limestone
Das and Chatterjee (2012)	1	Natural Sand	Natural Gravel

Table 3.12 MOR experimental database (continued)

Reference	Cement type	Filler type	f'_c
Fava et al. (2003)	Blended cement	GGBFS* and Limestone	Cylinder (150 mm × 300 mm)
Leemann and Hoffmann (2005)	Ordinary Portland Cement (OPC)	Fly ash	Prisms (120 mm × 120 mm × 360 mm)
Koehler and Fowler (2007)	PC-I/II, PC-III, PC-I	Fly Ash	Cylinder (100 mm × 200 mm)
Kim (2008)	PC-III	Fly Ash	Cylinder (100 mm × 200 mm)
Türkel and Kandemir (2010)	OPC	Fly Ash	Cylinder (100 mm × 200 mm)
Corinaldesi and Moriconi (2011)	Portland limestone blended cement type CEM II/ A-L 42.5 R	Limestone	Cubic (100 mm)
Khaeel et al. (2011)	OPC	Metakaolin	Cylinder (100 mm × 200 mm)
Vilanova et al. (2009)	Various	Various	Various
Mohammadhassani et al. (2012)	OPC	Silica fume	Cubic (100 mm)
Dehwah (2012)	OPC	Silica fume and Fly ash	Cubic (100 mm)
Das and Chatterjee (2012)	OPC	Fly ash	Cubic (150 mm)

Table 3.13 MOR models for CC

Reference	CC MOR Models
Carasquillo et al. (1981)	$f_{cr} = 0.94\sqrt{f'_c}$; $21MPa < f'_c < 83MPa$
Ahmad and Shah (1985)	$f_{cr} = 0.44 f'^{2/3}_c$
CEB-FIP (1990)	150 mm × 150 mm $f_{cr} = 2.1\left(\frac{f'_c - 8}{10}\right)^{2/3}$
	100 mm × 100 mm $f_{cr} = 2.33\left(\frac{f'_c - 8}{10}\right)^{2/3}$
ACI 363 (1992)	$f_{cr} = 0.97\sqrt{f'_c}$
Légeron and Paultre (2000)	$f_{cr} = 0.94\sqrt{f'_c}$ $f_{cr} = 0.5 f'^{2/3}_c$
Canadian Code (CSA A23.3, 2004)	$f_{cr} = 0.6\sqrt{f'_c}$; $20MPa < f'_c < 80MPa$
Leemann and Hoffmann (2005)	$f_{cr} = 0.11 f'_c$
New Zealand Code (NZS 3101, 2006)	Normal weight concrete $f_{cr} = 0.8\sqrt{f'_c}$

Table 3.13 MOR models for CC (continued)

Reference	CC MOR Models
AASHTO (2006)	Lower bound $f_{cr} = 0.63\sqrt{f_c'}$
	Upper bound $f_{cr} = 0.97\sqrt{f_c'}$
ACI Code (2008)	$f_{cr} = 0.62\sqrt{f_c'}$
	concrete for prestressed members $f_{cr} = 0.5\sqrt{f_c'}$

Table 3.14 MOR models for SCC

Reference	SCC MOR Models
Leemann and Hoffmann (2005)	$f_{cr} = 0.12 f_c'$
Kim (2008)	$f_{cr} = 0.95 f_c'^{0.75}$
Dehwah (2012)	$f_{cr} = 0.0368 f_c' + 4.2932$
Das and Chatterjee (2012)	$f_{cr} = 0.762\sqrt{f_c'}$
Mohammadhassani et al. (2012)	$f_{cr} = 0.6\sqrt{f_c'}$

Table 3.15 MOR models prediction properties for CC

Reference	CC MOR Models	
	Pred. / Exp.	R^2
Carasquillo et al. (1981)	1.028	0.80
Ahmad and Shah (1985)	0.957	0.70
CEB-FIP (1990)	0.984	0.68
ACI 363 (1992)	1.061	0.80
Légeron and Paultre (2000)	1.088	0.70
Canadian Code (CSA A23.3, 2004)	0.656	0.49
Leemann and Hoffmann (2005)	0.955	0.68
New Zealand Code (NZS 3101, 2006)	0.875	0.62
AASHTO (2006)	1.061	0.80
ACI Code (2008)	0.678	0.54

Table 3.16 MOR models prediction properties for SCC

Reference	SCC MOR Models	
	Pred. / Exp.	R^2
Leemann and Hoffmann (2005)	1.041	0.76
Kim (2008)	2.919	0.41
Dehwah (2012)	0.923	0.63
Das and Chatterjee (2012)	0.833	0.69
Mohammadhassani et al. (2012)	0.656	0.43
Proposed Model	1.032	0.85

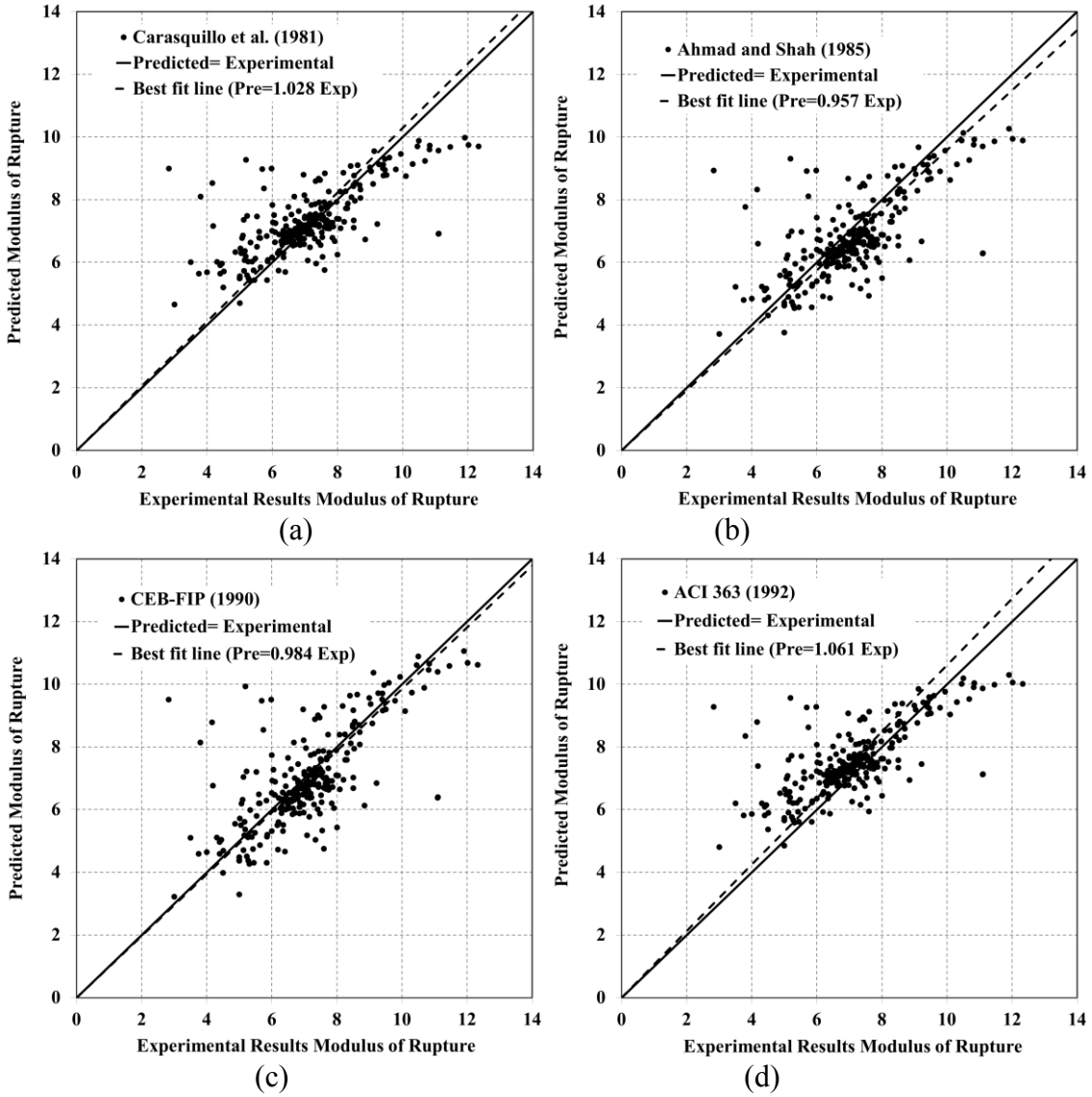

Figure 3.17 (a to d) Comparison of MOR for SCC experimental results versus calculated values for various CC prediction models

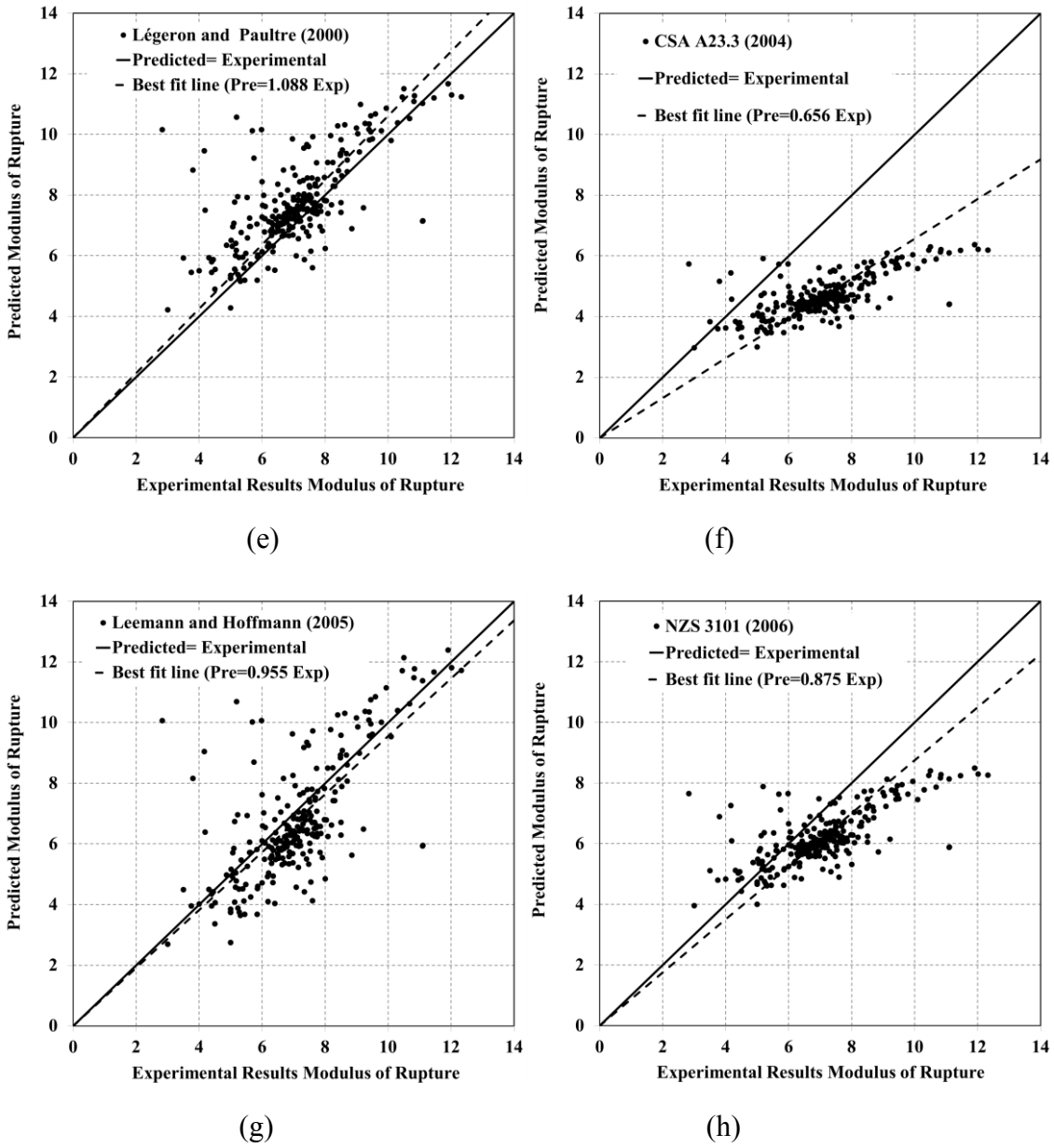

Figure 3.17 (e to h) Comparison of MOR for SCC experimental results versus calculated values for various CC prediction models

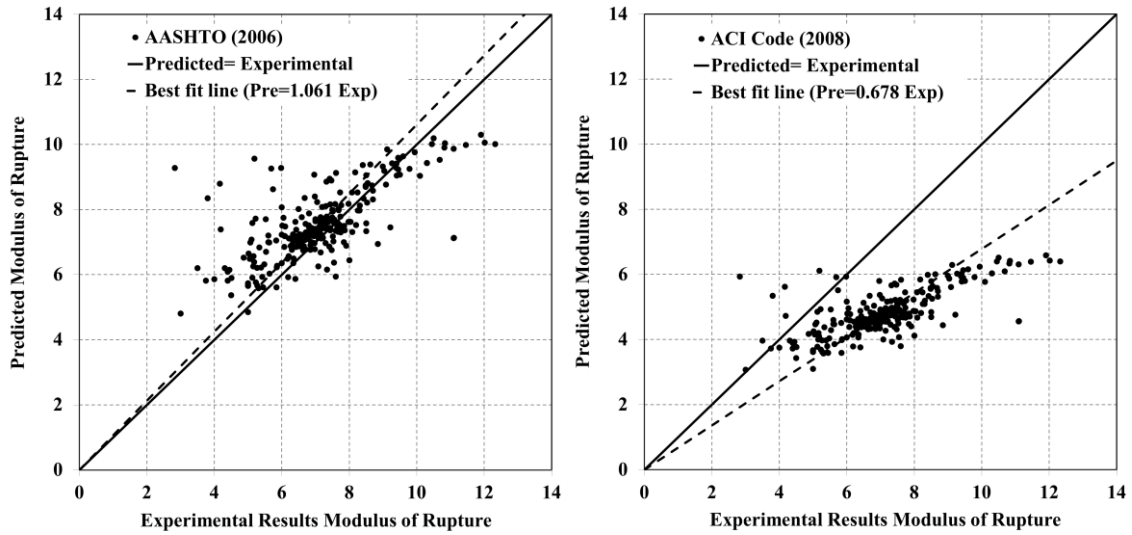

(i) (j)

Figure 3.17 (i to j) Comparison of MOR for SCC experimental results versus calculated values for various CC prediction models

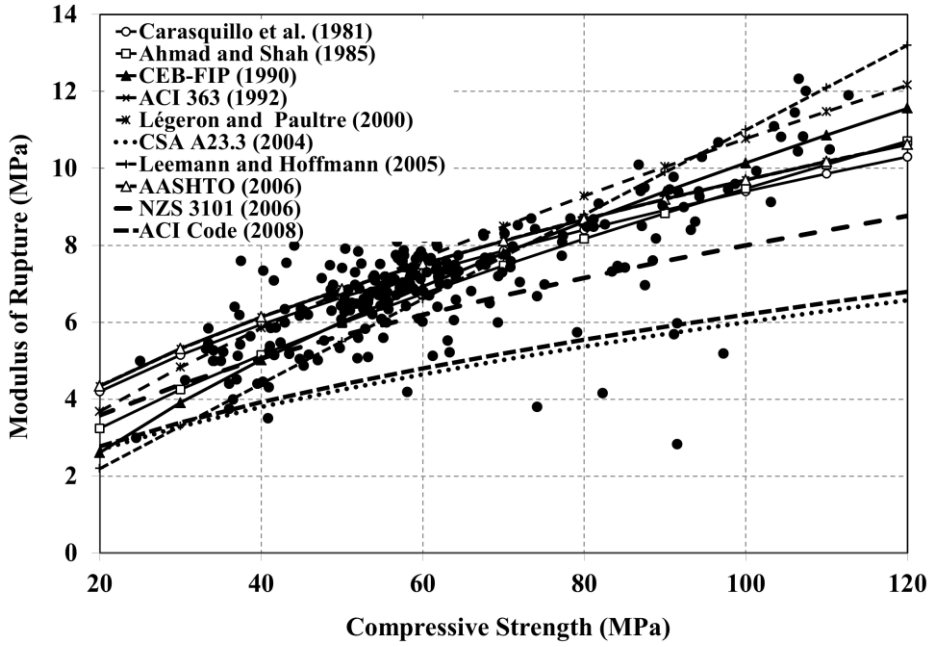

Figure 3.18 Comparison of MOR for SCC experimental results versus calculated values for various CC prediction models

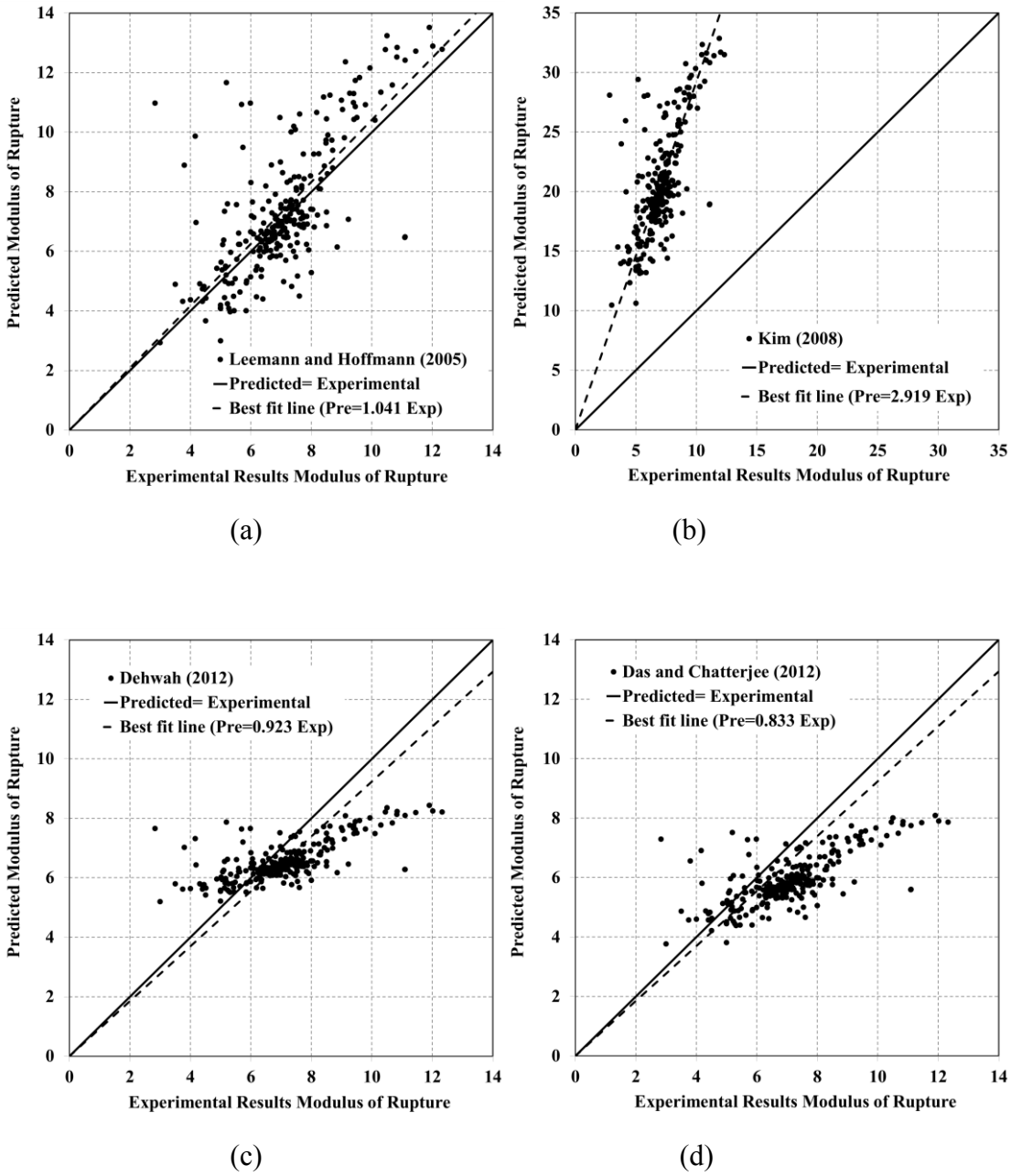

Figure 3.19 (a to d) Comparison of MOR for SCC experimental results versus calculated values for various SCC prediction models

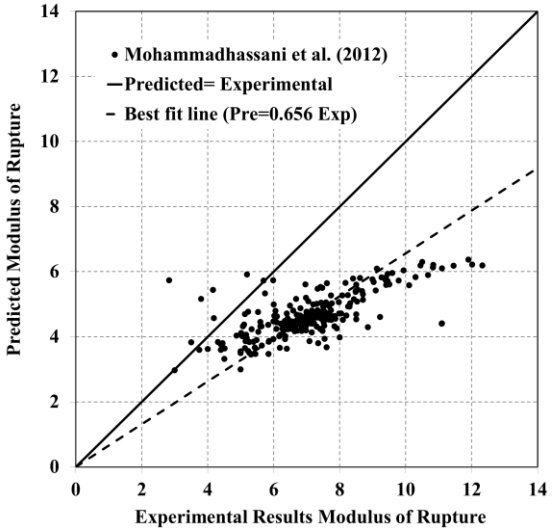

(e)

Figure 3.19(e) Comparison of MOR for SCC experimental results versus calculated values for various SCC prediction models

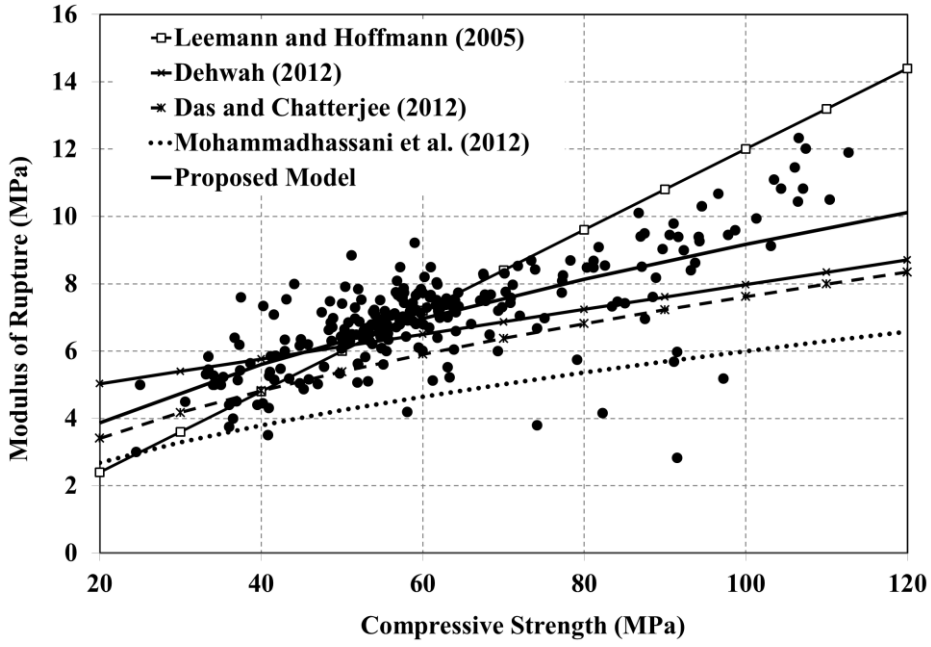

Figure 3.20 Comparison of MOR for SCC experimental results versus calculated values for various SCC prediction models and proposed model

3.5 COMPRESSIVE STRESS-STRAIN CURVE (CSSC)

Rational analysis and design of reinforced concrete structures are based on the realistic prediction of concrete stress-strain models. The highly non-linear behaviour of concrete in its post-elastic state, particularly after peak stress, makes the stress–strain model more sensitive. This is the main reason that most models that have been developed so far, are suited to their own test results and require specific computations to determine their essential parameters and hence cannot represent the stress-strain behaviour of concrete that has different characteristics and is prepared under different conditions. Consideration of the individual effects of these parameters on the shape of the stress-strain curve appears to be inadequate. The descending portion of the stress-strain curve is a key element in the non-linear analysis and design of reinforced concrete members under compressive load (Tasnimi, 2004). This is significant when increased strength and ductility are required to resist seismic load. The stress-strain curve of concrete under monotonic load could be considered the envelope of the cyclic behaviour of concrete (Karsan and Jirsa, 1969; Sakai and Kawashima, 2000; Barros et al., 2000). Consequently, a comprehensive mathematical model to represent the inclusive stress-strain curve is required for a rational design.

3.5.1 Experimental and Analytical Database for CSSC

Tables 3.17 and 3.19 are a general summary of the compressive stress-strain curves (CSSCs) of the concrete mixtures included in the database. Tables 3.17 and 3.18 also include information regarding the curing age, type of curing, type of the cement, type of the filler, and type of fine aggregate (FA) and coarse aggregate (CA). Dominant properties of the available mixes in the database are that the curing age is 28 days, type of curing is moist, type of cement is ordinary Portland cement, types of filler are fly ash and limestone, and type of aggregate for FA is natural sand and for CA is natural river gravel, crushed granite and limestone. Table 3.19 includes information regarding the compressive strength of concrete at different ages of SCC and CC for different mixtures of concrete. In the literature, several analytical and numerical models try to represent the compressive stress-strain curve for both SCC and CC mixtures. Tables 3.20 and 3.21 show various compressive stress-strain models for calculating the compressive stress-strain curve of SCC and CC, respectively. These models vary in complexity and precision in the calculations. In

a recent section that evaluated and compared the compressive stress-strain models of SCC and CC (Tables 3.17, 3.18, and 3.20) by Nejadi and Aslani (2011), the following conclusion is drawn: Collins and Mitchell (1991) and Mazars and Pijaudier-Cabot (1989) models provide a better prediction of CC and SCC compressive stress-strain data than other models.

3.5.2 Comparison of Proposed CSSC Model with Available CSSC Models

In a recent section that evaluated and compared the compressive stress-strain models of SCC and CC (Tables 3.17 to 3.20) by Nejadi and Aslani (2011), the following conclusion is drawn: Collins and Mitchell (1991) and Mazars and Pijaudier-Cabot (1989) models provide a better prediction of CC and SCC compressive stress-strain data than other models. Nevertheless, the Mazars and Pijaudier-Cabot (1989) model cannot model maximum compressive strength of concrete accurately. In the present section, the shape suggested by Carreira and Chu (1985) was introduced as the basic model equation. Because the equation is simple, the shape of the stress-strain curve is well represented, and it has good correlation with the experimental results of other researchers (e.g., Hognestad et al., 1951 and Kaar et al., 1987). It can be concluded that the equation is a verified equation. Therefore, the suggested model equation is based on Carreira and Chu's model, as given by Equations (3.4 to 3.11). In this stress-strain model, MOE equation (3.1) for SCC and CC are used:

$$\frac{\sigma_c}{f_c^{'}} = \frac{n\left(\frac{\varepsilon_c}{\varepsilon_c^{'}}\right)}{n-1+\left(\frac{\varepsilon_c}{\varepsilon_c^{'}}\right)^n} \tag{3.4}$$

$$n = n_1 = \left[1.02 - 1.17\left(E_{sec} / E_c\right)\right]^{-0.74} \quad if\ \varepsilon_c \le \varepsilon_c^{'} \tag{3.5}$$

$$n = n_2 = n_1 + \left(\lambda + 28 \times \mu\right) \quad if\ \varepsilon_c \ge \varepsilon_c^{'} \tag{3.6}$$

$$\lambda = \left(135.16 - 0.1744 f_c^{'}\right)^{-0.46} \tag{3.7}$$

$$\mu = 0.83\, exp\left(-911 / f_c^{'}\right) \tag{3.8}$$

$$E_{sec} = f_c' / \varepsilon_c' \tag{3.9}$$

$$\varepsilon_c' = \left(\frac{f_c'}{E_c}\right)\left(\frac{\psi}{\psi - 1}\right) \tag{3.10}$$

$$\psi = \frac{f_c'}{17} + 0.8 \tag{3.11}$$

where σ_c is concrete stress, f'_c maximum compressive strength of concrete, n material parameter that depends on the shape of the stress-strain curve, ε concrete strain, ε'_c strain corresponding with the maximum stress f'_c, n_1 modified material parameter at the ascending branch, n_2 modified material parameter at the descending branch, E_c modulus of elasticity, E_{sec} secant modulus of elasticity, and λ, μ coefficients of linear equation.

In Figures 3.21 to 3.25, comparisons between Kim et al. (1998), Rols et al. (1999), Peter et al. (2006), Dhonde et al. (2007), Babu et al. (2008), Prasad et al. (2009), Luo and Chao (2009) and Kumar et al. (2011) compressive stress-strain curve experimental results and calculated stress-strain prediction models (Collins and Mitchell, 1991; CEB-FIP, 1990; Prasad et al., 2009; Kumar et al., 2011) are shown.

As shown in Table 3.22, the proposed compressive stress-strain model in this section provides a better prediction of compressive stress-strain data, with a coefficient of correlation factor (R^2) compared to CEB-FIP (1990), Collins and Mitchell (1991), Prasad et al. (2009), and Kumar et al. (2011) stress-strain models (Figures 3.21 to 3.25) for both SCC and CC mixtures. In the proposed compressive stress-strain model, MOE (E_c) equations for each type of aggregate, filler, and concrete type (SCC or CC) are applicable. Based on the CSSC experimental results database (Tables 3.17 to 3.19), the major filler is fly ash and the major aggregate is river gravel and crushed granite aggregate.

Therefore, the proposed MOE models of SCC with fly ash filler and river gravel and crushed granite aggregate should be replaced in the CSSC model. E_{sec} / E_c has been used by many researchers as the most influential factor in determining the stress-strain curve. In this section, it is also used as the most important factor. The compressive stress-strain relationship suggested in this section accurately predicts the ascending branch of the stress-

strain curve compared to the experimental database. It also predicts the descending branch within a minimum range of deviations with reasonable accuracy.

Table 3.17 CSSC experimental database

Reference	No. of SCC mixtures	No. of CC mixtures	Curing Age (days)	Type of cement
Kim et al. (1998)	5	3	3,7, 28 and 90	Portland cement
Rols et al. (1999)	2	0	28	Portland cement
Peter et al. (2006)	2	1	3,14 and 28	Portland cement
Dhonde et al. (2007)	2	0	1,3, 7 and 28	Portland cement
Babu et al. (2008)	5	0	28	Portland cement
Prasad et al. (2009)	2	0	28	Portland cement
Luo and Chao (2009)	7	0	3,7, 14 and 28	Portland cement
Kumar et al. (2011)	3	0	28	Portland cement
Total of 32 mixtures	28	4		

Table 3.18 CSSC experimental database (continued)

Reference	Type of filler	Type of Aggregate	
		FA	CA
Kim et al. (1998)	Fly ash	Sea sand	Crushed stone
Rols et al. (1999)	Limestone	River sand with larger than 5 mm	River gravel with larger than 16 mm
Peter et al. (2006)	Flay Ash, Silica Fume, GGBS, Metakaoline and Limestone	River sand	Crushed granite with maximum size of 12.5 mm
Dhonde et al. (2007)	Fly ash	Well-graded, river-bed sand	Well-graded, rounded, river-bed with 19 mm nominal size
Babu et al. (2008)	Fly ash, GGBS and Rice husk ash	Natural river sand	Crushed granite angular aggregate of size 12.5 mm passing
Prasad et al. (2009)	Fly ash	Standard river sand	Crushed granite
Luo and Chao (2009)	Fly ash	Natural river sand	Crushed granite with maximum size of 20 mm
Kumar et al. (2011)	Fly ash and Silica fume	Natural river sand	Crushed granite

Table 3.19 CSSC experimental database (continued)

Reference	Compressive Strength (MPa)					
Kim et al. (1998)	Mix.	3 Days		7 Days	28 Days	90 Days
	SCC1	20.0		33.0	47.0	53.0
	SCC2	19.0		32.0	47.0	54.0
	SCC3	16.0		31.0	46.0	53.0
	SCC4	11.0		26.0	37.0	44.0
	CC	18.0		30.0	42.0	43.0
Rols et al. (1999)	Mix.	1 Day		7 Days	28 Days	90 Days
	SCC1	18.1		36.1	42.8	43.0
	SCC2	17.2		37.6	44.1	44.5
Peter et al. (2006)	Mix.	3 Days		14 Days	28 Days	
	SCC	25.0		51.0	57.0	
Dhonde et al. (2007)	Mix.	1 Day		3 Days	7 Days	28 Days
	SCC	24.9		30.2	37.7	51.4
Babu et al. (2008)	Mix.	SCC1	SCC2	SCC3	SCC4	SCC5
	28 Days	26.5	33.3	35.8	30.8	33.3
Prasad et al. (2009)	Mix.	SCC1		SCC2		
	28 Days	31.6		52.9		
Luo and Chao (2009)	Mix.	3 Days		7 Days	14 Days	28 Days
	SCC1	24.0		37.4	44.1	52.9
	SCC2	22.5		37.3	43.8	50.3
	SCC3	19.1		34.2	40.6	46.1
	SCC4	18.7		32.6	37.3	43.0
	SCC5	17.1		31.1	37.0	41.8
	SCC6	17.8		26.9	36.6	40.0
	SCC7	16.0		25.8	34.6	38.9
Kumar et al. (2011)	Mix.	SCC1		SCC2	SCC3	
	28 Days	35.0		55.0	70.0	

Table 3.20 Compressive stress-strain models for CC

Reference	Models
Hognestad (1951)	$\sigma_c = f_c^{'}\left[\frac{2\varepsilon_c}{\varepsilon_c^{'}} - \left(\frac{\varepsilon_c}{\varepsilon_c^{'}}\right)^2\right] \qquad \varepsilon_c \le \varepsilon_c^{'};$ $\sigma_c = f_c^{'}\left[1 - 0.15\left(\frac{\varepsilon_c - \varepsilon_c^{'}}{\varepsilon_u - \varepsilon_c^{'}}\right)\right] \qquad \varepsilon_c^{'} \le \varepsilon_c \le \varepsilon_u$
Smith and Young (1955)	$\sigma_c = E_c \varepsilon \, \varepsilon^{(1-\frac{\varepsilon}{\varepsilon_c^{'}})}$
Desayi and Krishnan (1964)	$\sigma_c = \frac{E_c \varepsilon}{1 + \left(\frac{\varepsilon}{\varepsilon_c^{'}}\right)^2}$
Saenz (1964)	$\sigma_c = \frac{E_c \varepsilon}{1 + \left(\frac{E_c}{E_p} - 2\right)\left(\frac{\varepsilon}{\varepsilon_c^{'}}\right) + \left(\frac{\varepsilon}{\varepsilon_c^{'}}\right)^2}; E_p = \frac{f_c^{'}}{\varepsilon_c^{'}}$
CEB-FIP (1990)	$0 \le \varepsilon \le \varepsilon_{\max}: \quad f_c = f_c'\left[\frac{\left(\frac{E_{it}}{E_o}\right)\left(\frac{\varepsilon}{\varepsilon_o}\right) - \left(\frac{\varepsilon}{\varepsilon_o}\right)^2}{1 + \left(\frac{E_{it}}{E_o} - 2\right)\left(\frac{\varepsilon}{\varepsilon_o}\right)}\right];$ $\varepsilon_{\max} = \varepsilon_o\left[\frac{1}{2}\left(\frac{1}{2}\frac{E_{it}}{E_o} + 1\right) + \sqrt{\frac{1}{2}\left(\frac{1}{2}\frac{E_{it}}{E_o} + 1\right)^2 - \frac{1}{2}}\right]$ $\varepsilon > \varepsilon_{\max}: f_c = \frac{f_c'}{\left[\frac{1}{(\varepsilon_{\max}/\varepsilon_o)}\zeta - \frac{2}{(\varepsilon_{\max}/\varepsilon_o)^2}\right]\left(\frac{\varepsilon}{\varepsilon_o}\right)^2 + \left[\frac{4}{(\varepsilon_{\max}/\varepsilon_o)} - \zeta\right]\frac{\varepsilon}{\varepsilon_o}};$ $E_{it} = 21500\left(f_c'/10\right)^{(1/3)}$ $\zeta = \frac{4\left[\left(\frac{\varepsilon_{\max}}{\varepsilon_o}\right)^2\left(\frac{E_{it}}{E_o} - 2\right) + 2\left(\frac{\varepsilon_{\max}}{\varepsilon_o}\right) - \frac{E_{it}}{E_o}\right]}{\left[\left(\frac{\varepsilon_{\max}}{\varepsilon_o}\right)\left(\frac{E_{it}}{E_o} - 2\right) + 1\right]^2};$ $E_o = f_c'/0.0022; \; \varepsilon_o = 0.0022$

Table 3.20 Compressive stress-strain models for CC (continued)

Reference	Models
Mazars and Pijaudier-Cabot (1989)	$\left\{\begin{array}{ll}\sigma = \varepsilon E_c & \varepsilon \le \varepsilon_0 \\ \sigma = \left[\varepsilon_0(1-A) + A\varepsilon e^{\left(\frac{\varepsilon 0-\varepsilon}{\varepsilon_c'}\right)}\right]E_c & \varepsilon > \varepsilon_0\end{array}\right\}$ $A = \frac{f_c' - \varepsilon_0 E_c}{E_c\left(\varepsilon_c' e^{\frac{\varepsilon_0}{\varepsilon_c'}-1} - \varepsilon_0\right)}$
Collins and Mitchell (1991)	$\frac{\sigma_c}{f_c'} = \frac{n}{n-1+\left(\frac{\varepsilon_c}{\varepsilon_c'}\right)^{nk}}\left(\frac{\varepsilon_c}{\varepsilon_c'}\right);$ $if \quad \varepsilon_c/\varepsilon_c' < 1 \quad k = 1 \quad ;$ $if \quad \varepsilon_c/\varepsilon_c' > 1 \quad k = 0.67 + \frac{f_c'}{62}\ Mpa$ $n = 0.8 + \frac{f_c'}{17}, \varepsilon_c' = \frac{f_c'}{E_c}\frac{n}{n-1},$ $E_c = 3320\sqrt{f_c'} + 6900$

Table 3.21 Compressive stress-strain models for SCC

Reference	Models
Prasad et al. (2009)	$Ascending\ portion: f_c = f_c' \frac{2.8662(\varepsilon/\varepsilon_0)}{1+0.8662(\varepsilon/\varepsilon_0)+(\varepsilon/\varepsilon_0)^2}$ $Descending\ portion: f_c = f_c' \frac{1.206(\varepsilon/\varepsilon_0)}{1-0.794(\varepsilon/\varepsilon_0)+(\varepsilon/\varepsilon_0)^2}$
Kumar et al. (2011)	$f_c = f_c'\left[\frac{\alpha(\varepsilon/\varepsilon_0)+(k\beta-1)(\varepsilon/\varepsilon_0)^2}{1+(\alpha-2)(\varepsilon/\varepsilon_0)+k\beta(\varepsilon/\varepsilon_0)^2}\right];$ $\beta = \frac{(\varepsilon_{80}/\varepsilon_0)^2 - (0.2\alpha+1.6)(\varepsilon_{80}/\varepsilon_0)}{0.2(\varepsilon_{80}/\varepsilon_0)^2}$ $\alpha = E_{it}\ \varepsilon_0/f_c';\ k = 1.85 - 0.025 f_c';$ $\varepsilon_0 = (0.0006)\left(f_c'\right)^{0.33};\ E_c = 5300\left(f_c'\right)^{0.46};$ $\varepsilon_{80} = (0.0015)\left(f_c'\right)^{0.16}$

Table 3.22 Coefficient of correlation factor (R^2) for compressive stress-strain models

Coefficient of correlation factor (R^2)						
Reference	Mix	CEB-FIP (1990)	Collins and Mitchell (1991)	Prasad et al. (2009)	Kumar et al. (2011)	Proposed Model
Kim et al. (1998)	CC	0.73	0.92	0.80	0.72	0.93
	SCC1	0.95	0.71	0.85	0.82	0.96
	SCC2	0.90	0.88	0.84	0.85	0.97
	SCC3	0.94	0.89	0.84	0.87	0.97
	SCC4	0.69	0.81	0.84	0.77	0.96
Rols et al. (1999)	SCC1	0.95	0.95	0.95	0.95	0.98
Peter et al. (2006)	SCC1	0.79	0.75	0.86	0.56	0.87
Dhonde et al. (2007)	SCC1	0.80	0.86	0.73	0.75	0.96
Babu et al. (2008)	SCC1	0.82	0.88	0.87	0.73	0.97
	SCC2	0.83	0.90	0.88	0.75	0.95
	SCC3	0.88	0.91	0.89	0.74	0.96
	SCC4	0.83	0.92	0.86	0.74	0.94
	SCC5	0.84	0.92	0.85	0.73	0.95
Prasad et al. (2009)	SCC1	0.76	0.90	0.92	0.63	0.91
	SCC2	0.74	0.89	0.93	0.64	0.92
Luo and Chao (2009)	SCC1	0.58	0.79	0.57	0.30	0.95
	SCC2	0.56	0.76	0.61	0.41	0.96
	SCC3	0.51	0.69	0.63	0.40	0.95
	SCC4	0.51	0.92	0.89	0.41	0.94
	SCC5	0.62	0.75	0.77	0.43	0.99
Kumar et al. (2011)	SCC1	0.70	0.87	0.63	0.95	0.92
	SCC2	0.88	0.86	0.67	0.96	0.91
	SCC3	0.63	0.88	0.66	0.95	0.91

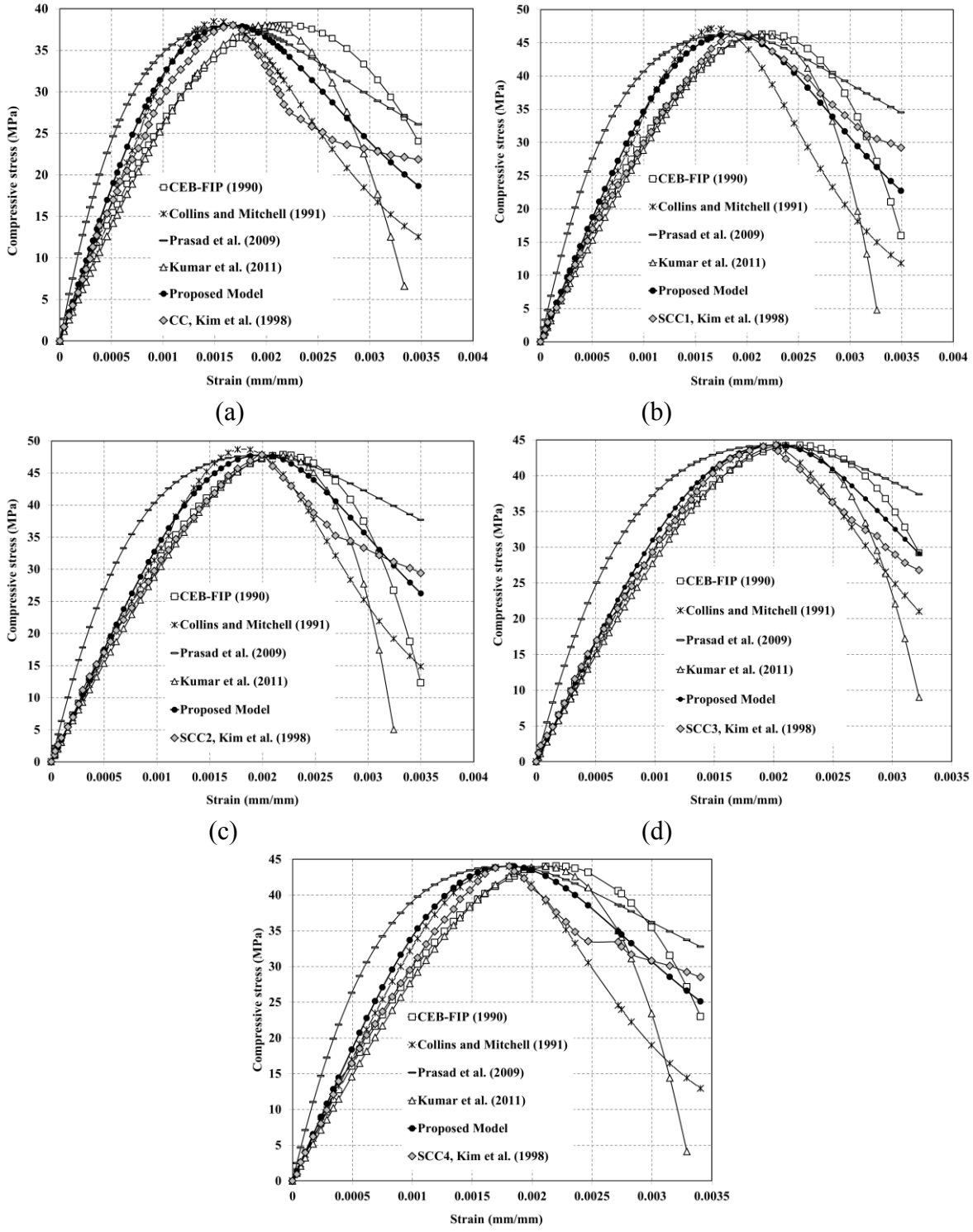

Figure 3.21 Comparison between Kim et al. (1998) experimental test with compressive stress-strain models

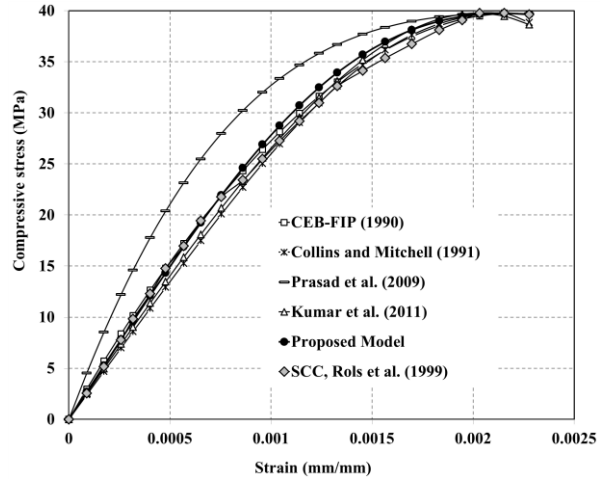

(a)

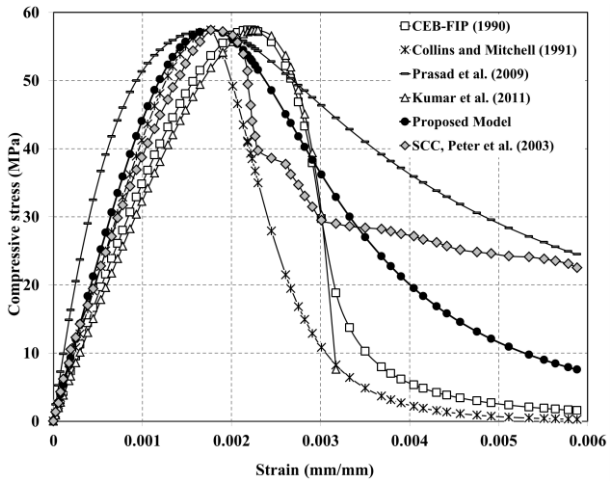

(b)

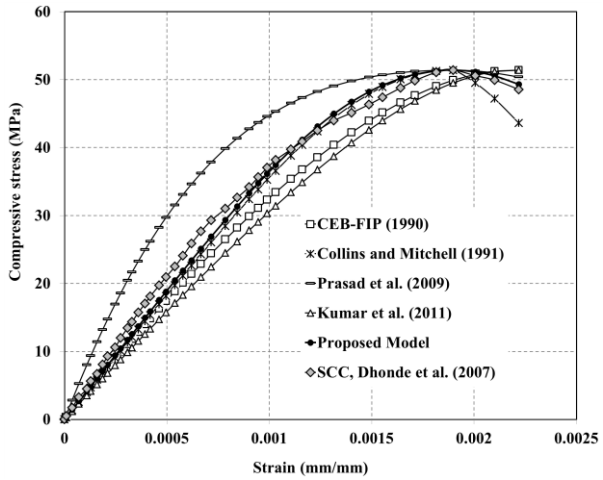

(c)

Figure 3.22 Comparison between Rols et al. (1999), Peter et al. (2006), and Dhonde et al. (2007) experimental test with compressive stress-strain models

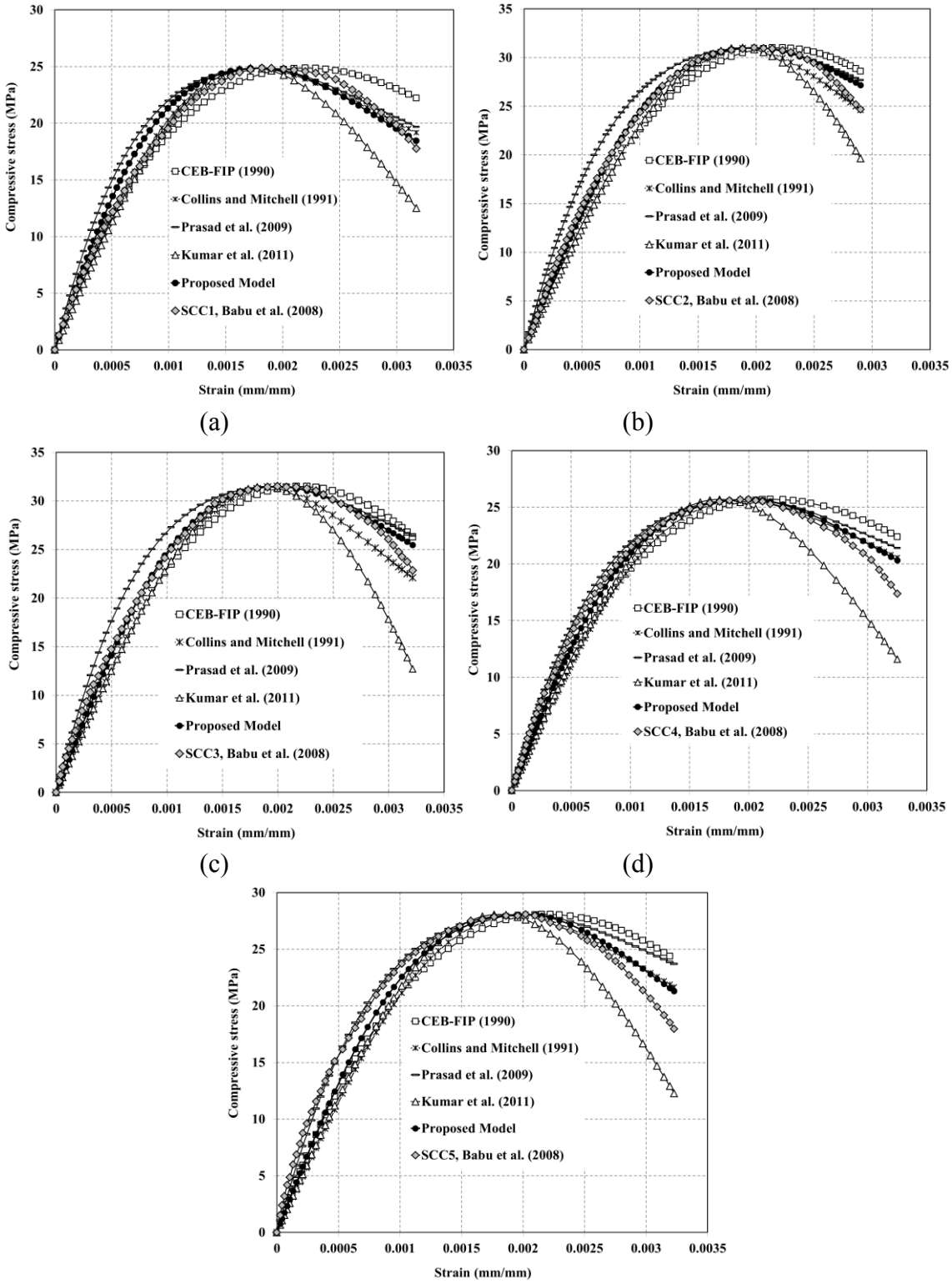

Figure 3.23 Comparison between Babu et al. (2008) experimental test with compressive stress-strain models

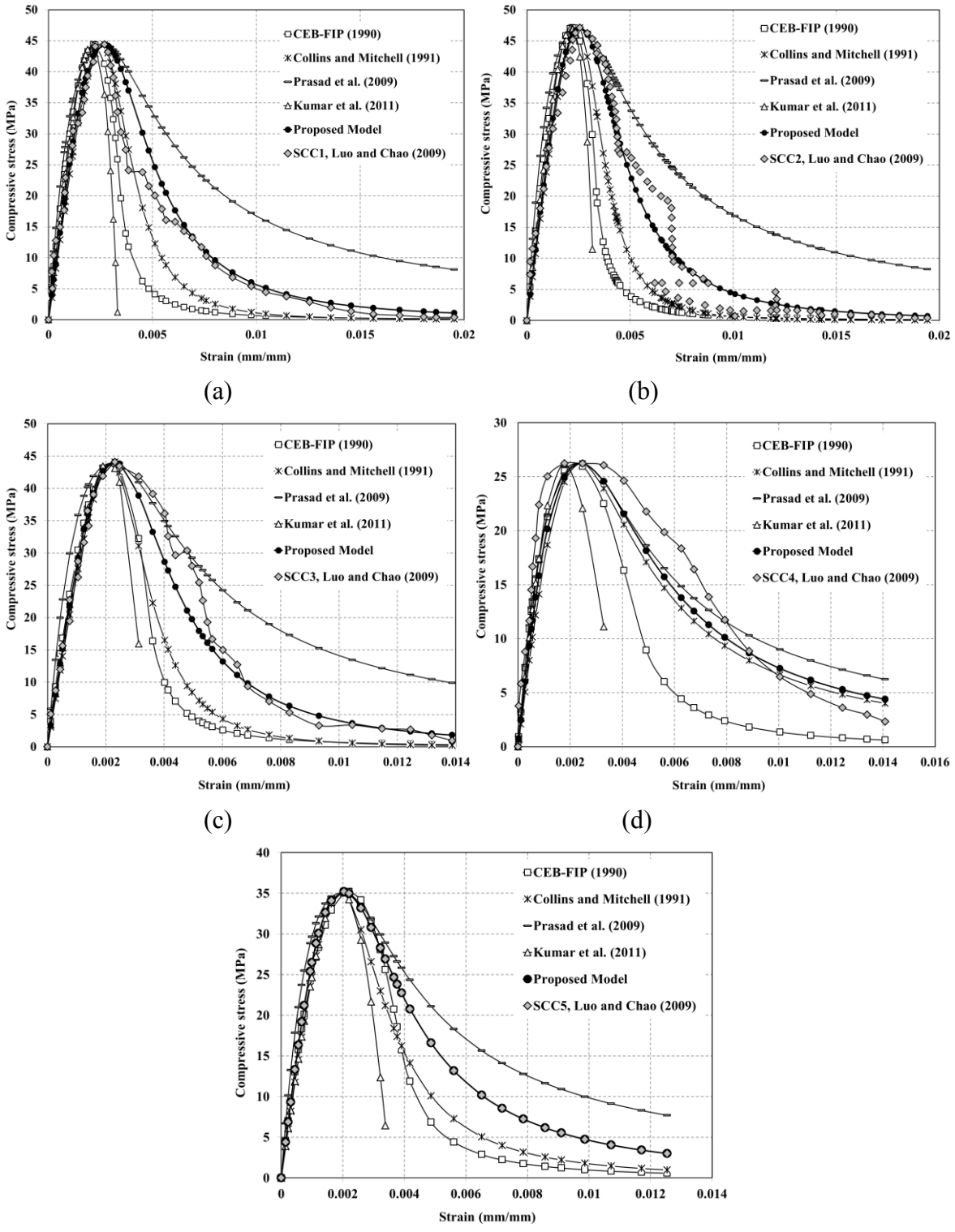

Figure 3.24 Comparison between Luo and Chao (2009) experimental test with compressive stress-strain models

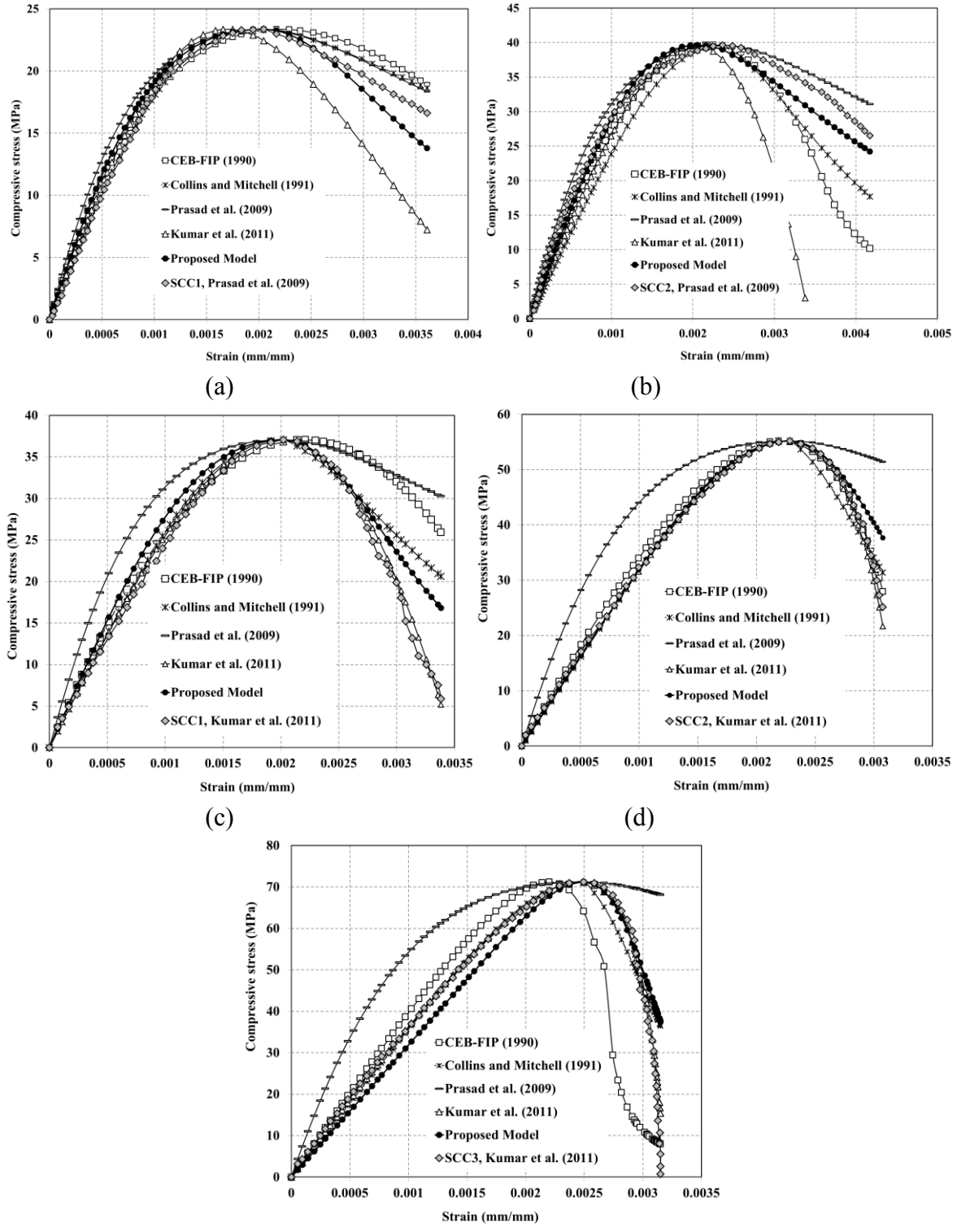

Figure 3.25 Comparison between Prasad et al. (2009) and Kumar et al. (2011) experimental test with compressive stress-strain models

3.6 BOND CHARACTERISTICS OF REINFORCING STEEL BARS EMBEDDED IN CC AND SCC

The objectives of this section are to: (a) develop a bond strength model based on the experimental results of the nine recent investigations on the SCC and CC that emphasize the influence of bar type, diameter of the steel bar, embedded length of the steel bar, concrete type, compressive strength of the concrete, and casting direction and (b) compare the proposed model, code provisions, and empirical equations via the experimental results of recent studies on the bond strength of SCC and CC. The comparison is based on the measured bond between reinforcing steel and concrete by utilizing the pullout test on the embedded bars at various heights in mock-up structural elements to assess the top-bar effect on single bars in small prismatic specimens and; conducting additional beam tests. For these purposes, the experimental results from the nine recent studies (i.e. Zhu et al., 2004; Castel et al., 2006; Almeida Filho et al., 2008; Hossain and Lachemi, 2008; Valcuende and Parra, 2009; Lachemi et al. , 2009; Hassan et al., 2010; and Desnerck et al., 2010) on the bond strength of SCC and CC are investigated and compared.

3.6.1 Experimental and Analytical Database for Bond Characteristics

An experimental results database from various published investigations is an effective tool for studying the applicability of the various bond estimation models for SCC. To apply the models to a particular concrete mixture accurately, it is necessary to use only investigations that are sufficiently consistent with the applied testing methodology. The SCC experimental results included in the database were gathered mainly from papers presented at various conferences and published articles. The database includes information regarding the composition of the mixtures, fresh properties of SCC, testing methodology, and conditions. Bond characteristics have not been investigated as much as the other aspects of SCC.

Tables 3.23 and 3.24 include general information about the concrete experimental tests, such as type of specimens and test, types of bar (BT; plain (P) and deformed (D)), diameter of the steel bar (d_b), embedded length of the steel bar (l_d), compressive strength of the concrete (f'_c), type of specimen utilized in the compressive strength test (TS f'_c), and

casting direction (CD). The CD includes vertical up casting direction (V-U), vertical down casting direction (V-D), and horizontal casting direction (H). Various admixtures are used in the mix design of SCC including superplaticizers (SP), high-range water reduces (HRWR), water reducer (WR), viscosity-modifying admixture (VMA), fly ash (FA), slag cement (SC), ground granulated blast slag (GGBS), and air-entraining admixtures (AEA). As shown in Tables 3.23 and 3.24, various types of specimens and tests have been investigated in the literature including the pullout test on prism specimens and cylinder specimens and beam test specimens. Moreover, various types of d_b, l_d, f'_c and CD were used; however, the bar type was only considered in Castel et al. (2006). From the experimental results database (Tables 3.23 and 3.24), the following conclusions can be made: (a) The ultimate and mean bond strengths are greater in SCC than in CC; (b) For the top cast bars, the local bond strength for SCC is less than that for CC, and (c) The bond strength of SCC is almost the same as that of CC when large bar diameters are used. In the literature, there are several analytical and numerical models that attempt to represent the bond stress response in the steel-concrete interface. Most of these models are based on results of experiments that investigated the concrete compressive strength, concrete cover (C), steel bar diameter, and embedment length. In them, researchers provided equations to calculate the average bond strength via linear or non-linear regressions. Table 3.26 shows some of the empirical equations (Orangun et al., 1977; Kemp and Wilhelm, 1979; Eligehausen, 1983; Kemp, 1986; Chapman and Shah, 1987; Harajli, 1994; Huang et al., 1996; Esfahani and Rangan, 1998; Pillai et al., 1999; Bae, 2006; CEB-FIP, 1990; 2010; Desnerck, 2011) that represent the bond behaviour without transverse reinforcement. The influence of the transverse reinforcement is typically added to the bond strength without reinforcement.

3.6.2 Comparison of Proposed Bond Model with Available Bond Models

Many researchers have examined relationships between pull-out load and compressive strength. All studies in this area have shown that the bond strength (stress) increases with the increased compressive strength of concrete. In this regard, ACI 318 (2008) proposes that the bond strength is linearly proportional to $(f'_c)^{0.5}$. It can be easily concluded from the earlier literature that the average bond stress reduces as the embedment length increases

due to the nonlinear stress distribution that exists between the rebar and the concrete. Another conclusion is that average bond stress decreases with larger rebar diameters. Different explanations exist for the decrease in bond stress due to the larger rebar diameters. In this section, the relationships proposed for the CC and SCC are based on regression analyses using existing experimental data, with the results expressed as Eqs. (3.12 to 3.15). Eqs. (3.12 and 3.13) consider plain rebar bond strength for CC and SCC, respectively, whereas Eqs. (3.14 and 3.15) consider deformed rebar bond strength for CC and SCC, respectively. In these equations the influences of concrete cover, bar diameter, embedment length, and compressive strength (at the curing age) parameters are considered.

$$\tau_{max} = \left(0.7 \left(\frac{c}{d_b} \right)^{0.6} + 4 \left(\frac{d_b}{l_d} \right) \right) (f_c')^{0.23} \tag{3.12}$$

$$\tau_{max} = \left(0.7 \left(\frac{c}{d_b} \right)^{0.6} + 5 \left(\frac{d_b}{l_d} \right) \right) (f_c')^{0.23} \tag{3.13}$$

$$\tau_{max} = \left(0.679 \left(\frac{c}{d_b} \right)^{0.6} + 3.88 \left(\frac{d_b}{l_d} \right) \right) (f_c')^{0.55} \tag{3.14}$$

$$\tau_{max} = \left(0.672 \left(\frac{c}{d_b} \right)^{0.6} + 4.8 \left(\frac{d_b}{l_d} \right) \right) (f_c')^{0.55} \tag{3.15}$$

Proposed bond strength models are related to compressive strength. Further, because the compressive strength test types of specimens in the database are different, the f'_c values should be corrected. In this section, the most used type of compressive strength test in the database (i.e. 100 mm × 200 mm cylindrical) is considered as main and other types of test results (i.e., 150 mm × 300 mm cylindrical and 150 mm cube) must convert to it. Yi et al. (2006) reported that the relationship between 100 mm × 200 mm cylindrical with 150 mm cube was: $f'_{cy}(100 \times 200) = (f'_{cu}(150) - 8.86) / 0.85$. Also, Carrasquillo et al. (1981) stated that the average ratio of compressive strength of 150 mm × 300 mm to 100 mm × 200 mm cylinders was 0.9, regardless of strength and test age. Figure 3.26 shows the comparisons of the SCC and CC bond strength measured from the experimental results (Tables 3.23 and 3.24) versus the calculated values from empirical equations (Table 3.25). Figure 3.26(m) shows the comparison of the SCC and CC bond strengths measured from the experimental

results (Tables 3.23 and 3.24) versus the calculated values from the proposed models (Eqs. 3.12 to 3.15).

In the analysis of reinforced concrete structures, the bond action between steel bars and concrete is often viewed as a bond-slip relationship. This relationship expresses the local bond stress at any location along a bar as a function of the local slip. Numerous bond-slip relationships have been proposed and formulated. However, given that bond-slip relationships are impacted by various factors that vary across bond tests, these proposed models are different. For example, in pullout tests, bond-slip relationships obtained from extremely short specimens are different from those obtained from longer ones. Even in the same specimen, the bond-slip relationship varies with the location along the bar if the free end slip exists. Table 3.26 shows several bond stress-slip prediction models (Barbosa, 2001; CEB-FIP, 1990; 2010; Huang et al., 1996; Harajli et al., 1995) described in the literature. According to Table 3.27, three of these models are based on and similar to the main curve of bond stress-slip, although the influencing parameters are different.

In this section, the proposed bond-slip main curve is similar to the CEB-FIP (1990), Huang et al. (1996), and Harajli et al. (1995) models but the τ_{max} parameter for SCC and CC are different (see Table 3.27). Figures 3.27 to 3.32 illustrate the capability of proposed bond strength equations with a combination of bond stress-slip compared with the findings of Valcuende and Parra (2009) (with different compressive strength and water to cement ratio), Hassan et al. (2010) (with different bar pullout positions (top, middle, and bottom) and age of concrete), and Desnerck et al. (2010) (with different diameter of bar) for both of SCC and CC. As shown in Figure 1(a-m), available bond strength prediction models (Orangun et al., 1977; Kemp and Wilhelm, 1979; Eligehausen, 1983; Kemp, 1986; Chapman and Shah, 1987; Harajli, 1994; Huang et al., 1996; Esfahani and Rangan, 1998; Pillai et al., 1999; Bae, 2006; CEB-FIP, 1990; 2010; Desnerck, 2011) generally underestimate the bond strength for both SCC and CC mixtures when compared to experimental results. Although Chapman and Shah (1987) has a more accurate prediction equation (see Figure 1(e)), the model tends to underestimate the bond strength. The proposed models for bond strength are consistent with the experimental results for both SCC and CC, as shown in Figure 1(m).

As shown in Table 3.28 for CC, the proposed model provides a better prediction of bond strength data with a coefficient of correlation factor (R^2) of 0.80 compared to 0.37 in Kemp (1986), 0.37 in Eligehausen et al. (1983), 0.38 in Desnerck (2011), 0.38 in Kemp and Wilhelm (1979), 0.38 in Esfahani and Rangan (1998), 0.39 in Harajli (1994), 0.40 in Huang et al. (1996), 0.41 in Pillai et al. (1999), 0.44 in Chapman and Shah (1987), 0.53 in CEB-FIP (1990), and 0.60 in Bae (2006). Also, as shown in the Table 3.28 for SCC, the proposed model provides a better prediction of bond strength data with a coefficient of correlation factor (R^2) of 0.81 compared to 0.27 in Orangun et al. (1977), 0.29 in Harajli (1994), 0.30 in the Pillai et al. (1999), 0.35 for the Kemp and Wilhelm (1979), 0.35 for the Eligehausen et al. (1983), 0.38 in Esfahani and Rangan (1998), 0.38 in Kemp (1986), 0.38 in Huang et al. (1996), 0.38 in Desnerck (2011), 0.43 in Chapman and Shah (1987), 0.50 in CEB-FIP (1990), and 0.51 in Bae (2006).

Compared to the experimental results (SCC and CC) of Valcuende and Parra (2009) (with different types of maximum compressive strength at 28 days and water-to-cement ratio), the available bond stress-slip models (Barbosa, 2001, CEB-FIP, 1999, Huang et al., 1996, and Harajli et al., 1995) underestimate the bond strength, as shown in Figures 2.27 and 2.28. However, the predicted values of the proposed model are more consistent with Valcuende and Parra's (2009) bond stress-slip experimental results, although there are several different factors (compressive strength, water-to-cement ratio, and concrete (for both SCC and CC)).

According to Figure 3.29, compared to the experimental results of Hassan et al. (2010) ((CC, top, 28 days) and (CC, middle, 14 days)), Huang et al.'s (1996) and Harajli et al.'s (1995) models are consistent the experimental results. On the contrary, Barbosa's (2001) model overestimates the values, whereas CEB-FIP's (1999) model underestimates them. According to Figure 3.29, compared to the experimental results of Hassan et al. (2010) (SCC, top, 28 days), Huang et al.'s (1996) and Barbosa's (2001) models are consistent. In addition, CEB-FIP's (1999) and Harajli et al.'s (1995) models underestimate the bond strength. According to Figure 3.29, in comparison with the experimental results of Hassan et al. (2010) ((SCC, middle, 14 days), (CC, bottom, 7 days) and (SCC, bottom, 7 days)), Barbosa's (2001) model has good agreement. Further, CEB-FIP's (1999), Huang et

al.'s (1996), and Harajli et al.'s (1995) models underestimate the values. However, the proposed model's prediction results for all of these conditions (with different bar pullout positions and age of concrete) are consistent with Hassan et al.'s (2010) bond stress-slip experimental results.

According to Figure 3.30, in comparison with experimental results (CC1, d_b = 25 mm), all of the models overestimate the bond strength. According to Figures 3.30 through 3.31, CEB-FIP's (1999) and Harajli et al.'s (1995) models have a good prediction, whereas Huang et al.'s (1996) and Barbosa's (2001) models overestimate the values in comparison to the experimental results of Desnerck et al. (2010) ((SCC1 and SCC2, d_b = 25 mm) and (CC1, SCC1, and SCC2, d_b = 40 mm)). The proposed relationship is consistent with Desnerck et al.'s (2010) test results, despite the different bar diameters (d_b = 12, 25, and 40 mm) and concrete types (CC1, SCC1, and SCC2).

There are several models to predict the ultimate bond strength, corresponding slip and equations in the literature to describe the bond stress-slip behaviour can be found mostly for conventional concrete with compressive strengths in the range of 20 MPa to 50 MPa. Comparisons between the available models and the experimental results database revealed a poor agreement. Therefore new proposals for bond strength and bond-slip curve are made. The proposed bond strength models in this section are covered bond strength predictions for the plain and deformed steel bars, the normal and high strength conventional and self-compacting concrete. Furthermore, the proposed bond-slip models are covered bond-slip behaviour predictions for the plain and deformed steel bars, the normal and high strength conventional and self-compacting concrete, and the confined and unconfined conventional and self-compacting concrete. Also, the proposed bond-slips models are shown to have good predictions for bond-slip experimental curves with different range of bar diameters, with different range of concrete age, with different steel bar pullout positions in the form works, with different types of maximum compressive strength at 28 days and with different water-to-cement ratios. This section presented proposed models based on the experimental results from eight recent investigations of SCC and CC. The proposed models have some limitations (e.g. more high strength SCC, confined SCC, and etc.) so additional tests are needed.

Table 3.23 SCC and CC bond experimental tests details

Reference	Mixture	Specimen type	BT
Zhu et al. (2004)	CC35	pull-out test of 100 x 100 x 150 (mm)	D
	CC60		D
	SCC35		D
	SCC60		D
Castel et al. (2006)	CC25	pull-out test of 100 x 100 x 500 (mm)	D and P
	CC40		D and P
	SCC25		D and P
	SCC40		D and P
Almeida Filho et al. (2008)	CC1	pull-out test of cylinder with 10 d_b diameter and height	D
	CC2		D
	SCC1		D
	SCC2		D
	CC1	beam specimen test	D
	CC2		D
	SCC1		D
	SCC2		D
Hossain and Lachemi, (2008)	CC	pull-out test of 900 x 200 x100 (mm)	D
	FA SCC		D
	SC SCC		D
	VMA SCC		D
Lachemi et al. (2009)	NG_NS	pull-out test of 200 x 200 x 100 (mm)	D
	BS_NS		D
	ES_NS		D
Valcuende and Parra (2009)	CC32-0.65	pull-out test of 200 mm cube	D
	CC32-0.55		D
	CC42-0.55		D
	CC42-0.45		D
	SCC 32-0.65		D
	SCC 32-0.55		D
	SCC 42-0.45		D
	CC32-0.65	square cross-section columns of 1500 x150 (mm)	D
	CC32-0.55		D
	CC42-0.55		D
	CC42-0.45		D
	SCC 32-0.65		D
	SCC 32-0.55		D
	SCC 42-0.55		D
	SCC 42-0.45		D
Hassan et al. (2010)	CC	pull-out test of 4000 x 1200 x 300 (mm)	D
	SCC		D
Desnerck et al. (2010)	CC1	beam specimen test type I	D
	SCC1		D
	SCC2		D
	CC1	beam specimen test type II	D
	SCC1		D
	SCC2		D
	CC1	beam specimen test type III	D
	SCC1		D
	SCC2		D

Table 3.24 SCC and CC bond experimental tests details (continued)

Reference	d_b(mm)	l_d (mm)	$f_c^{'}$ (MPa)	(TS $f_c^{'}$)	CD
Zhu et al. (2004)	12 and 20	120	37.00	150 mm cube	V-U
	12 and 20	120	61.50		V-U
	12 and 20	120	47.00		V-U
	12 and 20	120	79.50		V-U
Castel et al. (2006)	12	60	34.40	110 mm × 220 mm cylindrical	V-U, V-D, H
	12	60	48.80		V-U, V-D, H
	12	60	30.00		V-U, V-D, H
	12	60	43.70		V-U, V-D, H
Almeida Filho et al. (2008)	10 and 16	5 and 8	35.80	100 mm × 200 mm cylindrical	V-U
	10 and 16	5 and 8	62.25		V-U
	10 and 16	5 and 8	38.00		V-U
	10 and 16	5 and 8	70.76		V-U
	10 and 16	10 d_b	35.80		H
	10 and 16	10 d_b	62.25		H
	10 and 16	10 d_b	38.00		H
	10 and 16	10 d_b	70.76		H
Hossain and Lachemi, (2008)	25	100	53.00	100 mm × 200 mm cylindrical	V-U, H
	25	100	62.00		V-U, H
	25	100	39.00		V-U, H
	25	100	47.00		V-U, H
Lachemi et al. (2009)	15	100 and 200	38.80	100 mm × 200 mm cylindrical	V-U
	15	100 and 200	43.20		V-U
	15	100 and 200	43.60		V-U
Valcuende and Parra (2009)	16	80	27.75	150 mm × 300 mm cylindrical	V-U
	16	80	33.76		V-U
	16	80	42.40		V-U
	16	80	56.50		V-U
	16	80	30.21		V-U
	16	80	35.77		V-U
	16	80	61.15		V-U
	12	60	27.75		H
	12	60	33.76		H
	12	60	42.40		H
	12	60	56.50		H
	12	60	30.21		H
	12	60	35.77		H
	12	60	50.18		H
	12	60	61.15		H

Table 3.24 SCC and CC bond experimental tests details (continued)

Reference	d_b(mm)	l_d (mm)	f_c' (MPa)	(TS f'_c)	CD
Hassan et al. (2010)	20	150	47.00	100 mm × 200 mm cylindrical	H
	20	150	45.00		H
Desnerck et al. (2010)	12	60	51.80	150 mm × 300 mm cylindrical and 150 mm cube	H
	12	60	63.70		H
	12	60	57.50		H
	20 and 25	5 d_b	51.80		H
	20 and 25	5 d_b	63.70		H
	20 and 25	5 d_b	57.50		H
	32 and 40	5 d_b	51.80		H
	32 and 40	5 d_b	63.70		H
	32 and 40	5 db	57.50		H

Table 3.25 Analytical bond models

Reference	Bond strength equation	Units
Orangun et al. (1977)	$\tau_{max} = \left[1.22 + 3.23\frac{c}{d_b} + 53\frac{d_b}{l_d}\right]\sqrt{f'_c}$	Psi units
Kemp and Wilhelm (1979)	$\tau_{max} = \left[0.55 + 0.24\frac{c}{d_b}\right]\sqrt{f'_c} + 0.191\frac{A_t\, f_{yt}}{s\, d_b}$	SI units
Eligehausen et al. (1983)	$\tau_{max} = 0.75\sqrt{\frac{c}{d_b}}\sqrt{f'_c}$	SI units
Kemp (1986)	$\tau_{max} = 232.2 + 2.716\frac{c}{d_b}\sqrt{f'_c}$	Psi units
Chapman and Shah (1987)	$\tau_{max} = \left[3.5 + 3.4\left(\frac{c}{d_b}\right) + 57\left(\frac{d_b}{l_d}\right)\right]\sqrt{f'_c}$	Psi units
Harajli (1994)	$\tau_{max} = \left[1.2 + 3\left(\frac{c}{d_b}\right) + 50\left(\frac{d_b}{l_d}\right)\right]\sqrt{f'_c}$	Psi units
Huang et al. (1996)	$\tau_{max} = 0.45 f'_c$	SI units
Esfahani and Rangan (1998)	NSC: $\tau_{max} = 2.695\frac{\frac{c}{d_b} + 0.5}{\frac{c}{d_b} + 3.6}\sqrt{f'_c}$	SI units
	HSC: $\tau_{max} = 4.73\frac{\frac{c}{d_b} + 0.5}{\frac{c}{d_b} + 5.5}\sqrt{f'_c}$	
Pillai et al. (1999)	$\tau_{max} = \left[0.1 + 0.25\frac{c}{d_b} + 4.2\frac{d_b}{l_d} + 0.024\frac{A_{tr}\, f_{yt}}{s\, d_b}\right]\sqrt{f'_c}$	SI units

Table 3.25 Analytical bond models (continued)

<table>
<tr><th>Reference</th><th>Bond strength equation</th><th>Units</th></tr>
<tr><td>Bae (2006)</td><td>$$\tau_{max} = A\left(\frac{c}{d_b}\right)^{B} \times (f_c')^{\alpha},$$
$$\alpha = \begin{Bmatrix} 0.58 & Deformed\,Rebar \\ 0.21 & Plain\,Rebar \\ 0.45 & GFRP\,Rebar \end{Bmatrix},$$
<table><tr><th></th><th colspan="3">LWSCC</th><th>NWSCC</th></tr><tr><th>Constant</th><th>Deformed</th><th>GFRP</th><th>Plain</th><th>Deformed</th></tr><tr><td>A</td><td>0.85</td><td>0.48</td><td>0.3</td><td>0.74</td></tr><tr><td>B</td><td>0.17</td><td>0.68</td><td>0.88</td><td>0.52</td></tr></table>embedment length $<15d_b$ in mm</td><td>SI units</td></tr>
<tr><td>CEB-FIP (1990)</td><td>$$\tau_{max} = \begin{Bmatrix} 2.5\sqrt{f_c'} & \text{Confined} \\ 2.0\sqrt{f_c'} & \text{Unconfined} \end{Bmatrix}$$</td><td>SI units</td></tr>
<tr><td>Desnerck (2011)</td><td>$$\tau_{max} = \begin{Bmatrix} \left(1.762 + 0.514\frac{c}{d_b}\right)\sqrt{f_c'} & \text{SCC} \\ \left(1.940 + 0.291\frac{c}{d_b}\right)\sqrt{f_c'} & \text{CC} \end{Bmatrix}$$</td><td>SI units</td></tr>
</table>

Table 3.26 Analytical bond stress-slip models

Reference	Bond stress-slip equation	Units
Barbosa (2001)	$\tau = 19.36\, s^{0.51} \left(f_c' < 50 MPa\right)$ $\tau = 32.58\, s^{0.48} \left(f_c' \geq 50 MPa\right)$	SI units
CEB-FIP (1990), Huang et al. (1996) and Harajli et al. (1995)	$\tau = \begin{cases} \tau_{\max} \left(s / s_1\right)^{\alpha} & 0 \leq s \leq s_1 \\ \tau_{\max} & s_1 < s \leq s_2 \\ \tau_{\max} - \left(\tau_{\max} - \tau_u\right)\left(s - s_2 / s_3 - s_2\right) & s_2 < s \leq s_3 \\ \tau_u & s_3 < s \end{cases}$	SI units

CEB-FIP (1990)	Confined concrete	Unconfined concrete
s_1 (mm)	1.0	0.6
s_2 (mm)	3.0	0.6
s_3 (mm)	Distance between ribs	1.0
α	0.4	0.4
$\tau_{\max}$	2.5 $\sqrt{f_c'}$	2.0 $\sqrt{f_c'}$
τ_u	0.4 $\tau_{\max}$	0.15 $\tau_{\max}$
Huang et al. (1996)	High strength concrete	Normal strength concrete
s_1 (mm)	0.5	1
s_2 (mm)	1.5	3
s_3 (mm)	Distance between ribs	Distance between ribs
α	0.3	0.4
$\tau_{\max}$	0.4 f_{cm}	0.4 f_{cm}
τ_u	0.4 $\tau_{\max}$	0.4 $\tau_{\max}$
Harajli et al. (1995)	Concrete	-
s_1 (mm)	0.15 Distance between ribs	-
s_2 (mm)	0.35 Distance between ribs	-
s_3 (mm)	Distance between ribs	-
α	0.3	-
$\tau_{\max}$	2.57 $\sqrt{f_c'}$	-
τ_u	0.9 $\sqrt{f_c'}$	-

Table 3.27 Proposed parameters that included in bond stress-slip model

	High strength concrete	Normal strength concrete	Confined concrete	Unconfined concrete
s_1 (mm)	0.5	1.0	1.0	0.6
s_2 (mm)	1.5	3.0	3.0	0.6
s_3 (mm)	Distance between ribs	Distance between ribs	Distance between ribs	1.0
α	0.3	0.4	0.4	0.4
τ_{max} for CC with plain rebar	Eq. (2.12)			
τ_{max} for SCC with plain rebar	Eq. (2.13)			
τ_{max} for CC with deformed rebar	Eq. (2.14)			
τ_{max} for SCC with deformed rebar	Eq. (2.15)			
τ_u	0.4 τ_{max}	0.4 τ_{max}	0.4 τ_{max}	0.15 τ_{max}

Table 3.28 Coefficient of correlation factor (R^2) bond prediction models for CC and SCC

Reference	CC		SCC	
	Predicted/Experimental bond results	R^2	Predicted/Experimental bond results	R^2
Orangun et al. (1977)	0.75	0.40	0.71	0.27
Kemp and Wilhelm (1979)	0.56	0.38	0.53	0.35
Eligehausen et al. (1983)	0.56	0.37	0.52	0.36
Kemp (1986)	0.41	0.37	0.38	0.38
Chapman and Shah (1987)	0.87	0.44	0.83	0.43
Harajli (1994)	0.70	0.39	0.66	0.29
Huang et al. (1996)	1.25	0.44	1.30	0.46
Esfahani and Rangan (1998)	0.66	0.42	0.66	0.36
Pillai et al. (1999)	0.70	0.41	0.66	0.30
Bae (2006)	0.73	0.60	0.78	0.51
CEB-FIP (1990)	0.80	0.64	0.78	0.60
Desnerck (2011)	1.35	0.38	1.27	0.39
Proposed Model	1.00	0.88	1.07	0.86

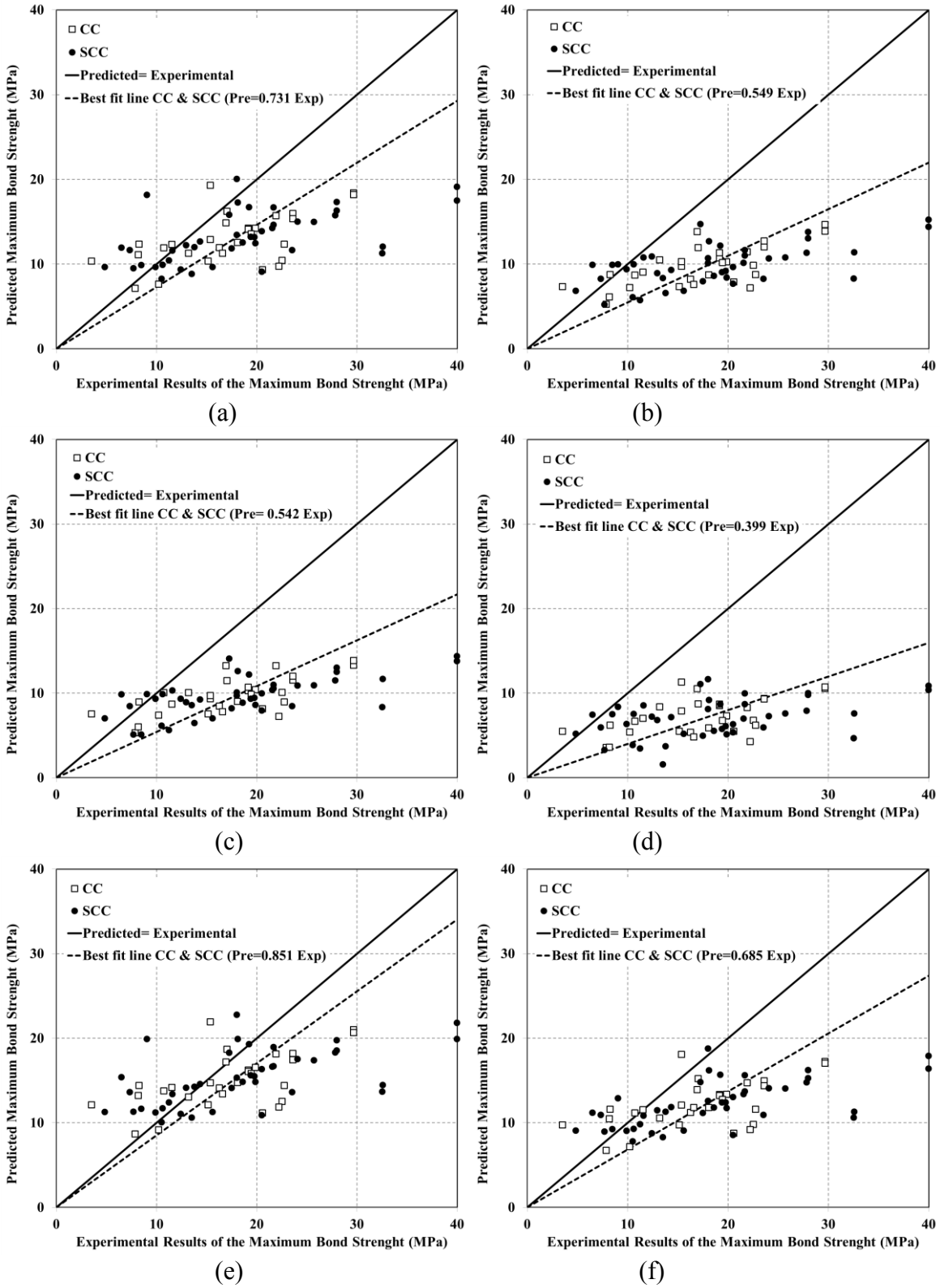

Figure 3.26 (a to f) Comparison of the experimental results versus calculated values from following models (a) Orangun et al. (1977), (b) Kemp and Wilhelm (1979), (c) Eligehausen (1983), (d) Kemp (1986), (e) Chapman and Shah (1987), (f) Harajli (1994)

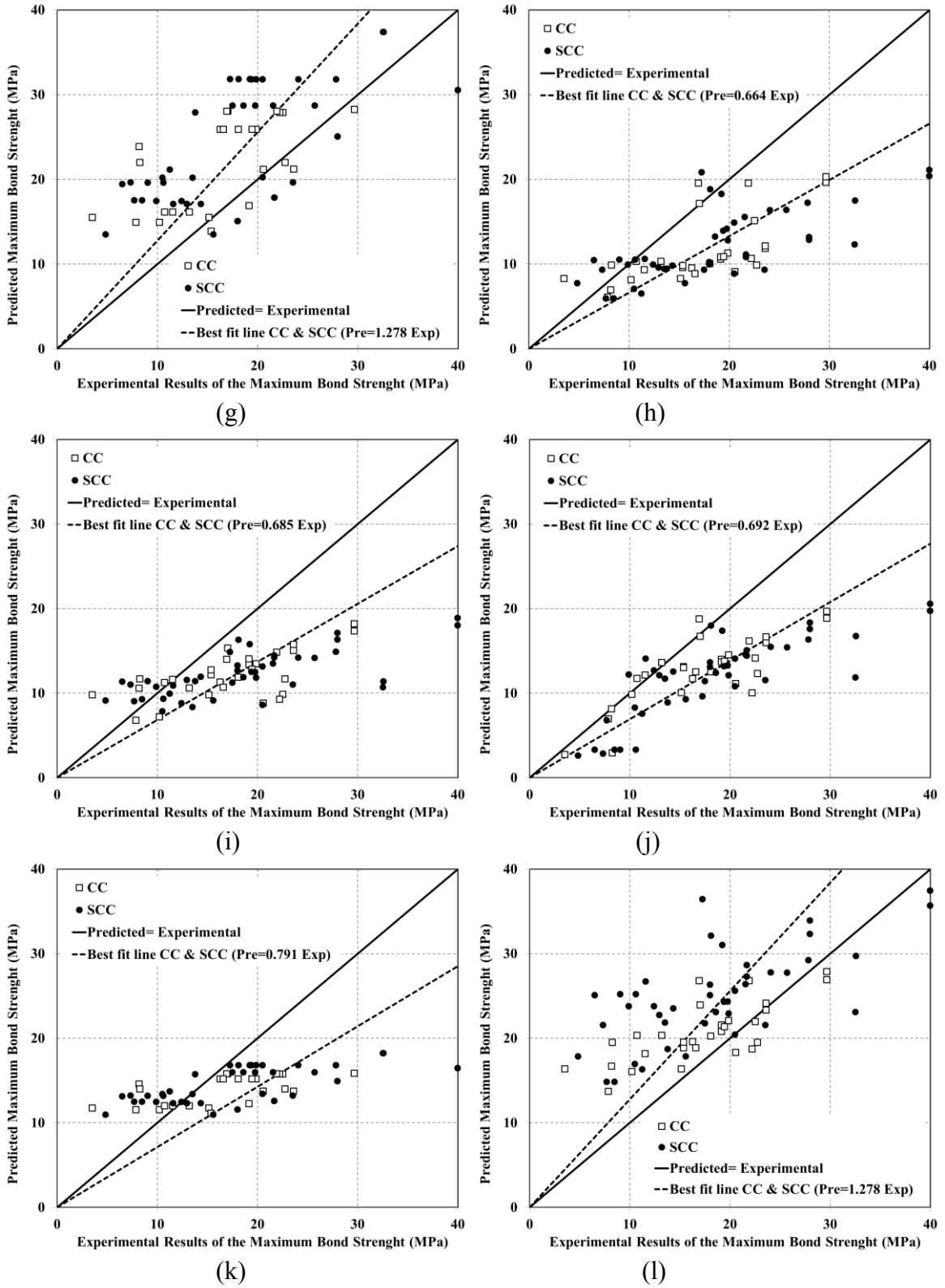

Figure 3.26 (g to l) Comparison of the experimental results versus calculated values from following models (g) Huang et al. (1996), (h) Esfahani and Rangan (1998), (i) Pillai et al. (1999), (j) Bae (2006), (k) CEB-FIP (1990), (l) Desnerck (2011)

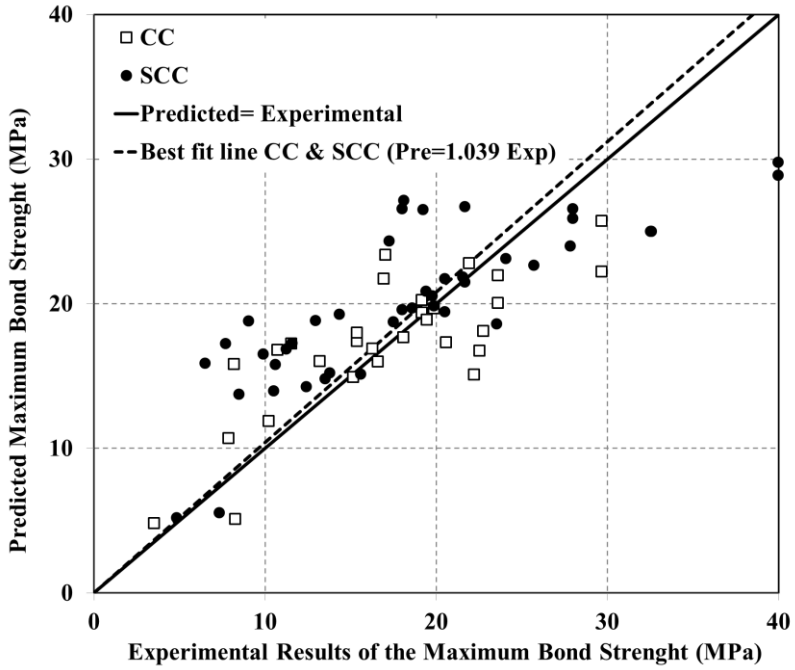

(m)

Figure 3.26 (m) Comparison of the experimental results versus calculated values from proposed model

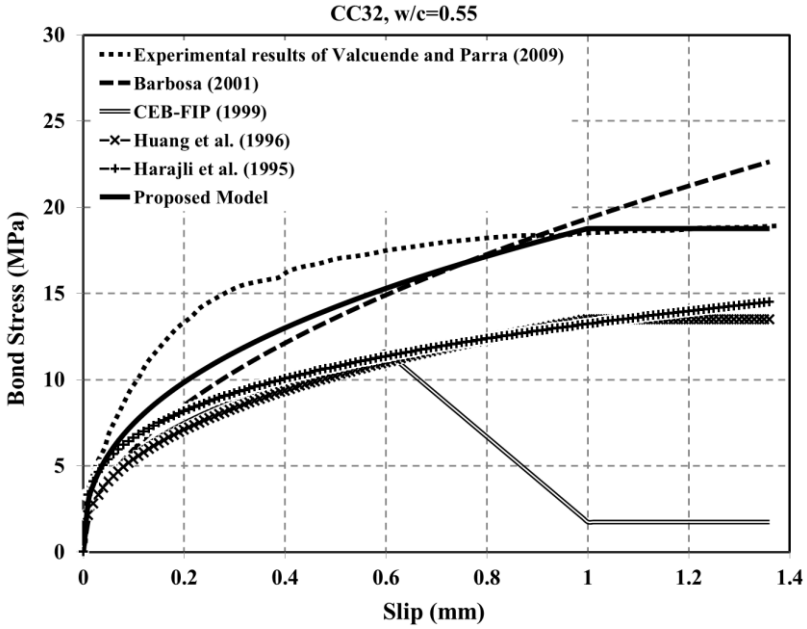

(a)

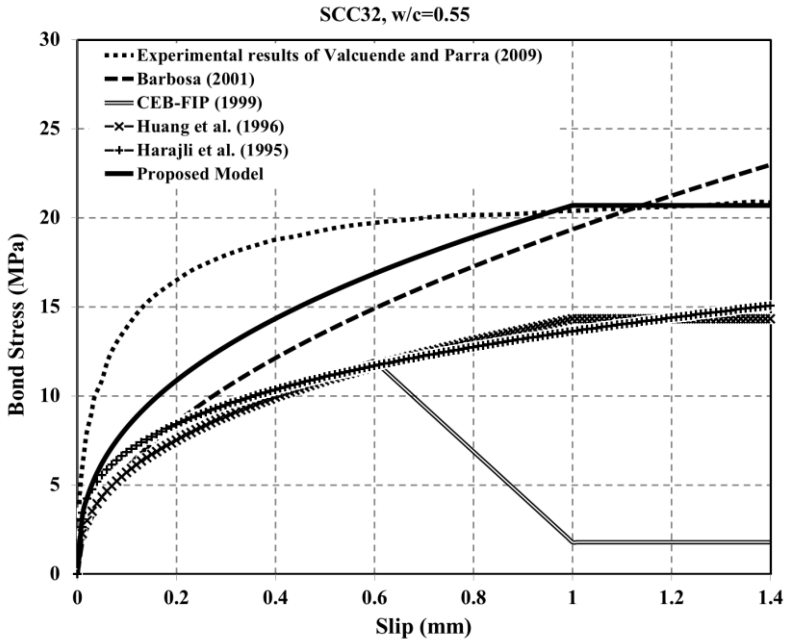

(b)

Figure 3.27 Bond stress versus slip curves of the equations compared with Valcuende and Parra (2009) experimental results of (a) CC, (b) SCC (f'_c= 32 MPa and w/c=0.55)

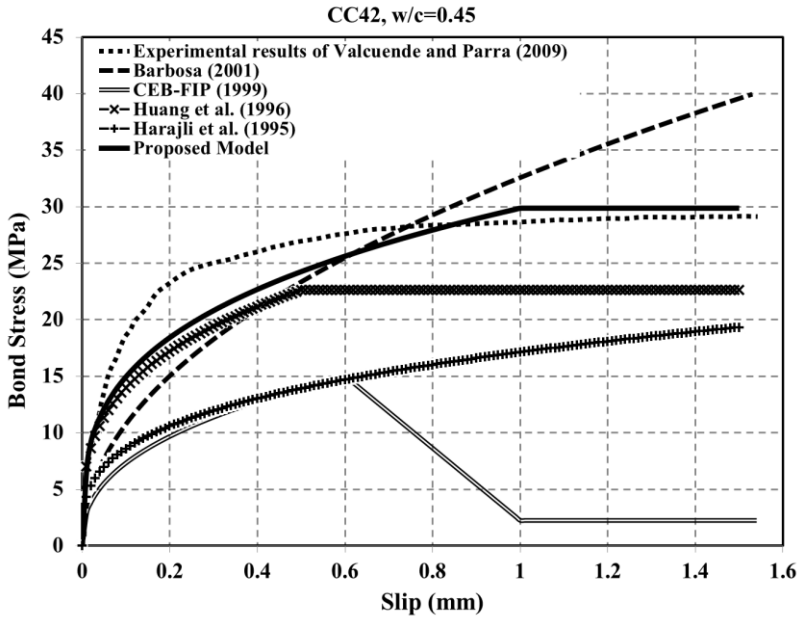

(a)

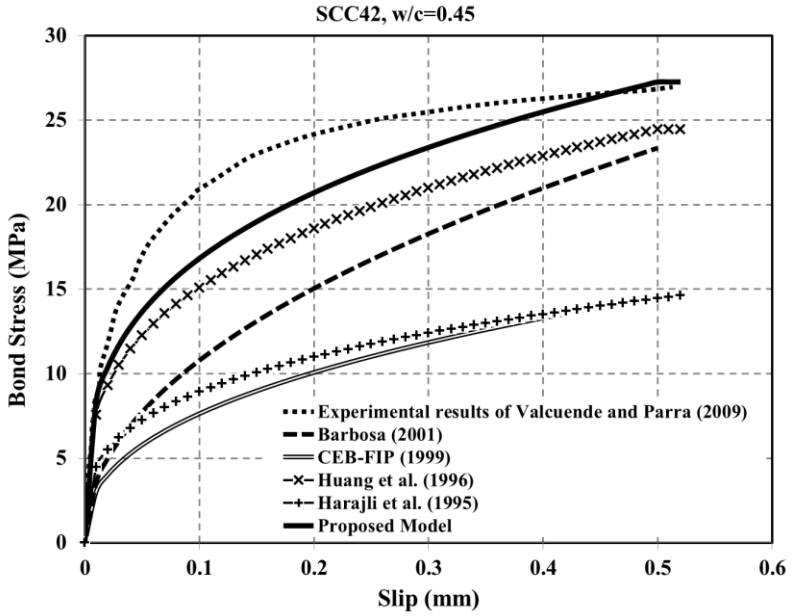

(b)

Figure 3.28 Bond stress versus slip curves of the equations compared with Valcuende and Parra (2009) experimental results of (a) CC, (b) SCC (f'_c= 42 MPa and w/c=0.45)

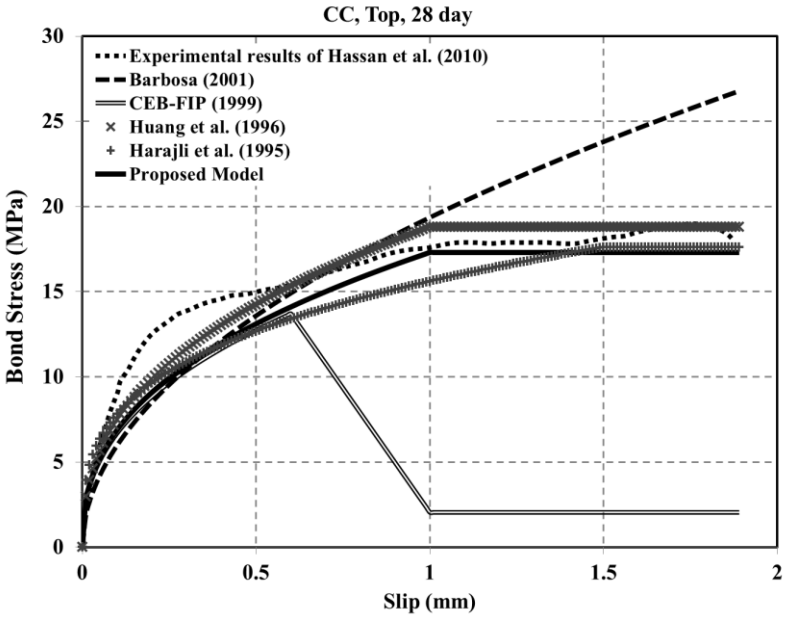

(a)

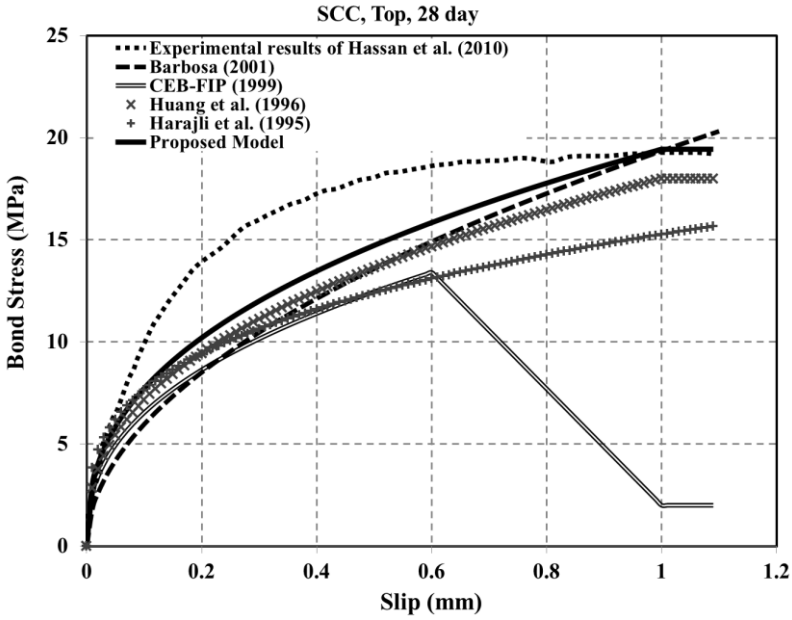

(b)

Figure 3.29 (a, b) Bond stress versus slip curves of the equations compared with Hassan et al. (2010) experimental results of (a) CC, (b) SCC (Top bar pullout at 28 days)

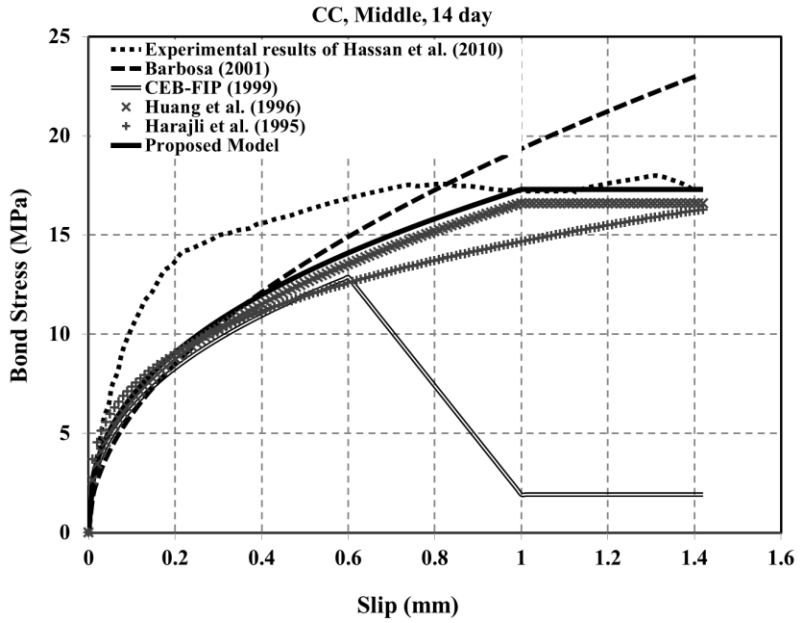

(c)

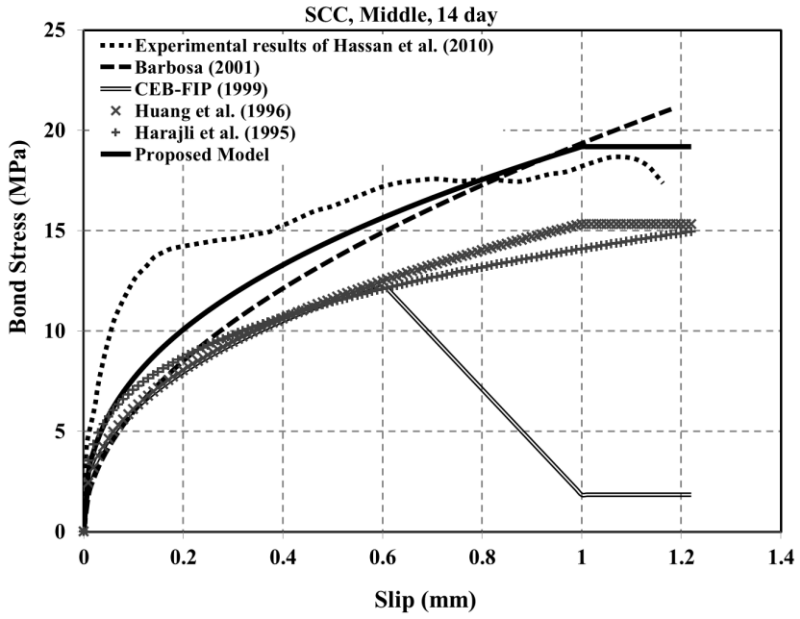

(d)

Figure 3.29 (c, d) Bond stress versus slip curves of the equations compared with Hassan et al. (2010) experimental results (c) CC, (d) SCC (Middle bar pullout at 14 days)

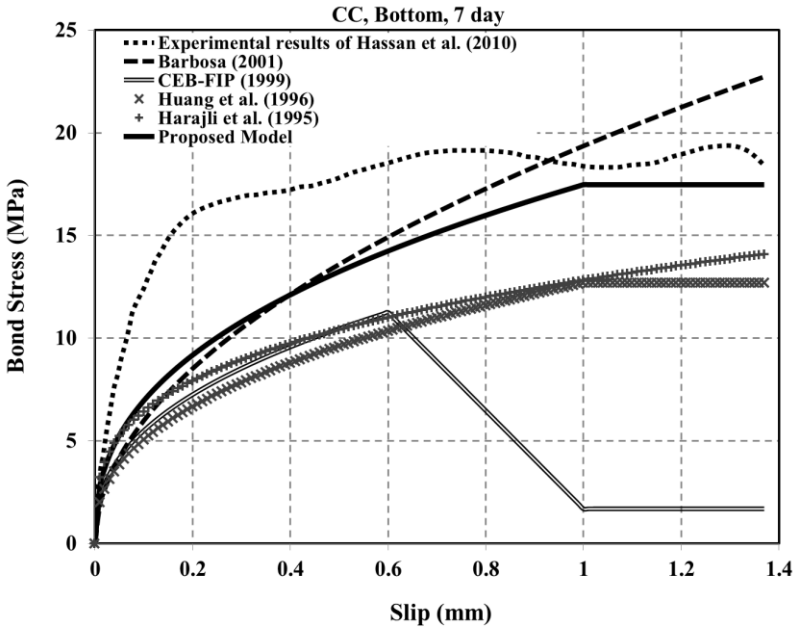

(e)

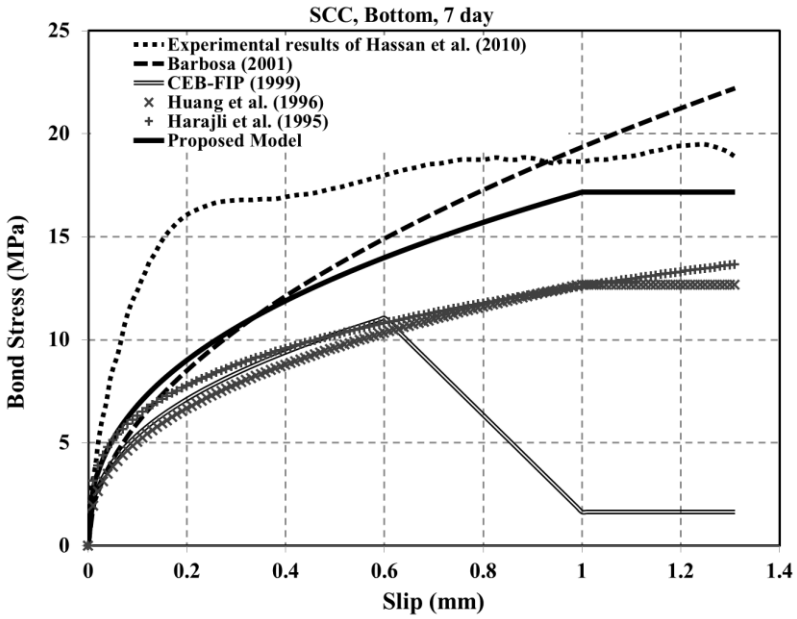

(f)

Figure 3.29 (e, f) Bond stress versus slip curves of the equations compared with Hassan et al. (2010) experimental results of (e) CC, (f) SCC (Bottom bar pullout at 7 days)

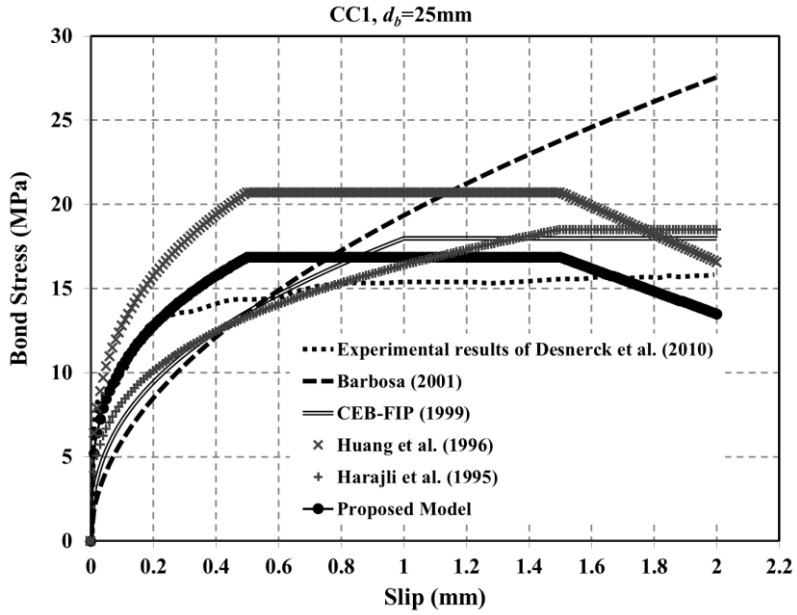

(a)

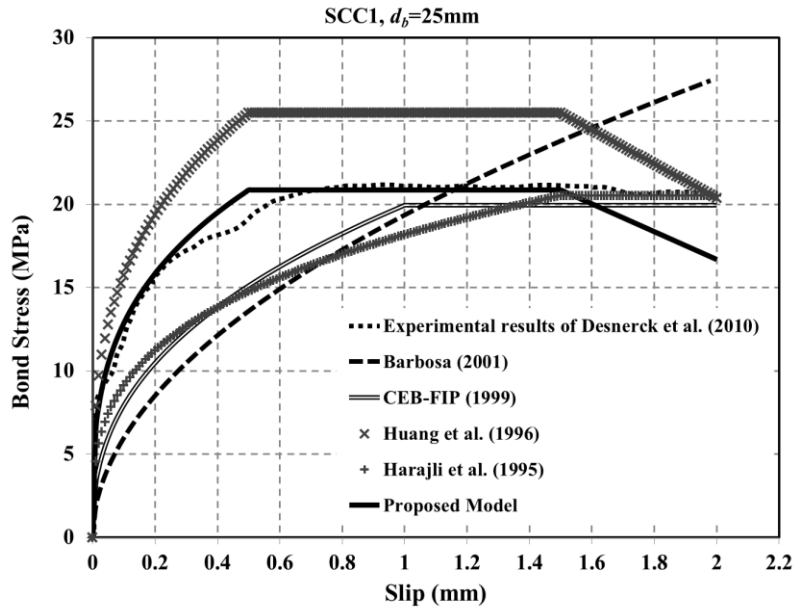

(b)

Figure 3.30 Bond stress versus slip curves of the equations compared with Desnerck et al. (2010) experimental results of (a) CC, (b) SCC1 (diameter of bar 25 mm)

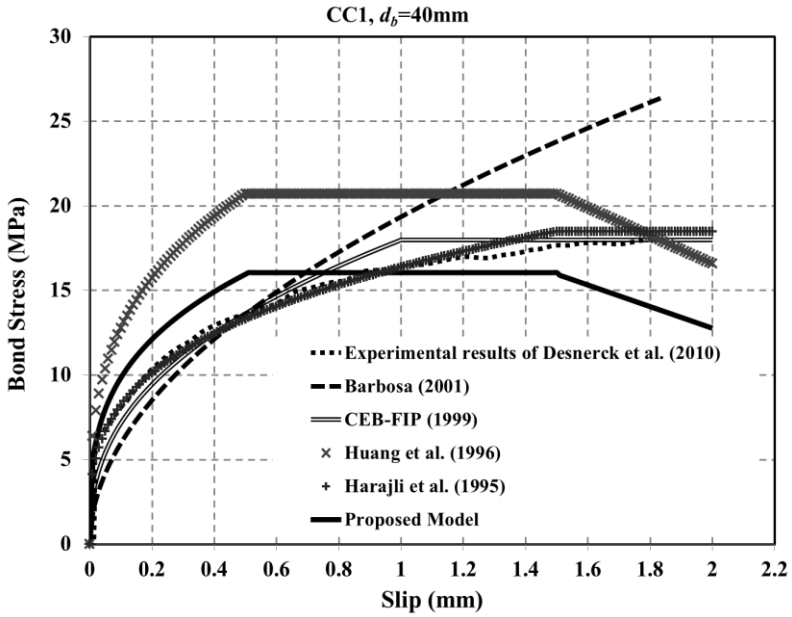

(a)

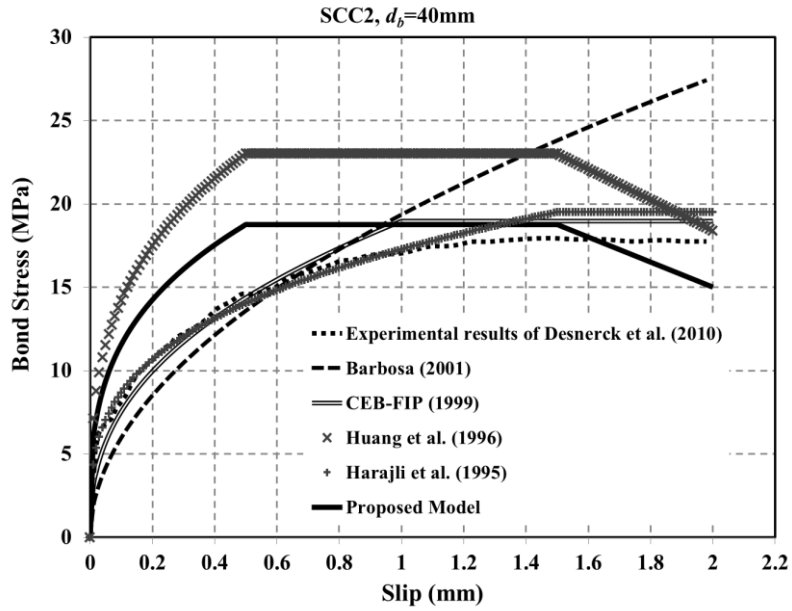

(b)

Figure 3.31 Bond stress versus slip curves of the equations compared with Desnerck et al. (2010) experimental results of (a) CC, (b) SCC2 (diameter of bar 40 mm)

3.7 STRESS-STRAIN BEHAVIOUR OF STEEL FIBRE REINFORCED SELF-COMPACTING CONCRETE

The use of Steel Fibre Reinforced Self-Compacting Concrete (SFRSCC) probably will increase in the next few years, since this composite material introduces several advantages on the concrete technology. In fact, the partial or total replacement of the conventional bar reinforcement by discrete fibres optimizes the construction process. The assembly of the reinforcement bars in the construction of concrete structures has a significant economic impact on the final cost of this type of construction, due to the man-labour consuming that it requires. In the developed societies, the cost of the man-labour is significant, so diminishing the man-labour will decrease the overall cost of the construction. For this reason, SFRSCC is a very promising construction material with a high potential of application, mainly in the cases where fibres can replace the conventional reinforcement. At the present time, however, the SFRSCC technology and the mechanical behaviour of the SFRSCC material are not yet fully developed and controlled (Cunha, 2006). In the fresh state, SFRSCC homogeneously spreads due to its own weight, without any additional compaction energy. To homogeneously fill a mould, SFRSCC has to fulfil high demands with regard to filling and passing ability, as well as segregation resistance. Driven by its own weight, the concrete has to fill a mould completely without leaving entrapped air even in the presence of dense steel bar reinforcement. All the concrete components have to be homogeneously distributed during the flow and at rest (Gräunewald, 2004).

The properties most benefited with the fibre addition to the concrete in the hardened state are the impact strength, the toughness and the energy absorption capacity. A detailed description of the benefits provided by the fibre addition to concrete can be found elsewhere (Balaguru and Shah, 1992, Casanova, 1996, ACI 544.1R, 1997). The fibre addition might also improve the shear resistance (Rosenbusch and Teutsch, 2003). Recently, Gräunewald (2004) compared the mechanical behaviour of SFRSCC to the behaviour of current fibre reinforced concrete (FRC). This author carried out bending and pull-out tests, and concluded that those properties were much better in the SFRSCC. The field of possible application of SFRSCC include: highways, industrial and airfield pavements; hydraulic structures, tunnel segments, bridges components and concrete

structures of complex geometry which present high difficulties in being reinforced by conventional steel bars, especially those which have a high degree of support redundancy.

The behaviour of structural members can be rationally predicted by the given material properties, cross-sectional properties, and loading conditions when computerized non-linear structural analysis techniques are employed. For this purpose, material properties can best be described by their stress-strain relationships. Available material models are not able to accurately simulate the behaviour of SFRSCC; more research should be done in this domain. The objectives of this section are: a) to propose new mechanical properties relationships for SFRSCC mixtures (i.e. compressive and tensile strengths, modulus of elasticity, and peak strain at maximum compressive strength), b) to propose new compressive and tensile stress-strain relationships for SFRSCC.

3.7.1 Experimental and Analytical Database for Stress-Strain Behaviour of SFRSCC

Using experimental results from various published investigations as a database is an effective tool for studying the applicability of the various SFRSCC mechanical properties. In order to apply the models to a particular concrete mixture accurately, it is necessary to use only the investigations that are adequately consistent with the applied testing methodology. The experimental results included in the database have been carried on mainly from the papers presented and published articles on SFRSCC. The database includes information regarding the composition of the mixtures, fresh properties of SFRSCC, testing methodology and conditions. However, it should be emphasized that the mechanical characteristics have not been investigated as much as the other aspects of SFRSCC, and the available published experimental data in the literature are still not very extensive.

Tables 3.29 and 3.30 are a general summary of the SFRSCC mechanical properties mixtures included in the database. The database includes 21 reference experimental results (i.e. Grünewald, 2004, Corinaldesi and Moriconi, 2004, Sahmaran et al., 2005, Cunha, 2006, Liao et al., 2006, Schumacher, 2006, Sengul et al., 2006, Dhonde et al., 2007, Ferrara et al., 2007, Aydin, 2007, Torrijos et al., 2008, El-Dieb, 2009, Buratti et al., 2010, Khaliq

and Kodur, 2011, Fantilli et al., 2011, Corinaldesi and Moriconi, 2011, Ding et al., 2012a, 2012b, Goel et al., 2012, Akcay and Tasdemir, 2012), van Zijl and Zeranka, 2012). Tables 1-3 also include additional information regarding the cement type, filler type, compressive strength test specimen type, aggregate type, fibre type, fibre shape, fibre aspect ratio, fibre length, mix label, fibre volume fraction (V_f), compressive strength at 28 days (f'_c), and fibre reinforcing index (R.I. = $V_f \times l_f / d_f$).

The stress-strain relationship of concrete essentially consists of two distinct branches; an ascending branch up to the peak stress followed by a descending branch until the concrete crushes. The key properties that are normally used to characterize the ascending branch of the curve are the initial tangent modulus, the compressive strength, and the strain at peak stress. In technical literature there are reported many analytical models developed to represent the stress-strain curves for plain concrete under compression. Among the most important and known models must be cited the models of Popovics (1973) and Carreira and Chu (1985). Since the models of the compressive behaviour of fibre-reinforced concrete were developed from models developed for plain concrete, it is necessary to include some parameters in these models to consider the influence of fibres on the properties of stress-strain curves. In Table 3.31 most of the SFRC compressive stress-strain relationships are summarized and include: Ezeldin et al. (1992), Hsu and Hsu (1994), Mansur et al. (1999), Nataraja et al. (1999), Neves and Almeida (2005), Bhargava et al. (2006), and Oliveira Júnior et al. (2010). Also, Table 3.32 shows SFRSCC compressive stress-strain relationship as Cunha (2006).

Ezeldin et al. (1992) proposed a model for complete stress-strain curve for non-silica-fume fibre reinforced concrete. Ezeldin et al.'s model (1992) is valid for the experimental stress-strain behaviour of fibre reinforced concrete with compressive strength ranging from 35 MPa to 85 MPa. Three fibre volume fractions 30 kg/m^3, 45 kg/m^3, and 60 kg/m^3 and three aspect ratios of 60, 75, and 100 were investigated. The influence of the fibre reinforcing parameters on the peak stress, corresponding strain, the secant modulus of elasticity, the toughness of concrete, and the curve shape were reported.

Empirical equations are proposed by Hsu and Hsu (1994) to represent the complete stress-strain relationships of high strength steel fibre concrete with compressive strength

exceeding 69 MPa. Hsu and Hsu's model (1994) is based on a series of compression tests that were conducted on 75×150 mm cylindrical specimens using a modified test method that gave the complete stress-strain behaviour for high-strength steel-fibre concrete with or without tie confinements. The volume fractions of steel fibre in the concrete were 0%, 0.5%, 0.75% and 1%, respectively. Various parameters were studied and their relationships were experimentally determined. Mansur et al. (1999), based on their test data, proposed an analytical model to generate the complete stress-strain curves of high-strength fibre reinforced concrete derived from cylinders and horizontally cast prisms. The concrete strength investigated ranges from 70 to 120 MPa. Other parameters include volume fraction of steel fibres and direction of casting in relation to the loading axis. Mansur et al. (1999) test results indicate that inclusion of fibres improves the strength and increases the strain at peak stress but results in a smaller initial tangent modulus for specimens cast in an upright (vertical) position.

Analytical models are proposed by Nataraja et al. (1999) to quantify the effect of fibre on compressive strength, strain at peak stress and the toughness of concrete in terms of the fibre reinforcing parameter. These models are based on the experimental investigations to generate the complete stress-strain curve experimentally for steel fibre reinforced concrete for compressive strength ranging from 30 to 50 MPa. Round crimped fibre with three volume fractions of 0.5%, 0.75% and 1.0% (39, 59, and 78 kg/m^3) and for two aspect ratios of 55 and 82 were considered. The effect of fibre addition to concrete on some of the major parameters namely peak stress, strain at peak stress, the toughness of concrete and the nature of the stress-strain curve is studied. Neves and Almeida (2005) proposed expressions to estimate the Young's modulus and the strain at peak stress, from the compressive strength results, knowing fibre volume, length and diameter. Also, an analytical model to predict the stress–strain relationship for steel fibre concrete in compression is also proposed by Neves and Almeida (2005). These relationships are achieved by using an experimental section to investigate the influence of matrix strength, fibre content and diameter on the compressive behaviour of steel fibre reinforced concrete. Concrete compressive strengths of 35 and 60 MPa, 0.38 and 0.55 mm fibre diameter, and 30 mm fibre length, were considered. The volume of fibre in the concrete was varied up to 1.5 %.

Bhargava et al. (2006) based on their test data, proposed a model to generate the complete stress-strain relationship for steel fibre reinforced high strength concrete. The experimental program consisted of testing 100×200 mm concrete cylinders. The experimental variables of this section were concrete strength levels (58.03 MPa and 76.80 MPa), volume fractions (0.5% to 2.0%) and aspect ratios (20 and 40) of flat crimped steel fibres. The effect of the mixed aspect ratio of fibres on the stress-strain behaviour of steel fibre high strength concrete was also studied by blending short and long fibres. Oliveira Júnior et al. (2010) presented a section on the compressive behaviour of steel fibre reinforced concrete. In this section, an analytical model for stress-strain curve for steel fibre reinforced concrete is derived for concretes with strengths of 40 MPa and 60 MPa at the age of 28 days. Those concretes were reinforced with steel fibres with hooked ends 35 mm long and with aspect ratio of 65.

Cunha (2006) has proposed stress-strain laws to model the behaviour of the SFRSCC from early in its development. Additionally empirical expressions to predict the principal mechanical properties were presented. The requirements established for this SFRSCC were the following: average compression strength at 24 hours greater than 20 MPa, equivalent flexural tensile strength greater than 2 MPa at this age, content of cement not exceeding 400 kg/m^3. In this work, the compressive softening behaviour of SFRSCC was investigated, within a structural point of view.

3.7.2 Comparison of Proposed SFRSCC Model with Available SFRSCC Models

In this section, the relationships proposed for the most significant properties of the SFRSCC (e.g. compressive strength (f'_{cf}), tensile strength (f_{ctf}), modulus of elasticity (E_{cf}), and strain at peak stress (ε'_{cf})) are based on regression analyses on existing experimental data, with the results expressed as Eq. (3.16 to 3.19).

For compressive strength:

$$f'_{cf} = \begin{cases} f'_c + 17.53(R.I.) & 35 \le f'_c < 60 \\ f'_c + 13.92(R.I.) & 60 \le f'_c \le 80 \\ f'_c + 122.20(R.I.) & 80 < f'_c \le 120 \end{cases} \quad (3.16)$$

where f'_{cf} is the compressive strength of SFRSCC (MPa), R.I. is the fibre reinforcing index (=$V_f \times l_f / d_f$) and f'_c is the compressive strength of normal concrete (MPa). Figures 3.32 shows proposed SFRSCC compressive strength relationship compared to the experimental results database for three different limitations of compressive strength 35 to 60 (MPa), 60 to 80 (MPa), and 80 to 120 (MPa).

For tensile strength:

$$f_{ctf} = \begin{Bmatrix} f_{ct} + 14.19(R.I.) & 35 \le f'_c < 60 \\ f_{ct} + 19.74(R.I.) & 60 \le f'_c \le 80 \\ f_{ct} + 18.37(R.I.) & 80 < f'_c \le 120 \end{Bmatrix} \quad (3.17)$$

where f_{ctf} is the tensile strength of SFRSCC (MPa), R.I. is the fibre reinforcing index (=$V_f \times l_f / d_f$) and f'_c is the compressive strength of normal concrete (MPa). Figures 3.33 shows proposed SFRSCC tensile strength relationship compared to the experimental results database for three different limitations of compressive strength 35 to 60 (MPa), 60 to 80 (MPa), and 80 to 120 (MPa).

For modulus of elasticity:

$$E_{cf} = E_c + 23.70(R.I.) \quad (3.18)$$

where E_{cf} is the modulus of elasticity of SFRSCC (GPa), R.I. is the fibre reinforcing index (=$V_f \times l_f / d_f$) and E_c is the secant modulus of elasticity of normal concrete (GPa). Figure 3.34 shows proposed SFRSCC modulus of elasticity relationship compared to the experimental results database by considering corresponding compressive strength compared to the modulus of elasticity.

For strain at peak stress:

$$\varepsilon'_{cf} = \varepsilon'_c + 0.003(R.I.) \quad (3.19)$$

where ε'_{cf} is the corresponding strain to the maximum stress of SFRSCC, R.I. is the fibre reinforcing index (=$V_f \times l_f / d_f$) and ε'_c is the corresponding strain to the maximum stress. Figure 3.35 shows proposed SFRSCC strain at peak stress relationship compared to the

experimental results database by considering corresponding compressive strength to the each strain at peak stress.

For compressive stress-strain curve:

The proposed compressive envelope curve is based on Carreira and Chu's model (1985), as given by Eqs. (3.20 to 3.27). In this compressive stress-strain relationship for normal and high strength SFRSCC the compressive strength (f'_{cf}) as Eq. (3.16), modulus of elasticity (E_{cf}) as Eq. (3.18) and strain at peak stress (ε'_{cf}) as Eq. (3.19) are used:

$$\frac{\sigma_{cf}}{f'_{cf}} = \frac{n_f \left(\frac{\varepsilon_{cf}}{\varepsilon'_{cf}} \right)}{n_f - 1 + \left(\frac{\varepsilon_{cf}}{\varepsilon'_{cf}} \right)^{n_f}} \tag{3.20}$$

$$n_f = n_{1f} = \left[1.02 - 1.17 \left(E_{\sec f} / E_{cf} \right) \right]^{-0.74} \quad if\ \varepsilon_{cf} \le \varepsilon'_{cf} \tag{3.21}$$

$$n_f = n_{2_f} = n_{1_f} + \left(\gamma + 28 \times \mu \right) \quad if\ \varepsilon_{c_f} \ge \varepsilon'_{cf} \tag{3.22}$$

$$\gamma_f = 3 \times \left(12.40 - 0.0166 f'_{cf} \right)^{-0.46} \tag{3.23}$$

$$\mu_f = 0.83 \exp\left(-911 / f'_{cf} \right) \tag{3.24}$$

$$E_{\sec f} = f'_{cf} / \varepsilon'_{cf} \tag{3.25}$$

$$\varepsilon'_c = \left(\frac{f'_c}{E_c} \right) \left(\frac{\psi}{\psi - 1} \right) \tag{3.26}$$

$$\psi = \frac{f'_c}{17} + 0.8 \tag{3.27}$$

Figures 3.36 to 3.38 show comparisons between Liao et al. (2006) (SFRSCC3 to SFRSCC6 mixtures), Cunha (2006) (SFRSCC1 and SFRSCC2 mixtures), and Dhonde et al. (2007) (SFRSCC2 and SFRSCC3 mixtures) experimental results and available compressive fibre reinforced stress-strain relationships database (Tables 3.32-3.33).

For tensile stress-strain curve:

Several expressions have been documented in the literature to represent the softening branch, including straight lines (Bažant and Oh, 1983), polylinear curves (Gustafsson, 1985 and Gylltoft, 1983, Hillerborg et al., 1976, Rots et al., 1985, and Petersson, 1981), exponential curves (Gopalaratman and Shah, 1985 and Sima et al., 2008), polynomial curves (Lin and Scordelis, 1975), Yankelevsky and Reinhardt, 1987, 1989), combinations of them (Cornelissen et al., 1985), a continuous damage-based formulation to represent post-peak stress-strain curves of concrete (Mazars, 1981) and tension softening in terms of prescribed drops (Scanalon, 1971). The proposed tensile envelope curve is a very simple model, as given by Eqs. (3.28-3.30). In this tensile stress-strain model for normal and high strength SFRSCC the tensile strength (f'_{ctf}) as Eq. (3.17), modulus of elasticity (E_{cf}) as Eq. (3.18) are used:

$$\sigma_{ctf} = E_{cf}\,\varepsilon_{ct} \qquad \varepsilon_{ct} < \varepsilon^* \tag{3.28}$$

$$\sigma_{ctf} = f_{ctf} \qquad \varepsilon_{ct} = \varepsilon^* \text{ to } 5.66\,\varepsilon^* \tag{3.29}$$

$$\sigma_{ctf} = f_{ctf}\left(\frac{5.66\,\varepsilon^*}{\varepsilon_{ct}}\right)^{0.78} \qquad \varepsilon_{ct} > 5.66\,\varepsilon^* \tag{3.30}$$

where ε^* is the corresponding strain to the 0.85 f_{ctf} and ε_{ct} is the tensile concrete strain in general. Figure 3.39 shows comparisons between Liao et al. (2006) (SFRSCC3 to SFRSCC6 mixtures) experimental results and proposed tensile fibre reinforced stress-strain relationship.

Experimental results database (Tables 3.29-3.31) shows that the major cement type that is used is ordinary Portland cement (ASTM C150-04), the major fillers that are used in the mix designs are fly ash and limestone, and compressive strength test specimen type is variable. Major aggregate types that used are crushed limestone, natural coarse aggregate and natural sand. Major type of fibre is Dramix and major shape is hooked end with different lengths and aspect ratios. In this section, the compressive strength test specimen type of 100 mm × 200 mm cylindrical is considered as main for compressive strength and

other types of test results (i.e. 150 mm × 300 mm cylindrical, 100 mm cube, and 150 mm cube) must convert to it. Yi et al. (2006) reported that the relationship between 100 mm × 200 mm cylindrical with 150 mm cube was: $f'_{cy}(100 \times 200) = (f'_{cu}(150)-8.86)/0.85$ and the relationship between 100 mm × 200 mm cylindrical with 100 mm cube was: $f'_{cy}(100 \times 200) = (f'_{cu}(100)-7.07)/0.95$. Also, Carrasquillo et al. (1981) stated that the average ratio of compressive strength of 150 mm × 300 mm to 100 mm × 200 mm cylinders was 0.9, regardless of strength and test age.

Comparisons of proposed relationships for compressive and tensile strength of SFRSCC with the experimental results database show that the proposed relationships for three different limitations of compressive strength are in good correlation with test results (see Figures 3.32 and 3.33). Coefficient of correlation factor (R^2) of proposed compressive relationships for 35 to 60 (MPa), 60 to 80 (MPa), and 80 to 120 (MPa) are 0.80, 0.86, and 0.91, respectively. Also, Coefficient of correlation factor (R^2) of proposed tensile relationships for 35 to 60 (MPa), 60 to 80 (MPa), and 80 to 120 (MPa) are 0.85, 0.81, and 0.90, respectively. Figure 3.34 shows proposed for normal and high strength SFRSCC modulus of elasticity relationship is in good agreement with the experimental test results. In Figure 3.34, experimental results show that E_{cf} related to largest compressive strength are placed in the largest R.I. axe. Coefficient of correlation factor (R^2) of modulus of elasticity relationship is 0.84. Figure 3.35 shows proposed SFRSCC strain at peak stress relationship is in good agreement with the experimental test results. In Figure 3.35, experimental results show that corresponding strain to the maximum stress of SFRSCC that related to largest compressive strength are placed in the smallest R.I. axis. Coefficient of correlation factor (R^2) of strain at peak stress relationship is 0.80.

Ezeldin et al. (1992), Nataraja et al. (1999), Mansur et al. (1999), Neves and Almeida (2005), and Bhargava et al. (2006) relationships do not have good prediction in both ascending and descending branches of stress-strain curve compared with Liao et al. (2006) experimental results for all mixtures (see Figure 3.36). In comparison with Cunha (2006) experimental results, these relationships have good prediction in ascending branch but in descending portion are overestimated (see Figure 3.37). Also, these relationships compared to Dhonde et al. (2007) experimental tests are overestimated (see Figure 3.38).

Hsu and Hsu (1994) relationship has good prediction in ascending branch but for descending branch prediction compared with Liao et al. (2006) experimental results for all mixtures, it is underestimated (see Figure 3.36). In comparison with Cunha (2006) experimental results, it has a good prediction in both ascending and descending portions (see Figure 3.37). Also, this relationship compared to Dhonde et al. (2007) experimental tests (it is just for ascending portion) is overestimated (see Figure 3.38).

Oliveira Júnior et al. (2010) and SFRSCC Cunha (2006) compressive stress-strain relationships have good prediction in ascending branch but for descending branch prediction compared with Liao et al. (2006) experimental results for all mixtures are underestimated except for SFRSCC3 mixture (as shown in Figure 3.36). In comparison with Liao et al. (2006) experimental results, these relationships have good prediction in both ascending and descending portions. Also, these relationships compared to Dhonde et al. (2007) experimental tests are overestimated (as shown in Figure 3.38).

The compressive SFRSCC stress–strain relationship suggested in this section calculates the ascending branch of the stress–strain curve in comparison with Liao et al. (2006), Cunha (2006) and Dhonde et al. (2007) appropriately. Also, it calculates the descending branch within a minimum range of deviations with a reasonably accuracy. Besides, simple proposed tensile SFRSCC stress–strain relationship estimates Liao et al. (2006) experimental results for both ascending and descending portions (as shown in Figure 3.39) in an accurate manner.

Table 3.29 SFRSCC experimental results database properties (including: cement type, filler type, compressive strength specimen type, and aggregate type)

Reference	Cement type	Filler type	f'_c Specimen type	Aggregate type
Grünewald (2004)	CEM III/A 52.5, CEM I 52.5 R	Silica fume	Cube (150 mm)	Natural crushed and round coarse aggregate and natural round sand
Corinaldesi and Moriconi (2004)	CEM II/ A-L 42.5 R	Limestone	Cube (100 mm)	Crushed limestone coarse aggregate and natural sand
Sahmaran et al. (2005)	OPC type I (ASTM C150-04)	Limestone	Cube (150 mm)	Crushed limestone and crushed sand
Cunha (2006)	CEM I 42.5R	Limestone	Cylinder (150 mm × 300 mm)	Crushed granite coarse aggregate and river sand
Liao et al. (2006)	ASTM Type III Portland	Fly ash	Cylinder (100 mm × 200 mm)	Crushed Limestone and Pea gravel, Silica Sand
Schumacher (2006)	CEM III/A 52.5, CEM I 52.5 R	Fly ash	Cube (150 mm)	Natural crushed and round coarse aggregate and natural round sand
Sengul et al. (2006)	OPC type I (ASTM C150-04)	Silica fume	-	-

Table 3.29 SFRSCC experimental results database properties (continued)

Reference	Cement type	Filler type	f'_c Specimen type	Aggregate type
Dhonde et al. (2007)	ASTM Type III Portland	Fly ash	Cylinder (150 mm × 300 mm)	Well-graded, rounded, river-bed, coarse aggregates and well-graded, river-bed sand
Ferrara et al. (2007)	OPC type I (ASTM C150-04)	Fly ash	Cylinder (100 mm × 200 mm)	-
Aydin (2007)	OPC type I (ASTM C150-04)	Quartz powder	Cylinder (100 mm × 200 mm)	Natural gravel aggregate and natural sand
Torrijos et al. (2008)	CEM II 32.5 R	Limestone	Cylinder (150 mm × 300 mm)	Crushed limestone aggregates
El-Dieb (2009)	OPC type I (ASTM C150-04)	Silica fume	Cube	Natural crushed stone coarse aggregate and crushed natural stone sand
Buratti et al. (2010)	II/A-L 32.5R	II/A-L 32.5R	-	-
Khaliq and Kodur (2011)	OPC type I (ASTM C150-04)	Fly ash	Cylinder (100 mm × 200 mm)	Crushed Limestone coarse aggregate and natural sand
Fantilli et al. (2011)	A-LL 42.5 R	Carbonate	Cylinder (70 mm × 140 mm)	Natural gravel aggregate and natural sand
Corinaldesi and Moriconi (2011)	CEM II/A-L 42.5 R	Limestone	Cube (100 mm)	Gravel and quartz sand
Ding et al. (2012a)	OPC type I (ASTM C150-04)	Fly ash	Cube (150 mm)	Crushed gravel and natural sand
Ding et al. (2012b)	OPC type I (ASTM C150-04)	Fly ash	Cube (150 mm)	Crushed limestone aggregate and natural sand
Goel et al. (2012)	OPC type I (ASTM C150-04)	Fly ash	Cube (150 mm)	Crushed stone aggregate and natural sand
Akcay and Tasdemir (2012)	OPC type I (ASTM C150-04)	Silica fume	Cylinder (100 mm × 200 mm)	Crushed stone coarse aggregate and natural sand
van Zijl and Zeranka (2012)	OPC type I (ASTM C150-04) and CEM II 32.5	Fly ash	Cube (100 mm)	Greywacke stone and Malmesbury sand

Table 3.30 SFRSCC experimental results database properties (including: fibre type, fibre shape, aspect ratio (l_f / d_f), and fibre length)

Reference	Fibre type	Shape	l_f/d_f	l_f(mm)
Grünewald (2004)	Dramix BP 80/60 C	Hooked	85.66	61.06
	Dramix BN 80/60 C		76.10	57.94
	Dramix BN 45/50 L		48.08	51.09
	Eurosteel 50/50		45.81	47.77
	Dramix BN 65/40 C		64.94	41.24
	Harex 01/32		32.82	32.40
	Dramix BP 80/30 C		78.50	30.48
	Dramix BN 45/30 L		46.34	28.80
	Harex 65/20		64.30	20.20
	Dramix OL 13/0.16		81.25	13.00
	Dramix OL 6/0.16		37.50	6.00
Corinaldesi and Moriconi (2004)	Straight steel fibres	Straight	27.50	11.00
Sahmaran et al. (2005)	Dramix ZP 305	Hooked	55.00	30.00
	Dramix OL 6/16	Straight	37.5	6.00
Cunha (2006)	Dramix RC-80/60-BN	Hooked	85.66	60.00
Liao et al. (2006)	Dramix RC-80/30-BP	Hooked	78.50	30.00
	Dramix ZP305		55.00	30.00
Schumacher (2006)	Dramix BN 80/60 C	Hooked	85.66	61.06
	Dramix BP 80/30 C		78.50	30.48
	Dramix BN 45/30 L		46.34	28.80
Sengul et al. (2006)	-	Hooked	54.54	30.00
Dhonde et al. (2007)	Dramix RC-80/60-BN	Hooked	80.00	60.00
	Dramix ZP305		55.00	30.00
Ferrara et al. (2007)	Dramix 65/35	Hooked	65.00	35.00
Aydin (2007)	Dramix OL 6/16	Hooked	37.5	6.00
Torrijos et al. (2008)	-	Hooked	50.00	50.00
El-Dieb (2009)	HELIX 5-25	Twisted	50.00	25.00
Buratti et al. (2010)	Steel A		66.66	50.00
Khaliq and Kodur (2011)	NOVOCON XR	Corrugated	33.33	38.00
Fantilli et al. (2011)	Dramix RC 65/35 BN	Hooked	63.63	35.00
Corinaldesi and Moriconi (2011)	-	Hooked	43.00	30.00
Ding et al. (2012a)	Dramix BN 80/60 C	Hooked	80.00	60.00
Ding et al. (2012b)	-	Hooked	63.63	35.00
Goel et al. (2012)	-	Circular corrugated	30.00	30.00
Akcay and Tasdemir (2012)	HSS	Hooked	40.00	6.00
	NSH		55.00	30.00
	HSH		55.00	30.00
van Zijl and Zeranka (2012)	Dramix ZP305	Hooked	55.00	30.00

Table 3.31 SFRSCC compressive strength results database properties (including: fibre type, fibre volume fraction (V_f), 28 days compressive strength, and fibre reinforcing index R.I.)

Reference	Mix Label	Fibre type	V_f (%)	f'_c (28 days) (MPa)	$R.I. = (V_f \times l_f/d_f)$
Grünewald (2004)	L-R-60-60	80/60	2.5	54.00	2.14
	L-R-30-60	80/30	2.5	57.60	1.96
	L-R-40-100	65/40	4.23	51.90	2.74
	L-R-30-140	45/30	6.3	55.80	2.92
	M-R-30-40	80/30	1.7	70.30	1.33
	M-R-20-60	65/20	2.57	75.60	1.65
	M-R-60-60	80/60	2.56	75.10	2.19
	M-R-30-60	80/30	2.56	72.30	2.01
	M-R-40-100	65/40	4.2	73.50	2.73
	M-R-30-140	45/30	5.84	78.10	2.70
	M-F-60-60	80/60	2.5	75.30	2.14
	M-F-30-140	45/30	5.84	71.70	2.70
	H-R-60-60	80/60	2.5	116.70	2.14
	H-R-13-125	OL13/0.16	5.1	120.30	4.14
	P1	45/30	2.5	52.20	1.16
	P2	45/30	5	55.50	2.31
	P3	80/30	2.5	114.40	1.96
Corinaldesi and Moriconi (2004)	SCC-0.40	Straight	0.6	44.00	1.65
Sahmaran et al. (2005)	2	Dramix ZP 305	2.0	49.50	1.10
	6	Dramix OL 6/16	2.0	58.90	0.75
Cunha (2006)	SFRSCC1	80/60-BN	0.55	69.70	0.47
	SFRSCC2		0.80	56.20	0.68
Liao et al. (2006)	SFRSCC1	ZP305	1.96	65.00	1.08
	SFRSCC2	80/30-BN	1.92	67.90	1.50
	SFRSCC3		1.47	65.00	1.15
	SFRSCC4		1.38	36.40	1.08
	SFRSCC5		1.50	43.60	1.18
	SFRSCC6		1.50	39.30	1.18
Schumacher (2006)	B45.45/30.60	45/30	2.50	55.70	1.16
	B45.45/30.120	45/30	5.00	56.40	2.32
	B45.80/30.60	80/30	2.50	56.10	1.96
	B45.80/60.60	80/60	2.50	60.70	2.14
	B105.80/30.60	80/30	2.50	116.70	1.96
	B105.80/60.60	80/60	2.50	116.70	2.14
Sengul et al. (2006)	V1350	-	1.50	86.0	0.81
	V1650		1.50	110.2	0.81
	V1900		1.50	124.2	0.81
	V2350		1.50	94.9	0.81
	V2650		1.50	123.7	0.81
	V2900		1.50	138.0	0.81

Table 3.31 SFRSCC compressive strength results database properties (continued)

Reference	Mix Label	Fibre type	V_f (%)	f'_c (28 days) (MPa)	$R.I. = (V_f \times l_f/d_f)$
Dhonde et al. (2007)	SFRSCC1	80/60-BP	0.50	83.00	0.4
	SFRSCC2	ZP305	0.50	84.30	0.27
	SFRSCC3	ZP305	1.00	90.00	0.55
Ferrara et al. (2007)	1FRC	Dramix 65/35	2.75	58.26	1.78
	2FRC		2.91	81.60	1.89
	3FRC		3.10	61.40	2.01
	4FRC		2.75	76.70	1.78
	5FRC		2.91	79.44	1.89
	6FRC		3.10	66.50	2.01
	7FRC		2.75	73.95	1.78
	8FRC		2.91	82.78	1.89
	9FRC		3.10	68.07	2.01
Aydin (2007)	M2	Dramix OL 6/16	0.25	18.47	0.09
	M3		0.50	24.21	0.18
	M4		0.75	22.57	0.28
	M5		1.00	39.25	0.37
	M6		1.25	18.70	0.46
	M7		1.50	25.89	0.56
	M8		1.75	24.41	0.65
	M9		2.00	44.44	0.75
Torrijos et al. (2008)	SFR-SCC 25	-	1.00	54.00	0.50
	SFR-SCC 50		2.00	54.00	1.00
El-Dieb (2009)	A	HELIX 5-25	0.08	116.74	0.04
	B		0.12	99.48	0.06
	C		0.52	96.65	0.26
Buratti et al. (2010)	SF25a	Steel A	0.32	40.1	0.21
	SF25b		0.32	42.2	0.21
	SF35a		0.45	39.9	0.30
	SF35b		0.45	40.1	0.30
Khaliq and Kodur (2011)	SCC-S	NOVOCON XR	1.75	57.00	0.58
Fantilli et al. (2011)	35SC0	Dramix RC 65/35 BN	0.45	34.50	0.28
	35SC1		0.45	37.30	0.28
	35SC3		0.45	42.50	0.28
	35SC10		0.45	67.80	0.28
	70SC0		0.90	21.80	0.57
	70SC1		0.90	29.50	0.57
	70SC3		0.90	38.30	0.57
	70SC10		0.90	64.90	0.57
Corinaldesi and Moriconi (2011)	S-RP	-	0.60	63.50	0.25
	S-LP		0.60	63.00	0.25
Ding et al. (2012a)	SF20	Dramix BN 80/60 C	0.44	36.00	0.35
	SF40		1.78	32.50	1.42
	SF60		2.60	41.20	2.08
Ding et al. (2012b)	SF40	-	0.51	64.00	0.32
	SF55		0.71	65.00	0.45

Table 3.31 SFRSCC compressive strength results database properties (continued)

Reference	Mix Label	Fibre type	V_f (%)	f'_c (28 days) (MPa)	$R.I. = (V_f \times l_f/d_f)$
Goel et al. (2012)	SCFRC-1	-	0.50	40.40	0.15
	SCFRC-2		1.00	43.10	0.30
	SCFRC-3		1.50	45.70	0.45
Akcay and Tasdemir (2012)	C0.75N	0.5% HSS + 0.25% NSH	0.75	116.3	0.33
	C0.75H	0.5% HSS + 0.25% HSH	0.75	122.2	0.33
	C1.5N	1.0% HSS + 0.5% NSH	1.50	118.6	0.67
	C1.5H	1.0% HSS + 0.5% HSH	1.50	123.6	0.67
van Zijl and Zeranka (2012)	HPNFRC	Dramix ZP305	0.50	63.3	0.28
			1.00	71	0.55
			1.50	75.9	0.82
	HPSCFRC		0.50	85.5	0.28
			1.00	85.9	0.55
			1.50	91.8	0.82
	NFRC		0.50	34.9	0.28
			1.00	42.6	0.55
			1.50	42.2	0.82
	SCFRC		0.50	57	0.28
			1.00	56.7	0.55
			1.50	58.4	0.82

Table 3.32 SFRC compressive stress-strain relationships database

Reference	Compressive stress-strain relationships for SFRC
Ezeldin et al. (1992)	$\sigma_{cf} = f'_{cf}\left(\frac{\beta\left(\frac{\varepsilon_c}{\varepsilon'_{cf}}\right)}{\beta - 1 + \left(\frac{\varepsilon_c}{\varepsilon'_{cf}}\right)^{\beta}}\right)$ $\beta = 1.093 + 0.7132(3R.I.)^{-0.926}$
Hsu and Hsu (1994)	$\sigma_{cf} = \frac{n\beta\varepsilon_c}{n\beta - 1 + \varepsilon_c^{n\beta}}$ $0 \le x < x_d$ $\sigma_{cf} = \eta_d \exp\left[-k_d\left(\varepsilon_c - x_d\right)^a\right]$ $x_d \le x$, $\eta_d = 0.6$, $k_d = 0.7$, $a = 0.8$ $\beta = \left[\frac{f'_c}{A}\right] + C$, $A = 1.717\left(V_f\right)^3 + 8.501$, $C = -0.26V_f + 2.742$, x_d : strain corresponding to $0.6f'_c$, $n = \begin{Bmatrix} 1.0 \text{ if } f'_c < 79.3, 1.5 \text{ if } 79.3 \le f'_c < 82.73, 2.0 \text{ if } f'_c \ge 82.73 & V_f = 0.5 \\ 1.0 \text{ if } f'_c < 79.3, 1.5 \text{ if } 79.3 \le f'_c < 86.18, 2.0 \text{ if } f'_c \ge 86.18 & V_f = 0.75 \\ 1.0 \text{ if } f'_c < 82.73, 1.5 \text{ if } f'_c \ge 82.73 & V_f = 1.0 \end{Bmatrix}$

Table 3.32 SFRC compressive stress-strain relationships database (continued)

Reference	Compressive stress-strain relationships for SFRC
Mansur et al. (1999)	$\sigma_{cf} = f'_{cf}\left[\dfrac{k_1\beta\left(\dfrac{\varepsilon_c}{\varepsilon'_{cf}}\right)}{k_1\beta - 1 + \left(\dfrac{\varepsilon_c}{\varepsilon'_{cf}}\right)^{k2\beta}}\right]$ $k_2 = \left(\dfrac{50}{f'_{cf}}\right)^{1.3}\left[1 - 0.11\left(\dfrac{V_f\, l}{\phi}\right)^{-1.1}\right]$, $E_{cf} = \left(10300 - 400V_f\right) f_o^{1/3}$, $\varepsilon'_{cf} = \left(0.0005 + 0.00000072\left(\dfrac{V_f\, l}{\phi}\right)\right)\left(f'_{cf}\right)^{0.35}$ For cylindrical specimens: $k_1 = \left(\dfrac{50}{f'_{cf}}\right)^{3.0}\left[1 + 2.5\left(\dfrac{V_f\, l}{\phi}\right)^{2.5}\right]$ For horizontally cast prisms: $k_1 = A\left\{\dfrac{40}{f'_{cf}}\right\}^{2.0}$, $k_2 = B\left\{\dfrac{40}{f'_{cf}}\right\}^{1.3}$ $A = 0.96$ and $B = 0.80$ for fibre concretes while $A = 1.00$ and $B = 1.00$ for plain concrete
Nataraja et al. (1999)	$\sigma_{cf} = f'_{cf}\left[\dfrac{\beta\left(\dfrac{\varepsilon_c}{\varepsilon'_{cf}}\right)}{\beta - 1 + \left(\dfrac{\varepsilon_c}{\varepsilon'_{cf}}\right)^{\beta}}\right]$, $\beta = 0.5811 + 1.93RI^{-0.7406}$
Neves and Almeida (2005)	$\sigma_{cf} = f'_{cf}\dfrac{\left(\dfrac{\varepsilon_c}{\varepsilon'_{cf}}\right)}{(1-p-q) + q\left(\dfrac{\varepsilon_c}{\varepsilon'_{cf}}\right) + p\left(\dfrac{\varepsilon_c}{\varepsilon'_{cf}}\right)^{(1-q)/p}}$, $p + q = 1 - \dfrac{f'_c}{E_c\,\varepsilon'_c}$, $E_{cf} = \left(10.5 - 0.22\,V_f\right) f_c^{1/3}$, $\varepsilon'_{cf} = 0.69 \times f'^{\left[0.29 + 0.0002 V_f\left(lf/d_f^2\right)\right]}_{cf}$, $\dfrac{1-q}{p} > 0$ Neves (2000): $p = 1 - 0.85 \times f'^{\left[-0.0013 \cdot V_f\left(lf/d_f^2\right)\right]}_{cf}$
Bhargava et al. (2006)	$\sigma_{cf} = f'_{cf}\left[\dfrac{k_1\beta\left(\dfrac{\varepsilon_{cf}}{\varepsilon'_{cf}}\right)}{k_1\beta - 1 + \left(\dfrac{\varepsilon_{cf}}{\varepsilon'_{cf}}\right)^{k2\beta}}\right]$, $\beta = \dfrac{1}{1 - \dfrac{f'_{cf}}{\varepsilon'_{cf}\,E_{if}}}$, Modifications: $\beta = \left[\dfrac{f'_{cf}}{A}\right]^3 + C$ $A = 50.35 + 22.31(R.I.)_s + 19.13(R.I.)_l$, $C = 2.04 - 0.313(R.I.)_s - 0.155(R.I.)_l$ For the ascending portion of the curve: $k_1 = 1$, $k_2 = 1$ For the descending portion of the curve: $k_1 = \left[\dfrac{D}{f'_{cf}}\right]^{3.79}$, $k_2 = \left[\dfrac{G}{f'_{cf}}\right]^{1.46}$ $D = 35.635 + 17.21(R.I.)_s + 9.11(R.I.)_l$, $G = 31.82 + 16.39(R.I.)_s + 9.35(R.I.)_l$
Oliveira Júnior et al. (2010)	$\sigma_{cf} = f'_{cf}\left[\dfrac{\beta\left(\dfrac{\varepsilon_c}{\varepsilon'_{cf}}\right)}{\beta - 1 + \left(\dfrac{\varepsilon_c}{\varepsilon'_{cf}}\right)^{\beta}}\right]$, $\beta = \left(0.0536 - 0.5754\,V_f\right) f'_{cf}$, $\varepsilon'_{cf} = \left(0.00048 + 0.01886\,V_f\right)\ln f'_{cf}$

Table 3.33 SFRSCC compressive stress-strain relationship database

Reference	Compressive stress-strain relationships for SFRSCC
Cunha (2006)	Fitted for SCC: $f_{cm}(t) = f_{cm,28}\exp\left\{0.052\left[1-\left(\frac{28}{t}\right)^{0.89}\right]\right\}$ Fitted for SCC: $E_c(t) = E_{c,28}\left\{\exp\left[0.1\left(1-\left(\frac{28}{t}\right)^{0.97}\right)\right]\right\}^{0.17}$ Fitted for SCC: $E_{ci} = 13\left(\frac{f_{cm}}{10}\right)^{0.6}$ Strain at peak stress: $\varepsilon_{c1} = \frac{\varepsilon_{c1,28}\frac{t}{28}}{\frac{t}{28}-0.008}$ Stress–strain model: $\sigma(\varepsilon_c) = f_{cm}\frac{\frac{E_{ci}}{E_{c1}}\frac{\varepsilon_c}{\varepsilon_{c1}}-\left(\frac{\varepsilon_c}{\varepsilon_{c1}}\right)^2}{1+\left(\frac{E_{ci}}{E_c}-2\right)\frac{\varepsilon_c}{\varepsilon_{c1}}} \qquad \varepsilon_c \le \varepsilon_{c,\lim}$ $\varepsilon_{c,\lim} = \varepsilon_{c1}\left[\frac{1}{2}\left[(1-\alpha)\frac{E_{ci}}{E_{c1}}+2\alpha\right]+\left[\frac{1}{4}\left[(1-\alpha)\frac{E_{ci}}{E_{c1}}+2\alpha\right]^2-\alpha\right]^{0.5}\right]$ $\sigma(\varepsilon_c) = f_{cm}\left[\left[\frac{1}{\frac{\varepsilon_{c,\lim}}{\varepsilon_{c1}}}\xi\left(\frac{1}{2\alpha}\right)^2-\frac{1}{\left(\frac{\varepsilon_c}{\varepsilon_{c1}}\right)^2}\frac{1}{\alpha}\right]\left(\frac{\varepsilon_c}{\varepsilon_{c1}}\right)^2+\left[\frac{1}{\frac{\varepsilon_{c,\lim}}{\varepsilon_{c1}}}\frac{2}{\alpha}-\xi\left(\frac{1}{2\alpha}\right)^2\right]\frac{\varepsilon_c}{\varepsilon_{c1}}\right]^{-1}$ $\xi = \frac{4\left[\left(\frac{\varepsilon_{c,\lim}}{\varepsilon_{c1}}\right)^2\left(\frac{E_{ci}}{E_{c1}}-2\right)+2\frac{\varepsilon_c}{\varepsilon_{c1}}-\frac{E_{ci}}{E_{c1}}\right]}{\left[\frac{\varepsilon_{c,\lim}}{\varepsilon_{c1}}\left(\frac{E_{ci}}{E_{c1}}-2\right)+1\right]^2}$ $\alpha = 0.9\exp\left\{0.005\left[1-\left(\frac{28}{t}\right)^{1.16}\right]\right\}$

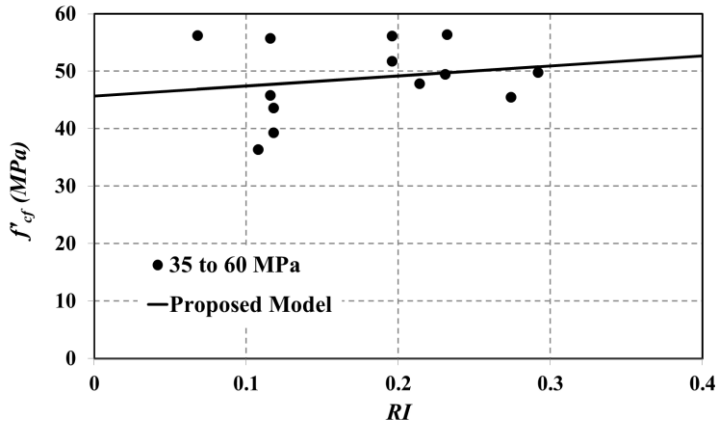

(a)

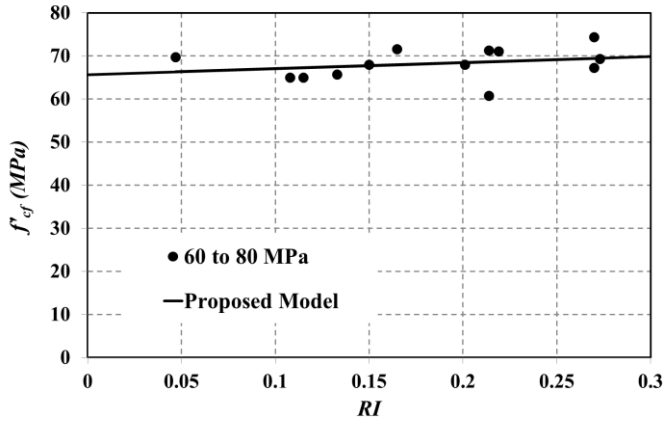

(b)

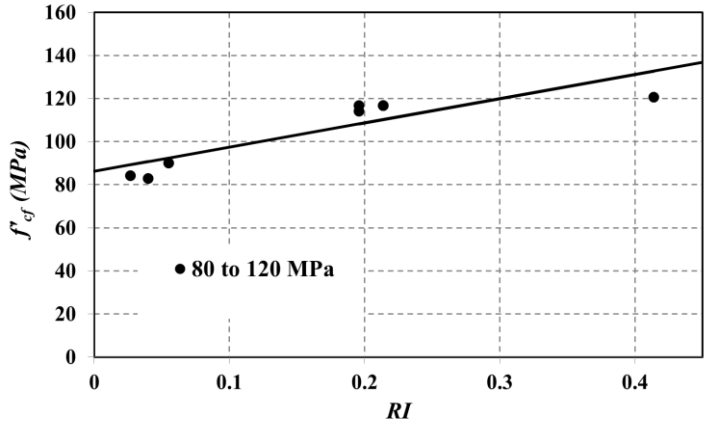

(c)

Figure 3.32 Proposed relationship for compressive strength of SFRSCC versus reinforcing index of fibre (a) 35-60, (b) 60-80, and (c) 80-120 MPa

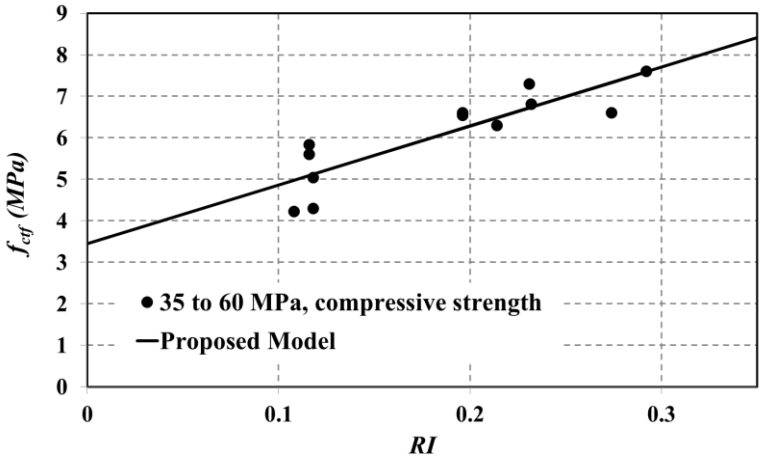

(a)

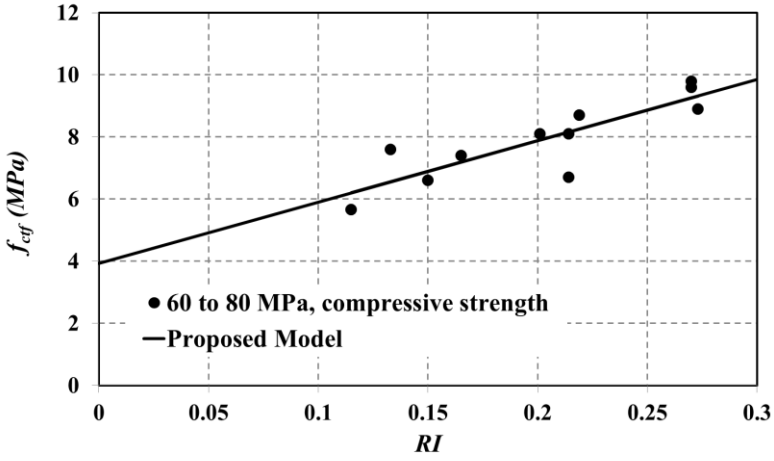

(b)

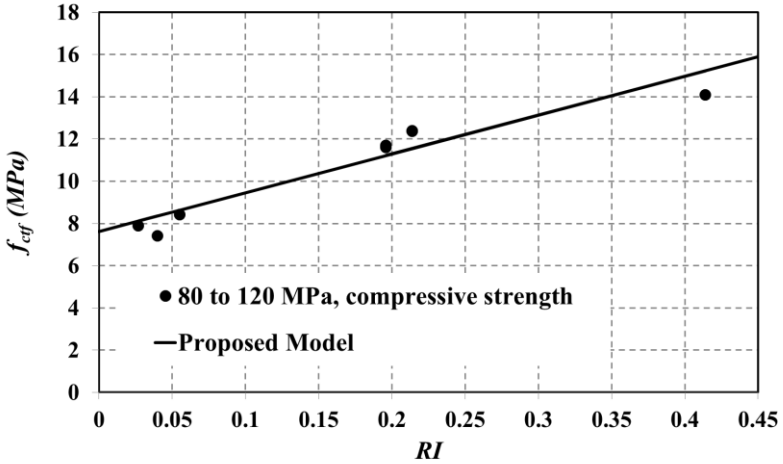

(c)

Figure 3.33 Proposed relationship for tensile strength of SFRSCC versus reinforcing index of fibre (a) 35-60, (b) 60-80, and (c) 80-120 MPa

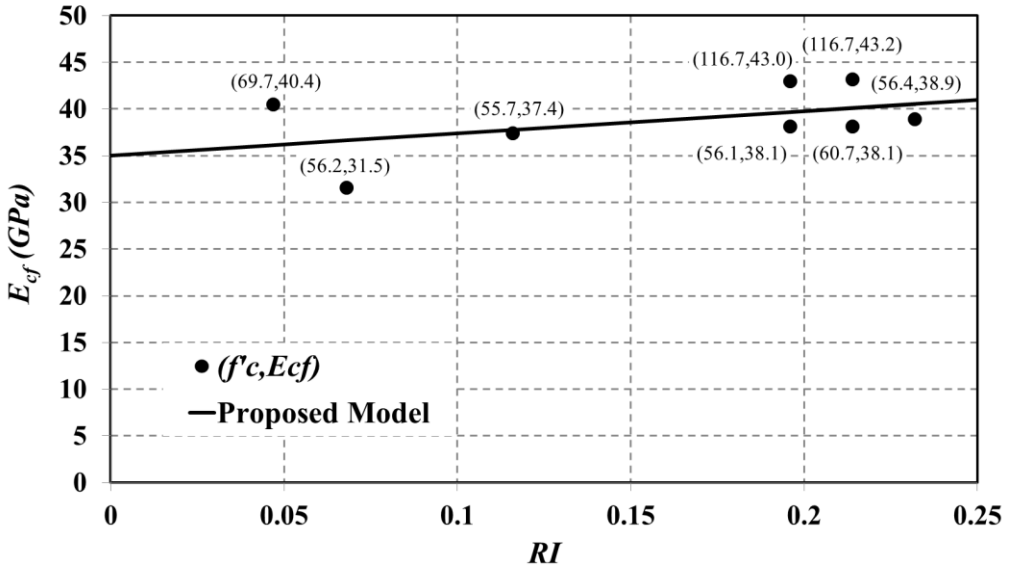

Figure 3.34 Proposed relationship for modulus of elasticity of SFRSCC versus reinforcing index of fibre

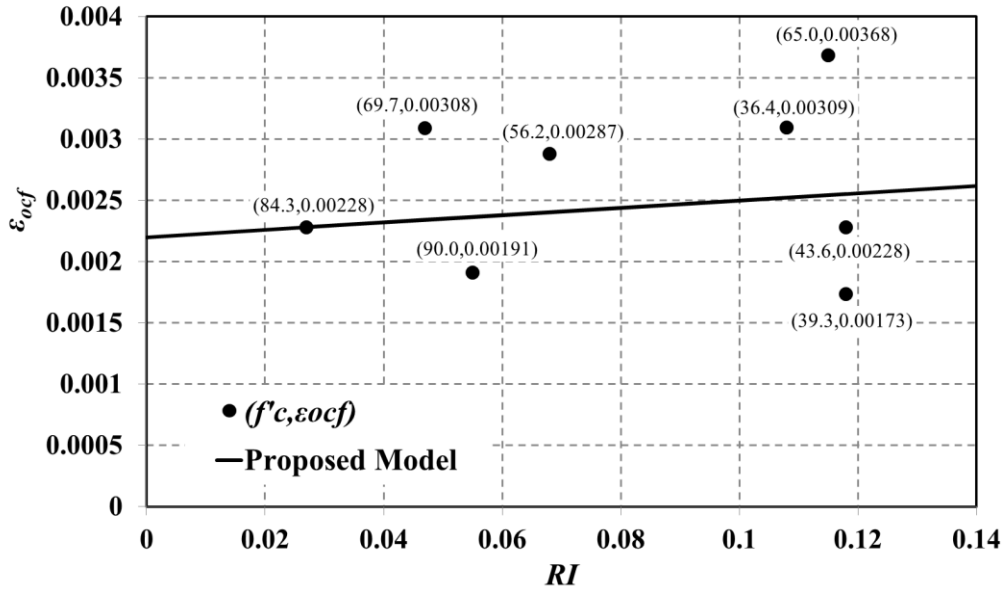

Figure 3.35 Proposed relationship for strain at peak stress of SFRSCC versus reinforcing index of fibre

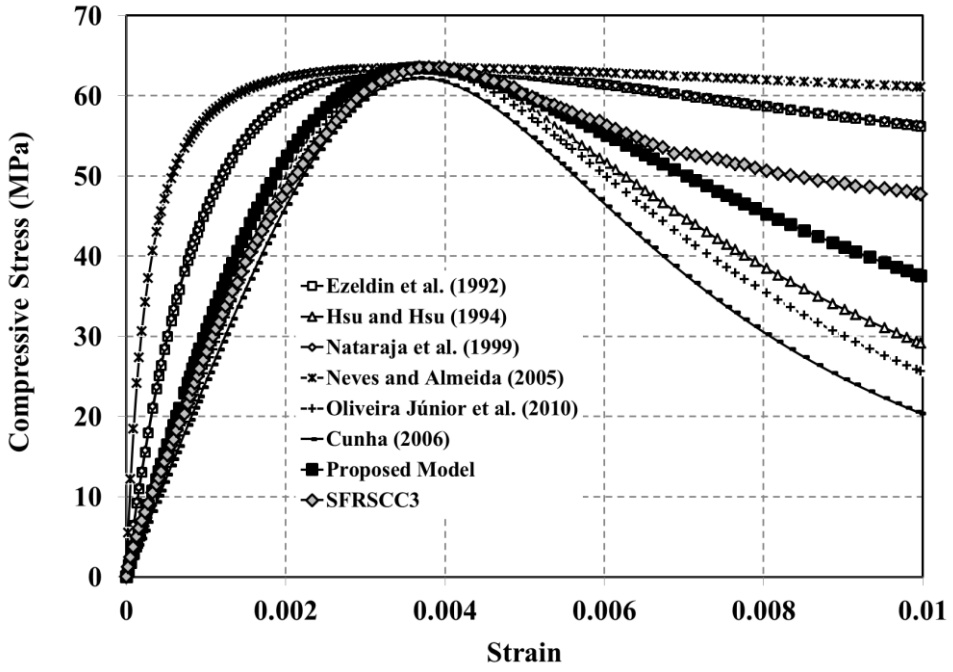

(a)

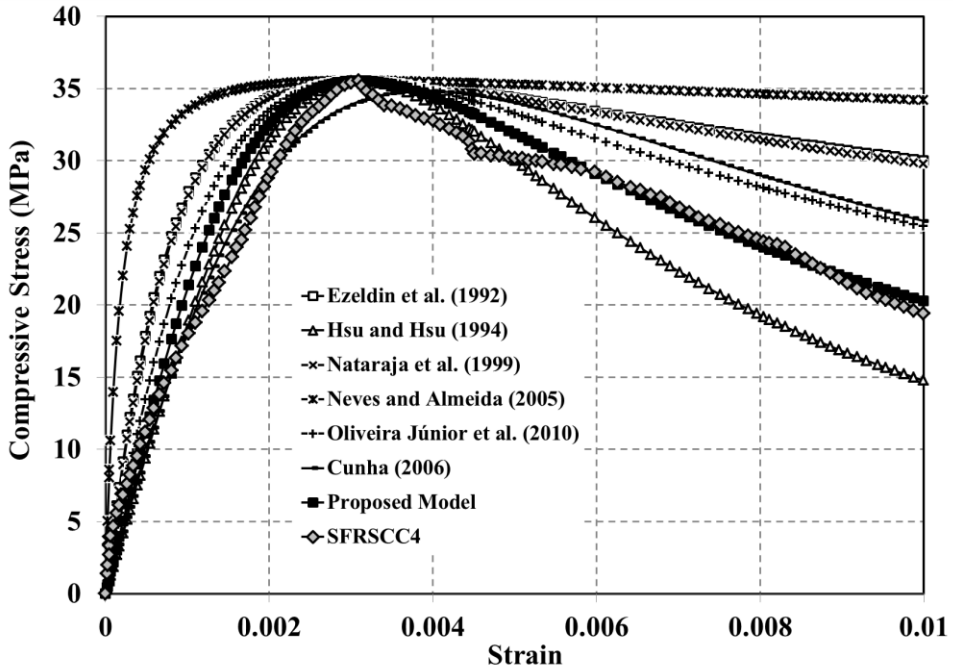

(b)

Figure 3.36 (a, b) Comparison between Liao et al. (2006) experimental tests with compressive stress-strain relationships (a) SFRSCC3, (b) SFRSCC4

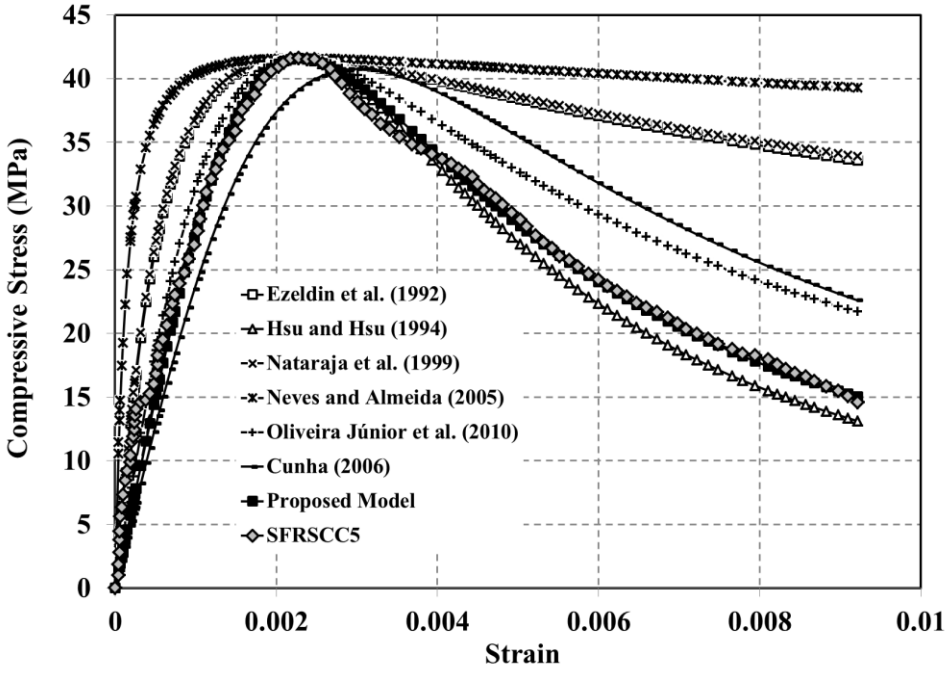

(c)

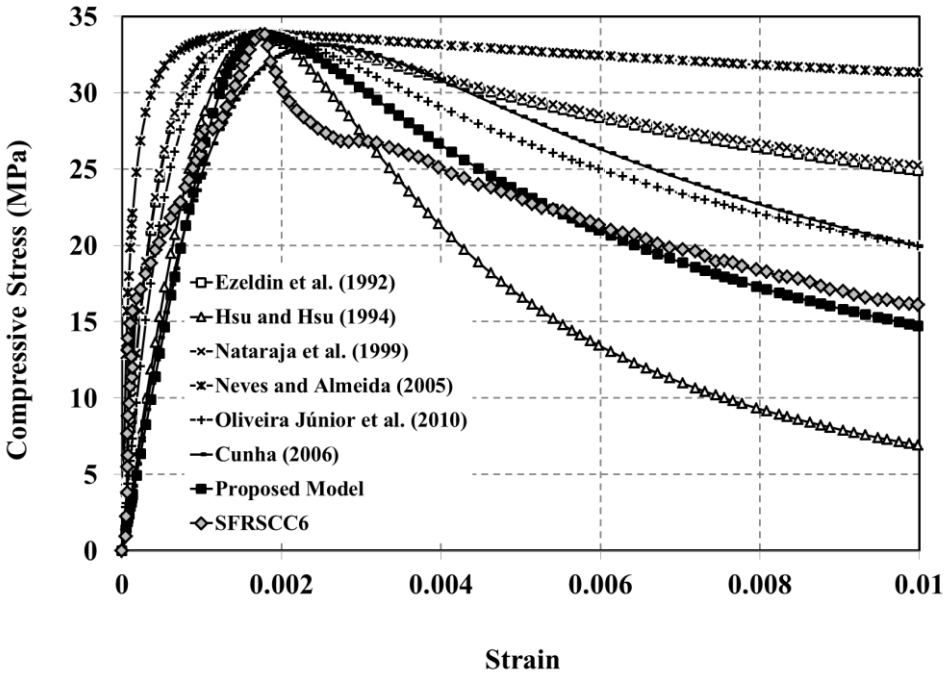

(d)

Figure 3.36(c, d) Comparison between Liao et al. (2006) experimental tests with compressive stress-strain relationships (c) SFRSCC5, and (d) SFRSCC6 mixtures

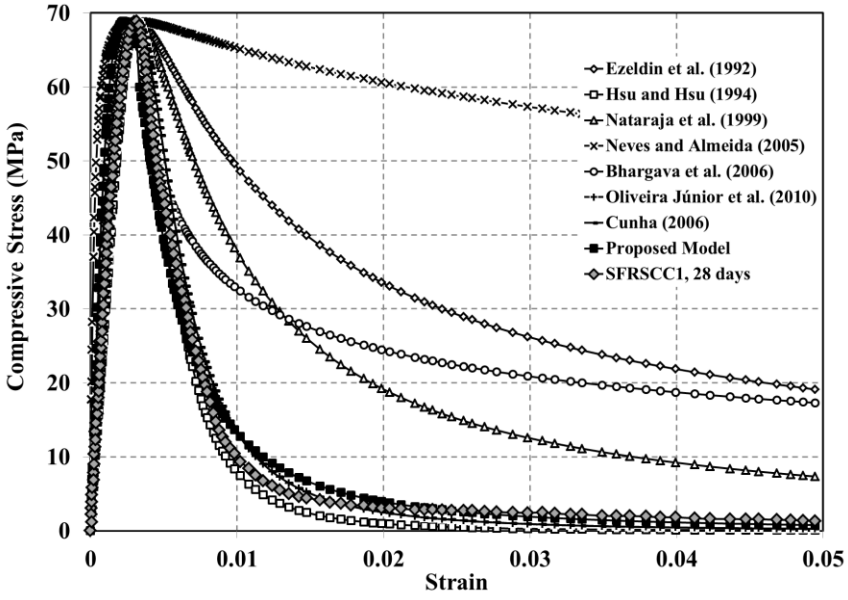

(a)

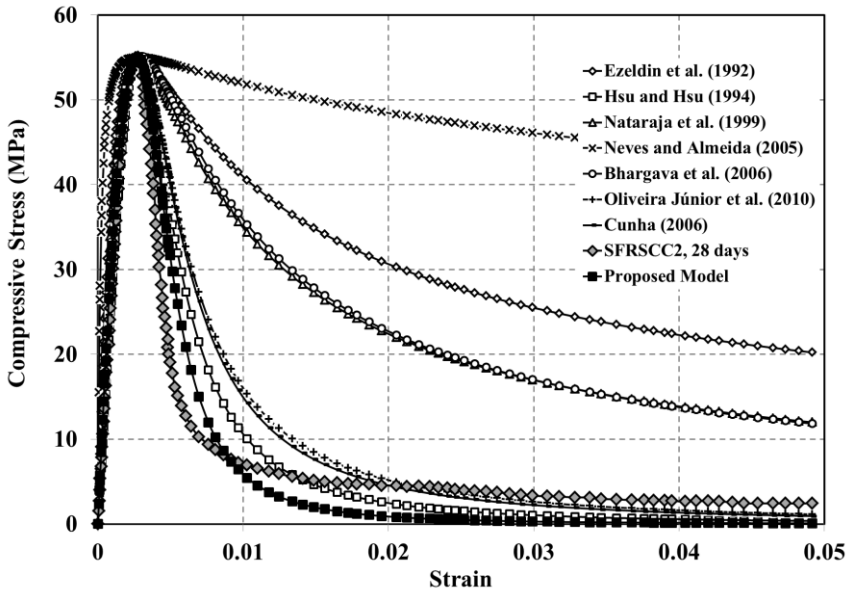

(b)

Figure 3.37 Comparison between Cunha (2006) experimental tests with compressive stress-strain relationships (a) SFRSCC1 and (b) SFRSCC2 mixtures

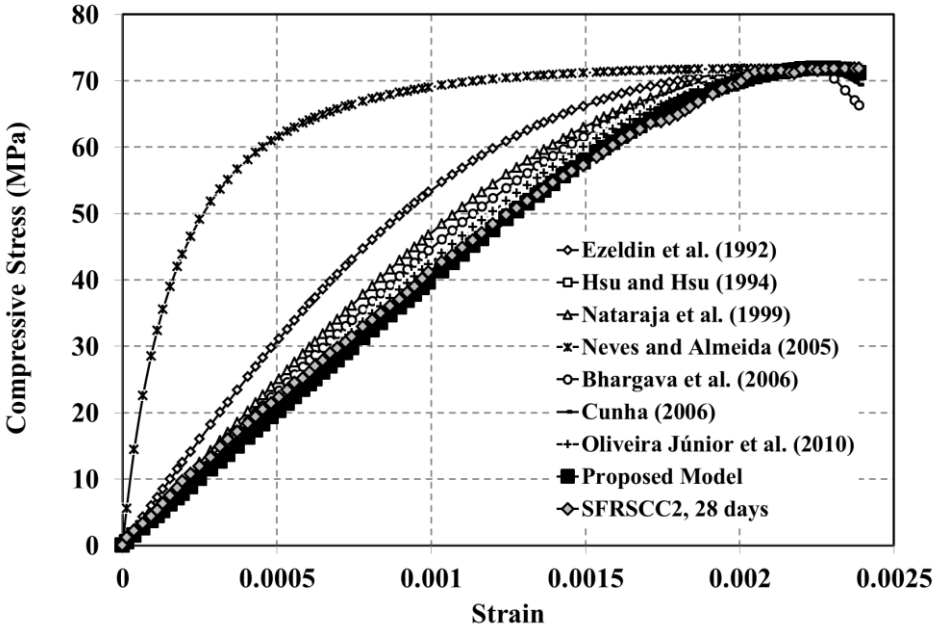

(a)

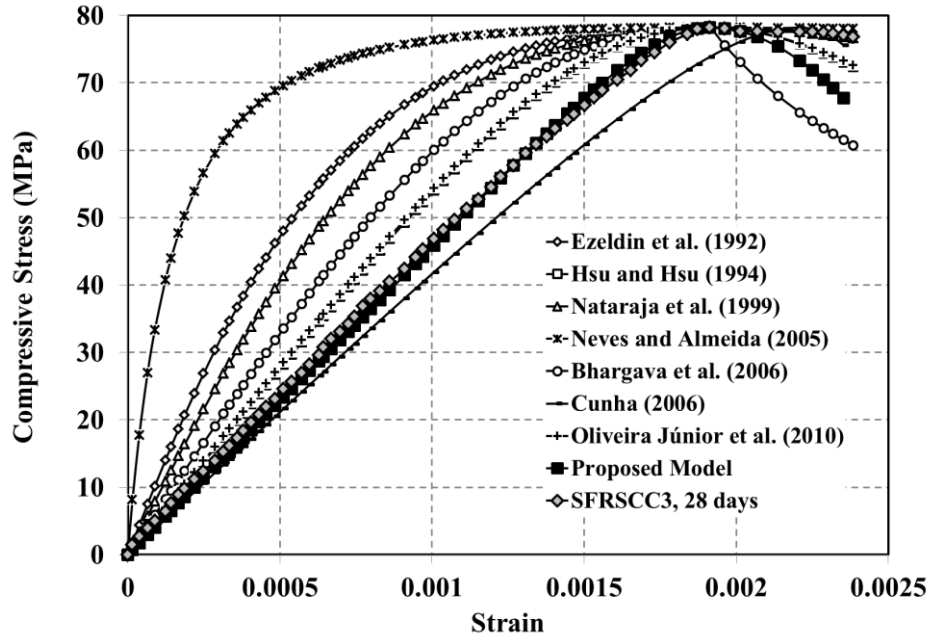

(b)

Figure 3.38 Comparison between Dhonde et al. (2007) experimental tests with compressive stress-strain relationships (a) SFRSCC2 and (b) SFRSCC3 mixtures

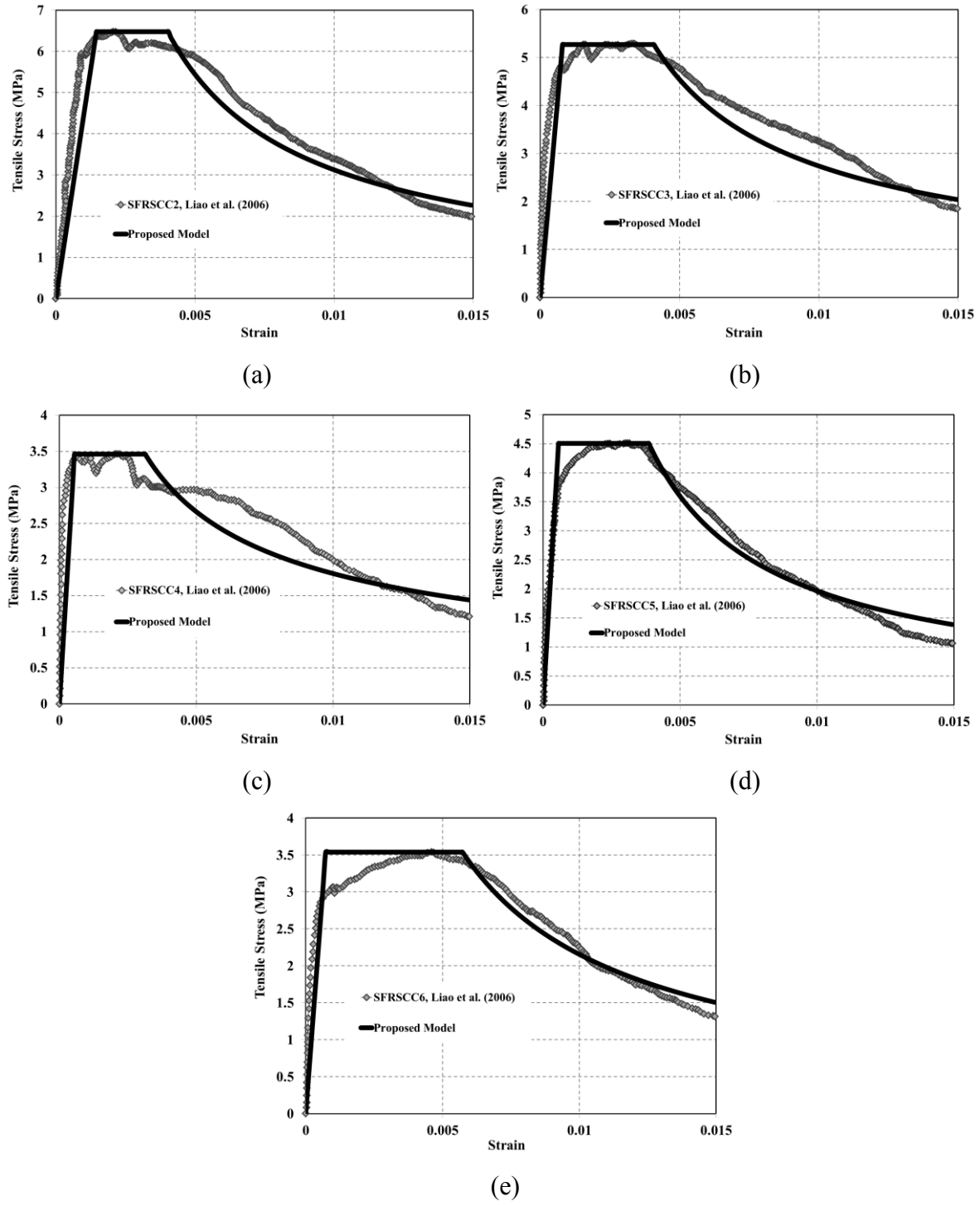

Figure 3.39 Comparison between Liao et al. (2006) experimental tests with proposed tensile stress-strain relationship (a) SFRSCC2, (b) SFRSCC3, (c) SFRSCC4, (d) SFRSCC5, and (e) SFRSCC6 mixtures

3.8 BOND CHARACTERISTICS OF STEEL FIBRE REINFORCED SELF-COMPACTING CONCRETE

In the fresh state, SFRSCC homogeneously spreads due to its own weight, without any additional compaction energy, due to filling and passing ability, as well as segregation resistance. In the hardened state, the addition of fibres to a brittle cementitious matrix mostly contributes to the improvement of the impact resistance and the energy absorption capacity (ACI Committee 544, 2008), because the fibres that bridge the cracks will allow stress transfer between the cracked planes and then retard the crack opening propagation. SFRC resists tensile forces through a composite action of the matrix and the fibres. A part of the tensile force is resisted by the matrix, while the other part is resisted by the fibres. Each of these resistances is determined by the stress transfer at the fibre–matrix interface, which is achieved by the bond defined as the shear stress acting at the interface. Before any cracking takes place, elastic stress transfer is dominant. At more advanced stages of loading, debonding across the interface usually takes place, and frictional slip governs the stress transfer at the interface. Therefore, the mechanical properties of SFRC, especially its tensile strength, tensile stress–strain curve, and toughness, are influenced by the bond characteristics at the fibre–matrix interface (Mandel et al., 1987, Stang and Shah, 1986, Armelin and Banthia, 1997, Li et al., 2002). Accordingly, it is necessary to study the bond properties between the matrix and fibre prior to examining the various mechanical properties of SFRC (Lee et al., 2010). The bond characteristics depend on several factors including the orientation of the fibres relative to the direction of the applied load, the embedded length of the fibres, the shape of the fibres, and strength of the matrix. Many researches concerning bond properties have been conducted to reveal the effects of the parameters related to fibre geometry or strength of the matrix (Chanvillard and Aïtcin, 1996, Sujivorakul et al. 2000, Ezeldin and Balaguru, 1989, Shannag et al. 1996, 1997, Orange et al., 1999, Morton and Groves, 1974, Bartos, 1981, Li et al. 1990). Several models to predict the pullout behaviour of fibres have been proposed (Wang et al., 1988, Stang et al. 1995, Lin et al. 1999, Nammur and Naaman, 1991, Naaman et al. 1991) so far. However, the inclination angle of a fibre in a cementitious matrix has a strong influence on the pullout resistance. Although several researchers have performed experiments to

investigate the effect of the fibre inclination angle, the focus was mostly on the peak pullout load. Thus, fibre inclination effect is still disputable (Armelin and Banthia, 1997, Morton and Groves, 1974, Bartos, 1981, Li et al. 1990). It is generally agreed that the effect of fibre inclination angle on the pullout load and pullout energy depends on the fibre aspect ratio (ratio of fibre length to equivalent fibre diameter), fibre shape (straight, hooked, corrugated etc.), and material properties such as yield strength whether the fibre material is metallic or synthetic (Lee et al., 2010). Based on the choice of criterion which is used for the fibre-matrix interfacial debonding, the theoretical analysis of the fibre pullout problem can be classified into two distinct approaches: strength-based and fracture mechanics-based approaches. Theoretical models based on the former approach use maximum interfacial shear stress as the interfacial debonding criterion. Therefore, when the interfacial shear stress exceeds the interfacial bond strength, debonding is supposed to occur. On the other hand, in the theoretical models based on the concepts of fracture mechanics, the debonded zone is considered as an interfacial crack, and the extension of the crack depends on the energy criterion that should be satisfied (Dubey, 1999).

Although the available research concerning the influence of steel fibres on the properties of SFRSCC is limited, this research investigates the bond characteristics between steel fibre and the matrix made of SCC. The objectives of the present section are: (a) to modify the aligned fibre pullout model based on the available experimental results of SFRSCC. (b) to propose a fibre pullout model allowing for the fibre inclination utilizing the available experimental results. (c) to include the influence of the different fibre types (smooth, hooked), fibre inclination and fibre embedment length influence in the fibre pullout models.

3.8.1 Experimental and Analytical Database for Bond Characteristics of SFRSCC

The experimental results included in the database are developed mainly from Grünewald (2004), Holschemacher and Klug (2005) and Cunha (2007) studies. It includes information regarding the composition of the mixtures, fresh properties of SFRSCC and testing methodology and conditions. However, it should be emphasized that this aspect has not been investigated as broadly as the other aspects of SFRSCC therefore the published

experimental data is still not very extensive (Dubey, 1999). Using experimental data results from different sources can frequently be problematic for the following reasons: 1. there is often insufficient information regarding the exact composition of the concrete mixtures; 2. the size of the specimens, curing conditions, and testing methodology vary between the different investigations and, in some cases, this information is not fully indicated; 3. in many cases, it is difficult to extract the relevant experimental values because the published results are incomplete or presented in graphical form and the data values have to be extrapolated. Table 3.34 presents a general summary of the fibre shape (smooth or hooked-end), fibre length (l_f) and diameter (d_f), outer radius of the matrix cylinder b, tensile strength of fibre, compressive strength of concrete (f'_c), inclination angle, fibre type, cement type, filler type and embedment length (l_b).

In Table 3.35, Grünewald's (2004) experimental results are summarized. The dataset includes the peak pullout force, the average force (the length of the hook is equal to the displacement which fibre requires to completely enter the straight channel) and the average frictional force (up to the slip at which the load rapidly dropped to zero). In addition, it includes different types of fibre, embedded lengths, different concrete types (SCC or conventional concrete CC) and different compressive strengths (45, 65, 105 MPa). In Table 3.36, the experimental results of Holschemacher and Klug (2005) are shown. It summarizes the peak pullout force, slip at peak pullout force for different types of fibre (long and short end hook, smooth, l_f/d_f=50 and l_f/d_f =62.5), concrete ages (3, 7 and 28 days) and concrete types (SCC or CC). In Table 3.37, Cunha's (2007) experimental results which include the peak pullout force, slip at peak pullout force for different types of fibre (hooked and smooth), inclination angle and embedment length are summarized.

From investigation conducted by Aslani and Nejadi (2011c; 2011d) on the bond characteristics of steel fibre in the SCC matrix experimental tests, the following conclusions can be derived: a) The maximum pullout force and the average force within the length of the hook of SCC are significantly higher than CC. The frictional resistance was also larger in most cases but a few results were found to be lower. b) The compressive strength of concrete influences the pullout loads but not in the expected order of magnitude. That means by increasing the concrete age and consequently the compressive strength the

ultimate load increases as well. c) The influence of a small inclination of the end hook seems to be more effective than the compressive strength of SCC. d) The slip at peak pullout force increases with the inclination angle for both hooked and smooth fibres. e) In the larger cross-sectional area under stress, fibres with lower aspect ratio (l_f/d_f) show higher pullout loads than fibres at a higher aspect ratio in SCC mixtures. f) The bond behaviour of fibres embedded in SCC is more efficient than of those fibres embedded in CC. g) In SCC, for both hooked and smooth aligned fibres, the configuration of the pullout load-slip curve was similar (regardless of the fibre embedded length). However, the peak load and the dissipated energy increase as expected. h) In the case of aligned fibres the influence of l_b is more significant on the smooth fibres, while relatively small increments are registered for the hooked end fibres. i) For both hooked and smooth fibres the highest maximum pullout load is observed for an inclination angle of 30°. However, the increase of the maximum pullout load with the inclination angle is more significant on the smooth fibre types. j) For SCC without fibres the direction of the casting pullout test specimens does not significantly influence the bond stress–slip relationship. k) The addition of steel fibres slightly influences the bond behaviour in the case of pullout bond failure and is expected to have a pronounced effect in the case of splitting bond failure.

3.8.2 Overview of the Theoretical Pullout Models

Cox (1952) has developed the first strength-based analytical model to describe the transfer of the stress between fibre and matrix. This model assumes that the tensile stress in the matrix is negligible if compared to those in the fibre and the shear stresses in the fibre. In addition, the shear stresses in the fibre are small compared to those in the matrix. Assuming compatibility of the fibre and matrix displacement at interface, i.e., no slip, Cox (1952) derived analytical expressions for the axial stress distribution in the fibre and the shear stress distribution at the interface. Greszczuk (1969) was the first to derive an interfacial debonding criterion using the shear-lag theory. The analytical model by Greszczuk (1969) was also based on similar assumptions as Cox (1952), but later postulated that at the instant when the shear strength of the interface is first attained, catastrophic debonding would occur over the entire embedded length of the fibre. However, in reality, debonding may be limited to the zone in which the elastic shear stress exceeds the adhesional shear bond

strength and in those circumstances, the process of load transfer will comprise the frictional shear transfer at the debonded zone and elastic shear transfer over the remaining length of the fibre. Greszczuk's model did not include the possibility of the existence of frictional bond, which constituted a major limitation of the model. Thus, his solution did not consider the stabilization of the debonding process that may take place due to the existence of frictional shear bond at the debonded interface. Further, Lawrence (1972) extended the theory developed by Greszczuk (1969) by taking into account the process of progressive debonding of the fibre-matrix interface. He suggested that the maximum fibre pullout load would occur at the instant when debonding of that part of fibre length where the elastic bond is still intact takes place in a catastrophic manner. The model developed by Lawrence (1972) includes the effects of both the interfacial elastic shear stresses and the frictional shear stresses, and it recognizes the conditions for either a gradual, or an instantaneous debonding of the interface. He has shown that the form of the distribution of the shear stress and the load along the fibre length depends upon the elastic properties of constituents and the fibre embedded length. In this model, interfacial frictional shear stresses over the entire debonded zone were assumed to remain constant.

Models developed by Gopalratnam and Shah (1987), Nammur et al. (1988), Gopalaratnam and Cheng (1988), Stang et al. (1990) also took into account the combined stress transfer mechanisms. It is apparent that the shear stresses (both elastic and frictional) that develop parallel to the fibre-matrix interface are of extreme importance in controlling the fibre-matrix stress transfer mechanism. However, stresses and strains may also develop normal to the fibre-matrix interface as a result of Poisson's effect, volume change, and multiaxial loading. They may induce considerable variations in the resistance of frictional slip, which is sensitive to normal stress. A comprehensive approach to the stress-transfer problem therefore requires simultaneous treatment of all the above-mentioned effects, including elastic shear transfer, frictional slip, debonding and normal stresses and strains. Analytical models developed by Takaku and Arridge (193) and Hsueh (1988, 1990a, 1990b) are more comprehensive than the previously cited models since these models take into consideration the influence of Poisson's contraction of the fibre on the pullout test. However, these aspects were considered in the analysis only after the occurrence of complete interfacial debonding (i.e., in the fibre pullout case as explained later). Thus, the

influence of Poisson's contraction during progressive debonding remained unaccounted, which constituted a major limitation of this model. The model by Hsueh (1988) considers Poisson's effect during progressive debonding, however the analysis and the closed-form solutions presented are complex to use. Furthermore, Nammur and Naaman (1989) proposed an analytical model of the bond at the interface between steel fibres and cementitious composites, assuming an idealized bond–slip relationship. The assumed relationship is bilinear and elastic-perfectly frictional. This model was limited with bond stress in the interface and does not deal with the pullout behaviour. Naaman et al. (1991a) proposed an analytical solution for the bond behaviour using the relationship between the bond behaviour curve and the shear stress–slip curve at the interface. The authors also adopted values of the post-debonding frictional stress on the slip based on experimental results instead of the constant value assumed in Nammur and Naaman (1989). The fibre pullout model introduced by Nammur et al. (1988) is a cohesive interface type model. A cohesive interface type model assumes that only relative displacements between the fibre and the matrix can activate the stress transfer at the interface. Also, in these types of models the interfacial traction is described as a function of the displacement discontinuity, and since there is a unique relationship between interface traction and interface displacement discontinuity, it is not required to distinguish between the debonded and bonded interface. Since the interfacial bond due to chemical adhesion is not a slip induced bond, the application of the assumed bond stress versus slip relationship in this model is limited to the cases where chemical adhesion is negligible. The other major limitation of this model is that it assumes a constant value of interfacial shear stress at the debonded face. Applying the bond stress versus slip constitutive relationship to a cylindrical fibre-matrix coaxial pullout model, relationships were derived for interfacial shear stress distribution, axial shear stress distribution, and fibre displacement at the various stages of pullout loading. Applying the shrink-fit theory to the problem and hypothesizing that the radial misfit between fibre and matrix decreases as fibre is pulled out of the matrix, Naaman et al. (1991a; 1991b) modified the previously developed model by Nammur et al. (1988). It has been shown that as is the fibre pulled out from the matrix, the interfacial frictional shear stress at the debonded interface decreases as a result of the decrease in radial misfit.

Numerous studies have been also conducted on deformed fibres with different shapes, such as hook-shaped fibres, and analytical models were proposed by Alwan et al. (1999), Chavillard (1999), and Sujivorakul et al. (2000). The above discussion brings to attention the inadequacy of the existing fibre pullout models, and also the fact that a need exists for a model that realistically captures the physical phenomenon occurring during the process of fibre pullout. To model the pullout behaviour of steel fibre in SFRSCC, this section applies the progressive debonding model for fibre pullout proposed by Dubey (1999), which appears to be the most suitable model for this composite. This fibre pullout model considers the evolution of the interfacial coefficient of friction during the process of fibre pullout. Additionally, the proposed model takes into account the following aspects that are either considered or ignored in the earlier models: 1) Dependence of the initial debonding stress on the embedded fibre length; 2) Radial dependence of the axial stress in the matrix; 3) Explicit inclusion of the interfacial properties such as the contact stress and the coefficient of friction; 4) Poisson's effect (in the event of a debonded fibre).

The Dubey (1999) model is briefly described below. This model has been explained in detail in Dubey (1999). Consider a fibre of radius a and length L embedded in the centre of the matrix coaxial cylinder with inner radius a and outer radius b. A cylindrical coordinate system is selected so that the z-axis corresponds to the fibre axial direction and r-axis corresponds to the radial direction. The embedded end of the fibre is located at z=0, and the other end where the fibre exits the matrix is located at z=L. The exit-end of the fibre (i.e., at z=L) is subjected to the tensile stress σ_0. Both fibre and matrix are assumed to be elastic. Recall that transfer of the stress between the fibre and the matrix is via interfacial shear stresses (see Figure A.1).

In this model, the entire pullout process can be divided into three stages:

1. As shown in Figure A.1, a fibre completely bonded along its length: During stage 1, fibre and matrix displacements at the interface remain compatible, and the resistance to fibre pullout is derived from the adhesional shear stresses at the interface. At the end of stage 1, debonding of the interface is initiated at the location where the fibre enters the matrix (see Appendix-A).

2. Figure A.2 shows that a fibre that is partially bonded along its embedded length: During stage 2, progressive debonding of the interface is initiated at the location where the fibre exits the matrix. The adhesional shear stresses at the bonded interface and the frictional shear stresses at the debonded interface resist the fibre pullout. At the end of stage 2, the fibre is completely debonded along its embedded length (see Appendix-A).

3. As shown in Figure A.3, the fibre is completely debonded over its embedded length and is pulled out: At the end of Stage 2, pullout of the fibre is initiated, and thereafter, the interfacial frictional shear stresses connect the pullout of the fibre from the matrix (see Appendix-A).

Dubey's model is capable of taking into account the evolution of the interfacial properties during the pullout process. This model captures the essential features of the pullout process, including the progressive interfacial debonding and Poisson's effect in the event of a debonded fibre.

Table 3.34 SFRSCC database for the included bond characteristics investigations

Reference	Smooth fibre	Hooked-end fibre	l_f(mm)	d_f(mm)	Outer radius of matrix cylinder b (mm)	Tensile strength of fibre (MPa)
Grünewald (2004)	no	yes	30, 60	0.38, 0.75	32.5	1050
Holschemacher and Klug (2005)	yes	yes	50	0.8, 1	50	1100
Cunha (2007)	yes	yes	60	0.75	40	1100
Reference	f'_c (MPa)	Inclination angle (°)	Fibre type	Cement type	Filler type	Embedment length l_b (mm)
Grünewald (2004)	45, 65, 105	-	Dramix 80/60 BP and Dramix 80/30 BP	CEM III 42.5 N and CEM I 52.5 R	Fly ash	10,30
Holschemacher and Klug (2005)	48, 67	30, 50	-	CEM I 42.5R	Fly ash	25, 17.5, 12.5
Cunha (2007)	59	0, 30, 60	DRAMIX R° RC-80/60-BN	CEM I 42.5R	Limestone	10, 20, 30

Table 3.35 Experimental results of Grünewald (2004)

l_b (mm)	Fibre type	Peak Pullout Force (N)					
		SCC (B45)	SCC (B65)	SCC (B105)	CC (B45)	CC (B65)	CC (B105)
10	80/30	177.6	193.2	181.4	131.9	164.4	176.6
30	80/60	496.0	614.9	624.8	510.4	529.3	626.5
10	80/60	557.4	590.4	661.6	498.9	488.9	611.9
l_b (mm)	Fibre type	Average Hook Force (N)					
		SCC (B45)	SCC (B65)	SCC (B105)	CC (B45)	CC (B65)	CC (B105)
10	80/30	109.3	110.9	103.8	73.5	87.2	106.6
30	80/60	386.8	462.2	464.7	383.7	403.5	446.3
10	80/60	378.2	427.5	446.4	353.9	360.4	424.0
l_b (mm)	Fibre type	Frictional Force (N)					
		SCC (B45)	SCC (B65)	SCC (B105)	CC (B45)	CC (B65)	CC (B105)
10	80/30	32.3	23.6	24.4	17.0	16.4	29.5
30	80/60	175.6	215.8	206.4	181.6	186.5	143.8
10	80/60	157.0	227.7	136.5	186.2	155.9	137.3

Table 3.36 Experimental results of Holschemacher and Klug (2005)

	Peak Pullout Force (N)	Slip at Peak Pullout Force (mm)
Mixture type	Hooked fibre (l_f/d_f=50)	Hooked fibre (l_f/d_f=50)
SCC	469.3	0.759
CC	316.0	1.130
Mixture type	Fibre (l_f/d_f=50)	Fibre (l_f/d_f=50)
SCC (Long end hook fibre)	544.4	1.251
SCC (Short end hook fibre)	610.6	1.063
SCC (Smooth fibre)	138.9	1.184
Concrete age	Long end hook fibre (l_f/d_f=50)	Long end hook fibre (l_f/d_f=50)
SCC (3 days)	455.8	1.426
SCC (7 days)	486.2	1.345
SCC (28 days)	546.5	1.244
Concrete age	Long end hook fibre (l_f/d_f=62.5)	Long end hook fibre (l_f/d_f=62.5)
SCC (3 days)	326.0	0.857
SCC (7 days)	300.7	1.148
SCC (28 days)	294.5	1.421

Table 3.37 Experimental results of Cunha (2007)

	l_b (mm)	Peak Pullout Force (N)		Slip at Peak Pullout Force (mm)	
		Hooked fibre	Smooth fibre	Hooked fibre	Smooth fibre
Angle (0°)	10	321.8	-	0.59	-
	20	347.8	77.4	0.65	0.12
	30	388.2	155.2	0.69	0.25
	l_b (mm)	Peak Pullout Force (N)		Slip at Peak Pullout Force (mm)	
		Hooked fibre	Smooth fibre	Hooked fibre	Smooth fibre
Angle (30°)	10	360.9	-	0.94	-
	20	400.1	173.5	1.00	0.19
	30	416.0	203.7	0.80	0.38
	l_b (mm)	Peak Pullout Force (N)		Slip at Peak Pullout Force (mm)	
		Hooked fibre	Smooth fibre	Hooked fibre	Smooth fibre
Angle (60°)	10	342.0	154.2	2.40	3.34
	20	335.2	172.8	2.33	2.02
	30	365.1	189.4	2.64	2.17

3.8.3 Calibration of the pullout model for bond characterization of SFRSCC

By using the database on bond characteristics of SFRSCC as shown in Tables 3.34-3.37, the interfacial properties were calibrated. The coefficient of friction versus pullout distance relationship was calculated from Eq. (3-10) as shown in Figure A.3. In this equation, the interval between p_{d1} and p_{d2} was chosen as 0.5 mm. Work of fibre pullout, W_p, when fibre pullout displacement increase from p_{d1} to p_{d2} can be calculated as following:

$$W_p = \frac{\left(P_{p_{d1}} - P_{p_{d2}}\right)}{2} \times \left(p_{d1} - p_{d2}\right) \tag{3.31}$$

where $P_{p_{d1}}$ and $P_{p_{d2}}$ are the pullout load corresponding to the pullout distance p_{d1} and p_{d2}, respectively. The evolution law for the coefficient of friction can be described by the following Eq.(3.32):

$$\mu = \left(\mu_i - \mu_{ss}\right)e^{-c\,pd} + \mu_{ss} \tag{3.32}$$

where μ_i is the initial coefficient of friction, μ_{ss} is steady state value of the coefficient of friction attained at large pullout distances and c is a constant that governs the rate at which the coefficient of friction decays with increase in pullout distance (Dubey, 1999).

By using experimental results of the database the coefficients of friction for smooth and hooked fibres by considering normal or high strength SCC are proposed as shown in Table 3.38. The coefficient of friction versus pullout distance curves obtained using equations in Table 3.38 for smooth and hooked fibres with different lengths (15 mm to 60 mm) and normal or high strength SCC are plotted in Figures 3.40 and 3.41. In these figures, it can be seen that the coefficient of friction, μ, decreases exponentially with increase in pullout distance. Table 3.39 compares the Grünewald (2004) experimental results including the measured peak pullout force with the predicted peak pullout force by utilizing the proposed coefficient of friction in the modified Dubey (1999) model. In addition, Figure 3.42 compares experimental results of Holschemacher and Klug (2005) including the load–slip curves and the predicted curves by using the proposed model for smooth and hooked fibre.

3.8.4 Calibration of the Pullout Model by Allowing for the Effect of Fibre Inclination Angle in the Bond Characterization of SFRSCC

Modelling was implemented through a comparison of the pullout test results according to change of the inclination of the fibres. The modelling for the bond behaviour of inclined fibres is based on the pullout model for the aligned fibre (as shown in Figs.A.1 to A.3). The modelling of the bond behaviour for inclined fibres considers the variation of load due to the snubbing effect and matrix spalling effect assumed that the fibre inclination angle (ϕ) is equal to zero (in the case where the fibres are not positioned in the tensile load direction and are inclined, the bridging force will be increased, this phenomenon is called the 'snubbing effect' (Lee et al., 2010; Li et al., 1990; Morton and Groves, 1976; Kanda and Li, 1998). This is accomplished by introducing the apparent bond strength ($\tau_{max(app)}$, $\tau_{f(app)}$) which is illustrated as a function of the inclination angle ϕ. In addition, the increase in the slip displacement is reflected by multiplying the corresponding slip to $\phi = 0$ by the coefficient β, which is also a function of the inclined angle ϕ. Table 3.40 gives the values of $\tau_{max(app)}$, $\tau_{f(app)}$ and β obtained through the comparison with the experimental results of Cunha (2007) for each fibre inclination angle, as well as the corresponding P_{max}. However, in this section, $\tau_{max(app)}$ is equal to $\tau_{f(app)}$ for each fibre inclination angle, since τ_{max} and τ_f are the same for the aligned fibres. Furthermore, the Levenberg–Marquardt algorithm

(Levenberg, 1944) is selected for the nonlinear regression analysis to fit the test results with the parameters $\tau_{max(app)}$ and $\tau_{f(app)}$. A parameter-section is also performed to minimize the sum of squares of errors, as shown in Eq. (3.33).

$$F\left(\tau_{\max(app)}, \tau_{f(app)}\right) = \sum_{1}^{n}\left(P_e - P_m\right)^2 \tag{3.33}$$

where n is the number of data sets, P_m is the measured pullout load from the pullout tests, and $P_e = \sigma_0 A_f$ is the calculated pullout load from Eq. (2-11) as shown in Figure A.2 including the parameters $\tau_{max(app)}$ and $\tau_{f(app)}$. The parameter β is determined by calculating $U_{peak}(\varphi)/U_{peak}(0)$ ratio obtained from the experiments as shown in Tables 3.37 and 3.40 where $U_{peak}(\varphi)$ denotes the peak slip displacement corresponding to the peak load with the inclination angle ϕ. $U_{peak}(0)$ is the peak slip displacement corresponding to the peak load for the aligned fibre. Primarily, this section attempts to express $\tau_{max(app)}$, $\tau_{f(app)}$ and β as a function of ϕ based on the results of Table 3.40. To express these quantities as a function of ϕ, an allowance for the snubbing and matrix spalling effects in P_{max} is made. The snubbing effect could be defined by the following Eqs. (2-5 and 2-7) as shown in Figure A.2.

$$P(\phi) = e^{f\phi}\, P(\phi = 0) \tag{3.34}$$

where f is the snubbing friction coefficient; the value of f varies with the type of the fibre and strength of the matrix. The matrix of spalling effect can be considered by the following equation, assuming that load reduction does not occur when $\phi = 0$ and the pullout force does not act on the fibre when $\phi = \pi/2$.

$$P(\phi) = (\cos\phi)^k\, P(\phi = 0) \tag{3.35}$$

where k is the spalling coefficient and ϕ is in radians. In order to apply the snubbing and matrix spalling effects to the bond behaviour, τ_{app} can be expressed as a function of ϕ using Eqs. (3.34 and 3.35) as follows:

$$\tau_{app}(\phi) = e^{f\phi}\,(\cos\phi)^k\, \tau(\phi = 0) \tag{3.36}$$

Comparison of the experimental results of Cunha (2007) for smooth and hooked steel fibre with two different fibre embedment lengths reveals that the best agreement can be proposed by utilizing Eq. (3.37) for fibre embedment lengths 10 mm and 20 mm; and for

embedment length 30 mm by utilizing Eq. (3.38) as presented below:

$$\tau_{app}(\phi) = e^{1.6\phi}(\cos\phi)^{1.4}\,\tau(\phi = 0) \tag{3.37}$$

$$\tau_{app}(\phi) = e^{0.8\phi}(\cos\phi)^{3}\,\tau(\phi = 0) \tag{3.38}$$

Figures 3.43 and 3.44 compare the shear strengths obtained by using the experimental results and Eq. (2-5) in Figure A.2. The apparent shear strengths are obtained by using Eqs. (3.37 and 3.38) for three different embedment length: 10 mm, 20 mm and 30 mm. In addition, $U(\phi)$ is defined by the following expression considering both the snubbing and the effect of matrix spalling effects.

$$U(\phi) = \beta\, U(\phi = 0) \tag{3.39}$$

$$\beta = 1 + \gamma\left(\frac{2\phi}{\pi}\right)^{n} \tag{3.40}$$

Comparison of the results determined by the above mentioned equations with the experimental results reveals that a good agreement can be achieved if: n = 1.8 and γ = 100 are proposed. Figure 3.45 shows the variation of slip coefficient, β, with respect to ϕ (Eq. (3.40)) using the proposed values of n and γ. Accordingly, the pullout behaviour of an inclined fibre can be expressed in three stages which are shown in Figures A.1 and A.2. Eqs. (3.41 and 3.42) represent the stage 1 when a fibre is completely bonded along the length of the fibre, while Eqs. (3.43 to 3.46) represent Stage 2, when the fibre is partially bonded along its embedded length and finally Eqs. (3.47 to 3.49) correspond to the behaviour in Stage 3 when the fibre is completely debonded over its embedded length. Apparent shear strengths that reflect the effects of a fibre inclination angle, such as snubbing and matrix spalling effects, on both load and slip displacement are adopted in the pulling out procedure.

Stage1*-Fibre completely bonded along the length of the fibre:*

$$\sigma_{\max} = \sigma_d(\phi) = \frac{-2\tau_{\max(app)}(\phi)(\gamma + \alpha - \gamma\eta\alpha + \alpha\eta)}{a\beta}\left[\frac{(\alpha - \gamma\eta\alpha + \alpha\eta)\cosh(\beta L)}{\sinh(\beta L)}\right]^{-1} \tag{3.41}$$

$$(\sigma_{\max}/U_b)(\phi) = \frac{[((\alpha - \gamma\eta\alpha + \alpha\eta)\cosh(\beta L))/\sinh(\beta L)]^{-1}}{E_f\,\alpha\beta\,[\{((\alpha - \gamma\eta\alpha + \alpha\eta)\cosh(\beta L))/\sinh(\beta L)\} + \gamma L]} \tag{3.42}$$

Stage 2*- Fibre partially bonded along its embedded length:*

Bond and frictional components of pullout stress:

$$\sigma_0(\phi) = \sigma_{0,bond}(\phi) + \sigma_{0,fric}(\phi) \tag{3.43}$$

$$\sigma_{0,bond}(\phi) = \sigma_d(\phi) \tag{3.44}$$

$$\sigma_{0,fric}(\phi) = \left[e^{\frac{-2\mu w l_d}{a}} - 1 \right] \sigma_d(\phi) + \frac{\sigma_c}{w} \left[e^{\frac{-2\mu w l_d}{a}} - 1 \right] \tag{3.45}$$

The total fibre displacement:

$$U_{pd}(\phi) = \frac{\sigma_d(\phi)}{E_f(\gamma + \alpha - \gamma\eta\alpha + \alpha\eta)} \left[(\alpha - \gamma\eta\alpha + \alpha\eta - \gamma) \frac{\cosh[\beta(L - l_d)] - 1}{\beta \sinh[\beta[L - l_d]]} + \gamma(L - l_d) \right] - \frac{\sigma_c l_d}{E_f w} - \frac{a}{2E_f \mu w} \left[\sigma_d(\phi) + \frac{\sigma_c}{w} \right] \left[e^{\frac{-2\mu W l_d}{a}} - 1 \right] \tag{3.46}$$

Stage 3*- Fibre completely debonded over its embedded length and pulling out:*

Interfacial frictional shear stress distribution: $\tau_f(\phi) = \mu\sigma_c(\phi) e^{\frac{-2w\mu z}{a}} \quad 0 \le z \le L - p_d$ (3.47)

Fibre pullout stress: $$\sigma_0(\phi) = \frac{-\sigma_c(\phi)}{w} \left[1 - e^{\frac{-2w\mu(L - p_d)}{a}} \right] \tag{3.48}$$

Fibre displacement:

$$U_{pd}(\phi) = p_d - \frac{\sigma_c(\phi)}{E_f w} \left[(L - p_d) + \frac{a}{2\mu w} \left\{ e^{\frac{-2\mu w(L - p_d)}{a}} - 1 \right\} + p_d \left\{ 1 - e^{\frac{-2\mu w(L - p_d)}{a}} \right\} \right] \tag{3.49}$$

Figure 3.46 compares the Cunha (2007) load-slip curves from the experiment with the predicted curves obtained from the proposed model using $\tau_{max(app)}$, $\tau_{f(app)}$ and β with different fibre inclination angles.

3.8.5 Results and Discussion

As shown in Figures 3.40 and 3.41, the proposed models for coefficient of friction versus pullout displacement (with different fibres type and strength classes of SCC) are in good

agreement with the experimental results. By utilizing the proposed models to determine the coefficient of friction of Dubey's (1999) pullout model for aligned fibres, this adapted model demonstrates a good capability for the prediction of the pullout behaviour of SFRSCC. Table 3.39 presents a comparison of the peak pullout force obtained by Grünewald (2004) versus the predicted peak pullout force using the modified pullout model. This modified model shows a good prediction capability when considering different fibre types and compressive strengths for SCC. Also, Figure 3.42 compares the experimental load-slip curves of Holschemacher and Klug (2005) with the predicted curves obtained by using the proposed model for different types of fibre (smooth and short-hooked or long-hooked) which provides a good prediction for a wide range of percentages.

Figures 3.43 and 3.44 illustrate the proposed τ_{app} models when allowing for the different types of fibre and embedment fibre lengths which demonstrate a good agreement with the experimental results. By using the proposed τ_{app} and β in the proposed pullout model for inclined fibres which are presented in Eqs.(3.41 to 3.49), a good prediction capability of the pullout behaviour of SFRSCC is demonstrated. Furthermore, Figure 3.46 shows that the proposed model is in good agreement with the experimental results for different inclination angles too.

The following conclusions can be drawn:

- The proposed models describe the coefficient of friction versus pullout displacement by allowing for different fibre types and strength of SFRSCC (normal and high); they demonstrate a good agreement with the experimental results. The observed decrease in coefficient of friction could be caused by matrix wear and consequent smoothening of the interface layer as the fibre pulls out of the matrix.
- Dubey's pullout model (1999) for aligned fibres was applied and calibrated with the proposed coefficient of friction for SFRSCC. The calibrated and modified model reveals good results for the different fibre types (smooth and hooked) and strength for SCC (normal and high).
- In order to take into account the effect of fibre inclination in the pullout model, apparent shear strengths ($\tau_{(app)}$) and slip coefficient (β) were introduced to express the variation of the pullout peak load and the augmentation of peak slip when the

inclination angle increases. They are expressed as functions of the inclination angle ϕ.

- The proposed pullout model was applicable for inclined fibres by introducing apparent shear strengths and slip coefficients which allowed the simulation of the experimental pullout load-slip curves accurately for both hooked and straight aligned fibres with different embedment lengths.

Table 3.38 Proposed models for the coefficient of friction μ

Coefficient of friction	Hooked fibre	
	Normal strength concrete	High strength concrete
μ_i	0.26	0.35
μ_{ss}	0.068	0.083
c	0.7	
μ	$0.192e^{-0.7pd}+0.068$	$0.267e^{-0.7pd}+0.083$
Coefficient of friction	Smooth fibre	
	Normal strength concrete	High strength concrete
μ_i	0.12	0.18
μ_{ss}	0.035	0.050
c	0.7	
μ	$0.085e^{-0.7pd}+0.035$	$0.13e^{-0.7pd}+0.050$

Table 3.39 Comparison of experimental peak pullout force (Grünewald, 2004) versus predicted peak pullout force by using proposed model

l_b (mm)	Fibre type	Peak Pullout Force (N)		
		SCC (B45)	SCC (B65)	SCC (B105)
10	80/30	177.6	193.2	181.4
30	80/60	496.0	614.9	624.8
10	80/60	557.4	590.4	661.6
l_b (mm)	Fibre type	Predicted Peak Pullout Force (N)		
		SCC (B45)	SCC (B65)	SCC (B105)
10	80/30	170.3	189.4	177.7
30	80/60	499.2	616.2	620.6
10	80/60	556.1	596.9	656.7

Table 3.40 Proposed values of $\tau_{max(app)}$, $\tau_{f(app)}$, β and the corresponding P_{max} obtained through comparison of the Cunha (2007) experimental results with respect to the inclination of fibres

	l_b (mm)	Peak Pullout Force (N)		$\tau_{max(app)}$, $\tau_{f(app)}$		β
		Hooked fibre	Smooth fibre	Hooked fibre	Smooth fibre	
Angle (0°)	10	321.8	-	1.61	-	1.0
	20	347.8	77.4	1.80	1.77	
	30	388.2	155.2	2.10	2.27	
	l_b (mm)	Peak Pullout Force (N)		$\tau_{max(app)}$, $\tau_{f(app)}$		β
		Hooked fibre	Smooth fibre	Hooked fibre	Smooth fibre	
Angle (30°)	10	360.9	-	4.31	-	9.0
	20	400.1	173.5	3.29	3.12	
	30	416.0	203.7	1.99	2.34	
	l_b (mm)	Peak Pullout Force (N)		$\tau_{max(app)}$, $\tau_{f(app)}$		β
		Hooked fibre	Smooth fibre	Hooked fibre	Smooth fibre	
Angle (60°)	10	342.0	154.2	2.62	3.07	62.40
	20	335.2	172.8	3.33	3.63	
	30	365.1	189.4	0.85	0.91	

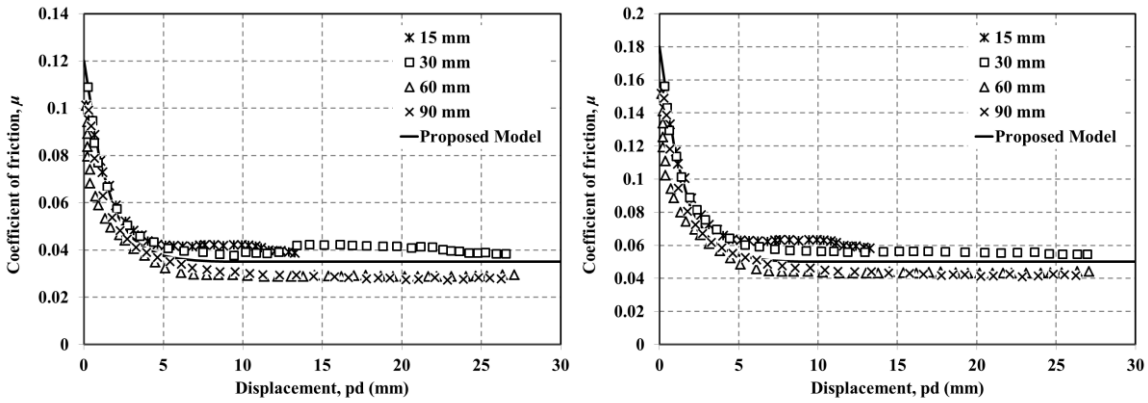

(a) (b)

Figure 3.40 Coefficient of friction versus pullout displacement curves for (a) smooth fibre and normal strength SCC (b) smooth fibre and high strength SCC

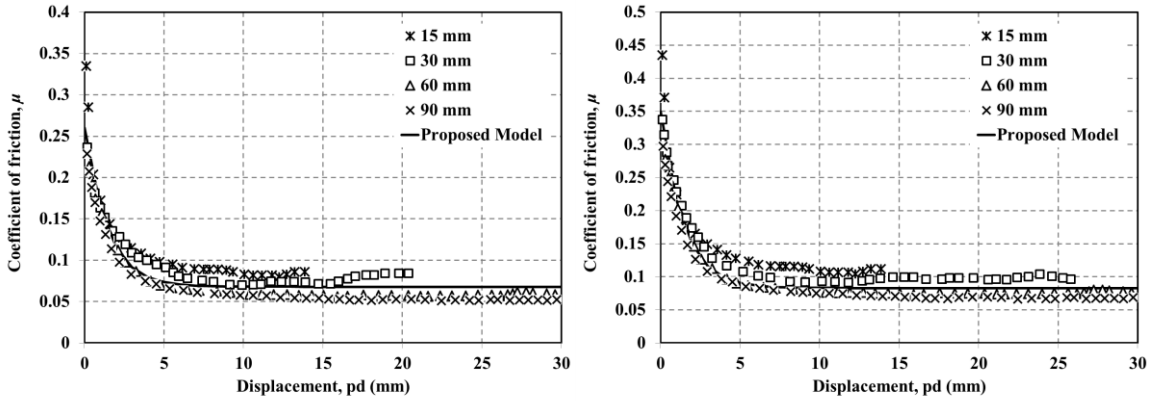

(a) (b)

Figure 3.41 Coefficient of friction versus pullout displacement curves for (a) hooked fibre and normal strength SCC (b) hooked fibre and high strength SCC

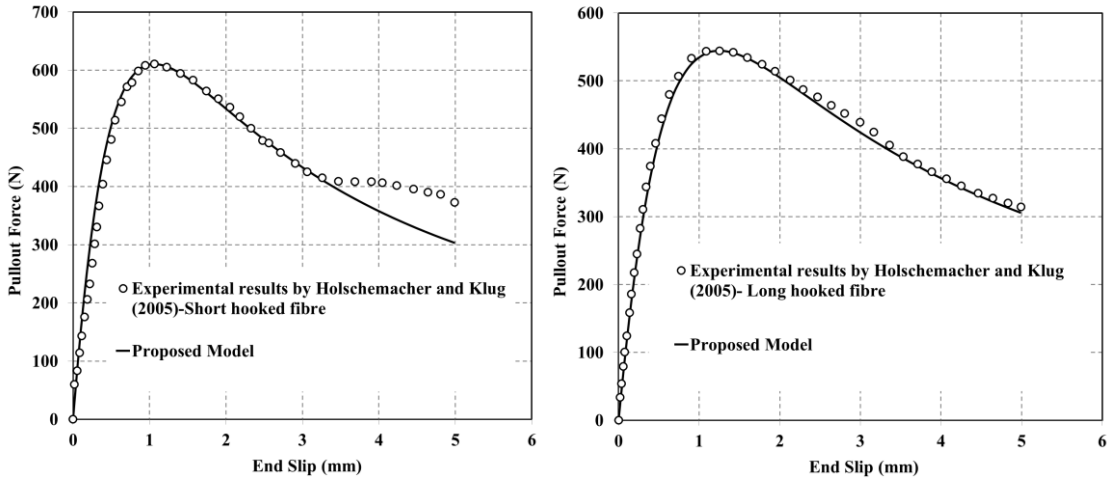

(a) l_f/d_f=50, short hooked fibre (b) l_f/d_f=50, long hooked fibre

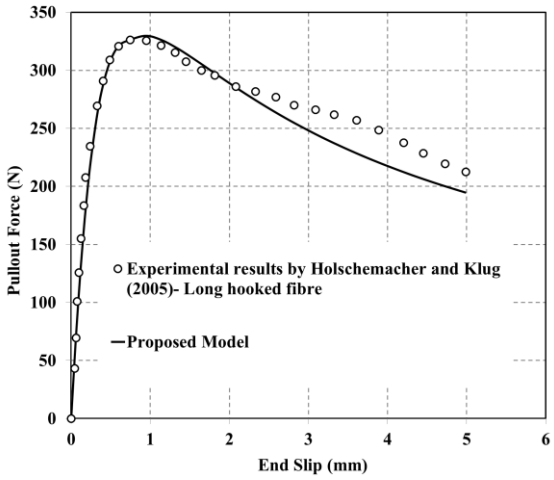

(c) l_f/d_f=62.5, long hooked fibre

Figure 3.42 Comparison of the experimentally obtained load–slip curves versus (Holschemacher and Klug, 2005) predicted curves by using the proposed model

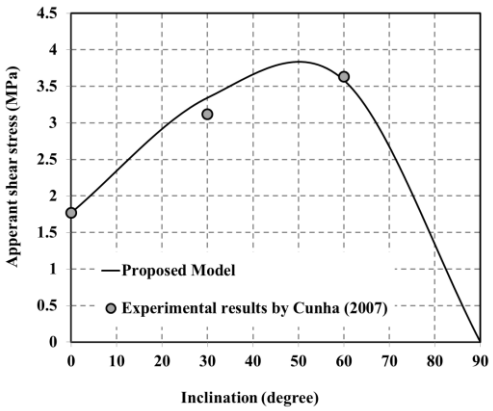

(a) l_b = 20 mm, smooth fibre

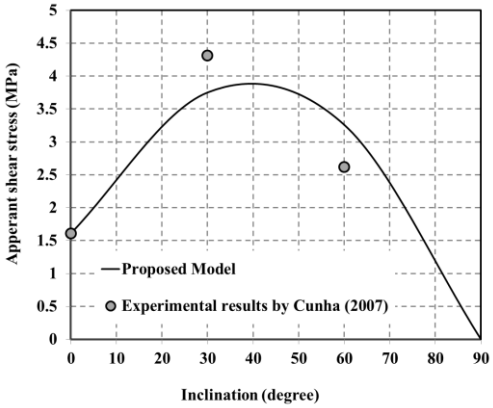

(b) l_b = 10 mm, hooked fibre

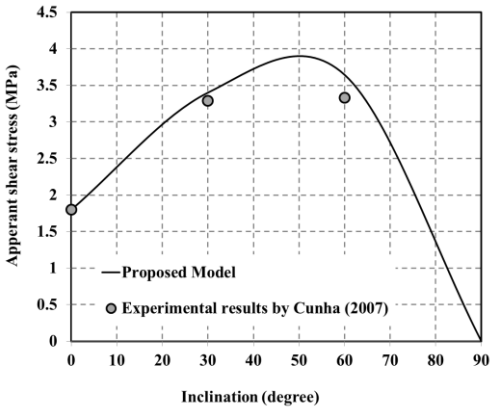

(c) l_b = 20 mm, hooked fibre

Figure 3.43 Comparison of the proposed apparent shear strengths (Eq. (3.37)) with shear strengths obtained by using the Cunha (2007) experimental results subjected to calibration according to inclination angle by using Eq. (2-11) in Figure A.2.

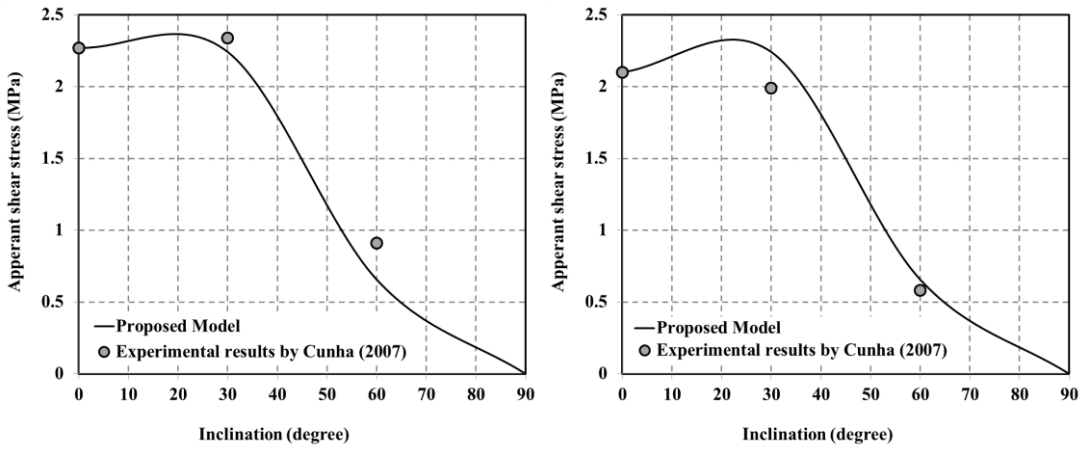

(a) l_b = 20 mm, smooth fibre (b) l_b = 10 mm, hooked fibre

Figure 3.44 Comparison of the proposed apparent shear strengths (Eq. (3.38)) with shear strengths obtained by using the Cunha (2007) experimental results subjected to calibration according to inclination angle by using Eq. (2-11) in Figure A.2.

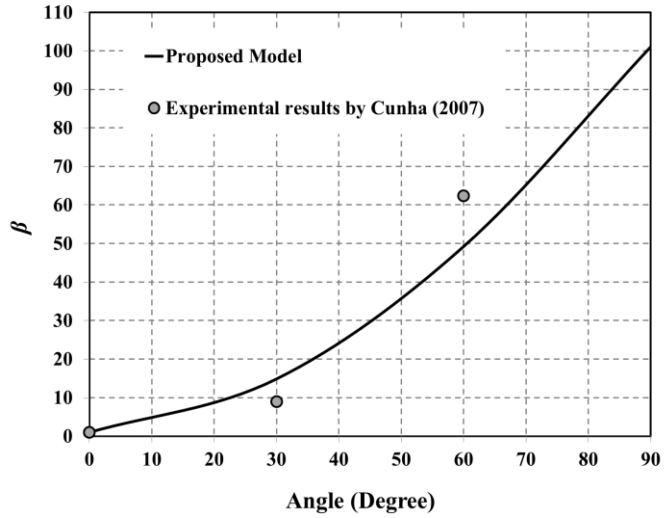

Figure 3.45 Comparison of the predicted curve for β by Eq. (3.40) with the experimentally obtained $U_{peak}(\varphi)/U_{peak}(0)$ ratios for different inclination angles

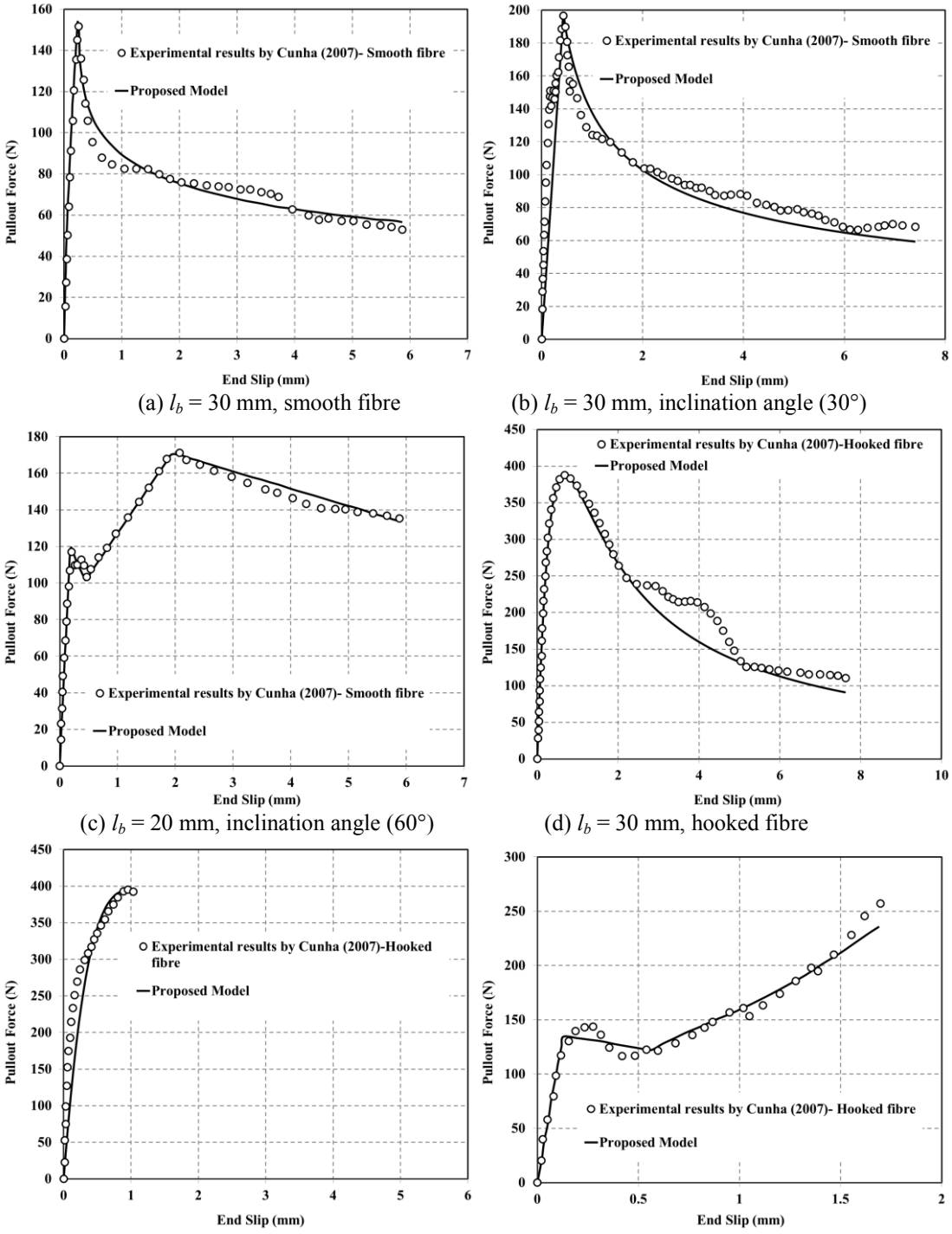

(a) l_b = 30 mm, smooth fibre

(b) l_b = 30 mm, inclination angle (30°)

(c) l_b = 20 mm, inclination angle (60°)

(d) l_b = 30 mm, hooked fibre

(e) l_b = 20 mm, inclination angle (30°)

(f) l_b = 20 mm, inclination angle (60°)

Figure 3.46 Comparison of the experimentally obtained load-slip curves (Cunha, 2007) versus the predicted curves by using the proposed model

CHAPTER 4

TIME-DEPENDENT BEHAVIOUR OF HARDENED CONCRETE

CHAPTER 4

TIME-DEPENDENT BEHAVIOUR OF HARDENED CONCRETE

4.1 INTRODUCTION

The time-dependent behaviour of concrete has been investigated by many researchers since it was first observed and reported almost a century ago. A concrete specimen subjected to load responds instantaneously and time-dependently. When concrete is subjected to a sustained load, deformation gradually increases with time due to creep. Concrete also deforms with time due to shrinkage. Creep strain is produced by sustained stress, while, shrinkage strains are independent of stress and are caused by the loss of water during the drying process or by chemical reactions in the hydrating cement paste. Any increase in deformation over time directly attributable to creep and shrinkage significantly affects the service load behaviour. In some cases these deformations are much larger than the initial deformations produced when the external loads are first applied. In reality, creep and shrinkage are interdependent but for most design calculations they are assumed to be independent and additive. The total concrete strain may be considered to consist of an instantaneous component occurring immediately after application of the stress but does not change unless the level of stress changes, a time-dependent and stress-dependent creep component, and a time-dependent but stress-independent shrinkage component (Nejadi, 2005).

The varying deformation of concrete over time may be illustrated by taking a uniaxially loaded specimen at constant temperature and under constant sustained stress σ_o first applied at time t_o. The total strain at any time $t > t_o$ is the sum of the instantaneous, creep and shrinkage components (Gilbert, 1988):

$$\varepsilon(t) = \varepsilon_e(t) + \varepsilon_c(t) + \varepsilon_{sh}(t) \tag{4.1}$$

In Figure 4.1 the components of strain in a specimen under a sustained compressive stress first applied at time t_o are illustrated diagrammatically. Shrinkage strains develop immediately after drying commences (when the concrete sets or moist curing has finished) and increases continuously at a decreasing rate. Applying the first stress at time t_o, the instantaneous strain component causes the strain diagram to jump suddenly, followed by an additional increase in strain caused by creep. The magnitude and development rate of each strain component must be known in order to accurate prediction of the varying behaviour of the concrete over time. Predicting the time-dependent deformation of a concrete structure is further complicated by the restraint provided by the reinforcement and the external supports, and the fact that the stress history in a concrete structure is rarely constant.

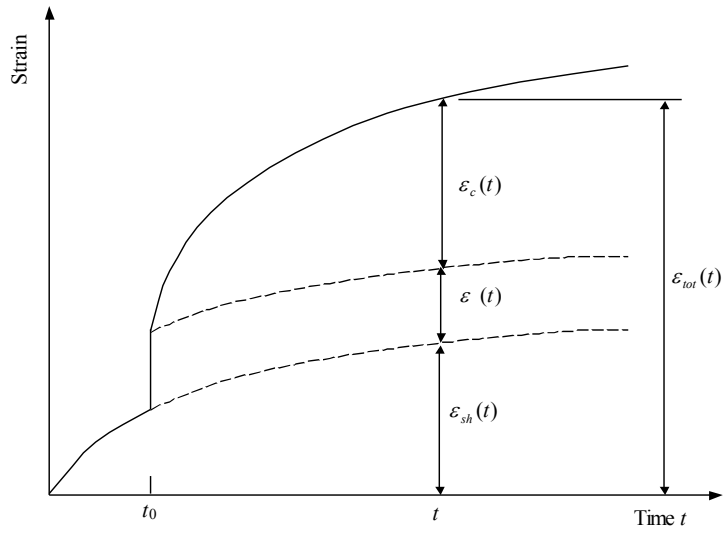

Figure 4.1 Concrete strain components under sustained stress

4.2 INSTANTANEOUS STRAIN

The magnitude of instantaneous strain $\varepsilon_e(t)$, occurring immediately after the application of compressive or tensile stress depends on the rate and magnitude of the applied stress and the properties and proportions of the concrete and its constituent materials. Figure 4.2 illustrates the uniaxial instantaneous strain versus compressive stress curve. When the applied stress is less than about half the compressive strength ($0.5f'_c$), the curve is essentially linear and the instantaneous strain is usually considered to be elastic (fully

recoverable). At higher stress levels the curve is non-linear and a significant proportion of the instantaneous strain is irrecoverable. Because compressive stresses in a concrete structure caused by service loads are low, seldom exceeding half the compressive strength, the secant modulus E_c does not vary significantly with stress in this low stress range, and is only slightly smaller than the initial tangent modulus. Therefore, it is common to assume that the instantaneous behaviour of concrete at service loads is entirely linear-elastic and the instantaneous strain is given by

$$\varepsilon_e(t) = \frac{\sigma(t)}{E_c} \tag{4.2}$$

As the concrete gains strength and hardness, the value of the elastic modulus E_c increases with time. The elastic modulus also depends on the stress rate and actually increases as the loading rate increases, ie the faster the load is applied, the larger the value of E_c. For engineering purposes, these variations are usually ignored and it is assumed that E_c is constant with time. When stress is slowly applied, over say one day's duration, additional deformation occurs because of the rapid and early development of creep. To estimate such a short-term deformation Gilbert (1988) suggested multiplying the elastic modulus given by Equation 2.4 by 0.8.

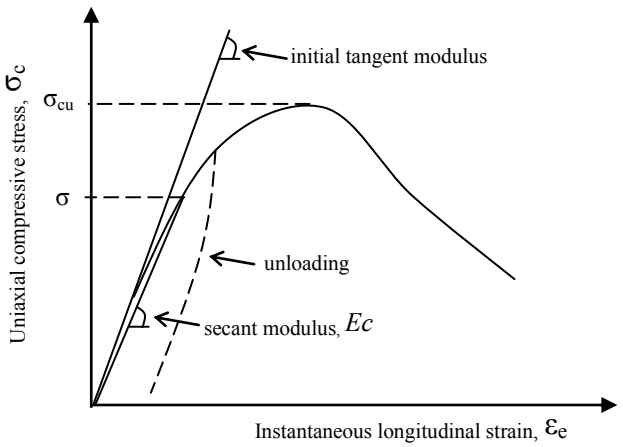

Figure 4.2 Typical stress vs instantaneous strain curve for concrete in compression (Gilbert, 1993)

Concrete's instantaneous behaviour in tension is also important and greatly affects the in-service performance of concrete structures. Before cracking occurs, the instantaneous strain in tension consists of elastic and inelastic components. In structural design, concrete is usually taken to be elastic-brittle in tension and, at stress levels less than the tensile strength, the instantaneous strain versus stress relationship is assumed to be linear. Cracking is assumed to occur when the tensile strength is reached and therefore the stress perpendicular to the crack is generally taken as zero. It is common practice to assume that the initial elastic modulus in tension is equal to that in compression, although the initial elastic modulus in tension is actually higher than in compression. Prior to cracking the instantaneous strain in tension may be calculated by means of Equation 4.2.

4.3 CREEP STRAIN

Under sustained loads, the deformation of a specimen gradually increases such that it may eventually be many times greater than its instantaneous value. The gradual development of strain with time is caused by creep and shrinkage. Creep strain is a time-dependent deformation produced at a gradually decreasing rate by sustained stress. Creep occurs in the hardened cement paste and is related to the movement of moisture and the slow growth of micro cracks.

Creep may be divided into two components, (a) under hygral equilibrium (no drying) conditions the time-dependent increase in strain in a loaded specimen is known as basic creep; (b) additional creep in excess of basic creep in a drying specimen is known as drying creep. Creep in a drying environment is the difference between the total time-dependent deformation of a loaded specimen and shrinkage of an identical but unloaded specimen. In this section, creep is considered as the time-dependent deformation in excess of shrinkage. Figure 4.1 shows the gradual development of creep strain with time. Creep strain increases rapidly immediately after first loading but the rate of increase in creep decreases with time. Approximately, 50% of the final creep develops within the first 2 or 3 months and about 90% of final creep after 2 or 3 years (Gilbert, 1993).

Figure 4.3 illustrates a typical strain-time curve of a concrete specimen subjected to a sustained load, with creep increasing at a decreasing rate under sustained stress. When the stress is removed, creep strain gradually reduces, and eventually tends to a constant. Creep strain is therefore often decomposed into two strain components; recoverable (or delayed elastic) creep and irrecoverable (or flow) creep. Most creep strain is irrecoverable, while the recoverable part is generally less than 30% of the total creep strain.

Many factors influence the magnitude and rate of creep development, including the properties of the concrete mix and its constituent materials. The composition of a concrete structure can be essentially defined by the water-cement ratio w/c, aggregate and cement types, and aggregate and cement contents. Creep is approximately proportional to the square of the w/c ratio when all other factors are kept constant.

An increase in the w/c ratio increases creep, on the contrary, an increase in either aggregate content or maximum aggregate size or the use of a stiffer aggregate type reduces creep. A rise in temperature also increases creep. In general, when the quality of the concrete increases there is a tendency towards lower creep (Nejadi, 2005).

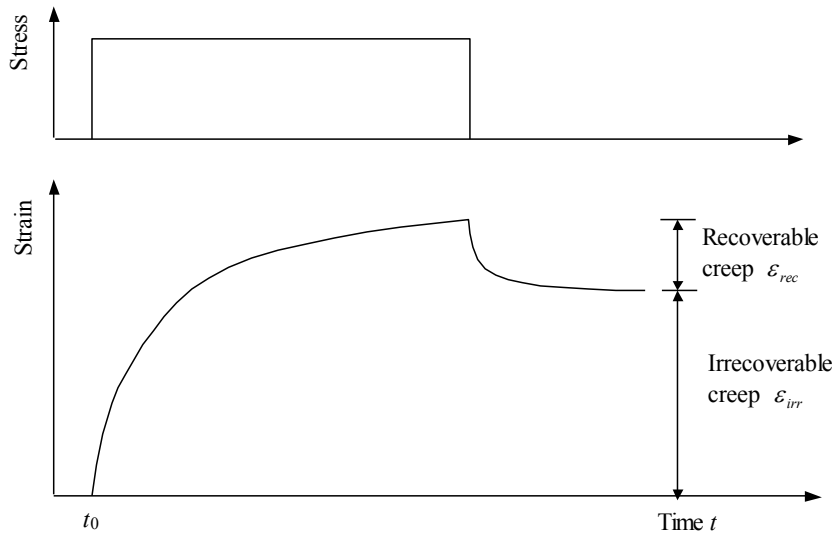

Figure 4.3 Strain versus time for specimen under constant stress

Creep is also influenced by the environmental conditions (i.e. relative humidity and specimen size), the duration of load and the age of the concrete at first loading. As the surface area-to-volume ratio increases, creep increases, and therefore creep is greater in thin members such as slabs, than in thicker members such as beams or columns. The magnitude of creep strain under sustained stress is strongly affected by the age of the concrete at first loading (Davis et al, 1934). As shown in Figure 4.4, concrete loaded at an early age creeps more than concrete loaded at a later age. Concrete is therefore a material that hardens over time although the tendency to creep never completely disappears, even in very old concrete.

4.3.1 Creep Coefficient

The capacity of concrete to creep is commonly defined as the creep coefficient. Under a constant sustained stress first applied at age t_o, the creep coefficient is the ratio of the creep strain at time t to the instantaneous elastic strain:

$$\varphi(t,t_o)=\frac{\varepsilon_c(t,t_o)}{\varepsilon_e(t_o)} \tag{4.3}$$

For stress levels less than about $0.5f'_c$ (the usual service stress range), the creep coefficient is a stress-independent quantity and a pure time function.

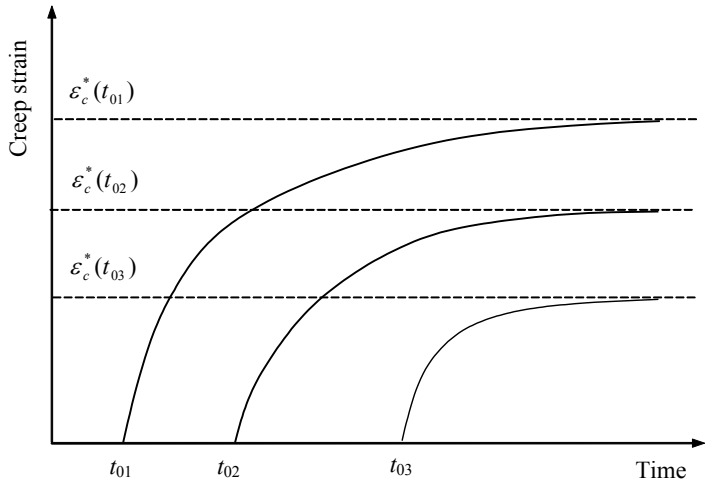

Figure 4.4 Effect of age at first loading on the creep strain (Gilbert, 1988)

The creep coefficient is assumed to approach a final value $\varphi^*(t_o)$, as time approaches infinity, which usually falls within 1.5-4.0 (Gilbert, 1988).

$$\varphi^*(t_o) = \varphi(\infty, t_o) = \frac{\varepsilon_c^*(t_o)}{\varepsilon_e(t_o)} \tag{4.4}$$

By testing or using one of the many predictive methods available in the literature (e.g., Clause 6.1.8 of AS3600-2009), the creep coefficient for a particular mix can readily be estimated. Under a constant sustained stress σ_o, the creep strain may be obtained as

$$\varepsilon_c(t, t_o) = \frac{\sigma_o}{E_c}\phi(t, t_o) \tag{4.5}$$

4.3.2 Creep in Tension

Creep in tension is of interest in many practical situations, especially in estimating the possibility of cracking due to shrinkage or thermal stresses. Tensile creep is thought to be a different mechanism from compressive creep even though the magnitudes are similar at the same stress levels.

The rate of creep in tension is initially higher than compression under the same stress, but long-term creep is lower in tension than in compression. It appears that creep in tension is proportional to applied stress up to a stress strength ratio of 0.5, and even higher than 0.5, and therefore from this perspective there is no difference between its behaviour in tension and in compression.

To assume identical creep coefficients in tension and compression for design purposes is quite common because it simplifies calculations without causing serious errors. Although difficulties with experimental techniques are the reason for a lack of universal agreement on tensile creep, further research into concrete in tensile creep is imperative (Nejadi, 2005).

4.4 SHRINKAGE STRAIN

Shrinkage is a reduction in volume caused by water moving out of a porous body, a movement that occurs in concrete throughout its life. Here, shrinkage is defined as the time-dependent strain measured at a constant temperature in an unloaded and unrestrained specimen. Concrete begins to shrink when drying commences and continues to increase with time at a decreasing rate, and is assumed to approach a final value as time approaches infinity (see Figure 4.5).

Shrinkage may be classified as plastic shrinkage, chemical shrinkage, thermal shrinkage, and drying shrinkage (Gilbert, 2002).While the concrete is still in its plastic state, water can be lost by evaporation from the surface or suction by the underlying dry concrete or soil. This contraction is known as plastic shrinkage because the concrete is still in the plastic state. Here moisture evaporates faster from the surface than can be replaced by bleed water from the lower layers, and surface cracking may occur. Steel reinforcement does not control this type of cracking because the bond between the concrete and steel has not yet developed.

Chemical shrinkage is related to the various chemical reactions within the cement paste and there are two different types of chemical shrinkage in concrete namely autogenous shrinkage and carbonation shrinkage. Under isothermal condition in the absence of hygral exchange with the ambient medium, the hydration of cement continues long after setting. This type of shrinkage, known as autogenous shrinkage or autogenous volume change, is a direct consequence of water withdrawn from the capillary pores by the hydration of un-hydrated cement, which in practice occurs inside a concrete mass. Autogenous shrinkage is an inherent characteristic of the material and is largely independent of specimen size (CEB, 1997).

The cement paste is also subjected to carbonation shrinkage resulting from the effects of carbon dioxide on the chemical changes of calcium-silicate hydrate, and the drying of the pores by removing absorbed water.

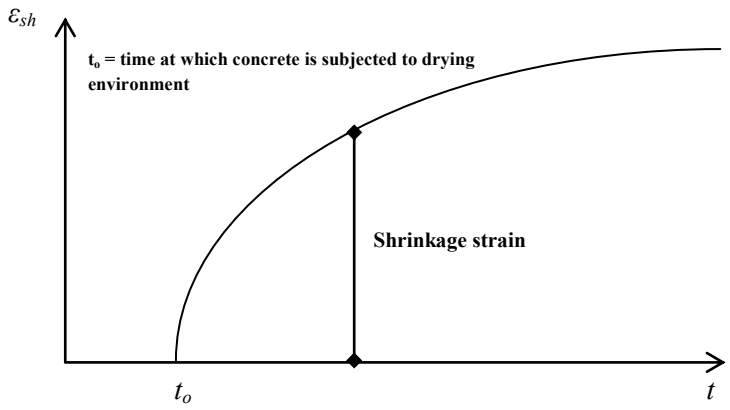

Figure 4.5 Typical shrinkage curve for concrete

Because atmospheric carbon dioxide does not penetrate more than about 12 mm into the surface of high-quality, low porosity concrete, carbonation shrinkage is of minor importance in the overall shrinkage of most concrete structures (ACI, 2003). During the setting process hydration of the cement causes heat to be generated, and as the concrete cools, thermal shrinkage occurs due to thermal contraction. Thermal shrinkage is important for mass concrete structures such as dams, but may be reduced by restricting temperature rise during hydration.

Withdrawal of water from concrete stored in unsaturated air causes drying shrinkage. This phenomenon may be defined as the time-dependent linear strain at constant temperature measured on an unloaded specimen which is allowed to dry and it may be considered proportional to the loss of water from concrete. The opposite phenomenon is swelling, which is an increase in volume caused by water absorption. Shrinkage and swelling represent water movement into and out of the concrete gel. Shrinkage however, is not a completely reversible process, if a specimen is saturated with water after full shrinkage it will not expand to its original volume.

The irreversible shrinkage may be considered as 30 to 60 percent of the ultimate first drying shrinkage (Helmuth and Turk, 1967). The reason of that is the gel pores are reduced due to additional bonds developing within them while drying. The irreversible shrinkage

residual may be reduced if most of the cement paste in the concrete is hydrated before drying (Neville, 1995).

Drying shrinkage is affected by all the factors that affect the drying process. The following factors influence the magnitude of the drying shrinkage:

- Aggregates provide restraint to shrinkage of the cement paste, depending on their quantity and type (properties). Concrete with high aggregate content and high quality (stiffer) aggregates are more resistant to shrinkage.
- The water/cement (w/c) ratio strongly affects shrinkage. The higher the w/c ratio, the higher the shrinkage effect.
- The rate and magnitude of shrinkage decreases as the volume (size) of the concrete element is increased, however, the duration of shrinkage is longer for larger members because the inside of an element takes longer to dry.
- Shrinkage is also affected by temperature and humidity; shrinkage is lower at high humidity and is stabilised at low temperatures. Results by Troxell et al. (1958) showed that the lower the relative humidity, the greater the ultimate shrinkage and rate of shrinkage.

4.5 SHRINKAGE OF SCC

Basically, the SCC consists of the same components as CC (cement, water, aggregates, admixtures, and mineral additions), but the final composition of the mixture and its fresh characteristics are different. In comparison with the CC, the SCC contains larger quantities of mineral fillers such as finely crushed limestone or fly ash, higher quantities of high-range water-reducing admixtures, and smaller maximum size of the coarse aggregate. These modifications in the composition of the mixture affect the behaviour of the concrete in its hardened state, including the shrinkage deformation.

As discussed earlier, the overall shrinkage of concrete corresponds to a combination of several shrinkages, that is, plastic shrinkage, autogenous shrinkage, drying shrinkage,

thermal shrinkage, and carbonation (chemical) shrinkage. In designing the CC, shrinkage is taken as drying shrinkage, which is the strain associated with the loss of moisture from the concrete under drying conditions. The CC with a relatively high water cementitious material ratio (w/c) (higher than 0.40) exhibits a relatively low autogenous shrinkage, with values less than 100 μstrain (Davis, 1940). In contrast, the SCC used in precast, prestressed applications has typically a low w/c ratio (0.32 to 0.40). Lower w/c values, coupled with a high content of binder, lead to greater autogenous shrinkage. Such shrinkage increases with the use of finely ground supplementary cementitious materials and fillers employed in the SCC. Therefore, both drying and autogenous shrinkage deformations have to be accounted for in the structural detailing of the reinforced concrete and the prestressed concrete members (Khayat and Long, 2010). Because the SCC has a higher paste volume (or higher sand to aggregate ratio) to achieve high workability and high early strength, several researchers have claimed larger shrinkage of the SCC for precast, prestressed concrete, resulting in larger prestress losses (Issa et al., 2005; Naito et al., 2006; Suksawang et al., 2006; Schindler et al., 2007). Although mechanical properties of the SCC are superior to those of the CC, shrinkage of SCC is significantly high (Issa et al., 2005). Naito et al. (2006) also found that the SCC exhibits higher shrinkage than the CC, which is due to the higher fine aggregate volume in the SCC, and that the shrinkage of the SCC and the CC was 40% and 6% higher than that of the ACI 209R (1997) prediction model, respectively.

Different methodologies are followed in different countries to obtain the SCC (Ouchi et al., 2003), and few studies are available concerning its long-term behaviour (Persson, 2001; 2005; Poppe and De Shutter, 2001; Seng and Shima, 2005; Mazzotti et al., 2006). It is not clear in the available studies if current international standards apply successfully for the SCC (Klug and Holschemaker, 2003; Vidal et al., 2005; Landsberger and Fernandez-Gomez, 2007). Moreover, it is not assessed if the long-term properties can be predicted with reference to the conventional mechanical and physical parameters only (such as strength, w/c), or the adoption of parameters concerning the mix design is needed.

The objectives of this section are: (1) To establish an experimental results database of shrinkage. (2) To review the accuracies of the CC shrinkage prediction models proposed by international codes of practice, including CEB-FIP (1990), ACI 209R (1997), Eurocode 2

(2001), JSCE (2002), AASHTO (2004; 2007) and AS 3600 (2009). (3) To review the accuracies of the SCC shrinkage prediction models proposed by Poppe and De Schutter (2005), Larson (2007), Cordoba (2007) and Khayat and Long (2010). (4) To propose a new prediction shrinkage model based on the comprehensive analysis of the available models and the experimental results database of both the CC and the SCC.

4.5.1 Experimental Database for Shrinkage of CC and SCC from the Literature

Tables 4.1 to 4.3 present a general summary of the concrete mixtures included in the database. The database comprises test results from 14 different investigations, with a total of 165 different SCC mixtures and 21 CC mixtures for shrinkage tests. Table 1 includes complimentary information regarding the age of the concrete (in days) when shrinkage begins (ACWSB), final age of the concrete, relative humidity (RH), type of the specimen, type of the cement and type of the filler. Table 4.2 includes information about the amount of the cement, filler and water, compressive strength (f'_c) and cement to powder (c/p) ratio for each mixtures that were used in different investigations. Figures 4.8 and 4.9 show the CC and SCC experimental results database that is summarized in Tables 4.1 and 4.2 (drying shrinkage vs. time). By considering experimental results of drying shrinkage in the database, the following conclusions are observed: (1) Increase in the water to binder ratio causes increase in the drying shrinkage. (2) The proper use of fly ash in the SCC can reduce drying shrinkage remarkably. (3) Increase in the volume of coarse aggregate can reduce drying shrinkage significantly. Additionally, the change in the sand volume ratio has little effect on the drying shrinkage of the medium strength SCC (Aslani and Nejadi, 2011e; 2011f).

4.5.2 Shrinkage Models for CC from the Literature

This section assesses the accuracy of seven models from the commonly used international codes to predict shrinkage strains without the need for shrinkage tests. These empirical models, which vary widely in their techniques, require certain intrinsic and/or extrinsic variables, such as mix proportions, material properties and age of loading as inputs. The

models considered are listed in Table 4.4, which also shows the factors required by each model. In this section the accuracies of the shrinkage prediction models proposed by the international codes of practice, including CEB-FIP (1990), ACI 209R (1997), Eurocode 2 (2001), JSCE (2002), AASHTO (2004; 2007) and AS 3600 (2009) are compared with the actual measured shrinkage strains in 165 SCC mixtures and 21 CC mixtures. Figures 4.7 to 4.13 show comparisons of the shrinkage by available SCC and CC models with the experimental results available in the literature (Tables 4.1 to 4.3).

4.5.3 Shrinkage Models for SCC from the Literature

Table 4.5 shows empirical models for calculating the shrinkage of SCC, which vary in complexity and precision in the calculations. Figures 4.15 to 4.18 show comparisons of the drying shrinkage by Poppe and De Schutter (2005), Larson (2007), Cordoba (2007) and Khayat and Long (2010) with the available shrinkage experimental results.

4.5.4 Proposed Shrinkage Model for SCC

The comparisons of different models and experimental database show that ACI 209R (1997), JSCE (2002) and AASHTO (2004) models have conservative drying shrinkage predictions. This section required certain intrinsic and/or extrinsic variables (i.e., mix proportions, material properties and age of loading) for the SCC which are shown in Table 4.4. Table 4.4 shows that JSCE (2002) drying shrinkage model gives good coverage of the intrinsic and/or extrinsic variables that are useful for calculating the drying shrinkage strain. Therefore, with the JSCE (2002) model as a basis, the current section has tried to include the c/p ratio into the formulas in order to obtain a better prediction of the time-dependent deformations of the normal strength and the high strength SCC. These results are shown in Eqs. (4.6 to 4.18).

Table 4.1 Shrinkage experimental database

Reference	No. of SCC mixtures	No. of CC mixtures	Age of concrete when shrinkage begins (days)	Final age of concrete (days)
Chopin et al. (2003)	5	1	1	365
Poppe and De Schutter (2005)	4	0	1	1400
Horta (2005)	6	0	1	200
Larson (2006)	1	0	1	520
Turcry et al. (2006)	3	3	1	120, 150, 210
Cordoba (2007)	4	1	1	365
Heirman et al. (2008)	7	1	1	98
Bhattacharya (2008)	6	2	1	90
Oliva and Cramer (2008)	11	4	1	350, 495
Hwang and Khayat (2009)	10	2	1	56
Ma et al. (2009)	16	0	1	120, 150
Loser and Leemann (2009)	13	3	1	91
Güneyisi et al. (2010)	63	2	1	50
Khayat and Long (2010)	16	2	1	300
Total of 186 mixtures	165	21		

Table 4.2 Shrinkage experimental database (continued)

Reference	R.H. (%)	Type of specimen (mm)	Type of cement	Type of filler
Chopin et al. (2003)	50	Cylinder (90 × 280)	CEM I	Limestone
Poppe and De Schutter (2005)	60	Prism (150×150×500)	CEM I 42, 5 R, CEM I 52,5	Limestone
Horta (2005)	50	Cylinder (150 × 300)	CEM I , CEM III	Fly ash and GGBFS
Larson (2006)	50	Prism (101.6×101.6×609.6) and Cylinder (114.3×609.6)	CEM III	Limestone
Turcry et al. (2006)	50	Prism (70×70×280)	CEM I 52.5, CEM II 42.5	Limestone
Cordoba (2007)	50	Cylinder (101.6 × 203.2), (101.6 × 1057.8)	CEM I/II	Fly ash and GGBFS
Heirman et al. (2008)	60	Cylinder (120 x 300)	CEM I 42.5 R, CEM III/A 42.5 N LA	Limestone
Bhattacharya (2008)	50	Prism (76.2×76.2×311.2)	CEM I	Limestone, Silica fume and Slag
Oliva and Cramer (2008)	50	Prism (101.6×101.6×285.75)	CEM I	GGBFS
Hwang and Khayat (2009)	50	Prism (75x75×285)	CSA type Gub-F/SF, Gub-S/SF and quaternary blended cement	Fly ash and Limestone
Ma et al. (2009)	60	Prism (100×100×515)	CEM I	Fly ash
Loser and Leemann (2009)	70	Prism (120×120×360)	CEM I 42.5 N, CEM II/A-LL 45.2 N	Fly ash and Silica fume
Güneyisi et al. (2010)	50	Prism (70×70×280)	CEM I	Fly ash, GGBFS, Silica fume and Metakaolin
Khayat and Long (2010)	50	Cylinder (150×300)	MS and HE (similar to ASTM C150 Type I/II and Type III)	Fly ash

Table 4.3 Mix properties of the shrinkage experimental database

Chopin et al. (2003)	Cement (kg/m^3)	Filler (kg/m^3)	c/p	w (kg/m^3)	f'_c (MPa)
SCC1	374	172	0.68	123	36.8
SCC2	344	256	0.57	131	36.5
SCC3	396	161	0.71	154	49.9
SCC4	396	177	0.69	115	36
SCC5	347	177	0.66	139	39.1
CC	348	-	1.00	132	35.6
Poppe and De Schutter (2005)	Cement (kg/m^3)	Filler (kg/m^3)	c/p	w (kg/m^3)	f'_c (MPa)
SCC1	300	300	0.50	165	59
SCC2	360	240	0.60	165	63.8
SCC3	400	200	0.67	165	73.7
SCC4	450	150	0.75	165	74.3
SCC5	360	240	0.60	165	66.6
SCC6	360	240	0.60	165	67.2
Horta (2005)	Cement (kg/m^3)	Filler (kg/m^3)	c/p	w (kg/m^3)	f'_c(MPa)
S-Slag/Ash	427	172	0.71	182	73.3
G-Slag	433	133	0.77	208	56.6
Tindall	445	-	1.00	171	57.3
7N	468	99	0.83	177	87
7BL	461	97	0.83	181	77.7
67M	458	91	0.83	175	78.2
Larson (2006)	Cement (kg/m^3)	Filler (kg/m^3)	c/p	w (kg/m^3)	f'_c (MPa)
SCC	446	-	1	224	51.7
CC	387	-	1	263	51.7
Turcry et al. (2006)	Cement (kg/m^3)	Filler (kg/m^3)	c/p	w (kg/m^3)	f'_c (MPa)
SCC1	330	110	0.75	180	40
SCC2	350	139	0.72	198	42
SCC3	350	150	0.70	187	48
CC1	280	-	1.00	170	37
CC2	350	-	1.00	175	41
CC3	360	-	1.00	170	53
Cordoba (2007)	Cement (kg/m^3)	Filler (kg/m^3)	c/p	w (kg/m^3)	f'_c (MPa)
KH	408	132.8	0.75	205.00	48.9
KM	418	136	0.75	210.00	48.2
CC	531	-	1	202.00	46.1
Heirman et al. (2008)	Cement (kg/m^3)	Filler (kg/m^3)	c/p	w (kg/m^3)	f', *cub150* (MPa)
SCC1	360	240	0.6	165	57.1
SCC3	360	240	0.6	165	69.2
SCC5	300	300	0.5	165	49
SCC14	360	240	0.6	144	68.4
SCC15	360	240	0.6	198	46.7
SCC16	360	240	0.6	165	73.3
SCC17	360	240	0.6	216	39.9

Table 4.3 Mix properties of the shrinkage experimental database (continued)

Bhattacharya (2008)	Cement (kg/m^3)	Filler (kg/m^3)	c/p	w (kg/m^3)	f'_c (MPa)
SCCA	386	112	0.78	154	61.9
SCCB	386	112	0.78	154	61.7
SCCC	386	112	0.78	154	58.0
SCCD	380	112	0.77	152	61.8
SCCE	386	112	0.78	161	67.4
SCCF	386	112	0.78	151	63.2
Hwang and Khayat (2009)	Cement (kg/m^3)	Filler (kg/m^3)	c/p	w (kg/m^3)	f'_c (MPa)
35-C1-BC	474	475	0.50	166	53.2
35-C2-BC	474	475	0.50	166	49.5
35-C3-BC	474	475	0.50	166	46.1
42-N-B1	476	475	0.50	200	34.7
42-C2-B1	476	475	0.50	200	46.1
42-C3-B1	476	475	0.50	200	39.9
42-N-B2	476	475	0.50	200	42.2
42-C3-B2	476	475	0.50	200	46
42-C3-B3	476	475	0.50	200	37.1
SCC180	476	475	0.50	200	41.1
HPC180	357	428	0.45	150	51.6
CC	436	455	0.49	183	38.5
Ma et al. (2009)	Cement (kg/m^3)	Filler (kg/m^3)	c/p	w (kg/m^3)	f'_c (MPa)
A1	386	166	0.70	166	44.1
A2	359	154	0.70	180	42.3
A3	335	144	0.70	192	33.6
B1	389	97	0.80	195	38.7
B2	335	144	0.70	192	35.2
B3	283	189	0.60	189	33.9
C1	394	131	0.75	210	30.4
C2	382	128	0.75	204	33.2
C3	370	125	0.75	198	35.9
C4	360	120	0.75	192	36.4
C5	348	117	0.75	186	39.1
C6	338	112	0.75	180	41.9
D1	390	130	0.75	208	51.7
D2	375	125	0.75	200	54.2
D3	360	120	0.75	192	53.3
D4	337	113	0.75	180	56.4
Loser and Leemann (2009)	Cement (kg/m^3)	Filler (kg/m^3)	c/p	w (kg/m^3)	f'_c (MPa)
SCC2	310	-	1	179	71.1
CC2	512	-	1	155	51.2

Table 4.3 Mix properties of the shrinkage experimental database (continued)

Güneyisi et al. (2010)	Cement (kg/m^3)	Filler (kg/m^3)	c/p	w (kg/m^3)	f'_c (MPa)
M1	550	-	1	176	80.9
M2	440	110	0.8	176	69.8
M3	330	220	0.6	176	60.9
M4	220	330	0.4	176	47.5
M5	440	110	0.8	176	75.1
M6	330	220	0.6	176	80.1
M7	220	330	0.4	176	78.1
M8	522.5	27.5	0.95	176	80.4
M9	495	55	0.9	176	85.7
M10	467.5	82.5	0.85	176	84.4
M11	522.5	27.5	0.95	176	96.3
M12	495	55	0.9	176	91.4
M13	467.5	82.5	0.85	176	98.6
M14	440	110	0.8	176	79.2
M15	330	220	0.6	176	67.2
M16	220	330	0.4	176	60
M17	440	110	0.8	176	81
M18	330	220	0.6	176	84.2
M19	220	330	0.4	176	67.5
M20	440	110	0.8	176	79.6
M21	330	220	0.6	176	87.6
M22	220	330	0.4	176	84.5
M23	440	110	0.8	176	89.7
M24	330	220	0.6	176	81.2
M25	220	330	0.4	176	83.1
M26	440	110	0.8	176	77
M27	330	220	0.6	176	62.3
M28	220	330	0.4	176	69.4
M29	522.5	27.5	0.95	176	93.9
M30	495	55	0.9	176	92.6
M31	467.5	82.5	0.85	176	94.4
M32	440	110	0.8	176	78.5
M33	330	220	0.6	176	74.1
M34	220	330	0.4	176	60.7
M35	440	110	0.8	176	90.6
M36	330	220	0.6	176	88.5
M37	220	330	0.4	176	74.1
M38	440	110	0.8	176	78.6
M39	330	220	0.6	176	72.7
M40	220	330	0.4	176	64.3
M41	440	110	0.8	176	91.2
M42	330	220	0.6	176	85.4
M43	220	330	0.4	176	76.5

Table 4.3 Mix properties of the shrinkage experimental database (continued)

Güneyisi et al. (2010)	Cement (kg/m^3)	Filler (kg/m^3)	c/p	w (kg/m^3)	f'_c (MPa)
M44	450	-	1	144	61.5
M45	360	90	0.8	144	52.1
M46	270	180	0.6	144	44.7
M47	180	270	0.4	144	30.3
M48	360	90	0.8	144	59
M49	270	180	0.6	144	58
M50	180	270	0.4	144	56.2
M51	427.5	22.5	0.95	144	60.7
M52	405	45	0.9	144	58.5
M53	382.5	67.5	0.85	144	71.1
M54	360	90	0.8	144	61.5
M55	270	180	0.6	144	46.9
M56	180	270	0.4	144	37.4
M57	360	90	0.8	144	60.1
M58	270	180	0.6	144	58.3
M59	180	270	0.4	144	57.6
M60	360	90	0.8	144	62.4
M61	270	180	0.6	144	53.6
M62	180	270	0.4	144	45.9
M63	360	90	0.8	144	60.6
M64	270	180	0.6	144	54.7
M65	180	270	0.4	144	44.2
Khayat and Long (2010)	Cement (kg/m^3)	Filler (kg/m^3)	c/p	w (kg/m^3)	f'_c (MPa)
1	390	440	0.47	133	62.5
2	530	440	0.55	180	62.5
3	390	440	0.47	133	62.5
4	530	440	0.55	180	62.5
5	390	440	0.47	156	62.5
6	530	440	0.55	212	62.5
7	390	440	0.47	156	62.5
8	530	440	0.55	212	62.5
9	390	500	0.44	133	62.5
10	530	500	0.51	180	62.5
11	390	500	0.44	133	62.5
12	530	500	0.51	180	62.5
13	390	500	0.44	156	62.5
14	530	500	0.51	212	62.5
15	390	500	0.44	156	62.5
16	530	500	0.51	212	62.5

Table 4.3 Mix properties of the shrinkage experimental database (continued)

Kim (2008)	Cement (kg/m^3)	Filler (kg/m^3)	c/p	w (kg/m^3)	f'_c (MPa)
S5G-3	376	177	0.68	152	63
S7G-4,5,6	427	107	0.80	123	79
S5L-3	380	253	0.60	171	65
S7L-4,5,6	427	107	0.80	133	88
C5G	371	-	1.00	134	65
C7G	415	-	1.00	119	73
C5L	356	-	1.00	149	59
C7L	403	-	1.00	133	72
Zheng et al. (2009)	Cement (kg/m^3)	Filler (kg/m^3)	c/p	w (kg/m^3)	f'_c (MPa)
SCC1	440	110	0.80	180	52.6
SCC2	250	300	0.45	154	46.5
SCC3	288	192	0.60	145	47.7
SCC4	312	208	0.60	156	51
SCC5	330	220	0.60	165	52
SCC6	330	220	0.60	155	43.8
SCC7	330	220	0.60	165	40.5
CC	525	0	1.00	200	41.3
Loser and Leemann (2009)	Cement (kg/m^3)	Filler (kg/m^3)	c/p	w (kg/m^3)	f'_c (MPa)
SCC2	310	-	1	179	71.1
CC2	512	-	1	155	51.2

- ***For normal strength SCC with range of applicability:***

$45\% \leq RH \leq 80\%$

$130\ kg/m^3 \leq w \leq 230\,kg/m^3$

$100\,mm \leq v/s \leq 300\,mm$

$40\% \leq w/c \leq 65\%$

$f'_c(28) \leq 55\,MPa$

$260\,kg/m^3 \leq c \leq 500\,kg/m^3$

$$\varepsilon'_{cs}(t,t_0) = \varepsilon'_{sh}\left[1-\exp\left\{-0.1(t-t_0)^{(-2.4(c/p)+2.3)}\right\}\right] \quad (4.6)$$

$$\varepsilon'_{sh} = \left[-50 + 78 \left\{ 1 - \exp\left(\frac{RH}{100} \right) \right\} + 38.3 \ln w - 0.92 \ln\left(\frac{w}{c} \right) - 5 \left[\ln\left(\frac{v/s}{10} \right) \right]^2 \right] \times \left(10^{-5}\right) \quad \text{for c/p} < 0.65 \quad (4.7)$$

$$\varepsilon'_{sh} = \left[-50 + 78 \left\{ 1 - \exp\left(\frac{RH}{100} \right) \right\} + 37.5 \ln w - 0.92 \ln\left(\frac{w}{c} \right) - 5 \left[\ln\left(\frac{v/s}{10} \right) \right]^2 \right] \times \left(10^{-5}\right) \quad \text{for c/p} \geq 0.65 \quad (4.8)$$

- ***For high strength SCC with range of applicability:***

$45\% \leq RH \leq 90\%$

$130\ kg/m^3 \leq w \leq 230\ kg/m^3$

$100\ mm \leq v/s \leq 300\ mm$

$40\% \leq w/c \leq 65\%$

$f'_c(28) \leq 80\ MPa$

$$\varepsilon'_{cs}(t,t_0) = \varepsilon'_{ds}(t,t_0) + \varepsilon'_{as}(t,t_0) \quad (4.9)$$

$$\varepsilon'_{ds}(t,t_0) = \frac{\varepsilon'_{ds\infty}(t-t_0)}{\beta + (t-t_0)} \quad (4.10)$$

$$\varepsilon'_{ds\infty} = \frac{\varepsilon'_{ds\rho}}{\eta\, t_0} \left(\times 10^{-6}\right) \quad (4.11)$$

$$\varepsilon'_{ds\rho} = \left[\frac{\alpha\,(1 - RH/100)\, w}{1 + 110 \exp\left\{ -\frac{400}{f'_c(28)} \right\}} \right] \times \left(0.015 + 1.35\,(c/p)\right)^{-1} \quad \text{for c/p} < 0.65 \quad (4.12)$$

$$\varepsilon'_{ds\rho} = \left[\frac{\alpha\,(1 - RH/100)\, w}{1 + 110 \exp\left\{ -\frac{410}{f'_c(28)} \right\}} \right] \times \left(0.015 + 1.05\,(c/p)\right)^{-1} \quad \text{for c/p} \geq 0.65 \quad (4.13)$$

$$\beta = \frac{4\, w \sqrt{v/s}}{100 + 0.7\, t_0} \tag{4.14}$$

$$\eta = \left[15 \exp\left(0.007\, f_c'(28)\right) + 0.25\, w \right] \times 10^{-4} \tag{4.15}$$

$$\varepsilon'_{as}(t, t_0) = \varepsilon'_{as}(t) - \varepsilon'_{as}(t_0) \tag{4.16}$$

$$\varepsilon'_{as}(t) = \gamma\, \varepsilon'_{as\infty} \left[1 - \exp\left\{ -a\,(t - t_s)^b \right\} \right] \times 10^{-6} \tag{4.17}$$

$$\varepsilon'_{as\infty} = 3070 \exp\left\{ -7.2(w/c) \right\} \tag{4.18}$$

α=11 for normal and low heat cement, α= 15 high early strength cement

where, for t_0, t' and t is replaced by: $t = \sum_{i=1}^{n} \Delta t_i \exp\left[13.65 - \frac{4000}{273 + T(\Delta t_i)/T_0} \right]$ t: is the temperature adjusted concrete age,t_0: starting drying concrete age Δt_i: is the number of days where a temperature T prevails, $T(\Delta t_i)$: is the temperature (°C) during the time period Δt_i, T_0=1 °C.γ: coefficient representing the influence of the cement and admixtures type (maybe 1 when only ordinary Portland cement is used).

w/c	a	b
0.20	1.2	0.4
0.23	1.5	0.4
0.30	0.6	0.5
0.40	0.1	0.7
>=0.50	0.03	0.8

Figure 4.20 shows comparison of the proposed drying shrinkagemodel with the available drying shrinkage experimental results.

Table 4.4 Summary of the factors accounted for by different prediction models

Models		CEB-FIP (1990)	ACI 209R (1997)	Eurocode 2 (2001)	JSCE (2002)	AASHTO (2004)	AASHTO (2007)	AS 3600 (2009)
Intrinsic Factors	Aggregate Type							
	A/C Ratio							
	Air Content		■					■
	Cement Content	■		■	■			
	Cement Type							
	Concrete Density		■					■
	Fine/Total Aggregate Ratio (Mass)		■					■
	Slump		■					■
	W/C Ratio				■			
	Water Content				■			
Extrinsic Factors	Age at First Loading	■	■	■	■	■	■	■
	Age of Sample				■			
	Applied Stress	■	■	■	■			■
	Characteristic Strength at Loading							
	Cross-section Shape				■			
	Curing Conditions							
	Compressive Strength at 28 Days	■	■	■	■	■	■	■
	Duration of Load	■	■	■	■			■
	Effective Thickness	■	■	■	■	■	■	■
	Elastic Modulus at Age of Loading							
	Elastic Modulus at 28 Days	■	■	■	■			■
	Relative Humidity	■	■	■	■	■	■	■
	Temperature				■			
	Time Drying Commences							

Table 4.5 Shrinkage models for SCC

<table>
<tr><th>Ref.</th><th>Modified Shrinkage Prediction Models</th><th>Main Model</th></tr>
<tr><td>Poppe and De Schutter (2005)</td><td>$$\varepsilon_{shr}(t,t_s)=\left[\frac{160}{1-\alpha(w/c)}+10\,\beta_{sc}\left(9-\frac{f_{cm}}{f_{cm0}}\right)\right].\left[-1.55\left(1-\left(RH/RH_0\right)^3\right)\right].\left[\frac{(t-t_s)/t_1}{45.5(h/h_0)^2+(t-t_s)/t_1}\right]^{\gamma}$$
$$\alpha=4.1(c/p)-1.8\quad \gamma=-2.5\,(c/p)+2.6$$
Other symbols as in Model Code 1990, c/p (cement to powder ratio)</td><td>CEB-FIP (1990)</td></tr>
<tr><td>Larson (2006)</td><td>For square specimens: $(\varepsilon_{sh})_t=\frac{t}{20+t}\times 550\times 10^{-6}$
For cylindrical specimens: $(\varepsilon_{sh})_t=\frac{t}{20+t}\times 600\times 10^{-6}$</td><td>ACI 209R (1997)</td></tr>
<tr><td>Cordoba (2007)**</td><td>$$(\varepsilon_{sh})_t=\frac{t^{\alpha}}{f+t^{\alpha}}(\varepsilon_{sh})_u$$
<table>
<tr><th></th><th colspan="3">2 Year Shrinkage Fit Coefficients</th></tr>
<tr><th>Mixtures</th><th>α</th><th>$f\,(days)$</th><th>$(\varepsilon_{sh})_u$</th></tr>
<tr><td>KM</td><td>0.75</td><td>56.9</td><td>847.1</td></tr>
<tr><td>KH</td><td>0.66</td><td>23.3</td><td>1033.8</td></tr>
<tr><td>REGULAR</td><td>0.71</td><td>29.7</td><td>990</td></tr>
<tr><td>Normal Values</td><td>0.94-1.10</td><td>20-130</td><td>415 $\mu\varepsilon$-1070 $\mu\varepsilon$</td></tr>
</table></td><td>ACI 209R (1997)</td></tr>
<tr><td>Khayat and Long (2010)</td><td>$$\varepsilon_{sh}=-k_s\,k_h\left(\frac{t}{55+t}\right)\left(0.56\times 10^3\right)\times A\,(steam-cured);$$
$$k_s=\left[\frac{\frac{t}{26e^{0.0142(V/S)}+t}}{\frac{t}{45+t}}\right]\left[\frac{1064-3.70(V/S)}{923}\right]$$
A is the cement factor: 0.918 for Type MS cement and 1.065 for Type HE + 20% fly ash.</td><td>AASHTO (2004)</td></tr>
</table>

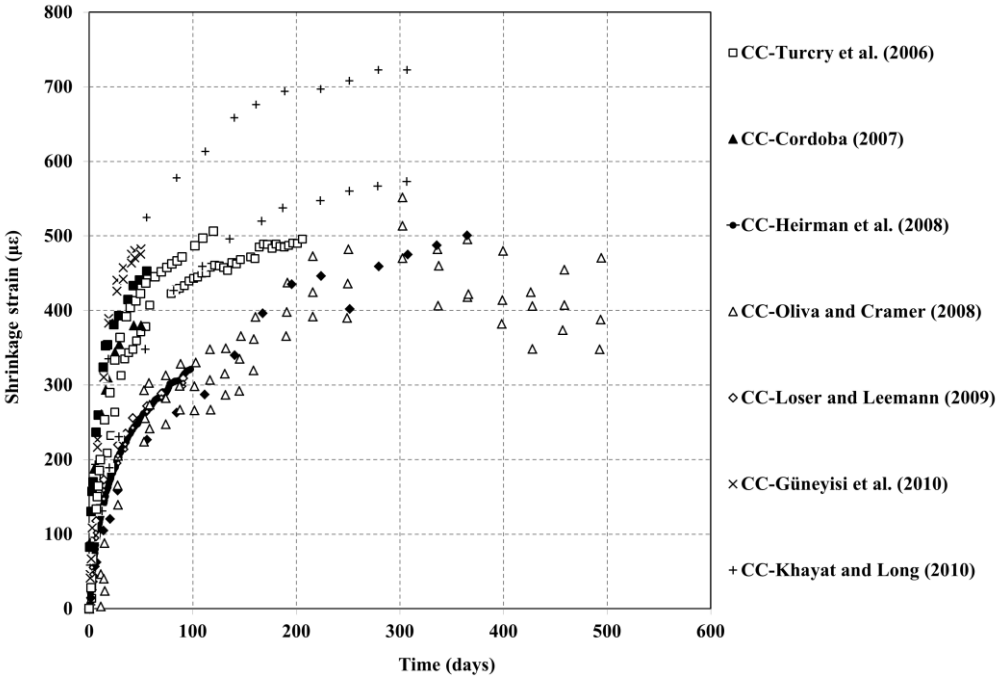

Figure 4.6 Experimental database that summarized for CC (drying shrinkage versus time (days))

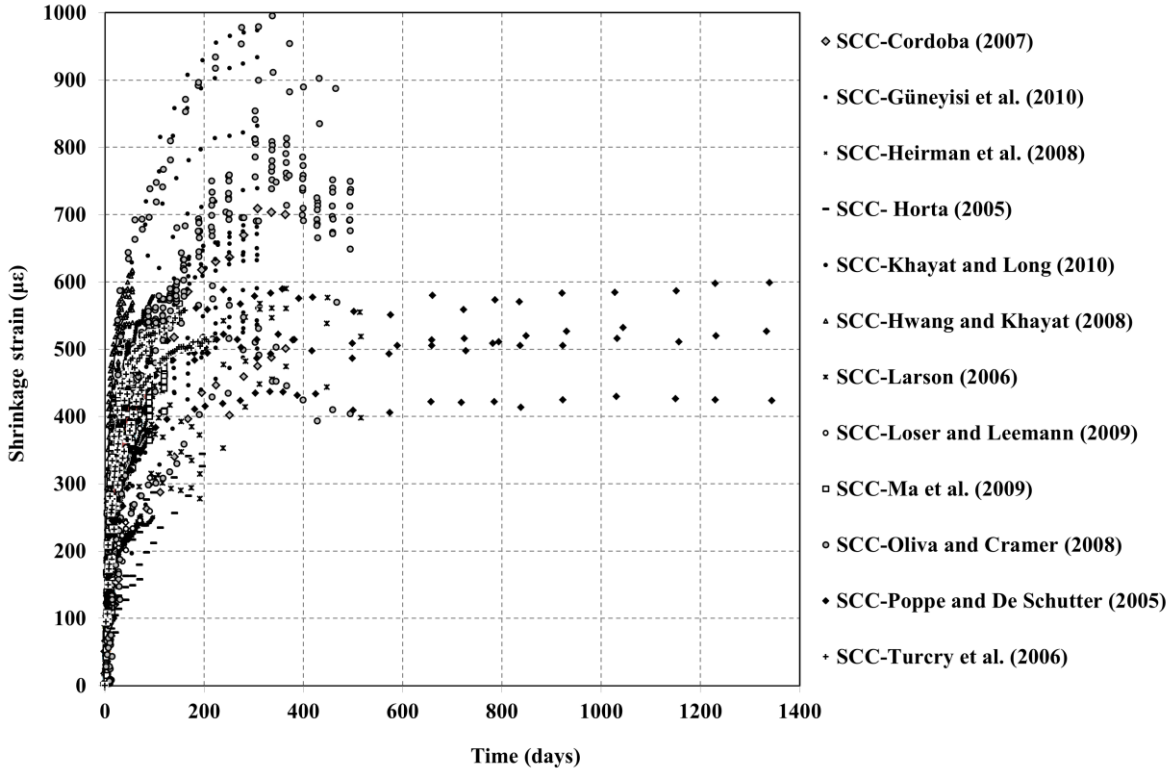

Figure 4.7 Experimental database that summarized for SCC (drying shrinkage versus time (days))

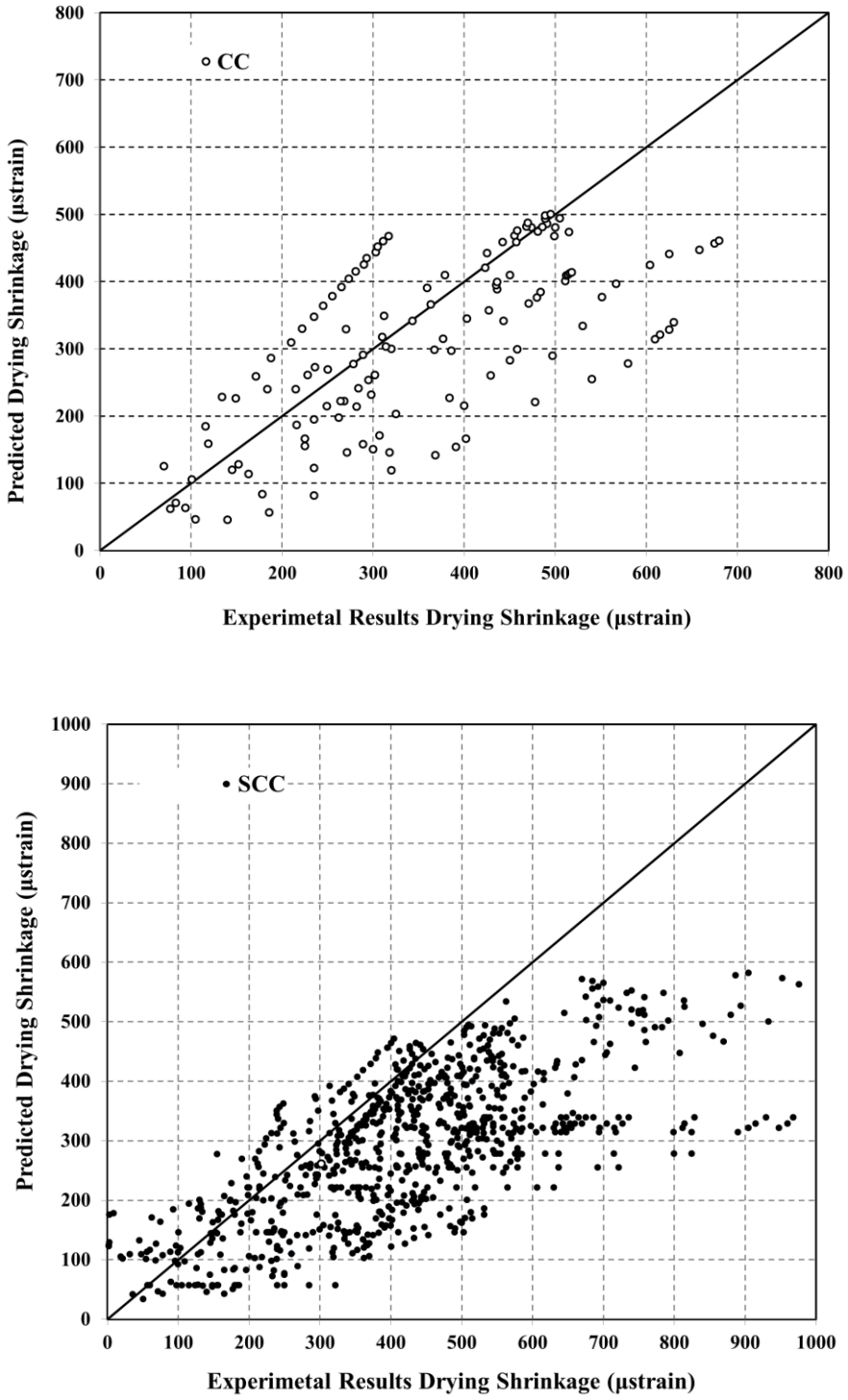

Figure 4.8 Comparison of the SCC and CC drying shrinkage from experimental results versus calculated values from CEB-FIP (1990) model

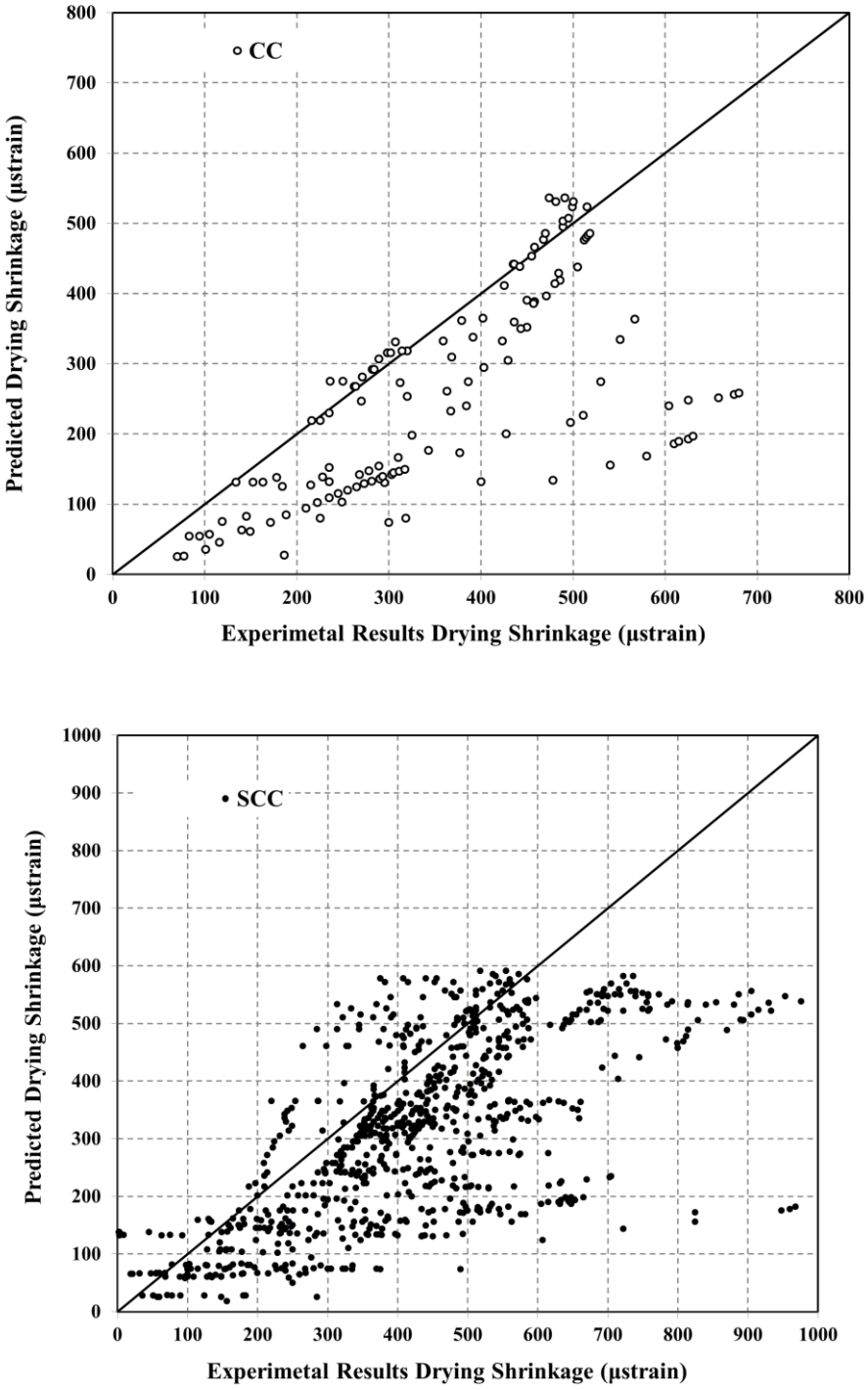

Figure 4.9 Comparison of the SCC and CC drying shrinkage from experimental results versus calculated values from ACI 209R (1997) model

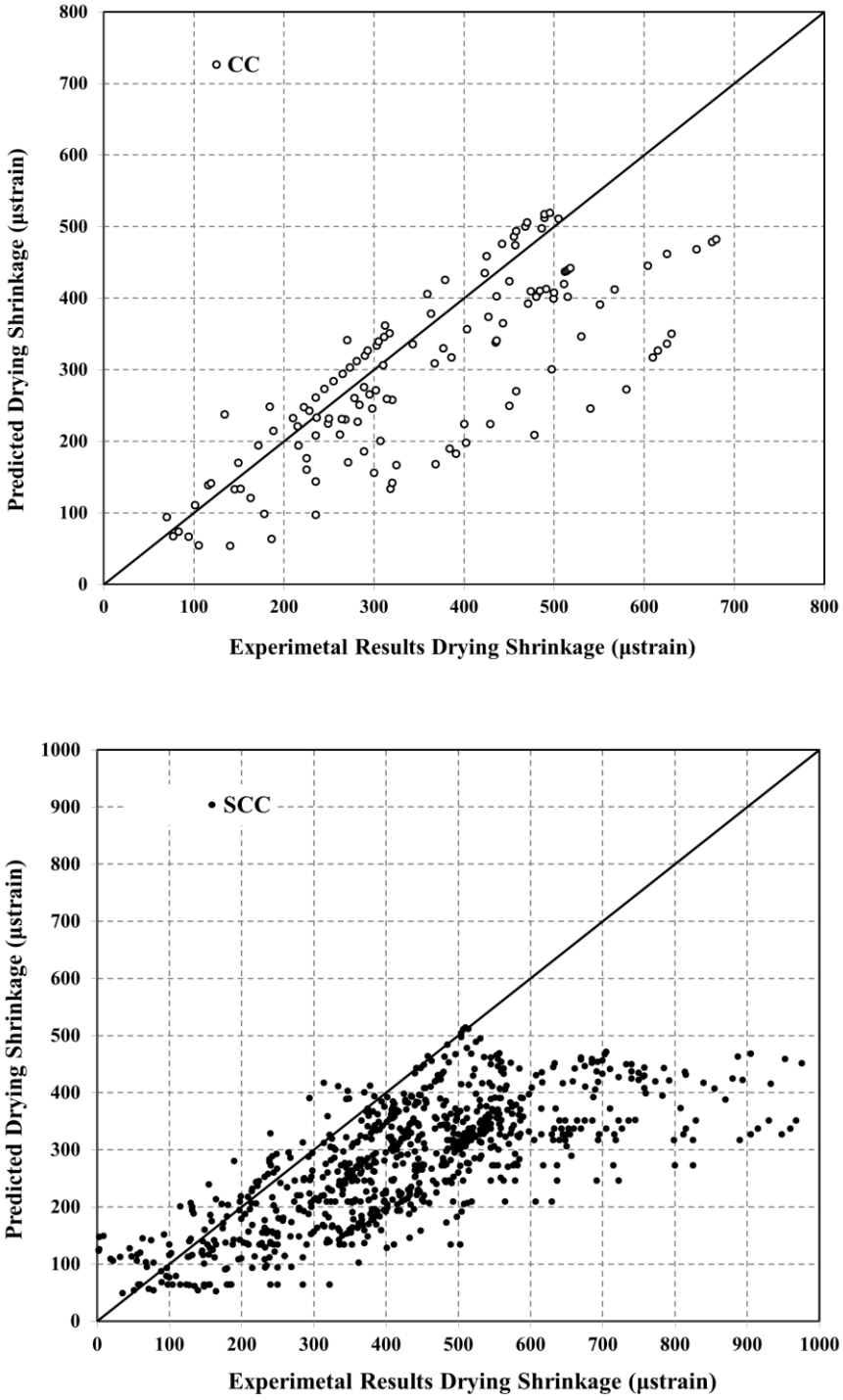

Figure 4.10 Comparison of the SCC and CC drying shrinkage from experimental results versus calculated values from Eurocode 2 (2001) model

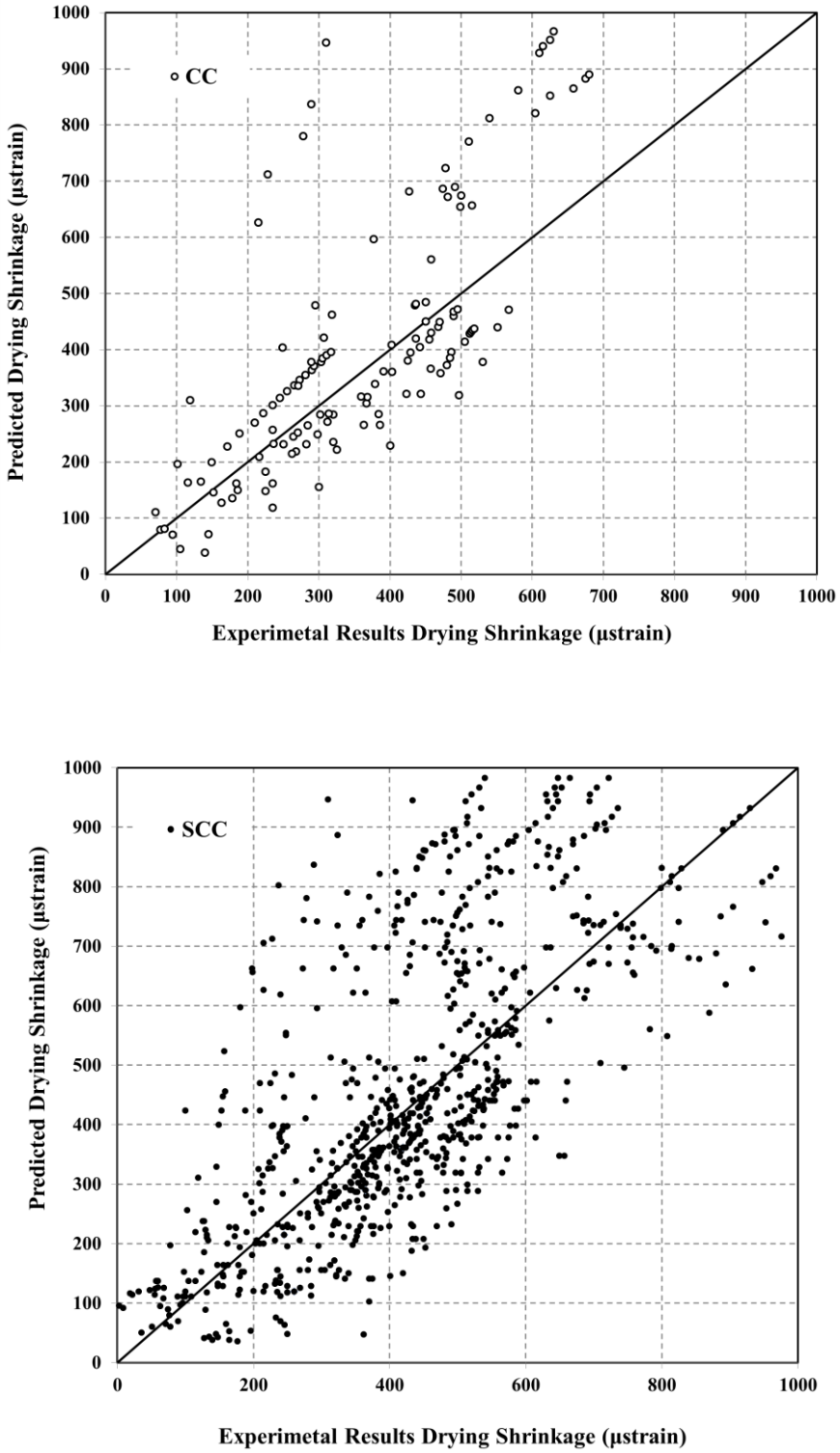

Figure 4.11 Comparison of the SCC and CC drying shrinkage from experimental results versus calculated values from JSCE (2002) model

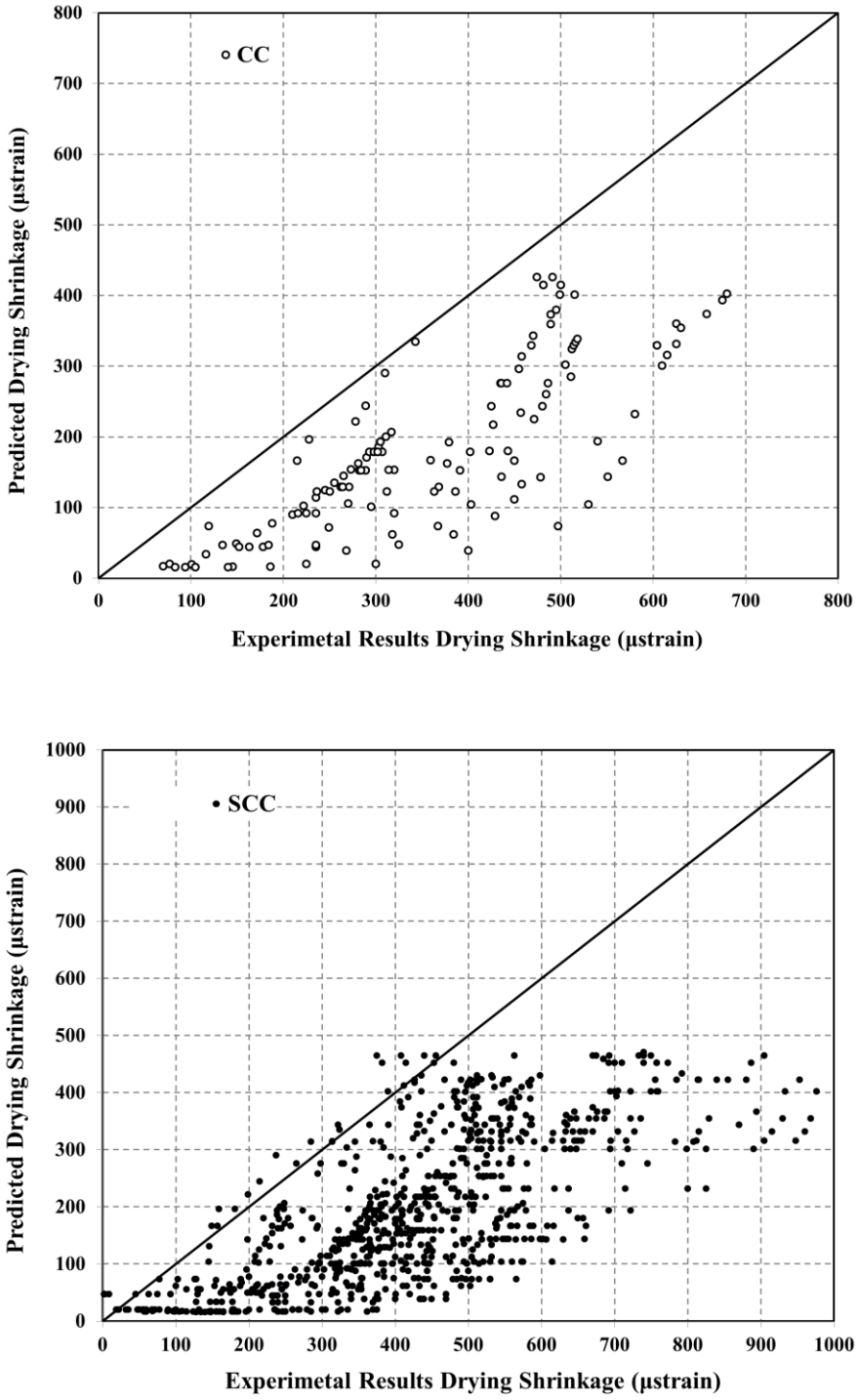

Figure 4.12 Comparison of the SCC and CC drying shrinkage from experimental results versus calculated values from AASHTO (2004) model

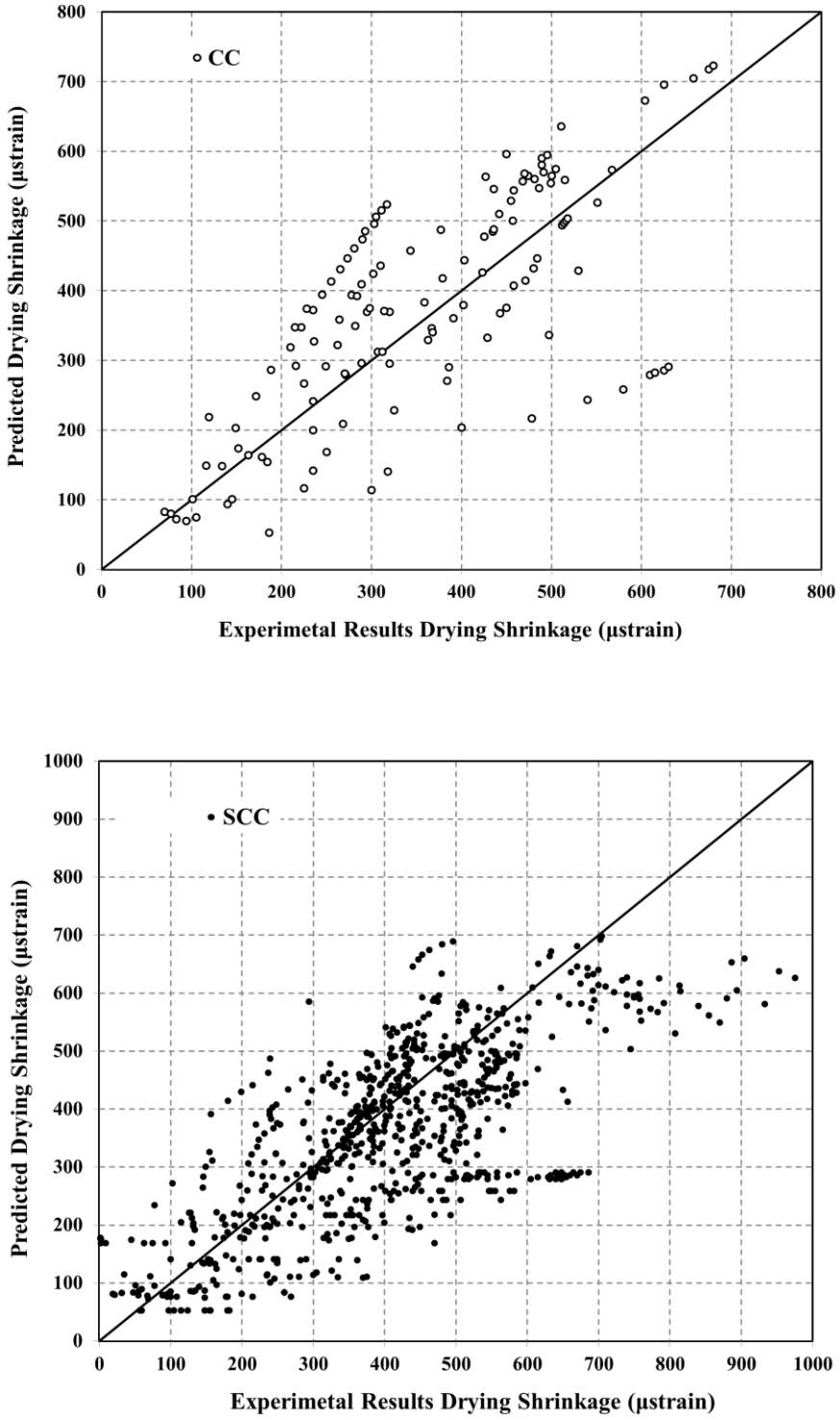

Figure 4.13 Comparison of the SCC and CC drying shrinkage from experimental results versus calculated values from AASHTO (2007) model

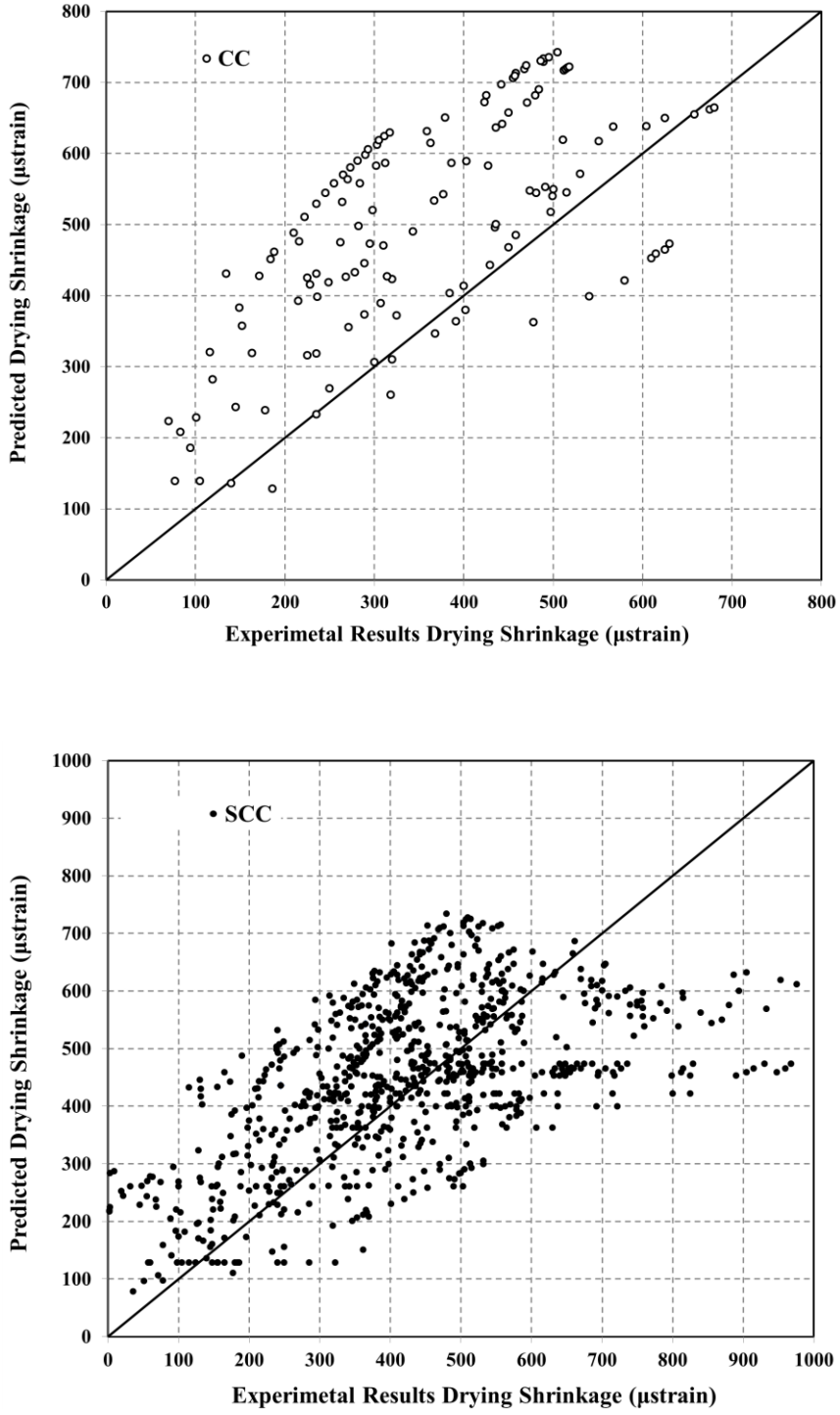

Figure 4.14 Comparison of the SCC and CC drying shrinkage from experimental results versus calculated values from AS 3600 (2009) model

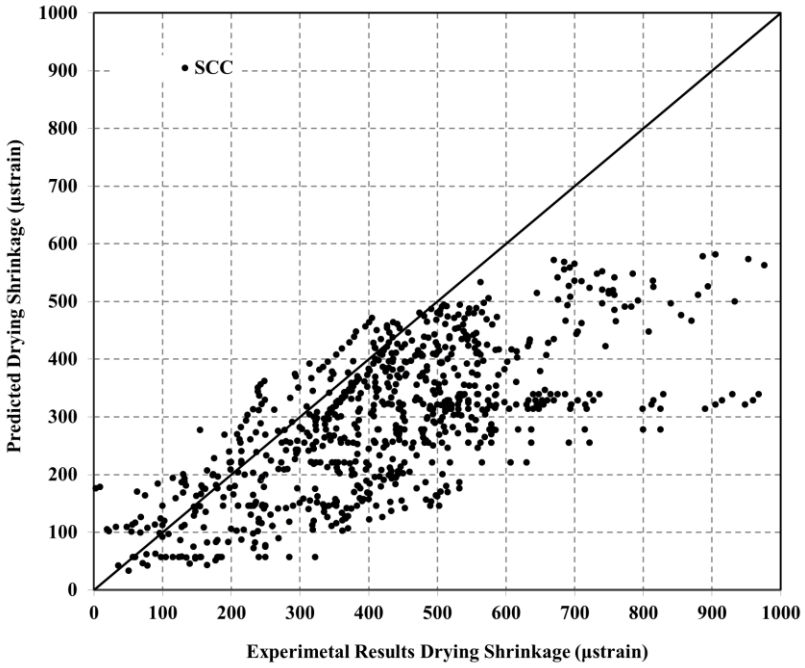

Figure 4.15 Comparison of the SCC drying shrinkage from experimental results versus calculated values from Poppe and De Schutter (2005) model

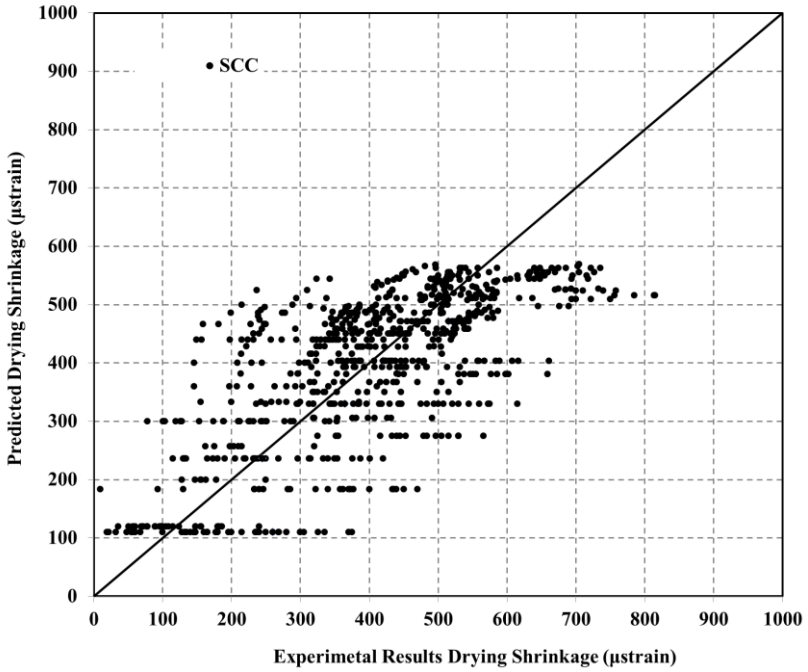

Figure 4.16 Comparison of the SCC drying shrinkage from experimental results versus calculated values from Larson (2006) model

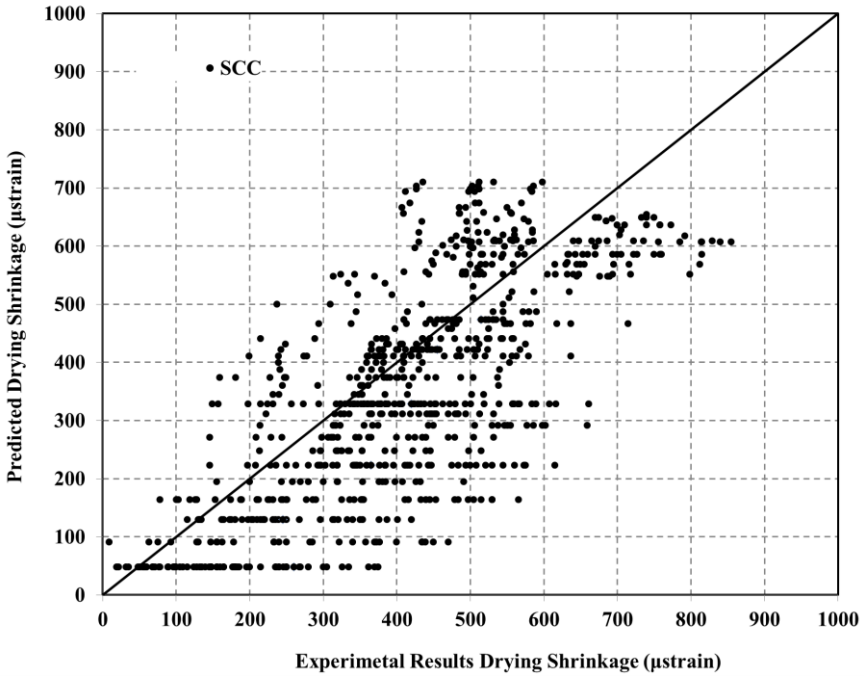

Figure 4.17 Comparison of the SCC drying shrinkage from experimental results versus calculated values from Cordoba (2007) model

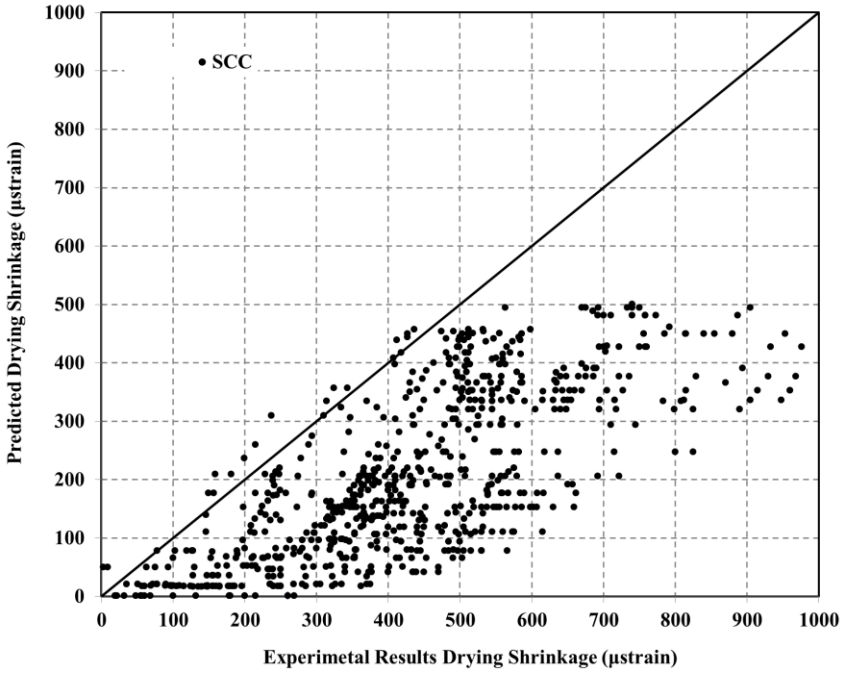

Figure 4.18 Comparison of the SCC drying shrinkage from experimental results versus calculated values from Khayat and Long (2010) model

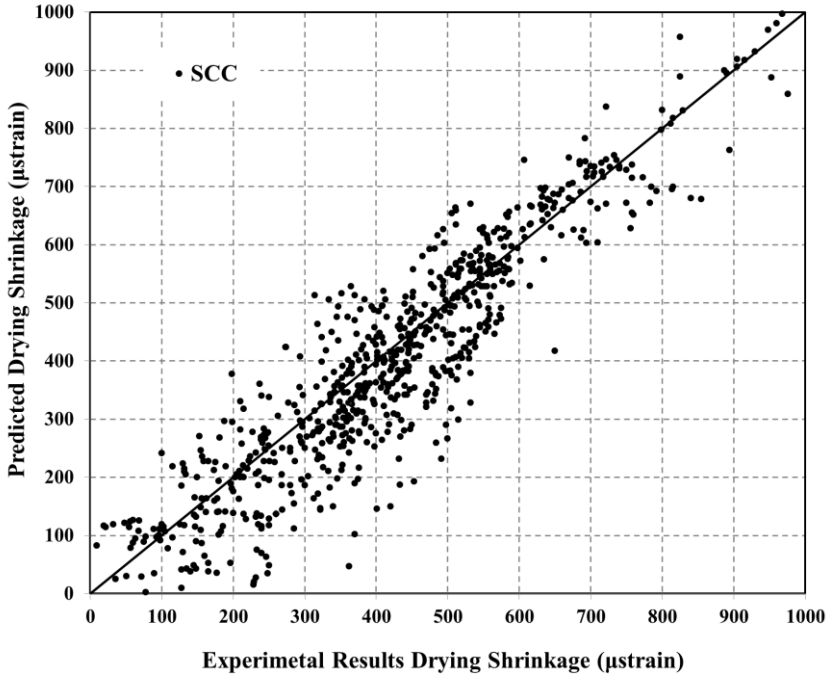

Figure 4.19 Comparison of proposed shrinkage SCC model with experimental results database

4.5.5 Discussion of the Shrinkage Models

As shown in Table 4.6 and Figures 4.8 to 4.14 for the CC mixture in the experimental database, the AASHTO (2007) and JSCE (2002) models provide a better prediction of the drying shrinkage strain with coefficient of correlation factors (R^2) of 0.88 and 0.84, respectively as compared to the other models. In addition, for the SCC mixture in the experimental database, the AASHTO (2007), JSCE (2002) and AS 3600 (2009) models provided a better prediction of drying shrinkage strain with R^2 of 0.86, 0.83 and 0.80, respectively as compared to the other models.

As shown in AASHTO (2007) and JSCE (2002), the CC models that have conservative predictions are different in the certain intrinsic and/or extrinsic variables. As shown in Table 4.4, the AASHTO (2007) model has not considered any intrinsic factors but the JSCE (2002) model has a good consideration of both the intrinsic and the extrinsic variables. The modified composition of the SCC in comparison with the CC has an influence on the shrinkage behaviour of the concrete. Therefore, it is important to include

some variables that have impact on this behaviour. By considering these variables, JSCE (2002) model can cover more reliable intrinsic and extrinsic variables for the SCC mixture.

It can be seen from Figures 4.15 and 4.18 that Poppe and De Schutter (2005) and Khayat and Long (2010)'s models overestimate the drying shrinkage of the SCC mixture. According to Larson (2007) and Cordoba (2007), the SCC drying shrinkage prediction models conservatively underestimate the shrinkage strain of SCC mixtures (Figures 4.16 and 4.17). In Poppe and De Schutter (2005), ACI 209R (1997), CEB-FIP (1990) and Le Roy et al. (1996)'s models are compared and it is found that CEB-FIP (1990) always leads to underestimation of the deformation. Since the CEB-FIP (1990) model shape of the shrinkage deformation is suitable, then this model is selected as a basic model. But, the modified model of CEB-FIP (1990) is just suitable for Poppe and De Schutter (2005)'s experimental results.

The Larson (2006)'s model is just a modification of ACI 209R (1997) model based on the SCC mixture database. This model does not cover intrinsic and extrinsic variables. In the Cordoba (2007)'s model, KL is the first mixture that was based on a mixture developed by Khayat (1995) and modified by Altan (1999). This mixture achieves the SCC performance by replacing some of the coarse aggregates with cement. The second mixture, labelled KM, was based on the KL but with a coarse aggregate content increased to 38%. Similarly, the third mixture, KH, was based on the first mixture, KL but has a coarse aggregate content of 39%. Cordoba (2007)'s model is based on the ACI 209R (1997) because it does not protect intrinsic and extrinsic variables. Khayat and Long (2010)'s shrinkage model is a modification of the AASHTO (2004) model. They have defined a factor that is related to the cement type used in the mixture design. As indicated in Table 4.4, the AASHTO (2004) model does not have any intrinsic factors.

As shown in Figure 4.19, the proposed new model has good prediction compared to the experimental database of SCC mixtures. In the experimental database, normal strength and high strength of the SCC mixtures are available. The SCC proposed new model has good agreement for both normal strength and high strength experimental results. Also, the c/p ratio included in the proposed model has an effective influence on the overall shrinkage

prediction. The experimental results of c/p ratios as shown in Table 4.3 are very variable but the proposed model can predict the drying shrinkage strain better.

Table 4.6 Coefficient of correlation factor (R^2) of shrinkage prediction models for CC and SCC

Shrinkage prediction models	CC	SCC
	R^2	R^2
CEB-FIP (1990)	0.70	0.57
ACI 209R (1992)	0.62	0.66
Eurocode 2 (2001)	0.72	0.55
JSCE (2002)	0.84	0.83
AASHTO (2004)	0.42	0.47
AASHTO (2007)	0.88	0.86
AS 3600 (2009)	0.65	0.80

4.6 CREEP OF SCC

Modifications in the SCC composition of the mixture affect the behaviour of the concrete in its hardened state, including the creep deformations too. Creep of SCC depends on the characteristics of aggregate stiffness and texture, w/c ratio, volume of paste, volume of coarse aggregate, cement type, admixture type, curing method, ratio of volume to surface area, environmental conditions, magnitude of loads, and age of first loading. According to Neville (1996) mostly the hydrated cement paste experiences creep, while the aggregate is the only portion which resists against creep. Therefore, creep is highly dependent on the stiffness of the chosen aggregate and its proportion within the mixture (Neville, 1996). As a result, since creep mainly occurs in the cement paste, main concern arises that SCC may exhibit higher creep because of its high paste content.

Because SCC has a higher paste volume (or higher sand to aggregate ratio) to achieve high workability and high early strength, several researchers have reported relatively large creep strains of SCC for precast, prestressed concrete, resulting in larger prestress losses

(Issa et al., 2005; Naito et al., 2006; Schindler et al., 2007; Suksawang et al., 2006). While the mechanical properties of SCC are superior to those of the CC, creep of SCC is significantly higher too (Issa et al., 2005). Naito et al. (2006) also found that the SCC exhibits higher creep than the CC, which is due to the high fine aggregate volume in SCC. Naito et al. (2006) found that the creep coefficient of SCC and CC was 40 and 6 precent higher than the ACI 209 (1992) prediction model, respectively. However, different methodologies are followed to obtain SCC in different countries (Ouchi et al., 2003) and limited number of studies are available concerning its long-term behaviour (Persson 2001, 2005; Poppe and De Shutter 2001; Seng and Shima, 2005; Mazzotti et al., 2006). It is not clear in the available studies if current international standards apply successfully for the SCC (Klug and Holschemaker, 2003; Vidal et al., 2005; Landsberger and F.-Gomez, 2007). Moreover, it is not assessed if long-term properties can be predicted with reference to conventional parameters only (like strength, w/c, etc) or adoption of the new parameters concerning the mix design are also needed.

The objectives of the present section are: (a) To establish an experimental results database of creep. (b) To review the accuracy of the CC creep prediction models proposed by international codes of practice, including: CEB-FIP (1990), ACI 209R (1997), Eurocode 2 (2001), JSCE (2002), AASHTO (2004), AASHTO (2007) and AS 3600 (2009). (c) To review the accuracy of the SCC creep prediction models proposed by Poppe and De Schutter (2005), Larson (2007) and Cordoba (2007). (d) To propose a new prediction creep model based on the comprehensive analysis of the available models and the experimental results database of both CC and SCC.

4.6.1 Experimental Database for Creep of CC and SCC from the Literature

The database comprises test results from 11 different investigations, with a total of 55 SCC and 16 CC mixtures for creep tests. Tables 4.7 and 4.8 also include complimentary information regarding the applied stress to the creep specimens, final age of the concrete (in days), relative humidity (RH), type of the specimen, type of the cement and the filler. Table 4.9 includes information about cement content, water, compressive strength and cement to powder (c/p) ratio for each mixtures that have been used in the different investigation.

Figures 4.20 and 4.21 show the CC and SCC experimental results database that is summarized in Tables 4.7 and 4.8. By reviewing the experimental results of creep in the database the following conclusions can be made: (1) by decreasing the water to binder ratio, increase in the creep strain is observed (2) increase in the proportion of the total aggregate in the mixture could cause decrease in the total creep (3) when the content of total aggregate and binder in concrete is held constant, the total creep decreases as coarse aggregate proportion increases.

4.6.2 Creep Models for CC from the Literature

This section assesses the accuracy of seven models commonly used international codes to predict creep strains. These empirical models, which vary widely in their techniques, require certain intrinsic and/or extrinsic variables, such as mix proportions, material properties and age of loading as input. The models considered are listed in Table 4.10, which also shows the factors required by each model. In this section the accuracy of the creep models proposed by the international codes of practice, including: CEB-FIP (1990), ACI 209R (1997), Eurocode 2 (2001), JSCE (2002), AASHTO (2004), AASHTO (2007) and AS 3600 (2009) are compared with the actual measured creep strains in 52 mixtures of SCC and 15 mixtures of CC. Figures 4.22 to 4.28 show comparison of the creep coefficient determined by the available CC models with the available experimental results in the literature (Tables 4.7 to 4.9).

4.6.3 Creep Models for SCC from the Literature

In Table 4.11 empirical models for calculating creep of the SCC are shown. These models vary in complexity, and precision in the calculations. Figures 4.29 to 4.31 show comparison of the creep coefficient by Poppe and De Schutter (2005), Larson (2006), and Cordoba (2007) with the measured creep coefficient in the experimental results.

4.6.4 Proposed Creep Model for SCC

The comparison of the different models and the experimental database shows that ACI 209R (1997), JSCE (2002) and AASHTO (2004) models have conservative creep coefficient predictions. In this section, based on required certain intrinsic and/or extrinsic variables (i.e., mix proportions, material properties and age of loading) for the SCC mixtures are shown in Table 4.12. Table 4.12 shows that JSCE (2002) creep model gives a good coverage of the intrinsic and/or extrinsic variables that are useful for calculating the creep strain. Therefore, with the JSCE (2002) model as a basis, an attempt is made to formulate some proposals to include the c/p (cement to powder) ratio in order to obtain a better prediction of the time-dependent deformations of the normal strength and the high strength SCC. These proposed models are presented below in Eq. (4.19) to Eq. (4.28), for normal strength and high strength SCC:

- ***For normal strength SCC with range of applicability:***

$45\% \le RH \le 80\%$

$130\ kg/m^3 \le w \le 230\,kg/m^3$

$100\,mm \le v/s \le 300\,mm$

$40\% \le w/c \le 65\%$

$f'_c(28) \le 55\,MPa$

$260\,kg/m^3 \le c \le 500\,kg/m^3$

$$\varepsilon'_{cc}(t,t',t_0) = \sigma'_{cp} \times \varepsilon'_{cr} \left[1-\exp\left\{-0.09\,(t-t')^{0.54}\right\}\right] \times (0.015+1.35\,(c/p))^{-1} \quad \text{for c/p} < 0.65 \qquad (4.19)$$

$$\varepsilon'_{cc}(t,t',t_0) = \sigma'_{cp} \times \varepsilon'_{cr} \left[1-exp\left\{-0.09\,(t-t')^{0.54}\right\}\right] \times (0.015+1.05\,(c/p))^{-1} \quad \text{for c/p} \ge 0.65 \qquad (4.20)$$

non-linear creep amplification function: $\sigma'_{cp} = \dfrac{\mu + \lambda.\sigma(t,t_0)^{\alpha}}{1-\kappa}$ (4.21)

where μ and λ and α are additional parameters to be obtained from a least square minimization procedure starting from experimental data (Mazzotti and Ceccoli, 2009) μ=0.90, λ=1.80, α=2.10; moreover, the stress function $\sigma(t, t_0)$ is the actual stress/strength ratio, being:

$$\sigma(t,t_0)=\frac{\sigma(t_0)}{f_{cm}(t)} \tag{4.22}$$

in the case of constant applied load. In Eq. (4.16), numerator and denominator indicate the effect of sustained load and the effect of a damage level due to instantaneous loading. The law $f_{cm}(t)$ representing the evolution with time of compression strength has been defined by modifying MC90 proposal according to expression:

$$f_{cm}(t)=f'_{c,28}.\exp\left[s'\left(1-\left(\frac{28}{t}\right)^{n}\right)\right] \tag{4.23}$$

where parameters s' and n have been specifically calibrated for each SCC concrete mix by using experimental results previously described. According to the available data, parameters s' and n range from 0.2–0.6, and 0.28–0.35, respectively (Mazzotti and Ceccoli, 2009). The adoption of function $\sigma(t, t_0)$ allows for variable rate of increase of mechanical properties be taken into account, particularly important for concretes loaded at early ages. Finally, the non-linear behavior during the load application has been introduced in Eq. (4.16) according to the conventional scalar damage index $\kappa = 1 - E/E_0$, where E is the secant stiffness at the end of loading and E_0 is the initial tangent stiffness. Usually damage index κ is about 0.10–0.15 or 0.22–0.35 for low ($0.35f_{cm}(t)$) or medium ($0.55f_{cm}(t)$) applied stress levels, respectively.

$$\varepsilon'_{cr}=\varepsilon'_{bc}+\varepsilon'_{dc} \tag{4.24}$$

$$\varepsilon'_{bc}=\left[17.5\,(c+w)^{2.0}\,(w/c)^{2.4}\,\{ln(t')\}^{-0.67}\right]\times10^{-10} \tag{4.25}$$

$$\varepsilon'_{dc}=\left[4500(w/c)^{4.2}\,(c+w)^{1.4}\left[ln\left(\frac{v/s}{10}\right)\right]^{-2.2}\left\{1-\frac{RH}{100}\right\}^{0.36}t_0^{-0.30}\right]\times10^{-10} \tag{4.26}$$

- ***For high strength SCC with range of applicability:***

$45\% \le RH \le 90\%$

$130\ kg/m^3 \le w \le 230\ kg/m^3$

$100\ mm \le v/s \le 300\ mm$

$40\% \le w/c \le 65\%$

$f'_c(28) \le 80\ MPa$

$$\varepsilon'_{cc}(t,t',t_0) = \sigma'_{cp} \times \left[\frac{4w(1-RH/100)+350}{12+f'_c(t')}\ ln(t-t'+1) \right] \times \left(10 \times (c/p)^{0.678}\right) \quad \text{for c/p} < 0.65 \qquad (4.27)$$

$$\varepsilon'_{cc}(t,t',t_0) = \sigma'_{cp} \times \left[\frac{4w(1-RH/100)+350}{12+f'_c(t')}\ \ln(t-t'+1) \right] \times \left(13 \times (c/p)^{0.701}\right) \quad \text{for c/p} \ge 0.65 \qquad (4.28)$$

where t_0,t' and t are the effective age (days) of concrete at the beginning of drying, at the beginning of loading, and during loading respectively; ε'_{cr} is the final value of creep strain per unit stress; ε'_{bc} is the final value of basic creep strain per unit stress; ε'_{dc} is the final value of drying creep strain per unit stress.

Figure 4.32 shows comparison of the proposed creep model with the available creep coefficient experimental results.

Table 4.7 Creep experimental results database

Reference	No. of SCC mixtures	No. of CC mixtures	Applied stress to the creep specimens	Final age of concrete (days)
Chopin et al. (2003)	5	1	40% or 60% of the compressive strength at 28 days	365
Poppe and De Schutter (2005)	6	0	1/3 of the compressive strength at 28 days	1400
Horta (2005)	6	0	40% of the compressive strength at 28 days	70, 200
Larson (2006)	1	0	40% of the compressive strength at 28 days	520
Turcry et al. (2006)	3	3	20% of the compressive strength at 7 days	65, 100
Cordoba (2007)	4	1	30% of the compressive strength at 28 days	365
Heirman et al. (2008)	7	1	±1/3 of the compressive strength at 28 days	70
Oliva and Cramer (2008)	11	4	40% of the compressive strength at 28 days	495
Kim (2008)	4	4	Changeable for each mixture	150
Zheng et al. (2009)	7	1	30% of the compressive strength at loading days	150
Loser and Leemann (2009)	1	1	Changeable for each mixture	91
Total of 71 mixtures	55	16		

Table 4.8 Creep experimental results database (continued)

Reference	R.H. (%)	Type of specimen (mm)	Type of cement	Type of Filler
Chopin et al. (2003)	50	Cylinder (90 × 280)	CEM I	Limestone
Poppe and De Schutter (2005)	60	Prism (150×150×500)	CEM I 42.5 R, CEM I 52.5	Limestone
Horta (2005)	50	Cylinder (150 × 300)	CEM I , CEM III	Fly ash and GGBFS
Larson (2006)	50	Prism (101.6×101.6×609.6) and Cylinder (114.3×609.6)	CEM III	Limestone
Turcry et al. (2006)	50	Cylinder (110 x 200)	CEM I 52.5, CEM II 42.5	Limestone
Cordoba (2007)	50	Cylinder (101.6 × 203.2), (101.6 × 1057.8)	CEM I/II	Fly ash and GGBFS
Heirman et al. (2008)	60	Cylinder (120 × 300)	CEM I 42.5 R, CEM III/A 42.5 N LA	Limestone
Oliva and Cramer (2008)	50	Cylinder (152.4 × 213.6)	CEM I	GGBFS
Kim (2008)	50	Cylinder (100×200)	CEM III	Fly ash and Limestone
Zheng et al. (2009)	60	Prism (100×100×400)	CEM I	Fly ash
Loser and Leemann (2009)	70	Prism (120×120×360)	CEM I 42.5 N, CEM II/A-LL 45.2 N	Fly ash and Limestone

Table 4.9 Mix properties of the creep experimental database

Chopin et al. (2003)	Cement (kg/m^3)	Filler (kg/m^3)	c/p	w (kg/m^3)	f'_c (MPa)
SCC1	374	172	0.68	123	36.8
SCC2	344	256	0.57	131	36.5
SCC3	396	161	0.71	154	49.9
SCC4	396	177	0.69	115	36
SCC5	347	177	0.66	139	39.1
CC	348	-	1.00	132	35.6
Poppe and De Schutter (2005)	Cement (kg/m^3)	Filler (kg/m^3)	c/p	w (kg/m^3)	f'_c (MPa)
SCC1	300	300	0.50	165	59
SCC2	360	240	0.60	165	63.8
SCC3	400	200	0.67	165	73.7
SCC4	450	150	0.75	165	74.3
SCC5	360	240	0.60	165	66.6
SCC6	360	240	0.60	165	67.2
Horta(2005)	Cement (kg/m^3)	Filler (kg/m^3)	c/p	w (kg/m^3)	f'_c (MPa)
S-Slag/Ash	427	172	0.71	182	73.3
G-Slag	433	133	0.77	208	56.6
Tindall	445	-	1.00	171	57.3
7N	468	99	0.83	177	87
7BL	461	97	0.83	181	77.7
67M	458	91	0.83	175	78.2
Larson (2006)	Cement (kg/m^3)	Filler (kg/m^3)	c/p	w (kg/m^3)	f'_c (MPa)
SCC	446	-	1	224	51.7
CC	387	-	1	263	51.7
Turcry et al. (2006)	Cement (kg/m^3)	Filler (kg/m^3)	c/p	w (kg/m^3)	f'_c (MPa)
SCC1	330	110	0.75	180	40
SCC2	350	139	0.72	198	42
SCC3	350	150	0.70	187	48
CC1	280	-	1.00	170	37
CC2	350	-	1.00	175	41
CC3	360	-	1.00	170	53
Cordoba (2007)	Cement (kg/m^3)	Filler (kg/m^3)	c/p	w (kg/m^3)	f'_c (MPa)
KH	408	132.8	0.75	205.00	48.9
KM	418	136	0.75	210.00	48.2
CC	531	-	1	202.00	46.1
Heirman et al. (2008)	Cement (kg/m^3)	Filler (kg/m^3)	c/p	w (kg/m^3)	f'_c, *cub150* (MPa)
SCC1	360	240	0.6	165	57.1
SCC3	360	240	0.6	165	69.2
SCC5	300	300	0.5	165	49
SCC14	360	240	0.6	144	68.4
SCC15	360	240	0.6	198	46.7
SCC16	360	240	0.6	165	73.3
SCC17	360	240	0.6	216	39.9

Table 4.9 Mix properties of the creep experimental database (continued)

Kim (2008)	Cement (kg/m^3)	Filler (kg/m^3)	c/p	w (kg/m^3)	f'_c (MPa)
S5G-3	376	177	0.68	152	63
S7G-4,5,6	427	107	0.80	123	79
S5L-3	380	253	0.60	171	65
S7L-4,5,6	427	107	0.80	133	88
C5G	371	-	1.00	134	65
C7G	415	-	1.00	119	73
C5L	356	-	1.00	149	59
C7L	403	-	1.00	133	72
Zheng et al. (2009)	Cement (kg/m^3)	Filler (kg/m^3)	c/p	w (kg/m^3)	f'_c (MPa)
SCC1	440	110	0.80	180	52.6
SCC2	250	300	0.45	154	46.5
SCC3	288	192	0.60	145	47.7
SCC4	312	208	0.60	156	51
SCC5	330	220	0.60	165	52
SCC6	330	220	0.60	155	43.8
SCC7	330	220	0.60	165	40.5
CC	525	0	1.00	200	41.3
Loser and Leemann (2009)	Cement (kg/m^3)	Filler (kg/m^3)	c/p	w (kg/m^3)	f'_c (MPa)
SCC2	310	-	1	179	71.1
CC2	512	-	1	155	51.2

Table 4.10 Summary of the factors accounted for by different prediction models

Models		CEB-FIP (1990)	ACI 209R (1997)	Eurocode 2 (2001)	JSCE (2002)	AASHTO (2004)	AASHTO (2007)	AS 3600 (2009)
Intrinsic Factors	Aggregate Type							
	A/C Ratio							
	Air Content		■					■
	Cement Content	■		■	■			
	Cement Type							
	Concrete Density		■					■
	Fine/Total Aggregate Ratio (Mass)		■					■
	Slump		■					■
	W/C Ratio				■			
	Water Content				■			
Extrinsic Factors	Age at First Loading	■	■	■	■	■	■	■
	Age of Sample				■			
	Applied Stress	■	■	■	■			■
	Characteristic Strength at Loading							
	Cross-section Shape				■			
	Curing Conditions							
	Compressive Strength at 28 Days	■	■	■	■	■	■	■
	Duration of Load	■	■	■	■			■
	Effective Thickness	■	■	■	■	■	■	■
	Elastic Modulus at Age of Loading							
	Elastic Modulus at 28 Days	■	■	■	■			■
	Relative Humidity	■	■	■	■	■	■	■
	Temperature				■			
	Time Drying Commences							

Table 4.11 Creep Models for SCC

<table>
<tr><th>Ref.</th><th>Creep Prediction Models</th><th>Main Model</th></tr>
<tr><td>Poppe and De Schutter (2005)</td><td>$$\varepsilon_{cr}(t,t_0)=\frac{\sigma_c(t_0)}{E_{ci}}\cdot\left[1+\frac{(1-(RH/RH_0))}{0.46(h/h_0)^{1/3}}\right]\cdot\frac{5.3}{(f_{cm}/f_{cm0})^{1/2}}\frac{1}{0.1+(t_0/t_1)^{0.2}}\cdot$$ $$\cdot\left[\frac{(t-t_0)/t_1}{\left(150\left(1+\left(1.2\frac{RH}{RH_0}\right)^{18}\right)\frac{h}{h_0}+250\right)+\frac{t-t_0}{t_1}}\right]^{0.3}\cdot\left[\frac{1}{0.01+1.37(c/p)}\right]$$ Other symbols as in Model Code 1990, c/p (cement to powder ratio)</td><td>CEB-FIP (1990)</td></tr>
<tr><td>Larson (2006)</td><td>For the specimens loaded at 1 day (for square and cylindrical specimens): $v_t=\frac{t^{0.7}}{16+t^{0.7}}(1.75)$
For the specimens loaded at 28 day (for square specimens): $v_t=\frac{t^{0.6}}{24+t^{0.6}}(2.00)$</td><td>ACI 209R (1997)</td></tr>
<tr><td>Cordoba (2007)</td><td>$$v_t=\frac{t^{\psi}}{d+t^{\psi}}v_u$$
<table>
<tr><th></th><th colspan="3">1 Year Creep Fit Coefficients</th><th colspan="3">2 Year Creep Fit Coefficients</th></tr>
<tr><th>Mixtures</th><th>ψ</th><th>$d\ (days)$</th><th>v_u</th><th>ψ</th><th>$d\ (days)$</th><th>v_u</th></tr>
<tr><td>KM</td><td>0.43</td><td>13.34</td><td>2.43</td><td>0.35</td><td>37.65</td><td>7.27</td></tr>
<tr><td>KH</td><td>0.44</td><td>16.95</td><td>5.08</td><td>N/A</td><td>N/A</td><td>N/A</td></tr>
<tr><td>REGULAR</td><td>0.39</td><td>8.22</td><td>1.25</td><td></td><td>8.54</td><td>1.31</td></tr>
<tr><td>Normal Values</td><td>0.4-0.8</td><td>6-30</td><td>1.3-4.15</td><td>0.4-0.8</td><td>6-30</td><td>1.3-4.15</td></tr>
</table></td><td>ACI 209R (1997)</td></tr>
</table>

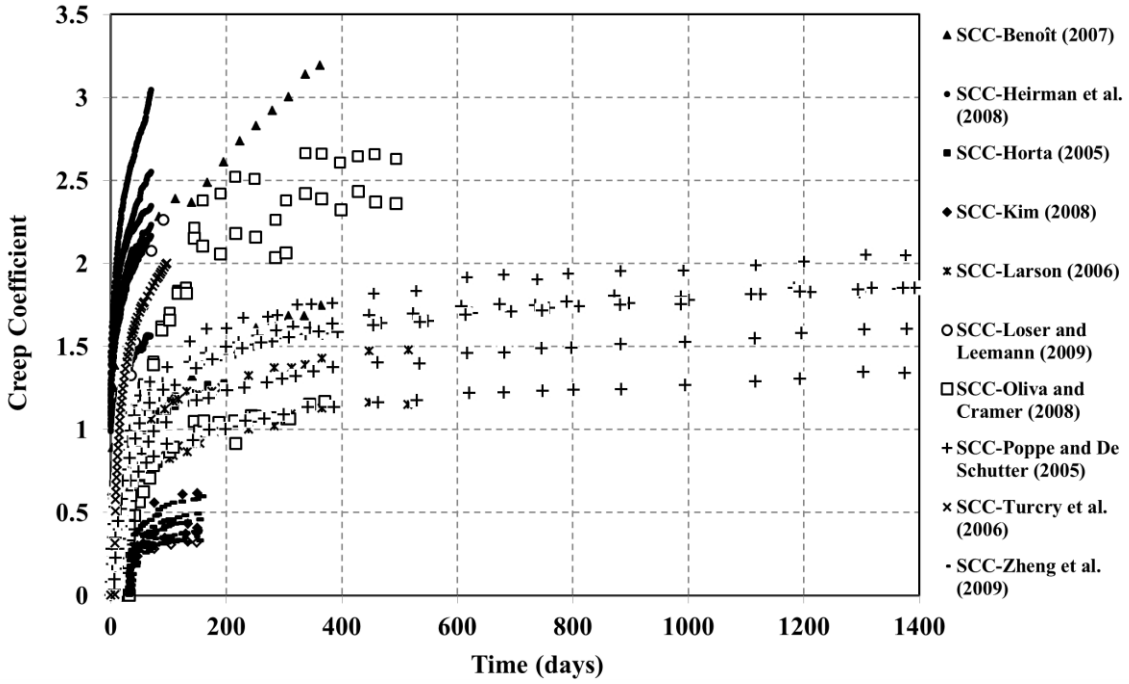

Figure 4.20 Experimental database that summarized for CC (creep coefficient versus time (days))

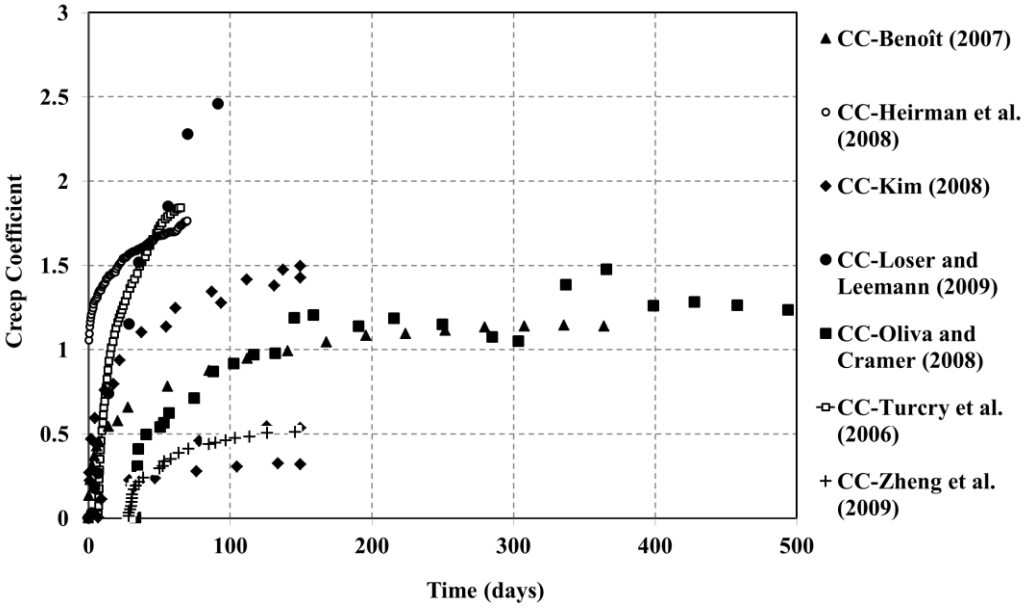

Figure 4.21 Experimental database that summarized for SCC (creep coefficient versus time (days))

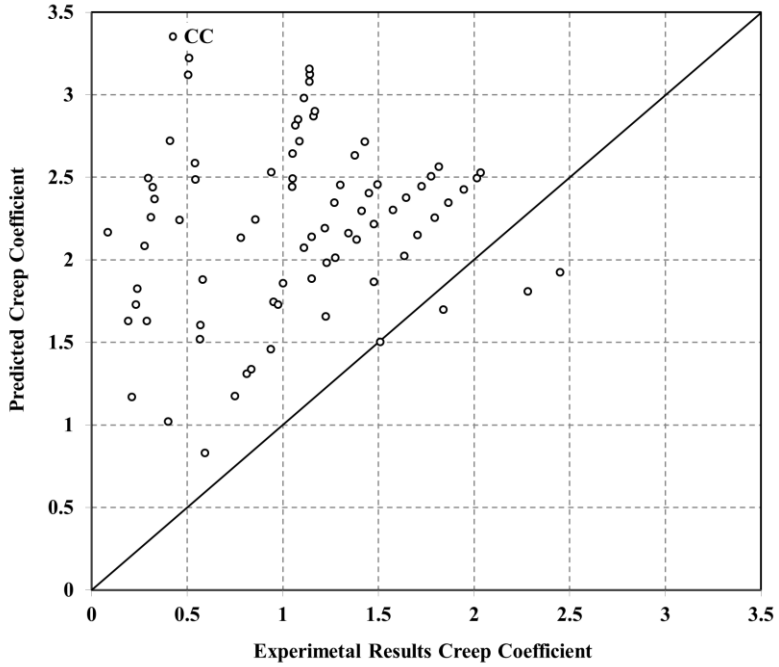

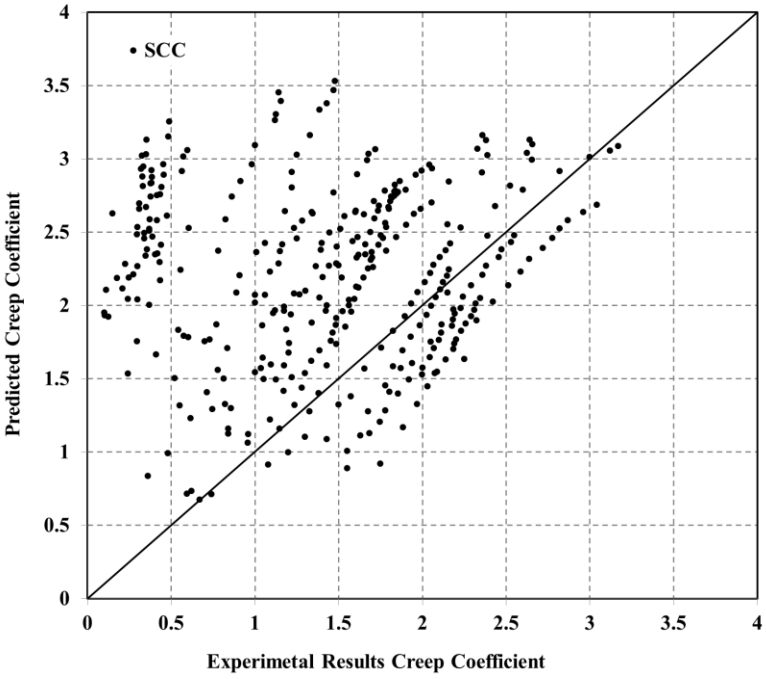

Figure 4.22 Comparison of the SCC and CC creep coefficient from experimental results versus calculated values from CEB-FIP (1990) model

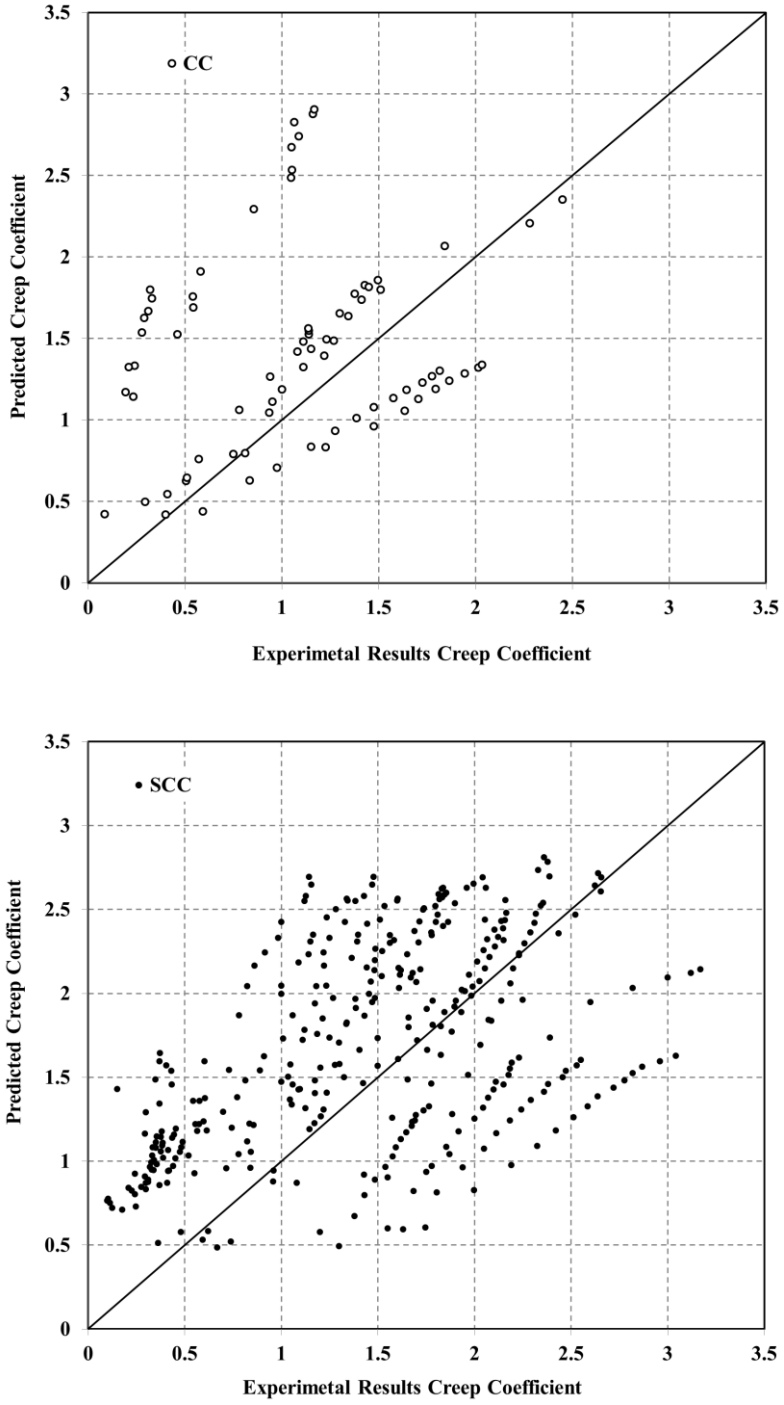

Figure 4.23 Comparison of the SCC and CC creep coefficient from experimental results versus calculated values from ACI 209R (1997) model

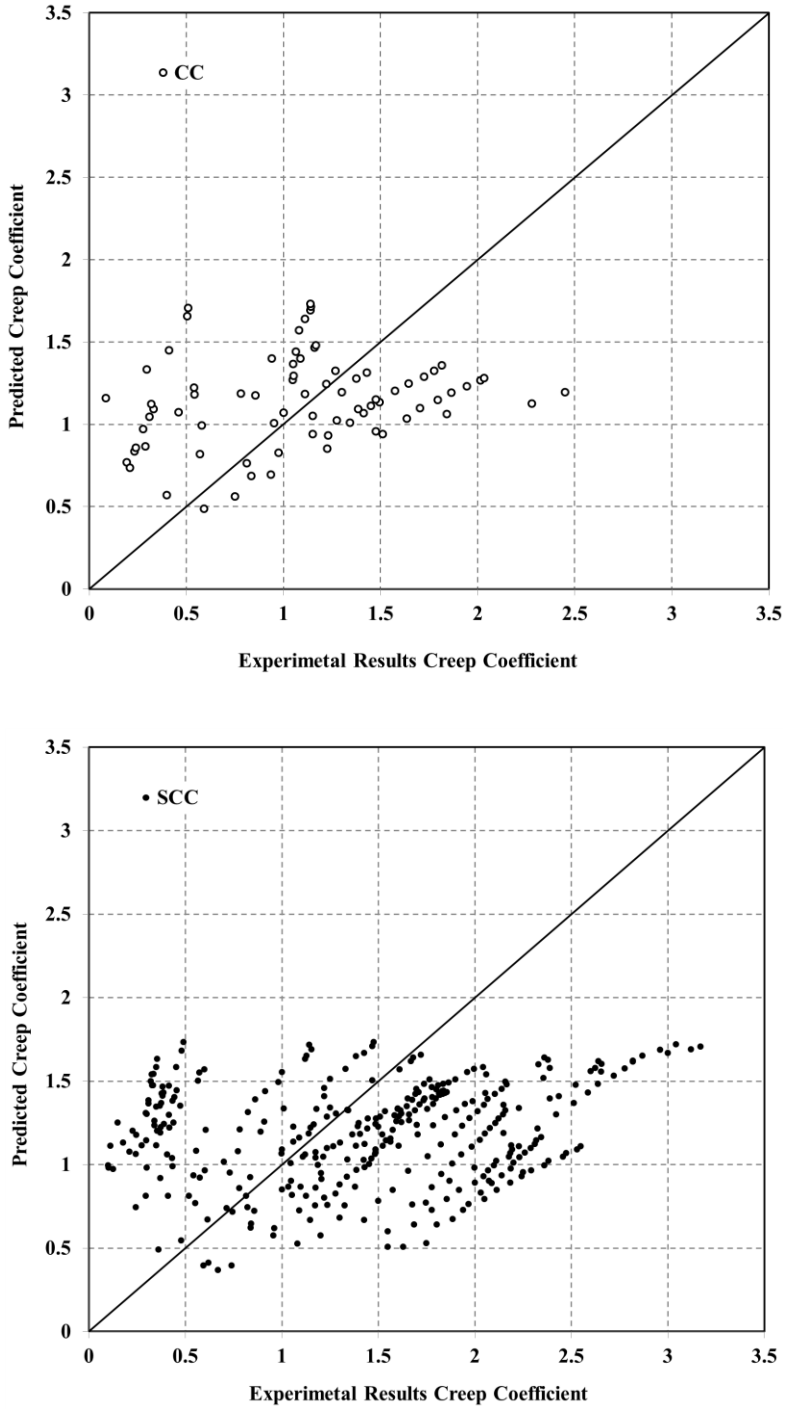

Figure 4.24 Comparison of the SCC and CC creep coefficient from experimental results versus calculated values from Eurocode 2 (2001) model

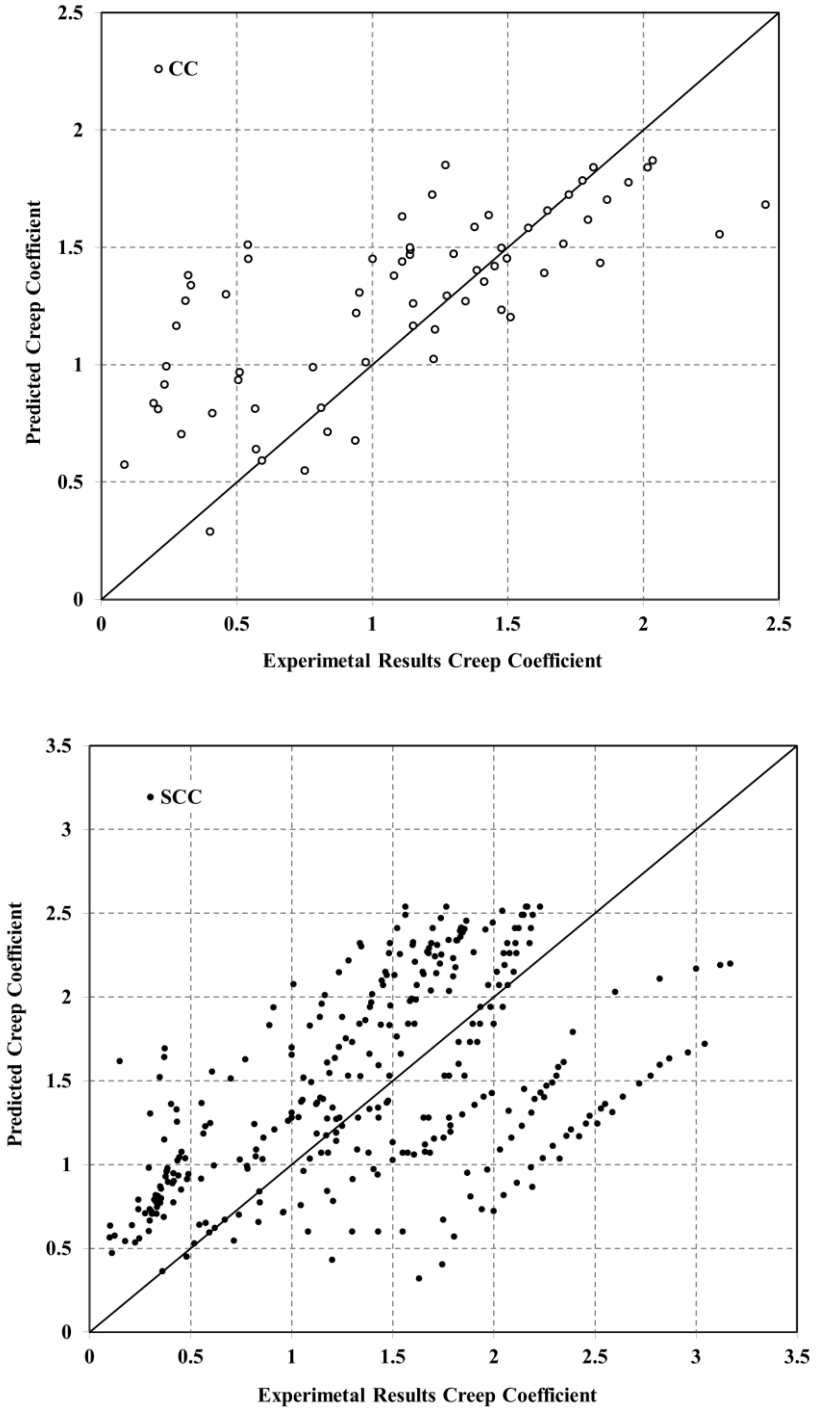

Figure 4.25 Comparison of the SCC and CC creep coefficient from experimental results versus calculated values from JSCE (2002) model

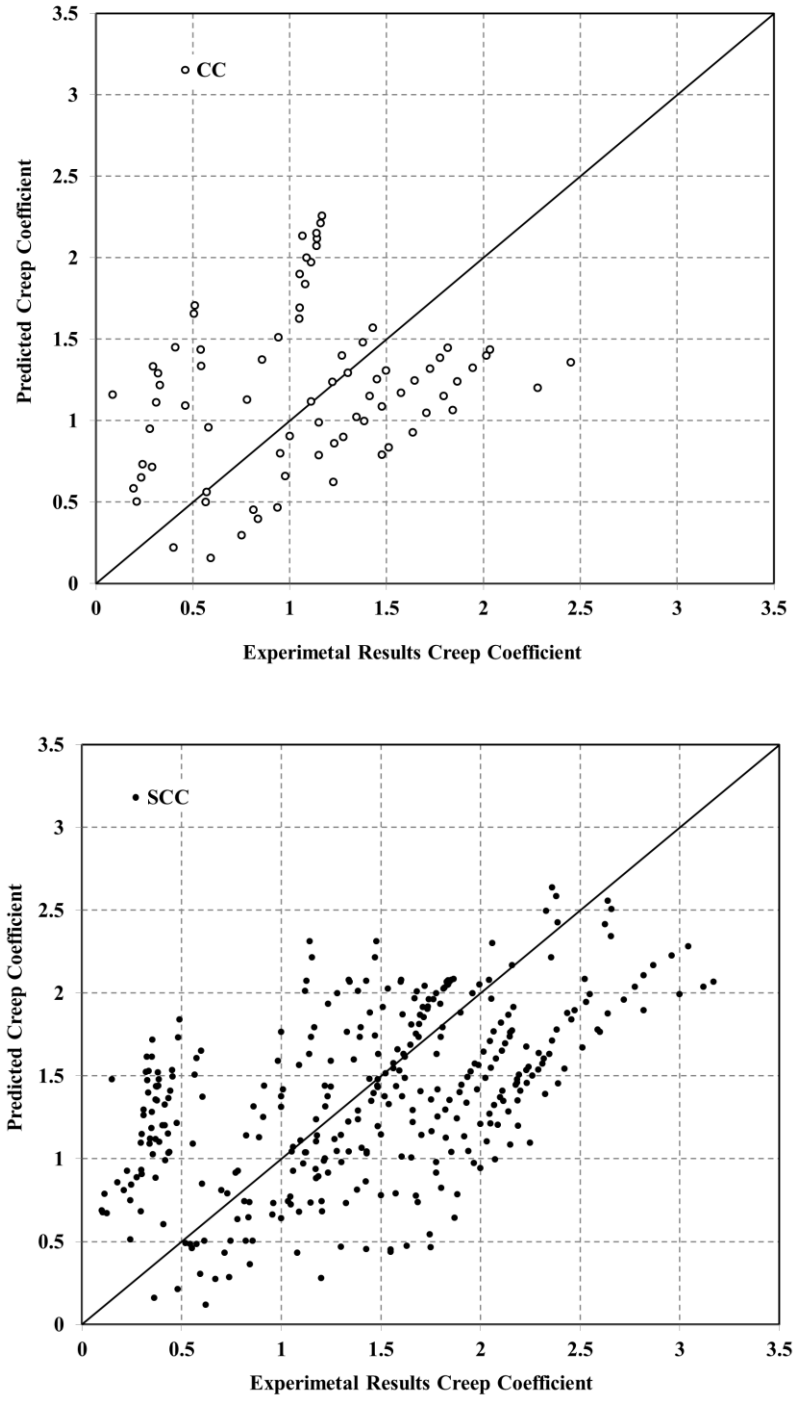

Figure 4.26 Comparison of the SCC and CC creep coefficient from experimental results versus calculated values from AASHTO (2004) model

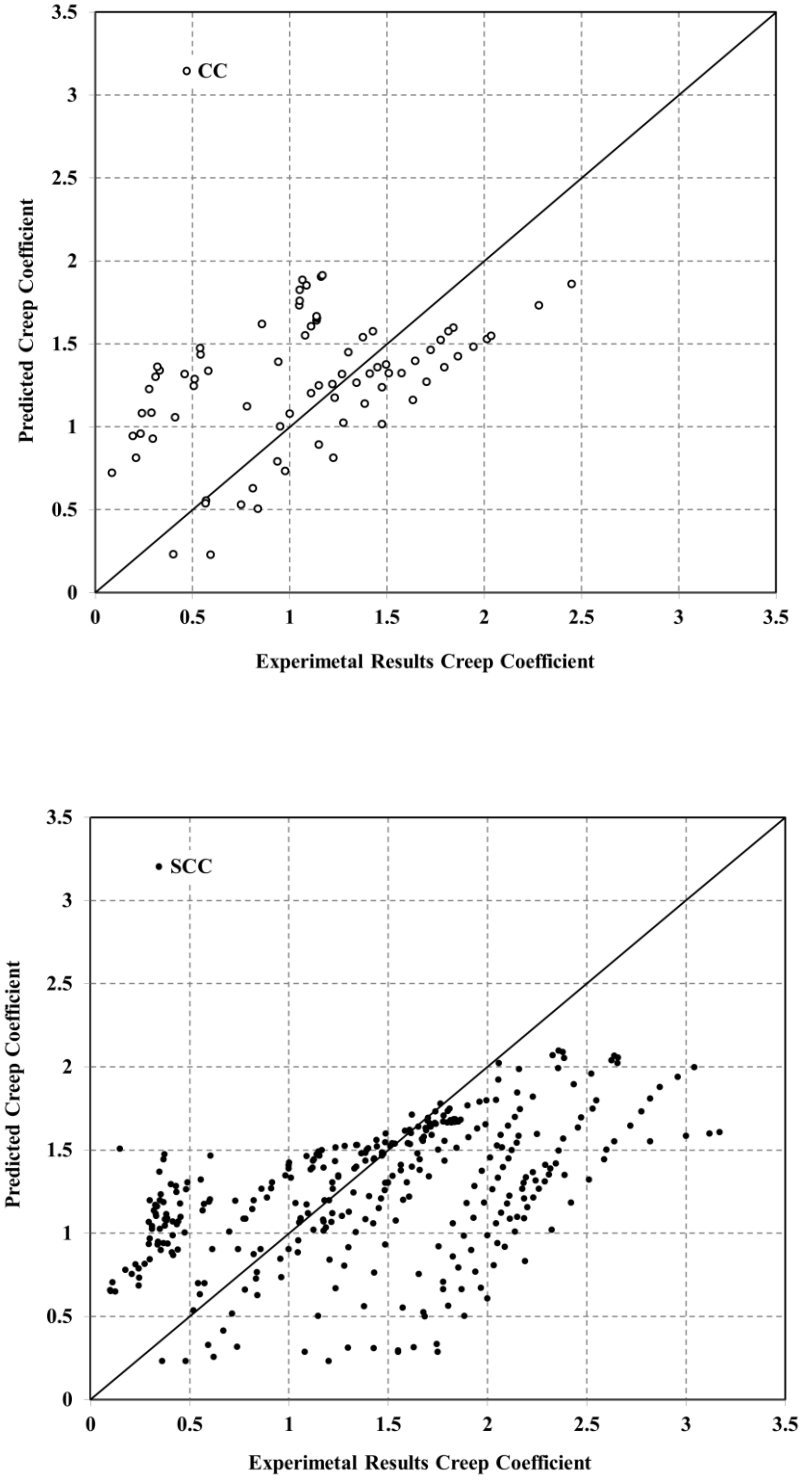

Figure 4.27 Comparison of the SCC and CC creep coefficient from experimental results versus calculated values from AASHTO (2007) model

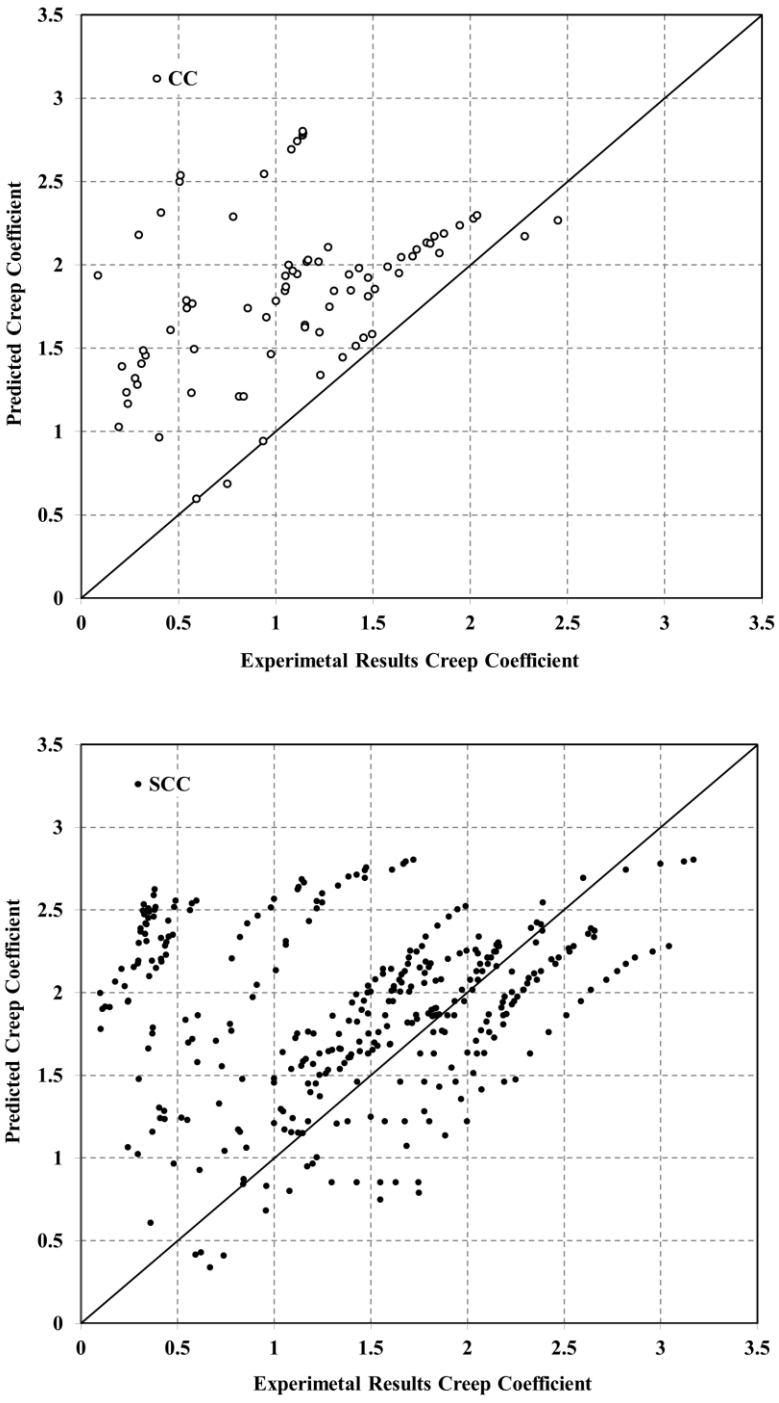

Figure 4.28 Comparison of the SCC and CC creep coefficient from experimental results versus calculated values from AS 3600 (2009) model

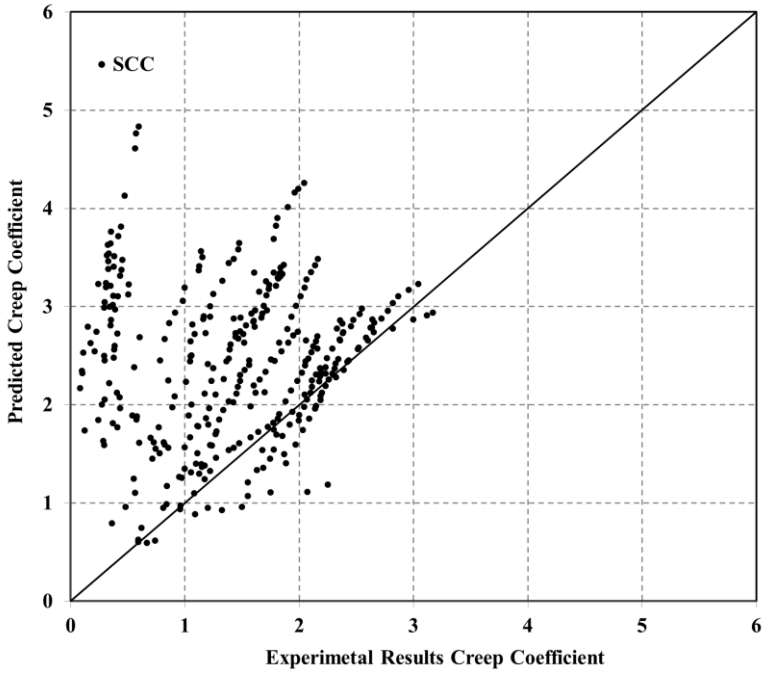

Figure 4.29 Comparison of the SCC creep coefficient from experimental results versus calculated values from Poppe and De Schutter (2005) model

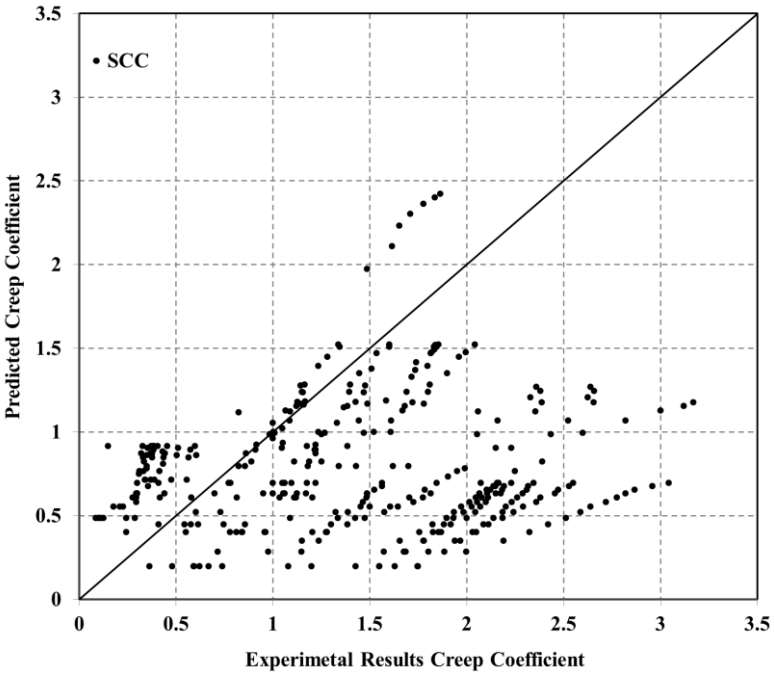

Figure 4.30 Comparison of the SCC creep coefficient from experimental results versus calculated values from Larson (2006) model

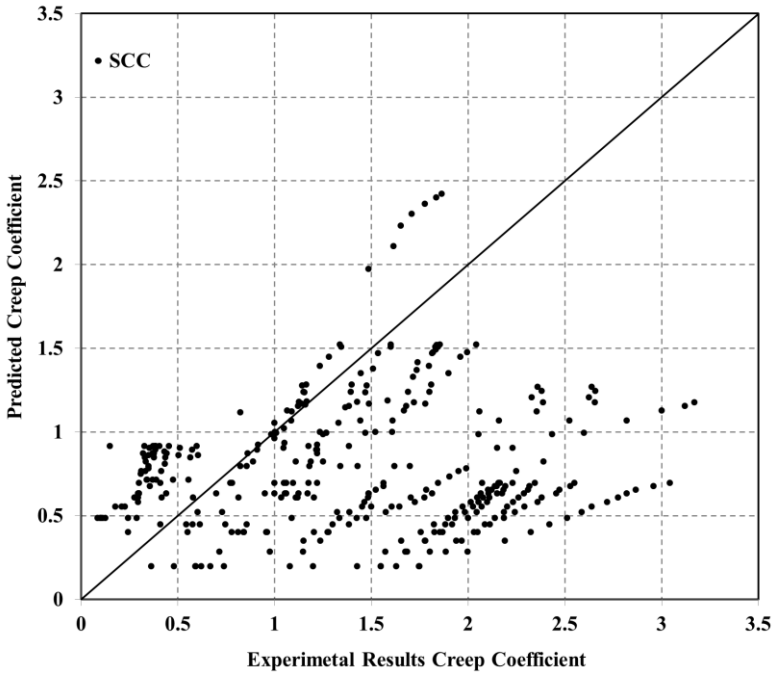

Figure 4.31 Comparison of the SCC creep coefficient from experimental results versus calculated values from Cordoba (2007) model

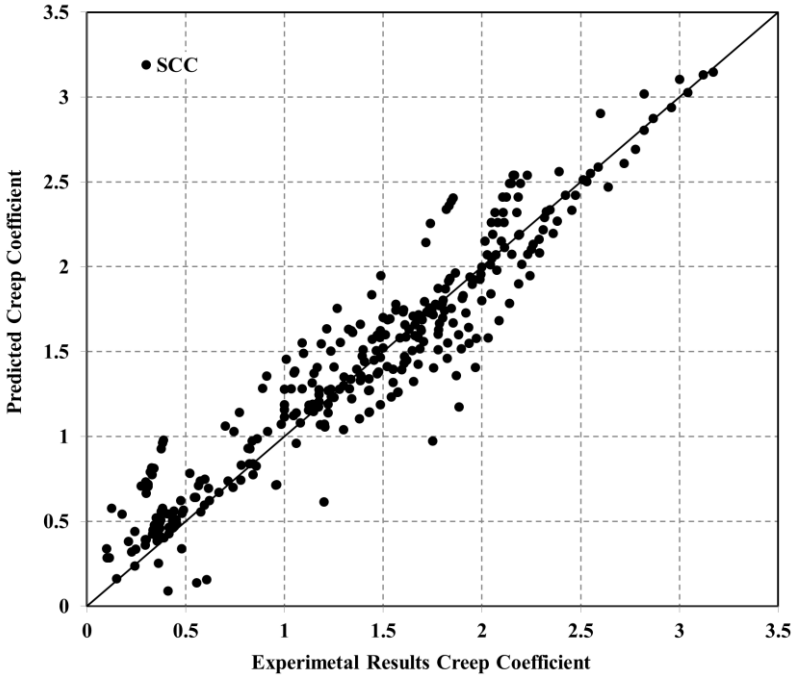

Figure 4.32 Comparison of proposed creep SCC model with experimental results database

4.6.5 Discussion of the Creep Models

As shown in Table 4.12 and Figures 4.22 to 4.28 for the CC mixture included in the experimental database, the AASHTO (2007), JSCE (2002), Eurocode 2 (2001) and AASHTO (2004) models provide better prediction of the creep strain with a coefficient of correlation factor (R^2) of 0.90, 0.89,0.89 and 0.86, respectively. Also, as shown in Table 4.12 and Figures 4.22 to 4.28 for SCC mixture in the experimental database, AASHTO (2004), JSCE (2002) and ACI 209R (1992) models provided better prediction of creep strain with a coefficient of correlation factor (R^2) of 0.87, 0.87 and 0.84, respectively.

As shown in AASHTO (2004), JSCE (2002) and ACI 209R (1992), the CC models that have conservative predictions are different in the certain intrinsic and/or extrinsic variables. As indicated in the Table 4.10, the AASHTO (2004) model has not any intrinsic factors but the JSCE (2002) and ACI 209R (1992) models have a good consideration of both the intrinsic and the extrinsic variables. The modified composition of the SCC in comparison with the CC has an influence on the creep behaviour of the concrete. Therefore, it is important to include some key variables that have impact on this behaviour. By considerations of these variables, JSCE (2002) model can cover more reliable intrinsic and extrinsic variables for the SCC mixture.

It can be seen from Figure 4.29 that Poppe and De Schutter (2005) model overestimates the creep coefficient of the SCC mixture. According to the Figure 4.30, Larson's (2006) creep prediction model underestimates the creep coefficient of the SCC mixture. According to Cordoba (2007) the SCC creep prediction model is more conservative underestimate for the creep strain of SCC experimental results (see Figure 4.31). In the Poppe and De Schutter (2005) investigation, ACI 209R (1997), CEB-FIP (1990) and Le Roy et al. (1996) models are compared and it is found that CEB-FIP (1990) always leads to underestimation of the deformation. But, the CEB-FIP model's creep deformation prediction trend is suitable then it is selected as a basis model. The modified model of CEB-FIP (1990) is just suitable for Poppe and De Schutter's experimental results.

The Larson's (2006) model is just a modification of ACI 209R (1997) model based on Larson's mixture. This model does not cover intrinsic and extrinsic variables. In the Cordoba's (2007) model, KL is first mixture that was based on a mixture developed by Khayat (1995) and modified by Altan (1999). This mixture achieves the SCC performance

by replacing some of the coarse aggregates with cement. The second mixture, labelled KM, was based on the KL but with a coarse aggregate content increased to 38%. Similarly, the third mixture, KH, was based on the KL but has a coarse aggregate content of 39%. Cordoba's model is based on ACI 209R (1997) and it does not cover intrinsic and extrinsic variables.

As shown in Figure 4.32, the proposed model provides good predictions compared to the experimental database of the SCC mixtures. In the experimental database, normal and high strength SCC mixtures are available and the SCC proposed model has good prediction for both normal and high strength experimental results. Also, the c/p ratio that is included in the proposed model has effective influence on the overall creep prediction. As can be seen in Table 4.9 this ratio varies over a wide range.

Table 4.12 Coefficient of correlation factor (R^2) CC creep prediction models for CC and SCC

Creep prediction models	**CC**	**SCC**
	R^2	R^2
CEB-FIP (1990)	0.41	0.58
ACI 209R (1992)	0.79	0.84
Eurocode 2 (2001)	0.89	0.80
JSCE (2002)	0.89	0.87
AASHTO (2004)	0.86	0.87
AASHTO (2007)	0.90	0.80
AS 3600 (2009)	0.70	0.75

CHAPTER 5

EXPERIMENTAL PROGRAM (PHASE I) – MATERIALS PROPERTIES OF PROPOSED SCC AND FRSCC

CHAPTER 5

EXPERIMENTAL PROGRAM (PHASE I) – MATERIALS PROPERTIES OF PROPOSED SCC AND FRSCC

5.1 INTRODUCTION

This Chapter describes experimental program on the characteristics of SCC and FRCSCC in the fresh and hardened states conducted in the Concrete Structures Laboratory, University of Technology, Sydney. For these purposes, four SCC mixes - plain SCC, steel, polypropylene, and hybrid FRSCC - are considered in the test program. In this section slump flow, T_{50cm} time, J-ring flow, V-funnel flow time, and L-box blocking ratio tests in the fresh states are performed. These tests are performed for checking the filling ability, passing ability and segregation resistance of SCC and FRSCC. In the hardened state, the properties include compressive and splitting tensile strengths, modulus of elasticity, modulus of rupture, and compressive stress-strain curve. These properties are tested at 3, 7, 14, 28, 56, and 91 days. Also, for better understanding of post-cracking behaviour of SCC and FRSCC prisms, flexural toughness analysis and energy dissipation in compression have been determined.

Since only a few correlations among the mechanical properties of SCC and FRSCC have been reported which are unclear, regression analyses were conducted on existing experimental data to propose splitting tensile strength, modulus of elasticity, and modulus of rupture models. Also, proposed compressive stress-strain and energy dissipation models for SCC and FRSCC are compared with the test results.

5.2 MATERIALS

5.2.1 Cement

In this experimental study, Shrinkage Limited Cement (SLC) corresponding to the AS 3972 (2010) standard was used. SLC is manufactured from specially prepared Portland cement clinker and gypsum. It may contain up to 5% of additions approved by AS 3972. The chemical, physical, and mechanical properties of the cement used in the experiments are shown in Table 5.1. The chemical, physical, and mechanical properties adhere to the limit values specified in AS 2350.2, 3, 4, 5, 8, and 11 (2006).

5.2.2 Fly Ash

It is important to increase the amount of paste in SCC because it is an agent to carry the aggregates. As a consequence, Eraring Fly Ash (EFA) has been used to increase the amount of paste. EFA is a natural pozzolan. It is a fine cream/grey powder that is low in lime content. However, since it is a very fine powder, in the presence of moisture it reacts chemically with calcium hydroxide at ordinary temperatures to form insoluble compounds possessing cementitious properties. The chemical and physical properties of EFA used in the experimental study are given in Table 5.2. The chemical, physical, and mechanical properties of the EFA used adhere to the limit values specified in AS 2350.2 (2006), AS 3583.1, 2, 3, 5, 6, 12, and 13 (1998).

5.2.3 Ground Granulated Blast Furnace Slag

Ground Granulated blast furnace slag (GGBFS) is another supplementary cementitious material that is used in combination with SLC. GGBFS initially used by Boral Company, Sydney-Australia, which compiles the AS 3582.2 (2001) specifications. The chemical and physical properties of GGBFS are given in Table 5.3.

Table 5.1 Chemical, physical, and mechanical properties of cement

Chemical properties	
CaO	64.5 %
SiO_2	19.3 %
Al_2O_3	5.2 %
Fe_2O_3	2.9 %
MgO	1.1 %
SO_3	2.9 %
K_2O	0.56 %
Na_2O	<0.01 %
Cl	0.02 %
LOI	2.8 %
Physical properties	
Autoclave Expansion	0.05 %
Fineness Index	405 m^2/kg
Mechanical properties	
Initial Setting Time	90 mins
Final Setting Time	135 mins
Soundness	1.0 mm
Drying Shrinkage	590 μstrain
f'_c (3 Days)	37.2 MPa
f'_c (7 Days)	47.3 MPa
f'_c (28 Days)	60.8 MPa

Table 5.2 Chemical and physical properties of Fly Ash

Chemical properties	
Al_2O_3	26.40 %
CaO	2.40 %
Fe_2O_3	3.20 %
K_2O	1.55 %
MgO	0.60 %
Mn_2O_3	<0.1 %
Na_2O	0.47 %
P_2O_5	0.20 %
SiO_2	61.40 %
SO_3	0.20 %
SrO	<0.1 %
TiO_2	1.00 %
Physical properties	
Moisture	<0.1 %
Fineness 45 micron	78% passed
Loss on Ignition	2.30 %
Sulfuric Anhydride	0.20 %
Alkali Content	0.50 %
Chloride Ion	<0.001 %
Relative Density	2.02 %
Relative Water Requirement	97 %
Relative Strength 28 Days	88 %

Table 5.3 Chemical and physical properties of GGBFS

Chemical properties	
Al_2O_3	14.30 %
Fe_2O_3	1.20 %
MgO	5.40 %
Mn_2O_3	1.50 %
SO_3	0.20 %
Cl	0.01 %
Insoluble Residue	0.50 %
LOI	-1.10 %
Physical properties	
Fineness Index	435 m^2/kg

5.2.4 Aggregate

In this study, crushed volcanic rock (i.e., latite) coarse aggregate was used with a maximum aggregate size of 10 mm. Nepean river gravel with a maximum size of 5 mm and Kurnell natural river sand. Fine aggregates were also implemented. Methods for sampling and testing aggregates were determined in accordance with AS 1141 (2011) and RTA (2006) and the results for coarse and fine aggregates are shown in Tables 5.4 to 5.6, respectively.

5.2.5 Admixtures

A new generation of superplasticiser, Glenium 27; viscosity-modifying admixture (VMA); and high-range water-reducing agent admixture were used in this study. Glenium 27 complies with AS 1478.1 (2000). In addition, High Range Water Reducer (HWR) and ASTM C494 (2000) types A and F were used. The Rheomac VMA 362 viscosity modifying admixture that was used in this study was a ready-to-use, liquid admixture that was specially developed for producing concrete with enhanced viscosity and controlled rheological properties. Pozzolith 80 was used as a high-range water-reducing agent admixture in the mixes. It reduces the quantity of water required to produce concrete of a given consistency and strength with greater economy. It meets AS 1478 (2000) Type WRRe, requirements for admixtures.

5.2.6 Fibres

In this study, two commercially available fibres, Dramix RC-80/60-BN type steel fibres and Synmix 65 type polypropylene (PP) fibres were used. The mechanical and physical properties of the steel and PP fibres are summarized in Table 5.7.

5.3 MIXTURE PROPORTIONS

One SCC control mixture, (N-SCC) and three different types of fibre-reinforced SCC mixtures were used in this study.(i) Fibre-reinforced SCC mixtures contain steel fibres, (D-SCC). (ii) Fibre-reinforced SCC mixtures contain PP fibres, (S-SCC); and (iii) Fibre-reinforced SCC mixtures contain hybrid (steel + PP) fibres, (DS-SCC). The content proportions of these mixtures are given in Table 5.8. These contents were chosen to attempt to keep compressive strength to a level applicable to construction.

Table 5.4 Properties of crushed latite volcanic rock coarse aggregate

Characteristics	Results
Sieve size	Passing (%)
13.2 (mm)	100
9.5 (mm)	89
6.7 (mm)	40
4.75 (mm)	7
2.36 (mm)	1
1.18 (mm)	1
Material finer than 75 micron (%)	1
Mis-shapen particles (%)	
Ratio 2:1	13
Ratio 3:1	1
Flakiness Index (%)	20
Uncompacted Bulk Density (t/m^3)	1.36
Compacted Bulk Density t/m^3	1.54
Moisture condition of the aggregate (%)	1.3
Particle Density (Dry) (t/m^3)	2.65
Particle Density (SSD) (t/m^3)	2.70
Apparent Particle Density (t/m^3)	2.79
Water Absorption (%)	1.9
Ave. Dry Strength (kN)	391
Ave. Wet Strength (kN)	293
Wet/Dry Strength Variation (%)	25
Test fraction (mm)	-9.5+6.7
The amount of significant breakdown (%) The size of testing cylinder = 150 mm diam.	<0.2
Los Angeles Value Grd. 'K' (%Loss)	13

Table 5.5 Properties of Nepean river gravel fine aggregate

Characteristics	Results
Sieve size	Passing (%)
6.7 (mm)	100
4.75 (mm)	99
2.36 (mm)	83
1.18 (mm)	64
600 (micron)	42
425 (micron)	28
300 (micron)	19
150 (micron)	8
Material finer than 75 micron (%)	3
Uncompacted Bulk Density (t/m^3)	1.52
Compacted Bulk Density (t/m^3)	1.64
Particle Density (Dry) (t/m^3)	2.58
Particle Density (SSD) (t/m^3)	2.60
Apparent Particle Density (t/m^3)	2.63
Water Absorption (%)	0.7
Silt Content (%)	7
Degradation Factor of Fine Aggregate The wash water after using permitted 500ml was: CLEAR	90
Moisture Content (%)	5.5
Method of Determining Voids Content	
% Voids	41.7
The mean Flow Time (Sec.)	26.5

Table 5.6 Properties of Kurnell natural river sand fine aggregate

Characteristics	Results
Sieve size	Passing (%)
1.18 (mm)	100
600 (micron)	98
425 (micron)	87
300 (micron)	46
150 (micron)	1
Material finer than 75 micron in aggregate by washing (%)	Nil
Uncompacted Bulk Density (t/m^3)	1.39
Compacted Bulk Density (t/m^3)	1.54
Particle Density (Dry) (t/m^3)	2.58
Particle Density (SSD) (t/m^3)	2.59
Apparent Particle Density (t/m^3)	2.62
Water Absorption (%)	0.6
Silt Content (%)	4

Table 5.7 The physical and mechanical properties of fibres

Fibre type	Fibre name	Density (kg/m^3)	Length (l)	Diameter (d)	Aspect ratio (l/d)
Steel	Dramix RC-80/60-BN	7850	60	0.75	80.0
Polipropylene (PP)	Synmix 65	905	65	0.85	76.5
Fibre type	Tensile strength (MPa)	Modulus of elasticity (GPa)	Cross-section form	Surface structure	
Steel	1050	200	Circular	Hooked end	
Polipropylene (PP)	250	3	Square	Rough	

Table 5.8 The proportions of the concrete mixtures (based on saturated surface dry condition)

Constituents	N-SCC	D-SCC	S-SCC	DS-SCC
Cement (kg/m^3)	160	160	160	160
Fly Ash (kg/m^3)	130	130	130	130
GGBFS (kg/m^3)	110	110	110	110
Cementitious content (kg/m^3)	400	400	400	400
Water (lit/m^3)	208	208	208	208
Water cementitious Ratio	0.52	0.52	0.52	0.52
Fine aggregate (kg/m^3)				
Coarse Sand	660	660	660	660
Fine Sand	221	221	221	221
Coarse aggregate (kg/m^3)	820	820	820	820
Admixtures (lit/m^3)				
Superplasticiser	4	4.86	4.73	4.5
VMA	1.3	1.3	1.3	1.3
High range water reducing agent	1.6	1.6	1.6	1.6
Fibre content (kg/m^3)				
Steel	-	30	-	15
PP	-	-	5	3

5.4 PREPARATION AND CURING CONDITION OF SAMPLES

The cylindrical moulds used were six ϕ150 mm × 300 mm for the determination of compressive and splitting tensile strengths per each age, and three cylindrical moulds ϕ150 mm × 300 mm for the determination of the modulus of elasticity per each age. Meanwhile, three 100 mm × 100 mm × 350 mm prism moulds were used for the determination of modulus of rupture per each age. Specimens for testing the hardened properties were prepared by direct pouring of concrete into moulds without compaction. The specimens were kept covered in a controlled chamber at 20 ± 2^{o}C for 24 h until demolding. Thereafter, the specimens are placed in water presaturated with lime at 20 ^{o}C. These specimens were tested at 3, 7, 14, 28, 56, and 91 days. For each test, separated specimens were used and surface of specimens were smoothed.

5.5 TEST METHODS OF SAMPLES

The compressive strength test, performed on ϕ150 mm × 300 mm cylinders, followed AS 1012.14 (1991) and ASTAM C39 (2000) standards. The cylinders were loaded in a testing machine under load control at the rate of 0.3 MPa/s until failure. The splitting tensile test, run on ϕ150 mm × 300 mm cylinders, was in accordance with the AS 1012.10 (2000) and ASTM C496 (2000) standards, although the ACI committee 544.2R (1999) does not recommends the use of the test on fibre-reinforced concrete. The running of the tests arose because the ratio of fibre length to cylinder diameter took a low value of 0.23 in the work and because some investigators have shown that the ASTM C496 test is applicable to fibre-reinforced concrete specimens.

The modulus of elasticity test that followed the AS 1012.17 (1997) and ASTM C469 was done to ϕ150 mm × 300 mm cylinders. The flexural strength (modulus of rupture, MOR) test, conducted using 100 mm × 100 mm × 350 mm test beams under third-point loading, followed the AS 1012.11 (2000) and ASTM C1018 test for flexural toughness and first-crack strength of fibre-reinforced concrete. The mid-span deflection was the average of the ones detected by the transducers through contact with brackets attached to the beam specimen.

5.6 PROPERTIES OF FRESH CONCRETE

Generally, most of the SCC experiments are carried out worldwide under laboratory conditions. These experiments include flow-ability, segregation, placement, and compaction of fresh concrete. Conventional workability tests are not sufficient for the evaluation of SCC. Some test methods to measure the flow-ability, segregation, placement, and compaction of SCC are developed and defined in the European guidelines (2005) and ACI 237R-07 (2007). These test methods include V-funnel, U-box, L-box and fill-box tests for specification, production and use as slump-flow.

In this study slump flow, T_{50cm} time, J-ring flow, V-funnel flow time, and L-box blocking ratio tests were performed. In order to reduce the effect of loss of workability on the variability of test results, the fresh properties of the mixes were determined within 30 min after mixing. The order of testing was as follows: 1. Slump flow test and measurement of T_{50cm} time; 2. J-ring flow test, measurement of difference in height of concrete inside and outside the J-ring and measurement of T_{50cm} time; 3. V-funnel flow tests at 10 s T_{10s} and 5 min T_{5min}; and 4. L-box test.

5.7 EXPERIMENTAL RESULTS

5.7.1 Properties of Fresh Concrete

The results of various fresh properties tested by the slump flow test (slump flow diameter and T_{50cm}); J-ring test (flow diameter); L-box test (time taken to reach 400 mm distance T_{400mm}, time taken to reach 600 mm distance T_{600mm}, time taken to reach 800 mm distance T_L, and ratio of heights at the two edges of L-box [H_2/H_1]); V-funnel test (time taken by concrete to flow through V-funnel after 10 s T_{10s}); the amount of entrapped air; and the specific gravity of mixes are given in Table 5.9. The slump flow test judges the capability of concrete to deform under its own weight against the friction of the surface with no restraint present. A slump flow value ranging from 500 to 700 mm for self-compacting concrete was suggested (European guidelines, 2005). At a slump flow > 700 mm the concrete might segregate, and at <500 mm, the concrete might have insufficient flow to

pass through highly congested reinforcements. All the mixes in the present study conform to the above range, because the slump flow of SCC is in the range of 600–700 mm. The slump flow time for the concrete to reach a diameter of 500 mm for all mixes was less than 4.5 s. The J-ring diameters were in the range of 560–655 mm. In addition to the slump flow test, a V-funnel test was also performed to assess the flowability and stability of SCC. V-funnel flow time is the elapsed time in seconds between the opening of the bottom outlet, depending when it is opened (T_{10s} and T_{5min}), and the time when light becomes visible at the bottom when observed from the top. According to the European guidelines (2005), a period ranging from 6 to 12 s is considered adequate for SCC. The V-funnel flow times in the experiment were in the range of 7-11 s. The test results of this investigation indicated that all mixes met the requirements of allowable flow time. The V-funnel flow time test results for the N-SCC mix was 6 s and for the D-SCC was 7 s and for other fibre reinforced SCC mixes were blocked, as expected.

The maximum size of coarse aggregate was restricted to 10 mm to avoid a blocking effect in the L-box for N-SCC mix. The gap between rebars in the L-box test was 35 mm. The L-box ratio H_2/H_1 for the N-SCC mix was above 0.8 which, according to the European guidelines and, for other mixes is blocked. A total spread over 700 mm was measured and no sign of segregation or considerable bleeding in any of the mixtures was detected as the mixtures showed good homogeneity and cohesion. A collection of photos about fresh property tests are included in Appendix-B.

Table 5.9 The SCC mixes workability characteristics

Workability characteristics	N-SCC	D-SCC	S-SCC	DS-SCC
Average spreading diameter (mm)	680	670	700	650
Flow time T_{50cm} (s)	2.7	3.8	2.5	3.2
Average J-Ring diameter (mm)	655	580	570	560
Flow time T_{50cm} J-Ring (s)	3.2	5	6	5
L-box test	0.87	Blocked	Blocked	Blocked
Flow time V-funnel (s)	6	7	Blocked	Blocked
V-funnel at $T_{5minutes}$ (s)	4	5	Blocked	Blocked
Entrapped air (%)	1.3	1.2	1.2	1.0
Specific gravity (kg/m^3)	2340	2274	2330	2385

5.7.2 Compressive Strength

Figure 5.1 and Table 5.10 present the compressive strength of N-SCC, D-SCC, S-SCC, and DS-SCC mixes achieved at different ages. Compressive strength samples with fibre mixes are higher than N-SCC mix. Samples with the S-SCC mix have lower compressive strength unlike the D-SCC and DS-SCC mixes. The average compressive strength of the DS-SCC mix is 18.90%, 3.83%, and 12.86% higher than the N-SCC, D-SCC, and S-SCC mixes, respectively. The results show that the D-SCC mix at three days was 32.57%, 26.13%, and 22.73% higher than the N-SCC, S-SCC and DS-SCC mixes respectively. Furthermore, the results indicate that the compressive strength of the DS-SCC mix at 91 days is 10.71%, 1.62%, and 8.32% higher than the N-SCC, D-SCC, and S-SCC mixes, respectively.

5.7.3 Tensile Strength

Figure 5.2 and Table 5.10 show the splitting tensile strengths of N-SCC, D-SCC, S-SCC, and DS-SCC mixes determined at different ages. The tensile strengths of the D-SCC and DS-SCC samples are higher than those of the N-SCC and S-SCC. The S-SCC mix has a lower tensile strength than N-SCC. The average tensile strength of the D-SCC mix is 23.52%, 27.19%, and 15.54% higher than that of the N-SCC, S-SCC, and DS-SCC mixes, respectively. Moreover, the results indicate that the tensile strength of the D-SCC mix at 91 days is 15.95%, 18.89%, and 11.76% higher than that of the N-SCC, S-SCC, and DS-SCC mixes, respectively.

5.7.4 Modulus of Elasticity

Figure 5.3 and Table 5.10 present the modulus of elasticity of N-SCC, D-SCC, S-SCC, and DS-SCC mixes attained at different ages. The average modulus of elasticity of DS-SCC mix is 2.67%, 4.75% and 3.49%, higher than that of the N-SCC, D-SCC, and S-SCC mixes, respectively. The results show that the N-SCC mix at 14 days age is 9.62%, 7.94%, and 3.03% higher than D-SCC, S-SCC, and DS-SCC mixes, respectively. Additionally, the results indicate that the tensile strength of the DS-SCC mix at 91 days is 0.86%, 1.41%, and 1.72% higher than that of the N-SCC, D-SCC, and S-SCC mixes, respectively.

5.7.5 Modulus of Rupture (flexural tensile strength)

Figure 5.4 and Table 5.10 illustrate the flexural tensile strengths of N-SCC, D-SCC, S-SCC, and DS-SCC mixes determined at different ages. The average flexural tensile strength of the D-SCC mix is 13.96%, 8.80%, and 8.89% higher than that of the N-SCC, S-SCC, and DS-SCC mixes, respectively. The results show that the S-SCC mix at seven days is 21.30%, 3.97% and 10.52% higher than the N-SCC, D-SCC, and DS-SCC mixes, respectively. Also, the results indicate that flexural tensile strength of D-SCC mix at 91 days is 1.30%, 6.44%, and 0.21% higher than that of the N-SCC, S-SCC, and DS-SCC mixes, respectively.

Table 5.10 Compressive strength, tensile strength, modulus of elasticity, and modulus of rupture of SCC mixtures at different ages

	Compressive strength (MPa)				Tensile strength (MPa)			
Age (days)	N-SCC	D-SCC	S-SCC	DS-SCC	N-SCC	D-SCC	S-SCC	DS-SCC
3	12.45	18.50	13.65	14.30	1.65	2.32	1.16	1.76
7	21.80	25.30	22.50	26.30	2.26	3.38	1.93	2.51
14	29.05	34.30	32.45	38.10	2.80	3.87	3.05	3.54
28	33.30	38.00	38.10	45.00	3.60	4.54	3.56	4.09
56	40.60	50.50	42.90	50.75	4.17	5.35	4.02	4.33
91	46.40	51.15	47.65	52.00	4.57	5.44	4.41	4.80
	Modulus of elasticity (GPa)				Modulus of rupture (MPa)			
Age (days)	N-SCC	D-SCC	S-SCC	DS-SCC	N-SCC	D-SCC	S-SCC	DS-SCC
3	25.23	24.45	25.36	26.78	2.50	3.35	3.13	2.47
7	27.84	26.57	27.87	30.13	3.35	4.10	4.26	3.81
14	32.24	29.14	29.68	31.26	4.66	5.40	4.60	4.80
28	35.39	35.76	35.76	36.10	5.00	6.37	5.00	5.40
56	35.58	36.44	36.32	37.03	5.87	6.72	6.50	6.52
91	37.79	37.58	37.47	38.12	7.13	7.23	6.76	7.21

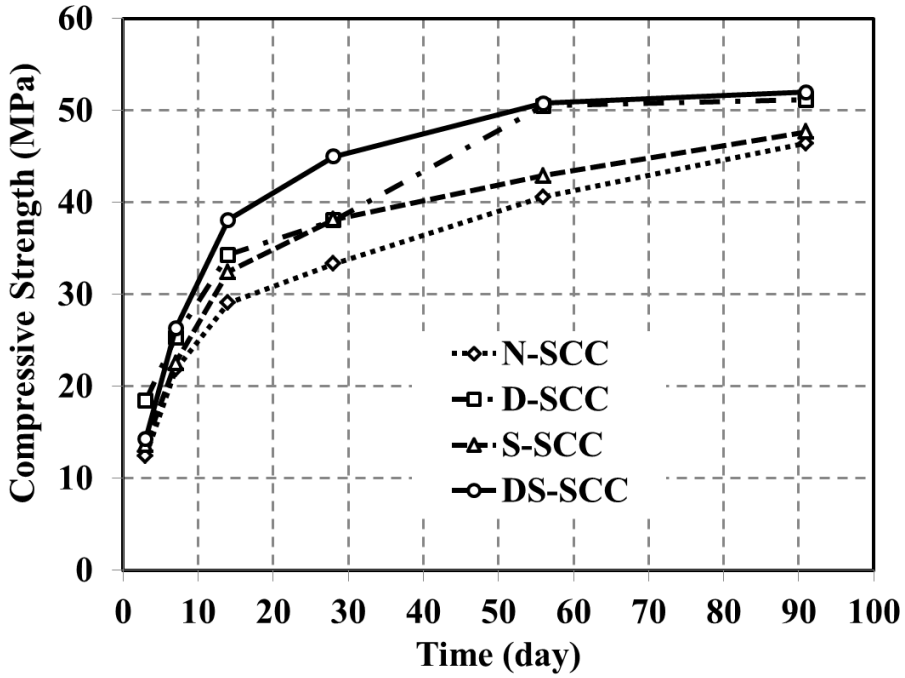

Figure 5.1 Compressive strengths of SCC mixtures at different ages

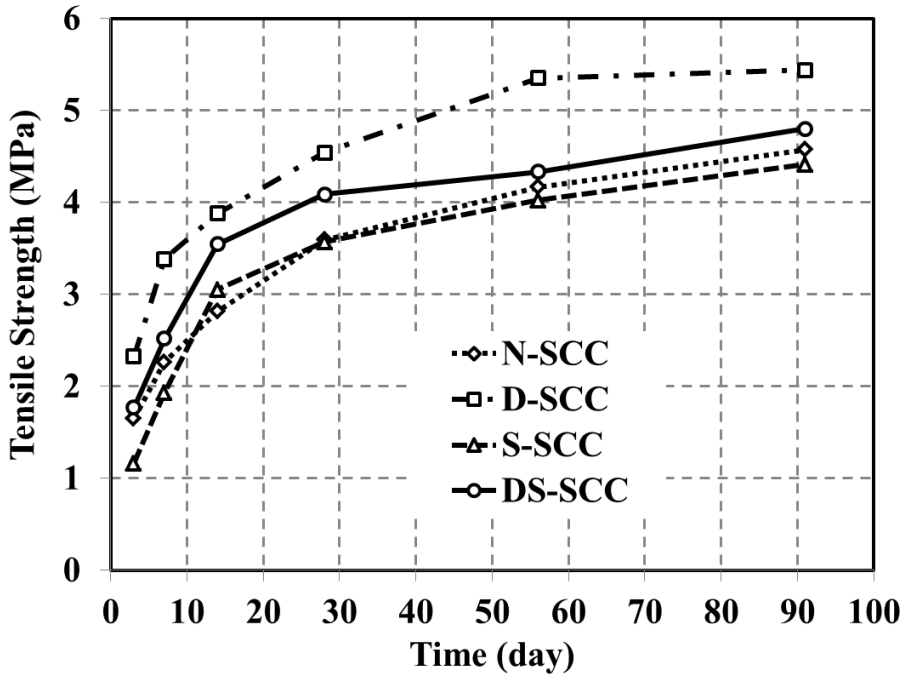

Figure 5.2 Tensile strengths of SCC mixtures at different ages

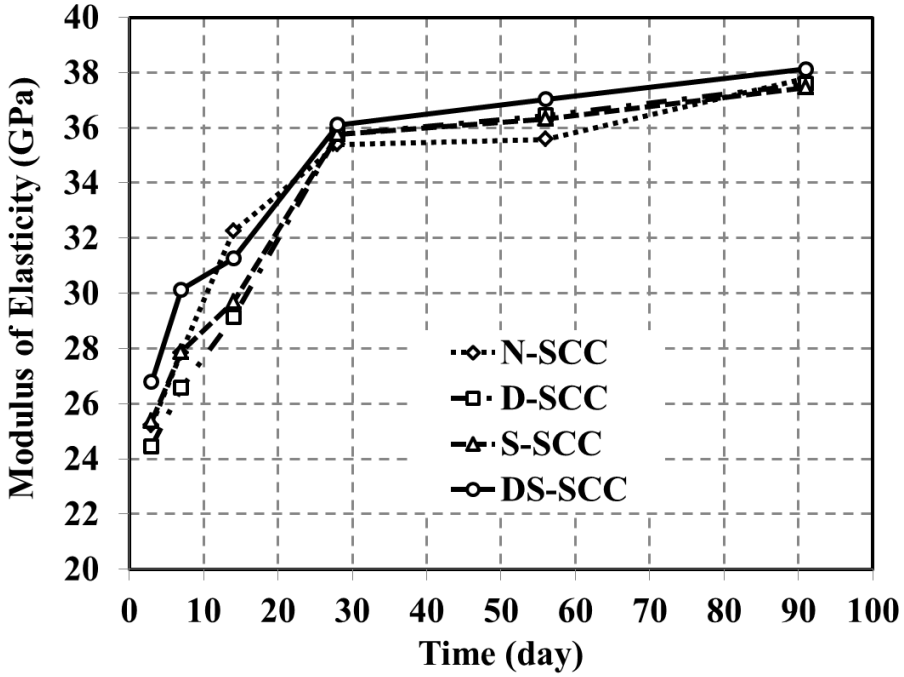

Figure 5.3 Modulus of elasticity of SCC mixtures at different ages

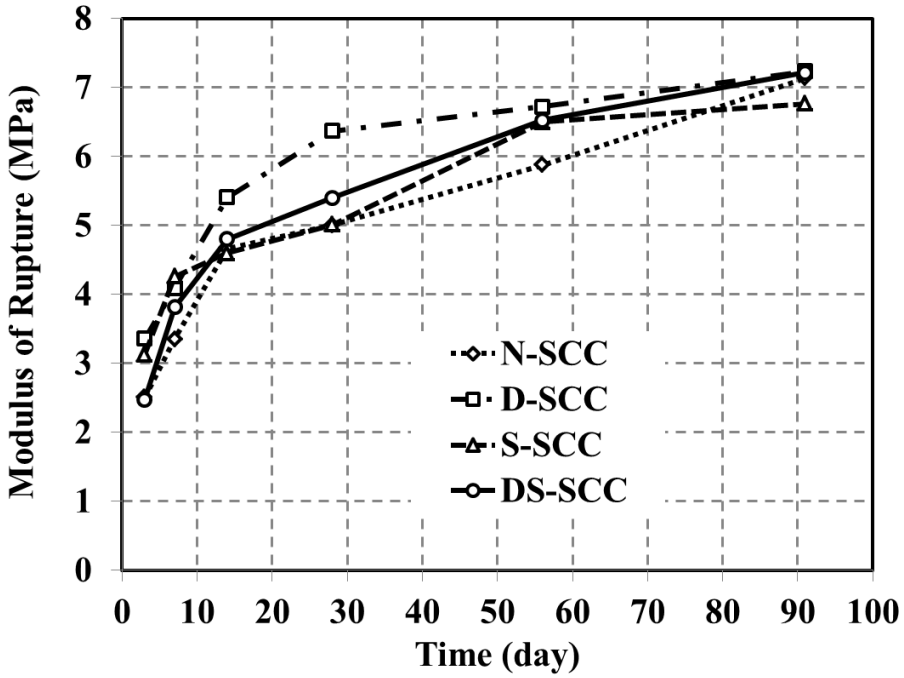

Figure 5.4 Modulus of rupture of SCC mixtures at different ages

5.7.6 Compressive Stress-Strain Curve

Complete stress–strain curves of the concrete of specimens were obtained from the compression tests of the cylinders with a controlled displacement rate. For each mix, three cylinders were tested. As the test results reproduced well, each stress–strain curves shown in Figures 5.5-5.8 represents the average results of the three tests. It should be noted that the axial strains of the concrete in compression were obtained from the full height shortening of the cylinders using LVDTs. The compression stress-strain curves at increasing ages of N-SCC, D-SCC, S-SCC, and DS-SCC mixes are shown in Figures 5.5-5.8. All the fibrous SCC mixes verified more substantial ductility than the corresponding N-SCC mix. Commonly, the nature of failure in compression for the N-SCC mix tended to be more sudden and brittle as the age of the concrete increased. On the other hand, by increasing the age, majority of the fibrous SCC mixes maintained their ductility and gradual failure mechanism.

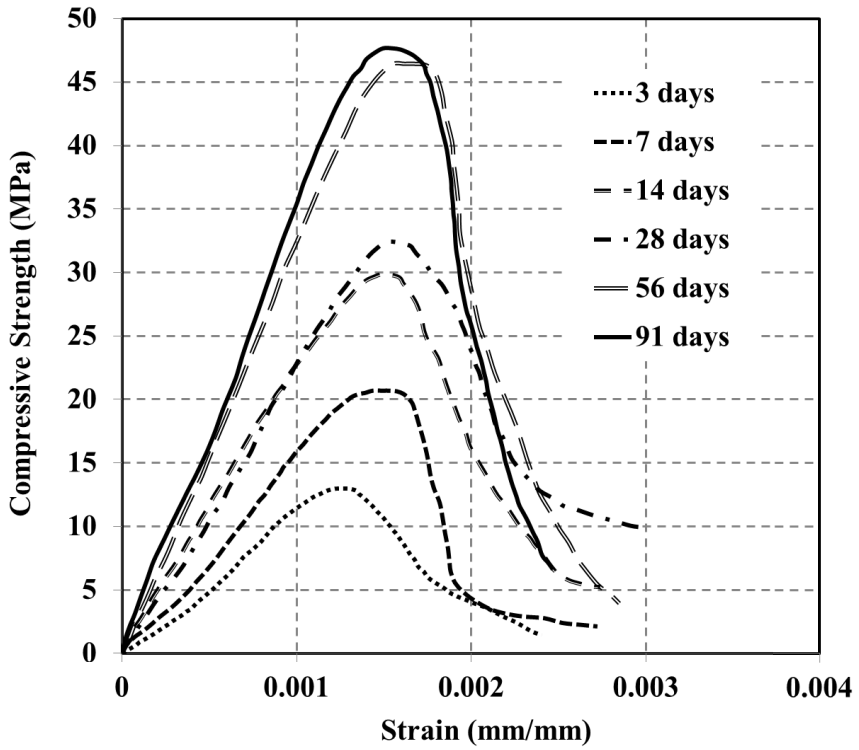

Figure 5.5 Compressive stress-strain curve of N-SCC mix at different ages

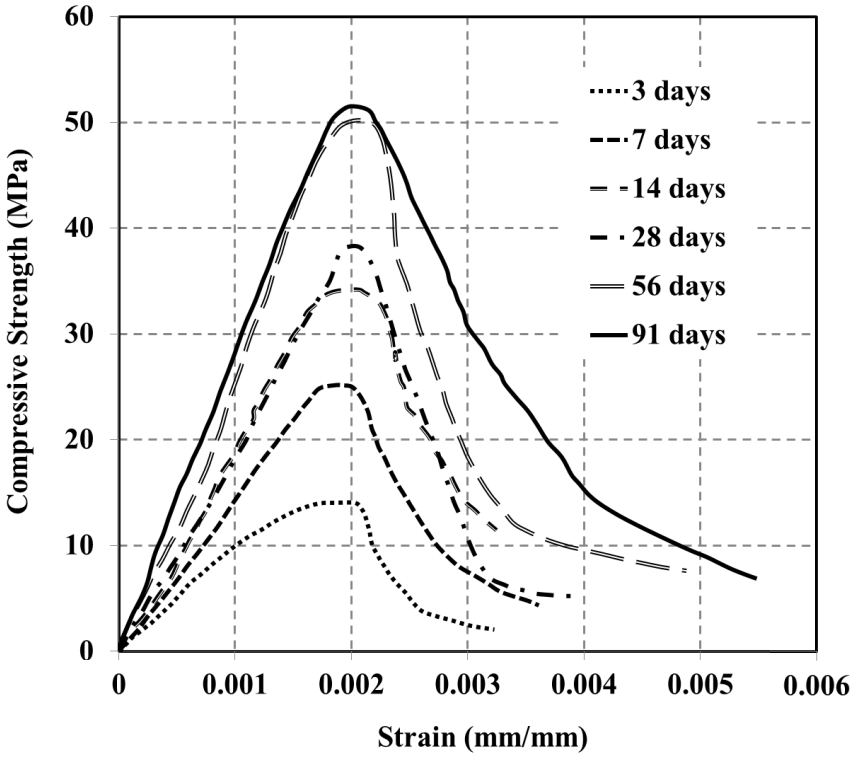

Figure 5.6 Compressive stress-strain curve of D-SCC mix at different ages

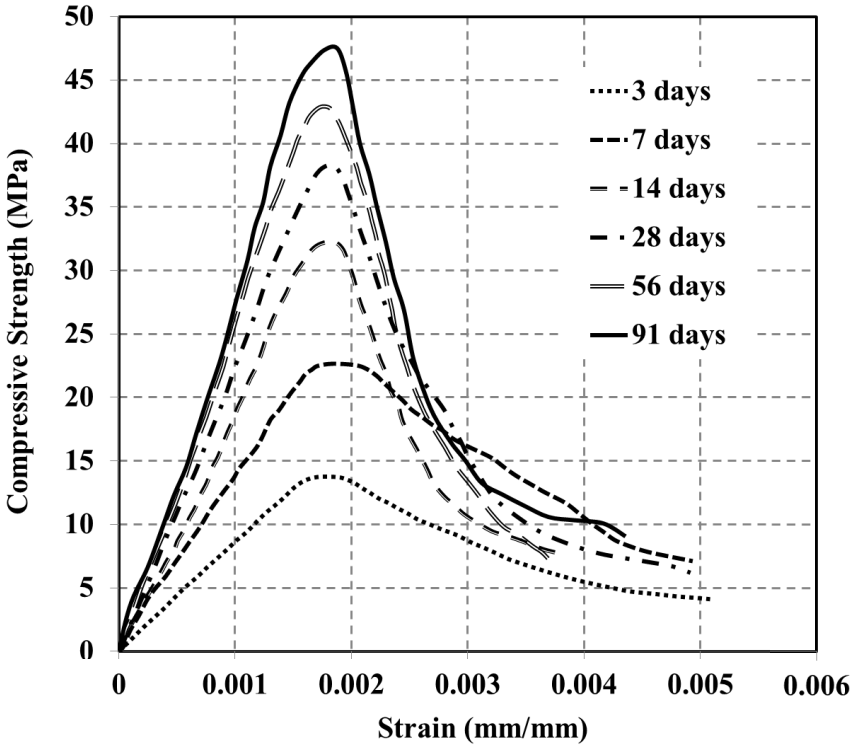

Figure 5.7 Compressive stress-strain curve of S-SCC mix at different ages

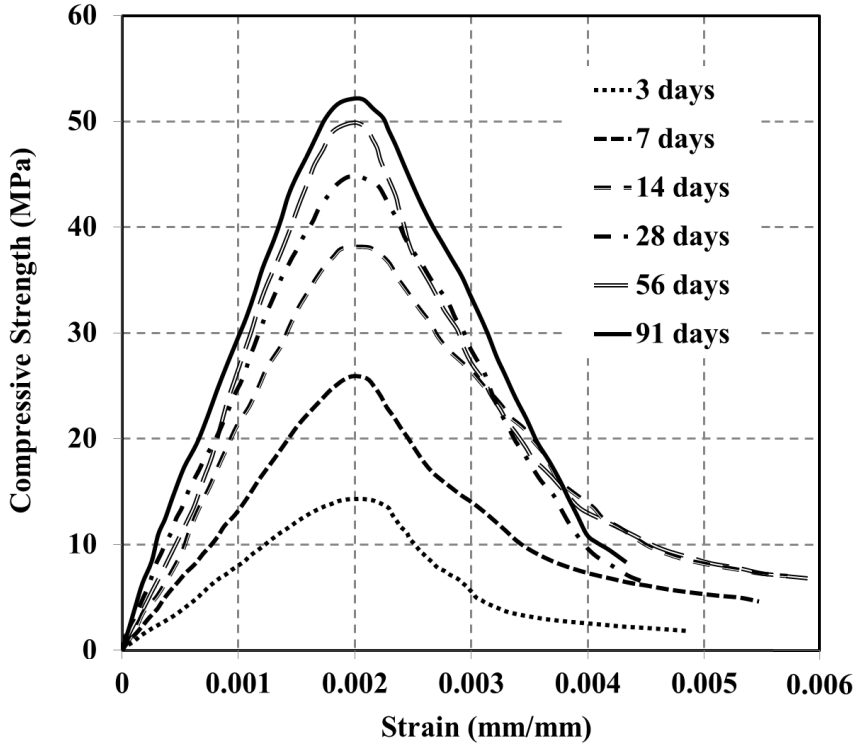

Figure 5.8 Compressive stress-strain curve of DS-SCC mix at different ages

5.7.7 Energy Dissipated under Compression

The energy absorption per unit volume under compression was determined as the under curve area of the stress (σ)/strain (ε) curve; the value was calculated using Eq. (5.1):

$$G_c = \int_0^{\varepsilon_u} \sigma \; d\varepsilon \tag{5.1}$$

The G_c value was always determined until an ultimate deformation, ε_u, of 0.05, where it was expected that the residual strength would be small. Table 5.11 and Figure 5.9 include the average values of G_c. In general, the concrete energy absorption increased with age. The major part of the energy is released in the softening phase that is also dependent on the fibre reinforcement mechanisms provided by fibres crossing the cracks. The efficiency of those mechanisms depend considerably on the fibre bond length and fibre orientation towards the cracks they bridge, whose homogeneity cannot be assumed between two, apparently, equal batches. The variation of the energy dissipated under compression with

the strain is represented in Figures 5.10-5.13. In general, G_c increased with strain more quickly for the older specimens, 56 and 91 days than for the specimens with 3, 7, 14 and 28 days.

Table 5.11 The energy dissipated under compression

G_c (MPa)	Mix	Age (days)					
		3	7	14	28	56	91
	N-SCC	0.658	0.833	1.228	1.255	1.544	1.612
	D-SCC	0.747	1.117	1.327	1.494	1.683	1.825
	S-SCC	0.701	0.988	1.304	1.421	1.617	1.745
	DS-SCC	0.762	1.239	1.359	1.535	1.700	1.865

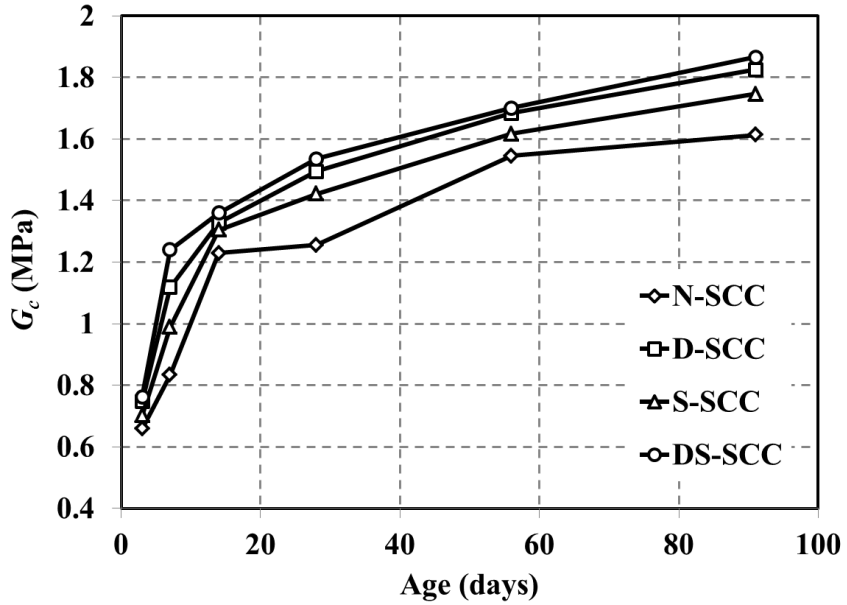

Figure 5.9 Energy dissipated under compression (G_c) at different ages

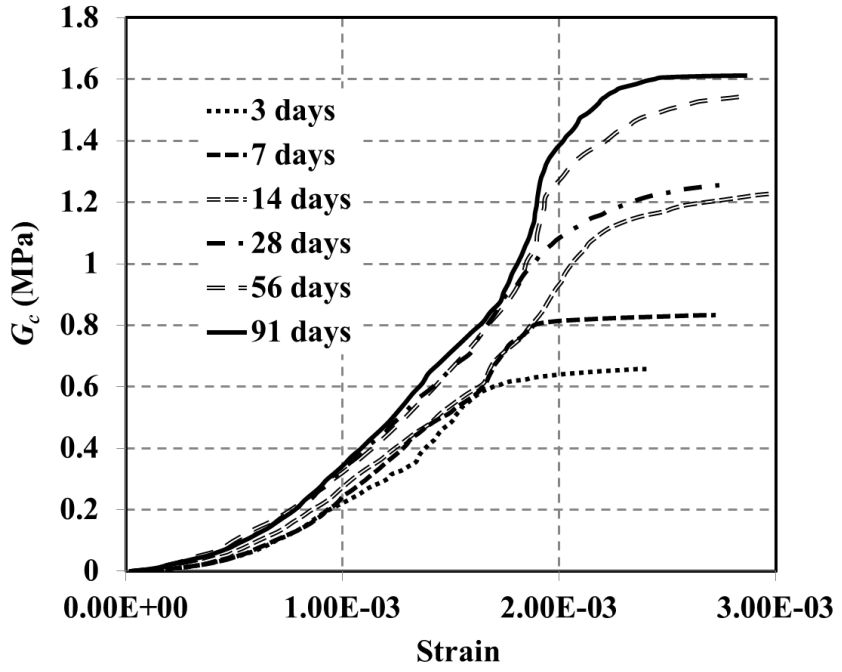

Figure 5.10 Energy dissipated under compression (G_c) versus strain of N-SCC mix at different ages

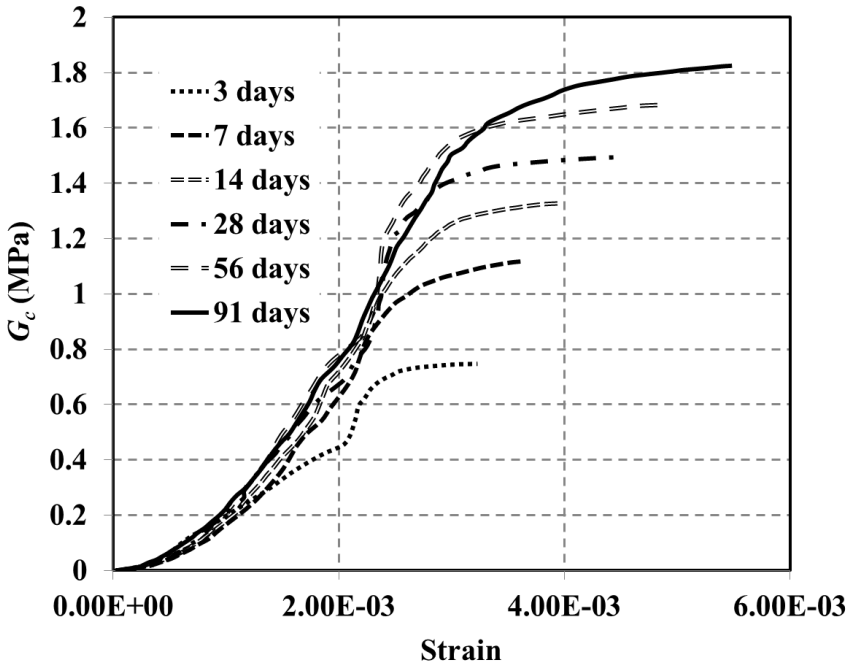

Figure 5.11 Energy dissipated under compression (G_c) versus strain of D-SCC mix at different ages

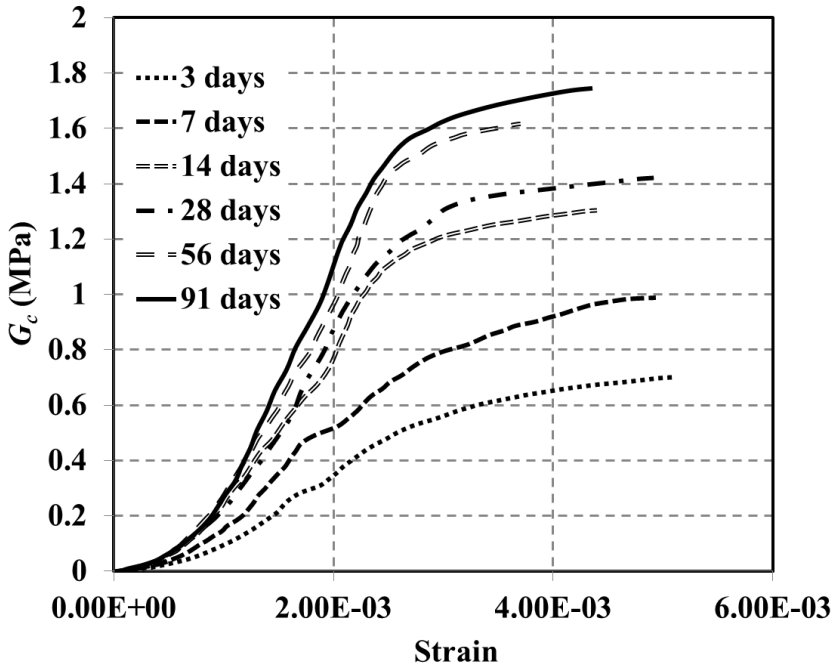

Figure 5.12 Energy dissipated under compression (G_c) versus strain of S-SCC mix at different ages

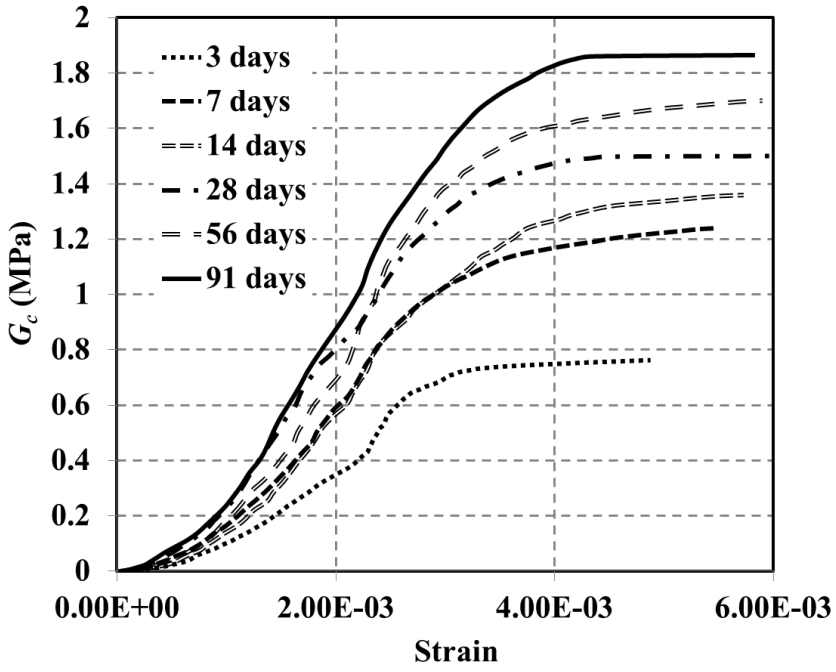

Figure 5.13 Energy dissipated under compression (G_c) versus strain of DS-SCC mix at different ages

5.8 ANALYTICAL RELATIONSHIPS FOR THE MECHANICAL PROPERTIES

5.8.1 Time-Dependent Mechanical Properties Relationships

To estimate the SCC mixes' compressive strength, tensile strength, modulus of elasticity, modulus of rupture, and energy dissipated under compression at various ages, Eqs. (5.2 to 5.6) are proposed based on regression analyses of the experimental data. Figure 5.14 shows that the proposed time-dependent relationships are in good agreement with the experimental results. Also, correlation coefficient factors (R^2) of the proposed models in comparison with experimental results are shown in Figure 5.14.

5.8.1.1 Compressive strength

$$f_{cm}(t) = \frac{f'_c}{\alpha} ln(t) + \beta \tag{5.2}$$

where:

Mix	f'_c	α	β
N-SCC	f'_{cN}	3.47	2.54
D-SCC	f'_{cfD}	3.75	6.66
S-SCC	f'_{cfS}	3.84	3.87
DS-SCC	f'_{cfDS}	3.96	4.54

where f'_{cN} is the N-SCC mix, f'_{cfD} is the D-SCC mix, f'_{cfS} is the S-SCC mix, and f'_{cfDS} is the DS-SCC mix compressive strengths; α and β are the empirical constants.

5.8.1.2 Tensile strength

$$f_{ctm}(t) = \frac{f_{ct}}{\gamma} ln(t) + \lambda \tag{5.3}$$

where:

Mix	f_{ct}	γ	λ
N-SCC	f_{ctN}	4.09	0.60
D-SCC	f_{ctfD}	4.87	1.43
S-SCC	f_{ctfS}	3.69	0.19
DS-SCC	f_{ctfDS}	4.60	0.91

where f_{ctN} is the N-SCC mix, f_{ctfD} is the D-SCC mix, f'_{ctfS} is the S-SCC mix, and f'_{ctfDS} is the DS-SCC mix tensile strengths; γ and λ are the empirical constants.

5.8.1.3 Modulus of elasticity

$$E_{cm}(t) = \frac{E_c}{\eta} ln(t) + \mu \tag{5.4}$$

where:

Mix	E_c	η	μ
N-SCC	E_{cN}	9.47	21.42
D-SCC	E_{cfD}	8.40	19.20
S-SCC	E_{cfS}	9.30	20.83
DS-SCC	E_{cfDS}	10.47	23.15

where E_{cN} is the N-SCC mix, E_{cfD} is the D-SCC mix, E_{cfS} is the S-SCC mix, and E_{cfDS} is the DS-SCC mix modulus of elasticity; η and μ are the empirical constants.

5.8.1.4 Modulus of rupture

$$f_{crm}(t) = \frac{f_{cr}}{\psi} ln(t) + \phi \tag{5.5}$$

where:

Mix	f_{cr}	ψ	ϕ
N-SCC	f_{crN}	3.89	1.00
D-SCC	f_{crfD}	5.39	2.07
S-SCC	f_{crfS}	4.75	1.96
DS-SCC	f_{crfDS}	3.99	1.08

where f_{crN} is the N-SCC mix, f_{crfD} is the D-SCC mix, f_{crfS} is the S-SCC mix, and f_{crfDS} is the DS-SCC mix modulus of rupture; ψ and ϕ are the empirical constants.

5.8.1.5 Energy dissipated under compression

$$G_{cm}(t) = \frac{G_c}{\omega} ln(t) + \rho \tag{5.6}$$

where:

Mix	G_c	ω	ρ
N-SCC	G_{cN}	4.33	0.340
D-SCC	G_{cfD}	4.91	0.476
S-SCC	G_{cfS}	4.69	0.411
DS-SCC	G_{cfDS}	5.16	0.541

where G_{cN} is the N-SCC mix, G_{cfD} is the D-SCC mix, G_{cfS} is the S-SCC mix, and G_{cfDS} is the DS-SCC mix modulus of rupture; ω and ρ are the empirical constants.

5.8.2 Compressive Strength-Related Mechanical Properties Relationships

Figure 5.15 illustrates tensile strength, modulus of elasticity, and modulus of rupture versus compressive strength. Eqs. (5.7 to 5.9) are proposed based on regression analyses of the experimental data to predict the SCC mixes' tensile strength, modulus of elasticity, and modulus of rupture based on the compressive strength. The bases of the proposed relationships are captured from Chapter 3 (Eqs. [3.1 to 3.3]). Figure 5.15 indicates the proposed compressive strength-related relationships of tensile strength, modulus of elasticity, and modulus of rupture are in good agreement with the experimental results.

5.8.2.1 Tensile strength

$$f_{ct} = \eta_1 \left(f'_c\right)^{\eta 2} \tag{5.7}$$

where:

Mix	f_{ct}	f'_c	η_1	η_2
N-SCC	f_{ctN}	f'_{cN}	0.204	0.8047
D-SCC	f_{ctfD}	f'_{cfD}	0.237	0.7999
S-SCC	f_{ctfS}	f'_{cfS}	0.067	1.0889
DS-SCC	f_{ctfDS}	f'_{cfDS}	0.226	0.7585

5.8.2.2 Modulus of elasticity

$$E_c = \kappa_1 \left(f_c'\right)^{\kappa 2} \tag{5.8}$$

where:

Mix	E_c	f'_c	κ_1	κ_2
N-SCC	E_{cN}	f'_{cN}	10.913	0.3226
D-SCC	E_{cfD}	f'_{cfD}	6.649	0.4383
S-SCC	E_{cfS}	f'_{cfS}	10.395	0.3271
DS-SCC	E_{cfDS}	f'_{cfDS}	12.895	0.2651

5.8.2.3 Modulus of rupture

$$f_{cr} = \delta_1 \left(f_c'\right)^{\delta 2} \tag{5.9}$$

where:

Mix	f_{cr}	f'_c	δ_1	δ_2
N-SCC	f_{crN}	f'_{cN}	0.325	0.7871
D-SCC	f_{crfD}	f'_{cfD}	0.376	0.7511
S-SCC	f_{crfS}	f'_{cfS}	0.670	0.5818
DS-SCC	f_{crfDS}	f'_{cfDS}	0.309	0.7714

5.8.3 Compressive Stress–Strain Relationship

In this study, a compressive stress–strain relationship (Eqs. [5.10 to 5.17]) for SCC mixes that is based on Chapter 3 models (Eqs. [3.4 to 3.11]) was developed by using the proposed compressive strength (Eq.[5.2]) and elastic modulus (Eqs.[5.4 and 5.8]) relationships. Figure 5.16 shows that the proposed stress-strain relationship fits the experimental results well. In Figure 5.16, typical 91 days age compressive stress-strain curve results are selected to compare with the proposed compressive stress-strain relationship.

$$\frac{\sigma_c}{f_c^{'}} = \frac{n\left(\frac{\varepsilon_c}{\varepsilon_c^{'}}\right)}{n-1+\left(\frac{\varepsilon_c}{\varepsilon_c^{'}}\right)^n} \tag{5.10}$$

$$n = n_1 = \left[1.02 - 1.17\left(E_{\sec} / E_c\right)\right]^{-0.74} \quad if\ \varepsilon_c \le \varepsilon_c^{'} \tag{5.11}$$

$$n = n_2 = n_1 + \left(\rho + 28 \times \omega\right) \quad if\ \varepsilon_c \ge \varepsilon_c^{'} \tag{5.12}$$

$$\chi = \left(135.16 - 0.1744 f_c^{'}\right)^{-0.46} \tag{5.13}$$

$$\xi = 0.83 \exp\left(-911 / f_c^{'}\right) \tag{5.14}$$

$$E_{\sec} = f_c' / \varepsilon_c' \tag{5.15}$$

$$\varepsilon_c' = \left(\frac{f_c'}{E_c}\right)\left(\frac{\nu}{\nu - 1}\right) \tag{5.16}$$

$$\nu = \frac{f_c'}{17} + 0.8 \tag{5.17}$$

where σ_c is concrete stress, f'_c maximum compressive strength of concrete, n material parameter that depends on the shape of the stress-strain curve, ε concrete strain, ε'_c strain corresponding with the maximum stress f'_c, n_1 modified material parameter at the ascending branch, n_2 modified material parameter at the descending branch, E_c modulus of elasticity, E_{sec} secant modulus of elasticity, and χ, ξ coefficients of linear equation.

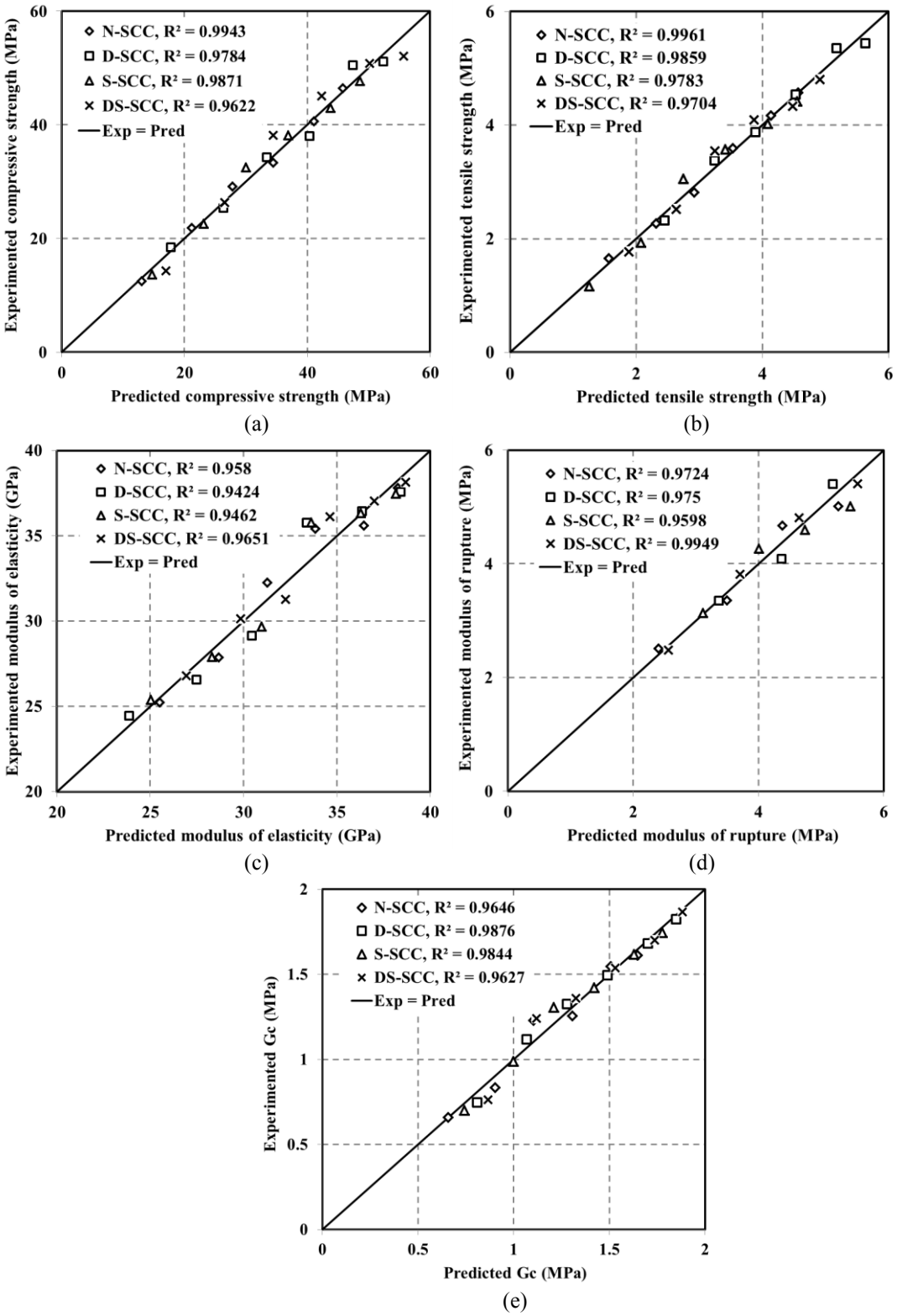

Figure 5.14 Predicted time-related mechanical properties values versus experimented values (a) compressive strength, (b) tensile strength, (c) modulus of elasticity, (d) modulus of rupture, and (e) energy dissipated under compression

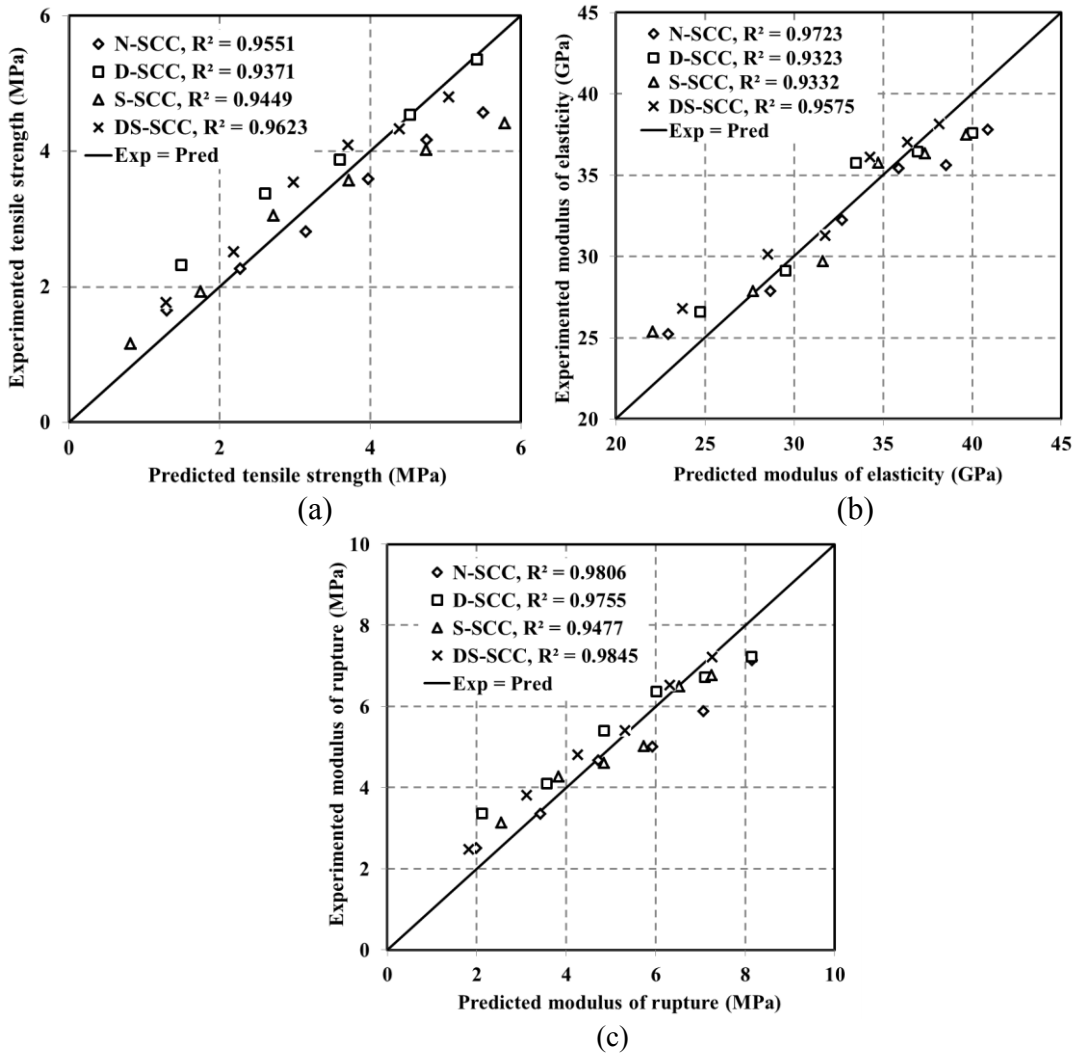

Figure 5.15 Predicted compressive strength-related mechanical properties values versus experimented values (a) tensile strength, (b) modulus of elasticity, and (c) modulus of rupture

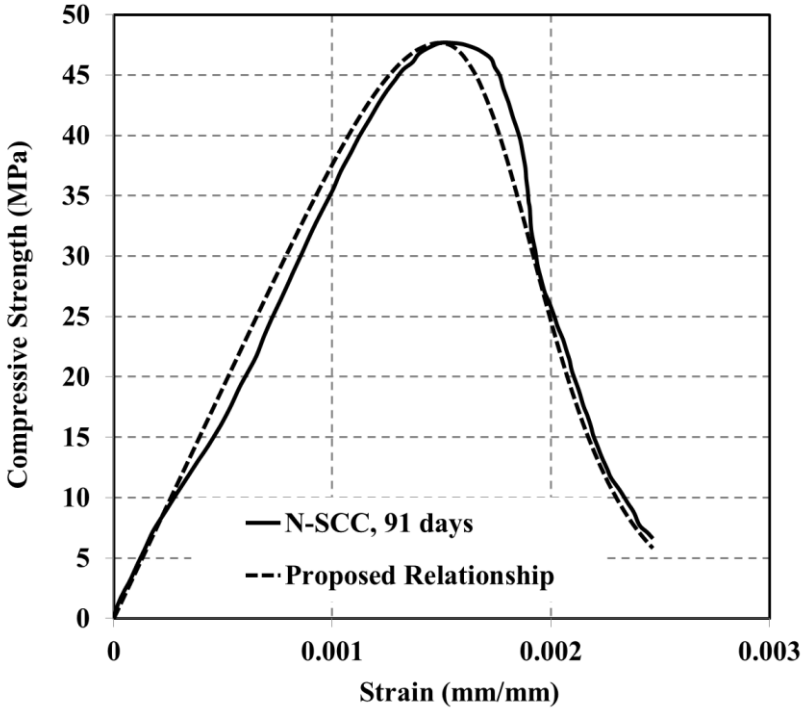

(a)

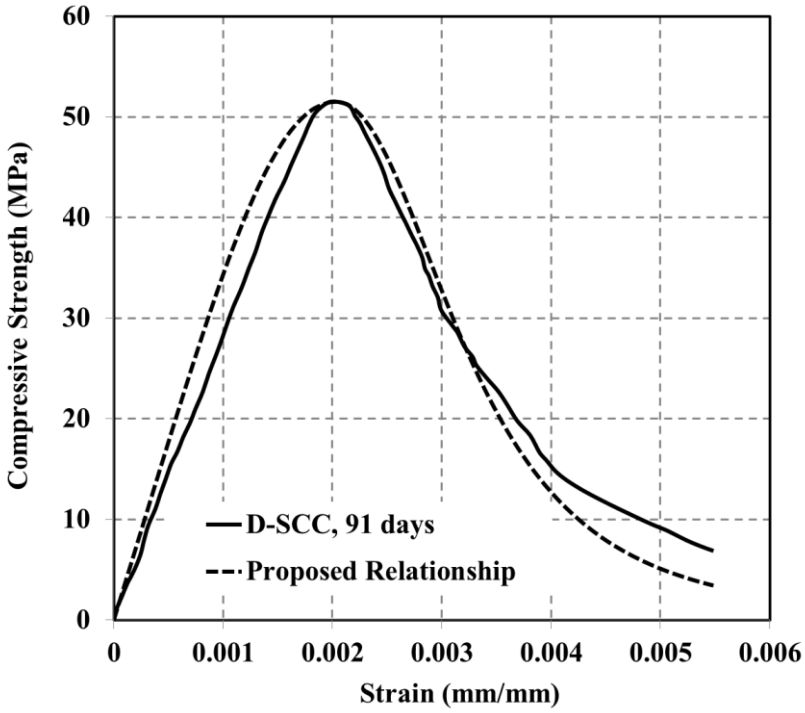

(b)

Figure 5.16(a, b) Comparison between experimented compressive stress-strain curve result with proposed relationship (a) N–SCC and (b) D–SCC

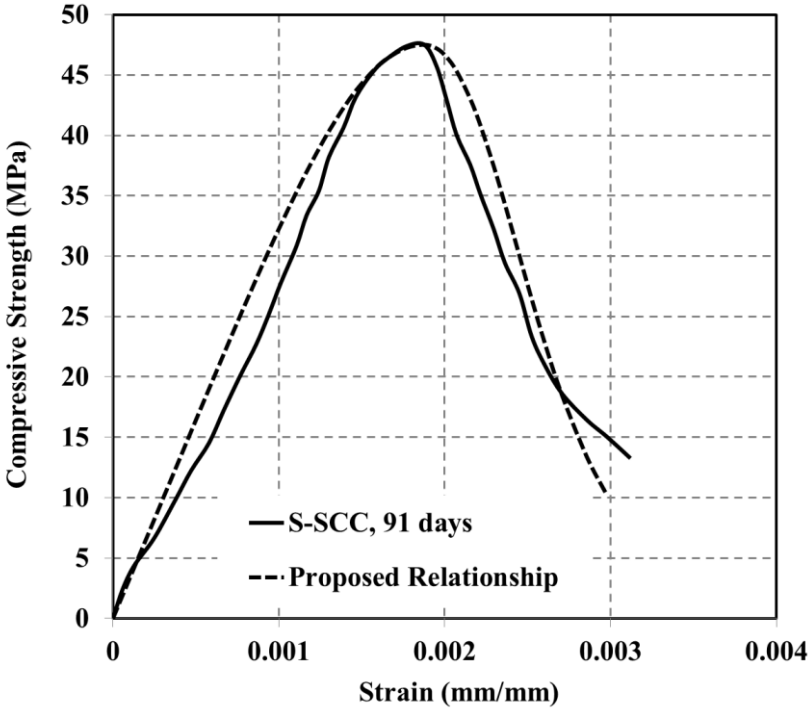

(c)

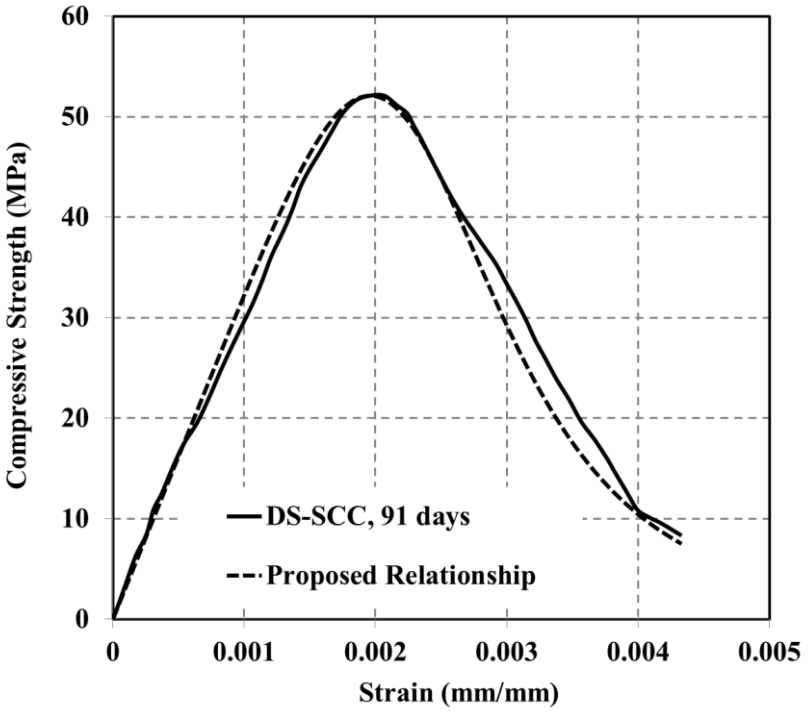

(d)

Figure 5.16(c, d) Comparison between experimented compressive stress-strain curve result with proposed relationship (c) S–SCC and (d) DS-SCC

5.9 FLEXURAL TOUGHNESS OF SCC AND FRSCC

The enhanced performance of fibre reinforced concrete over its unreinforced counterpart comes from its improved capacity to absorb energy during fracture (Banthia and Trottier, 1995). While a plain unreinforced matrix fails in a brittle manner at the cracking stresses, the ductile fibres in fibre reinforced concrete continue to carry stresses beyond the matrix cracking, which helps to maintain structural integrity and cohesiveness in the material. Further, if properly designed, fibres undergo pullout processes, and the fractional work needed for pullout leads to a significantly improved energy-absorption capability. Thus, fibre reinforced concrete exhibits better performance not only under static and quasi-statically applied loads but also under fatigue, impact, and impulsive loadings. This energy-absorption attribute of FRC is often termed "toughness" (Banthia and Trottier, 1995).

The actual influence of fibres on the toughness characteristics of FRSCC is not well understood. One reason for this is the inadequacies of standard toughness characterization experimental results. This section investigates the flexural toughness characteristics of SCC incorporating steel and polypropylene fibres. An extensive experimental program in the University of Technology Sydney (UTS) concrete laboratory has been carried out to monitor and record the compressive and flexural strengths of SCC and FRSCC cylinderal and prism specimens. For this purpose, four different SCC mixes including plain SCC, steel, polypropylene, and hybrid FRSCC mixes were considered in the test program. The compressive and flexural strengths were tested after 3, 7, 14, 28, 56, and 91 days. The flexural toughness parameters were obtained according to the ASTM C 1018 (2000), JSCE (1984), Banthia and Trottier (1995), and ACI 544 (1988) methods.

5.9.1 Flexural Toughness and Its Characterization

Methods to calculate the flexural toughness were according the ASTM C 1018 (2000), JSCE (1984), Banthia and Trottier (1995), and ACI 544 (1988) test methods. The differences between the methods and their specifications are described in Appendix-C. Flexural load-deflection curves for the N-SCC, D-SCC, S-SCC, and DS-SCC mixes are shown in Figures 5.17 to 5.20. These flexural load-deflection curves are captured at 3, 7, 14, 28, 56, and 91 days. Moreover, in Tables 5.12 to 5.15, first cracking load (FCL),

deflection at the first cracking (DFC), and flexural tensile strength (FTS) of these four mixes at different ages are presented. In this study, flexural toughness for the four proposed mixes at different ages is calculated:

As shown in Tables 5.12 to 5.15, the first cracking loads for the N-SCC, D-SCC, S-SCC, and DS-SCC mixes at age 91 days compared to age 3 days are raised to 63%, 60%, 63%, and 65%, respectively. Furthermore, the deflections at the first crack for the N-SCC, D-SCC, S-SCC, and DS-SCC mixes at age 91 days compared to age 3 days are raised to 75%, 56%, 72%, and 13%, respectively. Also, areas under curve up to first crack for the N-SCC, D-SCC, S-SCC, and DS-SCC mixes at age 91 days compared to age 3 days are raised to 70%, 57%, 65%, and 69%, respectively.

According to the ASTM C 1018 method (see Table 5.13 and Appendix-C), the toughness indexes "I_5, I_{10}, I_{20}, and I_{30}" of the D-SCC mix at age 91 days are "3.63, 6.28, 7.96, and 8.47" and compared to age 3 days are raised to 28%, 28%, 35%, and 38%, respectively. Also, the residual strength factors "$R_{5,10}$, $R_{10,20}$, and $R_{20,30}$" of the D-SCC mix at age 91 days are "52.97, 16.78, and 5.12" and compared to age 3 days are raised to 27%, 62%, and 94%, respectively.

From Table 5.14, the toughness indexes "I_5, I_{10}, I_{20}, and I_{30}" of the S-SCC mix at age 91 days are "1.88, 2.93, 4.20, and 4.41" and compared to age 3 days are raised to 0.5%, 26%, 34%, and 26%, respectively. Also, the residual strength factors "$R_{5,10}$, $R_{10,20}$, and $R_{20,30}$" of the S-SCC mix at age 91 days are "21.13, 12.64, and 2.13" and compared to age 3 days are raised to 71%, 55%, and 57%, respectively.

From Table 5.15, the toughness indexes "I_5, I_{10}, I_{20}, and I_{30}" of the DS-SCC mix at age 91 days are "3.52, 4.75, 5.59, and 5.61" and compared to age 3 days are raised to 7%, 15%, 23%, and 23%, respectively. Also, the residual strength factors "$R_{5,10}$, $R_{10,20}$, and $R_{20,30}$" of the DS-SCC mix at age 91 days are "24.63, 8.36, 0.25" and compared to age 3 days are raised to 40%, 65%, and 30%, respectively.

By utilizing the JSCE method (see Table 5.13 and Appendix-C), the flexural toughness factor (*FT*) of the D-SCC mix at age 91 days is 4.40 and compared to age 3 days is raised to 34%. Also, from Table 12 the *FT* of the S-SCC mix at age 91 days is 2.32 and compared to age 3 days is raised to 53%. About the *FT* of the DS-SCC mix at age 91 days is 4.47 and compared to age 3 days is raised to 43%.

According to Banthia and Trottier method (see Appendix-C), the post-cracking strength (PCS_m) at L/150 for D-SCC mix at age 91 days is 4.89 and compared to age 3 days is raised to 43%. PCS_m at L/150 for S-SCC mix at age 91 days is 1.62 and compared to age 3 days is raised to 55%. Also, PCS_m at L/150 for DS-SCC mix at age 91 days is 4.40 and compared to age 3 days is raised to 37%.

By utilizing the ACI 544 method, the toughness index (I_t) of the D-SCC mix at age 91 days is 9.20 and compared to age 3 days is raised to 11%. From Table 5.14 the I_t of the S-SCC mix at age 91 days is 3.94 and compared to age 3 days is raised to 40%. Moreover, the I_t of the DS-SCC mix at age 91 days is 4.70 and compared to age 3 days is raised to 44%. Based on the above mentioned flexural toughness results, it can be concluded that D-SCC mix has a better flexural toughness characteristic than DS-CC and S-SCC mixes.

The JSCE flexural toughness factors are less variable and more sensitive to both age and fibre content that the ASTM toughness indexes for the studied SCC mixes. They increase as the concrete age or fibre content increases. The characterization of flexural toughness based on the JSCE approach is very simple and is independent of the type of deflection measuring technique. No sophisticated instrumentation is required to determine the toughness factor. The calculated flexural toughness factor using this approach has good correlation with the fibre-reinforcing index. Also, based on the flexural toughness analyses by using ASTM C 1018, JSCE, Banthia and Trottier, and ACI 544 methods, it can be observed that D-SCC mix had a better flexural toughness characteristic than DS-CC and S-SCC mixes.

5.9.2 Flexural Load-Deflection Behaviour of D-SCC, S-SCC, and DS-SCC Mixes

Figures 5.21 to 5.23 shown the D-SCC, S-SCC, and DS-SCC mixes flexural load-deflection curves. The fibre SCC mixes behave almost perfectly elastic until first-cracking load. However, the load-carrying capacity drops immediately after cracking, then increases again with increase in deflection, reaches its maximum value, and then gradually decreases until fracture. As shown in Figures 5.21 to 5.23, first crack is occurred in 0.60 mm, 0.69 mm, 0.58 mm average deflection for the D-SCC, S-SCC, and DS-SCC mixes, receptively.

The average amount of load drops immediately after cracking for the D-SCC mix is 19%, for the S-SCC mix is 53%, and for the DS-SCC mix is 17% of first cracking load. The average differences between first cracking deflections to final deflections are 0.077 mm, 0.150 mm, and 0.091 mm for the D-SCC, S-SCC, and DS-SCC mixes, receptively.

These load-deflection characteristics may be explained as follows: Typical flexural load-deflection curves may be drawn as shown in Figures 5.21 to 5.23, which are divided into different regions based on the fracture process. Generally the load-deflection curve is divided into two parts; region (I) which is the elastic range before cracking, and region (II) which is the inelastic range until fracture. In region (I), it is considered that only concrete carries loads. The fibres do not contribute to load capacity except in special cases. In region (II), only fibres carry tensile stresses as in conventional reinforced concrete. This region may be subdivided into three parts: the region where load is transmitted from concrete to fibres (A), the region where fibres carry all the tensile forces, and thereby increase the load carrying capacity (B), and the region where the load carrying capacity decreases because of rupture or slipping of fibres until fracture (C). In region (A), the tensile forces carried by the concrete matrix are gradually transmitted to fibres after cracking. The amount of decrease (P_{cr}-P_0) is affected by fibre content, loading velocity and the strength of the concrete matrix. In region (B), the fibres carry all the tensile forces, and the load carrying capacity is recovered as fibres stretch with increase in deflection. The maximum load carrying capacity (P_{max}) which exceeds the cracking load may be reached, when a sufficient amount of fibre is incorporated. In region (C), fibre reinforced concrete gradually loses its load carrying capacity because of rupture or slipping of fibres and finally fracture occurs. From this discussion, it is clear that the behaviour of fibre reinforced concrete in region (II) is governed by the mechanical properties and content of the fibres.

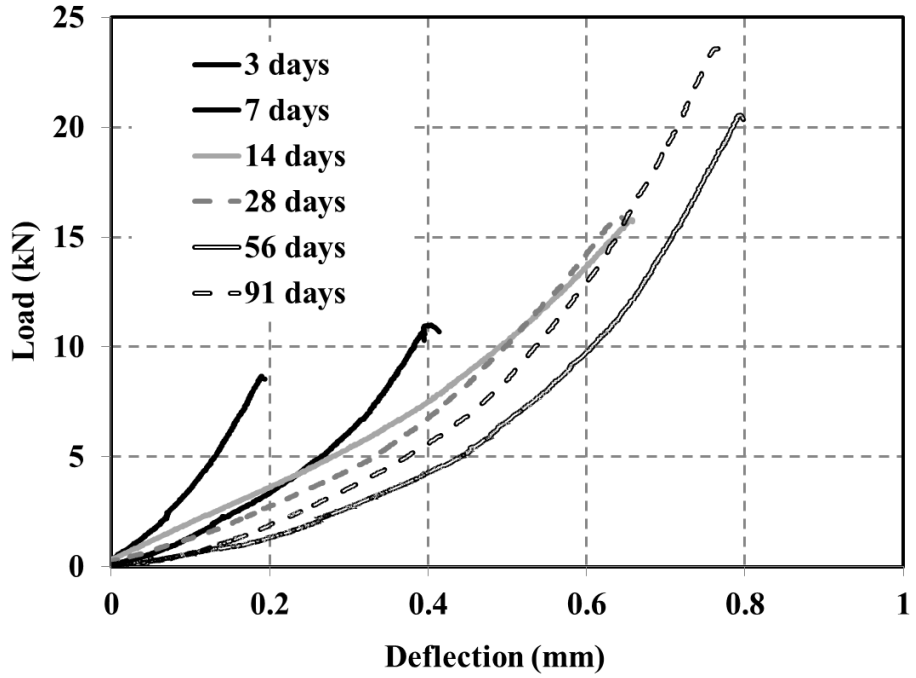

Figure 5.17 Flexural load-deflection behaviour of N-SCC mixture at different ages

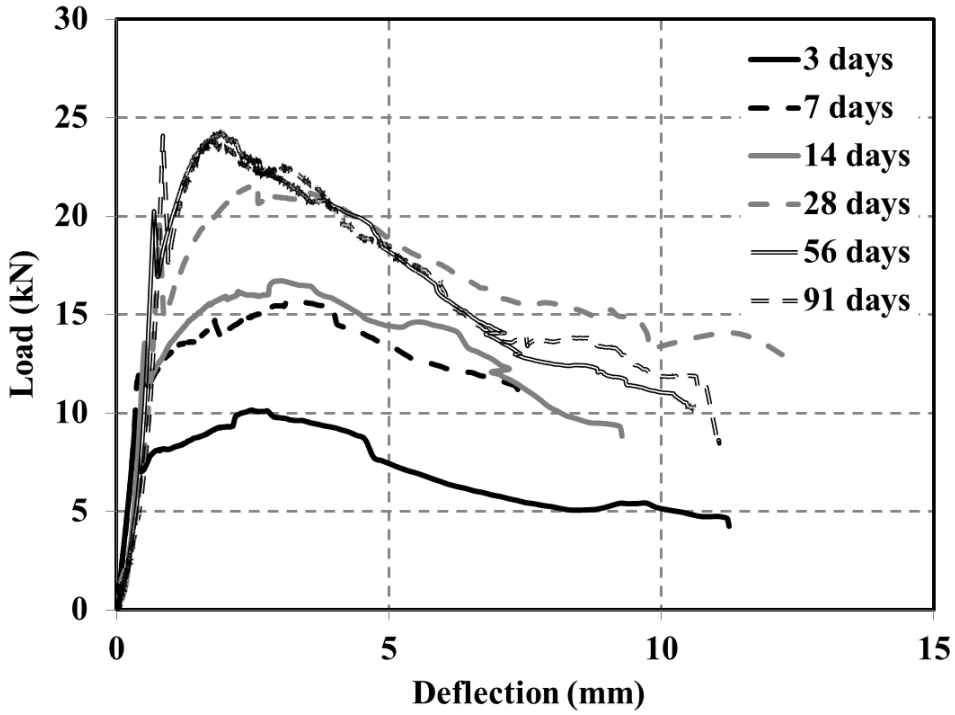

Figure 5.18 Flexural load-deflection behaviour of D-SCC mixture at different ages

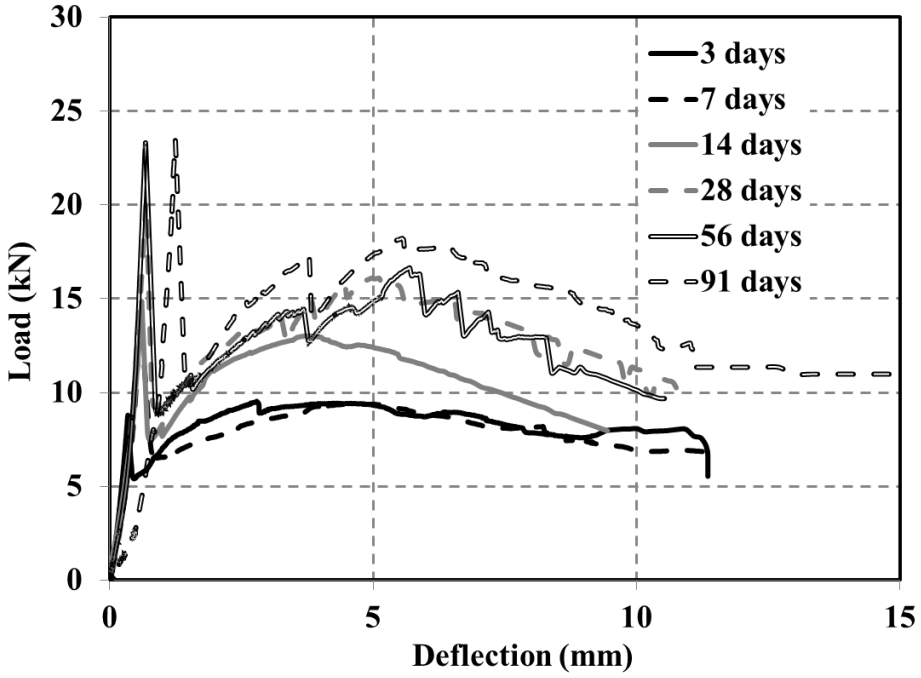

Figure 5.19 Flexural load-deflection behaviour of S-SCC mixture at different ages

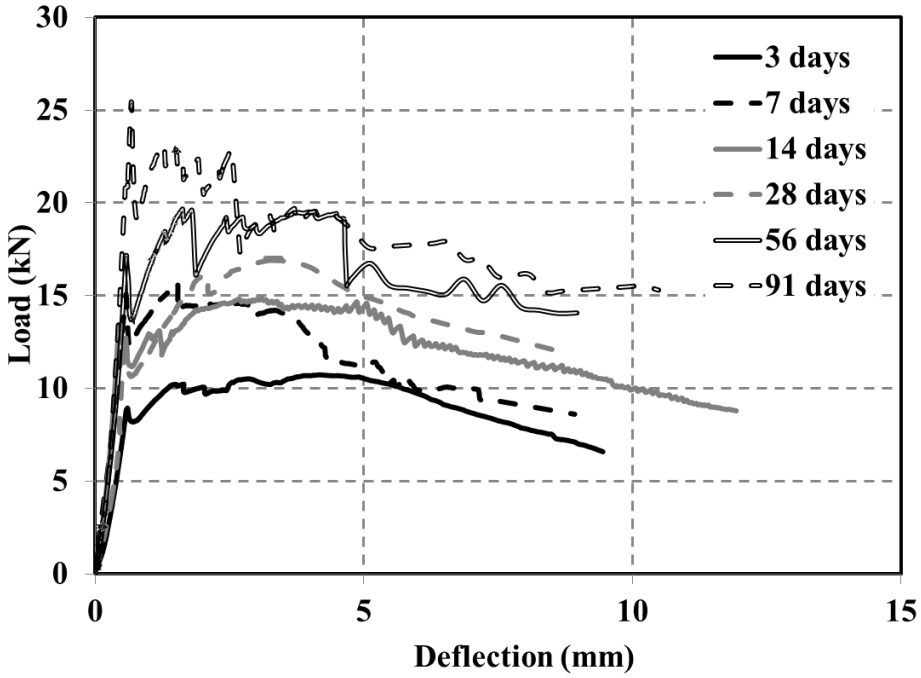

Figure 5.20 Flexural load-deflection behaviour of DS-SCC mixture at different ages

Table 5.12 Load-deflection and flexural strength properties of the N-SCC mix

N-SCC	Time (days)					
	3	7	14	28	56	91
FCL* (kN)	8.56	10.75	15.79	15.93	20.53	23.57
DFC** (mm)	0.187	0.394	0.655	0.643	0.793	0.762
FTS*** (MPa)	2.57	3.22	4.73	4.78	6.16	7.07
ASTM C1018						
Area under the curve						
δ	2.60	8.79	8.98	7.95	8.88	8.90

*First cracking load, ** Deflection at the first cracking, *** Flexural tensile strength

Table 5.13 Load-deflection and flexural strength properties of the D-SCC mix

D-SCC	Time (days)					
	3	7	14	28	56	91
FCL (kN)	9.52	11.60	13.54	19.56	20.26	24.10
FCD (mm)	0.347	0.380	0.515	0.788	0.690	0.795
FTS (MPa)	2.85	3.48	4.06	5.87	6.08	7.23
ASTM C 1018 (2000)						
Area under the curve						
δ	4.09	4.60	5.77	10.46	7.09	9.66
3δ	10.56	14.73	19.51	26.91	27.51	35.11
5.5δ	18.46	25.49	33.75	39.34	45.37	60.71
10.5δ	21.05	28.64	34.14	41.83	50.19	76.93
15.5δ	21.16	29.06	34.48	42.22	53.90	81.88
Toughness index						
I_5	2.58	3.19	3.38	2.57	3.88	3.63
I_{10}	4.51	5.53	5.84	3.76	6.40	6.28
I_{20}	5.14	6.21	5.91	4.00	7.08	7.96
I_{30}	5.17	6.30	5.97	4.03	7.60	8.47
Residual strength factor						
$R_{5,10}$	38.63	46.71	49.34	23.75	50.39	52.97
$R_{10,20}$	6.33	6.83	0.68	2.38	6.79	16.78
$R_{20,30}$	0.26	0.91	0.58	0.37	5.23	5.12
JSCE (1984)						
δ_{150}	2	2	2	2	2	2
D_f	19.30	25.15	26.81	22.64	26.53	29.32
FT	2.89	3.77	4.02	3.39	3.98	4.40
Banthia and Trottier (1995)						
L/m	L/150	L/150	L/150	L/150	L/150	L/150
$E_{post,m}$	15.21	20.54	21.04	12.18	19.44	19.65
PCS_m	2.76	3.80	4.25	3.01	4.45	4.89
L/m	L/200	L/200	L/200	L/200	L/200	L/200
$E_{post,m}$	10.36	15.26	13.04	6.70	11.61	11.55
PCS_m	2.69	4.08	3.97	2.82	4.30	4.91
L/m	L/300	L/300	L/300	L/300	L/300	L/300
$E_{post,m}$	6.07	8.15	5.67	1.78	3.62	1.16
PCS_m	2.79	3.93	3.51	2.52	3.50	1.69
L/m	L/400	L/400	L/400	L/400	L/400	L/400
$E_{post,m}$	3.76	4.67	2.34	-	0.11	-
PCS_m	2.80	3.78	2.99	-	0.55	-
ACI 544 (1988)						
I_t	8.18	3.34	3.84	5.30	6.07	9.20

Table 5.14 Load-deflection and flexural strength properties of the S-SCC mix

S-SCC	Time (days)					
	3	7	14	28	56	91
FCL (kN)	8.59	14.15	14.86	20.10	23.32	23.44
FCD (mm)	0.338	0.580	0.607	0.693	0.679	1.243
FTS (MPa)	2.57	4.24	4.45	6.03	6.99	7.03
ASTM C 1018 (2000)						
Area under the curve						
δ	3.27	4.55	3.63	5.06	9.55	8.32
3δ	6.13	7.33	10.27	10.84	19.72	15.67
5.5δ	7.12	9.22	14.21	15.42	27.65	24.46
10.5δ	8.98	10.63	17.86	17.59	34.86	34.98
15.5δ	10.61	11.76	18.15	18.07	35.06	36.76
Toughness index						
I_5	1.87	1.61	2.82	2.14	2.06	1.88
I_{10}	2.17	2.02	3.91	3.05	2.89	2.93
I_{20}	2.74	2.33	4.91	3.47	3.65	4.20
I_{30}	3.24	2.58	4.99	3.57	3.67	4.41
Residual strength factor						
$R_{5,10}$	6.06	8.30	21.67	18.09	16.61	21.13
$R_{10,20}$	5.66	3.09	10.03	4.30	7.55	12.64
$R_{20,30}$	4.98	2.48	0.81	0.93	0.20	2.13
JSCE (1984)						
δ_{150}	2	2	2	2	2	2
D_f	7.30	7.80	10.73	10.66	12.50	15.48
FT	1.09	1.17	1.61	1.60	1.87	2.32
Banthia and Trottier (1995)						
L/m	L/150	L/150	L/150	L/150	L/150	L/150
$E_{post,m}$	4.02	3.24	7.09	5.61	2.94	7.16
PCS_m	0.72	0.68	1.52	1.28	1.17	1.62
L/m	L/200	L/200	L/200	L/200	L/200	L/200
$E_{post,m}$	3.39	2.36	4.59	4.36	-	4.78
PCS_m	0.87	0.77	1.54	1.62	-	1.74
L/m	L/300	L/300	L/300	L/300	L/300	L/300
$E_{post,m}$	2.82	0.90	1.49	1.31	-	0.92
PCS_m	1.28	0.64	1.13	1.28	-	0.86
L/m	L/400	L/400	L/400	L/400	L/400	L/400
$E_{post,m}$	2.23	0.06	0.15	0.05	-	0.04
PCS_m	1.62	0.10	0.32	0.28	-	0.16
ACI 544 (1988)						
I_t	2.34	1.43	2.02	2.27	4.14	3.94

Table 5.15 Load-deflection and flexural strength properties of the DS-SCC mix

DS-SCC	Time (days)					
	3	7	14	28	56	91
FCL (kN)	8.85	13.00	13.44	15.06	17.17	25.45
FCD (mm)	0.584	0.562	0.459	0.575	0.581	0.675
FTS (MPa)	2.65	3.90	4.03	4.52	5.15	7.63
ASTM C 1018 (2000)						
Area under the curve						
δ	3.80	5.32	3.76	6.21	7.46	12.53
3δ	14.33	17.35	18.05	20.40	29.91	26.29
5.5δ	21.73	21.29	22.28	29.48	37.91	35.49
10.5δ	22.79	22.84	23.85	38.25	41.60	41.73
15.5δ	23.50	23.04	24.01	39.62	41.87	41.92
Toughness index						
I_5	3.26	3.76	4.79	3.28	2.38	3.52
I_{10}	4.00	5.71	5.91	4.74	3.02	4.75
I_{20}	4.29	5.99	6.33	6.16	3.32	5.59
I_{30}	4.32	6.18	6.37	6.38	3.34	5.61
Residual strength factor						
$R_{5,10}$	14.80	38.87	22.47	29.22	12.77	24.63
$R_{10,20}$	2.90	2.79	4.14	14.13	2.94	8.36
$R_{20,30}$	0.36	1.88	0.42	2.21	0.21	0.25
JSCE (1984)						
δ_{150}	2	2	2	2	2	2
D_f	16.73	19.27	21.19	22.80	28.27	29.83
FT	2.51	2.89	3.18	3.42	4.24	4.47
Banthia and Trottier (1995)						
L/m	L/150	L/150	L/150	L/150	L/150	L/150
$E_{post,m}$	12.93	13.94	17.42	16.59	17.30	20.81
PCS_m	2.74	2.90	3.39	3.49	3.91	4.40
L/m	L/200	L/200	L/200	L/200	L/200	L/200
$E_{post,m}$	8.14	10.38	15.76	11.48	12.65	15.49
PCS_m	2.66	3.32	4.54	3.72	4.60	5.05
L/m	L/300	L/300	L/300	L/300	L/300	L/300
$E_{post,m}$	3.34	4.08	3.00	4.88	5.17	6.39
PCS_m	2.41	2.79	1.66	3.44	4.70	4.57
L/m	L/400	L/400	L/400	L/400	L/400	L/400
$E_{post,m}$	1.15	1.36	1.16	1.71	0.46	1.88
PCS_m	2.08	2.18	1.19	2.94	1.87	3.35
ACI 544 (1988)						
I_t	2.60	2.62	4.14	4.98	4.70	4.72

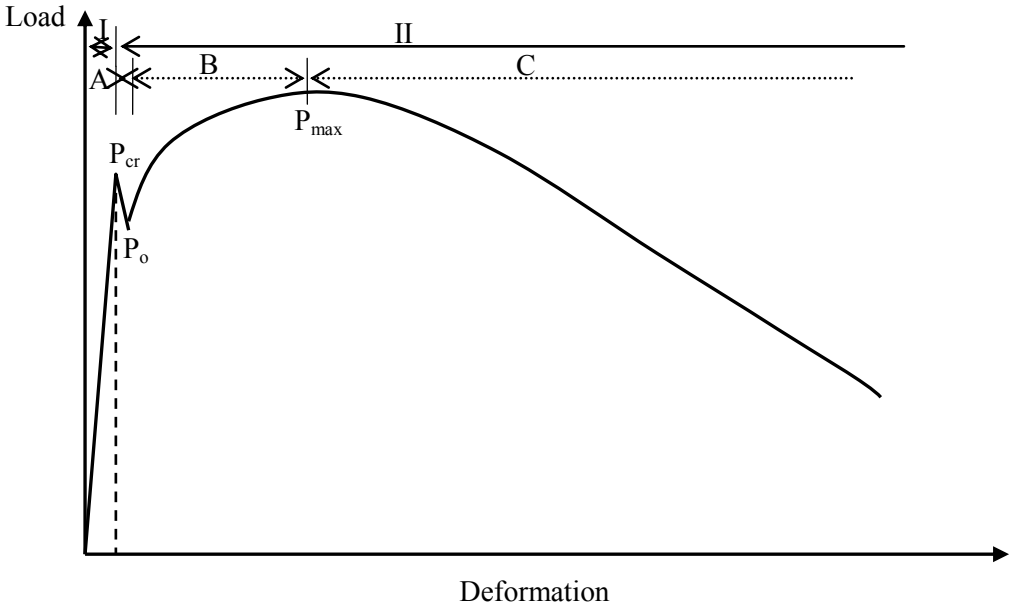

Figure 5.21 Flexural load-deformation behaviour of the D-SCC mix

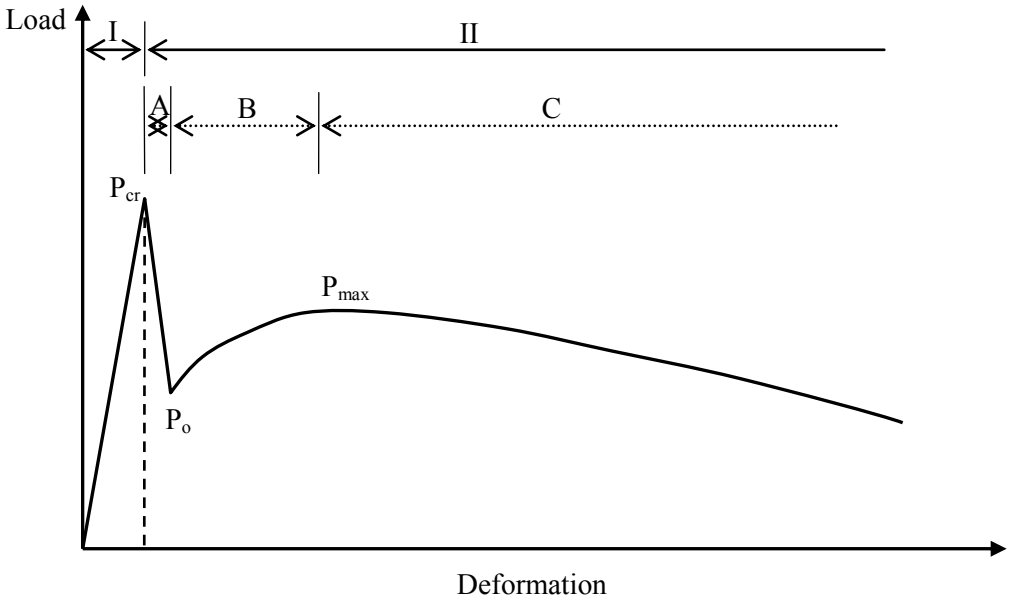

Figure 5.22 Flexural load-deformation behaviour of the S-SCC mix

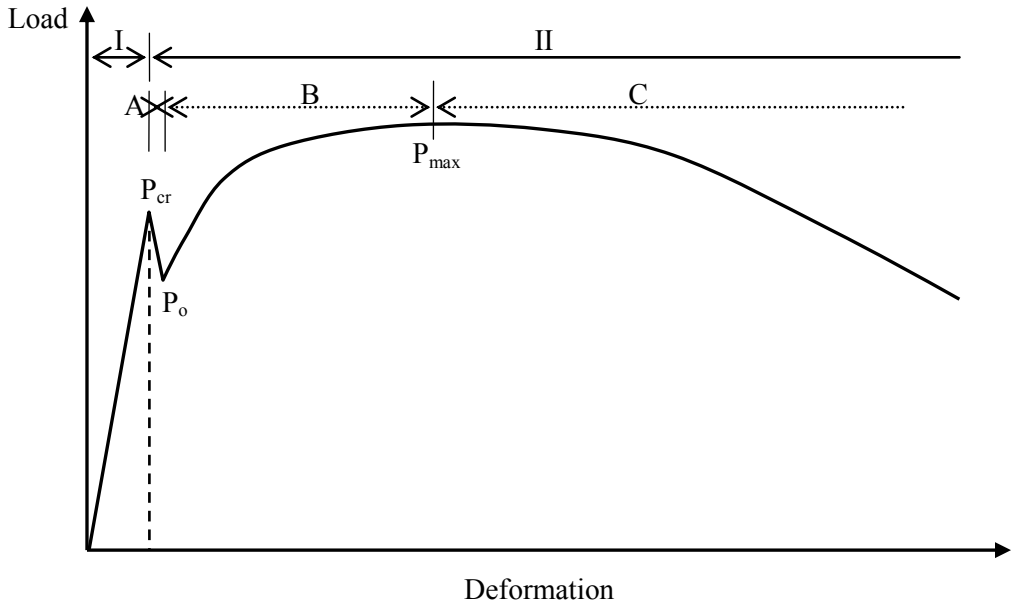

Figure 5.23 Flexural load-deformation behaviour of the DS-SCC mix

CHAPTER 6

EXPERIMENTAL PROGRAM (PHASE II) – SHORT TERM FLEXURAL CRACKING

CHAPTER 6

EXPERIMENTAL PROGRAM (PHASE II) – SHORT TERM FLEXURAL CRACKING

6.1 INTRODUCTION

Members subjected to bending moments develop flexural cracks in those regions subjected to tensile stresses. Unlike pure tension cracks, which are further uniform in width and extend fully through the members, flexural cracks are tapered and extend almost to the zero-strain axis (neutral axis). Flexural cracks are almost vertical, varying from a maximum width at the tensile face to zero near the neutral axis. Crack spacing is irregular because of random variations in the tensile strength of concrete from point to point. The extent of cracking in reinforced concrete flexural members depends mainly on the non-linear and inelastic properties of the concrete itself. When the applied loading is insufficient to cause cracking, the short-term behaviour of concrete beams is essentially linear and elastic. Even in prestressed concrete members, compressive stresses are rarely high enough to cause significant non-linearity. However, tensile cracking initiates a marked redistribution of internal stresses and structural behaviour becomes non-linear (Nejadi, 2005).

Many variables influence the width and spacing of flexural cracks in reinforced concrete members and there are a number of theoretical and semi-empirical approaches for the determination of the crack width and crack spacing. Generally, the width of a crack depends on the quantity, orientation, and distribution of the steel across the crack and the reinforcement cover. It also depends on the bond characteristics between the concrete and reinforcement bars at and in the vicinity of the crack. A local breakdown in the bond immediately adjacent to a crack complicates modelling (Nejadi, 2005).

In this Chapter, the results of short-term flexural load tests on eight reinforced SCC and FRSCC specimens slabs are presented. For this purpose, four SCC mixes – two plain SCC, two steel, two polypropylene, and two hybrid FRSCC slab specimens – are

considered in the test program. In this study, all testing and measurement requirements are based on the Nejadi (2005) research study and comparing the SCC and FRSCC experimental results with CC (Nejadi, 2005) experimental results. The tests were conducted to study the development of SCC and FRSCC flexural cracking under increasing short-term loads from first cracking through to flexural failure. Crack width, crack patterns, deflections at mid-span, steel strains and concrete surface strains at the steel levels were recorded at each load increment in the post-cracking range.

6.2 EXPERIMENTAL PROGRAM

Eight singly reinforced SCC and FRSCC slab specimens were cast and moist cured for 28 days. All the specimens were simply supported on a 3.5 m span and tested to failure to investigate the distribution and extent of primary and secondary cracking under short-term loading using two equal point loads applied at the third points on the span, at ages greater than 28 days. Crack widths were monitored on the side face of the specimens from initial cracking up to a load sufficient to cause the tensile steel to yield. The schematic diagram of the test set-up is shown in Figure 6.1.

Deflections at mid-span, crack widths, crack patterns, steel strains within the high moment region, and concrete surface strains at the steel level were recorded at each load increment in the post-cracking range and development of the primary crack pattern was monitored throughout the test. The concrete properties including the compressive and splitting tensile strengths, modulus of elasticity, and modulus of rupture at different ages were measured on companion specimens (as presented in Chapter 5).

The major objectives of the experimental program were:

(a) To gain a better understanding of the mechanisms associated with SCC and FRSCC flexural cracking of slabs, and the influence of those factors that affect the spacing and width of flexural cracks under short-term loading.

(b) To obtain benchmark, laboratory-controlled data to assist in the development of rational design-oriented procedures for the control of cracking and the calculation of crack widths in reinforced SCC and FRSCC slabs.

6.2.1 Test Parameters and Reinforcement Layouts

The parameter is varied in the tests, including the four SCC mixes – plain SCC, steel, polypropylene, and hybrid FRSCC. Details of the slab specimens are given in Table 6.1. Two identical specimens "a" and "b" were constructed for each SCC mix.

The slab specimens were each nominally 3500 mm long by 400 mm wide. In all slabs the nominal distance from the soffit to the centroid of the main reinforcement was 25 mm. Each slab is reinforced with 4N12. Details of the cross-sections and reinforcement layouts for slab specimens are shown in Figure 6.2.

6.2.2 Construction of Specimens and Test Procedures

All specimens were constructed in 3800 mm long formwork and were simply supported over a 3500 mm span. The variation of mechanical properties of concrete was measured on companion cylinders and prisms at ages 3, 7, 14, 28, 56, and 91 days. Eight electric resistance concrete strain gauges (60 mm) were glued on the side face of each specimen at the steel level to measure the concrete surface strains and eight electric resistance steel strain gauges (5 mm) were glued on middle rebar in the slab specimens for measuring the steel strains in the high moment region (as shown in Figure 6.2). A microscope with a magnification factor of 50 was used to measure the crack widths. Deflection at mid-span was measured using a MTS-Temposonics R-Series position sensor. The position sensor and

resistance strain gauge measurements were retrieved through a data acquisition system connected to a computer, while load was supplied by a hydraulic jack connected to an electrically powered pressure pump. Before casting each specimen, the inside surface of the mould was cleaned and coated with a thin layer of concrete release agent to prevent adhesion of the concrete (as shown in Figure 6.3). The SCC was placed into the mould in equal layers until each surface layer became smooth. Sufficient concrete was placed into the top layer to overfill the mould, after which the surface was stripped off and finished with a steel trowel. The companion specimens were also cast at the same time as the test specimens. Within two hours of casting the specimens were covered with wet hessian and plastic sheets and left in their moulds for 3 days. After 3 days they were removed and kept moist continuously by a thick covering of wet hessian. After 28 days the wet hessian was removed and the specimens were identified and tested at different ages. Each specimen was slowly and gradually loaded to failure over a period of approximately four hours. Figure 6.4 shows views of the experimental set-up. Each specimen was simply supported at each end before testing (Figure 6.4), and then one Temposonics R-Series position sensor was attached at the mid-span (see Figure 6.5) and linked to a computer. Electric resistance concrete strain gauges targets were glued to the concrete surface and initial strain measurements were recorded (see Figure 6.5).

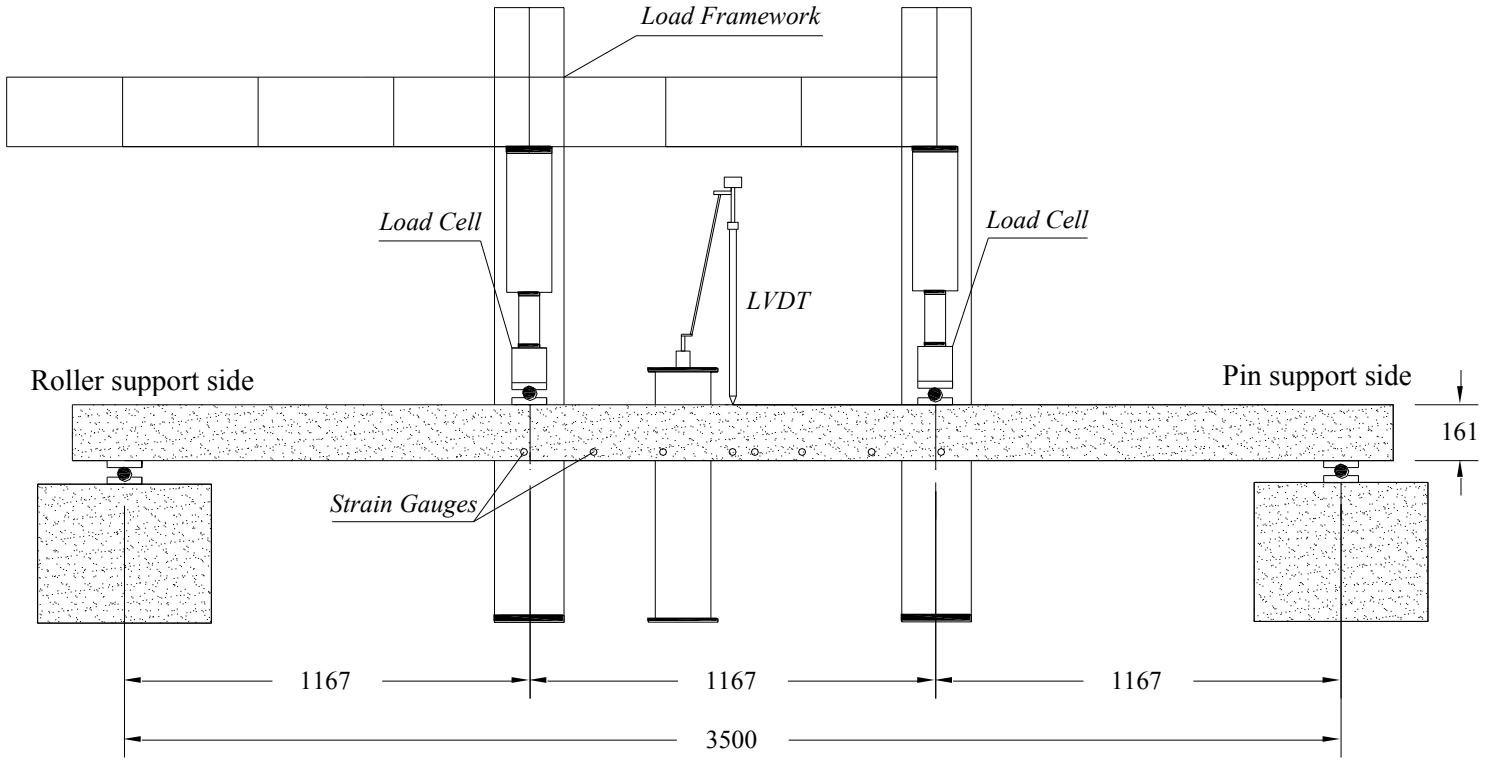

Figure 6.1 Test arrangement for all specimens

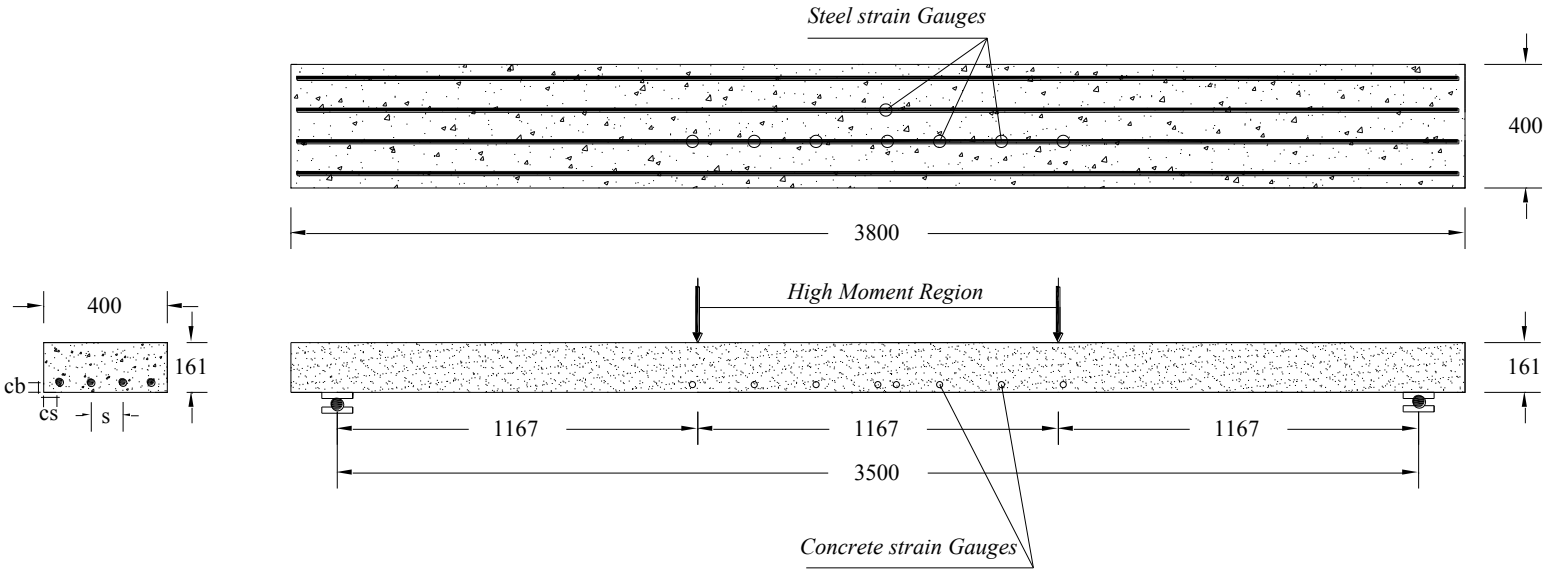

Figure 6.2 Dimensions and reinforcement details for slab specimens

Table 6.1 Details of slabs for short-term flexural tests

Specimen	No. of Bars	Bar Diam. (mm)	Steel Area (mm^2)	c_b (mm)	c_s (mm)	s (mm)
Slab -a	4	12	452	25	40	103
Slab -b	4	12	452	25	40	103

Figure 6.3 General view of slab mould before casting the SCC

Figure 6.4 General view of test set-up

Figure 6.5 General view of loading cells, concrete strain gauges, and LVDT test set-up

6.3 TEST RESULTS

Initial readings of the concrete and steel strains and the mid-span deflection were taken at zero load condition. The load was then applied in 3 kN increments for the slab specimens until approximately 70% of the calculated ultimate load was reached the same as testing procedure of Nejadi (2005). Every visible crack on the surface of the concrete was measured and the crack pattern was recorded at each load increment. The load was then increased monotonically in small increments to failure and crack widths and crack patterns were recorded at each load increment. In this section the experimental results taken from eight slabs are presented. These results include the measured material properties, the width and spacing of flexural cracking under short-term loading, and deflection at mid-span. The results are discussed in detail and a comparison between the specimens is also made. Graphs of concrete surface strain at steel level, steel strains, and some photos of tests are illustrated in Appendix-D.

6.3.1 Material Properties

As presented in Chapter 4, standard concrete cylinders (150 mm × 300 mm), and prisms (100 mm × 100 mm × 350 mm) were used to determine the compressive and tensile strengths, MOR and MOE of the concrete at ages 3, 7, 14, 28, 56, and 91 days. The results are presented in Table 6.2.

Table 6.2 Material properties of SCC and FRSCC

	Compressive strength (MPa)				Tensile strength (MPa)			
Age (days)	N-SCC	D-SCC	S-SCC	DS-SCC	N-SCC	D-SCC	S-SCC	DS-SCC
3	12.45	18.50	13.65	14.30	1.65	2.32	1.16	1.76
7	21.80	25.30	22.50	26.30	2.26	3.38	1.93	2.51
14	29.05	34.30	32.45	38.10	2.80	3.87	3.05	3.54
28	33.30	38.00	38.10	45.00	3.60	4.54	3.56	4.09
56	40.60	50.50	42.90	50.75	4.17	5.35	4.02	4.33
91	46.40	51.15	47.65	52.00	4.57	5.44	4.41	4.80
	MOE (GPa)				MOR (MPa)			
Age (days)	N-SCC	D-SCC	S-SCC	DS-SCC	N-SCC	D-SCC	S-SCC	DS-SCC
3	25.23	24.45	25.36	26.78	2.50	3.35	3.13	2.47
7	27.84	26.57	27.87	30.13	3.35	4.10	4.26	3.81
14	32.24	29.14	29.68	31.26	4.66	5.40	4.60	4.80
28	35.39	35.76	35.76	36.10	5.00	6.37	5.00	5.40
56	35.58	36.44	36.32	37.03	5.87	6.72	6.50	6.52
91	37.79	37.58	37.47	38.12	7.13	7.23	6.76	7.21

6.3.2 N-SCC-a and N-SCC-b

Slabs N-SCC-a and N-SCC-b containing 4N12 longitudinal tensile reinforcing bars, with 25 mm clear bottom cover were tested at ages 62 and 63 days respectively. Cracking first occurred approximately at load of P = 8 kN in both N-SCC-a and N-SCC-b. The number of cracks increased as the applied load increased and at approximately 70% of the ultimate load, 14 cracks were located inside the high moment region (H.M.R) for N-SCC-a, and 13 cracks for N-SCC-b respectively. The measured final average crack spacing at this load stage were 95 mm for N-SCC-a and 94 mm for N-SCC-b. The ratio of maximum crack width to average crack width at load stage P = 26 kN was 1.29 for N-SCC-a and 1.17 for N-SCC-b. The measured maximum and average crack widths within the high moment region at the bottom fibre of the slabs versus applied load are illustrated in Figures 6.6 and 6.7. The crack width history and final crack spacing are presented in Tables 6.3 and 6.4. The crack patterns at approximately 70% of the ultimate load for both slabs are illustrated in Figures 6.8 and 6.9.

The measured mid-span deflections of slabs N-SCC-a and N-SCC-b are plotted against load in Figures 6.10 and 6.11, respectively. As shown, slab series N-SCC illustrated good ductile behaviour with an extended flat plateau in the load-deflection curve. The ultimate strength was reached when P = 49 KN for N-SCC-a and P = 48.5 KN for N-SCC-b when crushing of the top compressive fibre occurred and corresponding deflections were 180 mm and 163 mm, respectively. Slab series N-SCC failed in flexure in the pure moment zone, with the compressive concrete crushing above a crack (see Figure 6.12).

Table 6.3 Crack history for slab N-SCC-a

	N-SCC-a		Load (kN)								
	Cracks	Distance from edge (roller side) (mm)	0	5	8	11	14	17	20	23	26
			Crack width (mm)								
	c-1	890							0.03	0.05	0.05
	c-2	1050							0.03	0.05	0.08
	c-3	1190						0.05	0.08	0.10	0.10
	c-4	1300			0.03	0.05	0.08	0.10	0.13	0.13	0.15
H.M.R	c-5	1410			0.03	0.03	0.05	0.08	0.10	0.13	0.15
H.M.R	c-6	1480			0.03	0.05	0.05	0.08	0.10	0.15	0.15
H.M.R	c-7	1550			0.03	0.05	0.08	0.10	0.13	0.15	0.18
H.M.R	c-8	1620			0.05	0.05	0.08	0.10	0.13	0.18	0.18
H.M.R	c-9	1680				0.05	0.10	0.13	0.15	0.18	0.20
H.M.R	c-10	1750				0.03	0.05	0.08	0.08	0.10	0.13
H.M.R	c-11	1800					0.05	0.05	0.08	0.10	0.10
H.M.R	c-12	1900			0.05	0.08	0.10	0.10	0.13	0.15	0.18
H.M.R	c-13	2030				0.03	0.05	0.05	0.08	0.08	0.10
H.M.R	c-14	2130			0.03	0.05	0.08	0.08	0.10	0.13	0.18
H.M.R	c-15	2210				0.03	0.05	0.08	0.10	0.13	0.15
H.M.R	c-16	2330			0.05	0.08	0.10	0.13	0.13	0.15	0.18
H.M.R	c-17	2390				0.03	0.05	0.08	0.10	0.13	0.15
H.M.R	c-18	2470				0.03	0.05	0.05	0.08	0.10	0.13
	c-19	2580			0.05	0.08	0.10	0.10	0.13	0.15	0.18
	c-20	2650			0.03	0.05	0.05	0.08	0.10	0.13	0.15
	c-21	2780				0.03	0.05	0.08	0.08	0.10	0.13
	c-22	2860				0.03	0.05	0.08	0.08	0.10	0.13
	c-23	2970				0.03	0.05	0.05	0.08	0.08	0.10
	c-24	3080							0.03	0.05	0.08

Table 6.4 Crack history for slab N-SCC-b

	N-SCC-b		Load (kN)								
	Cracks	Distance from edge (roller side) (mm)	0	5	8	11	14	17	20	23	26
			Crack width (mm)								
	c-1	900							0.03	0.05	0.08
	c-2	1070					0.03	0.05	0.08	0.08	0.10
	c-3	1160				0.03	0.05	0.05	0.08	0.10	0.13
	c-4	1250				0.03	0.05	0.08	0.10	0.13	0.13
	c-5	1320			0.05	0.05	0.05	0.10	0.13	0.13	0.18
H.M.R	c-6	1430			0.03	0.05	0.08	0.10	0.15	0.18	0.20
H.M.R	c-7	1510			0.05	0.05	0.08	0.13	0.15	0.18	0.18
H.M.R	c-8	1600			0.05	0.08	0.10	0.13	0.15	0.18	0.20
H.M.R	c-9	1680				0.03	0.05	0.08	0.10	0.13	0.15
H.M.R	c-10	1800			0.08	0.10	0.13	0.15	0.18	0.20	0.23
H.M.R	c-11	1860			0.05	0.08	0.10	0.13	0.15	0.18	0.20
H.M.R	c-12	1930			0.05	0.08	0.10	0.10	0.13	0.15	0.18
H.M.R	c-13	2010				0.05	0.08	0.10	0.13	0.15	0.18
H.M.R	c-14	2070			0.08	0.13	0.15	0.18	0.2	0.23	0.25
H.M.R	c-15	2200			0.05	0.05	0.08	0.10	0.13	0.15	0.18
H.M.R	c-16	2350			0.03	0.08	0.10	0.13	0.15	0.18	0.20
H.M.R	c-17	2410			0.03	0.05	0.13	0.15	0.18	0.18	0.20
	c-18	2500				0.05	0.08	0.13	0.15	0.18	0.20
	c-19	2600				0.03	0.05	0.08	0.08	0.10	0.13
	c-20	2730			0.03	0.05	0.08	0.10	0.13	0.13	0.15
	c-21	2800					0.03	0.03	0.05	0.08	0.10
	c-22	2900					0.03	0.05	0.05	0.08	0.08
	c-23	2980								0.03	0.05

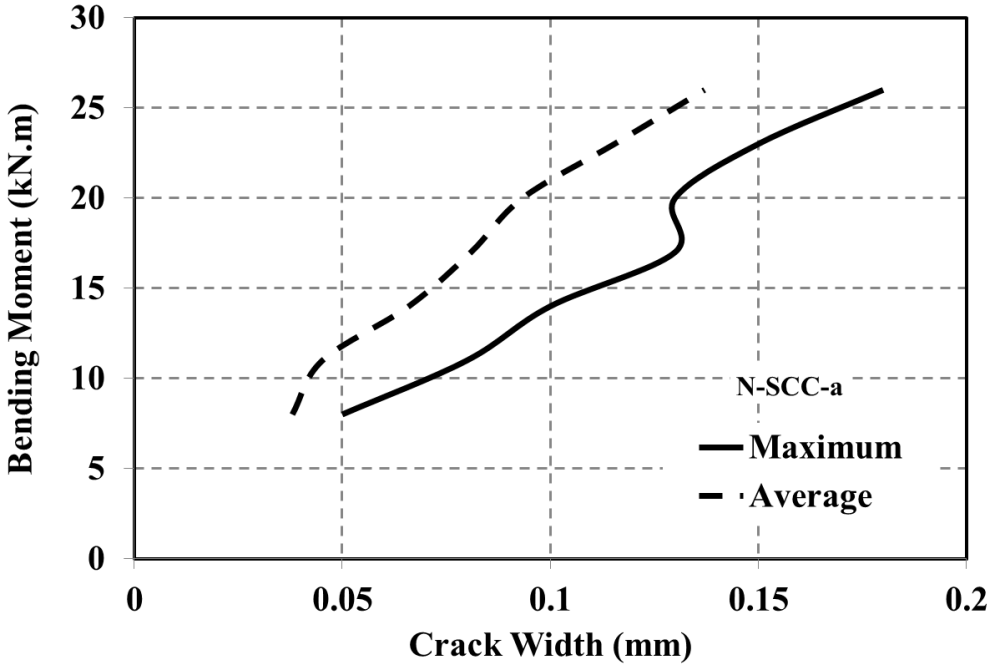

Figure 6.6 Crack width vs. applied bending moment for slab N-SCC-a

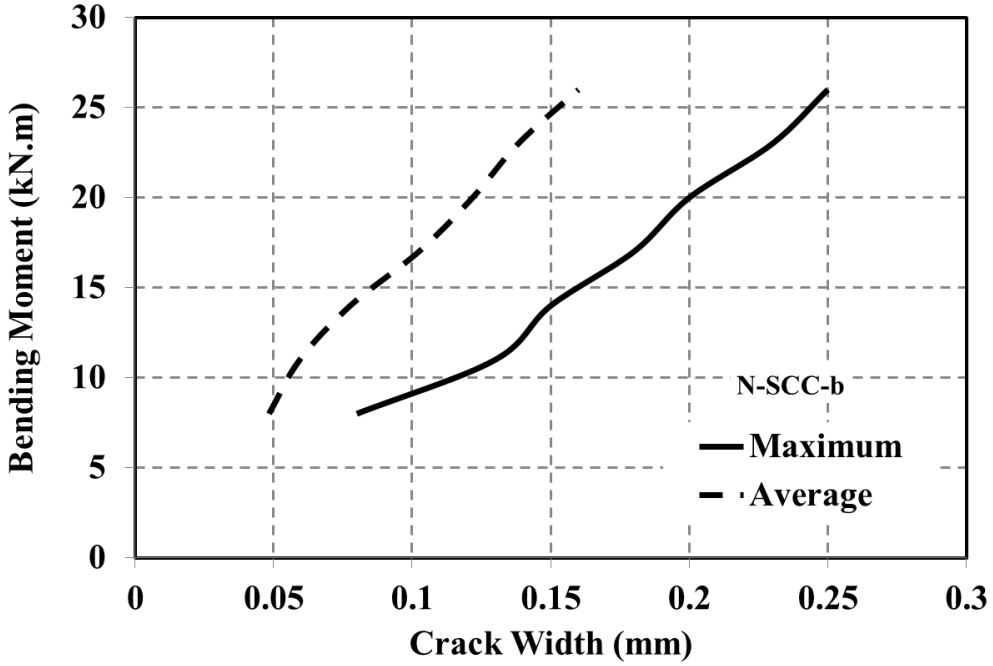

Figure 6.7 Crack width vs. applied bending moment for slab N-SCC-b

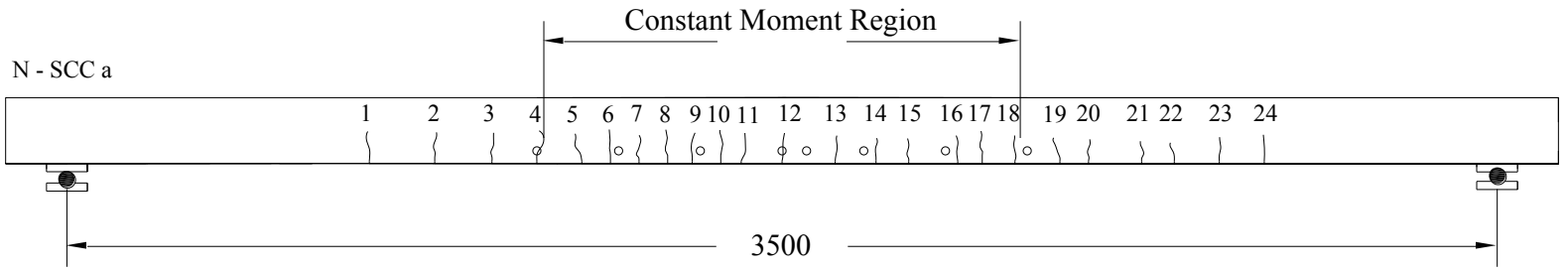

Figure 6.8 Crack pattern for slab N-SCC-a (4N12 c_b=25 mm) at load stage P = 26 kN

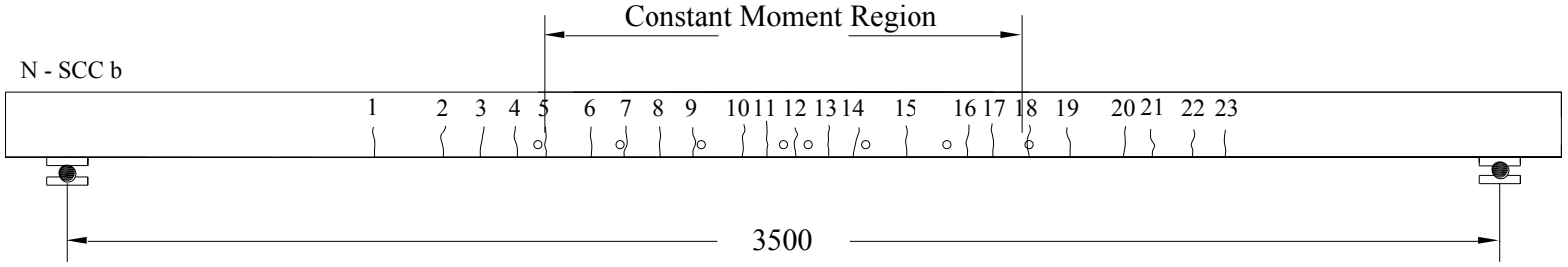

Figure 6.9 Crack pattern for slab N-SCC-b (4N12 c_b=25 mm) at load stage P = 26 kN

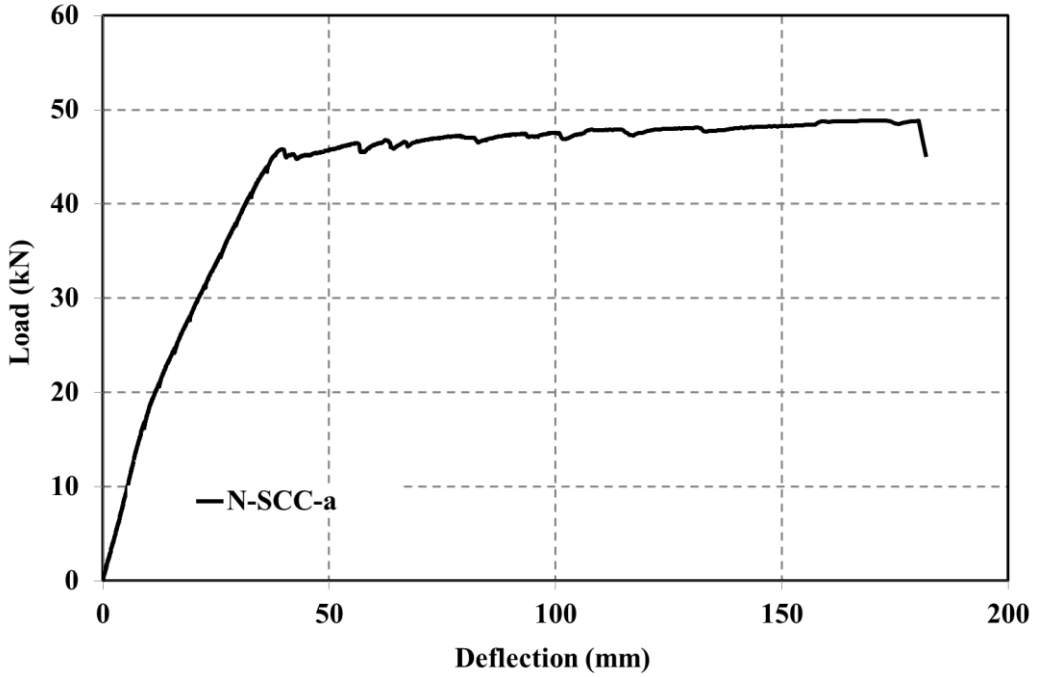

Figure 6.10 Load-deflection curve for slab N-SCC-a at mid-span

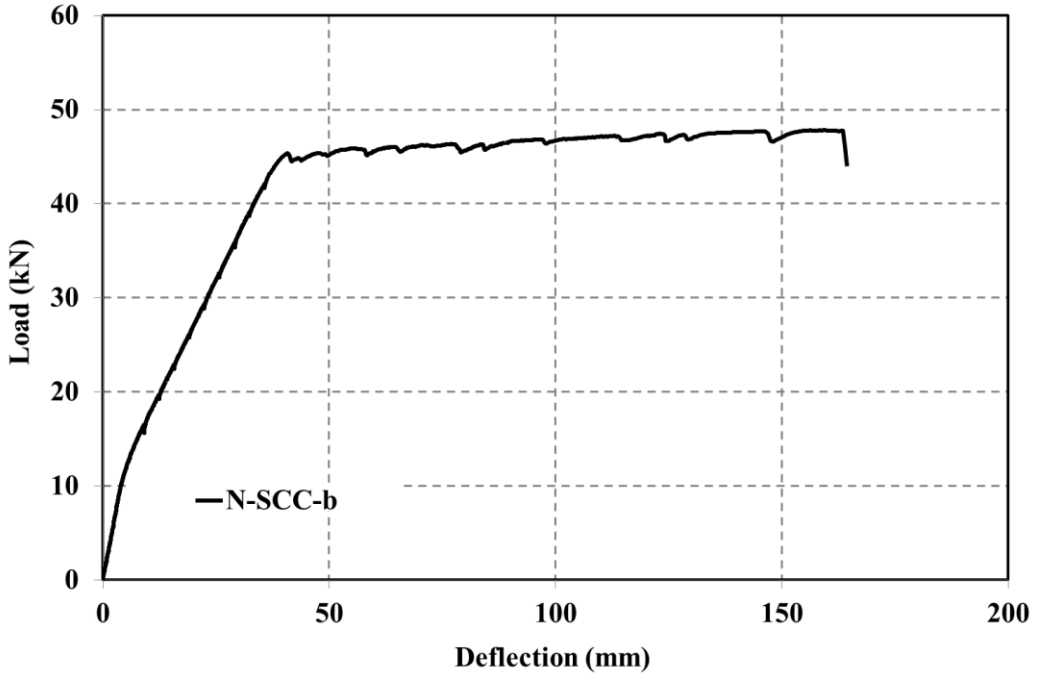

Figure 6.11 Load-deflection curve for slab N-SCC-b at mid-span

Figure 6.12 General view of slab N-SCC-a failure

6.3.3 D-SCC-a and D-SCC-b

Slabs D-SCC-a and D-SCC-b containing 4N12 longitudinal tensile reinforcing bars, with 25 mm clear bottom cover were tested at ages 65 and 66 days respectively. Cracking first occurred approximately at load of P = 8 kN in both D-SCC-a and D-SCC-b same as N-SCC series. The number of cracks increased as the applied load increased and at approximately 70% of the ultimate load, 11 cracks were located inside the high moment region (H.M.R) for D-SCC-a, and 13 cracks for D-SCC-b respectively. The measured final average crack spacing at this load stage were 106 mm for D-SCC-a and 96 mm for D-SCC-b. The ratio of maximum crack width to average crack width at load stage P = 26 kN was 1.10 for D-SCC-a and 1.33 for D-SCC-b. The measured maximum and average crack widths within the high moment region at the bottom fibre of the slabs versus applied load are illustrated in Figures 6.13 and 6.14. The crack width history and final crack spacing are presented in Tables 6.5 and 6.6. The crack patterns at approximately 70% of the ultimate load for both slabs are illustrated in Figures 6.15 and 6.16.

The measured mid-span deflections of slabs D-SCC-a and D-SCC-b are plotted against load in Figures 6.17 and 6.18, respectively. Maximum deflection at failure loading of D-SCC slab series is 25 and 14 mm higher than N-SCC slab series. It shows that D-SCC slab series are more ductile than N-SCC slab series. The ultimate strength was reached when P = 53 KN for D-SCC-a and P = 52 KN for D-SCC-b when crushing the top compressive fibre occurred and corresponding deflections were 205 mm and 177 mm, respectively.

Table 6.5 Crack history for slab D-SCC-a

	D-SCC-a		Load (kN)								
	Cracks	Distance from edge (roller side) (mm)	0	5	8	11	14	17	20	23	26
			Crack width (mm)								
	c-1	855								0.03	0.05
	c-2	965						0.03	0.03	0.05	0.08
	c-3	1085					0.03	0.03	0.05	0.08	0.10
	c-4	1205					0.03	0.05	0.08	0.10	0.10
	c-5	1300						0.05	0.08	0.10	0.13
H.M.R	c-6	1375					0.03	0.05	0.08	0.10	0.13
H.M.R	c-7	1450			0.03	0.05	0.05	0.08	0.08	0.10	0.10
H.M.R	c-8	1540			0.05	0.05	0.08	0.10	0.13	0.15	0.15
H.M.R	c-9	1635				0.05	0.08	0.10	0.10	0.13	0.15
H.M.R	c-10	1775			0.05	0.08	0.10	0.13	0.15	0.18	0.18
H.M.R	c-11	1905			0.03	0.03	0.05	0.08	0.10	0.13	0.15
H.M.R	c-12	2005			0.03	0.05	0.08	0.10	0.13	0.15	0.18
H.M.R	c-13	2080				0.03	0.05	0.08	0.10	0.13	0.15
H.M.R	c-14	2225				0.05	0.08	0.08	0.10	0.10	0.13
H.M.R	c-15	2350							0.05	0.08	0.10
H.M.R	c-16	2470					0.05	0.05	0.08	0.10	0.10
	c-17	2560				0.05	0.05	0.08	0.08	0.10	0.13
	c-18	2675				0.03	0.05	0.05	0.08	0.08	0.13
	c-19	2770					0.03	0.03	0.05	0.08	0.10
	c-20	2860						0.03	0.03	0.05	0.08
	c-21	2965						0.03	0.05	0.08	0.10
	c-22	3095								0.03	0.08

Table 6.6 Crack history for slab D-SCC-b

	D-SCC-b		Load (kN)								
	Cracks	Distance from edge (roller side) (mm)	0	5	8	11	14	17	20	23	26
			Crack width (mm)								
	c-1	970								0.03	0.03
	c-2	1090							0.03	0.05	0.08
	c-3	1160						0.03	0.05	0.08	0.10
	c-4	1240					0.03	0.05	0.08	0.10	0.13
H.M.R	c-5	1350			0.03	0.05	0.08	0.10	0.13	0.15	0.18
H.M.R	c-6	1410			0.03	0.05	0.08	0.10	0.13	0.15	0.18
H.M.R	c-7	1530			0.05	0.05	0.08	0.13	0.15	0.18	0.18
H.M.R	c-8	1630			0.03	0.05	0.08	0.13	0.15	0.18	0.2
H.M.R	c-9	1710			0.03	0.03	0.05	0.08	0.08	0.10	0.13
H.M.R	c-10	1800			0.05	0.05	0.08	0.10	0.10	0.13	0.15
H.M.R	c-11	1870			0.05	0.08	0.13	0.15	0.18	0.2	0.23
H.M.R	c-12	1970			0.05	0.05	0.10	0.13	0.18	0.2	0.2
H.M.R	c-13	2030			0.05	0.08	0.08	0.10	0.13	0.15	0.18
H.M.R	c-14	2110			0.03	0.05	0.08	0.10	0.13	0.13	0.15
H.M.R	c-15	2180			0.03	0.05	0.08	0.10	0.15	0.15	0.18
H.M.R	c-16	2280			0.03	0.03	0.05	0.08	0.10	0.10	0.15
H.M.R	c-17	2370				0.03	0.05	0.08	0.10	0.10	0.13
	c-18	2540						0.03	0.03	0.05	0.08
	c-19	2650							0.05	0.08	0.10
	c-20	2740							0.03	0.05	0.05
	c-21	2890								0.03	0.05

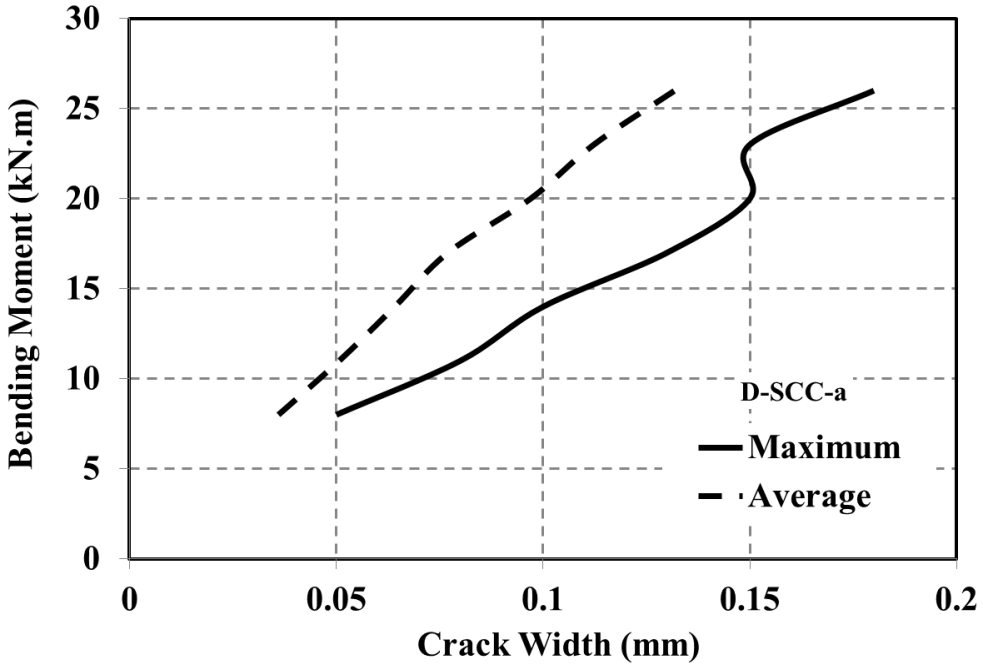

Figure 6.13 Crack width vs. applied bending moment for slab D-SCC-a

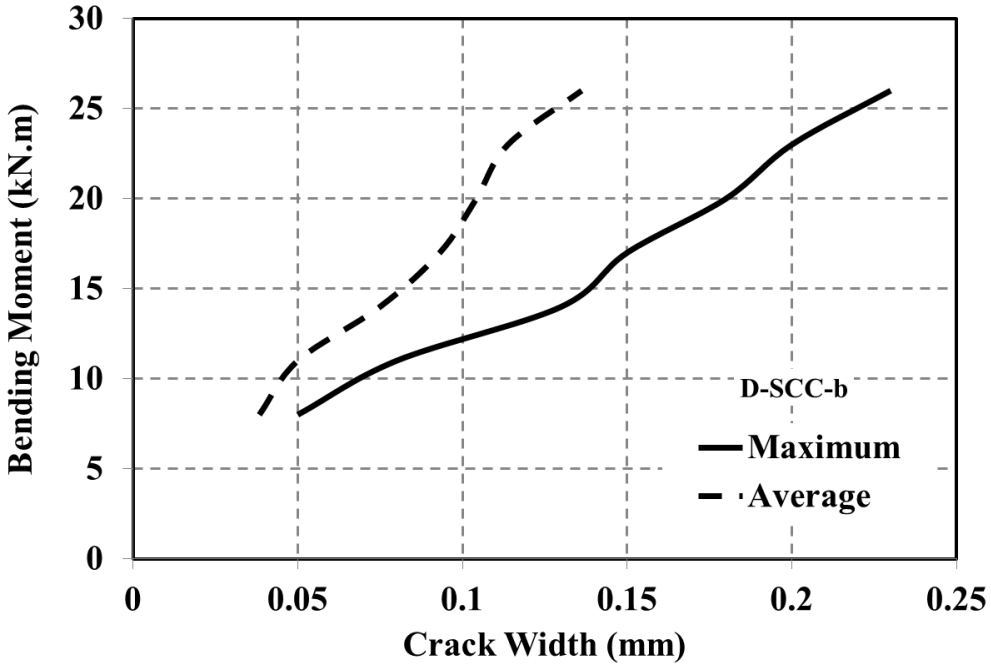

Figure 6.14 Crack width vs. applied bending moment for slab D-SCC-b

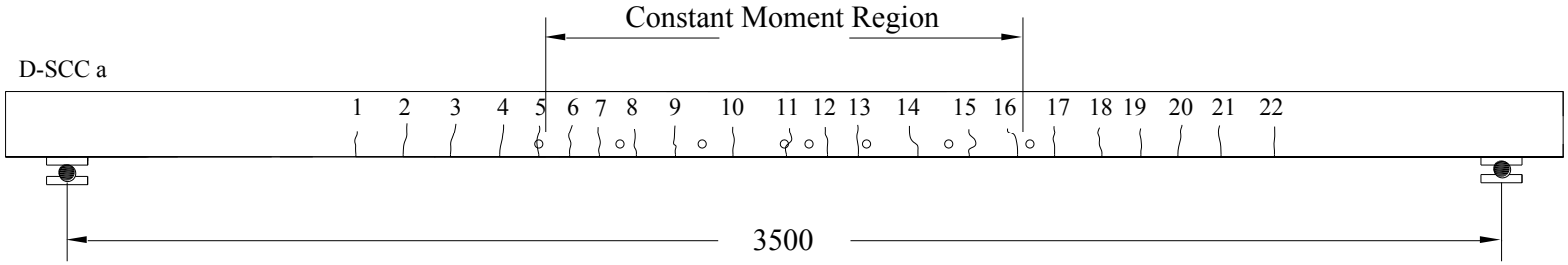

Figure 6.15 Crack pattern for slab D-SCC-a (4N12 c_b=25 mm) at load stage P = 26 kN

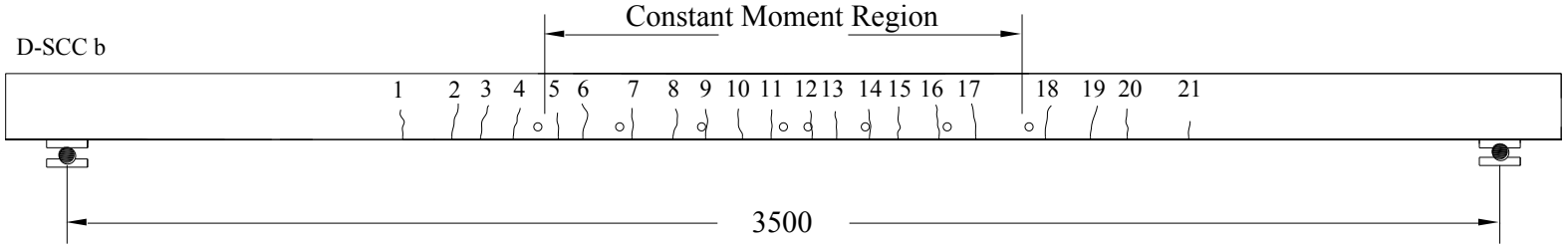

Figure 6.16 Crack pattern for slab D-SCC-b (4N12 c_b=25 mm) at load stage P = 26 kN

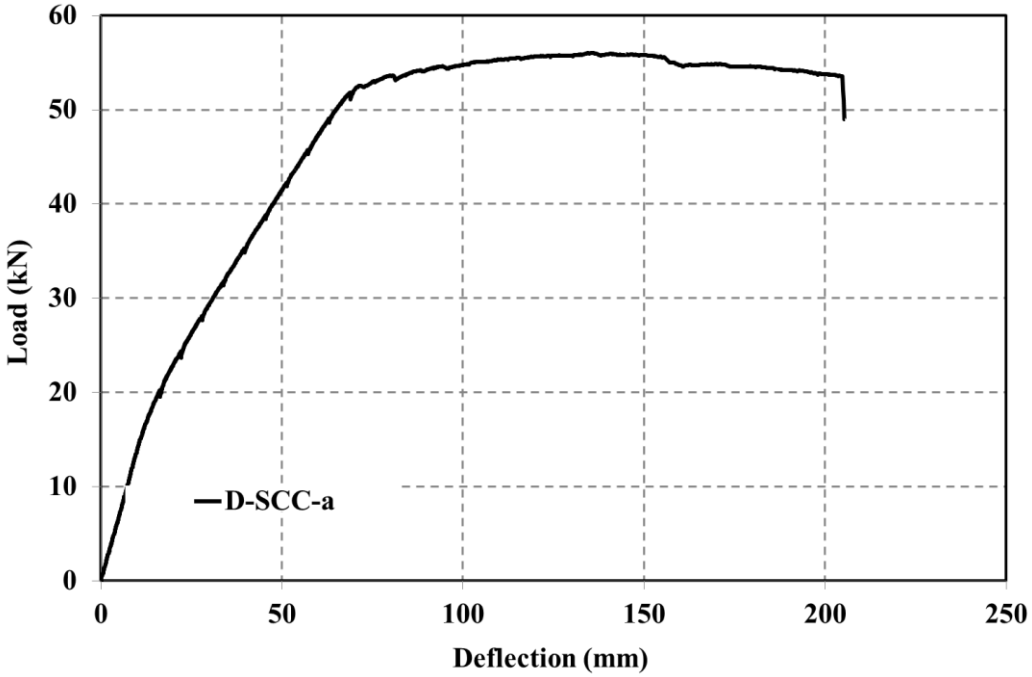

Figure 6.17 Load-deflection curve for slab D-SCC-a at mid-span

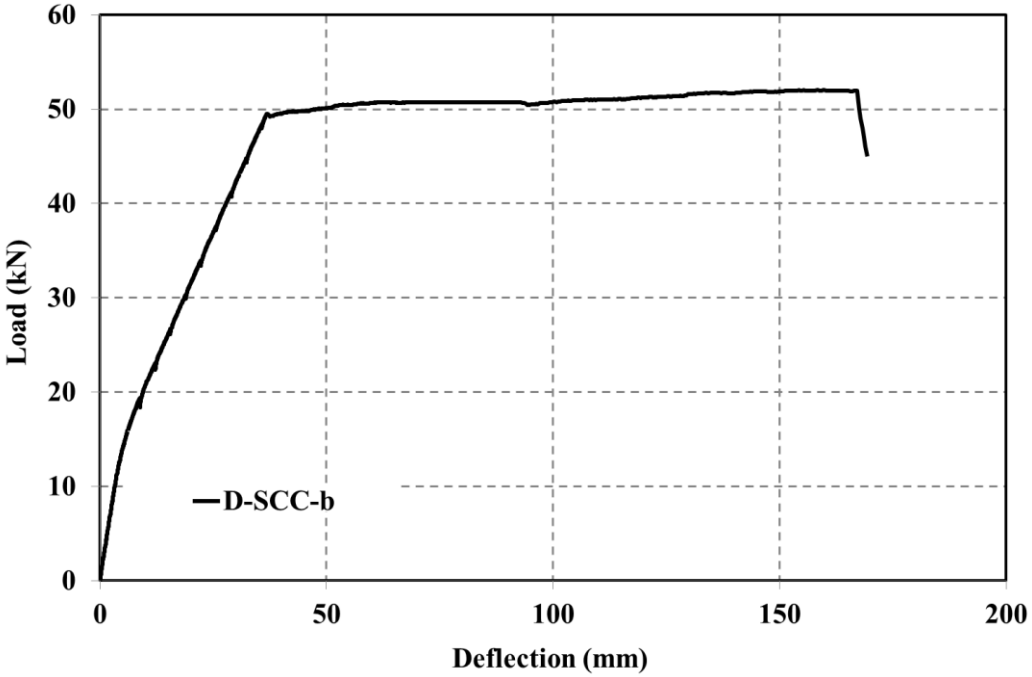

Figure 6.18 Load-deflection curve for slab D-SCC-b at mid-span

6.3.4 S-SCC-a and S-SCC-b

Slabs S-SCC-a and S-SCC-b containing 4N12 longitudinal tensile reinforcing bars, with 25 mm clear bottom cover were tested at ages 67 and 69 days respectively. Cracking first occurred approximately at load of P = 5 kN in both S-SCC-a and S-SCC-b. The number of cracks increased as the applied load increased and at approximately 70% of the ultimate load, 12 cracks were located inside the high moment region (H.M.R) for S-SCC-a, and 12 cracks for S-SCC-b respectively. The measured final average crack spacing at this load stage were 102 mm for S-SCC-a and 100 mm for S-SCC-b. The ratio of maximum crack width to average crack width at load stage P = 26 kN was 1.36 for S-SCC-a and 1.21 for S-SCC-b. The measured maximum and average crack widths within the high moment region at the bottom fibre of the slabs versus applied load are illustrated in Figures 6.19 and 6.20. The crack width history and final crack spacing are presented in Tables 6.5 and 6.6. The crack patterns at approximately 70% of the ultimate load for both slabs are illustrated in Figures 6.21 and 6.22.

The measured mid-span deflections of slabs S-SCC-a and S-SCC-b are plotted against load in Figures 6.23 and 6.24, respectively. Maximum deflection at failure loading of S-SCC slab series is 25 and 14 mm higher than N-SCC slab series. It shows that S-SCC slab series are more ductile than N-SCC slab series. The ultimate strength was reached when P = 50 KN for S-SCC-a and P = 48 KN for S-SCC-b when crushing the top compressive fibre occurred and corresponding deflections were 185 mm and 167 mm, respectively.

Table 6.7 Crack history for slab S-SCC-a

	S-SCC-a		Load (kN)								
	Cracks	Distance from edge (roller side) (mm)	0	5	8	11	14	17	20	23	26
			Crack width (mm)								
	c-1	870							0.03	0.05	0.05
	c-2	990							0.03	0.05	0.05
	c-3	1090						0.03	0.03	0.05	0.08
	c-4	1225				0.05	0.08	0.10	0.10	0.15	0.15
	c-5	1290			0.03	0.05	0.08	0.10	0.10	0.13	0.15
H.M.R	c-6	1370			0.03	0.05	0.08	0.10	0.13	0.13	0.15
H.M.R	c-7	1470			0.03	0.05	0.10	0.13	0.13	0.15	0.18
H.M.R	c-8	1570						0.03	0.05	0.05	0.08
H.M.R	c-9	1655		0.03	0.03	0.05	0.08	0.08	0.10	0.13	0.15
H.M.R	c-10	1750				0.03	0.03	0.05	0.08	0.10	0.13
H.M.R	c-11	1860			0.03	0.05	0.05	0.08	0.08	0.10	0.13
H.M.R	c-12	1950				0.03	0.05	0.08	0.10	0.10	0.18
H.M.R	c-13	2040		0.03	0.05	0.05	0.08	0.08	0.10	0.13	0.13
H.M.R	c-14	2150					0.03	0.03	0.08	0.08	0.10
H.M.R	c-15	2235		0.03	0.05	0.08	0.10	0.13	0.13	0.15	0.18
H.M.R	c-16	2340				0.03	0.03	0.05	0.08	0.10	0.10
H.M.R	c-17	2440			0.03	0.03	0.05	0.05	0.08	0.08	0.08
	c-18	2570				0.03	0.03	0.05	0.08	0.10	0.13
	c-19	2630				0.03	0.05	0.08	0.10	0.10	0.13
	c-20	2750				0.03	0.03	0.05	0.08	0.08	0.10
	c-21	2840						0.03	0.05	0.08	0.08
	c-22	3000							0.03	0.05	0.08

Table 6.8 Crack history for slab S-SCC-b

	S-SCC-b		Load (kN)								
	Cracks	Distance from edge (roller side) (mm)	0	5	8	11	14	17	20	23	26
			Crack width (mm)								
	c-1	970								0.03	0.05
	c-2	1040							0.03	0.05	0.08
	c-3	1130				0.03	0.03	0.05	0.08	0.10	0.13
	c-4	1280				0.03	0.05	0.08	0.08	0.10	0.15
	c-5	1300			0.03	0.05	0.08	0.10	0.10	0.13	0.15
H.M.R	c-6	1400			0.03	0.05	0.05	0.10	0.15	0.18	0.20
H.M.R	c-7	1500			0.05	0.08	0.10	0.15	0.18	0.18	0.23
H.M.R	c-8	1550			0.05	0.08	0.10	0.13	0.15	0.18	0.20
H.M.R	c-9	1630			0.03	0.05	0.08	0.10	0.13	0.13	0.15
H.M.R	c-10	1760		0.003	0.03	0.05	0.08	0.08	0.10	0.13	0.15
H.M.R	c-11	1830				0.03	0.08	0.10	0.15	0.18	0.20
H.M.R	c-12	1940			0.03	0.05	0.10	0.15	0.18	0.18	0.20
H.M.R	c-13	2000			0.05	0.08	0.10	0.13	0.15	0.20	0.23
H.M.R	c-14	2080			0.03	0.05	0.08	0.10	0.13	0.15	0.18
H.M.R	c-15	2140			0.03	0.05	0.08	0.13	0.13	0.18	0.20
H.M.R	c-16	2250			0.03	0.05	0.08	0.10	0.13	0.15	0.18
H.M.R	c-17	2390			0.03	0.05	0.08	0.10	0.13	0.15	0.15
	c-18	2510					0.05	0.05	0.08	0.10	0.13
	c-19	2610				0.03	0.05	0.05	0.08	0.10	0.13
	c-20	2730					0.03	0.05	0.05	0.05	0.08
	c-21	2850						0.03	0.03	0.05	0.08
	c-22	2950					0.03	0.05	0.05	0.08	0.08
	c-23	3100									0.05

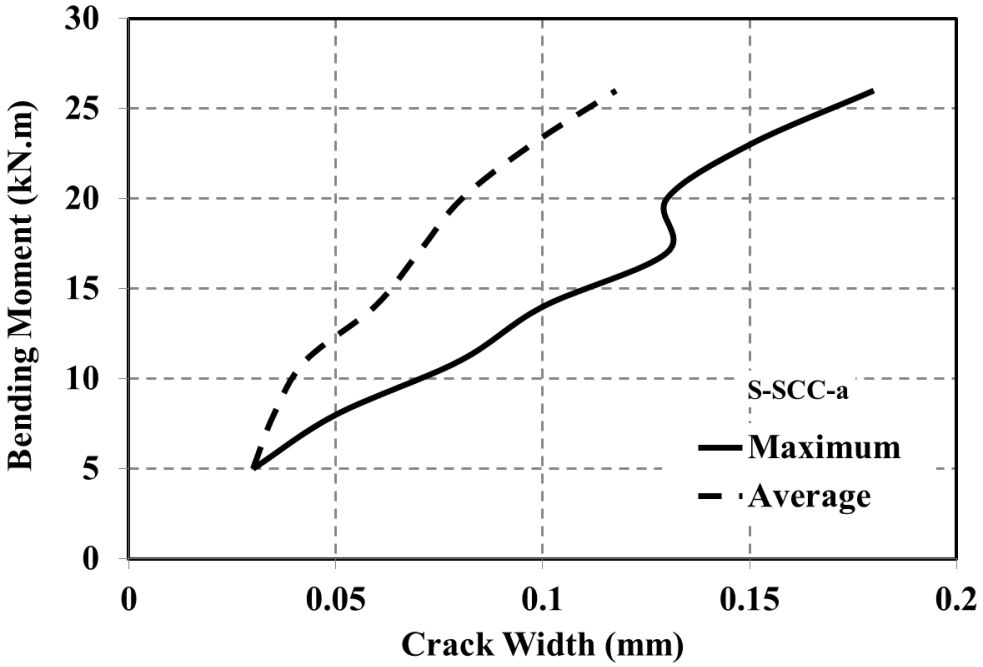

Figure 6.19 Crack width vs. applied bending moment for slab S-SCC-a

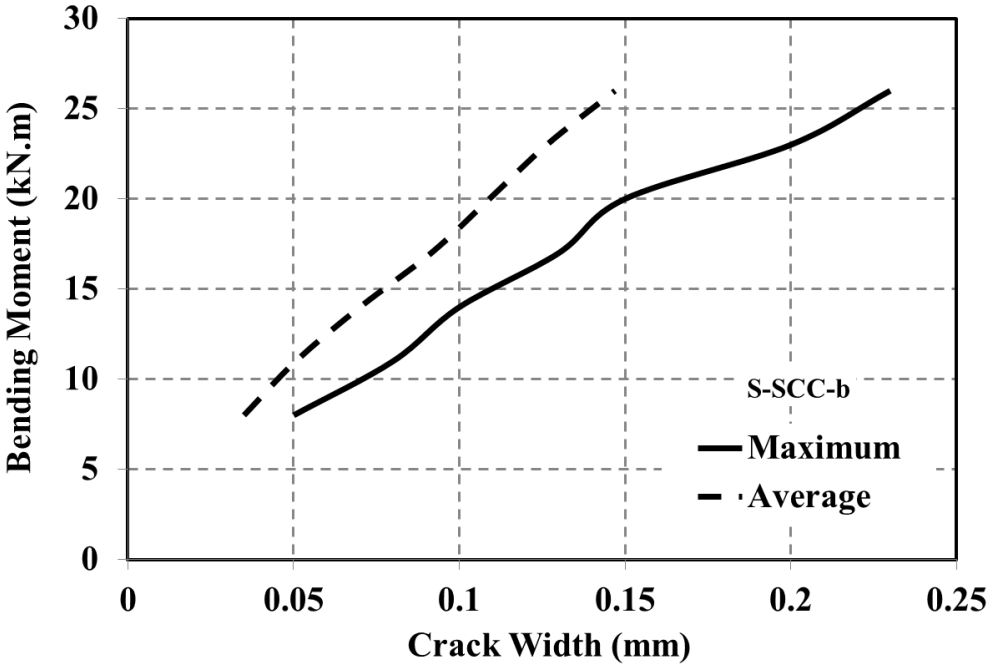

Figure 6.20 Crack width vs. applied bending moment for slab S-SCC-b

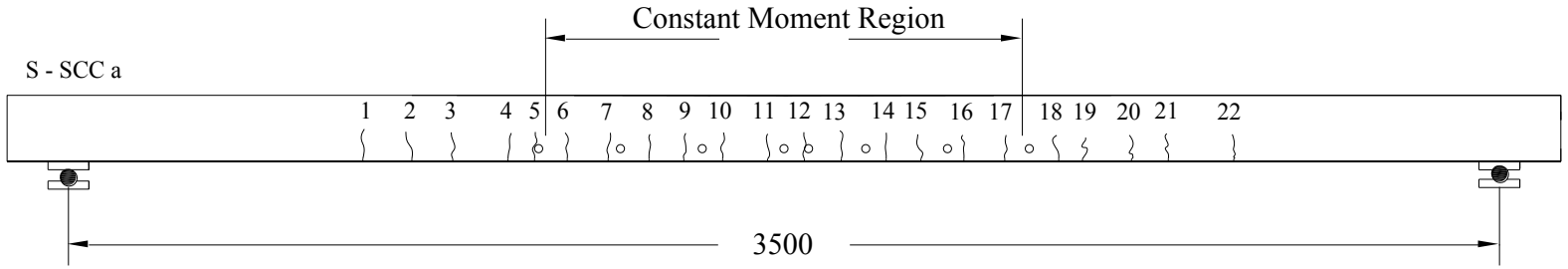

Figure 6.21 Crack pattern for slab S-SCC-a (4N12 c_b=25 mm) at load stage P = 26 kN

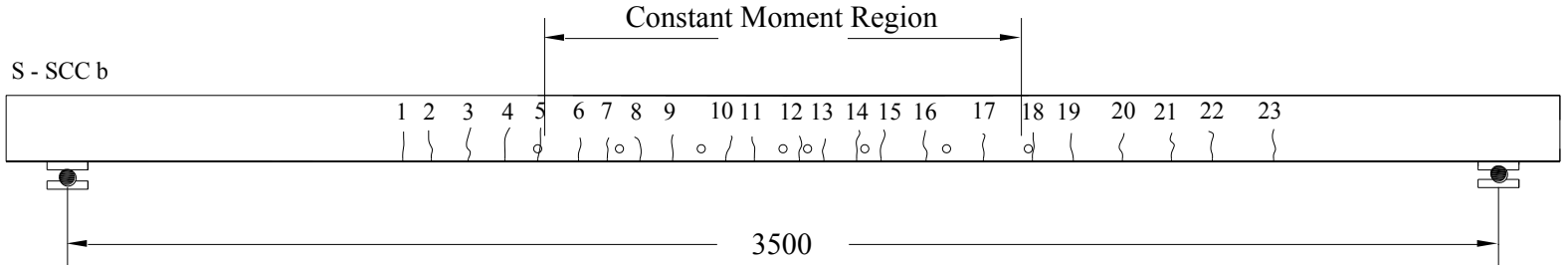

Figure 6.22 Crack pattern for slab S-SCC-b (4N12 c_b=25 mm) at load stage P = 26 kN

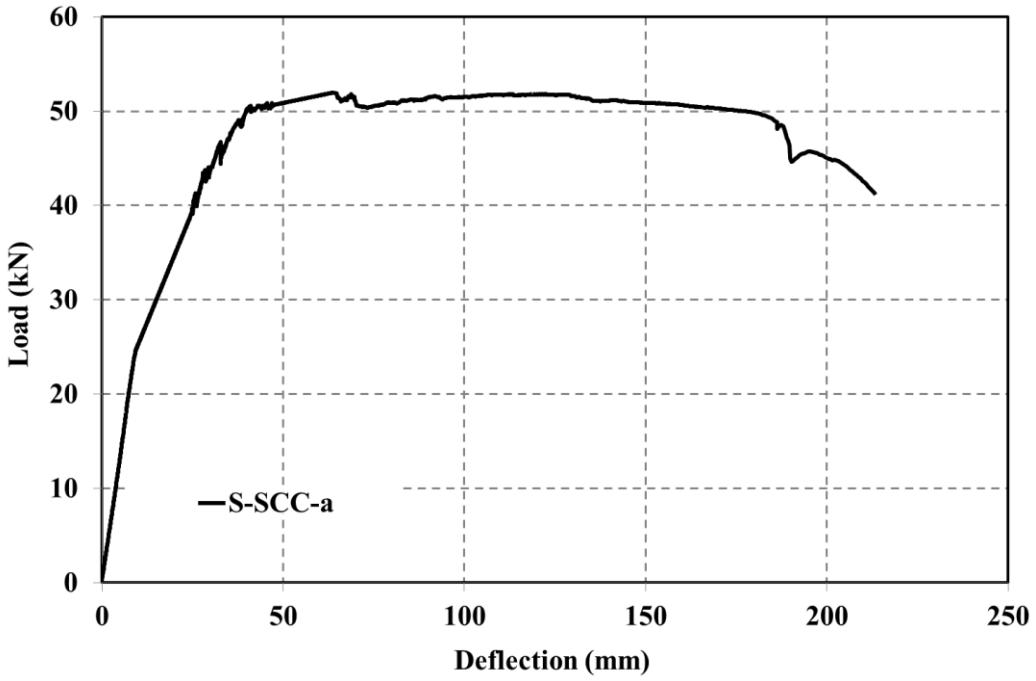

Figure 6.23 Load-deflection curve for slab S-SCC-a at mid-span

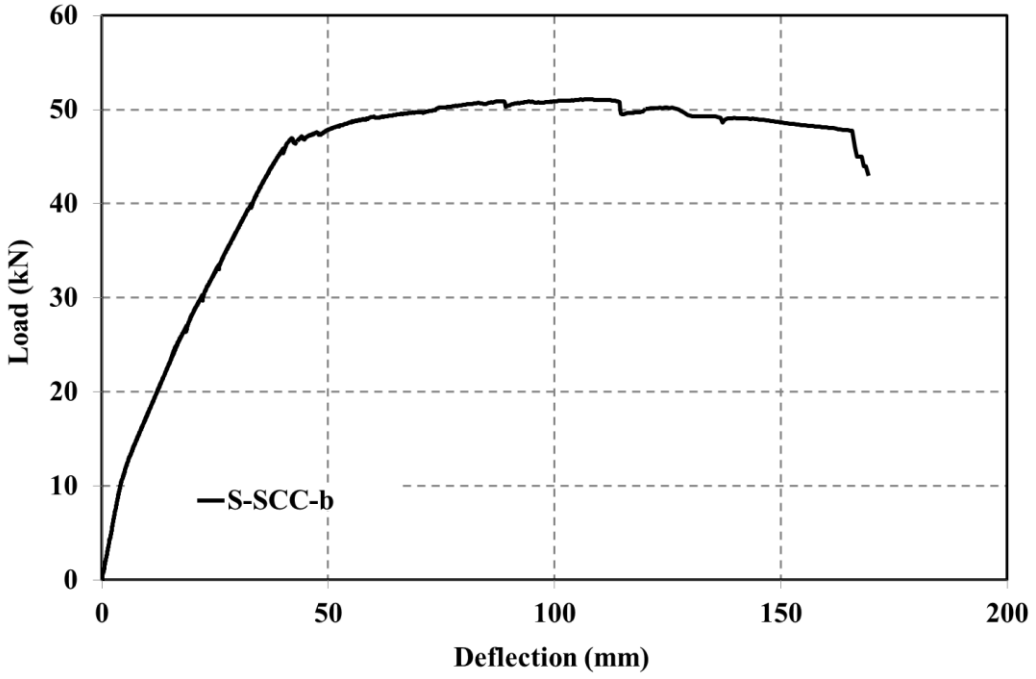

Figure 6.24 Load-deflection curve for slab S-SCC-b at mid-span

6.3.5 DS-SCC-a and DS-SCC-b

Slabs DS-SCC-a and DS-SCC-b containing 4N12 longitudinal tensile reinforcing bars, with 25 mm clear bottom cover were tested at ages 71 and 72 days respectively. Cracking first occurred approximately at load of P = 8 kN in both DS-SCC-a and DS-SCC-b. The number of cracks increased as the applied load increased and at approximately 70% of the ultimate load, 13 cracks were located inside the high moment region (H.M.R) for DS-SCC-a, and 12 cracks for DS-SCC-b respectively. The measured final average crack spacing at this load stage were 95 mm for DS-SCC-a and 98 mm for DS-SCC-b. The ratio of maximum crack width to average crack width at load stage P = 26 kN was 1.24 for DS-SCC-a and 1.15 for DS-SCC-b. The measured maximum and average crack widths within the high moment region at the bottom fibre of the slabs versus applied load are illustrated in Figures 6.25 and 6.26. The crack width history and final crack spacing are presented in Tables 6.9 and 6.10. The crack patterns at approximately 70% of the ultimate load for both slabs are illustrated in Figures 6.27 and 6.28.

The measured mid-span deflections of slabs DS-SCC-a and DS-SCC-b are plotted against load in Figures 6.29 and 6.30, respectively. Maximum deflection at failure loading of DS-SCC slab series is 40 and 19 mm higher than N-SCC slab series. It shows that DS-SCC slab series are more ductile than N-SCC slab series. The ultimate strength was reached when P = 56 KN for DS-SCC-a and P = 54 KN for DS-SCC-b when crushing the top compressive fibre occurred and corresponding deflections were 220 mm and 182 mm, respectively.

Table 6.9 Crack history for slab DS-SCC-a

	DS-SCC-a		Load (kN)								
	Cracks	Distance from edge (roller side) (mm)	0	5	8	11	14	17	20	23	26
			Crack width (mm)								
	c-1	850								0.03	0.03
	c-2	910								0.03	0.05
	c-3	1060								0.05	0.05
	c-4	1140				0.03	0.05	0.08	0.10	0.10	0.13
	c-5	1240				0.03	0.05	0.08	0.10	0.13	0.13
	c-6	1330				0.03	0.05	0.08	0.10	0.10	0.15
H.M.R	c-7	1485			0.03	0.05	0.08	0.10	0.13	0.13	0.15
H.M.R	c-8	1570							0.03	0.05	0.08
H.M.R	c-9	1670				0.03	0.08	0.08	0.10	0.13	0.15
H.M.R	c-10	1735				0.03	0.03	0.05	0.08	0.10	0.10
H.M.R	c-11	1830				0.03	0.05	0.08	0.08	0.10	0.13
H.M.R	c-12	1930				0.03	0.05	0.08	0.10	0.10	0.13
H.M.R	c-13	2010			0.05	0.05	0.08	0.08	0.10	0.10	0.13
H.M.R	c-14	2100				0.03	0.03	0.05	0.08	0.10	0.10
H.M.R	c-15	2200			0.05	0.08	0.10	0.13	0.13	0.15	0.15
H.M.R	c-16	2250			0.03	0.03	0.05	0.05	0.08	0.10	0.13
H.M.R	c-17	2340			0.03	0.03	0.05	0.08	0.08	0.10	0.10
H.M.R	c-18	2460					0.03	0.05	0.08	0.08	0.10
	c-19	2550			0.03	0.05	0.08	0.10	0.10	0.13	0.13
	c-20	2630						0.03	0.05	0.05	0.08
	c-21	2700				0.03	0.03	0.05	0.08	0.08	0.10
	c-22	2820						0.03	0.03	0.05	0.08
	c-23	2920									0.05
	c-24	3050								0.03	0.03

Table 6.10 Crack history for slab DS-SCC-b

	DS-SCC-b		Load (kN)								
	Cracks	Distance from edge (roller side) (mm)	0	5	8	11	14	17	20	23	26
			Crack width (mm)								
	c-1	930								0.03	0.05
	c-2	1070							0.03	0.05	0.05
	c-3	1110						0.03	0.05	0.08	0.08
	c-4	1170					0.03	0.05	0.08	0.08	0.10
	c-5	1320				0.03	0.05	0.05	0.08	0.10	0.13
H.M.R	c-6	1390			0.03	0.05	0.08	0.10	0.13	0.15	0.15
H.M.R	c-7	1500			0.05	0.05	0.08	0.10	0.13	0.15	0.18
H.M.R	c-8	1590			0.05	0.05	0.08	0.10	0.13	0.13	0.15
H.M.R	c-9	1680			0.03	0.05	0.08	0.08	0.10	0.13	0.15
H.M.R	c-10	1800			0.05	0.08	0.10	0.13	0.15	0.18	0.18
H.M.R	c-11	1910				0.03	0.05	0.08	0.10	0.13	0.15
H.M.R	c-12	1980			0.05	0.08	0.10	0.13	0.15	0.18	0.20
H.M.R	c-13	2080			0.03	0.05	0.08	0.08	0.10	0.13	0.15
H.M.R	c-14	2210				0.03	0.08	0.10	0.10	0.13	0.13
H.M.R	c-15	2300			0.05	0.05	0.08	0.10	0.13	0.15	0.18
H.M.R	c-16	2410			0.03	0.03	0.05	0.08	0.10	0.10	0.13
H.M.R	c-17	2480				0.05	0.05	0.08	0.10	0.10	0.13
	c-18	2570					0.03	0.03	0.05	0.08	0.10
	c-19	2640							0.05	0.08	0.08
	c-20	2780							0.03	0.05	0.05
	c-21	2910						0.03	0.05	0.05	0.08
	c-22	2970							0.03	0.05	0.08
	c-23	3100								0.03	0.03

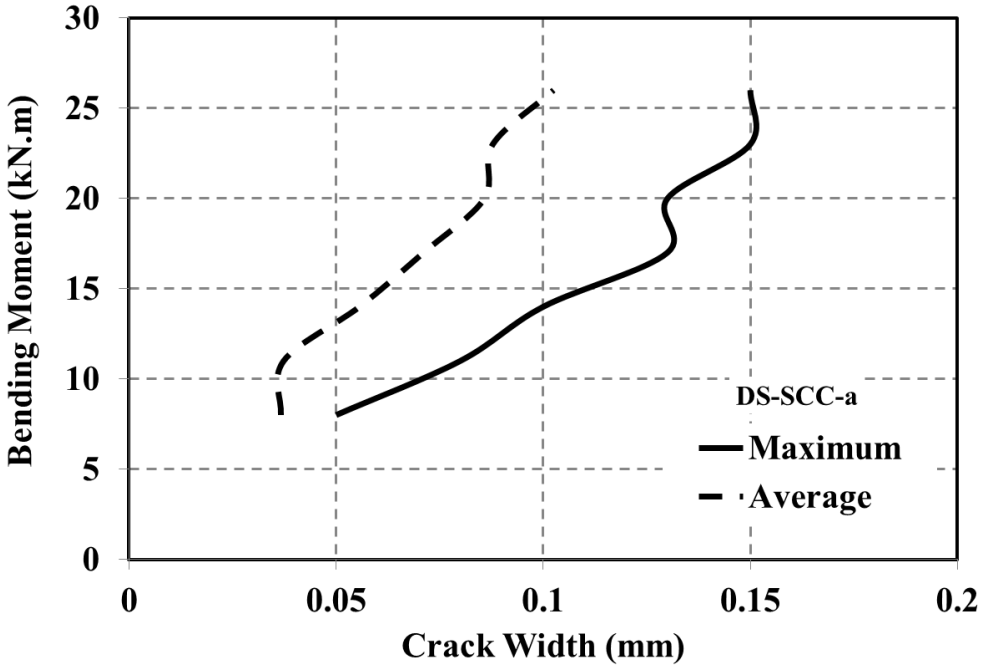

Figure 6.25 Crack width vs. applied bending moment for slab DS-SCC-a

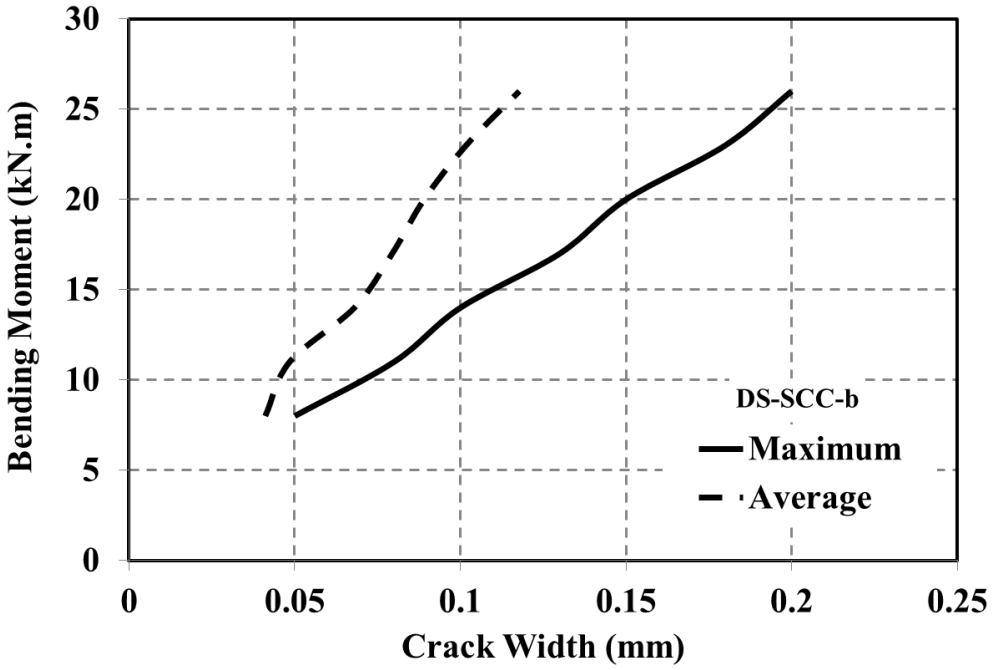

Figure 6.26 Crack width vs. applied bending moment for slab DS-SCC-b

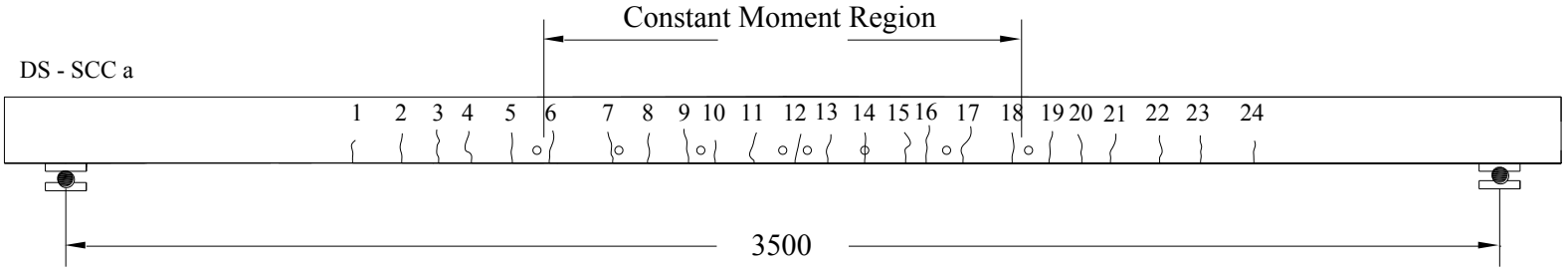

Figure 6.27 Crack pattern for slab DS-SCC-a (4N12 c_b=25 mm) at load stage P = 26 kN

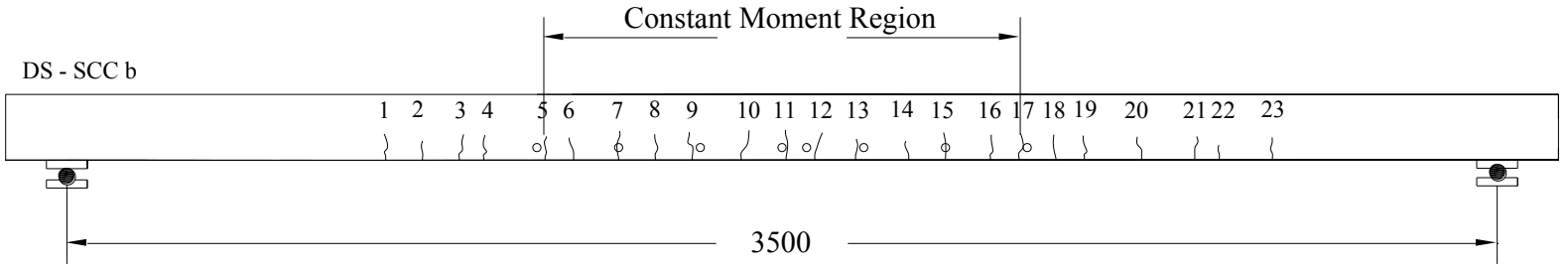

Figure 6.28 Crack pattern for slab DS-SCC-b (4N12 c_b=25 mm) at load stage P = 26 kN

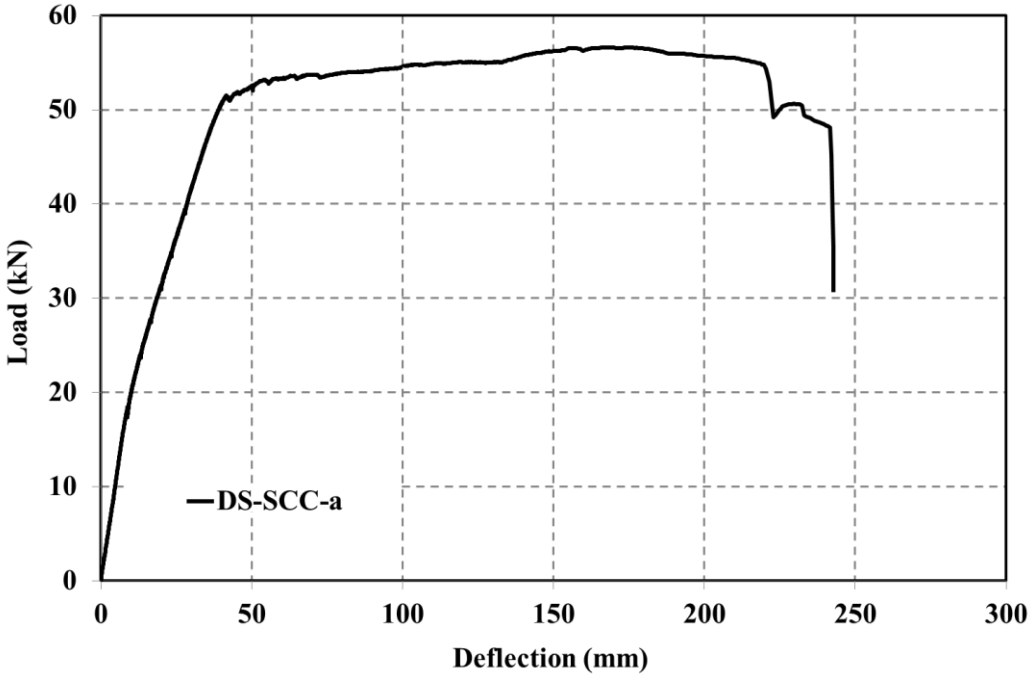

Figure 6.29 Load-deflection curve for slab DS-SCC-a at mid-span

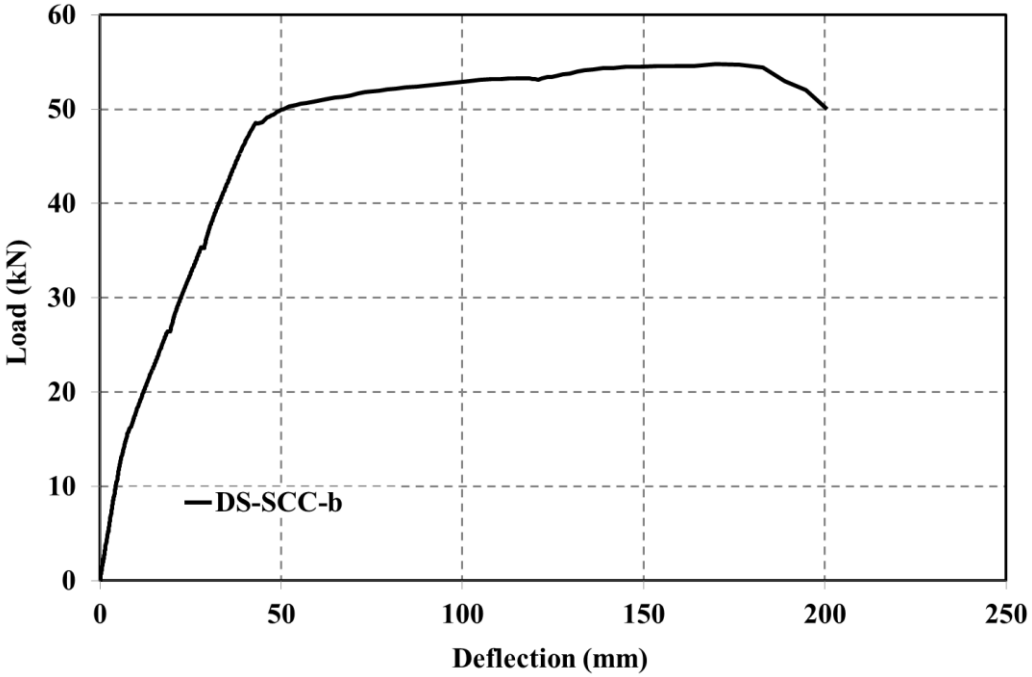

Figure 6.30 Load-deflection curve for slab DS-SCC-b at mid-span

6.3.6 N-CC-a and N-CC-b, Nejadi (2005)

Slabs N-CC-a and N-CC-b containing most longitudinal tensile reinforcing bars 4N12, with 25 mm clear bottom cover were tested at ages 62 and 63 days respectively. Cracking first occurred approximately at load of P = 8 kN in both N-CC-a and N-CC-b. The number of cracks increased as the applied load increased and at approximately 70% of the ultimate load, 14 cracks were located inside the high moment region for N-CC-a, and 12 cracks for N-CC-b respectively. The measured final average crack spacing at this load stage were 90 mm for N-CC-a and 117 mm for N-CC-b. The ratio of maximum crack width to average crack width at load stage P = 26 kN was 1.38 for N-CC-a and 1.28 for N-CC-b. The measured maximum and average crack widths within the high moment region at the bottom fibre of the slabs versus applied load are illustrated in Figures 6.31 and 6.32. The crack width history and final crack spacing are presented in Tables 6.11 and 6.12. The crack patterns at approximately 70% of the ultimate load for both slabs are illustrated in Figures 6.33 and 6.34.

The failure loads were P = 50 kN and P = 47 kN and corresponding deflections were 136 mm and 156 mm for N-CC-a and N-CC-b, respectively. The mid-span load-deflection curves for slab series 3 are presented in Figures 6.35 and 6.36.

Table 6.11 Crack history for slab N-CC-a (Nejadi, 2005)

	N-CC-a		Load (kN)								
	Cracks	Distance from edge (roller side) (mm)	0	5	8	11	14	17	20	23	26
			Crack width (mm)								
	c-1	612							0.03	0.03	0.05
	c-2	744								0.05	0.05
	c-3	927								0.05	0.05
	c-4	1063			0.03	0.05	0.08	0.10	0.13	0.15	0.18
	c-5	1153				0.05	0.08	0.10	0.13	0.15	0.15
	c-6	1285				0.05	0.08	0.10	0.13	0.15	0.15
H.M.R	c-7	1411			0.05	0.05	0.10	0.13	0.15	0.15	0.18
H.M.R	c-8	1462							0.05	0.05	0.08
H.M.R	c-9	1563			0.05	0.05	0.08	0.08	0.13	0.13	0.15
H.M.R	c-10	1639					0.03	0.05	0.08	0.10	0.10
H.M.R	c-11	1742			0.03	0.05	0.05	0.08	0.10	0.13	0.13
H.M.R	c-12	1822					0.05	0.08	0.10	0.13	0.15
H.M.R	c-13	1908			0.05	0.05	0.08	0.08	0.10	0.13	0.13
H.M.R	c-14	1988						0.03	0.08	0.10	0.10
H.M.R	c-15	2081			0.05	0.08	0.10	0.13	0.13	0.15	0.18
H.M.R	c-16	2210					0.03	0.05	0.08	0.13	0.13
H.M.R	c-17	2258				0.03	0.05	0.05	0.08	0.08	0.08
H.M.R	c-18	2314						0.03	0.05	0.08	0.10
H.M.R	c-19	2413			0.03	0.05	0.08	0.10	0.13	0.13	0.15
	c-20	2507					0.03	0.05	0.05	0.05	0.08
	c-21	2631					0.03	0.05	0.05	0.10	0.10
	c-22	2757						0.03	0.05	0.08	0.08
	c-23	2897								0.03	0.05

Table 6.12 Crack history for slab N-CC-b (Nejadi, 2005)

	N-CC-b		Load (kN)								
	Cracks	Distance from edge (roller side) (mm)	0	5	8	11	14	17	20	23	26
			Crack width (mm)								
	c-1	608							0.03	0.05	0.08
	c-2	697						0.03	0.05	0.08	0.10
	c-3	825					0.03	0.05	0.08	0.08	0.13
	c-4	936				0.03	0.05	0.08	0.10	0.10	0.13
	c-5	1051			0.05	0.05	0.05	0.10	0.13	0.13	0.18
	c-6	1175			0.03	0.05	0.08	0.13	0.15	0.15	0.20
H.M.R	c-7	1316			0.05	0.08	0.08	0.13	0.15	0.18	0.20
H.M.R	c-8	1438			0.03	0.05	0.08	0.10	0.13	0.15	0.18
H.M.R	c-9	1536				0.03	0.05	0.08	0.08	0.10	0.13
H.M.R	c-10	1616			0.05	0.08	0.08	0.10	0.10	0.13	0.15
H.M.R	c-11	1701					0.05	0.08	0.13	0.15	0.18
H.M.R	c-12	1827			0.05	0.08	0.10	0.13	0.18	0.2	0.23
H.M.R	c-13	1979			0.05	0.08	0.08	0.10	0.13	0.15	0.18
H.M.R	c-14	2124				0.05	0.08	0.10	0.13	0.15	0.15
H.M.R	c-15	2228				0.05	0.08	0.13	0.15	0.18	0.20
H.M.R	c-16	2359				0.03	0.05	0.08	0.08	0.10	0.13
H.M.R	c-17	2481				0.05	0.08	0.08	0.10	0.13	0.15
	c-18	2557								0.03	0.05
	c-19	2619					0.03	0.05	0.08	0.08	0.10
	c-20	2711									0.03
	c-21	2797								0.05	0.05
	c-22	2973					0.03	0.05	0.05	0.08	0.10
	c-23	3052									0.03
	c-24	3053									0.05

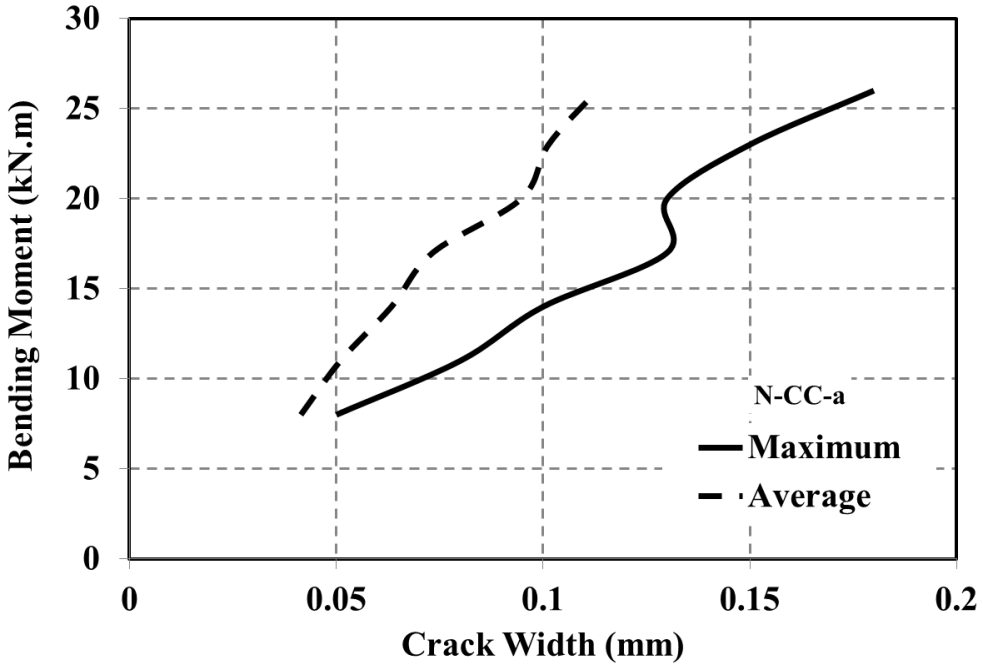

Figure 6.31 Crack width vs. applied bending moment for slab N-CC-a (Nejadi, 2005)

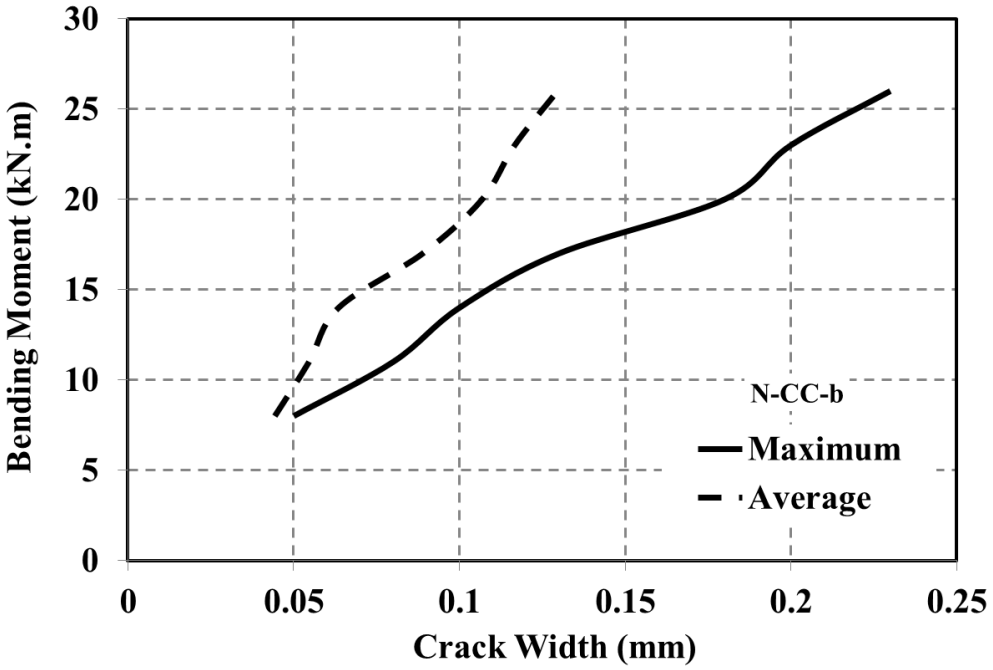

Figure 6.32 Crack width vs. applied bending moment for slab N-CC-b (Nejadi, 2005)

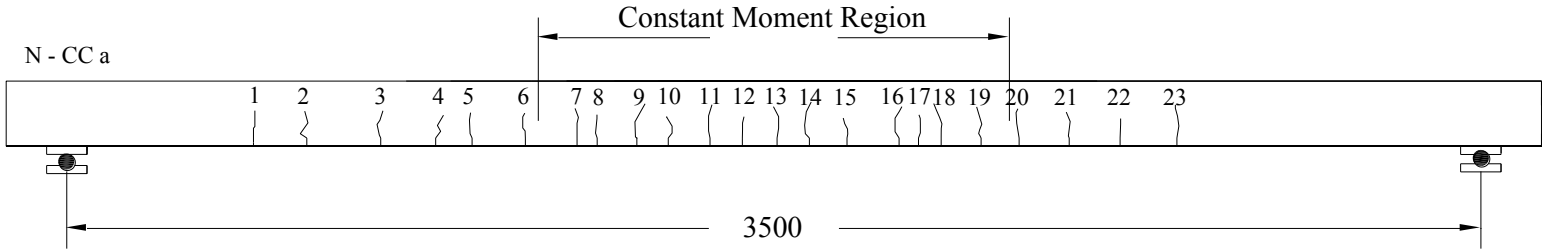

Figure 6.33 Crack pattern for slab N-CC-a (4N12 c_b=25 mm) at load stage P = 26 kN (Nejadi, 2005)

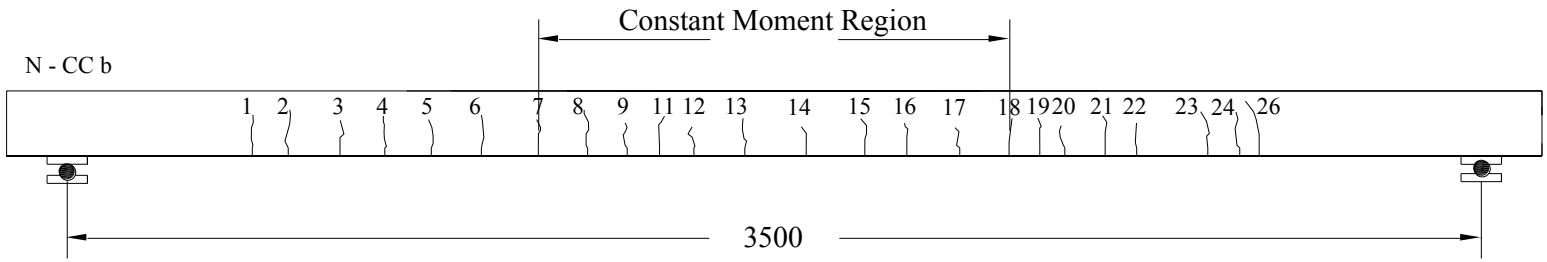

Figure 6.34 Crack pattern for slab N-CC-b (4N12 c_b=25 mm) at load stage P = 26 kN (Nejadi, 2005)

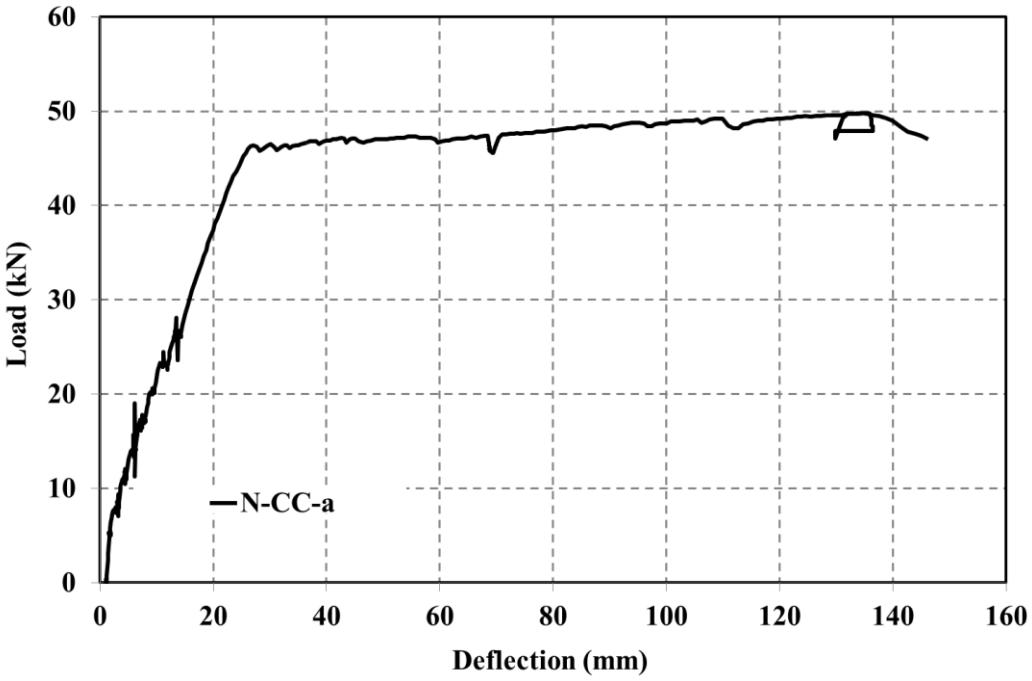

Figure 6.35 Load-deflection curve for slab N-CC-a at mid-span (Nejadi, 2005)

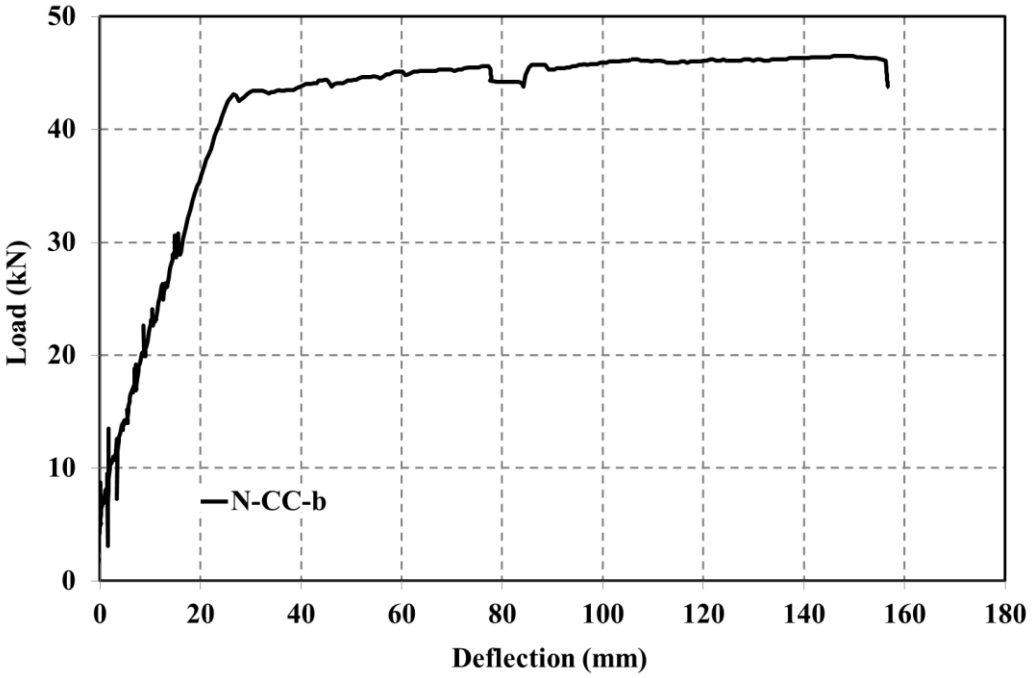

Figure 6.36 Load-deflection curve for slab N-CC-b at mid-span (Nejadi, 2005)

6.4 INSTANTANEOUS BOND SHEAR STRESS

The force in the bar is transmitted to the surrounding concrete by bond shear stress τ_b. Due to this transfer, the force in a reinforcing bar changes along its length. The transfer of forces across the interface by bond between concrete and steel is of fundamental importance to many aspects of reinforced concrete behaviour. Under service conditions $\sigma_s < f_{sy}$ and according to Marti et al. (1998), $\tau_b = 2\,f_{ct}$. To investigate the influence of the assumed bond shear stress on the predicted crack width, five different values for bond shear stress ($\tau_b = f_{ct}$, $\tau_b = 1.5\,f_{ct}$, $\tau_b = 2\,f_{ct}$, $\tau_b = 3\,f_{ct}$, and $\tau_b = \lambda_1\,\lambda_2\,\lambda_3\,f_{ct}$-Eq.[6.5]) have been considered. For each assumed bond shear stress, the crack widths were calculated and compared with the measured crack widths for each load increment. Instantaneous crack width calculations for concrete reinforced with bars are different from concrete reinforced with bars and fibres, following sections 6.4.1 and 6.4.2 described crack width calculations in both conditions.

6.4.1 Steel Bar Reinforcement Concrete

Nejadi (2005) proposed a model for predicting the maximum final crack width in reinforced concrete flexural members based on the Tension Chord Model of Marti et al. (1998). The model provides good agreement with the measured final spacing and width of cracks in a range of reinforced concrete beams and slabs tested in the laboratory under sustained service loads for periods in excess of 400 days (Gilbert and Nejadi, 2004). The notation associated with the model is shown in Figure 6.37.

As shown in Figure 6.36(a), consider a segment of a singly reinforced beam of rectangular section subjected to an in-service bending moment, M_s, greater than the cracking moment, M_{cr}. The spacing between the primary cracks is s, as shown in Figure 6.37(a). A typical cross-section between the cracks is shown in Figure 6.37(b) and a cross-section at a primary crack is shown in Figure 6.37(c). The cracked beam is idealised as a compression chord of depth kd and width b and a cracked tension chord consisting of the tensile reinforcement of area A_{st} surrounded by an area of tensile concrete (A_{ct}) as shown in Figure 6.37(d). The centroids of A_{st} and A_{ct} are assumed to coincide at a depth d below the top fibre of the section.

For the sections containing a primary crack (Figure 6.37(c)), A_{ct} = 0 and the depth of the compressive zone, kd, and the second moment of area about the centroidal axis (I_{cr}) may be determined from a cracked section analysis using modular ratio theory. Away from the crack, the area of the concrete in the tension chord of Figure 6.37(d) is assumed to carry a uniform tensile stress (σ_{ct}) that develops due to the bond stress (τ_b) that exists between the tensile steel and the surrounding concrete.

For the tension chord, the area of concrete between the cracks, A_{ct}, may be taken as:

$$A_{ct} = 0.5(D - kd)b^* \tag{6.1}$$

where b^* is the width of the section at the level of the centroid of the tensile steel (i.e. at the depth d) but not greater than the number of bars in the tension zone multiplied by $12d_b$. At each crack, the concrete carries no tension and the tensile steel stress is $\sigma_{st1} = T / A_{st}$, where:

$$T = \frac{n M_s (d - kd)}{I_{cr}} A_{st} \tag{6.2}$$

$$k = \sqrt{(n\rho)^2 + 2n\rho} - n\,\rho \tag{6.3}$$

where ρ is the tensile reinforcement ratio, A_{st} / bd. It should be noted that k (and hence the depth to the neutral axis kd) depends only on the modular ratio n and the reinforcement ratio ρ and is independent of the applied moment M. The depth to the neutral axis remains constant after cracking as the moment increases, until either the concrete compressive stress distribution becomes curvilinear or the reinforcing steel yields.

The second moment of area of the cracked section is:

$$I_{cr} = \frac{1}{2} b\, d^3\, k^2\, (1 - k/3) \tag{6.4}$$

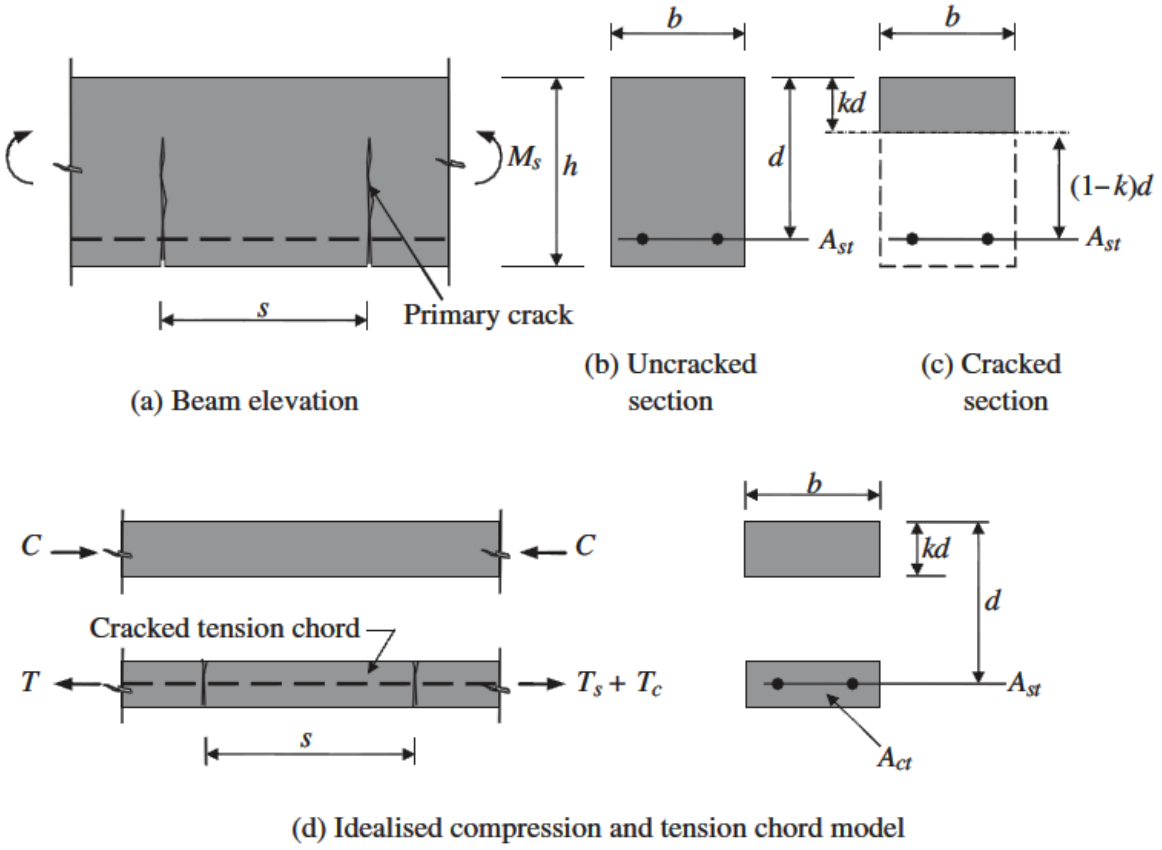

Figure 6.37 Cracked reinforced concrete beam and idealised tension chord model (Nejadi, 2005)

As the distance z from the crack in the direction of the tension chord increases, the stress in the steel reduces due to the bond shear stress τ_b between the steel and the surrounding tensile concrete. For reinforced concrete under service loads, where σ_{st1} is less than the yield stress f_y, Marti et al. (1998) assumed a rigid-plastic bond shear stress-slip relationship, with τ_b =2.0 f_{ct} at all values of slip, where f_{ct} is the direct tensile strength of the concrete. To account for the reduction in bond stress with time due to tensile creep and shrinkage, Gilbert (2008) took the bond stress to be τ_b = 2.0 f_{ct} for short-term calculations and τ_b = 1.0 f_{ct} when the final long-term crack width was to be determined. Experimental observations (Gilbert and Nejadi, 2004; Wu and Gilbert, 2009) indicate that τ_b reduces as the stress in the reinforcement increases and, consequently, the tensile stresses in the concrete between the cracks reduces (i.e. tension stiffening reduces with increasing steel stress). In reality, the magnitude of τ_b is affected by many factors, including steel stress, concrete cover, bar spacing, transverse reinforcement (stirrups), lateral pressure,

compaction of the concrete, size of bar deformations, tensile creep and shrinkage. It is recommended by Wu and Gilbert (2009) that in situations where the concrete cover and the clear spacing between the bars are greater than the bar diameter, the bond stress τ_b may be taken as:

$$\tau_b = \lambda_1 \lambda_2 \lambda_3 f_{ct} \tag{6.5}$$

where λ_1 accounts for the load duration with λ_1 =1.0 for short-term calculations and λ_1 = 0.7 for long-term calculations, λ_2 is a factor that accounts for the reduction in bond stress as the steel stress σ_{st1} (in MPa) increases and is given by (Wu and Gilbert, 2009):

$$\lambda_2 = 1.66 - 0.003\,\sigma_{st1} \geq 0.0 \tag{6.6}$$

and λ_3 is a factor that accounts for the very significant increase in bond stress that has been observed in laboratory tests for small diameter bars (Gilbert and Nejadi, 2004) and may be taken as:

$$\lambda_3 = 7.0 - 0.3\,d_b \geq 2.0 \quad (d_b \text{ in mm}) \tag{6.7}$$

An elevation of the tension chord is shown in Figure 6.38(a) and the stress variations in the concrete and steel in the tension chord are illustrated in Figure 6.38(b) and Figure 6.38(c), respectively. Following the approach of Marti et al. (1988), the concrete and steel tensile stresses in Figures 6.38(b) and 6.38(c), where $0 < z \leq s/2$, may be expressed as:

$$\sigma_{stz} = \frac{T}{A_{st}} - \frac{4\,\tau_b\,z}{d_b} \tag{6.8}$$

$$\sigma_{cz} = \frac{4\,\tau_b\,\rho_{tc}\,z}{d_b} \tag{6.9}$$

where ρ_{tc} is the reinforcement ratio of the tension chord (= A_{st}/A_{ct}) and d_b is the reinforcing bar diameter. Mid-way between the cracks, at $z = s/2$, the stresses are:

$$\sigma_{st2} = \frac{T}{A_{st}} - \frac{2\,\tau_b\,s}{d_b} \tag{6.10}$$

$$\sigma_{c2} = \frac{2\,\tau_b\,\rho_{tc}\,s}{d_b} \tag{6.11}$$

The maximum crack spacing immediately after loading, $s = s_{max}$, occurs when $\sigma_{c2} = f_{ct}$, and from Eq. 6.11:

$$s_{\max} = \frac{f_{ct}\,d_b}{2\,\tau_b\,\rho_{tc}} \tag{6.12}$$

If the spacing between two adjacent cracks just exceeds s_{max}, the concrete stress mid-way between the cracks will exceed f_{ct} and another crack will form between the two existing cracks. It follows that the minimum crack spacing is half the maximum value, that is, $s_{min} = s_{max}/2$.

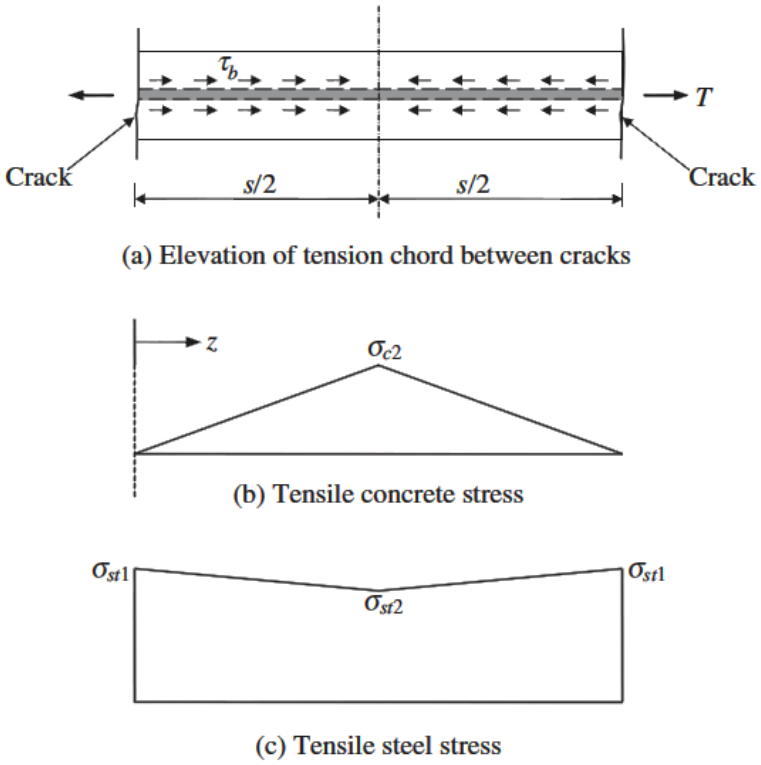

Figure 6.38 Tension chord – actions and stresses (Marti et al., 1998)

The instantaneous crack width $(w_i)_{tc}$ in the fictitious tension chord is the difference between the elongation of the tensile steel over the length s and the elongation of the concrete between the cracks and is given by:

$$\left(w_i\right)_{tc} = \frac{s}{E_s}\left[\frac{T}{A_{st}} - \frac{\tau_b\, s}{d_b}\left(1 + n\rho_{tc}\right)\right] \tag{6.13}$$

Depending on the dimensions of the cross-section and the concrete cover, the instantaneous crack width at the bottom concrete surface of the beam or slab, $(w_i)_{soffit}$, may be different from that given by Eq. (6.13) for the tension chord and may be obtained from:

$$\left(w_i\right)_{soffit} = k_{cover}\left(w_i\right)_{av} = \frac{k_{cover}s}{E_s}\left[\frac{T}{A_{st}} - \frac{\tau_b\, s}{d_b}\left(1 + n\rho_{tc}\right)\right] \tag{6.14}$$

where k_{cover} is a term to account for the dependence of crack width on the clear concrete cover c and may be taken as:

$$k_{cover} = \left(\frac{D - kd}{d - kd}\right)\left(\frac{5\,c}{\left(D - kd\right) - 2d_b}\right)^{0.3} \tag{6.15}$$

6.4.2 Reinforcement Concrete with Fibres

Leutbecher and Fehling (2008) have developed a cracking behaviour model based on the assumptions of constant bond stress and a parabolic relationship of concrete and steel strains between the cracks. To calculate crack widths, the assumption of parabolic strain development is used to determine mean steel and concrete strains. The maximum crack width is calculated as twice the transfer length multiplied by the difference between the concrete and steel mean strains:

$$w_{\max} = 2\,l_{es}\left(\varepsilon_{sm} - \varepsilon_{cm}\right) \tag{6.16}$$

where w_{max} is the maximum crack width, l_{es} is the transfer length, ε_{sm} is the mean steel strain, ε_{cm} is the mean concrete strain.

The Eq. (6.16) can be re-written for the initial crack as follows (see Figure 6.39):

$$w_{\max} = \frac{\left(\sigma^{i}_{cf,cr} - \sigma_{cf}\right) d_b}{5 E_s \ \tau_{sm} \ \rho_s^2} \left[\left(1 + \alpha_E \ \rho_S\right) \sigma^{i}_{cf,cr} - \sigma_{cf} \right] \tag{6.17}$$

where σ_{cf} is the stress in the fibre reinforced concrete, $\sigma^{i}_{cf,cr}$ is the imaginary cracking stress of the fibre reinforced concrete (see Eq.(6.29)), τ_{sm} is the average bond stress over load transmission length, d_b is the reinforcing bar diameter, E_s is the modulus of elasticity of reinforcing bar, ρ_s is the ratio of steel reinforcement, α_b is the shape coefficient of strain courses (α_b = 0.6 for short term loading, α_b = 0.4 for long term or repeated loading), α_E is the ratio of the modulus of elasticity of steel to concrete, $\alpha_E = E_s/E_c$. Figure 6.40 illustrates the various stresses used in this model.

For practical use, the bond stress often is assumed to be constant (rigid-plastic bond law), e.g. $\tau_{sm} = 1.8\, f_{ct}$ for N-CC. For HPC, the reference values according to Eq. (6.18) may be used depending on the crack width w and the relative rib area of the rebars f_R. If concrete splitting is avoided before reaching w, the proposed values do not depend significantly on the fibre content.

$$\tau_{sm} = \begin{Bmatrix} 1.2\, f_{ct} & f_R = 0.024, w = 0.05\ mm \\ 1.7\, f_{ct} & f_R = 0.024, w = 0.10\ mm \\ 2.0\, f_{ct} & f_R = 0.072, w = 0.05\ mm \\ 3.3\, f_{ct} & f_R = 0.072, w = 0.10\ mm \end{Bmatrix} \tag{6.18}$$

A similar equation can be used for stabilized cracking pattern (refer to Figure 6.41):

$$w_{\max} = \frac{\left(\sigma^{i}_{cf,cr} - \sigma_{cf}\right) d_b}{5 E_s \ \tau_{sm} \ \rho_s^2} \left[\sigma_s - 0.6 \frac{\sigma^{i}_{cf,cr}}{\rho_s} \left(1 + \alpha_E \ \rho_s\right) \sigma^{i}_{cf,cr} - 0.6 \frac{\sigma_{cf}}{\rho_s} \right] \tag{6.19}$$

where σ_s is the stress in the reinforcing bar at a crack. This can be calculated from the following equation:

$$\sigma_s = \frac{F}{A_s} - \frac{\sigma_{cf}}{\rho_s} \tag{6.20}$$

where F is the applied load, A_s is the cross-sectional area of the steel bars.

The maximum crack spacing stabilized cracking pattern can also be determined, using the following equation:

$$s_{r,\max} = \left(\sigma_{cf,cr}^{i} - \sigma_{cf0}\right) \frac{d_b}{2\,\tau_{sm}\,\rho_s} \tag{6.21}$$

where $s_{r,max}$ is the maximum crack spacing.

$$\sigma_{cf} = f_{ct}\left(1 - \frac{w\,f_{ct}}{2\,G_f}\right) + \sigma_{cf0}\left(2\sqrt{\frac{w}{w_0}} - \frac{w}{w_0}\right) \tag{6.22}$$

where w is the crack width, f_{ct} is the concrete matrix tensile strength, G_f is the fracture energy of the concrete matrix, σ_{cf0} is the maximum post-cracking stress, w_0 is the crack width corresponding to maximum post-cracking stress, mm.

During the fibre pullout phase, the fibre stress can be calculated from the following equation:

$$\sigma_{cf} = \sigma_{cf0}\left(1 - \frac{w}{l_f}\right) \tag{6.23}$$

where σ_{cf0} is the maximum post-cracking stress (whether strain hardening or strain softening – see Figure 6.40). The σ_{cf0} for fibres with a random orientation, it can be calculated as:

$$\sigma_{cf0} = \eta\; g\; \rho_f\; \frac{\tau_{fm}\; l_f}{d_f} \tag{6.24}$$

where η is the coefficient of fibre orientation; g is the coefficient of fibre efficiency (i.e. – damage factor), ρ_f is the volume fraction of fibres, l_f is the fibre length, d_f is the fibre diameter, τ_{fm} is the mean fibre-matrix bond stress. The mean fibre-matrix bond stress can be approximated as:

$$\tau_{fm} = 1.3\; f_{ctm} \tag{6.25}$$

where f_{ctm} is the mean tensile strength of the plain concrete matrix.

The fibre orientation and efficiency coefficients, η and g, respectively are more difficult to define and must be determined experimentally. σ_{cf0} can easily be determined from direct tension tests, and consequently the coefficient of fibre efficiency can be determined from these as follows:

$$g = \frac{\sigma_{cf\,0}\, d_f}{\eta\, \rho_f\, \tau_{fm}\, l_f} \tag{6.26}$$

However, the fibre orientation coefficient, η, must be derived from a large number of tests for a variety of fibre types. More study is required to create an adequate formulation.

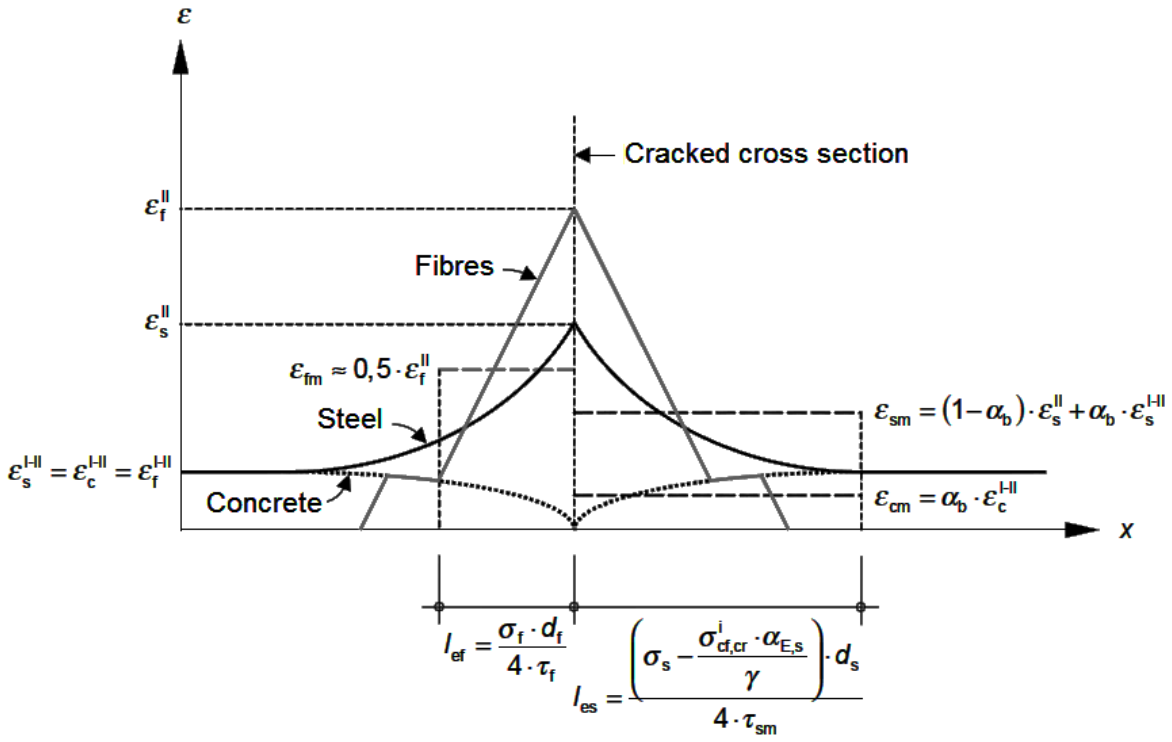

Figure 6.39 Strain development along reinforcing bar and fibres for initial crack (Leutbecher and Fehling, 2008)

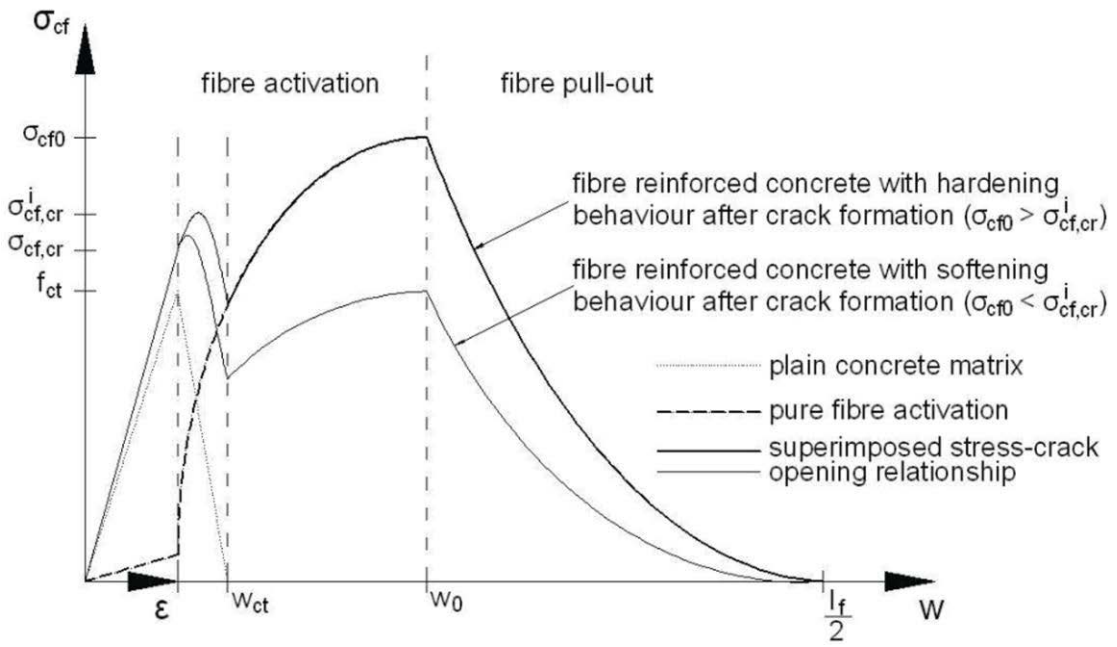

Figure 6.40 Stress-COD model (Leutbecher and Fehling, 2008)

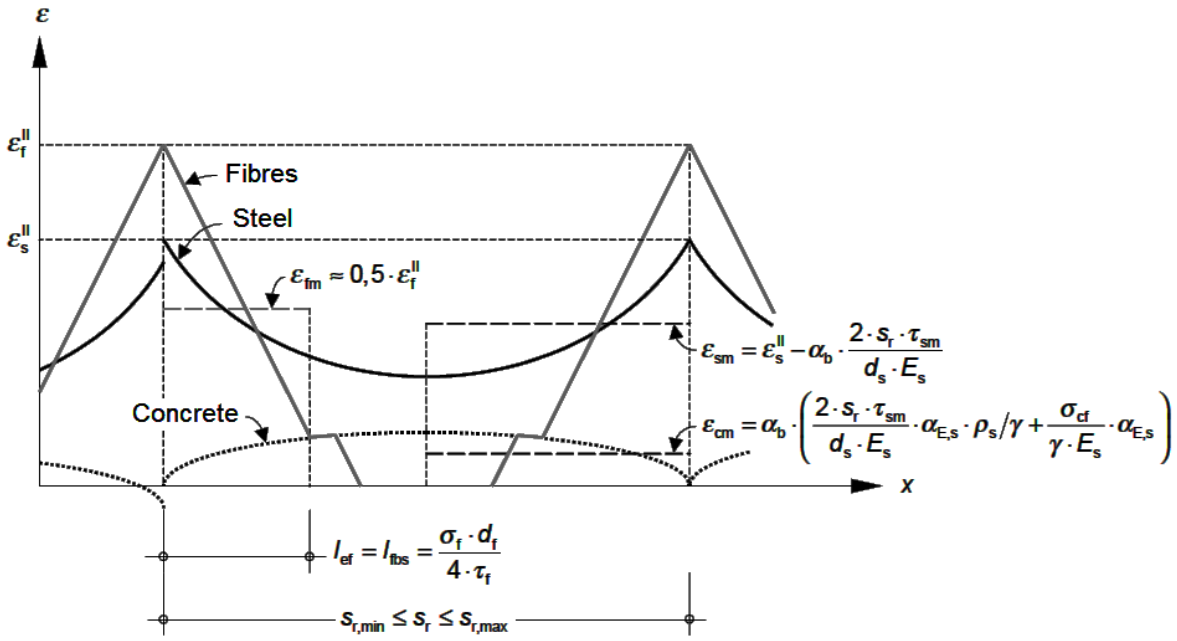

Figure 6.41 Strain development along reinforcing bar and fibres for stabilized cracking (Leutbecher and Fehling, 2008)

As stated earlier, w_0 is the crack width corresponding to the maximum post-cracking stress, σ_{cf0} and can be calculated from the following equation:

$$w_0 = \frac{\tau_{fm}\, l_f^2}{E_f\, d_f} \tag{6.27}$$

where E_f is the modulus of elasticity of the fibres.

The imaginary cracking stress, $\sigma^i_{cf,cr}$ is the maximum stress of the ascending fibre phase. It can be calculated by substituting the crack width corresponding to the maximum stress of the ascending fibre activation phase (Eq. (6.28)) into the equation for the fibre reinforced concrete stress (Eq. (6.22)):

$$w^* = \frac{w_0}{\left(1 + \frac{w_0\, f_{ct}^2\, g}{2\,\sigma_{cf\,0}\, G_f}\right)} \tag{6.28}$$

The Eq.(6.28) was determined by taking the derivation with respect σ_{cf} and setting it to zero. The imaginary cracking stress is then calculated using the following equation:

$$\sigma^i_{cf,cr} = f_{ct}\left(1 - \frac{w^* f_{ct}}{2\, G_f}\right) + \sigma_{cf\,0}\left(2\sqrt{\frac{w^*}{w_0}} - \frac{w^*}{w_0}\right) \tag{6.29}$$

By combining the above equations with the expression for the maximum crack width, w_{max}, the maximum crack width can be determined. However, since many of these equations are functions of the crack width, an iterative solution procedure must be adopted.

6.4.3 Calculation of Crack Width with Different Bond Shear Stress

For the N-SCC mix, Eq.(6.13) is used and for D-SCC, S-SCC, and DS-SCC mixes, Eq.(6.17) is used for crack width calculations. The results are presented in Tables 6.13 to 6.16. Measured and calculated maximum crack widths versus steel stress are illustrated in Figures 6.42 to 6.45. Also, the results of Nejadi (2005) are presented for comparison of CC with SCC mixtures in Figure 6.46 and Table 6.17.

Table 6.13 Measured and calculated maximum crack width for slab N-SCC series

(N-SCC)		Maximum Crack Width (mm)						
		Measured		Calculated (Eq. 6.13)				
M (kNm)	σ_{st} (MPa)	N-SCC-a	N-SCC-b	$\tau_b = f_{ct}$	$\tau_b = 1.5\, f_{ct}$	$\tau_b = 2\, f_{ct}$	$\tau_b = 3\, f_{ct}$	$\tau_b = \lambda_1\, \lambda_2\, \lambda_3\, f_{ct}$
7.00	60	0.05	0.08	0.034	0.022	0.017	0.011	0.008
8.80	84	0.08	0.13	0.090	0.060	0.045	0.030	0.022
10.5	93	0.10	0.15	0.143	0.095	0.072	0.048	0.039
12.3	142	0.13	0.18	0.199	0.133	0.099	0.066	0.060
14.0	201	0.13	0.20	0.252	0.168	0.126	0.084	0.085
15.8	262	0.18	0.23	0.309	0.206	0.154	0.103	0.117
17.5	337	0.20	0.25	0.362	0.241	0.181	0.121	0.157

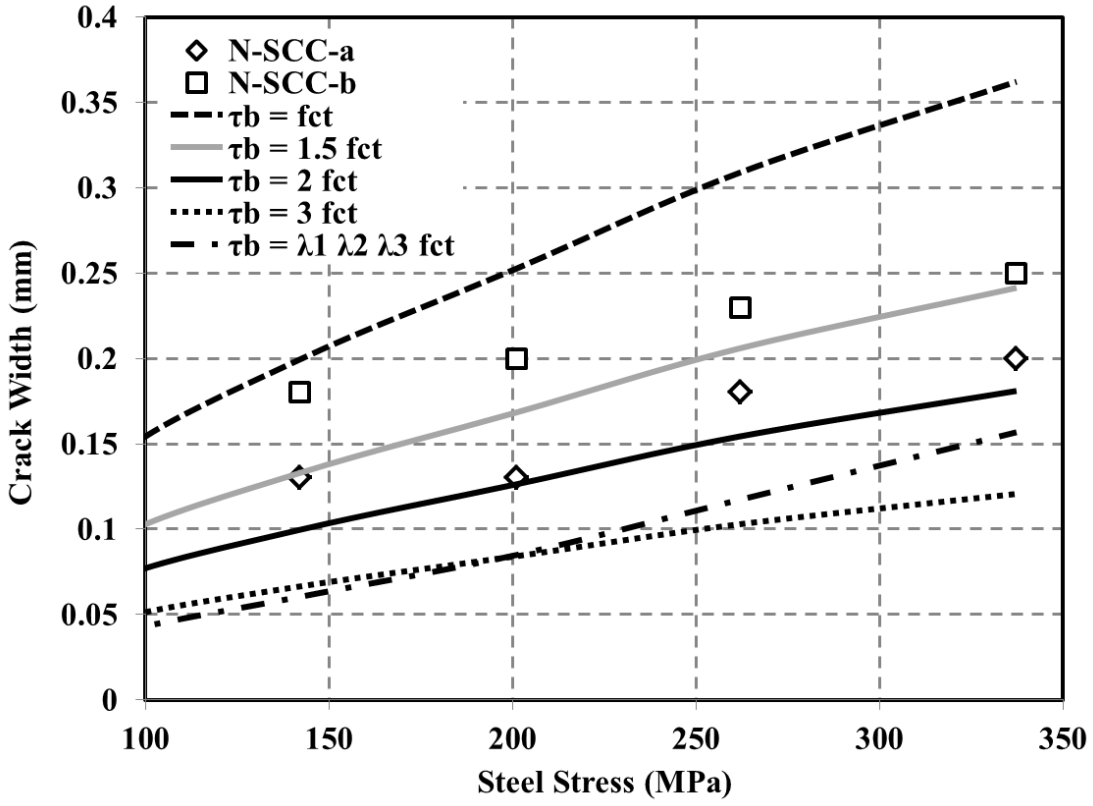

Figure 6.42 Comparison of different bond stresses for slab N-SCC series

Table 6.14 Measured and calculated maximum crack width for slab D-SCC series

(D-SCC)		Maximum Crack Width (mm)						
		Measured		Calculated (Eqs. 6.17, 6.18)				
M (kNm)	σ_{st} (MPa)	D-SCC-a	D-SCC-b	$\tau_b = f_{ct}$	$\tau_b = 1.5 f_{ct}$	$\tau_b = 2 f_{ct}$	$\tau_b = 3 f_{ct}$	$\tau_b = \lambda_1 \lambda_2 \lambda_3 f_{ct}$
7.00	60	0.05	0.05	0.027	0.018	0.013	0.009	0.006
8.80	85	0.08	0.08	0.071	0.047	0.036	0.024	0.018
10.5	111	0.10	0.13	0.113	0.075	0.057	0.038	0.032
12.3	139	0.13	0.15	0.158	0.105	0.079	0.053	0.048
14.0	186	0.15	0.18	0.200	0.133	0.100	0.067	0.067
15.8	253	0.18	0.20	0.245	0.163	0.122	0.082	0.093
17.5	323	0.18	0.23	0.287	0.191	0.143	0.096	0.124

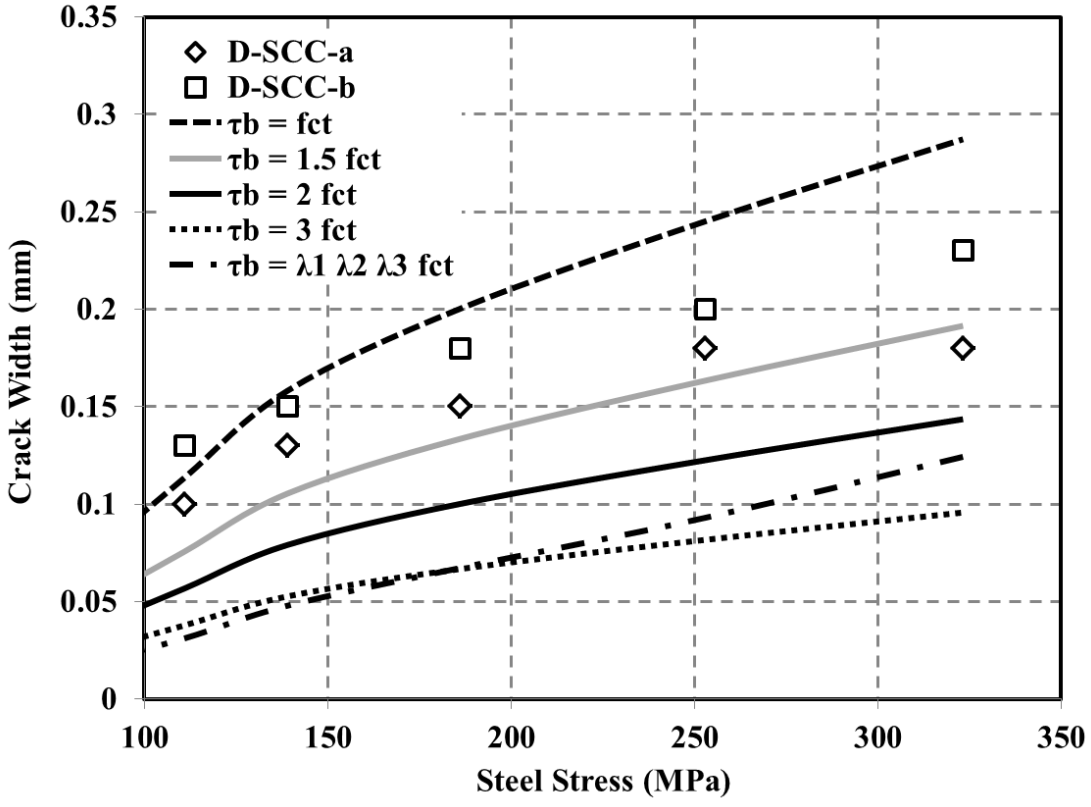

Figure 6.43 Comparison of different bond stresses for slab D-SCC series

Table 6.15 Measured and calculated maximum crack width for slab S-SCC series

(S-SCC)		Maximum Crack Width (mm)						
		Measured		Calculated (Eqs. 6.17, 6.18)				
M (kNm)	σ_{st} (MPa)	S-SCC-a	S-SCC-b	$\tau_b = f_{ct}$	$\tau_b = 1.5\, f_{ct}$	$\tau_b = 2\, f_{ct}$	$\tau_b = 3\, f_{ct}$	$\tau_b = \lambda_1\, \lambda_2\, \lambda_3\, f_{ct}$
7.00	62	0.05	0.08	0.034	0.022	0.017	0.011	0.008
8.80	100	0.08	0.08	0.091	0.060	0.045	0.030	0.023
10.5	137	0.10	0.10	0.145	0.096	0.072	0.048	0.040
12.3	178	0.13	0.15	0.202	0.134	0.101	0.067	0.061
14.0	218	0.13	0.18	0.255	0.170	0.128	0.085	0.085
15.8	289	0.15	0.20	0.312	0.208	0.156	0.104	0.118
17.5	344	0.18	0.23	0.366	0.244	0.183	0.122	0.158

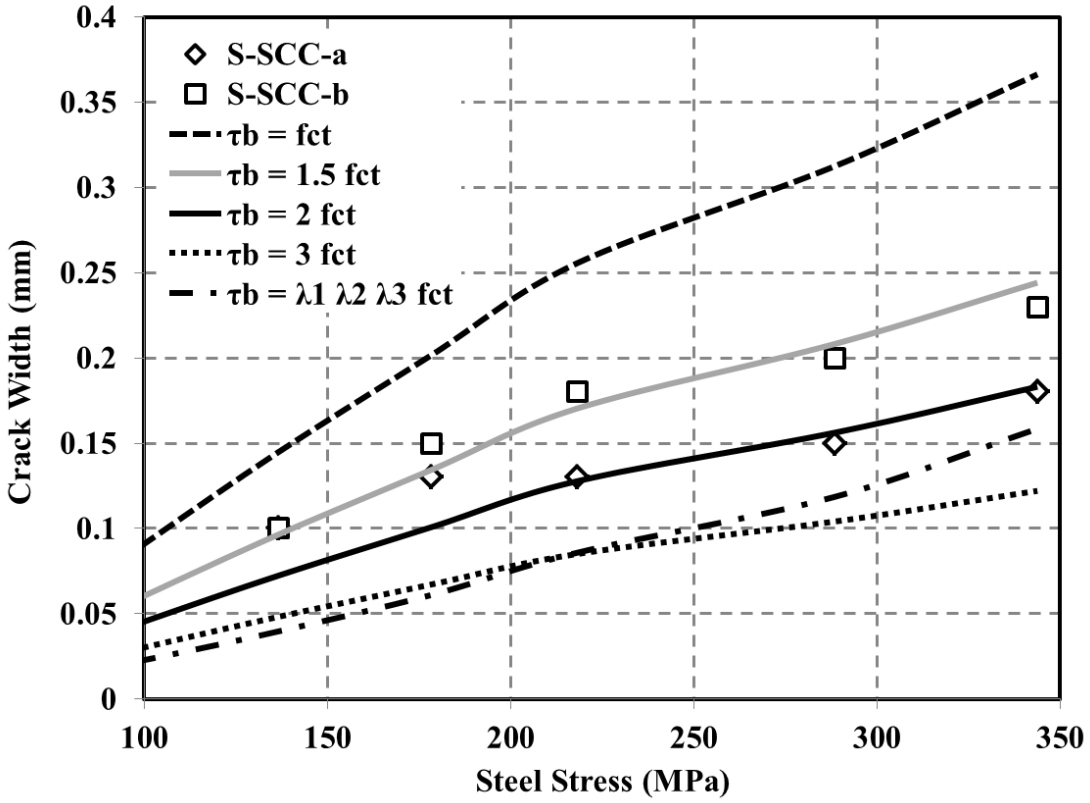

Figure 6.44 Comparison of different bond stresses for slab S-SCC series

Table 6.16 Measured and calculated maximum crack width for slab DS-SCC series

(DS-SCC)		Maximum Crack Width (mm)						
		Measured		Calculated (Eqs. 6.17, 6.18)				
M (kNm)	σ_{st} (MPa)	DS-SCC-a	DS-SCC-b	$\tau_b = f_{ct}$	$\tau_b = 1.5 f_{ct}$	$\tau_b = 2 f_{ct}$	$\tau_b = 3 f_{ct}$	$\tau_b = \lambda_1 \lambda_2 \lambda_3 f_{ct}$
7.00	108	0.05	0.05	0.029	0.020	0.015	0.010	0.007
8.80	138	0.08	0.08	0.079	0.053	0.039	0.026	0.020
10.5	168	0.10	0.10	0.126	0.084	0.063	0.042	0.034
12.3	203	0.13	0.13	0.176	0.117	0.088	0.058	0.053
14.0	232	0.13	0.15	0.222	0.148	0.111	0.074	0.074
15.8	276	0.15	0.18	0.272	0.181	0.136	0.090	0.103
17.5	320	0.15	0.20	0.319	0.212	0.159	0.106	0.167

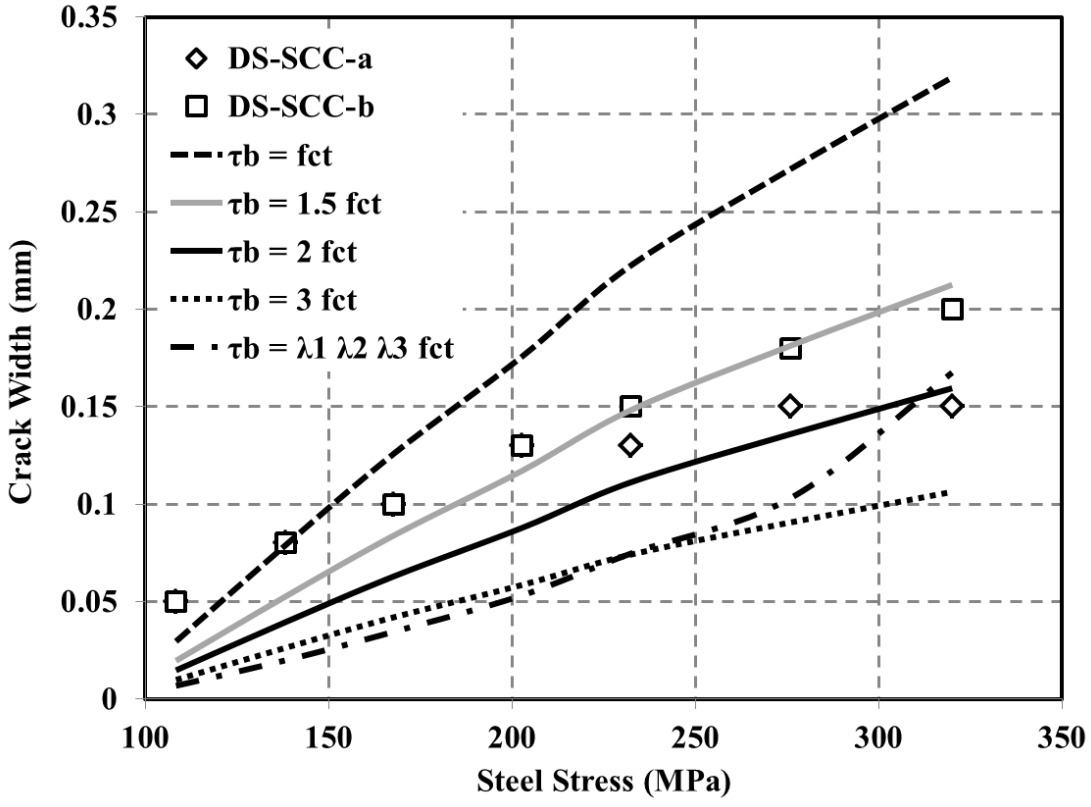

Figure 6.45 Comparison of different bond stresses for slab DS-SCC series

Table 6.17 Measured and calculated maximum crack width for slab N-CC series (Nejadi, 2005)

(N-CC)		Maximum Crack Width (mm)						
		Measured		Calculated (Eq. 6.13)				
M (kNm)	σ_{st} (MPa)	N-CC-a	N-CC-b	$\tau_b = f_{ct}$	$\tau_b = 1.5\, f_{ct}$	$\tau_b = 2\, f_{ct}$	$\tau_b = 3\, f_{ct}$	$\tau_b = \lambda_1 \lambda_2 \lambda_3 f_{ct}$
7.00	133	0.05	0.05	0.070	0.033	0.040	0.030	0.013
8.80	166	0.08	0.08	0.120	0.084	0.060	0.040	0.036
10.5	199	0.10	0.10	0.170	0.132	0.080	0.060	0.062
12.3	232	0.13	0.13	0.220	0.182	0.110	0.070	0.096
14.0	265	0.15	0.18	0.270	0.230	0.130	0.090	0.138
15.8	298	0.15	0.20	0.320	0.281	0.160	0.110	0.195
17.5	331	0.18	0.23	0.370	0.329	0.190	0.120	0.269

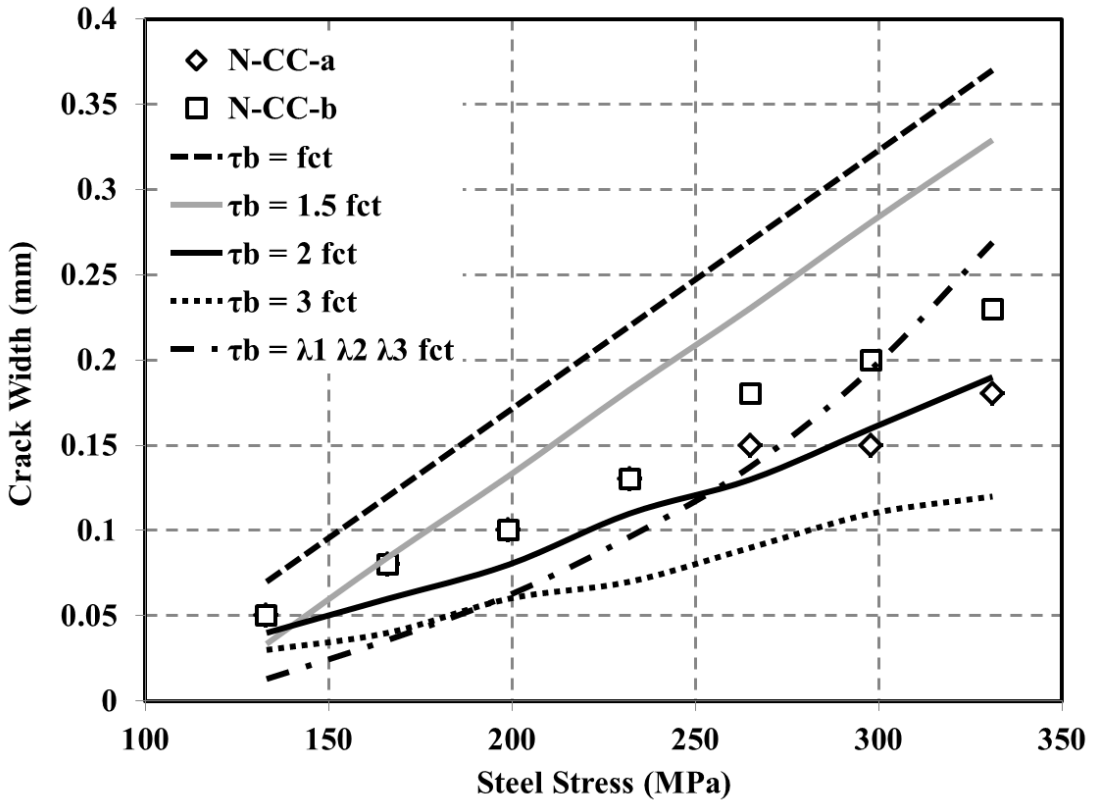

Figure 6.46 Comparison of different bond stresses for slab N-CC series (Nejadi, 2005)

6.5 SUMMARY AND CONCLUSIONS

The results from the short-term flexural test programme on reinforced SCC slab specimens were presented in Sections 6.3.2 through 6.3.6. In addition, the results are summarised in Table 6.18. Overall conclusions based on the short-term flexural test experimental results can be made as follows:

- The DS-SCC slabs show the lowest maximum and average final crack widths comparing to the other mixture slabs.
- The DS-SCC slabs bear maximum failure load and deflection comparing to the other mixture slabs.
- The S-SCC slabs decrease maximum and average final crack widths comparing to N-SCC slabs but not much changed comparing to N-CC slabs.
- Using PP fibres in SCC do not change failure loading much but it increases the ductility of the slab specimens comparing to the N-SCC and N-CC slabs.
- Using steel fibres in SCC decrease maximum and average final crack widths comparing to the N-SCC and N-CC slabs.
- The D-SCC slabs decrease final average spacing comparing to the other mixtures slabs.

Table 6.18 Summary of the results from short-term flexural test

Specimen	Testing age (days)	$(w_{max})_{final}$ (mm)	$(w_{ave})_{final}$ (mm)	$(s_{ave})_{final}$ (mm)	Failure Load (kN)	Deflection at failure load (mm)	w_{max} / w_{ave}
N-SCC-a	62	0.20	0.154	95	49.0	180	1.29
N-SCC-b	63	0.25	0.195	94	48.5	163	1.17
D-SCC-a	65	0.18	0.138	106	53.0	205	1.10
D-SCC-b	66	0.23	0.172	96	52.0	177	1.33
S-SCC-a	67	0.18	0.132	102	50.0	185	1.36
S-SCC-b	69	0.23	0.189	100	48.0	167	1.21
DS-SCC-a	71	0.15	0.120	95	56.0	220	1.24
DS-SCC-b	72	0.20	0.156	98	54.0	182	1.15
N-CC-a	62	0.18	0.130	90	50.0	136	1.38
N-CC-b	63	0.23	0.180	117	47.0	156	1.28

6.5.1 Cracking Behaviour

When a reinforced concrete beam is subjected to a gradually increasing moment, two basic types of flexural cracks occur (Beeby, 1970):

As the load is gradually increased, primary cracks occur and penetrate almost to the neutral axis (h_o), after which the primary crack pattern is established and controlled by the crack height h_o. From St. Venant's principal, the concrete tensile stresses reduce within the distance h_o on both sides of the crack, hence the next crack will form at a distance from the crack equal to or greater than h_o and therefore the minimum crack spacing is h_o and the maximum is $2h_o$. Secondary or cover-controlled cracks occur between the primary cracks as the load is increased. According to the 'no-slip' theory, secondary cracks are wedge-shaped cracks with zero width at the bar surface, that is a linear relationship exists between crack width and distance from the bar. Thus, the effective crack height is c_o directly over the bar, where c_o is the minimum cover to the tensile reinforcement. Using the same reasoning the crack spacing for secondary cracks will vary between c_o and $2c_o$.

The development and width of flexural cracks in each specimen were carefully monitored under gradually increasing loads up to failure. The first crack appeared in the pure flexure zone within the high moment region. Subsequent cracks appeared with the basic primary crack pattern establishing itself quite rapidly. Secondary cracks appeared between the primary cracks, as the load increased, and a few new cracks occurred at high overload stages.

From a comparison of the results it was also observed that crack widths were directly proportional to applied load and consequently to stress in the steel. In addition to the above, the average of all observed crack widths at approximately 70% of the ultimate load was taken and compared with the maximum observed crack width at that load stage.

As Table 6.18 shows, final maximum and average crack widths for N-SCC slab series are slightly more than N-CC slab series and final average spacing of N-SCC-a slab is 5 mm higher than N-CC-a but final average spacing of N-SCC-b slab is 23 mm less than N-CC-b.

In the D-SCC slab series compared to the N-SCC and N-CC slab series, final maximum crack widths for D-SCC slab series are slightly less than N-SCC slab series and equal to N-CC slab series. Final average crack widths for D-SCC slab series are less than N-SCC and N-CC slab series. Final average spacing of D-SCC-a slab is 11 mm higher than N-SCC-a and final average spacing of D-SCC-b slab is 2 mm higher than N-SCC-b. Final average spacing of D-SCC-a slab is 16 mm higher than N-CC-a but final average spacing of D-SCC-b slab is 21 mm less than N-CC-b.

In the S-SCC slab series compared to the N-SCC and N-CC slab series, final maximum crack widths for S-SCC slab series are slightly less than N-SCC slab series and equal to N-CC slab series. Final average crack widths for S-SCC slab series are less than N-SCC and N-CC slab series. Final average spacing of S-SCC-a slab is 7 mm higher than N-SCC-a and final average spacing of S-SCC-b slab is 6 mm higher than N-SCC-b. Final average spacing of S-SCC-a slab is 12 mm higher than N-CC-a but final average spacing of S-SCC-b slab is 17 mm less than N-CC-b.

Finally, in the DS-SCC slab series compared to the N-SCC and N-CC slab series, final maximum crack widths for DS-SCC slab series are less than N-SCC and N-CC slab series. Final average crack widths for DS-SCC slab series are less than N-SCC and N-CC slab series. Final average spacing of DS-SCC-a slab is equal to N-SCC-a and final average spacing of DS-SCC-b slab is 4 mm higher than N-SCC-b. Final average spacing of DS-SCC-a slab is 5 mm higher than N-CC-a but final average spacing of DS-SCC-b slab is 19 mm less than N-CC-b.

6.5.2 Deflection

In general, when a section cracks, its moment of inertia decreases, leading to a decrease in slab stiffness. From plotted mid-span deflection against load curves, deflection behaviour of all slab specimens under gradually increased loads were identical. Initially, the specimens were uncracked and stiff, but by increasing the load, cracking occurred when the moment at mid-span exceeded the cracking moment. After cracking, the specimens exhibited elastic behaviour until the reinforcement yielded at mid-span, leading to a large

increase in deflection with little change in load until the compressive concrete crushed and the specimens collapsed. Ductility is an important structural property because it ensures that large deformations and deflections occur under overload conditions. Good ductility can be achieved if the quantity of reinforcement is kept small, e.g. $\rho < 0.02$ and ductile reinforcement is used.

Failure loading of the N-SCC slab series is 1 kN less than the N-CC-a and failure loading of the N-SCC-b is 1.5 kN higher than the N-CC-b. Maximum deflection at failure loading of the N-SCC slab series is 44 and 7 mm higher than the N-CC slab series. It shows that the N-SCC slab series are more ductile than the N-CC slab series.

Failure loading of the D-SCC-a is 4 and 3 kN higher than the N-SCC-a and N-CC-a and failure loading of the D-SCC-b is 3.5 and 5 kN higher than the N-SCC-b and N-CC-b. Maximum deflection at failure loading of the D-SCC slab series is 25 and 14 mm higher than the N-SCC slab series and it is 69 and 21 mm higher than N-SCC slab series. It shows that D-SCC slab series are more ductile than the N-SCC and N-CC slab series.

Failure loading of the S-SCC-a is nearly equal to the N-SCC and N-CC slab series. Maximum deflection at failure loading of S-SCC slab series is 25 and 14 mm higher than the N-SCC slab series and it is 69 and 21 mm higher than N-CC slab series. It shows that S-SCC slab series are more ductile than the N-SCC and N-CC slab series.

Failure loading of the DS-SCC-a is 7 and 6 kN higher than the N-SCC-a and N-CC-a and failure loading of the DS-SCC-b is 5.5 and 7 kN higher than the N-SCC-b and N-CC-b. Maximum deflection at failure loading of the DS-SCC slab series is 40 and 19 mm higher than the N-SCC slab series and it is 84 and 26 mm higher than the N-SCC slab series. It shows that the DS-SCC slab series are more ductile than the N-SCC and N-CC slab series.

6.5.3 Bond Shear Stress

Bond can be considered as the shear stress or force between a bar and the surrounding concrete. The bond shear stress τ_b depends on several factors, including the tensile strength and cover of concrete, steel stress, bar size and spacing, confining effects, and load history.

Subsequently, the location, spacing, and width of cracks, the internal distribution of forces, tension stiffening, and the strength of the member depend directly on the bond characteristics between the steel and surrounding concrete.

Five different values for bond shear stress ($\tau_b = f_{ct}$, $\tau_b = 1.5\, f_{ct}$, $\tau_b = 2\, f_{ct}$, $\tau_b = 3\, f_{ct}$, and $\tau_b = \lambda_1\, \lambda_2\, \lambda_3\, f_{ct}$-Eq.[6.5]) have been considered and the corresponding crack widths were calculated and compared with the experimental results for each load increment. It should be mentioned that throughout the test, crack widths were monitored at two levels on the side of each specimens, i.e., the steel level and bottom fibre.

In general, cracking in reinforced concrete is a random phenomenon with every experimental result subjected to both systematic and random errors. For example, repeated measurements of the crack widths during each load increment differed, even when the measurements were performed by the same microscope, under the same conditions. The measurements varied according to the exact location of the measurement on the crack, as the crack side faces are irregular and not parallel. The adopted expressions for the bond shear stress τ_b for the SCC slab series under short-term loading and for the different in-service steel stress ranges have been presented in Table 6.19 and Figure 6.47.

.

Table 6.19 Adopted bond stresses for SCC slab series

Slab series	τ_b	
	$f_{sy} > \sigma_{s.max} \geq 180$ MPa	$\sigma_{s.max} < 180$ MPa
N-SCC	$1.50\, f_{ct}$	$1.50\, f_{ct}$
D-SCC	$1.30\, f_{ct}$	$1.25\, f_{ct}$
S-SCC	$1.70\, f_{ct}$	$1.50\, f_{ct}$
DS-SCC	$1.60\, f_{ct}$	$1.50\, f_{ct}$

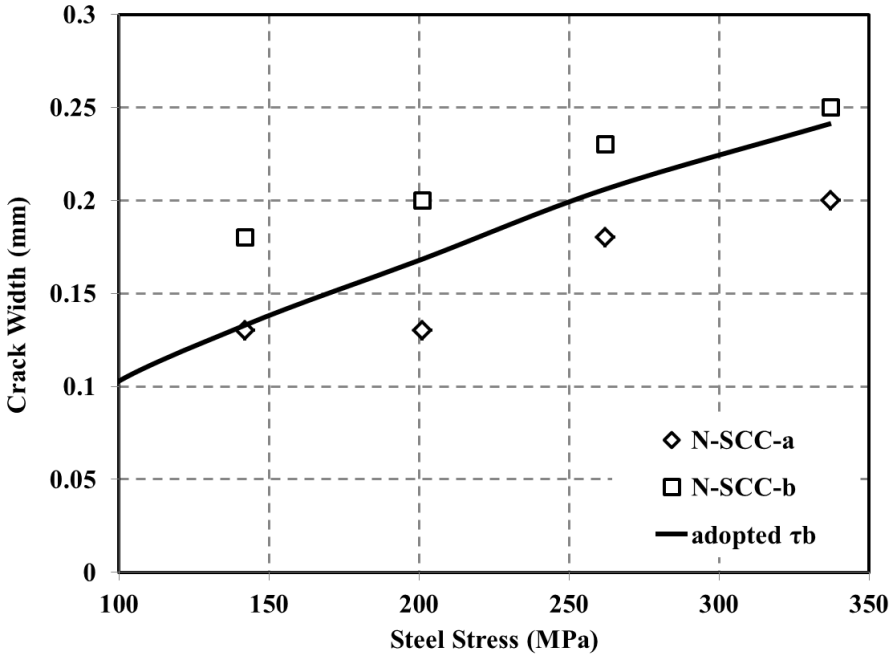

(a)

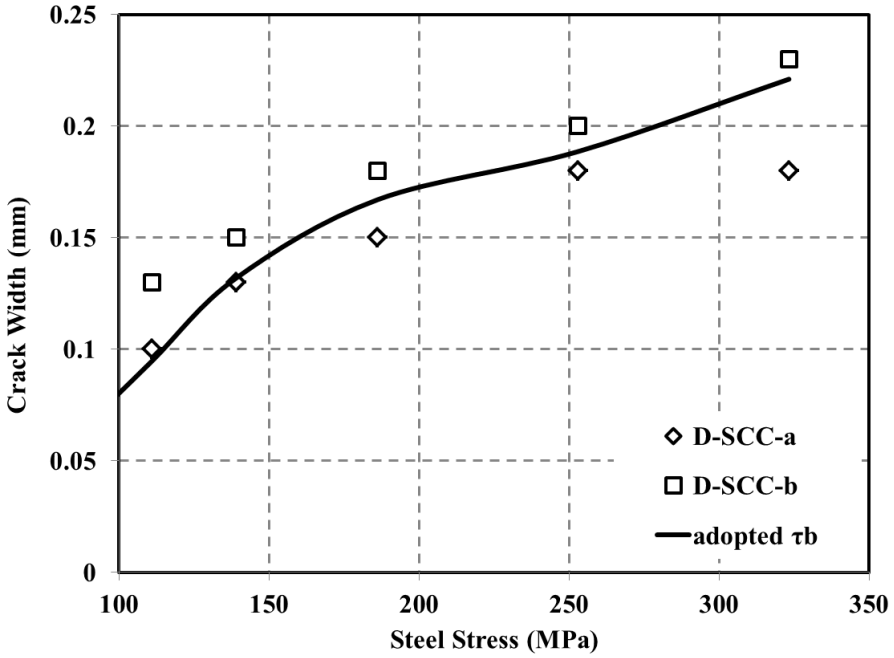

(b)

Figure 6.47(a, b) Adopted bond stresses for (a) N-SCC, (b) D-SCC slab series

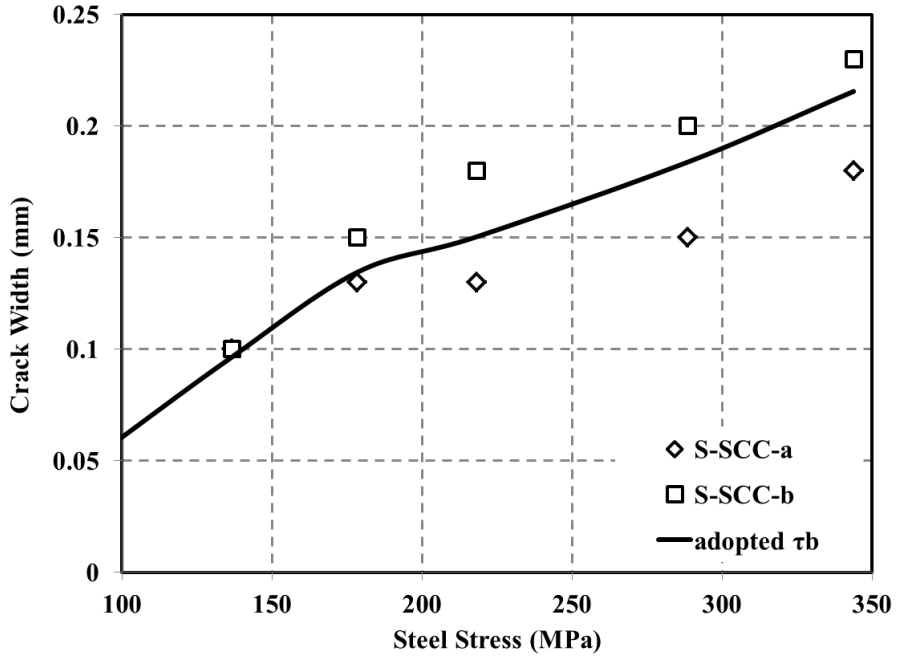

(c)

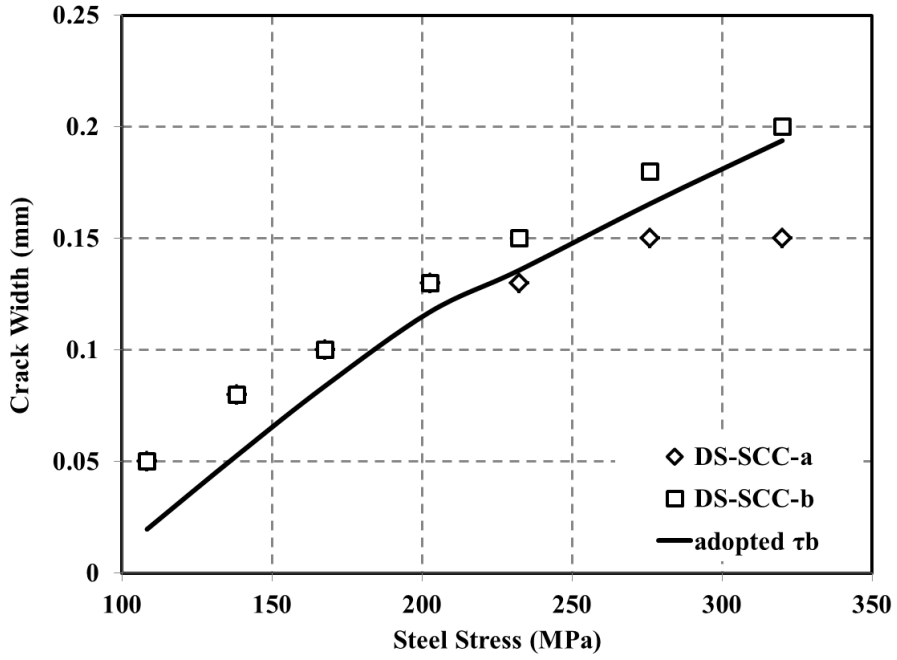

(d)

Figure 6.47(c, d) Adopted bond stresses for (c) S-SCC, (d) DS-SCC slab series

CHAPTER 7

EXPERIMENTAL PROGRAM (PHASE III) – LONG TERM FLEXURAL CRACKING

CHAPTER 7

EXPERIMENTAL PROGRAM (PHASE III) – LONG TERM FLEXURAL CRACKING

7.1 INTRODUCTION

The performance of reinforced concrete structures under sustained loads particularly in the post-cracking range is a key design concern. If sections are designed according to strength requirements only, the behaviour of the structure under sustained service loads may be unsatisfactory. For example, at service loads, deflections of the member may be excessively large or the width of the cracks may be improper, even nevertheless the degree of the safety against collapse is acceptable.

For a concrete structure to be serviceable, cracking must be controlled and deflection must not be excessive. Service load behaviour depends primarily on the properties of the concrete and these are often not known reliably at the design stage. As mentioned in the design of concrete structures, it is necessary to check the serviceability of the structure in the post-cracking range. The behaviour in this range is complicated by the effects of several factors, which are difficult to assess from analytical considerations only. Of prime importance are the effects of tension stiffening, random development of primary and secondary cracks, and the degree of bond breakdown (Nejadi, 2005).

According to the existing literature, the increase in crack width occurs at a decreasing rate with time due to long-term or cyclic loading and this increase can be up to twice the initial value within a few years. However, under most conditions, the spacing of cracks does not change with time at constant levels of stress. The test results compiled by Illston and Stevencs (1972) show that, under sustained loads the increase in crack width is caused by shrinkage of the concrete and by the time-dependent change of curvature. They also found that, there was a breakdown of bond with sustained loading.

Nejadi (2005) has conducted a comprehensive experimental and analytical research about the time-dependent development of flexural cracking including crack widths and crack spacing in conventional reinforced concrete members'. Nejadi's (2005) test results show that in the beam specimens, the maximum crack width within the high moment region increases rapidly in the first few weeks of loading when the creep and shrinkage strain developed rapidly. The rate of increases in crack width in the beams with a high sustained load is greater than for beams with a lower sustained load. Change in the cover does not affect the final maximum crack width as much as in instantaneous behaviour. In Nejadi's (2005) slab specimens, a comparison of the results in different regions with different moment levels shows that under sustained loads, maximum and minimum crack width are proportional to the bending moment, and crack width increases linearly as the applied moment increases. Also, the largest increase in crack width occurs in those regions subjected to low levels of bending moment; because cracks take more time to develop. The average ratio of the final maximum crack width to the final average crack width for all specimens (6 beams and 6 slabs) is 1.5. Also, Nejadi's (2005) experimental results show that deflection at mid-span increases rapidly over the first 1 to 2 months after loading with more than 60% of the final deflection occurring within this period. This rapid increase in deflection is caused by the loss of stiffness due to the development of time-dependent cracking and the increase in deformation caused by creep and shrinkage.

Little information is available in the literature regarding development the time-dependent of SCC and FRSCC flexural cracking and the effect of long-term on crack widths and crack spacing. Following tests have been down for monitoring the long-term behaviour of SCC and FRSCC beams but no one consider long-term behaviour of SCC and FRSCC slabs.

Xiao-jie et al. (2008) have performed long-term experimental tests of SCC beams. The shrinkage strain of SCC increases as the age increases. The shrinkage strain curves converge after 6 months. Also, under the same environmental conditions, the shrinkage-time curve of SCC is very similar to that of CC. The shrinkage strain of SCC after one year is about 450×10^{-6}. The creep coefficient of reinforced SCC beams for deflection after 18 months is about 1.6, which is very close to the normal reinforced CC beams.

Mazzotti and Savoia (2009) have performed set of long-term creep tests on reinforced SCC beams. The results show that the long-term behaviour of SCC is qualitatively similar to the case of CC, both in terms of total shrinkage and creep strains. The creep strain attains an almost constant increase rate (in the time log scale) after approximately 2 months from casting. Nevertheless, creep and shrinkage are much greater for the specific SCC evaluated in this study than in the case of normal-slump concrete (e.g. CC). Also, the long-term deflection rate of beams under flexure is almost constant (in the time log scale) after the same period of time. On the contrary, the tensile strain rate in concrete close to the transverse cracks reduces after a few months from loading, suggesting the crack opening stabilization. Most of the irreversible deflection and tensile strain are due to the shrinkage effect during the test. Moreover, crack widths increase only very slightly under the long-term loading, and their contribution to the long-term beam deflection is negligible.

Buratti et al. (2010) have conducted series of long-term experimental tests for FRSCC beams. The performed tests showed that the magnitude of the delayed deformation can be high, up to 150% of the instantaneous counterpart. The rate of delayed deformation increase at lower rates for the FRSCC beams than for the plain SCC beam containing standard reinforcing bars. In particular, the lowest long-term damage was obtained for the specimen containing a combination of steel fibres of different sizes and of synthetic fibres usually employed to reduce shrinkage.

The major objective of the long-term flexural test conducted in this study was to assess the influence of the factors that affect the width and spacing of flexural cracking under sustained loads and obtain laboratory controlled data on the time-dependent response of *one-way slabs* made of SCC and FRSCC as a benchmark in order to develop and calibrate a proposed flexural cracking analytical model.

7.2 EXPERIMENTAL PROGRAM

A total of eight SCC and FRSCC slabs with the same cross-section and details as for the short-term tests were monitored for up to 240 days to measure the time-dependent development of cracking and deformations under service loads. For this purpose, four SCC mixes – two plain SCC, two steel, two polypropylene, and two hybrid FRSCC slab specimens – are considered in the test program. A general view of the test specimens is shown in Figure 7.1. The steel strains within the high moment regions, the concrete surface strains at the tensile steel level, deflection at the mid-span, crack widths and crack spacing were recorded throughout the testing period. The compressive and tensile strength of the concrete were measured on companion specimens (in the form of concrete cylinders, prisms and unreinforced blocks) at various times, together with the elastic modulus, creep coefficient and free shrinkage in the concrete.

All slab specimens were subjected to different gravity loads, consisting of self-weight plus superimposed sustained loads via carefully constructed and arranged concrete blocks supported off the top (of the specimens). To provide the sustained loading, rectangular concrete blocks of predetermined size and weights were cast and weighed prior to the commencement of the test. The blocks were suitably arranged on the top surface of each specimen to achieve the desired sustained load level (see Figure 7.2).

Figure 7.1 General view of flexural long-term tests under load

Figure 7.2 Loading slab specimens by concrete blocks

Two sustained load levels were considered, namely 50% and 30% of the ultimate design load, and designated load conditions ‘a’ and ‘b’, respectively. The slab specimens were subjected to uniformly distributed sustained loads, UDL + self-weight. All measurements were taken within the high moment region, i.e. the middle third of the span for beams and for slabs where M ≥ 90% Mmax. For long-term tests the loading arrangement and high moment regions are shown in Figure 7.3.

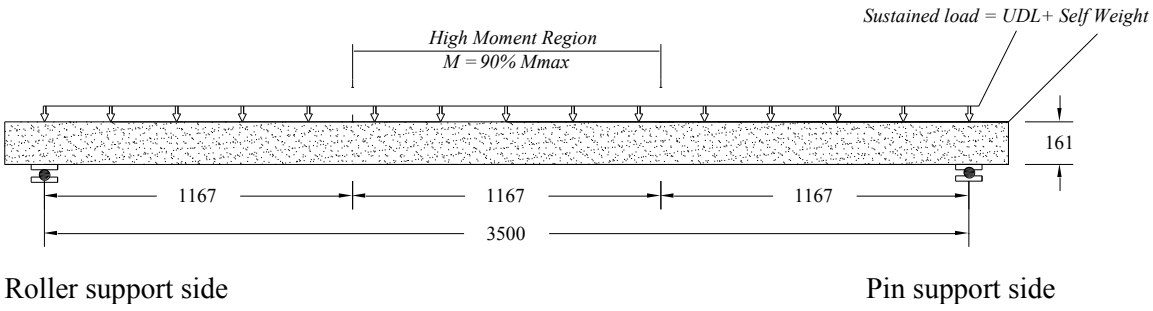

Figure 7.3 Illustrative sustained loads slab specimens

7.2.1 Test Parameters and Reinforcement Layouts

Details of the cross-section, steel reinforcement layouts and cross-sectional dimensions for each specimen were presented in Section 5.2 (Note: short-term and long-term specimens were identical). Details of the parameters varied in the long-term flexural tests are given in Table 7.1. All specimens were constructed in 3800 mm long formwork and were simply supported by two short steel columns on a 3500 mm span (Figure 7.4). For the slab specimens, two identical specimens were constructed for each combination of variables, with one loaded to 50% of its ultimate capacity (type 'a') and one loaded to 30% of its ultimate capacity (type 'b').

Table 7.1 Details of slab specimens for long-term flexural test

Specimen	No. of Bars	Bar Diam. (mm)	Load (UDL) (kN/m)	c_b (mm)	c_s (mm)	s (mm)
Slab-a	4	12	5.8	25	40	103
Slab-b	4	12	3.9	25	40	103

Figure 7.4 Supports for slabs

7.2.2 Construction of Specimens and Test Procedures

In total, 8 slab specimens were cast and tested under sustained loads. Each of the specimens was moist cured for a period of 14 days and then subjected to a constant sustained load. Cracking and deformation were monitored throughout the test. For these long-term tests, the variation of mechanical properties of SCC and FRSCC was measured on companion cylinders and prisms. To measure the steel strains in the critical moment regions (e.g. high moment regions, see Figure 7.3), 8 electric resistance strain gauges were attached to one of the main reinforcement bars. The strain gauges were connected to a HBM amplifier. To measure the concrete surface strains, 8 electric resistance strain gauges were glued onto the side face of each specimen at the steel level. While a microscope with a magnification factor of 40 was used to measure the crack widths. The development, propagation, extent, and width of cracking were observed and recorded throughout the test. Deflection at mid-span was measured using a Linear Variable Displacement Transducer (LVDT).

The inside surface of the mould was cleaned and thinly coated with a concrete release agent to prevent adhesion of the concrete. The SCC was placed into the mould in equal layers until each surface layer became smooth. Sufficient concrete was placed into the top layer to overfill the mould, after which the surface was stripped off and finished with a steel trowel. To measure the concrete material properties, companion specimens were also cast in the form of cylinders and prisms at the same time. The companion specimens were exposed to the same environmental, curing, and drying conditions as the test specimens. Creep coefficient and shrinkage strain for four SCC mixes was obtained. The specimens were left in their moulds for 3 days, and then removed from the mould and kept continuously moist by a thick covering of wet Hessian to minimise the loss of moisture from the concrete. After 14 days the covers and wet Hessian were removed, strain gauges were glued to the concrete surface and initial strain measurements were recorded. Slab specimens were uniformly loaded by the concrete blocks using wooden timbers as loading pads.

7.3 TEST RESULTS

The experimental results taken from 8 slabs are presented in this section. Results include the measured material properties, the extent, distribution and width of cracking with time within the high moment regions, and time-dependent deflection at mid-span. The experimental results for slab specimens are discussed and a comparison of the results is also made. The raw data measured of concrete surface, steel strains and some photos of tests throughout the experimental programme are presented in Appendix-E.

7.3.1 Material Properties

As presented in Chapter 4, standard concrete cylinders (150 mm × 300 mm), and prisms (100 mm × 100 mm × 350 mm) were used to determine the compressive and tensile strengths, MOR and MOE of the concrete at ages 3, 7, 14, 28, 56, and 91 days. The results are presented in Table 7.2. The measured creep coefficients for SCC loaded at age 14 days and shrinkage strain is presented are Tables 7.3-7.4 and in Figures 7.5 and 7.6.

Table 7.2 Material properties of SCC and FRSCC

	Compressive strength (MPa)				Tensile strength (MPa)			
Age (days)	N-SCC	D-SCC	S-SCC	DS-SCC	N-SCC	D-SCC	S-SCC	DS-SCC
3	12.45	18.50	13.65	14.30	1.65	2.32	1.16	1.76
7	21.80	25.30	22.50	26.30	2.26	3.38	1.93	2.51
14	29.05	34.30	32.45	38.10	2.80	3.87	3.05	3.54
28	33.30	38.00	38.10	45.00	3.60	4.54	3.56	4.09
56	40.60	50.50	42.90	50.75	4.17	5.35	4.02	4.33
91	46.40	51.15	47.65	52.00	4.57	5.44	4.41	4.80
	MOE (GPa)				MOR (MPa)			
Age (days)	N-SCC	D-SCC	S-SCC	DS-SCC	N-SCC	D-SCC	S-SCC	DS-SCC
3	25.23	24.45	25.36	26.78	2.50	3.35	3.13	2.47
7	27.84	26.57	27.87	30.13	3.35	4.10	4.26	3.81
14	32.24	29.14	29.68	31.26	4.66	5.40	4.60	4.80
28	35.39	35.76	35.76	36.10	5.00	6.37	5.00	5.40
56	35.58	36.44	36.32	37.03	5.87	6.72	6.50	6.52
91	37.79	37.58	37.47	38.12	7.13	7.23	6.76	7.21

Table 7.3 The measured creep coefficient for SCC and CC mixtures

Age (days)	15	17	20	21	28	35	42	70	98	126	154	182	210	240
	Creep coefficient, φ_{cc}													
N-SCC*	0.36	0.7	0.96	1.01	1.15	1.28	1.36	1.55	1.7	1.76	1.82	1.85	1.91	1.96
D-SCC	0.39	0.52	0.67	0.73	1.02	1.12	1.2	1.43	1.6	1.67	1.72	1.76	1.82	1.86
S-SCC	0.36	0.59	0.75	0.78	0.96	1.12	1.19	1.41	1.50	1.58	1.64	1.72	1.77	1.82
DS-SCC	0.20	0.35	0.55	0.60	0.74	0.85	0.95	1.10	1.21	1.27	1.32	1.38	1.41	1.45
N-CC**	0.1	0.17	0.35	0.36	0.55	0.75	0.83	1.07	1.15	1.25	1.33	1.37	1.42	1.49

* N-SCC: normal SCC mixture, ** N-CC: normal conventional concrete (Nejadi, 2005)

Table 7.4 The measured free shrinkage for unreinforced SCC and CC mixtures

Age (days)	15	17	20	21	28	35	42	70	98	126	154	182	210	240
	Shrinkage strain (microstrain)													
N-SCC	12	52	121	150	242	329	403	567	693	756	793	827	848	870
D-SCC	42	105	166	204	339	419	479	631	713	757	803	816	830	844
S-SCC	22	81	119	150	251	348	404	565	650	709	749	780	811	823
DS-SCC	36	95	172	210	310	394	436	596	688	758	830	849	869	882
N-CC	15	41	97	109	227	315	341	526	598	724	748	769	778	785

The final creep coefficients for N-SCC, D-SCC, S-SCC, DS-SCC, and N-CC mixtures were 1.96, 1.86, 1.82, 1.45, and 1.49 after 240 days. There are very interesting results here the creep coefficient of DS-SCC mixture has same trend like N-CC. But, the other SCC mixtures have different behaviour. The maximum creep coefficient is related to N-SCC without any fibres in the mixture. The creep coefficient of N-SCC mixture at age 240 days is 5%, 7%, 26%, and 24% higher than D-SCC, S-SCC, DS-SCC, and N-CC mixtures, respectively.

Also, the creep coefficients of the D-SCC and S-SCC mixtures have close trend. The D-SCC mixture creep coefficient is just 2% higher than S-SCC mixture at age 240 days. presented in Appendix-F

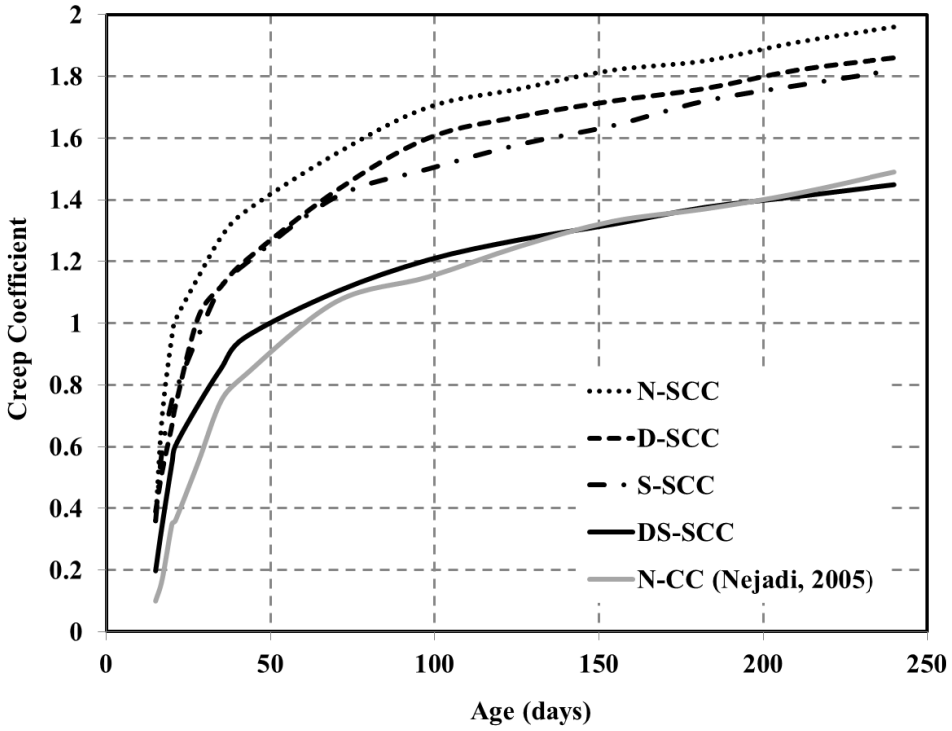

Figure 7.5 Creep coefficient for SCC and CC mixtures

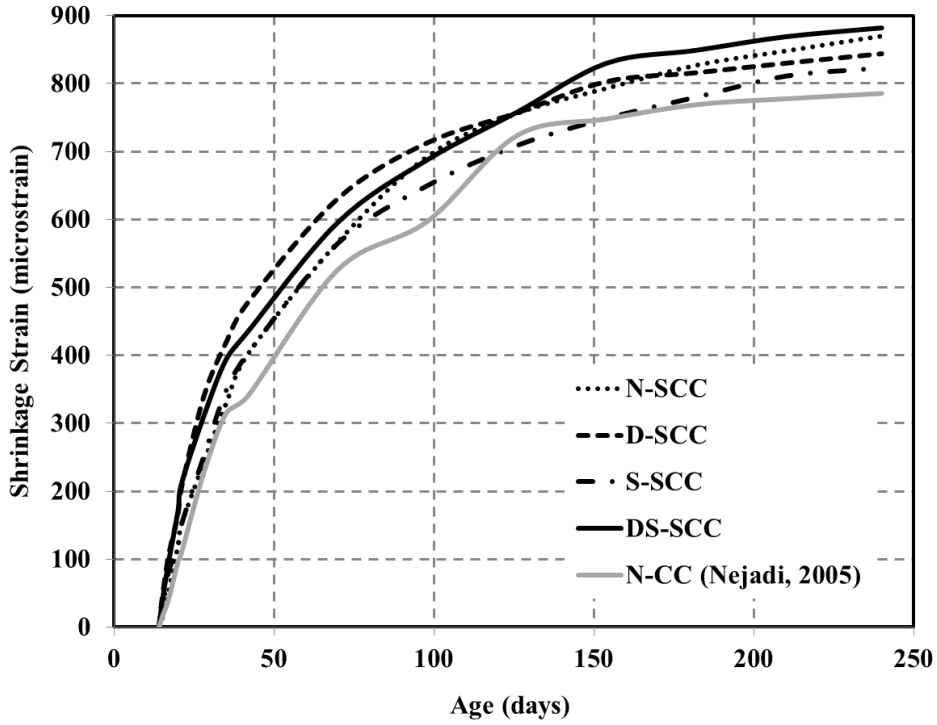

Figure 7.6 Free shrinkage for unreinforced SCC and CC mixtures

After the commencement of drying, the shrinkage strain developed rapidly within the first two or three months and more than 50% of shrinkage occurred during this period. The maximum measured final shrinkage strain or N-SCC, D-SCC, S-SCC, DS-SCC, and N-CC mixtures were 870, 844, 823, 882, and 785 microstrains after 240 days. The maximum measured final shrinkage strain for SCC mixtures are not much different from each other. Also, the S-SCC mixture has the lowest final shrinkage strain that is 5.7%, 2.5%, and 7% lower than N-SCC, D-SCC, and DS-SCC mixtures. The raw data measured of creep and shrinkage of SCC mixes and some photos of tests throughout the experimental programme are presented in Appendix-F.

7.3.2 N-SCC-a and N-SCC-b

Slabs N-SCC-a and N-SCC-b (plain SCC mixture) containing 4N12 longitudinal tensile reinforcing bars with 25 mm clear bottom cover were subjected to uniformly distributed sustained loads for 240 days. For N-SCC-a, the sustained uniform load was 5.8 kN/m plus self-weight, and for N-SCC-b, 3.9 kN/m plus self-weight.

7.3.2.1 Cracking Behaviour

The slab lengths were divided into seven different regions namely; Region 1 (where $M \geq 0.99M_{max}$), Region 2 (where $0.99M_{max} > M \geq 0.9M_{max}$), Region 3 (where $0.9M_{max} > M \geq 0.8M_{max}$), Region 4 (where $0.8M_{max} > M \geq 0.7M_{max}$), Region 5 (where $0.7M_{max} > M \geq 0.6M_{max}$), Region 6 (where $0.6M_{max} > M \geq 0.5M_{max}$) and Region 7 (where $M < 0.5M_{max}$). The development, extent and width of cracks were observed and measured within Regions 1 to 6 immediately after the first loading and during the remainder of the test period. To compare the maximum crack width located in different regions with different moment levels, the measured maximum and average crack widths at commencement of the test ($t = 0$) and at the end ($t = 240$ days) for slabs N-SCC-a and N-SCC-b are presented in Tables 7.5 and 7.6.

Tables 7.5 and 7.6 show that for long-term loading, maximum and average crack widths are proportional to the bending moment, and the crack width increases linearly by increasing the moment. The results suggest that the largest percentage increase in crack

width is in those regions subjected to low levels of bending moment, because the cracks take more time to develop. The visible cracks were developed at age 14 days where the primary crack pattern was established at first loading of slabs. The measured maximum instantaneous crack widths within Region 2 (where $0.99M_{max}>M\geq0.9M_{max}$), were 0.10 mm and 0.07 mm for N-SCC-a and N-SCC-b, respectively. The instantaneous average crack spacing within this region were 147 mm and 138 mm, respectively.

The width of cracks gradually increased with time and additional cracks mainly due to shrinkage developed within the primary crack pattern. The final average crack spacing therefore reduced with time. The measured maximum final crack widths at age 240 days within Region 2 were 0.24 mm and 0.18 mm for N-SCC-a and N-SCC-b, respectively, and the final average crack spacing were 123 mm and 100 mm respectively. The ratios of final to instantaneous crack spacing were 0.83 for N-SCC-a and 0.72 for N-SCC-b. The ratio of maximum final crack width to the final average crack width was 1.0 and 1.125 for N-SCC-a and N-SCC-b, respectively. The final crack pattern for two identical slabs N-SCC-a and N-SCC-b are illustrated in Figures 7.7 and 7.8 and Tables 7.7 and 7.8, respectively.

Table 7.5 Crack width at different regions for slab N-SCC-a

N-SCC-a		*t* = 0		*t* = 240 days	
M_{max}= 11.24 kNm	M (kNm)	Max.	Avge.	Max.	Avge.
$M \geq 0.99\ M_{max}$	11.13	0.11	0.11	0.24	0.24
$M \geq 0.90\ M_{max}$	10.12	0.10	0.10	0.23	0.23
$M \geq 0.80\ M_{max}$	8.99	0.10	0.09	0.22	0.20
$M \geq 0.70\ M_{max}$	7.87	0.10	0.09	0.20	0.19

Table 7.6 Crack width at different regions for slab N-SCC-b

N-SCC-b		*t* = 0		*t* = 240 days	
M_{max}= 8.33 kNm	M (kNm)	Max.	Avge.	Max.	Avge.
$M \geq 0.99\ M_{max}$	8.25	0.08	0.07	0.18	0.16
$M \geq 0.90\ M_{max}$	7.50	0.07	0.07	0.16	0.10
$M \geq 0.80\ M_{max}$	6.66	0.06	0.06	0.16	0.12
$M \geq 0.70\ M_{max}$	5.83	0.06	0.05	0.12	0.11

Table 7.7 The measured crack widths for slab N-SCC-a

N-SCC-a		Crack width (mm)	
Crack Number	Distance from edge (roller side) (mm)	t = 0 days	t = 240 days
1	670	0.04	0.12
2	750	0.05	0.14
3	850	0.06	0.14
4	965	0.05	0.10
5	1047	0.08	0.18
6	1180	-	0.08
7	1240	0.09	0.18
8	1350	0.09	0.16
9	1425	0.08	0.16
10	1530	0.10	0.20
11	1637	0.1	0.20
12	1757	0.1	0.23
13	1880	0.11	0.24
14	1990	0.1	0.22
15	2074	0.08	0.18
16	2190	0.08	0.18
17	2300	0.07	0.14
18	2360	0.07	0.14
19	2435	0.06	0.14
20	2510	0.04	0.14
21	2585	0.04	0.18
22	2717	0.05	0.14
23	2826	0.05	0.12
24	2916	0.03	0.10
25	3000	0.03	0.10
26	3090	-	0.06

Table 7.8 The measured crack widths for slab N-SCC-b

N-SCC-b		Crack width (mm)	
Crack Number	Distance from edge (roller side) (mm)	t = 14 days	t = 240 days
1	725	-	0.08
2	872	-	0.08
3	903	-	0.12
4	1060	0.04	0.12
5	1210	0.05	0.12
6	1275	-	0.08
7	1380	0.05	0.14
8	1470	-	0.08
9	1532	-	0.07
10	1580	0.05	0.12
11	1650	0.06	0.12
12	1770	0.06	0.14
13	1870	0.08	0.18
14	1960	0.07	0.16
15	2070	0.07	0.14
16	2120	0.04	0.10
17	2190	0.05	0.12
18	2320	-	0.06
19	2423	0.06	0.18
20	2573	0.06	0.14
21	2653	-	0.08
22	2750	0.03	0.10
23	2850	0.04	0.10
24	2940	-	0.06
25	3023	0.03	0.06
26	3095	-	0.03

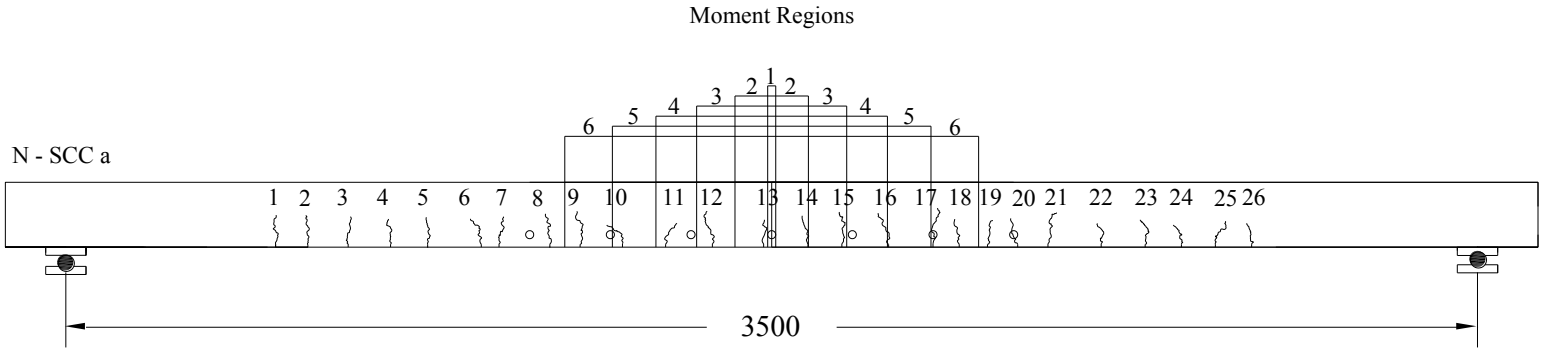

Figure 7.7 Final crack pattern for slab N-SCC-a

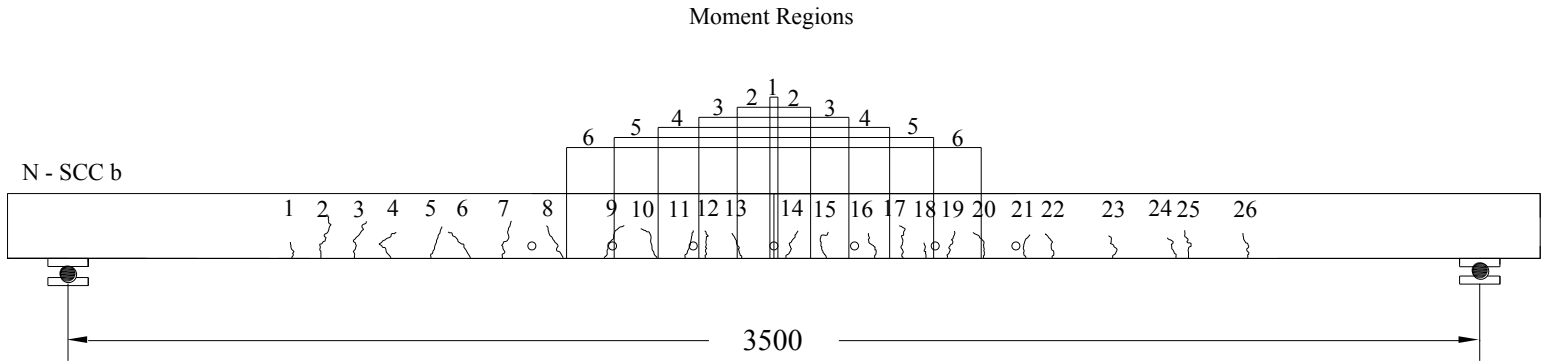

Figure 7.8 Final crack pattern for slab N-SCC-b

7.3.2.2 Deflection

Deflections were monitored and recorded immediately after loading and throughout the test period by a dial gauge installed at the middle of the each span. In Figure 7.9 the measured deflections at the mid-span of slabs N-SCC-a and N-SCC-b versus time are illustrated. The measured long-term deflection of N-SCC-a and N-SCC-b at age 240 days were 24.75 mm and 18.08 mm respectively, which are 2.04 and 3.07 times the corresponding instantaneous deflections, respectively. The ratio of deflections at different ages to instantaneous deflection at mid-span for slabs N-SCC-a and N-SCC-b are presented in Table 7.9.

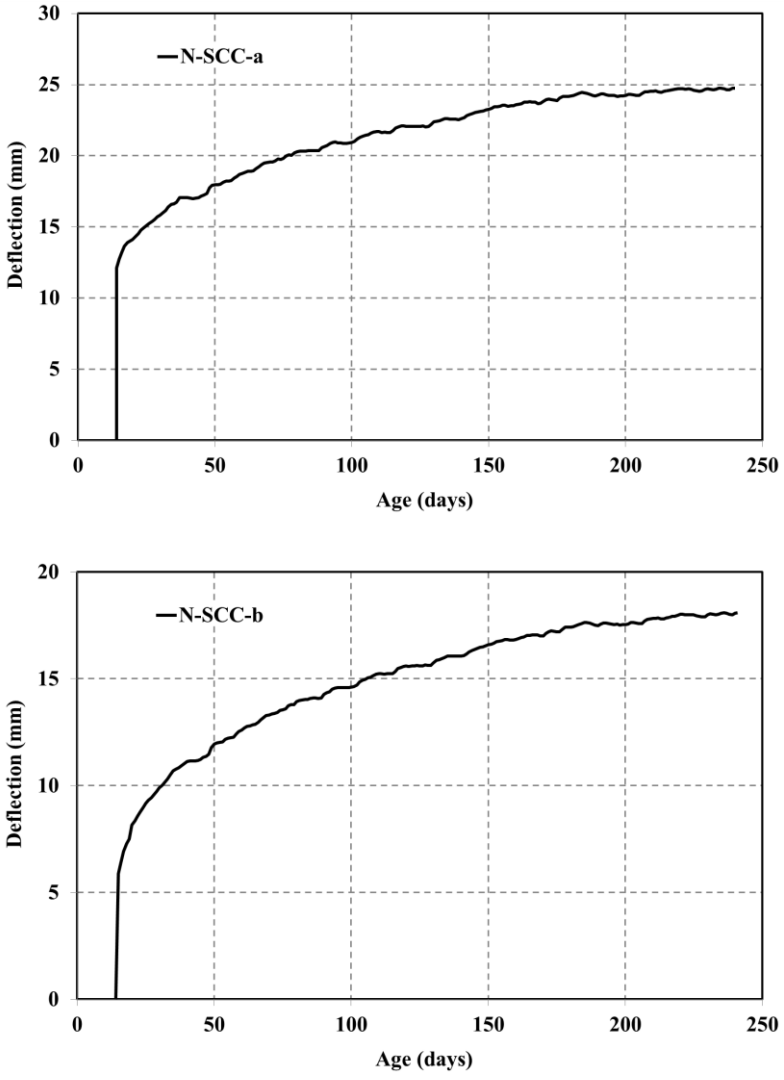

Figure 7.9 Deflection of slabs N-SCC-a and N-SCC-b

Table 7.9 Ratio of deflections at different ages to instantaneous deflection for slabs N-SCC-a and N-SCC-b

Age (days)	14	21	28	45	60	95	122	200	240
N-SCC-a	1.00	1.18	1.28	1.42	1.55	1.73	1.82	2.00	2.04
N-SCC-b	1.00	1.42	1.63	1.91	2.14	2.48	2.65	2.98	3.07

7.3.3 D-SCC-a and D-SCC-b

Slabs D-SCC-a and D-SCC-b (steel fibre SCC mixture) containing 4N12 longitudinal tensile reinforcing bars with 25 mm clear bottom cover were subjected to uniformly distributed sustained loads for 240 days. For D-SCC-a, the sustained uniform load was 5.8 kN/m plus self-weight, and for D-SCC-b, 3.9 kN/m plus self-weight.

7.3.3.1 Cracking Behaviour

To compare the maximum crack width located in different regions with different moment levels, the measured maximum and average crack widths at commencement of the test (t = 0) and at the end (t = 240 days) for slabs D-SCC-a and D-SCC-b are presented in Tables 7.10 and 7.11.

Tables 7.10 and 7.11 show that for long-term loading, maximum and average crack widths are proportional to the bending moment, and the crack width increases linearly by increasing the moment. The results suggest that the largest percentage increase in crack width is in those regions subjected to low levels of bending moment, because the cracks take more time to develop. The visible cracks were developed at age 14 days where the primary crack pattern was established at first loading of slabs. The measured maximum instantaneous crack widths within Region 2 (where $0.99M_{max}>M\geq0.9M_{max}$), were 0.09 mm and 0.07 mm for D-SCC-a and D-SCC-b, respectively. The instantaneous average crack spacing within this region were 124 mm and 131 mm, respectively.

The width of cracks gradually increased with time and additional cracks mainly due to shrinkage developed within the primary crack pattern. The final average crack spacing

therefore reduced with time. The measured maximum final crack widths at age 240 days within Region 2 were 0.22 mm and 0.14 mm for D-SCC-a and D-SCC-b, respectively, and the final average crack spacing were 100 mm and 90 mm respectively. The ratios of final to instantaneous crack spacing were 0.80 for D-SCC-a and 0.68 for D-SCC-b. The ratio of maximum final crack width to the final average crack width was 1.0 and 1.076 for D-SCC-a and D-SCC-b, respectively. The final crack pattern for two identical slabs D-SCC-a and D-SCC-b are illustrated in Figures 7.12 and 7.13 and Tables 7.10 and 7.11, respectively.

Table 7.10 Crack width at different regions for slab D-SCC-a

D-SCC-a		$t = 0$		$t = 240$ days	
M_{max}= 11.24 kNm	M (kNm)	Max.	Avge.	Max.	Avge.
$M \geq 0.99\ M_{max}$	11.13	0.11	0.11	0.22	0.22
$M \geq 0.90\ M_{max}$	10.12	0.09	0.09	0.18	0.18
$M \geq 0.80\ M_{max}$	8.99	0.09	0.08	0.16	0.15
$M \geq 0.70\ M_{max}$	7.87	0.08	0.07	0.14	0.14

Table 7.11 Crack width at different regions for slab D-SCC-b

D-SCC-b		$t = 0$		$t = 240$ days	
M_{max}= 8.33 kNm	M (kNm)	Max.	Avge.	Max.	Avge.
$M \geq 0.99\ M_{max}$	8.25	-	-	-	-
$M \geq 0.90\ M_{max}$	7.50	0.07	0.065	0.14	0.13
$M \geq 0.80\ M_{max}$	6.66	0.06	0.055	0.12	0.11
$M \geq 0.70\ M_{max}$	5.83	0.06	0.055	0.10	0.10

Table 7.12 The measured crack widths for slab D-SCC-a

D-SCC-a		Crack width (mm)	
Crack Number	Distance from edge (roller side) (mm)	t = 14 days	t = 240 days
1	725	-	0.10
2	820	0.06	0.12
3	940	0.06	0.14
4	1010	0.05	0.08
5	1100	0.06	0.12
6	1195	0.08	0.14
7	1350	0.08	0.12
8	1440	0.06	0.16
9	1515	0.09	0.14
10	1603	0.07	0.14
11	1668	0.08	0.14
12	1730	0.09	0.16
13	1830	0.11	0.22
14	1905	0.09	0.18
15	1972	0.08	0.14
16	2100	0.08	0.14
17	2206	0.07	0.14
18	2280	0.07	0.12
19	2390	0.08	0.16
20	2530	-	0.12
21	2555	0.05	0.10
22	2655	-	0.06
23	2750	0.05	0.10
24	2870	0.04	0.10
25	2980	-	0.08
26	3035	-	0.06

Table 7.13 The measured crack widths for slab D-SCC-b

D-SCC-b		Crack width (mm)	
Crack Number	Distance from edge (roller side) (mm)	t = 14 days	t = 240 days
1	630	-	0.05
2	765	-	0.04
3	860	-	0.05
4	935	-	0.08
5	1013	0.04	0.10
6	1085	0.02	0.03
7	1140	0.05	0.10
8	1275	0.05	0.10
9	1385	0.06	0.12
10	1490	0.05	0.10
11	1577	0.06	0.10
12	1705	0.05	0.10
13	1794	0.07	0.14
14	1860	0.06	0.12
15	1960	0.06	0.12
16	2015	0.05	0.10
17	2124	0.06	0.07
18	2155	-	0.08
19	2265	0.06	0.10
20	2390	0.06	0.12
21	2480	-	0.10
22	2570	0.05	0.10
23	2700	0.05	0.06
24	2800	0.05	0.08
25	2910	-	0.04
26	3010	-	0.02

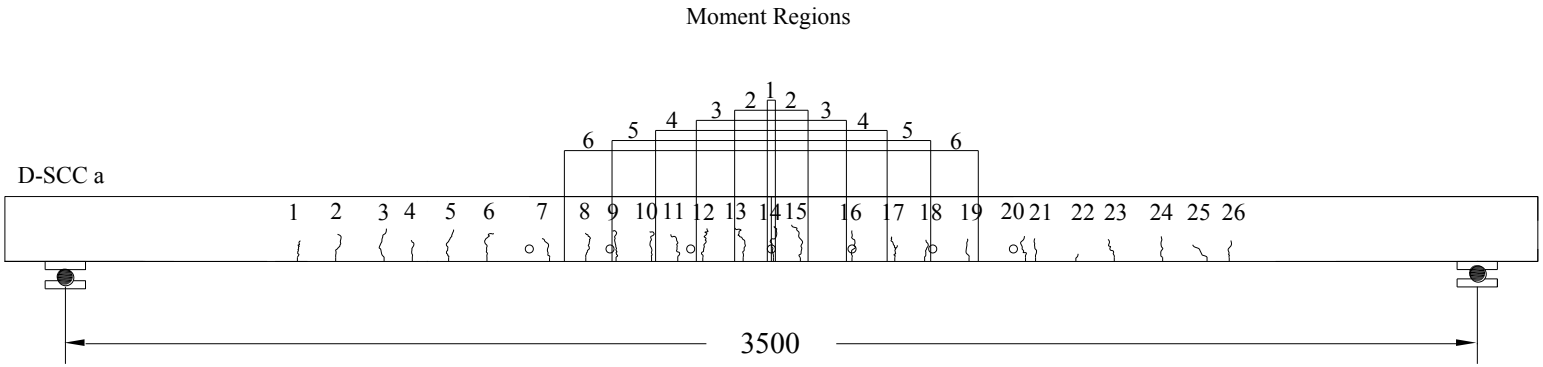

Figure 7.10 Final crack pattern for slab D-SCC-a

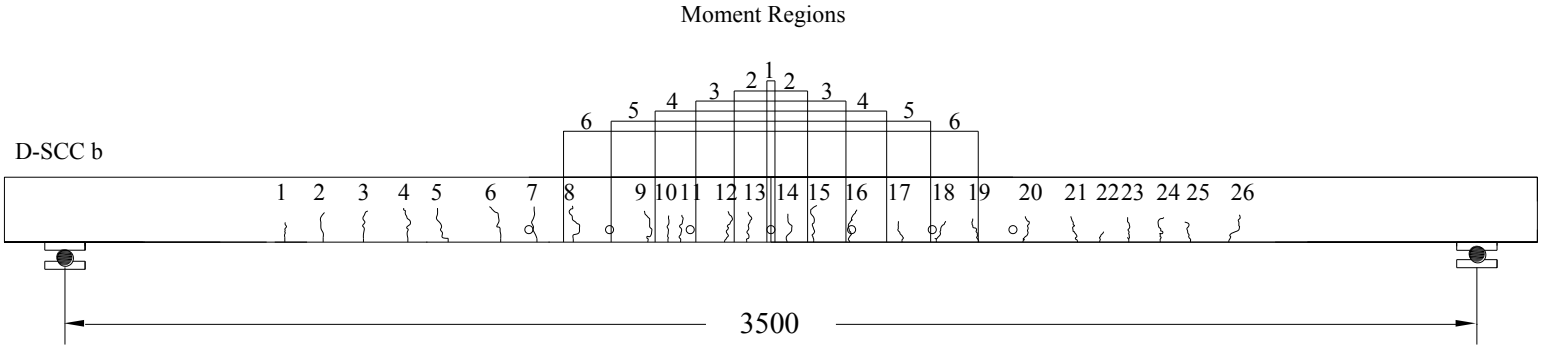

Figure 7.11 Final crack pattern for slab D-SCC-b

7.3.3.2 Deflection

Deflections were monitored and recorded immediately after loading and throughout the test period by a dial gauge installed at the middle of the each span. In Figure 7.12 the measured deflections at the mid-span of slabs D-SCC-a and D-SCC-b versus time are illustrated. The measured long-term deflection of D-SCC-a and D-SCC-b at age 240 days were 17.75 mm and 16.78 mm respectively, which are 2.32 and 2.21 times the corresponding instantaneous deflections, respectively. The ratio of deflections at different ages to instantaneous deflection at mid-span for slabs D-SCC-a and D-SCC-b are presented in Table 7.14.

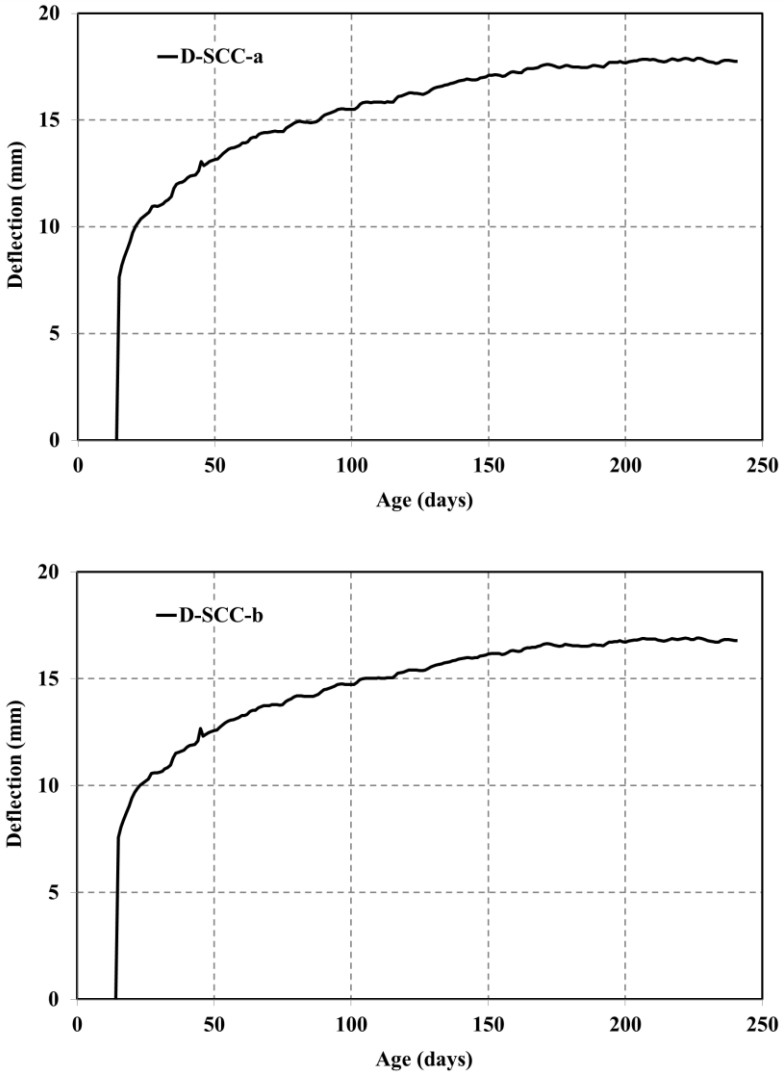

Figure 7.12 Deflection of slabs D-SCC-a and D-SCC-b

Table 7.14 Ratio of deflections at different ages to instantaneous deflection for slabs D-SCC-a and D-SCC-b

Age (days)	14	21	28	45	60	95	122	200	240
D-SCC-a	1.00	1.31	1.43	1.71	1.82	2.03	2.13	2.31	2.32
D-SCC-b	1.00	1.28	1.40	1.67	1.75	1.94	2.03	2.20	2.21

7.3.4 S-SCC-a and S-SCC-b

Slabs S-SCC-a and S-SCC-b (polypropylene fibre SCC mixture) containing 4N12 longitudinal tensile reinforcing bars with 25 mm clear bottom cover were subjected to uniformly distributed sustained loads for 240 days. For S-SCC-a, the sustained uniform load was 5.8 kN/m plus self-weight, and for S-SCC-b, 3.9 kN/m plus self-weight.

7.3.4.1 Cracking Behaviour

To compare the maximum crack width located in different regions with different moment levels, the measured maximum and average crack widths at commencement of the test (t = 0) and at the end (t = 240 days) for slabs S-SCC-a and S-SCC-b are presented in Tables 7.15 and 7.16.

Tables 7.15 and 7.16 show that for long-term loading, maximum and average crack widths are proportional to the bending moment, and the crack width increases linearly by increasing the moment. The results suggest that the largest percentage increase in crack width is in those regions subjected to low levels of bending moment, because the cracks take more time to develop. The visible cracks were developed at age 14 days where the primary crack pattern was established at first loading of slabs. The measured maximum instantaneous crack widths within Region 2 (where $0.99M_{max}>M\geq0.9M_{max}$), were 0.12 mm and 0.06 mm for S-SCC-a and S-SCC-b, respectively. The instantaneous average crack spacing within this region were 121 mm and 127 mm, respectively.

The width of cracks gradually increased with time and additional cracks mainly due to shrinkage developed within the primary crack pattern. The final average crack spacing therefore reduced with time. The measured maximum final crack widths at age 240 days within Region 2 were 0.22 mm and 0.15 mm for S-SCC-a and S-SCC-b, respectively, and the final average crack spacing were 95 mm and 85 mm respectively. The ratios of final to instantaneous crack spacing were 0.78 for S-SCC-a and 0.68 for S-SCC-b. The ratio of maximum final crack width to the final average crack width was 1.1 and 1.0 for S-SCC-a and S-SCC-b, respectively. The final crack pattern for two identical slabs S-SCC-a and S-SCC-b are illustrated in Figures 7.13 and 7.14 and Tables 7.17 and 7.18, respectively.

Table 7.15 Crack width at different regions for slab S-SCC-a

S-SCC-a		$t = 0$		$t = 240$ days	
M_{max}= 11.24 kNm	M (kNm)	Max.	Avge.	Max.	Avge.
$M \geq 0.99\ M_{max}$	11.13	-	-	-	-
$M \geq 0.90\ M_{max}$	10.12	0.12	0.10	0.22	0.20
$M \geq 0.80\ M_{max}$	8.99	0.10	0.09	0.20	0.19
$M \geq 0.70\ M_{max}$	7.87	0.09	0.09	0.18	0.18

Table 7.16 Crack width at different regions for slab S-SCC-b

S-SCC-b		$t = 0$		$t = 240$ days	
M_{max}= 8.33 kNm	M (kNm)	Max.	Avge.	Max.	Avge.
$M \geq 0.99\ M_{max}$	8.25	0.07	0.065	0.15	0.15
$M \geq 0.90\ M_{max}$	7.50	0.06	0.060	0.14	0.14
$M \geq 0.80\ M_{max}$	6.66	0.06	0.045	0.12	0.12
$M \geq 0.70\ M_{max}$	5.83	0.03	0.030	0.11	0.11

Table 7.17 The measured crack widths for slab S-SCC-a

S-SCC-a		Crack width (mm)	
Crack Number	Distance from edge (roller side) (mm)	t = 14 days	t = 240 days
1	710	-	0.07
2	830	-	0.08
3	905	0.03	0.10
4	1040	0.04	0.14
5	1150	0.07	0.20
6	1225	-	0.08
7	1295	0.07	0.14
8	1373	0.07	0.20
9	1502	0.05	0.16
10	1563	0.08	0.18
11	1722	0.09	0.18
12	1792	0.10	0.20
13	1843	0.12	0.22
14	1965	0.08	0.18
15	2005	0.09	0.18
16	2120	0.09	0.18
17	2197	0.09	0.16
18	2320	0.09	0.16
19	2400	0.06	0.14
20	2490	0.05	0.10
21	2572	0.07	0.18
22	2700	0.07	0.14
23	2800	0.04	0.10
24	2865	-	0.08
25	2965	0.03	0.12
26	3060	-	0.10

Table 7.18 The measured crack widths for slab S-SCC-b

S-SCC-b		Crack width (mm)	
Crack Number	Distance from edge (roller side) (mm)	t = 14 days	t = 240 days
1	780	-	0.05
2	840	-	0.06
3	920	-	0.06
4	996	-	0.08
5	1090	-	0.12
6	1205	0.02	0.14
7	1310	0.04	0.09
8	1393	0.03	0.12
9	1470	0.05	0.10
10	1618	0.04	0.12
11	1765	0.03	0.11
12	1845	0.03	0.12
13	1905	0.06	0.14
14	1975	0.07	0.15
15	2063	0.06	0.15
16	2185	0.06	0.12
17	2295	0.03	0.10
18	2410	0.06	0.12
19	2520	0.04	0.12
20	2605	0.05	0.10
21	2645	0.04	0.11
22	2695	0.05	0.08
23	2760	-	0.10
24	2870	-	0.10
25	2990	-	0.08
26	3095	-	0.07
27	3155	-	0.06

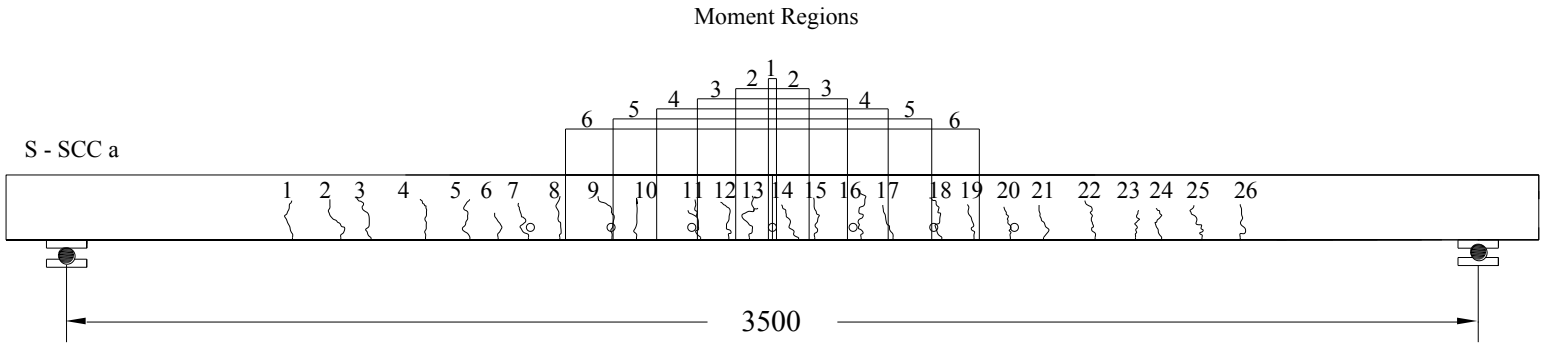

Figure 7.13 Final crack pattern for slab S-SCC-a

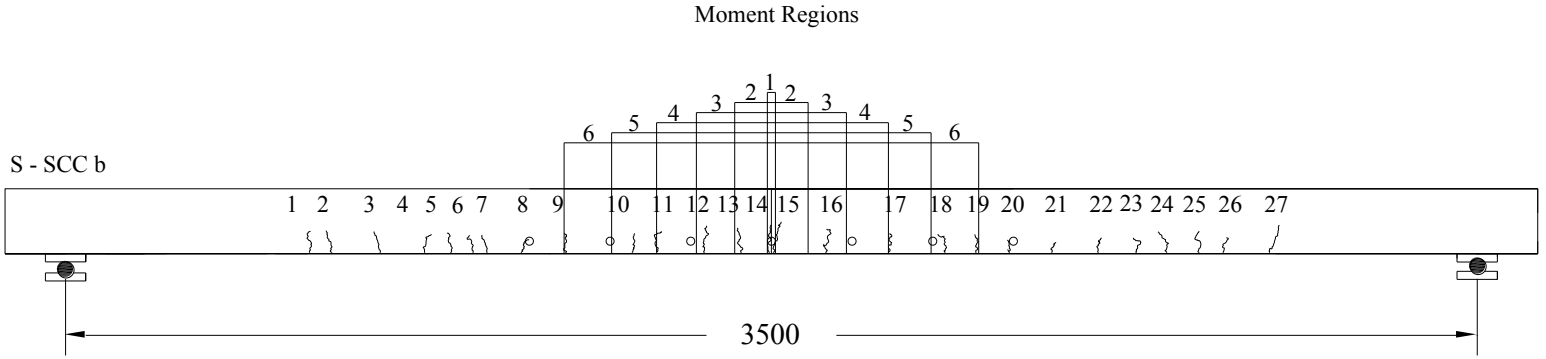

Figure 7.14 Final crack pattern for slab S-SCC-b

7.3.4.2 Deflection

Deflections were monitored and recorded immediately after loading and throughout the test period by a dial gauge installed at the middle of the each span. In Figure 7.15 the measured deflections at the mid-span of slabs S-SCC-a and S-SCC-b versus time are illustrated. The measured long-term deflection of S-SCC-a and S-SCC-b at age 240 days were 22.26 mm and 20.24 mm respectively, which are 3.47 and 6.95 times the corresponding instantaneous deflections, respectively. The ratio of deflections at different ages to instantaneous deflection at mid-span for slabs S-SCC-a and S-SCC-b are presented in Table 7.19.

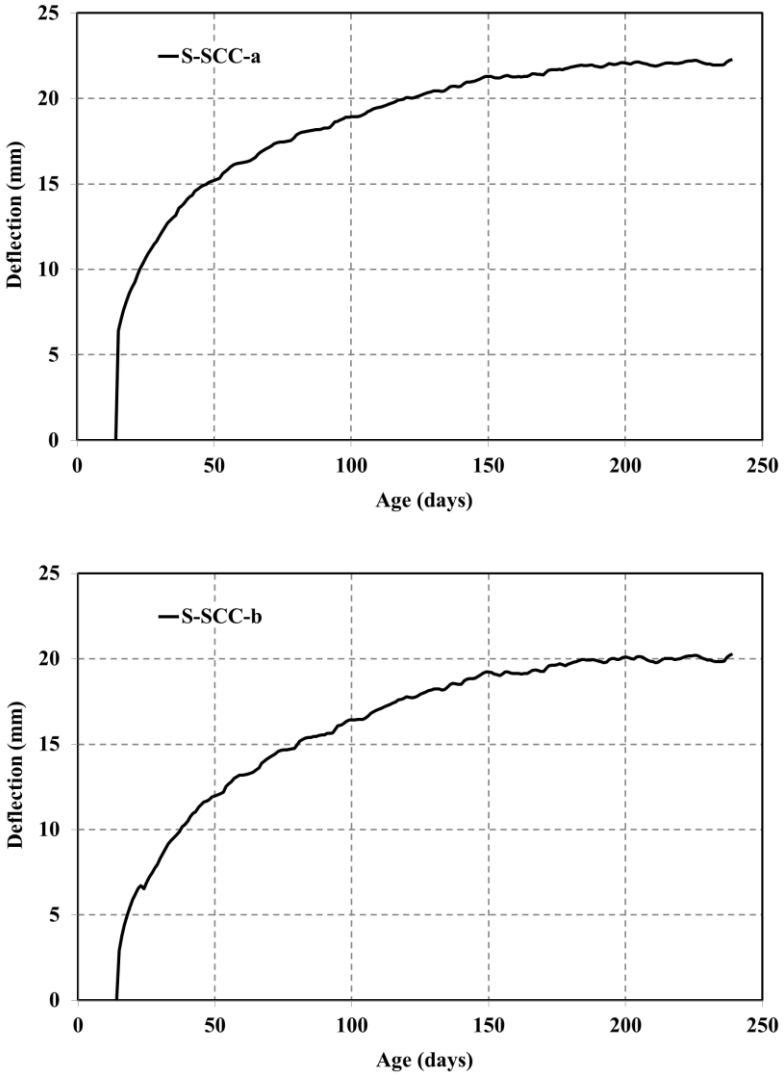

Figure 7.15 Deflection of slabs S-SCC-a and S-SCC-b

Table 7.19 Ratio of deflections at different ages to instantaneous deflection for slabs S-SCC-a and S-SCC-b

Age (days)	14	21	28	45	60	95	122	200	240
S-SCC-a	1.00	1.44	1.79	2.31	2.53	2.91	3.12	3.44	3.47
S-SCC-b	1.00	2.15	2.66	3.94	4.53	5.52	6.09	6.91	6.95

7.3.5 DS-SCC-a and DS-SCC-b

Slabs DS-SCC-a and DS-SCC-b (steel and polypropylene fibres SCC mixture) containing 4N12 longitudinal tensile reinforcing bars with 25 mm clear bottom cover were subjected to uniformly distributed sustained loads for 240 days. For DS-SCC-a, the sustained uniform load was 5.8 kN/m plus self-weight, and for DS-SCC-b, 3.9 kN/m plus self-weight.

7.3.5.1 Cracking Behaviour

To compare the maximum crack width located in different regions with different moment levels, the measured maximum and average crack widths at commencement of the test (t = 0) and at the end (t = 240 days) for slabs DS-SCC-a and DS-SCC-b are presented in Tables 7.20 and 7.21.

Tables 7.20 and 7.21 show that for long-term loading, maximum and average crack widths are proportional to the bending moment, and the crack width increases linearly by increasing the moment. The results suggest that the largest percentage increase in crack width is in those regions subjected to low levels of bending moment, because the cracks take more time to develop. The visible cracks were developed at age 14 days where the primary crack pattern was established at first loading of slabs. The measured maximum instantaneous crack widths within Region 2 (where $0.99M_{max}>M\geq0.9M_{max}$), were 0.10 mm and 0.06 mm for DS-SCC-a and DS-SCC-b, respectively. The instantaneous average crack spacing within this region were 129 mm and 133 mm, respectively.

The width of cracks gradually increased with time and additional cracks mainly due to shrinkage developed within the primary crack pattern. The final average crack spacing therefore reduced with time. The measured maximum final crack widths at age 240 days within Region 2 were 0.20 mm and 0.14 mm for DS-SCC-a and DS-SCC-b, respectively, and the final average crack spacing were 102 mm and 88 mm respectively. The ratios of final to instantaneous crack spacing were 0.79 for DS-SCC-a and 0.66 for DS-SCC-b. The ratio of maximum final crack width to the final average crack width was 1.0 and 1.12 for DS-SCC-a and DS-SCC-b, respectively. The final crack pattern for two identical slabs DS-SCC-a and DS-SCC-b are illustrated in Figures 7.16 and 7.17 and Tables 7.22 and 7.23, respectively.

Table 7.20 Crack width at different regions for slab DS-SCC-a

DS-SCC-a		$t = 0$		$t = 240$ days	
M_{max}= 11.24 kNm	M (kNm)	Max.	Avge.	Max.	Avge.
$M \geq 0.99\ M_{max}$	11.13	0.100	0.100	0.200	0.200
$M \geq 0.90\ M_{max}$	10.12	-	-	-	-
$M \geq 0.80\ M_{max}$	8.99	0.100	0.090	0.200	0.190
$M \geq 0.70\ M_{max}$	7.87	0.080	0.075	0.180	0.170

Table 7.21 Crack width at different regions for slab DS-SCC-b

DS-SCC-b		$t = 0$		$t = 240$ days	
M_{max}= 8.33 kNm	M (kNm)	Max.	Avge.	Max.	Avge.
$M \geq 0.99\ M_{max}$	8.25	-	-	-	-
$M \geq 0.90\ M_{max}$	7.50	0.060	0.055	0.140	0.125
$M \geq 0.80\ M_{max}$	6.66	0.050	0.050	0.120	0.120
$M \geq 0.70\ M_{max}$	5.83	0.050	0.045	0.110	0.105

Table 7.22 The measured crack widths for slab DS-SCC-a

DS-SCC-a		Crack width (mm)	
Crack Number	Distance from edge (roller side) (mm)	t = 14 days	t = 240 days
1	700	-	0.04
2	765	0.03	0.10
3	865	0.03	0.11
4	987	0.04	0.11
5	1100	0.05	0.10
6	1180	0.04	0.10
7	1250	0.07	0.13
8	1360	0.06	0.14
9	1467	0.06	0.13
10	1560	0.08	0.16
11	1656	0.07	0.16
12	1760	0.10	0.20
13	1900	0.10	0.20
14	1995	0.08	0.18
15	2100	0.08	0.18
16	2210	0.06	0.14
17	2310	0.07	0.14
18	2380	0.07	0.13
19	2490	-	0.20
20	2570	0.04	0.12
21	2655	0.08	0.20
22	2780	0.05	0.11
23	2870	-	0.10
24	2942	0.06	0.14
25	3050	0.04	0.10

Table 7.23 The measured crack widths for slab DS-SCC-b

DS-SCC-b		Crack width (mm)	
Crack Number	Distance from edge (roller side) (mm)	t = 14 days	t = 240 days
1	770	-	0.04
2	860	0.02	0.08
3	986	0.02	0.05
4	1095	0.03	0.10
5	1160	-	0.04
6	1230	0.04	0.10
7	1350	0.03	0.08
8	1450	0.04	0.09
9	1540	0.04	0.08
10	1610	0.04	0.10
11	1699	0.04	0.10
12	1810	0.04	0.10
13	1880	0.05	0.12
14	1970	0.06	0.14
15	2047	0.06	0.12
16	2135	0.05	0.11
17	2190	0.05	0.11
18	2260	-	0.07
19	2335	0.06	0.12
20	2395	0.02	0.08
21	2440	-	0.05
22	2510	0.04	0.10
23	2618	0.05	0.11
24	2760	-	0.06
25	2825	0.03	0.06
26	2960	-	0.04
27	3070	0.02	0.05

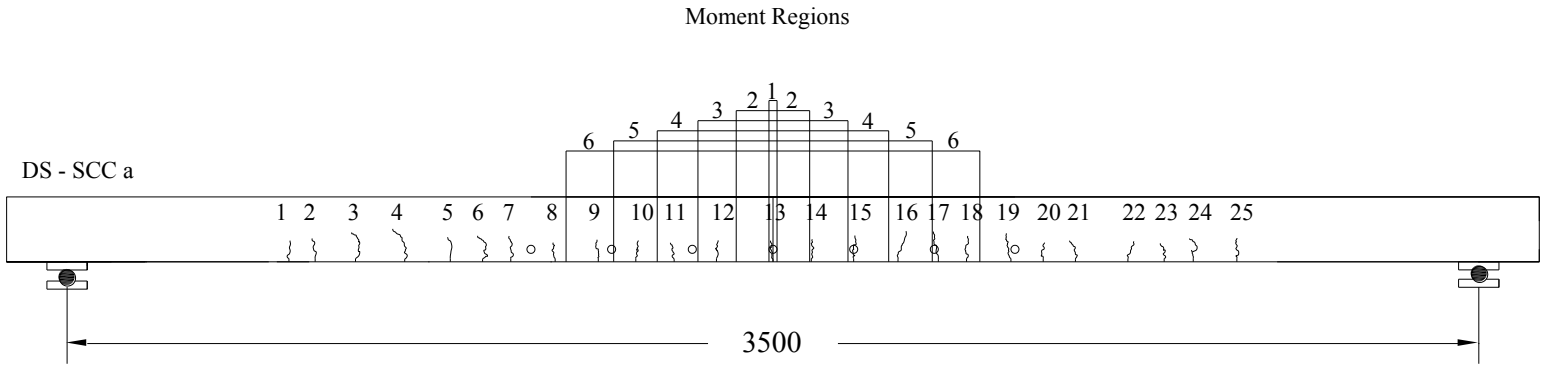

Figure 7.16 Final crack pattern for slab DS-SCC-a

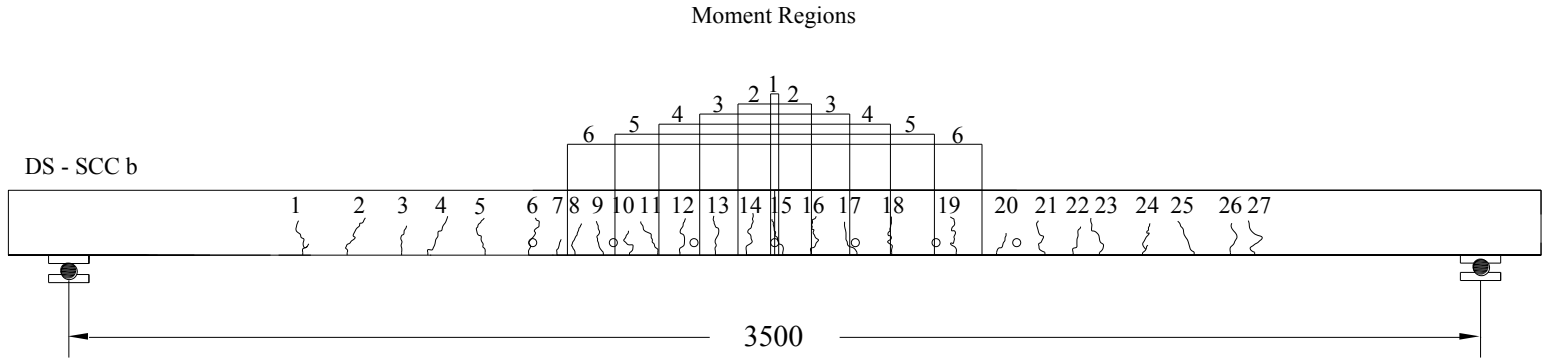

Figure 7.17 Final crack pattern for slab DS-SCC-b

7.3.5.2 Deflection

Deflections were monitored and recorded immediately after loading and throughout the test period by a dial gauge installed at the middle of the each span. In Figure 7.18 the measured deflections at the mid-span of slabs DS-SCC-a and DS-SCC-b versus time are illustrated. The measured long-term deflection of DS-SCC-a and DS-SCC-b at age 240 days were 21.30 mm and 15.83 mm respectively, which are 2.37 and 3.08 times the corresponding instantaneous deflections, respectively. The ratio of deflections at different ages to instantaneous deflection at mid-span for slabs DS-SCC-a and DS-SCC-b are presented in Table 7.24.

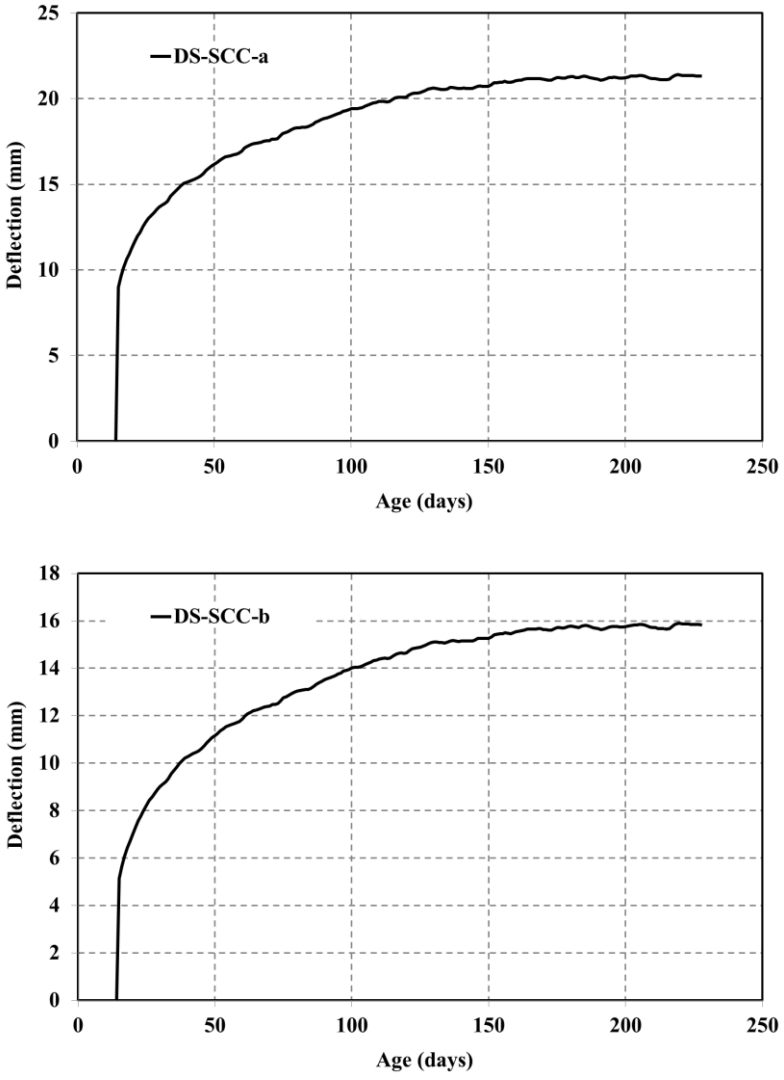

Figure 7.18 Deflection of slabs DS-SCC-a and DS-SCC-b

Table 7.24 Ratio of deflections at different ages to instantaneous deflection for slabs DS-SCC-a and DS-SCC-b

Age (days)	14	21	28	45	60	95	122	200	240
DS-SCC-a	1.00	1.30	1.48	1.72	1.89	2.13	2.26	2.36	2.37
DS-SCC-b	1.00	1.42	1.70	2.06	2.31	2.67	2.88	3.06	3.08

7.3.6 N-CC-a and N-CC-b, Nejadi (2005)

Slabs N-CC-a and N-CC-b (CC mixture) containing 4N12 longitudinal tensile reinforcing bars with 25 mm clear bottom cover were subjected to uniformly distributed sustained loads for 240 days. For N-CC-a, the sustained uniform load was 5.8 kN/m plus self-weight, and for N-CC-b, 3.9 kN/m plus self-weight.

7.3.6.1 Cracking Behaviour

To compare the maximum crack width located in different regions with different moment levels, the measured maximum and average crack widths at commencement of the test (t = 0) and at the end (t = 394 days) for slabs N-CC-a and N-CC-b are presented in Tables 7.25 and 7.26.

Tables 7.25 and 7.26 show that for long-term loading, maximum and average crack widths are proportional to the bending moment, and the crack width increases linearly by increasing the moment. The results suggest that the largest percentage increase in crack width is in those regions subjected to low levels of bending moment, because the cracks take more time to develop. The visible cracks were developed at age 14 days where the primary crack pattern was established at first loading of slabs. The measured maximum instantaneous crack widths within Region 2 (where $0.99M_{max}>M\geq0.9M_{max}$), were 0.10 mm and 0.05 mm for N-CC-a and N-CC-b, respectively. The instantaneous average crack spacing within this region were 153 mm and 141 mm, respectively.

The width of cracks gradually increased with time and additional cracks mainly due to shrinkage developed within the primary crack pattern. The final average crack spacing therefore reduced with time. The measured maximum final crack widths at age 394 days within Region 2 were 0.25 mm and 0.20 mm for N-CC-a and N-CC-b, respectively, and the final average crack spacing were 102 mm and 136 mm respectively. The ratios of final to instantaneous crack spacing were 0.67 for N-CC-a and 0.96 for N-CC-b. The ratio of maximum final crack width to the final average crack width was 1.47 and 1.17 for N-CC-a and N-CC-b, respectively. The final crack pattern for two identical slabs N-CC-a and N-CC-b are illustrated in Figures 7.19 and 7.20, respectively.

Table 7.25 Crack width at different regions for slab N-CC-a (Nejadi, 2005)

N-CC-a		$t = 0$		$t = 394$ days	
M_{max}= 11.24 kNm	M (kNm)	Max.	Avge.	Max.	Avge.
$M \geq 0.99\ M_{max}$	11.13	0.10	0.10	0.25	0.17
$M \geq 0.90\ M_{max}$	10.12	0.10	0.09	0.2	0.15
$M \geq 0.80\ M_{max}$	8.99	0.08	0.07	0.18	0.15
$M \geq 0.70\ M_{max}$	7.87	0.05	0.05	0.18	0.14

Table 7.26 Crack width at different regions for slab N-CC-b (Nejadi, 2005)

N-CC-b		$t = 0$		$t = 394$ days	
M_{max}= 8.33 kNm	M (kNm)	Max.	Avge.	Max.	Avge.
$M \geq 0.99\ M_{max}$	8.25	0.08	0.07	0.20	0.17
$M \geq 0.90\ M_{max}$	7.50	0.05	0.05	0.18	0.13
$M \geq 0.80\ M_{max}$	6.66	0.05	0.04	0.13	0.11

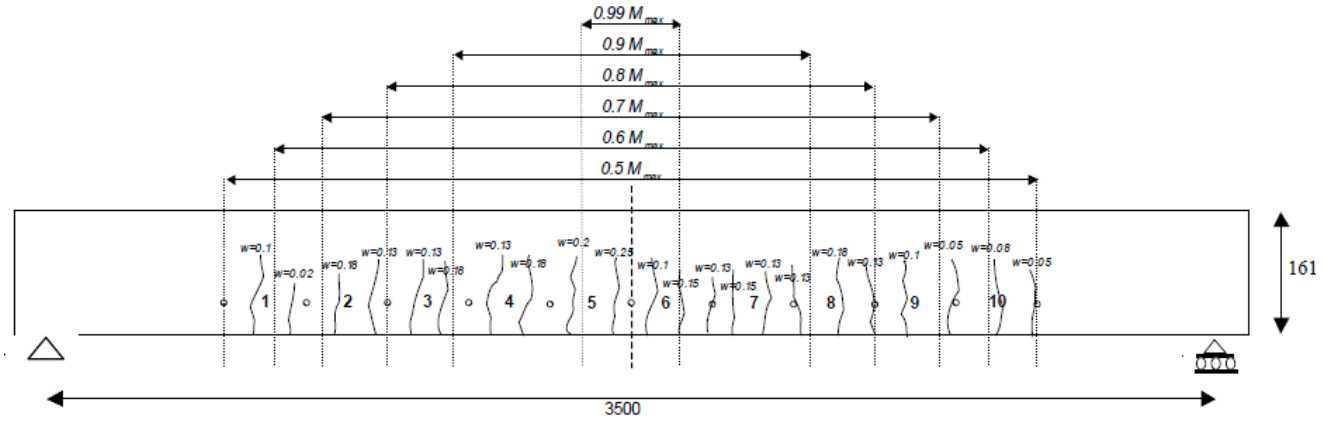

Figure 7.19 Final crack pattern for slab N-CC-a (Nejadi, 2005) - Not scaled

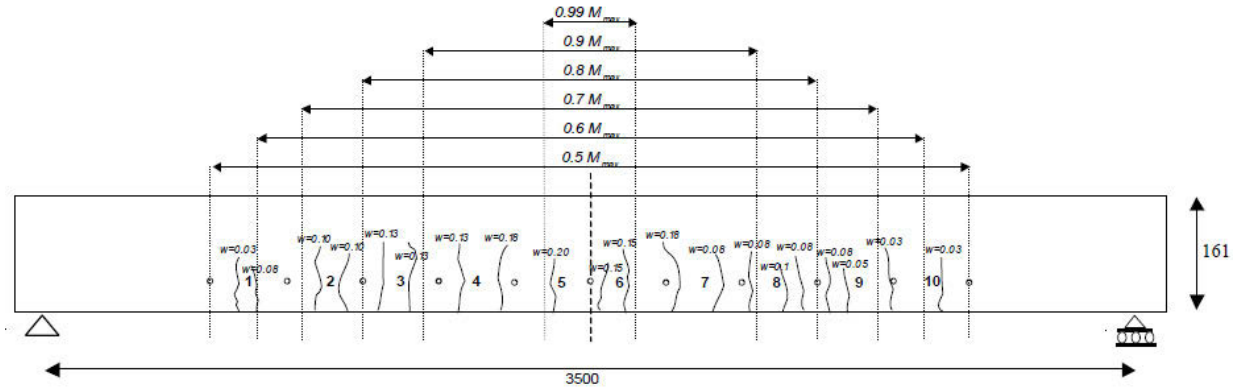

Figure 7.20 Final crack pattern for slab N-CC-b (Nejadi, 2005) - Not scaled

7.3.6.2 Deflection

Deflections were monitored and recorded immediately after loading and throughout the test period by a dial gauge installed at the middle of the each span. In Figure 7.21 the measured deflections at the mid-span of slabs N-CC-a and N-CC-b versus time are illustrated. The measured long-term deflection of N-CC-a and N-CC-b at age 394 days were 32.5 mm and 22.90 mm respectively, which are 2.75 and 4.54 times the corresponding instantaneous deflections, respectively. The ratio of deflections at different ages to instantaneous deflection at mid-span for slabs N-CC-a and N-CC-b are presented in Table 7.27.

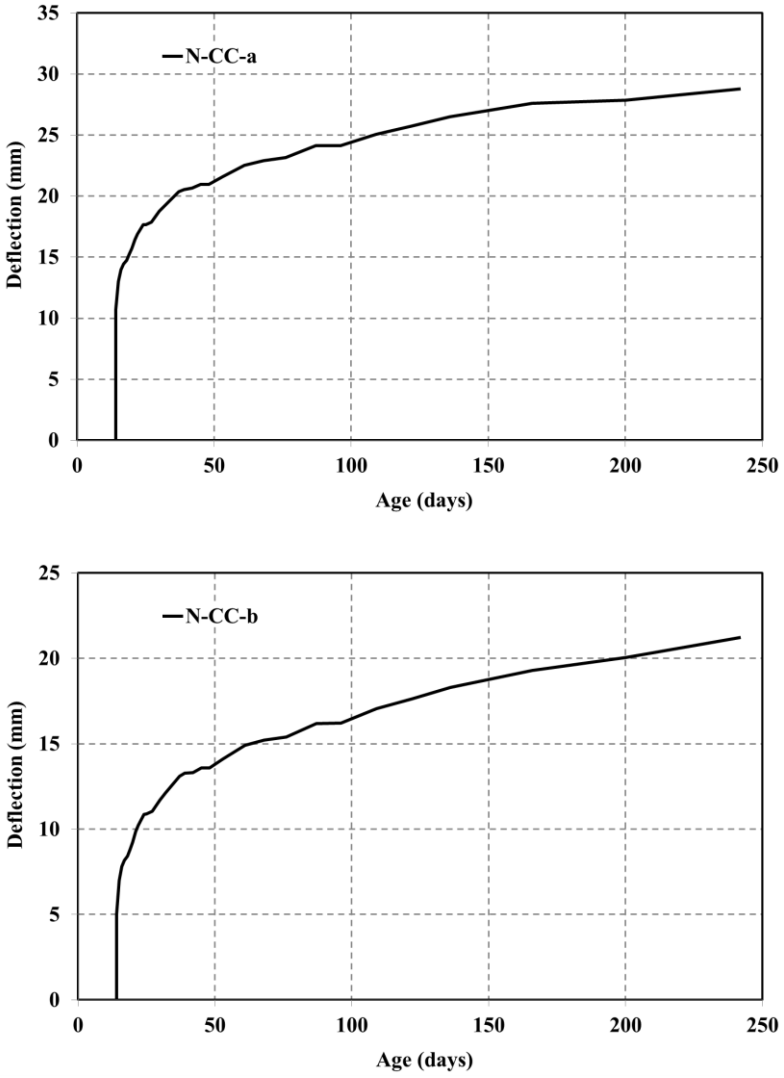

Figure 7.21 Deflection of slabs N-CC-a and N-CC-b (Nejadi, 2005)

Table 7.27 Ratio of deflections at different ages to instantaneous deflection for slabs N-CC-a and N-CC-b (Nejadi, 2005)

Age (days)	14	21	28	45	60	95	122	200	285	330	394
N-CC-a	1.00	1.54	1.67	1.96	2.10	2.25	2.40	2.61	2.72	2.77	2.79
N-CC-b	1.00	1.96	2.19	2.69	2.96	3.21	3.50	3.98	4.35	4.45	4.54

7.4 TIME-DEPENDENT BOND SHEAR STRESS

Following the procedures presented in Section 6.4 to investigate the influence of the assumed bond shear stress on the predicted crack width, five different values for bond shear stress ($\tau_b = f_{ct}$, $\tau_b = 1.5\ f_{ct}$, $\tau_b = 2\ f_{ct}$, $\tau_b = 3\ f_{ct}$, and $\tau_b = \lambda_1\ \lambda_2\ \lambda_3\ f_{ct}$) were considered. Following the CEB proposal which accounts for the breakdown of tension stiffening under long-term or cyclic loading, each value was reduced by a factor of one half ($\tau_b(t) = 0.5\ f_{ct}$, $\tau_b(t) = f_{ct}$ and $\tau_b(t) = 1.5\ f_{ct}$) for time-dependent behaviour. Time-dependent crack width calculations for concrete reinforced with bars only are different from concrete reinforced with bars and fibres, as described in sections 7.4.1 and 7.4.2.

7.4.1 Steel Bar Reinforcement Concrete

According to section 6.4.1, maximum crack width calculation for long-term behaviour can be presented as follows: Under sustained load, additional cracks occur between widely spaced cracks (usually when $0.67 s_{max} < s \leq s_{max}$). The additional cracks are due to the combined effect of tensile creep rupture and shrinkage. As a consequence, the number of cracks increases and the maximum crack spacing reduces with time. The final maximum crack spacing, s^* is only about two-thirds of that given by Eq. 6.12, but the final minimum crack spacing remains about half of the value given by Eq. 6.12.

$$s^* = \frac{2}{3} \times \frac{f_{ct}\ d_b}{2\ \tau_b\ \rho_{tc}} \tag{7.1}$$

As Nejadi (2005) presented, experimental observations indicate that τ_b decreases with time, probably as a result of shrinkage-induced slip and tensile creep. Hence, the stress in

the tensile concrete between the cracks gradually reduces. Furthermore, although creep and shrinkage will cause a small increase in the resultant tensile force T in the real beam and a slight reduction in the internal lever arm, this effect is relatively small and is ignored in the tension chord model presented here. The final crack width is the elongation of the steel over the distance between the cracks minus the extension of the concrete caused by σ_{cz} plus the shortening of the concrete between the cracks due to shrinkage. For a final maximum crack spacing of s^*, the final maximum crack width at the member soffit is:

$$\left(w^*\right)_{soffit} = \frac{s^*}{E_s}\left[\frac{T}{A_{st}} - \frac{\tau_b\, s^*}{d_b}\left(1 + n_e\, \rho_{tc}\right) - \varepsilon_{sh}\, E_s\right] \tag{7.2}$$

the effective modular ratio: $n_e = \dfrac{E_s}{E_e}$ (7.3)

the effective modulus: $E_e = \dfrac{E_c}{\left(1 + \varphi(t,\tau)\right)}$ (7.4)

where ε_{sh} is the shrinkage strain in the tensile concrete (and is a negative value); E_c and E_s are the elastic moduli of the concrete and steel respectively; and $\varphi(t,\tau)$ is the creep coefficient of the concrete.

7.4.2 Steel Bar Reinforcement Concrete with Fibres

Following the section 6.4.2, maximum crack width calculation for long-term behaviour is presented as follows: Leutbecher and Fehling (2008) have derived a cracking behaviour model based on the assumptions of constant bond stress and a parabolic development of concrete and steel strains between the cracks. Eq. (6.19) can be re-written for the stabilized cracking as (refer to Figure 7.22):

$$w_s = s_r\left(\varepsilon_{sm} - \varepsilon_{cm}\right) = s_r\left[\frac{\sigma_s}{E_s} - \alpha_b\left(\frac{2\, s_r\, \tau_{sm}}{d_s\, E_s}\left(1 + \alpha_{E,s}\, \rho_s / \gamma\right) + \frac{\sigma_{cf}}{\gamma\, E_s}\,\alpha_{E,s} - \varepsilon^*_{f,shr}\,\alpha_{E,f}\,\eta\,\rho_f\right) - \varepsilon^*_{shr}\right] \tag{7.5}$$

$$s_{r,max} = \left(\sigma^i_{cf,cr} - \sigma_{cf0}\right)\frac{d_s}{2\,\tau_{sm}\,\rho_s} \tag{7.6}$$

$$\varepsilon^{*}_{shr} = \varepsilon_{s,shr}\left(1+\alpha_{E,s}\ \rho_s / \gamma\right)+\varepsilon_{f,shr}\ \alpha_{E,f}\ \eta\ \rho_f \tag{7.7}$$

$$\varepsilon^{*}_{f,shr} = \varepsilon_{f,shr}\ \gamma \tag{7.8}$$

$$\gamma = 1+\rho_f\ \left(\eta\ \alpha_{E,f}-1\right) \tag{7.9}$$

where σ_{cf} is the stress in the fibre reinforced concrete (Eqs. 6.22 and 6.23), $\varepsilon_{f,shr}$ is the shrinkage shortening of the fibres, τ_{sm} is the average bond stress over load transmission length, d_b is the reinforcing bar diameter, E_s is the modulus of elasticity of reinforcing bar, ρ_s is the reinforcing ratio of steel reinforcement, ρ_f is the fibre content, η is the fibre orientation coefficient; α_b is the shape coefficient of strain courses (α_b = 0.6 for short term loading, α_b = 0.4 for long term or repeated loading); $\alpha_{E,s}$ is the ratio of the modulus of elasticity of steel to the modulus of elasticity of concrete. $\alpha_{E,s} = E_s/E_c$; $\alpha_{E,f}$ is the ratio of the modulus of elasticity of fibre to the modulus of elasticity of concrete. $\alpha_{E,f} = E_f/E_c$. Refer to Figure 7.22 for definitions of the various stresses used in this model.

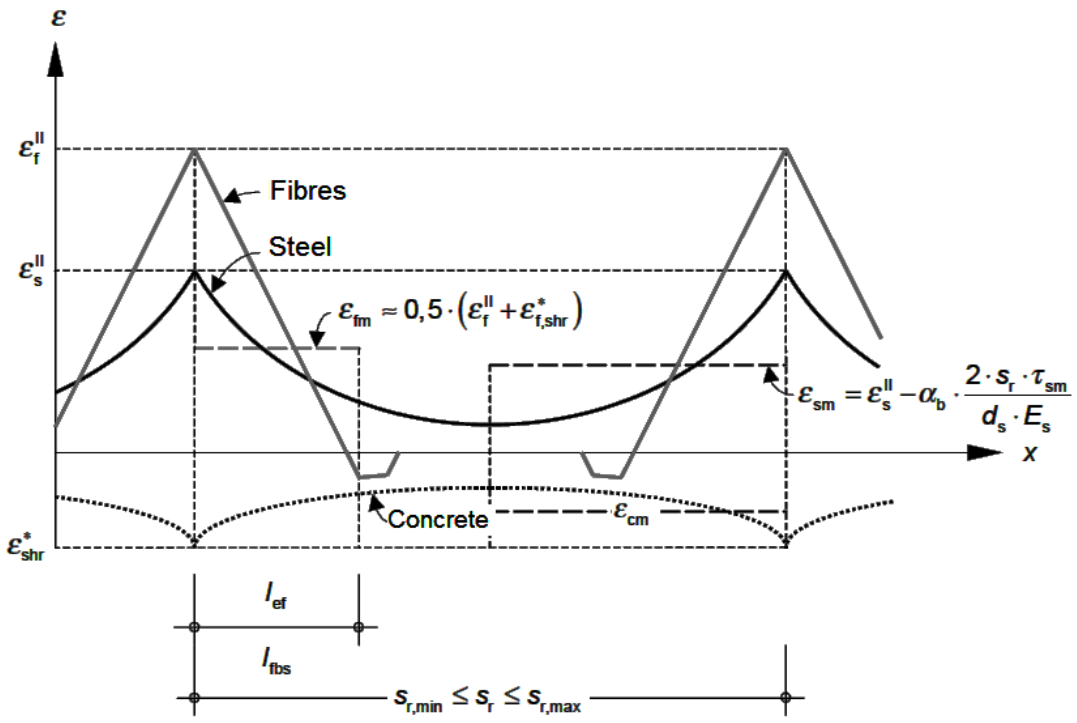

Figure 7.22 Stabilized cracking - Qualitative distribution of strains for the bar and fibres reinforcement and for the matrix, considering the influence of shrinkage (Leutbecher and Fehling, 2008)

7.4.3 Crack Width Calculations with Different Bond Shear Stress

For N-SCC mix, Eq.(7.2) is used for time-dependent crack width calculations and for D-SCC, S-SCC, and DS-SCC mixes, Eq.(7.5) is used. The results are presented in Tables 7.28 to 7.31. Measured and calculated maximum crack widths versus steel stress are illustrated in Figures 7.23 to 7.26. Also, the results of Nejadi (2005) are presented for comparison with SCC mixtures in Figure 7.27 and Table 7.32.

Table 7.28 Measured and calculated maximum crack width for slab N-SCC series

	N-SCC			Bond Stress			
	M (kNm)	σ_{st} (MPa)	Experiment	$\tau_b = 0.5\ f_{ct}$	$\tau_b = f_{ct}$	$\tau_b = 1.5\ f_{ct}$	$\tau_b = \lambda_1\ \lambda_2\ \lambda_3\ f_{ct}$
			w_{max} (mm)	w_{max} (mm)			
N-SCC-a	11.13	207.94	0.24	0.658	0.329	0.219	0.151
	10.12	189.07	0.23	0.616	0.308	0.205	0.133
	8.99	167.96	0.22	0.569	0.284	0.190	0.115
	7.87	147.03	0.20	0.522	0.261	0.174	0.100
N-SCC-b	8.25	154.13	0.18	0.538	0.269	0.179	0.105
	7.50	140.12	0.16	0.507	0.253	0.169	0.095
	6.66	124.43	0.16	0.472	0.236	0.157	0.085
	5.83	108.92	0.12	0.437	0.219	0.146	0.076

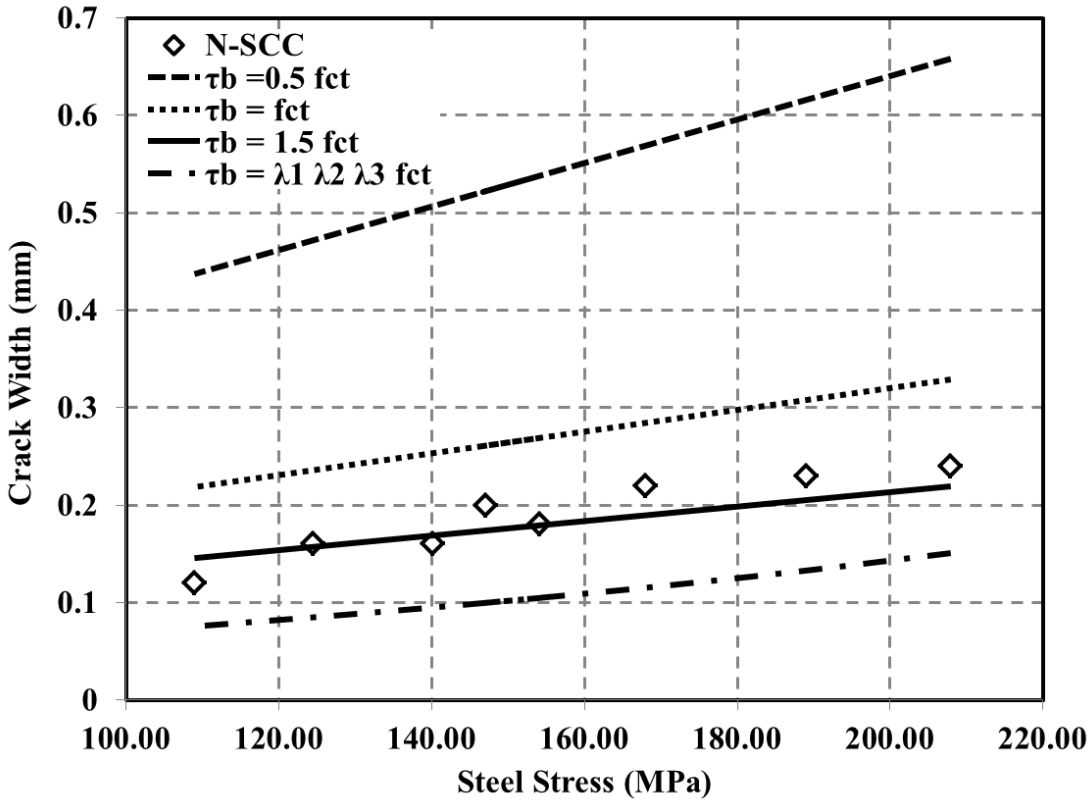

Figure 7.23 Comparison of different bond stresses for slab N-SCC series

Table 7.29 Measured and calculated maximum crack width for slab D-SCC series

	D-SCC			Bond Stress			
	M (kNm)	σ_{st} (MPa)	Experiment w_{max} (mm)	$\tau_b = 0.5\, f_{ct}$	$\tau_b = f_{ct}$	$\tau_b = 1.5\, f_{ct}$	$\tau_b = \lambda_1\, \lambda_2\, \lambda_3\, f_{ct}$
				w_{max} (mm)			
D-SCC-a	11.13	207.85	0.22	0.552	0.276	0.184	0.126
	10.12	188.99	0.18	0.513	0.256	0.171	0.111
	8.99	167.88	0.16	0.469	0.235	0.156	0.095
	7.87	146.97	0.14	0.426	0.213	0.142	0.081
D-SCC-b	8.25	154.06	-	0.441	0.220	0.147	0.086
	7.50	140.06	0.14	0.412	0.206	0.137	0.077
	6.66	124.37	0.12	0.380	0.190	0.127	0.068
	11.13	207.85	0.22	0.552	0.276	0.184	0.126

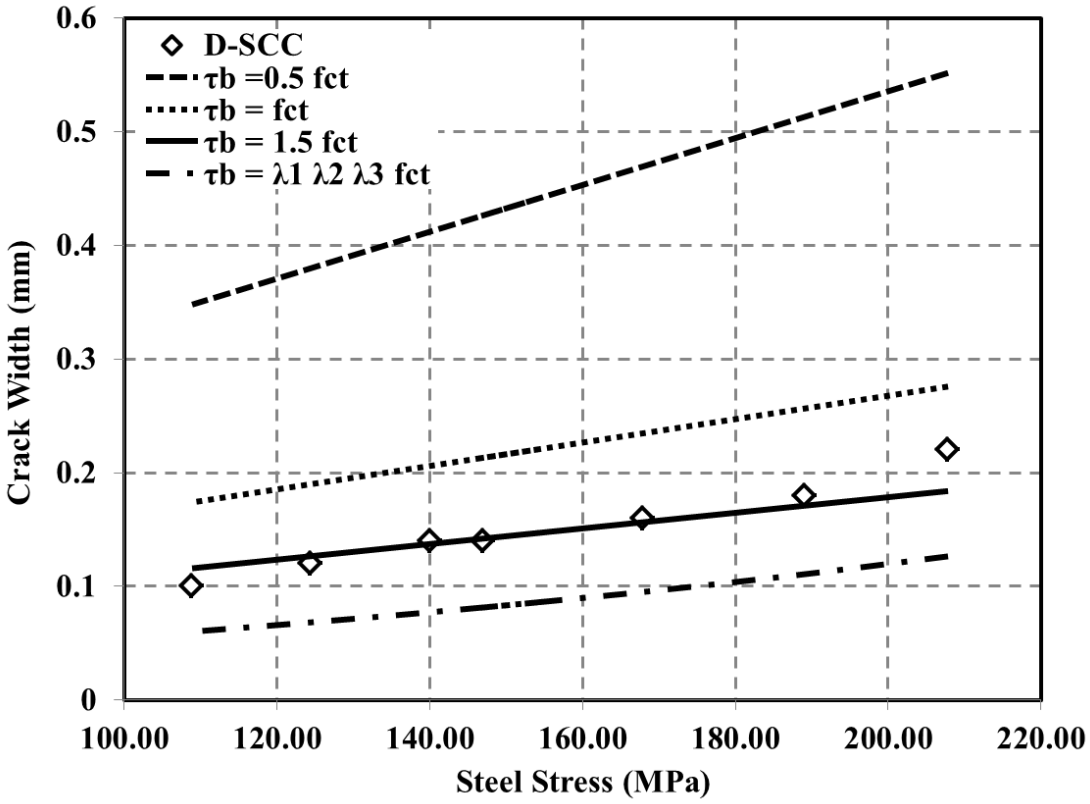

Figure 7.24 Comparison of different bond stresses for slab D-SCC series

Table 7.30 Measured and calculated maximum crack width for slab S-SCC series

	S-SCC			Bond Stress			
	M (kNm)	σ_{st} (MPa)	Experiment w_{max} (mm)	$\tau_b = 0.5\, f_{ct}$	$\tau_b = f_{ct}$	$\tau_b = 1.5\, f_{ct}$	$\tau_b = \lambda_1\, \lambda_2\, \lambda_3\, f_{ct}$
				w_{max} (mm)			
S-SCC-a	11.13	207.85	-	0.642	0.321	0.214	0.147
	10.12	188.99	0.22	0.602	0.301	0.201	0.130
	8.99	167.88	0.20	0.557	0.278	0.186	0.113
	7.87	146.97	0.18	0.512	0.256	0.171	0.098
S-SCC-b	8.25	154.06	0.15	0.527	0.264	0.176	0.103
	7.50	140.06	0.14	0.497	0.249	0.166	0.093
	6.66	124.37	0.12	0.463	0.232	0.154	0.116
	5.83	108.87	0.11	0.430	0.215	0.143	0.074

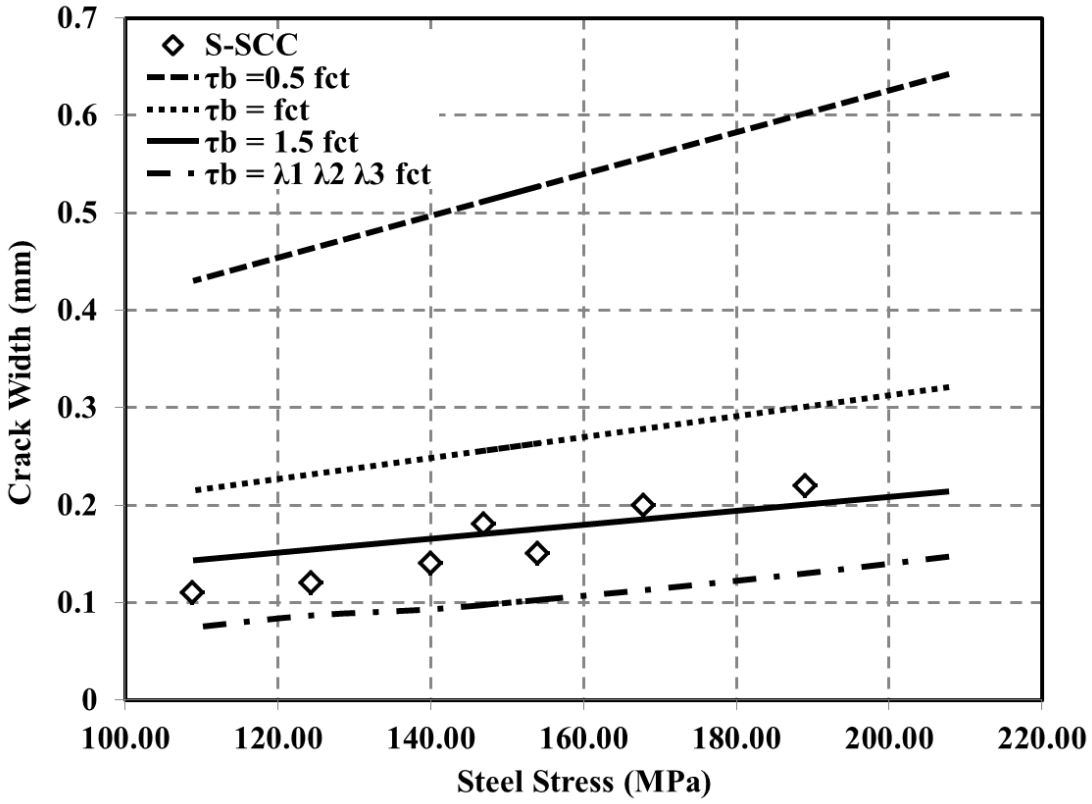

Figure 7.25 Comparison of different bond stresses for slab S-SCC series

Table 7.31 Measured and calculated maximum crack width for slab DS-SCC series

	DS-SCC			Bond Stress			
	M (kNm)	σ_{st} (MPa)	Experiment w_{max} (mm)	$\tau_b = 0.5\, f_{ct}$	$\tau_b = f_{ct}$	$\tau_b = 1.5\, f_{ct}$	$\tau_b = \lambda_1\, \lambda_2\, \lambda_3\, f_{ct}$
				w_{max} (mm)			
DS-SCC-a	11.13	207.77	0.20	0.621	0.311	0.207	0.142
	10.12	188.91	-	0.581	0.291	0.194	0.131
	8.99	167.82	0.20	0.536	0.268	0.179	0.113
	7.87	146.91	0.18	0.491	0.245	0.164	0.094
DS-SCC-b	8.25	154.00	-	0.506	0.253	0.169	0.099
	7.50	140.00	0.14	0.476	0.238	0.159	0.089
	6.66	124.32	0.12	0.442	0.221	0.147	0.080
	5.83	108.83	0.11	0.409	0.205	0.136	0.071

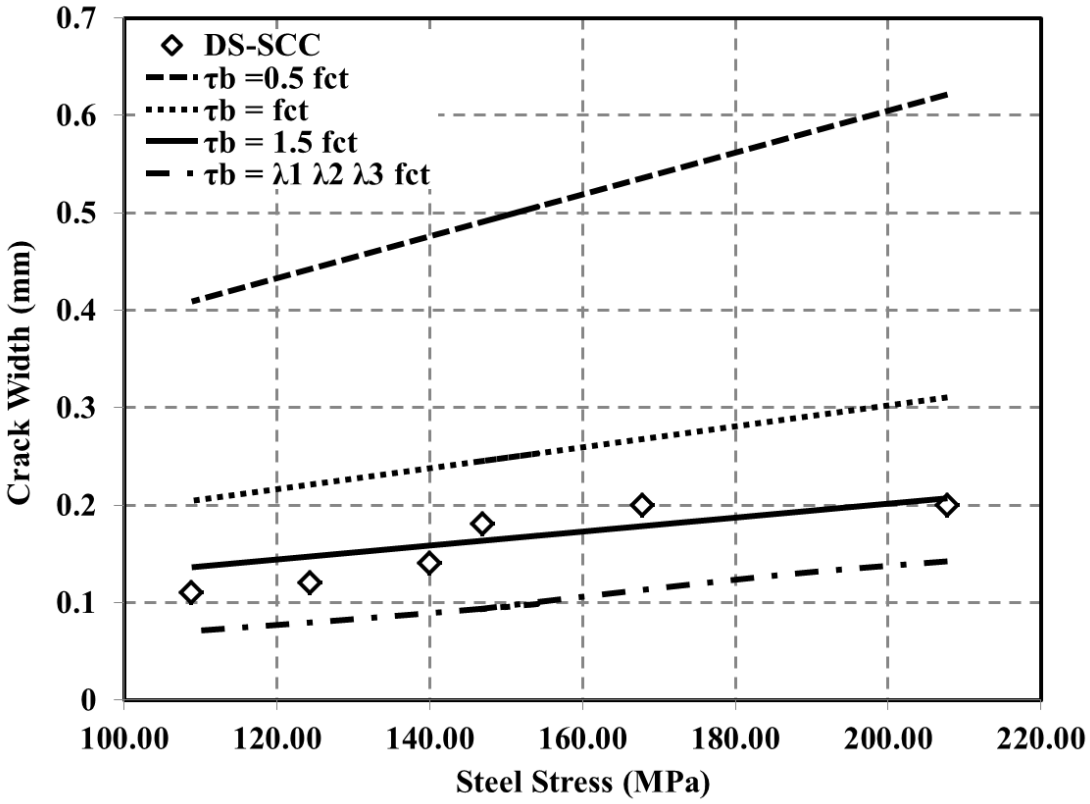

Figure 7.26 Comparison of different bond stresses for slab DS-SCC series

Table 7.32 Measured and calculated maximum crack width for slab N-CC series

	N-CC			Bond Stress			
	M (kNm)	σ_{st} (MPa)	Experiment w_{max} (mm)	$\tau_b = 0.5\,f_{ct}$	$\tau_b = f_{ct}$	$\tau_b = 1.5\,f_{ct}$	$\tau_b = \lambda_1\,\lambda_2\,\lambda_3\,f_{ct}$
				w_{max} (mm)			
N-CC-a	11.13	211.18	0.25	0.639	0.320	0.213	0.148
	10.12	192.01	0.20	0.598	0.299	0.199	0.130
	8.99	170.57	0.18	0.553	0.276	0.184	0.113
	7.87	149.32	0.18	0.507	0.254	0.169	0.098
N-CC-b	8.25	156.53	0.20	0.523	0.261	0.174	0.103
	7.50	142.30	0.18	0.492	0.246	0.164	0.093
	6.66	126.36	0.13	0.458	0.229	0.153	0.083

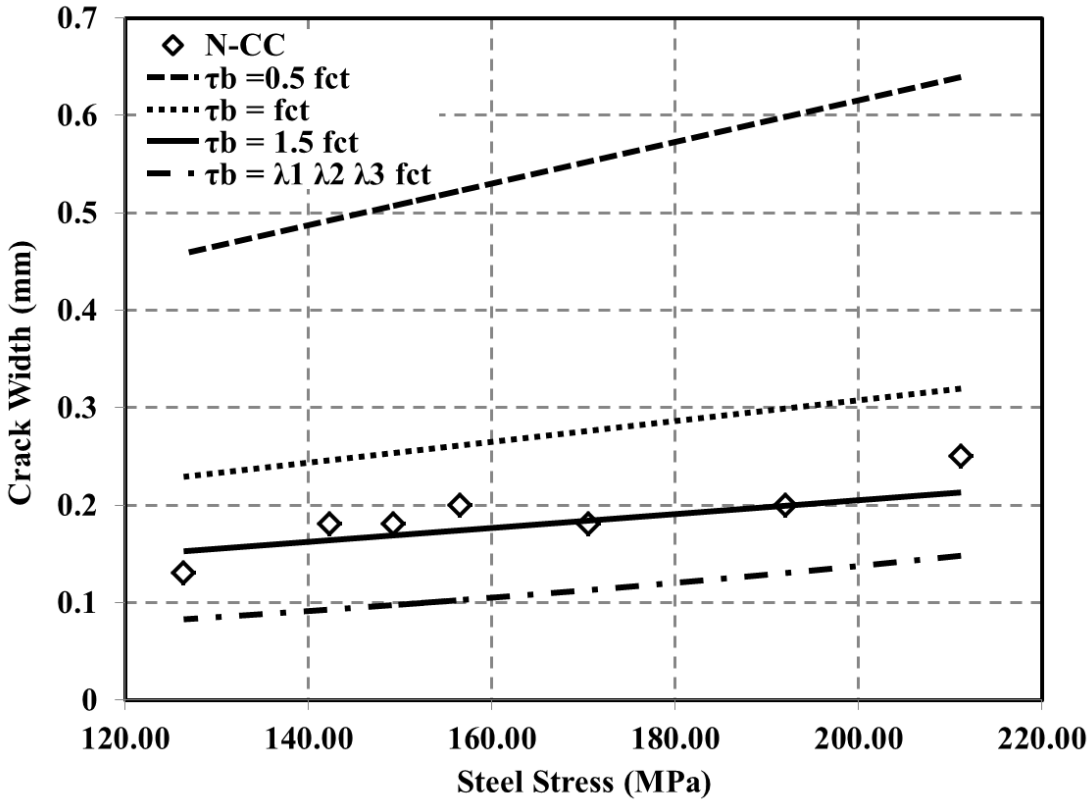

Figure 7.27 Comparison of different bond stresses for slab N-CC series

7.5 SUMMARY AND CONCLUSIONS

The results from a long-term flexural test programme on reinforced SCC slab specimens were presented in Sections 7.3.2 through 7.3.6. The results are summarised in Table 7.33.

Table 7.33 Summary of the results from long-term flexural test

Specimen	Instantaneous				Time-dependent				$(s_{rm})_{final}$ / $(s_{rm})_{inst.}$
	w_{min} (mm)	w_{ave} (mm)	w_{max} (mm)	$s_{rm,ave}$ (mm)	w_{min} (mm)	w_{ave} (mm)	w_{max} (mm)	$s_{rm,ave}$ (mm)	
N-SCC-a	0.03	0.07	0.11	99	0.06	0.15	0.24	97	0.98
N-SCC-b	0.03	0.05	0.08	100	0.03	0.11	0.18	95	0.95
D-SCC-a	0.04	0.07	0.11	96	0.06	0.13	0.22	95	0.99
D-SCC-b	0.02	0.05	0.07	99	0.02	0.09	0.14	95	0.96
S-SCC-a	0.03	0.07	0.12	96	0.07	0.15	0.22	94	0.98
S-SCC-b	0.02	0.04	0.07	93	0.05	0.10	0.15	91	0.98
DS-SCC-a	0.03	0.06	0.10	102	0.04	0.14	0.20	98	0.96
DS-SCC-b	0.02	0.04	0.06	94	0.04	0.09	0.14	90	0.96
N-CC-a	0.05	0.09	0.10	153	0.10	0.15	0.22	102	0.67
N-CC-b	0.03	0.04	0.08	141	0.08	0.14	0.20	136	0.96

7.5.1 Cracking Behaviour

As Table 7.33 shows, the instantaneous minimum, average, and maximum crack widths for the N-SCC slab series are close to N-CC slab series and instantaneous average spacing of N-SCC-a slab is 54 mm less than N-CC-a and instantaneous average spacing of N-SCC-b slab is 41 mm less than N-CC-b. Moreover, time-dependent minimum, average, and maximum crack widths for N-SCC-a slab are slightly more than N-CC-a slab but crack widths for N-SCC-b slab are slightly less than N-CC-b slab. Also, time-dependent average spacing of N-SCC-a slab is 5 mm less than N-CC-a and time-dependent average spacing of

N-SCC-b slab is 41 mm less than N-CC-b. These results are shown that crack spacing by using SCC is much less than CC.

Instantaneous minimum, average, and maximum crack widths for the D-SCC, S-SCC, and DS-SCC slab series are close to N-SCC and N-CC slab series crack widths. But, time-dependent minimum, average, and maximum crack widths for D-SCC, S-SCC, and DS-SCC slab series are slightly less than N-SCC slab series and are close to N-CC slab series crack widths. Also, same as N-SCC slab series, other SCC mixture slab series average crack spacing are much higher than N-SCC slab series average crack spacing. The final and instantaneous crack spacing and the ratio of final to instantaneous values are presented in Table 7.33.

The average ratios of final to instantaneous crack spacing for N-SCC, D-SCC, S-SCC, DS-SCC, and N-CC slab series are 0.96, 0.97, 0.98, 0.96, and 0.82, respectively. Also, the overall average ratio of final to instantaneous crack spacing for SCC mixture slab series is 0.97.

7.5.2 Deflection

The measured instantaneous and final deflections (at t = 0 and t = 240 days, respectively) and their ratios are presented in Table 7.34. Table 7.34 shows that the ratio of final to instantaneous deflection for a lower load condition ‘b’ is greater than the higher load condition ‘a’. This was due to a small instantaneous deflection under a low level sustained load and the subsequently greater influence of shrinkage and other load-independent effects.

Based on the comparison of the results between slab series N-SCC and series N-CC it may be concluded that the slab series N-SCC’s instantaneous deflection is close to N-CC but the final deflections of N-SCC slab series are less than N-CC slab series. The final deflection of N-SCC-a is 7.5 mm less than N-CC-a and the final deflection of N-SCC-b is 3.8 mm less than N-CC-b. About the instantaneous deflection of the other SCC mixtures slab series, all of them are less than N-SCC and N-CC slab series. Also, the S-SCC slab

series instantaneous deflections surprisingly are less than the other SCC slab series instantaneous deflections.

The D-SCC slab series have the minimum final deflections compared to the all other slab series. The D-SCC-a final deflection is 7 and 14.3 mm is less than the N-SCC-a and N-CC-a slabs and the D-SCC-b final deflection is 1.3 and 5.1 mm is less than the N-SCC-b and N-CC-b slabs. The main reason for this reduction of final deflection is using steel fibre in the mixture. After the D-SCC slab series minimum final deflection, DS-SCC slab series hold the less final defections compared to the N-SCC, N-CC, and S-SCC slab series.

Table 7.34 Measured final and instantaneous deflection at mid-span

Specimen	Instan. Deflection (mm)	Final Deflection (mm)	Final Deflection / Instan. Deflection
N-SCC-a	12.11	24.76	2.04
N-SCC-b	5.89	18.08	3.07
D-SCC-a	7.65	17.76	2.32
D-SCC-b	7.59	16.78	2.21
S-SCC-a	6.41	22.27	3.47
S-SCC-b	2.91	20.25	6.95
DS-SCC-a	8.98	21.31	2.37
DS-SCC-b	5.14	15.83	3.08
N-CC-a	11.80	32.10	2.72
N-CC-b	5.04	21.92	4.35

7.5.3 Bond Shear Stress

The force in the bar is transmitted to the surrounding concrete by bond shear stress. Experimental results indicate that bond shear stress τ_b decreases with increasing steel stress and reduces under a sustained load. For a given type of reinforcement the bond shear stress τ_b may be considered proportional to f_{ct}. Four different values for bond shear stress ($\tau_b = 0.5\ f_{ct}$, $\tau_b = f_{ct}$, $\tau_b = 1.5\ f_{ct}$, and $\tau_b = \lambda_1\ \lambda_2\ \lambda_3\ f_{ct}$) have been considered and the corresponding crack widths were calculated and compared with the experimental results for each load increment. It should be mentioned that throughout the test, crack widths were monitored at

two levels on the side of each specimens, i.e., the steel level and bottom fibre. Considering this and comparing the best fit between the calculated values and measured crack widths, the expressions for the bond shear stress τ_b for SCC slab series are presented in Eq. (7.10) and Figure 7.28, under long-term loading and for the different in-service steel stress ranges have been adopted for the analytical model.

$$\tau_b = 1.5 f_{ct} \tag{7.10}$$

Presented Eq. (7.10) is based on the comprehensive analyses and comparisons that are summarized and presented in Tables 7.28 to 7.31 and Figures 7.23 to 7.26.

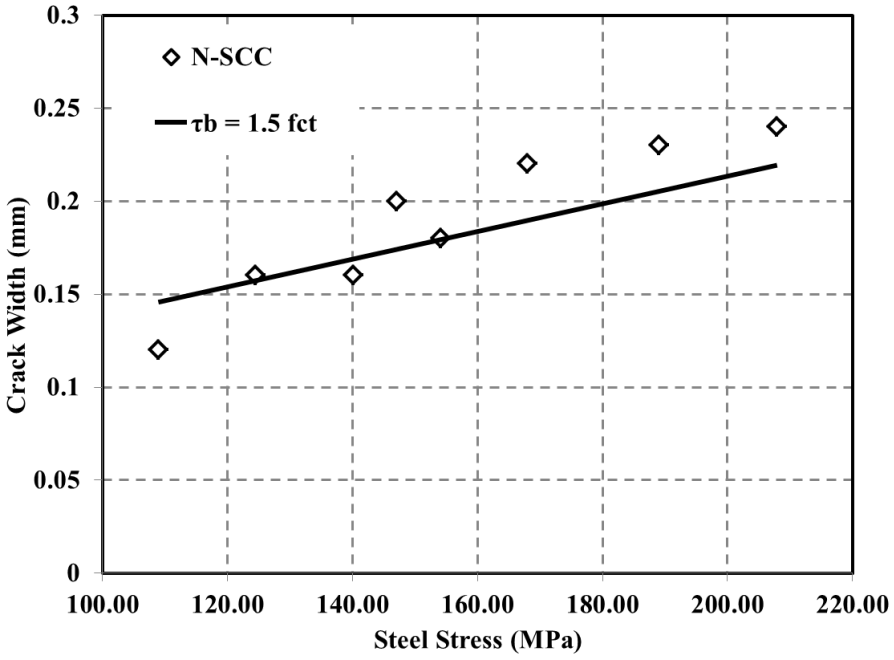

(a)

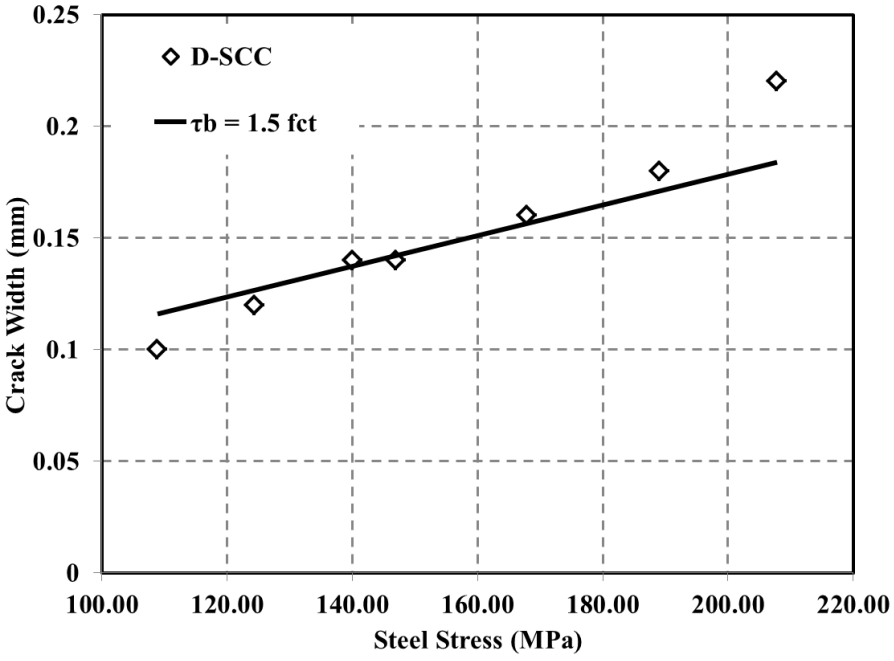

(b)

Figure 7.28 (a, b) Adopted bond stresses for (a) N-SCC, (b) D-SCC slab series

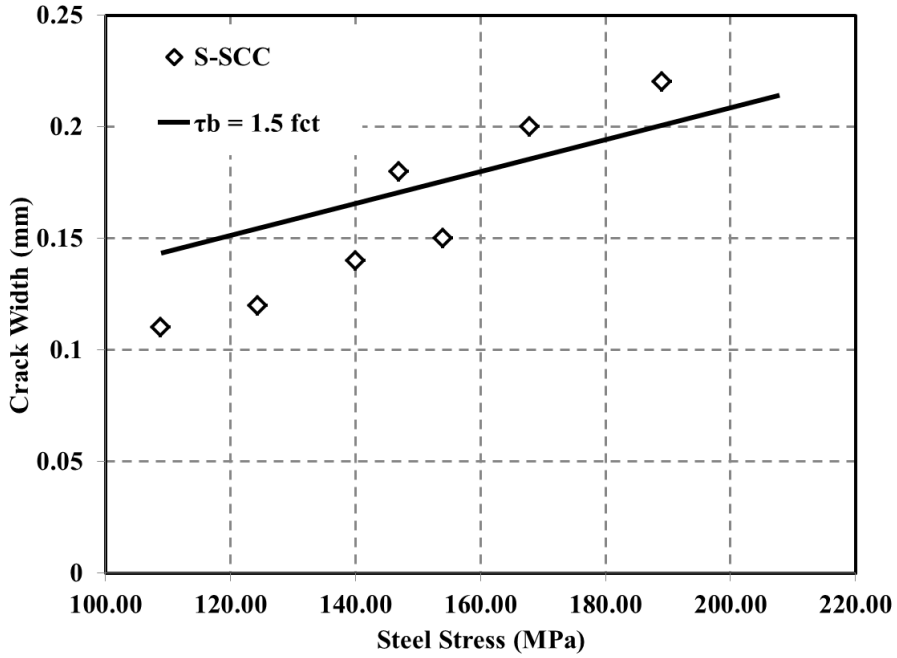

(c)

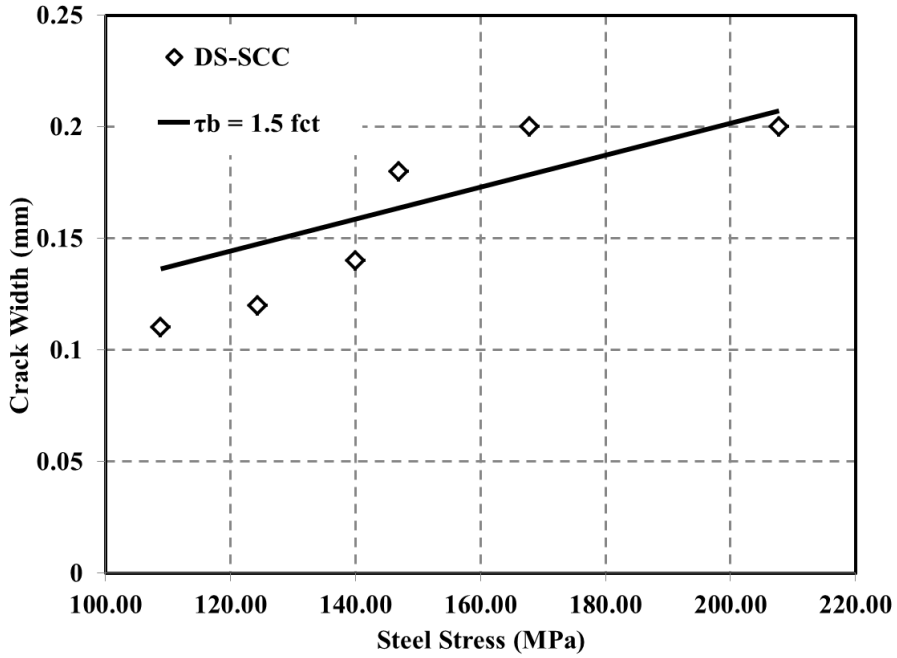

(d)

Figure 7.28 (c, d) Adopted bond stresses for (c) S-SCC, (d) DS-SCC slab series

CHAPTER 8

ANALYTICAL MODELS FOR INSTANTANEOUS AND TIME-DEPENDENT FLEXURAL CRACKING OF SCC AND FRSCC

CHAPTER 8

ANALYTICAL MODELS FOR INSTANTANEOUS AND TIME-DEPENDENT FLEXURAL CRACKING OF SCC AND FRSCC

8.1 INTRODUCTION

The aim in this chapter is to develop analytical models for flexural cracking that describes in appropriate detail the observed cracking behaviour of the reinforced concrete flexural members tested in this study and presented in Chapters 6 and 7. The crack width and crack spacing calculation procedures outlined in five international codes, namely Eurocode 2 (1991), CEB-FIP (1990), ACI318-99 (1999), Eurocode 2 (2004), and fib-Model Code (2010), are presented and crack widths and crack spacings are accordingly calculated. Then, the results are compared with the proposed analytical models and the measured experimental values, and discussed in detail separately.

When a reinforced concrete member is subjected to a bending moment as shown in Figure 8.1, two types of stresses (longitudinal and lateral stresses) act on the tensile zones of the concrete surrounding the tensile reinforcement. As the longitudinal bending stress acts, the tensile zone undergoes a lateral contraction before cracking, resulting in lateral compression between the reinforcing bar and the concrete around it. When a flexural crack starts to develop, this biaxial lateral compression has to disappear at the crack because the longitudinal tension in the concrete becomes zero. The stress in the concrete is dynamically transferred to the reinforcing bar and the tensile stress in the concrete becomes zero at the cracked section. The position of the neutral axis rises at the cracked section in order to maintain equilibrium at that section (Nejadi, 2005).

Tensile stress is present in the concrete between the cracks, because tension is transferred from the steel to the concrete by bond. The distribution of tensile stress in the concrete and the steel depends on the magnitude and distribution of bond stress between the cracks. Longitudinal bond stress exists between the concrete and the tensile reinforcement

in the regions adjacent to each crack and this gradually builds up the stress in the concrete on either side of the crack. Further loading causes the tensile stress to increase until the tensile strength of the concrete at the next weakest section of the reinforced concrete member is exceeded and this section also cracks. With increasing load, this process continues until the distance between the cracks is not large enough for the extreme fibre tensile stress to reach the tensile strength of the concrete and hence to cause cracking. Once this stage is reached, the crack pattern has stabilized and further loading just widens the existing cracks. The distance between two adjacent cracks at this stage is called the stabilized crack spacing. The width of each of the two cracks in Figure 8.1 is essentially a function of the difference in elongation between the reinforcing bars and the surrounding concrete in tension over a length distance between two adjacent cracks (Nejadi, 2005).

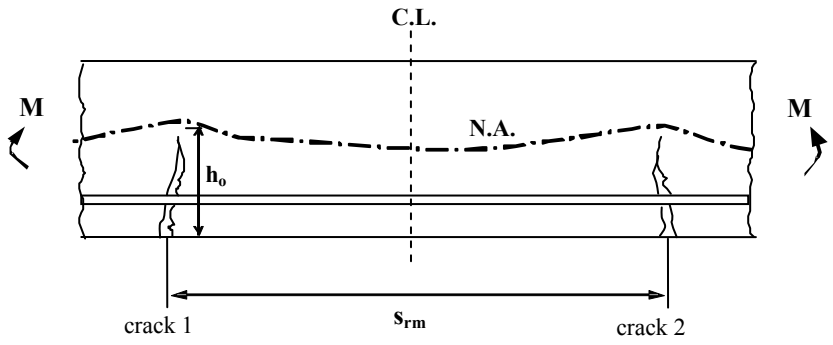

Figure 8.1 Flexural cracking in reinforced concrete one-way slabs, crack development geometry (Nejadi, 2005)

8.2 Crack Width and Crack Spacing According to the Codes of Practice

In this section, the crack width and crack spacing calculation procedures outlined in five international concrete codes, namely Eurocode 2 (1991), CEB-FIP (1990), ACI318-99 (1999), Eurocode 2 (2004), ACI 318-08, and fib-Model Code (2010), are presented. Results are compared with the analytical model proposed here and with the measured experimental values in Tables 8.1 and 8.2. Crack width is not specifically mentioned as a design parameter in AS 3600. AS 3600 (2009) is adopted the Eurocode 2 recommendations. In AS 3600 (2009), Section 9.4, “Crack control of slabs” is described as follow:

Cracking in reinforced slabs subject to flexure shall be deemed to be controlled if the appropriate requirements in below items are satisfied. For areas of slabs fully enclosed within a building except for a brief period of weather exposure during construction and, where it is assessed that crack control is not required, only Item (a) and Item (b) need be satisfied.

a) The minimum area of reinforcement in a tensile zone of a slab supported by columns at their corners complies with $0.24\left(D/d\right)^2 f'_{ct.f}/f_{sy}$ or of a slab supported by beams or walls on four sides complies with $0.19\left(D/d\right)^2 f'_{ct.f}/f_{sy}$.

b) The centre-to-centre spacing of bars in each direction shall not exceed the lesser of 2.0 D_s or 300 mm. Bars with a diameter less than half the diameter of the largest bar in the cross-section shall be ignored.

c) The calculated tensile steel stress shall not exceed the larger of the maximum steel stresses.

d) The calculated tensile steel stress shall not exceed $0.8 f_{sy}$.

8.2.1. Eurocode 2 (1991) Model

According to Eurocode 2 (1991) the average crack width, w_m may be calculated as follow:

$$w_m = s_{rm}\,\zeta\,\varepsilon_{s2} \tag{8.1}$$

$$\zeta = 1-\beta_1\,\beta_2\left(\frac{M_{cr}}{M_{max}}\right)^2 \tag{8.2}$$

$$\beta_1 = \begin{Bmatrix} 1.0 & \text{for high bond bars} \\ 0.5 & \text{for plain bars} \end{Bmatrix} \tag{8.3}$$

$$\beta_2 = \begin{Bmatrix} 1.0 & \text{for first loading} \\ 0.5 & \text{for loads applied in a sustained manner} \end{Bmatrix} \tag{8.4}$$

where ε_{s2} is the maximum steel strain at the crack, s_{rm} is the average crack spacing, M_{cr} is the cracking moment, M_{max} is the maximum moment in the section.

The code defines the design or characteristic maximum crack width, w_k as:

$$w_k = \beta_{ec}\, w_m \tag{8.5}$$

where β_{ec} is a coefficient relating the average crack width to the design value and equals 1.7 for load induced flexural cracking.

The average final crack spacing, s_{rm} is calculated by means of:

$$s_{rm} = 50 + k_1\, k_2\, \frac{d_b}{4\,\rho_{ef}} \tag{8.6}$$

where k_1 is a coefficient depending upon bond quality and k_2 is a coefficient depending upon the shape of the strain diagram as follows:

$$k_1 = \begin{cases} 0.8 & \text{for high bond bars} \\ 1.6 & \text{for plain bars} \end{cases} \tag{8.7}$$

$$k_2 = \begin{cases} 0.5 & \text{in the case of bending without axial forces} \\ 1.0 & \text{in the case of axial tension} \end{cases} \tag{8.8}$$

and d_b is the bar diameter; ρ_{ef} is the effective steel ratio ($\rho_{ef} = A_{st} / A_{cef}$); A_{cef} is the effective tension area which is generally equal to the width of the section at the level of the tensile steel multiplied by 2.5 times the distance from the tension face of the section to the centroid of A_{st}. However, the height of the effective area should not be greater than $(D - d_n)/3$.

For considering steel fibre in the concrete, the following crack spacing developed in RILEM TC-162-TDF (2003):

$$s_{rm} = \left(50 + 0.25 k_1\, k_2\, \frac{d_b}{\rho_{ef}}\right)\left(\frac{50}{L/\phi}\right) \tag{8.9}$$

where L is the length of the steel fibre; ϕ is the diameter of the steel fibre; $\left(\frac{50}{L/\phi}\right) \leq 1.0$ is the fibre contribution to the average final crack spacing; and L/ϕ is the slenderness ratio of steel fibres.

8.2.2. CEB-FIP (1990) Model

According to CEB-FIP (1990), for all stages of cracking the design crack width may be calculated by means of the following equation:

$$w_k = l_{s,max}\left(\varepsilon_{s2} - \beta_{mc}\,\varepsilon_{sr2} - \varepsilon_{cs}\right) \tag{8.10}$$

where $l_{s,max}$ is the length over which slip between steel and concrete occurs, ε_{s2} is the maximum steel strain at the crack, ε_{sr2} is the steel strain at the crack, under a force causing stress equal to f_{ctm} within A_{cef}, ε_{cs} is the free shrinkage of concrete, β_{mc} is the empirical coefficient to assess the average strain within $l_{s,max}$.

$$\beta_m = \begin{cases} 0.60 & \text{for short - term or instantaneous loading} \\ 0.38 & \text{for long - term or repeated loading} \end{cases} \tag{8.11}$$

$$l_{s,max} = \frac{d_b}{3.6\,\rho_{ef}} \tag{8.12}$$

$$\varepsilon_{sr2} = \frac{f_{ctm}}{E_s\,\rho_{ef}}\left(1 + n\,\rho_{ef}\right) \tag{8.13}$$

where f_{ctm} is the mean value of axial tensile strength and may be estimated from the mean splitting tensile strength.

$$f_{ctm} = 0.9\,f_{ct} \tag{8.14}$$

ρ_{ef} and A_{cef} may be calculated according to Eurocode 2 (1991).

8.2.3. ACI318-99 (1999) Model

The American Concrete Institute, ACI controls flexural cracking by limiting the stress in the steel at a cracked section due to service load to 60 percent of the specified yield strength. A parameter *z* is defined with dimensions of kN/mm as:

$$z = f_s \sqrt[3]{d_c A_e} \times 10^{-3} \tag{8.15}$$

where f_s is the steel stress at service load, which is calculated for a fully cracked section (state 2); d_c is the distance from centre of bar to extreme tension fibre; A_e is the effective tension area of concrete surrounding the flexural tension reinforcement and having the same centroid as that of reinforcement, divided by the number of bars.

The ACI method is based on the Gergely-Lutz expression for maximum crack width, w_{max}. The Gergely-Lutz equation predicts the maximum crack width as:

$$w_{max} = 0.011 \beta_{ac} z \tag{8.16}$$

The parameter β_{ac} is the ratio of the distances from the neutral axis to the extreme tension fibre and from the neutral axis to the centroid of the main reinforcement and may be expressed as:

$$\beta_{ac} = \frac{D - d_n}{d - d_n} \tag{8.17}$$

where D is the overall depth of a cross-section, d_n is the depth of compression zone in a fully cracked section, and d is the depth to the tensile reinforcement.

Derivation of Eq. (8.14) involves the assumption that the maximum crack spacing is:

$$\left(s_{rm}\right)_{max} = 4 t_e \tag{8.18}$$

where t_e is an increased effective cover. Based on the work of Broms and Lutz, the effective concrete cover is:

$$t_e = d_c \sqrt{1+\left(\frac{s}{4\,d_c}\right)^2} \tag{8.19}$$

where s is the bar spacing.

8.2.4. Eurocode 2 (2004) Model

In the 2004 version of Eurocode 2, the crack width in a reinforced concrete member is calculated from:

$$w = s_{r.max}\left(\varepsilon_{sm} - \varepsilon_{cm}\right) \tag{8.20}$$

where $s_{r.max}$ is the maximum crack spacing, ε_{sm} is the mean strain in the reinforcement at the design loads, including the effects of tension stiffening and any imposed deformations; ε_{cm} is the mean strain in the concrete between the cracks. The difference between the mean strain in the reinforcement and the mean strain in the concrete may be taken as:

$$\varepsilon_{sm} - \varepsilon_{cm} = \frac{\sigma_{st1}}{E_s} - k_t \frac{f_{ct,eff}}{E_s\,\rho_{eff}}\left(1 + n\,\rho_{eff}\right) \geq 0.6\frac{\sigma_{st1}}{E_s} \tag{8.21}$$

where k_t is a factor that depends on the duration of load and equals 0.6 for short term loading and 0.4 for long-term loading; n is the modular ratio E_s / E_c, $f_{ct,eff}$ is the mean value of the axial tensile strength of concrete at the time cracking is expected, $\rho_{eff}\left(= A_s / A_{c,eff}\right)$ and $A_{c,eff}$ is the effective area of the tensile concrete surrounding the tensile reinforcement of depth equal to 2.5 times the distance from the tension face of the section to the centroid of the tensile reinforcement (i.e. $2.5(D-d)$), but not greater than $(D-kd)/3$ or $D/2$. For reinforced concrete sections with bonded reinforcement fixed at reasonably close centres, the maximum final crack width may be calculated from:

$$s_{r,max} = 3.4\,c + 0.425 k_1\,k_2\,\frac{d_b}{\rho_{eff}} \tag{8.22}$$

in which c is the clear cover to the longitudinal reinforcement, k_1 is a coefficient equal to 0.8 for deformed bars and 1.6 for plain round bars, k_2 is a coefficient that takes into

account the form of the strain distribution on the cross-section and equals 0.5 for bending and 1.0 for direct tension.

Alternatively, cracking is deemed to be controlled by Eurocode 2 (2004) if the quantity of tensile reinforcement in a beam or slab is greater than the minimum value given in $A_{s,min}$ and if either the bar diameter and/or the bar spacing is limited to the maximum values given in Tables 8.1 and 8.2, respectively. The minimum area of steel for crack control is:

$$A_{s,min} = k_c \, f_{ct,eff} \frac{A_{ct}}{f_s} \tag{8.23}$$

where k_c depends on the stress distribution prior to cracking and equals 1.0 for pure tension and 0.4 for pure bending, A_{ct} is the cross-sectional area of concrete in the tensile zone, i.e. the area in tension just before the formation of the first crack, and f_s is the maximum stress permitted in the reinforcement immediately after crack formation and is the lesser of the yield stress f_y and the value given in Table 8.1. If the area of steel in the tension zone exceeds the minimum value given by Eq. (8.23), cracking is deemed to be controlled if either Tables 8.1 or 8.2 are satisfied. The steel stress used in these tables is the steel stress on the cracked section due to the quasi-permanent loads.

Table 8.1 Maximum bar diameters for crack control

Steel stress (MPa)	Maximum bar diameter (mm)		
	Crack width, w = 0.4 mm	Crack width, w = 0.3 mm	Crack width, w = 0.2 mm
160	40	32	25
200	32	25	16
240	20	16	12
280	16	12	8
320	12	10	6
360	10	8	5
400	8	6	4
450	6	5	–

Table 8.2 Maximum bar spacing for crack control

Steel stress (MPa)	Maximum bar diameter (mm)		
	Crack width, w = 0.4 mm	Crack width, w = 0.3 mm	Crack width, w = 0.2 mm
160	300	300	200
200	300	250	150
240	250	200	100
280	200	150	50
320	150	100	–
360	100	50	–

8.2.5. fib-Model Code (2010)

In this model, for all stages of cracking, the design crack width w_d may be calculated by:

$$w_d = l_{s,max}\left(\varepsilon_{sm} - \varepsilon_{cm} - \varepsilon_{cs}\right) \tag{8.24}$$

where $l_{s,max}$ denotes the length over which slip between concrete and steel occurs: steel and concrete strains, which occur within this length, contribute to the width of the crack, $l_{s,max}$ is calculated by means of Eq. (8.25), ε_{sm} is the average steel strain over the length $l_{s,max}$, ε_{cm} is the average concrete strain over the length $l_{s,max}$, ε_{cs} denotes the strain of the concrete due to shrinkage.

For the length $l_{s,max}$ the following expression can be derived:

$$l_{s,max} = \frac{1}{4}\frac{f_{ctm}}{\tau_{bm}}\frac{d_b}{\rho_s} \tag{8.25}$$

The general equation for the design (maximum) value of the crack width is:

$$w_d = \frac{1}{2}\frac{d_b}{\rho_{s,ef}}\frac{f_{ctm}}{\tau_{bm}}\left(\sigma_s - \beta\,\sigma_{sr} + \eta_r\,\varepsilon_r\,E_s\right) \tag{8.26}$$

where σ_s is the steel stress in a crack, σ_{sr} is the maximum steel stress in a crack in the crack formation stage, which is:

$$\sigma_{sr} = \frac{f_{ctm}}{\rho_{s,ef}} \left(1 + \alpha_e \, \rho_s\right) \tag{8.27}$$

where $\rho_{s,ef} = \frac{A_s}{A_{c,ef}}$ with $A_{c,ef}$ is the effective area of concrete in tension, τ_{bm} is the mean bond strength between reinforcing bars and concrete, α_e is modular ratio (E_s / E_c), β is empirical coefficient to assess the mean strain over $l_{s,max}$, η_r is a coefficient that takes into account the shrinkage contribution. The value for τ_{bm} and the coefficients β and η_r can be taken from Table 8.3.

Table 8.3 Values for τ_{bm} and the coefficients β and η_r for deformed reinforcing bars

	Crack formation stage	Stabilized cracking stage
Short term, instantaneous loading	$\tau_{bm} = 1.8\, f_{ctm}(t)$	$\tau_{bm} = 1.8\, f_{ctm}(t)$
	$\beta = 0.6$	$\beta = 0.6$
	$\alpha = 0$	$\alpha = 0$
Long term, repeated loading	$\tau_{bm} = 1.35\, f_{ctm}(t)$	$\tau_{bm} = 1.8\, f_{ctm}(t)$
	$\beta = 0.6$	$\beta = 0.4$
	$\eta_r = 0$	$\eta_r = 1$

8.3 FLEXURAL CRACKING MODEL FOR CC BY NEJADI (2005)

In the Nejadi's proposed model, Tension Chord Model, T.C.M (Marti et al, 1998) has been incorporated into the idealized model to represent the tensile zone of the cracked member. Obviously, as the applied moment M increases, the tension stiffening effect decreases and the contribution of the tensile concrete between the cracks to the stiffness of the member decreases. This phenomenon can be modelled by reducing the effective tensile area of the concrete, A_{cti} or by reducing the average concrete tensile stress, σ_{cti} as moment increases. In the present section, A_{cti} is assumed to be constant after cracking and independent of the applied moment and time. However, σ_{cti} is assumed to depend on the applied moment and reduces with time due to creep and shrinkage.

From the Nejadi's (2005) experimental and numerical study, the effective tensile area of concrete, A_{cti} surrounding the flexural tensile reinforcement and having the same centroid as that of reinforcement may be expressed as follows:
For slabs:

$$A_{ct} = 2\, n_b\, d_c\, R_f\, s \tag{8.28}$$

where

$$R_f = 0.31\,(n_b - 1) \le 1 \tag{8.29}$$

D is the depth of section, b is the width of section, d_n is the depth of compression zone in a fully cracked section, d_c is the distance from the centre of reinforcement bar to extreme tensile fibre, s is the bar spacing, n_b is the number of reinforcing bar ($n_b \geq 2$).

According to the T.C.M. (Marti et al, 1998), the concrete in the tension chord is assumed to carry a uniform average tensile stress, σ_{cti}. The instantaneous average tensile stress, σ_{cti} under short-term service loads can be determined from below Equation as follow:

$$\sigma_{cti} = \frac{\tau_{bi}\, s_{rm}\, \rho_{ef}}{d_b} \tag{8.30}$$

where τ_{bi} is the short-term bond stress, ρ_{ef} is the effective reinforcement ratio (ratio of tensile reinforcement area to the area of the effective concrete in tension, A_{st}/A_{cti}), A_{st} is the cross-sectional area of tensile steel reinforcement, A_{cti} is the intact area of tensile concrete; s_{rm} is the average crack spacing, and d_b is the nominal diameter of the tensile reinforcing bars.

The force in the bar is transmitted to the surrounding concrete by bond shear stress, τ_b. Due to this force transfer, the force in a reinforcing bar changes along its length. The bond shear stress depends on several factors, including the concrete tensile strength and cover, steel stress, bar size and spacing, confining effects, and load history. From the Nejadi (2005) experimental results presented, bond shear stress τ_b decreases with increasing steel stress and reduces under sustained load with time. Marti et al (1998) is assumed $\tau_{bi} = \tau_{bo} = 2\, f_{ct}$ for the service load range ($\sigma_s < f_{sy}$) and f_{ct} is the direct tensile strength of concrete.

As it is mentioned in Chapter 6, Section 6.4.1, Nejadi (2005) in accordance with the experimental study proposed below Equation for the bond shear stress:

$$\tau_b = \lambda_1 \lambda_2 \lambda_3 f_{ct} \tag{8.31}$$

where λ_1 accounts for the load duration with λ_1 =1.0 for short-term calculations and λ_1 = 0.7 for long-term calculations, λ_2 is a factor that accounts for the reduction in bond stress as the steel stress σ_{st1} (in MPa) increases:

$$\lambda_2 = 1.66 - 0.003\sigma_{st1} \geq 0.0 \tag{8.32}$$

and λ_3 is a factor that accounts for the very significant increase in bond stress that has been observed in laboratory tests for small diameter bars (Gilbert and Nejadi, 2004) and may be taken as:

$$\lambda_3 = 7.0 - 0.3\, d_b \geq 2.0 \quad (d_b \text{ in mm}) \tag{8.33}$$

Also, as mentioned in Chapter 6, Section 6.4.1, Nejadi (2005) proposed instantaneous crack width model as:

$$(w_i)_{tc} = \frac{s}{E_s}\left[\frac{T}{A_{st}} - \frac{\tau_b\, s}{d_b}(1 + n\rho_{tc})\right] \tag{8.34}$$

Moreover, the proposed time-dependent crack width model by Nejadi (2005) that is mentioned in Chapter 7, Section 7.4.1 is as below Equation:

$$(w^*)_{soffit} = \frac{s^*}{E_s}\left[\frac{T}{A_{st}} - \frac{\tau_b\, s^*}{d_b}(1 + n_e\, \rho_{tc}) - \varepsilon_{sh}\, E_s\right] \tag{8.35}$$

8.4 PROPOSED FLEXURAL CRACKING MODELS FOR SCC AND FRSCC

The proposed models in this study for prediction of instantaneous and time-dependent crack widths for SCC and FRSCC are based on the proposed models by Leutbecher (2007) that are summarized through Sections 8.4.1 to 8.4.4. The Leutbecher and Fehling's proposed

models are include instantaneous and time-dependent crack widths for initial crack and stabilized cracking phases. These models are proposed for conventional reinforced concrete (CRC) and CRC with fibres. The flexural cracking modelling of fibre reinforced concrete is very complicated but the proposed model by Leutbecher (2007) are very convenient and effective for both instantaneous and time-dependent cracking modelling of this type of concrete. The proposed models of Leutbecher (2007) are more suitable when they are combined with the proposed effective tensile area of concrete Eq. (8.28) by Nejadi (2005) and the calculated results are more in agreement with the measured experimental results. Also, in accordance with the experimental study presented in Sections 6.4 and 7.4, the proposed bond shear stress for short-term and long-term behaviour which have been applied in the crack width and spacing calculations based on the Leutbecher (2007)'s models can be presented as follows:

For short-term:

$$\text{N-SCC: } \tau_b = \begin{Bmatrix} 1.50\, f_{ct} & \sigma_{s,max} < 180\, MPa \\ 1.50\, f_{ct} & f_{sy} > \sigma_{s,max} \geq 180\, MPa \end{Bmatrix} \tag{8.36}$$

$$\text{D-SCC: } \tau_b = \begin{Bmatrix} 1.25\, f_{ct} & \sigma_{s,max} < 180\, MPa \\ 1.30\, f_{ct} & f_{sy} > \sigma_{s,max} \geq 180\, MPa \end{Bmatrix} \tag{8.37}$$

$$\text{S-SCC: } \tau_b = \begin{Bmatrix} 1.50\, f_{ct} & \sigma_{s,max} < 180\, MPa \\ 1.70\, f_{ct} & f_{sy} > \sigma_{s,max} \geq 180\, MPa \end{Bmatrix} \tag{8.38}$$

$$\text{DS-SCC: } \tau_b = \begin{Bmatrix} 1.50\, f_{ct} & \sigma_{s,max} < 180\, MPa \\ 1.60\, f_{ct} & f_{sy} > \sigma_{s,max} \geq 180\, MPa \end{Bmatrix} \tag{8.39}$$

All the N-SCC, D-SCC, S-SCC, DS-SCC mixtures for the long-term behaviour:

$$\tau_b = 1.5\, f_{ct} \tag{8.40}$$

The proposed models for calculation of instantaneous and time-dependent crack widths for SCC and FRSCC are presented in Section 8.4.5.

8.4.1. Calculation of Instantaneous and Time-dependent Crack Widths in Conventional Reinforced Concrete - Initial Cracking

Leutbecher (2007) have derived a cracking model based on the assumptions of constant bond stress and a parabolic development of concrete and steel strains between the cracks. To calculate crack widths, the assumption of parabolic strain development is used to determine mean steel and concrete strains. The maximum crack width is calculated as twice the transfer length multiplied by the difference between the concrete and steel mean strains. The calculation of the instantaneous crack widths of RC member (Figure 8.2) follows below the steps:

$F = F_c + F_s = \sigma_c\, A_c + \sigma_s\, A_s \qquad \varepsilon_c = \varepsilon_s \qquad \sigma_c = E_c\, \varepsilon_c^I$ and $\sigma_s = E_s\, \varepsilon_s^I$:

$$\sigma_c = \frac{F}{A_c \left(1 + \alpha_E\, \rho_s\right)} \tag{8.42}$$

$$F_{cr} = A_c \left(1 + \alpha_E\, \rho_s\right) f_{ct} \tag{8.43}$$

$$\sigma_s = \left(1 + \alpha_E\, \rho_s\right) \frac{f_{ct}}{\rho_s} \tag{8.44}$$

$$l_{es} = \frac{\sigma_s\, d_b}{4\, \tau_{sm} \left(1 + \alpha_E\, \rho_s\right)} = \frac{f_{ct}\, d_b}{4\, \tau_{sm}\, \rho_s} \tag{8.45}$$

$$w = 2\, l_{es} \left(\varepsilon_{sm} - \varepsilon_{cm}\right) \tag{8.46}$$

$$\varepsilon_{sm} = \left(1 - \alpha_b\right) \varepsilon_s^{II} + \alpha_b\, \varepsilon_s^I \tag{8.47}$$

$$\varepsilon_{cm} = \alpha_b\, \varepsilon_c^I = \alpha_b\, \varepsilon_s^I \tag{8.48}$$

$$w = \frac{\left(1 - \alpha_b\right) \sigma_s^2\, d_b}{2\, E_s\, \tau_{sm} \left(1 + \alpha_E\, \rho_s\right)} = \frac{\left(1 - \alpha_b\right) f_{ct}^2\, d_b}{2\, E_s\, \tau_{sm}\, \rho_s^2} \left(1 + \alpha_E\, \rho_s\right) \tag{8.49}$$

where w_{max} is the maximum crack width, l_{es} is the transfer length, ε_{sm} is the mean steel strain, ε_{cm} is the mean concrete strain, F_{cr} is the cracking force, σ_s is the steel stress, τ_{sm} is the average bond stress over the load transmission length, f_{ct} is the concrete matrix tensile strength, d_s is the reinforcing bar diameter, E_s is the modulus of elasticity of reinforcing bar,

ρ_s is the reinforcing ratio of steel reinforcement; α_b is the shape coefficient of the strains (α_b = 0.6 for short term loading, α_b = 0.4 for long term or repeated loading), α_E is the ratio of the modulus of elasticity of steel to the modulus of elasticity of concrete ($\alpha_E = E_s/E_c$). Figure 8.1 shows definitions of the various strains that are used in this model.

The calculation of crack widths of RC member with initial crack by considering the influence of shrinkage and creep (Figure 8.3) can be presented as follows:

shrinkage strain without creep effect: $\varepsilon_{s.shr} = \dfrac{\varepsilon_{cs}}{1+\alpha_E\ \rho_s}$ (8.50)

shrinkage strain with creep effect: $\varepsilon_{s.shr} = \dfrac{\varepsilon_{cs}}{1+\alpha_E\ \rho_s\ (1+\rho\varphi)}$ (8.51)

where ρ is the relaxation coefficient equal to 0.8 and φ is the creep coefficient.

$$F_{cr} = A_c\,(1+\alpha_E\ \rho_s)\left(f_{ct} + \varepsilon_{s,shr}\ E_s\ \rho_s\right) \tag{8.52}$$

$$\sigma_s = (1+\alpha_E\ \rho_s)\left(\frac{f_{ct}}{\rho_s} + \varepsilon_{s,shr}\ E_s\right) \tag{8.53}$$

$$\varepsilon^*_{s.shr} = \varepsilon_{s.shr}(1+\alpha_E\ \rho_s) \tag{8.54}$$

$$l_{es} = \frac{\left(\dfrac{\sigma_s}{1+\alpha_E\ \rho_s} - \varepsilon_{s,shr}\ E_s\right) d_b}{4\ \tau_{sm}} = \frac{f_{ct}\ d_b}{4\ \tau_{sm}\ \rho_s} \tag{8.55}$$

$$\varepsilon_{sm} = (1-\alpha_b)\,\varepsilon_s^{II} + \alpha_b\ \varepsilon_s^{I} \tag{8.56}$$

$$\varepsilon_{cm} = (1-\alpha_b)\,\varepsilon^*_{s,shr} + \alpha_b\ \varepsilon_c^{I} = (1-\alpha_b)\,\varepsilon^*_{s,shr} + \alpha_b\ \varepsilon_s^{I} \tag{8.57}$$

$$w = 2\frac{\left(\dfrac{\sigma_s}{1+\alpha_E\ \rho_s} - \varepsilon_{s,shr}\ E_s\right) d_b}{4\tau_{sm}}\left[(1-\alpha_b)\varepsilon_s^{II} - (1-\alpha_b)\varepsilon^*_{s,shr}\right] \tag{8.58}$$

$$w = \frac{(1-\alpha_b)\left(\dfrac{\sigma_s}{1+\alpha_E\ \rho_s} - \varepsilon_{s,shr}\ E_s\right)^2 d_b}{2\ E_s\ \tau_{sm}}\left[1+\alpha_E\ \rho_s\right] \tag{8.59}$$

Figure 8.2 shows definitions of the various strains that are used in this model.

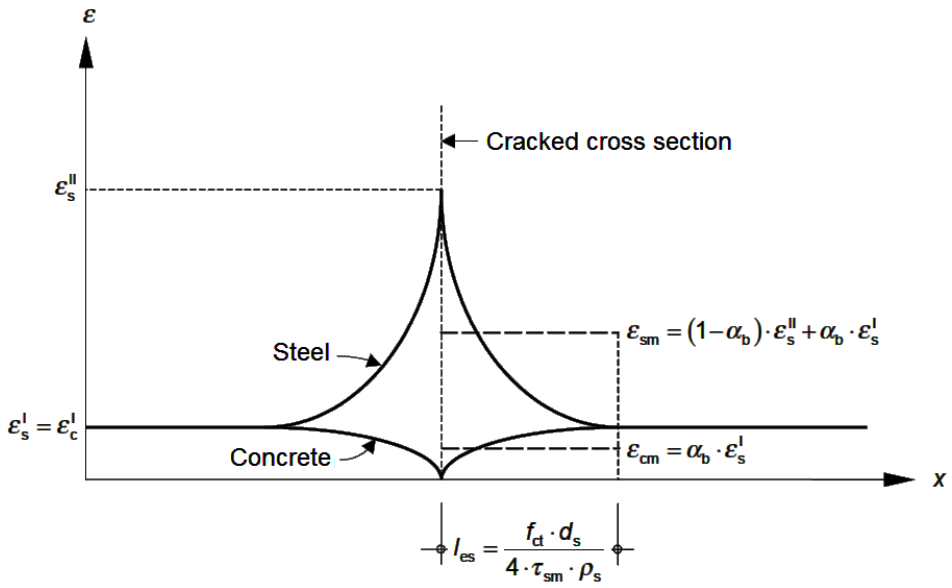

Figure 8.2 Initial crack - Qualitative distribution of strains for the steel bar and the matrix (Leutbecher, 2007)

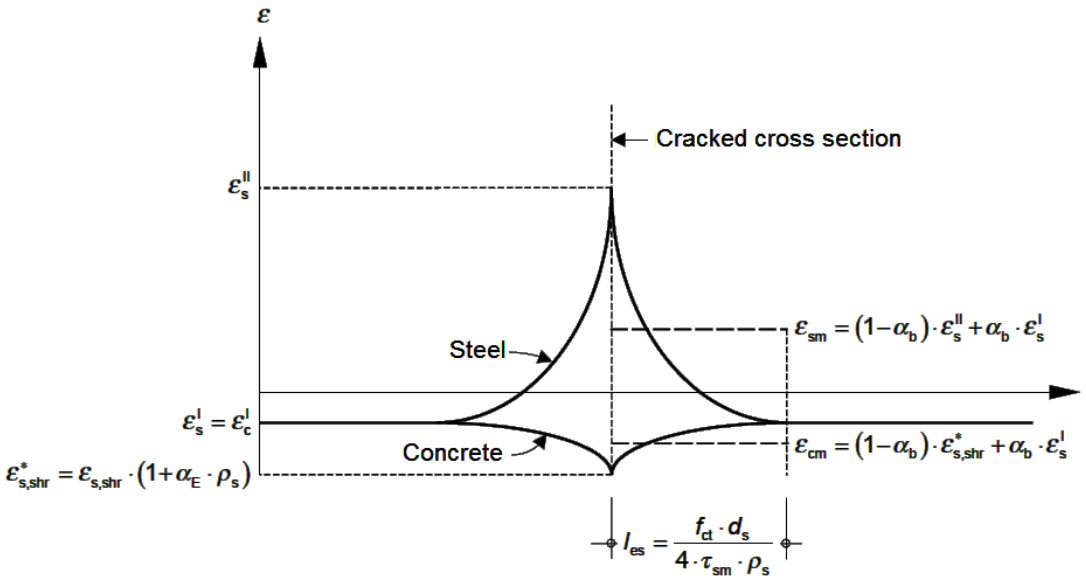

Figure 8.3 Initial crack - Qualitative distribution of strains for the steel bar and the matrix, considering the influence of shrinkage (Leutbecher, 2007)

8.4.2. Calculation of Instantaneous and Time-dependent Crack Widths in Conventional Reinforced Concrete - Stabilized Cracking

Similarly, Leutbecher (2007) cracking model is applicable to the stabilizing cracking too. Calculation of crack widths of CRC member with stabilized cracking (Figure 8.4) can be shown as follows:

For $s_r = s_{r,max} = 2\,l_{es}$:

$$\varepsilon_{sm} = \varepsilon_s^{II} - \alpha_b \frac{f_{ct}}{\rho_s\, E_s} \tag{8.60}$$

$$\varepsilon_{cm} = \alpha_b \frac{f_{ct}}{E_c} = \alpha_b \frac{f_{ct}}{\rho_s\, E_s}\, \alpha_E\, \rho_s \tag{8.61}$$

$$w_{max} = s_{r,max}\left(\varepsilon_{sm} - \varepsilon_{cm}\right) = \frac{f_{ct}\, d_b}{2\, E_s\, \tau_{sm}\, \rho_s}\left[\sigma_s - \alpha_b \frac{f_{ct}}{\rho_s}\left(1 + \alpha_E\, \rho_s\right)\right] \tag{8.62}$$

For $s_{r,min} = l_{es} \le s_r < s_{r,max} = 2\,l_{es}$:

$$\varepsilon_{sm} = \varepsilon_s^{II} - \alpha_b \frac{2\, s_r\, \tau_{sm}}{d_b\, E_s} \tag{8.63}$$

$$\varepsilon_{cm} = \alpha_b \frac{2\, s_r\, \tau_{sm}\, \rho_s}{d_b\, E_s} = \alpha_b \frac{2\, s_r\, \tau_{sm}}{d_s\, E_s}\, \alpha_E\, \rho_s \tag{8.64}$$

$$w = s_r\left(\varepsilon_{sm} - \varepsilon_{cm}\right) = \frac{s_r}{E_s}\left[\sigma_s - \alpha_b \frac{2\, s_r\, \tau_{sm}}{d_b}\left(1 + \alpha_E\, \rho_s\right)\right] \tag{8.65}$$

Calculation of the crack widths for CRC member with stabilized cracking by considering the influence of shrinkage (Figure 8.5) follows the below steps:

For $s_r = s_{r,max} = 2\,l_{es}$:

$$\varepsilon_{sm} = \varepsilon_s^{II} - \alpha_b \frac{f_{ct}}{\rho_s\, E_s} \tag{8.66}$$

$$\varepsilon_{cm} = \alpha_b \frac{f_{ct}}{\rho_s E_s} \alpha_E \rho_S + \varepsilon^*_{s,shr} \tag{8.67}$$

$$w_{max} = s_{r,max} \left(\varepsilon_{sm} - \varepsilon_{cm}\right) = \frac{f_{ct}\, d_b}{2\, E_s\, \tau_{sm}\, \rho_s} \left[\sigma_s - \left(\alpha_b \frac{f_{ct}}{\rho_s} + \varepsilon_{s,shr}\, E_s\right)\left(1 + \alpha_E \rho_s\right)\right] \tag{8.68}$$

For $s_{r,min} = l_{es} \le s_r < s_{r,max} = 2\, l_{es}$:

$$\varepsilon_{sm} = \varepsilon_s^{II} - \alpha_b \frac{2 s_r\, \tau_{sm}}{d_b\, E_s} \tag{8.69}$$

$$\varepsilon_{cm} = \alpha_b \frac{s_r\, 2\, \tau_{sm}}{d_b\, E_s} \alpha_E \rho_S + \varepsilon^*_{s,shr} \tag{8.70}$$

$$w = s_r \left(\varepsilon_{sm} - \varepsilon_{cm}\right) = \frac{s_r}{E_s} \left[\sigma_s - \left(\alpha_b \frac{2\, s_r\, \tau_{sm}}{d_b} + \varepsilon_{s,shr}\, E_s\right)\left(1 + \alpha_E\, \rho_s\right)\right] \tag{8.71}$$

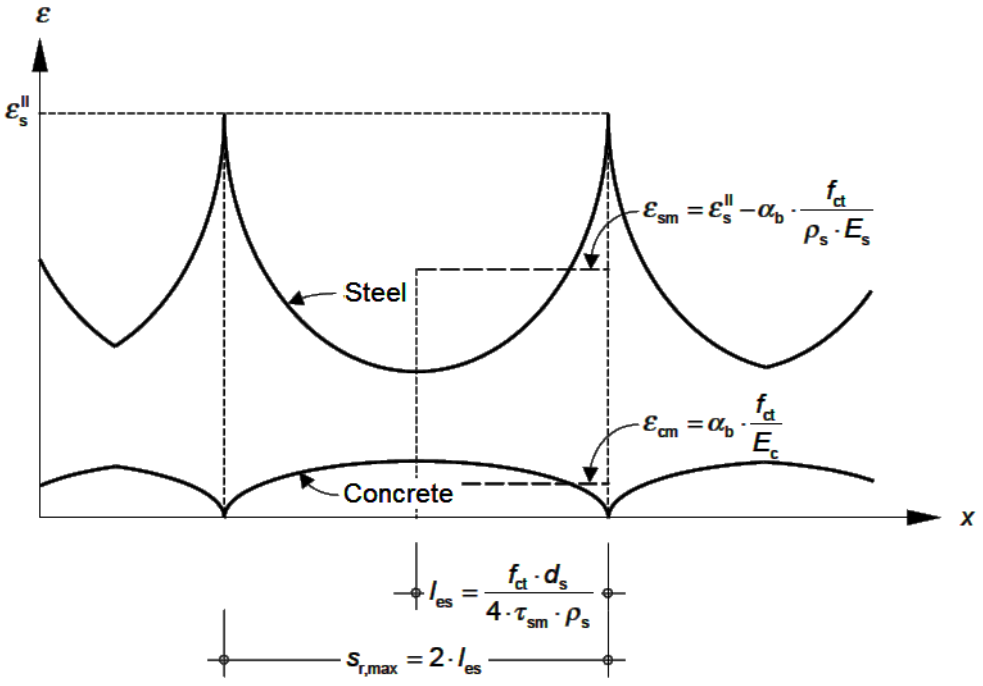

Figure 8.4 Stabilized cracking - Qualitative distribution of strains for the steel bar and the matrix (Leutbecher, 2007)

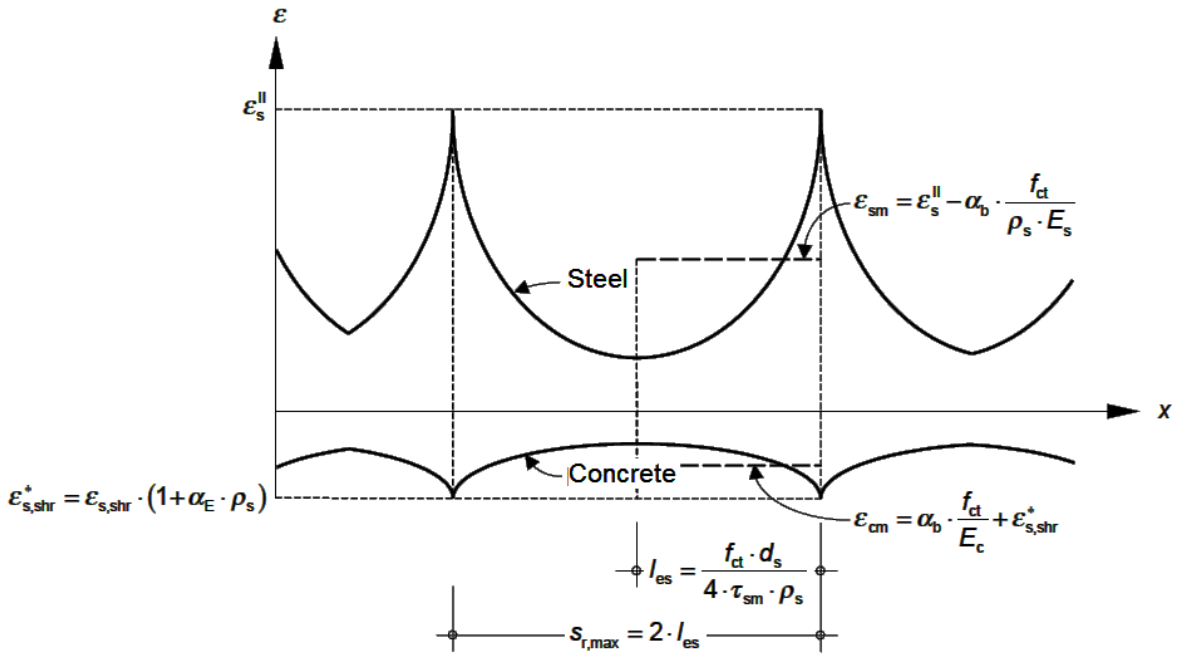

Figure 8.5 Stabilized cracking - Qualitative distribution of strains for the steel bar and the matrix, considering the influence of shrinkage (Leutbecher, 2007)

8.4.3. Calculation of Instantaneous and Time-dependent Crack Widths in Conventional Reinforced Concrete with Fibres - Initial Cracking

Calculation of the instantaneous crack widths of CRC with fibres member with initial crack (Figure 8.6) can be presented as follows:

$$F_{cr} = A_c \left(1 + \alpha_{E,s}\ \rho_s / \gamma\right)\left(\sigma^i_{cf,cr} + \varepsilon_{s,shr}\ E_s\ \rho_s\right) \tag{8.72}$$

$$\sigma^i_{c,cr} = \left(1 + \alpha_{E,s}\ \rho_s / \gamma\right)\left(\sigma^i_{cf,cr} + \varepsilon_{s,shr}\ E_s\ \rho_s\right) \tag{8.73}$$

$$\sigma^i_{cf,cr} = \frac{E_f^2\ d_f}{16\,\tau_f\ l_f}\left(1 - \sqrt{1 + \frac{16\,\tau_f}{E_f\ d_f}\left(w - \frac{l_f}{2}\right)}\right)^2 \tag{8.74}$$

$$\alpha_{E,s} = \frac{E_s}{E_c} \tag{8.75}$$

$$\rho_s = \frac{A_s}{A_c} \tag{8.76}$$

$$\gamma = 1 + \rho_f \left(\eta \, \alpha_{E,f} - 1 \right) \tag{8.77}$$

where ρ_f is the fibre content and η is the fibre orientation coefficient.

$$w_s = 2 \, l_{es} \left(\varepsilon_{sm} - \varepsilon_{cm} \right) = \frac{\left(1 - \alpha_b \right) \left[\sigma_s - \dfrac{\sigma_{cf,cr}^{i} \, \alpha_{E,s}}{\gamma} \right] d_b}{2 \, E_s \, \tau_{sm}} \left(\sigma_s \right) \tag{8.78}$$

Calculation of the crack widths of CRC with fibres member with initial crack by considering the influence of shrinkage (Figure 8.7) can be shown as follows:

$$\varepsilon_{shr}^{*} = \varepsilon_{s,shr} \left(1 + \alpha_{E,s} \, \rho_s / \gamma \right) + \varepsilon_{f,shr} \, \alpha_{E,f} \, \eta \, \rho_f \tag{8.79}$$

where $\varepsilon_{f,shr}$ is the shrinkage shortening of the fibres.

$$\alpha_{E,f} = \frac{E_f}{E_c} \tag{8.80}$$

$$\varepsilon_s^{I-II} = \varepsilon_c^{I-II} = \varepsilon_{s,shr} \left(1 + \alpha_{E,s} \, \rho_s / \gamma \right) + \frac{\sigma_{cf,cr}^{i} \, \alpha_{E,s}}{\gamma \, E_s} \tag{8.81}$$

$$l_{es} = \frac{\left[\sigma_s - \varepsilon_{s,shr} \, E_s \left(1 + \alpha_{E,s} \, \rho_s / \gamma \right) - \dfrac{\sigma_{cf,cr}^{i} \, \alpha_{E,s}}{\gamma} \right] d_b}{4 \, \tau_{sm}} \tag{8.82}$$

$$\varepsilon_{sm} = \left(1 - \alpha_b \right) \varepsilon_s^{II} + \alpha_b \, \varepsilon_s^{I-II} \tag{8.83}$$

$$\varepsilon_{cm} = \left(1 - \alpha_b \right) \varepsilon_{shr}^{II} + \alpha_b \, \varepsilon_c^{I-II} \tag{8.84}$$

$$w_s = 2 \, l_{es} \left(\varepsilon_{sm} - \varepsilon_{cm} \right) = \frac{\left(1 - \alpha_b \right) \left[\sigma_s - \varepsilon_{s,shr} \, E_s \left(1 + \alpha_{E,s} \, \rho_s / \gamma \right) - \dfrac{\sigma_{cf,cr}^{i} \, \alpha_{E,s}}{\gamma} \right] d_b}{2 \, E_s \, \tau_{sm}} \left(\sigma_s - \varepsilon_{shr}^{*} \, E_s \right) \tag{8.85}$$

Fibre activation phase (refer to Figure 6.40):

$$l_{ef} = \frac{\left(\sigma_f - \varepsilon_{f,shr}^{*} \, E_f \right) d_f}{4 \, \tau_f} \le \frac{\sigma_f \, d_f}{8 \, \tau_f} + \frac{l_f}{4} \tag{8.86}$$

Fibre pullout phase (refer to Figure 6.40):

$$l_{fbs} = \frac{\sigma_f \, d_f}{8 \, \tau_f} \tag{8.87}$$

$$\varepsilon^*_{f,shr} = \varepsilon_{f,shr} \, \gamma \tag{8.88}$$

Fibre activation phase:

$$w_f = \frac{\left(\sigma_f - \varepsilon^*_{f,shr} \, E_f\right) d_f}{4 \, E_f \, \tau_f} \left(\sigma_f + \varepsilon^*_{f,shr} \, E_f - 2 \, \varepsilon^*_{shr} \, E_f\right) \tag{8.89}$$

Fibre pullout phase:

$$w_f = \frac{l_f}{2} - \frac{\sigma_f \, d_f}{4 \, \tau_f} + \frac{\left(\sigma_f - \varepsilon^*_{f,shr} \, E_f\right) d_f}{4 \, E_f \, \tau_f} \left(\sigma_f + \varepsilon^*_{f,shr} \, E_f - 2 \, \varepsilon^*_{shr} \, E_f\right) \tag{8.90}$$

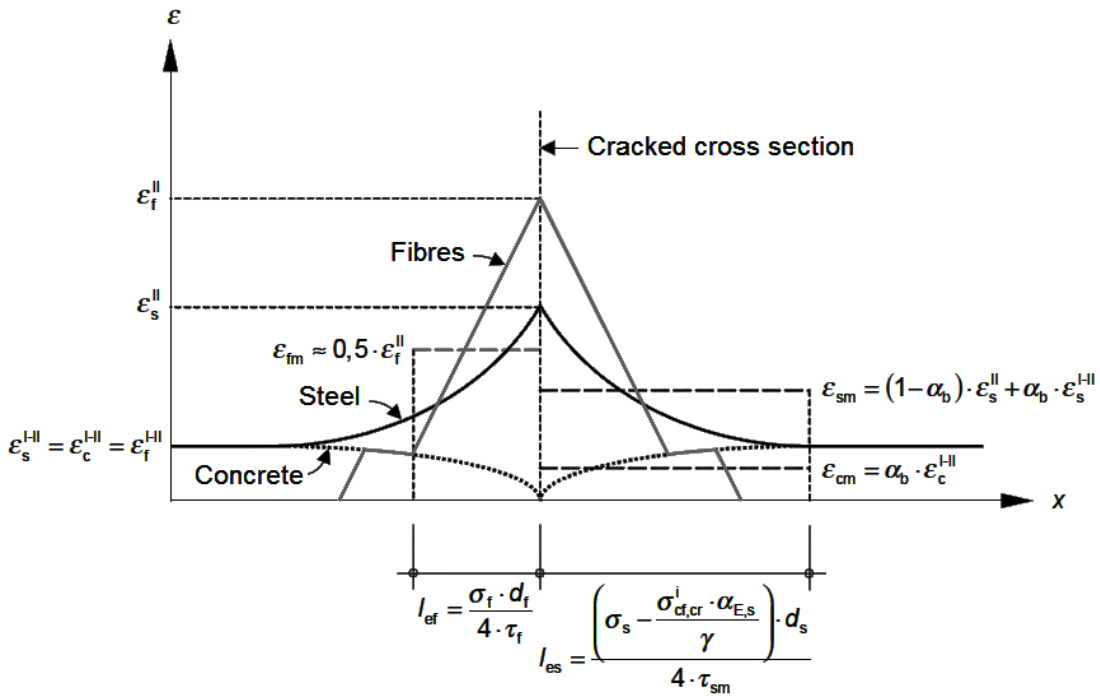

Figure 8.6 Initial crack - Qualitative distribution of strains for the steel bar and fibres reinforcement and the matrix (Leutbecher, 2007)

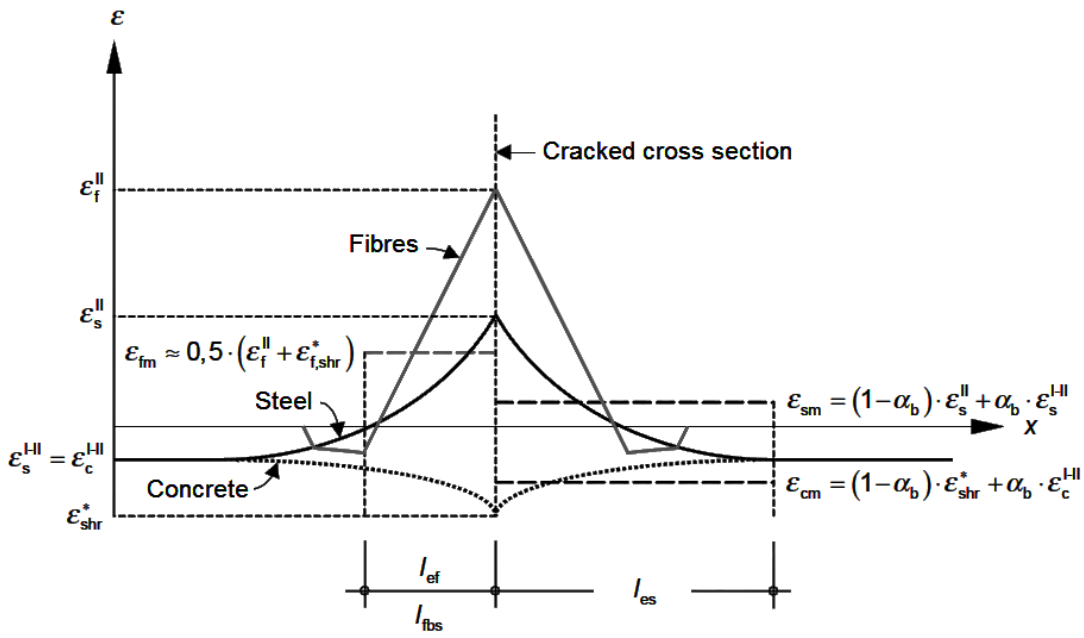

Figure 8.7 Initial crack - Qualitative distribution of strains for the steel bar and fibres reinforcement and the matrix, considering the influence of shrinkage (Leutbecher, 2007)

8.4.4. Calculation of Instantaneous and Time-dependent Crack Widths in Conventional Reinforced Concrete with Fibres - Stabilized Cracking

Calculation of the instantaneous crack widths of CRC with fibres member with stabilized cracking (Figure 8.8) can be presented as follows:

$$\varepsilon_{sm} = \varepsilon_s^{II} - \alpha_b \frac{2\, s_r\, \tau_{sm}}{d_b\, E_s} \tag{8.91}$$

$$\varepsilon_{cm} = \alpha_b \left(\frac{2\, s_r\, \tau_{sm}}{d_b\, E_s} \alpha_{E,s}\, \rho_s / \gamma + \frac{\sigma_{cf}}{\gamma\, E_s} \alpha_{E,s} \right) \tag{8.92}$$

$$w_s = s_r\, (\varepsilon_{sm} - \varepsilon_{cm}) = s_r \left[\frac{\sigma_s}{E_s} - \alpha_b \left(\frac{2\, s_r\, \tau_{sm}}{d_b\, E_s} (1 + \alpha_{E,s}\, \rho_s / \gamma) + \frac{\sigma_{cf}}{\gamma\, E_s} \alpha_{E,s} \right) \right] \tag{8.93}$$

Calculation of the crack widths of CRC with fibres member with stabilized cracking by considering the influence of shrinkage (Figure 8.9) can be shown as follows:

$$\varepsilon_{sm} = \varepsilon_s^{II} - \alpha_b \frac{2\, s_r\, \tau_{sm}}{d_b\, E_s} \tag{8.94}$$

$$\varepsilon_{cm} = \alpha_b \left(\frac{2\, s_r\, \tau_{sm}}{d_b\, E_s} \alpha_{E,s}\, \rho_s / \gamma + \frac{\sigma_{cf}}{\gamma\, E_s} \alpha_{E,s} - \varepsilon^*_{f,shr}\, \alpha_{E,f}\, \eta\, \rho_f \right) + \varepsilon^*_{shr} \tag{8.95}$$

$$w_s = s_r \left(\varepsilon_{sm} - \varepsilon_{cm}\right) =$$
$$s_r \left[\frac{\sigma_s}{E_s} - \alpha_b \left(\frac{2\, s_r\, \tau_{sm}}{d_b\, E_s} \left(1 + \alpha_{E,s}\, \rho_s / \gamma\right) + \frac{\sigma_{cf}}{\gamma\, E_s} \alpha_{E,s} - \varepsilon^*_{f,shr}\, \alpha_{E,f}\, \eta\, \rho_f \right) - \varepsilon^*_{shr} \right] \tag{8.96}$$

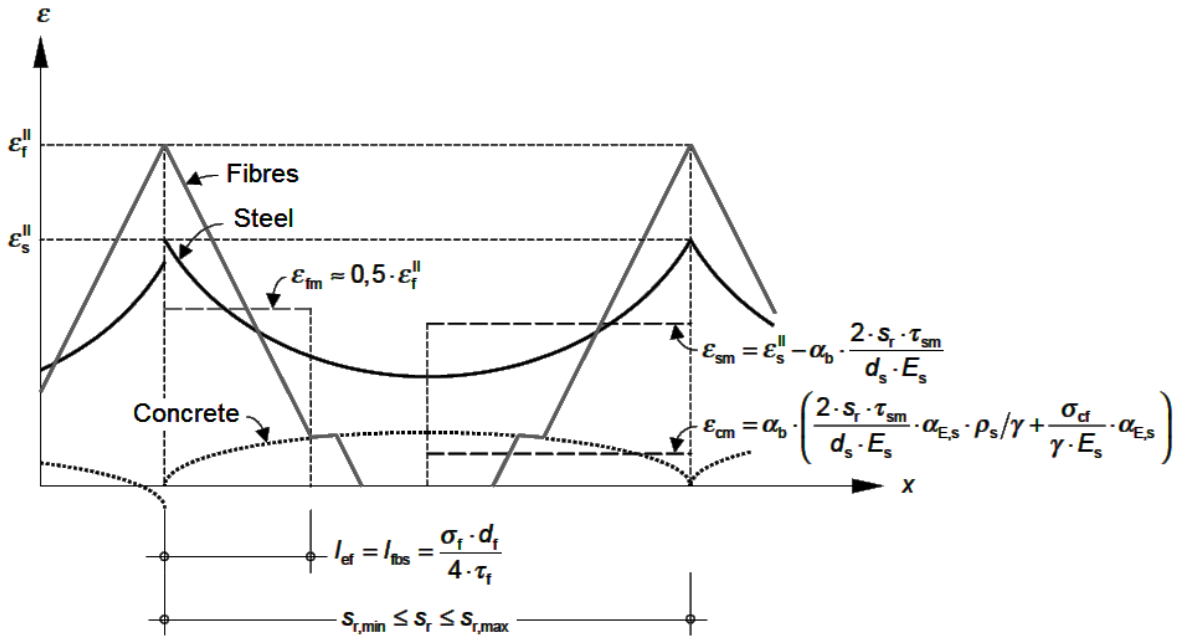

Figure 8.8 Stabilized cracking - Qualitative distribution of strains for the steel bar and fibres reinforcement and the matrix (Leutbecher, 2007)

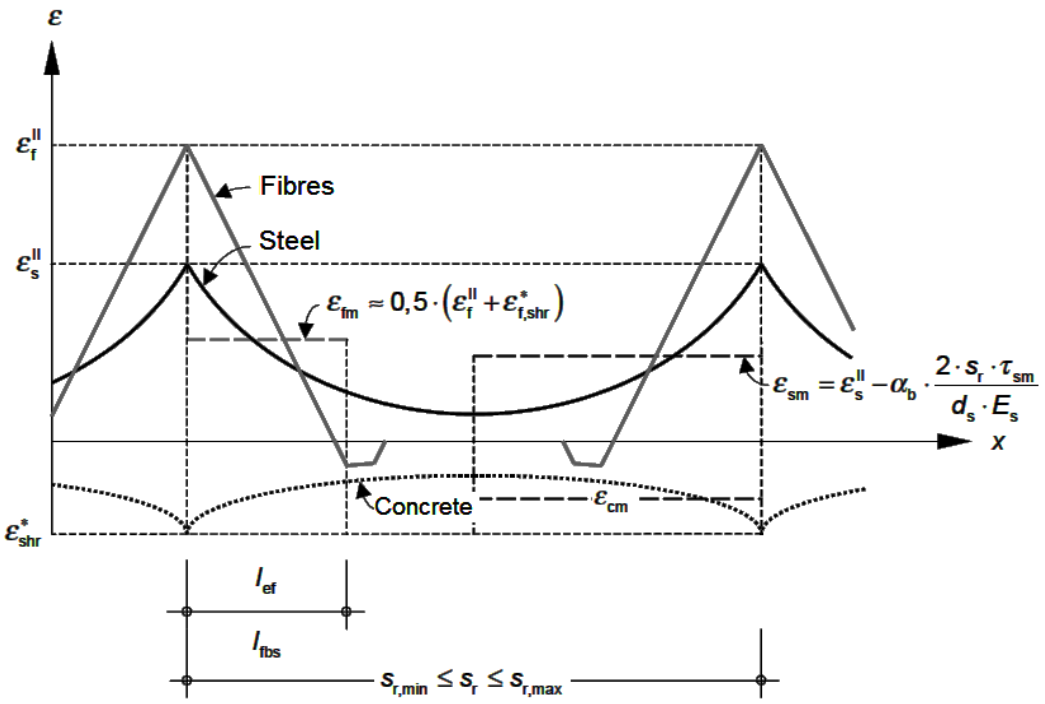

Figure 8.9 Stabilized cracking - Qualitative distribution of strains for the steel bar and fibres reinforcement and the matrix, considering the influence of shrinkage (Leutbecher, 2007)

8.4.5. Proposed Models for Calculation of Instantaneous and Time-dependent Crack Widths and Crack Spacing for SCC and FRSCC

Proposed SCC and FRSCC flexural cracking models - instantaneous and time-dependent behaviour are presented through Eqs. (8.97 to 8.107). In these equations, the proposed these bond shear stress models, Eqs. (8.36 to 8.40), should be used.

SCC instantaneous crack width initial crack phase:

$$w = \frac{0.25\, f_{ct}^2\, d_b}{E_s\, \tau_b\, \rho_s^2}\left(1+\frac{E_s}{E_c}\rho_s\right) \tag{8.97}$$

where

N-SCC: $\tau_b = \begin{Bmatrix} 1.50\, f_{ct} & \sigma_{s,max} < 180\, MPa \\ 1.50\, f_{ct} & f_{sy} > \sigma_{s,max} \geq 180\, MPa \end{Bmatrix}$

D-SCC: $\tau_b = \begin{Bmatrix} 1.25\, f_{ct} & \sigma_{s,max} < 180\, MPa \\ 1.30\, f_{ct} & f_{sy} > \sigma_{s,max} \geq 180\, MPa \end{Bmatrix}$

S-SCC: $\tau_b = \begin{Bmatrix} 1.50\, f_{ct} & \sigma_{s,max} < 180\, MPa \\ 1.70\, f_{ct} & f_{sy} > \sigma_{s,max} \geq 180\, MPa \end{Bmatrix}$

DS-SCC: $\tau_b = \begin{Bmatrix} 1.50\, f_{ct} & \sigma_{s,max} < 180\, MPa \\ 1.60\, f_{ct} & f_{sy} > \sigma_{s,max} \geq 180\, MPa \end{Bmatrix}$

SCC time-dependent crack width initial crack phase:

$$w = \frac{0.25 \left(\dfrac{\sigma_s}{1 + \dfrac{E_s}{E_c}\rho_s} - \varepsilon_{s,shr}\, E_s \right)^2 d_b}{E_s\, \tau_b} \left[1 + \frac{E_s}{E_c}\, \rho_s \right] \tag{8.98}$$

where for the N-SCC, D-SCC, S-SCC, DS-SCC mixtures

$\tau_b = 1.5\, f_{ct}$

SCC instantaneous crack width stabilized cracking phase:

$$w = \frac{s_r}{E_s} \left[\sigma_s - \frac{s_r\, \tau_b}{d_b} \left(1 + \frac{E_s}{E_c}\, \rho_s \right) \right] \tag{8.99}$$

where

N-SCC: $\tau_b = \begin{Bmatrix} 1.50\, f_{ct} & \sigma_{s,max} < 180\, MPa \\ 1.50\, f_{ct} & f_{sy} > \sigma_{s,max} \geq 180\, MPa \end{Bmatrix}$

D-SCC: $\tau_b = \begin{Bmatrix} 1.25\, f_{ct} & \sigma_{s,max} < 180\, MPa \\ 1.30\, f_{ct} & f_{sy} > \sigma_{s,max} \geq 180\, MPa \end{Bmatrix}$

S-SCC: $\tau_b = \begin{Bmatrix} 1.50\, f_{ct} & \sigma_{s,max} < 180\, MPa \\ 1.70\, f_{ct} & f_{sy} > \sigma_{s,max} \geq 180\, MPa \end{Bmatrix}$

DS-SCC: $\tau_b = \begin{Bmatrix} 1.50\, f_{ct} & \sigma_{s,max} < 180\, MPa \\ 1.60\, f_{ct} & f_{sy} > \sigma_{s,max} \geq 180\, MPa \end{Bmatrix}$

SCC time-dependent crack width stabilized cracking phase:

$$w = \frac{s_r}{E_s}\left[\sigma_s - \left(\frac{s_r\ \tau_b}{d_b} + \varepsilon_{s,shr}\ E_s\right)\left(1 + \frac{E_s}{E_c}\rho_s\right)\right] \tag{8.100}$$

where for the N-SCC, D-SCC, S-SCC, DS-SCC mixtures

$\tau_b = 1.5\, f_{ct}$

FRSCC instantaneous crack width initial crack phase:

$$w_s = \frac{0.25\left[\sigma_s - \dfrac{\sigma^i_{cf,cr}\dfrac{E_s}{E_c}}{\gamma}\right] d_b}{E_s\ \tau_b}(\sigma_s) \tag{8.101}$$

where

N-SCC: $\tau_b = \begin{Bmatrix} 1.50\, f_{ct} & \sigma_{s,max} < 180\, MPa \\ 1.50\, f_{ct} & f_{sy} > \sigma_{s,max} \geq 180\, MPa \end{Bmatrix}$

D-SCC: $\tau_b = \begin{Bmatrix} 1.25\, f_{ct} & \sigma_{s,max} < 180\, MPa \\ 1.30\, f_{ct} & f_{sy} > \sigma_{s,max} \geq 180\, MPa \end{Bmatrix}$

S-SCC: $\tau_b = \begin{Bmatrix} 1.50\, f_{ct} & \sigma_{s,max} < 180\, MPa \\ 1.70\, f_{ct} & f_{sy} > \sigma_{s,max} \geq 180\, MPa \end{Bmatrix}$

DS-SCC: $\tau_b = \begin{Bmatrix} 1.50\, f_{ct} & \sigma_{s,max} < 180\, MPa \\ 1.60\, f_{ct} & f_{sy} > \sigma_{s,max} \geq 180\, MPa \end{Bmatrix}$

FRSCC time-dependent crack width initial crack phase:

$$w_s = \frac{0.25\left[\sigma_s - \varepsilon_{s,shr}\ E_s\left(1+\frac{E_s}{E_c}\rho_s/\gamma\right) - \frac{\sigma_{cf,cr}^{i}\frac{E_s}{E_c}}{\gamma}\right] d_b}{E_s\ \tau_b}\left(\sigma_s - \varepsilon_{shr}^{*}\ E_s\right) \tag{8.102}$$

where for the N-SCC, D-SCC, S-SCC, DS-SCC mixtures

$\tau_b = 1.5\ f_{ct}$

FRSCC instantaneous crack width stabilized cracking phase:

$$w_s = s_r\left[\frac{\sigma_s}{E_s} - \left(\frac{s_r\ \tau_b}{d_b\ E_s}\left(1+\frac{E_s}{E_c}\rho_s/\gamma\right) + \frac{\sigma_{cf}}{\gamma\ E_c}\right)\right] \tag{8.103}$$

where

N-SCC: $\tau_b = \begin{Bmatrix} 1.50\ f_{ct} & \sigma_{s,max} < 180\ MPa \\ 1.50\ f_{ct} & f_{sy} > \sigma_{s,max} \geq 180\ MPa \end{Bmatrix}$

D-SCC: $\tau_b = \begin{Bmatrix} 1.25\ f_{ct} & \sigma_{s,max} < 180\ MPa \\ 1.30\ f_{ct} & f_{sy} > \sigma_{s,max} \geq 180\ MPa \end{Bmatrix}$

S-SCC: $\tau_b = \begin{Bmatrix} 1.50\ f_{ct} & \sigma_{s,max} < 180\ MPa \\ 1.70\ f_{ct} & f_{sy} > \sigma_{s,max} \geq 180\ MPa \end{Bmatrix}$

DS-SCC: $\tau_b = \begin{Bmatrix} 1.50\ f_{ct} & \sigma_{s,max} < 180\ MPa \\ 1.60\ f_{ct} & f_{sy} > \sigma_{s,max} \geq 180\ MPa \end{Bmatrix}$

FRSCC time-dependent crack width stabilized cracking phase:

$$w_s = s_r\left[\frac{\sigma_s}{E_s} - \left(\frac{s_r\ \tau_{sm}}{d_b\ E_s}\left(1+\frac{E_s}{E_c}\rho_s/\gamma\right) + \frac{\sigma_{cf}}{\gamma\ E_c} - \varepsilon_{f,shr}^{*}\frac{E_f}{E_c}\eta\,\rho_f\right) - \varepsilon_{shr}^{*}\right] \tag{8.104}$$

where for the N-SCC, D-SCC, S-SCC, DS-SCC mixtures

$\tau_b = 1.5\ f_{ct}$

SCC and FRSCC instantaneous and time-dependent crack spacing:

$$(s_r)_{max} = \frac{f_{ct}\, d_b}{2\, \tau_b\, \rho_{ef}} \tag{8.105}$$

$$(s_r)_{min} = \frac{1}{2}(s_r)_{max} \tag{8.106}$$

$$(s_r)_{ave} = \frac{(s_r)_{max} + (s_r)_{min}}{2} \tag{8.107}$$

For short-term:

N-SCC: $\tau_b = \begin{Bmatrix} 1.50\, f_{ct} & \sigma_{s,max} < 180\, MPa \\ 1.50\, f_{ct} & f_{sy} > \sigma_{s,max} \geq 180\, MPa \end{Bmatrix}$

D-SCC: $\tau_b = \begin{Bmatrix} 1.25\, f_{ct} & \sigma_{s,max} < 180\, MPa \\ 1.30\, f_{ct} & f_{sy} > \sigma_{s,max} \geq 180\, MPa \end{Bmatrix}$

S-SCC: $\tau_b = \begin{Bmatrix} 1.50\, f_{ct} & \sigma_{s,max} < 180\, MPa \\ 1.70\, f_{ct} & f_{sy} > \sigma_{s,max} \geq 180\, MPa \end{Bmatrix}$

DS-SCC: $\tau_b = \begin{Bmatrix} 1.50\, f_{ct} & \sigma_{s,max} < 180\, MPa \\ 1.60\, f_{ct} & f_{sy} > \sigma_{s,max} \geq 180\, MPa \end{Bmatrix}$

All the N-SCC, D-SCC, S-SCC, DS-SCC mixtures for the long-term behaviour:

$\tau_b = 1.5\, f_{ct}$

8.5 SUMMARY AND CONCLUSIONS

Rational analytical models are presented for predicting the crack width and crack spacing of flexural SCC and FRSCC slabs. The proposed analytical models were used to predict crack width and crack spacing of 8 flexural slabs under sustained service loads for periods up to 240 days. It should be emphasized that, cracking in reinforced concrete is a random phenomenon and measured crack widths and crack spacings in structural members show

large scatter. Considering this, good agreement was both obtained between the measured experimental values and the predicted values; for instantaneous and time-dependent behaviour as shown in Figures 8.10 to 8.25.

In order to make a comparison between the models, crack width and crack spacing were also calculated in accordance with Eurocode 2 (1991), CEB-FIP (1990), ACI318-99 (1999), Eurocode 2 (2004), fib-Model Code (2010), Nejadi (2005), Leutbecher (2007), and proposed model in this study. Comparison between the experimental results, proposed analytical model and international codes are presented in Tables 8.4 and 8.7 and illustrated in Figures 8.10 to 8.25.

8.5.1 Crack Width

The instantaneous behaviour of Eurocode 2 (1991) overestimates the crack width for slab specimens at all steel stress levels (Figures 8.10 to 8.17). However, for long-term behaviour, it underestimates actual crack widths (Figures 8.17 to 8.25).

The instantaneous crack widths calculated in accordance with CEB-FIP (1990) at in-service steel stress levels up to 250 MPa underestimates the crack width for slab specimens (Figures 8.10 to 8.17). However, for time-dependent behaviour, the method slightly underestimates the crack width at steel stress levels lower than 200 MPa and for slabs with widely spaced tensile reinforcement bars (Figures 8.17 to 8.25).

The instantaneous crack widths calculated in accordance with ACI318-99 (1999) at steel stress levels up to 250 MPa shows that ACI318 overestimates the crack width for slab specimens at all steel stress levels (Figures 8.10 to 8.17). Since in this code the time-dependent effect of shrinkage has not been considered, ACI318-99 (1999) underestimates the long-term crack width (Figures 8.17 to 8.25).

For the instantaneous behaviour, Eurocode 2 (2004) slightly underestimates the crack width for slab specimens at all steel stress levels (Figures 8.10 to 8.17). However, for long-term behaviour, it more underestimates actual crack widths (Figures 8.17 to 8.25).

The instantaneous crack widths calculated in accordance with fib-Model Code (2010) at in-service steel stress levels up to 250 MPa slightly overestimates the crack width for

slab specimens (Figures 8.10 to 8.17). However, for time-dependent behaviour, the method underestimates the crack width at steel stress levels lower than 200 MPa and for slabs with widely spaced tensile reinforcement bars (Figures 8.17 to 8.25).

The instantaneous crack widths calculated in accordance with Nejadi (2005) and Leutbecher (2007) at in-service steel stress levels up to 250 MPa underestimate the crack width for slab specimens (Figures 8.10 to 8.17). However, for time-dependent behaviour, the methods slightly underestimate the crack width at steel stress levels lower than 200 MPa and for slabs with widely spaced tensile reinforcement bars (Figures 8.16 to 8.24).

The crack widths calculated in accordance with Proposed Model at steel stress levels up to 250 MPa shows that, for short-term cracking and time-dependent behaviour, Proposed Model predicts crack widths in good agreement with measured experimental results at all steel stress levels (Figures 8.10 to 8.25).

8.5.2 Crack Spacing

According to Section 7.5, instantaneous crack spacing reduces with time under sustained load due to creep and shrinkage. Eurocode 2 (1991), CEB-FIP (1990), fib-Model Code (2010), and Leutbecher (2007) give equations corresponds to the design or characteristic maximum crack width and consider the limit values of maximum crack width under quasi-permanent loading as satisfactory for reinforced concrete members. Therefore, crack spacing calculated in accordance with the above mentioned models corresponds to the quasi-permanent loading and underestimates the instantaneous crack spacing, but provides reasonable agreement with the measured final long-term crack spacing.

The crack spacing calculated in accordance with ACI318-99 (1999) and Eurocode 2 (2004) overestimate the short-term and long-term crack spacing.

Due to the random nature of cracking, great accuracy in calculating the crack spacing is not achievable. Nevertheless, the instantaneous and final average crack spacing predicted by the Proposed Model is in good agreement with the measured instantaneous and final average crack spacing.

Table 8.4 Comparison between crack widths experimental results, proposed analytical model and codes for instantaneous behaviour

	Instantaneous Behaviour							
	N-SCC-a	N-SCC-b	D-SCC-a	D-SCC-b	S-SCC-a	S-SCC-b	DS-SCC-a	DS-SCC-b
Experimental Results	0.1100	0.0800	0.1100	0.0700	0.1200	0.0700	0.1000	0.0600
Eurocode 2 (1991)	0.1396	0.0831	0.1396	0.0831	0.1396	0.0831	0.1396	0.0831
CEB-FIP (1990)	0.0741	0.0392	0.0591	0.0566	0.0748	0.0473	0.0664	0.0399
ACI318-99 (1999)	0.1785	0.1311	0.1783	0.1310	0.1783	0.1310	0.1782	0.1309
Eurocode 2 (2004)	0.0961	0.0509	0.0767	0.0314	0.1066	0.0613	0.0969	0.0517
fib-Model Code (2010)	0.1213	0.0981	0.1093	0.0743	0.1180	0.0996	0.1173	0.0997
Nejadi (2005)	0.0857	0.0543	0.0886	0.0561	0.1003	0.0558	0.0768	0.0573
Leutbecher (2007)	0.0667	0.0319	0.0506	0.0292	0.0772	0.0424	0.0610	0.0261
Proposed Model	0.1040	0.0751	0.1057	0.0685	0.1184	0.0657	0.0933	0.0575

Table 8.5 Comparison between crack spacings experimental results, proposed analytical model and codes for instantaneous behaviour

	Instantaneous Behaviour							
	N-SCC-a	N-SCC-b	D-SCC-a	D-SCC-b	S-SCC-a	S-SCC-b	DS-SCC-a	DS-SCC-b
Experimental Results	99.000	100.000	96.000	99.000	96.000	93.000	102.000	94.000
Eurocode 2 (1991)	94.634	94.634	94.634	94.634	94.634	94.634	94.634	94.634
CEB-FIP (1990)	82.656	82.656	82.656	82.656	82.656	82.656	82.656	82.656
ACI318-99 (1999)	161.199	161.199	161.199	161.199	161.199	161.199	161.199	161.199
Eurocode 2 (2004)	160.878	160.878	160.878	160.878	160.878	160.878	160.878	160.878
fib-Model Code (2010)	82.656	82.656	82.656	82.656	82.656	82.656	82.656	82.656
Nejadi (2005)	155.614	156.614	131.272	131.272	131.272	131.272	131.394	131.394
Leutbecher (2007)	82.656	82.656	82.656	82.656	82.656	82.656	82.656	82.656
Proposed Model	111.585	112.585	111.721	111.721	111.721	111.721	111.843	111.843

Table 8.6 Comparison between crack widths experimental results, proposed analytical model and codes for time-dependent behaviour

	Time-dependent Behaviour							
	N-SCC-a	N-SCC-b	D-SCC-a	D-SCC-b	S-SCC-a	S-SCC-b	DS-SCC-a	DS-SCC-b
Experimental Results	0.2400	0.1800	0.2200	0.1400	0.2200	0.1500	0.2000	0.1400
Eurocode 2 (1991)	0.1551	0.1042	0.1551	0.1042	0.1551	0.1042	0.1551	0.1043
CEB-FIP (1990)	0.2030	0.1681	0.1905	0.1444	0.1978	0.1676	0.1999	0.1703
ACI318-99 (1999)	0.1785	0.1311	0.1783	0.1310	0.1783	0.1310	0.1782	0.1309
Eurocode 2 (2004)	0.1209	0.0757	0.1201	0.0627	0.1215	0.0763	0.1142	0.0690
fib-Model Code (2010)	0.1340	0.1108	0.1254	0.0943	0.1306	0.1106	0.1318	0.1123
Nejadi (2005)	0.1551	0.1061	0.1412	0.0944	0.1576	0.1083	0.1525	0.1039
Leutbecher (2007)	0.1962	0.1613	0.1823	0.1474	0.1975	0.1626	0.1942	0.1592
Proposed Model	0.2224	0.1806	0.2026	0.1431	0.2270	0.1551	0.2089	0.1570

Table 8.7 Comparison between crack spacings experimental results, proposed analytical model and codes for time-dependent behaviour

	Time-dependent Behaviour							
	N-SCC-a	N-SCC-b	D-SCC-a	D-SCC-b	S-SCC-a	S-SCC-b	DS-SCC-a	DS-SCC-b
Experimental Results	97.000	95.000	95.000	95.000	94.000	91.000	98.000	90.000
Eurocode 2 (1991)	94.634	94.634	94.634	94.634	94.634	94.634	94.634	94.634
CEB-FIP (1990)	82.656	82.656	82.656	82.656	82.656	82.656	82.656	82.656
ACI318-99 (1999)	161.199	161.199	161.199	161.199	161.199	161.199	161.199	161.199
Eurocode 2 (2004)	160.878	160.878	160.878	160.878	160.878	160.878	160.878	160.878
fib-Model Code (2010)	82.656	82.656	82.656	82.656	82.656	82.656	82.656	82.656
Nejadi (2005)	109.904	109.904	92.600	92.600	92.600	92.600	92.584	92.584
Leutbecher (2007)	82.656	82.656	82.756	82.756	82.756	82.756	82.847	82.847
Proposed Model	102.077	102.077	100.077	100.077	100.077	100.077	100.062	100.062

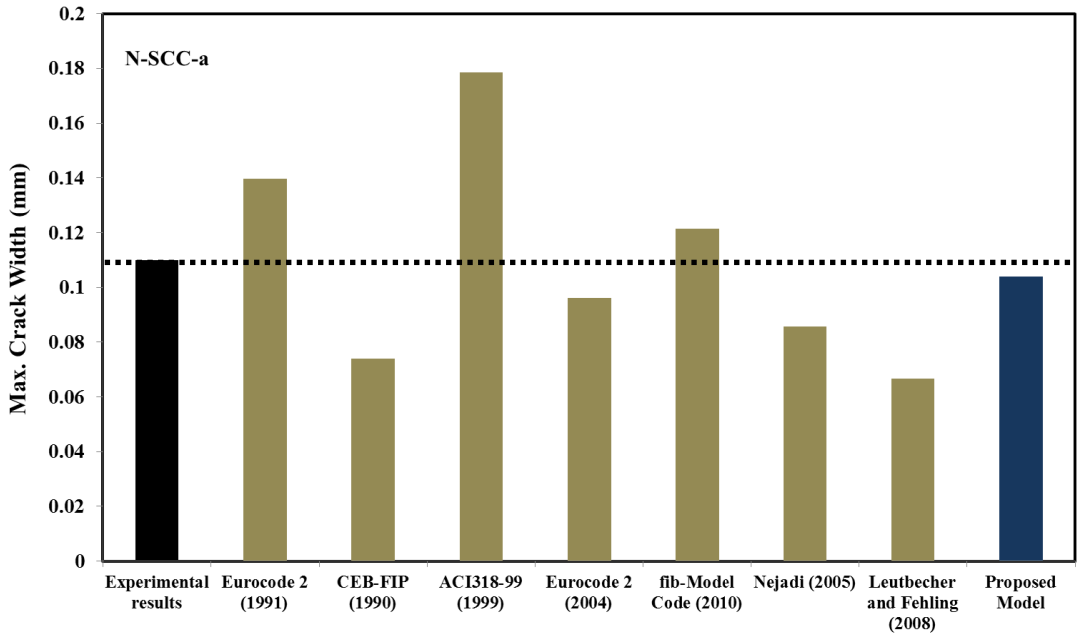

Figure 8.10 Comparison between experimental results, proposed model and available models for slab N-SCC-a (Instantaneous behaviour)

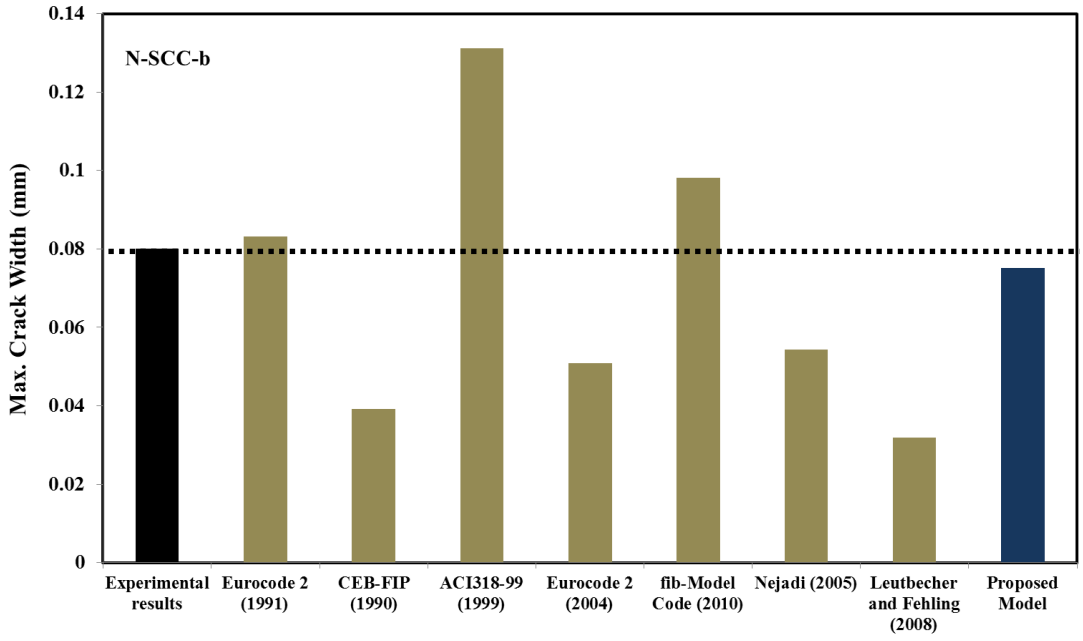

Figure 8.11 Comparison between experimental results, proposed model and available models for slab N-SCC-b (Instantaneous behaviour)

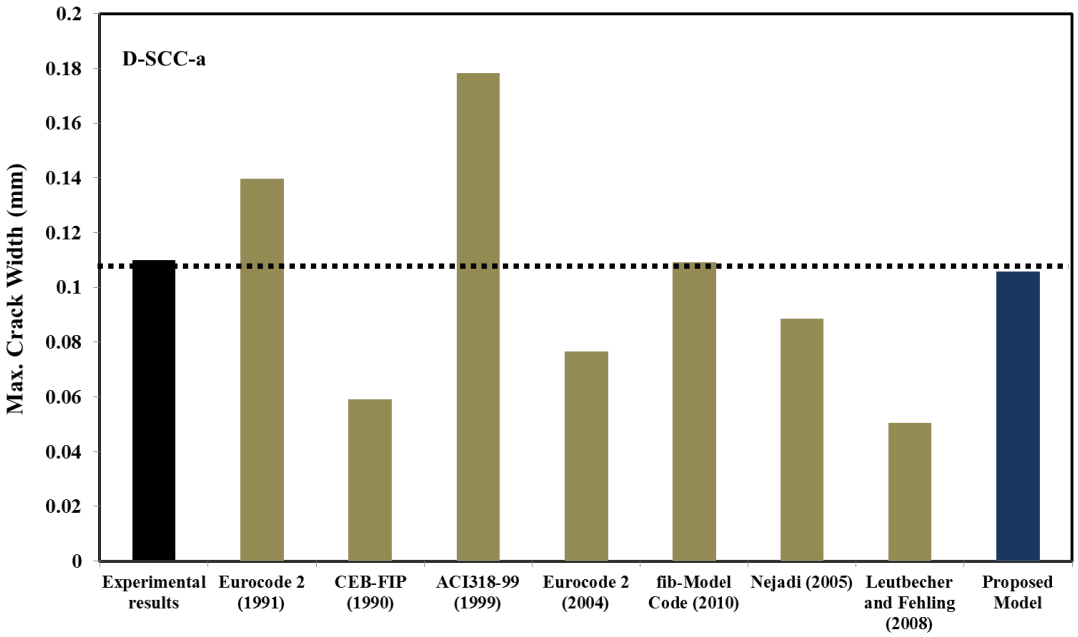

Figure 8.12 Comparison between experimental results, proposed model and available models for slab D-SCC-a (Instantaneous behaviour)

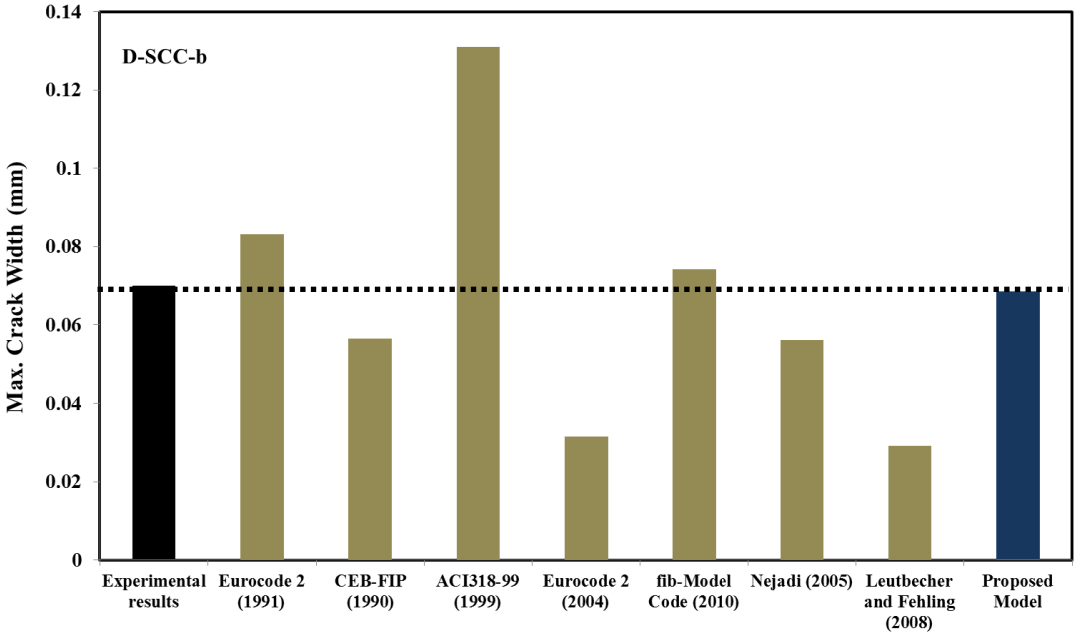

Figure 8.13 Comparison between experimental results, proposed model and available models for slab D-SCC-b (Instantaneous behaviour)

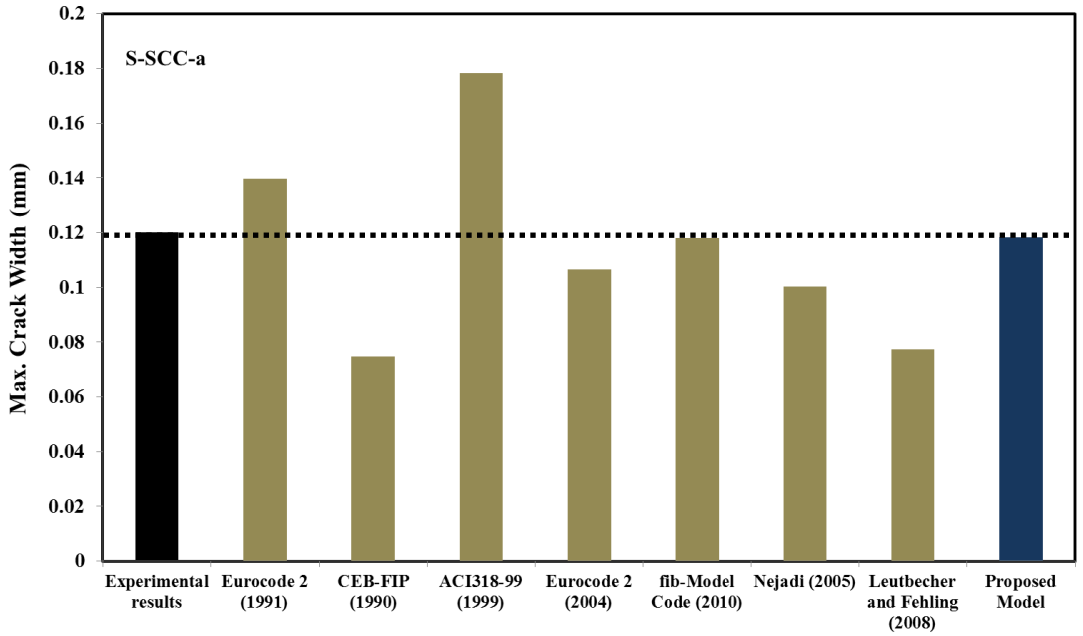

Figure 8.14 Comparison between experimental results, proposed model and available models for slab S-SCC-a (Instantaneous behaviour)

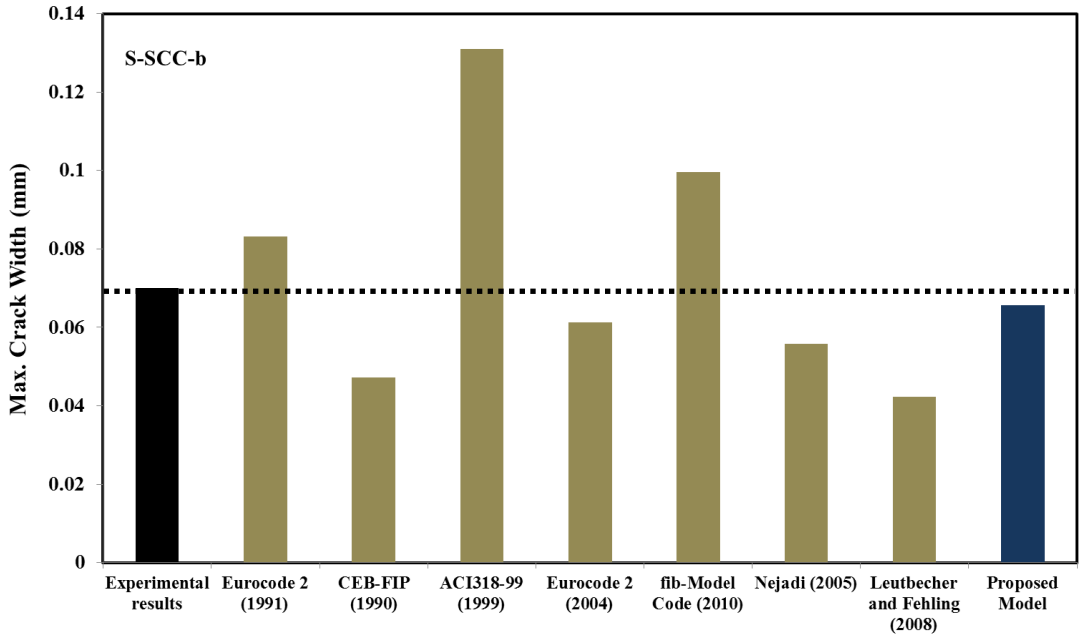

Figure 8.15 Comparison between experimental results, proposed model and available models for slab S-SCC-b (Instantaneous behaviour)

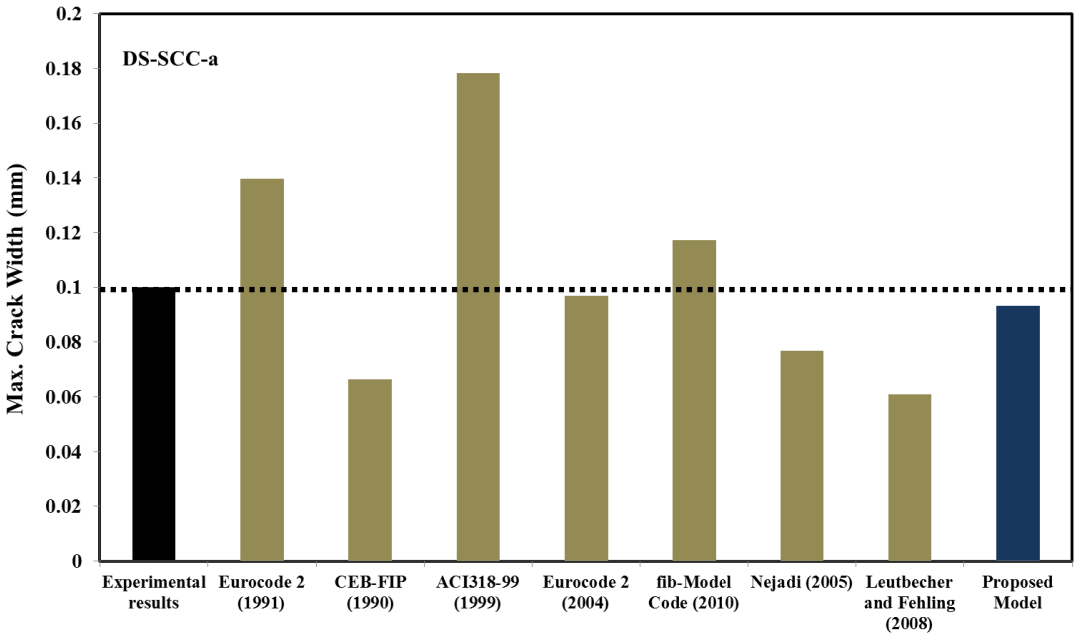

Figure 8.16 Comparison between experimental results, proposed model and available models for slab DS-SCC-a (Instantaneous behaviour)

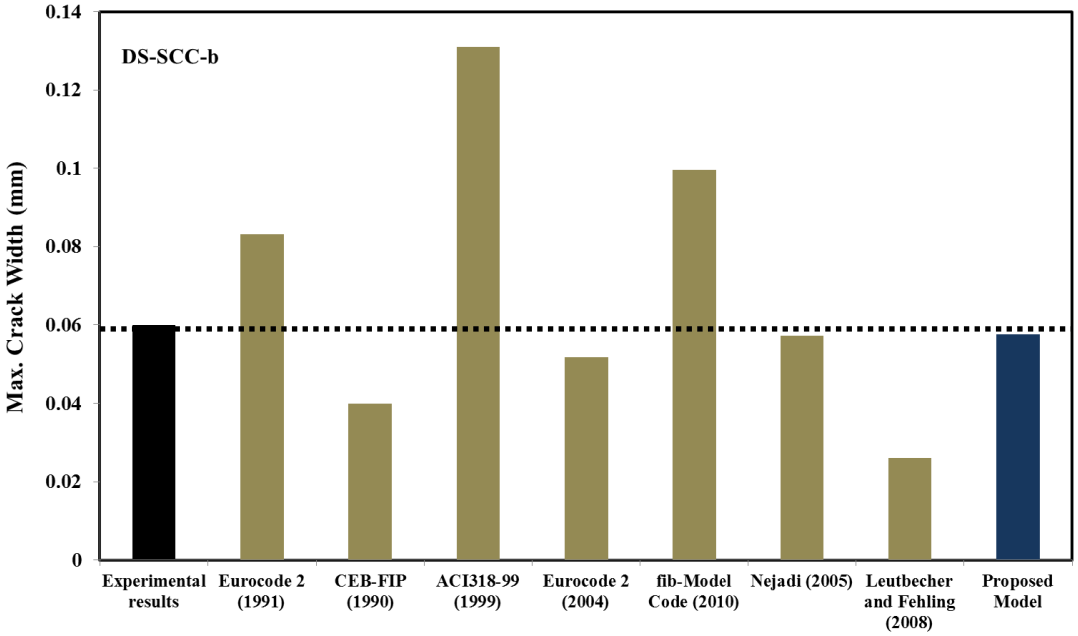

Figure 8.17 Comparison between experimental results, proposed model and available models for slab DS-SCC-b (Instantaneous behaviour)

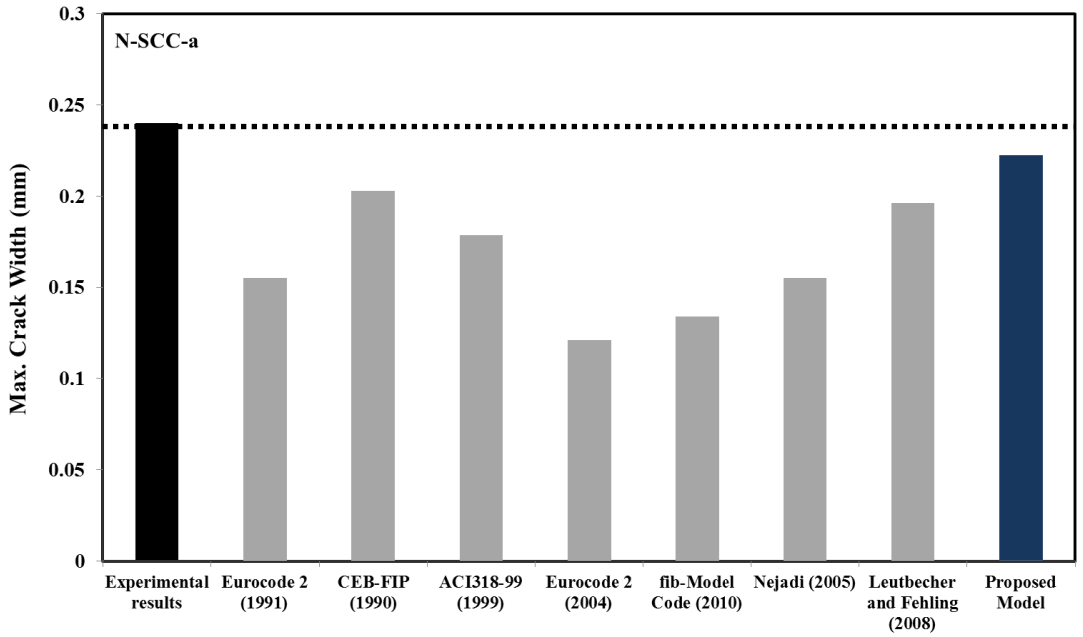

Figure 8.18 Comparison between experimental results, proposed model and available models for slab N-SCC-a (Time-dependent behaviour)

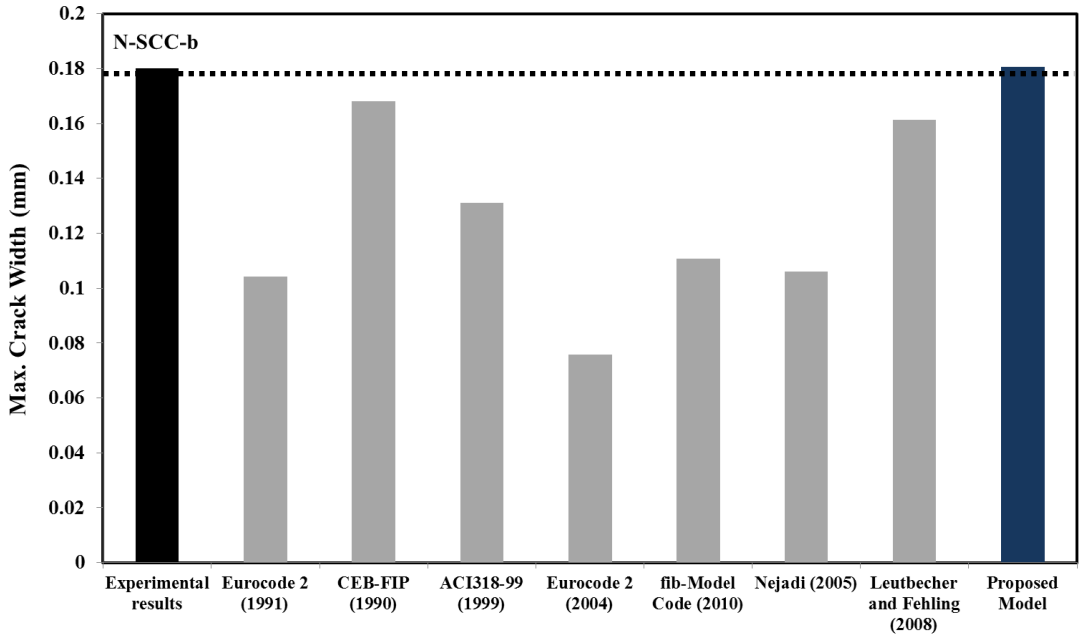

Figure 8.19 Comparison between experimental results, proposed model and available models for slab N-SCC-b (Time-dependent behaviour)

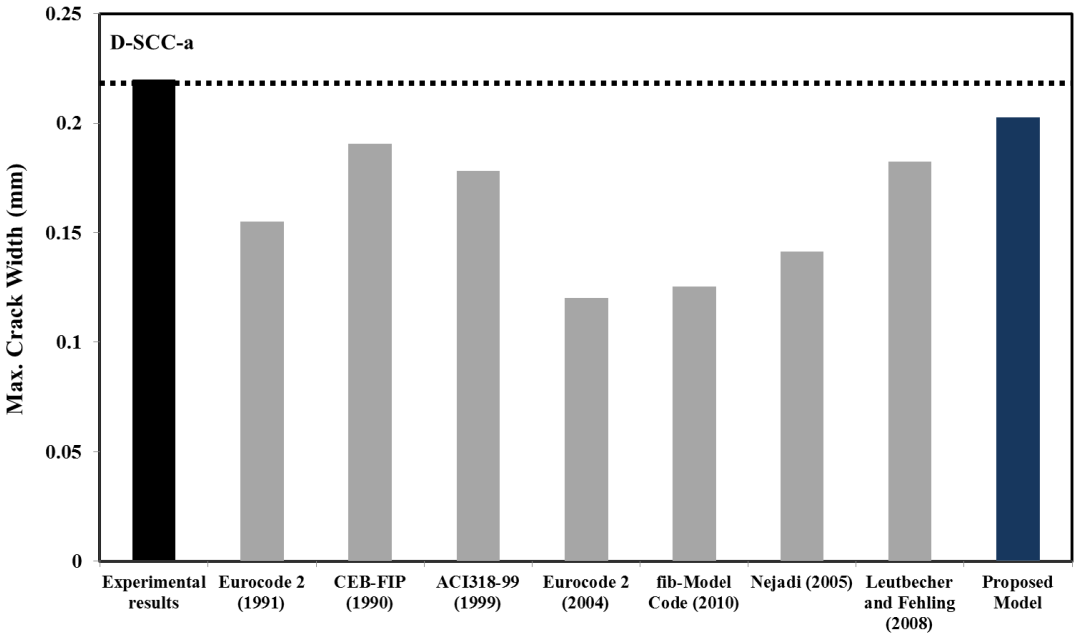

Figure 8.20 Comparison between experimental results, proposed model and available models for slab D-SCC-a (Time-dependent behaviour)

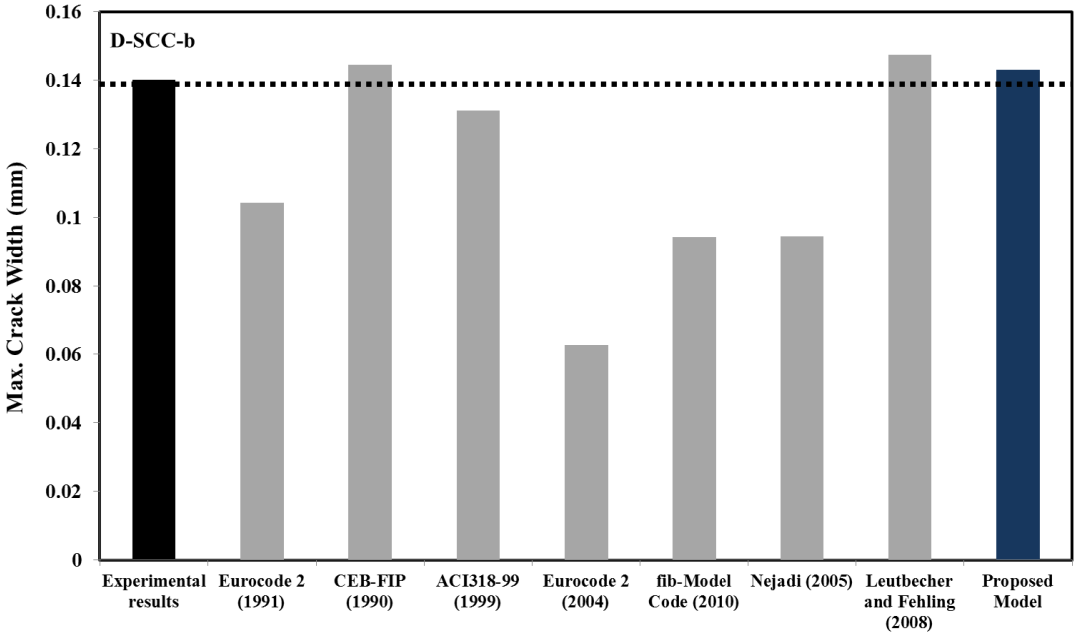

Figure 8.21 Comparison between experimental results, proposed model and available models for slab D-SCC-b (Time-dependent behaviour)

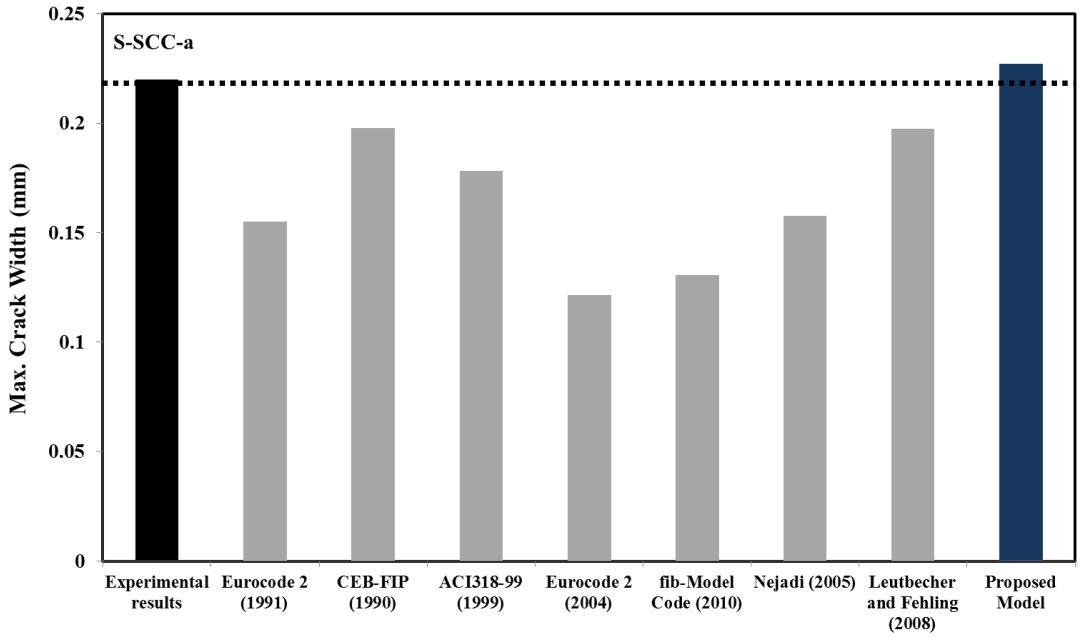

Figure 8.22 Comparison between experimental results, proposed model and available models for slab S-SCC-a (Time-dependent behaviour)

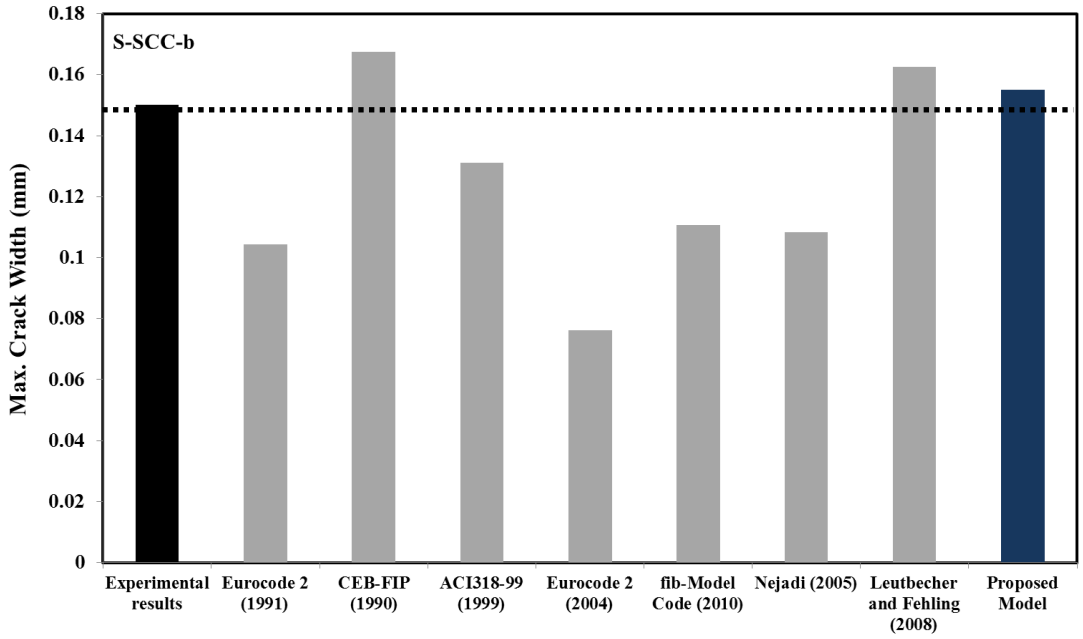

Figure 8.23 Comparison between experimental results, proposed model and available models for slab S-SCC-b (Time-dependent behaviour)

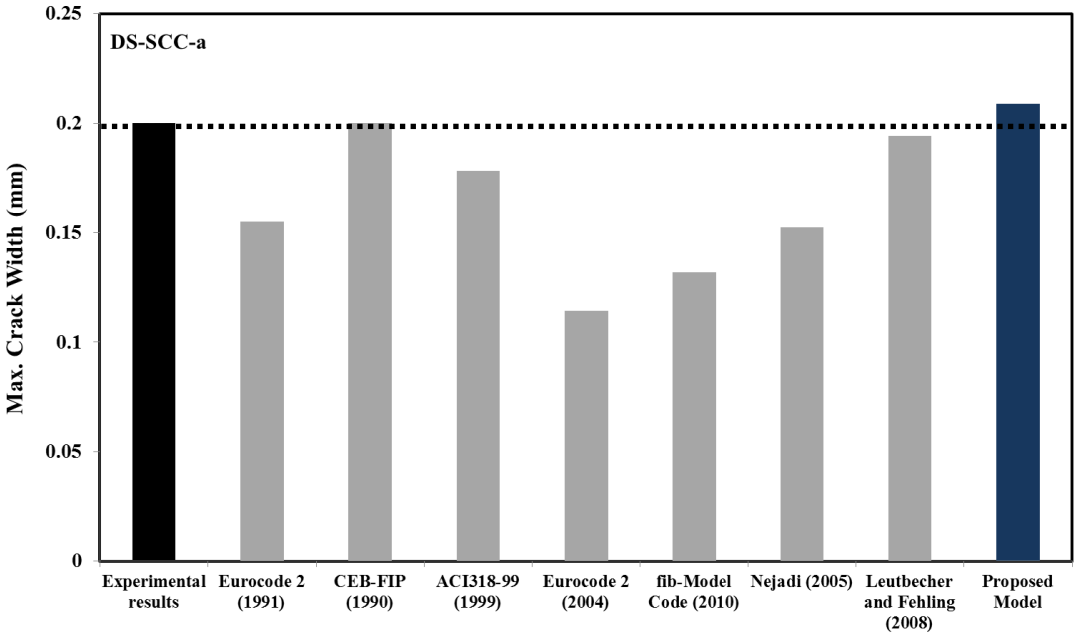

Figure 8.24 Comparison between experimental results, proposed model and available models for slab DS-SCC-a (Time-dependent behaviour)

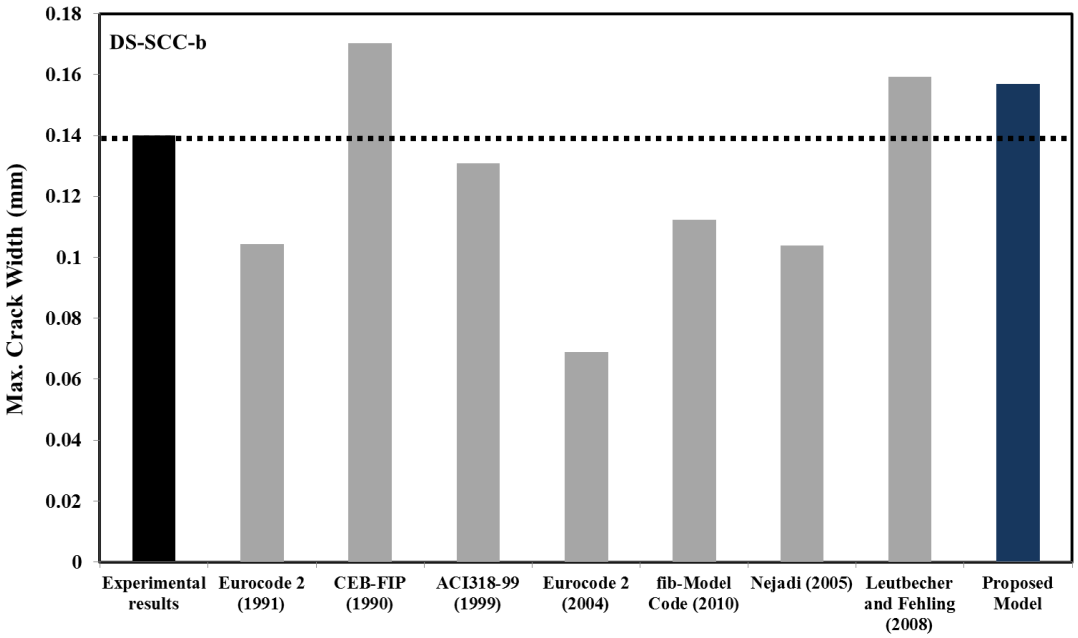

Figure 8.25 Comparison between experimental results, proposed model and available models for slab DS-SCC-b (Time-dependent behaviour)

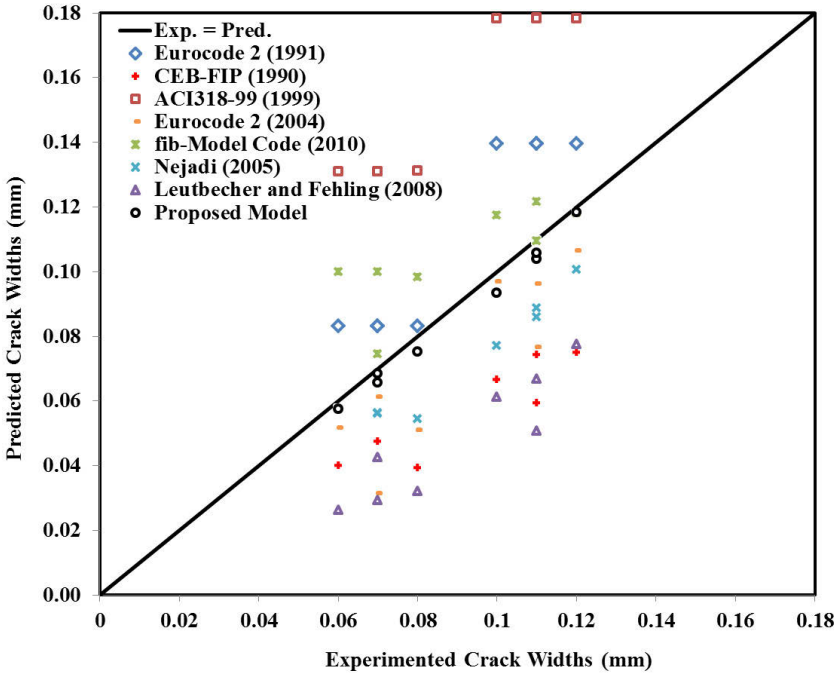

Figure 8.26 Comparison between crack widths experimental results, proposed analytical model and codes for instantaneous behaviour

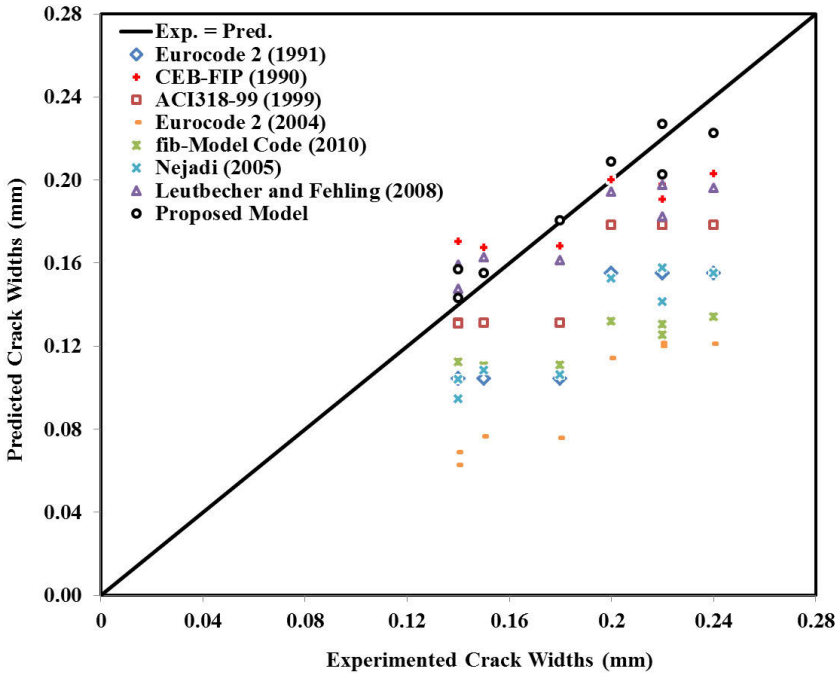

Figure 8.27 Comparison between crack widths experimental results, proposed analytical model and codes for time-dependent behaviour

CHAPTER 9

FINITE ELEMENT MODELLING OF CRACKING BEHAVIOUR OF CONVENTIONAL STEEL REINFORCED AND FIBRE REINFORCED SELF-COMPACTING CONCRETE SLABS

CHAPTER 9

FINITE ELEMENT MODELLING OF CRACKING BEHAVIOUR OF CONVENTIONAL STEEL REINFORCED AND FIBRE REINFORCED SELF-COMPACTING CONCRETE SLABS

9.1 INTRODUCTION

The utility of reinforced concrete as a composite structural material is derived from the combination of concrete that is strong in compression and reinforcing steel which is strong and ductile in tension. Maintaining composite action requires perfect transfer of load between the concrete and steel. To better understanding of the reinforced concrete and its composite behaviour, many experimental programs have been developed that provided a firm basis for design equations. Activities that aim to predict the real behaviour of reinforced concrete members and structures have been intensively conducted in laboratories. However, to establish the global behaviour of an entire structure by experimental means would require the fabrication of the entire structure or at least a significant portion of that structure within the laboratory. Such a test specimen would be physically very difficult to be constructed. Although the alternative option could be scaling down the members with reproduced loading condition, it brings problems of changing of material behaviour in the model. Moreover, experimental test limitations also come from the nonlinearity nature of the reinforced concrete that includes:

- Reinforced concrete is a composite material made up of two materials, concrete and steel, with very different physical and mechanical properties;
- Concrete exhibits nonlinear behaviour even under low level loading due to nonlinear material behaviour, environmental effects, cracking, biaxial stiffening and strain softening;

- Reinforcing steel and concrete interact in a complex way through bond-slip and aggregate interlock.

These complex phenomena have led to engineers and scientists devoting many efforts to develop analytical solutions by using numerical methods. With the application of the Finite Element Method (FEM) to reinforced concrete structures, a numerical loading and testing can be performed upon structures that cannot be modelled for laboratory study. Applications of the FEM to model the behaviour of reinforced concrete structures, including tensile cracking, crushing, tension stiffening, multi-axial nonlinear concrete properties, creep, shrinkage, concrete-steel interaction, etc., have been undertaken by a number of investigators (Yi, 2006).

To conduct finite element analysis for reinforced concrete members the required knowledge in the material behaviour as well as the techniques of FEM are essential. Since the first finite element study in reinforced concrete members conducted by Ngo and Scordelis in 1967, a number of finite element programs, both for commercial purpose and produced in-house, have been popularly used. Since it is not an easy job to develop a complicated finite element program, the current trend in the finite element analysis of reinforced concrete members and structures is to implement new material models or new numerical methods into existing general purpose finite element models. New material models and new numerical methods reported in the open literature certainly make the current analysis programs more efficient and more updated. However, it is impossible for these existing finite element programs to include all new features that have not been considered when they were under development.

This study concerns the effective modelling of conventional reinforced concrete slabs and fibre reinforced self-compacting concrete slabs. The FEM will be used to model the slabs with the aid of a computer program to process the finite element model. The models will be critiqued on their ability to properly replicate real cracking and deflection behaviour in practice models. There are multiple methods for determining the deflection of beams as well as calculating crack spacing and crack width with regard to short term loading and under sustained load.

In this Chapter, non-linear modelling and finite element models of the reinforced concrete structures subjected to sustained service loads are presented briefly. Also, the FEM software (ATENA), developed by (Cervenka et al., 2005) that has been used for time-dependent analysis of reinforced concrete in this research is presented in summary. In the FEM parametric study, the hardened properties models, bond-slip models, and creep and shrinkage models for SCC and FRSCC in this proposed study are used together with the default ATENA models, to simulate and analysis of instantaneous and time-dependent cracking behaviours SCC and FRSCC one-way slabs.

9.2 NONLINEAR MODELLING OF CONCRETE STRUCTURES

Reinforced concrete is well known for its non-linear behaviour. The non-linearity in reinforced concrete originates from the non-linear stress-strain relationship of plain concrete. The structural behaviour is further complicated by cracking of concrete which causes a considerable redistribution of stresses within the intact concrete as well as the stress transfer from concrete to steel reinforcement. The FEM is the most often adopted numerical tool to simulate the non-linear behaviour of reinforced concrete structures. Rational and reliable representations of cracking of concrete must be used in conjunction with the FEM in order to accurately describe the structural behaviour.

In this section as shown in Figures 9.1 to 9.6, the following sub-sections are summarized for non-linear modelling of the concrete structures: general modelling approaches of cracking in concrete structures, constitutive models for concrete, fracture models for concrete, regularization of spurious strain localization, modelling of steel reinforcement, modelling of steel-concrete bond, and computational creep modelling. The above mentioned non-linear modelling sub-sections are very extensive and comprehensive in the literature (Chong, 2004, Yi, 2006, Lam, 2007). In this study, most important parameters that have major effect on our numerical modelling are considered and applied.

Figure 9.1 is summarized the available FEM modelling approaches of cracking in concrete structures, constitutive concrete models, and fracture concrete models. Two major approaches are available in the literature for the modelling of cracking in concrete

structures, namely the discrete crack approach and the smeared crack approach. One very important aspect in smeared crack modelling of concrete is the development of constitutive models that are capable to describe the behaviour of concrete. In the broad sense, the constitutive models of concrete may be classified into two categories: the macroscopic phenomenological models and the micromechanical models (see Figure 9.1).

Figure 9.2 shows FEM regularization of spurious strain localization. The earliest continuum modelling of cracking in concrete was based on the strength criterion. In these models, the concrete tensile response is characterized by a linear elastic pre-peak stress-strain relation and is followed by a sudden drop in stress to zero upon initiation of cracking. However, these models suffer from the severe deficiency of mesh size dependence. Numerical results for the same structure vary notably for finite element discretizations of different mesh sizes especially in the case of localized cracking with little or no reinforcement. Bažant and Cedolin (1979) pointed out that objective results could only be obtained based on an energy criterion by considering the energy release rate G_f and, hence, promoted the use of tension softening model for cracked concrete, that is, by the inclusion of a descending branch of the tensile stress-strain curve. Nevertheless, proper regularization tools must be employed in conjunction with the tension softening model in order to conserve the energy dissipation rate in crack formation.

Figures 9.3 and 9.4 indicate available FEM steel reinforcement modelling and steel-concrete bond modelling methods. Figure 9.5 illustrates available FEM creep modelling models for concrete. Moreover, continuum modelling of reinforced concrete structures, material constitutive modelling, and non-linear finite element implementations are summarized in Figure 9.6.

9.3 FINITE ELEMENT MODELS FOR REINFORCED CONCRETE

The main scope of this study is to develop a constitutive model which can provide reliable predictions of long-term cracking behaviour of reinforced SCC and FRSCC structures so that to facilitate a parametric study of cracking behaviour. In this way, the parameters affecting the development of a crack with time may be identified and quantified. For this

purpose, the most important finite element models for continuum modelling and material constitutive models are summarized in Figure 9.7.

9.4 FINITE ELEMENT MODELLING SOFTWARE

In this study for analysis of the long-term behaviour of reinforced SCC and FRSCC one-way slabs, the program that has been selected is ATENA. The main reasons for selecting ATENA can be summarized as follows:

a) Most of the creep models are included.

b) Shrinkage behaviour of reinforced concrete members can be considered.

c) User defined applications of some hardened mechanical properties of concrete such as compressive strength, tensile strength, modulus of elasticity, bond stress, tension stiffing factor, cark width, etc.

d) It is suitable for fibre reinforced concrete modelling.

e) Parallel ATENA-GiD software that can be used for interfacing with ATENA (ATENA is used for the analysis itself and the software GiD is used for the data preparation and the mesh generation).

Elasticity based material model (SBETA), fracture–plastic material model, and creep and shrinkage analysis algorithm that have been used in ATENA are summarized in Figures 9.8 to 9.11.

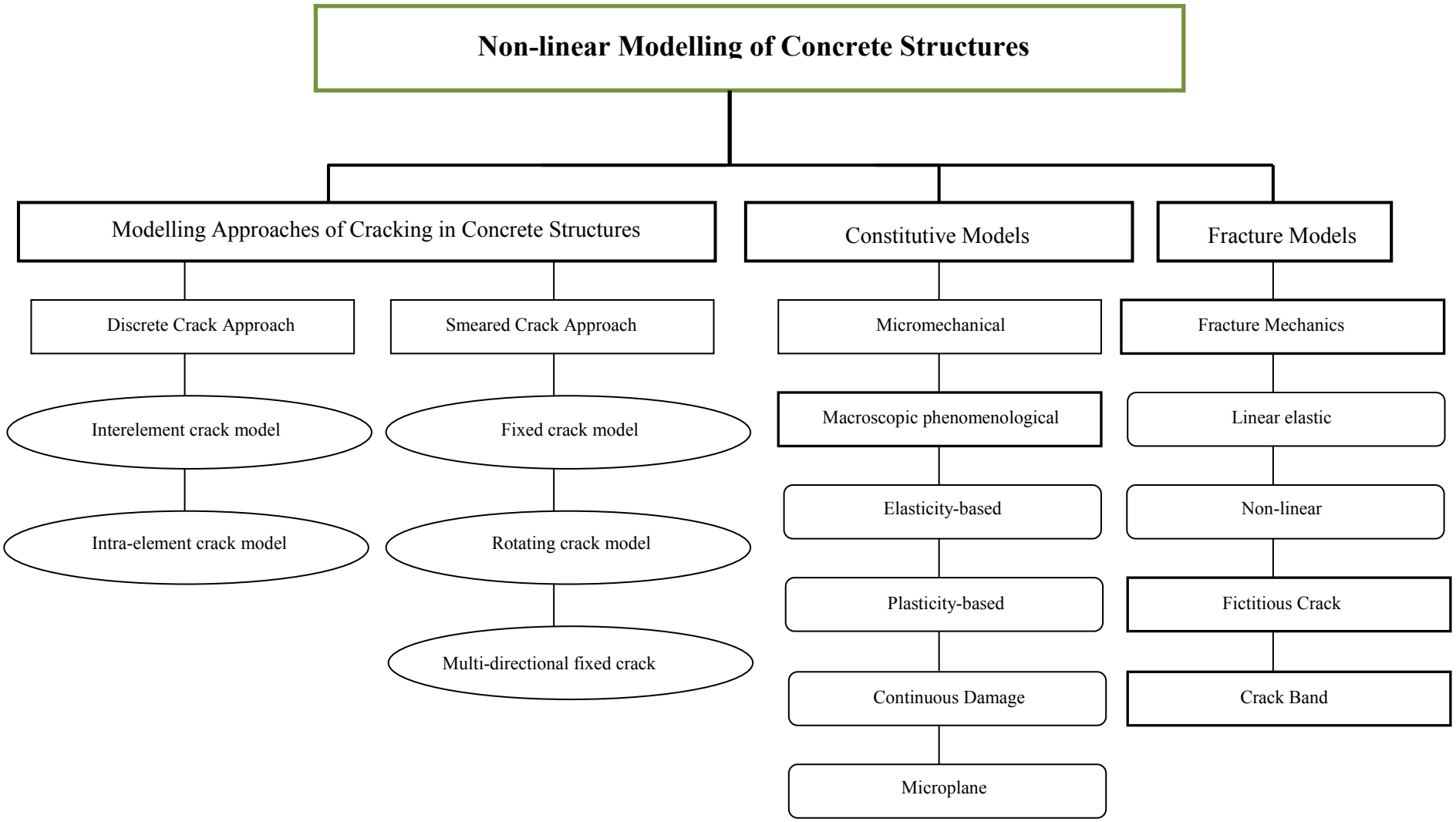

Figure 9.1 Non-linear modelling of concrete structures: Cracking approaches, constitutive models and fracture models (Chong, 2004)

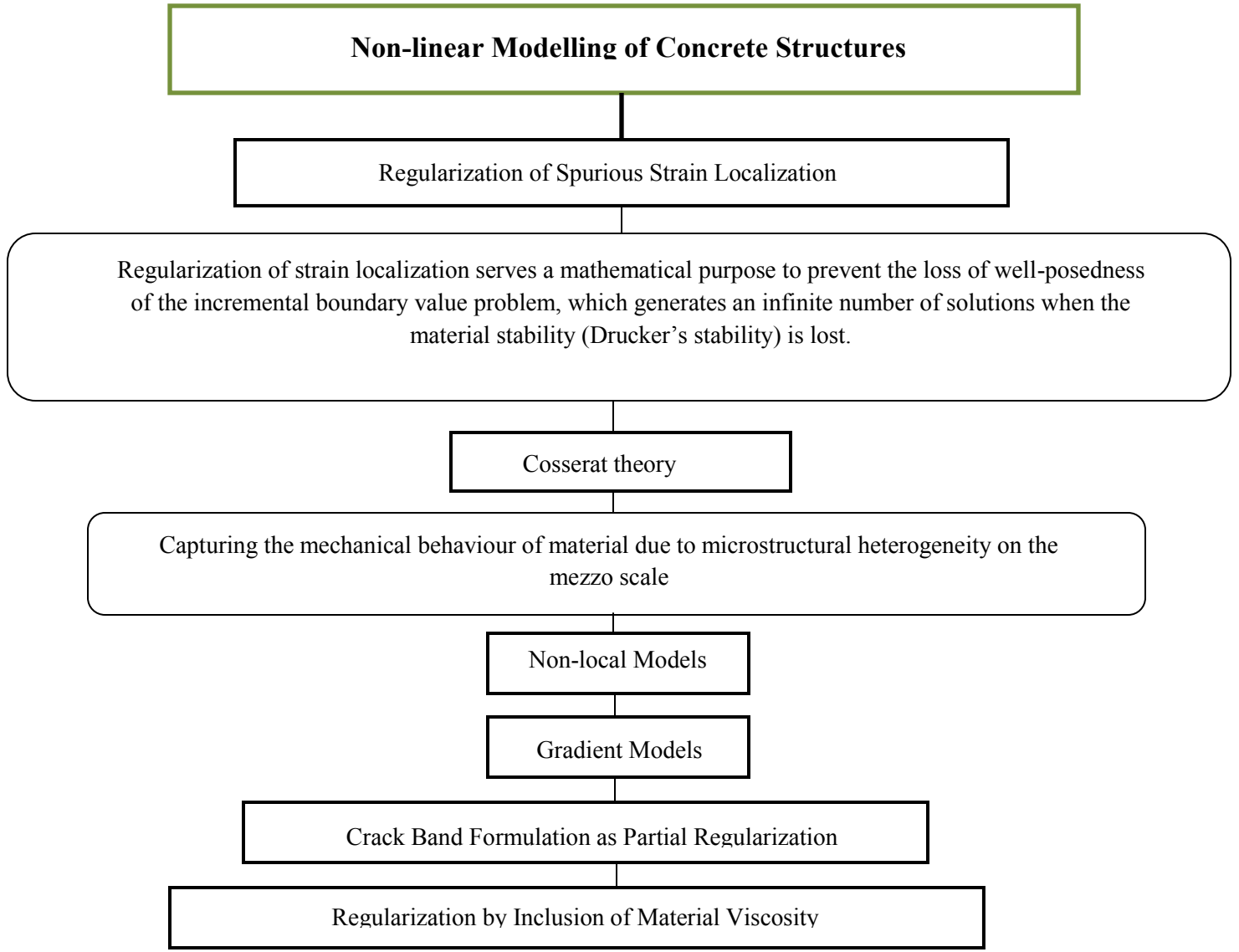

Figure 9.2 Non-linear modelling of concrete structures: Regularization of spurious strain localization (Chong, 2004)

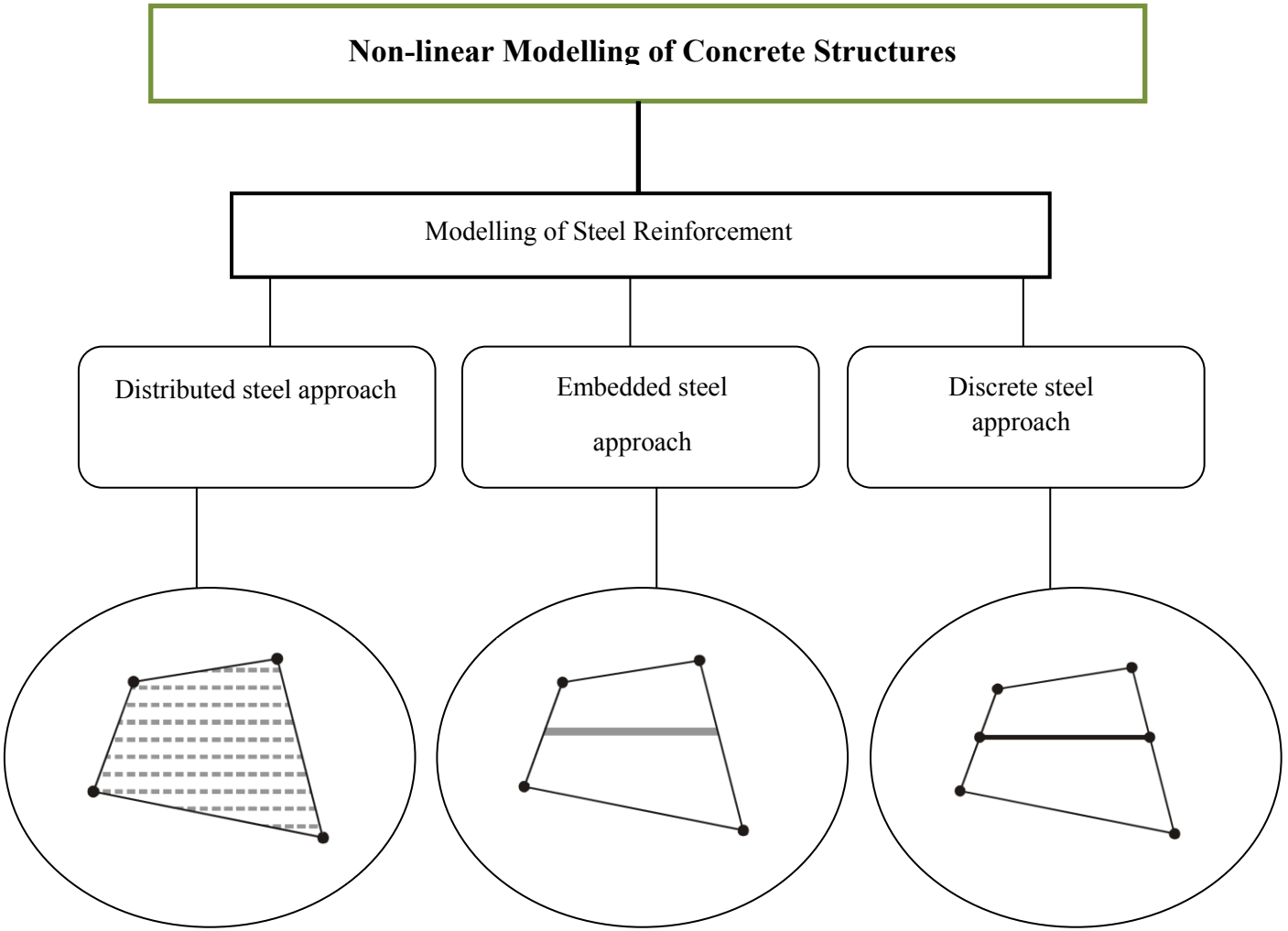

Figure 9.3 Non-linear modelling of concrete structures: Modelling of steel reinforcement (Chong, 2004)

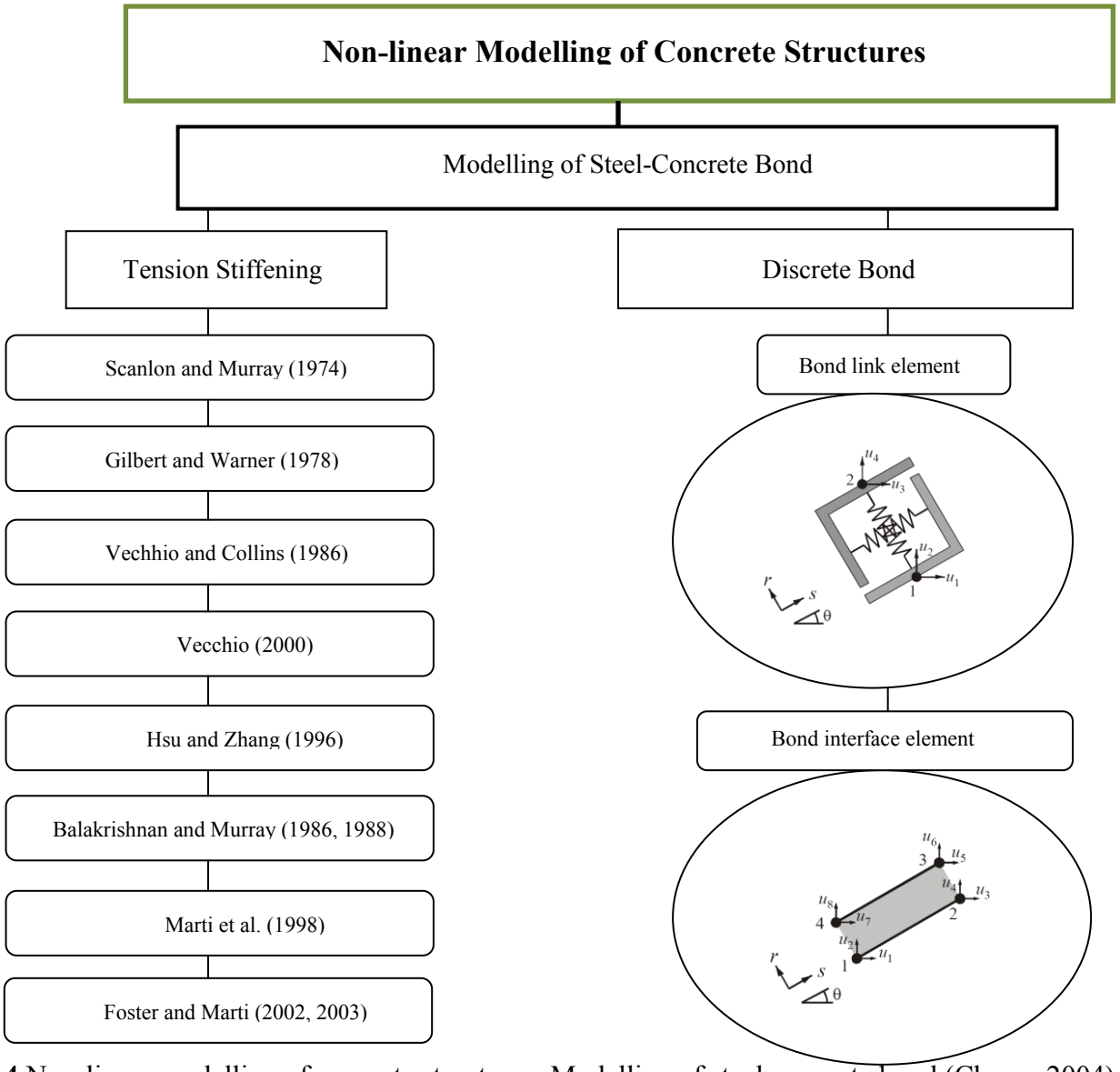

Figure 9.4 Non-linear modelling of concrete structures: Modelling of steel-concrete bond (Chong, 2004)

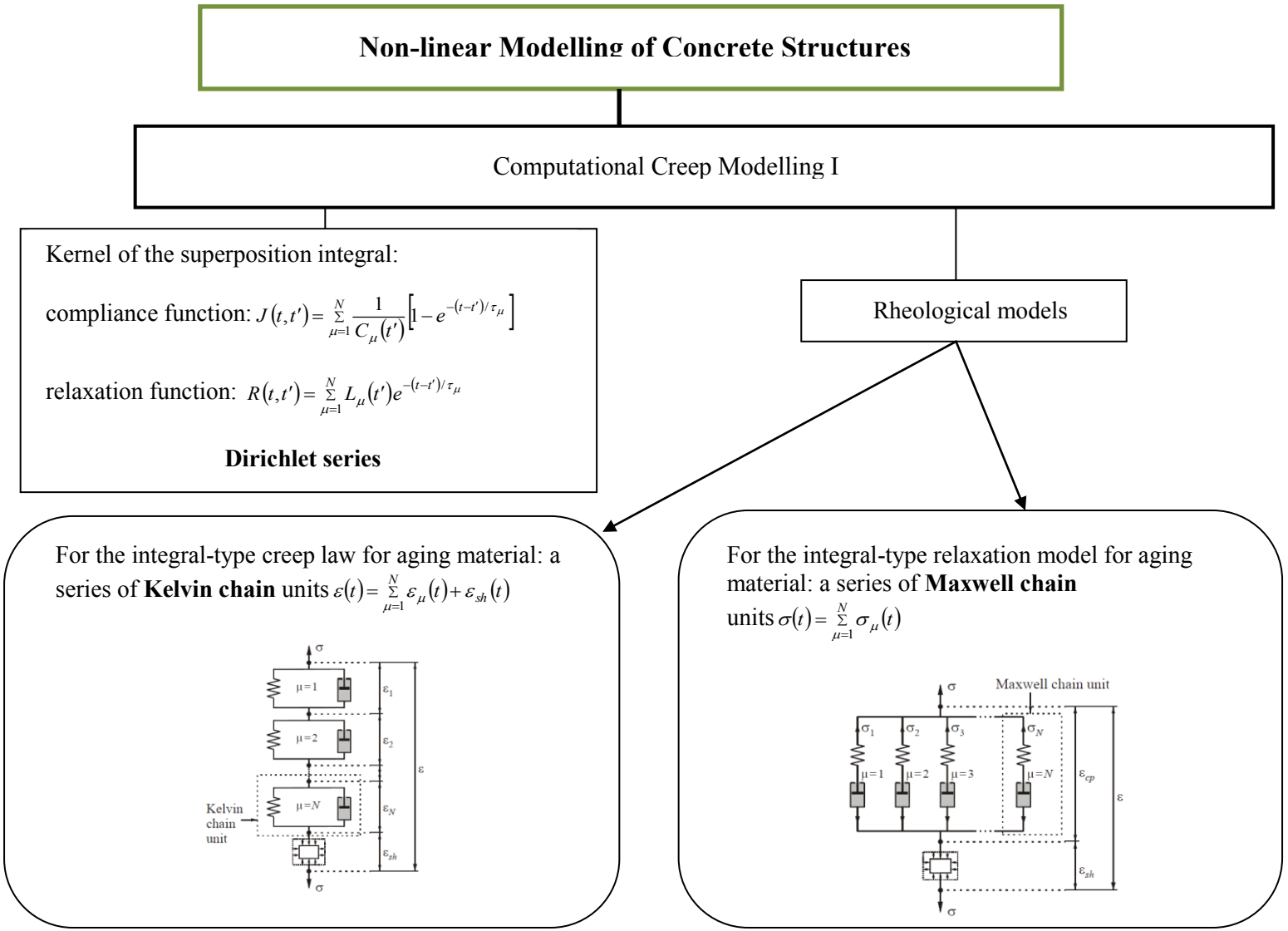

Figure 9.5 Non-linear modelling of concrete structures: Computational creep modelling part I (Chong, 2004)

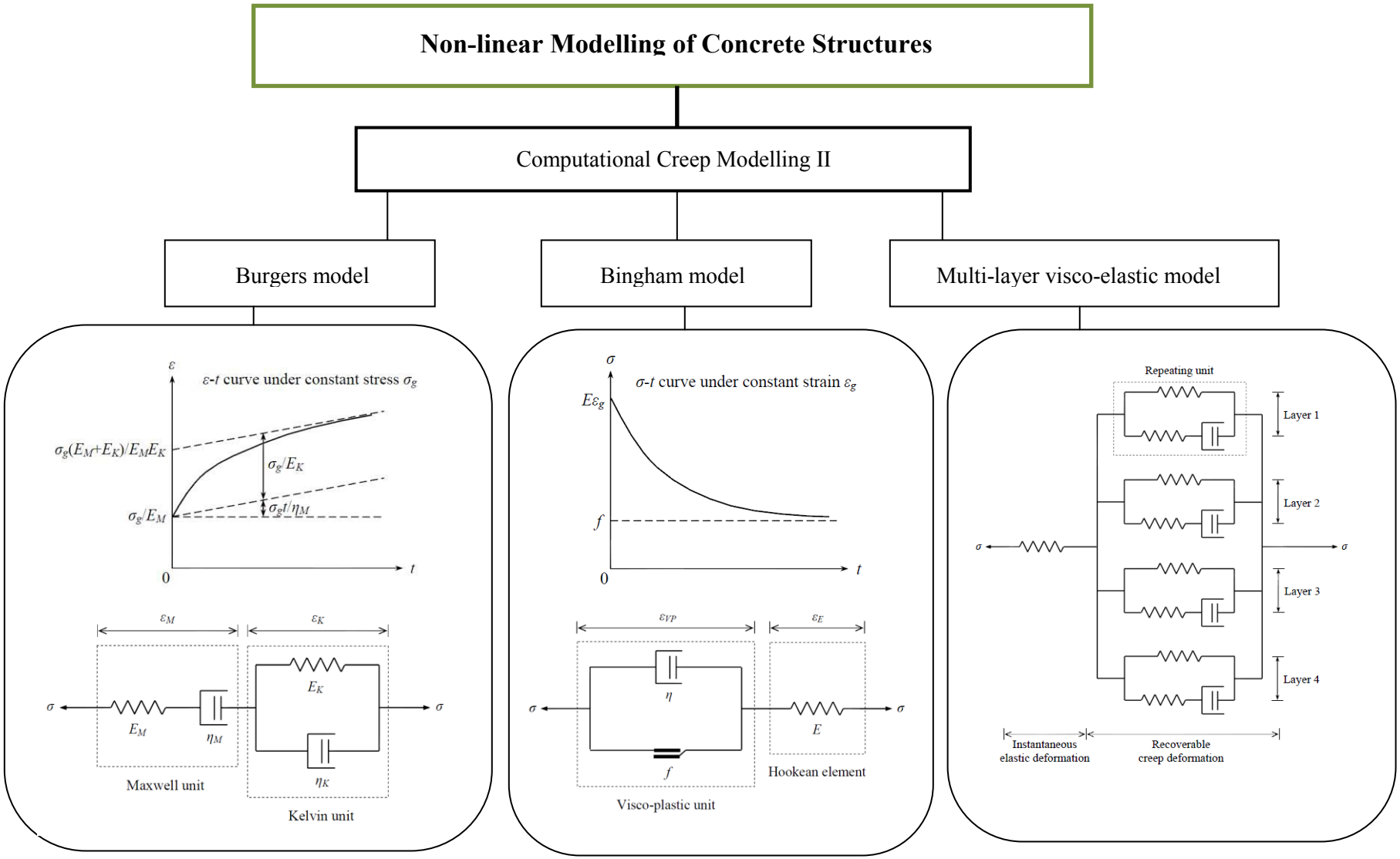

Figure 9.6 Non-linear modelling of concrete structures: Computational creep modelling part II (Lam, 2007)

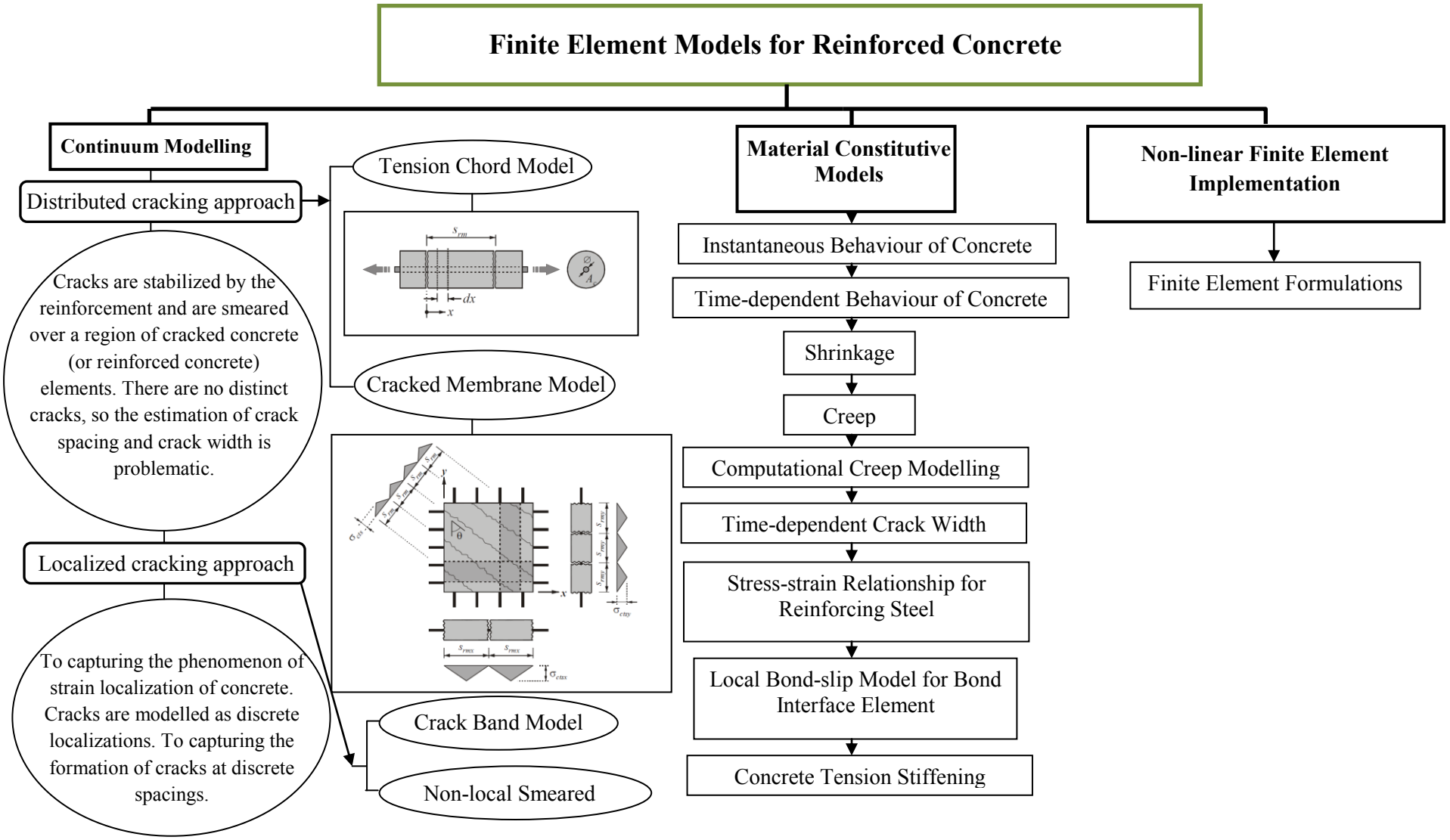

Figure 9.7 Finite element models for reinforced concrete (ATENA, 2012)

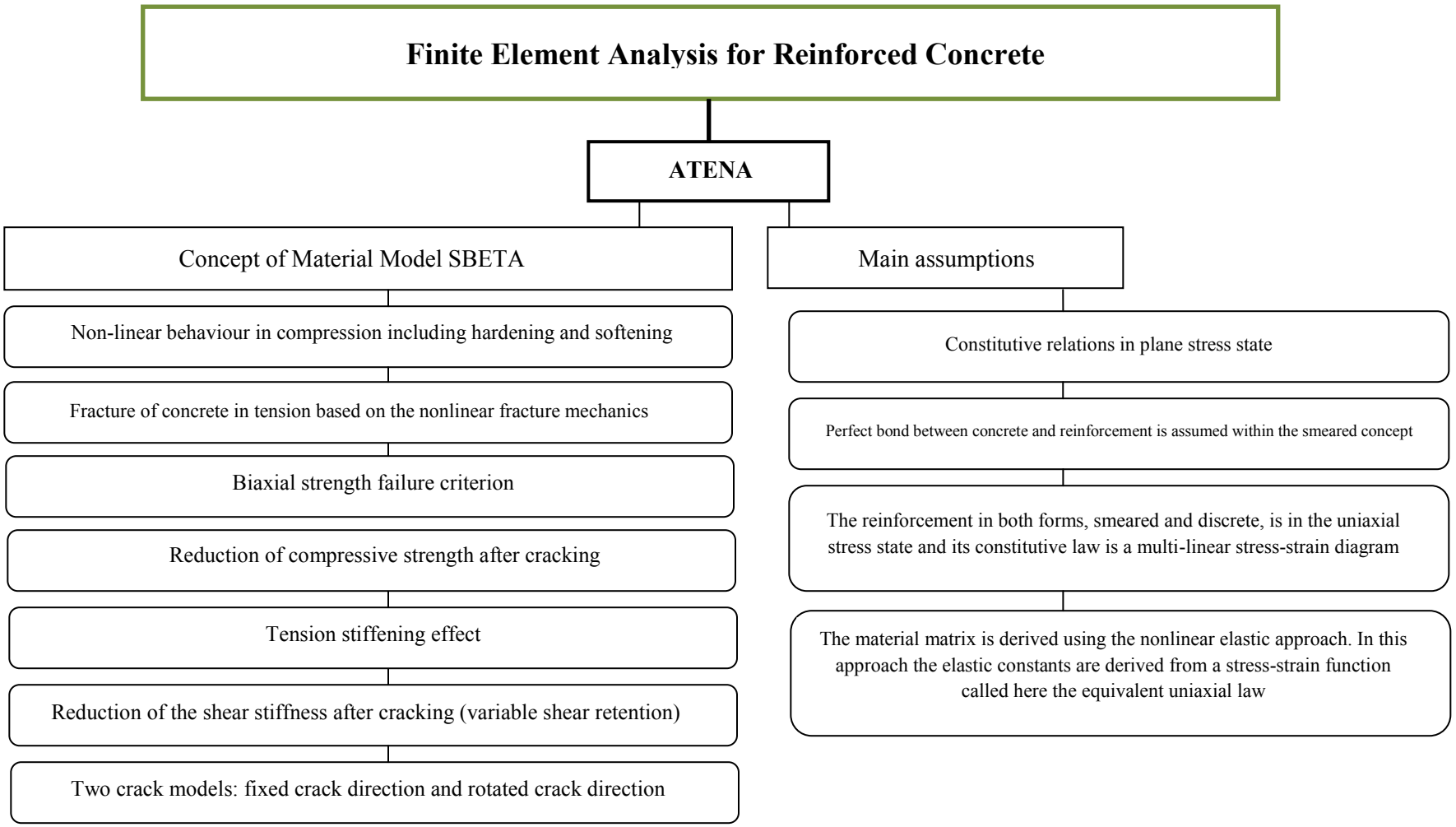

Figure 9.8 ATENA, constitutive model SBETA I (ATENA, 2012)

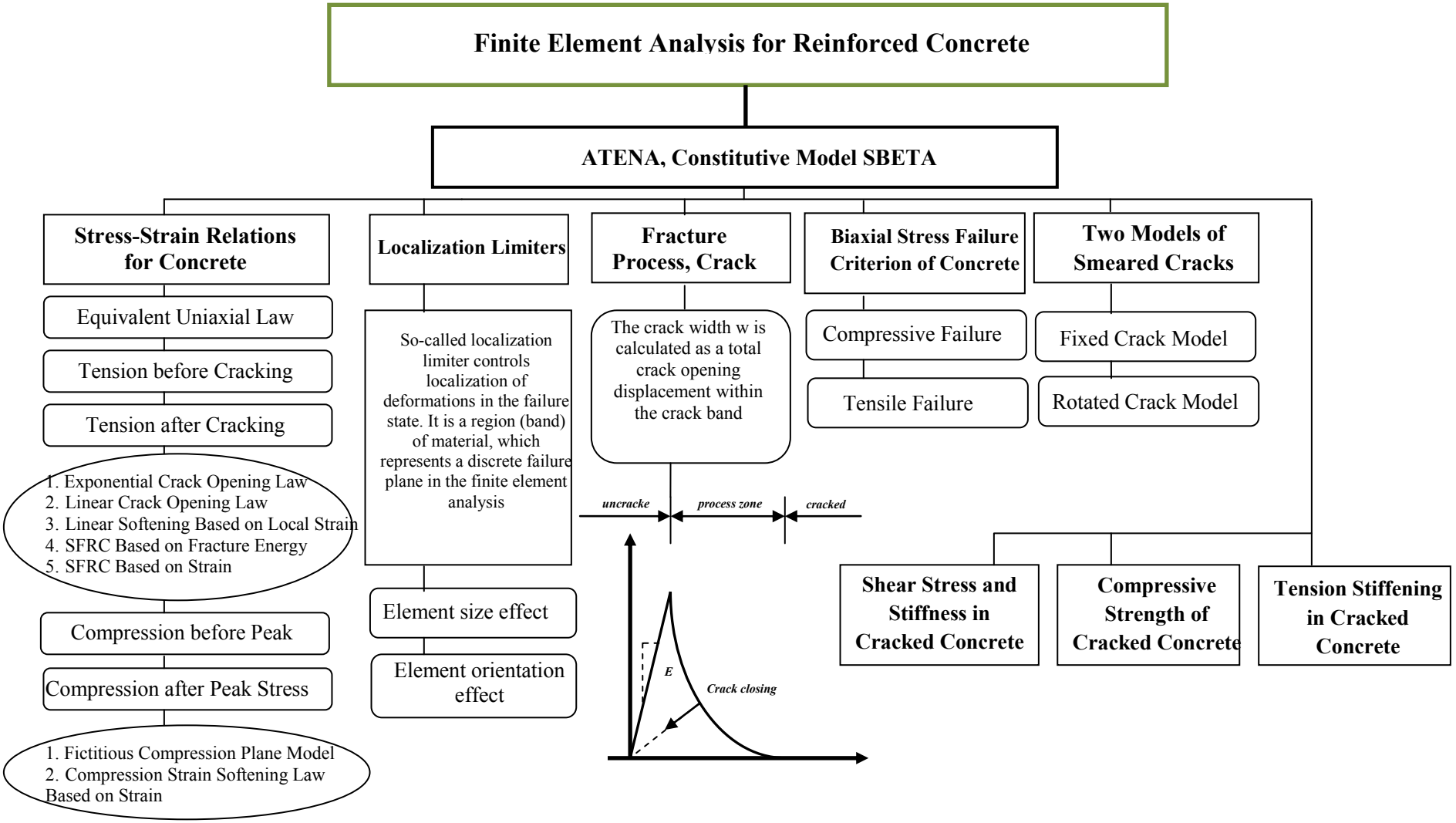

Figure 9.9 ATENA, constitutive model SBETA II (ATENA, 2012)

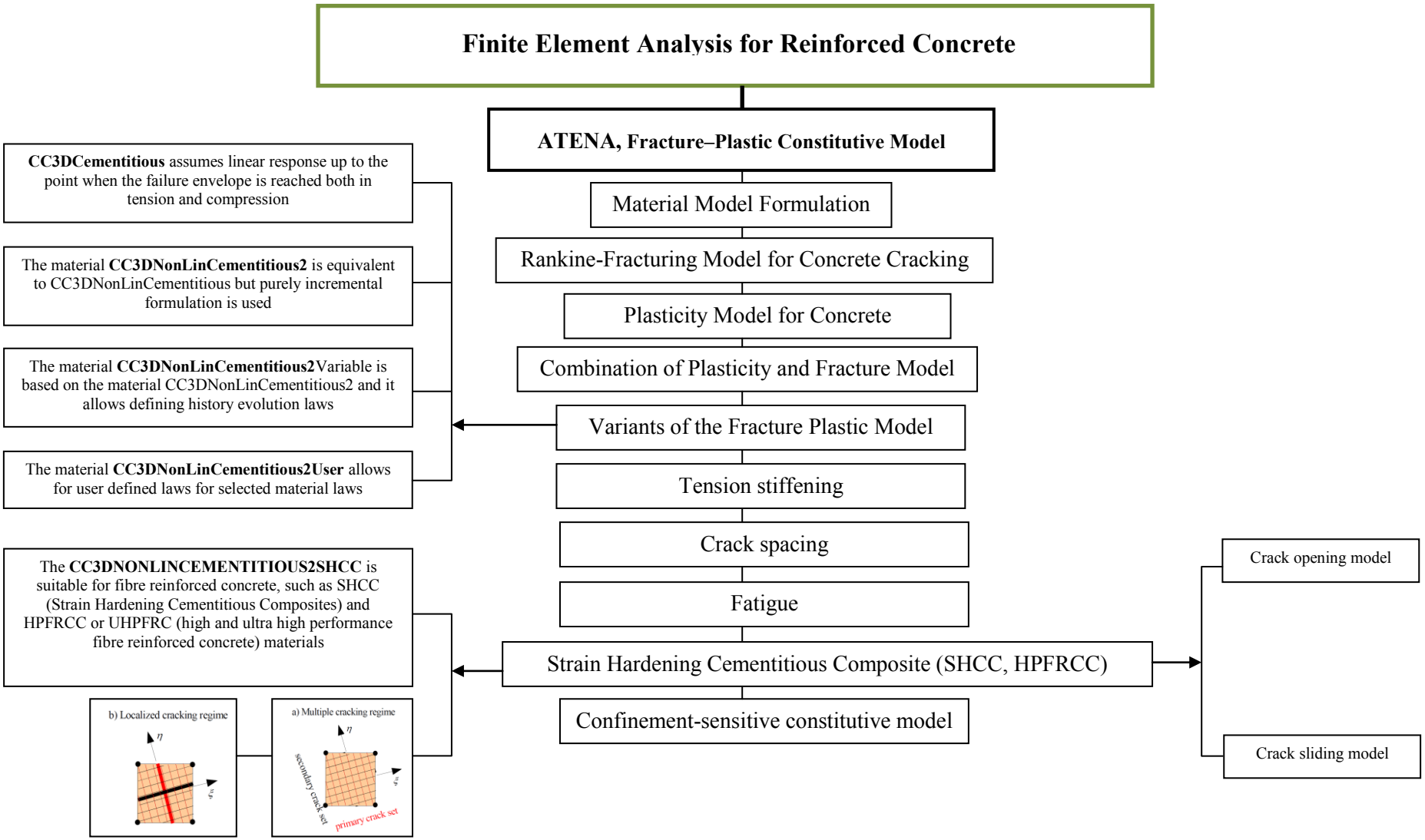

Figure 9.10 ATENA, Fracture–Plastic Constitutive Model (ATENA, 2012)

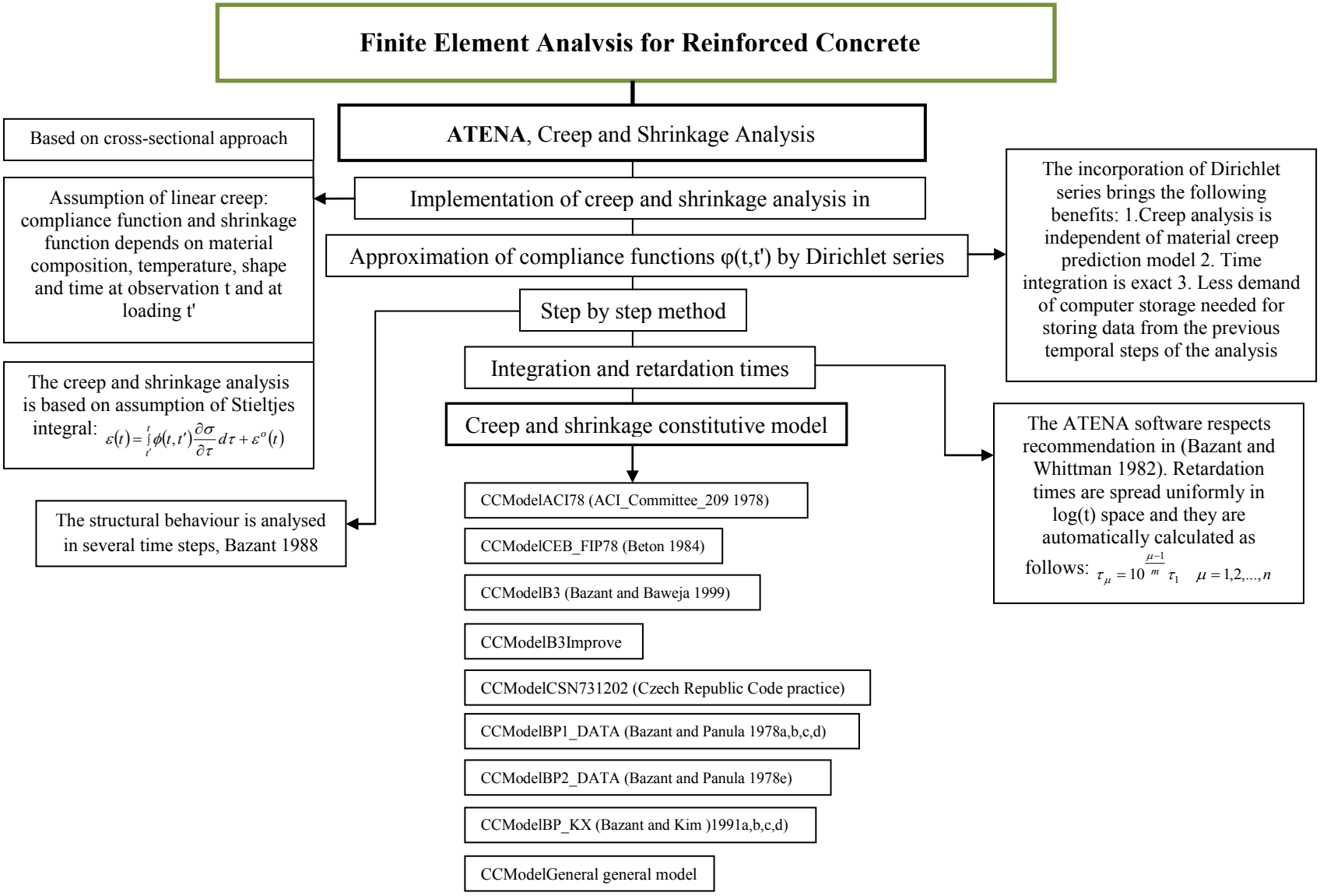

Figure 9.11 ATENA, Creep and Shrinkage Analysis (ATENA, 2012)

9.5 FEM MODELLING OF SCC AND FRSCC SLABS

9.5.1 Criteria for Element Choice

CCIsoBrick an 8-noded hexahedron element shown in Figure 9.12 is used for the concrete element for both the SCC and FRSCC models. Two-dimensional elements are not suitable as the model requires a three-dimensional mesh. Tetrahedral elements (see Figure 9.13) are not suitable too due to their inability to properly calculate stress and strain of concrete independently (Cook, 1995). Cracking behaviour may also be affected by the choice of tetrahedral elements as cracks would need to propagate through the pairs of tetrahedral elements as cracks cannot go through a corner of an element. Shell elements are not chosen due to their limitations in properly replicating stress and strain compared to brick elements (Cook, 1995).

The CCIsoBrick element is chosen in 8-noded configuration to reduce the computation time required to process the model. CCIsoBrick allows for a 20 node element however by using the 8-node CCIsoBrick element in a structured mesh with relatively small element size and by utilising the quadratic option for the element an appropriate trade-off between computation time and accuracy will be achieved.

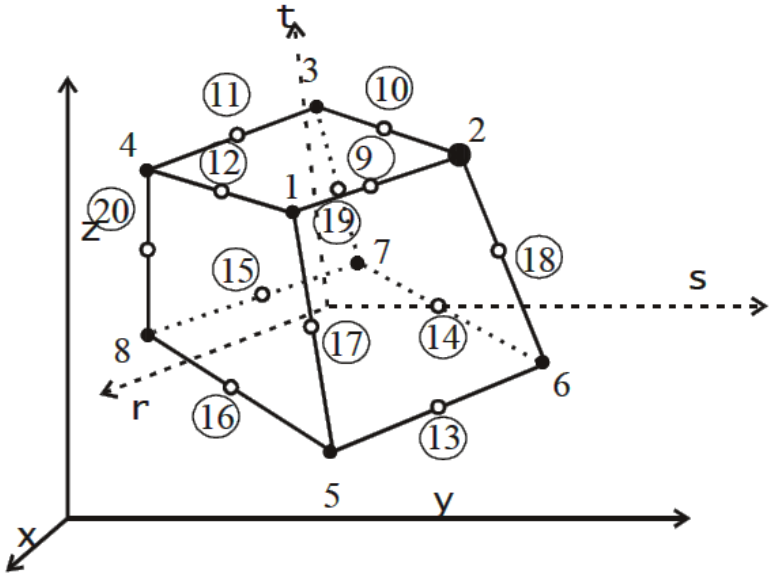

Figure 9.12 Geometry of CCIsoBrick element (ATENA, 2012)

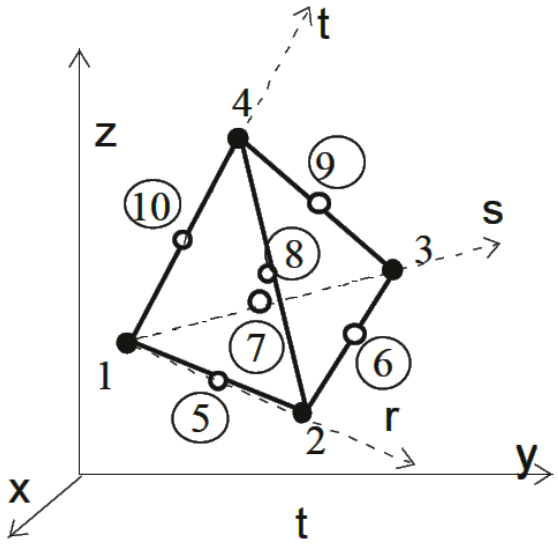

Figure 9.13 Geometry of CCIsoTetra element (ATENA, 2012)

9.5.2 Verification of the Element

9.5.2.1 Height of the Element

According to the mesh study in the ATENA Engineering Example manual (Cervenka et al., 2011), CCIsoQuad should be modelled with a minimum of 4 elements through the thickness (see Figure 9.14). The CCIsoQuad is a two dimensional elemental version of CCIsoBrick. This is because in finite elements a three dimensional element is built up from two dimensional element faces, (Cook, 1995).

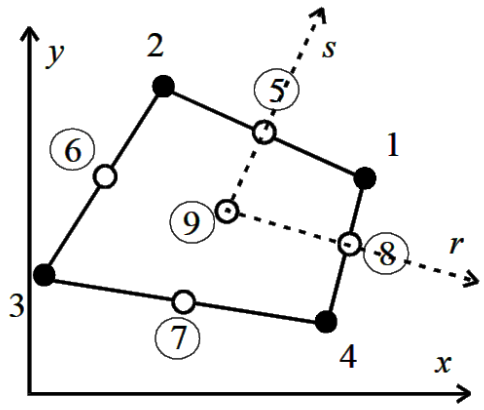

Figure 9.14 Geometry of CCIsoQuad element (ATENA, 2012)

9.5.2.2 Width of the Element

A crack can only propagate through an element by intersecting its face and not adjacent to an element interface. As a result, an element cannot differentiate between one or multiple cracks (Cervenka et al., 2012). Therefore, it can be seen that mesh size directly impacts crack spacing, as larger elements will induce larger crack spacing. In Figure 9.15(c) section it is shown that at the extreme tension face of the slab, at the cracked there is no stress within the concrete. This increases to a maximum stress roughly equidistant between to cracks and then decreases down to zero at the next crack (Nejadi, 2005). This is due to the interaction between the concrete and steel reinforcement where the maximum stress of the steel is at a crack where it carries all of the tensile force and then reduces between the cracks as some of the tensile force is transferred into the concrete, an effect called "tension stiffening". The smallest cracking spacing in the slab models was a spacing of 95 mm. Assuming for simplicity that the model needs to replicate a minimum crack spacing of 100 mm, an element width of 25 mm is chosen. This allows for four elements between cracks, which will accommodate the change in stress between cracks. Estimation of stress change within the element is represented by quadratic distribution based on the stress at each end node. Allowing a minimum of one element within the maximum stress and then another element within the stress transition before cracking of the element will better represent the change in stress by reducing the differences in stress between each element.

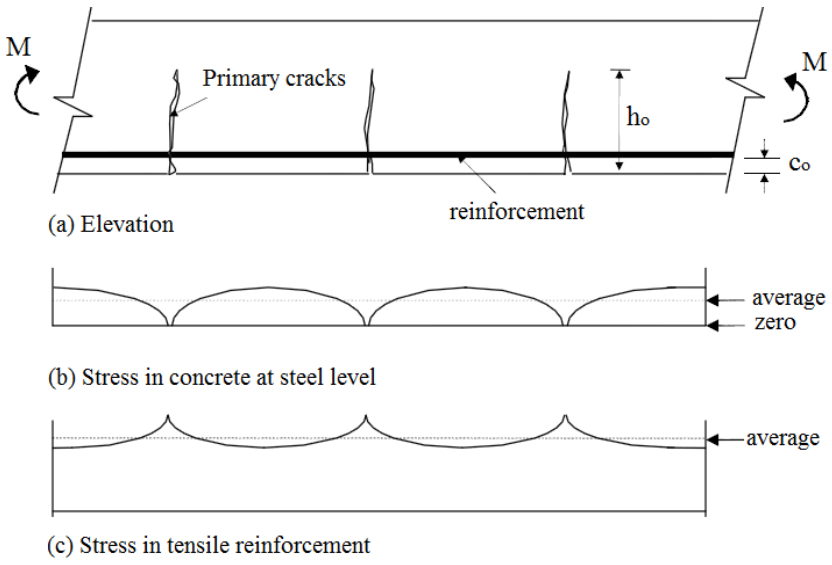

Figure 9.15 Stresses at steel level in a cracked reinforced concrete member

9.5.3 Loading Plates

Conventionally, a finite element model will implement loading plates into the model similar to the loading plates that are used in the experimental model. However, in the finite element model the plates are perfectly bonded to the slab. This creates a scenario where the stiffness of the plate is transferred into the slab as the displacement of the mesh within each element is linked at a common interface. When using conventional loading plates, it is shown that the loading plates would transfer stiffness into the slab, creating localized areas of increased stiffness.

The Figure 9.16 shows an uneven distribution of tensile stresses during the onset of an initial crack. Cracking occurs between the loading plates as the concrete has an inferred higher tensile strength under the plates. Figure 9.16 is a screenshot of an early design of slab showing the onset of cracking. Blue areas represent a reduction of strength of 0.1 MPa due to cracking.

As this is the first irritation in the model showing the initial cracking, should start at the far left edge and be uniformly distributed. Random loading was 15% of the ultimate load. To remediate this scenario, the loading plates were removed pressure equal to the load on each loading plate was applied to the footprint area of the loading plate. As there is no loading plate the stiffness of the slab is uniform throughout.

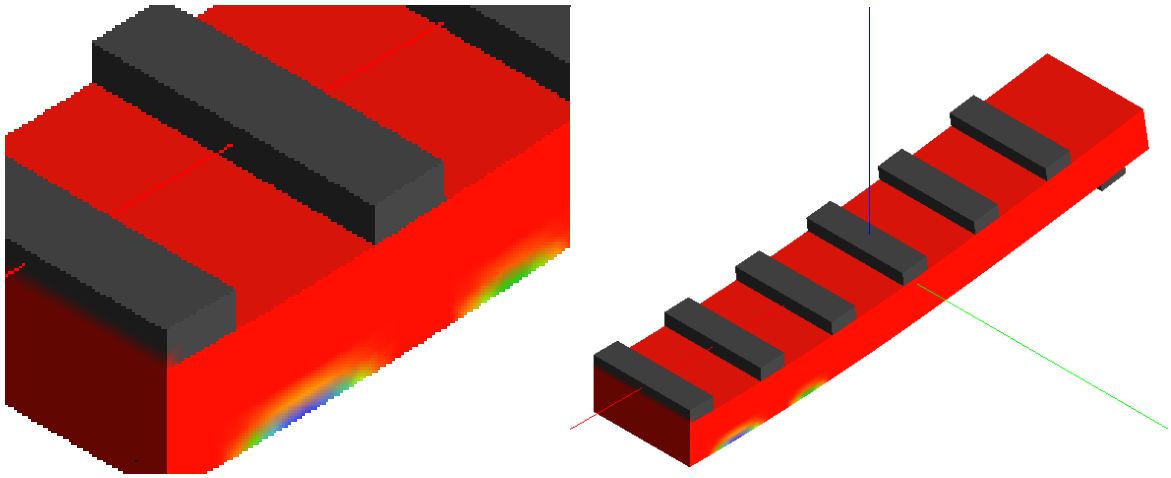

Figure 9.16 Slab tensile strength - Red = 2.9 MPa, Blue = 2.8 MPa (onset of cracking)

Figure 9.17 is a screenshot of an early design of slab showing the onset of cracking by using the same model as before but without loading plates and by using pressure to load the model. Early cracking is shown as a function of the moment at the extreme tensile face of the slab. The uniform tensile softening on the underside of the slab suggests that in Figure 9.16 the plates were increasing the stiffness of the slab.

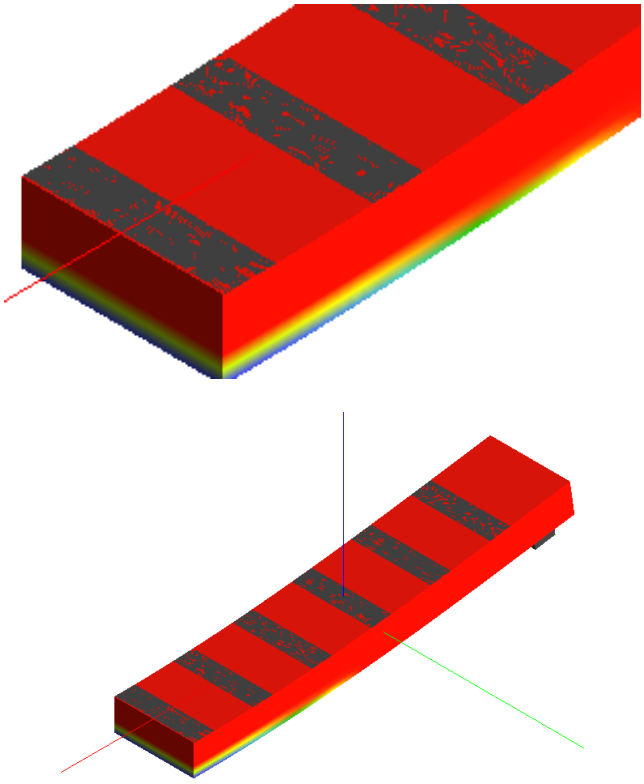

Figure 9.17 Slab tensile strength - Red = 2.9 MPa, Blue = 2.8 MPa (onset of cracking)

9.5.4 Slab Modelling Process

Two sets of models will be made for the all SCC slab series. The first set will be modelled in the "ATENA Static" environment and the second set will be modelled in the "ATENA Creep" environment. The sets represent the instantaneous and time-dependent behaviours respectively. The instantaneous behaviour modelling only day 0 (i.e. the first day that the slabs have been loaded) while the time-dependent behaviour modelling from 0 to 240 days.

Differences in the model process for instantaneous and time-dependent behaviours will be determined, otherwise the modelling process is the same for each set.

9.5.4.1 Dimension of Slabs

To save processing time, symmetry of the model will be used to the advantage and only half of the model from end to mid-span will be modelled. This can be achieved in finite element models by apply the appropriate boundary conditions which in this case will prevent movement in the *x* and *y* axis and rotation at the mid-span cut face. From the study of the accuracy of the ISoBrick element and the need to properly capture stress profile at extreme tensile face, the size of the elements should ideally be at least 25 mm × 25 mm × 25 mm. To accommodate an element width of 25 mm, it has been assumed that the total length of the slabs is 3800 mm, providing an overhang of 150 mm at each end. The total dimensions of the slab will be as depicted. The wireframe shown in Figure 9.18 is typical for the all slabs.

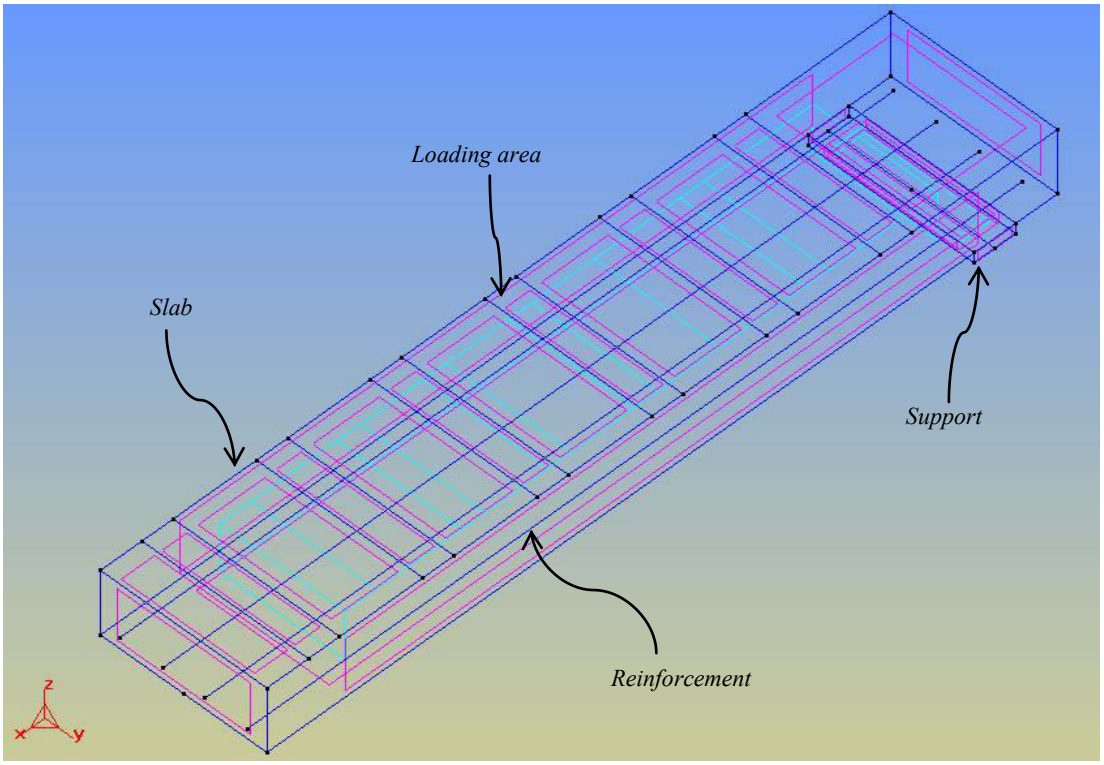

Figure 9.18 GiD wireframe slabs showing reinforcement and loading areas

9.5.4.2 Material Properties

The one of the purposes of this study is utilizing the proposed material properties models in Chapters 3, 4, and 5 (including mechanical properties, bond stress, creep and shrinkage) in the ATENA and running the program with the SCC and FRSCC slabs. ATENA's concrete material models are shown in Figure 9.10.

The *CC3DCementitious* material model assumes linear response up to the point when the failure envelope is reached both in tension and compression. This means that there is no hardening regime. The material model of *CC3DNonLinCementitious* on the contrary assumes a hardening regime before the compressive strength is reached. The material model of *CC3DNonLinCementitious2* is equivalent to the CC3DNonLinCementitious material model but purely incremental formulation is used (in CC3DNonLinCementitious a total formulation is used for the fracturing part of the model). Therefore, this material model can be used in creep calculations or when it is necessary to change material properties during the analysis. The material model of *CC3DNonLinCementitious2Variable* is based on the material CC3DNonLinCementitious2 and it allows defining History Evolution Laws for selected material parameters.

The material model of *CC3DNonLinCementitious2User* allows for user defined laws for selected material laws such as: diagrams for tensile and softening behaviour, shear retention factor and the effect of lateral compression on tensile strength.

The *CC3DNonLinCementitious2SHCC* material model is suitable for fibre reinforced concrete, such as SHCC (Strain Hardening Cementitious Composites) and HPFRCC or UHPFRC (High and Ultrahigh Performance Fibre Reinforced Concrete) respectively. The tensile softening regime and the shear retention factor are modified based on the model, proposed in Kabele (2002). This model is based on a notion of a Representative Volume Element (RVE), which contains distributed multiple cracks (hardening) as well as localized cracks (softening).

In this study first the material model of *CC3DNonLinCementitious2* model is used for a general analysis. The main reasons for using this model are creep calculations and when it is necessary to change the material properties during the analysis. The implemented material properties are summarized in Figure 9.19. The presented data is the default values

of ATENA software. The required data for SCC and FRSCC properties is used from Table 5.10. After this general process, we used *CC3DNonLinCementitious2User* and *CC3DNonLinCementitious2SHCC* material models. By using these models, we can utilize the developed models for mechanical properties of SCC and FRSCC in chapters 4 and 5. Figure 9.20 shows the user defined tension, compression, shear, tension-compression and fibre reinforcement of *CC3DNonLinCementitious2User* and *CC3DNonLinCementitious2SHCC* concrete models. The proposed relationships in Chapter 3 are used in this section.

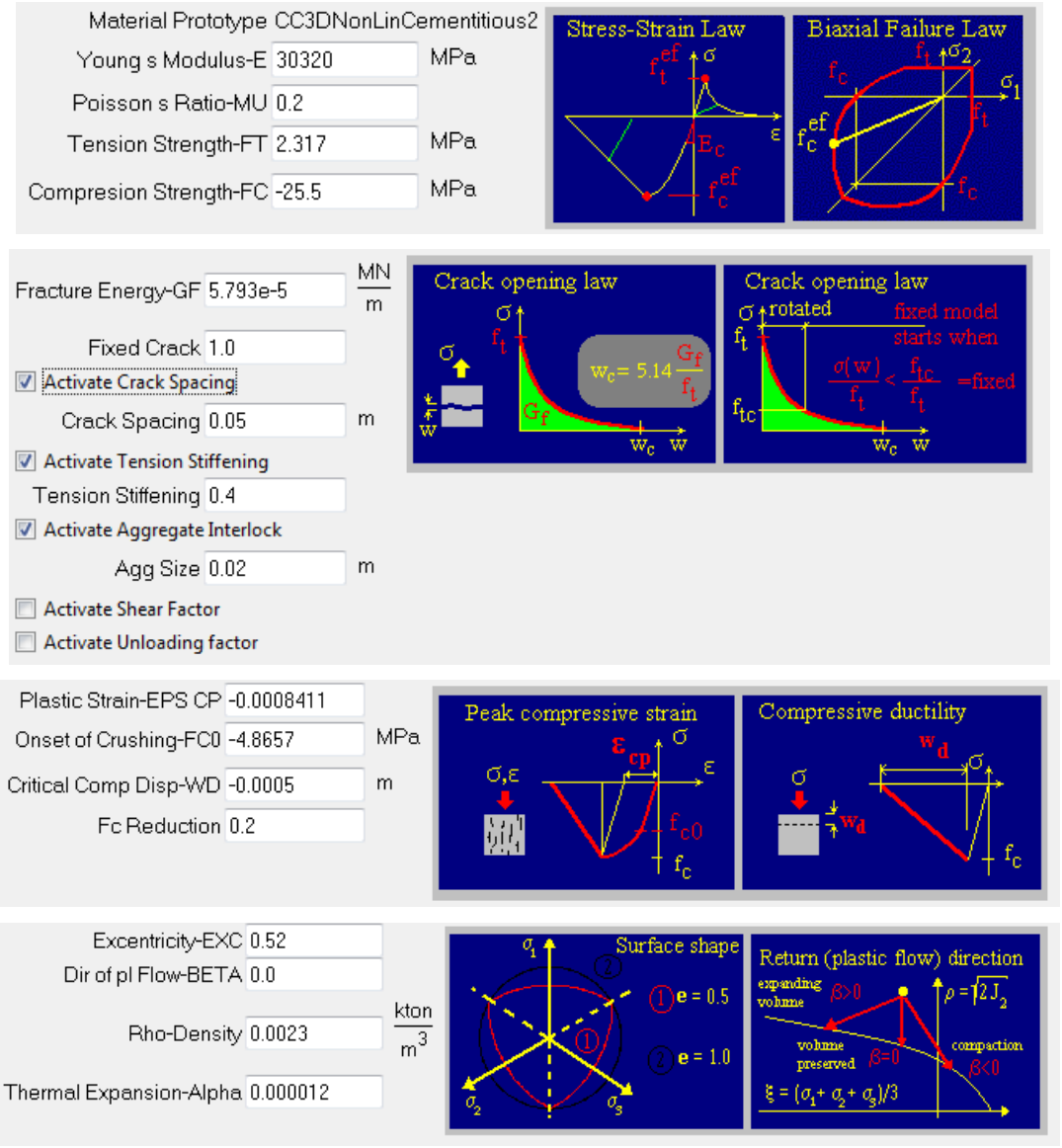

Figure 9.19 Material properties for CC3DNonLinCementitious2 (ATENA, 2012)

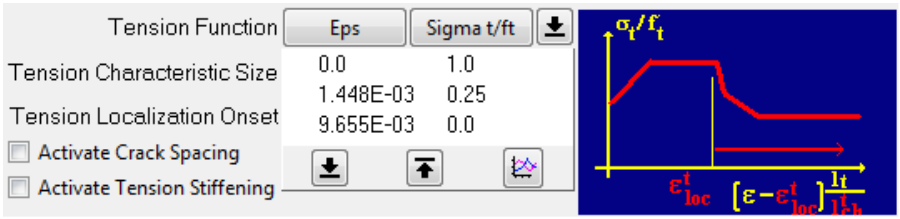

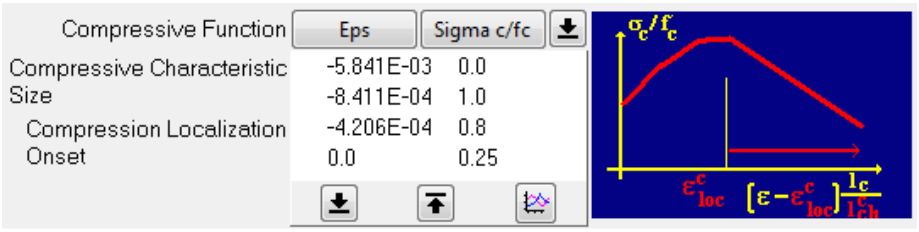

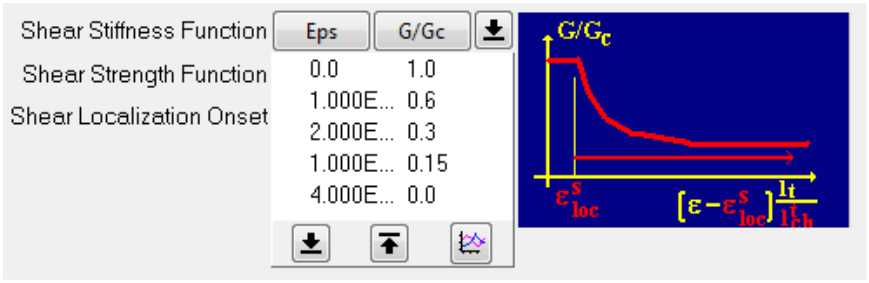

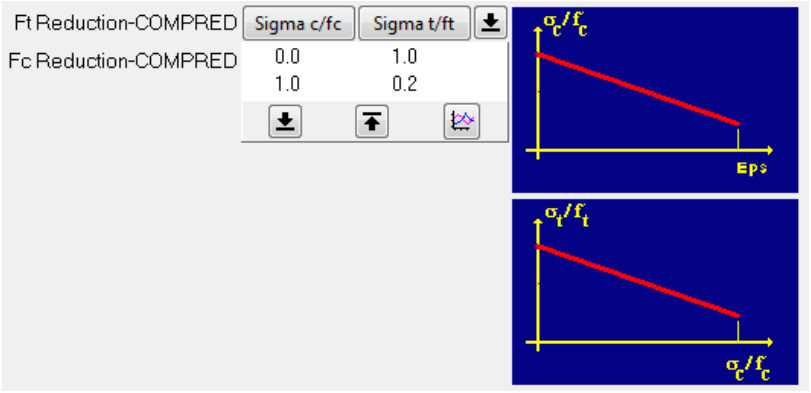

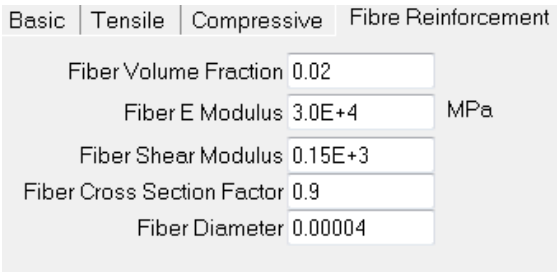

Figure 9.20 Material properties for CC3DNonLinCementitious2User and CC3DNonLinCementitious2SHCC (ATENA, 2012)

ATENA's reinforcement material model is shown in Figure 9.3. The multi-linear law consisting of four lines is adapted in ATENA. This law allows modelling of the all four stages of steel behaviour including: elastic state, yield plateau, hardening and fracture. The multi-line is defined by four points, which can be specified by the user's input. The described stress-strain laws can be used for the discrete as well as the smeared reinforcement. The smeared reinforcement requires two additional parameters including: the reinforcing ratio and angle of direction. For more information about this model see Figure 9.21.

In addition, ATENA contains three bond-slip models according to the CEB-FIB model code 1990, slip law by Bigaj and the user defined law. In the first two models, the laws are generated based on the concrete compressive strength, reinforcement diameter and reinforcement type. The important parameters are also the confinement conditions and the quality of the concrete casting. We have used the user defined law for bond-slip model. The proposed bond-slip model for SCC in Chapter 4 is used for this purpose (see Figure 9.22).

9.5.4.3 Creep and Shrinkage in ATENA

ATENA provides a powerful method for creep and shrinkage analysis for most of the problems from engineering practice. It is based on so called cross-sectional approach, meaning that the analysis builds upon creep and shrinkage behaviour of the whole cross section rather than behaviour of individual material points only. The reason for selecting this method is as follows: There are available numerous models for predicting creep and shrinkage behaviour of a concrete cross section, whereas there is very little evidence about the creep and shrinkage behaviour at material point level. The second reason is, its accuracy suffices for most analyses of the engineering practice and it is cheaper in terms of computational cost. Creep and shrinkage processes are summarized in Figure 9.11.

The CCStructureCreep module currently supports the following models:

1. CCModelACI78 (ACI_Committee_209 1978), recommended by ACI, by now already obsolete,

2. CCModelCEB_FIP78 (Beton 1984), recommended by CEB committee, by now already obsolete,

3. CCModelB3 (Bazant and Baweja 1999), developed by Bazant and Al Manaseer in 1996, very efficient model recognized world-wide,

4. CCModelB3Improved, same as the above, improved to account for temperature history, probably the best model available in ATENA,

5. CCModelCSN731202, model developed by CSN 731202 Code of practice in Czech Republic,

6. CCModelBP1_DATA (Bazant and Panula 1978a; Bazant and Panula 1978d; Bazant and Panula 1978b; Bazant and Panula 1978c), relatively efficient and complex model; now it is superceeded by CCModelBP_KX or CCModelB3,

7. CCModelBP2_DATA (Bazant and Panula 1978e), simplified version of the above model,

8. CCModelBP_KX (Bazant and Kim 1991a; Bazant and Kim 1991b; Bazant and Kim 1991c; Bazant and Kim 1991d), powerful model with accounts for humidity and temperature history etc., for practical use it may-be too advanced,

9. CCModelGeneral general model into which experimentally obtained $\Phi(t,t')$ and ε_r^0 function can be input.

As it is recommended CCModelB3Improved model as the best model available in ATENA is selected for the time-dependent analyses. Also, for applying proposed creep and shrinkage models of SCC, we modified the input file that is run with CCModelB3Improved model by using our proposed model as input data. The input data for B3Improved model is presented in Table 9.1.

Besides, in the B3Improved model, the shrinkage effect can be activated as shown in Figure 9.23. The shrinkage strain for SCC mixtures (see Table 7.4) can be added to the ATENA creep environment easily. Also, the proposed SCC shrinkage model can be applied to the FEM modelling by this method.

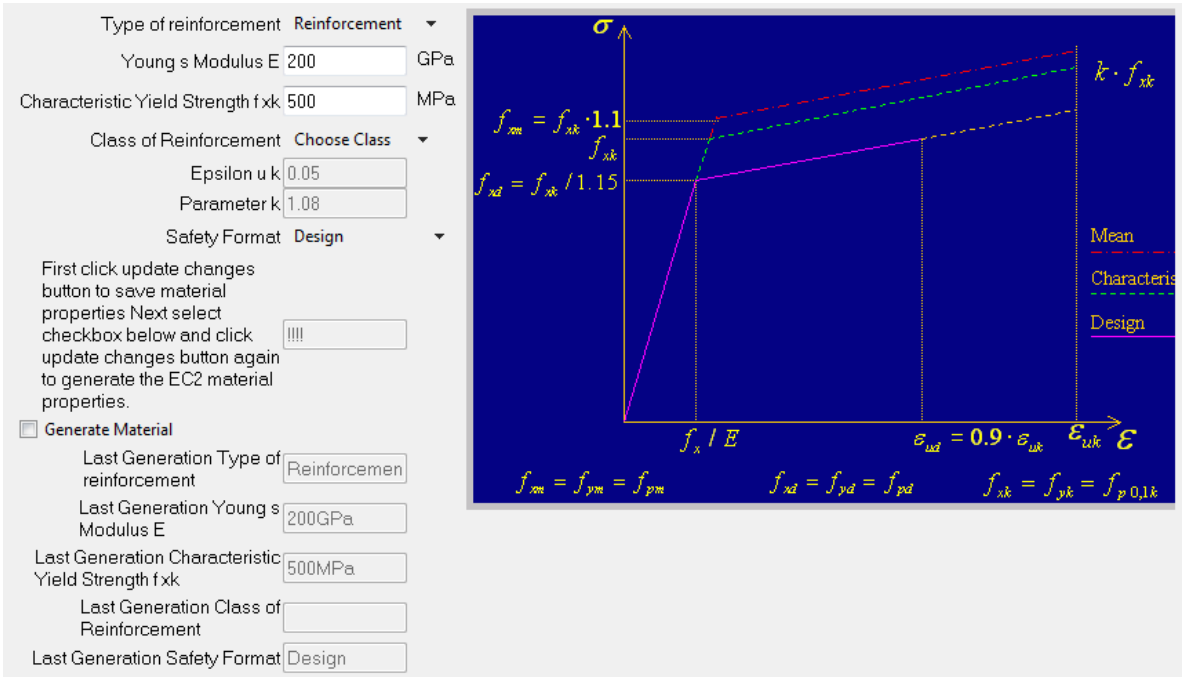

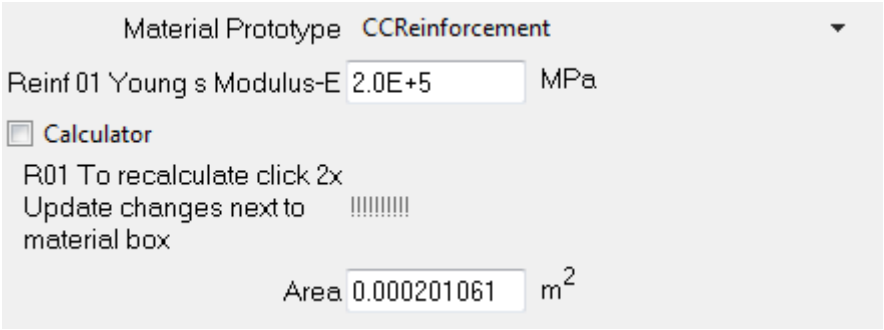

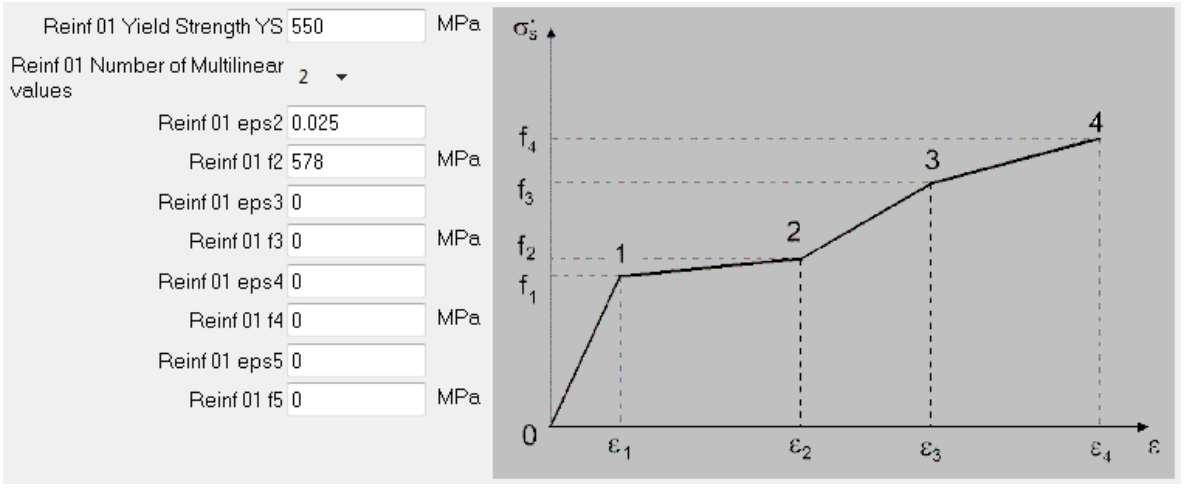

Figure 9.21 Reinforcement material model details (ATENA, 2012)

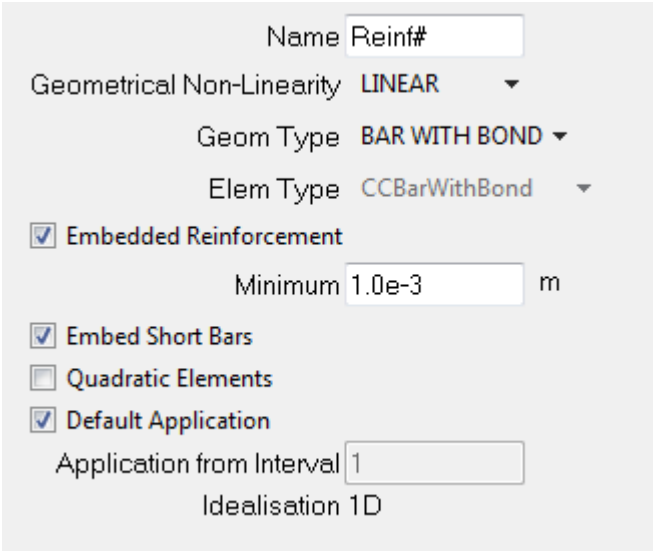

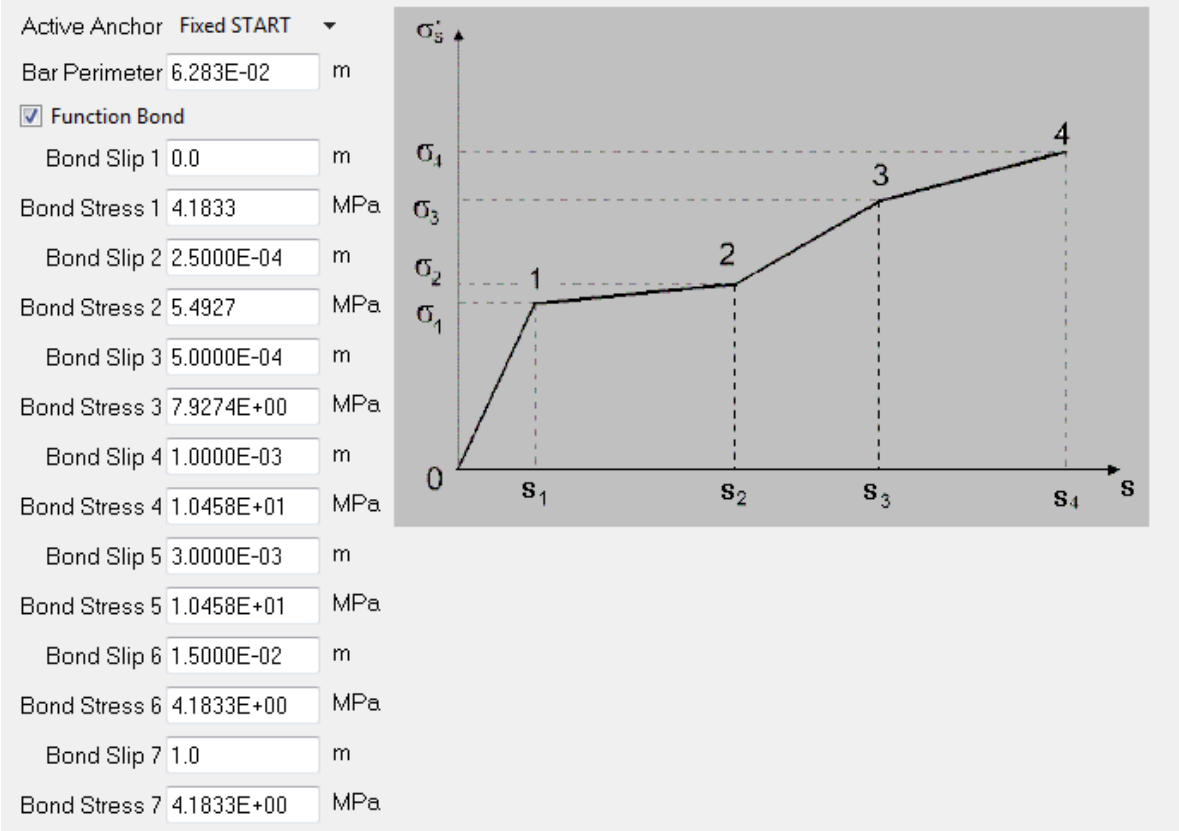

Figure 9.22 Reinforcement with bond model details (ATENA, 2012)

Table 9.1 B3Improved model input data

Concrete Slab – Program Material Group: Model B3 Improved					
Concrete Type	N-CC	N-SCC	D-SCC	S-SCC	DS-SCC
Thickness (volume/surface area)	0.0556				
Humidity	0.50	0.55	0.55	0.55	0.55
Density (kg/m^3)	2350	2340	2274	2330	2385
Aggregate/Cement Ratio	7.04	10.63	10.63	10.63	10.63
Water/Cement Ratio	0.63	0.52	0.52	0.52	0.52
Shape Factor	slab				
Curing	Water				
End of Curing Time (days)	13.9				
Base Material	Cementitious 2, CC3DNonLinCementitious2User and CC3DNonLinCementitious2SHCC				
Geometrical Non-linearity	Non-Linear				
Element Idealisation	3D				
Quadratic Element	Yes				

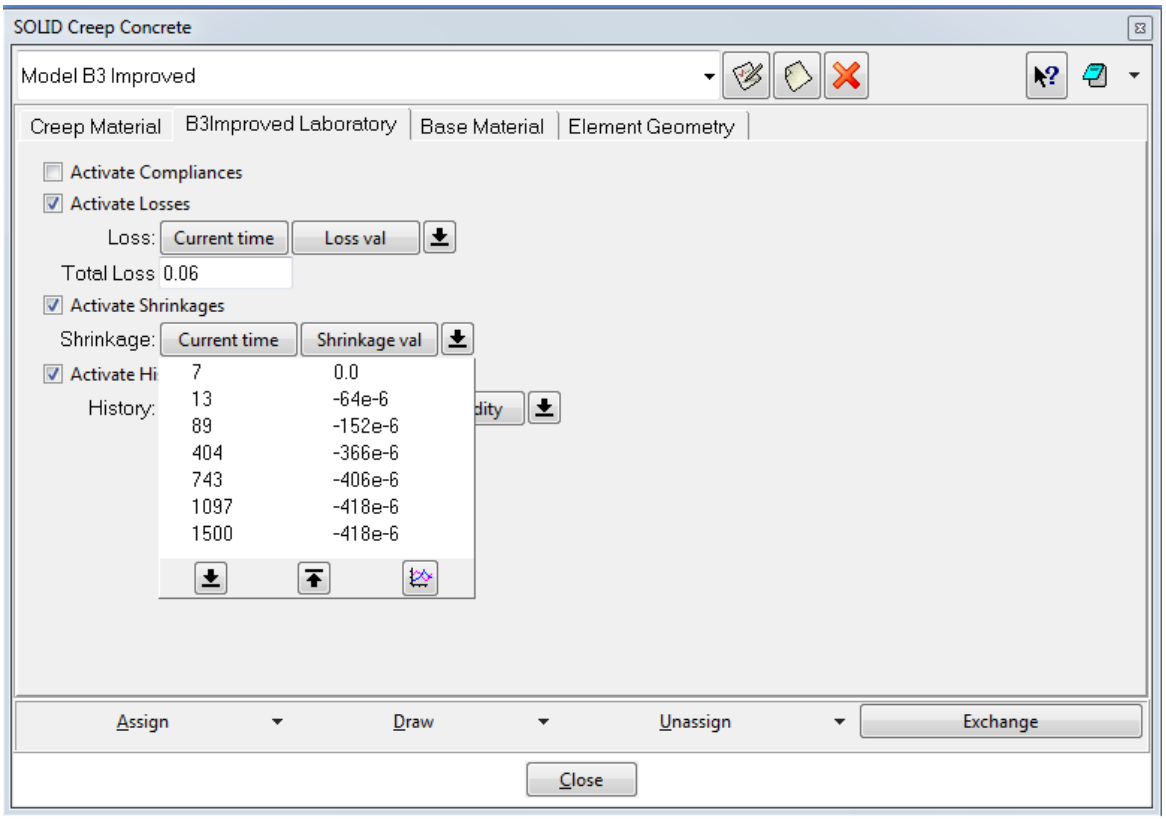

Figure 9.23 Shrinkage in the ATENA creep environment (ATENA, 2012)

9.5.4.4 Applied Mesh

The mesh of the concrete slab is 25.83 mm × 25 mm × 25 mm hexahedra elements and the mesh of the support is 25 mm × 25 mm × 25 mm. The placement and size of the supports and the loading areas are such that they integrate into the mesh of the slab without overlap. Although, ATENA uses complex boundary conditions where the nodes of two contacting components do not need to be shared because the boundary conditions of adjacent nodes are affected by proximity to each other. The mesh of contacting components has been matched so that the size of the component in contact with the other surface is not made larger by affecting nodes beyond its immediate proximity. ATENA requires that steel mesh reinforcement is designed as one long element, although during processing the reinforcement element is divided to best suit the surrounding concrete mesh. Total number of linear elements, hexahedra elements, and nodes for each slab meshing is presented in Table 9.2 and Figure 9.24.

Table 9.2 Summary of mesh size

Number of elements and nods in slab	Steel	Concrete	Whole slab mesh
	Linear Elements	Hexahedra Elements	Nodes
	4	7360	9341

9.5.4.5 Boundary Conditions

The slab's assigned self-weight is 0.024MN/m^3, self-weight of the reinforcement and the support slab was omitted. Since only a symmetric half of the beam is analysed, it is necessary to enforce the fixed condition along the right side of the beam. It means that the horizontal displacements along *x*-axis should be equal to zero. Load was applied as pressure over the loading area, which was calculated as the total UDL being applied over half of the beam divided by the total area of the loading areas. The cut face of the mid-span was restricted in movement with respect to the *x* and *y* axis. The ends of the reinforcement which intersected the cut face were also restricted from movement in the *x* axis, this was to prevent the reinforcement pulling on the concrete surface which is introduced as it is a half model. The steel support was prevented from moving in the *y* and *z* axis but free in rotation, thus acting as a roller support. The support and the slab were bonded by a perfect bond. The applied boundary conditions are presented in Figure 9.25.

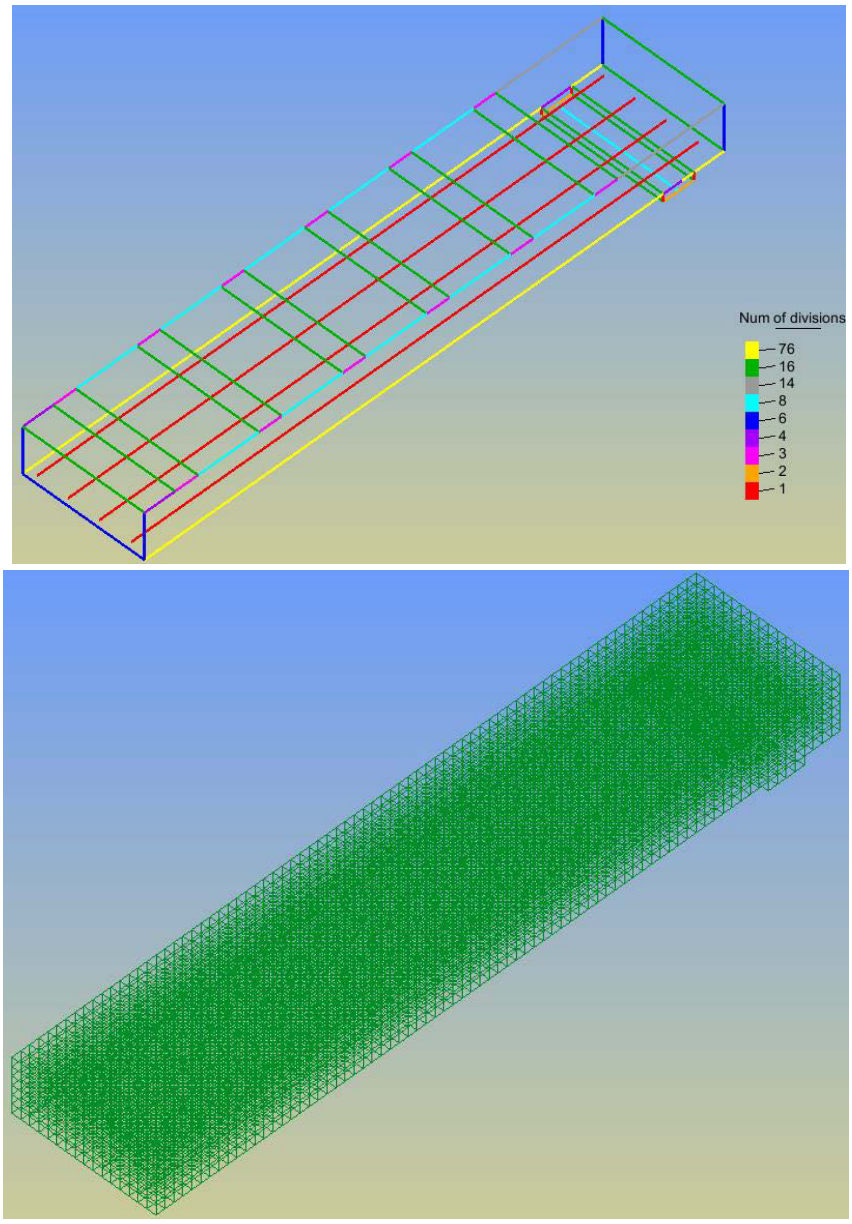

Figure 9.24 Visual representation of meshing

9.5.4.6 Loading Intervals

The models for instantaneous were loaded in 1 interval consisting of 20 sub intervals, with each interval having a limit of 500 irritations. 20 sub intervals and large limit on irritations was so that the non-linear displacement and cracking behaviour of the model could be properly captured. The time-dependent model had 2 intervals. Interval 1 started at day 14.0 and ended at day 14.2 to replicate initial loading of the specimen. Interval 2 started at day

14.2 and ended at day 240. Loads were removed in interval 2 as per the manual instructions to simulate creep behaviour in the model.

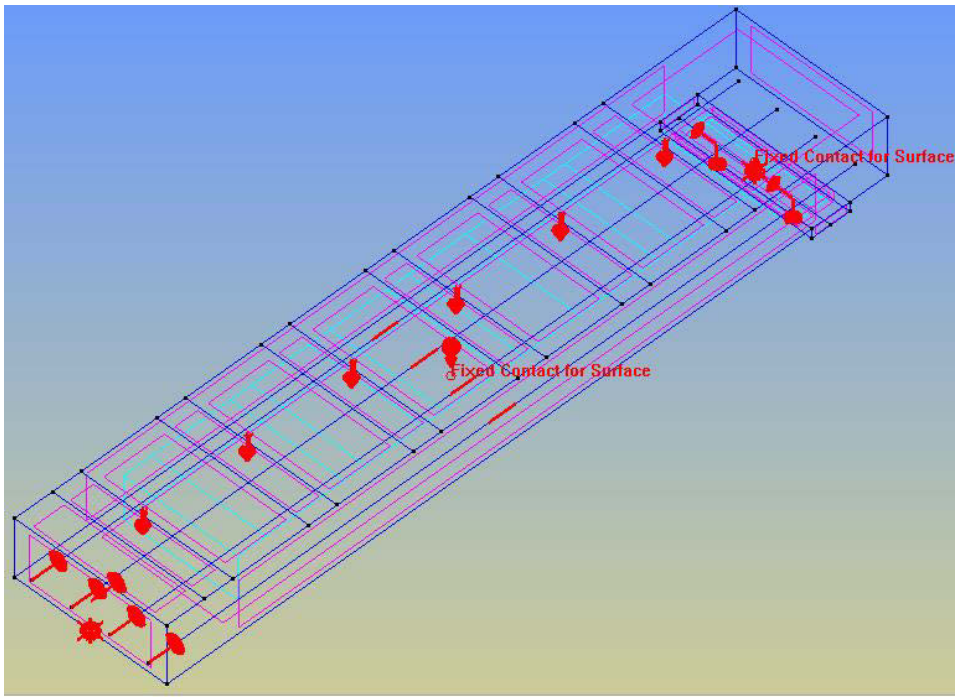

Figure 9.25 Visual representation of boundary conditions

9.6 PARAMETRIC STUDY OF THE SCC AND FRSCC ONE-WAY SLABS BY FEM ANALYSIS

A comprehensive parametric study has been conducted to study the instantaneous and time-dependent behaviours of the SCC and FRSCC one-way slabs.

The process of the parametric study is as follows:

1. Using the default models of ATENA software (i.e. CC3DNonLinCementitious2 for material, CCModelB3Improved for creep and shrinkage, and bond-slip).
2. Applying default ATENA's CCModelB3Improved creep and shrinkage model then using the CC3DNonLinCementitious2User by utilizing the proposed models in presented in chapter 3, and default ATENA's bond-slip model.

3. Using default ATENA's CCModelB3Improved creep and shrinkage model then using the CC3DNonLinCementitious2User and bond-slip model by utilizing the proposed models in presented in chapter 3.
4. Using proposed creep and shrinkage models by utilizing the proposed models in presented in chapter 4 and using the CC3DNonLinCementitious2User and bond-slip model by utilizing the proposed models in presented in chapter 3.

The results from parametric study have been presented in Figures 9.26 to 9.35 and Tables 9.3 and 9.4. Figures 9.26 to 9.35 show the deflection versus age from the FEM analysis of the parametric study. Also, Tables 9.3 and 9.4 show the instantaneous and time-dependent crack widths from the parametric study. More details of the FEM parametric study including crack width, deflection of the slabs are presented in Appendix-G.

Figure 9.36 shows comparison of the final deflections from the FEM parametric analyses. The results show that by using each proposed model (e.g. material properties, bond-slip, and creep and shrinkage), accuracy of the deflection prediction increases. Also, when the analysis is combined with the proposed models the accuracy of the deflection prediction is in the best agreement with the experimental results.

Moreover, Figures 9.37 and 9.38 and Tables 9.3 and 9.4 show comparisons of the instantaneous and time-dependent crack widths. The comparisons show that by using the proposed models in this study, accuracy of crack widths prediction results increases. Also, when the analysis is combined with the all proposed models the accuracy of the results is in the best agreement with the experimental results. Typical FEM analysis results are shown in Figures 9.39 to 9.41.

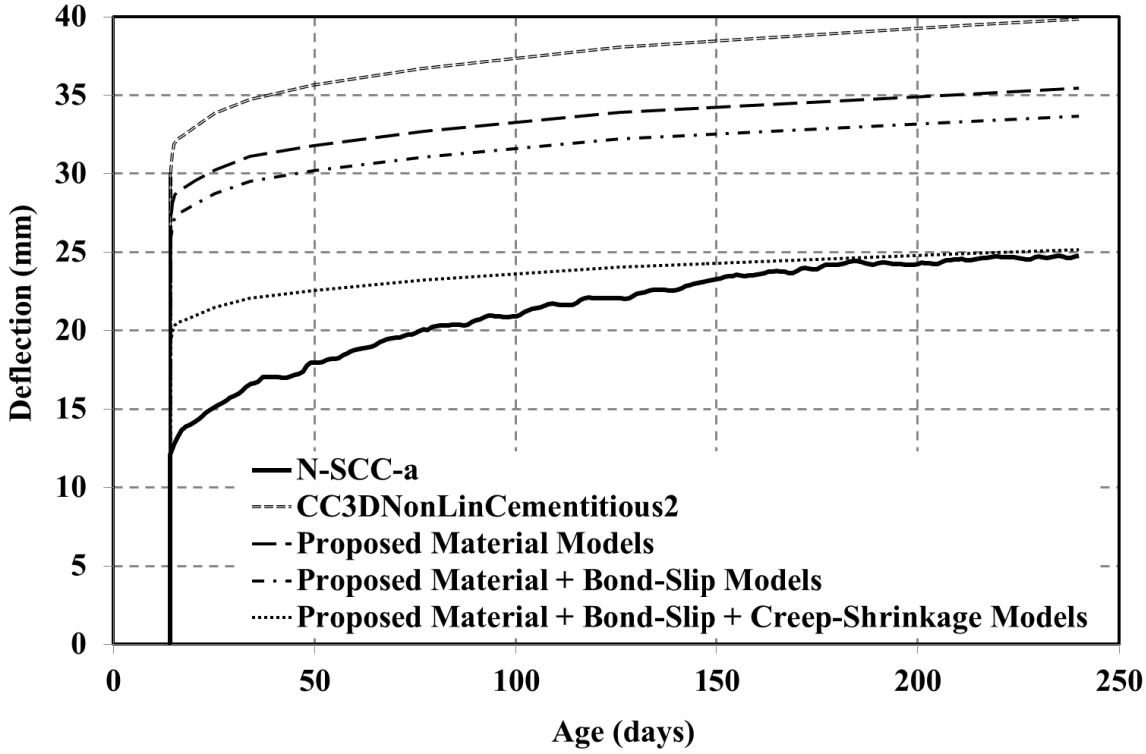

Figure 9.26 Deflection-age behaviour of slab N-SCC-a

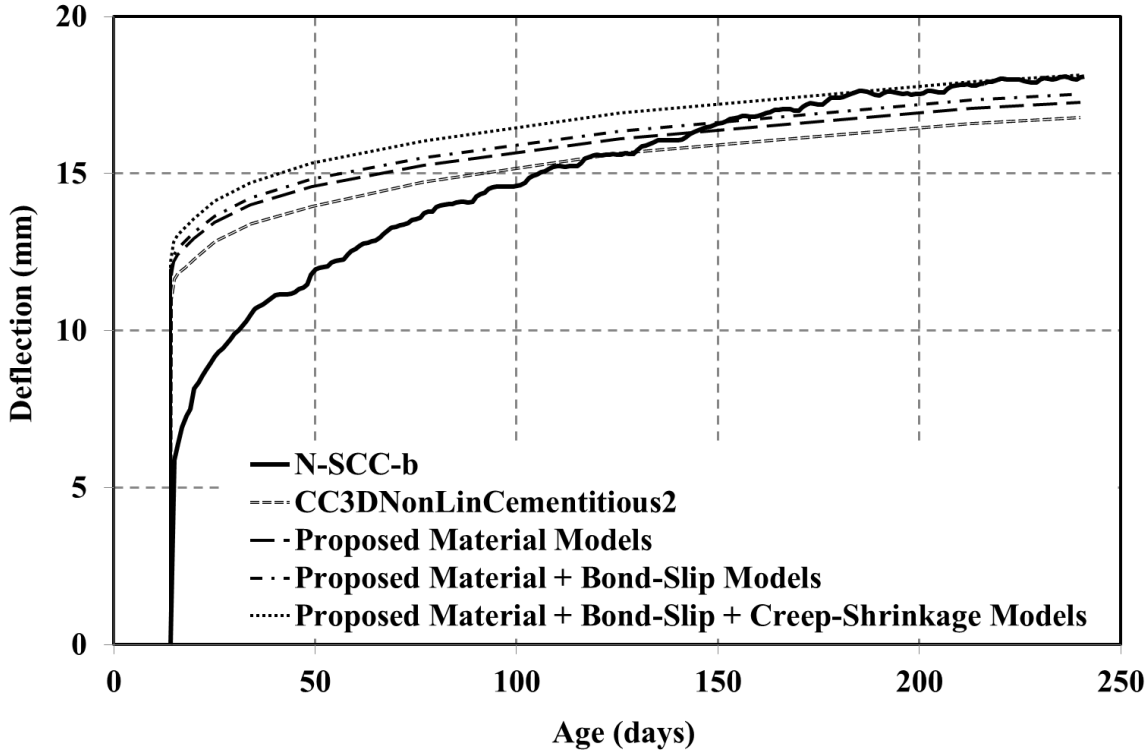

Figure 9.27 Deflection-age behaviour of slab N-SCC-b

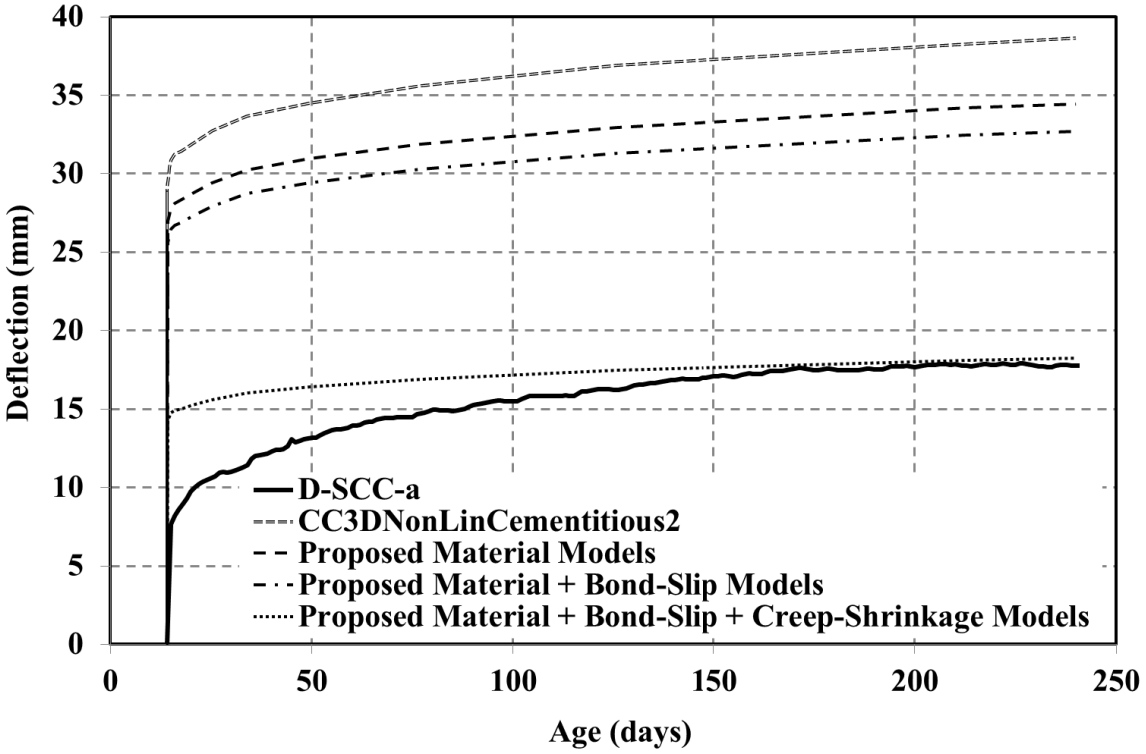

Figure 9.28 Deflection-age behaviour of slab D-SCC-a

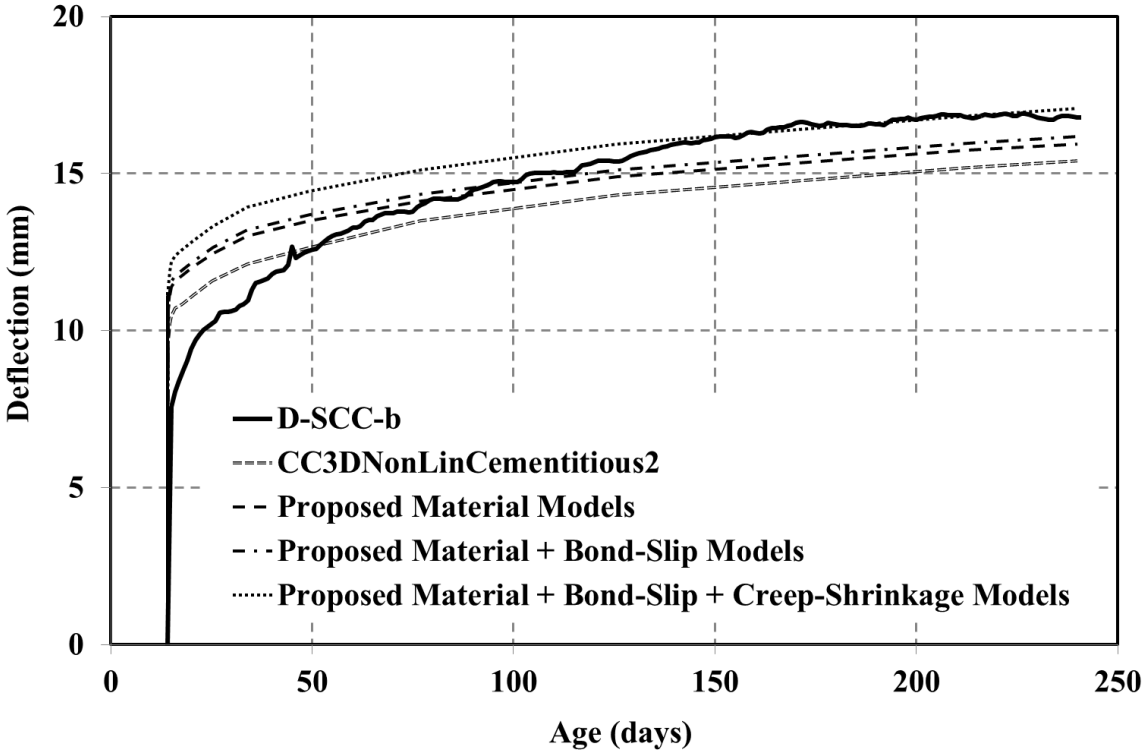

Figure 9.29 Deflection-age behaviour of slab D-SCC-b

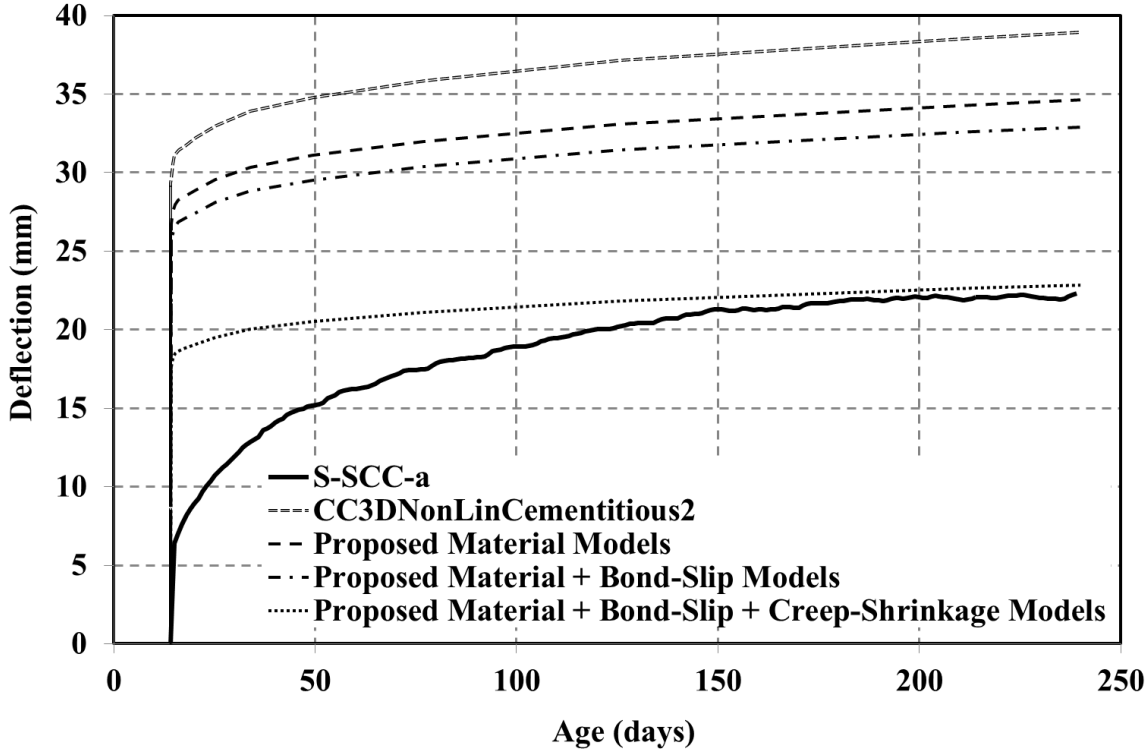

Figure 9.30 Deflection-age behaviour of slab S-SCC-a

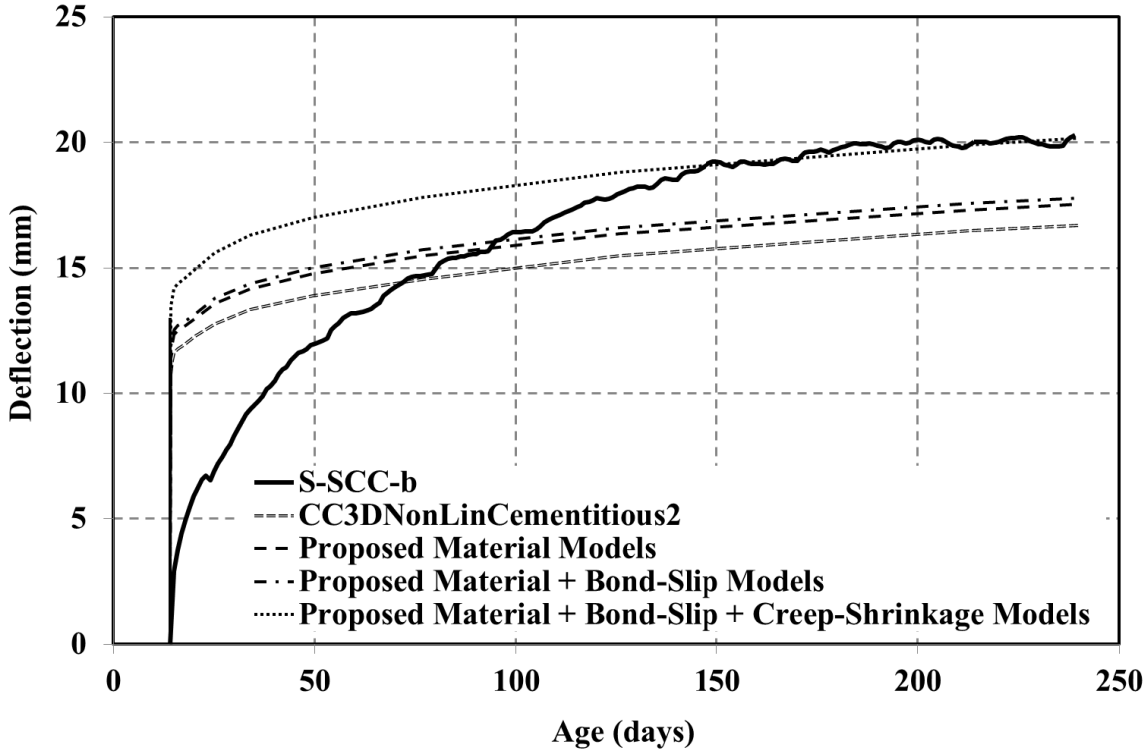

Figure 9.31 Deflection-age behaviour of slab S-SCC-b

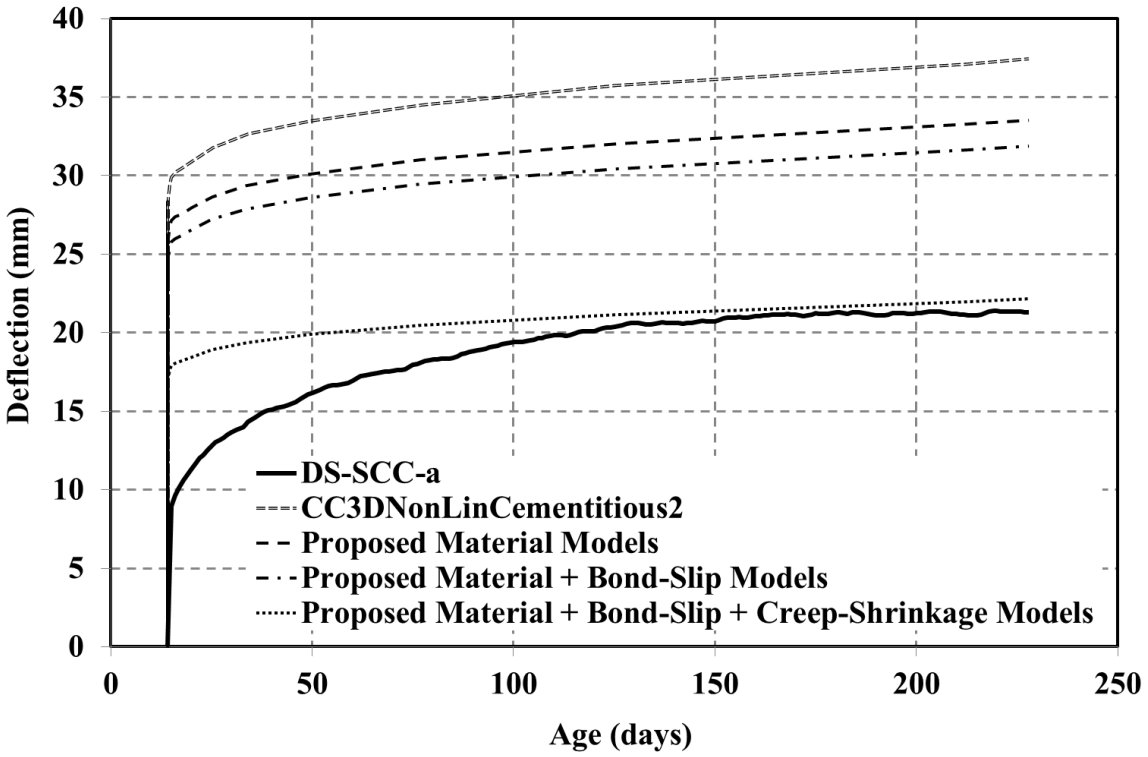

Figure 9.32 Deflection-age behaviour of slab DS-SCC-a

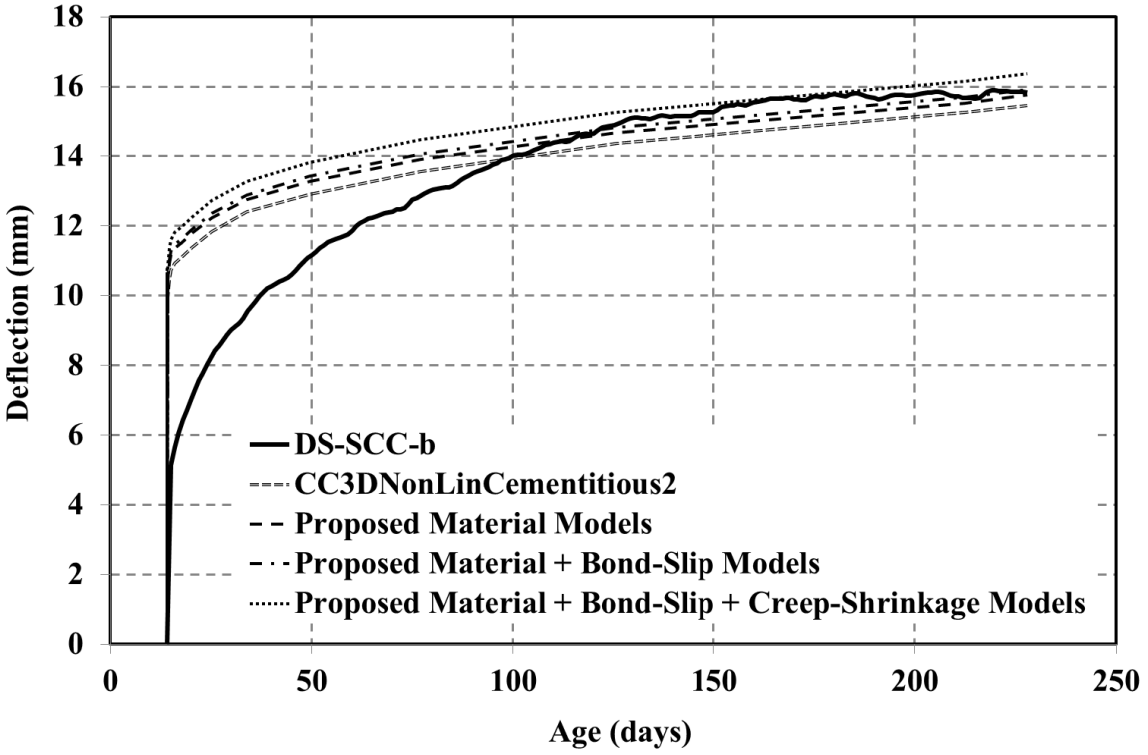

Figure 9.33 Deflection-age behaviour of slab DS-SCC-b

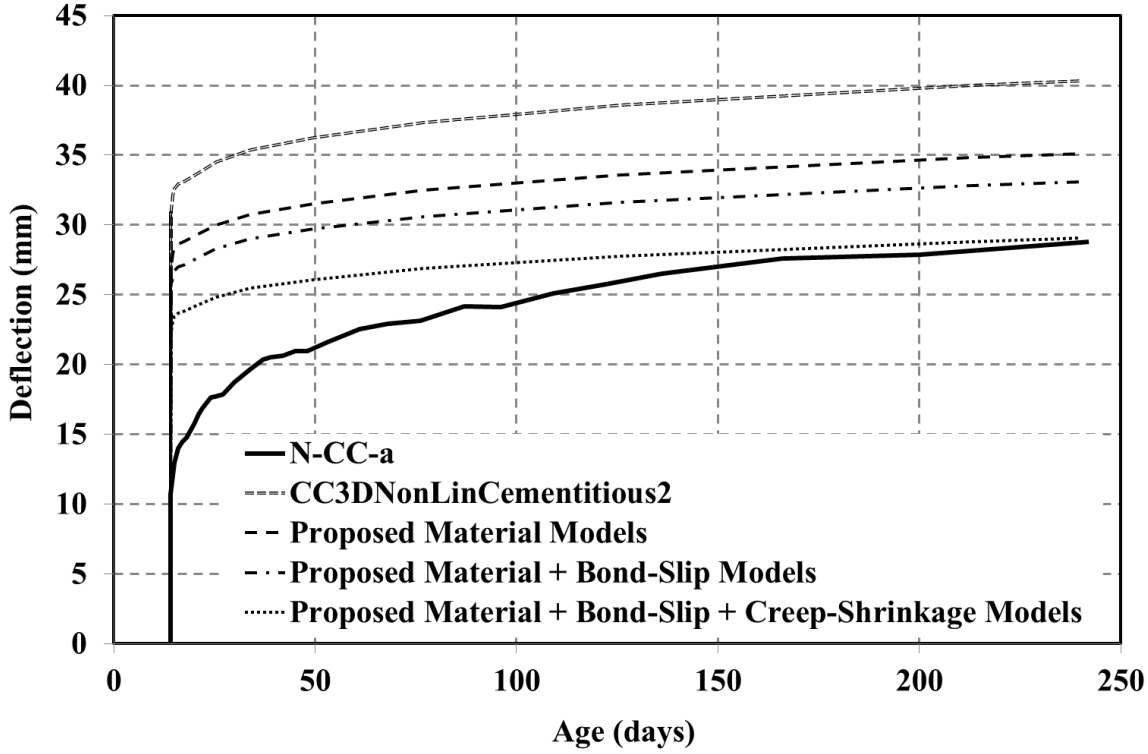

Figure 9.34 Deflection-age behaviour of slab N-CC-a

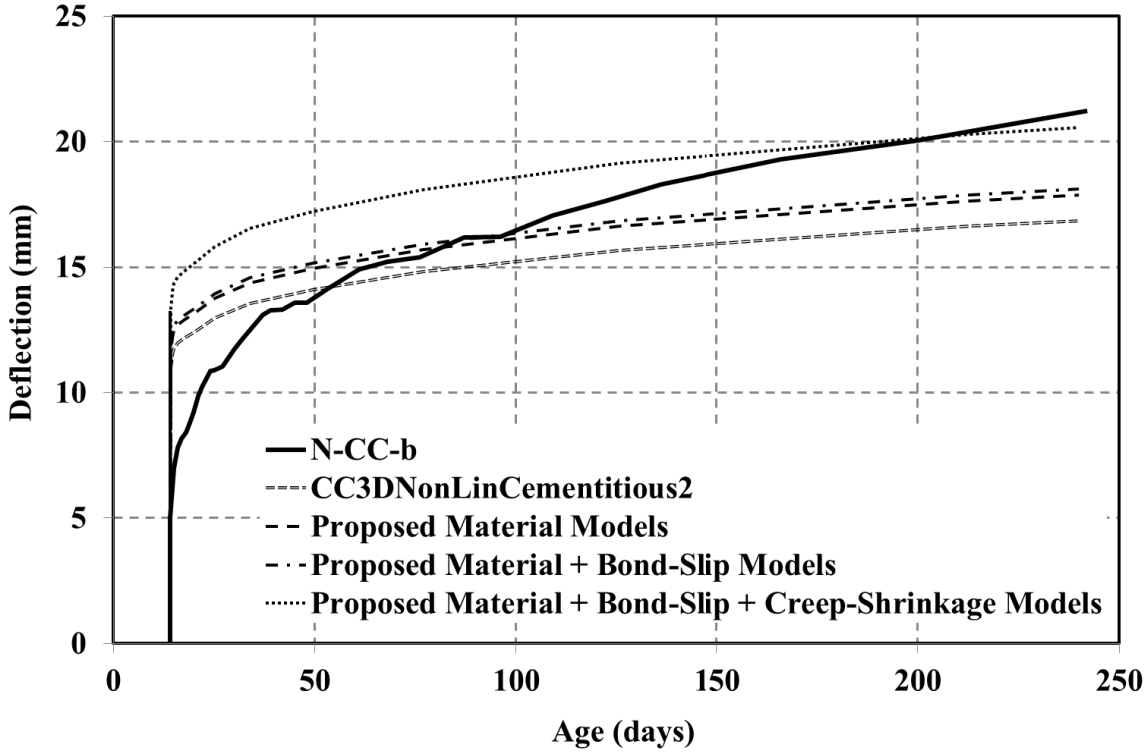

Figure 9.35 Deflection-age behaviour of slab N-CC-b

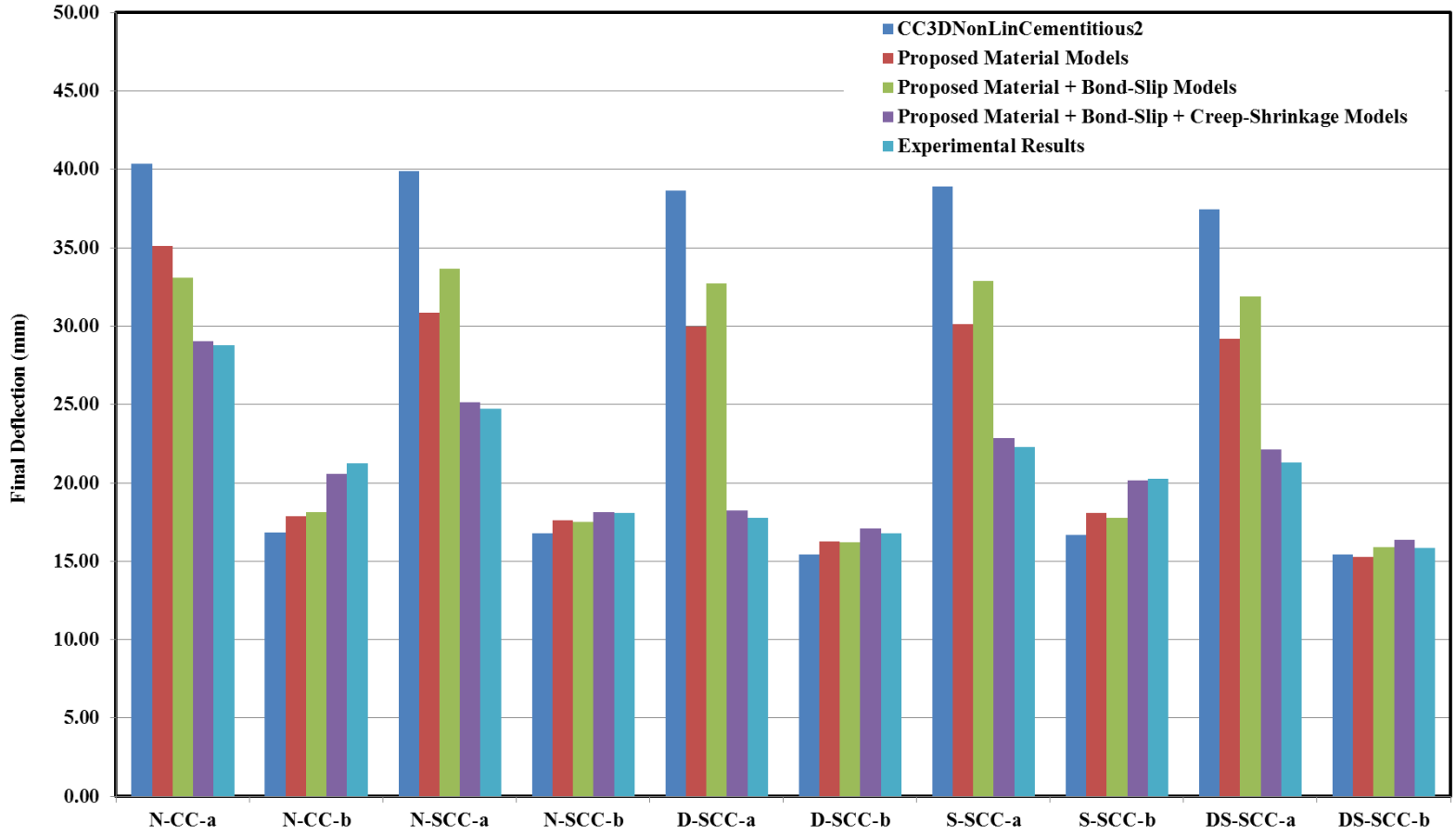

Figure 9.36 Final deflection comparisons for all concrete mixes

Table 9.3 Comparison between crack widths experimental results, proposed analytical model and codes for instantaneous behaviour

	Instantaneous Behaviour (mm)									
	N-SCC-a	N-SCC-b	D-SCC-a	D-SCC-b	S-SCC-a	S-SCC-b	DS-SCC-a	DS-SCC-b	N-CC-a	N-CC-b
Experimental Results	0.11	0.08	0.11	0.07	0.12	0.07	0.10	0.06	0.10	0.08
CC3DNonLinCementitious2	0.17	0.15	0.17	0.15	0.17	0.16	0.16	0.14	0.16	0.14
Proposed Material Models	0.15	0.13	0.15	0.13	0.15	0.14	0.12	0.11	0.12	0.13
Proposed Material + Bond-Slip Models	0.14	0.12	0.14	0.12	0.14	0.13	0.11	0.10	0.11	0.12
Proposed Material + Bond-Slip + Creep-Shrinkage Models	0.12	0.10	0.12	0.09	0.12	0.09	0.11	0.09	0.11	0.10

Table 9.4 Comparison between crack widths experimental results, proposed analytical model and codes for time-dependent behaviour

	Time-dependent Behaviour (mm)									
	N-SCC-a	N-SCC-b	D-SCC-a	D-SCC-b	S-SCC-a	S-SCC-b	DS-SCC-a	DS-SCC-b	N-CC-a	N-CC-b
Experimental Results	0.24	0.18	0.22	0.14	0.22	0.15	0.20	0.14	0.22	0.20
CC3DNonLinCementitious2	0.32	0.25	0.32	0.20	0.31	0.21	0.29	0.19	0.32	0.27
Proposed Material Models	0.28	0.22	0.28	0.18	0.27	0.18	0.24	0.16	0.28	0.23
Proposed Material + Bond-Slip Models	0.27	0.21	0.27	0.17	0.26	0.17	0.22	0.15	0.27	0.22
Proposed Material + Bond-Slip + Creep-Shrinkage Models	0.25	0.19	0.24	0.16	0.23	0.16	0.21	0.14	0.25	0.21

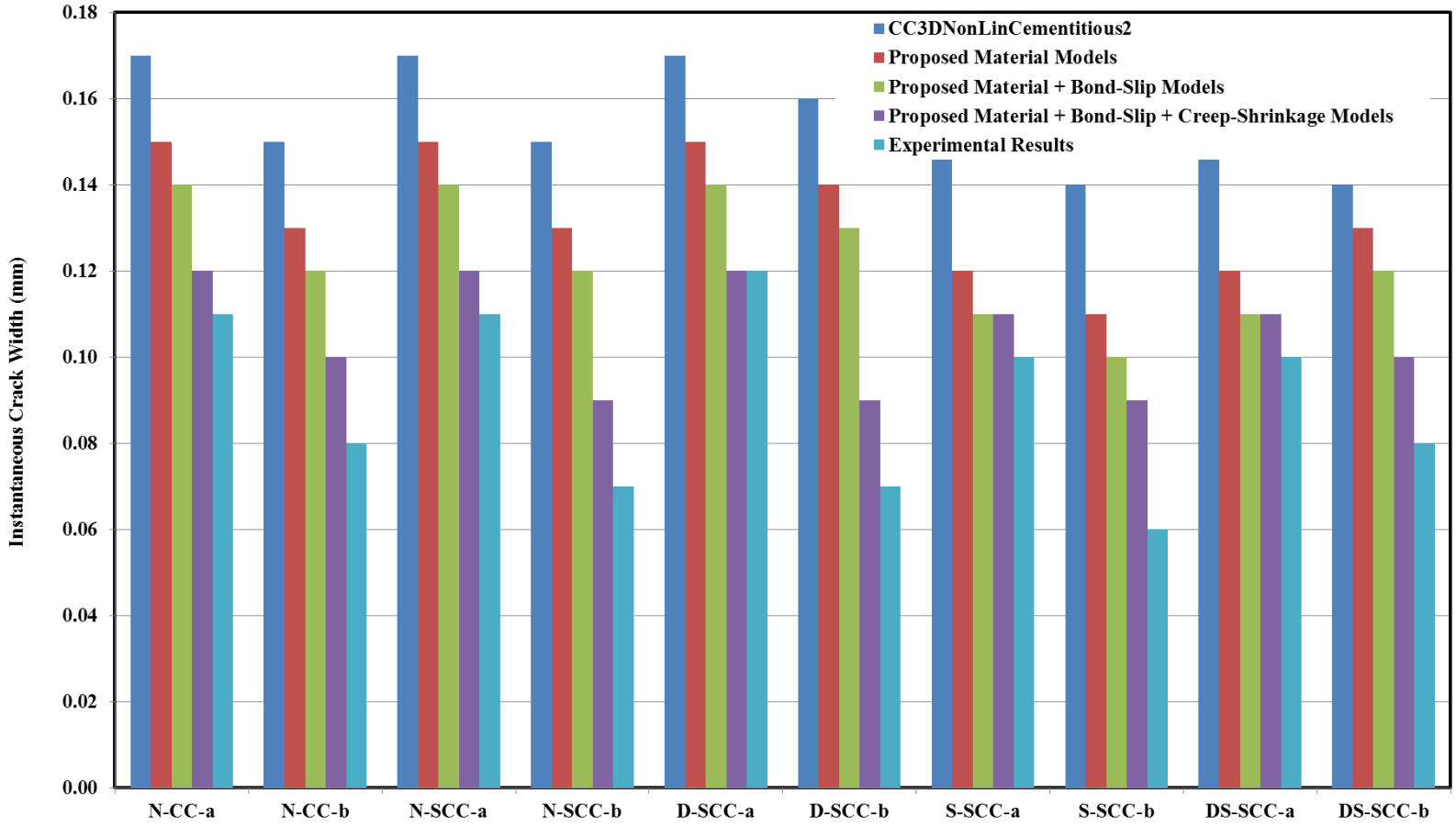

Figure 9.37 Instantaneous crack widths comparisons for all concrete mixes

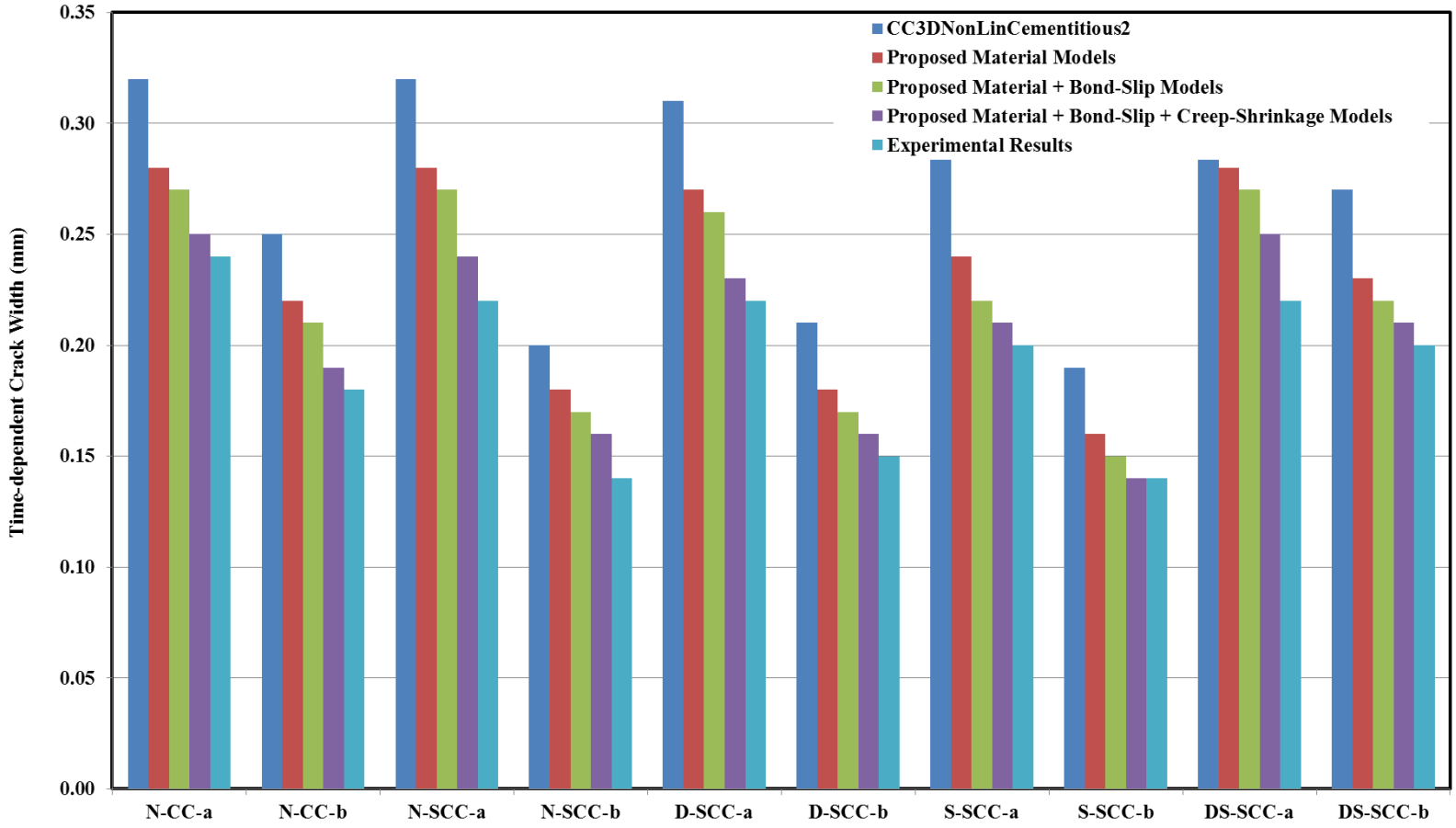

Figure 9.38 Time-dependent crack widths comparisons for all concrete mixes

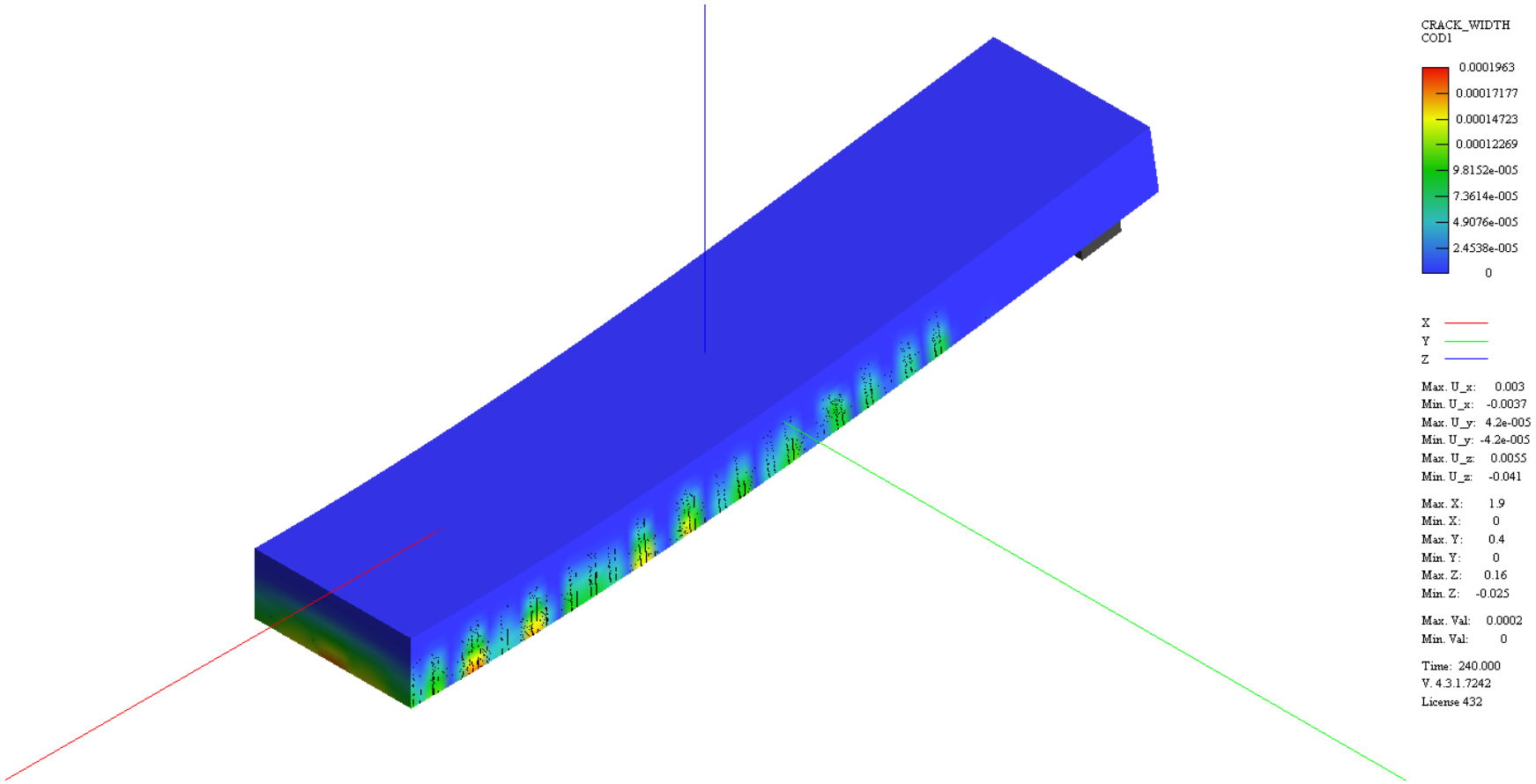

Figure 9.39 Typical FEM time-dependent crack width result for N-SCC-a slab

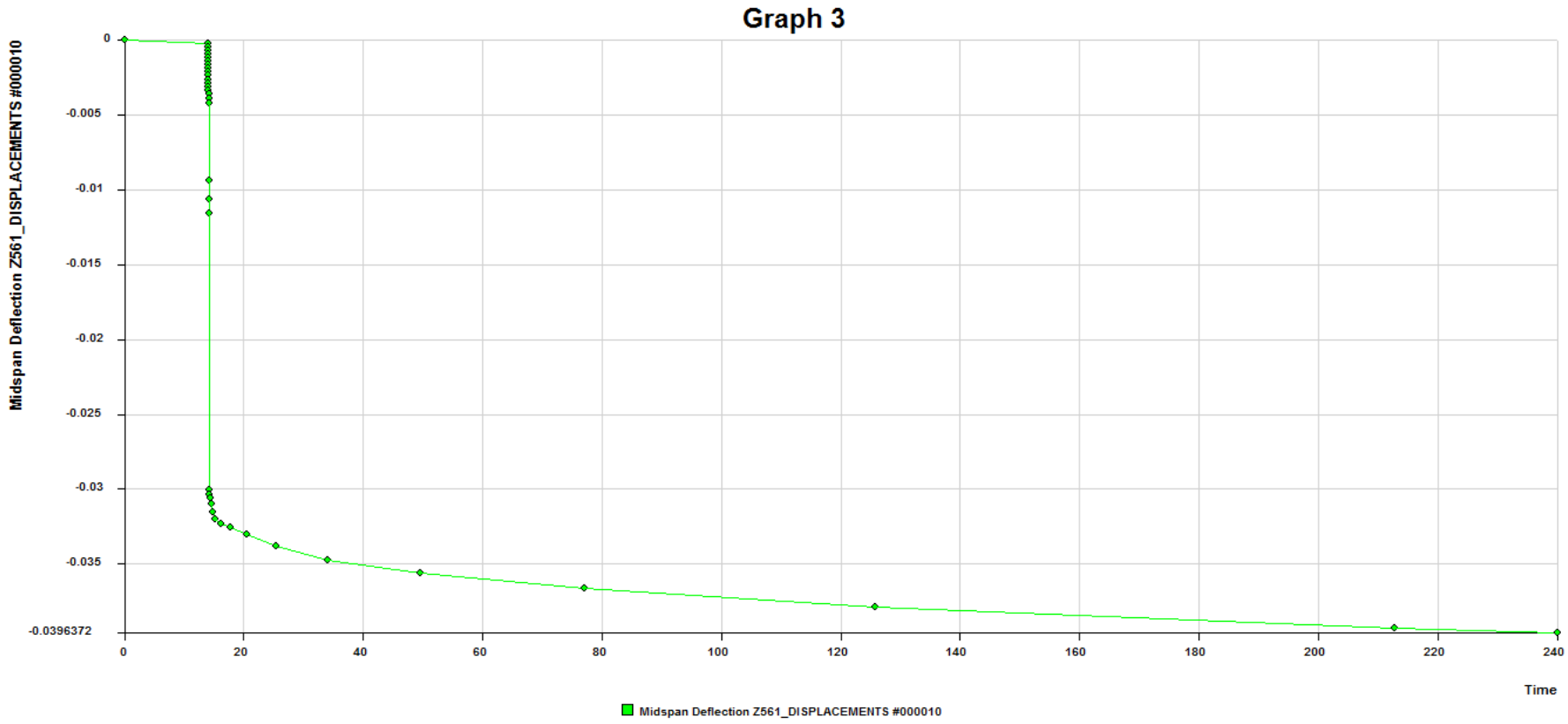

Figure 9.40 Typical FEM time-dependent deflection result for N-SCC-a slab

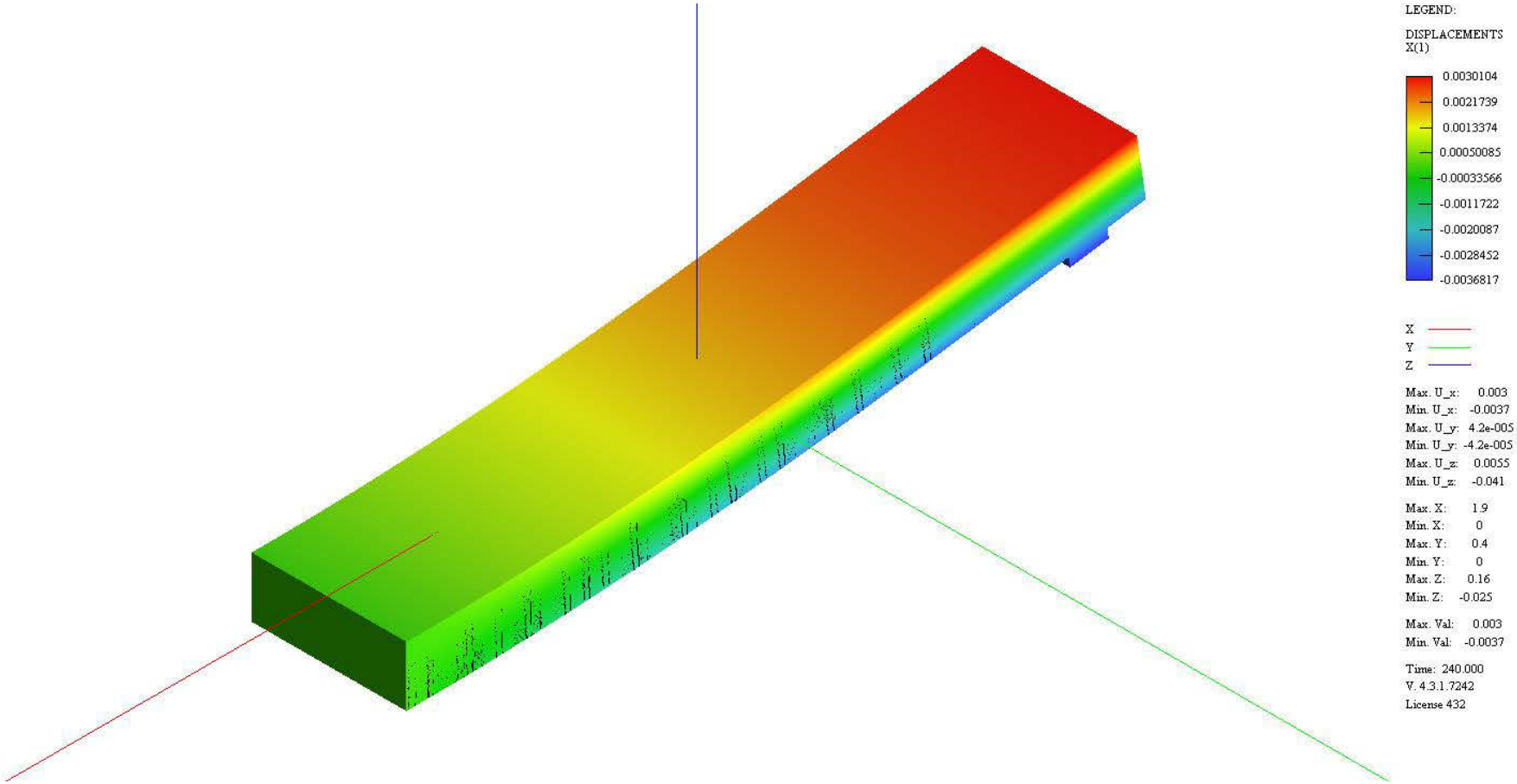

Figure 9.41 Typical FEM time-dependent displacement result for N-SCC-a slab

CHAPTER 10

SUMMARY AND CONCLUSIONS

CHAPTER 10

SUMMARY AND CONCLUSIONS

10.1 SUMMARY

In this study, cracking in reinforced self-compacting and fibre reinforced self-compacting concrete slabs with particular emphasis on the development of flexural cracking due to the combined effects of constant sustained service loads and shrinkage have been investigated both experimentally and analytically. The results have been compared with the conventional concrete slabs flexural cracking behaviour available in the literature.

The history and development, advantages, limitations, key drivers of development, fresh properties, mechanical properties, bond characteristics, shrinkage and creep of the SCC members have been presented.

Moreover, the hardened properties of SCC and FRSCC, including the mechanical properties, bond characteristics, shrinkage, and creep have been investigated. Also, the hardened properties of SCC and FRSCC with those of CC and FRC have been compared and new models for the hardened properties of SCC and FRSCC were proposed and compared with the available models in the literature.

A series of short-term tests was conducted on the one-way reinforced self-compacting and fibre reinforced self-compacting concrete slabs to study the development of flexural cracking under monotonically increasing loads. The location and width of the flexural cracks were carefully monitored under the increasing load up to failure for each load increment. Deflections at mid-span, crack patterns, crack widths, steel strains, and concrete surface strains at the steel level were recorded in the instantaneous cracking and post-cracking range. A second series of long-term tests on the one-way reinforced self-compacting and fibre reinforced self-compacting concrete slabs under sustained loads was also conducted to study the development of flexural cracking caused by the combined effects of constant sustained service loads and shrinkage. Deflections at mid-span, crack

patterns, crack widths, steel strains and concrete surface strains at the steel level were recorded both immediately after loading and up to 240 days under sustained loads. The concrete properties including the compressive strength, tensile strength, elastic modulus, and modulus of rupture of the SCC and FRSCC at different ages were also measured on the companion specimens.

Analytical models were developed to simulate SCC and FRSCC instantaneous and time-dependent flexural cracking. The tension chord model for CC (Nejadi, 2005) was modified for SCC and used in the proposed model to study the SCC tension zone of a flexural member and the effect of creep and shrinkage with time. Also, tension chord model for FRC (Leutbecher, 2007) was modified and used in the proposed model to study the FRSCC tension zone of a flexural member and the effect of creep and shrinkage with time.

Moreover, the crack width and spacing calculation procedures of the codes of practice including Eurocode 2 (1991), CEB-FIP (1990), ACI318-99 (1999), Eurocode 2 (2004), fib-Model Code (2010), Nejadi (2005), Leutbecher (2007), were assessed and some deficiencies in the existing approaches exposed. A comparison between the experimental results, proposed analytical model, and codes of practice models was presented for the one-way slab specimens for both instantaneous and time-dependent behaviour. Finally, a comprehensive parametric study for the instantaneous and time-dependent behaviour of the slabs by FEM analyses has been conducted. In this parametric study, the proposed SCC and FRSCC models for hardened properties, bond characteristics, creep, and shrinkage models have been utilized in the FEM analyses.

10.2 CONCLUSIONS

The following conclusions can be drawn from the work presented in this study:

10.2.1 Hardened Concrete Properties

10.2.1.1 Material Properties

According to the discussion of the presented models in chapter 3 regarding the Modulus of Elasticity (MOE), Tensile Strength (TS), Modulus of Rupture (MOR), Compressive Stress-Strain Curve (CSSC) models for CC and SCC, the following conclusions can be made:

- In general, without considering the types of aggregates and fillers, there are small differences between the SCC and CC models. However, when the types of aggregates and fillers change, the amount of the differences change too.
- Mostly, the differences between CC and SCC models for MOE and TS are dependent to the compressive strength. Differences for high compressive strength concrete more than 80 MPa are low, but for the normal compressive strength concrete, more than 45 MPa are significant. In this study general models are proposed. These MOE and TS models are applicable to both SCC and CC accurately.
- For CC, the Carasquillo et al. (1981), ACI 363 (1992), AASHTO (2006) models for MOR are conservative in general. Overall, predictions of these models are not accurate enough comparing to the test results.
- For SCC, the Leemann and Hoffmann (2005) model for MOR is conservative but is not accurate enough.
- The available MOR models for SCC are based on the specific researchers' experimental results in the literature. The proposed MOR model for SCC in this study is tried to solve this problem.
- The proposed MOE models for each type of aggregate, filler, and concrete type (SCC or CC) are applicable to the proposed SCC compressive stress-strain model.
- Based on the CSSC experimental database, the major filler is fly ash and the major aggregate is river gravel and crushed granite aggregate. Therefore, the proposed MOE models of SCC with fly ash filler and river gravel and crushed granite aggregate should be included in the CSSC model.
- The proposed compressive stress-strain model is based on the Carreira and Chu's model (1984) with several modifications (i.e., changing the ascending and descending portions) which is in good agreement with the experimental results for both SCC and CC mixtures.
- The compressive SCC stress-strain relationship suggested in this study accurately predicts the ascending branch of the stress-strain curve compared to the experimental database. It also predicts the descending branch within a minimum range of deviations with reasonable accuracy.

10.2.1.2 Bond characteristics of reinforcing steel bars embedded in CC and SCC

According to the discussion presented in chapter 3 regarding the bond characteristics of embedded reinforcing steel bars in CC and SCC, the following conclusions can be made:

- Based on the experimental database from the literature:
  - The ultimate and mean bond strengths are greater in SCC than in CC.
  - For the top cast bars, the local bond strength for SCC is greater than that for CC.
  - The bond strength of SCC is as high as the bond strength for CC when large bar diameters are used. For smaller bar diameters, the bond strength of SCC is slightly higher.
  - The corresponding slip to the maximum bond strength increases by increasing the bar diameters.
- By comparison of the code provisions and equations of the bond strength it can be concluded that the same procedures of CC can be used for SCC too. Thus bond properties of SCC are similar to the CC.
- Most of the available bond strength models in the literature are not accurate enough to evaluate the SCC and CC bond characteristics. The proposed bond strength models in this study are based on regression analyses on existing experimental data that is in good agreement with the experimental test results for both SCC and CC.
- In the proposed bond stress-slip model, the main curve is similar to the ones used in CEB-FIP's (1999), Huang et al.'s (1996), and Harajli et al.'s (1995) models, but the bond strength models for SCC and CC are different. Although there are several different factors (compressive strength, water-to-cement ratio, bar pullout positions, age of concrete, and bar diameter), the predicted values from the proposed SCC models in this study are consistent with Valcuende and Parra's (2009), Hassan et al.'s (2010), and Desnerck et al.'s (2010) bond stress-slip experimental results.
- The predicted values of the proposed SCC bond stress-slip model accurately are verified that this model can predict good the bond stress-slip curve for normal and high strength SCC and CC for the various conditions (such as different bar pullout positions, different ages of concrete, different compressive strength, and different bar diameters).

10.2.1.3 Stress-strain behaviour of SFRSCC

According to the discussion presented in chapter 3 regarding the stress-strain behaviour of SFRSCC, the following conclusions can be made:

- Available SFRC and SFRSCC compressive stress-strain relationships in the literature are not in good agreement with the experimental results especially descending portion of the stress-strain curve.
- Nonlinear regression analyses have been conducted in order to develop SFRSCC for the mechanical properties of SFRC and SFRSCC mixes (e.g. compressive strength, tensile strength, modulus of elasticity, and strain at peak stress).
- Normalized mechanical SFRSCC properties data are more compatible with the nonlinear regression analyses rather than just mechanical SFRSCC properties data.
- Proposed SFRSCC relationships are more suitable for SFRSCC mixtures results in the database that used ordinary Portland cement; fly ash and limestone fillers; limestone, natural coarse aggregate and natural sand; and hooked end fibres.
- The proposed SFRSCC stress-strain compressive relationship proposed in this study is based on the several modifications (i.e. changing the ascending and descending portions). In this compressive stress-strain relationship for normal and high strength SFRSCC the proposed compressive strength, modulus of elasticity and strain at peak stress models are used.
- The proposed SFRSCC tensile envelope curve is a simple relationship based on the normal and high strength SFRSCC tensile stress-strain model, the proposed SFRSCC tensile strength and modulus of elasticity models are used.

10.2.1.4 Bond characteristics of SFRSCC

According to the discussion presented in chapter 3 regarding the bond characteristic of SFRSCC, the following conclusions can be made:

- The proposed models for the bond characteristic describe the coefficient of friction versus pullout displacement by allowing for the different fibre types and strength of SFRSCC (normal and high). They proved a good agreement with the experimental

results. The observed decrease in the coefficient of friction could be caused by matrix wear and consequent smoothening of the interface layer as the fibre pulls out of the matrix.

- Dubey's pullout model (1999) for aligned fibres was applied and calibrated with the proposed coefficient of friction for SFRSCC. The calibrated and modified model reveals a good agreement with the test results for the different fibre types (smooth and hooked) and SCC strength (normal and high).
- To take into account the effect of fibre inclination in the pullout model, apparent shear strengths ($\tau_{(app)}$) and slip coefficient (β) are introduced to express the variation of the pullout peak load and the augmentation of peak slip when the inclination angle increases. They are expressed as functions of the inclination angle.
- The proposed pullout models are applicable for inclined fibres by introducing the apparent shear strengths and slip coefficients which allow simulation of the experimental pullout load-slip curves accurately for both hooked and straight aligned fibres with different embedment lengths.

10.2.2 Time-Dependent Behaviour of Hardened Concrete

10.2.2.1 Shrinkage of SCC

According to the discussion presented in chapter 4 regarding the shrinkage behaviour of SCC, the following conclusions can be made:

- The AASHTO (2007), JSCE (2002) and AS 3600 (2009) shrinkage models provide a better prediction of the shrinkage strain for SCC mixtures compared to the other models. But, these models are different in the certain intrinsic and/or extrinsic variables which JSCE (2002) model is better in this case.
- The AASHTO (2007) and JSCE (2002) shrinkage models provide better prediction of the shrinkage strain for CC mixtures compared to the other models.
- Larson (2007) and Cordoba (2007)'s shrinkage models for SCC underestimate the shrinkage strain of SCC mixtures. These models are a modification of the ACI

209R (1997) model. Also, these models are a general model of ACI 209R (1997) because they do not cover intrinsic and extrinsic variables.

- The proposed SCC shrinkage model proves a good prediction of the shrinkage strain for normal strength and high strength of the SCC mixtures compared to the experimental database.

10.2.2.2 Creep of SCC

According to the discussion presented in chapter 4 regarding the creep behaviour of SCC, the following conclusions can be made:

- The AASHTO (2004), JSCE (2002) and ACI 209R (1992) creep models provide a better prediction of the creep strain for SCC mixtures compared to the other models. However, these models are different in the certain intrinsic and/or extrinsic variables which JSCE (2002) model is better in this case.
- The AASHTO (2007), JSCE (2002), Eurocode 2 (2001) and AASHTO (2004) creep models provide a better prediction of the creep strain for CC mixtures too compared to the other models.
- Cordoba (2007) creep prediction model for SCC underestimates the creep strain of SCC mixtures. This model is a modification of the ACI 209R (1997) model. Also, these models are a general model of ACI 209R (1997) because they do not cover intrinsic and extrinsic variables.
- Proposed SCC creep model proves a good prediction of the creep strain for normal and high strength of the SCC mixtures compared to the experimental database.

10.2.3 Experimental Program (Phase I) – Material Properties of SCC and FRSCC

- An experimental program was performed consisting of four different SCC mixtures as follows: include normal SCC (N-SCC), steel fibre-reinforced SCC (D-SCC), PP fibre-reinforced SCC (S-SCC), and hybrid fibre-reinforced SCC (DS-SCC).

- The CS, TS, MOE, MOR, and CSSC are tested and recorded at ages of 3, 7, 14, 28, 56 and 91 days. For these properties, differences between SCC mixes show that the differences decrease with time.

- The average CS of the DS-SCC mixture is higher than that of the N-SCC, D-SCC, and S-SCC mixtures. The results indicate that CS of the DS-SCC mixture at 91 days is 10.71%, 1.62% and 8.32% higher than that of the N-SCC, D-SCC, and S-SCC mixtures respectively.

- The average TS of the D-SCC mixture is higher than that of the DS-SCC, N-SCC, and S-SCC mixtures. The results show that the TS of D-SCC mixture at 91 days is 15.95%, 18.89%, and 11.76% higher than that of the N-SCC, S-SCC, and DS-SCC mixtures, respectively.

- The average MOE of the DS-SCC mixture is higher than that of the N-SCC, D-SCC, and S-SCC mixture. The results indicate that MOE of DS-SCC mixture at 91 days is 0.86%, 1.41%, and 1.72% higher than that of the N-SCC, D-SCC, and S-SCC mixture, respectively.

- The average MOR of the D-SCC mixture is higher than that of the N-SCC, S-SCC, and DS-SCC mixture. The results indicate that the MOR of the D-SCC mixture at 91 days is 1.30%, 6.44%, and 0.21% higher than that of the N-SCC, S-SCC, and DS-SCC mixtures, respectively.

- Analytical expressions to predict the most significant mechanical properties (i.e., compressive strength, tensile strength, modulus of elasticity, and modulus of rupture) of the SCC mixtures at any age, arbitrary are presented.

- The proposed compressive stress–strain relationship in this study is developed by using the proposed compressive strength and elastic modulus models that are in good agreement with the experimental results for the developed SCC mixtures.

- The JSCE (1984) flexural toughness factors are more sensitive to both age and fibre content comparing to the ASTM toughness indexes for the SCC mixtures. They increase as concrete age or fibre content increase.

- The characterization of flexural toughness based on the JSCE (1984) approach is very simple and is independent of the type of deflection measuring method. No sophisticated instrumentation is required to determine the toughness factor. The

determination of first crack, which is very difficult to identify, is not required in this method. The flexural toughness factor calculated using this approach has provided a good correlation with the fibre-reinforcing index.

- Based on the flexural toughness analyses by using ASTM C 1018 (2000), JSCE (1984), Banthia and Trottier (1995), and ACI 544 (1988) methods, it can be concluded that D-SCC mixture shows better flexural toughness behaviour than DS-CC and S-SCC mixtures.

10.2.4 Experimental Program (Phase II) – Short Term Flexural Cracking

The results from the short-term flexural test programme on reinforced SCC slab specimens are summarised in Table 10.1. Overall conclusions based on the short-term flexural test experimental results can be made as follows:

- The DS-SCC slabs show the lowest maximum and average final crack widths compared to the other mixture slabs.
- The DS-SCC slabs bear maximum failure load and deflection compared to the other mixture slabs.
- In the S-SCC slabs maximum and average final crack widths are decreased compared to the N-SCC slabs but not too much change comparing to the N-CC slabs.
- By using PP fibres in SCC the failure loading does not change much too, but it increases the ductility of the slab specimens comparing to the N-SCC and N-CC slabs.
- By using steel fibres in SCC maximum and average final crack widths are decreased compared to the N-SCC and N-CC slabs.
- In the D-SCC slabs final average spacing is decreased compared to the other mixtures slabs.

- The adopted expressions for the bond shear stress τ_b for the SCC slab series under short-term loading and for the different in-service steel stress ranges have been presented in Table 10.2.

Table 10.1 Summary of the results from short-term flexural test

Specimen	Testing age (days)	$(w_{max})_{final}$ (mm)	$(w_{ave})_{final}$ (mm)	$(s_{ave})_{final}$ (mm)	Failure Load (kN)	Deflection at failure load (mm)	w_{max}/w_{ave}
N-SCC-a	62	0.20	0.154	95	49.0	180	1.29
N-SCC-b	63	0.25	0.195	94	48.5	163	1.17
D-SCC-a	65	0.18	0.138	106	53.0	205	1.10
D-SCC-b	66	0.23	0.172	96	52.0	177	1.33
S-SCC-a	67	0.18	0.132	102	50.0	185	1.36
S-SCC-b	69	0.23	0.189	100	48.0	167	1.21
DS-SCC-a	71	0.15	0.120	95	56.0	220	1.24
DS-SCC-b	72	0.20	0.156	98	54.0	182	1.15
N-CC-a*	62	0.18	0.130	90	50.0	136	1.38
N-CC-b*	63	0.23	0.180	117	47.0	156	1.28

* Nejadi's (2005) experimental results for CC

Table 10.2 Adopted bond stresses for SCC slab series

Slab series	τ_b	
	$f_{sy} > \sigma_{s.max} \geq 180$ MPa	$\sigma_{s.max} < 180$ MPa
N-SCC	$1.50\, f_{ct}$	$1.50\, f_{ct}$
D-SCC	$1.30\, f_{ct}$	$1.25\, f_{ct}$
S-SCC	$1.70\, f_{ct}$	$1.50\, f_{ct}$
DS-SCC	$1.60\, f_{ct}$	$1.50\, f_{ct}$

10.2.5 Experimental Program (Phase III) – Long Term Flexural Cracking

- The creep coefficient of DS-SCC mixture has the same trend like the N-CC. But, the other SCC mixtures shpw different behaviour. The creep coefficient of the N-SCC mixture at age 240 days is 5%, 7%, 26%, and 24% higher than the D-SCC, S-SCC, DS-SCC, and N-CC mixtures, respectively. Also, the creep coefficients of the D-SCC and S-SCC mixtures have similar trend. The D-SCC mixture creep coefficient is just 2% higher than the S-SCC mixture at age 240 days.

- The maximum measured final shrinkage strains of the N-SCC, D-SCC, S-SCC, DS-SCC, and N-CC mixtures are 870, 844, 823, 882, and 785 microstrains after 240 days. The maximum measured final shrinkage strains for the different SCC mixtures are not much different from each other. Also, the S-SCC mixture has the lowest final shrinkage strain that is 5.7%, 2.5%, and 7% lower than the N-SCC, D-SCC, and DS-SCC mixtures.

- The results from long-term flexural test programme on reinforced SCC slab specimens are summarised in Table 10.3. Overall conclusions according to the long-term flexural test results can be made as follows:

- The instantaneous minimum, average, and maximum crack widths for the N-SCC slabs are close to the N-CC slabs. Moreover, time-dependent minimum, average, and maximum crack widths for N-SCC-a slab are slightly more than N-CC-a slab but crack widths for N-SCC-b slab are slightly less than N-CC-b slab. These results confirm that the crack spacing by using SCC is much smaller than CC.

- Instantaneous minimum, average, and maximum crack widths for the D-SCC, S-SCC, and DS-SCC slabs are close to the N-SCC and N-CC slabs crack widths. But, time-dependent minimum, average, and maximum crack widths for the D-SCC, S-SCC, and DS-SCC slabs are slightly smaller than the N-SCC slabs and close to the N-CC slabs' crack widths. Also, other SCC mixture slas average crack spacings are much higher than N-SCC slabs.

Table 10.3 Summary of the results from long-term flexural test

Specimen	Instantaneous				Time-dependent				$(s_{rm})_{final}$ / $(s_{rm})_{inst.}$
	w_{min} (mm)	w_{ave} (mm)	w_{max} (mm)	$s_{rm,ave}$ (mm)	w_{min} (mm)	w_{ave} (mm)	w_{max} (mm)	$s_{rm,ave}$ (mm)	
N-SCC-a	0.03	0.07	0.11	99	0.06	0.15	0.24	97	0.98
N-SCC-b	0.03	0.05	0.08	100	0.03	0.11	0.18	95	0.95
D-SCC-a	0.04	0.07	0.11	96	0.06	0.13	0.22	95	0.99
D-SCC-b	0.02	0.05	0.07	99	0.02	0.09	0.14	95	0.96
S-SCC-a	0.03	0.07	0.12	96	0.07	0.15	0.22	94	0.98
S-SCC-b	0.02	0.04	0.07	93	0.05	0.10	0.15	91	0.98
DS-SCC-a	0.03	0.06	0.10	102	0.04	0.14	0.20	98	0.96
DS-SCC-b	0.02	0.04	0.06	94	0.04	0.09	0.14	90	0.96
N-CC-a	0.05	0.09	0.10	153	0.10	0.15	0.22	102	0.67
N-CC-b	0.03	0.04	0.08	141	0.08	0.14	0.20	136	0.96

- The measured instantaneous and final deflections (at t = 0 and t = 240 days) and their ratios are presented in Table 10.4.

- Based on the comparison of the results between slab series N-SCC and series N-CC presented in Table 10.4, it can be concluded that the slabs N-SCC's instantaneous deflection is close to the N-CC slabs, but the final deflections of the N-SCC slabs are less than the N-CC slabs. Also, the instantaneous deflections of the other SCC slabs are less than the N-SCC and N-CC slabs all of them. Also, the S-SCC slabs instantaneous deflections surprisingly are less than the other SCC slabs instantaneous deflections.

- The D-SCC slabs have the minimum final deflection compared to the other slab series. The DS-SCC slabs have the less final defection compared to the N-SCC, N-CC, and S-SCC slabs except the D-SCC slabs.

Table 10.4 Measured final and instantaneous deflection at mid-span

.

Specimen	Instan. Deflection (mm)	Final Deflection (mm)	Final Deflection / Instan. Deflection
N-SCC-a	12.11	24.76	2.04
N-SCC-b	5.89	18.08	3.07
D-SCC-a	7.65	17.76	2.32
D-SCC-b	7.59	16.78	2.21
S-SCC-a	6.41	22.27	3.47
S-SCC-b	2.91	20.25	6.95
DS-SCC-a	8.98	21.31	2.37
DS-SCC-b	5.14	15.83	3.08
N-CC-a	11.80	32.10	2.72
N-CC-b	5.04	21.92	4.35

- Four different relationships for bond shear stress ($\tau_b = 0.5\, f_{ct}$, $\tau_b = f_{ct}$, $\tau_b = 1.5\, f_{ct}$, and $\tau_b = \lambda_1\, \lambda_2\, \lambda_3\, f_{ct}$) have been considered and the corresponding crack widths are calculated and compared with the experimental results. It should be mentioned that throughout the test, crack widths are monitored at two levels on the side of each specimens. Considering those values and comparing the best fit between the calculated values and measured crack widths, the expressions for the bond shear stress τ_b for SCC slabs are presented by Eq. (10.1), under long-term loading and for the different in-service steel stress ranges have been adopted for the analytical model.

$$\tau_b = 1.5\, f_{ct} \tag{10.1}$$

10.2.6 Analytical Model for Instantaneous and Time-Dependent Flexural Cracking of SCC and FRSCC

- The instantaneous model of Eurocode 2 (1991) overestimates the crack width for slab specimens at all steel stress levels. However, for long-term behaviour, it underestimates actual crack widths.

- The instantaneous crack widths calculated in accordance with CEB-FIP (1990) at in-service steel stress levels up to 250 MPa underestimates the crack width for slab specimens. However, for time-dependent cracking, this method slightly underestimates the crack width at steel stress levels lower than 200 MPa and for slabs with widely spaced tensile reinforcement bars.

- The instantaneous crack widths calculated in accordance with ACI318-99 (1999) at steel stress levels up to 250 MPa overestimates the crack width for slab specimens at all steel stress levels. Since in this code the time-dependent effect of shrinkage has not been considered, ACI318-99 (1999) underestimates the long-term crack width always.

- The instantaneous behaviour of Eurocode 2 (2004) slightly underestimates the crack width for slab specimens at all steel stress levels. However, for long-term behaviour, it underestimates actual crack widths significantly.

- The instantaneous crack widths calculated in accordance with fib-Model Code (2010) at in-service steel stress levels up to 250 MPa slightly overestimates the crack width for slab specimens. However, for time-dependent cracking, this method underestimates the crack width at steel stress levels lower than 200 MPa and for slabs with widely spaced tensile reinforcement bars.

- The instantaneous crack widths calculated in accordance with Nejadi (2005) and Leutbecher (2007) at in-service steel stress levels up to 250 MPa underestimate the crack width for slab specimens. However, for time-dependent cracking, these methods slightly underestimate the crack width at steel stress levels lower than 200 MPa and for slabs with widely spaced tensile reinforcement bars.

- The crack widths calculated in accordance with proposed model (in chapter 8) at steel stress levels up to 250 MPa shows that, for short-term and time-dependent cracking, proposed model predicts crack widths which are in good agreement with the measured experimental results at all steel stress levels.

- The crack spacing calculated in accordance with ACI318-99 (1999) and Eurocode 2 (2004) generally overestimate the short-term and long-term crack spacing.

- Instantaneous crack spacing reduces with time under sustained load due to creep and shrinkage effects. Eurocode 2 (1991), CEB-FIP (1990), fib-Model Code (2010), and Leutbecher (2007) consider the limit values of maximum crack width under quasi-permanent loading for reinforced concrete members. Therefore, crack spacing calculated in accordance with the above mentioned models corresponds to the quasi-permanent loading and underestimates the instantaneous crack spacing, but provides reasonable agreement with the measured final long-term crack spacing.

- Due to the random nature of cracking, great accuracy in calculating the crack spacing is not achievable. Nevertheless, the instantaneous and final average crack spacing predicted by the proposed model in this study proves good agreement with the measured instantaneous and final average crack spacing.

10.2.7 Finite Element Modelling of Cracking Behaviour of Conventional Steel Reinforced and Fibre Reinforced Self-Compacting Concrete Slabs

Reinforced concrete structures FEM analysis process and development is summarized in chapter 9.

- A comprehensive FEM parametric study for calibration of the proposed SCC and FRSCC models in this research has been conducted.

- The FEM parametric study results indicate that by using the proposed SCC models in this study for material properties, bond-slip and creep and shrinkage, the accuracy of the deflection and crack widths calculations increase. Also, when the analysis is conducted by including the proposed models in this study all together the accuracy of the deflection and crack widths calculation are in the highest agreement with the experimental results.

10.3 RECOMMENDATIONS FOR FUTURE RESEARCH

The following areas of research concerning self-compacting concrete members remain relatively unexplored and could form the basis for future studies:

- The analytical and experimental results presented in this thesis are aimed to investigate the flexural behaviour of SCC and FRSCC members. Therefore the shear failure is not taken into account. However, shear failure always play important role in the reinforced concrete structures. More research is needed to develop a suitable shear failure mechanism to treat the collapse of SCC and FRSCC members due to shear failure.

- Researchers should perform additional studies on the restrained SCC and FRSCC slab specimens to assess the effects of drying shrinkage on direct tension cracking. This could provide benchmark data for restrained SCC and FRSCC slabs.

- An extensive experimental program could be conducted to investigate the long-term behaviour of the precast prestressed SCC members.

- An experimental program could be conducted to study the reversed cyclic and repeating loading effects in the short-term and long-term behaviour of the SCC and FRSCC members.

- An experimental program could be conducted to study the serviceability behaviour of members reinforced SCC with fibre-reinforced polymers.

- An experimental program could be conducted to study the durability of SCC, mainly the freeze/thaw resistance and the chloride penetration, and to a lesser extent the interaction between sea-water and SCC (in terms of sulphate attack).

REFERENCES

REFERENCES

AASHTO 2004, *Bridge design specifications and commentary*, American Association of Highway and Transportation Officials (AASHTO), Washington, D.C.

AASHTO 2006, *Interim bridge design specifications and commentary*, American Association of Highway and Transportation Officials (AASHTO), Washington, D.C.

AASHTO. 2007, *Interim bridge design specifications and commentary*, American Association of Highway and Transportation Officials (AASHTO), Washington, D.C.

ACI 209R. 1992, *Prediction of creep, shrinkage, and temperature effects in concrete structures*, ACI 209R-92, American Concrete Institute, Farmington Hills, Michigan.

ACI Committee 224. 2003, *Control of cracking in concrete structures*, ACI Manual of Concrete Practice Part 2 - 2003, USA.

AC1 232.2R-03. 2004, *Use of fly ash in concrete*, ACI Committee 232.

ACI 233R-95. 2000, *Ground granulated blast-furnace slag as a cementitious constituent in concrete*, ACI Committee 233.

ACI 237R-07. 2007, *Self-consolidating concrete*, American Concrete Institute, Farmington Hills.

ACI 318. 2005, *Building code requirements for structural concrete*, American Concrete Institute, Farmington Hills.

ACI 318-08, 2008, Building code requirements for structural concrete, ACI 318-08, Detroit, American Concrete Institute.

ACI 544.1R. 1997, *State-of-the-art report on fiber reinforced concrete*, Technical report, American Concrete Institute.

ACI Committee 544. 1988, 'Measurement of properties of fiber reinforced concrete', *ACI Materials Journal*, vol. 85, no. 6, pp. 583-589.

ACI 544.2R. 1999, *State-of-the-art report on fiber reinforced concrete*, Technical report, American Concrete Institute.

Aitcin, P.C., & Mehta, P.K. 1990, 'Effect of coarse aggregate characteristics on mechanical properties of high-strength concrete', *ACI Materials Journal*, vol. 87, no. 2, pp. 103-107.

Akcay, B. & Tasdemir, M.A. 2012, 'Mechanical behaviour and fibre dispersion of hybrid steel fibre reinforced self-compacting concrete', *Construction and Building Materials,* vol. 28, no.1, pp. 287–293.

Almeida Filho, F.M. 2006, *Contribution to study of the bond between steel bars and self-compacting concrete*, Doctoral Thesis, Universidade de Sao Paulo (in Portuguese).

Almeida Filho, F.M., Debs, M.H.C. & El Debs, A.L. 2008, 'Bond-slip behavior of self-compacting concrete and vibrated concrete using pullout and beam tests', *Materials and Structures*, vol. 41, no. 6, pp.1073–1089.

Alwan, J.M., Naaman, A.E., Guerrero, P. 1999, 'Effect of mechanical clamping on the pullout response of hooked steel fibers embedded in cementitious matrices', *Concrete Science Engineering*, vol. 1, no. 1, pp.15–25.

Andrawes, B., Shin, M. & Pozolo, A. 2009, Transfer and development length of prestressing tendons in full-scale aashto prestressed concrete girders using self-consolidating concrete, Research Report ICT-09-038, University of Illinois at Urbana-Champaign.

Armelin, H.S. & Banthia, N. 1997, 'Predicting the flexural post cracking performance of steel fiber reinforced concrete from the pullout of single fibers', *ACI Materials Journal*, vol. 94, no. 1, pp.18–31.

AS 1012.13. 1992, *Determination of the drying shrinkage of concrete for samples prepared in the field or in the laboratory*, Standards Australia.

AS 1012.14. 1991, *Method for securing and testing from hardened concrete for compressive strength*, Standards Australia.

AS 1012.16. 1996, *Determination of creep of concrete cylinders in compression*, Standards Australia.

AS 1012.17. 1997, *Determination of the static chord modulus of elasticity and Poisson's ratio of concrete specimens*, Standards Australia.

AS 1141. 2011, *Methods for sampling and testing aggregates - Particle size distribution - Sieving method*, Standards Australia.

AS 1478.1. 2000, *Chemical admixtures for concrete, mortar and grout - Admixtures for concrete*, Standards Australia.

AS 2350. 2006, *Methods of testing portland and blended cements*, Standards Australia.

AS 3582.2. 2001, *Supplementary cementitious materials for use with portland and blended cement - Slag - Ground granulated iron blast-furnace*, Standards Australia.

AS 3583. 1998, *Methods of test for supplementary cementitious materials for use with portland cement*, Standards Australia.

AS 3600. 2009, *Concrete structures*, Australian Standards.

AS 3972. 2010, General purpose and blended cements, Standards Australia.

ASCE Committee 447. 1982, State-of-the-art report on finite element analysis of reinforced concrete, ASCE, New York.

ASCE Committee 447. 1993, Finite element analysis of reinforced concrete structures II., ASCE, New York, 717 pp.

Aslani, F. & Nejadi, S. 2011a, 'Comparison of the analytical models to determine modulus of elasticity of self-compacting concrete and conventional concrete', *Structural Engineering World Congress (SEWC)*, Como, Italy, pp.1-10.

Aslani, F. & Nejadi, S. 2011b, 'Evaluation and comparison of the analytical models to determine tensile strength of self-compacting concrete and conventional concrete', *Structural Engineering World Congress (SEWC)*, Como, Italy, pp.1-11.

Aslani, F. & Nejadi, S. 2011c, 'Evaluation and comparison of experimental results to determine the bond characteristics of steel fiber reinforced self-compacting concrete', *Structural Engineering World Congress (SEWC)*, Como, Italy, pp.1-7.

Aslani, F. & Nejadi, S. 2011d, 'Evaluation and comparison of analytical models to determine the bond characteristics of steel fibre reinforced self-compacting concrete', The *9th Symposium on High Performance Concrete*, Rotorua, New Zealand, pp.1-8.

Aslani, F. & Nejadi, S. 2011e, 'Comparison of shrinkage prediction models for self-compacting and conventional concrete', The *9th Symposium on High Performance Concrete*, Rotorua, New Zealand, pp.1-10.

Aslani, F. & Nejadi, S. 2011f, 'Comparison of creep prediction models for self-compacting and conventional concrete', *The 9th Symposium on High Performance Concrete*, Rotorua, New Zealand, pp.1-10.

Assie, S., Escadeillas, G., & Marchese, G. 2003, 'Durability of Self Compacting Concrete', *RILEM Proceedings PRO 33*, pp.655-662.

ASTM standards. 2000, *Concrete and aggregates*, vol. 04.02.

ASTM C31-11b. 2000, *Standard test methods for sampling and testing fly ash or natural pozzolans for use in portland-cement concrete*, ASTM standards 2000 (Annual book).

ASTM C183-08. 2000, *Standard practice for sampling and the amount of testing of hydraulic cement*, ASTM standards 2000 (Annual book).

ASTM C989-06. 2000, *Standard specification for ground granulated blast-furnace slag for use in concrete and mortars*," ASTM standards 2000 (Annual book).

ASTM C 1018. 2000, '*Standard test methods for flexural toughness and first crack strength of fiber reinforced concrete (using beam with third point loading)*', ASTM, vol. 4.02, pp. 637-644.

ASTM C1077-13. 2000, *Standard practice for agencies testing concrete and concrete aggregates for use in construction and criteria for testing agency evaluation*, ASTM standards 2000 (Annual book).

ATENA. 2012, *program documentation*, Theory.

Aydin, A.C. 2007, 'Self compactability of high volume hybrid fiber reinforced concrete', *Construction and Building Materials,* vol. 21, no. 6, pp. 1149–1154.

Babu, T.S., Rao, M.V.S. & Seshu, D.R. 2008, 'Mechanical properties and stress–strain behavior of self-compacting concrete with and without glass fibres', *Asian Civil Eng (Building and Housing)*, vol. 9, no. 5, pp.457–472.

Balaguru, P.N. & Shah, S.P. 1992, *Fiber reinforced cement composites*, McGraw-Hill Inc, New York.

Banthia, N. & Trottier, J.F. 1995, 'Test Methods for Flexural Toughness Characterization of Fiber Reinforced Concrete: Some Concerns and a Proposition', *ACI Materials Journal*, vol. 92, no. 1, pp. 48-57.

Banthia, N. & Trottier, J.F. 1995, 'Concrete reinforced with deformed steel fibers: Part II. Toughness characterisation', *ACI Materials Journal*, vol. 92, no. 3, pp. 146-154.

Barragán, B.E. 2002, *Failure and toughness of steel fiber reinforced concrete under tension and shear*, PhD Thesis, UPC, Barcelona.

Bažant Z, Huet C & Müller H. 1994, *Comment on recent analysis of concrete creep linearity and applicability of principle of superposition*, Materials and Structures, vol. 27, no. 6, pp. 359-361.

Bazant, Z.P. & Oh, B.H. 1983, 'Crack band theory for fracture of concrete', *Material and Structures,* vol. 16, no. 94, pp. 155-177.

Bhargava, P., Sharma, U.K. & Kaushik, K. 2005, 'Compressive stress-strain behavior of small scale steel fibre reinforced high strength concrete cylinders', *Journal of Advanced Concrete Technology,* vol. 4, no. 1, pp. 109-121.

Bhattacharya, A. 2008, *Effects of aggregate grading and admixtures/fillers on fresh and hardened properties of self-consolidating concrete*, MSc Thesis, West Virginia University.

Bonen, D. & Shah, S.P. 2004, 'The effects of formulation on the properties of self-consolidating concrete', *Concrete Science and Engineering*: A Tribute to Arnon Bentur, Proc. of the Int. RILEM Symp., RILEM Publications, Bagneux, France, pp.43-56.

Bouzoubaa, N. & Lachemi, M. 2001, 'Self-compacting concrete incorporating high volumes of class f fly ash', *Cement and Concrete Research*, vol. 31, no. 3, pp.413-442.

Buratti, N., Mazzotti, C. & Savoia, M. 2010, 'long-term behaviour of fibre-reinforced self-compacting concrete beams', *Design, Production and Placement of Self-Consolidating Concrete*, SCC2010, Montreal, Canada. vol. 1, pp. 439-450

Buratti, N., & Claudio, M. 2009, 'Long term behaviour of self-comapcting fibre-reinforced concrete beams', *Second International Symposium on Design, Performance and Use of Self-Consolidating Concrete*, SCC'2009-China, Beijing, China.

Burgueño, R., & Haq, M. 2007, 'Effect of SCC mixture proportioning on transfer and development length of prestressing strand', *Self-Consolidating Concrete for Precast Prestressed Applications*, SP-247, American Concrete Institute, Fajardo, Puerto Rico, 105-116.

Carino, N.J. & Lew, H.S. 1982, 'Re-examination of the relation between splitting tensile and compressive strength of normal weight concrete', *ACI Journal*, vol. 88, no. 2, pp.214-219.

Carreira, D.J. & Chu, K.H. 1984, 'Stress– strain relationship for plain concrete in compression', *ACI Journal*, vol. 82, no. 6, 1985, pp. 797–804.

Carrasquillo, R., Nilson, A., & Slate, F. 1981, Properties of high strength concrete subject to short-term loads, *ACI Journal,* vol. 78, no. 3, pp. 171-178.

Casanova, P. 1996, *Bétons renforcés de fibres métalliques du materiau μa la structure*, Ph.D. thesis, Ecole nationale dês Ponts et Chaussées (in French).

Castel, A., Vidal, T., Viriyametanont, K. & François, R. 2006, 'Effect of reinforcing bar orientation and location on bond with self-consolidating concrete', *ACI Structural Journal*, vol. 103, no. 4, pp.559-67.

CEB. 1996, *RC elements under cyclic loading*, Thomas Telford, London, 190 pp.

CEB-FIP. 1990, High-strength concrete state of the art report, Thomas Telford, London.

CEB. 1997, *Serviceability models*, Bulletin d'Information No. 235, Comite Euro-International du Beton (CEB), Lausanne, Switzerland. 265 pp.

Cervenka, V., Jendele, L. & Cervenka, J. 2005, *ATENA program documentation, part 1: theory*, Prague.

Chan, Y. W., Chern, J. C., Hong, C. Y. & Lue, J. W. 2004, 'The Analysis of Shrinkage Behavior of SCC and OPC under Various Weather Conditions', *RILEM Proceedings PRO 17*, pp.493-506.

Chanvillard, G. 1999, 'Modeling the pullout of wire-drawn steel fibers', Cement and Concrete Research, vol. 29, no. 7, pp.1027–37.

Chapman, R.A. & Shah, S.P. 1987, 'Early-age bond strength in reinforced concrete', *ACI Materials Journal*, vol. 84, no. 6, pp.501-510.

Chong, K.T. 2004, *Numerical modelling of time-dependent cracking and deformation of reinforced concrete structures*, PhD Thesis, University of New South Wales.

Chopin, D., Francy, O., Lebourgeois, S. & Rougeau, P. 2003, 'Creep and shrinkage of heat-cured self-compacting concrete (SCC)', *3rd International Symposium on Self-Compacting Concrete*, Reykjavik, Iceland, pp. 672-683.

Collins, M.P. & Mitchell, D. 1991, *Prestressed concrete structures*, Prentice-Hall, New Jersey.

Cordoba, B. 2007, *Creep and shrinkage of self-consolidating concrete (SCC)*, MSc Thesis, University of Wyoming.

Cornelissen, H.A.W., Hordijk, D.A. & Reinhardt, H.W. 1985, 'Experiments and theory for the application of fracture mechanics to normal and lightweight concrete', *Proc. Int. Conf. on Fracture Mechanics of Concrete*, F.H.Wittman, ed., Elsevier, Amsterdam.

Corinaldesi, V. & Moriconi, G. 2004, 'Durable fiber reinforced self-compacting concrete', *Cement and Concrete Research,* vol. 34, no. 2, pp. 249–254.

Corinaldesi, V. & Moriconi, G. 2011, 'Characterization of self-compacting concretes prepared with different fibers and mineral additions', *Cement & Concrete Composites,* vol. 33, no. 5, pp. 596–601.

Cunha, V. 2006, *Compression behaviour of steel fibre reinforced self-compacting concrete – age influence and modelling*, Report 06-DEC/E-04, University of Minho.

Cunha, V. 2007, *Pullout behaviour of hooked-end steel fibres in self-compacting concrete*, Report 07-DEC/E06, University of Minho.

D'Ambrosia, M. D., Lange, D. A., & Brinks, A. J. 2005, 'Restrained shrinkage and creep of self-consolidating concrete', *Proc. of the Second North American Conf. on the Des. and Use of Self Consolidating Concr. and the Fourth Int. RILEM Symp. on Self-Consolidating Concr.*, Center for Advanced Cement-Based Materials (ACBM), Chicago, 921-928.

Daoud, A., Lorrain, M. & Laborderie, C. 20'3, "Anchorage and cracking behaviour of self-compacting concrete', In: Wallevik O, Nielsson I, editors. *Proceedings of the 3rd*

international RILEM symposium on self-compacting concrete, Reykjavik: RILEM Publications S.A.R.L., p.692–702.

Davis, R.E., Davis, H.E. & Hamilton, J.S. 1934, 'Plastic flow of concrete under sustained stress', *ASTM Proc. 34*, Part 2, pp. 354-386.

Dehn, F., Holschemacher, K., & Weiße, D. 2000, Self-compacting concrete (SCC) time development of the material properties and the bond behaviour, University of Leipzig, Germany.

Desnerck, P., De Schutter, G. & Taerwe, L. 2010, 'Bond behaviour of reinforcing bars in self-compacting concrete: experimental determination by using beam tests' *Materials and Structures*, vol. 43, no. 1, pp.53-62.

Deutscher Beton-Verein EV, 1996, DBV-Merkblatt. *Bemessungsgrundlagen für Stahlfaserbeton im Tunnelbau*, Eigenverlag.

Dhonde, H.B., Mo, Y.L., Hsu, T.C.T. & Vogel, J. 2007, 'Fresh and hardened properties of self-consolidating fiber-reinforced concrete', *ACI Material Journal*, vol. 104, no. 5, pp.491-500.

Dinakar, P., Babu, K.G. & Santhanam, M. 2008, 'Mechanical properties of high-volume fly ash self-compacting concrete mixtures' *Structural Concrete*, vol. 9, no. 2, pp.109-116.

Ding, Y., Zhang, F., Torgal, F. & Zhang, Y. 2012a, 'Shear behaviour of steel fibre reinforced self-consolidating concrete beams based on the modified compression field theory', *Composite Structures,* vol. 94, no. 8, pp. 2440–2449.

Ding, Y., Azevedo, C., Aguiar, J.B., Jalali, S. 2012b, 'Study on residual behaviour and flexural toughness of fibre cocktail reinforced self-compacting high performance concrete after exposure to high temperature', *Construction and Building Materials,* vol. 26, no. 1, pp. 21–31.

Domone, P.L. 2007a, 'A review of the hardened mechanical properties of self-compacting concrete', *Cement and Concrete Composites*, vol. 29, no. 1, pp.1–12.

Dubey, A. 1999, Fiber reinforced concrete: characterization of flexural toughness & some studies on fiber-matrix bond-slip interaction, PhD Thesis, University of British Columbia.

El-Dieb, A.S. 2009, 'Mechanical, durability and microstructural characteristics of ultra-high-strength self-compacting concrete incorporating steel fibers', Materials and Design, vol. 30, no. 10, pp. 4286–4292.

Erkmen, B., Shield, C.K., & French, C.E. 2007, Time-dependent behavior of fullscale self-consolidating concrete precast prestressed girders', *Self-Consolidating Concrete for Precast Prestressed Applications*, SP-247, American Concrete Institute, Fajardo, Puerto Rico, pp.139-154.

Ezeldin, A.S. & Balaguru, P.N. 1992, 'Normal- and high- strength fiber-reinforced concrete under compression', *ASCE, Journal of Materials in Civil Engineering,* vol. 4, no. 4, pp. 415-429.

Eurocode 2. British Standards Institution, 1992, '*Design of concrete structures – Part 1: General rules and rules for buildings*', – DD ENV 1992-1-1:1992. European Committee for Standardization, Brussels.

Eurocode 2. British Standards Institution, 2004, 'Design of concrete structures – Part 1-1: General rules and rules for buildings', – BS EN 1992-1-1:2004. European Committee for Standardization, Brussels.

European guidelines, (2005). "The European guidelines for self-compacting concrete."

Fantilli, A.P., Vallini, P. & Chiaia, B. 2011, 'Ductility of fiber-reinforced self-consolidating concrete under multi-axial compression,' *Cement & Concrete Composites,* vol. 33, no. 4, pp. 520–527.

Fava, C., Bergol, L., Fornasier, G., Giangrasso, F. & Rocco, C. 2003, 'Fracture behaviour of self-compacting concrete', In: Wallevik O, Nielsson I, editors. *Proceedings of the 3rd international RILEM symposium on self-compacting concrete*, Reykjavik: RILEM Publications S.A.R.L., p.628–636.

Felekoglu, B., Turkel, S. & Baradan, B. 2007, 'Effect of water/cement ratio on the fresh and hardened properties of self-compacting concrete', *Building and Environment*, vol. 42, no. 4, pp.1795-1802.

Ferrara, L., Park, Y.D., & Shah, S.P. 2007, 'A method for mix-design of fiber-reinforced self-compacting concrete', *Cement and Concrete Research,* vol. 37, no. 6, pp. 957–971.

Ferraris, C.F., Brower, L., Ozyildirim, C. & Daezko, J., 2000, 'Workability of self-compacting concrete', *Proceedings, PCI/FHWA/FIB international symposium on high performance concrete*, pp. 398–407.

FHWA and NCBC. 2005, 'Q&A: What is the status on the use of self-consolidating concrete in bridges?', *HPC bridge views, the Federal Highway Administration and the National Concr. Bridge Counc.*, Skokie, Illinois, pp.1-4.

FIB model code. 2010, First complete draft Volume 1, fib Bulletin 55.

Gardner, N.J. 1990, 'Relationship of the punching shear capacity of reinforced concrete slabs with concrete strength', *ACI Structural Journal*, vol. 87, no. 1, pp.66-71.

Gilbert, R.I. 1993, Designing concrete structures for serviceability, The Munro centre for Civil & Environmental Engineering, University of New South Wales, Sydney, Australia, 109 pp.

Gilbert, R.I. 1998, 'Serviceability considerations and requirements for high performance reinforced concrete slabs', *International Conference on HPHSC*, Perth, Australia, pp. 425-435.

Gilbert, R.I. 2002, 'Creep and shrinkage models for high strength concrete- proposal for inclusion in AS3600', *Australian Journal of Structural Engineering*, vol. 4, no. 2, pp. 95-106.

Gilbert, R.I. 2008, 'Control of flexural cracking in reinforced concrete', *ACI Structural Journal*, vol. 105, no. 3, pp. 301–307.

Gilbert, R.I. & Nejadi, S. 2004, *An Experimental Study of Flexural Cracking in Reinforced Concrete Members under Sustained Loads*, UNICIV Report No. R-435, School of Civil and Environmental Engineering, University of New South Wales, Sydney, Australia.

Girgis, A. F., & Tuan, C.Y. 2004, *Bond strength of self-consolidating concrete for prestress concrete applications*, Rep. No. SPR-P1(04) P571, University of Nebraska, Lincoln.

Glanville, W.H. & Thomas, F.G. 1939, 'Studies in reinforced concrete-iv. further investigation on creep or flow of concrete under load', *Building Research Technical Paper,* no. 21, London, 44 pp.

Goel, S., Singh, S.P., & Singh, P. 2012, 'Flexural fatigue strength and failure probability of self-compacting fibre reinforced concrete beams', *Engineering Structures,* vol. 40, pp. 131–140.

Goodier, C.I. 2003, 'Development of self-compacting concrete', *Structures and Building*, vol. 156, no. SB4, pp. 405-414.

Gopalaratnam, V.S., & Shah, S.P. 1985, 'Softening response of plain concrete in direct tension', *ACI Journal Proc,* vol. 82, no. 3, pp. 310-323.

Grünewald, S. 2004, *Performance-based design of self-compacting fibre reinforced concrete*, Ph.D. thesis, TU Delft, Netherlands.

Güneyisi, Gesoğlu, M. & Özbay, E. 2010, 'Strength and drying shrinkage properties of self-compacting concretes incorporating multi-system blended mineral admixtures', *Construction and Building Materials*, vol. 24, no.10, pp.1878-1887.

Gustafsson, P.J. 1985, *Fracture mechanics studies of non-yielding materials like concrete*, REPORT TVBM-1007, Dept. of Civ. Engrg., Lund Inst.of Tech., Sweden.

Gvosdev, A.A. 1966, 'Creep of concrete', *Mekhanica Tverdogo Tela*, Moscow, pp. 137-152.

Gylltoft, K. 1983, *Fracture mechanics models for fatigue in concrete structures,* Thesis Presented to Div.of Struct. Engrg., University of Technology, at Lulea, Sweden, in Partial Fulfillment of the Requirements for the Degree of Doctor of Philosophy.

Hamilton, H. R., & Labonte, T. 2005, *Self-consolidating concrete (SCC) structural investigation*, Rep. No. 455404712, Department of Civil and Coastal Engineering, University of Florida, Gainesville.

Han, N., 1996, Time dependent behaviour of high strength concrete, PhD Thesis, Delft University.

Harajli, M.H., Hout, M. & Jalkh, W. 1995, 'Local bond stress-slip behaviour of reinforcing bars em1bedded in plain and fibre concrete', *ACI Materials Journal*, vol. 92, no. 4, pp.343-53.

Hassan, A.A.A., Hossain, K.M.A. & Lachemi, M. 2010, 'Bond strength of deformed bars in large reinforced concrete members cast with industrial self-consolidating concrete mixture', *Construction and Building Materials*, vol. 24, no. 4, pp520–530.

Hatt, W.K. 1907, 'Notes on the effects of time element in loading reinforced concrete beams', *ASTM Proc. 7*, pp. 421-433.

Hauke, B. 2001, 'Self-compacting concrete for precast concrete products in Germany', In: Ozawa K, Ouchi M, editors. *Proceedings of the 2nd international RILEM symposium on self-compacting concrete*, Tokyo: COMS Engineering Corporation, p.633–642.

Heirman, G., Vandewalle, L., Van Gemerta, D., Boel, V., Audenaert, K., De Schutter, G., Desmetd, B. & Vantomme, J. 2008, 'Time-dependent deformations of limestone powder type self-compacting concrete', *Engineering Structures*, vol.30, no.10, pp. 2945-2956.

Hillerborg, A., Modeer, M., & Petersson, P.E. 1976, 'Analysis of crack formation and crack growth in concrete by means of fracture mechanics and finite element', *Cement and Concrete Research,* vol. 6, no. 6, pp. 773-782.

Holschemacher, K. & Klug, Y. 2005, 'Pull-out behaviour of steel fibres in self-compacting concrete', *First International Symposium on Design, Performance and Use of Self-Consolidating Concrete*, China, pp.523-532.

Horta, A. 2005, *Evaluation of self-consolidating concrete for bridge structures applications,* MSc Thesis, Georgia Institute of Technology.

Hossain, K.M.A. & Lachemi, M. 2008, 'Bond behavior of self-consolidating concrete with mineral and chemical admixtures', *ASCE, Journal of Materials in Civil Engineering*, vol. 20, no. 9, pp.608-16.

Hu, C. & Barcelo, L. 1998, 'Investigation on the shrinkage of self-compacting concrete for building construction', *Proceedings of the 1st Symposium International Conference on Self-Compacting Concrete*, Kochi, Japan, pp.228-242.

Hu, D., & Xie, Y. 2005, 'Testing and prediction of creep behavior of high performance self-compacting concrete-from material to structures', *First International Symposium on Design, Performance and Use of Self-Consolidating Concrete*, China, pp.491-498.

Huang, Z., Engström, B. & Magnusson, J. 1996, Experimental investigation of the bond and anchorage behaviour of deformed bars in high strength concrete, Report 94:4, Chalmers University of Technology.

Hsu, L.S. & Hsu, C.T.T. (1994), "Stress-strain behavior of steel-fibre high-strength concrete under compression", *ACI Structural Journal,* vol. 91, no. 4, pp. 448-457.

Illston, J.M. & Stevens, R.F. 1972, 'Long-term cracking in reinforced concrete beams, *Proceedings, Institutions of Civil Engineers*, Part 2, vol. 53, pp. 445-459.

Issa, M., Alhassan, M., Shabila, H., & Krozel, J. 2005, 'Laboratory performance evaluation of self-consolidating concrete', *Proceeding of the Second North American Conference*

on the Des. and Use of Self Consolidating Concrete and the Fourth Int. RILEM Symposium on Self-Consolidating Concrete, Center for Advanced Cement-Based Materials (ACBM), Chicago, pp.857-862.

JSCE. 2002, Standard specifications for concrete structure.

JSCE Standard SF-4. 1984, *Method of test for flexural strength and flexural toughness of fiber reinforced concrete*, pp. 58-66.

Kim, Y.H. 2008, *Characterization of self-consolidating concrete for the design of precast, pretensioned bridge superstructure elements*, PhD Thesis, Texas A&M University.

Kim, J.-K., Han, S.H., Park, Y.D. & Noh, J.H. 1998, 'Material properties of self-flowing concrete', *ASCE, Journal of Material in Civil Engineering*, vol. 10, no. 4, pp.244-249.

Khaliq, W., & Kodur, V. 2011, 'Thermal and mechanical properties of fiber reinforced high performance self-consolidating concrete at elevated temperatures', *Cement and Concrete Research,* vol. 41, no. 11, pp. 1112-1122.

Khayat, K.H. 1996, 'Effects of antiwashout admixtures on properties of hardened concrete', *ACI Materials Journal*, vol. 93, no. 2, pp. 134-146.

Khayat, K.H. 1998, 'Viscosity enhancing admixtures for cement-based materials: overview', *Cement and Concrete Composites*, vol. 20, no. 2-3, pp. 171-188.

Khayat, K.H. & Long, W.J. 2010, 'Shrinkage of precast, prestressed self-consolidating concrete', *ACI Materials Journal*, vol. 107, no. 3, pp. 231-238.

Khayat, K.H. & Roussel, Y. 2000, 'Testing and performance of fiber-reinforced, self-consolidating concrete', *Materials and Structures*, vol. 33, no. 6, pp. 391-397.

Klug, Y. & Holschemacher, K. 2003, 'Comparison of the hardened properties of self-compacting and normal vibrated concrete', *RILEM Proceedings PRO 33*, pp. 596-605.

Köning, G., Holsechemacher, K., Dehn, F. & Weibe, D. 2001, 'Self-compacting concrete-time development of material properties and bond behaviour', In: Ozawa K, Ouchi M,

editors. *Proceedings of the 2nd international RILEM symposium on self-compacting concrete*, Tokyo: COMS Engineering Corporation, pp.507–516.

Kooiman, A.G. 2000, *Modelling steel fibre reinforced concrete for structural design*, Dissertation, Technische Universiteit Delft; 2000.

Kumar, R., Singh, B. & Bhargava, P. 2011, 'Flexural capacity predictions of self-compacting concrete beams using stress–strain relationship in axial compression', *Magazine of Concrete Research*, vol. 36, no. 1, pp.49-59.

Lachemi, M, Bae, S., Hossain, K.M.A. & Sahmaran, M. 2009, 'Steel–concrete bond strength of lightweight self-consolidating concrete', *Materials and Structures*, vol. 42, no. 7, pp.1015–1023.

Lam, N.P. 2007, *Constitutive modeling and finite element analysis of reinforced concrete structures*, PhD Thesis, University of Hong Kong.

Larson, K. 2006, *Evaluation the time-dependent deformation and bond characteristics of a self-consolidating concretet mix and the implication for pretensioned bridge applications*, PhD Thesis, Kansas state university.

Lee, Y., Kang, S-T. & Kim, J-K. 2010, 'Pullout behavior of inclined steel fiber in an ultra-high strength cementitious matrix', *Construction and Building Materials*, vol. 24, no. 10, pp.2030–2041.

Leemann, A. & Hoffmann, C. 2005, 'Properties of self-compacting and conventional concrete – differences and similarities', *Magazine of Concrete Research*, vol. 57, no. 6, pp.315-319.

Leemann, A., Lura, P. & Loser, R. 2011, 'Shrinkage and creep of SCC - The influence of paste volume and binder composition, *Construction and Building Materials*, vol. 25, no. 5, pp.2283-2289.

Leutbecher, T. 2007, *Rissbildung und Zugtragverhalten von mit Stabstahl und Fasern bewehrtem Ultrahochfesten Beton (UHPC)*, Doktors der Ingebieurwissenschaften genehmigte Dissertation, der Universitat Kassel.

Leutbecher, T. & Fehling, E. 2008, 'Crack formation and tensile behaviour of uhpc reinforced with a combination of rebars and fibres', In: Schmidt, M., Fehling, E., Stürwald, S. (eds.) *Ultra High Performance Concrete (UHPC), Second International Symposium on Ultra High Performance Concrete*. Structural Materials and Engineering Series, vol. 10, pp. 497–504.

Li, V.C., Wu, C., Wang, S., Ogawa, A. & Saito, T. 2002, 'Interface tailoring for strain-hardening polyvinyl alcohol-engineered cementitious composites (PVA-ECC)', *ACI Materials Journal*, vol. 99, no. 5, pp.463–472.

Liao, W.-C., Chao, S.-H., Park, S.-Y., & Naaman, A.E. 2006, 'Self-consolidating high performance fiber reinforced concrete (schpfrc) - preliminary investigation', Report UMCEE 06-02, Department of Civil and Environmental Engineering University of Michigan Ann Arbor, USA, p.68.

Lin, C.S., & Scordelis, A. 1975, 'Non linear analysis of rc shells of general forms', *ASCE, Journal of Structural Engineering,* vol. 101, no. ST3, pp. 523-538.

Lorman, W.R. 1940, 'The theory of concrete creep', *Proceedings ASTM*, vol. 40, pp. 1082-1102.

Loser, R. & Leemann, A. 2009, 'Shrinkage and restrained shrinkage cracking of self-compacting concrete compared to conventionally vibrated concrete', *Materials and Structures*, vol. 42, no. 1, pp.71-82.

Luo, S. & Chao, P. 2009, 'Effect of fly ash on the stress-strain behaviour of self-compacting concrete', *Second International Symposium on Design, Performance and Use of Self-Consolidating Concrete*, Beijing, China, pp.710-716.

Ma, K., Xie, Y., Long, G. & Luo, Y. 2009, 'Drying shrinkage of medium strength SCC', *Second International Symposium on Design, Performance and Use of Self-Consolidating Concrete* SCC'2099, China, pp.657-663.

MacDonanld, K. A., & Lukkarila, M. R. 2002, 'Impact of production and proportioning on microstructure and properties of self-consolidating concrete', *Proc. of the First North American Conf. on the Des. and Use of Self Consolidating Concr.*, Center for Advanced Cement Based Materials (ACBM), Chicago, pp. 9-14.

Mandel, J., Wei, S. & Said, S. 1987, 'Studies of the properties of the fiber–matrix interface in steel fiber reinforced mortar', *ACI Materials Journal*, vol. 84, no. 2, pp.101–109.

Mansur, M.A., Chin, M.S., & Wee, T.H. 1999, 'Stress-strain relationship of high-strength fiber concrete in compression', *ASCE, Journal of Materials in Civil Engineering,* vol. 11, no. 1, pp. 21-29.

Madrio, H. & Chirgwin, G., 2011, 'RTA Study on the use of self-compacting concrete', *Austroads Bridge Conference, 8th*, 2011, Sydney, New South Wales, Australia.

Martin, H. 1982, 'Bond performance of ribbed bars (pullout tests)–influence of concrete composition and consistency', In: Bartos P, editor. *Bond in concrete*, pp.89–99.

Marti, P., Alvarez, M., Kaufmann, W., & Sigrist V. 1998, Tension chord model for structural concrete', *Struct Eng Int*, vol. 4, pp. 287-298.

Mazars, J. 1981, 'Mechanical damage and fracture of concrete structures', *Advanced in Fracture Research, ICFS, Cannes*, vol. 4, pp. 1499-1506.

Mazars, J. & Pijaudier-Cabot, G. 1989, 'Continuum damage theory, application to concrete', *ASCE Engineering Mechanics*, vol. 115, no. 2, pp.345-365.

Mazzotti, C. & Savoia, M. 2009, 'Long-Term Deflection of Reinforced Self-Consolidating Concrete Beams', *ACI Structural Journal*, vol. 6, no. 6, pp 772-781.

Naik, T.R., Kumar, R., Ramme, B.W. & Conpolat, F., 'Development of high-strength, economical self-consolidating concrete', *Construction and Building Materials*, vol. 30, pp. 463-469.

Nagataki, S. & Fujiwara, H., 1995, 'Self-compacting property of highly-flowable concrete', *Proceedings, second CANMET/ACI international symposium on advances in concrete technology*, SP-154, pp. 301- 314.

Nataraja, M.C., Dhang, N., & Gupta, A.P. 1999, 'Stress-strain curves for steel-fiber reinforced concrete under compression', *Cement and Concrete Composites,* vol. 21, no. 5-6, pp. 383-390.

Naito, C. J., Parent, G., & Brunn, G. 2006, 'Performance of bulb-tee girders made with self-consolidating concrete', *PCI Journal*, vol. 51, no. 6, pp.72-85.

Nejadi, S. 2005, Time-dependent cracking and crack control in reinforced concrete structures, PhD Thesis, University of New South Wales.

Nejadi, S. & Aslani, F. 2011, 'Evaluation and comparison of the compressive stress-strain relationships of self-compacting concrete and conventional concrete', *Concrete 2011, Building a Sustainable Future*, Perth, Australia, pp.1-10.

Neves, R.D., & Fernandes de Almeida J.C.O. 2005, 'Compressive behaviour of steel fibre reinforced concrete', *Structural Concrete,* vol. 6, no. 1, pp. 1-8.

Neville, A.M. 1995, *Properties of concrete*, Fourth Edition, Pearson Education Limited, England, 844 pp.

Neville, A. M. 1996, *Properties of concrete*, 4th Edition, John Wiley and Sons, Inc., New York, New York.

Neville, A.M., Dilger, W.H. & Brooks, J.J. 1983, *Creep of plain and structural concrete*, London New York: Construction Press.

Ngo, D. & Scordelis, A.C. 1967, 'Finite element analysis of reinforced concrete beams', *ACI Journal*, vol. 82, no. 2, pp.162-169.

Noghabai, K. 1988, *Effect of tension softening on the performance of concrete computational studies*, PhD Thesis, Dept. of Civil and Mining Eng., Division of Structural Eng., Lülea University of Technology, Sweden.

Okamura, H. 1999. 'Self-compacting high-performance concrete', *ACI Material Journal*, vol. 96, no. 3, pp.346-353.

Okamura, H. & Ozawa, K. 1995, Mix design for self-compacting concrete', *Concrete Libr JSCE*, vol. 25, pp.107–20.

Okamura, H. & Ouchi, M. 2003, 'Self Compacting Concrete', *Journal of Advanced Concrete Technology*, vol. 1, no. 1, pp. 5-15.

Oliva, M.G. & Cramer, S. 2008, *Self-consolidating concrete: creep and shrinkage characteristics*, Report, University of Wisconsin.

Oliveira Júnior, L.A., Santos Borges, V.E., Danin, A.R., Ramos Machado, D.V., Lima Araújo, D., El Debs, M.K., & Rodrigues, P.F., 2010, 'Stress-strain curves for steel fiber-reinforced concrete in compression', *Revista Matéria*, vol. 15, no. 2, pp. 260–266.

Ozawa, K., Maekawa, K., Kunishima, m., & Okamura, H., 1989, 'Development of high performance concrete based on the durability design of structures', *Proceedings of the 2nd East-Asia and Pacific Conference on Structural Engineering and Construction*, vol. 1, pp. 445-450.

Ozawa, K., Sakata, N. & Okamura, H. 1995, 'Evaluation of self-compactability of fresh concrete using the funnel test', *Concrete Libr JSCE*, vol. 25, pp.59–75.

Ozyildrim, C. 2007, 'Bulb T-beams with self-consolidating concrete on route 33 in Virginia', *Transportation Research Record*, 2020, 76-82.

Parra, C.J. 2005, *Experimental study of self-compacted concrete in hardened state*, PhD thesis, Polytechnic University of Valencia.

Parra, C., Valcuende & M., Gómez, F. 2011, "Splitting tensile strength and modulus of elasticity of self-compacting concrete', *Construction and Building Material*, vol. 25, no. 1, pp.201-207.

Persson, B. 2001, 'A comparison between mechanical properties of SCC and the corresponding properties of normal concrete', *Cement and Concrete Research*, vol. 31, no. 2, pp.193–198.

Persson, B. 2005, 'Creep of self-compacting concrete', *in CONCREEP 7, Proc. Int. Conf.*, Nantes: pp. 535–540.

Peter, J.A., Lakshmanan & N., Manoharan, P.D. 2006, 'Investigation on the static behaviour of self-compacting concrete underreamed piles', *ASCE, Journal of Material in Civil Engineering*, vol. 18, no. 3, pp.408–414.

Petersson, P.E. 1981, *Crack growth and development of fracture zone in plain concrete and similar materials*, Rep. No.TVBM-1006, Lund Institute of Technology, Lund, Sweden.

Pineaud, A., Cabrillac, R., Remond, S., Pimienta, P., & Rivillon, P. 2005, 'Mechanical properties of self- compacting concrete - influence of composition parameters', *Proc. of the Second North American Conf. on the Des. and Use of Self Consolidating Concr. and the Fourth Int. RILEM Symp. on Self-Consolidating Concr.*, Center for Advanced Cement-Based Materials (ACBM), Chicago, 863-868.

Pons, G., Proust, E., & Assie, S. 2003, 'Creep and shrinkage of self-compacting concrete: a different behaviour compared with vibrated concrete?" *RILEM Proceedings PRO 33*, pp.645-654.

Poppe, A.M. & De Schutter, G. 2001, 'Creep and shrinkage of self-compacting concrete', *Proceedings of the Sixth International Conference CONCREEP-6*, pp.563–568.

Poppe, A-M. & De Schutter, G. 2005, 'Creep and shrinkage of self-compacting concrete', *First International Symposium on Design, Performance and Use of Self-Consolidating Concrete* SCC2005, China, pp.329-336.

Popovics, S. 1973, 'A numerical approach to the complete stress-strain curve of concrete', *Cement and Concrete Research*, vol. 3, no. 4, pp. 583-599.

Prasad, M.L.V., Kumar, P.R. & Oshima, T. 2009, 'Development of analytical stress-strain model for glass fiber reinforced self-compacting concrete', *International Journal of Mechanics of Solids*, vol. 4, no. 1, pp.25-37.

Raphael, J.M. 1984, 'Tensile strength of concrete', *ACI Journal*, vol. 81, no. 2, pp.158-165.

Reinhardt, H.W. & Rinder, T. 2006, 'Tensile creep of high-strength concrete' *Journal of Advanced Concrete Technology*, vol. 4, no. 2, pp. 277-283.

Ravindrarajah, R.S., Farrokhzadi, F. & Lahoud, A., 2003, 'Properties of flowing concrete and self-compacting concrete with high-performance superplasticiser', *Proceedings of the 3rd International RILEM Symposium*, vol 1, pp. 1048.

RILEM TC 162-TDF. 2002, Test and design methods for steel fibre reinforced concrete, Final recommendations, *Materials and Structures*, vol. 35. pp. 579–582.

Rols, S., Ambroise, J. & Pera, J. 1999, 'Effect of different viscosity agents on the properties of self-leveling concrete', *Cement and Concrete Research*, vol. 29, no. 2, pp.261–266.

Rosenbusch, J. & Teutsch., M. 2003, 'Shear design with method, test and design methods for steel fibre reinforced concrete - background and experiences', Edited by Schnutgen and Vandewalle, *RILEM publication PRO 31*, pp.105-118.

Rots, J.G., Nauta, P., Kusters, G.M.A., & Blaauwendraad, J. 1985, 'Smeared Crack Approach and Fracture Localization in Concrete', *Heron,* vol. 30, no. 1, pp. 1-48.

RTA (Regional Transportation Authority). 2006, *Materials test methods*, vol. 1.

Sahmaran, M., Yurtseven, A., & Yaman, I.O. 2005, 'Workability of hybrid fiber reinforced self-compacting concrete', *Building and Environment,* vol. 40, no. 12, pp. 1672–1677.

Scanlon, A. 1971, *Time dependent deflections of reinforced concrete slabs*, PhD Thesis, University of Alberta, Edmonton.

Schindler, A. K., Barnes, R. W., Roberts, J. B., & Rodriguez, S. 2007, 'Properties of self-consolidating concrete for prestressed members', *ACI Material Journal*, vol. 104, no. 1, pp. 53-61.

Schumacher, P. 2008, *Rotation capacity of self-compacting steel fiber reinforced concrete*, PhD Thesis, Delft University of Technology.

Sengul, C., Akkaya, Y., & Tasdemir, M.A. 2006, 'Fracture behavior of high performance fiber reinforced self-compacting concrete', M.S. Konsta-Gdoutos, (ed.), *Measuring, Monitoring and Modeling Concrete Properties*, pp. 171–177.

Sonebi, M., Bartos, P.J.M., Zhu, W., Gibbs, J. & Tamimi, A., 2000, 'Final report task 4 on the SSC project; project no. E 96-3801', Self-compacting concrete: properties of hardened concrete, University of Paisley, Scotland.

Stang, H. & Shah, S.P. 1986, 'Failure of fiber-reinforced composites by pull-out fracture', *Journal of Materials Science*, vol. 21, no. 3, pp.953–957.

Sujivorakul, C., Waas, A.M. & Guerrero, P. 2000, 'Pull-out of a smooth fiber with an end anchorage', *ASCE Journal of Materials in Civil Engineering*, vol. 126, no. 9, pp.986–993.

Tasnimi, A.A. (2004). 'Mathematical model for complete stress–strain curve prediction of normal, light-weight and high-strength concretes', *Magazine of Concrete Research*, vol. 56, no. 1, pp.23-34.

Topçu, B.I. & Uygunoğlu, T. 2010, 'Effect of aggregate type on properties of hardened self-consolidating lightweight concrete (SCLC)', *Construction and Building Material,* vol. 24, no. 7, pp.1286-1295.

Torrijos, M.C., Barragán, B.E., & Zerbino, R.L. 2008, 'Physical–mechanical properties, and mesostructure of plain and fibre reinforced self-compacting concrete', *Construction and Building Materials,* vol. 22, no. 8, pp. 1780–1788.

Turcry, P., Loukili, A. & Haidar, K. 2002, 'Mechanical properties, plastic shrinkage and free deformations of self-consolidating concrete', *Proceedings of the 1st North American Conference on the Design and Use of Self-Consolidating Concrete*, Center for Advanced Cement-Based Materials, Northwestern University, Evanston, IL, pp.301-306.

Turcry, P., Loukili, A., Haidar, K., Pijaudier-Cabot, G., & Belarbi, A. 2006, 'Cracking tendency of self-compacting concrete subjected to restrained shrinkage: experimental study and modelling', *ASCE, Journal of Materials in Civil Engineering*, vol. 18, no. 1, pp.46-54.

Valcuende, M. & Parra, C. 2009, 'Bond behaviour of reinforcement in self-compacting concretes', *Construction and Building Materials*, vol. 23, no. 1, pp.162–170.

van Zijl G.P.A.G., & Zeranka, S. 2012, 'The impact of rheology on the mechanical performance of steel fiber-reinforced concrete', G.J. Parra-Montesinos, H.W. Reinhardt, and A.E. Naaman (Eds.): *HPFRCC 6*, pp. 59–66.

Vieira, M., & Bettencourt, A. 2003, 'Deformability of hardened SCC', *RILEM Proceedings PRO 33*, pp. 606-618.

Vitek, J.L. 2003, 'Long-term deformations of self-compacting concrete', *3rd International Symposium on Self-Compacting Concrete*, Reykjavik, Iceland.

Walraven, J. 2005, 'Self-compacting concrete: challenge for designer and researcher', Combining the 2nd North American Conference on the Des. and Use of Self-Consolidating Concrete and the 4th Int. RILEM Symposium on Self-Compacting Concrete, Center for Advanced Cement-Based Materials (ACBM), Chicago, pp.431-446.

Woolson, I.H. 1905, 'Some remarkable tests indicating flow of concrete under pressure', Engineering News 54, no. 18.

Wu, H.Q. & Gilbert, R.I. 2009, 'Modelling short-term tension stiffening in reinforced concrete prisms using a continuum-based finite element model', *Engineering Structures*, vol. 31, no. 10, pp. 2380–2391.

Xiao-jie, L., Zhi-wu, Y. & Li-zhong, J. 2008, 'Long term behavior of self-compacting reinforced concrete beams', *Journal of Central South University of Technology,* vol. 15, no. 3, pp.423-428.

Xie, Y., Li, Y. & Long, G. 2005, 'Influence of aggregate on properties of self-consolidating concrete', *RILEM Proceedings PRO 42*, pp.161-171.

Yankelevsky, D.Z. & Reinhardt, H.W. 1987, 'Response of plain concrete to cyclic tension', *ACI Material Journal,* vol. 84, no. 5, pp. 365-373.

Yankelevsky, D.Z., & Renhardt, H.W. 1989, 'Uniaxial behavior of concrete in cyclic tension', *ASCE, Journal of Structural Engineering,* vol. 115, no. 1, pp. 166-182.

Yi, W. 2006, *Post-crack and post-peak behavior of reinforced concrete members by nonlinear finite element analysis*, PhD Thesis, University of Hong Kong.

Yi, S.T., Yang, E.I., & Choi, J.C. 2006, 'Effect of specimen sizes, specimen shapes, and placement directions on compressive strength of concrete', *Nuclear Engineering and Design*, vol. 236, no. 2, pp. 115–127.

Zheng, J., Chao, P. & Luo, S. 2009, 'Experimental study on factors influencing creep of self-compacting concrete', *Second International Symposium on Design, Performance and Use of Self-Consolidating Concrete*, SCC'2009, China, pp.703-709.

Zhu, W., Sonebi, M., Bartos & P.J.M. 2004, 'Bond and interfacial properties of reinforcement in self-compacting concrete', *Materials and Structures*, vol. 37, no. 7, pp.442-48.

APPENDICES

APPENDIX A

FIBRE PULLOUT TEST

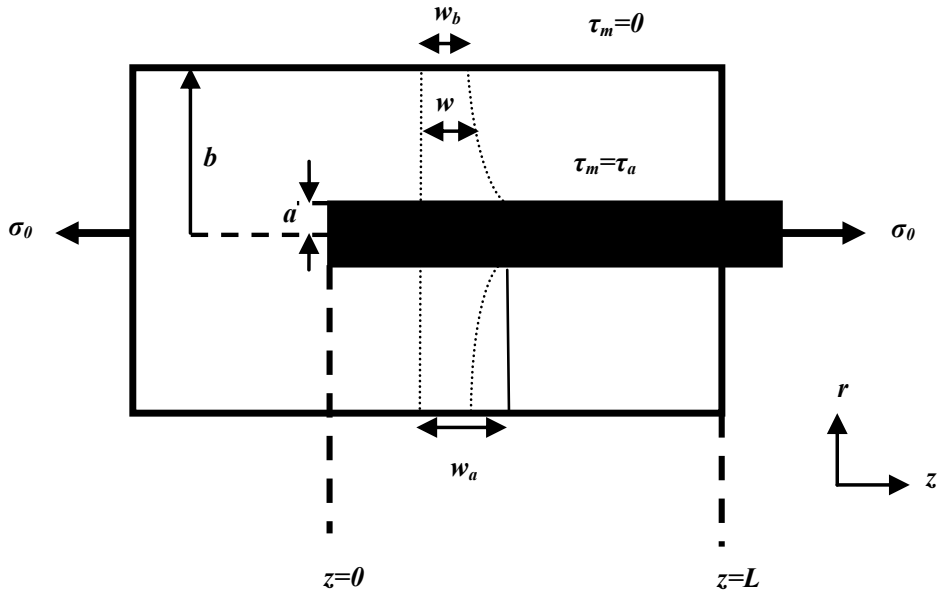

The matrix shear stress, τ_m, at any radial distance, r, can be expressed as:

$$\tau_m = \left[\frac{b-r}{b-a}\right]\frac{a}{r}\tau_a \qquad r \geq a \tag{1-1}$$

If w_m represents the displacement of matrix in the axial direction, the corresponding shear stress in the matrix (ignoring the radial displacements) is given by:

$$\tau_m = \frac{E_m}{2(1+v_m)}\frac{dw_m}{dr} \tag{1-2}$$

The interfacial shear stress:

$$\tau_a = \frac{E_m(w_b - w_a)}{2(1+v_m)a\left[\frac{b}{(b-a)}\log\left(\frac{b}{a}\right)-1\right]} \tag{1-3}$$

w_a and w_b are the axial displacement in the matrix at $r=a$ and $r=b$; The shear stress in the matrix:

$$\tau_m = \frac{E_m \left(w_b - w_a\right)\left(b - r\right)}{2\left(1 + v_m\right) r \left[b \log\left(\frac{b}{a}\right) - \left(b - a\right)\right]} \tag{1-4}$$

$$w_m = w_a + \frac{w_b - w_a}{b \log\left(\frac{b}{a}\right) - \left(b - a\right)} \left[b \log\left(\frac{r}{a}\right) + a - r \right] \tag{1-5}$$

The axial stress in the matrix:

$$\sigma_m = E_m \frac{d\, w_m}{d\, z} \tag{1-6}$$

$$\sigma_m = \frac{E_m}{E_f}\sigma_f + \frac{\sigma_b - \frac{E_m}{E_f}\sigma_f}{\left[b \log\left(\frac{b}{a}\right) - \left(b - a\right)\right]} \left[b \log\left(\frac{r}{a}\right) + a - r \right] \tag{1-7}$$

The axial stress in the matrix $\sigma_{m=b}$,

$$\sigma_b = \frac{\sigma_0}{\eta} - \left[\frac{\gamma + \alpha - \gamma\,\eta\,\alpha}{\gamma\,\eta} \right] \sigma_f \tag{1-8}$$

$$\alpha = \frac{E_m}{E_f} \tag{1-9}$$

$$\gamma = \frac{a^2}{b^2 - a^2} \tag{1-10}$$

$$\eta = \frac{2}{a^2 \left[b \log\left(\frac{b}{a}\right) - \left(b - a\right)\right]} \left\{ b \left[\frac{b^2}{2} \log\left(\frac{b}{a}\right) - \frac{\left(b^2 - a^2\right)}{4} \right] + \frac{a\left(b^2 - a^2\right)}{2} - \frac{\left(b^3 - a^3\right)}{3} \right\} \tag{1-11}$$

Fiber Axial Stress Distribution:

$$\sigma_f = \frac{\sigma_0}{\gamma + \alpha - \gamma\,\eta\,\alpha + \alpha\,\eta} \left[\left(\alpha - \gamma\,\eta\,\alpha + \alpha\,\eta\right) \frac{\sinh\left(\beta\, z\right)}{\sinh\left(\beta\, L\right)} - \gamma \frac{\sinh\left[\beta\left(L - z\right)\right]}{\sinh\left(\beta\, L\right)} + \gamma \right] \tag{1-12}$$

$$\beta = \left[\frac{\theta}{\gamma \eta} (\gamma + \alpha - \gamma \eta \alpha) + \alpha \theta \right]^{1/2} \tag{1-13}$$

Interfacial Shear Stress Distribution:

$$\tau_a = \frac{-a \beta \sigma_0}{2(\gamma + \alpha - \gamma \eta \alpha + \alpha \eta)} \left[(\alpha - \gamma \eta \alpha + \alpha \eta) \frac{\cosh(\beta z)}{\sinh(\beta L)} + \gamma \frac{\cosh[\beta (L - z)]}{\sinh(\beta L)} \right] \tag{1-14}$$

Fiber Displacement:

$$U_b = \frac{\sigma_0}{E_f (\gamma + \alpha - \gamma \eta \alpha + \alpha \eta)} \left[(\alpha - \gamma \eta \alpha + \alpha \eta - \gamma) \frac{\cosh(\beta L)}{\beta \sinh(\beta L)} + \gamma L \right] \tag{1-15}$$

For a two-sided pullout test, fiber displacement is given by:

$$U_b = \frac{2\sigma_0}{E_f (\gamma + \alpha - \gamma \eta \alpha + \alpha \eta)} \left[(\alpha - \gamma \eta \alpha + \alpha \eta - \gamma) \frac{\cosh(\beta L)}{\beta \sinh(\beta L)} + \gamma L \right] \tag{1-16}$$

Debounding criterion and initial debounding stress:

$$\sigma_d = \frac{-2\tau_s (\gamma + \alpha - \gamma \eta \alpha + \alpha \eta)}{a \beta} \left[\frac{(\alpha - \gamma \eta \alpha + \alpha \eta) \cosh(\beta L)}{\sinh(\beta L)} \right]^{-1} \tag{1-17}$$

Figure A.1 Stage 1-Fiber completely bonded along the length of the fibre with the relevant calculations

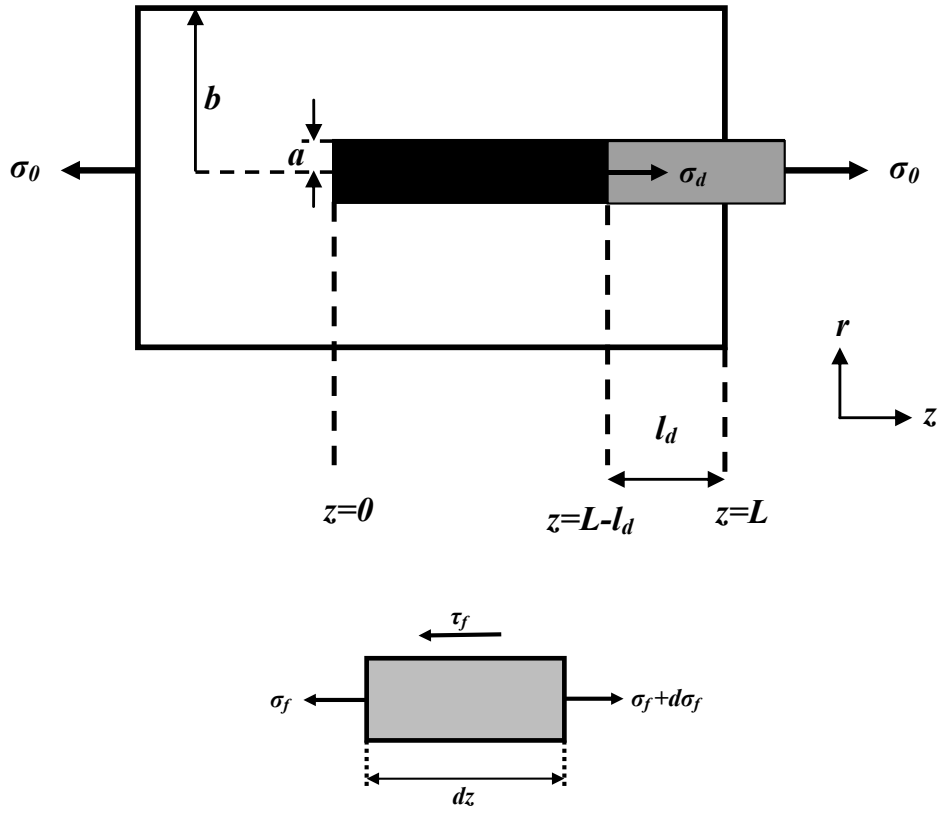

For an unstressed fibre, the relationship between the interfacial contact pressure, σ_c, and the radial fibre-matrix misfit, δ_r:

$$\sigma_c = -\frac{\delta_r}{\frac{a}{E_m}\left[\frac{a^2+b^2}{b^2-a^2}+v_m\right]+\frac{a}{E_f}\left[1-v_f\right]} \tag{2-1}$$

$$\Delta a = a\, v_f \frac{\sigma_f}{E_f} \tag{2-2}$$

$$\sigma_{cp} = -\frac{\left(\delta_r-\Delta a\right)}{\frac{a}{E_m}\left[\frac{a^2+b^2}{b^2-a^2}+v_m\right]+\frac{a}{E_f}\left[1-v_f\right]} \tag{2-3}$$

The resultant contact pressure:

$$\sigma_{cp} = \frac{-\delta_r}{\frac{a}{E_m}\left[\frac{a^2+b^2}{b^2-a^2}+v_m\right]+\frac{a}{E_f}\left[1-v_f\right]} + \frac{v_f\,\sigma_f}{\frac{E_f}{E_m}\left[\frac{a^2+b^2}{b^2-a^2}+v_m\right]+\left[1-v_f\right]} \tag{2-4}$$

$$\sigma_{cp} = \sigma_c + w\sigma_f \tag{2-5}$$

$$w = \frac{v_f}{\frac{E_f}{E_m}\left[\frac{a^2+b^2}{b^2-a^2}+v_m\right]+\left[1-v_f\right]} \tag{2-6}$$

The fibre axial stress:

$$\sigma_f = -\frac{\sigma_c}{w} + \left[\sigma_d + \frac{\sigma_c}{w}\right] e^{\frac{2w\mu(L-l_d)}{a}}\, e^{\frac{-2w\mu z}{a}} \tag{2-7}$$

The distribution of interfacial shear stress:

$$\tau_f = \mu\sigma_{cp} = \mu\left(\sigma_c + w\sigma_f\right) \tag{2-8}$$

The relationship between the fibre pullout stress, σ_0, and the debonded length, l_d:

$$\sigma_0 = -\frac{\sigma_c}{w} + \left[\sigma_d + \frac{\sigma_c}{w}\right] e^{\frac{-2\mu w l_d}{a}} \tag{2-9}$$

The total fibre displacement:

$$U_{pd} = \frac{\sigma_d}{E_f\left(\gamma+\alpha-\gamma\eta\alpha+\alpha\eta\right)}\left[\left(\alpha-\gamma\eta\alpha+\alpha\eta-\gamma\right)\frac{\cosh\left[\beta\left(L-l_d\right)\right]-1}{\beta\sinh\left[\beta\left[L-l_d\right]\right]}+\gamma\left(L-l_d\right)\right] - \frac{\sigma_c\, l_d}{E_f\, w} - \frac{a}{2E_f\,\mu w}\left[\sigma_d+\frac{\sigma_c}{w}\right]\left[e^{\frac{-2\mu W l_d}{a}}-1\right] \tag{2-10}$$

Bond and frictional components of pullout stress:

$$\sigma_0 = \sigma_{0,bond} + \sigma_{0,fric} \tag{2-11}$$

$$\sigma_{0,bond} = \sigma_d \tag{2-12}$$

$$\sigma_{0,fric} = \left[e^{\frac{-2\mu w l_d}{a}} - 1\right]\sigma_d + \frac{\sigma_c}{w}\left[e^{\frac{-2\mu w l_d}{a}} - 1\right] \tag{2-13}$$

Catastrophic debonding:

$$\frac{d\sigma_0}{dl_d} \le 0 \; ; \; \left|\frac{d\sigma_{0,fric}}{dl_d}\right| \le \left|\frac{d\sigma_{0,bond}}{dl_d}\right| \tag{2-14}$$

$$\frac{d\sigma_0}{dl_d} = \left\{-\frac{2\mu w x_1}{a x_2} - \frac{\beta x_4}{x_2} + \frac{\beta x_1 x_3}{x_2^2} - \frac{2\mu\sigma_c}{a}\right\} e^{\frac{-2\mu w l_d}{a}} \tag{2-15}$$

$$x_1 = \frac{-2\tau_s(\gamma + \alpha - \gamma\eta\alpha + \alpha\eta)}{a\beta}\sinh\left[\beta(L - l_d)\right] \tag{2-16}$$

$$x_2 = (\alpha - \gamma\eta\alpha + \alpha\eta)\cosh\left[\beta(L - l_d)\right] + \gamma \tag{2-17}$$

$$x_3 = (\alpha - \gamma\eta\alpha + \alpha\eta)\sinh\left[\beta(L - l_d)\right] \tag{2-18}$$

$$x_4 = \frac{-2\tau_s(\alpha - \gamma\eta\alpha + \alpha\eta)}{a\beta}\cosh\left[\beta(L - l_d)\right] \tag{2-19}$$

Figure A.2 Stage 2- Fibre partially bonded along its embedded length with the relevant calculations

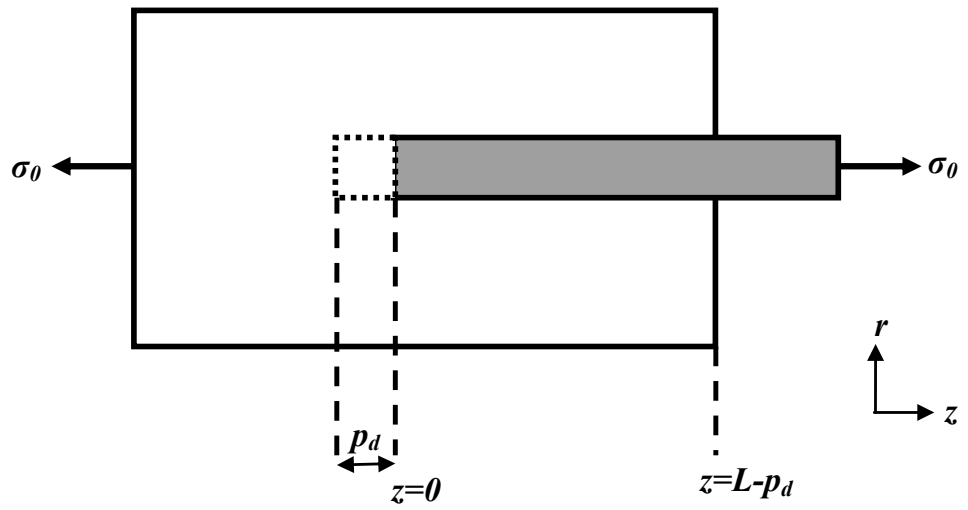

The governing differential equation of stress transfer for the pullout case has been derived by Takaku and Arridge (1973):

$$\frac{d\sigma_f}{dz} + \frac{2\mu}{a} w\sigma_f = \frac{-2\mu}{a}\sigma_c \tag{3-1}$$

Fiber axial stress distribution:

$$\sigma_f = -\frac{\sigma_c}{w}\left[1 - e^{\frac{-2\mu w z}{a}}\right] \quad 0 \le z \le L - p_d \tag{3-2}$$

Interfacial frictional shear stress distribution:

$$\tau_f = \mu\sigma_{cp} = \mu\left(\sigma_c + w\sigma_f\right) \tag{3-3}$$

$$\tau_f = \mu\sigma_c e^{\frac{-2w\mu z}{a}} \quad 0 \le z \le L - p_d \tag{3-4}$$

Fiber pullout stress:

$$\sigma_0 = \frac{-\sigma_c}{w}\left[1 - e^{\frac{-2w\mu\left(L-p_d\right)}{a}}\right] \tag{3-5}$$

The initial frictional pullout stress:

$$\sigma_0 = \frac{-\sigma_c}{w}\left[1 - e^{\frac{-2w\mu L}{a}}\right] \tag{3-6}$$

Fiber displacement:

$$U_{pd} = p_d - \frac{\sigma_c}{E_f w}\left[(L - p_d) + \frac{a}{2\mu w}\left\{e^{\frac{-2\mu w(L-p_d)}{a}} - 1\right\} + p_d\left\{1 - e^{\frac{-2\mu w(L-p_d)}{a}}\right\}\right] \tag{3-7}$$

The resultant contact stress:

$$\sigma_{cp} = \sigma_c + w\sigma_f \tag{3-8}$$

The interfacial contact stress:

$$\sigma_c = -w\sigma_{0,asymptotic} \tag{3-9}$$

The work of fibre pullout, μ is the interfacial coefficient of friction:

$$W_p = -\frac{\pi a^2 \sigma_c}{w}\left\{p_{d2} - p_{d1} - \frac{a}{2w\mu}e^{\frac{-2w\mu L}{a}}\left[e^{\frac{-2w\mu p_{d2}}{a}} - e^{\frac{-2w\mu p_{d1}}{a}}\right]\right\} \tag{3-10}$$

The adhesional bond strength:

$$\frac{d\sigma_d}{dL} = \frac{-2\tau_s(\gamma + \alpha - \gamma\eta\alpha + \alpha\eta)}{a\beta}\left\{\frac{[(\alpha - \gamma\eta\alpha + \alpha\eta)\cosh(\beta L) + \gamma]\beta\cosh(\beta L)}{[(\alpha - \gamma\eta\alpha + \alpha\eta)\cosh(\beta L) + \gamma]^2} - \frac{\beta(\alpha - \gamma\eta\alpha + \alpha\eta)\sinh^2(\beta L)}{[(\alpha - \gamma\eta\alpha + \alpha\eta)\cosh(\beta L) + \gamma]^2}\right\} \tag{3-11}$$

$$\left(\frac{d\sigma_d}{dL}\right)_{L=0} = -\frac{2\tau_s}{d} \tag{3-12}$$

$$\tau_s = -\frac{a}{2}\left(\frac{d\sigma_d}{dL}\right)_{L=0} \tag{3-13}$$

Figure A.3 Stage 3- Fibre completely debonded over its embedded length and pulling out with the relevant calculations

APPENDIX B

FRESH PROPERTY TESTS OF SCC

In this study slump flow, T_{50cm} time, J-ring flow, V-funnel flow time, and L-box blocking ratio tests were performed. In order to reduce the effect of loss of workability on the variability of test results, the fresh properties of the mixes were determined within 30 min after mixing.

The order of testing was as follows: 1. Slump flow test and measurement of T_{50cm} time; 2. J-ring flow test, measurement of difference in height of concrete inside and outside the J-ring and measurement of T_{50cm} time; 3. V-funnel flow tests at 10 s T10s and 5 min T5min; and 4. L-box test.

Figure B.1 Slump flow test

Figure B.2 Slump flow test measurement

Figure B.3 J-ring test-1

Figure B.4 J-ring test-2

Figure B.5 J-ring test measurement-1

Figure B.6 J-ring test measurement-2

Figure B.7 J-ring test measurement-3

Figure B.8 L-Box test-1

Figure B.9 L-Box test-2

Figure B.10 L-Box test-3

Figure B.11 L-Box test-4

Figure B.12 L-Box test measurement-1

Figure B.13 L-Box test measurement-2

Figure B.14 V-Funnel test-1

Figure B.16 V-Funnel test-2

APPENDIX C

FLEXURAL TOUGHNESS TEST METHODS AND CALCULATIONS

C.1. ASTM C 1018 standard test method

The ASTM C 1018 (2000) standard method is based on determining the amount of energy required first to deflect and crack an FRC beam loaded at its third points, and then to further deflect the beam out to selected multiples of the first-crack deflection (Figure C.1). Toughness indexes I_5, I_{10}, I_{20}, I_{30}, etc., are then calculated by taking the ratios of the energy absorbed to a certain multiple of first-crack deflection and the energy consumed up to the occurrence of first crack. Expressed in general terms:

I_N = Energy absorbed up to a certain multiple of first - crack deflection/Energy absorbed up to the first crack

The subscript N in these indexes is based on the elasto-plastic analogy such that, for a perfectly elasto-plastic material, the index I_N would have a value equal to N. Here, the given FRC is compared with a conceptual material that behaves in an ideally elasto-plastic manner. Implicitly, the scheme also assumes that plain concrete is ideally brittle and, hence, the various toughness indexes in its case assume a constant value of 1. The strength remaining in the material is characterized by the residual strength factors (R) derived from the toughness indexes (Figure C.1). Expressed in general terms $R_{M,N}$, the residual strength factor between Indexes I_M and I_N ($N > M$) is expressed as $R_{M,N} = C\,[I_N - I_M]$

where constant $C = 100/(N - M)$ chosen such that for an ideally elasto-plastic material the residual strength factors assume a value equal to the stress at which the elastic-to-plastic transition takes place. Plain concrete, with its ideally brittle response, therefore, has residual strength factors equal to zero. Both toughness indexes and the residual strength factors provide information on the shape of the load-deflection plot and are presumably

independent of the specimen size and other testing variables. Notice that an accurate assessment of the energy at first crack is of critical importance, since its use is made later in the determination of all performance parameters. Equally important is an exact determination of the beam deflections both before and after the first crack.

C.2. JSCE standard SF-4 method

In this technique, the area under the load-versus-deflection plot up to a load point deflection of span/150 is obtained. From this measure of flexural toughness, a flexural toughness factor (*FT*) is calculated as shown in Figure C.2. Note that the *FT* has the units of stress such that its value indicates, in a way, the post-matrix cracking residual strength of the material when loaded to an arbitrary deflection of span/150. Clearly, the flexural toughness factor is dependent on specimen geometry and other testing variables. The chosen deflection of span/150 for its calculation is purely arbitrary and not based on serviceability considerations.

Flexural toughness factor, *FT*, stress concept is calculated from the Eq. (1).

$$FT = k\frac{L}{bh^2}\frac{D_f}{\delta_{150}} \tag{1}$$

where k = 1.0, since it is a four point bending test with equal distance amongst the point loads, b and h are the width and the height of the beam cross section, D_f is the energy dissipated up to the deflection $\delta_{150} = L/150$, where L is the beam span length.

C.3. Banthia and Trottier's method

In Banthia and Trottier's (1995) method identification of first crack is not required (Figure C.3). This method procedure is as follows: 1. Obtain the load-deflection curve with accurate deflection measurements device. 2. Locate the peak load and divide the curve into two regions: the pre-peak region (before the occurrence of the peak load) and the post-peak region (after the peak load). Note the value of the load at the peak and measure the area under the curve up to the peak load. This measure of energy is termed as pre-peak energy and denoted as E_{pre}. 3. Locate points on the curve in the post-peak region with specimen deflections equal to various fractions of the span L/m_1, L/m_2, etc. The suggested fractions are between $L/3000$ and $L/150$. Measure the areas under the curve up to these deflections, denoted as $E_{total,m}$ (measured at a deflection of L/m). 4. Subtract the pre-peak energy E_{pre} from the various values of $E_{total,m}$ to obtain the post-peak energy values to a deflection of L/m, $E_{post,m}$. 5. Calculate the post-crack strength (PCS_m) in the postpeak region at the various deflections. The PCS_m at a deflection of L/m, is defined as Eq. (2):

$$PCS_m = \frac{\left(E_{post,m}\right)L}{\left((L/m)-\delta_{peak}\right)bh^2} \tag{2}$$

C.4. ACI 544 method

To characterize toughness enhancement provided by fiber reinforcement mechanisms, ACI 544 proposed the concept of toughness index, $I_{(ACI)Old}$, which is the ratio between the energy dissipated by the FRC up to a deflection of 1.9 mm, and the energy consumed up to crack initiation, δ_{cr}, see Figure C.4 (Gopalaratnam et al., 1991). This approach has,

however, two deficiencies: the necessity of evaluating δ_{cr} with high accuracy, which is too difficult to assure, and the inexistence of a justification for the deflection limit value of 1.9 mm, under the framework of the limit state analysis required by design model codes. Attempting to overcome this drawback, ACI recommended the replacement of $I_{(ACI)Old}$ by the I_t index, see Fig.A.4. However, to evaluate I_t, the tests with the FRC and its corresponding plain concrete specimens should be carried out up to the total dissipation of the energy, which is difficult or even impossible to attain using flexural test set-ups. To evaluate the total energy dissipated in the fracture process of FRC materials, it should be carried out direct tensile tests in very high stiff, servo-controlled equipments (Barragán, 2002; Noghabai, 1998). However, this is a very time consuming test, since the energy is only totally dissipated at very large crack opening displacement (Noghabai, 1998). Furthermore, behind a certain deflection/crack-opening level, the energy dissipated has no interest from the design point of view, which declines the design utility of the I_t index.

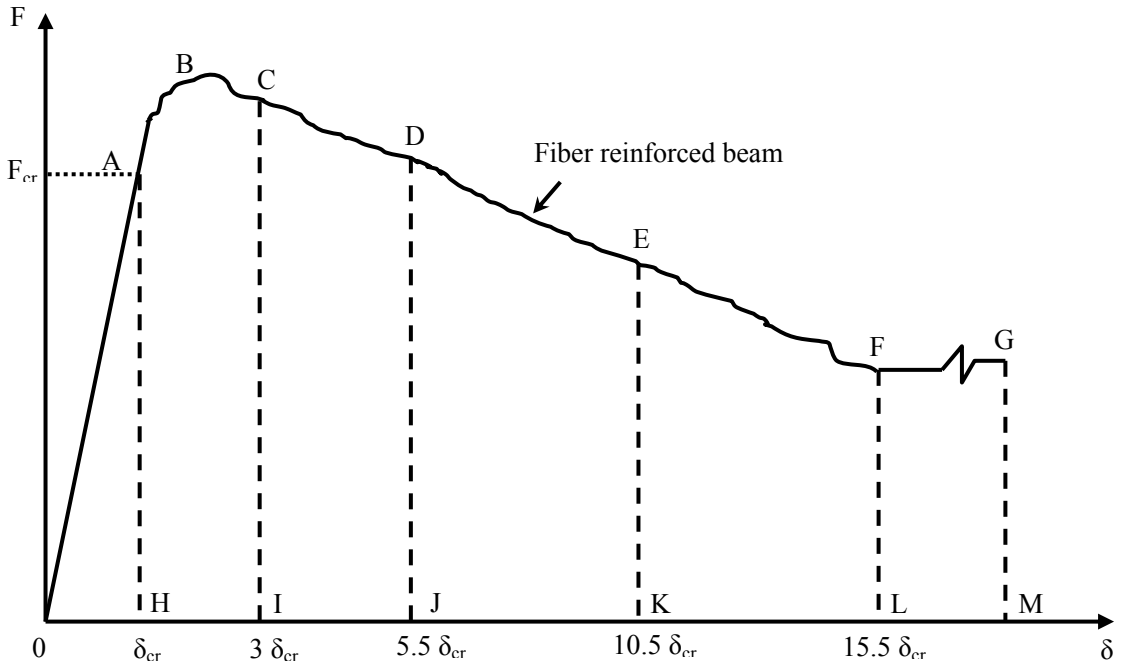

$$I_5 = \frac{\text{AREA}_{\text{OABCIO}}}{\text{AREA}_{\text{OAHO}}}$$

$$I_{10} = \frac{\text{AREA}_{\text{OABDJO}}}{\text{AREA}_{\text{OAHO}}} \qquad R_{5,10} = 20\,(I_{10} - I_5)$$

$$I_{20} = \frac{\text{AREA}_{\text{OABEKO}}}{\text{AREA}_{\text{OAHO}}} \qquad R_{10,20} = 10\,(I_{20} - I_{10})$$

$$I_{30} = \frac{\text{AREA}_{\text{OABFLO}}}{\text{AREA}_{\text{OAHO}}} \qquad R_{20,30} = 10\,(I_{30} - I_{20})$$

Figure C.1 Toughness indexes proposed by ASTM C 1018 (2000)

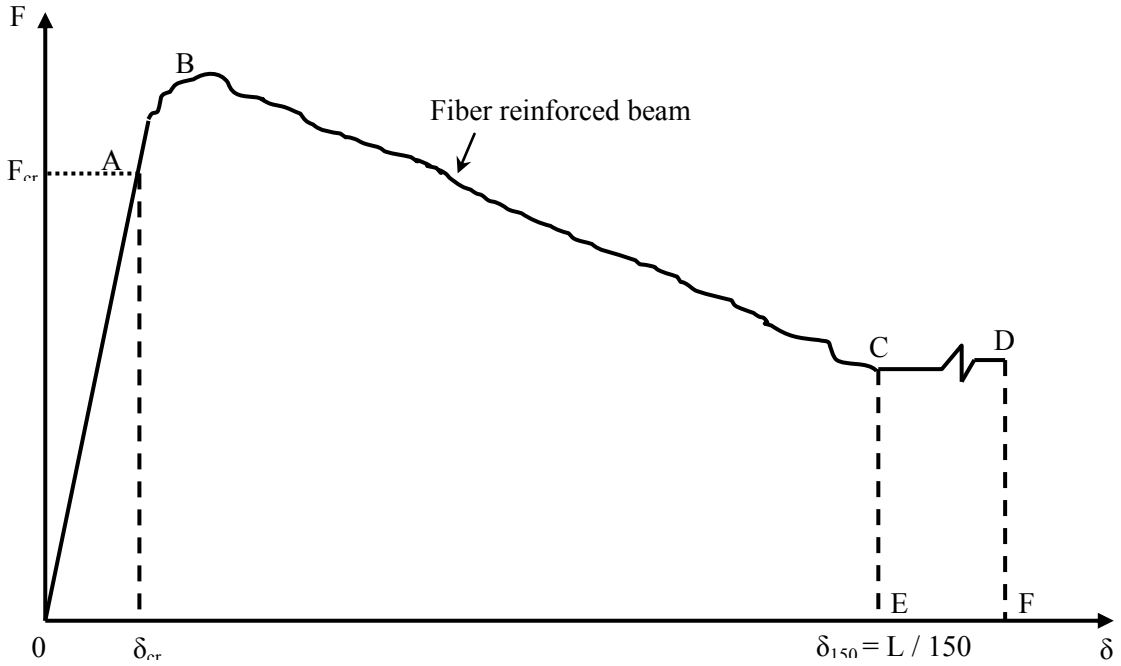

$$D_f = \text{AREA}_{\text{OABCEO}}$$

Figure C.2 JSCE (1984) flexural toughness factor

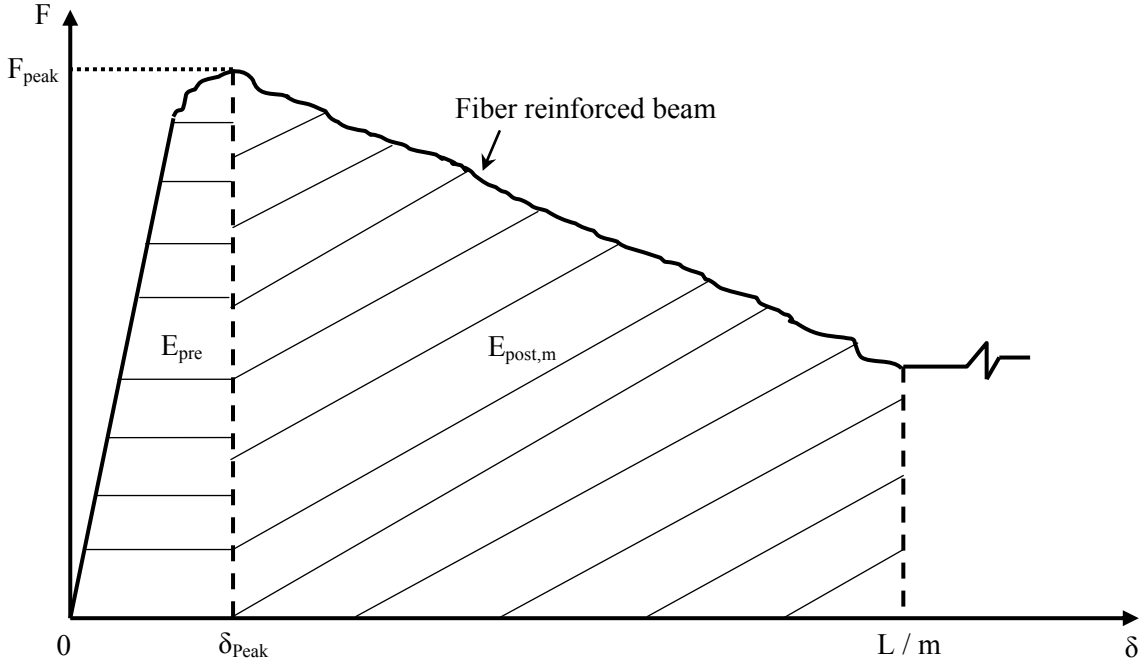

Figure C.3 Banthia and Trottier (1995) flexural toughness factor

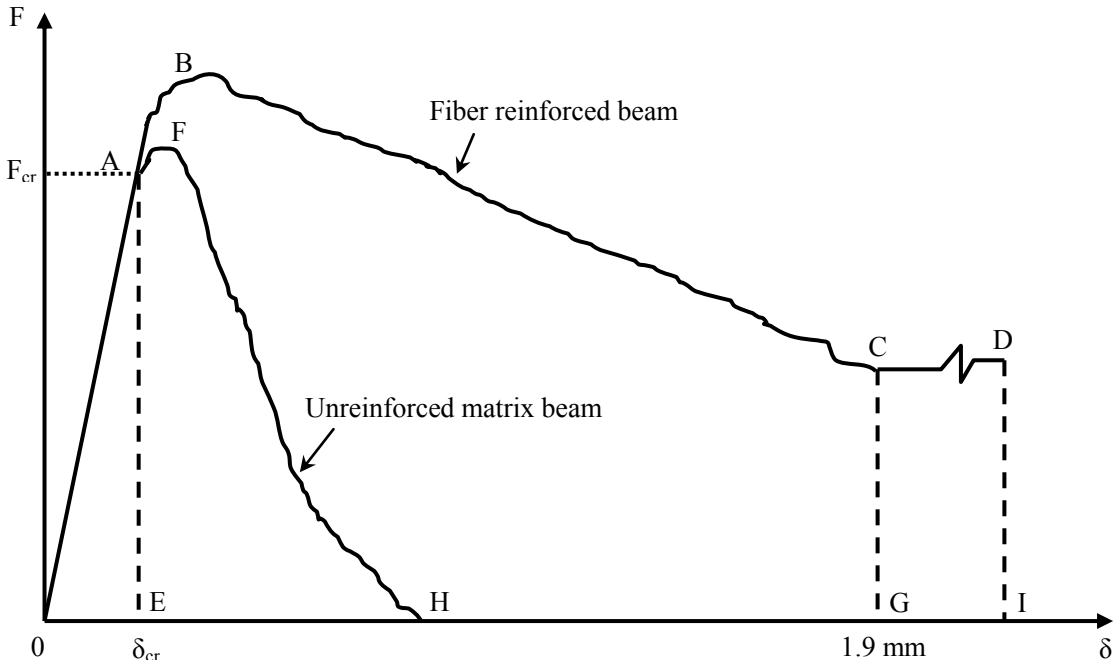

$$I_{(ACI)Old} = \frac{\text{AREA}_{\text{OABCGO}}}{\text{AREA}_{\text{OAEO}}} \qquad I_t = \frac{\text{AREA}_{\text{OABDIO}}}{\text{AREA}_{\text{OAFHO}}}$$

Figure C.4 Toughness indexes proposed by ACI 544 (1988)

APPENDIX D

RAW DATA AND GRAPHS OF SHORT-TERM TESTS

Table D.1 Concrete surface strain at steel level for slab N-SCC-a

N-SCC-a								
	SURFACE STRAIN (Microstrain)							
P(kN)	1	2	3	4	5	6	7	8
0	0	0	0	0	0	0	0	0
5	81.40	60.02	101.53	152.37	182.28	83.84	99.09	113.81
8	120.41	103.14	158.06	246.16	301.03	143.53	161.04	212.99
11	221.34	177.06	233.37	343.54	424.48	194.22	234.64	315.96
14	453.48	351.90	401.84	566.97	673.28	299.12	404.01	552.23
17	687.65	588.82	613.43	740.85	855.71	500.50	588.41	736.11
20	846.35	824.45	816.58	809.06	1067.99	700.78	709.89	808.24
23	1004.38	1073.03	1017.97	895.56	1292.73	912.08	881.55	899.71
26	1185.94	1325.07	1218.48	1040.59	1492.25	1126.31	1058.06	1053.07
29	2018.80	2262.92	2061.94	1692.40	2357.70	1923.49	1746.21	1742.35

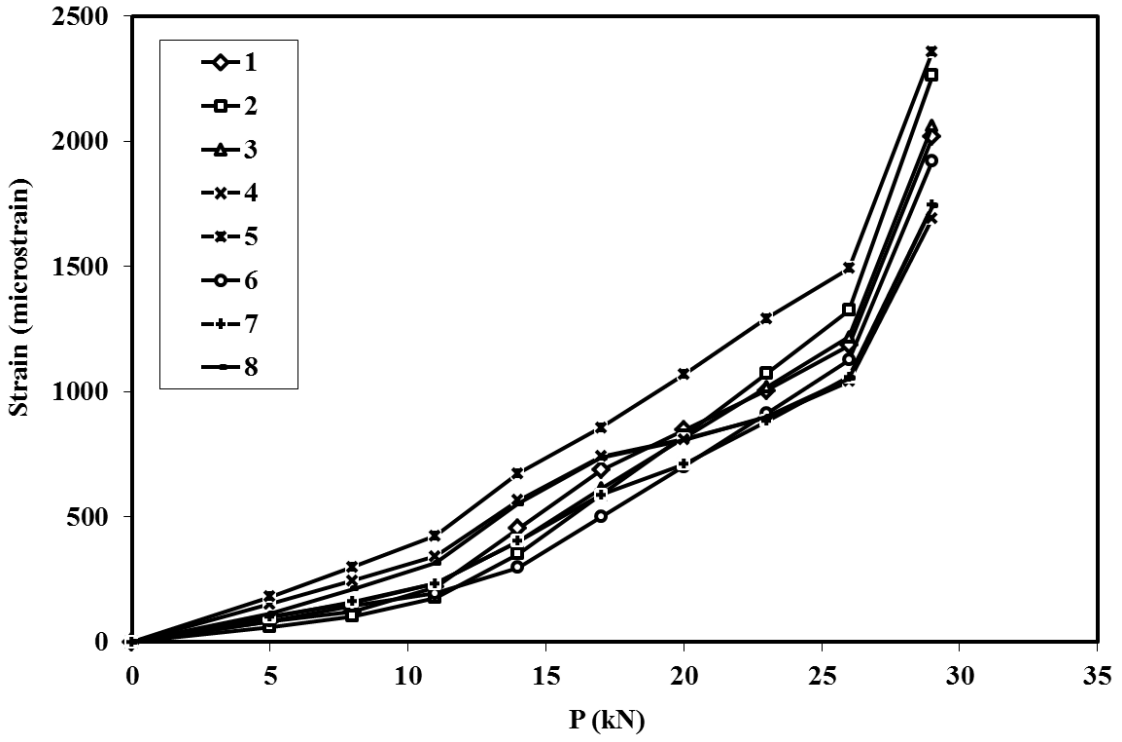

Figure D.1 Concrete surface strain at steel level for slab N-SCC-a

Table D.2 Concrete surface strain at steel level for slab N-SCC-b

N-SCC-b								
	SURFACE STRAIN (Microstrain)							
P(kN)	1	2	3	4	5	6	7	8
0	0	0	0	0	0	0	0	0
5	70.56	96.58	86.70	148.70	209.52	96.37	113.89	102.37
8	115.40	146.14	151.67	256.51	346.01	164.98	185.10	196.16
11	231.41	231.11	238.24	368.44	487.91	223.24	269.70	293.54
14	498.24	432.07	431.89	625.25	773.88	302.45	464.37	516.97
17	767.40	704.39	675.09	825.12	983.57	493.07	676.34	690.85
20	949.82	975.23	908.60	903.52	1227.58	682.66	815.96	759.06
23	1131.46	1260.96	1140.08	1002.95	1485.89	882.67	1013.28	845.56
26	1340.14	1550.65	1370.55	1169.64	1715.23	1085.46	1216.16	990.59
29	2297.46	2628.65	2340.05	1918.85	2710.00	1840.05	2007.14	1642.40

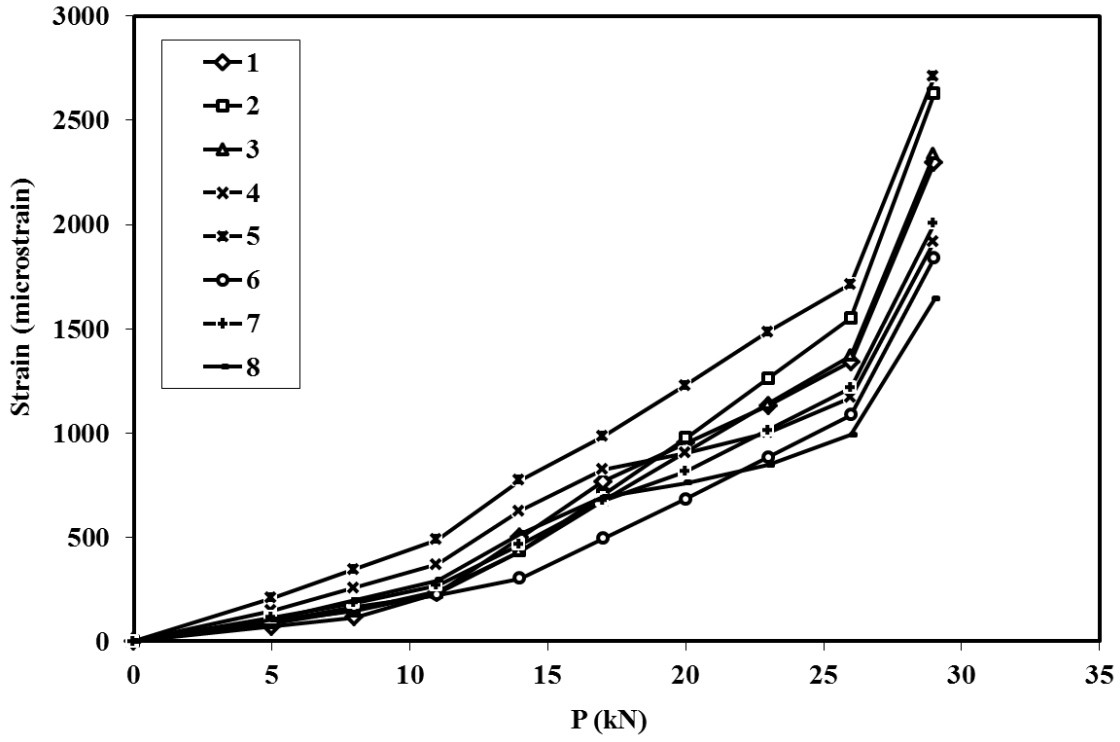

Figure D.2 Concrete surface strain at steel level for slab N-SCC-b

Table D.3 Concrete surface strain at steel level for slab D-SCC-a

D-SCC-a								
	SURFACE STRAIN (Microstrain)							
P(kN)	1	2	3	4	5	6	7	8
0	0	0	0	0	0	0	0	0
5	73.26	57.62	91.38	141.43	164.05	75.45	89.18	65.14
8	108.37	96.43	142.25	225.85	270.93	129.18	144.94	123.38
11	199.20	162.96	210.04	313.48	382.03	174.80	211.17	192.56
14	408.13	320.31	361.66	514.57	605.95	265.86	363.61	351.77
17	618.88	533.54	552.09	671.07	770.14	442.84	529.57	525.11
20	761.72	745.61	734.93	732.45	961.19	618.85	638.90	639.29
23	903.94	969.33	916.17	810.31	1163.45	804.54	793.39	800.66
26	1067.34	1196.16	1096.63	940.83	1343.03	992.81	952.25	966.57
29	1816.92	2040.23	1855.75	1527.46	2121.93	1693.39	1571.59	1613.44

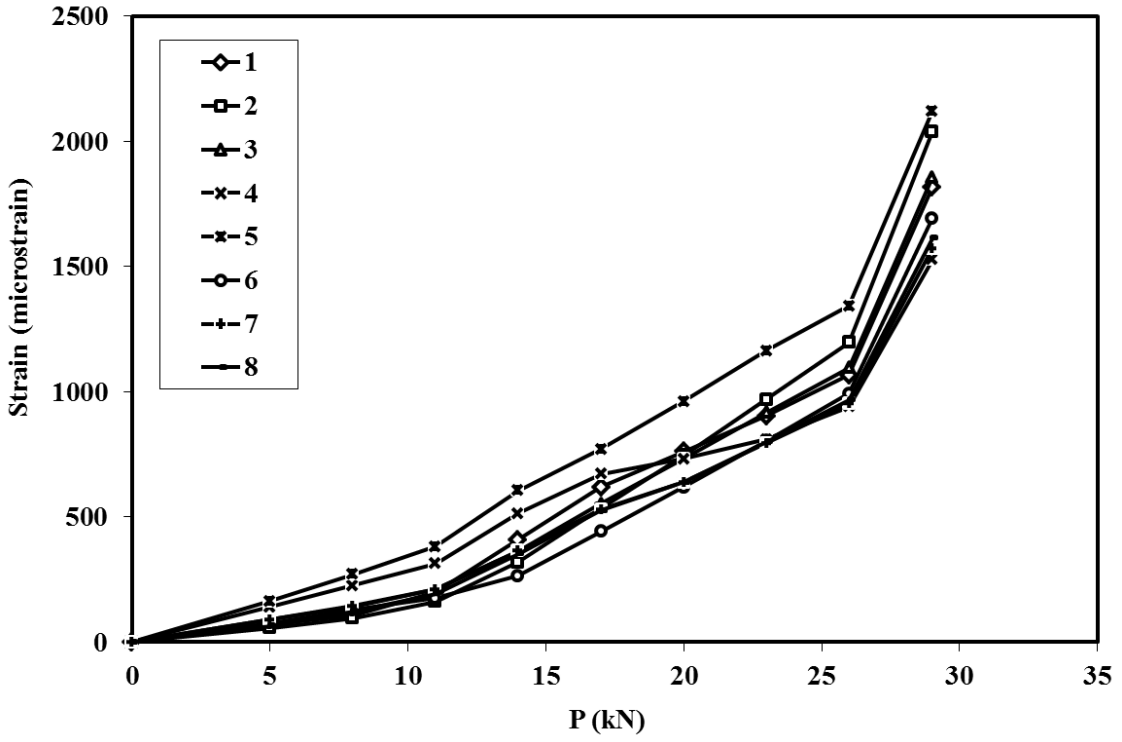

Figure D.3 Concrete surface strain at steel level for slab D-SCC-a

Table D.4 Concrete surface strain at steel level for slab D-SCC-b

D-SCC-b								
P(kN)	SURFACE STRAIN (Microstrain)							
	1	2	3	4	5	6	7	8
0	0	0	0	0	0	0	0	0
5	33.07	88.85	75.36	136.81	192.76	88.66	104.78	120.43
8	74.33	134.45	135.14	235.99	318.33	151.78	170.30	204.85
11	181.06	212.62	214.78	338.96	448.88	205.38	248.12	292.48
14	426.54	397.51	392.93	575.23	711.97	302.11	427.22	493.57
17	674.17	648.04	616.68	759.11	904.89	492.51	622.23	650.07
20	841.99	897.21	831.51	831.24	1129.37	681.88	750.69	711.45
23	1009.10	1160.08	1044.47	922.71	1367.02	881.66	932.21	789.31
26	1201.09	1426.60	1256.51	1076.07	1578.01	1084.22	1118.87	919.83
29	2081.83	2418.36	2148.45	1765.35	2493.20	1837.95	1846.57	1506.46

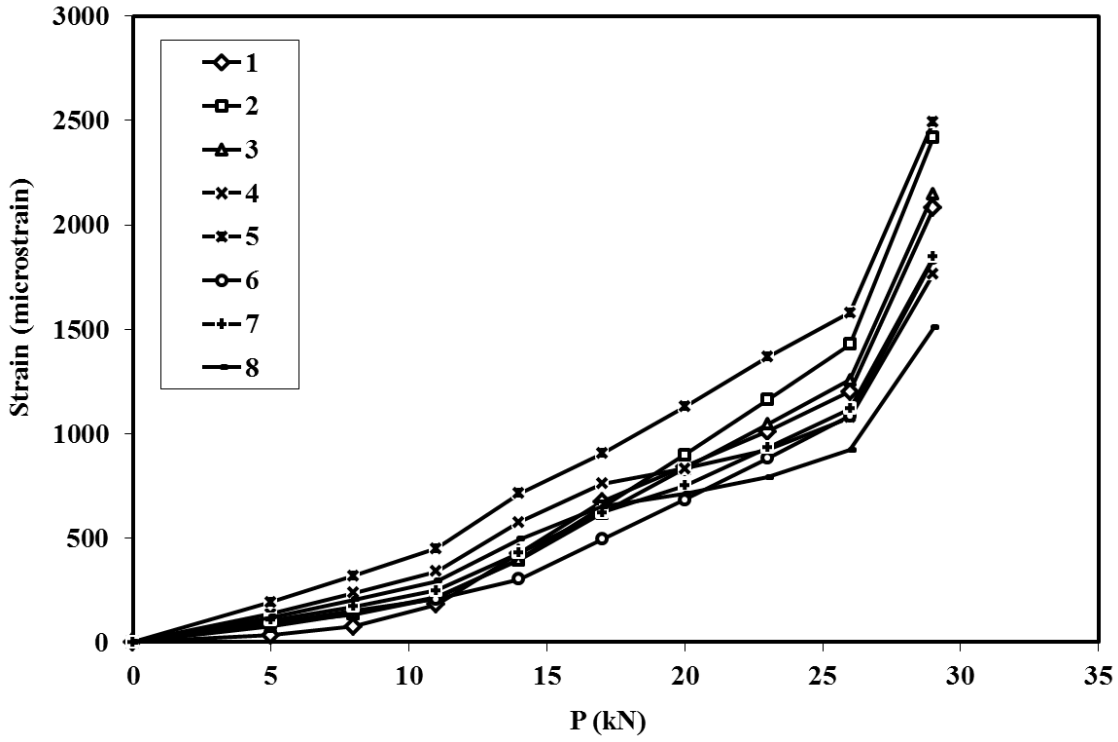

Figure D.4 Concrete surface strain at steel level for slab D-SCC-b

Table D.5 Concrete surface strain at steel level for slab S-SCC-a

S-SCC-a								
	SURFACE STRAIN (Microstrain)							
P(kN)	1	2	3	4	5	6	7	8
0	0	0	0	0	0	0	0	0
5	59.61	78.98	70.44	121.61	151.34	78.81	72.14	118.50
8	96.28	119.51	123.57	209.77	262.97	134.92	130.38	222.53
11	191.16	189.00	194.37	301.31	379.01	182.57	199.56	330.54
14	409.37	353.35	352.73	511.33	612.88	318.01	358.77	578.37
17	629.49	576.05	551.62	674.78	784.37	518.45	532.11	771.24
20	778.67	797.55	742.59	738.90	983.91	717.79	646.29	846.89
23	927.22	1031.21	931.89	820.21	1195.16	928.09	807.66	942.84
26	1097.88	1268.12	1120.37	956.53	1382.72	1141.31	973.57	1103.71
29	1880.78	2149.71	1913.23	1569.24	2196.24	1934.74	1620.44	1826.69

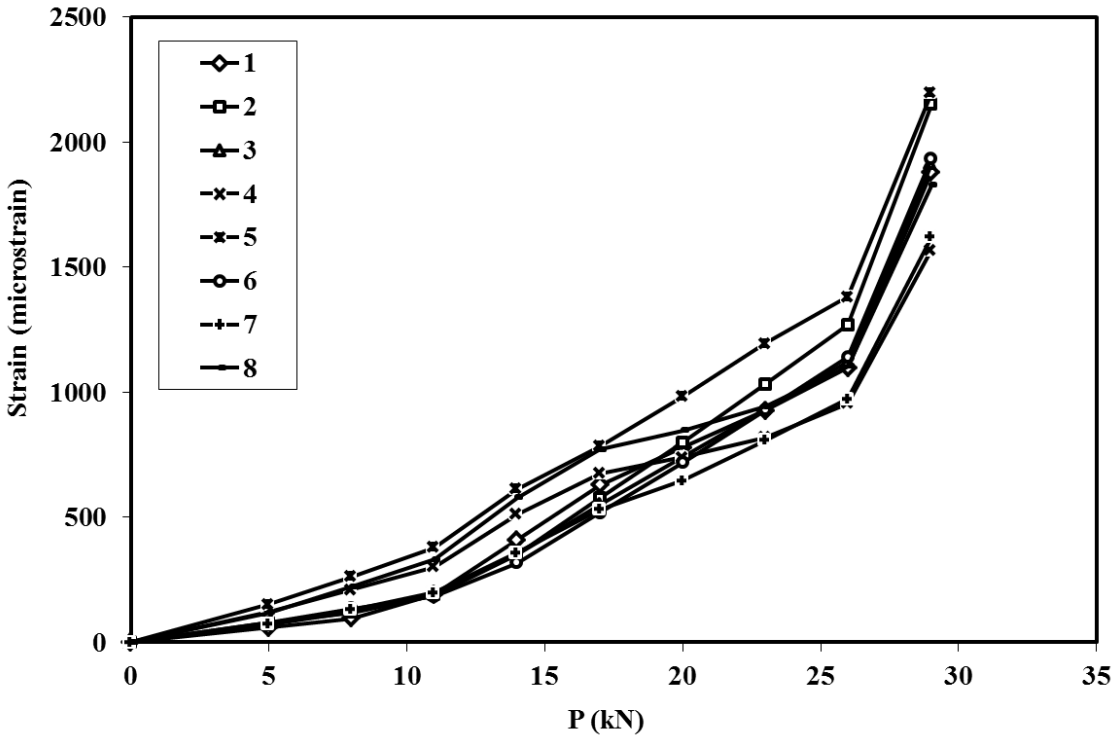

Figure D.5 Concrete surface strain at steel level for slab S-SCC-a

Table D.6 Concrete surface strain at steel level for slab S-SCC-b

S-SCC-b								
P(kN)	SURFACE STRAIN (Microstrain)							
	1	2	3	4	5	6	7	8
0	0	0	0	0	0	0	0	0
5	90.28	76.90	112.62	143.50	184.82	92.99	109.90	103.96
8	133.55	124.73	175.32	247.53	316.54	159.21	178.62	184.62
11	245.51	206.72	258.86	355.54	453.47	215.43	260.26	268.36
14	503.00	400.65	445.72	603.37	729.44	356.58	448.12	460.51
17	762.74	663.44	680.41	796.24	931.79	590.46	652.66	610.05
20	938.77	924.80	905.75	871.89	1167.25	823.07	787.40	668.71
23	1114.06	1200.52	1129.12	967.84	1416.53	1068.47	977.81	743.11
26	1315.43	1480.08	1351.53	1128.71	1637.84	1317.27	1173.59	867.83
29	2239.25	2520.35	2287.10	1851.69	2597.79	2243.11	1936.89	1428.39

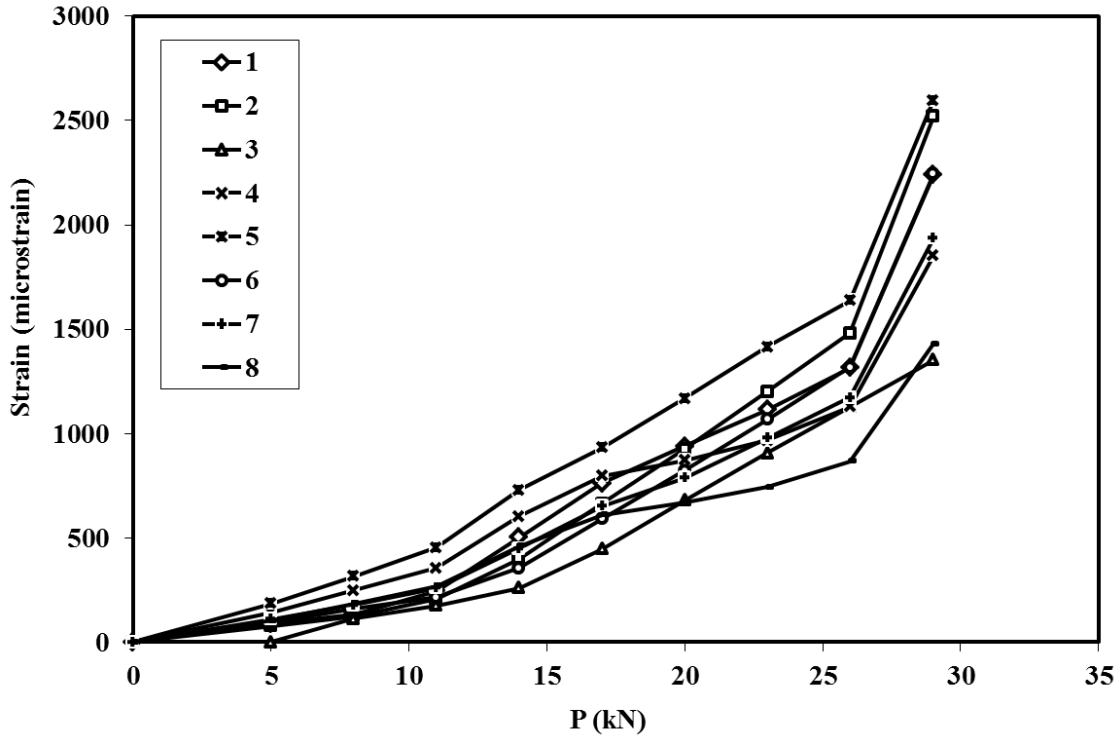

Figure D.6 Concrete surface strain at steel level for slab S-SCC-b

Table D.7 Concrete surface strain at steel level for slab DS-SCC-a

DS-SCC-a								
	SURFACE STRAIN (Microstrain)							
P(kN)	1	2	3	4	5	6	7	8
0	0	0	0	0	0	0	0	0
5	55.70	72.26	87.32	93.96	156.76	72.10	100.10	60.10
8	89.25	109.34	135.93	174.62	258.89	123.44	153.38	111.44
11	176.05	172.91	200.70	258.36	365.06	167.03	216.68	155.03
14	375.69	323.28	345.58	450.51	579.02	355.61	362.34	450.83
17	577.08	527.03	527.55	600.05	735.91	579.73	520.93	618.15
20	713.56	729.67	702.26	658.71	918.47	802.64	625.39	833.51
23	849.47	943.45	875.45	733.11	1111.75	1037.79	773.02	1081.98
26	1005.60	1160.20	1047.89	857.83	1283.34	1276.22	924.82	1071.34
29	1721.87	1966.75	1773.27	1418.39	2027.62	2163.43	1516.63	1813.91

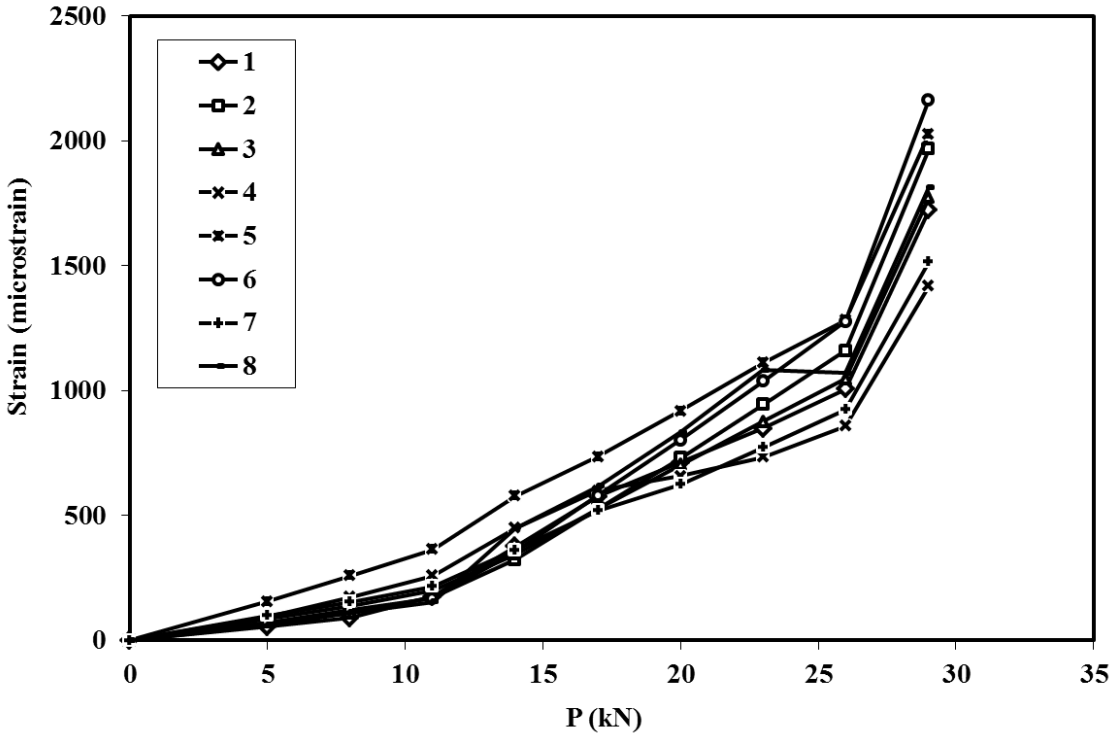

Figure D.7 Concrete surface strain at steel level for slab DS-SCC-a

Table D.8 Concrete surface strain at steel level for slab DS-SCC-b

DS-SCC-b								
P(kN)	SURFACE STRAIN (Microstrain)							
	1	2	3	4	5	6	7	8
0	0	0	0	0	0	0	0	0
5	81.40	70.52	101.53	129.37	166.50	83.84	99.09	107.84
8	120.41	113.64	158.06	223.16	285.25	143.53	161.04	167.53
11	221.34	187.56	233.37	320.54	408.70	194.22	234.64	218.22
14	453.48	362.40	401.84	543.97	657.50	300.80	404.01	425.40
17	687.65	599.32	613.43	717.85	839.93	497.44	588.41	560.75
20	846.35	834.95	816.58	786.06	1052.21	693.01	709.89	734.95
23	1004.38	1083.53	1017.97	872.56	1276.95	899.33	881.55	935.94
26	1185.94	1335.57	1218.48	1017.59	1476.47	1108.52	1058.06	927.33
29	2018.80	2273.42	2061.94	1669.40	2341.92	1886.94	1746.21	1342.66

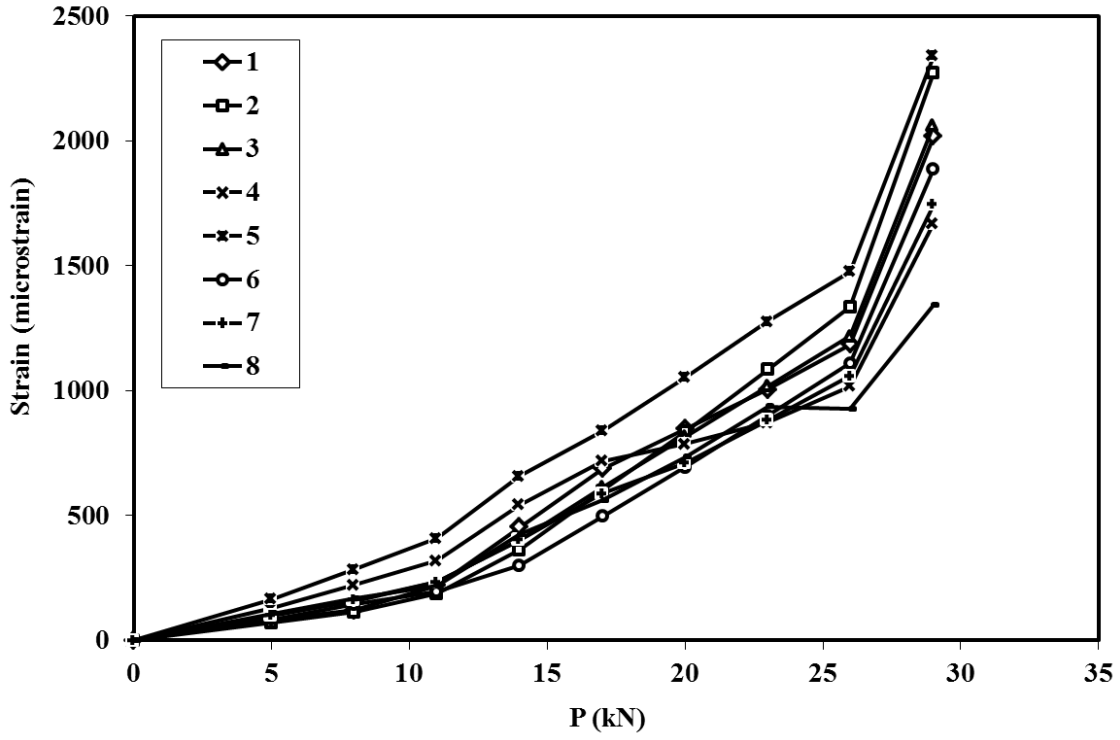

Figure D.8 Concrete surface strain at steel level for slab DS-SCC-b

Table D.9 Steel strain for slab N-SCC-a

N-SCC-a								
P(kN)	STEEL STRAIN (Microstrain)							
	1	2	3	4	5	6	7	8
0	0	0	0	0	0	0	0	0
5	68.06	85.79	65.36	87.13	89.50	79.37	60.82	76.19
7	98.85	128.51	102.26	129.85	120.38	113.59	91.85	109.31
8.8	119.32	150.58	117.14	160.61	154.39	139.27	112.95	135.68
10.5	137.74	177.51	141.48	189.16	173.87	164.96	130.33	156.30
12.3	169.68	213.58	164.02	215.29	210.88	196.09	155.99	186.74
14	186.21	234.74	185.19	237.88	237.55	214.37	174.93	205.25
15.8	222.13	272.94	215.70	276.62	272.94	250.10	206.10	241.81
17.5	258.04	302.89	245.01	310.96	312.73	276.49	245.35	271.56
20	320.56	364.28	305.39	375.87	365.40	339.68	312.36	333.08
22	370.16	413.30	351.06	426.33	420.72	390.99	369.37	379.86
25	470.88	492.84	438.21	514.81	515.67	483.41	471.13	467.26
27	528.98	547.95	492.18	571.37	559.39	540.66	528.40	516.95
29	577.04	599.34	550.86	622.71	602.91	591.07	590.15	567.77
31	645.16	658.83	609.20	691.28	682.49	660.24	666.95	627.07

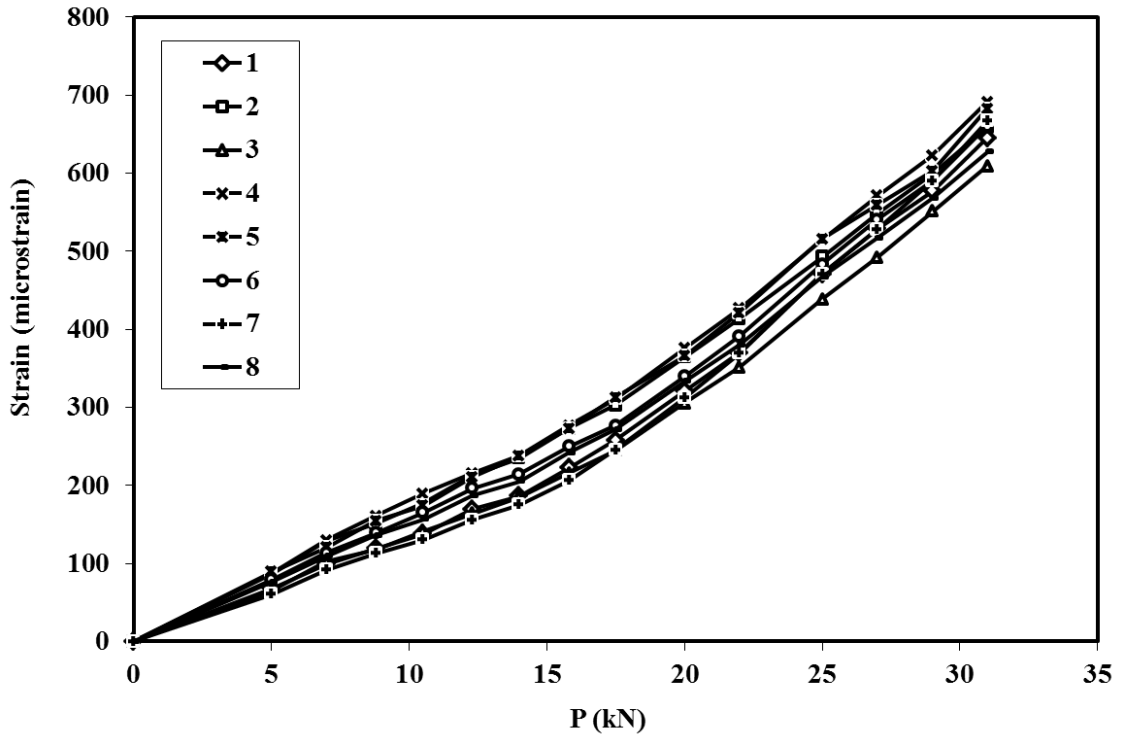

Figure D.9 Steel strain for slab N-SCC-a

Table D.10 Steel strain for slab N-SCC-b

N-SCC-b								
P(kN)	STEEL STRAIN (Microstrain)							
	1	2	3	4	5	6	7	8
0	0	0	0	0	0	0	0	0
5	32.47	67.39	53.91	44.84	18.97	42.32		38.22
7	47.96	90.71	68.14	60.23	28.20	50.67		51.25
8.8	68.62	121.60	99.77	83.63	46.14	82.14		71.87
10.5	82.55	152.39	112.43	92.77	58.50	97.41		88.93
12.3	121.01	204.43	153.00	142.05	75.20	135.50		129.13
14	156.39	261.02	199.04	200.97	110.26	176.31		174.99
15.8	207.53	326.62	258.44	261.96	131.79	233.15		234.09
17.5	250.82	386.66	310.37	337.29	166.93	309.60		295.44
20	316.74	482.87	405.62	441.31	223.45	441.50		415.88
22	372.95	556.16	473.92	525.10	248.59	523.72		488.16
25	456.85	666.16	580.78	641.58	301.50	653.18		609.88
27	503.68	737.36	642.66	716.16	338.45	733.47		680.44
29	516.77	805.40	717.85	785.59	366.26	808.92		756.73
31	544.77	880.16	792.84	873.21	401.00	892.81		825.36

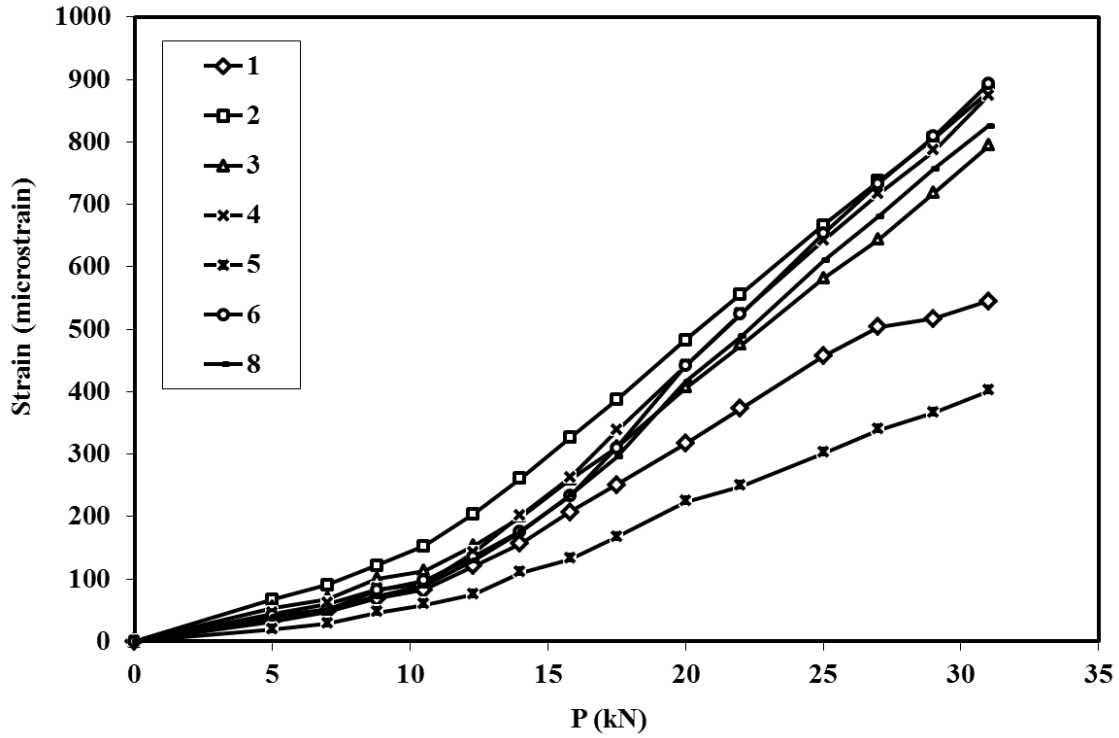

Figure D.10 Steel strain for slab N-SCC-b

Table D.11 Steel strain for slab D-SCC-a

D-SCC-a								
P(kN)	STEEL STRAIN (Microstrain)							
	1	2	3	4	5	6	7	8
0	0	0	0	0	0	0	0	0
5	54.00	83.87	48.79	82.56	83.29	41.38	52.89	31.74
7	83.16	120.69	75.52	121.74	130.73	67.97	79.86	52.96
8.8	100.79	151.43	94.48	144.71	156.19	81.36	98.46	65.21
10.5	122.72	178.62	113.67	171.87	191.05	91.64	120.20	78.49
12.3	137.18	203.78	126.75	197.13	230.25	109.25	136.06	88.97
14	163.75	235.99	151.16	220.26	256.11	126.75	160.84	107.62
15.8	199.53	274.91	180.49	253.35	290.87	147.17	191.28	125.04
17.5	242.31	317.04	209.38	296.62	338.97	183.22	230.66	152.95
20	310.84	378.21	266.90	355.18	403.03	232.98	299.95	195.36
22	372.84	433.87	329.30	416.00	459.90	282.34	364.41	236.65
25	474.32	446.91	430.13	515.55	563.06	374.06	468.13	315.39
27	550.16	593.01	498.10	584.76	630.74	439.36	540.36	383.26
29	621.83	655.23	573.10	657.49	710.02	512.54	617.62	448.26
31	692.12	731.65	655.14	721.98	774.79	575.34	687.39	516.80

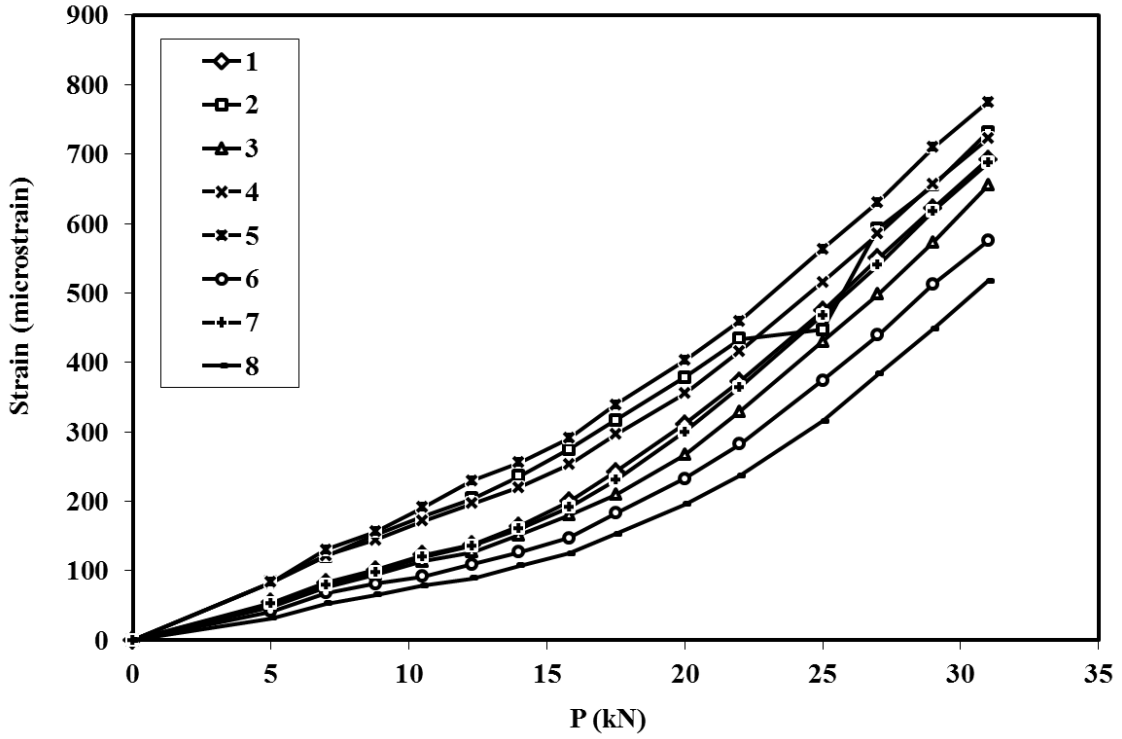

Table D.11 Steel strain for slab D-SCC-a

Table D.12 Steel strain for slab D-SCC-b

D-SCC-b								
P(kN)	STEEL STRAIN (Microstrain)							
	1	2	3	4	5	6	7	8
0	0	0	0	0	0	0	0	0
5	52.00	55.35	47.33	51.55	53.40	41.72	42.84	28.38
7	56.64	63.21	59.32	68.57	59.57	54.33	51.07	36.06
8.8	78.83	87.26	72.27	81.02	84.55	72.65	64.67	48.94
10.5	107.51	107.49	97.34	104.85	110.88	85.98	79.19	59.50
12.3	142.07	142.41	121.25	135.87	139.00	122.70	106.89	78.91
14	188.46	185.50	155.78	184.23	186.18	163.95	137.78	103.16
15.8	250.92	231.75	202.59	244.54	252.86	222.86	186.91	128.68
17.5	323.04	304.27	262.10	314.92	323.23	294.14	263.90	181.23
20	450.37	415.73	364.62	429.67	431.80	401.36	367.23	260.22
22	549.01	509.29	451.10	511.91	523.77	486.37	442.94	335.56
25	728.24	654.65	623.51	647.56	649.68	619.10	565.96	465.21
27	822.29	742.83	710.05	734.67	734.48	694.37	653.50	543.13
29	906.27	821.64	789.65	810.52	808.68	778.78	729.16	624.32
31	993.82	910.35	890.90	887.85	900.62	864.98	826.21	712.84

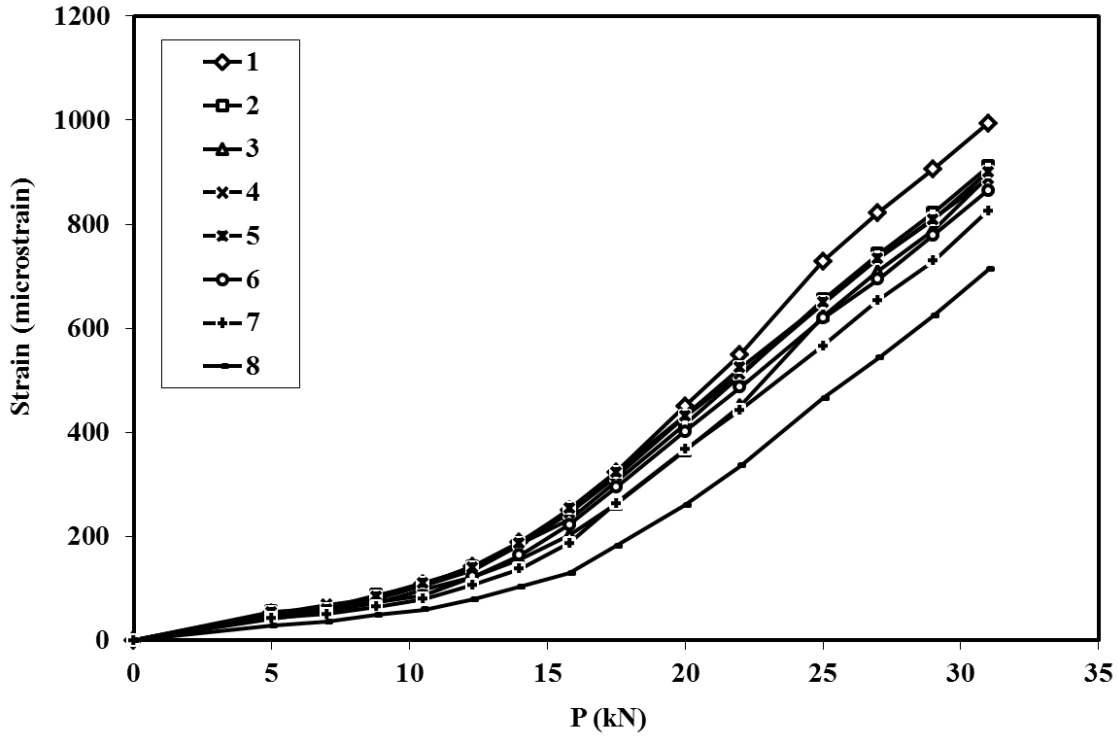

Figure D.12 Steel strain for slab D-SCC-b

Table D.13 Steel strain for slab S-SCC-a

S-SCC-a								
P(kN)	STEEL STRAIN (Microstrain)							
	1	2	3	4	5	6	7	8
0	0	0	0	0	0	0	0	0
5	49.41	48.42	62.25	62.38	41.62	45.94	57.04	48.30
7	73.53	65.09	88.10	84.99	56.03	63.39	74.06	64.78
8.8	84.00	76.30	102.86	100.15	71.12	77.45	91.53	81.30
10.5	105.45	90.65	123.57	119.84	90.15	94.82	108.36	97.73
12.3	123.29	105.78	143.06	137.69	103.42	107.64	127.21	110.76
14	137.43	129.24	161.17	146.21	111.29	124.38	145.58	125.67
15.8	160.79	135.15	182.10	165.86	131.11	140.06	165.69	146.97
17.5	265.09	235.57	297.21	285.96	249.99	267.64	323.12	309.92
20	328.05	331.82	360.51	354.16	316.05	340.60	402.73	377.34
22	387.74	392.33	422.73	414.62	386.64	401.62	467.23	433.28
25	466.36	467.63	496.99	493.08	462.13	470.69	535.94	491.56
27	499.43	498.41	536.22	524.99	497.28	504.23	566.75	517.52
29	565.81	556.55	592.99	590.37	570.22	567.81	627.93	579.17
31	647.23	633.36	684.77	687.69	668.57	659.89	723.06	669.89

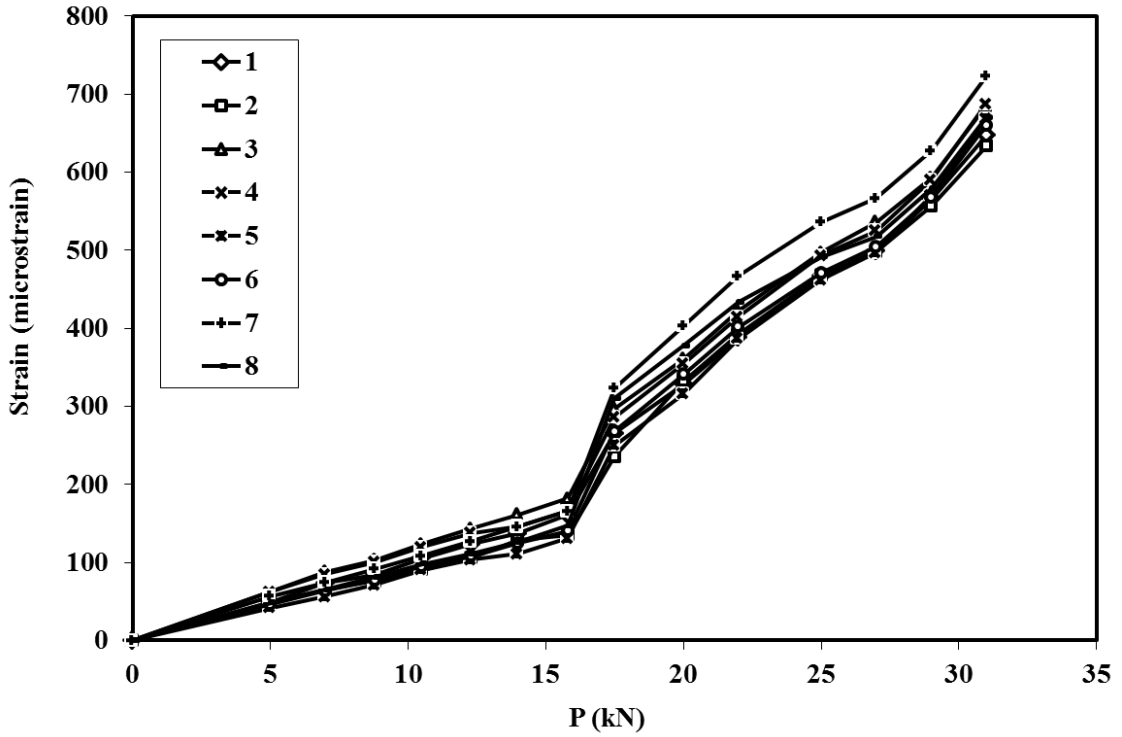

Figure D.13 Steel strain for slab S-SCC-a

Table D.14 Steel strain for slab S-SCC-b

S-SCC-b								
P(kN)	STEEL STRAIN (Microstrain)							
	1	2	3	4	5	6	7	8
0	0	0	0	0	0	0	0	0
5		42.59	40.29	43.22	18.83	38.44	31.34	33.73
7		61.98	60.41	64.08	35.62	56.22	43.23	46.27
8.8		99.96	102.03	100.72	75.57	91.51	73.74	71.30
10.5		136.58	142.21	145.61	123.52	137.01	118.16	100.45
12.3		178.41	189.02	189.17	173.77	176.35	170.97	150.87
14		218.08	233.31	236.72	228.13	225.25	223.06	203.99
15.8		288.52	281.68	286.30	272.95	277.53	265.75	246.58
17.5		343.77	335.67	335.15	322.66	329.74	314.99	298.63
20		476.20	470.17	453.44	447.63	458.60	436.30	415.21
22		557.80	550.64	527.57	521.23	535.88	505.06	484.41
25		661.28	653.17	617.94	623.21	632.10	594.35	574.91
27		732.64	724.99	685.19	694.39	702.82	659.58	638.71
29		807.31	801.22	753.41	762.47	774.92	727.50	704.31
31		874.43	868.52	812.24	832.16	837.43	787.42	763.08

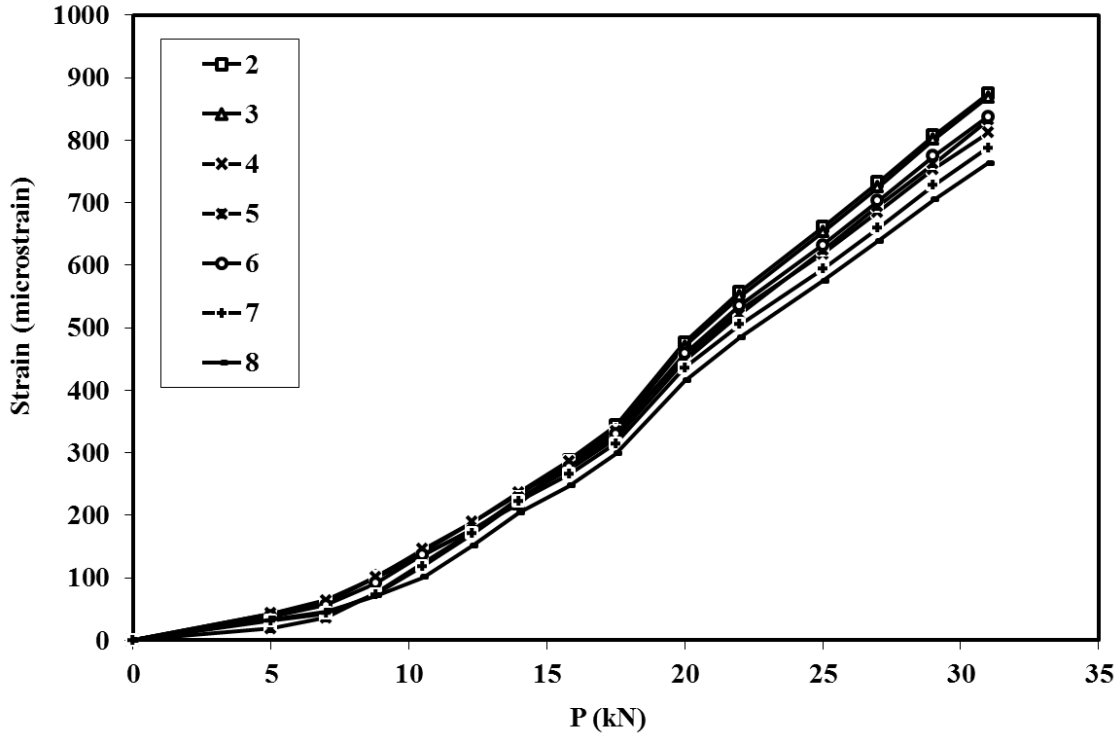

Figure D.14 Steel strain for slab S-SCC-b

Table D.15 Steel strain for slab DS-SCC-a

DS-SCC-a								
P(kN)	STEEL STRAIN (Microstrain)							
	1	2	3	4	5	6	7	8
0	0	0	0	0	0	0	0	0
5	61.60	90.79	65.07	65.94	66.85	53.24	44.24	46.77
7	89.44	123.15	95.96	98.43	97.55	76.47	67.88	69.31
8.8	111.94	149.28	115.45	116.88	113.71	92.14	79.93	84.99
10.5	136.78	180.52	145.23	145.71	144.75	115.47	99.40	104.86
12.3	157.69	205.45	162.34	163.50	157.51	128.93	107.82	119.23
14	182.75	234.63	189.81	188.58	183.37	149.57	129.51	140.67
15.8	211.23	266.92	218.66	212.06	211.66	169.00	145.50	162.34
17.5	239.24	299.14	242.96	240.61	236.79	193.13	167.77	186.32
20	426.41	501.42	412.47	409.41	409.71	354.90	331.60	343.20
22	491.15	571.16	472.19	470.19	469.76	416.30	389.65	407.24
25	452.94	518.72	415.17	409.99	406.48	351.80	326.14	366.67
27	509.39	586.24	474.28	468.21	456.87	412.07	378.08	426.48
29	567.81	652.82	531.34	526.59	513.84	474.31	433.38	485.48
31	622.58	715.90	600.59	584.88	571.87	545.50	501.61	545.17

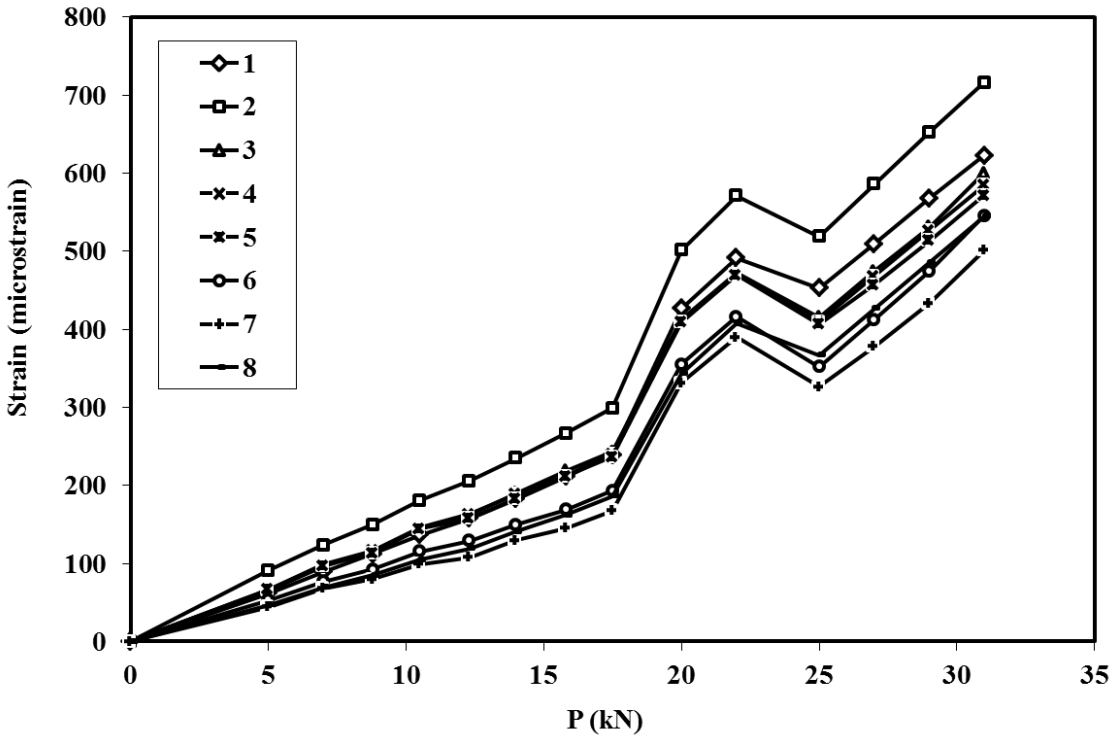

Figure D.15 Steel strain for slab DS-SCC-a

Table D.16 Steel strain for slab DS-SCC-b

DS-SCC-b								
P(kN)	STEEL STRAIN (Microstrain)							
	1	2	3	4	5	6	7	8
0	0	0	0	0	0	0	0	0
5	37.95	78.80	62.28	45.72	48.00	42.78	51.57	39.78
7	51.69	108.29	85.97	57.33	65.22	55.89	69.30	52.64
8.8	68.88	138.29	108.44	73.15	76.21	71.14	87.17	69.32
10.5	87.93	167.75	133.70	90.86	102.04	89.18	107.56	84.31
12.3	108.48	202.64	163.89	112.66	127.61	109.30	130.48	105.53
14	128.38	232.41	187.72	129.49	154.53	130.09	155.03	125.35
15.8	164.52	276.06	233.31	164.82	193.05	167.31	193.29	158.10
17.5	217.72	323.52	287.80	214.64	250.01	216.84	236.37	206.40
20	296.27	392.74	365.06	287.54	334.70	288.61	299.74	276.46
22	365.95	455.09	433.83	366.33	416.04	362.46	357.10	340.35
25	480.73	559.91	548.54	500.71	548.45	482.56	477.62	448.64
27	555.49	630.33	627.23	584.33	637.61	557.64	555.09	526.34
29	616.35	691.98	700.56	646.69	706.64	615.79	615.11	594.58
31	678.96	755.47	773.93	710.58	775.98	676.92	682.84	663.17

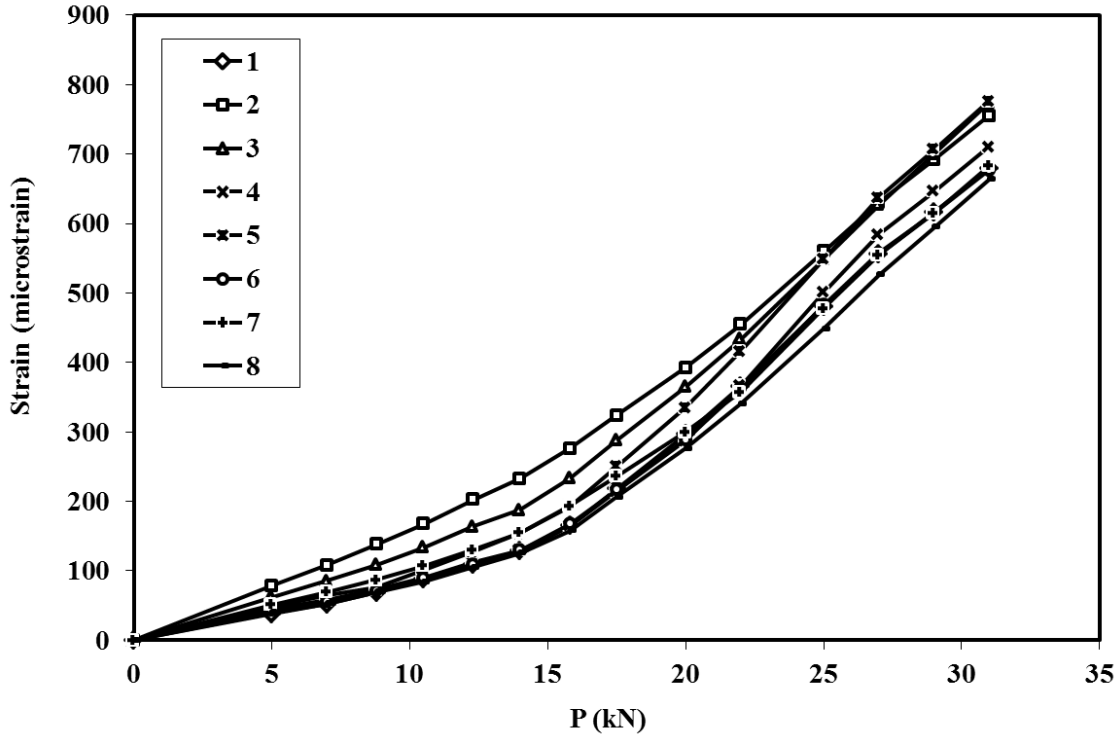

Figure D.16 Steel strain for slab DS-SCC-b

Figure D.17 Short-term typical experimental test view-1

Figure D.18 Short-term typical experimental test view-2

Figure D.19 Short-term typical experimental test view-3

Figure D.20 Short-term typical experimental test view-4

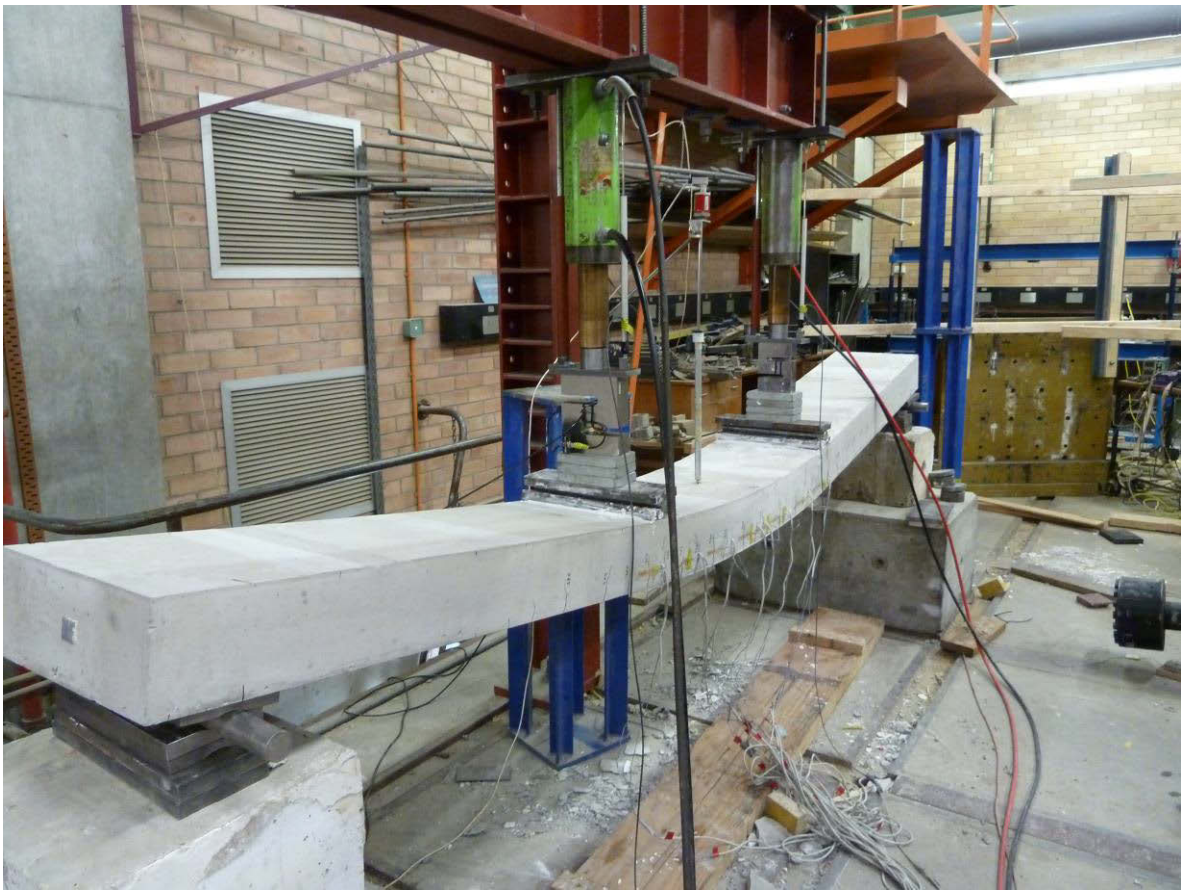

Figure D.21 Short-term typical experimental test view-5

APPENDIX E

EXPERIMENTAL DATA FOR LONG-TERM TESTS

Table E.1 Concrete surface strain at steel level for slab N-SCC-a

Slab N-SCC-a		CONCRETE SURFACE STRAIN BY SG															
		1		2		3		4		5		6		7		8	
Date	Age	Reading	Strain	Reading	Strain	Reading	Strain	Reading	Strain	Reading	Strain	Reading	Strain	Reading	Strain	Reading	Strain
21/03/2012	14	413.0		849.9		1065.4		593.2		1228.3		273.0		767.8		497.0	
21/03/2012	14	569.7		976.3		1213.0		734.9		1404.8		339.5		912.1		500.7	
22/03/2012	15	570.5	0.8	978.9	2.4	1225.9	12.2	740.8	5.6	1410.0	5.0	341.0	1.4	914.8	2.6	503.0	2.2
23/03/2012	16	570.8	1.1	989.0	12.0	1245.1	30.4	754.0	18.1	1438.8	32.3	257.0	-78.3	925.0	12.3	510.4	9.2
24/03/2012	17	706.1	129.3	1083.3	101.4	1344.6	124.7	930.6	185.5	1631.8	215.2	381.4	39.7	1091.1	169.7	513.2	11.8
25/03/2012	18	721.7	144.2	1092.3	109.9	1360.3	139.7	960.1	213.5	1674.5	255.7	370.0	28.9	1124.3	201.1	518.0	16.3
26/03/2012	19	730.8	152.7	1101.9	119.0	1369.8	148.6	973.9	226.5	1698.2	278.1	367.2	26.2	1140.0	216.0	507.4	6.3
27/03/2012	20	701.1	124.6	1062.2	81.4	1343.2	123.4	963.1	216.3	1717.0	295.9	360.5	19.8	1132.6	209.1	510.0	8.7
28/03/2012	21	715.1	137.9	1066.0	85.0	1326.9	108.0	952.4	206.2	1708.2	287.6	355.2	14.9	1136.6	212.8	511.7	10.4
29/03/2012	22	719.2	141.8	1069.0	87.8	1356.0	135.6	970.3	223.1	1690.4	270.7	350.6	10.5	1097.6	175.9	517.5	15.9
30/03/2012	23	721.4	143.8	1073.2	91.8	1370.3	149.1	987.9	239.8	1725.2	303.7	339.6	0.1	1093.6	172.1	503.4	2.5
31/03/2012	24	729.4	151.4	1076.4	94.8	1365.0	144.1	995.2	246.8	1765.9	342.3	345.8	6.0	1086.5	165.3	505.3	4.3
1/04/2012	25	735.8	157.5	1079.2	97.5	1357.0	136.5	985.8	237.8	1786.4	361.7	358.4	17.9	1080.6	159.8	508.7	7.5
2/04/2012	26	739.0	160.5	1086.0	103.9	1371.8	150.5	1010.0	260.8	1794.1	369.1	364.8	24.0	1094.3	172.7	509.6	8.4
3/04/2012	27	745.1	166.3	1087.5	105.3	1369.7	148.5	1050.2	298.9	1817.4	391.1	362.6	21.9	1159.6	234.7	506.5	5.5
4/04/2012	28	744.3	165.5	1086.5	104.4	1382.2	160.4	1063.6	311.6	1839.4	412.0	368.0	27.0	1202.8	275.6	515.9	14.4
5/04/2012	29	722.7	145.1	1064.4	83.5	1357.7	137.2	1044.1	293.1	1828.3	401.4	379.0	37.4	1182.3	256.2	506.3	5.3
6/04/2012	30	709.6	132.6	1048.7	68.6	1337.2	117.8	1034.3	283.8	1827.7	400.9	378.9	37.3	1168.4	243.0	509.0	7.9
7/04/2012	31	718.9	141.5	1049.8	69.7	1339.1	119.5	1046.5	295.3	1839.1	411.6	369.9	28.8	1175.5	249.7	509.4	8.2
8/04/2012	32	718.7	141.3	1047.5	67.5	1336.0	116.6	1050.4	299.1	1848.3	420.4	354.3	14.0	1177.5	251.6	512.2	10.9
9/04/2012	33	716.3	139.0	1044.1	64.2	1332.0	112.8	1052.6	301.1	1861.7	433.1	356.6	16.2	1183.0	256.8	514.1	12.6
10/04/2012	34	754.8	175.5	1076.7	95.1	1369.6	148.5	1100.0	346.1	1914.2	482.8	382.2	40.4	1226.4	297.9	514.2	12.7
11/04/2012	35	769.8	189.7	1087.3	105.2	1383.6	161.7	1120.9	365.9	1936.0	503.5	395.4	52.9	1243.8	314.4	514.9	13.4
12/04/2012	36	773.7	193.4	1091.8	109.5	1391.1	168.8	1127.0	371.7	1941.9	509.1	397.0	54.5	1246.4	316.9	516.1	14.6
13/04/2012	37	768.0	188.0	1084.5	102.5	1383.6	161.7	1125.3	370.1	1942.7	509.8	402.2	59.4	1240.3	311.1	516.5	15.0
16/04/2012	40	791.1	209.9	1097.2	114.6	1401.6	178.8	1153.6	396.9	1980.2	545.4	401.6	58.8	1263.9	333.5	516.6	15.1
17/04/2012	41	741.1	162.5	1053.9	73.5	1349.4	129.3	1102.4	348.4	1934.6	502.2	403.0	60.2	1214.3	286.5	517.2	15.6
18/04/2012	42	737.1	158.7	1048.1	68.0	1345.8	125.9	1099.3	345.4	1929.0	496.9	416.7	73.1	1207.7	280.2	517.6	16.0
19/04/2012	43	738.9	160.5	1047.5	67.4	1347.9	127.9	1100.0	346.1	1927.0	495.0	408.3	65.2	1205.2	277.9	517.8	16.2
20/04/2012	44	732.0	153.8	1038.4	58.8	1339.5	119.9	1091.8	338.3	1918.6	487.0	426.2	82.2	1195.3	268.5	519.1	17.4
21/04/2012	45	706.9	130.1	1014.3	35.9	1314.3	96.1	1067.2	315.0	1896.8	466.4	441.3	96.5	1173.0	247.4	519.9	18.2
22/04/2012	46	699.7	123.2	1005.6	27.8	1305.8	88.0	1060.3	308.4	1893.2	463.0	456.4	110.8	1164.4	239.2	520.2	18.4

23/04/2012	47	704.9	128.2	1011.1	32.9	1311.1	93.0	1067.4	315.1	1901.8	471.1	432.7	88.3	1168.1	242.7	520.7	19.0
24/04/2012	48	731.9	153.8	1033.7	54.4	1334.4	115.1	1098.0	344.1	1933.1	500.7	428.3	84.1	1195.4	268.6	521.1	19.3
25/04/2012	49	725.4	147.7	1022.5	43.7	1321.4	102.8	1101.2	347.2	1952.9	519.6	449.9	104.7	1195.8	268.9	521.2	19.4
26/04/2012	50	751.4	172.3	1049.2	69.0	1347.9	127.9	1119.2	364.2	1991.2	555.8	443.5	98.6	1226.3	297.8	521.2	19.4
27/04/2012	51	784.6	203.7	1074.3	92.8	1374.9	153.5	1145.2	389.0	2016.3	579.7	460.3	114.5	1250.4	320.7	521.3	19.5
28/04/2012	52	777.8	197.3	1068.1	87.0	1368.1	147.0	1138.3	382.4	2009.6	573.3	460.5	114.6	1243.3	314.0	522.9	21.0
29/04/2012	53	773.6	193.3	1062.5	81.7	1362.7	142.0	1134.3	378.6	2006.5	570.4	445.1	100.1	1238.7	309.6	523.3	21.4
30/04/2012	54	781.2	200.5	1069.7	88.5	1370.8	149.6	1146.0	389.7	2021.8	584.8	430.3	86.1	1248.5	318.9	523.3	21.4
1/05/2012	55	778.6	198.0	1065.4	84.4	1365.3	144.4	1143.1	387.0	2020.6	583.7	442.3	97.4	1245.7	316.3	523.6	21.7
2/05/2012	56	781.5	200.8	1066.6	85.5	1367.1	146.1	1144.5	388.3	2020.7	583.8	450.7	105.4	1246.0	316.6	523.8	21.9
3/05/2012	57	780.3	199.7	1065.4	84.5	1364.7	143.8	1144.9	388.7	2020.8	583.9	466.8	120.6	1245.1	315.7	524.0	22.1
4/05/2012	58	786.7	205.7	1068.7	87.6	1369.7	148.6	1156.7	399.8	2038.3	600.5	497.7	149.9	1253.9	324.0	524.0	22.1
5/05/2012	59	781.0	200.3	1065.3	84.3	1365.5	144.6	1157.2	400.3	2047.9	609.5	485.5	138.4	1252.1	322.3	524.3	22.3
6/05/2012	60	784.2	203.4	1066.0	85.0	1366.1	145.1	1159.4	402.4	2055.0	616.4	467.0	120.8	1255.2	325.3	524.6	22.7
7/05/2012	61	799.6	218.0	1078.1	96.4	1380.5	158.8	1174.6	416.8	2071.4	631.9	485.4	138.3	1269.7	339.0	524.9	23.0
8/05/2012	62	812.4	230.1	1089.3	107.1	1392.5	170.1	1188.5	430.0	2084.7	644.5	500.3	152.4	1281.7	350.4	525.1	23.1
9/05/2012	63	815.5	233.0	1089.5	107.3	1392.0	169.7	1190.1	431.5	2086.8	646.5	474.4	127.9	1282.7	351.4	525.2	23.2
10/05/2012	64	810.9	228.7	1084.3	102.4	1389.0	166.8	1186.8	428.3	2083.7	643.6	483.4	136.4	1278.5	347.3	525.2	23.2
11/05/2012	65	803.8	221.9	1076.1	94.5	1382.3	160.5	1180.2	422.1	2077.8	637.9	499.7	151.8	1270.6	339.8	525.4	23.4
12/05/2012	66	813.3	231.0	1082.9	101.0	1389.9	167.7	1190.1	431.4	2092.2	651.6	503.2	155.1	1280.6	349.3	525.6	23.5
13/05/2012	67	803.1	221.2	1076.0	94.5	1381.5	159.7	1189.5	430.9	2097.5	656.6	490.5	143.1	1280.6	349.3	525.9	23.8
14/05/2012	68	825.3	242.3	1095.1	112.6	1401.7	178.8	1215.8	455.8	2124.2	681.9	503.9	155.8	1305.9	373.3	525.9	23.9
15/05/2012	69	829.2	246.1	1099.0	116.3	1405.2	182.2	1219.5	459.3	2133.1	690.4	495.7	148.1	1311.5	378.6	526.5	24.4
16/05/2012	70	830.4	247.1	1102.0	119.1	1408.4	185.3	1214.5	454.6	2137.9	694.9	491.6	144.1	1311.7	378.8	526.6	24.5
17/05/2012	71	835.9	252.4	1108.3	125.1	1413.8	190.4	1227.4	466.9	2146.5	703.0	514.3	165.7	1318.2	385.0	526.6	24.5
18/05/2012	72	829.0	245.8	1098.7	116.0	1408.2	185.1	1222.9	462.6	2138.7	695.6	517.7	168.8	1312.5	379.5	526.7	24.6
19/05/2012	73	832.3	249.0	1097.9	115.3	1407.2	184.1	1220.4	460.2	2141.0	697.8	535.5	185.8	1308.4	375.7	527.2	25.1
20/05/2012	74	835.0	251.6	1097.9	115.2	1406.2	183.1	1224.2	463.8	2149.4	705.7	518.9	170.0	1310.6	377.8	527.3	25.2
21/05/2012	75	832.9	249.5	1095.5	112.9	1405.1	182.2	1216.5	456.5	2144.3	701.0	516.0	167.3	1305.2	372.7	527.8	25.7
22/05/2012	76	835.9	252.4	1096.1	113.5	1407.7	184.6	1226.0	465.5	2149.7	706.1	538.9	189.0	1308.4	375.7	528.5	26.4
23/05/2012	77	844.3	260.3	1102.0	119.1	1414.3	190.8	1235.2	474.2	2167.9	723.4	534.4	184.7	1320.4	387.0	528.8	26.6
24/05/2012	78	842.2	258.3	1100.4	117.6	1412.8	189.4	1223.5	463.1	2167.9	723.3	529.6	180.2	1318.5	385.2	528.9	26.7
25/05/2012	79	838.3	254.6	1099.0	116.3	1410.5	187.3	1228.2	467.6	2163.6	719.3	534.8	185.1	1314.4	381.3	529.4	27.2
26/05/2012	80	846.9	262.8	1103.7	120.7	1416.6	193.0	1244.4	483.0	2179.2	734.0	558.1	207.2	1325.0	391.4	529.5	27.3
27/05/2012	81	845.6	261.6	1102.3	119.4	1414.8	191.3	1246.4	484.8	2179.8	734.6	555.5	204.7	1323.2	389.7	529.7	27.5
28/05/2012	82	860.3	275.5	1116.6	133.0	1428.9	204.7	1264.5	502.0	2194.4	748.4	535.5	185.8	1336.2	402.1	530.7	28.4
29/05/2012	83	843.9	259.9	1099.8	117.0	1411.3	188.0	1246.8	485.2	2177.9	732.8	525.3	176.1	1317.4	384.2	532.2	29.8

30/05/2012	84	850.0	265.7	1105.2	122.1	1417.2	193.6	1255.7	493.6	2183.7	738.3	522.8	173.7	1323.3	389.8	532.4	30.0
31/05/2012	85	845.1	261.1	1098.1	115.4	1409.9	186.6	1251.2	489.4	2179.9	734.7	511.6	163.1	1316.9	383.7	532.9	30.5
1/06/2012	86	852.7	268.3	1106.3	123.2	1415.5	192.0	1258.6	496.4	2186.6	741.0	525.8	176.5	1323.6	390.0	533.8	31.4
2/06/2012	87	836.3	252.7	1087.9	105.7	1399.3	176.7	1241.5	480.2	2166.1	721.6	528.0	178.6	1305.8	373.2	533.9	31.5
3/06/2012	88	840.2	256.4	1088.7	106.5	1404.1	181.1	1245.1	483.6	2167.7	723.2	518.5	169.7	1307.3	374.6	534.0	31.5
4/06/2012	89	838.3	254.7	1084.9	102.9	1401.8	179.0	1244.0	482.5	2165.8	721.4	509.5	161.1	1304.7	372.2	534.2	31.7
5/06/2012	90	859.4	274.6	1104.6	121.6	1421.1	197.2	1272.4	509.5	2200.5	754.2	499.9	152.0	1332.3	398.3	534.8	32.3
6/06/2012	91	853.1	268.7	1099.7	116.9	1411.6	188.3	1265.7	503.1	2196.6	750.5	501.0	153.0	1323.6	390.1	535.0	32.5
7/06/2012	92	863.9	278.9	1109.4	126.1	1421.7	197.8	1278.2	515.0	2210.3	763.5	491.3	143.9	1336.3	402.1	535.1	32.6
8/06/2012	93	875.4	289.8	1117.3	133.6	1432.6	208.2	1293.2	529.2	2226.9	779.3	500.4	152.5	1350.0	415.1	535.3	32.8
9/06/2012	94	876.0	290.3	1116.9	133.3	1432.0	207.6	1294.6	530.6	2231.0	783.2	497.2	149.4	1349.7	414.8	535.9	33.3
10/06/2012	95	874.3	288.7	1115.8	132.2	1432.0	207.6	1293.4	529.4	2229.4	781.6	485.8	138.6	1346.7	412.0	536.2	33.6
11/06/2012	96	861.7	276.8	1104.4	121.4	1419.8	196.1	1279.6	516.3	2212.9	766.0	499.1	151.3	1331.8	397.9	536.2	33.6
12/06/2012	97	859.2	274.5	1102.2	119.3	1415.5	192.0	1276.5	513.4	2208.8	762.1	507.9	159.6	1329.3	395.5	536.6	34.0
13/06/2012	98	862.7	277.8	1101.7	118.8	1418.3	194.6	1276.9	513.8	2209.8	763.1	494.5	146.9	1329.7	395.9	536.9	34.3
14/06/2012	99	861.7	276.8	1100.0	117.2	1416.7	193.1	1275.6	512.5	2208.3	761.6	500.6	152.6	1329.6	395.8	537.2	34.5
15/06/2012	100	858.0	273.3	1096.8	114.1	1414.0	190.5	1271.2	508.4	2206.4	759.8	510.2	161.8	1327.5	393.8	537.4	34.8
16/06/2012	101	854.6	270.1	1093.3	110.8	1411.0	187.7	1269.2	506.5	2204.4	757.9	515.5	166.8	1323.3	389.8	538.1	35.5
17/06/2012	102	852.5	268.1	1091.3	109.0	1409.5	186.3	1271.3	508.4	2208.3	761.6	523.4	174.3	1324.9	391.4	539.2	36.5
18/06/2012	103	882.5	296.5	1116.8	133.1	1433.7	209.2	1303.4	538.9	2245.0	796.4	544.5	194.3	1355.4	420.3	539.2	36.5
19/06/2012	104	886.2	300.1	1116.4	132.8	1433.3	208.9	1308.4	543.6	2250.6	801.7	524.6	175.4	1357.5	422.3	539.7	36.9
20/06/2012	105	886.0	299.9	1117.8	134.1	1432.3	207.9	1309.1	544.3	2254.0	805.0	528.2	178.8	1359.2	423.8	540.7	37.9
21/06/2012	106	896.4	309.7	1125.0	140.9	1442.2	217.3	1320.6	555.2	2265.8	816.2	525.8	176.6	1368.0	432.2	541.1	38.2
22/06/2012	107	881.2	295.3	1112.2	128.8	1428.2	204.0	1306.1	541.4	2256.6	807.4	524.1	175.0	1354.3	419.2	541.4	38.6
23/06/2012	108	888.3	302.1	1118.5	134.7	1437.0	212.3	1316.6	551.4	2267.7	817.9	511.9	163.4	1364.5	428.9	541.4	38.6
24/06/2012	109	890.6	304.2	1118.4	134.6	1439.0	214.2	1321.8	556.4	2271.3	821.3	516.8	168.0	1368.2	432.4	541.7	38.8
25/06/2012	110	890.4	304.1	1118.6	134.8	1438.2	213.5	1322.0	556.5	2271.4	821.5	522.7	173.6	1366.0	430.2	541.8	38.9
26/06/2012	111	880.2	294.4	1109.9	126.6	1428.7	204.5	1308.0	543.2	2259.7	810.3	520.0	171.0	1353.4	418.3	542.6	39.7
27/06/2012	112	879.6	293.8	1108.2	125.0	1427.3	203.2	1307.3	542.6	2254.6	805.5	533.2	183.6	1349.9	415.1	543.2	40.3
28/06/2012	113	878.3	292.6	1106.7	123.6	1425.6	201.5	1307.4	542.7	2254.7	805.6	493.8	146.2	1349.1	414.2	543.3	40.4
29/06/2012	114	870.5	285.2	1099.1	116.3	1416.8	193.2	1297.9	533.7	2246.4	797.7	526.2	177.0	1338.4	404.1	544.0	41.0
30/06/2012	115	866.8	281.7	1094.9	112.3	1414.6	191.1	1294.5	530.5	2242.5	794.0	534.2	184.5	1336.9	402.7	544.1	41.1
1/07/2012	116	877.0	291.3	1103.1	120.1	1422.5	198.6	1305.4	540.7	2259.4	810.0	514.6	166.0	1350.1	415.2	544.9	41.9
2/07/2012	117	886.9	300.7	1112.2	128.8	1431.7	207.3	1318.1	552.8	2275.6	825.4	527.0	177.7	1361.4	425.9	545.8	42.7
3/07/2012	118	900.7	313.8	1122.9	138.9	1442.5	217.5	1336.2	569.9	2295.7	844.5	547.8	197.4	1376.7	440.5	545.9	42.8
4/07/2012	119	898.6	311.8	1122.0	138.1	1440.6	215.8	1337.4	571.1	2297.4	846.1	521.0	172.0	1375.9	439.7	546.1	43.0
5/07/2012	120	889.6	303.3	1116.0	132.3	1432.8	208.4	1328.5	562.6	2287.5	836.6	497.4	149.7	1367.2	431.4	546.4	43.3

6/07/2012	121	884.1	298.0	1113.1	129.6	1430.4	206.1	1322.6	557.0	2282.4	831.9	524.1	174.9	1361.7	426.2	547.0	43.9
7/07/2012	122	890.6	304.2	1117.4	133.7	1435.6	211.0	1328.8	562.9	2287.6	836.8	528.4	179.0	1366.8	431.0	547.5	44.4
8/07/2012	123	882.0	296.1	1107.4	124.2	1427.1	203.0	1316.4	551.2	2277.3	827.0	517.2	168.4	1356.2	421.0	548.1	44.9
9/07/2012	124	897.6	310.8	1119.2	135.4	1438.7	214.0	1333.4	567.3	2287.7	836.9	515.3	166.6	1367.3	431.5	548.4	45.2
10/07/2012	125	889.0	302.7	1108.6	125.3	1428.5	204.3	1323.7	558.1	2276.3	826.1	514.5	165.8	1356.0	420.8	550.3	47.0
11/07/2012	126	875.8	290.1	1098.0	115.3	1416.4	192.9	1311.2	546.3	2264.9	815.3	528.6	179.2	1344.0	409.4	550.8	47.4
12/07/2012	127	888.9	302.6	1107.8	124.6	1427.4	203.2	1322.7	557.2	2276.8	826.6	522.0	172.9	1353.8	418.7	550.8	47.5
13/07/2012	128	881.0	295.1	1101.1	118.3	1420.7	196.9	1315.4	550.2	2266.7	816.9	514.0	165.4	1345.4	410.7	555.2	51.7
14/07/2012	129	857.5	272.8	1081.1	99.3	1400.0	177.3	1298.0	533.8	2247.9	799.2	521.3	172.3	1328.1	394.3	556.2	52.6
15/07/2012	130	868.3	283.1	1088.2	106.0	1407.6	184.4	1307.2	542.4	2267.4	817.7	515.0	166.3	1341.7	407.2	556.3	52.7
16/07/2012	131	896.5	309.8	1112.7	129.2	1432.6	208.2	1340.2	573.8	2302.2	850.6	515.0	166.3	1367.2	431.4	557.0	53.3
17/07/2012	132	892.5	306.0	1108.8	125.6	1426.6	202.5	1335.5	569.3	2298.6	847.2	510.8	162.4	1361.6	426.1	557.4	53.7
18/07/2012	133	891.1	304.7	1107.4	124.3	1424.7	200.7	1332.5	566.5	2301.5	849.9	478.9	132.1	1362.2	426.7	557.8	54.1
19/07/2012	134	895.2	308.5	1110.5	127.1	1429.3	205.0	1339.3	572.9	2308.4	856.5	504.3	156.2	1367.6	431.8	558.6	54.8
20/07/2012	135	904.4	317.3	1117.7	134.0	1436.9	212.3	1349.8	582.8	2317.8	865.5	506.7	158.5	1376.4	440.1	561.6	57.7
21/07/2012	136	892.7	306.2	1110.7	127.3	1427.4	203.2	1335.2	569.0	2306.7	854.9	505.4	157.2	1364.0	428.4	563.6	59.6
22/07/2012	137	880.8	294.9	1101.2	118.3	1418.4	194.7	1323.2	557.7	2296.6	845.3	491.9	144.5	1354.0	418.9	563.8	59.8
23/07/2012	138	880.8	294.9	1099.3	116.5	1417.7	194.1	1321.8	556.3	2294.0	842.8	476.0	129.4	1351.5	416.5	568.1	63.9
24/07/2012	139	874.4	288.9	1096.9	114.3	1415.2	191.7	1319.3	553.9	2287.8	837.0	485.2	138.1	1348.1	413.3	568.5	64.3
25/07/2012	140	882.8	296.8	1099.9	117.1	1418.3	194.7	1325.4	559.7	2289.8	838.9	475.6	129.0	1352.3	417.3	569.6	65.3
26/07/2012	141	892.2	305.8	1105.6	122.5	1424.5	200.5	1334.8	568.7	2301.4	849.9	472.0	125.5	1358.6	423.2	569.9	65.6
27/07/2012	142	888.7	302.4	1100.9	118.1	1420.2	196.5	1333.3	567.3	2303.6	852.0	467.8	121.6	1358.4	423.1	572.6	68.1
28/07/2012	143	898.0	311.2	1108.2	125.0	1426.8	202.7	1343.5	576.9	2318.8	866.4	481.5	134.5	1367.7	431.9	573.3	68.8
29/07/2012	144	902.6	315.6	1114.2	130.7	1432.6	208.2	1350.3	583.3	2328.6	875.6	491.6	144.1	1374.8	438.6	573.7	69.2
30/07/2012	145	908.8	321.5	1117.6	133.9	1436.1	211.5	1355.1	587.9	2334.8	881.6	500.5	152.5	1380.7	444.2	573.8	69.3
31/07/2012	146	911.3	323.8	1119.5	135.7	1437.8	213.1	1358.1	590.7	2337.7	884.3	500.6	152.7	1381.7	445.2	574.5	69.9
1/08/2012	147	914.7	327.0	1121.9	138.0	1440.4	215.6	1361.0	593.5	2340.9	887.3	459.3	113.5	1384.5	447.9	574.5	69.9
2/08/2012	148	914.4	326.7	1119.8	135.9	1438.1	213.4	1359.2	591.7	2341.5	887.9	480.3	133.4	1383.4	446.8	578.8	74.0
3/08/2012	149	921.4	333.5	1126.7	142.5	1444.3	219.2	1367.9	600.0	2350.0	895.9	478.0	131.2	1389.6	452.7	587.6	82.4
4/08/2012	150	918.8	330.9	1122.0	138.1	1438.6	213.9	1364.7	597.0	2349.3	895.3	506.7	158.5	1386.5	449.7	588.5	83.2
5/08/2012	151	914.8	327.1	1118.8	135.0	1434.4	209.9	1362.0	594.4	2348.4	894.4	499.0	151.1	1382.7	446.2	589.4	84.1
6/08/2012	152	909.7	322.3	1114.7	131.1	1430.2	205.9	1363.4	595.8	2345.5	891.7	472.5	126.0	1380.5	444.0	593.9	88.3
7/08/2012	153	932.2	343.7	1134.4	149.8	1451.8	226.3	1390.2	621.2	2368.0	913.0	472.6	126.1	1403.2	465.6	599.1	93.3
8/08/2012	154	932.6	344.0	1135.8	151.2	1452.2	226.7	1389.4	620.4	2367.3	912.3	499.0	151.1	1402.1	464.5	599.1	93.3
9/08/2012	155	920.9	332.9	1126.8	142.6	1443.2	218.2	1377.3	609.0	2359.1	904.5	525.0	175.8	1392.1	455.0	603.0	97.0
10/08/2012	156	932.6	344.0	1135.8	151.1	1452.6	227.2	1393.3	624.1	2373.1	917.8	480.3	133.4	1400.5	463.0	604.1	98.0
11/08/2012	157	912.1	324.6	1119.9	136.1	1436.7	212.0	1368.6	600.7	2351.5	897.4	415.9	72.4	1381.8	445.2	604.7	98.5

12/08/2012	158	900.7	313.8	1111.0	127.6	1428.7	204.5	1357.4	590.0	2338.6	885.1	457.2	111.6	1371.8	435.8	608.6	102.2
13/08/2012	159	915.4	327.7	1119.3	135.5	1436.9	212.2	1372.6	604.4	2349.3	895.3	412.6	69.3	1382.5	445.9	608.6	102.3
14/08/2012	160	926.4	338.1	1128.8	144.5	1446.6	221.5	1383.6	614.9	2360.5	905.9	405.2	62.2	1394.0	456.8	611.3	104.8
15/08/2012	161	929.7	341.3	1132.7	148.2	1448.1	222.9	1385.9	617.0	2368.4	913.4	422.8	78.9	1400.2	462.7	612.8	106.3
16/08/2012	162	928.4	340.0	1132.9	148.4	1446.8	221.7	1388.1	619.2	2370.6	915.4	413.0	69.6	1400.9	463.4	615.1	108.5
17/08/2012	163	918.7	330.8	1125.9	141.8	1440.5	215.6	1379.0	610.5	2364.8	910.0	354.6	14.3	1393.0	455.9	618.4	111.6
18/08/2012	164	911.0	323.5	1116.8	133.1	1430.7	206.4	1374.5	606.3	2359.7	905.1	361.3	20.6	1386.1	449.3	619.3	112.4
19/08/2012	165	917.8	330.0	1122.7	138.8	1439.1	214.3	1379.8	611.3	2366.1	911.2	418.6	74.9	1390.6	453.6	623.1	116.0
20/08/2012	166	936.4	347.6	1134.6	150.0	1452.0	226.5	1397.4	628.0	2380.3	924.6	460.6	114.7	1403.0	465.3	630.5	123.0
21/08/2012	167	918.0	330.2	1120.1	136.3	1436.1	211.5	1381.3	612.7	2364.2	909.4	494.1	146.5	1386.2	449.4	634.0	126.3
22/08/2012	168	902.6	315.6	1107.0	123.9	1424.0	200.0	1361.3	593.7	2349.5	895.5	518.3	169.5	1371.3	435.3	636.6	128.8
23/08/2012	169	908.0	320.7	1108.9	125.6	1428.6	204.4	1368.1	600.2	2345.7	891.8	528.1	178.8	1371.8	435.7	637.0	129.1
24/08/2012	170	903.4	316.3	1102.8	119.9	1422.6	198.7	1367.5	599.6	2343.7	890.0	498.3	150.5	1369.5	433.6	637.4	129.5
25/08/2012	171	910.6	323.2	1111.0	127.6	1428.9	204.7	1374.3	606.1	2358.4	903.9	440.4	95.6	1381.6	445.1	637.9	130.1
26/08/2012	172	923.8	335.7	1122.0	138.0	1437.1	212.4	1387.4	618.5	2374.9	919.5	491.0	143.6	1391.1	454.0	639.0	131.0
27/08/2012	173	938.2	349.3	1134.0	149.4	1447.2	222.0	1403.1	633.3	2388.5	932.4	496.7	149.0	1399.6	462.1	641.1	133.1
28/08/2012	174	921.2	333.2	1118.4	134.7	1431.3	207.0	1382.9	614.2	2369.5	914.4	454.4	108.9	1381.9	445.3	642.1	134.0
29/08/2012	175	915.6	327.9	1114.7	131.2	1428.7	204.5	1376.1	607.8	2362.3	907.6	484.9	137.8	1377.5	441.2	642.7	134.6
30/08/2012	176	918.4	330.6	1115.5	131.9	1430.6	206.3	1379.2	610.7	2364.0	909.2	502.4	154.4	1379.6	443.2	646.4	138.1
31/08/2012	177	929.7	341.3	1123.7	139.6	1437.4	212.7	1398.1	628.7	2383.4	927.6	502.4	154.3	1395.8	458.6	652.4	143.8
1/09/2012	178	941.0	352.0	1131.4	146.9	1445.3	220.2	1407.2	637.3	2394.9	938.5	480.0	133.2	1403.8	466.1	653.2	144.5
2/09/2012	179	924.8	336.6	1118.6	134.8	1431.3	207.0	1390.9	621.8	2379.2	923.6	504.0	155.9	1388.2	451.3	654.0	145.3
3/09/2012	180	933.6	344.9	1126.2	142.0	1440.3	215.5	1400.2	630.6	2386.2	930.3	488.4	141.1	1396.3	459.0	659.1	150.1
4/09/2012	181	936.0	347.3	1128.4	144.2	1440.2	215.4	1398.7	629.2	2389.3	933.2	485.7	138.5	1398.7	461.3	662.1	152.9
5/09/2012	182	931.3	342.8	1121.8	137.9	1433.5	209.0	1401.4	631.8	2388.4	932.3	507.2	159.0	1395.5	458.2	662.1	153.0
6/09/2012	183	945.1	355.9	1133.3	148.7	1443.0	218.1	1418.3	647.7	2403.9	947.0	503.0	154.9	1408.8	470.8	663.6	154.4
7/09/2012	184	959.1	369.2	1146.7	161.5	1457.0	231.3	1432.6	661.3	2422.2	964.4	498.4	150.6	1424.5	485.8	670.5	161.0
8/09/2012	185	956.4	366.6	1146.8	161.5	1456.5	230.9	1424.0	653.2	2422.1	964.3	503.3	155.3	1422.5	483.9	672.2	162.5
9/09/2012	186	937.5	348.7	1128.8	144.5	1440.0	215.2	1403.3	633.6	2401.8	945.0	525.3	176.1	1402.4	464.8	676.7	166.8
10/09/2012	187	930.0	341.6	1121.9	138.0	1433.2	208.8	1397.8	628.4	2391.7	935.4	522.8	173.7	1393.2	456.1	688.5	177.9
11/09/2012	188	931.6	343.1	1122.3	138.3	1436.4	211.8	1398.6	629.2	2386.3	930.3	504.0	155.9	1390.0	453.0	693.0	182.3
12/09/2012	189	923.9	335.8	1118.0	134.2	1432.6	208.2	1388.7	619.8	2378.5	922.9	494.4	146.8	1386.6	449.8	693.9	183.1
13/09/2012	190	918.2	330.4	1111.6	128.2	1426.8	202.7	1380.3	611.7	2370.6	915.5	492.1	144.6	1379.1	442.7	696.9	185.9
14/09/2012	191	936.5	347.7	1124.5	140.5	1439.9	215.1	1405.5	635.7	2389.2	933.1	481.5	134.5	1396.4	459.1	697.6	186.6
15/09/2012	192	936.9	348.1	1127.3	143.1	1437.5	212.8	1402.7	633.0	2394.3	937.9	494.9	147.2	1399.3	461.9	698.8	187.8
16/09/2012	193	932.4	343.9	1124.6	140.5	1435.8	211.3	1397.7	628.2	2389.0	932.9	496.9	149.2	1392.8	455.6	700.4	189.3
17/09/2012	194	928.9	340.5	1119.7	135.9	1432.9	208.5	1393.7	624.5	2381.7	926.0	488.0	140.7	1382.2	445.6	702.2	190.9

18/09/2012	195	921.9	333.9	1115.2	131.6	1428.9	204.6	1390.4	621.3	2374.9	919.5	479.6	132.7	1380.1	443.7	705.3	193.9
19/09/2012	196	926.8	338.5	1117.6	133.9	1431.7	207.4	1393.5	624.3	2376.9	921.4	470.5	124.2	1385.1	448.4	708.0	196.4
20/09/2012	197	923.7	335.6	1116.5	132.8	1427.9	203.8	1393.2	624.0	2375.1	919.8	471.5	125.1	1382.4	445.8	708.1	196.6
21/09/2012	198	925.1	336.9	1112.9	129.4	1427.2	203.1	1393.9	624.7	2367.2	912.2	462.4	116.5	1377.2	440.9	708.7	197.1
22/09/2012	199	917.7	329.9	1106.6	123.4	1420.8	197.0	1391.4	622.3	2362.6	907.8	470.9	124.6	1371.1	435.1	712.5	200.7
23/09/2012	200	913.3	325.7	1106.9	123.7	1419.4	195.7	1386.4	617.5	2360.5	905.9	467.9	121.7	1371.3	435.3	713.2	201.4
24/09/2012	201	928.7	340.3	1119.9	136.0	1433.5	209.0	1403.0	633.3	2378.7	923.1	457.2	111.5	1388.0	451.2	716.2	204.2
25/09/2012	202	937.1	348.3	1122.8	138.8	1434.7	210.2	1409.4	639.3	2386.3	930.4	469.8	123.4	1393.2	456.0	724.1	211.7
26/09/2012	203	929.0	340.6	1115.8	132.2	1426.0	201.9	1398.4	628.9	2377.5	922.0	478.1	131.3	1380.6	444.1	726.0	213.5
27/09/2012	204	930.2	341.7	1117.9	134.1	1431.1	206.7	1401.4	631.8	2376.8	921.3	465.4	119.3	1381.7	445.1	728.7	216.1
28/09/2012	205	919.2	331.4	1107.5	124.3	1420.9	197.1	1387.3	618.4	2366.0	911.1	471.1	124.7	1371.0	435.0	735.2	222.2
29/09/2012	206	907.1	319.9	1096.5	113.9	1410.2	186.9	1379.9	611.4	2354.2	900.0	480.2	133.3	1360.4	425.0	737.6	224.5
30/09/2012	207	923.6	335.5	1114.7	131.2	1427.0	202.9	1404.6	634.8	2379.9	924.3	485.2	138.1	1384.7	448.0	738.6	225.5
1/10/2012	208	937.4	348.6	1125.0	140.9	1435.5	211.0	1412.4	642.2	2393.9	937.5	492.6	145.1	1395.1	457.8	740.9	227.7
2/10/2012	209	924.2	336.1	1112.4	128.9	1422.2	198.4	1397.2	627.8	2383.6	927.8	512.5	163.9	1381.1	444.6	754.4	240.5
3/10/2012	210	937.1	348.3	1123.2	139.2	1433.1	208.6	1408.7	638.7	2393.1	936.8	493.8	146.2	1392.2	455.1	755.2	241.2
4/10/2012	211	933.1	344.5	1119.3	135.5	1428.6	204.3	1406.6	636.7	2388.6	932.5	497.1	149.4	1386.1	449.4	757.4	243.3
5/10/2012	212	944.9	355.6	1127.5	143.2	1437.1	212.5	1422.5	651.8	2405.7	948.7	494.9	147.2	1396.7	459.3	758.7	244.5
6/10/2012	213	926.6	338.4	1115.8	132.2	1426.2	202.1	1404.0	634.2	2384.2	928.4	493.3	145.8	1379.9	443.4	761.9	247.6
7/10/2012	214	922.1	334.1	1116.5	132.8	1427.3	203.2	1404.0	634.3	2382.5	926.7	481.8	134.8	1380.6	444.1	767.0	252.4
8/10/2012	215	931.6	343.1	1122.1	138.2	1428.8	204.6	1412.0	641.8	2391.7	935.5	486.4	139.2	1387.3	450.5	769.2	254.5
9/10/2012	216	932.2	343.6	1122.7	138.8	1428.2	204.0	1409.8	639.7	2392.8	936.5	492.0	144.5	1390.2	453.2	769.6	254.9
10/10/2012	217	942.5	353.4	1129.1	144.7	1435.5	211.0	1417.8	647.4	2404.3	947.4	489.4	142.1	1398.6	461.2	771.2	256.4
11/10/2012	218	935.9	347.2	1121.3	137.4	1428.7	204.4	1409.6	639.5	2396.7	940.2	501.8	153.9	1387.9	451.1	774.0	259.0
12/10/2012	219	968.2	377.8	1150.3	164.9	1463.5	237.5	1449.2	677.0	2426.6	968.6	464.8	118.7	1423.2	484.5	774.8	259.8
13/10/2012	220	952.7	363.1	1136.8	152.1	1447.7	222.5	1434.0	662.6	2414.2	956.8	495.3	147.6	1407.3	469.4	781.7	266.4
14/10/2012	221	944.3	355.2	1130.8	146.4	1440.5	215.7	1421.5	650.9	2407.6	950.5	502.8	154.7	1400.9	463.4	783.1	267.7
15/10/2012	222	953.9	364.2	1137.3	152.6	1447.8	222.6	1428.1	657.1	2412.3	955.0	484.4	137.3	1405.4	467.6	784.5	269.0
16/10/2012	223	945.0	355.7	1126.8	142.6	1435.5	211.0	1420.3	649.7	2402.0	945.3	496.0	148.3	1393.2	456.1	786.9	271.2
17/10/2012	224	933.6	344.9	1114.6	131.1	1424.0	200.1	1410.8	640.7	2393.5	937.2	515.5	166.8	1381.6	445.1	788.4	272.7
18/10/2012	225	942.5	353.4	1126.4	142.2	1436.0	211.4	1418.5	647.9	2400.4	943.7	490.4	143.0	1393.7	456.5	789.9	274.1
19/10/2012	226	946.6	357.3	1128.6	144.3	1441.4	216.5	1420.3	649.6	2397.0	940.4	468.2	121.9	1391.8	454.8	792.4	276.4
20/10/2012	227	918.1	330.3	1103.3	120.3	1417.3	193.7	1398.1	628.6	2370.4	915.3	493.3	145.7	1367.7	431.9	795.4	279.3
21/10/2012	228	907.1	319.9	1092.2	109.8	1404.6	181.6	1387.3	618.4	2356.5	902.1	497.3	149.5	1357.0	421.8	795.6	279.5
22/10/2012	229	914.5	326.9	1097.6	114.9	1411.2	187.9	1394.1	624.9	2363.7	908.9	486.7	139.5	1365.5	429.8	798.3	282.1
23/10/2012	230	935.1	346.4	1114.7	131.1	1426.9	202.8	1413.7	643.4	2387.1	931.1	485.0	137.9	1387.1	450.3	802.4	286.0
24/10/2012	231	938.8	349.9	1123.6	139.6	1433.6	209.1	1416.7	646.2	2396.7	940.2	484.2	137.1	1393.3	456.2	805.1	288.5

25/10/2012	232	924.2	336.0	1110.1	126.7	1419.5	195.7	1399.3	629.8	2381.2	925.5	497.5	149.8	1375.4	439.2	806.6	289.9
26/10/2012	233	921.6	333.6	1106.8	123.6	1414.6	191.1	1396.9	627.5	2377.1	921.6	491.3	143.8	1372.3	436.2	807.3	290.6
27/10/2012	234	930.3	341.9	1115.3	131.7	1423.5	199.6	1409.0	639.0	2386.4	930.4	483.8	136.7	1383.2	446.5	812.5	295.5
28/10/2012	235	931.8	343.3	1118.4	134.6	1425.8	201.8	1411.3	641.2	2393.7	937.3	490.6	143.2	1386.2	449.4	819.1	301.8
29/10/2012	236	934.1	345.5	1124.2	140.1	1432.0	207.6	1413.3	643.1	2399.9	943.3	484.7	137.6	1390.6	453.6	819.9	302.5
30/10/2012	237	931.8	343.3	1117.9	134.2	1426.4	202.3	1408.4	638.4	2390.1	934.0	484.7	137.6	1381.1	444.6	820.7	303.3
31/10/2012	238	926.7	338.5	1108.7	125.4	1421.2	197.4	1406.6	636.7	2377.5	922.0	480.8	133.9	1371.6	435.6	825.1	307.4
1/11/2012	239	945.1	355.9	1122.7	138.7	1436.6	212.0	1425.3	654.4	2390.1	933.9	450.7	105.4	1390.9	453.9	832.8	314.8
2/11/2012	240	938.6	349.7	1121.7	137.8	1433.5	209.0	1426.7	655.7	2396.8	940.3	474.7	128.1	1392.7	455.6	837.6	319.3

Table E.2 Concrete surface strain at steel level for slab N-SCC-b

Slab N-SCC-b		CONCRETE SURFACE STRAIN BY SG															
		1		2		3		4		5		6		7		8	
Date	Age	Reading	Strain	Reading	Strain	Reading	Strain	Reading	Strain	Reading	Strain	Reading	Strain	Reading	Strain	Reading	Strain
21/03/2012	14	302.9		1141.7		919.4		949.6		942.8		624.3		926.4		695.5	
21/03/2012	14	303.0		721.0		974.1		2224.8		127.3		560.7		1724.2		1376.1	
22/03/2012	15	305.6	2.5	739.6	17.7	979.2	4.8	2433.3	197.6	128.6	1.2	514.0	-44.3	1861.4	130.0	1487.9	105.9
23/03/2012	16	305.9	2.8	746.8	24.5	993.7	18.7	2486.3	247.9	130.5	3.0	492.7	-64.4	1907.4	173.6	1528.2	144.2
24/03/2012	17	306.4	3.2	756.9	34.0	1042.7	65.1	2571.8	328.9	129.8	2.4	500.9	-56.6	1975.2	237.8	1594.2	206.7
25/03/2012	18	303.3	0.2	773.5	49.8	1043.3	65.7	2605.1	360.5	130.4	2.9	481.7	-74.9	1998.2	259.7	1621.2	232.2
26/03/2012	19	304.5	1.4	756.1	33.3	1044.2	66.5	2625.3	379.6	124.6	-2.6	473.4	-82.7	2008.5	269.5	1637.3	247.6
27/03/2012	20	305.8	2.6	757.7	34.8	1041.0	63.4	2666.5	418.6	136.9	9.1	445.6	-109.0	2063.8	321.8	1679.0	287.0
28/03/2012	21	306.0	2.8	783.6	59.3	1037.6	60.2	2676.2	427.9	144.2	16.0	441.2	-113.2	2065.2	323.2	1688.8	296.4
29/03/2012	22	303.2	0.1	754.0	31.3	1031.2	54.1	2666.9	419.0	139.0	11.0	410.5	-142.4	2047.6	306.5	1677.9	286.0
30/03/2012	23	303.5	0.5	740.5	18.5	1026.2	49.5	2706.7	456.8	138.6	10.7	423.7	-129.8	2079.2	336.5	1714.6	320.8
31/03/2012	24	305.1	2.0	751.2	28.6	1024.8	48.1	2741.1	489.3	138.7	10.8	432.3	-121.6	2118.1	373.4	1746.9	351.4
1/04/2012	25	305.1	2.0	764.2	41.0	1020.3	43.9	2746.9	494.8	158.4	29.4	414.2	-138.8	2117.8	373.1	1751.8	356.1
2/04/2012	26	305.5	2.3	767.6	44.2	1019.1	42.7	2714.9	464.5	155.8	27.0	368.4	-182.3	2077.5	334.9	1722.3	328.1
3/04/2012	27	305.6	2.4	765.6	42.3	1024.0	47.3	2710.6	460.5	146.7	18.3	347.3	-202.2	2073.5	331.1	1716.6	322.7
4/04/2012	28	306.2	3.0	763.8	40.6	1025.3	48.6	2732.5	481.2	146.8	18.5	352.0	-197.8	2076.1	333.5	1732.6	337.9
5/04/2012	29	307.3	4.1	760.0	37.0	1010.4	34.4	2717.2	466.7	143.3	15.2	320.1	-228.0	2066.6	324.5	1718.1	324.1
6/04/2012	30	307.6	4.3	760.7	37.6	1009.0	33.2	2713.0	462.7	147.2	18.8	295.8	-251.0	2068.2	326.1	1715.4	321.5
7/04/2012	31	307.6	4.3	758.5	35.5	1017.0	40.7	2718.1	467.6	164.0	34.8	292.9	-253.8	2073.6	331.1	1727.8	333.3
8/04/2012	32	307.7	4.4	756.5	33.7	1017.2	40.9	2723.6	472.8	169.3	39.8	278.9	-267.1	2080.8	337.9	1732.6	337.8
9/04/2012	33	307.7	4.4	754.0	31.3	1016.9	40.6	2728.3	477.3	155.6	26.8	261.8	-283.3	2087.8	344.7	1737.2	342.2
10/04/2012	34	308.4	5.1	753.4	30.7	1013.9	37.8	2767.5	514.4	155.9	27.0	265.0	-280.2	2114.4	369.8	1771.0	374.3
11/04/2012	35	309.4	6.1	751.0	28.4	1026.9	50.1	2788.4	534.2	159.5	30.5	265.7	-279.6	2142.8	396.7	1791.4	393.6
12/04/2012	36	309.7	6.3	755.1	32.4	1036.0	58.7	2790.4	536.1	154.9	26.1	270.8	-274.8	2132.7	387.2	1799.1	400.9
13/04/2012	37	310.2	6.8	731.7	10.1	1031.7	54.6	2789.8	535.6	153.1	24.5	257.8	-287.0	2130.3	384.9	1796.6	398.6
16/04/2012	40	310.7	7.2	747.9	25.5	1050.3	72.3	2816.2	560.5	163.6	34.4	252.0	-292.6	2146.4	400.2	1820.3	421.0
17/04/2012	41	311.0	7.5	765.4	42.1	1009.4	33.5	2777.3	523.7	167.0	37.6	224.4	-318.7	2110.5	366.1	1788.1	390.5
18/04/2012	42	311.5	8.1	768.1	44.7	1009.2	33.4	2769.5	516.3	169.2	39.7	227.9	-315.4	2101.7	357.8	1784.8	387.4
19/04/2012	43	311.6	8.1	752.4	29.7	1017.1	40.8	2764.5	511.5	182.0	51.8	240.2	-303.8	2104.4	360.4	1785.6	388.2
20/04/2012	44	311.7	8.3	744.7	22.5	1013.4	37.3	2752.8	500.4	174.3	44.5	235.9	-307.9	2085.9	342.8	1777.1	380.1
21/04/2012	45	311.8	8.3	763.4	40.2	990.6	15.7	2740.1	488.4	173.1	43.4	220.7	-322.2	2086.3	343.2	1765.3	368.9
22/04/2012	46	312.5	9.0	756.0	33.2	978.4	4.1	2738.4	486.8	174.6	44.8	205.7	-336.5	2086.1	343.0	1762.6	366.3

23/04/2012	47	312.8	9.3	763.4	40.2	983.2	8.6	2747.3	495.2	179.3	49.3	204.6	-337.6	2077.6	334.9	1767.8	371.3
24/04/2012	48	313.2	9.6	742.5	20.4	999.8	24.4	2776.9	523.3	180.7	50.6	209.4	-333.0	2122.2	377.2	1791.1	393.4
25/04/2012	49	313.3	9.7	747.5	25.1	966.9	-6.8	2789.6	535.3	187.0	56.6	154.7	-384.8	2137.2	391.5	1796.6	398.5
26/04/2012	50	313.4	9.8	755.0	32.2	987.7	13.0	2801.9	547.0	187.5	57.0	147.5	-391.6	2127.3	382.1	1809.7	410.9
27/04/2012	51	313.4	9.8	758.4	35.5	1018.9	42.5	2812.0	556.6	181.2	51.1	159.3	-380.4	2151.1	404.6	1821.1	421.8
28/04/2012	52	314.0	10.4	765.6	42.3	1018.0	41.6	2803.9	548.9	183.8	53.5	161.1	-378.7	2142.1	396.1	1817.4	418.2
29/04/2012	53	314.0	10.4	762.8	39.6	1014.4	38.2	2798.7	544.0	188.9	58.4	153.2	-386.2	2135.4	389.7	1812.2	413.3
30/04/2012	54	314.1	10.5	755.2	32.4	1014.6	38.5	2813.8	558.3	200.1	69.0	141.7	-397.1	2141.2	395.2	1821.6	422.3
1/05/2012	55	314.2	10.6	752.3	29.7	1012.2	36.1	2811.3	555.9	202.1	70.9	137.9	-400.7	2137.1	391.4	1820.7	421.4
2/05/2012	56	314.3	10.7	758.1	35.1	1017.5	41.2	2810.8	555.4	205.8	74.4	143.2	-395.7	2138.1	392.3	1822.3	422.9
3/05/2012	57	314.4	10.8	751.4	28.8	1020.4	43.9	2809.1	553.8	207.1	75.7	144.9	-394.1	2133.0	387.4	1823.7	424.2
4/05/2012	58	314.5	10.9	745.4	23.1	1014.8	38.7	2824.4	568.3	205.1	73.8	123.0	-414.9	2147.8	401.5	1833.1	433.1
5/05/2012	59	314.7	11.1	749.5	27.1	1006.9	31.1	2831.9	575.5	206.9	75.4	109.2	-427.9	2149.3	402.9	1839.3	439.0
6/05/2012	60	314.8	11.1	754.3	31.6	1003.2	27.7	2838.2	581.4	208.9	77.3	104.2	-432.6	2168.8	421.4	1847.1	446.4
7/05/2012	61	314.8	11.2	767.7	44.3	1015.1	38.9	2850.6	593.1	220.2	88.0	105.6	-431.3	2168.3	420.9	1858.6	457.3
8/05/2012	62	315.3	11.6	745.5	23.3	1024.9	48.2	2860.8	602.8	230.8	98.1	107.3	-429.7	2184.2	436.0	1867.8	466.0
9/05/2012	63	315.4	11.7	738.2	16.4	1025.4	48.7	2862.7	604.6	234.1	101.2	107.0	-430.0	2189.1	440.6	1870.0	468.1
10/05/2012	64	315.4	11.8	741.2	19.2	1023.3	46.7	2856.2	598.4	228.4	95.8	101.9	-434.9	2180.8	432.7	1864.5	462.9
11/05/2012	65	315.5	11.8	739.4	17.4	1018.6	42.2	2848.5	591.2	226.3	93.8	94.6	-441.8	2176.6	428.8	1858.3	457.0
12/05/2012	66	315.6	11.9	741.8	19.8	1019.8	43.4	2864.2	606.0	227.0	94.5	90.9	-445.3	2203.4	454.2	1871.7	469.7
13/05/2012	67	315.6	11.9	736.9	15.0	1004.3	28.7	2867.6	609.3	226.7	94.2	66.6	-468.3	2190.6	442.1	1871.0	469.1
14/05/2012	68	315.8	12.1	730.5	9.0	1021.1	44.6	2891.5	632.0	231.4	98.6	72.7	-462.6	2211.9	462.2	1891.3	488.3
15/05/2012	69	316.0	12.3	745.7	23.4	1021.2	44.7	2900.9	640.8	228.1	95.5	67.2	-467.7	2224.4	474.1	1897.6	494.3
16/05/2012	70	316.1	12.4	747.6	25.2	1024.7	48.0	2899.3	639.3	231.1	98.3	68.3	-466.7	2220.1	470.0	1899.5	496.1
17/05/2012	71	316.2	12.5	743.2	21.1	1037.3	59.9	2913.1	652.4	239.5	106.3	83.9	-451.9	2245.0	493.6	1916.6	512.3
18/05/2012	72	316.2	12.5	734.7	13.0	1028.4	51.5	2906.3	646.0	243.8	110.4	72.7	-462.5	2231.2	480.6	1907.2	503.4
19/05/2012	73	316.3	12.6	736.0	14.2	1026.5	49.7	2902.7	642.6	242.5	109.2	65.1	-469.7	2229.2	478.7	1906.0	502.3
20/05/2012	74	316.3	12.6	746.5	24.2	1020.3	43.9	2913.6	652.8	259.3	125.1	55.7	-478.7	2250.8	499.1	1916.2	511.9
21/05/2012	75	316.5	12.8	729.7	8.2	1024.0	47.3	2905.3	645.0	273.0	138.1	60.0	-474.6	2228.2	477.7	1911.4	507.3
22/05/2012	76	317.1	13.3	718.9	-2.0	1023.3	46.7	2909.4	648.9	270.4	135.6	53.6	-480.6	2237.9	486.9	1915.4	511.1
23/05/2012	77	317.3	13.5	727.7	6.4	1016.9	40.6	2930.4	668.8	266.2	131.6	41.3	-492.3	2254.7	502.8	1932.0	526.9
24/05/2012	78	317.5	13.7	737.7	15.9	1017.4	41.1	2927.4	666.0	269.2	134.5	35.6	-497.7	2249.8	498.2	1930.3	525.2
25/05/2012	79	317.5	13.7	725.0	3.8	1025.1	48.4	2918.6	657.6	272.5	137.6	43.7	-490.0	2246.7	495.3	1927.6	522.7
26/05/2012	80	318.1	14.3	730.4	8.9	1018.0	41.6	2938.5	676.5	257.2	123.1	29.1	-503.8	2256.5	504.5	1942.8	537.1
27/05/2012	81	318.2	14.4	756.0	33.2	1011.0	35.0	2937.6	675.6	264.4	130.0	22.6	-510.0	2265.5	513.0	1940.6	535.0
28/05/2012	82	318.5	14.7	723.5	2.4	1030.4	53.4	2948.0	685.5	264.4	130.0	32.4	-500.7	2280.9	527.6	1949.8	543.8
29/05/2012	83	318.5	14.7	735.2	13.5	1021.7	45.2	2931.8	670.1	266.5	131.9	26.9	-505.9	2273.0	520.2	1937.5	532.1

30/05/2012	84	318.8	15.0	731.1	9.6	1030.7	53.7	2940.2	678.1	262.9	128.6	37.1	-496.3	2275.9	522.9	1946.6	540.8
31/05/2012	85	319.1	15.3	734.7	13.0	1023.2	46.6	2935.5	673.6	267.9	133.2	27.3	-505.6	2265.2	512.8	1942.0	536.4
1/06/2012	86	319.2	15.3	743.7	21.5	1036.1	58.8	2938.8	676.8	268.8	134.1	36.8	-496.6	2258.9	506.8	1949.6	543.5
2/06/2012	87	319.6	15.7	736.6	14.8	1023.9	47.3	2916.5	655.6	273.3	138.3	25.1	-507.6	2238.9	487.8	1933.1	527.9
3/06/2012	88	319.6	15.7	741.4	19.3	1028.6	51.7	2918.7	657.7	285.8	150.2	36.4	-496.9	2249.7	498.1	1936.4	531.1
4/06/2012	89	320.3	16.4	730.5	9.0	1028.2	51.3	2915.2	654.4	285.5	149.9	31.6	-501.5	2241.1	490.0	1931.8	526.6
5/06/2012	90	320.5	16.6	733.5	11.8	1032.2	55.1	2950.1	687.5	289.4	153.7	18.1	-514.3	2264.3	511.9	1957.1	550.7
6/06/2012	91	320.6	16.6	722.4	1.4	1024.4	47.7	2942.5	680.3	288.2	152.5	6.2	-525.6	2255.8	503.9	1951.7	545.5
7/06/2012	92	320.6	16.7	742.4	20.3	1031.6	54.5	2961.6	698.4	281.3	145.9	11.6	-520.4	2279.4	526.2	1966.1	559.2
8/06/2012	93	320.6	16.7	750.6	28.1	1033.4	56.3	2977.7	713.6	285.3	149.8	4.2	-527.5	2317.9	562.7	1981.6	573.9
9/06/2012	94	320.7	16.7	749.6	27.2	1029.1	52.1	2980.9	716.7	286.2	150.6	-0.9	-532.3	2323.0	567.6	1984.1	576.3
10/06/2012	95	320.8	16.8	752.1	29.5	1028.6	51.7	2977.8	713.7	292.4	156.5	-1.0	-532.4	2313.5	558.5	1981.6	573.9
11/06/2012	96	321.1	17.1	760.0	37.0	1025.0	48.3	2961.3	698.1	291.3	155.4	1.0	-530.5	2282.8	529.5	1970.8	563.7
12/06/2012	97	321.3	17.3	757.1	34.2	1027.9	51.0	2955.7	692.7	305.2	168.6	5.0	-526.7	2270.7	517.9	1968.8	561.8
13/06/2012	98	321.8	17.8	763.4	40.2	1034.3	57.1	2956.7	693.8	306.8	170.1	15.0	-517.3	2281.1	527.8	1972.3	565.0
14/06/2012	99	322.0	17.9	770.2	46.7	1038.4	61.0	2951.1	688.4	307.5	170.8	16.9	-515.5	2272.7	519.9	1968.5	561.5
15/06/2012	100	322.3	18.3	758.6	35.7	1036.2	58.9	2946.2	683.8	317.7	180.4	10.8	-521.2	2258.5	506.4	1963.0	556.2
16/06/2012	101	322.8	18.7	760.2	37.2	1032.8	55.7	2943.7	681.4	320.6	183.2	5.5	-526.2	2259.2	507.1	1961.8	555.1
17/06/2012	102	323.0	18.9	761.6	38.5	1026.5	49.7	2948.6	686.1	331.8	193.9	-4.8	-536.0	2268.9	516.3	1965.8	558.9
18/06/2012	103	323.0	18.9	766.0	42.6	1037.8	60.5	2985.6	721.1	337.3	199.1	-9.4	-540.3	2304.5	550.1	1994.0	585.6
19/06/2012	104	323.4	19.3	766.0	42.7	1032.5	55.4	2994.7	729.7	343.4	204.8	-20.4	-550.8	2322.0	566.6	1998.9	590.2
20/06/2012	105	324.0	19.9	758.6	35.6	1031.5	54.5	2998.9	733.7	340.7	202.2	-21.0	-551.3	2323.1	567.6	2002.4	593.6
21/06/2012	106	324.4	20.3	756.4	33.5	1038.0	60.6	3007.3	741.7	333.2	195.1	-22.1	-552.4	2344.4	587.9	2010.8	601.6
22/06/2012	107	324.7	20.5	752.9	30.3	1020.6	44.2	2996.9	731.9	329.4	191.6	-36.0	-565.5	2312.9	558.0	2000.5	591.8
23/06/2012	108	325.2	21.0	758.3	35.4	1021.9	45.3	3009.9	744.1	327.2	189.5	-34.3	-563.9	2344.7	588.1	2012.6	603.2
24/06/2012	109	325.3	21.1	764.2	40.9	1023.9	47.2	3013.8	747.9	328.2	190.4	-41.3	-570.6	2359.7	602.3	2015.1	605.6
25/06/2012	110	325.9	21.7	754.8	32.1	1023.0	46.4	3015.1	749.1	333.5	195.5	-41.9	-571.2	2359.8	602.4	2015.3	605.8
26/06/2012	111	325.9	21.7	755.4	32.7	1014.3	38.2	3002.3	736.9	340.5	202.1	-44.8	-573.9	2336.8	580.6	2003.9	595.1
27/06/2012	112	326.5	22.3	752.0	29.4	1022.6	46.0	2993.4	728.5	334.5	196.4	-36.0	-565.6	2335.8	579.7	2001.0	592.3
28/06/2012	113	326.7	22.4	741.9	19.9	1021.1	44.6	2995.5	730.5	345.9	207.2	-34.9	-564.5	2332.4	576.4	2002.9	594.1
29/06/2012	114	327.7	23.4	743.0	20.9	1017.1	40.8	2983.0	718.7	357.4	218.1	-38.2	-567.7	2306.0	551.5	1992.3	584.0
30/06/2012	115	327.8	23.5	761.1	38.0	1016.5	40.3	2980.3	716.1	362.9	223.3	-37.7	-567.1	2307.1	552.5	1993.6	585.3
1/07/2012	116	328.5	24.2	771.5	47.9	1014.0	37.9	2996.3	731.3	355.8	216.6	-50.4	-579.2	2318.0	562.8	2004.7	595.8
2/07/2012	117	329.2	24.9	766.5	43.1	1023.6	47.0	3025.0	758.4	366.5	226.7	-56.6	-585.1	2362.3	604.8	2027.1	617.0
3/07/2012	118	329.5	25.1	760.7	37.6	1022.6	46.0	3035.5	768.4	356.0	216.7	-58.4	-586.8	2370.7	612.7	2035.1	624.6
4/07/2012	119	329.9	25.5	768.2	44.7	1017.5	41.2	3038.4	771.2	367.1	227.2	-62.4	-590.5	2369.2	611.3	2036.2	625.6
5/07/2012	120	330.3	25.8	770.1	46.6	1016.7	40.5	3031.2	764.4	357.2	217.9	-57.3	-585.8	2359.9	602.6	2031.7	621.4

6/07/2012	121	330.5	26.1	759.0	36.1	1022.3	45.7	3016.3	750.2	363.5	223.9	-59.0	-587.3	2346.3	589.6	2020.1	610.4
7/07/2012	122	331.8	27.3	774.8	51.0	1026.7	49.9	3018.0	751.8	354.3	215.1	-58.4	-586.8	2343.3	586.8	2021.6	611.8
8/07/2012	123	331.9	27.3	775.2	51.4	1020.4	44.0	3003.0	737.6	361.4	221.8	-65.7	-593.7	2322.0	566.6	2010.7	601.4
9/07/2012	124	332.4	27.9	783.5	59.3	1036.0	58.7	3017.5	751.3	374.0	233.8	-49.5	-578.4	2350.3	593.5	2026.5	616.5
10/07/2012	125	332.9	28.3	780.6	56.5	1027.6	50.7	3009.5	743.8	366.7	226.9	-52.1	-580.8	2347.4	590.7	2020.2	610.5
11/07/2012	126	335.4	30.7	777.5	53.6	1019.7	43.3	2999.0	733.8	373.1	232.9	-54.4	-583.0	2338.6	582.4	2013.0	603.7
12/07/2012	127	335.8	31.1	790.4	65.8	1027.4	50.6	3011.0	745.2	384.1	243.4	-51.3	-580.1	2339.5	583.2	2022.6	612.7
13/07/2012	128	335.9	31.2	784.3	60.0	1026.0	49.3	3001.5	736.2	391.1	250.0	-48.8	-577.7	2320.6	565.2	2016.3	606.8
14/07/2012	129	337.3	32.5	783.1	58.9	1004.2	28.6	2985.5	721.0	386.5	245.7	-61.5	-589.8	2281.4	528.2	2002.6	593.8
15/07/2012	130	337.4	32.6	787.2	62.8	999.4	24.0	3004.0	738.6	394.2	253.0	-79.2	-606.5	2313.9	558.9	2015.1	605.6
16/07/2012	131	337.6	32.8	790.8	66.2	1014.7	38.5	3041.0	773.6	404.0	262.2	-76.8	-604.2	2368.5	610.6	2045.8	634.7
17/07/2012	132	339.1	34.2	782.0	57.8	1011.6	35.6	3036.5	769.4	415.3	272.9	-80.5	-607.7	2367.6	609.8	2041.2	630.4
18/07/2012	133	339.9	34.9	793.0	68.3	1005.1	29.4	3036.4	769.3	401.6	260.0	-89.0	-615.8	2355.3	598.2	2039.1	628.4
19/07/2012	134	340.7	35.7	808.9	83.3	1003.8	28.2	3045.5	777.9	400.8	259.2	-92.7	-619.3	2368.0	610.3	2046.5	635.4
20/07/2012	135	341.6	36.6	798.0	73.0	1010.4	34.5	3057.2	788.9	405.9	264.1	-88.8	-615.6	2390.2	631.2	2058.4	646.7
21/07/2012	136	342.6	37.5	790.7	66.1	1005.1	29.4	3041.6	774.2	399.2	257.7	-93.8	-620.3	2354.1	597.0	2044.6	633.6
22/07/2012	137	344.3	39.1	810.2	84.5	996.9	21.6	3035.4	768.3	420.3	277.7	-92.2	-618.8	2348.0	591.3	2040.4	629.6
23/07/2012	138	345.4	40.1	819.5	93.4	994.8	19.7	3030.2	763.4	422.9	280.1	-92.8	-619.4	2335.9	579.8	2036.7	626.1
24/07/2012	139	346.3	41.0	823.1	96.8	1004.2	28.6	3020.6	754.3	431.7	288.5	-88.5	-615.3	2336.6	580.5	2030.8	620.5
25/07/2012	140	346.3	41.0	828.7	102.1	1015.9	39.7	3014.2	748.3	437.1	293.7	-83.0	-610.1	2340.7	584.3	2028.5	618.4
26/07/2012	141	346.8	41.5	815.9	90.0	1014.1	37.9	3023.1	756.7	438.7	295.2	-86.6	-613.6	2340.5	584.1	2034.3	623.8
27/07/2012	142	347.3	42.0	808.3	82.8	1003.6	28.0	3034.7	767.6	437.4	293.9	-96.6	-623.0	2362.9	605.4	2042.2	631.4
28/07/2012	143	348.8	43.4	807.6	82.1	1001.7	26.2	3050.6	782.7	435.5	292.1	-108.5	-634.3	2372.4	614.3	2052.4	641.0
29/07/2012	144	348.9	43.5	824.4	98.0	1002.4	26.9	3057.4	789.2	441.2	297.5	-111.6	-637.2	2368.5	610.6	2057.3	645.7
30/07/2012	145	349.5	44.0	819.1	93.0	1004.6	29.0	3065.3	796.7	453.5	309.1	-113.0	-638.5	2392.7	633.7	2066.8	654.7
31/07/2012	146	350.4	44.9	835.3	108.3	1006.7	31.0	3070.4	801.5	472.9	327.6	-110.6	-636.3	2403.6	644.0	2071.2	658.8
1/08/2012	147	351.2	45.7	832.6	105.8	1009.2	33.4	3073.0	804.0	472.4	327.1	-111.8	-637.4	2406.0	646.2	2072.8	660.3
2/08/2012	148	351.2	45.7	816.9	90.9	1000.9	25.5	3077.8	808.5	468.1	323.0	-116.0	-641.4	2410.8	650.7	2076.2	663.6
3/08/2012	149	351.3	45.7	825.3	98.8	1009.2	33.3	3078.6	809.3	472.8	327.4	-118.5	-643.8	2413.4	653.2	2077.3	664.6
4/08/2012	150	351.3	45.8	834.3	107.4	1000.3	24.9	3078.1	808.8	483.0	337.2	-130.0	-654.7	2406.7	646.9	2074.8	662.3
5/08/2012	151	351.9	46.4	842.5	115.2	993.1	18.1	3077.8	808.5	491.7	345.4	-135.6	-660.0	2399.6	640.2	2073.2	660.7
6/08/2012	152	352.9	47.3	836.8	109.7	988.7	13.8	3082.1	812.6	492.1	345.7	-138.8	-663.1	2396.7	637.4	2075.9	663.2
7/08/2012	153	353.2	47.6	845.2	117.8	1004.5	28.9	3100.6	830.1	483.0	337.1	-129.7	-654.4	2433.9	672.7	2096.5	682.8
8/08/2012	154	353.6	48.0	843.2	115.8	1008.0	32.2	3095.6	825.3	489.4	343.2	-130.6	-655.2	2431.1	670.1	2090.8	677.4
9/08/2012	155	355.5	49.8	843.3	115.9	996.2	21.0	3091.1	821.1	538.8	390.0	-138.7	-662.9	2413.9	653.7	2084.3	671.3
10/08/2012	156	357.1	51.2	842.8	115.4	1002.8	27.2	3101.4	830.9	533.6	385.1	-137.4	-661.7	2436.5	675.2	2096.8	683.1
11/08/2012	157	357.8	52.0	839.3	112.1	994.1	19.0	3079.7	810.3	534.6	386.1	-143.8	-667.8	2397.3	638.0	2076.5	663.8

12/08/2012	158	357.9	52.0	842.3	115.0	994.0	18.9	3059.8	791.5	550.9	401.5	-143.3	-667.2	2368.4	610.6	2062.7	650.8
13/08/2012	159	359.6	53.7	851.6	123.8	1000.8	25.3	3068.8	800.0	566.7	416.5	-139.6	-663.7	2387.7	628.8	2071.5	659.1
14/08/2012	160	360.3	54.2	852.6	124.7	1012.2	36.2	3079.7	810.4	572.0	421.5	-132.1	-656.7	2408.4	648.5	2081.6	668.7
15/08/2012	161	360.3	54.3	841.9	114.6	1010.0	34.1	3082.5	813.0	560.3	410.4	-144.9	-668.8	2389.4	630.5	2077.9	665.2
16/08/2012	162	361.9	55.8	840.5	113.3	1006.2	30.5	3089.6	819.7	559.1	409.3	-146.1	-669.9	2392.4	633.4	2083.5	670.4
17/08/2012	163	362.6	56.4	843.7	116.4	998.4	23.1	3090.2	820.3	589.5	438.1	-149.5	-673.2	2374.4	616.3	2083.2	670.2
18/08/2012	164	363.0	56.9	851.3	123.5	983.2	8.7	3092.3	822.2	598.7	446.8	-160.1	-683.2	2353.5	596.5	2083.0	670.0
19/08/2012	165	363.6	57.4	862.9	134.5	992.6	17.6	3095.8	825.5	610.2	457.7	-156.6	-679.9	2377.1	618.8	2088.7	675.4
20/08/2012	166	366.4	60.0	858.2	130.1	1004.0	28.4	3104.6	833.9	606.7	454.4	-151.1	-674.7	2412.5	652.4	2100.5	686.6
21/08/2012	167	366.9	60.5	859.5	131.3	991.1	16.2	3093.2	823.1	607.1	454.7	-155.3	-678.6	2393.4	634.3	2089.3	676.0
22/08/2012	168	366.9	60.6	869.1	140.4	981.3	6.9	3084.9	815.2	601.5	449.4	-153.0	-676.5	2361.9	604.5	2080.0	667.2
23/08/2012	169	370.2	63.7	875.1	146.1	990.7	15.8	3078.0	808.7	618.1	465.2	-137.5	-661.8	2358.1	600.9	2083.5	670.4
24/08/2012	170	376.2	69.3	864.0	135.6	985.8	11.1	3069.2	800.4	632.3	478.7	-144.4	-668.3	2352.0	595.1	2076.3	663.7
25/08/2012	171	378.9	71.9	869.5	140.8	983.7	9.2	3078.2	808.9	635.2	481.4	-165.0	-687.9	2357.3	600.1	2077.8	665.1
26/08/2012	172	381.9	74.7	889.1	159.4	988.3	13.5	3095.1	824.9	659.4	504.4	-169.1	-691.7	2348.4	591.6	2091.3	677.9
27/08/2012	173	382.1	75.0	892.1	162.2	997.2	22.0	3106.8	836.0	692.0	535.3	-165.2	-688.0	2375.2	617.1	2102.6	688.6
28/08/2012	174	382.8	75.6	886.1	156.5	988.2	13.4	3094.5	824.4	686.8	530.3	-162.9	-685.8	2357.2	599.9	2094.0	680.5
29/08/2012	175	384.5	77.2	896.4	166.2	992.1	17.1	3087.0	817.2	708.8	551.2	-155.0	-678.4	2339.4	583.1	2090.9	677.5
30/08/2012	176	384.5	77.3	903.8	173.3	993.8	18.7	3086.6	816.9	756.7	596.5	-152.6	-676.1	2351.1	594.2	2090.3	676.9
31/08/2012	177	385.0	77.7	888.9	159.1	986.7	11.9	3103.1	832.5	774.1	613.0	-174.2	-696.6	2385.5	626.8	2100.6	686.7
1/09/2012	178	385.5	78.1	899.1	168.9	989.8	14.9	3120.7	849.2	764.7	604.1	-172.8	-695.2	2414.8	654.6	2116.9	702.1
2/09/2012	179	385.5	78.1	897.3	167.2	978.7	4.4	3114.3	843.1	750.6	590.8	-173.6	-696.0	2400.2	640.7	2109.4	695.1
3/09/2012	180	386.5	79.2	894.4	164.4	989.9	15.0	3117.4	846.0	779.9	618.5	-166.6	-689.3	2415.8	655.5	2113.2	698.6
4/09/2012	181	386.7	79.3	899.6	169.3	993.0	18.0	3109.2	838.3	787.0	625.2	-174.2	-696.6	2399.1	639.7	2103.5	689.4
5/09/2012	182	387.9	80.4	903.0	172.5	981.9	7.4	3111.5	840.5	813.3	650.2	-184.7	-706.5	2403.4	643.8	2103.3	689.2
6/09/2012	183	389.1	81.6	909.3	178.5	989.7	14.8	3131.1	859.0	819.2	655.8	-180.7	-702.8	2430.0	669.0	2120.4	705.5
7/09/2012	184	390.9	83.3	901.8	171.4	996.7	21.4	3145.6	872.7	835.3	671.1	-182.0	-703.9	2446.2	684.3	2133.6	718.0
8/09/2012	185	391.2	83.6	902.9	172.4	993.9	18.8	3147.4	874.5	827.0	663.2	-181.9	-703.9	2445.2	683.3	2133.6	718.0
9/09/2012	186	392.3	84.6	903.3	172.8	976.4	2.2	3135.5	863.2	844.3	679.6	-185.8	-707.6	2414.9	654.6	2123.1	708.0
10/09/2012	187	392.6	84.9	910.2	179.4	976.1	2.0	3123.5	851.9	887.6	720.7	-182.1	-704.1	2395.5	636.3	2115.3	700.6
11/09/2012	188	395.0	87.2	912.9	181.9	986.2	11.5	3113.3	842.2	886.2	719.3	-168.0	-690.7	2400.2	640.7	2113.2	698.7
12/09/2012	189	395.7	87.9	907.2	176.6	988.1	13.3	3105.0	834.3	888.1	721.1	-154.8	-678.1	2389.1	630.3	2110.1	695.7
13/09/2012	190	396.4	88.5	919.4	188.1	989.5	14.7	3086.8	817.1	889.5	722.5	-155.3	-678.6	2362.8	605.3	2096.2	682.5
14/09/2012	191	396.9	89.0	923.8	192.3	997.2	22.0	3105.5	834.8	897.2	729.8	-153.0	-676.5	2398.0	638.6	2113.7	699.1
15/09/2012	192	397.0	89.1	925.7	194.0	994.6	19.5	3107.5	836.6	894.6	727.3	-168.7	-691.4	2353.0	596.0	2108.4	694.1
16/09/2012	193	397.9	89.9	926.6	194.9	992.4	17.4	3097.3	827.0	892.4	725.2	-171.1	-693.6	2318.5	563.3	2101.9	688.0
17/09/2012	194	404.6	96.3	948.1	215.3	998.7	23.3	3086.2	816.5	898.7	731.1	-164.1	-687.0	2326.7	571.0	2098.3	684.5

18/09/2012	195	409.8	101.2	945.2	212.5	999.5	24.1	3078.2	808.9	899.5	731.9	-154.4	-677.8	2337.3	581.1	2094.0	680.4
19/09/2012	196	410.1	101.5	946.6	213.9	1004.4	28.8	3077.4	808.1	904.4	736.6	-152.2	-675.7	2353.1	596.1	2093.5	680.0
20/09/2012	197	410.8	102.2	953.2	220.1	1007.9	32.0	3078.2	808.9	907.9	739.8	-150.6	-674.2	2348.7	591.9	2092.8	679.3
21/09/2012	198	411.3	102.6	944.1	211.5	1007.1	31.3	3079.6	810.2	907.1	739.1	-137.3	-661.6	2386.7	627.9	2099.5	685.7
22/09/2012	199	411.8	103.1	954.3	221.2	1003.5	27.9	3073.8	804.7	903.5	735.7	-142.1	-666.2	2386.7	628.0	2093.7	680.2
23/09/2012	200	413.5	104.7	958.8	225.4	1005.3	29.7	3068.4	799.6	905.3	737.5	-142.8	-666.8	2370.2	612.3	2090.2	676.9
24/09/2012	201	414.2	105.4	961.8	228.3	1014.8	38.6	3086.2	816.5	914.8	746.4	-139.9	-664.1	2386.5	627.8	2103.8	689.7
25/09/2012	202	415.5	106.6	958.7	225.3	1010.1	34.2	3096.0	825.8	910.1	742.0	-148.9	-672.5	2412.9	652.7	2109.2	694.8
26/09/2012	203	416.5	107.6	954.8	221.7	1006.8	31.1	3090.2	820.2	906.8	738.9	-150.7	-674.2	2394.4	635.2	2104.8	690.6
27/09/2012	204	416.6	107.6	954.9	221.8	1011.3	35.3	3087.4	817.6	911.3	743.1	-143.0	-667.0	2384.2	625.6	2105.1	690.9
28/09/2012	205	416.6	107.6	962.8	229.2	1003.5	27.9	3077.5	808.2	903.5	735.7	-141.5	-665.6	2369.5	611.7	2099.3	685.4
29/09/2012	206	417.1	108.1	964.5	230.9	997.7	22.4	3065.5	796.9	897.7	730.2	-142.7	-666.7	2360.3	602.9	2091.6	678.1
30/09/2012	207	418.4	109.4	970.8	236.8	1001.7	26.2	3084.9	815.2	901.7	734.0	-159.4	-682.5	2380.5	622.1	2101.3	687.4
1/10/2012	208	418.9	109.8	971.4	237.4	1000.2	24.8	3105.0	834.3	900.2	732.6	-165.7	-688.5	2401.0	641.5	2114.8	700.2
2/10/2012	209	419.0	109.9	966.8	233.0	985.1	10.5	3095.7	825.5	885.1	718.3	-173.1	-695.5	2374.8	616.6	2104.1	690.0
3/10/2012	210	419.5	110.4	978.7	244.3	1001.2	25.8	3104.0	833.4	901.2	733.6	-162.2	-685.2	2382.6	624.0	2114.3	699.6
4/10/2012	211	420.1	111.0	973.6	239.4	996.8	21.5	3102.7	832.1	896.8	729.4	-161.3	-684.3	2366.2	608.5	2114.4	699.8
5/10/2012	212	420.3	111.2	976.6	242.3	1002.4	26.9	3110.5	839.5	902.4	734.7	-166.8	-689.5	2412.8	652.7	2119.1	704.2
6/10/2012	213	421.2	112.0	972.5	238.4	999.7	24.3	3096.0	825.8	899.7	732.1	-155.8	-679.1	2398.3	638.9	2111.4	696.9
7/10/2012	214	421.5	112.3	987.2	252.3	1006.4	30.7	3089.6	819.7	906.4	738.5	-148.8	-672.5	2369.7	611.8	2109.3	694.9
8/10/2012	215	423.2	114.0	977.2	242.9	1006.1	30.4	3100.1	829.7	906.1	738.2	-154.7	-678.1	2374.3	616.2	2114.6	699.9
9/10/2012	216	424.1	114.8	988.0	253.1	1000.7	25.3	3110.9	839.9	900.7	733.1	-151.1	-674.6	2384.9	626.3	2121.7	706.7
10/10/2012	217	424.6	115.2	978.2	243.8	1004.3	28.7	3119.0	847.5	904.3	736.5	-152.9	-676.3	2398.8	639.4	2127.4	712.1
11/10/2012	218	427.8	118.3	991.2	256.1	994.1	19.0	3111.4	840.4	894.1	726.8	-158.5	-681.6	2389.3	630.4	2120.6	705.6
12/10/2012	219	427.9	118.4	976.9	242.6	1023.6	46.9	3137.6	865.2	923.6	754.7	-142.0	-666.0	2435.5	674.2	2146.9	730.6
13/10/2012	220	429.3	119.7	987.8	252.9	1003.7	28.1	3131.6	859.5	903.7	735.9	-154.8	-678.1	2401.5	641.9	2136.7	720.9
14/10/2012	221	429.4	119.8	996.0	260.7	999.7	24.3	3117.2	845.9	899.7	732.1	-162.4	-685.4	2370.9	613.0	2126.3	711.1
15/10/2012	222	429.8	120.2	994.8	259.5	1009.2	33.3	3116.9	845.6	909.2	741.1	-156.5	-679.8	2364.0	606.5	2126.2	711.0
16/10/2012	223	431.1	121.4	998.4	263.0	1001.2	25.8	3110.0	839.1	901.2	733.6	-159.0	-682.1	2375.6	617.4	2120.8	705.9
17/10/2012	224	433.3	123.5	1004.5	268.7	990.1	15.2	3102.7	832.1	890.1	723.0	-168.8	-691.4	2383.1	624.5	2112.4	697.9
18/10/2012	225	434.4	124.5	1007.0	271.1	1008.8	32.9	3098.6	828.3	908.8	740.7	-164.0	-686.9	2362.6	605.1	2111.9	697.4
19/10/2012	226	434.8	124.9	1006.6	270.7	1018.9	42.5	3102.6	832.0	918.9	750.3	-141.6	-665.7	2387.0	628.2	2121.9	706.9
20/10/2012	227	435.0	125.1	1016.3	279.9	1004.3	28.7	3083.8	814.2	904.3	736.5	-142.0	-666.0	2367.5	609.7	2107.9	693.6
21/10/2012	228	435.1	125.2	1025.2	288.4	1001.4	25.9	3063.1	794.6	901.4	733.7	-147.2	-671.0	2350.9	594.0	2092.9	679.4
22/10/2012	229	439.5	129.4	1030.4	293.3	1005.0	29.4	3067.1	798.4	905.0	737.2	-148.3	-672.0	2364.4	606.8	2094.6	681.0
23/10/2012	230	442.2	132.0	1021.2	284.6	1010.0	34.1	3090.8	820.9	910.0	741.9	-155.4	-678.7	2397.5	638.2	2108.4	694.1
24/10/2012	231	444.6	134.2	1023.5	286.8	1010.8	34.8	3105.9	835.2	910.8	742.6	-153.1	-676.5	2400.8	641.3	2121.0	706.0

25/10/2012	232	444.9	134.5	1024.4	287.6	1001.2	25.7	3085.4	815.7	901.2	733.5	-161.8	-684.8	2370.2	612.3	2103.3	689.2
26/10/2012	233	444.9	134.5	1013.4	277.2	1004.5	28.9	3079.7	810.3	904.5	736.7	-156.2	-679.5	2371.8	613.8	2100.7	686.8
27/10/2012	234	446.0	135.6	1032.7	295.5	1012.0	36.0	3087.3	817.6	912.0	743.8	-149.8	-673.4	2355.7	598.5	2109.0	694.7
28/10/2012	235	446.1	135.6	1034.1	296.8	1012.6	36.5	3094.4	824.3	912.6	744.3	-158.0	-681.2	2365.5	607.8	2111.4	696.9
29/10/2012	236	446.8	136.2	1040.4	302.8	1017.0	40.7	3094.3	824.1	917.0	748.5	-162.0	-685.0	2357.3	600.1	2109.7	695.3
30/10/2012	237	447.3	136.8	1044.9	307.0	1012.1	36.1	3085.4	815.8	912.1	743.9	-160.6	-683.7	2353.6	596.6	2104.0	689.9
31/10/2012	238	449.4	138.8	1047.7	309.6	1014.6	38.4	3079.4	810.0	914.6	746.2	-148.9	-672.5	2375.1	617.0	2102.7	688.7
1/11/2012	239	450.7	140.0	1043.8	306.0	1031.1	54.0	3091.4	821.4	931.1	761.8	-129.3	-654.0	2410.3	650.3	2117.2	702.4
2/11/2012	240	453.3	142.5	1037.6	300.2	1019.4	43.0	3097.0	826.7	919.4	750.8	-148.8	-672.5	2400.6	641.2	2114.9	700.2

Table E.3 Concrete surface strain at steel level for slab D-SCC-a

Slab D-SCC-a		CONCRETE SURFACE STRAIN BY SG															
		1		2		3		4		5		6		7		8	
Date	Age	Reading	Strain	Reading	Strain	Reading	Strain	Reading	Strain	Reading	Strain	Reading	Strain	Reading	Strain	Reading	Strain
4/04/2012	14	-966.8		1072.4		1145.8		1028.7		760.4		1027.9		1022.5		510.5	
4/04/2012	14	310.1		365.3		1289.6		1220.5		775.8		322.3		1128.7		137.0	
5/04/2012	15	312.4	2.2	398.2	31.2	1403.4	107.9	1409.9	179.5	836.0	57.1	330.3	7.6	1200.7	68.2	146.4	8.9
6/04/2012	16	324.5	13.7	411.9	44.2	1406.2	110.5	1439.7	207.7	813.4	35.7	340.6	17.4	1208.1	75.2	157.8	19.7
7/04/2012	17	344.9	33.0	405.8	38.5	1430.0	133.1	1477.6	243.6	817.6	39.7	331.9	9.1	1238.3	103.9	150.0	12.3
8/04/2012	18	342.0	30.2	386.0	19.6	1438.4	141.1	1504.4	269.1	816.1	38.2	334.5	11.6	1266.8	130.9	152.5	14.7
9/04/2012	19	330.5	19.4	384.6	18.3	1446.1	148.3	1526.5	290.0	809.3	31.7	330.1	7.4	1270.6	134.5	151.8	14.0
10/04/2012	20	335.7	24.3	400.0	32.9	1510.3	209.2	1595.5	355.4	862.1	81.8	352.8	29.0	1316.6	178.1	161.6	23.4
11/04/2012	21	330.8	19.6	390.1	23.6	1545.9	243.0	1634.3	392.1	886.8	105.2	348.7	25.0	1343.5	203.6	159.3	21.1
12/04/2012	22	350.8	38.6	408.3	40.8	1567.5	263.4	1655.9	412.7	905.8	123.2	340.0	16.8	1358.4	217.8	153.0	15.2
13/04/2012	23	364.1	51.2	392.0	25.3	1570.9	266.6	1657.9	414.6	901.7	119.3	340.8	17.5	1358.0	217.4	158.9	20.8
16/04/2012	26	363.8	50.9	399.9	32.9	1619.9	313.1	1723.8	477.0	926.5	142.8	332.4	9.6	1403.5	260.5	152.1	14.3
17/04/2012	27	353.5	41.2	401.6	34.4	1561.5	257.8	1662.5	418.9	865.8	85.3	334.3	11.4	1340.5	200.8	152.9	15.1
18/04/2012	28	337.9	26.4	397.0	30.1	1560.8	257.1	1658.8	415.4	864.1	83.7	353.1	29.2	1336.5	197.0	161.1	22.9
19/04/2012	29	353.0	40.6	401.0	33.9	1567.9	263.8	1661.3	417.7	873.0	92.1	363.1	38.7	1342.4	202.6	169.9	31.1
20/04/2012	30	368.4	55.3	394.6	27.8	1563.3	259.5	1655.2	412.0	862.4	82.1	344.7	21.3	1339.2	199.5	161.2	22.9
21/04/2012	31	381.0	67.2	398.2	31.2	1543.7	240.9	1637.9	395.6	844.2	64.8	346.9	23.3	1329.7	190.5	159.6	21.4
22/04/2012	32	367.9	54.8	386.8	20.4	1534.4	232.1	1634.8	392.6	832.1	53.3	352.6	28.8	1321.7	183.0	162.9	24.6
23/04/2012	33	358.2	45.6	387.2	20.8	1542.1	239.4	1643.7	401.1	837.2	58.2	345.0	21.6	1326.5	187.5	160.4	22.2
24/04/2012	34	348.0	35.9	379.3	13.3	1571.3	267.0	1681.2	436.6	858.0	77.9	346.4	22.9	1350.9	210.7	161.5	23.2
25/04/2012	35	337.0	25.5	378.7	12.7	1563.4	259.6	1684.4	439.6	828.2	49.7	351.1	27.3	1335.1	195.7	164.0	25.6
26/04/2012	36	346.0	34.0	379.8	13.8	1573.5	269.1	1697.4	452.0	833.2	54.4	355.6	31.6	1327.0	188.0	165.9	27.4
27/04/2012	37	346.7	34.7	382.8	16.6	1588.8	283.6	1716.4	470.0	846.0	66.5	351.7	27.9	1347.8	207.7	166.1	27.6

28/04/2012	38	348.8	36.7	400.3	33.2	1588.6	283.4	1713.3	467.1	844.8	65.4	366.6	42.0	1351.9	211.6	174.2	35.3
29/04/2012	39	343.7	31.8	371.1	5.5	1582.7	277.9	1708.7	462.7	836.9	57.9	355.8	31.8	1345.6	205.6	166.6	28.1
30/04/2012	40	349.6	37.4	375.7	9.9	1596.8	291.3	1728.3	481.3	843.5	64.1	354.0	30.1	1354.1	213.6	162.7	24.3
1/05/2012	41	352.8	40.5	379.1	13.1	1593.2	287.8	1724.2	477.4	837.8	58.7	360.5	36.3	1347.7	207.6	158.7	20.6
2/05/2012	42	363.2	50.3	390.0	23.5	1596.1	290.6	1728.0	481.0	841.0	61.8	364.0	39.5	1352.2	211.9	165.3	26.8
3/05/2012	43	367.7	54.6	374.4	8.7	1594.4	289.0	1725.2	478.4	839.8	60.7	363.2	38.8	1350.1	209.9	166.5	27.9
4/05/2012	44	353.0	40.7	368.4	2.9	1602.4	296.6	1739.0	491.4	836.8	57.8	370.6	45.8	1351.5	211.1	170.6	31.8
5/05/2012	45	333.0	21.7	365.0	-0.2	1590.2	285.0	1730.9	483.7	818.3	40.3	370.7	45.9	1337.9	198.3	172.1	33.3
6/05/2012	46	340.4	28.7	378.5	12.5	1593.1	287.7	1735.5	488.1	812.6	34.9	357.2	33.1	1336.3	196.8	160.7	22.5
7/05/2012	47	333.7	22.4	381.6	15.5	1610.8	304.4	1757.9	509.4	827.9	49.4	360.9	36.6	1346.6	206.5	163.0	24.7
8/05/2012	48	331.4	20.2	373.7	8.0	1633.2	325.7	1780.9	531.2	845.9	66.5	367.9	43.3	1364.5	223.5	166.7	28.1
9/05/2012	49	352.4	40.1	373.3	7.6	1636.7	329.0	1785.2	535.2	847.9	68.3	377.1	52.0	1368.9	227.7	175.7	36.7
10/05/2012	50	353.3	41.0	381.8	15.7	1633.0	325.5	1780.0	530.3	842.6	63.3	379.4	54.1	1364.6	223.6	176.4	37.3
11/05/2012	51	351.0	38.8	383.1	16.9	1623.8	316.8	1770.6	521.4	832.5	53.7	382.1	56.7	1357.7	217.0	181.4	42.1
12/05/2012	52	346.8	34.8	373.9	8.2	1634.1	326.6	1785.2	535.2	836.1	57.1	379.6	54.3	1369.2	228.0	179.3	40.1
13/05/2012	53	347.0	34.9	379.6	13.6	1629.7	322.4	1780.9	531.1	821.3	43.1	377.5	52.3	1351.2	210.9	176.5	37.5
14/05/2012	54	349.3	37.1	372.7	7.1	1651.5	343.1	1807.3	556.2	839.3	60.2	375.3	50.2	1366.0	224.9	176.3	37.2
15/05/2012	55	355.4	42.9	374.9	9.1	1653.0	344.5	1811.4	560.0	836.3	57.3	378.0	52.8	1370.6	229.3	176.5	37.5
16/05/2012	56	359.5	46.8	374.9	9.2	1655.4	346.7	1816.8	565.2	844.9	65.4	387.1	61.5	1341.0	201.3	180.7	41.4
17/05/2012	57	366.3	53.3	395.9	29.0	1673.3	363.7	1831.0	578.6	856.5	76.5	397.9	71.7	1390.8	248.4	188.2	48.5
18/05/2012	58	373.1	59.8	410.8	43.1	1665.8	356.6	1824.2	572.2	846.6	67.1	404.7	78.1	1382.6	240.7	189.3	49.6
19/05/2012	59	387.5	73.3	371.3	5.7	1660.4	351.5	1818.6	566.8	840.4	61.2	398.3	72.1	1380.7	238.9	187.4	47.7
20/05/2012	60	392.8	78.4	379.4	13.4	1665.9	356.7	1826.3	574.1	837.2	58.2	393.5	67.5	1380.0	238.2	187.6	47.9
21/05/2012	61	401.9	87.0	375.9	10.1	1663.7	354.6	1821.9	570.0	841.5	62.3	390.9	65.1	1379.0	237.3	189.3	49.5
22/05/2012	62	397.1	82.5	378.4	12.4	1666.2	357.0	1824.8	572.8	841.3	62.0	390.8	64.9	1379.7	237.9	187.0	47.4
23/05/2012	63	386.8	72.7	380.9	14.8	1677.4	367.7	1840.7	587.8	843.1	63.8	399.2	72.9	1374.3	232.8	193.0	53.1
24/05/2012	64	379.5	65.8	381.5	15.4	1676.0	366.3	1838.3	585.5	837.6	58.6	391.7	65.8	1366.8	225.7	188.0	48.4
25/05/2012	65	370.7	57.4	378.5	12.6	1673.3	363.7	1832.7	580.3	840.9	61.7	391.0	65.1	1377.8	236.1	189.7	49.9

26/05/2012	66	355.0	42.6	373.1	7.5	1681.9	371.9	1847.5	594.3	840.2	61.0	402.3	75.8	1374.8	233.3	196.8	56.7
27/05/2012	67	366.1	53.1	373.7	8.0	1680.7	370.7	1849.2	595.9	834.1	55.3	410.1	83.2	1373.0	231.6	202.4	62.0
28/05/2012	68	374.1	60.7	369.2	3.7	1693.7	383.0	1863.6	609.5	848.3	68.7	399.8	73.5	1388.1	245.9	185.9	46.4
29/05/2012	69	371.8	58.5	382.5	16.3	1678.7	368.9	1843.6	590.6	834.0	55.1	418.5	91.2	1372.5	231.1	195.3	55.3
30/05/2012	70	368.0	54.9	380.4	14.3	1690.2	379.8	1854.6	601.0	845.9	66.4	436.6	108.4	1389.2	246.9	213.0	72.1
31/05/2012	71	405.4	90.3	383.4	17.2	1683.4	373.3	1848.7	595.4	837.9	58.8	435.3	107.1	1376.0	234.4	213.3	72.4
1/06/2012	72	421.9	106.0	387.8	21.4	1690.3	379.9	1853.4	599.9	846.8	67.3	421.0	93.6	1377.9	236.2	193.6	53.6
2/06/2012	73	399.5	84.8	393.8	27.0	1672.9	363.4	1831.4	579.0	829.7	51.1	432.9	104.8	1351.6	211.3	211.3	70.4
3/06/2012	74	387.9	73.8	388.3	21.9	1675.7	366.0	1831.7	579.2	831.6	52.9	436.6	108.4	1365.8	224.8	219.0	77.7
4/06/2012	75	412.2	96.7	396.6	29.7	1673.4	363.8	1828.9	576.7	829.6	51.0	416.0	88.9	1362.1	221.3	203.0	62.6
5/06/2012	76	388.1	73.9	396.0	29.1	1692.5	382.0	1855.7	602.1	840.1	60.9	420.6	93.2	1385.2	243.1	211.4	70.5
6/06/2012	77	376.6	63.1	387.4	21.0	1684.0	373.8	1848.7	595.4	829.7	51.1	420.2	92.8	1371.4	230.1	208.3	67.6
7/06/2012	78	390.5	76.2	392.2	25.6	1701.8	390.7	1871.8	617.3	843.8	64.5	424.5	96.9	1390.4	248.1	210.0	69.2
8/06/2012	79	374.4	61.0	396.9	29.9	1710.9	399.4	1884.9	629.7	843.1	63.8	422.4	94.9	1402.8	259.8	206.7	66.1
9/06/2012	80	376.2	62.7	381.8	15.7	1709.3	397.9	1887.3	632.0	841.1	61.9	425.5	97.8	1401.2	258.3	212.7	71.8
10/06/2012	81	360.1	47.4	382.9	16.7	1710.2	398.7	1888.2	632.9	843.4	64.1	428.2	100.4	1399.4	256.6	213.6	72.6
11/06/2012	82	354.0	41.6	381.1	15.0	1699.2	388.3	1873.2	618.6	838.5	59.4	426.4	98.7	1384.8	242.7	208.9	68.1
12/06/2012	83	353.3	40.9	373.8	8.1	1697.4	386.6	1865.1	611.0	839.2	60.0	442.1	113.6	1374.2	232.7	215.5	74.4
13/06/2012	84	362.7	49.9	367.2	1.9	1700.2	389.3	1867.6	613.3	842.3	63.0	440.8	112.3	1382.6	240.7	215.7	74.6
14/06/2012	85	394.0	79.5	378.3	12.3	1702.4	391.3	1866.0	611.8	844.5	65.1	443.0	114.5	1375.6	234.1	220.5	79.1
15/06/2012	86	409.1	93.8	396.0	29.1	1697.5	386.7	1860.8	606.9	839.8	60.6	444.1	115.4	1368.8	227.6	218.8	77.5
16/06/2012	87	403.0	88.1	387.1	20.7	1694.3	383.7	1855.7	602.0	833.8	55.0	436.7	108.5	1366.1	225.1	210.2	69.4
17/06/2012	88	389.0	74.8	392.3	25.6	1687.6	377.2	1855.2	601.6	823.2	44.9	445.2	116.5	1367.1	226.0	215.3	74.2
18/06/2012	89	388.5	74.3	389.9	23.3	1713.3	401.7	1892.5	637.0	841.5	62.2	443.6	115.0	1392.8	250.3	214.5	73.5
19/06/2012	90	378.7	65.0	383.9	17.7	1713.5	401.8	1897.8	642.0	837.4	58.4	445.4	116.7	1396.5	253.9	220.1	78.8
20/06/2012	91	362.1	49.3	386.8	20.4	1716.1	404.3	1900.0	644.1	837.6	58.6	443.4	114.8	1395.1	252.5	212.3	71.3
21/06/2012	92	363.2	50.3	398.8	31.8	1721.6	409.5	1907.7	651.3	838.9	59.8	460.8	131.3	1406.7	263.5	229.2	87.4
22/06/2012	93	366.6	53.5	397.4	30.5	1708.4	397.0	1893.9	638.2	826.5	48.1	460.1	130.7	1387.5	245.4	228.2	86.5

23/06/2012	94	378.9	65.2	393.4	26.6	1720.6	408.6	1907.9	651.6	831.6	52.9	461.0	131.5	1403.1	260.1	227.1	85.4
24/06/2012	95	365.2	52.3	377.5	11.6	1720.5	408.5	1909.6	653.2	827.5	49.0	469.3	139.3	1402.2	259.2	233.6	91.6
25/06/2012	96	373.3	59.9	384.6	18.4	1721.7	409.7	1913.1	656.4	829.8	51.2	467.8	137.9	1404.6	261.5	224.1	82.6
26/06/2012	97	375.0	61.5	397.3	30.3	1709.9	398.4	1900.6	644.6	822.3	44.1	481.9	151.3	1395.1	252.5	237.3	95.1
27/06/2012	98	380.8	67.0	390.4	23.8	1708.0	396.6	1894.5	638.8	822.9	44.7	487.1	156.3	1393.7	251.2	245.7	103.0
28/06/2012	99	415.8	100.2	396.2	29.3	1707.2	395.9	1894.1	638.4	824.2	45.8	494.5	163.2	1390.2	247.9	252.0	109.0
29/06/2012	100	413.6	98.1	383.5	17.3	1699.0	388.1	1880.2	625.3	816.3	38.4	492.4	161.2	1375.2	233.6	249.8	106.9
30/06/2012	101	412.0	96.6	392.1	25.4	1695.1	384.4	1876.3	621.6	813.8	36.0	483.2	152.5	1377.1	235.5	243.5	101.0
1/07/2012	102	406.1	91.0	391.2	24.6	1701.2	390.2	1888.2	632.8	814.7	36.8	477.3	147.0	1389.2	247.0	241.7	99.3
2/07/2012	103	404.9	89.8	389.6	23.1	1724.0	411.8	1916.8	660.0	826.2	47.8	478.6	148.2	1410.5	267.1	242.4	99.9
3/07/2012	104	403.3	88.4	399.6	32.6	1731.2	418.6	1925.5	668.2	829.8	51.2	478.1	147.7	1410.7	267.3	239.0	96.6
4/07/2012	105	394.4	79.9	390.8	24.2	1731.3	418.8	1926.8	669.4	828.8	50.2	483.4	152.8	1406.4	263.3	240.3	97.9
5/07/2012	106	377.4	63.8	388.5	22.0	1726.7	414.3	1923.3	666.1	829.6	51.0	487.3	156.4	1402.9	259.9	242.9	100.4
6/07/2012	107	377.8	64.1	399.6	32.6	1716.9	405.0	1909.6	653.1	822.1	43.9	477.0	146.6	1393.2	250.7	227.6	85.9
7/07/2012	108	377.2	63.6	411.3	43.6	1718.9	407.0	1911.8	655.3	824.1	45.8	491.3	160.2	1393.6	251.1	241.9	99.4
8/07/2012	109	391.0	76.7	401.0	33.8	1705.9	394.6	1897.4	641.6	813.0	35.2	500.8	169.2	1380.7	238.9	244.4	101.8
9/07/2012	110	410.4	95.0	407.9	40.4	1721.8	409.7	1912.7	656.0	828.2	49.6	505.8	173.9	1400.9	258.0	249.3	106.5
10/07/2012	111	404.5	89.5	417.3	49.3	1714.3	402.6	1901.8	645.7	820.5	42.3	496.7	165.3	1392.3	249.9	243.2	100.7
11/07/2012	112	433.9	117.4	406.8	39.3	1694.4	383.7	1879.8	624.9	801.2	24.1	504.4	172.6	1370.9	229.6	257.1	113.9
12/07/2012	113	431.9	115.4	403.5	36.3	1717.8	405.9	1903.1	646.9	823.5	45.2	493.6	162.4	1390.8	248.4	244.2	101.6
13/07/2012	114	430.1	113.8	405.3	38.0	1709.1	397.7	1892.6	637.0	819.1	41.0	504.6	172.8	1382.6	240.7	255.3	112.1
14/07/2012	115	404.4	89.4	412.5	44.7	1689.3	378.9	1869.3	614.9	801.0	23.9	489.6	158.6	1360.5	219.8	241.3	98.9
15/07/2012	116	408.7	93.4	412.7	45.0	1696.0	385.3	1881.0	626.1	800.6	23.5	501.1	169.5	1370.4	229.1	251.3	108.3
16/07/2012	117	402.2	87.3	426.3	57.9	1723.4	411.2	1921.2	664.1	821.1	43.0	489.0	158.0	1404.7	261.6	236.6	94.4
17/07/2012	118	410.0	94.7	415.5	47.6	1717.3	405.5	1918.3	661.3	815.4	37.5	497.6	166.2	1401.5	258.6	244.6	102.0
18/07/2012	119	389.3	75.1	407.5	40.0	1716.0	404.2	1916.9	660.1	811.5	33.8	510.0	177.9	1393.4	250.9	256.3	113.1
19/07/2012	120	401.5	86.6	418.4	50.4	1721.6	409.5	1924.5	667.2	814.5	36.7	501.2	169.6	1401.1	258.2	245.2	102.5
20/07/2012	121	401.1	86.3	435.1	66.2	1731.8	419.2	1935.6	677.8	821.0	42.9	508.1	176.1	1410.2	266.8	253.3	110.2

21/07/2012	122	415.8	100.2	430.7	62.0	1718.0	406.1	1921.9	664.8	813.4	35.7	514.7	182.4	1389.0	246.7	259.9	116.5
22/07/2012	123	410.1	94.8	441.6	72.4	1714.9	403.2	1917.0	660.1	811.5	33.8	524.1	191.3	1387.6	245.4	262.3	118.8
23/07/2012	124	405.5	90.5	444.4	75.0	1710.8	399.2	1911.2	654.6	810.2	32.6	518.1	185.6	1385.1	243.0	259.2	115.8
24/07/2012	125	422.9	106.9	426.4	57.9	1705.0	393.8	1901.9	645.8	804.0	26.7	527.7	194.7	1381.3	239.5	267.0	123.2
25/07/2012	126	423.3	107.3	429.6	61.0	1705.8	394.5	1897.9	642.0	803.9	26.6	538.2	204.6	1380.9	239.1	281.0	136.5
26/07/2012	127	417.2	101.5	436.7	67.7	1712.3	400.7	1904.4	648.2	807.7	30.3	548.7	214.6	1383.8	241.8	283.1	138.5
27/07/2012	128	425.0	108.9	447.2	77.6	1713.4	401.8	1909.7	653.2	805.0	27.7	534.9	201.6	1384.5	242.5	268.2	124.3
28/07/2012	129	419.7	103.9	448.2	78.6	1720.5	408.5	1921.6	664.5	807.1	29.7	531.7	198.5	1393.6	251.1	269.1	125.2
29/07/2012	130	405.6	90.6	450.7	81.0	1723.1	410.9	1928.4	670.9	810.4	32.8	536.2	202.7	1398.0	255.3	272.9	128.8
30/07/2012	131	419.1	103.3	448.4	78.8	1728.3	415.9	1935.8	678.0	810.8	33.2	522.2	189.5	1402.9	259.9	258.5	115.2
31/07/2012	132	421.7	105.8	445.3	75.9	1732.4	419.8	1941.4	683.3	813.4	35.6	549.6	215.5	1404.4	261.3	279.4	134.9
1/08/2012	133	424.6	108.5	441.1	71.9	1738.4	425.4	1948.0	689.5	818.4	40.4	552.3	218.0	1408.9	265.6	280.3	135.8
2/08/2012	134	448.2	130.9	443.0	73.7	1737.1	424.2	1950.2	691.6	817.7	39.7	563.2	228.3	1411.1	267.7	290.3	145.3
3/08/2012	135	443.1	126.0	445.4	76.0	1737.9	425.0	1950.9	692.3	817.6	39.6	568.2	233.1	1411.0	267.6	295.3	150.0
4/08/2012	136	458.6	140.8	446.2	76.7	1734.3	421.6	1947.3	688.8	812.6	34.9	569.3	234.2	1404.6	261.5	292.4	147.3
5/08/2012	137	447.3	130.0	450.2	80.5	1732.5	419.8	1945.9	687.6	811.0	33.3	559.0	224.4	1404.3	261.2	279.3	134.9
6/08/2012	138	440.9	124.0	446.4	76.9	1737.1	424.2	1948.8	690.3	811.5	33.8	551.9	217.7	1403.1	260.1	269.6	125.6
7/08/2012	139	442.2	125.2	444.6	75.2	1753.3	439.6	1968.4	708.9	824.0	45.7	563.5	228.6	1417.0	273.3	276.8	132.6
8/08/2012	140	462.5	144.4	449.5	79.9	1750.2	436.6	1967.3	707.8	823.3	45.0	587.9	251.8	1410.2	266.8	298.9	153.4
9/08/2012	141	482.5	163.4	452.9	83.1	1743.5	430.3	1962.6	703.3	819.0	41.0	609.7	272.4	1409.1	265.8	313.2	167.0
10/08/2012	142	485.8	166.6	468.5	97.8	1747.9	434.5	1968.1	708.5	819.4	41.3	610.9	273.6	1408.6	265.3	314.4	168.2
11/08/2012	143	474.3	155.6	459.0	88.8	1733.3	420.6	1951.8	693.1	809.7	32.1	607.1	270.0	1395.2	252.6	311.2	165.1
12/08/2012	144	489.8	170.4	457.5	87.5	1726.1	413.8	1938.8	680.8	804.8	27.5	614.1	276.7	1393.3	250.8	317.5	171.1
13/08/2012	145	485.8	166.6	467.2	96.6	1732.7	420.1	1945.0	686.6	810.1	32.5	622.3	284.4	1400.3	257.5	320.1	173.5
14/08/2012	146	485.6	166.4	471.8	101.0	1743.7	430.5	1954.3	695.5	818.6	40.6	633.8	295.3	1410.6	267.2	331.0	183.9
15/08/2012	147	479.0	160.1	447.9	78.3	1743.3	430.1	1955.7	696.8	816.1	38.2	631.1	292.8	1408.0	264.8	331.2	184.0
16/08/2012	148	498.3	178.4	454.4	84.5	1749.0	435.5	1960.6	701.5	819.1	41.1	619.0	281.3	1415.9	272.2	318.6	172.1
17/08/2012	149	491.6	172.0	476.8	105.8	1746.4	433.1	1958.8	699.8	815.9	38.0	631.2	292.9	1415.5	271.8	327.3	180.4

18/08/2012	150	486.5	167.2	481.6	110.2	1749.0	435.5	1960.1	701.0	815.4	37.6	684.5	343.3	1411.9	268.4	375.2	225.8
19/08/2012	151	500.4	180.4	468.1	97.5	1749.3	435.7	1963.6	704.3	816.1	38.2	679.9	339.0	1415.3	271.6	361.8	213.1
20/08/2012	152	513.6	192.8	485.3	113.8	1756.9	443.0	1972.8	713.1	822.2	44.0	679.9	339.0	1424.1	280.0	358.8	210.2
21/08/2012	153	513.3	192.6	490.7	118.9	1747.6	434.2	1963.4	704.1	815.6	37.7	702.9	360.8	1412.8	269.3	376.3	226.8
22/08/2012	154	547.0	224.6	471.3	100.5	1743.2	430.0	1955.1	696.2	814.3	36.5	727.8	384.4	1406.9	263.7	388.9	238.7
23/08/2012	155	554.7	231.9	484.2	112.7	1740.3	427.2	1948.1	689.7	815.5	37.6	733.5	389.8	1406.2	263.0	387.4	237.3
24/08/2012	156	549.2	226.6	485.7	114.2	1730.3	417.8	1935.9	678.1	804.2	26.9	719.8	376.8	1397.9	255.2	375.2	225.8
25/08/2012	157	532.4	210.7	494.9	122.9	1735.1	422.4	1942.0	683.8	803.4	26.1	718.0	375.1	1403.8	260.7	376.6	227.1
26/08/2012	158	523.0	201.8	495.7	123.7	1744.8	431.5	1956.7	697.8	812.3	34.6	771.5	425.8	1409.7	266.3	436.2	283.6
27/08/2012	159	520.8	199.7	499.7	127.5	1757.8	443.9	1971.6	711.9	820.6	42.5	788.9	442.3	1420.5	276.6	435.6	283.1
28/08/2012	160	513.0	192.3	498.6	126.4	1744.1	430.8	1960.4	701.2	813.4	35.6	813.3	465.4	1409.3	266.0	438.7	285.9
29/08/2012	161	443.3	126.3	484.4	112.9	1741.4	428.3	1953.1	694.4	814.7	36.8	811.5	463.7	1403.4	260.4	433.4	280.9
30/08/2012	162	490.4	170.9	489.0	117.3	1746.5	433.1	1954.0	695.3	816.1	38.2	822.8	474.4	1404.6	261.5	440.4	287.6
31/08/2012	163	491.8	172.3	491.8	119.9	1753.3	439.6	1962.9	703.7	814.3	36.5	817.4	469.3	1416.9	273.2	425.9	273.8
1/09/2012	164	503.0	182.9	504.2	131.7	1764.8	450.5	1980.5	720.3	820.8	42.7	850.4	500.6	1423.8	279.7	447.9	294.7
2/09/2012	165	534.6	212.8	507.0	134.3	1759.0	444.9	1976.2	716.2	818.3	40.2	881.5	530.1	1415.7	272.1	457.2	303.5
3/09/2012	166	595.6	270.6	504.3	131.8	1766.7	452.2	1982.9	722.6	825.2	46.8	900.0	547.6	1425.6	281.5	460.9	307.0
4/09/2012	167	604.5	279.1	515.7	142.6	1756.6	442.7	1973.7	713.9	816.9	39.0	952.4	597.3	1422.5	278.5	498.5	342.7
5/09/2012	168	610.6	284.9	515.6	142.5	1756.3	442.4	1969.9	710.3	809.8	32.2	974.5	618.2	1417.5	273.8	544.6	386.3
6/09/2012	169	642.5	315.0	517.8	144.5	1771.8	457.1	1987.6	727.1	822.4	44.1	979.3	622.8	1432.1	287.6	548.4	390.0
7/09/2012	170	660.1	331.7	507.6	135.0	1780.6	465.5	1998.4	737.3	828.2	49.6	980.7	624.1	1430.3	285.9	549.2	390.7
8/09/2012	171	654.0	326.0	529.5	155.7	1783.1	467.8	2000.7	739.5	830.6	51.9	973.2	617.0	1429.4	285.1	545.0	386.7
9/09/2012	172	672.0	343.0	524.5	150.9	1769.4	454.8	1988.0	727.4	820.8	42.7	971.2	615.1	1421.1	277.2	543.8	385.6
10/09/2012	173	692.4	362.4	526.5	152.8	1765.7	451.3	1981.0	720.8	819.7	41.6	969.0	613.0	1422.6	278.6	542.7	384.5
11/09/2012	174	714.4	383.2	528.4	154.7	1761.9	447.7	1973.5	713.7	820.0	41.9	968.9	612.9	1415.1	271.5	542.6	384.5
12/09/2012	175	750.1	417.1	516.4	143.3	1761.7	447.5	1967.4	707.9	821.2	43.1	963.7	608.0	1404.7	261.6	539.7	381.7
13/09/2012	176	713.2	382.1	524.2	150.7	1752.3	438.6	1951.2	692.6	814.6	36.7	971.9	615.7	1392.5	250.1	544.2	386.0
14/09/2012	177	704.7	374.1	534.7	160.6	1767.0	452.6	1968.2	708.7	823.1	44.9	969.6	613.6	1414.6	271.0	543.0	384.8

15/09/2012	178	730.6	398.6	543.7	169.1	1762.9	448.7	1963.5	704.2	819.6	41.6	965.2	609.4	1407.4	264.2	540.5	382.5
16/09/2012	179	750.0	417.0	540.5	166.1	1754.9	441.1	1954.0	695.2	815.1	37.3	963.3	607.6	1400.6	257.7	539.4	381.5
17/09/2012	180	763.3	429.6	534.2	160.1	1751.5	437.8	1950.4	691.8	813.2	35.4	963.7	608.0	1397.0	254.3	539.7	381.7
18/09/2012	181	761.8	428.2	537.0	162.8	1752.2	438.6	1944.4	686.1	814.3	36.5	963.4	607.7	1386.3	244.2	539.5	381.5
19/09/2012	182	755.8	422.5	547.4	172.6	1751.7	438.0	1944.5	686.2	813.6	35.8	964.5	608.8	1387.7	245.6	540.1	382.1
20/09/2012	183	754.7	421.4	550.3	175.4	1753.7	439.9	1943.7	685.5	815.4	37.5	966.0	610.2	1390.2	247.8	541.0	382.9
21/09/2012	184	763.3	429.6	555.5	180.3	1756.5	442.6	1946.8	688.4	818.9	40.8	964.0	608.2	1390.8	248.4	539.8	381.8
22/09/2012	185	777.3	442.8	551.7	176.7	1752.7	439.0	1940.2	682.1	813.2	35.4	961.7	606.1	1384.8	242.8	538.5	380.6
23/09/2012	186	744.6	411.8	539.4	165.1	1748.5	435.0	1933.6	675.9	810.1	32.5	969.0	613.0	1376.0	234.5	542.7	384.5
24/09/2012	187	721.9	390.4	554.5	179.3	1761.9	447.7	1949.0	690.5	821.5	43.3	970.3	614.3	1397.5	254.8	543.4	385.2
25/09/2012	188	741.6	409.0	550.9	176.0	1764.2	449.9	1957.1	698.2	821.9	43.7	967.0	611.1	1407.3	264.1	541.5	383.4
26/09/2012	189	745.7	412.9	556.3	181.0	1758.2	444.2	1951.0	692.4	817.3	39.3	967.7	611.7	1396.7	254.1	541.9	383.8
27/09/2012	190	774.6	440.3	545.3	170.6	1759.4	445.3	1949.9	691.4	820.3	42.2	962.9	607.2	1399.3	256.6	539.2	381.3
28/09/2012	191	796.8	461.4	560.8	185.3	1750.8	437.2	1939.7	681.7	814.7	36.9	958.0	602.6	1391.3	248.9	536.5	378.7
29/09/2012	192	754.8	421.6	557.6	182.3	1741.8	428.7	1928.9	671.4	807.3	29.8	965.6	609.8	1380.7	238.9	540.7	382.7
30/09/2012	193	714.1	383.0	568.8	193.0	1755.6	441.7	1938.9	680.9	811.2	33.5	971.4	615.3	1392.5	250.0	544.0	385.8
1/10/2012	194	736.5	404.2	554.8	179.7	1766.2	451.8	1959.2	700.2	820.1	42.0	967.0	611.1	1411.7	268.2	541.5	383.4
2/10/2012	195	721.1	389.6	570.3	194.4	1758.2	444.2	1951.1	692.5	811.4	33.7	972.0	615.9	1404.0	261.0	544.3	386.1
3/10/2012	196	731.6	399.6	561.6	186.1	1767.3	452.8	1963.9	704.6	822.9	44.7	970.9	614.8	1416.0	272.3	543.7	385.5
4/10/2012	197	714.6	383.4	567.9	192.1	1765.3	451.0	1961.6	702.5	820.5	42.3	973.2	617.0	1414.9	271.3	545.0	386.7
5/10/2012	198	744.3	411.6	572.6	196.6	1769.5	454.9	1969.4	709.9	821.1	42.9	969.4	613.4	1419.2	275.3	542.9	384.7
6/10/2012	199	758.7	425.2	570.4	194.4	1762.6	448.4	1959.3	700.2	818.4	40.4	968.7	612.7	1406.2	263.0	542.5	384.3
7/10/2012	200	733.5	401.3	580.3	203.8	1761.2	447.1	1949.1	690.6	818.6	40.5	972.1	616.0	1399.1	256.3	544.4	386.2
8/10/2012	201	714.2	383.0	584.5	207.8	1767.5	453.1	1960.0	700.9	824.8	46.5	976.1	619.8	1412.7	269.2	546.6	388.3
9/10/2012	202	701.1	370.6	590.0	213.0	1774.7	459.9	1968.4	708.9	832.8	54.0	979.3	622.8	1421.0	277.1	548.4	390.0
10/10/2012	203	718.4	387.1	593.1	215.9	1780.6	465.4	1978.1	718.0	835.4	56.5	976.1	619.8	1427.8	283.5	546.6	388.3
11/10/2012	204	648.7	321.0	598.6	221.1	1774.8	460.0	1968.8	709.3	828.3	49.8	991.7	634.6	1419.7	275.8	555.4	396.6
12/10/2012	205	662.0	333.5	608.3	230.4	1803.2	486.8	2005.9	744.4	854.0	74.2	986.6	629.7	1445.3	300.1	552.5	393.8

13/10/2012	206	687.4	357.6	624.0	245.3	1793.9	478.0	1997.5	736.4	845.4	66.0	981.2	624.6	1429.7	285.3	549.5	391.0
14/10/2012	207	695.3	365.2	604.4	226.7	1784.1	468.7	1984.2	723.8	840.1	60.9	982.4	625.7	1420.3	276.4	550.1	391.6
15/10/2012	208	718.9	387.5	613.5	235.3	1786.2	470.7	1985.4	725.0	841.3	62.1	978.2	621.7	1423.0	279.0	547.8	389.4
16/10/2012	209	737.2	404.8	616.8	238.4	1778.5	463.4	1977.6	717.6	832.6	53.9	970.7	614.6	1413.7	270.2	543.6	385.4
17/10/2012	210	743.7	411.0	604.1	226.4	1764.9	450.6	1964.3	705.0	818.4	40.3	972.1	615.9	1402.1	259.2	544.4	386.1
18/10/2012	211	740.4	407.8	630.1	251.0	1767.4	453.0	1961.3	702.1	821.3	43.1	974.3	618.0	1400.0	257.2	545.6	387.3
19/10/2012	212	771.7	437.5	628.7	249.7	1771.4	456.7	1965.8	706.4	827.8	49.3	968.9	612.9	1402.0	259.1	542.6	384.5
20/10/2012	213	806.4	470.4	639.2	259.6	1761.7	447.5	1949.9	691.3	819.6	41.5	961.3	605.7	1384.9	242.9	538.3	380.4
21/10/2012	214	802.8	467.0	648.6	268.5	1747.9	434.4	1931.5	673.9	807.4	29.9	962.9	607.2	1367.4	226.2	539.2	381.3
22/10/2012	215	747.0	414.2	651.3	271.1	1750.7	437.1	1933.0	675.3	807.1	29.6	972.3	616.1	1370.6	229.3	544.5	386.2
23/10/2012	216	727.3	395.4	640.2	260.6	1767.8	453.3	1953.2	694.5	819.1	41.1	975.9	619.6	1389.9	247.6	546.5	388.2
24/10/2012	217	769.2	435.1	633.2	253.9	1774.4	459.5	1964.1	704.8	826.9	48.5	966.8	610.9	1400.8	258.0	541.4	383.3
25/10/2012	218	785.4	450.6	640.0	260.4	1757.8	443.8	1946.6	688.2	812.9	35.2	964.3	608.6	1391.7	249.3	540.0	382.0
26/10/2012	219	768.2	434.2	662.0	281.2	1753.3	439.6	1941.0	682.9	809.5	31.9	969.2	613.2	1385.0	242.9	542.8	384.6
27/10/2012	220	759.7	426.1	674.5	293.1	1762.2	448.0	1947.6	689.1	818.1	40.1	969.4	613.4	1384.0	242.0	542.9	384.7
28/10/2012	221	757.5	424.1	679.6	297.9	1762.6	448.4	1950.2	691.6	816.3	38.4	969.0	613.0	1383.3	241.3	542.6	384.5
29/10/2012	222	768.0	434.0	680.1	298.4	1761.7	447.6	1950.6	692.0	815.8	37.9	969.4	613.4	1389.3	247.0	542.8	384.7
30/10/2012	223	789.7	454.6	691.7	309.4	1762.5	448.3	1950.2	691.6	816.7	38.8	965.6	609.7	1393.5	251.0	540.7	382.7
31/10/2012	224	751.0	418.0	696.2	313.7	1755.6	441.7	1943.6	685.4	811.5	33.9	977.9	621.4	1385.8	243.7	547.6	389.2
1/11/2012	225	750.6	417.6	707.2	324.1	1778.0	463.0	1961.2	702.1	829.9	51.3	973.3	617.1	1403.7	260.6	545.0	386.8
2/11/2012	226	750.8	417.7	711.5	328.2	1769.6	455.0	1955.1	696.3	819.2	41.1	972.0	615.8	1393.3	250.8	544.3	386.1
3/11/2012	227	765.0	431.2	699.0	316.4	1767.2	452.8	1956.5	697.6	818.8	40.7	971.2	615.1	1391.2	248.8	543.8	385.6
4/11/2012	228	797.6	462.1	715.2	331.7	1765.7	451.3	1952.7	694.0	820.3	42.2	967.2	611.3	1388.2	246.0	541.6	383.5
5/11/2012	229	814.2	477.9	758.7	373.0	1758.5	444.5	1941.1	683.0	816.8	38.8	965.1	609.3	1382.4	240.5	540.5	382.4
6/11/2012	230	839.1	501.4	747.2	362.1	1754.7	440.9	1932.6	675.0	813.5	35.7	960.1	604.6	1377.1	235.4	537.6	379.8
7/11/2012	231	831.7	494.5	750.4	365.0	1745.6	432.3	1918.7	661.8	804.4	27.1	963.0	607.4	1367.0	225.9	539.3	381.3
8/11/2012	232	856.5	517.9	770.6	384.2	1751.0	437.4	1922.7	665.6	813.2	35.4	957.4	602.0	1374.2	232.7	536.1	378.3
9/11/2012	233	837.4	499.8	791.3	403.9	1740.7	427.6	1908.8	652.3	803.1	25.9	960.8	605.2	1363.7	222.8	538.1	380.1

10/11/2012	234	816.2	479.8	802.3	414.2	1746.9	433.5	1914.9	658.2	808.9	31.4	962.6	607.0	1368.8	227.6	539.1	381.1
11/11/2012	235	782.4	447.7	797.3	409.5	1750.3	436.7	1920.9	663.9	810.0	32.4	969.4	613.4	1372.4	231.0	542.8	384.7
12/11/2012	236	784.1	449.3	804.3	416.2	1762.5	448.3	1937.1	679.2	820.4	42.3	969.1	613.2	1386.4	244.3	542.7	384.6
13/11/2012	237	803.2	467.4	863.4	472.2	1762.1	447.9	1937.6	679.7	821.3	43.1	964.6	608.8	1389.0	246.7	540.2	382.1
14/11/2012	238	775.8	441.4	886.9	494.5	1753.8	440.0	1929.8	672.2	813.9	36.1	973.8	617.6	1382.4	240.5	545.4	387.1
15/11/2012	239	825.9	489.0	909.1	515.5	1770.6	456.0	1946.2	687.9	833.8	55.0	962.8	607.2	1399.2	256.4	539.2	381.2
16/11/2012	240	812.3	476.0	913.3	519.5	1750.6	437.0	1922.5	665.4	813.4	35.6	965.5	609.7	1376.4	234.8	540.7	382.6

Table E.4 Concrete surface strain at steel level for slab D-SCC-b

Slab D-SCC-b		CONCRETE SURFACE STRAIN BY SG															
		1		2		3		4		5		6		7		8	
Date	Age	Reading	Strain	Reading	Strain	Reading	Strain	Reading	Strain	Reading	Strain	Reading	Strain	Reading	Strain	Reading	Strain
4/04/2012	14	780.7		1364.2		852.6		1102.5		913.4		1486.4		526.1		848.6	
4/04/2012	14	1139.7		617.9		106.0		298.3		730.0		1608.7		366.2		430.2	
5/04/2012	15	1440.8	285.4	624.7	6.4	113.7	7.3	301.1	2.6	755.6	24.2	1734.8	119.6	423.0	53.9	463.9	31.9
6/04/2012	16	1488.4	330.5	626.2	7.8	118.8	12.2	302.1	3.6	765.2	33.3	1757.7	141.3	431.9	62.3	462.8	31.0
7/04/2012	17	1541.4	380.8	628.1	9.6	118.2	11.5	311.5	12.4	780.2	47.6	1792.2	174.0	443.3	73.1	469.2	37.0
8/04/2012	18	1582.5	419.7	621.3	3.2	110.1	3.8	309.6	10.7	795.7	62.3	1815.4	196.0	451.3	80.7	484.5	51.5
9/04/2012	19	1620.9	456.1	632.3	13.6	108.9	2.7	309.4	10.5	795.6	62.2	1832.7	212.4	458.0	87.0	477.2	44.6
10/04/2012	20	1696.5	527.8	642.3	23.1	111.8	5.5	306.4	7.6	826.8	91.7	1885.6	262.5	478.7	106.6	470.7	38.4
11/04/2012	21	1746.4	575.1	636.0	17.1	113.0	6.6	308.1	9.2	841.6	105.7	1917.0	292.2	490.3	117.6	467.8	35.6
12/04/2012	22	1768.6	596.1	639.8	20.7	117.1	10.5	309.3	10.4	859.0	122.3	1938.7	312.8	496.8	123.8	472.3	39.9
13/04/2012	23	1781.1	607.9	634.3	15.5	121.1	14.3	316.7	17.4	854.3	117.8	1940.5	314.5	497.4	124.4	467.1	35.0
16/04/2012	26	1845.6	669.1	643.2	23.9	112.8	6.4	318.9	19.5	869.5	132.2	1981.5	353.4	517.1	143.1	470.0	37.7
17/04/2012	27	1799.4	625.3	644.9	25.5	124.7	17.7	324.3	24.6	837.3	101.8	1939.9	314.0	498.8	125.7	478.8	46.1
18/04/2012	28	1790.8	617.1	641.1	22.0	132.6	25.2	322.9	23.3	840.7	104.9	1938.7	312.9	497.7	124.6	465.7	33.7
19/04/2012	29	1788.9	615.4	643.2	23.9	136.5	28.9	323.8	24.1	856.4	119.8	1946.6	320.3	498.4	125.3	459.0	27.3
20/04/2012	30	1787.9	614.4	634.1	15.3	128.8	21.6	328.6	28.6	859.6	122.8	1946.3	320.0	496.6	123.6	462.2	30.3
21/04/2012	31	1782.8	609.6	638.3	19.3	142.3	34.4	329.8	29.8	848.8	112.6	1936.4	310.6	491.4	118.7	466.0	34.0
22/04/2012	32	1786.6	613.1	654.3	34.4	131.7	24.4	337.9	37.5	836.8	101.2	1933.8	308.2	490.4	117.8	468.9	36.7
23/04/2012	33	1798.3	624.3	658.4	38.4	139.5	31.7	349.8	48.8	839.3	103.6	1943.5	317.4	493.1	120.3	451.5	20.2
24/04/2012	34	1835.5	659.5	647.9	28.4	132.7	25.3	352.5	51.3	846.2	110.2	1966.3	339.0	504.3	131.0	453.4	22.0
25/04/2012	35	1846.9	670.3	652.4	32.7	146.7	38.6	345.3	44.5	805.7	71.7	1958.8	331.9	505.3	131.9	450.0	18.8
26/04/2012	36	1858.8	681.6	652.9	33.2	136.0	28.4	346.5	45.7	803.9	70.1	1976.0	348.2	509.2	135.6	454.7	23.2
27/04/2012	37	1882.5	704.1	647.0	27.5	141.4	33.6	345.7	44.9	819.1	84.5	1992.4	363.7	514.9	141.0	443.5	12.6
28/04/2012	38	1875.7	697.6	637.1	18.1	155.1	46.6	344.2	43.5	823.4	88.5	1994.7	365.9	514.0	140.1	451.1	19.8
29/04/2012	39	1880.0	701.7	645.7	26.4	149.5	41.2	349.8	48.8	815.1	80.6	1983.2	355.0	512.6	138.8	465.6	33.5
30/04/2012	40	1897.3	718.1	648.7	29.2	154.0	45.4	347.6	46.7	804.0	70.2	1988.5	360.0	518.5	144.4	479.9	47.1
1/05/2012	41	1893.6	714.6	648.4	28.9	163.7	54.6	352.6	51.5	805.8	71.9	1989.9	361.4	517.2	143.2	480.8	48.0
2/05/2012	42	1901.7	722.3	666.7	46.2	170.7	61.3	360.0	58.4	817.6	83.0	1998.2	369.2	518.4	144.3	482.3	49.4
3/05/2012	43	1902.9	723.4	653.9	34.1	172.6	63.1	364.7	62.9	820.5	85.8	1999.2	370.2	517.6	143.5	479.9	47.1
4/05/2012	44	1916.0	735.9	646.9	27.5	177.4	67.7	357.6	56.2	801.9	68.1	2000.7	371.6	521.7	147.4	474.3	41.8
5/05/2012	45	1912.8	732.8	647.8	28.3	189.8	79.5	361.8	60.2	793.5	60.2	1999.5	370.5	519.3	145.1	476.4	43.8
6/05/2012	46	1930.2	749.3	665.8	45.3	200.2	89.3	384.0	81.2	794.4	61.1	2005.1	375.8	520.6	146.4	480.7	47.9

7/05/2012	47	1949.1	767.1	658.8	38.7	191.2	80.7	382.4	79.7	797.1	63.6	2020.3	390.2	527.4	152.8	484.6	51.5
8/05/2012	48	1964.5	781.8	671.0	50.3	192.3	81.8	369.0	67.0	803.5	69.6	2033.9	403.0	534.3	159.4	484.6	51.6
9/05/2012	49	1962.1	779.6	673.0	52.2	197.6	86.8	380.0	77.4	805.7	71.8	2037.1	406.1	535.6	160.6	489.6	56.3
10/05/2012	50	1956.3	774.1	652.6	32.9	193.8	83.2	383.0	80.2	805.6	71.7	2037.6	406.6	534.0	159.1	491.4	58.0
11/05/2012	51	1956.0	773.7	659.4	39.3	220.2	108.2	367.2	65.3	803.9	70.0	2033.1	402.3	531.2	156.4	491.2	57.8
12/05/2012	52	1975.0	791.7	670.0	49.4	223.0	110.9	373.8	71.6	802.9	69.1	2042.4	411.1	535.6	160.6	501.2	67.3
13/05/2012	53	1979.0	795.5	686.4	64.9	227.4	115.1	373.2	71.0	782.1	49.4	2040.0	408.8	534.3	159.3	494.8	61.2
14/05/2012	54	1996.2	811.8	687.9	66.3	234.8	122.1	376.0	73.6	786.8	53.8	2064.2	431.7	542.2	166.8	488.9	55.7
15/05/2012	55	2001.4	816.8	692.2	70.4	239.1	126.1	374.0	71.7	790.5	57.3	2069.9	437.2	543.4	168.0	490.7	57.4
16/05/2012	56	2000.7	816.1	693.2	71.4	233.9	121.3	379.1	76.5	801.1	67.4	2070.1	437.4	545.1	169.6	492.8	59.3
17/05/2012	57	2010.7	825.6	687.6	66.0	232.4	119.8	379.4	76.9	817.3	82.7	2081.8	448.4	549.3	173.6	493.5	60.0
18/05/2012	58	2005.3	820.5	681.9	60.7	237.2	124.3	384.0	81.2	810.2	76.0	2066.7	434.2	547.3	171.7	500.0	66.2
19/05/2012	59	1999.5	815.0	688.5	66.9	255.7	141.9	392.5	89.3	804.3	70.5	2066.4	433.8	545.6	170.0	504.7	70.6
20/05/2012	60	2017.0	831.5	696.8	74.8	282.5	167.3	393.8	90.4	804.7	70.8	2078.9	445.7	547.9	172.2	503.4	69.4
21/05/2012	61	2001.0	816.4	704.8	82.3	286.2	170.8	396.7	93.3	807.2	73.2	2078.4	445.2	546.6	171.0	501.5	67.6
22/05/2012	62	2004.3	819.5	710.0	87.3	280.5	165.4	393.3	90.0	803.1	69.3	2080.1	446.8	547.4	171.8	518.9	84.1
23/05/2012	63	2027.5	841.5	702.7	80.3	285.0	169.6	382.2	79.5	798.5	64.9	2092.8	458.9	552.2	176.4	516.0	81.4
24/05/2012	64	2024.0	838.2	697.3	75.2	299.7	183.6	384.9	82.0	799.6	66.0	2095.2	461.2	551.5	175.7	512.2	77.7
25/05/2012	65	2018.4	832.9	698.5	76.3	317.9	200.8	389.6	86.5	809.1	74.9	2094.1	460.1	549.8	174.1	509.0	74.7
26/05/2012	66	2034.8	848.4	696.0	74.0	318.8	201.7	398.1	94.6	801.7	68.0	2102.7	468.3	554.3	178.3	515.7	81.1
27/05/2012	67	2035.6	849.2	709.4	86.7	308.8	192.2	399.9	96.3	800.7	67.0	2105.3	470.7	554.8	178.8	528.8	93.5
28/05/2012	68	2041.9	855.1	701.0	78.7	318.7	201.6	406.3	102.3	811.5	77.2	2117.4	482.2	559.1	182.9	520.0	85.1
29/05/2012	69	2026.2	840.3	701.0	78.7	370.7	250.8	406.9	102.9	802.3	68.5	2102.4	468.0	553.1	177.2	517.1	82.4
30/05/2012	70	2039.9	853.2	711.2	88.4	367.8	248.2	414.0	109.6	811.1	76.9	2109.7	474.9	556.4	180.3	522.3	87.3
31/05/2012	71	2031.1	844.9	718.6	95.4	368.6	248.9	426.3	121.3	806.9	72.9	2108.4	473.7	554.6	178.6	517.8	83.0
1/06/2012	72	2035.0	848.6	706.5	83.9	383.6	263.1	420.0	115.4	818.6	84.0	2115.6	480.5	556.0	180.0	520.7	85.8
2/06/2012	73	2013.2	827.9	719.1	95.9	397.6	276.4	432.7	127.4	806.4	72.5	2096.1	462.0	549.4	173.7	527.2	92.0
3/06/2012	74	2012.4	827.2	734.4	110.4	399.0	277.7	439.3	133.6	818.0	83.5	2101.3	467.0	549.5	173.8	534.5	98.9
4/06/2012	75	2012.2	827.0	731.4	107.5	391.1	270.3	443.9	138.0	815.9	81.5	2098.0	463.8	548.7	173.0	519.2	84.4
5/06/2012	76	2047.8	860.7	722.3	98.9	396.1	275.0	438.1	132.5	811.9	77.6	2116.3	481.2	556.7	180.6	512.8	78.3
6/06/2012	77	2041.3	854.6	734.4	110.4	438.6	315.2	429.4	124.2	800.6	66.9	2110.3	475.5	554.6	178.6	513.9	79.3
7/06/2012	78	2059.7	872.1	739.0	114.7	470.4	345.4	424.4	119.5	806.5	72.5	2121.7	486.3	561.5	185.2	506.2	72.0
8/06/2012	79	2078.5	889.8	721.9	98.5	493.4	367.2	427.9	122.8	808.9	74.8	2133.1	497.1	565.5	188.9	499.3	65.5
9/06/2012	80	2081.4	892.6	731.1	107.2	496.8	370.4	428.6	123.5	808.5	74.4	2136.3	500.2	566.2	189.6	513.1	78.6
10/06/2012	81	2074.4	886.0	730.3	106.5	510.1	383.0	434.4	128.9	810.9	76.7	2137.1	500.9	566.5	189.9	521.1	86.1
11/06/2012	82	2047.7	860.6	731.5	107.6	514.9	387.6	440.1	134.4	810.7	76.5	2127.0	491.3	562.0	185.6	519.3	84.4
12/06/2012	83	2045.9	859.0	731.9	108.0	546.3	417.4	439.8	134.1	817.7	83.2	2125.7	490.0	559.5	183.3	530.2	94.8

13/06/2012	84	2041.2	854.5	739.5	115.2	579.4	448.7	452.2	145.9	825.7	90.7	2127.8	492.0	560.3	184.0	519.6	84.7
14/06/2012	85	2040.4	853.8	739.1	114.9	601.1	469.3	458.5	151.8	828.9	93.7	2126.2	490.5	559.8	183.5	517.3	82.5
15/06/2012	86	2038.6	852.0	737.0	112.9	605.6	473.5	461.7	154.8	824.3	89.4	2123.1	487.6	558.3	182.1	508.5	74.3
16/06/2012	87	2037.4	850.9	744.4	119.9	589.4	458.2	450.1	143.9	818.0	83.4	2122.7	487.2	556.7	180.6	520.1	85.2
17/06/2012	88	2044.8	857.9	742.5	118.0	585.2	454.2	462.4	155.5	808.1	74.0	2117.1	481.9	556.6	180.5	514.9	80.3
18/06/2012	89	2086.8	897.7	749.2	124.4	594.8	463.3	451.5	145.2	813.2	78.9	2142.5	506.0	567.8	191.1	524.7	89.6
19/06/2012	90	2090.6	901.3	750.4	125.6	596.8	465.2	457.2	150.5	806.5	72.5	2145.5	508.9	569.3	192.6	528.3	93.0
20/06/2012	91	2092.1	902.8	743.4	118.9	601.0	469.1	451.5	145.2	806.4	72.4	2148.4	511.6	570.0	193.2	521.1	86.1
21/06/2012	92	2102.1	912.2	748.6	123.8	613.8	481.3	462.7	155.8	809.7	75.5	2152.3	515.3	572.3	195.4	525.4	90.3
22/06/2012	93	2090.0	900.7	750.5	125.6	609.2	477.0	455.4	148.8	799.8	66.1	2146.4	509.7	568.2	191.5	518.3	83.6
23/06/2012	94	2106.6	916.5	754.6	129.5	614.0	481.5	460.2	153.4	804.6	70.7	2155.5	518.3	572.4	195.5	524.0	88.9
24/06/2012	95	2106.4	916.3	745.5	120.9	616.0	483.4	472.7	165.3	800.6	66.9	2154.2	517.1	572.9	196.0	521.5	86.5
25/06/2012	96	2105.5	915.4	764.6	139.0	618.5	485.7	469.2	161.9	802.5	68.7	2159.3	521.9	573.9	196.9	527.5	92.2
26/06/2012	97	2084.1	895.2	764.6	139.0	614.4	481.9	473.3	165.8	802.7	68.9	2153.3	516.2	570.2	193.4	530.0	94.7
27/06/2012	98	2082.3	893.5	765.4	139.8	613.9	481.4	485.3	177.3	809.8	75.6	2150.3	513.4	568.3	191.6	534.1	98.5
28/06/2012	99	2080.6	891.8	771.8	145.8	619.3	486.5	489.5	181.2	810.9	76.7	2151.8	514.9	568.2	191.5	535.5	99.8
29/06/2012	100	2071.9	883.6	767.3	141.6	619.8	487.0	493.0	184.5	810.4	76.3	2144.2	507.6	564.1	187.6	536.0	100.3
30/06/2012	101	2075.4	886.9	778.4	152.1	627.4	494.2	499.9	191.0	810.9	76.7	2143.2	506.6	562.9	186.5	542.3	106.3
1/07/2012	102	2092.8	903.4	786.2	159.5	628.3	495.1	506.3	197.1	804.2	70.4	2150.1	513.2	566.5	189.9	549.6	113.2
2/07/2012	103	2115.7	925.1	791.5	164.5	627.1	493.9	517.6	207.9	804.9	71.0	2163.8	526.2	575.0	198.0	551.6	115.1
3/07/2012	104	2131.0	939.6	788.9	162.1	632.9	499.5	510.6	201.2	806.9	72.9	2172.8	534.8	577.6	200.5	548.1	111.7
4/07/2012	105	2125.7	934.6	776.7	150.5	631.6	498.2	511.9	202.5	803.9	70.0	2175.8	537.5	578.0	200.8	548.8	112.4
5/07/2012	106	2112.8	922.3	776.7	150.5	633.0	499.5	516.0	206.4	807.3	73.3	2173.8	535.7	577.0	199.8	551.5	114.9
6/07/2012	107	2100.6	910.8	782.3	155.8	633.1	499.6	511.8	202.3	809.0	74.8	2166.7	529.0	572.9	195.9	547.4	111.1
7/07/2012	108	2103.6	913.6	784.4	157.8	641.4	507.5	534.6	223.9	810.7	76.4	2169.1	531.2	573.6	196.6	554.2	117.5
8/07/2012	109	2095.2	905.7	787.6	160.8	628.4	495.1	536.7	225.9	802.9	69.1	2158.0	520.7	569.2	192.5	547.0	110.7
9/07/2012	110	2112.3	921.9	789.0	162.1	632.6	499.2	533.2	222.6	818.4	83.8	2170.6	532.6	573.8	196.8	544.5	108.3
10/07/2012	111	2101.9	912.0	776.7	150.5	644.0	509.9	542.9	231.8	816.3	81.8	2164.8	527.2	570.5	193.7	550.8	114.3
11/07/2012	112	2085.3	896.3	794.7	167.5	633.6	500.1	550.9	239.4	805.7	71.7	2148.7	511.8	563.9	187.5	559.8	122.9
12/07/2012	113	2113.3	922.8	798.9	171.5	631.1	497.7	552.2	240.7	818.1	83.5	2167.3	529.5	570.9	194.1	550.9	114.4
13/07/2012	114	2098.9	909.1	803.4	175.8	646.7	512.5	552.1	240.5	822.9	88.0	2162.6	525.0	567.8	191.1	559.4	122.5
14/07/2012	115	2078.6	890.0	792.0	165.0	658.0	523.2	562.2	250.1	807.9	73.9	2145.2	508.5	560.8	184.5	573.7	136.0
15/07/2012	116	2101.4	911.6	803.5	175.9	649.7	515.3	578.2	265.3	795.2	61.8	2155.5	518.3	564.3	187.8	573.5	135.8
16/07/2012	117	2136.5	944.8	792.3	165.2	655.6	521.0	602.6	288.4	805.6	71.6	2180.6	542.1	576.4	199.2	559.8	122.8
17/07/2012	118	2133.9	942.4	802.3	174.7	663.2	528.1	607.1	292.7	802.1	68.3	2177.0	538.7	575.5	198.4	566.3	129.0
18/07/2012	119	2135.2	943.6	794.2	167.0	665.2	530.0	600.6	286.5	795.5	62.0	2176.3	538.0	575.1	198.0	565.9	128.7
19/07/2012	120	2138.8	947.0	803.1	175.5	660.8	525.8	603.5	289.2	795.0	61.6	2180.2	541.7	577.3	200.2	550.1	113.7

20/07/2012	121	2144.1	952.1	795.6	168.4	667.0	531.7	617.1	302.2	801.2	67.5	2188.3	549.4	580.7	203.3	559.9	123.0
21/07/2012	122	2133.8	942.3	800.6	173.1	665.1	529.9	632.3	316.5	797.3	63.8	2181.1	542.5	576.6	199.4	558.4	121.5
22/07/2012	123	2129.9	938.5	811.7	183.7	667.1	531.8	634.3	318.4	799.7	66.1	2179.0	540.6	575.1	198.0	558.5	121.6
23/07/2012	124	2125.0	934.0	806.5	178.7	666.2	531.0	625.6	310.2	799.9	66.3	2175.3	537.1	573.3	196.4	555.2	118.5
24/07/2012	125	2110.9	920.6	810.2	182.2	663.5	528.4	637.2	321.2	800.1	66.5	2168.1	530.3	570.6	193.7	559.8	122.8
25/07/2012	126	2109.5	919.2	821.0	192.5	665.7	530.5	691.8	372.9	805.3	71.4	2166.4	528.6	569.4	192.6	561.9	124.8
26/07/2012	127	2122.6	931.7	823.7	195.0	675.6	539.9	687.7	369.1	803.7	69.9	2174.8	536.6	571.3	194.5	559.0	122.1
27/07/2012	128	2129.7	938.4	825.8	197.1	682.7	546.6	685.9	367.4	794.5	61.1	2173.2	535.1	572.9	196.0	567.2	129.9
28/07/2012	129	2138.9	947.1	828.3	199.4	684.7	548.5	702.0	382.6	788.9	55.8	2181.0	542.5	576.5	199.3	562.3	125.2
29/07/2012	130	2148.6	956.2	838.2	208.8	684.3	548.1	719.0	398.7	789.9	56.8	2186.5	547.7	578.5	201.3	561.9	124.8
30/07/2012	131	2153.0	960.5	852.0	221.9	680.2	544.3	720.8	400.5	791.6	58.4	2188.9	550.0	580.7	203.4	559.5	122.6
31/07/2012	132	2153.6	961.1	840.7	211.1	681.5	545.5	710.6	390.8	796.7	63.2	2193.7	554.6	582.4	205.0	553.9	117.2
1/08/2012	133	2159.4	966.5	840.4	210.8	684.8	548.6	714.2	394.1	797.9	64.4	2197.8	558.5	584.4	206.9	554.2	117.6
2/08/2012	134	2158.0	965.2	843.5	213.8	686.7	550.4	756.7	434.5	796.1	62.7	2198.8	559.4	585.0	207.5	557.6	120.8
3/08/2012	135	2162.2	969.1	838.3	208.9	697.4	560.6	785.9	462.1	796.2	62.7	2200.4	560.9	585.3	207.7	564.8	127.6
4/08/2012	136	2163.8	970.7	861.7	231.0	701.4	564.3	809.2	484.3	788.9	55.8	2198.4	559.0	584.2	206.7	561.1	124.1
5/08/2012	137	2167.6	974.3	862.4	231.7	706.7	569.4	813.1	487.9	788.0	55.0	2198.8	559.4	583.8	206.3	576.8	138.9
6/08/2012	138	2167.2	973.9	867.8	236.8	696.7	559.9	825.4	499.6	783.8	51.0	2199.1	559.7	584.6	207.1	575.9	138.1
7/08/2012	139	2185.9	991.6	874.0	242.7	696.9	560.0	828.0	502.0	797.0	63.5	2213.8	573.6	590.5	212.7	579.9	141.9
8/08/2012	140	2176.1	982.4	878.1	246.6	703.5	566.4	858.6	531.0	798.2	64.7	2212.9	572.7	590.2	212.3	589.4	150.9
9/08/2012	141	2176.7	982.9	874.5	243.2	703.3	566.2	888.1	559.0	794.0	60.6	2210.0	570.0	588.8	211.0	580.7	142.7
10/08/2012	142	2176.6	982.9	870.9	239.8	712.5	574.8	907.1	577.0	796.4	62.9	2215.1	574.8	590.4	212.6	591.5	152.9
11/08/2012	143	2163.8	970.7	871.9	240.7	712.6	574.9	906.3	576.2	789.9	56.8	2199.6	560.2	585.5	207.9	596.2	157.3
12/08/2012	144	2152.4	959.9	892.2	259.9	710.9	573.4	932.6	601.2	793.8	60.4	2195.1	555.8	581.6	204.2	599.5	160.4
13/08/2012	145	2154.9	962.3	911.5	278.3	704.4	567.2	919.1	588.4	796.0	62.5	2200.8	561.2	583.5	206.0	600.0	160.9
14/08/2012	146	2166.4	973.1	909.1	276.0	715.2	577.4	917.2	586.6	804.5	70.6	2210.5	570.5	586.3	208.7	591.5	152.9
15/08/2012	147	2171.0	977.5	896.9	264.4	717.0	579.1	910.2	580.0	795.2	61.8	2207.0	567.2	586.7	209.0	587.7	149.3
16/08/2012	148	2178.9	985.0	902.6	269.8	719.4	581.4	892.9	563.6	795.4	62.0	2212.0	571.9	588.2	210.4	591.4	152.8
17/08/2012	149	2179.7	985.8	924.4	290.5	724.9	586.6	905.8	575.8	794.6	61.2	2211.1	571.1	587.6	209.9	593.4	154.7
18/08/2012	150	2183.8	989.6	941.4	306.6	721.2	583.1	903.7	573.8	789.9	56.7	2210.1	570.0	588.0	210.3	596.4	157.6
19/08/2012	151	2186.5	992.2	941.3	306.5	719.2	581.2	890.8	561.6	794.1	60.8	2218.9	578.4	589.1	211.3	594.1	155.4
20/08/2012	152	2183.3	989.2	929.6	295.4	722.1	584.0	886.7	557.6	796.6	63.1	2223.9	583.1	591.8	213.9	586.8	148.4
21/08/2012	153	2176.6	982.9	940.9	306.1	721.4	583.3	904.0	574.1	795.7	62.2	2216.6	576.2	589.0	211.2	603.4	164.1
22/08/2012	154	2171.5	978.0	991.1	353.7	714.3	576.6	884.8	555.9	798.2	64.7	2210.9	570.9	586.5	208.9	599.4	160.4
23/08/2012	155	2157.4	964.6	985.8	348.7	723.4	585.2	855.8	528.4	807.7	73.6	2211.0	570.9	584.4	206.9	600.7	161.6
24/08/2012	156	2152.3	959.8	987.5	350.3	733.1	594.4	845.9	519.0	800.4	66.8	2206.8	567.0	580.8	203.4	588.9	150.5
25/08/2012	157	2169.5	976.1	1002.9	364.9	735.0	596.2	861.9	534.2	791.4	58.2	2210.3	570.3	582.6	205.1	605.4	166.1

26/08/2012	158	2181.3	987.3	1015.8	377.1	731.6	592.9	850.5	523.4	791.6	58.4	2214.5	574.2	587.0	209.3	593.8	155.1
27/08/2012	159	2195.1	1000.4	1015.7	377.0	733.7	595.0	862.2	534.5	796.9	63.4	2225.7	584.9	591.5	213.6	595.2	156.4
28/08/2012	160	2173.0	979.4	1004.4	366.3	729.0	590.5	872.6	544.3	796.0	62.6	2217.1	576.7	588.1	210.4	586.9	148.6
29/08/2012	161	2168.5	975.2	1005.4	367.3	730.2	591.7	847.2	520.3	801.9	68.2	2214.6	574.3	585.9	208.3	591.7	153.1
30/08/2012	162	2167.4	974.1	1040.8	400.8	740.2	601.1	831.8	505.7	802.0	68.3	2217.5	577.1	586.2	208.6	576.8	139.0
31/08/2012	163	2181.9	987.9	1067.1	425.7	739.7	600.6	825.5	499.7	793.1	59.8	2226.8	586.0	588.9	211.1	579.8	141.8
1/09/2012	164	2194.3	999.6	1086.3	443.9	739.3	600.3	843.7	516.9	794.2	60.8	2233.1	591.9	594.1	216.1	587.3	148.9
2/09/2012	165	2188.2	993.8	1086.9	444.6	735.3	596.4	833.4	507.2	795.6	62.2	2231.1	590.0	592.8	214.9	589.7	151.2
3/09/2012	166	2196.7	1001.9	1098.3	455.3	743.0	603.7	809.3	484.4	801.6	67.9	2236.3	594.9	594.9	216.8	594.8	156.0
4/09/2012	167	2187.2	992.9	1101.8	458.7	756.7	616.8	834.0	507.8	796.3	62.8	2230.3	589.2	592.1	214.2	593.0	154.3
5/09/2012	168	2190.0	995.5	1127.4	482.9	752.9	613.1	825.7	499.9	784.0	51.2	2225.0	584.2	591.0	213.1	592.1	153.5
6/09/2012	169	2211.1	1015.5	1156.7	510.7	754.4	614.6	816.6	491.2	789.9	56.8	2240.1	598.5	596.3	218.1	599.7	160.7
7/09/2012	170	2223.7	1027.5	1173.9	527.0	755.1	615.2	799.2	474.8	791.3	58.1	2246.5	604.6	599.5	221.2	608.0	168.5
8/09/2012	171	2222.1	1026.0	1181.1	533.8	758.2	618.2	808.5	483.5	791.8	58.6	2247.6	605.7	600.2	221.8	606.4	167.0
9/09/2012	172	2208.8	1013.3	1206.0	557.4	755.5	615.6	829.1	503.1	789.9	56.8	2238.1	596.6	596.4	218.2	614.5	174.7
10/09/2012	173	2199.3	1004.4	1216.4	567.3	747.6	608.1	833.0	506.7	793.4	60.1	2235.9	594.5	594.3	216.2	599.4	160.4
11/09/2012	174	2187.2	992.8	1211.6	562.7	739.7	600.6	823.2	497.5	804.7	70.8	2234.0	592.7	592.1	214.1	601.7	162.6
12/09/2012	175	2173.6	980.0	1234.5	584.4	740.0	600.9	849.7	522.6	812.4	78.1	2233.1	591.9	590.2	212.4	605.4	166.1
13/09/2012	176	2160.3	967.4	1188.9	541.2	735.7	596.9	812.3	487.2	811.3	77.1	2222.9	582.2	585.4	207.8	593.4	154.7
14/09/2012	177	2181.5	987.5	1189.3	541.6	748.2	608.7	807.6	482.7	816.1	81.6	2238.2	596.7	590.5	212.6	610.1	170.6
15/09/2012	178	2183.3	989.2	1200.4	552.1	749.1	609.6	823.5	497.8	806.2	72.2	2237.8	596.3	589.0	211.3	608.8	169.3
16/09/2012	179	2178.1	984.2	1218.3	569.1	746.2	606.8	844.6	517.7	806.5	72.5	2230.6	589.5	586.2	208.6	612.7	173.0
17/09/2012	180	2170.7	977.2	1233.8	583.8	740.3	601.2	862.8	535.0	808.7	74.6	2225.1	584.3	585.1	207.5	617.6	177.6
18/09/2012	181	2155.6	962.9	1243.6	593.0	739.1	600.1	869.6	541.5	813.1	78.7	2222.6	581.9	583.3	205.8	616.9	176.9
19/09/2012	182	2152.3	959.8	1265.8	614.1	736.9	598.0	904.4	574.5	815.2	80.8	2224.7	583.9	583.3	205.9	610.8	171.2
20/09/2012	183	2149.5	957.1	1257.6	606.3	728.5	590.0	891.8	562.5	816.9	82.3	2226.1	585.3	583.1	205.6	610.2	170.6
21/09/2012	184	2155.4	962.8	1261.4	609.9	732.7	594.0	890.5	561.3	826.1	91.1	2227.4	586.5	584.1	206.5	610.6	171.0
22/09/2012	185	2149.2	956.9	1278.0	625.6	732.2	593.5	918.4	587.7	819.3	84.7	2222.8	582.1	582.1	204.6	622.1	181.9
23/09/2012	186	2139.3	947.5	1267.4	615.6	725.1	586.8	892.0	562.7	818.2	83.6	2220.2	579.7	580.1	202.8	636.2	195.3
24/09/2012	187	2165.3	972.1	1255.8	604.6	731.7	593.1	876.4	547.9	826.0	91.0	2235.4	594.0	584.7	207.2	637.1	196.2
25/09/2012	188	2177.5	983.7	1267.4	615.6	736.0	597.1	891.8	562.5	821.1	86.3	2239.8	598.2	587.1	209.4	630.3	189.7
26/09/2012	189	2161.8	968.8	1267.2	615.4	731.2	592.6	890.9	561.6	818.5	83.9	2233.1	591.9	585.3	207.7	632.3	191.6
27/09/2012	190	2165.1	971.9	1268.3	616.4	732.2	593.5	876.9	548.4	825.2	90.3	2231.6	590.5	585.0	207.4	640.0	198.8
28/09/2012	191	2157.8	965.0	1246.8	596.1	734.4	595.6	847.9	520.9	823.6	88.8	2223.7	582.9	581.9	204.5	660.8	218.6
29/09/2012	192	2139.1	947.3	1236.6	586.4	743.5	604.2	834.7	508.4	821.3	86.5	2215.3	575.0	578.7	201.4	659.6	217.4
30/09/2012	193	2168.4	975.0	1217.4	568.2	744.1	604.8	802.0	477.4	811.3	77.1	2226.3	585.5	581.7	204.3	644.6	203.2
1/10/2012	194	2186.2	991.9	1237.2	587.0	754.2	614.4	839.7	513.1	812.0	77.7	2239.8	598.2	587.8	210.0	643.3	202.0

2/10/2012	195	2178.4	984.6	1233.7	583.7	744.0	604.7	835.8	509.4	806.2	72.2	2230.0	589.0	585.3	207.8	681.4	238.1
3/10/2012	196	2191.3	996.8	1227.9	578.1	745.8	606.4	821.4	495.8	818.6	84.0	2241.4	599.7	589.2	211.4	672.4	229.6
4/10/2012	197	2189.1	994.7	1244.3	593.7	752.2	612.5	839.7	513.1	818.8	84.1	2238.4	596.9	588.5	210.7	669.9	227.2
5/10/2012	198	2201.2	1006.2	1255.0	603.8	746.1	606.7	861.8	534.1	814.4	80.0	2241.5	599.8	590.8	213.0	682.3	239.0
6/10/2012	199	2174.8	981.2	1255.7	604.5	740.5	601.4	865.3	537.4	819.2	84.5	2233.7	592.5	587.8	210.1	693.8	249.9
7/10/2012	200	2172.8	979.2	1256.5	605.3	741.5	602.3	871.3	543.1	825.2	90.3	2232.9	591.6	584.7	207.2	692.6	248.7
8/10/2012	201	2196.7	1001.9	1255.0	603.9	738.5	599.5	868.7	540.6	826.8	91.7	2242.2	600.5	588.0	210.3	679.2	236.1
9/10/2012	202	2207.4	1012.1	1235.8	585.7	740.0	600.9	844.7	517.9	830.4	95.2	2248.6	606.5	590.5	212.7	678.0	234.8
10/10/2012	203	2211.9	1016.3	1287.6	634.8	747.0	607.5	897.8	568.2	830.9	95.7	2251.8	609.6	593.4	215.4	715.5	270.4
11/10/2012	204	2205.1	1009.8	1251.2	600.3	726.7	588.3	851.0	523.9	824.8	89.9	2244.9	603.1	590.7	212.8	721.2	275.8
12/10/2012	205	2225.8	1029.5	1230.2	580.4	740.5	601.4	836.5	510.1	845.3	109.3	2268.1	625.1	601.8	223.3	735.6	289.5
13/10/2012	206	2223.5	1027.3	1241.9	591.5	747.4	607.9	857.6	530.1	832.7	97.3	2262.1	619.3	599.2	220.9	728.8	283.1
14/10/2012	207	2213.8	1018.0	1235.9	585.8	742.6	603.4	850.6	523.5	830.1	94.9	2253.4	611.1	595.2	217.1	728.3	282.6
15/10/2012	208	2211.0	1015.4	1218.8	569.6	748.8	609.2	813.9	488.7	836.5	100.9	2254.7	612.3	595.6	217.5	716.9	271.7
16/10/2012	209	2204.1	1008.9	1225.8	576.1	759.2	619.2	832.1	506.0	830.1	94.9	2247.2	605.3	593.3	215.3	734.9	288.8
17/10/2012	210	2197.0	1002.1	1264.6	613.0	754.3	614.5	882.5	553.7	819.7	85.0	2237.7	596.2	589.3	211.5	751.1	304.2
18/10/2012	211	2193.5	998.9	1268.0	616.1	738.9	599.9	877.0	548.5	825.1	90.1	2237.4	596.0	588.4	210.6	755.5	308.3
19/10/2012	212	2188.6	994.2	1258.2	606.8	739.7	600.6	846.3	519.4	836.4	100.9	2241.4	599.7	589.7	211.9	789.0	340.1
20/10/2012	213	2176.7	983.0	1261.5	610.0	747.5	608.0	858.7	531.2	833.9	98.4	2231.5	590.4	585.0	207.4	539.0	103.2
21/10/2012	214	2150.8	958.3	1255.4	604.3	746.2	606.8	868.0	539.9	824.0	89.1	2215.4	575.1	579.4	202.2	525.1	89.9
22/10/2012	215	2160.9	968.0	1254.3	603.2	746.8	607.3	868.3	540.2	824.3	89.4	2218.9	578.4	579.9	202.6	527.2	92.0
23/10/2012	216	2191.8	997.3	1243.0	592.5	743.4	604.2	845.9	519.0	820.7	86.0	2235.6	594.3	586.0	208.3	535.1	99.4
24/10/2012	217	2198.4	1003.5	1253.3	602.2	750.3	610.7	848.8	521.7	827.4	92.3	2244.8	602.9	589.2	211.4	539.5	103.6
25/10/2012	218	2180.9	986.9	1262.0	610.5	748.2	608.7	854.1	526.8	824.4	89.5	2231.0	589.9	584.0	206.5	530.3	94.9
26/10/2012	219	2170.8	977.3	1249.1	598.3	744.1	604.8	846.6	519.7	825.3	90.3	2226.1	585.3	582.3	204.9	530.6	95.2
27/10/2012	220	2180.7	986.7	1245.3	594.7	748.9	609.3	843.1	516.3	828.5	93.4	2231.3	590.2	584.3	206.7	533.1	97.6
28/10/2012	221	2189.1	994.6	1254.5	603.4	752.0	612.3	855.4	528.0	823.6	88.7	2234.3	593.0	585.1	207.5	529.8	94.5
29/10/2012	222	2190.5	996.0	1260.7	609.2	748.4	608.8	862.3	534.6	823.0	88.2	2234.2	592.9	585.2	207.6	525.7	90.5
30/10/2012	223	2179.7	985.8	1297.6	644.3	747.1	607.7	910.8	580.5	828.7	93.5	2232.4	591.2	585.1	207.5	527.5	92.2
31/10/2012	224	2169.9	976.5	1265.0	613.3	727.9	589.4	865.5	537.6	828.5	93.4	2225.4	584.6	583.1	205.6	530.3	94.9
1/11/2012	225	2186.4	992.2	1262.1	610.6	743.0	603.8	849.9	522.8	846.1	110.1	2242.1	600.4	588.4	210.6	555.9	119.1
2/11/2012	226	2190.3	995.8	1270.7	618.8	744.2	604.9	849.3	522.2	828.5	93.4	2238.8	597.3	586.5	208.9	540.2	104.3
3/11/2012	227	2182.5	988.4	1276.3	624.0	739.7	600.7	868.3	540.2	826.8	91.8	2236.9	595.5	587.0	209.3	534.1	98.5
4/11/2012	228	2170.7	977.3	1292.8	639.7	737.1	598.2	903.4	573.5	833.3	97.9	2234.1	592.8	585.8	208.2	533.5	97.9
5/11/2012	229	2160.1	967.2	1288.9	636.0	730.7	592.1	902.2	572.4	837.0	101.4	2224.9	584.1	582.3	204.9	535.1	99.5
6/11/2012	230	2152.4	959.9	1308.0	654.1	732.6	593.9	940.3	608.5	840.9	105.1	2219.4	578.9	579.8	202.5	542.1	106.1
7/11/2012	231	2140.5	948.6	1311.0	656.9	720.3	582.2	942.1	610.2	836.4	100.9	2209.1	569.2	575.6	198.5	541.4	105.4

8/11/2012	232	2145.1	953.0	1324.5	669.8	719.7	581.7	957.8	625.1	844.8	108.8	2215.3	575.0	576.8	199.7	550.7	114.2
9/11/2012	233	2134.1	942.6	1312.4	658.2	711.7	574.1	937.9	606.2	841.8	106.0	2206.0	566.2	572.6	195.7	549.0	112.6
10/11/2012	234	2141.2	949.3	1310.3	656.3	716.9	579.0	947.2	615.1	845.4	109.4	2212.2	572.1	574.5	197.5	556.1	119.3
11/11/2012	235	2152.5	959.9	1309.2	655.2	716.3	578.4	941.1	609.3	839.5	103.8	2217.8	577.4	576.3	199.2	552.0	115.5
12/11/2012	236	2169.9	976.4	1297.3	644.0	717.9	580.0	920.4	589.7	841.6	105.8	2229.6	588.6	581.1	203.8	551.2	114.7
13/11/2012	237	2170.3	976.9	1332.0	676.9	723.7	585.5	978.9	645.0	842.6	106.7	2229.7	588.7	581.3	203.9	550.3	113.8
14/11/2012	238	2160.0	967.1	1310.5	656.4	705.8	568.6	936.0	604.5	838.3	102.6	2222.1	581.5	578.9	201.7	544.0	107.9
15/11/2012	239	2169.7	976.3	1321.9	667.2	718.6	580.7	946.8	614.7	856.7	120.1	2236.9	595.5	583.9	206.4	560.9	123.9
16/11/2012	240	2146.7	954.5	1300.2	646.7	713.8	576.1	910.7	580.4	844.3	108.3	2217.3	576.9	576.8	199.6	546.8	110.5

Table E.5 Concrete surface strain at steel level for slab S-SCC-a

Slab S-SCC-a		CONCRETE SURFACE STRAIN BY SG															
		1		2		3		4		5		6		7		8	
Date	Age	Reading	Strain	Reading	Strain	Reading	Strain	Reading	Strain	Reading	Strain	Reading	Strain	Reading	Strain	Reading	Strain
26/04/2012	14	1079.8		417.3		1008.5		899.6		923.4		1762.9		200.6		820.6	
26/04/2012	14	1102.1		541.3		1153.8		1205.8		1206.0		1795.2		1098.8		962.1	
27/04/2012	15	1177.4	71.3	691.6	142.5	1340.7	177.2	1305.5	94.5	1532.4	309.4	1819.7	23.2	1184.1	80.8	1107.9	138.2
28/04/2012	16	1236.1	127.0	730.4	179.3	1378.9	213.3	1345.9	132.8	1565.4	340.7	1820.6	24.1	1214.2	109.4	1112.5	142.6
29/04/2012	17	1278.7	167.3	778.3	224.6	1418.3	250.7	1382.7	167.7	1593.2	367.1	1822.6	26.0	1244.2	137.8	1131.7	160.7
30/04/2012	18	1294.9	182.7	837.9	281.2	1443.8	274.9	1420.0	203.1	1610.1	383.1	1904.3	103.4	1282.4	174.0	1145.8	174.1
1/05/2012	19	1291.5	179.5	860.2	302.3	1454.4	285.0	1433.2	215.5	1614.7	387.4	1886.5	86.5	1291.0	182.2	1142.7	171.2
2/05/2012	20	1300.5	188.0	890.2	330.8	1487.2	316.0	1452.9	234.2	1634.5	406.2	1893.1	92.8	1310.3	200.4	1144.4	172.8
3/05/2012	21	1303.7	191.0	909.7	349.2	1513.8	341.2	1473.3	253.6	1649.8	420.6	1894.7	94.4	1330.9	220.0	1162.3	189.8
4/05/2012	22	1289.5	177.6	942.1	379.9	1526.0	352.8	1505.0	283.7	1662.2	432.4	1877.0	77.6	1360.7	248.2	1182.3	208.7
5/05/2012	23	1265.5	154.9	949.5	387.0	1524.1	351.0	1508.2	286.6	1658.6	429.0	1847.4	49.5	1363.8	251.1	1167.4	194.6
6/05/2012	24	1252.6	142.6	963.6	400.3	1537.4	363.6	1523.5	301.2	1674.9	444.4	1832.5	35.4	1373.6	260.5	1162.6	190.0
7/05/2012	25	1263.2	152.7	986.6	422.1	1565.6	390.3	1548.5	324.9	1702.1	470.3	1834.9	37.6	1396.0	281.7	1161.7	189.2
8/05/2012	26	1273.5	162.4	1011.9	446.1	1586.4	410.0	1578.1	352.9	1727.6	494.5	1841.9	44.3	1419.9	304.3	1178.8	205.4
9/05/2012	27	1267.5	156.8	1023.6	457.2	1592.8	416.1	1590.7	364.9	1738.9	505.2	1839.5	41.9	1432.7	316.5	1187.0	213.1
10/05/2012	28	1265.4	154.8	1032.4	465.5	1603.0	425.8	1598.5	372.3	1747.9	513.6	1890.8	90.6	1441.7	325.0	1187.0	213.2
11/05/2012	29	1265.0	154.3	1051.4	483.5	1614.0	436.2	1609.9	383.1	1753.5	519.0	2083.0	272.8	1452.1	334.9	1191.0	216.9
12/05/2012	30	1256.1	145.9	1065.0	496.5	1621.2	443.0	1625.7	398.1	1762.8	527.8	2093.7	283.0	1465.9	347.9	1206.0	231.2
13/05/2012	31	1244.1	134.5	1079.7	510.4	1629.5	450.9	1641.4	412.9	1778.2	542.3	2087.1	276.6	1480.0	361.3	1201.1	226.6
14/05/2012	32	1242.7	133.2	1090.4	520.5	1652.9	473.0	1660.5	431.0	1797.2	560.4	2091.5	280.8	1504.9	384.9	1216.6	241.3
15/05/2012	33	1232.2	123.3	1096.1	526.0	1651.9	472.1	1677.4	447.0	1801.6	564.5	2083.3	273.1	1518.6	397.9	1203.8	229.1
16/05/2012	34	1241.3	131.9	1110.2	539.3	1668.8	488.1	1681.0	450.4	1810.2	572.7	2101.3	290.1	1520.7	399.9	1198.0	223.6
17/05/2012	35	1227.8	119.1	1103.0	532.4	1663.0	482.6	1688.5	457.5	1801.1	564.1	2101.8	290.6	1522.3	401.4	1163.6	190.9
18/05/2012	36	1224.7	116.2	1113.1	542.0	1664.8	484.3	1695.1	463.8	1806.6	569.3	2119.0	307.0	1530.5	409.2	1164.9	192.2
19/05/2012	37	1216.6	108.5	1121.2	549.7	1664.7	484.2	1698.3	466.8	1811.5	573.9	2114.9	303.1	1535.7	414.1	1165.2	192.5
20/05/2012	38	1210.4	102.6	1143.3	570.6	1667.5	486.9	1713.2	481.0	1827.9	589.5	2111.8	300.1	1545.7	423.6	1170.3	197.3
21/05/2012	39	1206.0	98.4	1135.9	563.6	1659.3	479.2	1703.7	472.0	1823.1	585.0	2116.4	304.4	1547.9	425.6	1158.6	186.3
22/05/2012	40	1202.3	95.0	1146.5	573.7	1668.5	487.8	1716.7	484.3	1835.0	596.2	2121.8	309.6	1559.8	436.9	1164.1	191.4
23/05/2012	41	1195.8	88.8	1165.0	591.2	1672.7	491.9	1734.9	501.5	1853.6	613.8	2113.8	302.0	1571.9	448.5	1168.0	195.2
24/05/2012	42	1189.3	82.6	1162.4	588.8	1662.7	482.3	1736.5	503.0	1846.0	606.6	2099.7	288.6	1569.5	446.1	1153.4	181.3
25/05/2012	43	1186.1	79.6	1161.4	587.8	1664.0	483.6	1732.6	499.4	1842.8	603.6	2117.8	305.8	1575.2	451.5	1151.7	179.8
26/05/2012	44	1169.5	63.9	1177.7	603.2	1662.0	481.7	1746.5	512.5	1852.8	613.1	2105.3	293.9	1579.0	455.1	1154.7	182.5

27/05/2012	45	1168.3	62.7	1184.3	609.5	1663.0	482.6	1754.2	519.8	1861.9	621.7	2105.2	293.9	1581.5	457.5	1159.0	186.6
28/05/2012	46	1178.9	72.7	1201.6	625.9	1679.9	498.6	1770.5	535.3	1877.8	636.8	2125.9	313.4	1593.3	468.7	1165.0	192.3
29/05/2012	47	1170.7	65.0	1189.5	614.4	1671.7	490.9	1763.0	528.2	1867.0	626.6	2124.1	311.7	1598.8	473.9	1150.3	178.4
30/05/2012	48	1176.5	70.4	1196.1	620.7	1680.9	499.6	1769.6	534.4	1872.2	631.5	2133.0	320.2	1611.6	486.0	1157.6	185.3
31/05/2012	49	1165.7	60.2	1190.5	615.4	1678.1	497.0	1773.1	537.8	1870.2	629.6	2127.0	314.5	1605.0	479.8	1147.3	175.5
1/06/2012	50	1162.3	57.0	1192.6	617.4	1672.5	491.6	1772.1	536.8	1864.6	624.3	2125.7	313.3	1610.0	484.6	1143.2	171.6
2/06/2012	51	1162.5	57.2	1192.2	617.0	1672.5	491.7	1768.7	533.6	1863.2	623.0	2128.4	315.8	1606.3	481.0	1144.6	173.0
3/06/2012	52	1161.7	56.4	1190.3	615.2	1674.9	493.9	1766.6	531.6	1860.7	620.6	2132.3	319.5	1611.1	485.5	1147.5	175.7
4/06/2012	53	1155.0	50.1	1189.1	614.0	1671.2	490.4	1767.1	532.1	1858.6	618.6	2130.5	317.8	1616.4	490.6	1143.7	172.2
5/06/2012	54	1151.9	47.1	1218.8	642.3	1686.4	504.8	1790.2	554.0	1887.0	645.5	2124.6	312.3	1640.7	513.6	1151.2	179.2
6/06/2012	55	1136.1	32.2	1203.5	627.7	1674.7	493.8	1788.6	552.4	1875.3	634.5	2109.3	297.7	1632.5	505.8	1132.0	161.0
7/06/2012	56	1140.4	36.3	1217.9	641.3	1684.4	502.9	1799.2	562.5	1889.6	648.0	2114.5	302.7	1643.6	516.3	1138.4	167.1
8/06/2012	57	1142.5	38.2	1236.7	659.1	1699.4	517.1	1817.0	579.3	1907.7	665.2	2118.4	306.4	1663.7	535.5	1152.4	180.4
9/06/2012	58	1139.9	35.8	1235.6	658.1	1698.8	516.6	1822.0	584.1	1908.9	666.3	2112.8	301.0	1663.9	535.6	1153.6	181.5
10/06/2012	59	1144.1	39.7	1238.9	661.3	1704.3	521.8	1824.9	586.9	1909.8	667.1	2116.8	304.8	1666.6	538.1	1154.1	182.0
11/06/2012	60	1132.7	28.9	1232.9	655.5	1695.0	513.0	1811.2	573.9	1896.4	654.4	2117.7	305.7	1655.0	527.2	1142.7	171.1
12/06/2012	61	1105.7	3.3	1229.9	652.7	1686.9	505.3	1804.8	567.8	1890.8	649.1	2118.6	306.5	1645.6	518.2	1135.1	163.9
13/06/2012	62	1117.5	14.6	1234.0	656.6	1697.2	515.1	1809.2	571.9	1895.9	653.9	2129.8	317.2	1653.8	526.0	1145.7	174.0
14/06/2012	63	1120.5	17.4	1234.0	656.6	1698.5	516.3	1809.9	572.6	1894.8	652.9	2134.1	321.2	1659.7	531.7	1146.9	175.2
15/06/2012	64	1113.9	11.2	1229.5	652.3	1693.7	511.7	1806.6	569.5	1891.2	649.5	2126.7	314.2	1653.9	526.1	1140.2	168.8
16/06/2012	65	1114.2	11.5	1233.5	656.1	1699.0	516.8	1808.6	571.4	1894.7	652.8	2127.5	315.0	1656.3	528.4	1144.2	172.6
17/06/2012	66	1102.1	0.0	1230.3	653.1	1690.6	508.8	1809.6	572.4	1888.7	647.1	2112.6	300.9	1666.2	537.8	1132.3	161.3
18/06/2012	67	1134.9	31.0	1247.0	669.0	1704.4	521.9	1830.3	591.9	1907.4	664.8	2109.5	297.9	1675.9	546.9	1137.5	166.2
19/06/2012	68	1150.0	45.4	1252.8	674.5	1712.5	529.6	1843.0	604.0	1919.0	675.9	2107.0	295.5	1683.4	554.1	1143.2	171.7
20/06/2012	69	1146.3	41.8	1253.4	675.0	1709.9	527.1	1844.9	605.8	1919.2	676.0	2105.8	294.4	1684.4	555.0	1133.5	162.4
21/06/2012	70	1147.8	43.3	1261.9	683.1	1717.3	534.1	1852.5	613.0	1929.2	685.5	2105.8	294.4	1695.3	565.4	1144.3	172.7
22/06/2012	71	1137.9	33.9	1252.8	674.5	1707.5	524.9	1847.6	608.3	1925.0	681.5	2090.8	280.2	1679.7	550.6	1136.0	164.9
23/06/2012	72	1139.7	35.6	1265.8	686.8	1715.5	532.4	1856.0	616.3	1934.4	690.4	2099.6	288.5	1699.6	569.4	1141.7	170.2
24/06/2012	73	1135.2	31.3	1274.1	694.6	1718.2	535.0	1860.9	621.0	1938.4	694.2	2101.3	290.1	1716.2	585.2	1147.7	175.9
25/06/2012	74	1137.9	33.9	1274.4	695.0	1720.1	536.8	1863.2	623.1	1938.4	694.2	2102.7	291.4	1717.4	586.3	1150.4	178.4
26/06/2012	75	1133.6	29.8	1261.5	682.7	1705.7	523.1	1848.4	609.2	1925.5	682.0	2095.4	284.5	1708.0	577.5	1135.2	164.1
27/06/2012	76	1138.2	34.2	1259.8	681.0	1711.2	528.4	1844.0	605.0	1924.3	680.8	2108.0	296.5	1705.3	574.9	1137.9	166.6
28/06/2012	77	1135.5	31.6	1257.4	678.8	1708.3	525.5	1844.7	605.6	1923.9	680.5	2106.1	294.7	1706.2	575.7	1134.4	163.3
29/06/2012	78	1139.4	35.3	1258.6	679.9	1707.9	525.2	1838.8	600.0	1921.6	678.3	2108.6	297.1	1697.7	567.6	1134.3	163.2
30/06/2012	79	1135.5	31.7	1257.3	678.7	1709.0	526.3	1839.6	600.7	1915.8	672.8	2106.9	295.4	1698.7	568.6	1129.7	158.8
1/07/2012	80	1127.3	23.9	1269.9	690.6	1714.1	531.1	1849.0	609.7	1925.4	681.9	2097.8	286.9	1702.7	572.4	1129.4	158.6
2/07/2012	81	1126.1	22.7	1288.4	708.1	1725.4	541.8	1872.8	632.3	1944.5	700.0	2103.9	292.6	1727.5	595.9	1148.3	176.5

3/07/2012	82	1124.7	21.3	1290.0	709.7	1721.6	538.2	1872.5	632.0	1945.1	700.6	2096.4	285.5	1726.9	595.3	1141.5	170.1
4/07/2012	83	1124.4	21.1	1292.9	712.5	1724.6	541.1	1875.7	635.0	1945.9	701.4	2093.0	282.3	1726.0	594.5	1141.6	170.1
5/07/2012	84	1120.4	17.3	1280.8	701.0	1715.2	532.1	1869.0	628.7	1937.7	693.6	2091.7	281.1	1725.9	594.4	1129.3	158.5
6/07/2012	85	1118.5	15.5	1273.4	694.0	1710.8	528.0	1863.0	623.0	1931.0	687.3	2090.3	279.7	1723.6	592.2	1123.8	153.3
7/07/2012	86	1123.0	19.7	1279.1	699.4	1714.8	531.7	1867.8	627.5	1937.3	693.2	2097.0	286.1	1724.5	593.1	1128.6	157.8
8/07/2012	87	1115.8	12.9	1270.3	691.0	1706.1	523.5	1860.6	620.7	1929.1	685.4	2092.0	281.3	1713.4	582.6	1121.0	150.6
9/07/2012	88	1125.8	22.4	1279.5	699.8	1721.2	537.8	1869.6	629.2	1938.8	694.6	2105.7	294.3	1727.7	596.1	1137.0	165.7
10/07/2012	89	1127.3	23.8	1273.7	694.3	1721.6	538.2	1866.3	626.1	1936.4	692.3	2106.7	295.3	1725.3	593.8	1135.2	164.0
11/07/2012	90	1109.8	7.2	1255.7	677.2	1704.4	521.9	1847.8	608.5	1915.3	672.3	2088.9	278.3	1707.4	576.9	1113.4	143.4
12/07/2012	91	1119.9	16.9	1271.7	692.4	1719.5	536.2	1863.2	623.1	1931.4	687.6	2091.3	280.7	1718.0	586.8	1120.5	150.2
13/07/2012	92	1120.6	17.5	1268.0	688.8	1713.3	530.3	1854.3	614.7	1922.0	678.7	2091.8	281.1	1703.2	572.9	1113.8	143.8
14/07/2012	93	1114.0	11.3	1263.6	684.7	1707.4	524.7	1851.9	612.5	1914.8	671.9	2085.8	275.4	1705.2	574.8	1106.2	136.6
15/07/2012	94	1103.7	1.5	1278.6	698.9	1713.0	530.0	1867.4	627.1	1928.0	684.4	2079.4	269.4	1711.1	580.4	1106.6	137.0
16/07/2012	95	1114.4	11.6	1300.6	719.7	1735.8	551.6	1894.2	652.6	1956.2	711.1	2092.8	282.1	1740.6	608.3	1131.0	160.1
17/07/2012	96	1124.1	20.8	1305.7	724.6	1744.7	560.1	1892.8	651.2	1964.6	719.0	2097.9	286.9	1738.9	606.7	1136.3	165.1
18/07/2012	97	1142.6	38.3	1328.3	746.0	1765.5	579.8	1893.8	652.1	1985.7	739.1	2103.6	292.3	1733.4	601.5	1156.0	183.8
19/07/2012	98	1145.4	41.0	1339.8	756.9	1774.5	588.3	1903.0	660.8	1993.0	746.0	2107.6	296.1	1748.7	616.0	1161.7	189.2
20/07/2012	99	1147.5	43.0	1348.2	764.8	1780.6	594.1	1914.8	672.1	2003.4	755.8	2113.1	301.3	1768.0	634.3	1169.6	196.7
21/07/2012	100	1145.1	40.7	1333.6	751.0	1770.4	584.4	1901.2	659.2	1992.6	745.6	2104.6	293.2	1760.1	626.8	1152.6	180.5
22/07/2012	101	1142.2	38.0	1323.6	741.5	1765.5	579.8	1894.9	653.2	1988.2	741.4	2104.2	292.9	1758.1	624.9	1148.6	176.7
23/07/2012	102	1122.7	19.4	1299.5	718.7	1744.9	560.3	1889.6	648.1	1964.4	718.9	2096.3	285.4	1748.0	615.3	1128.8	158.0
24/07/2012	103	1097.5	-4.4	1276.0	696.4	1717.9	534.7	1886.5	645.2	1937.2	693.1	2088.9	278.4	1746.2	613.7	1102.4	133.0
25/07/2012	104	1104.8	2.5	1282.1	702.2	1724.8	541.2	1889.3	647.9	1938.5	694.3	2100.5	289.4	1754.7	621.7	1109.3	139.6
26/07/2012	105	1097.6	-4.3	1279.0	699.3	1722.9	539.4	1889.2	647.8	1942.4	698.0	2091.9	281.2	1747.1	614.5	1103.2	133.7
27/07/2012	106	1117.4	14.4	1313.9	732.4	1752.4	567.4	1902.9	660.7	1971.6	725.7	2096.7	285.8	1758.6	625.4	1130.9	160.0
28/07/2012	107	1139.5	35.4	1345.2	762.0	1781.9	595.4	1914.6	671.9	2004.2	756.6	2092.4	281.8	1767.4	633.7	1158.6	186.2
29/07/2012	108	1133.9	30.1	1339.1	756.3	1777.8	591.4	1914.3	671.6	2000.5	753.1	2086.6	276.2	1758.8	625.6	1152.7	180.6
30/07/2012	109	1134.6	30.8	1349.9	766.5	1784.4	597.8	1921.7	678.6	2009.4	761.5	2090.9	280.3	1778.4	644.1	1159.0	186.7
31/07/2012	110	1132.5	28.7	1341.4	758.5	1781.7	595.1	1922.9	679.8	2008.2	760.4	2089.6	279.0	1786.7	652.0	1156.1	183.9
1/08/2012	111	1137.5	33.6	1350.8	767.3	1787.1	600.3	1932.2	688.6	2016.4	768.2	2096.4	285.5	1797.2	662.0	1161.4	188.9
2/08/2012	112	1136.7	32.8	1353.1	769.5	1789.6	602.6	1934.9	691.1	2019.2	770.8	2097.0	286.1	1797.5	662.3	1162.8	190.2
3/08/2012	113	1134.6	30.8	1352.9	769.3	1789.7	602.7	1937.0	693.1	2018.4	770.1	2102.9	291.7	1798.4	663.1	1163.4	190.8
4/08/2012	114	1135.3	31.4	1357.5	773.6	1794.2	607.0	1941.2	697.1	2024.2	775.6	2110.0	298.4	1796.0	660.9	1165.3	192.6
5/08/2012	115	1131.4	27.7	1354.4	770.8	1792.0	604.9	1940.9	696.8	2027.1	778.3	2114.7	302.8	1790.6	655.7	1161.5	189.0
6/08/2012	116	1131.3	27.7	1361.1	777.1	1794.2	607.0	1943.1	698.9	2030.9	781.9	2126.9	314.4	1788.5	653.8	1157.2	185.0
7/08/2012	117	1136.6	32.6	1379.3	794.4	1804.2	616.5	1955.6	710.7	2042.0	792.4	2157.5	343.4	1821.2	684.8	1168.2	195.4
8/08/2012	118	1136.8	32.9	1366.4	782.1	1798.6	611.2	1950.2	705.6	2037.1	787.8	2173.5	358.6	1820.5	684.1	1166.5	193.8

9/08/2012	119	1134.2	30.4	1361.6	777.6	1794.5	607.3	1946.9	702.4	2037.2	787.9	2177.3	362.2	1806.6	670.9	1165.0	192.3
10/08/2012	120	1126.1	22.7	1367.7	783.4	1790.9	603.9	1947.5	703.1	2035.0	785.8	2184.4	368.9	1817.7	681.3	1158.4	186.1
11/08/2012	121	1125.8	22.4	1354.5	770.9	1776.2	589.9	1932.0	688.4	2021.2	772.7	2189.7	373.9	1800.4	665.0	1148.3	176.5
12/08/2012	122	1124.3	21.0	1346.9	763.7	1771.3	585.3	1923.5	680.3	2017.1	768.8	2202.1	385.7	1793.8	658.8	1145.0	173.4
13/08/2012	123	1131.4	27.8	1357.5	773.7	1786.5	599.7	1936.1	692.2	2025.9	777.1	2219.0	401.7	1809.7	673.8	1155.1	182.9
14/08/2012	124	1131.4	27.7	1367.6	783.2	1792.0	604.9	1941.9	697.8	2028.1	779.2	2225.7	408.1	1817.6	681.3	1159.2	186.8
15/08/2012	125	1122.6	19.4	1366.6	782.3	1789.1	602.2	1946.0	701.6	2028.5	779.6	2217.8	400.5	1813.5	677.4	1153.2	181.1
16/08/2012	126	1121.8	18.7	1373.7	789.0	1793.9	606.7	1943.5	699.3	2031.8	782.8	2225.2	407.6	1812.1	676.1	1157.2	184.9
17/08/2012	127	1114.6	11.8	1374.7	790.0	1786.2	599.4	1940.9	696.8	2026.2	777.5	2225.1	407.5	1802.9	667.4	1153.5	181.4
18/08/2012	128	1116.5	13.6	1385.3	800.1	1793.0	605.8	1952.1	707.4	2036.4	787.1	2237.4	419.2	1812.3	676.3	1159.0	186.6
19/08/2012	129	1117.8	14.9	1383.2	798.1	1792.7	605.6	1953.8	709.0	2037.9	788.6	2250.3	431.4	1821.7	685.1	1157.6	185.3
20/08/2012	130	1115.6	12.8	1385.5	800.2	1795.1	607.8	1959.7	714.6	2036.7	787.4	2256.2	437.0	1829.2	692.3	1156.1	183.8
21/08/2012	131	1097.9	-4.1	1359.1	775.2	1770.7	584.8	1945.4	701.1	2014.2	766.1	2245.3	426.6	1814.3	678.2	1126.5	155.8
22/08/2012	132	1098.5	-3.4	1357.3	773.5	1766.5	580.7	1937.6	693.7	2012.0	764.0	2255.0	435.9	1806.3	670.5	1126.5	155.8
23/08/2012	133	1105.5	3.2	1354.9	771.2	1769.7	583.8	1930.6	687.0	2005.6	757.9	2274.8	454.6	1805.9	670.2	1128.7	157.9
24/08/2012	134	1097.3	-4.6	1349.4	766.0	1765.4	579.7	1927.6	684.2	2000.5	753.0	2278.3	457.9	1799.0	663.7	1122.8	152.3
25/08/2012	135	1087.8	-13.6	1360.6	776.6	1763.5	577.9	1937.0	693.1	2010.0	762.1	2302.7	481.0	1805.4	669.7	1119.2	148.9
26/08/2012	136	1083.1	-18.0	1366.7	782.4	1762.6	577.1	1943.7	699.5	2014.8	766.7	2324.3	501.5	1811.4	675.4	1117.5	147.3
27/08/2012	137	1091.4	-10.1	1376.6	791.8	1775.6	589.3	1959.5	714.5	2027.1	778.3	2362.2	537.5	1826.5	689.7	1129.9	159.0
28/08/2012	138	1094.1	-7.6	1367.7	783.3	1770.3	584.4	1951.0	706.4	2020.3	771.8	2381.8	556.0	1818.3	682.0	1126.2	155.5
29/08/2012	139	1093.5	-8.2	1360.6	776.6	1766.8	581.1	1942.4	698.2	2010.7	762.8	2388.6	562.5	1813.3	677.2	1120.7	150.3
30/08/2012	140	1096.6	-5.2	1369.6	785.1	1773.4	587.3	1947.6	703.1	2014.4	766.3	2397.9	571.2	1818.7	682.3	1127.5	156.8
31/08/2012	141	1084.8	-16.4	1379.8	794.8	1776.0	589.8	1962.4	717.2	2026.2	777.5	2419.8	592.1	1818.0	681.7	1129.3	158.4
1/09/2012	142	1089.7	-11.8	1389.1	803.6	1788.0	601.1	1977.8	731.8	2038.5	789.1	2470.9	640.5	1853.3	715.2	1138.5	167.2
2/09/2012	143	1083.5	-17.6	1375.9	791.1	1772.7	586.7	1960.2	715.1	2027.5	778.6	2479.3	648.5	1846.7	708.9	1125.8	155.2
3/09/2012	144	1092.7	-9.0	1387.1	801.8	1783.4	596.7	1971.4	725.7	2035.0	785.8	2494.3	662.6	1851.0	712.9	1135.8	164.6
4/09/2012	145	1086.6	-14.8	1381.8	796.7	1775.7	589.4	1966.0	720.6	2028.2	779.4	2490.0	658.6	1842.0	704.5	1131.6	160.7
5/09/2012	146	1079.9	-21.1	1385.8	800.5	1781.1	594.6	1969.1	723.6	2029.0	780.1	2486.3	655.1	1841.9	704.3	1135.7	164.5
6/09/2012	147	1082.3	-18.8	1398.3	812.3	1793.3	606.1	1981.1	734.9	2040.9	791.4	2501.0	669.0	1852.4	714.2	1147.1	175.3
7/09/2012	148	1080.9	-20.1	1405.2	818.9	1795.6	608.3	1993.7	746.8	2047.3	797.5	2535.8	702.0	1865.1	726.4	1147.5	175.7
8/09/2012	149	1073.9	-26.8	1401.2	815.1	1784.6	597.9	1992.0	745.2	2043.7	794.1	2553.3	718.6	1865.1	726.3	1137.2	166.0
9/09/2012	150	1071.4	-29.1	1390.0	804.5	1771.9	585.9	1978.3	732.2	2036.9	787.6	2556.8	721.9	1858.4	720.0	1128.9	158.1
10/09/2012	151	1079.3	-21.6	1389.2	803.8	1775.7	589.5	1973.2	727.4	2036.0	786.7	2570.6	734.9	1853.0	714.9	1132.2	161.3
11/09/2012	152	1087.0	-14.4	1384.6	799.4	1781.4	594.9	1966.7	721.3	2027.2	778.4	2592.3	755.5	1851.5	713.5	1132.2	161.2
12/09/2012	153	1077.1	-23.8	1371.0	786.5	1763.9	578.3	1956.4	711.5	2008.7	760.8	2595.6	758.7	1839.5	702.1	1112.8	142.9
13/09/2012	154	1086.6	-14.7	1375.2	790.4	1770.0	584.1	1953.9	709.1	2011.4	763.4	2611.5	773.8	1838.7	701.3	1114.6	144.5
14/09/2012	155	1089.3	-12.2	1385.2	800.0	1778.6	592.2	1968.4	722.9	2019.5	771.1	2614.1	776.2	1852.7	714.6	1122.7	152.2

15/09/2012	156	1076.2	-24.6	1385.6	800.3	1769.5	583.6	1962.5	717.3	2019.5	771.1	2599.3	762.2	1841.7	704.2	1113.9	143.9
16/09/2012	157	1077.1	-23.7	1378.4	793.5	1759.1	573.7	1951.2	706.6	2012.4	764.4	2600.8	763.6	1832.8	695.7	1112.4	142.4
17/09/2012	158	1088.4	-13.1	1379.5	794.6	1763.8	578.2	1949.2	704.7	2010.5	762.6	2615.0	777.0	1838.5	701.1	1117.9	147.7
18/09/2012	159	1095.7	-6.1	1380.7	795.7	1766.1	580.4	1951.3	706.7	2008.0	760.2	2620.1	781.9	1831.8	694.8	1122.8	152.3
19/09/2012	160	1095.2	-6.6	1379.1	794.1	1770.0	584.1	1953.3	708.6	2006.3	758.6	2623.3	785.0	1833.5	696.3	1121.1	150.7
20/09/2012	161	1095.9	-5.9	1379.4	794.5	1771.9	585.8	1956.3	711.4	2005.9	758.2	2625.5	787.0	1841.4	703.9	1122.2	151.7
21/09/2012	162	1102.7	0.5	1377.3	792.5	1775.9	589.7	1951.6	707.0	2007.7	759.9	2630.2	791.4	1843.7	706.0	1124.3	153.8
22/09/2012	163	1103.5	1.3	1380.0	795.0	1776.0	589.7	1953.2	708.5	2004.2	756.6	2632.1	793.3	1841.9	704.4	1123.5	153.0
23/09/2012	164	1101.1	-1.0	1377.6	792.7	1771.1	585.1	1944.4	700.1	1999.2	751.9	2630.5	791.8	1834.9	697.7	1116.5	146.3
24/09/2012	165	1099.2	-2.8	1386.7	801.3	1775.8	589.6	1951.9	707.2	2005.5	757.9	2629.7	791.0	1842.7	705.1	1120.3	150.0
25/09/2012	166	1097.1	-4.8	1389.6	804.1	1781.0	594.5	1956.3	711.4	2013.5	765.4	2629.4	790.7	1841.5	704.0	1123.6	153.1
26/09/2012	167	1096.1	-5.7	1382.4	797.3	1774.7	588.5	1948.2	703.7	2007.0	759.2	2627.8	789.2	1836.1	698.9	1116.1	146.0
27/09/2012	168	1102.1	0.0	1379.9	794.9	1774.2	588.0	1941.2	697.1	2004.8	757.1	2633.1	794.2	1838.9	701.5	1115.7	145.6
28/09/2012	169	1104.2	1.9	1376.7	791.8	1772.4	586.3	1936.8	692.9	2001.9	754.4	2637.4	798.3	1829.7	692.7	1112.3	142.3
29/09/2012	170	1104.1	1.9	1374.1	789.5	1768.8	582.9	1939.0	695.0	1995.2	748.1	2639.3	800.1	1829.7	692.7	1108.3	138.6
30/09/2012	171	1093.7	-8.0	1389.7	804.2	1773.9	587.8	1951.7	707.0	2007.7	759.9	2630.7	791.9	1842.4	704.8	1111.8	141.9
1/10/2012	172	1087.8	-13.6	1392.4	806.8	1777.0	590.7	1959.5	714.4	2017.3	769.0	2625.1	786.7	1843.6	705.9	1115.0	144.9
2/10/2012	173	1082.5	-18.7	1379.8	794.8	1768.9	583.0	1947.7	703.2	2008.4	760.6	2618.6	780.5	1834.1	696.9	1103.9	134.4
3/10/2012	174	1086.7	-14.6	1384.4	799.2	1773.9	587.8	1954.2	709.4	2010.8	762.8	2624.4	786.0	1843.2	705.6	1103.6	134.1
4/10/2012	175	1089.8	-11.7	1384.2	799.0	1774.7	588.5	1952.5	707.8	2011.6	763.6	2628.0	789.4	1838.6	701.2	1106.9	137.2
5/10/2012	176	1087.0	-14.3	1388.3	802.9	1780.6	594.1	1963.0	717.7	2019.4	771.0	2627.5	788.9	1848.3	710.4	1111.9	142.0
6/10/2012	177	1090.8	-10.7	1378.2	793.3	1773.6	587.5	1952.2	707.5	2005.1	757.4	2638.0	798.8	1841.3	703.8	1105.2	135.6
7/10/2012	178	1084.5	-16.7	1369.7	785.2	1760.1	574.6	1942.4	698.2	1993.5	746.4	2639.6	800.4	1833.5	696.4	1093.9	124.9
8/10/2012	179	1085.8	-15.5	1382.0	796.9	1767.3	581.5	1954.4	709.6	2003.7	756.1	2641.6	802.3	1838.8	701.4	1100.5	131.2
9/10/2012	180	1083.3	-17.8	1382.5	797.4	1767.9	582.0	1953.2	708.5	2005.1	757.5	2637.8	798.7	1843.9	706.2	1098.8	129.6
10/10/2012	181	1090.9	-10.7	1393.5	807.8	1778.2	591.8	1963.8	718.5	2016.4	768.1	2645.5	806.0	1853.3	715.1	1110.2	140.4
11/10/2012	182	1083.0	-18.2	1382.0	796.9	1770.2	584.3	1954.7	709.9	2007.2	759.4	2640.0	800.8	1845.4	707.7	1101.6	132.2
12/10/2012	183	1104.7	2.4	1410.9	824.3	1796.7	609.3	1985.1	738.7	2034.8	785.6	2667.9	827.2	1880.8	741.2	1127.9	157.1
13/10/2012	184	1099.5	-2.5	1400.6	814.5	1789.5	602.5	1978.3	732.3	2032.1	783.1	2658.6	818.4	1873.6	734.4	1120.6	150.2
14/10/2012	185	1094.0	-7.7	1392.5	806.8	1776.9	590.6	1962.3	717.1	2022.9	774.3	2651.1	811.3	1859.3	720.8	1109.9	140.1
15/10/2012	186	1097.4	-4.5	1390.2	804.7	1778.8	592.4	1964.4	719.0	2018.5	770.1	2655.7	815.6	1858.9	720.5	1110.6	140.8
16/10/2012	187	1095.1	-6.7	1385.7	800.4	1777.0	590.7	1962.5	717.3	2015.0	766.9	2658.3	818.1	1852.5	714.4	1109.9	140.1
17/10/2012	188	1083.5	-17.7	1375.6	790.8	1767.3	581.5	1954.1	709.3	2006.2	758.5	2648.4	808.7	1849.7	711.7	1096.9	127.8
18/10/2012	189	1093.0	-8.7	1381.9	796.8	1774.5	588.3	1953.8	709.0	2010.1	762.2	2658.6	818.4	1850.2	712.2	1100.5	131.2
19/10/2012	190	1098.1	-3.8	1379.4	794.5	1773.2	587.1	1952.3	707.6	2006.4	758.7	2632.2	793.4	1845.9	708.2	1103.6	134.1
20/10/2012	191	1102.1	-0.1	1376.5	791.7	1772.4	586.3	1953.0	708.2	1998.9	751.5	2613.0	775.1	1847.3	709.5	1102.0	132.6
21/10/2012	192	1096.4	-5.4	1366.7	782.4	1762.4	576.8	1940.8	696.7	1986.1	739.4	2609.0	771.3	1840.2	702.7	1091.7	122.8

22/10/2012	193	1091.9	-9.7	1366.5	782.2	1758.5	573.1	1941.0	696.9	1984.6	738.0	2603.4	766.0	1839.4	702.0	1088.8	120.1
23/10/2012	194	1095.4	-6.4	1387.2	801.9	1774.2	588.1	1961.1	716.0	2006.9	759.2	2607.4	769.9	1858.1	719.7	1104.7	135.1
24/10/2012	195	1089.7	-11.8	1381.0	796.0	1771.1	585.2	1955.7	710.8	2006.2	758.5	2602.8	765.5	1855.2	717.0	1097.0	127.9
25/10/2012	196	1092.7	-8.9	1376.0	791.2	1769.4	583.5	1950.1	705.5	2001.5	754.0	2606.2	768.7	1852.3	714.2	1092.1	123.3
26/10/2012	197	1095.0	-6.8	1372.8	788.2	1766.0	580.3	1949.4	704.9	1995.7	748.6	2609.4	771.8	1848.6	710.7	1090.5	121.7
27/10/2012	198	1094.5	-7.2	1378.6	793.7	1768.0	582.2	1948.5	704.0	1997.0	749.7	2612.2	774.4	1853.7	715.6	1091.6	122.8
28/10/2012	199	1084.8	-16.5	1375.1	790.4	1765.1	579.4	1953.5	708.7	1998.2	750.9	2601.3	764.1	1856.8	718.4	1084.0	115.6
29/10/2012	200	1088.5	-13.0	1376.1	791.3	1769.2	583.3	1955.1	710.2	2002.7	755.2	2603.7	766.3	1856.2	717.8	1085.8	117.2
30/10/2012	201	1096.8	-5.1	1379.6	794.7	1773.9	587.7	1957.4	712.4	2003.7	756.1	2580.9	744.7	1851.4	713.3	1093.6	124.7
31/10/2012	202	1102.0	-0.1	1375.2	790.5	1771.1	585.1	1952.6	707.9	1996.3	749.1	2561.3	726.2	1849.3	711.3	1098.1	128.9
1/11/2012	203	1113.5	10.8	1384.7	799.4	1779.5	593.1	1962.3	717.1	2004.2	756.6	2573.1	737.4	1859.9	721.3	1110.3	140.5
2/11/2012	204	1096.6	-5.2	1384.9	799.6	1771.7	585.7	1962.7	717.4	2002.5	755.0	2558.0	723.1	1859.5	721.0	1097.1	127.9
3/11/2012	205	1090.9	-10.7	1373.3	788.7	1766.4	580.7	1958.1	713.1	1996.8	749.6	2553.6	718.9	1856.5	718.2	1087.2	118.6
4/11/2012	206	1093.6	-8.1	1368.9	784.5	1762.3	576.7	1948.3	703.8	1991.0	744.1	2555.5	720.7	1847.4	709.5	1080.5	112.2
5/11/2012	207	1110.6	8.0	1373.5	788.9	1768.3	582.4	1948.7	704.2	1992.8	745.8	2572.8	737.0	1847.9	710.0	1091.4	122.5
6/11/2012	208	1113.3	10.6	1369.4	784.9	1763.1	577.5	1947.8	703.4	1986.0	739.4	2581.5	745.3	1841.6	704.0	1090.8	122.0
7/11/2012	209	1117.8	14.8	1364.8	780.6	1759.5	574.1	1947.5	703.1	1980.6	734.2	2585.2	748.8	1836.7	699.4	1090.1	121.3
8/11/2012	210	1126.3	22.9	1367.3	782.9	1761.3	575.8	1948.0	703.5	1981.1	734.7	2594.4	757.5	1833.2	696.1	1094.3	125.3
9/11/2012	211	1126.1	22.7	1360.5	776.5	1755.4	570.2	1943.6	699.4	1972.4	726.5	2594.7	757.8	1829.5	692.6	1090.3	121.5
10/11/2012	212	1125.0	21.7	1365.6	781.4	1754.9	569.8	1949.3	704.7	1972.8	726.9	2594.9	758.0	1834.4	697.3	1090.0	121.2
11/11/2012	213	1120.2	17.1	1372.1	787.5	1758.6	573.3	1955.7	710.8	1980.5	734.1	2592.2	755.4	1836.7	699.4	1091.5	122.6
12/11/2012	214	1119.4	16.3	1379.4	794.4	1765.5	579.8	1967.2	721.7	1990.9	744.0	2590.9	754.2	1846.1	708.3	1096.6	127.5
13/11/2012	215	1116.1	13.2	1374.4	789.7	1764.3	578.7	1962.7	717.5	1987.9	741.1	2586.4	749.9	1841.7	704.2	1092.8	123.9
14/11/2012	216	1115.3	12.5	1371.7	787.1	1762.3	576.8	1958.6	713.5	1985.7	739.1	2583.6	747.3	1841.6	704.1	1087.8	119.1
15/11/2012	217	1125.9	22.6	1375.7	790.9	1767.9	582.1	1963.0	717.8	1989.8	742.9	2592.2	755.4	1845.4	707.7	1093.4	124.5
16/11/2012	218	1119.5	16.5	1365.6	781.3	1755.7	570.5	1950.3	705.7	1976.5	730.3	2585.8	749.4	1831.2	694.2	1083.3	114.9
17/11/2012	219	1118.7	15.7	1369.5	785.0	1755.6	570.5	1954.2	709.4	1977.0	730.8	2587.1	750.6	1833.9	696.7	1086.1	117.5
18/11/2012	220	1113.3	10.5	1365.6	781.3	1751.1	566.2	1950.0	705.4	1973.6	727.6	2580.2	744.1	1827.3	690.5	1076.4	108.4
19/11/2012	221	1111.0	8.4	1369.9	785.4	1752.5	567.4	1954.2	709.4	1977.1	730.9	2579.1	743.0	1835.2	698.0	1079.6	111.4
20/11/2012	222	1116.7	13.8	1379.2	794.3	1764.1	578.5	1967.5	722.0	1989.7	742.9	2585.9	749.5	1851.3	713.3	1090.4	121.6
21/11/2012	223	1120.4	17.3	1382.5	797.4	1769.8	583.8	1976.3	730.4	1995.8	748.6	2588.8	752.2	1862.0	723.4	1096.6	127.5
22/11/2012	224	1095.9	-5.9	1355.0	771.3	1742.4	557.9	1959.9	714.8	1968.7	722.9	2564.6	729.3	1843.2	705.5	1069.4	101.7
23/11/2012	225	1078.6	-22.3	1344.0	760.9	1728.1	544.3	1959.6	714.5	1955.2	710.2	2547.3	712.9	1844.2	706.5	1051.1	84.4
24/11/2012	226	1094.8	-7.0	1358.8	775.0	1741.5	557.1	1977.2	731.2	1966.7	721.1	2562.9	727.7	1864.6	725.9	1062.8	95.4
25/11/2012	227	1124.2	20.9	1381.1	796.1	1762.8	577.2	1988.8	742.2	1984.3	737.8	2591.9	755.1	1877.5	738.1	1087.1	118.5
26/11/2012	228	1101.1	-0.9	1351.6	768.1	1730.4	546.6	1957.9	713.0	1950.5	705.7	2570.0	734.4	1842.4	704.8	1056.9	89.8
27/11/2012	229	1118.1	15.1	1360.3	776.3	1740.5	556.1	1971.7	726.0	1956.0	710.9	2591.9	755.2	1857.8	719.4	1073.1	105.2

28/11/2012	230	1124.6	21.2	1363.0	778.9	1740.8	556.4	1975.5	729.6	1956.1	711.0	2599.2	762.1	1865.1	726.3	1076.0	107.9
29/11/2012	231	1113.6	10.9	1347.3	764.0	1724.5	541.0	1962.7	717.4	1940.2	695.9	2589.5	752.9	1849.5	711.6	1059.1	92.0
30/11/2012	232	1114.1	11.3	1346.0	762.8	1718.6	535.4	1957.5	712.5	1932.1	688.2	2590.8	754.2	1837.6	700.3	1058.6	91.5
1/12/2012	233	1147.1	42.6	1373.9	789.2	1744.5	559.9	1981.6	735.4	1956.3	711.2	2621.3	783.1	1863.5	724.8	1085.7	117.1
2/12/2012	234	1149.6	44.9	1372.3	787.7	1742.6	558.1	1981.2	735.0	1953.2	708.2	2618.5	780.4	1863.3	724.6	1081.4	113.0
3/12/2012	235	1119.3	16.3	1338.2	755.4	1707.7	525.1	1952.0	707.3	1921.2	677.9	2588.0	751.5	1831.6	694.6	1047.9	81.3
4/12/2012	236	1089.5	-12.0	1324.4	742.3	1681.9	500.6	1933.1	689.4	1897.2	655.2	2560.6	725.5	1814.7	678.6	1022.3	57.1
5/12/2012	237	1078.3	-22.6	1349.3	765.9	1690.5	508.8	1948.5	704.0	1913.4	670.6	2557.4	722.5	1836.8	699.5	1028.7	63.1
6/12/2012	238	1075.6	-25.1	1362.6	778.5	1699.9	517.6	1957.2	712.3	1927.2	683.6	2565.5	730.2	1845.8	708.0	1033.6	67.8
7/12/2012	239	1141.1	36.9	1432.3	844.6	1768.7	582.9	1950.3	705.7	1997.6	750.3	2632.7	793.8	1838.6	701.2	1096.2	127.1
8/12/2012	240	1187.8	81.2	1478.8	888.7	1811.9	623.7	1949.9	705.3	2034.9	785.7	2685.7	844.0	1839.7	702.2	1138.7	167.4

Table E.6 Concrete surface strain at steel level for slab S-SCC-b

Slab S-SCC-b		CONCRETE SURFACE STRAIN BY SG															
		1		2		3		4		5		6		7		8	
Date	Age	Reading	Strain	Reading	Strain	Reading	Strain	Reading	Strain	Reading	Strain	Reading	Strain	Reading	Strain	Reading	Strain
26/04/2012	14	1554.2		1772.7		-352.6		1520.4		-1362.1		1141.2		1468.5		2525.3	
26/04/2012	14	1559.1		1803.2		-321.4		1562.0		603.8		1139.2		1498.7		2520.8	
27/04/2012	15	1590.3	29.5	1930.7	120.8	-230.4	86.3	1672.8	105.0	785.7	172.4	1113.5	-24.4	1593.5	89.8	2584.3	60.2
28/04/2012	16	1612.5	50.6	1985.2	172.5	-197.0	117.9	1717.6	147.5	799.1	185.1	1091.4	-45.4	1626.9	121.6	2637.9	111.0
29/04/2012	17	1631.6	68.7	2026.5	211.6	-169.7	143.8	1758.5	186.3	803.5	189.3	1071.1	-64.6	1660.3	153.2	2684.0	154.7
30/04/2012	18	1656.2	92.0	2069.3	252.2	-138.5	173.4	1800.0	225.6	783.9	170.7	1056.8	-78.1	1702.7	193.4	2733.3	201.4
1/05/2012	19	1660.3	95.9	2082.4	264.7	-132.7	178.9	1814.6	239.5	814.1	199.4	1031.4	-102.2	1712.2	202.4	2753.3	220.4
2/05/2012	20	1676.6	111.3	2106.3	287.3	-117.0	193.8	1836.6	260.3	839.8	223.7	1022.4	-110.8	1733.6	222.7	2783.1	248.6
3/05/2012	21	1689.4	123.5	2129.6	309.4	-103.0	207.0	1859.2	281.7	853.8	237.0	1010.0	-122.5	1756.6	244.4	2812.3	276.4
4/05/2012	22	1708.7	141.8	2160.6	338.8	-85.2	223.9	1894.5	315.2	870.1	252.4	988.5	-142.8	1789.7	275.8	2846.6	308.9
5/05/2012	23	1705.4	138.7	2162.1	340.1	-93.7	215.8	1898.0	318.5	877.5	259.5	952.5	-177.0	1793.1	279.0	2854.5	316.3
6/05/2012	24	1716.9	149.6	2178.8	356.0	-84.2	224.8	1915.0	334.6	850.0	233.4	927.4	-200.8	1804.0	289.4	2876.9	337.6
7/05/2012	25	1737.8	169.3	2210.1	385.7	-60.8	247.0	1942.8	360.9	820.4	205.3	927.3	-200.9	1828.9	313.0	2915.4	374.0
8/05/2012	26	1765.0	195.2	2239.3	413.4	-35.9	270.6	1975.7	392.1	820.0	204.9	927.4	-200.8	1855.4	338.1	2951.0	407.8
9/05/2012	27	1775.2	204.8	2252.5	425.9	-27.5	278.6	1989.7	405.4	845.3	228.9	920.9	-207.0	1869.7	351.7	2970.1	425.9
10/05/2012	28	1784.4	213.5	2277.9	449.9	-20.8	285.0	1998.4	413.7	845.2	228.8	911.3	-216.1	1879.7	361.1	2986.0	441.0
11/05/2012	29	1792.2	220.9	2303.8	474.5	-15.9	289.6	2011.0	425.7	840.1	224.0	901.1	-225.7	1891.3	372.1	3001.2	455.4
12/05/2012	30	1800.5	228.7	2321.9	491.6	-8.4	296.7	2028.6	442.3	847.1	230.6	881.8	-244.0	1906.6	386.6	3022.3	475.4
13/05/2012	31	1808.7	236.5	2349.7	517.9	-2.7	302.1	2046.0	458.8	865.4	248.0	863.2	-261.6	1922.2	401.4	3045.3	497.1
14/05/2012	32	1832.3	258.9	2382.8	549.4	14.9	318.8	2067.2	478.9	836.8	220.9	859.7	-264.9	1949.9	427.6	3074.4	524.7
15/05/2012	33	1847.6	273.5	2402.5	568.0	25.6	328.9	2086.0	496.7	862.4	245.1	850.1	-274.1	1965.2	442.1	3094.4	543.7
16/05/2012	34	1852.4	278.0	2408.1	573.4	29.4	332.5	2090.0	500.5	882.4	264.1	845.8	-278.2	1967.5	444.3	3106.9	555.6
17/05/2012	35	1855.2	280.7	2411.1	576.2	28.5	331.7	2098.3	508.4	880.9	262.7	834.9	-288.4	1969.3	446.0	3117.0	565.2
18/05/2012	36	1859.9	285.1	2421.0	585.5	36.6	339.4	2105.6	515.3	863.0	245.8	836.6	-286.8	1978.3	454.6	3127.7	575.3
19/05/2012	37	1860.2	285.4	2428.9	593.1	33.5	336.4	2109.2	518.7	871.6	253.8	819.5	-303.1	1984.1	460.1	3132.7	580.0
20/05/2012	38	1872.4	296.9	2448.5	611.7	42.2	344.7	2125.8	534.4	881.7	263.4	804.7	-317.1	1995.2	470.6	3148.7	595.2
21/05/2012	39	1868.2	292.9	2444.6	608.0	38.7	341.3	2115.2	524.4	886.0	267.5	801.3	-320.3	1997.6	472.9	3148.1	594.6
22/05/2012	40	1876.5	300.8	2462.1	624.5	47.3	349.5	2129.7	538.1	875.7	257.8	794.8	-326.5	2010.9	485.5	3162.5	608.3
23/05/2012	41	1892.1	315.6	2494.9	655.6	58.1	359.8	2149.9	557.2	881.0	262.8	777.8	-342.6	2024.4	498.3	3189.3	633.7
24/05/2012	42	1892.8	316.3	2497.9	658.5	55.0	356.8	2151.7	558.9	868.2	250.6	767.2	-352.6	2021.7	495.7	3193.7	637.8
25/05/2012	43	1890.6	314.2	2496.2	656.8	50.0	352.0	2147.4	554.9	878.3	260.2	769.0	-350.9	2028.0	501.7	3191.6	635.8
26/05/2012	44	1896.3	319.6	2523.7	682.9	58.2	359.8	2162.8	569.5	875.6	257.7	746.3	-372.5	2032.2	505.7	3211.6	654.9

27/05/2012	45	1903.1	326.0	2532.2	691.0	62.8	364.2	2171.3	577.6	869.1	251.5	743.9	-374.7	2035.0	508.4	3222.8	665.5
28/05/2012	46	1919.0	341.1	2547.8	705.8	77.6	378.3	2189.4	594.8	882.0	263.7	752.9	-366.2	2048.1	520.8	3243.3	684.9
29/05/2012	47	1910.6	333.2	2536.0	694.6	63.3	364.7	2181.1	586.9	879.0	260.9	745.5	-373.3	2054.2	526.6	3234.7	676.7
30/05/2012	48	1915.8	338.1	2542.3	700.5	69.7	370.7	2188.5	593.8	879.1	261.0	748.4	-370.5	2068.4	540.0	3241.4	683.1
31/05/2012	49	1916.4	338.7	2545.4	703.5	68.9	370.0	2192.4	597.5	878.0	259.9	738.6	-379.7	2061.1	533.1	3247.2	688.5
1/06/2012	50	1915.0	337.3	2545.2	703.3	67.6	368.8	2191.2	596.4	881.7	263.5	735.8	-382.4	2066.7	538.4	3248.8	690.0
2/06/2012	51	1907.5	330.2	2540.2	698.6	62.4	363.9	2187.5	592.9	881.2	263.0	733.7	-384.4	2062.6	534.5	3244.2	685.7
3/06/2012	52	1908.0	330.6	2538.0	696.5	61.5	363.0	2185.1	590.6	878.6	260.5	734.6	-383.5	2067.9	539.5	3240.3	682.0
4/06/2012	53	1908.5	331.2	2541.0	699.3	61.6	363.0	2185.7	591.2	890.4	271.7	728.8	-389.0	2073.8	545.1	3243.5	685.0
5/06/2012	54	1925.9	347.6	2581.0	737.2	79.5	380.0	2211.4	615.6	885.8	267.3	709.0	-407.8	2100.7	570.7	3276.8	716.6
6/06/2012	55	1921.6	343.5	2579.4	735.7	72.3	373.2	2209.6	613.8	883.2	264.9	698.4	-417.9	2091.6	562.0	3276.9	716.7
7/06/2012	56	1933.0	354.3	2593.6	749.1	84.3	384.5	2221.3	625.0	872.1	254.4	699.0	-417.3	2104.0	573.7	3291.9	731.0
8/06/2012	57	1950.1	370.6	2614.7	769.2	97.7	397.3	2241.1	643.7	880.9	262.7	691.7	-424.2	2126.4	595.0	3311.5	749.5
9/06/2012	58	1954.1	374.4	2619.7	773.9	98.6	398.1	2246.7	649.0	881.3	263.0	688.7	-427.0	2126.5	595.1	3318.7	756.3
10/06/2012	59	1958.5	378.5	2622.2	776.3	100.2	399.6	2249.9	652.1	882.4	264.1	691.6	-424.3	2129.5	597.9	3325.3	762.6
11/06/2012	60	1946.4	367.0	2610.7	765.3	87.0	387.1	2234.7	637.7	891.7	272.9	688.5	-427.3	2116.6	585.7	3314.3	752.1
12/06/2012	61	1937.5	358.7	2604.9	759.9	81.9	382.3	2227.6	630.9	889.5	270.8	686.7	-429.0	2106.2	575.8	3309.6	747.7
13/06/2012	62	1943.2	364.0	2608.5	763.3	86.2	386.4	2232.4	635.5	890.4	271.7	696.8	-419.4	2115.3	584.5	3313.7	751.6
14/06/2012	63	1942.8	363.6	2607.6	762.4	85.1	385.4	2233.2	636.2	889.0	270.4	697.6	-418.7	2121.9	590.7	3312.0	750.0
15/06/2012	64	1937.2	358.3	2605.7	760.6	80.9	381.3	2229.6	632.8	886.5	268.0	688.1	-427.6	2115.5	584.6	3310.3	748.4
16/06/2012	65	1938.5	359.6	2610.6	765.3	82.5	382.9	2231.7	634.8	882.9	264.6	683.5	-431.9	2118.1	587.1	3316.3	754.1
17/06/2012	66	1939.3	360.3	2615.8	770.2	79.4	380.0	2232.9	636.0	896.6	277.6	663.9	-450.6	2129.1	597.6	3316.0	753.8
18/06/2012	67	1951.0	371.5	2646.4	799.2	92.6	392.4	2255.8	657.7	893.1	274.2	651.0	-462.8	2139.8	607.7	3340.4	776.9
19/06/2012	68	1961.8	381.7	2660.6	812.7	101.3	400.7	2270.0	671.1	885.8	267.3	647.8	-465.8	2148.2	615.7	3355.2	790.9
20/06/2012	69	1964.3	384.1	2662.8	814.8	101.9	401.3	2272.2	673.2	892.1	273.3	642.6	-470.7	2149.3	616.7	3359.8	795.3
21/06/2012	70	1975.2	394.3	2673.6	825.0	108.9	407.9	2280.6	681.2	887.1	268.6	642.0	-471.4	2161.5	628.2	3371.7	806.6
22/06/2012	71	1966.1	385.8	2669.3	820.9	100.7	400.1	2275.1	675.9	892.3	273.5	632.9	-480.0	2144.1	611.7	3371.9	806.7
23/06/2012	72	1977.4	396.5	2679.8	830.9	106.6	405.7	2284.4	684.8	891.4	272.6	629.4	-483.2	2166.2	632.7	3381.0	815.4
24/06/2012	73	1984.3	403.0	2688.7	839.4	111.0	409.9	2289.9	690.0	885.1	266.7	622.5	-489.8	2184.7	650.2	3388.5	822.5
25/06/2012	74	1987.8	406.3	2693.2	843.6	114.0	412.8	2292.4	692.3	890.5	271.8	624.8	-487.6	2186.0	651.5	3395.8	829.4
26/06/2012	75	1974.7	393.9	2681.7	832.7	100.7	400.1	2276.1	676.9	881.3	263.0	618.2	-493.8	2175.6	641.6	3386.7	820.8
27/06/2012	76	1972.4	391.7	2677.2	828.4	96.7	396.3	2271.1	672.2	869.7	252.1	625.6	-486.9	2172.6	638.8	3381.0	815.4
28/06/2012	77	1972.7	392.0	2677.6	828.8	94.8	394.6	2271.9	672.9	897.0	278.0	623.4	-488.9	2173.5	639.7	3382.3	816.6
29/06/2012	78	1965.5	385.2	2671.7	823.2	89.5	389.5	2265.4	666.7	889.8	271.1	627.2	-485.4	2164.1	630.7	3377.1	811.7
30/06/2012	79	1961.0	380.9	2669.6	821.2	85.7	385.9	2266.2	667.5	899.4	280.2	621.7	-490.5	2165.2	631.8	3374.1	808.9
1/07/2012	80	1966.8	386.5	2687.3	837.9	90.3	390.3	2276.7	677.4	899.1	280.0	599.3	-511.8	2169.6	635.9	3386.0	820.1
2/07/2012	81	1991.4	409.8	2726.4	875.1	126.2	424.3	2303.1	702.5	911.7	291.9	596.4	-514.5	2197.2	662.1	3414.5	847.2

3/07/2012	82	1991.0	409.4	2730.3	878.8	111.3	410.2	2302.8	702.2	901.0	281.8	585.6	-524.8	2196.5	661.4	3419.3	851.7
4/07/2012	83	1994.8	412.9	2735.9	884.1	114.0	412.7	2306.3	705.6	889.9	271.2	583.5	-526.8	2195.6	660.5	3426.9	858.9
5/07/2012	84	1988.3	406.8	2729.0	877.5	106.5	405.6	2298.9	698.5	899.9	280.7	584.8	-525.5	2195.5	660.5	3421.6	853.9
6/07/2012	85	1981.2	400.0	2720.7	869.6	98.6	398.2	2292.2	692.2	899.6	280.4	586.0	-524.4	2192.9	658.0	3413.8	846.5
7/07/2012	86	1985.0	403.7	2726.3	874.9	101.5	400.9	2297.6	697.3	904.3	284.8	584.7	-525.6	2193.9	659.0	3418.8	851.2
8/07/2012	87	1976.2	395.4	2716.5	865.6	92.3	392.2	2289.6	689.7	896.6	277.6	579.9	-530.2	2181.6	647.3	3408.7	841.6
9/07/2012	88	1986.4	405.0	2725.8	874.5	101.4	400.7	2299.5	699.1	901.9	282.6	589.8	-520.8	2197.4	662.3	3417.2	849.6
10/07/2012	89	1983.6	402.4	2721.9	870.8	97.7	397.3	2295.9	695.6	901.0	281.8	589.0	-521.5	2194.8	659.8	3414.9	847.5
11/07/2012	90	1964.9	384.6	2703.0	852.9	77.2	377.9	2275.3	676.2	904.2	284.8	573.5	-536.3	2174.9	641.0	3395.1	828.8
12/07/2012	91	1978.6	397.6	2721.8	870.7	93.2	393.0	2292.4	692.3	900.1	280.9	583.7	-526.6	2186.6	652.1	3413.1	845.8
13/07/2012	92	1962.6	382.4	2711.5	861.0	82.5	382.9	2282.6	683.0	895.1	276.2	586.3	-524.1	2170.3	636.6	3402.3	835.6
14/07/2012	93	1955.0	375.2	2709.6	859.1	79.7	380.2	2279.9	680.5	894.8	275.8	581.4	-528.8	2172.5	638.7	3398.8	832.3
15/07/2012	94	1971.4	390.8	2744.5	892.2	87.1	387.3	2297.1	696.8	889.6	270.9	560.7	-548.4	2179.0	644.9	3416.3	848.8
16/07/2012	95	1998.8	416.7	2798.3	943.2	109.0	408.0	2326.9	725.1	888.1	269.5	562.2	-546.9	2211.7	675.9	3449.0	879.8
17/07/2012	96	1999.2	417.1	2800.3	945.1	108.7	407.7	2325.3	723.6	887.8	269.3	560.7	-548.4	2209.8	674.1	3451.1	881.8
18/07/2012	97	1999.4	417.3	2805.4	949.9	107.9	406.9	2326.4	724.6	891.7	272.9	552.1	-556.5	2203.8	668.3	3455.1	885.6
19/07/2012	98	2007.8	425.3	2817.1	961.0	114.7	413.4	2336.6	734.3	892.8	274.0	549.3	-559.2	2220.8	684.4	3465.6	895.6
20/07/2012	99	2020.2	437.1	2830.5	973.7	122.5	420.8	2349.8	746.7	902.3	282.9	551.0	-557.5	2242.3	704.8	3476.4	905.8
21/07/2012	100	2005.9	423.5	2824.3	967.8	112.7	411.5	2334.7	732.4	903.8	284.4	549.5	-559.0	2233.4	696.4	3468.7	898.5
22/07/2012	101	2002.7	420.4	2820.0	963.7	108.7	407.7	2327.7	725.8	906.6	287.1	550.2	-558.4	2231.3	694.4	3464.2	894.2
23/07/2012	102	1995.1	413.2	2814.0	958.1	102.6	401.9	2321.7	720.1	922.7	302.3	546.9	-561.5	2220.0	683.7	3457.8	888.2
24/07/2012	103	1994.5	412.7	2806.2	950.7	97.9	397.5	2318.3	716.9	914.8	294.9	551.2	-557.4	2218.0	681.8	3451.7	882.4
25/07/2012	104	1996.3	414.4	2808.8	953.1	98.9	398.4	2321.4	719.8	900.6	281.3	560.4	-548.6	2227.5	690.8	3453.0	883.6
26/07/2012	105	1994.1	412.3	2815.4	959.4	99.3	398.8	2321.3	719.8	907.1	287.6	550.7	-557.9	2219.0	682.7	3456.7	887.1
27/07/2012	106	2007.8	425.3	2845.5	987.9	110.6	409.5	2336.5	734.1	913.3	293.4	544.0	-564.2	2231.8	694.9	3470.4	900.1
28/07/2012	107	2015.3	432.3	2887.0	1027.2	115.2	413.8	2349.5	746.5	907.1	287.5	531.5	-576.1	2241.6	704.1	3484.6	913.6
29/07/2012	108	2014.2	431.4	2890.3	1030.4	113.3	412.1	2349.2	746.2	904.0	284.5	523.2	-583.9	2232.0	695.1	3487.3	916.1
30/07/2012	109	2025.8	442.3	2908.8	1047.9	119.4	417.9	2357.5	754.0	906.1	286.6	519.9	-587.0	2253.7	715.7	3496.8	925.1
31/07/2012	110	2026.9	443.4	2917.7	1056.3	118.7	417.2	2358.8	755.3	904.6	285.2	517.5	-589.4	2263.0	724.5	3500.8	928.9
1/08/2012	111	2037.6	453.6	2929.1	1067.2	127.9	425.9	2369.2	765.1	898.8	279.6	525.6	-581.7	2274.7	735.6	3512.5	940.0
2/08/2012	112	2041.1	456.8	2933.5	1071.3	129.4	427.3	2372.1	767.9	895.8	276.9	518.9	-588.0	2275.1	735.9	3517.6	944.8
3/08/2012	113	2041.2	457.0	2934.7	1072.5	129.3	427.2	2374.5	770.1	901.9	282.6	518.1	-588.8	2276.0	736.8	3519.4	946.5
4/08/2012	114	2041.5	457.2	2941.3	1078.7	128.3	426.3	2379.1	774.5	903.3	283.9	513.4	-593.3	2273.4	734.3	3524.2	951.1
5/08/2012	115	2038.1	454.0	2942.8	1080.2	123.6	421.8	2378.8	774.2	899.2	280.0	506.8	-599.4	2267.3	728.6	3524.8	951.7
6/08/2012	116	2042.5	458.2	2954.8	1091.5	127.8	425.8	2381.2	776.5	907.6	288.0	507.2	-599.1	2265.0	726.4	3530.3	956.9
7/08/2012	117	2058.8	473.6	2982.3	1117.6	136.3	433.8	2395.1	789.7	893.9	275.0	506.6	-599.7	2301.4	760.8	3543.4	969.3
8/08/2012	118	2054.9	469.9	2979.3	1114.7	132.0	429.8	2389.2	784.1	911.5	291.7	504.9	-601.3	2300.6	760.1	3541.6	967.6

9/08/2012	119	2050.8	466.0	2979.9	1115.3	128.7	426.7	2385.4	780.5	915.1	295.2	500.4	-605.5	2285.1	745.4	3540.1	966.2
10/08/2012	120	2054.2	469.3	2988.7	1123.6	126.9	424.9	2386.1	781.2	921.3	300.9	488.4	-617.0	2297.4	757.1	3542.5	968.5
11/08/2012	121	2040.2	456.0	2976.3	1111.9	116.9	415.5	2368.9	764.9	920.0	299.8	491.6	-613.9	2278.2	738.9	3530.8	957.3
12/08/2012	122	2032.2	448.4	2963.0	1099.3	109.6	408.6	2359.5	755.9	913.9	293.9	491.2	-614.2	2270.9	731.9	3520.6	947.7
13/08/2012	123	2046.0	461.4	2976.3	1111.9	121.7	420.0	2373.4	769.1	923.0	302.6	499.1	-606.7	2288.6	748.7	3534.6	961.0
14/08/2012	124	2052.7	467.8	2982.8	1118.1	125.9	424.0	2379.9	775.3	924.8	304.3	499.5	-606.4	2297.4	757.0	3542.6	968.6
15/08/2012	125	2053.6	468.7	2997.8	1132.3	126.8	424.9	2384.4	779.6	927.1	306.5	491.4	-614.0	2292.8	752.7	3546.7	972.4
16/08/2012	126	2055.5	470.5	3004.5	1138.6	125.7	423.9	2381.7	777.0	922.6	302.2	486.5	-618.8	2291.2	751.2	3548.6	974.3
17/08/2012	127	2053.7	468.8	3004.0	1138.2	122.3	420.6	2378.7	774.2	915.2	295.2	481.8	-623.2	2281.0	741.5	3545.9	971.7
18/08/2012	128	2061.3	475.9	3022.3	1155.5	128.3	426.3	2391.2	786.0	913.7	293.8	475.6	-629.0	2291.5	751.4	3559.8	984.9
19/08/2012	129	2063.9	478.5	3021.6	1154.8	128.5	426.5	2393.1	787.8	900.4	281.1	477.9	-626.9	2301.8	761.3	3561.9	986.8
20/08/2012	130	2067.6	482.0	3025.0	1158.1	131.4	429.2	2399.6	794.0	905.0	285.5	476.0	-628.7	2310.2	769.2	3565.8	990.6
21/08/2012	131	2056.4	471.3	3010.4	1144.3	120.0	418.4	2383.8	778.9	906.1	286.6	473.0	-631.5	2293.7	753.6	3555.5	980.8
22/08/2012	132	2050.3	465.6	3002.2	1136.5	117.0	415.6	2375.2	770.8	909.8	290.1	478.1	-626.7	2284.7	745.1	3547.7	973.4
23/08/2012	133	2039.3	455.1	2990.3	1125.2	108.5	407.6	2367.3	763.4	903.5	284.1	485.3	-619.9	2284.4	744.7	3536.2	962.5
24/08/2012	134	2035.2	451.2	2993.6	1128.3	104.2	403.4	2364.0	760.2	898.3	279.2	478.5	-626.3	2276.7	737.4	3531.2	957.8
25/08/2012	135	2049.3	464.7	3034.5	1167.1	114.7	413.3	2374.5	770.1	894.0	275.1	464.2	-639.8	2283.8	744.1	3549.9	975.4
26/08/2012	136	2052.5	467.6	3050.0	1181.8	115.1	413.8	2381.9	777.2	903.5	284.1	450.5	-652.8	2290.4	750.4	3558.2	983.4
27/08/2012	137	2066.0	480.5	3066.8	1197.7	127.7	425.7	2399.5	793.9	918.0	297.9	459.3	-644.5	2307.2	766.4	3572.6	997.0
28/08/2012	138	2058.6	473.4	3052.4	1184.0	120.9	419.2	2390.0	784.9	911.7	291.9	463.0	-641.0	2298.1	757.8	3563.7	988.6
29/08/2012	139	2050.4	465.7	3040.3	1172.6	112.3	411.1	2380.4	775.8	903.7	284.3	467.4	-636.8	2292.5	752.4	3554.1	979.5
30/08/2012	140	2051.1	466.3	3046.8	1178.8	115.5	414.1	2386.2	781.2	902.3	283.0	473.5	-631.1	2298.5	758.1	3557.6	982.7
31/08/2012	141	2065.0	479.5	3094.2	1223.7	123.3	421.5	2402.6	796.8	899.1	280.0	452.1	-651.4	2297.8	757.4	3573.8	998.1
1/09/2012	142	2084.1	497.6	3119.2	1247.3	139.1	436.5	2419.8	813.1	894.4	275.5	454.5	-649.0	2337.1	794.6	3593.8	1017.1
2/09/2012	143	2071.7	485.8	3100.8	1229.9	126.6	424.7	2400.2	794.5	903.5	284.1	446.3	-656.8	2329.6	787.6	3583.0	1006.9
3/09/2012	144	2081.7	495.3	3105.8	1234.6	134.8	432.4	2412.7	806.4	905.2	285.7	459.5	-644.3	2334.4	792.2	3591.9	1015.3
4/09/2012	145	2076.5	490.4	3100.9	1230.0	131.1	428.9	2406.7	800.7	895.8	276.8	456.7	-647.0	2324.5	782.7	3589.5	1013.0
5/09/2012	146	2077.8	491.6	3108.3	1237.0	130.9	428.8	2410.1	803.9	891.6	272.9	447.8	-655.4	2324.3	782.6	3591.9	1015.3
6/09/2012	147	2088.3	501.5	3128.5	1256.2	138.1	435.6	2423.5	816.6	892.1	273.3	445.8	-657.3	2335.9	793.6	3605.7	1028.3
7/09/2012	148	2094.8	507.8	3144.5	1271.4	139.5	436.9	2437.4	829.8	893.7	274.8	438.1	-664.6	2350.1	807.1	3614.4	1036.6
8/09/2012	149	2092.7	505.7	3142.6	1269.6	133.7	431.4	2435.5	828.0	903.7	284.3	434.0	-668.5	2350.1	807.0	3615.1	1037.3
9/09/2012	150	2085.3	498.7	3130.4	1258.0	128.1	426.1	2420.3	813.6	904.1	284.7	435.0	-667.5	2342.7	800.0	3606.4	1029.0
10/09/2012	151	2082.8	496.4	3120.4	1248.5	127.0	425.0	2414.7	808.3	911.8	292.0	444.2	-658.9	2336.7	794.3	3602.9	1025.7
11/09/2012	152	2075.6	489.6	3108.5	1237.2	120.1	418.5	2407.5	801.4	909.1	289.5	452.5	-651.0	2335.0	792.7	3593.7	1017.0
12/09/2012	153	2063.2	477.8	3091.7	1221.3	108.6	407.6	2396.0	790.5	906.5	287.0	449.5	-653.8	2321.7	780.1	3578.5	1002.6
13/09/2012	154	2061.1	475.8	3087.3	1217.1	107.2	406.3	2393.2	787.9	917.4	297.3	461.9	-642.1	2320.7	779.2	3573.4	997.8
14/09/2012	155	2074.6	488.6	3119.5	1247.7	118.3	416.8	2409.4	803.2	914.6	294.7	459.3	-644.5	2336.3	794.0	3585.7	1009.4

15/09/2012	156	2073.0	487.1	3139.1	1266.2	118.5	417.0	2402.8	797.0	922.5	302.1	445.0	-658.1	2324.1	782.4	3590.7	1014.1
16/09/2012	157	2063.5	478.1	3128.2	1255.9	110.2	409.2	2390.2	785.1	923.8	303.3	445.1	-657.9	2314.2	773.0	3583.0	1006.9
17/09/2012	158	2062.0	476.7	3119.8	1247.9	108.9	407.9	2388.0	783.0	918.8	298.6	458.9	-644.9	2320.5	779.0	3578.7	1002.8
18/09/2012	159	2055.6	470.6	3112.2	1240.7	106.7	405.9	2390.4	785.2	920.6	300.3	466.7	-637.5	2313.2	772.0	3573.5	997.8
19/09/2012	160	2057.3	472.2	3114.3	1242.8	106.2	405.3	2392.6	787.3	900.7	281.4	468.4	-635.8	2315.0	773.7	3571.7	996.1
20/09/2012	161	2063.1	477.7	3120.9	1249.0	111.1	410.0	2395.9	790.5	904.3	284.9	474.1	-630.5	2323.8	782.1	3577.8	1001.9
21/09/2012	162	2056.7	471.7	3113.7	1242.2	105.8	404.9	2390.7	785.5	913.2	293.3	477.2	-627.5	2326.3	784.5	3569.4	994.0
22/09/2012	163	2057.4	472.3	3117.6	1245.9	107.8	406.9	2392.4	787.2	911.9	292.1	478.2	-626.6	2324.4	782.6	3569.8	994.3
23/09/2012	164	2051.2	466.4	3113.6	1242.1	103.5	402.8	2382.7	777.9	908.1	288.4	477.2	-627.5	2316.5	775.2	3567.1	991.8
24/09/2012	165	2054.2	469.3	3157.7	1283.9	105.8	405.0	2391.0	785.8	922.8	302.4	467.1	-637.1	2325.3	783.5	3571.1	995.6
25/09/2012	166	2059.5	474.3	3195.1	1319.3	105.6	404.8	2395.9	790.4	922.3	301.9	452.7	-650.7	2323.9	782.2	3577.2	1001.4
26/09/2012	167	2053.5	468.6	3183.4	1308.3	100.3	399.8	2386.9	781.9	918.8	298.6	451.5	-651.9	2317.9	776.5	3573.9	998.2
27/09/2012	168	2046.6	462.1	3173.3	1298.6	93.8	393.6	2379.1	774.6	916.0	296.0	455.3	-648.3	2321.0	779.4	3566.0	990.7
28/09/2012	169	2041.8	457.5	3166.8	1292.5	88.8	388.9	2374.2	769.9	924.1	303.6	460.2	-643.6	2310.7	769.7	3558.9	984.0
29/09/2012	170	2038.8	454.7	3170.9	1296.4	85.9	386.1	2376.7	772.2	908.6	288.9	465.1	-639.0	2310.8	769.7	3555.0	980.3
30/09/2012	171	2047.2	462.6	3356.3	1472.1	95.5	395.2	2390.8	785.6	911.4	291.6	441.0	-661.9	2324.8	783.1	3570.0	994.6
1/10/2012	172	2056.3	471.2	3417.9	1530.5	101.6	400.9	2399.4	793.8	925.6	305.1	429.1	-673.1	2326.2	784.4	3584.8	1008.5
2/10/2012	173	2047.4	462.8	3406.9	1520.1	93.9	393.7	2386.3	781.3	918.6	298.4	423.1	-678.9	2315.6	774.4	3578.4	1002.4
3/10/2012	174	2053.7	468.8	3409.8	1522.8	100.9	400.3	2393.5	788.2	920.3	300.0	431.5	-670.8	2325.8	784.0	3585.5	1009.2
4/10/2012	175	2050.6	465.8	3432.4	1544.3	96.6	396.2	2391.7	786.5	914.4	294.4	430.6	-671.7	2320.7	779.2	3580.8	1004.8
5/10/2012	176	2066.2	480.6	3589.9	1693.5	105.7	404.8	2403.3	797.5	906.5	286.9	432.0	-670.4	2331.4	789.3	3594.9	1018.1
6/10/2012	177	2053.5	468.5	3653.9	1754.2	93.4	393.2	2391.3	786.1	909.2	289.5	441.2	-661.7	2323.7	782.0	3580.1	1004.1
7/10/2012	178	2038.8	454.7	3739.5	1835.3	84.3	384.6	2380.5	775.8	906.0	286.5	437.7	-665.0	2315.1	773.8	3566.7	991.4
8/10/2012	179	2051.5	466.7	3963.4	2047.6	98.0	397.5	2393.7	788.4	920.6	300.3	441.3	-661.6	2320.9	779.3	3582.5	1006.4
9/10/2012	180	2054.7	469.7	3988.9	2071.7	98.4	397.9	2392.5	787.2	916.2	296.1	436.6	-666.0	2326.5	784.7	3585.1	1008.9
10/10/2012	181	2065.8	480.3	4029.5	2110.2	105.8	405.0	2404.2	798.4	912.6	292.8	438.2	-664.5	2337.0	794.6	3595.7	1018.9
11/10/2012	182	2053.1	468.2	4070.0	2148.6	96.3	396.0	2394.1	788.8	912.3	292.5	429.5	-672.7	2328.2	786.3	3589.3	1012.8
12/10/2012	183	2086.8	500.1	4189.5	2261.9	123.7	421.9	2427.9	820.8	913.4	293.5	449.6	-653.6	2367.6	823.6	3613.8	1036.1
13/10/2012	184	2079.2	493.0	4220.0	2290.8	119.9	418.3	2420.4	813.7	911.9	292.0	436.2	-666.4	2359.6	816.0	3616.2	1038.3
14/10/2012	185	2061.6	476.2	4219.8	2290.6	107.5	406.6	2402.6	796.8	902.6	283.3	429.6	-672.6	2343.6	800.9	3605.0	1027.7
15/10/2012	186	2064.2	478.7	4223.2	2293.8	108.7	407.7	2404.8	798.9	904.9	285.4	440.4	-662.5	2343.3	800.5	3604.1	1026.9
16/10/2012	187	2057.8	472.6	4233.1	2303.2	102.5	401.8	2402.8	797.0	908.4	288.8	436.6	-666.0	2336.1	793.8	3596.1	1019.3
17/10/2012	188	2051.3	466.5	4263.6	2332.1	95.9	395.6	2393.4	788.1	907.9	288.3	427.8	-674.4	2333.0	790.8	3591.9	1015.3
18/10/2012	189	2056.1	471.1	4274.1	2342.1	100.1	399.6	2393.1	787.8	903.5	284.1	438.0	-664.7	2333.6	791.4	3594.5	1017.7
19/10/2012	190	2052.3	467.5	4268.7	2337.0	90.3	390.3	2391.4	786.2	915.2	295.2	444.6	-658.5	2328.8	786.8	3582.5	1006.3
20/10/2012	191	2050.7	465.9	4268.2	2336.5	90.8	390.7	2392.2	786.9	918.4	298.3	455.8	-647.8	2330.3	788.3	3578.8	1002.8
21/10/2012	192	2039.3	455.2	4254.8	2323.8	81.5	382.0	2378.6	774.1	922.6	302.3	453.4	-650.1	2322.5	780.8	3565.8	990.6

22/10/2012	193	2036.0	452.0	4308.5	2374.7	79.6	380.1	2378.9	774.4	923.2	302.7	449.5	-653.8	2321.6	780.0	3562.8	987.7
23/10/2012	194	2058.2	473.1	4459.8	2518.0	100.4	399.8	2401.3	795.5	920.1	299.8	445.1	-658.0	2342.3	799.6	3588.7	1012.3
24/10/2012	195	2052.5	467.7	4485.6	2542.6	97.8	397.4	2395.2	789.8	922.7	302.3	432.7	-669.7	2339.2	796.6	3591.2	1014.6
25/10/2012	196	2045.9	461.4	4479.5	2536.8	90.9	390.8	2389.0	783.9	912.7	292.8	437.1	-665.6	2335.9	793.5	3584.2	1008.0
26/10/2012	197	2044.7	460.3	4476.6	2534.0	91.6	391.5	2388.2	783.2	914.8	294.8	445.2	-657.8	2331.8	789.7	3577.9	1002.1
27/10/2012	198	2044.7	460.2	4479.2	2536.5	90.7	390.7	2387.2	782.2	927.2	306.6	445.3	-657.7	2337.5	795.1	3580.4	1004.4
28/10/2012	199	2044.3	459.9	4482.0	2539.2	90.9	390.8	2392.8	787.5	917.7	297.5	434.0	-668.5	2340.9	798.3	3584.9	1008.7
29/10/2012	200	2048.2	463.6	4486.4	2543.3	95.1	394.8	2394.5	789.1	908.0	288.4	436.0	-666.6	2340.2	797.6	3591.7	1015.1
30/10/2012	201	2049.6	464.9	4486.4	2543.3	94.5	394.2	2397.1	791.6	914.3	294.4	446.6	-656.6	2334.9	792.6	3589.1	1012.6
31/10/2012	202	2050.3	465.6	4479.5	2536.7	87.0	387.1	2391.8	786.5	918.3	298.1	452.6	-650.9	2332.5	790.3	3579.4	1003.4
1/11/2012	203	2059.3	474.1	4484.9	2541.9	94.2	394.0	2402.6	796.8	933.4	312.5	463.6	-640.4	2344.3	801.5	3583.5	1007.4
2/11/2012	204	2056.0	471.0	4486.2	2543.1	92.0	391.9	2403.0	797.1	942.6	321.1	441.6	-661.3	2343.9	801.2	3585.7	1009.4
3/11/2012	205	2052.9	468.0	4483.1	2540.1	88.2	388.2	2397.9	792.4	934.8	313.8	435.3	-667.2	2340.5	797.9	3584.9	1008.6
4/11/2012	206	2043.2	458.9	4474.1	2531.6	81.2	381.6	2387.0	782.0	935.4	314.4	439.3	-663.4	2330.4	788.4	3576.7	1000.8
5/11/2012	207	2041.7	457.4	4473.6	2531.1	82.7	383.0	2387.4	782.4	932.3	311.4	460.6	-643.3	2331.0	788.9	3573.9	998.2
6/11/2012	208	2039.0	454.9	4466.0	2523.9	75.1	375.9	2386.5	781.5	932.7	311.8	465.3	-638.8	2324.0	782.2	3559.8	984.9
7/11/2012	209	2038.5	454.4	4461.9	2520.1	71.7	372.6	2386.1	781.2	931.5	310.6	471.6	-632.8	2318.6	777.2	3553.4	978.8
8/11/2012	210	2039.0	454.8	4462.1	2520.3	73.2	374.0	2386.6	781.7	929.2	308.5	481.2	-623.8	2314.6	773.4	3550.4	976.0
9/11/2012	211	2032.3	448.5	4453.9	2512.5	66.7	367.9	2381.8	777.1	925.7	305.1	479.8	-625.1	2310.6	769.6	3538.3	964.5
10/11/2012	212	2037.9	453.8	4455.2	2513.8	69.4	370.4	2388.1	783.0	935.8	314.7	476.8	-627.9	2316.0	774.7	3538.9	965.0
11/11/2012	213	2043.9	459.5	4463.0	2521.1	73.7	374.5	2395.2	789.8	926.4	305.8	468.0	-636.3	2318.5	777.1	3548.1	973.8
12/11/2012	214	2055.3	470.3	4477.6	2535.0	84.4	384.7	2408.0	801.9	941.2	319.8	466.1	-638.1	2329.0	787.0	3564.6	989.4
13/11/2012	215	2048.9	464.2	4473.7	2531.3	78.6	379.1	2403.0	797.2	945.6	324.0	460.9	-643.0	2324.1	782.4	3561.7	986.7
14/11/2012	216	2046.7	462.2	4472.4	2530.0	77.0	377.7	2398.4	792.8	945.7	324.1	460.7	-643.2	2324.1	782.3	3560.4	985.4
15/11/2012	217	2050.0	465.2	4476.8	2534.2	84.0	384.3	2403.4	797.5	943.6	322.1	472.8	-631.7	2328.2	786.3	3564.3	989.1
16/11/2012	218	2034.8	450.8	4461.8	2520.0	69.3	370.3	2389.3	784.2	939.7	318.4	466.2	-638.0	2312.5	771.4	3547.0	972.8
17/11/2012	219	2040.0	455.8	4464.0	2522.0	71.4	372.3	2393.6	788.2	941.8	320.4	466.8	-637.4	2315.4	774.1	3549.1	974.7
18/11/2012	220	2034.0	450.1	4460.5	2518.8	67.5	368.6	2388.9	783.8	943.7	322.2	459.0	-644.7	2308.1	767.2	3548.1	973.7
19/11/2012	221	2037.7	453.6	4466.8	2524.8	70.3	371.3	2393.5	788.2	939.5	318.2	456.5	-647.2	2316.9	775.6	3553.0	978.4
20/11/2012	222	2054.8	469.8	4484.0	2541.0	83.7	384.0	2408.4	802.3	938.9	317.7	463.0	-641.0	2334.8	792.5	3570.7	995.2
21/11/2012	223	2066.2	480.6	4495.5	2551.9	92.1	392.0	2418.1	811.5	935.2	314.2	471.0	-633.4	2346.7	803.8	3583.2	1007.0
22/11/2012	224	2048.8	464.2	4479.6	2536.9	74.8	375.6	2399.9	794.3	942.2	320.8	458.4	-645.3	2325.7	783.9	3566.5	991.2
23/11/2012	225	2049.7	465.0	4479.6	2536.9	74.0	374.9	2399.6	793.9	938.2	317.0	452.5	-651.0	2326.9	785.0	3566.8	991.5
24/11/2012	226	2070.4	484.6	4498.2	2554.5	95.7	395.4	2419.1	812.4	942.6	321.2	479.0	-625.8	2349.6	806.5	3586.9	1010.5
25/11/2012	227	2082.5	496.1	4510.9	2566.5	112.7	411.5	2432.0	824.7	955.5	333.4	506.7	-599.6	2363.9	820.1	3599.8	1022.7
26/11/2012	228	2046.9	462.4	4476.8	2534.2	78.2	378.8	2397.7	792.2	969.6	346.8	487.0	-618.3	2324.9	783.1	3559.2	984.3
27/11/2012	229	2060.1	474.9	4487.6	2544.5	90.8	390.7	2413.0	806.7	966.2	343.5	508.2	-598.1	2342.0	799.4	3567.1	991.8

28/11/2012	230	2062.9	477.5	4488.2	2545.0	95.4	395.1	2417.2	810.6	966.4	343.7	516.5	-590.3	2350.1	807.0	3565.7	990.5
29/11/2012	231	2050.6	465.8	4474.4	2531.9	81.9	382.3	2403.0	797.2	970.6	347.7	508.5	-597.8	2332.8	790.6	3549.8	975.4
30/11/2012	232	2044.8	460.3	4467.6	2525.5	74.7	375.5	2397.2	791.7	973.7	350.7	507.7	-598.6	2319.6	778.1	3539.3	965.5
1/12/2012	233	2070.1	484.3	4490.2	2546.9	100.7	400.1	2424.0	817.1	980.4	357.0	538.9	-569.0	2348.4	805.4	3560.4	985.4
2/12/2012	234	2068.6	482.9	4487.8	2544.6	99.0	398.5	2423.6	816.7	994.2	370.1	537.7	-570.1	2348.1	805.1	3556.8	982.1
3/12/2012	235	2036.4	452.4	4458.8	2517.2	66.7	367.9	2391.1	785.9	1010.8	385.8	509.0	-597.4	2312.9	771.8	3524.8	951.7
4/12/2012	236	2013.0	430.2	4437.8	2497.2	41.5	344.0	2370.1	766.0	1010.2	385.2	476.9	-627.8	2294.1	754.0	3501.5	929.6
5/12/2012	237	2029.3	445.7	4455.9	2514.4	50.9	353.0	2387.3	782.3	1001.2	376.7	455.6	-648.0	2318.7	777.3	3523.2	950.2
6/12/2012	238	2042.7	458.4	4471.6	2529.2	59.8	361.3	2396.9	791.4	1009.8	384.9	447.9	-655.3	2328.6	786.7	3544.0	969.9
7/12/2012	239	2057.9	472.8	4469.0	2526.8	55.0	356.9	2389.3	784.2	1017.5	392.2	441.6	-661.3	2320.7	779.1	3545.6	971.4
8/12/2012	240	2041.9	457.6	4468.6	2526.4	57.5	359.2	2388.8	783.7	1029.6	403.7	452.6	-650.9	2321.9	780.2	3546.9	972.6

Table E.7 Concrete surface strain at steel level for slab DS-SCC-a

Slab DS-SCC-a		CONCRETE SURFACE STRAIN BY SG															
		1		2		3		4		5		6		7		8	
Date	Age	Reading	Strain	Reading	Strain	Reading	Strain	Reading	Strain	Reading	Strain	Reading	Strain	Reading	Strain	Reading	Strain
16/05/2012	14	1902.2		486.7		759.1		-265.2		439.3				507.2		173.0	
16/05/2012	14	2550.7		748.3		1200.0		140.9		250.2				899.3		591.0	
17/05/2012	15	2900.3	331.3	1134.4	366.0	1507.3	291.3	475.0	316.7	649.5	378.5			1297.6	377.5	888.0	281.5
18/05/2012	16	2980.1	406.9	1159.6	389.9	1524.6	307.7	510.7	350.5	695.9	422.4			1367.7	444.0	907.4	299.9
19/05/2012	17	3050.1	473.3	1151.4	382.1	1537.0	319.5	545.2	383.2	740.7	464.9			1412.0	486.0	901.1	293.9
20/05/2012	18	3020.5	445.3	1148.1	378.9	1558.0	339.3	569.2	406.0	772.0	494.5			1462.4	533.8	898.5	291.5
21/05/2012	19	2604.8	51.3	1141.6	372.8	1536.8	319.2	550.0	387.8	747.1	470.9			1472.5	543.4	893.5	286.8
22/05/2012	20	3003.5	429.2	1148.2	379.1	1570.6	351.3	597.6	432.9	808.8	529.5			1520.2	588.6	898.6	291.6
23/05/2012	21	2946.4	375.0	1161.6	391.8	1616.5	394.8	628.2	461.9	848.7	567.3			1568.3	634.1	908.9	301.4
24/05/2012	22	3068.8	491.0	1153.6	384.2	1616.1	394.4	633.5	467.0	855.6	573.8			1592.3	656.8	902.8	295.6
25/05/2012	23	3098.5	519.2	1150.0	380.8	1608.6	387.3	623.6	457.6	842.7	561.6			1604.9	668.8	900.0	292.9
26/05/2012	24	3329.2	737.9	1167.2	397.1	1643.5	420.5	667.7	499.4	900.1	616.0			1634.3	696.7	913.2	305.5
27/05/2012	25	3359.5	766.6	1182.2	411.3	1662.5	438.4	674.0	505.4	908.2	623.7			1660.9	721.9	924.8	316.4
28/05/2012	26	3391.4	796.8	1201.9	429.9	1679.0	454.1	704.7	534.4	948.1	661.5			1688.9	748.5	939.9	330.7
29/05/2012	27	2930.9	360.3	1187.4	416.2	1663.7	439.6	681.9	512.9	918.5	633.5			1692.1	751.4	928.8	320.2
30/05/2012	28	2958.5	386.5	1196.3	424.7	1674.6	449.9	718.2	547.2	965.7	678.2			1711.7	770.1	935.6	326.7
31/05/2012	29	2900.2	331.3	1195.9	424.3	1671.1	446.6	696.8	527.0	937.9	651.8			1732.8	790.1	935.3	326.4
1/06/2012	30	3094.5	515.4	1194.9	423.3	1664.7	440.5	704.7	534.4	948.1	661.5			1746.4	803.0	934.5	325.6
2/06/2012	31	3230.8	644.6	1188.2	417.0	1660.3	436.4	712.7	542.0	958.5	671.4			1747.8	804.3	929.4	320.8
3/06/2012	32	2984.2	410.9	1184.3	413.3	1675.8	451.0	742.1	569.9	996.8	707.6			1754.6	810.7	926.4	317.9
4/06/2012	33	2893.0	324.4	1185.8	414.8	1676.4	451.6	748.9	576.3	1005.6	716.0			1763.1	818.8	927.6	319.0
5/06/2012	34	2710.4	151.3	1211.3	438.9	1703.4	477.2	774.3	600.4	1038.5	747.2			1802.0	855.6	947.1	337.6
6/06/2012	35	2788.2	225.1	1198.0	426.3	1686.1	460.8	744.6	572.2	999.9	710.6			1791.9	846.1	936.9	327.9
7/06/2012	36	2635.5	80.3	1209.0	436.7	1714.1	487.3	787.9	613.3	1056.2	764.0			1816.9	869.7	945.4	335.9
8/06/2012	37	2978.2	405.2	1227.3	454.1	1733.9	506.1	843.8	666.3	1128.9	832.9			1850.9	902.0	959.5	349.3
9/06/2012	38	2693.3	135.1	1224.4	451.3	1736.4	508.5	831.7	654.8	1113.2	818.0			1855.3	906.2	957.2	347.1
10/06/2012	39	3040.7	464.4	1226.3	453.1	1738.5	510.5	806.7	631.1	1080.7	787.2			1860.2	910.9	958.7	348.6
11/06/2012	40	2907.9	338.5	1210.6	438.2	1719.3	492.3	774.1	600.2	1038.3	747.0			1831.8	883.9	946.6	337.1
12/06/2012	41	2754.1	192.8	1204.2	432.1	1697.7	471.8	745.7	573.3	1001.4	712.0			1817.9	870.8	941.7	332.4
13/06/2012	42	2712.5	153.4	1210.9	438.5	1715.9	489.1	791.0	616.2	1060.3	767.8			1840.4	892.1	946.8	337.3
14/06/2012	43	2898.4	329.5	1207.7	435.4	1708.3	481.9	801.9	626.6	1074.5	781.3			1837.6	889.4	944.3	334.9
15/06/2012	44	2936.7	365.8	1201.6	429.7	1691.9	466.3	790.9	616.1	1060.1	767.7			1836.8	888.7	939.7	330.5

16/06/2012	45	2943.0	371.8	1204.8	432.7	1693.5	467.8	810.3	634.5	1085.4	791.6			1846.9	898.3	942.2	332.9
17/06/2012	46	2933.4	362.7	1199.3	427.5	1722.6	495.4	828.9	652.1	1109.5	814.5			1865.2	915.5	937.9	328.8
18/06/2012	47	2935.0	364.2	1215.4	442.7	1733.3	505.5	843.1	665.6	1128.0	832.0			1882.7	932.1	950.3	340.6
19/06/2012	48	2943.0	371.8	1224.9	451.7	1739.5	511.5	848.8	671.1	1135.5	839.1			1899.3	947.9	957.6	347.5
20/06/2012	49	2983.3	410.0	1222.5	449.6	1741.6	513.4	851.4	673.5	1138.8	842.2			1902.9	951.3	955.8	345.8
21/06/2012	50	3023.7	448.3	1232.0	458.5	1748.8	520.2	884.7	705.1	1182.1	883.3			1927.3	974.4	963.0	352.7
22/06/2012	51	3089.1	510.3	1221.5	448.5	1747.6	519.1	841.7	664.3	1126.3	830.4			1906.4	954.6	955.0	345.0
23/06/2012	52	3126.7	545.9	1225.9	452.7	1743.2	514.9	872.0	693.0	1165.6	867.6			1929.1	976.1	958.4	348.3
24/06/2012	53	3147.2	565.3	1228.9	455.6	1748.5	520.0	899.8	719.4	1201.7	901.9			1951.1	997.0	960.7	350.5
25/06/2012	54	3153.1	570.9	1231.8	458.4	1757.8	528.8	900.9	720.4	1203.1	903.2			1957.8	1003.4	963.0	352.6
26/06/2012	55	3132.1	551.1	1220.0	447.1	1751.7	523.0	867.8	689.0	1160.1	862.5			1927.5	974.6	953.8	343.9
27/06/2012	56	3047.9	471.3	1213.9	441.4	1752.3	523.6	870.6	691.7	1163.8	866.0			1929.0	976.1	949.2	339.5
28/06/2012	57	2907.1	337.8	1212.8	440.3	1753.7	524.9	872.0	693.0	1165.6	867.7			1924.6	971.8	948.3	338.7
29/06/2012	58	2827.9	262.7	1209.2	436.9	1755.0	526.1	863.8	685.3	1155.0	857.6			1911.6	959.6	945.5	336.1
30/06/2012	59	2916.3	346.5	1202.2	430.2	1751.3	522.6	853.0	675.1	1141.0	844.3			1914.5	962.3	940.1	330.9
1/07/2012	60	2973.8	401.0	1207.6	435.4	1747.7	519.2	861.4	682.9	1151.8	854.6			1933.4	980.2	944.3	334.9
2/07/2012	61	3032.1	456.2	1230.9	457.5	1759.5	530.4	915.4	734.2	1222.0	921.1			1974.2	1018.9	962.2	351.9
3/07/2012	62	3062.0	484.6	1224.9	451.8	1756.5	527.5	913.7	732.5	1219.8	919.0			1976.7	1021.3	957.6	347.5
4/07/2012	63	3139.3	557.9	1225.8	452.6	1756.2	527.3	907.2	726.4	1211.4	911.1			1977.3	1021.9	958.3	348.2
5/07/2012	64	3255.0	667.6	1218.8	446.0	1752.0	523.3	893.6	713.5	1193.6	894.2			1965.1	1010.2	952.9	343.1
6/07/2012	65	3383.8	789.7	1210.3	437.9	1748.5	520.0	898.7	718.4	1200.4	900.6			1962.0	1007.3	946.4	336.9
7/07/2012	66	3422.0	825.8	1215.1	442.5	1755.8	526.9	905.9	725.1	1209.6	909.4			1970.5	1015.3	950.1	340.4
8/07/2012	67	3346.5	754.2	1202.9	430.9	1750.6	521.9	900.9	720.5	1203.2	903.3			1959.6	1005.1	940.7	331.5
9/07/2012	68	3218.7	633.2	1213.7	441.1	1762.9	533.6	926.8	745.0	1236.9	935.2			1973.6	1018.3	949.0	339.3
10/07/2012	69	3047.8	471.1	1208.9	436.6	1765.3	535.9	932.5	750.4	1244.3	942.2			1964.2	1009.4	945.3	335.8
11/07/2012	70	2880.1	312.2	1184.1	413.1	1751.6	522.9	913.5	732.3	1219.5	918.8			1940.8	987.2	926.2	317.8
12/07/2012	71	2875.7	308.0	1203.0	431.1	1759.6	530.5	912.6	731.5	1218.4	917.7			1953.7	999.5	940.8	331.6
13/07/2012	72	2850.4	284.0	1193.3	421.8	1753.3	524.5	894.2	714.1	1194.5	895.0			1933.2	980.0	933.3	324.5
14/07/2012	73	2839.0	273.2	1187.2	416.0	1743.2	514.9	865.4	686.8	1157.0	859.5			1928.4	975.5	928.6	320.0
15/07/2012	74	2858.2	291.4	1198.9	427.2	1749.0	520.4	894.2	714.0	1194.4	895.0			1952.5	998.3	937.6	328.6
16/07/2012	75	2883.1	315.1	1226.5	453.3	1764.3	534.9	927.3	745.5	1237.6	935.9			1996.5	1040.0	958.8	348.7
17/07/2012	76	2870.6	303.1	1217.8	445.0	1761.5	532.2	907.4	726.6	1211.6	911.3			1993.1	1036.8	952.2	342.3
18/07/2012	77	2863.5	296.4	1212.5	440.1	1757.3	528.3	898.0	717.7	1199.4	899.7			1989.5	1033.4	948.1	338.5
19/07/2012	78	2867.7	300.5	1222.2	449.2	1761.9	532.7	917.4	736.0	1224.6	923.6			1999.6	1043.0	955.5	345.6
20/07/2012	79	2880.2	312.2	1231.8	458.3	1767.2	537.7	935.3	753.0	1247.8	945.6			2022.3	1064.5	962.9	352.6
21/07/2012	80	2875.2	307.6	1221.0	448.1	1758.4	529.4	908.1	727.2	1212.5	912.1			1999.2	1042.5	954.6	344.7
22/07/2012	81	2888.3	319.9	1215.3	442.7	1756.6	527.6	894.5	714.3	1194.8	895.3			1997.4	1040.8	950.3	340.5

23/07/2012	82	2917.9	348.0	1209.1	436.8	1758.2	529.2	894.9	714.7	1195.4	895.9			1988.6	1032.5	945.5	336.0
24/07/2012	83	2942.3	371.1	1197.5	425.8	1752.8	524.0	878.9	699.6	1174.6	876.2			1988.5	1032.5	936.5	327.5
25/07/2012	84	2960.0	387.9	1199.6	427.8	1759.8	530.7	911.6	730.6	1217.1	916.5			1990.3	1034.2	938.1	329.1
26/07/2012	85	2968.4	395.8	1201.3	429.4	1761.0	531.8	912.1	731.0	1217.7	917.0			1986.5	1030.6	939.5	330.3
27/07/2012	86	2991.6	417.9	1216.2	443.5	1768.2	538.6	913.9	732.7	1220.1	919.3			2011.6	1054.3	950.9	341.2
28/07/2012	87	3011.7	436.9	1226.7	453.5	1770.3	540.6	929.4	747.4	1240.2	938.3			2027.3	1069.2	959.0	348.9
29/07/2012	88	3029.2	453.5	1219.3	446.5	1765.9	536.4	916.4	735.1	1223.3	922.4			2021.0	1063.2	953.3	343.4
30/07/2012	89	3088.5	509.8	1227.7	454.4	1772.9	543.1	931.6	749.5	1243.0	941.1			2041.3	1082.5	959.8	349.6
31/07/2012	90	3139.5	558.1	1223.3	450.2	1768.5	538.9	917.3	736.0	1224.5	923.5			2037.7	1079.1	956.4	346.3
1/08/2012	91	3169.4	586.4	1227.9	454.7	1774.0	544.2	924.0	742.3	1233.2	931.7			2047.2	1088.1	959.9	349.7
2/08/2012	92	3205.2	620.4	1231.2	457.7	1777.2	547.2	918.8	737.4	1226.5	925.4			2054.3	1094.8	962.5	352.1
3/08/2012	93	3239.8	653.1	1231.3	457.9	1774.8	544.9	920.2	738.7	1228.2	927.0			2055.5	1095.9	962.6	352.2
4/08/2012	94	3269.3	681.1	1232.0	458.5	1773.1	543.3	909.1	728.2	1213.8	913.4			2055.7	1096.2	963.1	352.7
5/08/2012	95	3306.3	716.2	1228.5	455.2	1767.1	537.6	914.2	733.0	1220.5	919.7			2045.5	1086.5	960.4	350.1
6/08/2012	96	3360.5	767.5	1233.4	459.9	1761.2	532.0	920.7	739.2	1228.9	927.6			2043.2	1084.3	964.2	353.7
7/08/2012	97	3383.1	788.9	1249.6	475.2	1772.9	543.0	945.4	762.6	1261.1	958.2			2067.0	1106.9	976.6	365.5
8/08/2012	98	3398.8	803.8	1239.9	466.0	1768.2	538.6	932.8	750.6	1244.6	942.6			2059.9	1100.1	969.2	358.5
9/08/2012	99	3461.3	863.1	1239.3	465.4	1760.7	531.5	917.5	736.2	1224.8	923.7			2048.4	1089.3	968.7	358.0
10/08/2012	100	3554.6	951.5	1235.8	462.1	1765.0	535.6	915.6	734.3	1222.2	921.4			2048.1	1089.0	966.0	355.5
11/08/2012	101	3657.9	1049.4	1221.3	448.4	1747.8	519.3	895.8	715.6	1196.6	897.0			2028.1	1070.0	954.9	344.9
12/08/2012	102	3703.8	1092.9	1215.9	443.3	1742.7	514.4	878.4	699.1	1174.0	875.6			2020.7	1063.0	950.7	341.0
13/08/2012	103	3707.5	1096.5	1225.9	452.7	1758.4	529.3	919.5	738.1	1227.4	926.2			2041.9	1083.0	958.3	348.2
14/08/2012	104	3714.5	1103.1	1233.2	459.6	1766.7	537.2	948.7	765.8	1265.4	962.2			2051.7	1092.4	964.0	353.6
15/08/2012	105	3712.8	1101.5	1238.3	464.5	1762.3	533.0	921.5	740.0	1230.0	928.7			2052.9	1093.5	967.9	357.3
16/08/2012	106	3715.3	1103.8	1239.0	465.2	1761.9	532.7	925.6	743.8	1235.3	933.7			2056.4	1096.8	968.5	357.8
17/08/2012	107	3736.7	1124.1	1234.7	461.1	1754.5	525.6	925.9	744.2	1235.7	934.1			2051.6	1092.2	965.2	354.7
18/08/2012	108	3754.4	1140.9	1245.3	471.1	1754.7	525.9	929.3	747.3	1240.1	938.3			2061.3	1101.5	973.3	362.4
19/08/2012	109	3754.1	1140.6	1237.7	463.9	1758.0	529.0	930.5	748.5	1241.7	939.8			2069.7	1109.4	967.5	356.9
20/08/2012	110	3744.6	1131.7	1242.6	468.5	1770.2	540.5	953.5	770.2	1271.5	968.0			2073.3	1112.8	971.2	360.4
21/08/2012	111	3719.3	1107.6	1228.0	454.7	1759.7	530.5	926.3	744.5	1236.1	934.5			2057.7	1098.0	960.0	349.8
22/08/2012	112	3718.3	1106.7	1229.5	456.1	1762.4	533.1	908.5	727.6	1213.0	912.6			2060.6	1100.7	961.1	350.9
23/08/2012	113	3707.0	1096.0	1226.9	453.6	1772.5	542.7	922.8	741.2	1231.6	930.2			2060.1	1100.3	959.1	349.0
24/08/2012	114	3689.2	1079.1	1216.6	443.9	1765.7	536.3	908.2	727.4	1212.7	912.3			2049.6	1090.4	951.2	341.5
25/08/2012	115	3690.7	1080.5	1224.9	451.7	1752.5	523.7	860.0	681.7	1150.0	852.9			2060.3	1100.5	957.6	347.5
26/08/2012	116	3691.0	1080.8	1230.5	457.1	1749.1	520.5	896.2	715.9	1197.0	897.5			2066.8	1106.7	962.0	351.6
27/08/2012	117	3692.2	1082.0	1242.9	468.9	1761.2	532.0	931.7	749.6	1243.2	941.2			2085.5	1124.4	971.5	360.7
28/08/2012	118	3674.1	1064.8	1234.8	461.1	1763.1	533.8	902.3	721.8	1205.0	905.0			2081.4	1120.5	965.2	354.7

29/08/2012	119	3654.6	1046.3	1224.8	451.7	1763.8	534.5	891.4	711.4	1190.9	891.6			2070.1	1109.8	957.5	347.4
30/08/2012	120	3642.6	1035.0	1229.0	455.7	1762.6	533.4	896.1	715.8	1196.9	897.3			2073.8	1113.3	960.8	350.5
31/08/2012	121	3651.5	1043.4	1236.9	463.1	1754.3	525.5	935.1	752.9	1247.7	945.4			2086.2	1125.0	966.8	356.3
1/09/2012	122	3663.1	1054.4	1254.3	479.7	1771.0	541.3	970.6	786.5	1293.7	989.1			2108.2	1145.9	980.3	369.0
2/09/2012	123	3648.2	1040.2	1236.6	462.9	1761.4	532.2	938.5	756.0	1252.0	949.6			2092.4	1130.9	966.6	356.1
3/09/2012	124	3638.2	1030.8	1248.9	474.6	1773.2	543.4	952.2	769.0	1269.8	966.4			2105.2	1143.1	976.1	365.0
4/09/2012	125	3621.3	1014.7	1242.7	468.7	1772.0	542.3	944.1	761.4	1259.3	956.5			2100.7	1138.8	971.3	360.5
5/09/2012	126	3617.5	1011.1	1239.6	465.7	1776.8	546.8	964.6	780.8	1286.0	981.8			2105.2	1143.0	968.9	358.2
6/09/2012	127	3615.6	1009.4	1246.7	472.4	1784.0	553.6	975.4	791.0	1300.0	995.1			2110.0	1147.6	974.4	363.4
7/09/2012	128	3602.5	996.9	1250.8	476.3	1779.8	549.6	964.8	781.0	1286.3	982.1			2106.8	1144.5	977.5	366.4
8/09/2012	129	3592.2	987.2	1244.9	470.8	1776.6	546.6	948.7	765.7	1265.3	962.1			2104.7	1142.6	973.0	362.1
9/09/2012	130	3549.6	946.8	1236.7	463.0	1767.2	537.6	936.1	753.8	1248.9	946.6			2097.3	1135.6	966.7	356.1
10/09/2012	131	3508.9	908.2	1237.1	463.3	1769.7	540.1	948.4	765.4	1264.9	961.8			2102.4	1140.4	967.0	356.4
11/09/2012	132	3472.7	873.9	1241.8	467.8	1779.2	549.1	964.2	780.4	1285.5	981.3			2102.0	1140.0	970.6	359.9
12/09/2012	133	3447.5	850.0	1225.5	452.3	1770.9	541.2	934.0	751.7	1246.1	944.0			2081.4	1120.5	958.0	347.9
13/09/2012	134	3446.0	848.6	1229.8	456.4	1781.1	550.8	939.2	756.8	1253.0	950.5			2077.8	1117.0	961.4	351.1
14/09/2012	135	3453.2	855.5	1240.9	466.9	1779.7	549.5	976.9	792.5	1302.0	997.0			2098.0	1136.2	969.9	359.2
15/09/2012	136	3433.4	836.7	1238.7	464.9	1769.8	540.2	930.1	748.0	1241.1	939.2			2095.1	1133.5	968.3	357.6
16/09/2012	137	3411.9	816.3	1228.9	455.5	1764.5	535.1	927.4	745.5	1237.6	935.9			2080.8	1119.9	960.7	350.4
17/09/2012	138	3405.3	810.0	1228.8	455.5	1771.1	541.3	954.4	771.1	1272.7	969.2			2073.1	1112.6	960.6	350.4
18/09/2012	139	3392.7	798.0	1227.4	454.1	1769.9	540.2	963.4	779.6	1284.4	980.3			2068.3	1108.1	959.5	349.3
19/09/2012	140	3383.0	788.9	1228.2	454.9	1773.1	543.3	967.3	783.3	1289.5	985.1			2069.0	1108.7	960.1	349.9
20/09/2012	141	3382.4	788.3	1234.5	460.9	1775.1	545.2	965.0	781.2	1286.6	982.3			2072.8	1112.3	965.0	354.5
21/09/2012	142	3366.8	773.5	1234.4	460.8	1780.2	550.0	985.3	800.4	1312.9	1007.3			2072.9	1112.4	964.9	354.5
22/09/2012	143	3359.7	766.8	1239.0	465.1	1777.6	547.6	995.5	810.1	1326.1	1019.8			2074.0	1113.4	968.4	357.8
23/09/2012	144	3340.6	748.7	1234.1	460.5	1768.9	539.2	967.6	783.7	1289.9	985.5			2065.8	1105.7	964.7	354.2
24/09/2012	145	3329.4	738.0	1239.3	465.4	1768.8	539.2	980.4	795.8	1306.5	1001.2			2075.3	1114.7	968.7	358.0
25/09/2012	146	3324.1	733.0	1241.2	467.3	1770.8	541.1	997.1	811.6	1328.2	1021.8			2082.9	1121.9	970.2	359.4
26/09/2012	147	3309.0	718.7	1234.9	461.2	1768.5	539.0	977.6	793.1	1302.8	997.7			2074.1	1113.6	965.3	354.8
27/09/2012	148	3296.6	707.0	1231.9	458.4	1769.4	539.8	989.4	804.3	1318.3	1012.4			2063.4	1103.5	963.0	352.6
28/09/2012	149	3298.1	708.4	1229.0	455.7	1765.9	536.4	973.6	789.3	1297.7	992.9			2059.9	1100.1	960.8	350.5
29/09/2012	150	3288.5	699.3	1226.8	453.6	1764.3	534.9	973.6	789.3	1297.7	992.8			2057.5	1097.9	959.1	348.9
30/09/2012	151	3289.9	700.6	1240.4	466.4	1756.4	527.4	966.8	782.9	1288.8	984.4			2070.2	1109.9	969.5	358.8
1/10/2012	152	3345.4	753.2	1246.1	471.9	1759.3	530.2	985.9	801.0	1313.7	1008.0			2084.3	1123.2	973.9	363.0
2/10/2012	153	3356.7	763.9	1231.0	457.5	1756.0	527.1	979.9	795.3	1305.9	1000.7			2071.1	1110.7	962.3	351.9
3/10/2012	154	3356.7	763.9	1238.4	464.6	1757.8	528.8	980.8	796.2	1307.1	1001.7			2080.3	1119.4	968.0	357.4
4/10/2012	155	3362.3	769.3	1237.3	463.6	1757.6	528.6	992.9	807.6	1322.8	1016.6			2081.7	1120.8	967.2	356.6

5/10/2012	156	3355.8	763.1	1245.6	471.4	1773.7	543.8	1008.0	821.9	1342.4	1035.2			2103.2	1141.2	973.5	362.6
6/10/2012	157	3334.4	742.8	1234.6	461.0	1771.8	542.1	1006.3	820.3	1340.2	1033.2			2084.2	1123.1	965.1	354.6
7/10/2012	158	3303.0	713.1	1225.5	452.3	1762.2	532.9	986.2	801.2	1314.0	1008.3			2063.8	1103.8	958.0	347.9
8/10/2012	159	3298.5	708.7	1240.0	466.1	1763.4	534.1	987.3	802.3	1315.5	1009.7			2072.2	1111.7	969.3	358.6
9/10/2012	160	3325.0	733.9	1238.1	464.3	1757.0	528.0	989.4	804.3	1318.2	1012.3			2076.2	1115.5	967.8	357.1
10/10/2012	161	3332.5	741.0	1249.3	474.9	1764.2	534.8	1000.6	814.9	1332.8	1026.1			2088.9	1127.6	976.4	365.3
11/10/2012	162	3319.5	728.7	1236.6	462.9	1755.9	526.9	1000.1	814.4	1332.1	1025.5			2080.8	1119.9	966.6	356.1
12/10/2012	163	3348.5	756.2	1271.4	495.8	1785.8	555.4	1036.4	848.9	1379.3	1070.2			2119.5	1156.6	993.4	381.4
13/10/2012	164	3325.5	734.4	1266.3	491.1	1784.8	554.4	1036.9	849.4	1380.0	1070.9			2111.4	1149.0	989.5	377.7
14/10/2012	165	3298.0	708.3	1253.5	478.9	1770.7	541.0	1022.1	835.3	1360.7	1052.6			2092.0	1130.5	979.6	368.3
15/10/2012	166	3294.8	705.2	1255.3	480.6	1776.1	546.1	1023.1	836.3	1362.0	1053.9			2092.5	1131.0	981.0	369.7
16/10/2012	167	3292.3	702.9	1251.0	476.6	1776.6	546.6	1024.4	837.5	1363.7	1055.4			2083.9	1122.8	977.7	366.6
17/10/2012	168	3283.1	694.2	1239.2	465.3	1764.1	534.8	1020.1	833.4	1358.1	1050.1			2081.5	1120.6	968.6	357.9
18/10/2012	169	3282.8	693.9	1243.4	469.4	1770.7	540.9	1021.7	834.9	1360.3	1052.2			2080.7	1119.9	971.9	361.0
19/10/2012	170	3260.2	672.4	1236.1	462.4	1778.5	548.4	1022.5	835.7	1361.3	1053.1			2076.6	1116.0	966.2	355.7
20/10/2012	171	3263.7	675.8	1235.7	462.0	1776.6	546.6	1013.4	827.1	1349.5	1041.9			2072.3	1111.9	965.9	355.4
21/10/2012	172	3257.8	670.2	1225.9	452.7	1764.5	535.1	999.1	813.5	1330.8	1024.2			2060.5	1100.7	958.4	348.3
22/10/2012	173	3239.2	652.5	1223.7	450.6	1758.7	529.6	993.5	808.2	1323.5	1017.4			2064.1	1104.1	956.7	346.6
23/10/2012	174	3264.5	676.6	1246.5	472.2	1771.6	541.8	1030.2	843.0	1371.3	1062.6			2084.7	1123.7	974.2	363.3
24/10/2012	175	3324.4	733.3	1241.3	467.4	1754.7	525.8	1012.6	826.3	1348.4	1040.9			2076.2	1115.5	970.3	359.5
25/10/2012	176	3347.9	755.6	1233.7	460.1	1749.2	520.6	1007.0	821.0	1341.1	1034.0			2069.7	1109.4	964.4	354.0
26/10/2012	177	3353.5	760.9	1230.7	457.3	1756.1	527.1	1011.5	825.2	1346.9	1039.5			2069.7	1109.4	962.1	351.8
27/10/2012	178	3341.3	749.3	1236.5	462.8	1759.6	530.4	1010.8	824.6	1346.0	1038.7			2070.3	1110.0	966.6	356.0
28/10/2012	179	3325.9	734.7	1236.1	462.4	1753.5	524.7	1007.7	821.6	1342.0	1034.8			2064.7	1104.7	966.3	355.7
29/10/2012	180	3342.2	750.2	1242.4	468.3	1755.6	526.7	1009.9	823.7	1344.9	1037.6			2068.4	1108.2	971.0	360.3
30/10/2012	181	3351.8	759.3	1244.0	469.9	1762.9	533.6	1008.4	822.3	1342.9	1035.7			2074.9	1114.3	972.3	361.5
31/10/2012	182	3335.1	743.4	1236.9	463.1	1775.9	545.9	1021.1	834.3	1359.4	1051.3			2074.7	1114.2	966.8	356.3
1/11/2012	183	3331.8	740.4	1248.0	473.7	1785.4	554.9	1039.2	851.5	1382.9	1073.7			2087.0	1125.8	975.4	364.4
2/11/2012	184	3313.1	722.6	1243.5	469.4	1769.3	539.6	1036.1	848.5	1378.9	1069.8			2076.7	1116.0	972.0	361.1
3/11/2012	185	3379.7	785.8	1232.5	459.0	1760.2	531.0	1023.4	836.6	1362.4	1054.2			2069.3	1109.0	963.5	353.1
4/11/2012	186	3372.8	779.2	1227.1	453.8	1753.8	525.0	1007.1	821.1	1341.3	1034.2			2057.2	1097.5	959.3	349.1
5/11/2012	187	3362.7	769.6	1234.9	461.3	1767.1	537.6	1008.1	822.0	1342.5	1035.3			2062.4	1102.4	965.3	354.8
6/11/2012	188	3370.8	777.3	1226.2	453.0	1766.9	537.4	1010.2	824.1	1345.3	1038.0			2056.5	1096.9	958.6	348.5
7/11/2012	189	3374.0	780.3	1224.5	451.4	1765.5	536.1	1013.5	827.1	1349.5	1042.0			2053.9	1094.5	957.3	347.3
8/11/2012	190	3374.2	780.5	1228.6	455.3	1768.8	539.1	1020.7	833.9	1358.9	1050.9			2048.1	1088.9	960.5	350.3
9/11/2012	191	3365.7	772.5	1221.8	448.8	1764.6	535.2	1022.6	835.7	1361.3	1053.2			2044.2	1085.3	955.2	345.2
10/11/2012	192	3383.4	789.3	1224.8	451.7	1761.9	532.6	1024.4	837.5	1363.8	1055.5			2054.2	1094.7	957.6	347.5

11/11/2012	193	3394.2	799.5	1231.0	457.6	1759.5	530.4	1027.6	840.5	1367.8	1059.4			2058.6	1098.9	962.3	352.0
12/11/2012	194	3453.4	855.6	1241.7	467.7	1765.4	536.0	1042.3	854.4	1386.9	1077.5			2060.2	1100.4	970.6	359.8
13/11/2012	195	3475.8	876.9	1235.2	461.6	1762.2	532.9	1036.7	849.1	1379.7	1070.6			2058.2	1098.5	965.5	355.0
14/11/2012	196	3475.0	876.1	1234.3	460.6	1760.9	531.7	1036.5	849.0	1379.5	1070.4			2054.3	1094.8	964.8	354.3
15/11/2012	197	3479.5	880.3	1244.0	469.9	1767.4	537.8	1038.9	851.2	1382.6	1073.4			2052.4	1093.0	972.3	361.5
16/11/2012	198	3459.8	861.6	1226.7	453.5	1756.3	527.3	1027.2	840.1	1367.4	1058.9			2040.1	1081.4	959.0	348.9
17/11/2012	199	3464.4	866.0	1228.7	455.4	1764.1	534.7	1033.7	846.3	1375.8	1066.9			2053.3	1093.9	960.5	350.3
18/11/2012	200	3447.3	849.8	1224.4	451.3	1750.1	521.5	1028.9	841.8	1369.6	1061.0			2044.7	1085.7	957.2	347.1
19/11/2012	201	3452.1	854.4	1229.4	456.0	1749.3	520.7	1032.8	845.5	1374.7	1065.8			2046.5	1087.4	961.1	350.8
20/11/2012	202	3473.5	874.7	1242.8	468.8	1765.6	536.2	1041.1	853.3	1385.5	1076.1			2060.5	1100.7	971.4	360.6
21/11/2012	203	3485.8	886.3	1253.9	479.3	1780.5	550.2	1053.5	865.1	1401.6	1091.3			2078.7	1117.9	979.9	368.7
22/11/2012	204	3479.0	879.9	1235.7	462.1	1772.5	542.7	1041.8	853.9	1386.3	1076.9			2060.6	1100.8	966.0	355.4
23/11/2012	205	3473.0	874.1	1231.0	457.6	1767.7	538.2	1038.8	851.1	1382.4	1073.2			2063.1	1103.2	962.3	352.0
24/11/2012	206	3485.8	886.3	1260.4	485.4	1780.3	550.0	1058.3	869.6	1407.8	1097.2			2083.1	1122.1	984.9	373.4
25/11/2012	207	3505.6	905.1	1288.7	512.2	1793.8	562.9	1071.8	882.4	1425.4	1113.9			2099.1	1137.3	1006.7	394.0
26/11/2012	208	3477.3	878.2	1248.7	474.3	1777.9	547.8	1041.2	853.4	1385.6	1076.2			2060.1	1100.3	975.9	364.9
27/11/2012	209	3496.5	896.4	1260.8	485.8	1795.1	564.1	1055.2	866.6	1403.7	1093.4			2070.2	1109.9	985.3	373.7
28/11/2012	210	3500.4	900.2	1266.7	491.4	1792.9	562.1	1056.8	868.2	1405.8	1095.4			2073.4	1112.9	989.8	378.0
29/11/2012	211	3490.5	890.8	1249.1	474.7	1774.5	544.6	1039.8	852.1	1383.8	1074.4			2059.8	1100.0	976.2	365.1
30/11/2012	212	3496.6	896.5	1243.6	469.5	1774.2	544.3	1035.0	847.5	1377.5	1068.5			2054.3	1094.8	972.0	361.1
1/12/2012	213	3529.2	927.4	1278.4	502.5	1794.8	563.9	1061.7	872.8	1412.2	1101.4			2084.7	1123.6	998.8	386.5
2/12/2012	214	3532.0	930.1	1279.6	503.6	1794.0	563.1	1057.9	869.2	1407.3	1096.7			2086.9	1125.7	999.7	387.4
3/12/2012	215	3505.9	905.4	1236.3	462.6	1767.3	537.8	1029.1	842.0	1369.9	1061.3			2056.5	1096.9	966.4	355.8
4/12/2012	216	3484.1	884.7	1206.2	434.0	1740.2	512.1	1009.1	823.0	1343.8	1036.6			2037.4	1078.7	943.2	333.9
5/12/2012	217	3508.3	907.6	1218.4	445.6	1761.8	532.6	1025.9	838.9	1365.7	1057.3			2056.4	1096.8	952.6	342.8
6/12/2012	218	3516.2	915.2	1231.1	457.7	1768.6	539.0	1033.7	846.3	1375.8	1066.9			2068.3	1108.1	962.4	352.1
7/12/2012	219	3503.1	902.7	1226.0	452.8	1764.4	535.0	1022.0	835.2	1360.6	1052.4			2060.9	1101.1	958.5	348.3
8/12/2012	220	3507.9	907.3	1226.8	453.5	1769.2	539.6	1026.5	839.4	1366.4	1058.0			2064.6	1104.6	959.0	348.9
9/12/2012	221	3519.9	918.6	1241.6	467.6	1780.2	550.0	1038.8	851.1	1382.4	1073.2			2068.9	1108.6	970.5	359.7
10/12/2012	222	3493.4	893.5	1212.3	439.8	1751.9	523.2	1015.2	828.7	1351.7	1044.1			2041.9	1083.1	947.9	338.3
11/12/2012	223	3499.3	899.1	1218.4	445.7	1749.7	521.1	1013.6	827.3	1349.7	1042.2			2043.2	1084.2	952.7	342.8
12/12/2012	224	3514.2	913.2	1234.9	461.3	1767.1	537.6	1023.3	836.5	1362.3	1054.1			2054.7	1095.2	965.3	354.8
13/12/2012	225	3495.0	895.0	1217.2	444.5	1749.0	520.4	1009.5	823.3	1344.3	1037.1			2036.6	1078.0	951.7	341.9
14/12/2012	226	3498.6	898.4	1207.7	435.4	1753.1	524.3	1007.1	821.0	1341.2	1034.1			2032.1	1073.7	944.4	335.0
15/12/2012	227	3496.0	896.0	1207.8	435.6	1752.5	523.7	1006.6	820.6	1340.6	1033.6			2042.9	1084.0	944.5	335.1
28/12/2012	240	3492.1	892.3	1205.9	433.7	1746.1	517.7	1006.4	820.4	1340.3	1033.2			2038.1	1079.5	943.0	333.6

Table E.8 Concrete surface strain at steel level for slab DS-SCC-b

Slab DS-SCC-b		CONCRETE SURFACE STRAIN BY SG															
		1		2		3		4		5		6		7		8	
Date	Age	Reading	Strain	Reading	Strain	Reading	Strain	Reading	Strain	Reading	Strain	Reading	Strain	Reading	Strain	Reading	Strain
16/05/2012	14	958.2		6447.2		776.4		934.4		578.6		1689.7		-537.9		296.9	
16/05/2012	14	302.2		1152.4		916.6		1166.5		700.2		1008.1		105.2		105.8	
17/05/2012	15	523.2	209.4	1731.6	549.0	1110.0	183.3	1459.1	277.4	1019.6	302.8	1130.8	116.3	588.1	457.7	224.3	112.3
18/05/2012	16	535.0	220.6	1769.4	584.8	1148.9	220.2	1501.0	317.0	1056.7	337.9	1146.9	131.5	571.9	442.4	241.7	128.8
19/05/2012	17	536.8	222.4	1757.1	573.2	1160.3	230.9	1522.5	337.5	1092.6	371.9	1142.6	127.5	576.6	446.9	272.1	157.7
20/05/2012	18	547.5	232.5	1752.1	568.4	1164.5	235.0	1547.5	361.2	1117.6	395.6	1151.1	135.5	573.7	444.1	252.0	138.6
21/05/2012	19	572.7	256.4	1742.3	559.2	1158.7	229.4	1560.5	373.4	1097.6	376.7	1155.1	139.3	572.9	443.3	235.4	122.9
22/05/2012	20	596.8	279.2	1752.3	568.6	1167.9	238.2	1582.7	394.6	1147.1	423.6	1238.3	218.2	568.0	438.7	223.3	111.4
23/05/2012	21	599.5	281.7	1772.4	587.6	1184.2	253.6	1604.2	414.9	1178.9	453.8	1227.8	208.2	559.3	430.4	216.5	105.0
24/05/2012	22	577.0	260.5	1760.5	576.4	1189.4	258.5	1611.5	421.8	1184.4	459.0	1234.2	214.3	570.5	441.1	229.2	117.0
25/05/2012	23	582.1	265.2	1754.9	571.1	1217.6	285.3	1620.6	430.5	1174.2	449.3	1247.5	226.9	569.5	440.1	239.1	126.4
26/05/2012	24	590.8	273.5	1780.8	595.7	1226.1	293.3	1641.2	449.9	1220.0	492.8	1216.3	197.3	577.4	447.6	231.0	118.7
27/05/2012	25	583.0	266.2	1803.3	616.9	1235.1	301.8	1651.7	459.9	1226.6	499.0	1204.8	186.4	577.5	447.7	229.6	117.4
28/05/2012	26	570.0	253.8	1832.8	644.9	1250.2	316.1	1668.5	475.8	1258.4	529.2	1247.1	226.5	563.6	434.5	245.9	132.8
29/05/2012	27	585.6	268.6	1811.1	624.3	1254.9	320.7	1666.0	473.5	1234.8	506.8	1229.4	209.7	573.1	443.6	226.6	114.5
30/05/2012	28	558.2	242.6	1824.4	637.0	1264.3	329.6	1678.6	485.4	1272.5	542.5	1241.5	221.2	568.5	439.1	234.8	122.3
31/05/2012	29	534.1	219.8	1823.8	636.4	1262.8	328.2	1686.2	492.6	1250.3	521.4	1242.8	222.4	573.5	443.9	245.3	132.2
1/06/2012	30	541.0	226.3	1822.3	635.0	1268.5	333.5	1690.1	496.3	1258.5	529.2	1239.0	218.8	574.7	445.1	242.1	129.2
2/06/2012	31	551.1	235.9	1812.4	625.5	1269.0	334.0	1691.7	497.9	1266.8	537.1	1223.9	204.5	581.9	451.9	225.9	113.9
3/06/2012	32	543.4	228.6	1806.4	619.9	1275.2	339.9	1698.9	504.6	1297.4	566.1	1210.4	191.7	580.1	450.2	224.2	112.2
4/06/2012	33	540.7	226.0	1808.8	622.1	1278.5	343.0	1701.3	506.9	1304.4	572.8	1191.0	173.3	581.2	451.2	229.6	117.3
5/06/2012	34	542.3	227.6	1846.9	658.3	1295.5	359.2	1727.1	531.4	1330.8	597.8	1173.1	156.4	572.5	442.9	229.4	117.2
6/06/2012	35	551.4	236.2	1827.0	639.4	1287.1	351.1	1724.2	528.6	1299.9	568.5	1156.1	140.3	584.3	454.1	231.4	119.0
7/06/2012	36	550.4	235.2	1843.5	655.1	1298.9	362.3	1738.7	542.4	1345.0	611.2	1153.1	137.4	576.3	446.5	270.1	155.8
8/06/2012	37	553.1	237.8	1871.0	681.1	1314.6	377.2	1753.2	556.1	1403.1	666.3	1153.1	137.4	568.4	439.1	277.9	163.1
9/06/2012	38	543.0	228.3	1866.5	676.9	1315.9	378.4	1757.1	559.8	1390.6	654.4	1152.2	136.6	570.7	441.3	234.9	122.4
10/06/2012	39	542.4	227.7	1869.5	679.7	1319.4	381.8	1760.5	563.1	1364.6	629.7	1152.9	137.2	567.8	438.5	250.9	137.6
11/06/2012	40	547.0	232.0	1845.9	657.4	1312.2	374.9	1747.9	551.1	1330.6	597.6	1147.5	132.1	577.7	447.9	226.1	114.0
12/06/2012	41	551.5	236.3	1836.3	648.2	1349.8	410.6	1740.8	544.4	1301.1	569.6	1144.6	129.4	585.5	455.3	227.5	115.4
13/06/2012	42	558.1	242.5	1846.3	657.7	1491.2	544.6	1754.5	557.3	1348.2	614.3	1194.2	176.3	575.5	445.8	213.5	102.2
14/06/2012	43	561.0	245.2	1841.5	653.1	1492.3	545.7	1756.2	559.0	1359.6	625.0	1281.1	258.8	577.0	447.2	238.3	125.6
15/06/2012	44	554.7	239.3	1832.4	644.5	1485.9	539.6	1748.9	552.0	1348.1	614.1	1246.8	226.3	586.9	456.6	251.8	138.4

16/06/2012	45	542.9	228.2	1837.2	649.1	1490.5	544.0	1753.3	556.2	1368.3	633.3	1230.8	211.0	588.0	457.6	217.4	105.8
17/06/2012	46	537.0	222.5	1828.9	641.2	1494.6	547.8	1761.8	564.3	1387.6	651.6	1212.6	193.8	596.7	465.9	218.5	106.8
18/06/2012	47	527.1	213.1	1853.1	664.1	1502.9	555.7	1774.7	576.5	1402.4	665.6	1187.1	169.6	592.2	461.6	216.8	105.2
19/06/2012	48	505.2	192.4	1867.3	677.6	1511.3	563.6	1785.3	586.6	1408.4	671.3	1166.0	149.7	587.8	457.4	237.4	124.8
20/06/2012	49	499.4	186.8	1863.8	674.3	1514.0	566.2	1788.7	589.8	1411.0	673.8	1142.9	127.8	588.6	458.2	234.2	121.8
21/06/2012	50	510.4	197.3	1877.9	687.7	1521.7	573.5	1797.6	598.2	1445.7	706.7	1131.5	116.9	584.3	454.1	252.3	138.9
22/06/2012	51	529.1	215.0	1862.2	672.8	1513.8	566.1	1792.8	593.7	1401.0	664.3	1107.1	93.8	591.5	461.0	258.1	144.4
23/06/2012	52	516.3	202.9	1868.8	679.1	1523.2	574.9	1799.6	600.1	1432.5	694.1	1097.7	84.9	591.3	460.8	253.7	140.2
24/06/2012	53	499.6	187.0	1873.4	683.4	1528.2	579.7	1805.8	606.0	1461.4	721.5	1095.3	82.6	592.9	462.3	251.8	138.4
25/06/2012	54	489.4	177.4	1877.8	687.5	1531.8	583.1	1812.3	612.2	1462.5	722.6	1098.6	85.8	588.8	458.5	259.2	145.4
26/06/2012	55	486.8	175.0	1860.0	670.7	1523.5	575.2	1804.7	604.9	1428.1	690.0	1116.9	103.1	596.5	465.7	262.9	149.0
27/06/2012	56	499.4	186.9	1850.9	662.1	1522.2	574.0	1801.3	601.7	1431.0	692.8	1157.2	141.3	599.7	468.7	262.7	148.8
28/06/2012	57	498.4	186.0	1849.1	660.4	1522.1	573.9	1804.0	604.3	1432.5	694.1	1145.7	130.4	600.0	469.0	274.3	159.8
29/06/2012	58	490.1	178.1	1843.8	655.3	1517.2	569.3	1799.4	599.9	1424.0	686.1	1137.8	122.9	600.4	469.4	276.2	161.6
30/06/2012	59	488.2	176.3	1833.2	645.3	1514.5	566.7	1795.2	595.9	1412.8	675.4	1130.1	115.6	608.0	476.6	267.1	152.9
1/07/2012	60	507.6	194.7	1841.4	653.1	1520.9	572.7	1802.2	602.5	1421.4	683.6	1110.7	97.2	613.6	481.9	261.1	147.2
2/07/2012	61	510.3	197.2	1876.3	686.2	1539.8	590.7	1823.0	622.3	1477.6	736.9	1111.3	97.7	601.2	470.2	265.0	150.9
3/07/2012	62	514.9	201.6	1867.3	677.6	1538.5	589.5	1824.3	623.5	1475.8	735.2	1105.1	91.9	604.8	473.6	268.7	154.5
4/07/2012	63	514.2	200.9	1868.7	678.9	1540.7	591.5	1831.8	630.6	1469.1	728.8	1102.6	89.5	600.5	469.5	248.9	135.6
5/07/2012	64	498.4	185.9	1858.2	669.0	1552.2	602.5	1826.2	625.3	1454.9	715.4	1099.7	86.8	606.7	475.3	267.0	152.8
6/07/2012	65	482.7	171.0	1845.4	656.9	1548.1	598.5	1818.0	617.6	1460.3	720.5	1096.0	83.3	615.4	483.6	281.8	166.8
7/07/2012	66	472.9	161.8	1852.7	663.8	1555.0	605.1	1822.0	621.3	1467.7	727.5	1093.5	80.9	610.5	479.0	265.0	150.9
8/07/2012	67	484.1	172.3	1834.3	646.3	1546.6	597.1	1812.0	611.9	1462.6	722.7	1088.1	75.8	621.0	489.0	262.4	148.5
9/07/2012	68	481.0	169.4	1850.5	661.7	1560.8	610.6	1821.6	621.0	1489.5	748.2	1100.1	87.2	611.8	480.2	273.7	159.1
10/07/2012	69	462.1	151.5	1843.3	654.9	1559.4	609.2	1820.0	619.5	1495.4	753.8	1102.2	89.2	614.4	482.7	269.1	154.8
11/07/2012	70	483.2	171.5	1806.1	619.6	1545.2	595.9	1805.9	606.1	1475.6	735.0	1092.1	79.6	632.4	499.7	257.2	143.5
12/07/2012	71	503.3	190.6	1834.6	646.6	1554.6	604.7	1814.5	614.2	1474.7	734.2	1090.2	77.8	621.0	488.9	257.3	143.6
13/07/2012	72	475.0	163.7	1819.9	632.7	1553.1	603.3	1803.3	603.6	1455.6	716.0	1086.0	73.8	627.3	494.9	280.2	165.4
14/07/2012	73	472.6	161.5	1810.8	624.1	1551.6	601.9	1795.1	595.9	1425.6	687.6	1068.0	56.8	634.8	502.0	287.3	172.0
15/07/2012	74	471.0	159.9	1828.4	640.8	1560.9	610.6	1812.1	611.9	1455.5	716.0	1056.1	45.5	633.9	501.2	278.6	163.8
16/07/2012	75	477.9	166.6	1869.7	679.9	1579.4	628.2	1837.2	635.7	1490.0	748.7	1058.4	47.6	616.8	484.9	277.8	163.0
17/07/2012	76	486.3	174.5	1856.7	667.6	1573.6	622.7	1834.9	633.5	1469.3	729.0	1059.6	48.7	619.2	487.2	283.9	168.8
18/07/2012	77	487.2	175.3	1848.8	660.1	1571.4	620.7	1833.0	631.7	1459.6	719.8	1046.0	35.9	625.4	493.1	267.3	153.1
19/07/2012	78	477.4	166.0	1863.3	673.8	1581.4	630.1	1840.0	638.4	1479.7	738.8	1059.6	48.8	624.6	492.4	289.9	174.5
20/07/2012	79	471.2	160.1	1877.7	687.5	1595.7	643.7	1849.2	647.1	1498.3	756.5	1128.1	113.7	620.6	488.5	272.5	158.1
21/07/2012	80	461.2	150.6	1861.5	672.1	1587.2	635.6	1843.6	641.8	1470.0	729.7	1111.2	97.7	625.0	492.7	273.6	159.1
22/07/2012	81	466.5	155.7	1853.0	664.1	1584.5	633.1	1837.9	636.4	1455.8	716.3	1100.9	88.0	628.9	496.4	272.6	158.1

23/07/2012	82	477.2	165.8	1843.6	655.2	1580.1	628.9	1831.6	630.4	1456.3	716.7	1091.0	78.6	636.1	503.2	277.1	162.4
24/07/2012	83	488.0	176.1	1826.2	638.7	1581.7	630.4	1826.2	625.3	1439.6	700.9	1082.0	70.0	640.4	507.3	281.5	166.5
25/07/2012	84	504.9	192.1	1829.4	641.7	1587.8	636.2	1827.3	626.3	1473.7	733.2	1092.3	79.8	636.4	503.5	265.1	151.1
26/07/2012	85	496.6	184.3	1832.0	644.1	1579.7	628.5	1827.3	626.4	1474.2	733.6	1087.5	75.2	637.7	504.8	266.9	152.7
27/07/2012	86	494.9	182.6	1854.3	665.3	1599.4	647.1	1840.1	638.5	1476.0	735.4	1087.0	74.8	631.0	498.4	257.8	144.1
28/07/2012	87	485.7	173.9	1870.1	680.3	1609.0	656.3	1850.4	648.3	1492.1	750.7	1098.1	85.3	628.4	496.0	252.3	138.9
29/07/2012	88	485.3	173.5	1859.0	669.7	1607.1	654.5	1852.3	650.1	1478.6	737.9	1130.5	116.0	631.7	499.0	241.2	128.4
30/07/2012	89	495.9	183.6	1871.5	681.6	1619.5	666.2	1859.0	656.4	1494.4	752.8	1124.0	109.8	631.1	498.5	271.6	157.2
31/07/2012	90	500.6	188.0	1864.9	675.4	1621.6	668.2	1861.8	659.0	1479.6	738.8	1117.0	103.2	632.6	499.9	271.9	157.4
1/08/2012	91	507.7	194.7	1871.9	682.0	1629.1	675.3	1869.5	666.3	1486.6	745.4	1111.1	97.6	625.8	493.5	277.3	162.5
2/08/2012	92	510.0	196.9	1876.8	686.6	1633.1	679.1	1873.3	669.9	1481.2	740.3	1102.2	89.2	626.6	494.3	278.5	163.7
3/08/2012	93	493.5	181.3	1877.0	686.8	1631.6	677.7	1873.7	670.3	1482.6	741.6	1095.0	82.4	626.5	494.1	299.5	183.6
4/08/2012	94	493.2	181.0	1877.9	687.7	1633.8	679.7	1880.0	676.3	1471.1	730.7	1087.5	75.2	625.4	493.1	273.5	159.0
5/08/2012	95	500.1	187.6	1872.7	682.8	1628.4	674.7	1881.6	677.8	1476.4	735.7	1078.7	66.8	630.0	497.5	270.7	156.3
6/08/2012	96	485.8	174.0	1880.1	689.8	1631.1	677.2	1882.6	678.8	1483.1	742.1	1073.0	61.5	627.4	495.0	311.1	194.6
7/08/2012	97	472.2	161.1	1904.4	712.8	1643.7	689.2	1890.0	685.8	1508.9	766.5	1074.1	62.6	622.2	490.1	289.6	174.3
8/08/2012	98	474.4	163.2	1889.9	699.0	1642.1	687.6	1889.1	685.0	1495.7	754.0	1072.8	61.3	623.3	491.1	280.0	165.2
9/08/2012	99	495.8	183.5	1888.9	698.1	1638.6	684.3	1890.0	685.8	1479.8	739.0	1072.2	60.8	622.6	490.4	296.0	180.3
10/08/2012	100	500.7	188.1	1883.7	693.1	1641.7	687.3	1884.2	680.2	1477.8	737.1	1065.2	54.1	633.5	500.8	292.4	176.9
11/08/2012	101	482.5	170.8	1862.0	672.6	1632.0	678.1	1873.8	670.4	1457.3	717.6	1092.5	79.9	639.4	506.4	260.9	147.0
12/08/2012	102	489.4	177.4	1853.9	664.9	1626.0	672.4	1866.0	663.0	1439.2	700.5	1091.1	78.6	646.1	512.8	314.2	197.6
13/08/2012	103	464.4	153.7	1868.8	679.0	1634.7	680.7	1874.7	671.3	1481.9	741.0	1101.6	88.6	634.4	501.6	364.8	245.5
14/08/2012	104	453.0	142.9	1879.8	689.5	1641.0	686.6	1880.3	676.6	1512.3	769.8	1333.2	308.2	630.5	498.0	371.5	251.8
15/08/2012	105	457.7	147.3	1887.4	696.7	1642.8	688.4	1886.8	682.7	1484.0	743.0	1352.5	326.4	625.5	493.2	333.1	215.5
16/08/2012	106	468.2	157.3	1888.6	697.8	1643.2	688.7	1886.7	682.7	1488.2	747.0	1367.5	340.6	629.1	496.6	330.2	212.8
17/08/2012	107	476.3	165.0	1882.0	691.6	1638.9	684.6	1881.0	677.3	1488.6	747.3	1376.7	349.3	636.2	503.3	351.2	232.7
18/08/2012	108	475.0	163.7	1897.9	706.7	1649.0	694.2	1890.0	685.8	1492.1	750.6	1416.9	387.5	628.7	496.2	343.3	225.2
19/08/2012	109	476.6	165.3	1886.5	695.9	1650.7	695.8	1890.2	686.0	1493.4	751.8	1438.0	407.5	629.8	497.2	306.3	190.1
20/08/2012	110	483.9	172.2	1893.9	702.8	1663.7	708.2	1894.8	690.3	1517.2	774.4	1430.8	400.7	631.5	498.9	347.7	229.4
21/08/2012	111	469.6	158.6	1872.0	682.1	1661.7	706.2	1890.3	686.1	1488.9	747.6	1428.0	398.0	636.5	503.6	305.9	189.7
22/08/2012	112	480.0	168.5	1874.2	684.2	1662.9	707.4	1886.9	682.8	1470.4	730.1	1438.0	407.5	635.1	502.3	274.6	160.0
23/08/2012	113	470.2	159.2	1870.3	680.5	1672.3	716.2	1878.6	674.9	1485.3	744.2	1518.3	483.6	638.3	505.4	281.1	166.2
24/08/2012	114	489.7	177.7	1854.9	665.9	1672.4	716.4	1877.2	673.7	1470.2	729.8	1504.9	470.9	644.1	510.8	306.7	190.5
25/08/2012	115	489.0	177.0	1867.3	677.6	1674.1	718.0	1889.1	684.9	1420.0	682.3	1488.2	455.0	640.1	507.1	283.1	168.1
26/08/2012	116	483.5	171.8	1875.8	685.7	1679.4	723.0	1891.8	687.5	1457.6	718.0	1477.1	444.5	645.9	512.5	257.3	143.6
27/08/2012	117	480.1	168.6	1894.4	703.3	1693.0	735.9	1900.8	696.0	1494.6	753.0	1482.1	449.2	636.6	503.7	258.2	144.5
28/08/2012	118	467.9	157.0	1882.2	691.7	1692.4	735.4	1897.2	692.6	1464.0	724.0	1484.0	451.1	637.7	504.7	283.1	168.1

29/08/2012	119	474.8	163.5	1867.2	677.5	1693.7	736.6	1889.0	684.8	1452.7	713.3	1478.6	445.9	642.5	509.3	282.6	167.6
30/08/2012	120	497.0	184.6	1873.5	683.5	1697.1	739.8	1893.7	689.3	1457.5	717.9	1477.3	444.7	634.6	501.8	301.7	185.7
31/08/2012	121	509.1	196.1	1885.3	694.7	1701.2	743.7	1901.3	696.5	1498.1	756.4	1460.3	428.5	637.5	504.6	284.8	169.7
1/09/2012	122	490.8	178.7	1911.5	719.5	1717.1	758.8	1913.7	708.3	1535.0	791.3	1463.0	431.2	631.7	499.0	284.0	168.9
2/09/2012	123	476.8	165.5	1884.9	694.3	1710.3	752.3	1903.6	698.6	1501.6	759.7	1458.8	427.2	640.8	507.7	290.0	174.7
3/09/2012	124	488.7	176.8	1903.4	711.8	1715.9	757.6	1909.3	704.0	1515.8	773.1	1465.5	433.5	630.7	498.1	280.9	166.0
4/09/2012	125	478.0	166.6	1894.1	703.0	1709.9	751.9	1906.5	701.4	1507.5	765.2	1463.7	431.8	633.6	500.9	284.5	169.4
5/09/2012	126	476.9	165.6	1889.3	698.5	1708.2	750.3	1910.2	705.0	1528.8	785.4	1462.0	430.2	636.5	503.6	284.9	169.8
6/09/2012	127	483.5	171.8	1900.0	708.7	1718.1	759.7	1920.0	714.2	1540.0	796.1	1463.1	431.2	630.1	497.6	274.1	159.6
7/09/2012	128	493.3	181.1	1906.2	714.5	1725.4	766.6	1926.7	720.5	1529.0	785.7	1456.4	424.9	629.1	496.6	273.3	158.8
8/09/2012	129	496.9	184.5	1897.4	706.2	1725.1	766.3	1924.7	718.7	1512.2	769.7	1447.5	416.4	633.8	501.1	277.4	162.7
9/09/2012	130	508.4	195.4	1885.1	694.5	1723.9	765.2	1917.8	712.1	1499.1	757.3	1449.8	418.6	639.2	506.2	280.5	165.7
10/09/2012	131	501.6	189.0	1885.6	695.0	1729.9	770.9	1915.6	710.0	1511.9	769.4	1456.5	425.0	637.3	504.4	278.3	163.5
11/09/2012	132	491.2	179.1	1892.8	701.7	1736.7	777.3	1914.5	709.0	1528.4	785.0	1448.3	417.2	635.2	502.4	290.5	175.1
12/09/2012	133	484.9	173.1	1868.2	678.5	1733.7	774.5	1904.3	699.3	1496.9	755.2	1429.5	399.4	640.0	507.0	289.3	174.0
13/09/2012	134	484.4	172.7	1874.6	684.6	1744.7	784.9	1902.2	697.3	1502.4	760.4	1430.7	400.6	632.1	499.5	290.3	174.9
14/09/2012	135	493.0	180.8	1891.3	700.4	1752.2	792.0	1911.2	705.9	1541.6	797.6	1429.4	399.4	626.3	493.9	283.6	168.5
15/09/2012	136	502.4	189.8	1888.1	697.3	1744.5	784.7	1913.2	707.8	1492.9	751.4	1416.2	386.8	635.4	502.6	293.4	177.8
16/09/2012	137	506.0	193.1	1873.3	683.3	1744.6	784.8	1900.5	695.7	1490.1	748.7	1402.9	374.2	645.5	512.2	297.3	181.5
17/09/2012	138	496.9	184.5	1873.2	683.2	1756.1	795.7	1899.6	694.9	1518.2	775.3	1425.2	395.4	641.4	508.3	296.0	180.3
18/09/2012	139	500.9	188.3	1871.0	681.2	1762.4	801.7	1899.0	694.3	1527.5	784.2	1441.0	410.3	638.6	505.6	288.9	173.6
19/09/2012	140	510.8	197.7	1872.2	682.3	1763.8	803.0	1895.8	691.3	1531.6	788.1	1447.4	416.3	640.8	507.7	267.3	153.1
20/09/2012	141	513.1	199.9	1881.8	691.3	1766.4	805.5	1894.9	690.5	1529.2	785.9	1448.5	417.4	635.6	502.8	280.0	165.2
21/09/2012	142	509.7	196.7	1881.6	691.2	1775.4	814.0	1893.6	689.2	1550.3	805.8	1464.0	432.1	634.2	501.4	300.9	184.9
22/09/2012	143	511.4	198.3	1888.4	697.7	1780.9	819.2	1896.3	691.8	1560.9	815.9	1465.0	433.0	631.2	498.6	313.7	197.1
23/09/2012	144	509.7	196.7	1881.1	690.7	1782.5	820.8	1890.9	686.6	1531.9	788.4	1458.4	426.8	635.5	502.7	313.9	197.3
24/09/2012	145	511.7	198.6	1888.9	698.1	1786.8	824.8	1895.6	691.1	1545.2	801.0	1448.8	417.7	637.8	504.8	317.3	200.5
25/09/2012	146	508.7	195.7	1891.9	700.9	1786.7	824.7	1902.7	697.8	1562.5	817.4	1443.3	412.5	639.1	506.1	309.2	192.8
26/09/2012	147	520.0	206.4	1882.3	691.9	1787.6	825.6	1898.3	693.7	1542.3	798.2	1445.2	414.3	645.2	511.9	308.3	192.0
27/09/2012	148	526.1	212.2	1877.8	687.6	1788.8	826.7	1893.9	689.4	1554.6	809.9	1449.9	418.7	647.0	513.6	319.2	202.3
28/09/2012	149	526.2	212.3	1873.6	683.6	1786.8	824.8	1887.5	683.5	1538.2	794.3	1452.3	421.0	644.6	511.3	318.2	201.4
29/09/2012	150	532.5	218.2	1870.2	680.4	1791.3	829.0	1886.2	682.2	1538.1	794.3	1455.6	424.1	644.2	510.9	317.6	200.8
30/09/2012	151	522.7	209.0	1890.5	699.7	1793.7	831.4	1893.8	689.4	1531.1	787.6	1435.1	404.7	646.0	512.6	318.8	201.9
1/10/2012	152	517.9	204.4	1899.2	707.9	1796.9	834.4	1906.4	701.3	1551.0	806.4	1433.1	402.8	646.1	512.8	309.2	192.8
2/10/2012	153	520.1	206.5	1876.5	686.3	1788.3	826.3	1894.0	689.6	1544.7	800.5	1427.5	397.5	661.6	527.4	311.4	194.9
3/10/2012	154	522.9	209.2	1887.6	696.8	1787.4	825.4	1890.1	685.9	1545.7	801.4	1430.7	400.6	656.3	522.4	305.8	189.6
4/10/2012	155	528.6	214.5	1886.0	695.4	1789.2	827.1	1892.9	688.5	1558.2	813.3	1432.2	402.0	655.5	521.6	316.0	199.2

5/10/2012	156	524.4	210.6	1898.4	707.1	1802.6	839.7	1909.1	703.9	1573.9	828.2	1443.0	412.2	643.3	510.0	310.0	193.6
6/10/2012	157	524.6	210.7	1881.9	691.4	1787.5	825.5	1899.7	695.0	1572.2	826.5	1446.2	415.3	653.6	519.8	300.9	185.0
7/10/2012	158	533.5	219.2	1868.2	678.5	1770.1	809.0	1886.1	682.1	1551.2	806.7	1434.5	404.1	662.9	528.6	305.4	189.3
8/10/2012	159	540.2	225.5	1890.0	699.2	1769.8	808.7	1899.8	695.1	1552.4	807.8	1439.3	408.6	651.9	518.2	298.2	182.4
9/10/2012	160	530.9	216.7	1887.1	696.4	1771.1	809.9	1895.4	690.9	1554.6	809.8	1435.4	405.0	655.7	521.8	302.8	186.8
10/10/2012	161	545.6	230.7	1904.0	712.4	1787.9	825.9	1901.1	696.3	1566.2	820.9	1442.3	411.5	647.2	513.8	312.4	195.9
11/10/2012	162	551.9	236.7	1884.9	694.3	1781.2	819.5	1898.4	693.7	1565.7	820.4	1436.3	405.8	658.9	524.9	315.6	198.9
12/10/2012	163	548.6	233.6	1937.1	743.8	1813.9	850.5	1924.0	718.0	1603.5	856.2	1448.3	417.2	629.0	496.6	333.0	215.4
13/10/2012	164	545.2	230.3	1929.5	736.6	1812.2	848.9	1925.1	719.0	1604.0	856.7	1445.2	414.3	632.3	499.7	323.4	206.3
14/10/2012	165	557.6	242.1	1910.2	718.3	1794.9	832.5	1905.0	700.0	1588.5	842.1	1431.4	401.2	649.0	515.5	320.4	203.4
15/10/2012	166	552.4	237.2	1912.9	720.9	1794.1	831.7	1890.0	685.8	1589.6	843.1	1437.4	406.9	647.2	513.8	331.2	213.6
16/10/2012	167	540.5	225.8	1906.6	714.8	1788.0	825.9	1891.5	687.2	1591.0	844.3	1440.0	409.4	651.2	517.5	335.1	217.4
17/10/2012	168	546.8	231.8	1888.7	697.9	1791.3	829.1	1889.1	685.0	1586.5	840.1	1439.3	408.7	658.9	524.8	300.3	184.4
18/10/2012	169	543.0	228.3	1895.2	704.0	1793.1	830.8	1893.5	689.1	1588.2	841.7	1444.5	413.6	655.5	521.7	300.4	184.5
19/10/2012	170	542.1	227.4	1884.1	693.6	1795.5	833.0	1898.5	693.8	1589.0	842.5	1457.7	426.1	649.8	516.3	323.9	206.7
20/10/2012	171	546.8	231.9	1883.6	693.0	1801.7	839.0	1905.4	700.4	1579.6	833.6	1460.6	428.9	640.4	507.3	337.4	219.6
21/10/2012	172	548.9	233.8	1868.8	679.1	1800.7	838.0	1896.7	692.2	1564.6	819.4	1455.5	424.1	643.4	510.1	325.6	208.4
22/10/2012	173	558.4	242.8	1865.5	675.9	1799.1	836.5	1894.6	690.1	1558.8	813.9	1458.2	426.6	646.5	513.1	353.1	234.4
23/10/2012	174	554.3	238.9	1899.7	708.3	1804.6	841.7	1913.6	708.2	1597.0	850.1	1456.6	425.1	634.6	501.8	354.4	235.6
24/10/2012	175	568.9	252.7	1892.0	701.0	1798.4	835.8	1909.2	703.9	1578.7	832.7	1450.4	419.3	644.1	510.8	333.9	216.2
25/10/2012	176	572.8	256.4	1880.6	690.2	1795.9	833.4	1899.6	694.8	1572.9	827.2	1741.6	695.3	647.7	514.2	351.0	232.5
26/10/2012	177	569.7	253.5	1876.1	686.0	1801.7	838.9	1898.0	693.4	1577.5	831.6	1891.2	837.1	644.8	511.5	347.8	229.4
27/10/2012	178	573.5	257.1	1884.8	694.2	1807.1	844.0	1898.9	694.2	1576.8	830.9	1887.2	833.3	642.9	509.7	361.5	242.4
28/10/2012	179	566.9	250.9	1884.2	693.6	1799.9	837.2	1897.9	693.3	1573.6	827.9	1877.5	824.0	650.5	516.9	372.3	252.6
29/10/2012	180	573.2	256.8	1893.5	702.5	1809.1	845.9	1899.8	695.0	1575.9	830.1	1901.4	846.7	646.5	513.1	371.5	251.9
30/10/2012	181	570.4	254.1	1896.0	704.9	1807.0	843.9	1898.4	693.8	1574.3	828.6	1908.6	853.6	643.1	509.9	377.3	257.4
31/10/2012	182	571.5	255.2	1885.3	694.7	1823.5	859.6	1904.5	699.5	1587.5	841.1	1933.5	877.1	637.6	504.6	352.6	234.0
1/11/2012	183	575.7	259.2	1902.1	710.6	1834.6	870.1	1922.2	716.3	1606.3	858.9	1938.6	882.0	624.9	492.6	361.2	242.1
2/11/2012	184	587.3	270.2	1895.3	704.2	1826.9	862.8	1921.4	715.5	1603.1	855.9	1918.9	863.2	637.2	504.3	375.6	255.8
3/11/2012	185	583.6	266.7	1878.8	688.5	1817.5	853.9	1916.7	711.1	1590.0	843.4	1912.8	857.5	648.9	515.4	384.0	263.8
4/11/2012	186	589.8	272.6	1870.6	680.7	1818.7	855.0	1913.6	708.2	1573.0	827.3	1909.7	854.5	652.3	518.6	386.8	266.4
5/11/2012	187	590.7	273.5	1882.4	691.9	1831.2	866.9	1916.0	710.4	1574.0	828.3	1922.7	866.9	637.1	504.2	382.6	262.4
6/11/2012	188	597.2	279.5	1869.3	679.5	1832.9	868.5	1915.5	709.9	1576.3	830.4	1931.9	875.7	636.3	503.5	401.4	280.2
7/11/2012	189	608.7	290.5	1866.8	677.1	1836.6	872.0	1915.1	709.5	1579.6	833.6	1941.6	884.8	631.4	498.8	393.6	272.9
8/11/2012	190	609.5	291.2	1873.0	683.0	1842.0	877.1	1916.6	711.0	1587.1	840.7	1949.5	892.3	621.1	489.0	395.2	274.3
9/11/2012	191	616.5	297.8	1862.7	673.2	1842.5	877.6	1909.6	704.4	1589.1	842.5	1946.8	889.7	622.9	490.7	386.7	266.3
10/11/2012	192	616.4	297.8	1867.3	677.6	1848.2	883.0	1912.7	707.3	1591.0	844.4	1940.2	883.5	623.1	490.9	412.6	290.8

11/11/2012	193	604.0	286.0	1876.6	686.4	1852.9	887.5	1919.1	713.3	1594.3	847.5	1931.5	875.2	623.7	491.5	406.8	285.3
12/11/2012	194	604.7	286.7	1892.6	701.6	1857.5	891.8	1928.5	722.3	1609.6	862.0	1927.8	871.7	618.5	486.6	411.2	289.5
13/11/2012	195	604.9	286.9	1882.8	692.3	1853.8	888.3	1925.3	719.2	1603.7	856.5	1924.9	869.0	626.0	493.7	403.7	282.4
14/11/2012	196	593.3	275.9	1881.4	691.0	1856.0	890.4	1925.5	719.5	1603.6	856.3	1930.8	874.6	625.8	493.5	403.6	282.3
15/11/2012	197	600.9	283.1	1896.1	704.9	1860.3	894.5	1927.9	721.7	1606.1	858.7	1941.2	884.5	614.8	483.0	416.1	294.2
16/11/2012	198	600.6	282.8	1870.1	680.3	1855.3	889.8	1911.6	706.2	1593.9	847.1	1952.2	894.9	629.0	496.5	415.4	293.5
17/11/2012	199	601.6	283.8	1873.1	683.1	1856.6	890.9	1918.8	713.1	1600.6	853.5	1951.2	893.9	626.8	494.4	441.2	318.0
18/11/2012	200	617.9	299.2	1866.5	676.9	1853.4	887.9	1916.3	710.7	1595.7	848.8	1940.2	883.5	633.0	500.3	445.9	322.4
19/11/2012	201	628.9	309.6	1874.1	684.1	1857.8	892.1	1918.5	712.8	1599.7	852.7	1935.8	879.3	632.5	499.8	423.1	300.8
20/11/2012	202	638.8	319.0	1894.3	703.2	1865.8	899.7	1931.6	725.2	1608.4	860.9	1940.5	883.8	619.2	487.2	444.0	320.6
21/11/2012	203	639.4	319.6	1910.8	718.9	1874.6	908.0	1940.0	733.2	1621.2	873.0	1965.7	907.7	608.6	477.2	471.9	347.0
22/11/2012	204	643.3	323.3	1883.6	693.1	1865.7	899.6	1929.2	722.9	1609.0	861.5	1984.1	925.1	627.1	494.7	472.4	347.5
23/11/2012	205	648.9	328.6	1876.5	686.3	1864.6	898.6	1928.6	722.4	1605.9	858.5	1975.2	916.7	630.9	498.3	475.6	350.6
24/11/2012	206	663.1	342.1	1920.6	728.1	1883.0	916.0	1947.5	740.3	1626.2	877.8	1991.6	932.2	603.7	472.5	468.4	343.7
25/11/2012	207	662.8	341.8	1963.0	768.4	1898.0	930.2	1958.7	750.9	1640.3	891.1	2001.7	941.8	576.3	446.6	458.4	334.2
26/11/2012	208	677.7	355.9	1903.1	711.5	1883.3	916.3	1933.4	727.0	1608.5	861.0	1995.1	935.5	606.6	475.3	477.9	352.8
27/11/2012	209	677.6	355.7	1921.3	728.8	1895.0	927.4	1938.0	731.3	1623.0	874.7	2003.0	943.0	586.1	455.9	477.6	352.5
28/11/2012	210	691.6	369.1	1930.1	737.1	1901.7	933.7	1940.6	733.7	1624.7	876.3	2002.3	942.4	578.2	448.4	488.9	363.2
29/11/2012	211	718.3	394.4	1903.6	712.0	1897.7	930.0	1930.1	723.8	1607.0	859.6	1998.8	939.0	589.6	459.2	483.0	357.6
30/11/2012	212	728.0	403.6	1895.4	704.2	1898.8	931.0	1925.9	719.8	1602.0	854.8	2000.7	940.8	594.1	463.4	499.3	373.0
1/12/2012	213	752.2	426.5	1947.6	753.7	1923.8	954.7	1943.2	736.2	1629.8	881.1	2006.4	946.2	561.1	432.2	508.8	382.0
2/12/2012	214	769.7	443.1	1949.4	755.4	1928.5	959.1	1942.0	735.1	1625.8	877.4	2001.0	941.1	560.2	431.3	534.4	406.3
3/12/2012	215	785.4	458.0	1884.4	693.9	1911.3	942.8	1919.4	713.6	1595.9	849.0	1990.5	931.1	593.3	462.6	529.2	401.4
4/12/2012	216	807.7	479.1	1839.3	651.1	1900.1	932.2	1902.7	697.8	1575.1	829.3	1969.4	911.1	625.6	493.3	548.1	419.2
5/12/2012	217	839.2	508.9	1857.6	668.4	1910.4	941.9	1916.7	711.1	1592.5	845.8	1954.2	896.8	631.4	498.8	533.1	405.1
6/12/2012	218	881.2	548.8	1876.7	686.5	1926.5	957.2	1928.1	721.9	1600.7	853.6	1945.4	888.4	628.2	495.7	533.7	405.6
7/12/2012	219	921.6	587.1	1869.0	679.3	1924.8	955.6	1928.3	722.1	1588.4	842.0	1939.2	882.6	637.4	504.5	574.6	444.3
8/12/2012	220	957.2	620.9	1870.1	680.3	1932.5	962.9	1929.4	723.1	1593.1	846.4	1953.4	896.0	632.3	499.6	588.4	457.5
9/12/2012	221	962.1	625.5	1892.5	701.5	1944.1	973.9	1934.6	728.0	1605.9	858.5	1977.9	919.2	610.3	478.8	630.9	497.7
10/12/2012	222	970.2	633.1	1848.4	659.7	1928.1	958.8	1917.8	712.1	1581.4	835.3	1959.0	901.3	634.9	502.1	649.7	515.5
11/12/2012	223	981.6	643.9	1857.7	668.5	1931.0	961.5	1920.5	714.7	1579.8	833.7	1950.3	893.1	634.0	501.3	650.8	516.7
12/12/2012	224	983.1	645.4	1882.4	691.9	1943.3	973.1	1925.4	719.3	1589.9	843.3	1971.9	913.5	619.9	487.9	677.7	542.2
13/12/2012	225	993.5	655.3	1855.8	666.7	1934.7	965.0	1916.5	710.9	1575.5	829.7	1972.2	913.8	632.7	500.0	687.0	550.9
14/12/2012	226	990.1	652.0	1841.5	653.2	1931.7	962.2	1910.7	705.4	1572.9	827.3	1990.2	930.9	641.1	508.0	707.1	570.0
15/12/2012	227	995.2	656.8	1841.7	653.3	1933.9	964.3	1910.6	705.3	1572.5	826.9	1983.4	924.4	640.3	507.2	718.0	580.3
28/12/2012	240	1000.4	661.8	1838.8	650.6	1933.9	964.3	1909.1	703.8	1572.2	826.6	1987.4	928.3	636.3	503.5	719.8	582.0

Table E.9 Steel strain for slab N-SCC-a

Slab N-SCC-a		STEEL STRAIN BY SG															
		1		2		3		4		5		6		7		8	
Date	Age	Reading	Strain	Reading	Strain	Reading	Strain	Reading	Strain	Reading	Strain	Reading	Strain	Reading	Strain	Reading	Strain
21/03/2012	14	-1173.3		-1400.2		-1373.4		-1523.7		-261.0		-638.1		-1098.1		-1864.7	
21/03/2012	14	-905.2		-1047.5		-1034.2		-1249.4		-465.4		-1396.2		-861.2		-1613.4	
22/03/2012	15	-904.7	0.5	-1030.7	15.9	-1021.7	11.9	-1240.3	8.6	-459.8	5.3	-1379.3	16.0	-841.8	18.4	-1610.5	2.8
23/03/2012	16	-850.3	52.0	-1005.8	39.5	-1010.7	22.2	-1201.8	45.1	-454.8	10.0	-1364.5	30.0	-801.7	56.4	-1586.0	26.0
24/03/2012	17	-785.4	113.6	-918.2	122.5	-917.8	110.3	-1104.3	137.5	-413.0	49.6	-1239.1	148.9	-758.1	97.7	-1502.7	105.0
25/03/2012	18	-774.6	123.8	-898.4	141.3	-904.5	122.9	-1087.3	153.7	-407.0	55.3	-1221.1	165.9	-738.7	116.1	-1489.6	117.4
26/03/2012	19	-763.9	133.9	-894.0	145.5	-897.4	129.6	-1077.3	163.1	-403.8	58.3	-1211.5	175.0	-715.6	138.0	-1481.6	125.0
27/03/2012	20	-800.6	99.2	-915.7	124.9	-934.1	94.9	-1110.6	131.5	-420.3	42.7	-1261.0	128.1	-758.5	97.4	-1520.8	87.8
28/03/2012	21	-817.1	83.5	-933.8	107.8	-949.7	80.1	-1125.3	117.7	-427.4	36.0	-1282.1	108.1	-774.9	81.8	-1537.3	72.1
29/03/2012	22	-845.1	57.0	-960.3	82.6	-977.0	54.2	-1151.7	92.6	-439.7	24.4	-1319.0	73.2	-801.5	56.6	-1568.0	43.1
30/03/2012	23	-811.6	88.7	-955.4	87.2	-965.1	65.5	-1306.5	-54.2	-434.3	29.5	-1302.9	88.4	-798.4	59.6	-1556.3	54.1
31/03/2012	24	-802.5	97.4	-932.7	108.8	-953.2	76.8	-1466.9	-206.2	-428.9	34.5	-1286.8	103.6	-783.5	73.7	-1540.8	68.8
1/04/2012	25	-793.0	106.3	-920.4	120.5	-934.0	95.0	-1476.8	-215.6	-420.3	42.7	-1260.9	128.2	-764.0	92.1	-1529.6	79.4
2/04/2012	26	-784.2	114.7	-907.2	133.0	-925.0	103.5	-1532.5	-268.3	-416.2	46.6	-1248.7	139.7	-754.9	100.7	-1514.2	94.1
3/04/2012	27	-773.7	124.7	-893.3	146.1	-910.9	116.8	-1300.6	-48.5	-409.9	52.6	-1229.8	157.7	-746.3	109.0	-1502.3	105.4
4/04/2012	28	-763.2	134.6	-883.0	155.9	-900.5	126.7	-1073.6	166.6	-405.2	57.0	-1215.7	171.1	-729.3	125.0	-1491.4	115.6
5/04/2012	29	-787.2	111.8	-906.3	133.8	-926.1	102.5	-1096.7	144.7	-416.7	46.1	-1250.2	138.4	-750.8	104.7	-1514.1	94.2
6/04/2012	30	-804.4	95.5	-921.5	119.4	-944.9	84.6	-1111.1	131.1	-425.2	38.1	-1275.6	114.3	-766.4	89.8	-1530.8	78.3
7/04/2012	31	-798.6	101.0	-913.6	126.9	-939.5	89.8	-1105.7	136.2	-422.8	40.4	-1268.3	121.2	-759.0	96.9	-1527.0	81.9
8/04/2012	32	-802.1	97.7	-917.5	123.2	-942.8	86.6	-1107.5	134.5	-424.3	39.0	-1272.8	116.9	-763.1	93.0	-1529.9	79.2
9/04/2012	33	-805.9	94.1	-918.3	122.4	-948.8	81.0	-1110.5	131.7	-427.0	36.4	-1280.9	109.3	-767.1	89.2	-1535.6	73.8
10/04/2012	34	-768.2	129.8	-874.1	164.3	-914.0	113.9	-1073.3	166.9	-411.3	51.3	-1233.9	153.8	-732.8	121.7	-1502.8	104.9
11/04/2012	35	-756.6	140.8	-862.1	175.7	-900.2	127.0	-1062.0	177.7	-405.1	57.2	-1215.3	171.5	-719.1	134.7	-1488.5	118.4
12/04/2012	36	-748.4	148.6	-854.3	183.1	-891.6	135.2	-1054.2	185.0	-401.2	60.8	-1203.7	182.5	-710.0	143.3	-1482.1	124.5
13/04/2012	37	-755.9	141.5	-862.1	175.7	-900.2	127.0	-1061.2	178.4	-405.1	57.1	-1215.3	171.4	-716.8	136.9	-1490.2	116.8
16/04/2012	40	-758.4	139.2	-844.8	192.1	-880.3	145.9	-1040.7	197.8	-396.1	65.6	-1188.4	196.9	-700.7	152.2	-1469.1	136.8
17/04/2012	41	-805.7	94.3	-889.1	150.1	-927.5	101.1	-1086.6	154.3	-417.4	45.5	-1252.2	136.5	-743.8	111.3	-1516.5	91.9
18/04/2012	42	-806.5	93.6	-890.2	149.1	-929.8	99.0	-1088.7	152.3	-418.4	44.5	-1255.2	133.6	-744.5	110.6	-1518.7	89.8
19/04/2012	43	-801.2	98.6	-883.1	155.8	-923.2	105.2	-1083.5	157.3	-415.5	47.3	-1246.4	142.0	-736.6	118.1	-1512.8	95.3
20/04/2012	44	-802.7	97.1	-888.5	150.6	-929.2	99.6	-1089.4	151.7	-418.1	44.8	-1254.4	134.4	-741.7	113.2	-1517.8	90.6
21/04/2012	45	-829.0	72.2	-914.2	126.3	-954.3	75.8	-1113.4	128.9	-429.4	34.1	-1288.3	102.3	-766.1	90.2	-1543.5	66.3
22/04/2012	46	-845.2	56.9	-924.9	116.2	-965.5	65.1	-1124.0	118.8	-434.5	29.3	-1303.5	87.9	-777.3	79.5	-1553.9	56.4

23/04/2012	47	-842.6	59.3	-919.4	121.4	-960.7	69.7	-1118.7	123.9	-432.3	31.4	-1296.9	94.1	-772.1	84.5	-1549.0	61.1
24/04/2012	48	-826.7	74.4	-899.9	139.9	-941.9	87.5	-1097.0	144.5	-423.9	39.4	-1271.6	118.1	-753.1	102.5	-1529.2	79.9
25/04/2012	49	-849.1	53.1	-925.2	115.9	-964.5	66.1	-1111.2	131.0	-434.0	29.7	-1302.1	89.2	-777.5	79.3	-1552.9	57.3
26/04/2012	50	-833.3	68.1	-899.9	139.8	-938.0	91.2	-1087.3	153.7	-422.1	41.0	-1266.3	123.1	-756.7	99.1	-1529.1	79.9
27/04/2012	51	-798.4	101.2	-872.5	165.9	-909.7	118.0	-1058.4	181.0	-409.4	53.1	-1228.1	159.3	-723.9	130.2	-1502.1	105.5
28/04/2012	52	-794.6	104.8	-874.2	164.2	-911.7	116.1	-1061.0	178.5	-410.3	52.2	-1230.8	156.7	-726.2	128.0	-1505.0	102.8
29/04/2012	53	-787.4	111.6	-878.9	159.8	-916.8	111.2	-1066.4	173.4	-412.6	50.1	-1237.7	150.2	-731.1	123.3	-1508.8	99.2
30/04/2012	54	-780.1	118.5	-876.1	162.4	-914.1	113.9	-1061.9	177.7	-411.3	51.2	-1234.0	153.7	-728.8	125.5	-1506.1	101.8
1/05/2012	55	-774.0	124.4	-878.5	160.2	-917.1	111.0	-1065.4	174.4	-412.7	50.0	-1238.1	149.9	-732.1	122.3	-1509.7	98.3
2/05/2012	56	-771.1	127.1	-873.9	164.5	-914.0	113.9	-1061.3	178.3	-411.3	51.3	-1233.9	153.8	-727.1	127.1	-1506.4	101.4
3/05/2012	57	-778.4	120.1	-871.8	166.5	-912.9	115.0	-1060.0	179.5	-410.8	51.7	-1232.4	155.2	-726.4	127.8	-1505.5	102.3
4/05/2012	58	-783.5	115.4	-874.8	163.7	-916.3	111.7	-1061.1	178.5	-412.3	50.3	-1237.0	150.8	-730.4	124.0	-1508.9	99.1
5/05/2012	59	-792.6	106.7	-880.9	157.9	-923.7	104.8	-1063.8	176.0	-415.7	47.1	-1247.0	141.4	-736.4	118.3	-1515.8	92.5
6/05/2012	60	-797.1	102.4	-884.6	154.4	-927.5	101.2	-1065.8	174.0	-417.4	45.5	-1252.1	136.6	-740.6	114.3	-1517.9	90.5
7/05/2012	61	-786.3	112.7	-870.6	167.6	-914.8	113.2	-1051.9	187.2	-411.6	50.9	-1234.9	152.8	-728.4	125.9	-1502.9	104.8
8/05/2012	62	-759.6	138.0	-859.2	178.4	-902.8	124.5	-1041.6	197.0	-406.3	56.0	-1218.8	168.1	-719.7	134.1	-1491.4	115.7
9/05/2012	63	-683.7	210.0	-858.3	179.3	-898.8	128.3	-1040.9	197.7	-404.5	57.7	-1213.4	173.2	-719.6	134.2	-1489.2	117.7
10/05/2012	64	-584.0	304.5	-861.4	176.4	-901.7	125.6	-1044.1	194.6	-405.8	56.5	-1217.3	169.5	-723.3	130.7	-1492.7	114.5
11/05/2012	65	-562.1	325.2	-867.9	170.2	-908.5	119.2	-1050.9	188.1	-408.8	53.6	-1226.4	160.9	-729.4	125.0	-1499.6	107.9
12/05/2012	66	-559.6	327.6	-863.9	174.0	-904.5	122.9	-1044.5	194.2	-407.0	55.3	-1221.1	165.9	-724.0	130.1	-1495.3	112.0
13/05/2012	67	-575.8	312.2	-875.0	163.5	-915.1	112.9	-1053.6	185.6	-411.8	50.8	-1235.4	152.4	-736.4	118.3	-1506.1	101.7
14/05/2012	68	-556.9	330.1	-856.0	181.5	-896.0	131.0	-1035.0	203.2	-403.2	59.0	-1209.6	176.9	-717.7	136.0	-1486.7	120.1
15/05/2012	69	-546.9	339.7	-851.4	185.9	-893.4	133.4	-1032.5	205.6	-402.0	60.1	-1206.1	180.2	-707.4	145.8	-1483.1	123.6
16/05/2012	70	-548.2	338.3	-850.4	186.8	-892.0	134.8	-1026.9	210.9	-401.4	60.7	-1204.1	182.0	-711.7	141.7	-1480.4	126.1
17/05/2012	71	-550.5	336.2	-840.0	196.7	-883.7	142.6	-1018.1	219.2	-397.7	64.2	-1193.0	192.6	-701.5	151.4	-1472.2	133.9
18/05/2012	72	-585.2	303.3	-849.1	188.1	-890.6	136.1	-1018.9	218.5	-400.8	61.2	-1202.3	183.7	-710.4	142.9	-1480.5	126.0
19/05/2012	73	-621.3	269.1	-850.6	186.6	-894.5	132.4	-1026.9	210.8	-402.5	59.6	-1207.6	178.7	-712.1	141.3	-1481.6	125.0
20/05/2012	74	-632.2	258.8	-854.2	183.2	-897.1	130.0	-1029.8	208.2	-403.7	58.5	-1211.0	175.5	-715.2	138.4	-1485.6	121.2
21/05/2012	75	-638.9	252.5	-851.1	186.2	-893.6	133.2	-1028.4	209.4	-402.1	60.0	-1206.4	179.9	-714.0	139.5	-1482.7	124.0
22/05/2012	76	-640.0	251.4	-848.7	188.4	-891.8	135.0	-1027.9	210.0	-401.3	60.8	-1203.9	182.3	-712.2	141.3	-1481.4	125.1
23/05/2012	77	-641.2	250.2	-849.4	187.7	-891.3	135.4	-1025.6	212.2	-401.1	60.9	-1203.3	182.8	-713.9	139.6	-1481.2	125.3
24/05/2012	78	-644.5	247.1	-849.6	187.5	-893.6	133.2	-1028.1	209.7	-402.1	60.0	-1206.4	179.9	-717.6	136.1	-1483.4	123.3
25/05/2012	79	-640.0	251.3	-844.7	192.2	-889.6	137.1	-1025.1	212.6	-400.3	61.7	-1200.9	185.1	-713.7	139.9	-1476.9	129.4
26/05/2012	80	-637.9	253.3	-846.5	190.5	-893.1	133.8	-1025.5	212.2	-401.9	60.2	-1205.6	180.6	-715.6	138.1	-1479.7	126.7
27/05/2012	81	-643.1	248.4	-849.5	187.7	-896.7	130.4	-1028.2	209.7	-403.5	58.7	-1210.5	176.0	-716.0	137.7	-1482.1	124.5
28/05/2012	82	-628.1	262.7	-832.7	203.5	-879.2	147.0	-1010.5	226.5	-395.6	66.1	-1186.9	198.4	-701.3	151.5	-1465.8	140.0
29/05/2012	83	-646.6	245.1	-844.7	192.2	-891.3	135.4	-1024.1	213.6	-401.1	60.9	-1203.3	182.8	-715.8	137.9	-1478.6	127.8

30/05/2012	84	-658.9	233.4	-836.5	200.0	-882.6	143.7	-1016.4	220.9	-397.2	64.7	-1191.5	194.0	-706.6	146.5	-1469.9	136.1
31/05/2012	85	-704.3	190.5	-843.6	193.3	-890.9	135.8	-1023.7	213.9	-400.9	61.1	-1202.7	183.4	-713.1	140.4	-1478.8	127.6
1/06/2012	86	-705.8	189.0	-832.2	204.0	-881.5	144.7	-1015.0	222.1	-396.7	65.1	-1190.0	195.4	-704.1	148.9	-1467.9	138.0
2/06/2012	87	-725.8	170.1	-846.1	190.9	-895.0	131.9	-1030.3	207.7	-402.8	59.4	-1208.3	178.1	-715.3	138.3	-1481.1	125.5
3/06/2012	88	-731.9	164.3	-842.8	194.0	-890.1	136.6	-1024.5	213.2	-400.5	61.5	-1201.6	184.4	-705.5	147.6	-1477.7	128.6
4/06/2012	89	-736.1	160.3	-846.6	190.4	-892.9	133.9	-1026.2	211.5	-401.8	60.2	-1205.5	180.7	-707.4	145.8	-1480.4	126.1
5/06/2012	90	-722.4	173.3	-836.7	199.7	-881.0	145.2	-1013.8	223.3	-396.5	65.3	-1189.4	196.0	-698.7	154.0	-1468.2	137.7
6/06/2012	91	-729.9	166.2	-842.6	194.2	-888.7	137.9	-1018.6	218.7	-399.9	62.1	-1199.7	186.2	-707.2	146.0	-1475.8	130.5
7/06/2012	92	-715.5	179.8	-833.0	203.3	-880.1	146.1	-1010.1	226.8	-396.0	65.7	-1188.1	197.2	-697.9	154.8	-1466.8	139.0
8/06/2012	93	-702.6	192.1	-828.3	207.8	-875.6	150.4	-1004.3	232.3	-394.0	67.7	-1182.0	203.0	-692.8	159.7	-1462.5	143.1
9/06/2012	94	-707.4	187.5	-830.5	205.7	-877.2	148.8	-1003.9	232.7	-394.7	67.0	-1184.2	200.9	-693.8	158.6	-1463.5	142.1
10/06/2012	95	-735.4	160.9	-830.6	205.5	-875.2	150.7	-1004.1	232.5	-393.8	67.8	-1181.5	203.5	-695.7	156.9	-1463.9	141.7
11/06/2012	96	-775.2	123.2	-834.0	202.3	-881.1	145.1	-1012.1	225.0	-396.5	65.3	-1189.5	195.8	-704.5	148.6	-1471.0	135.0
12/06/2012	97	-769.6	128.5	-831.9	204.3	-880.5	145.7	-1012.4	224.6	-396.2	65.6	-1188.6	196.7	-704.4	148.7	-1468.5	137.3
13/06/2012	98	-759.8	137.8	-830.9	205.3	-875.5	150.4	-1009.7	227.2	-394.0	67.7	-1182.0	203.0	-697.2	155.5	-1466.1	139.7
14/06/2012	99	-749.9	147.2	-829.9	206.2	-875.7	150.2	-1008.7	228.1	-394.1	67.6	-1182.2	202.8	-694.2	158.3	-1466.3	139.5
15/06/2012	100	-755.1	142.3	-833.1	203.2	-880.7	145.5	-1013.4	223.7	-396.3	65.5	-1188.9	196.5	-697.6	155.0	-1470.2	135.7
16/06/2012	101	-774.2	124.2	-837.4	199.1	-884.5	141.9	-1017.2	220.1	-398.0	63.8	-1194.1	191.5	-702.4	150.5	-1473.4	132.7
17/06/2012	102	-794.4	105.1	-842.7	194.0	-888.6	138.0	-1021.2	216.3	-399.9	62.1	-1199.6	186.3	-706.6	146.6	-1478.3	128.1
18/06/2012	103	-775.2	123.2	-824.3	211.6	-868.3	157.2	-998.6	237.7	-390.8	70.7	-1172.3	212.2	-686.3	165.8	-1458.6	146.8
19/06/2012	104	-769.0	129.1	-824.4	211.5	-869.5	156.1	-998.9	237.4	-391.3	70.2	-1173.8	210.7	-687.5	164.7	-1461.6	143.9
20/06/2012	105	-777.4	121.1	-823.4	212.4	-869.4	156.2	-997.5	238.8	-391.2	70.3	-1173.7	210.9	-687.6	164.5	-1461.4	144.1
21/06/2012	106	-778.1	120.4	-817.9	217.6	-863.2	162.1	-990.7	245.2	-388.4	72.9	-1165.3	218.8	-681.0	170.9	-1455.2	150.0
22/06/2012	107	-788.8	110.3	-831.5	204.7	-878.8	147.3	-1005.8	230.9	-395.4	66.3	-1186.3	198.9	-701.5	151.4	-1468.0	137.9
23/06/2012	108	-790.8	108.4	-826.8	209.1	-873.2	152.6	-998.3	238.0	-393.0	68.7	-1178.9	206.0	-693.0	159.4	-1464.6	141.1
24/06/2012	109	-798.7	100.9	-828.6	207.5	-873.8	152.0	-996.7	239.5	-393.2	68.4	-1179.6	205.3	-694.3	158.2	-1465.6	140.1
25/06/2012	110	-797.9	101.7	-826.6	209.3	-873.0	152.8	-995.4	240.7	-392.9	68.8	-1178.6	206.3	-697.7	155.0	-1465.1	140.6
26/06/2012	111	-801.9	97.9	-830.9	205.2	-879.7	146.4	-1003.6	233.0	-395.9	65.9	-1187.6	197.7	-705.5	147.6	-1472.1	134.0
27/06/2012	112	-798.5	101.1	-827.4	208.6	-874.7	151.1	-1001.5	235.0	-393.6	68.0	-1180.9	204.0	-697.3	155.4	-1468.3	137.6
28/06/2012	113	-800.2	99.5	-827.8	208.2	-874.9	150.9	-1002.0	234.5	-393.7	67.9	-1181.2	203.8	-697.8	154.9	-1468.9	137.0
29/06/2012	114	-806.2	93.9	-831.1	205.1	-881.6	144.6	-1009.4	227.4	-396.7	65.1	-1190.2	195.2	-705.4	147.7	-1475.0	131.2
30/06/2012	115	-811.7	88.6	-833.6	202.7	-884.6	141.8	-1012.6	224.4	-398.1	63.8	-1194.2	191.4	-707.7	145.5	-1477.2	129.1
1/07/2012	116	-813.4	87.0	-833.2	203.1	-882.9	143.4	-1009.4	227.5	-397.3	64.5	-1191.9	193.6	-704.8	148.2	-1474.7	131.5
2/07/2012	117	-810.8	89.5	-829.1	206.9	-879.0	147.1	-1003.4	233.2	-395.6	66.2	-1186.7	198.6	-698.6	154.1	-1469.9	136.1
3/07/2012	118	-808.4	91.7	-822.1	213.6	-868.1	157.5	-992.7	243.3	-390.6	70.9	-1171.9	212.6	-688.6	163.6	-1461.0	144.5
4/07/2012	119	-810.1	90.2	-824.6	211.3	-869.1	156.5	-993.5	242.5	-391.1	70.4	-1173.3	211.3	-690.3	162.0	-1462.6	143.0
5/07/2012	120	-812.8	87.6	-827.2	208.8	-873.8	152.1	-998.9	237.4	-393.2	68.4	-1179.6	205.3	-695.4	157.2	-1466.2	139.5

6/07/2012	121	-810.8	89.4	-824.8	211.1	-872.9	152.9	-998.8	237.5	-392.8	68.8	-1178.5	206.4	-695.0	157.6	-1463.7	141.9
7/07/2012	122	-806.2	93.8	-820.6	215.0	-868.9	156.7	-993.9	242.1	-391.0	70.5	-1173.0	211.5	-690.1	162.2	-1459.5	145.9
8/07/2012	123	-804.3	95.6	-828.1	207.9	-876.9	149.1	-1001.3	235.2	-394.6	67.1	-1183.9	201.2	-696.3	156.3	-1466.1	139.6
9/07/2012	124	-786.4	112.6	-814.2	221.1	-862.0	163.2	-988.7	247.1	-387.9	73.4	-1163.7	220.3	-679.3	172.4	-1448.4	156.4
10/07/2012	125	-792.8	106.5	-821.7	214.0	-870.2	155.4	-996.8	239.4	-391.6	69.9	-1174.8	209.8	-684.2	167.8	-1456.3	148.9
11/07/2012	126	-802.7	97.2	-830.1	206.0	-880.6	145.5	-1006.9	229.9	-396.3	65.5	-1188.9	196.5	-693.0	159.4	-1466.4	139.4
12/07/2012	127	-791.3	108.0	-820.4	215.2	-871.2	154.5	-996.2	240.0	-392.0	69.5	-1176.1	208.6	-684.3	167.7	-1454.5	150.6
13/07/2012	128	-795.8	103.7	-822.2	213.5	-877.5	148.5	-1000.9	235.5	-394.9	66.8	-1184.7	200.5	-686.7	165.4	-1457.4	147.9
14/07/2012	129	-816.3	84.3	-843.9	193.0	-899.1	128.0	-1022.7	214.9	-404.6	57.6	-1213.8	172.9	-707.2	146.0	-1477.1	129.3
15/07/2012	130	-816.9	83.7	-842.7	194.1	-893.7	133.2	-1018.5	218.8	-402.2	59.9	-1206.5	179.8	-710.8	142.6	-1474.5	131.7
16/07/2012	131	-799.5	100.2	-825.1	210.8	-874.5	151.4	-999.0	237.4	-393.5	68.1	-1180.5	204.4	-690.1	162.2	-1458.4	146.9
17/07/2012	132	-801.2	98.6	-829.7	206.4	-877.0	149.0	-1002.0	234.5	-394.7	67.0	-1184.0	201.1	-693.1	159.3	-1462.2	143.4
18/07/2012	133	-804.1	95.8	-832.7	203.5	-880.8	145.4	-1004.4	232.2	-396.3	65.4	-1189.0	196.3	-696.8	155.8	-1465.3	140.5
19/07/2012	134	-803.0	96.8	-831.7	204.5	-879.3	146.9	-1002.4	234.1	-395.7	66.1	-1187.0	198.2	-694.2	158.3	-1464.0	141.7
20/07/2012	135	-799.3	100.3	-825.9	210.0	-873.2	152.6	-995.9	240.2	-392.9	68.7	-1178.8	206.0	-686.2	165.9	-1454.3	150.9
21/07/2012	136	-804.6	95.3	-831.5	204.7	-881.0	145.2	-1002.3	234.2	-396.4	65.4	-1189.3	196.1	-690.9	161.4	-1461.4	144.1
22/07/2012	137	-812.1	88.2	-838.0	198.6	-889.7	137.0	-1011.6	225.4	-400.4	61.6	-1201.1	184.9	-701.5	151.4	-1467.5	138.3
23/07/2012	138	-812.3	88.0	-835.7	200.7	-889.9	136.8	-1012.6	224.5	-400.5	61.5	-1201.4	184.6	-703.5	149.5	-1467.6	138.2
24/07/2012	139	-809.9	90.3	-835.5	200.9	-886.8	139.7	-1011.4	225.6	-399.1	62.9	-1197.2	188.6	-700.4	152.4	-1466.6	139.2
25/07/2012	140	-803.8	96.1	-827.7	208.3	-880.0	146.1	-1003.7	232.9	-396.0	65.8	-1188.1	197.3	-690.0	162.2	-1459.8	145.6
26/07/2012	141	-798.4	101.2	-824.4	211.4	-876.7	149.3	-998.7	237.6	-394.5	67.2	-1183.5	201.6	-684.9	167.1	-1456.1	149.1
27/07/2012	142	-807.1	93.0	-834.3	202.1	-884.2	142.1	-1005.9	230.8	-397.9	64.0	-1193.7	191.9	-691.7	160.7	-1468.4	137.5
28/07/2012	143	-804.7	95.2	-834.1	202.2	-882.4	143.9	-1003.1	233.4	-397.1	64.8	-1191.2	194.3	-689.5	162.8	-1466.5	139.2
29/07/2012	144	-800.3	99.4	-831.3	204.9	-879.0	147.1	-1000.4	236.0	-395.5	66.2	-1186.6	198.6	-689.0	163.2	-1463.0	142.6
30/07/2012	145	-801.2	98.6	-829.2	206.9	-877.0	149.0	-997.2	239.1	-394.7	67.0	-1184.0	201.1	-688.7	163.5	-1461.2	144.3
31/07/2012	146	-800.2	99.5	-828.7	207.4	-874.8	151.1	-993.4	242.6	-393.7	68.0	-1181.0	204.0	-685.7	166.3	-1458.7	146.7
1/08/2012	147	-797.7	101.9	-827.9	208.1	-872.4	153.3	-989.0	246.8	-392.6	69.0	-1177.8	207.0	-683.6	168.4	-1455.8	149.4
2/08/2012	148	-802.9	96.9	-830.0	206.2	-876.2	149.8	-992.1	243.8	-394.3	67.4	-1182.9	202.2	-688.0	164.2	-1459.5	145.9
3/08/2012	149	-795.3	104.2	-825.6	210.3	-869.5	156.1	-984.4	251.2	-391.3	70.2	-1173.9	210.7	-681.2	170.7	-1452.9	152.2
4/08/2012	150	-800.5	99.2	-831.5	204.7	-876.1	149.9	-989.8	246.1	-394.2	67.4	-1182.7	202.3	-687.1	165.0	-1458.4	146.9
5/08/2012	151	-805.3	94.7	-834.9	201.5	-880.6	145.5	-995.8	240.3	-396.3	65.5	-1188.9	196.5	-695.0	157.6	-1462.4	143.1
6/08/2012	152	-810.8	89.5	-841.6	195.1	-885.7	140.7	-1001.7	234.8	-398.6	63.3	-1195.7	190.0	-702.3	150.6	-1466.8	139.0
7/08/2012	153	-792.5	106.8	-824.7	211.1	-866.3	159.1	-981.4	254.0	-389.8	71.6	-1169.5	214.8	-681.9	170.0	-1449.0	155.8
8/08/2012	154	-792.1	107.2	-826.2	209.7	-864.6	160.8	-979.3	256.0	-389.1	72.3	-1167.2	217.0	-679.0	172.7	-1446.2	158.6
9/08/2012	155	-800.8	98.9	-832.5	203.7	-876.0	150.0	-992.7	243.4	-394.2	67.5	-1182.6	202.4	-691.1	161.3	-1455.5	149.7
10/08/2012	156	-794.0	105.4	-829.0	207.1	-867.7	157.8	-982.8	252.7	-390.5	71.0	-1171.4	213.1	-679.2	172.6	-1448.4	156.5
11/08/2012	157	-805.0	95.0	-838.7	197.9	-885.5	141.0	-1000.1	236.3	-398.5	63.4	-1195.4	190.3	-693.7	158.8	-1462.4	143.1

12/08/2012	158	-808.9	91.3	-844.5	192.4	-891.5	135.3	-1010.6	226.4	-401.2	60.9	-1203.5	182.7	-693.7	158.8	-1466.4	139.3
13/08/2012	159	-797.8	101.8	-836.5	199.9	-878.9	147.2	-998.3	238.0	-395.5	66.2	-1186.6	198.7	-681.3	170.6	-1455.2	150.0
14/08/2012	160	-787.9	111.2	-826.9	209.1	-867.4	158.1	-985.0	250.6	-390.3	71.1	-1171.0	213.4	-671.2	180.1	-1445.5	159.2
15/08/2012	161	-788.6	110.5	-828.9	207.2	-870.0	155.7	-987.3	248.4	-391.5	70.0	-1174.5	210.1	-679.8	172.0	-1443.8	160.8
16/08/2012	162	-789.7	109.5	-829.9	206.2	-871.2	154.5	-989.3	246.5	-392.1	69.5	-1176.2	208.5	-685.7	166.4	-1446.1	158.6
17/08/2012	163	-798.2	101.4	-835.7	200.7	-880.1	146.1	-1000.1	236.3	-396.0	65.7	-1188.1	197.2	-693.6	158.8	-1452.9	152.2
18/08/2012	164	-810.4	89.9	-845.3	191.7	-892.7	134.1	-1011.5	225.5	-401.7	60.4	-1205.1	181.1	-705.0	148.1	-1464.3	141.4
19/08/2012	165	-801.0	98.7	-840.1	196.6	-885.5	141.0	-1004.7	231.9	-398.5	63.4	-1195.4	190.3	-694.3	158.3	-1458.0	147.4
20/08/2012	166	-787.6	111.5	-828.9	207.1	-871.3	154.4	-989.3	246.5	-392.1	69.5	-1176.3	208.4	-679.2	172.6	-1444.9	159.8
21/08/2012	167	-799.9	99.8	-842.9	193.9	-884.8	141.6	-1002.3	234.2	-398.2	63.7	-1194.5	191.2	-691.9	160.5	-1456.5	148.8
22/08/2012	168	-810.8	89.5	-847.8	189.3	-895.9	131.1	-1018.7	218.6	-403.1	59.0	-1209.4	177.0	-706.0	147.1	-1466.4	139.4
23/08/2012	169	-801.3	98.4	-832.8	203.5	-884.4	142.0	-1008.7	228.2	-398.0	63.9	-1193.9	191.7	-690.0	162.3	-1459.9	145.5
24/08/2012	170	-808.4	91.7	-841.0	195.7	-887.8	138.7	-1010.4	226.5	-399.5	62.4	-1198.6	187.3	-693.2	159.3	-1463.3	142.3
25/08/2012	171	-809.2	91.0	-846.8	190.2	-886.9	139.6	-1009.9	227.0	-399.1	62.8	-1197.3	188.5	-696.9	155.7	-1455.7	149.5
26/08/2012	172	-802.0	97.8	-842.6	194.2	-884.7	141.7	-1006.0	230.7	-398.1	63.8	-1194.3	191.3	-692.1	160.3	-1450.9	154.1
27/08/2012	173	-793.2	106.2	-831.0	205.1	-873.7	152.2	-998.9	237.5	-393.1	68.5	-1179.4	205.4	-681.4	170.5	-1440.5	163.9
28/08/2012	174	-803.5	96.4	-836.8	199.7	-885.1	141.4	-1012.6	224.4	-398.3	63.6	-1194.8	190.8	-691.9	160.5	-1453.1	151.9
29/08/2012	175	-805.9	94.1	-832.2	204.0	-883.6	142.8	-1015.6	221.6	-397.6	64.2	-1192.8	192.7	-688.9	163.3	-1452.5	152.5
30/08/2012	176	-802.3	97.5	-831.6	204.6	-881.9	144.4	-1013.2	223.9	-396.8	65.0	-1190.5	194.9	-685.8	166.3	-1450.6	154.3
31/08/2012	177	-801.3	98.5	-838.6	198.0	-880.2	146.0	-1013.7	223.4	-396.1	65.7	-1188.3	197.1	-687.3	164.8	-1448.6	156.2
1/09/2012	178	-795.6	103.8	-834.5	201.8	-876.0	149.9	-1010.9	226.1	-394.2	67.5	-1182.6	202.4	-679.7	172.1	-1445.2	159.5
2/09/2012	179	-809.0	91.2	-843.3	193.5	-889.8	136.9	-1028.9	209.0	-400.4	61.6	-1201.2	184.8	-692.6	159.8	-1457.0	148.3
3/09/2012	180	-797.2	102.4	-835.1	201.3	-877.7	148.3	-1023.7	213.9	-395.0	66.7	-1184.9	200.2	-682.8	169.1	-1447.3	157.4
4/09/2012	181	-795.3	104.2	-836.8	199.7	-876.8	149.2	-1024.3	213.4	-394.6	67.1	-1183.7	201.4	-682.6	169.3	-1445.6	159.1
5/09/2012	182	-802.5	97.4	-848.5	188.6	-883.4	142.9	-1033.5	204.7	-397.5	64.3	-1192.6	192.9	-690.1	162.2	-1453.3	151.8
6/09/2012	183	-791.6	107.7	-837.3	199.2	-871.9	153.8	-1022.4	215.1	-392.3	69.2	-1177.0	207.7	-682.5	169.4	-1444.4	160.2
7/09/2012	184	-783.3	115.5	-824.7	211.2	-863.4	161.9	-1011.4	225.6	-388.5	72.8	-1165.6	218.5	-674.8	176.7	-1434.3	169.8
8/09/2012	185	-786.0	113.0	-826.9	209.1	-865.9	159.5	-1012.5	224.5	-389.6	71.8	-1168.9	215.4	-676.2	175.4	-1435.3	168.9
9/09/2012	186	-801.6	98.2	-843.2	193.6	-883.0	143.3	-1030.0	208.0	-397.4	64.5	-1192.1	193.5	-692.2	160.2	-1451.7	153.3
10/09/2012	187	-802.6	97.3	-846.3	190.7	-885.3	141.2	-1033.4	204.8	-398.4	63.5	-1195.1	190.6	-693.0	159.5	-1455.6	149.6
11/09/2012	188	-795.1	104.3	-832.7	203.6	-878.5	147.5	-1027.2	210.6	-395.3	66.4	-1186.0	199.2	-684.3	167.7	-1451.0	154.0
12/09/2012	189	-795.1	104.3	-829.5	206.6	-877.4	148.6	-1028.4	209.5	-394.9	66.9	-1184.6	200.6	-679.8	171.9	-1450.1	154.9
13/09/2012	190	-799.7	100.0	-831.9	204.3	-881.9	144.4	-1032.3	205.8	-396.8	65.0	-1190.5	194.9	-680.1	171.6	-1451.4	153.6
14/09/2012	191	-787.5	111.5	-822.7	213.0	-868.0	157.5	-1017.2	220.1	-390.6	70.9	-1171.8	212.6	-666.7	184.3	-1440.1	164.3
15/09/2012	192	-797.0	102.6	-827.1	208.9	-871.0	154.7	-1020.0	217.5	-391.9	69.6	-1175.8	208.9	-674.7	176.8	-1441.1	163.4
16/09/2012	193	-796.0	103.5	-821.4	214.3	-876.3	149.7	-1024.9	212.7	-394.3	67.4	-1183.0	202.1	-677.3	174.3	-1443.2	161.3
17/09/2012	194	-790.0	109.2	-819.5	216.0	-877.3	148.7	-1025.6	212.2	-394.8	66.9	-1184.4	200.8	-667.5	183.6	-1443.4	161.1

18/09/2012	195	-788.3	110.8	-821.7	214.0	-876.9	149.1	-1027.4	210.4	-394.6	67.1	-1183.9	201.2	-668.5	182.7	-1444.7	159.9
19/09/2012	196	-784.5	114.4	-819.7	215.9	-872.2	153.5	-1017.7	219.6	-392.5	69.1	-1177.5	207.3	-671.4	179.9	-1439.8	164.6
20/09/2012	197	-786.3	112.7	-821.1	214.5	-873.8	152.0	-1016.3	221.0	-393.2	68.4	-1179.6	205.2	-674.1	177.4	-1440.1	164.3
21/09/2012	198	-782.5	116.3	-820.2	215.4	-870.1	155.6	-1012.5	224.6	-391.5	70.0	-1174.6	210.0	-662.0	188.8	-1440.0	164.4
22/09/2012	199	-786.7	112.3	-822.5	213.2	-875.2	150.7	-1016.9	220.3	-393.8	67.8	-1181.5	203.5	-663.3	187.6	-1445.1	159.5
23/09/2012	200	-786.2	112.8	-821.1	214.6	-877.0	149.0	-1015.8	221.5	-394.7	67.0	-1184.0	201.1	-658.9	191.8	-1444.4	160.2
24/09/2012	201	-773.8	124.6	-809.5	225.5	-863.7	161.6	-1002.7	233.9	-388.7	72.7	-1166.0	218.1	-628.2	220.9	-1432.6	171.4
25/09/2012	202	-775.5	123.0	-810.7	224.4	-863.2	162.1	-1000.1	236.3	-388.4	72.9	-1165.3	218.8	-624.0	224.8	-1433.1	170.9
26/09/2012	203	-781.4	117.3	-815.6	219.8	-870.6	155.1	-1006.6	230.1	-391.8	69.8	-1175.3	209.4	-627.6	221.4	-1439.7	164.7
27/09/2012	204	-774.5	123.9	-811.2	223.9	-865.5	159.9	-1001.4	235.1	-389.5	72.0	-1168.4	215.9	-622.9	225.9	-1435.0	169.1
28/09/2012	205	-781.7	117.1	-816.6	218.8	-874.3	151.6	-1011.1	225.9	-393.4	68.2	-1180.3	204.7	-626.6	222.4	-1443.0	161.6
29/09/2012	206	-791.3	107.9	-824.5	211.3	-881.8	144.5	-1019.6	217.8	-396.8	65.0	-1190.4	195.0	-637.6	212.0	-1452.2	152.9
30/09/2012	207	-784.1	114.8	-814.1	221.2	-870.8	154.9	-1009.4	227.5	-391.8	69.7	-1175.5	209.1	-631.9	217.4	-1439.3	165.0
1/10/2012	208	-777.6	120.9	-810.6	224.5	-865.9	159.5	-1003.4	233.1	-389.7	71.8	-1169.0	215.3	-632.9	216.4	-1435.2	168.9
2/10/2012	209	-788.9	110.2	-822.7	213.0	-880.1	146.1	-1017.1	220.1	-396.0	65.7	-1188.1	197.2	-654.9	195.5	-1448.4	156.5
3/10/2012	210	-778.0	120.6	-809.5	225.5	-867.8	157.7	-1003.8	232.8	-390.5	71.0	-1171.5	212.9	-676.0	175.6	-1435.0	169.1
4/10/2012	211	-780.3	118.4	-811.6	223.6	-871.6	154.1	-1007.3	229.4	-392.2	69.3	-1176.7	208.0	-694.8	157.7	-1439.0	165.3
5/10/2012	212	-773.7	124.6	-805.4	229.4	-863.2	162.1	-996.9	239.4	-388.4	73.0	-1165.3	218.9	-706.4	146.7	-1433.7	170.4
6/10/2012	213	-780.3	118.4	-811.0	224.1	-871.2	154.5	-1004.1	232.5	-392.1	69.5	-1176.2	208.5	-715.9	137.7	-1440.3	164.1
7/10/2012	214	-777.1	121.4	-806.6	228.3	-867.2	158.3	-1000.5	235.9	-390.2	71.2	-1170.7	213.7	-725.6	128.5	-1435.4	168.8
8/10/2012	215	-774.6	123.8	-804.9	229.9	-865.7	159.7	-997.3	238.9	-389.6	71.8	-1168.8	215.5	-726.5	127.7	-1432.5	171.5
9/10/2012	216	-774.9	123.5	-804.9	229.9	-866.7	158.8	-998.0	238.2	-390.0	71.4	-1170.0	214.3	-728.5	125.8	-1433.7	170.4
10/10/2012	217	-770.5	127.7	-799.8	234.8	-859.9	165.2	-990.7	245.2	-387.0	74.3	-1160.9	223.0	-732.5	122.0	-1429.1	174.7
11/10/2012	218	-779.0	119.6	-807.9	227.1	-868.2	157.3	-998.5	237.8	-390.7	70.8	-1172.1	212.4	-739.5	115.4	-1436.7	167.5
12/10/2012	219	-750.6	146.5	-781.2	252.4	-839.3	184.7	-968.0	266.7	-377.7	83.1	-1133.1	249.3	-710.9	142.5	-1408.2	194.6
13/10/2012	220	-765.8	132.1	-799.2	235.4	-856.2	168.8	-984.1	251.4	-385.3	75.9	-1155.8	227.8	-729.3	125.0	-1425.0	178.7
14/10/2012	221	-772.4	125.8	-800.2	234.4	-863.7	161.6	-992.6	243.4	-388.7	72.7	-1166.0	218.2	-740.8	114.1	-1429.1	174.7
15/10/2012	222	-763.9	134.0	-789.8	244.3	-857.0	168.0	-985.3	250.3	-385.6	75.6	-1156.9	226.8	-722.7	131.3	-1421.0	182.4
16/10/2012	223	-772.4	125.9	-799.7	234.9	-865.4	160.0	-993.7	242.4	-389.4	72.0	-1168.2	216.1	-724.1	130.0	-1429.1	174.7
17/10/2012	224	-784.1	114.7	-812.8	222.5	-877.0	149.0	-1004.5	232.1	-394.7	67.0	-1184.0	201.1	-727.6	126.6	-1442.8	161.7
18/10/2012	225	-770.0	128.2	-798.1	236.3	-864.5	160.8	-992.7	243.3	-389.0	72.4	-1167.1	217.1	-681.4	170.5	-1429.5	174.4
19/10/2012	226	-761.6	136.1	-792.2	241.9	-857.5	167.5	-985.2	250.4	-385.9	75.4	-1157.6	226.1	-655.0	195.4	-1422.6	180.9
20/10/2012	227	-784.9	114.0	-813.5	221.8	-874.9	151.0	-1007.9	228.9	-393.7	68.0	-1181.1	203.9	-670.8	180.5	-1442.2	162.3
21/10/2012	228	-796.1	103.4	-822.3	213.4	-882.6	143.7	-1014.6	222.6	-397.2	64.7	-1191.5	194.0	-681.4	170.5	-1450.6	154.3
22/10/2012	229	-790.5	108.7	-819.0	216.5	-876.6	149.4	-1007.7	229.1	-394.5	67.2	-1183.4	201.6	-710.4	143.0	-1443.9	160.7
23/10/2012	230	-779.1	119.5	-807.5	227.4	-863.9	161.4	-992.3	243.6	-388.8	72.6	-1166.3	217.9	-713.7	139.8	-1431.8	172.2
24/10/2012	231	-776.1	122.3	-800.0	234.6	-860.5	164.6	-987.9	247.9	-387.2	74.1	-1161.7	222.3	-711.2	142.2	-1426.8	176.9

25/10/2012	232	-784.5	114.4	-809.6	225.5	-872.4	153.3	-998.4	237.9	-392.6	69.0	-1177.8	207.0	-726.8	127.4	-1437.9	166.4
26/10/2012	233	-784.2	114.7	-809.9	225.1	-872.2	153.6	-998.6	237.7	-392.5	69.1	-1177.4	207.3	-728.8	125.5	-1438.4	165.9
27/10/2012	234	-779.8	118.9	-803.5	231.2	-864.8	160.6	-991.1	244.9	-389.1	72.3	-1167.4	216.8	-729.1	125.2	-1430.7	173.2
28/10/2012	235	-781.7	117.0	-801.8	232.8	-863.6	161.7	-990.8	245.1	-388.6	72.8	-1165.8	218.3	-733.3	121.2	-1429.1	174.7
29/10/2012	236	-776.7	121.8	-795.9	238.5	-859.6	165.5	-987.0	248.7	-386.8	74.5	-1160.4	223.4	-755.9	99.8	-1424.3	179.3
30/10/2012	237	-776.6	121.9	-797.8	236.7	-861.9	163.3	-989.5	246.3	-387.8	73.5	-1163.5	220.5	-758.9	97.0	-1428.0	175.8
31/10/2012	238	-778.9	119.7	-804.5	230.3	-866.6	158.9	-994.5	241.6	-390.0	71.5	-1169.9	214.5	-755.8	99.9	-1434.4	169.7
1/11/2012	239	-760.6	137.1	-790.7	243.4	-848.4	176.1	-976.6	258.6	-381.8	79.2	-1145.4	237.7	-737.0	117.7	-1418.8	184.5
2/11/2012	240	-771.4	126.8	-797.3	237.1	-854.8	170.0	-982.1	253.4	-384.7	76.5	-1154.0	229.6	-744.0	111.1	-1424.4	179.2

Table E.10 Steel strain for slab N-SCC-b

Slab N-SCC-b		STEEL STRAIN BY SG															
		1		2		3		4		5		6		7		8	
Date	Age	Reading	Strain	Reading	Strain	Reading	Strain	Reading	Strain	Reading	Strain	Reading	Strain	Reading	Strain	Reading	Strain
21/03/2012	14	-320.1		-623.4		-730.2		109.4		2223.9		90.1		-337.8		-311.0	
22/03/2012	15	-228.5	86.9	-536.4	82.5	-652.2	73.9	202.8	88.5	2434.1	199.2	178.2	83.5	-254.7	78.8	-233.7	73.3
23/03/2012	16	-205.5	108.6	-511.1	106.5	-631.5	93.6	220.7	105.5	2487.4	249.8	193.6	98.1	-231.7	100.6	-215.4	90.6
24/03/2012	17	-143.5	167.4	-448.6	165.7	-578.1	144.2	270.7	152.9	2568.5	326.6	244.3	146.2	-177.1	152.4	-170.9	132.7
25/03/2012	18	-128.9	181.3	-429.5	183.9	-566.6	155.1	283.5	165.0	2605.3	361.5	255.3	156.6	-164.6	164.2	-161.8	141.4
26/03/2012	19	-118.0	191.6	-421.0	191.9	-559.6	161.7	291.3	172.4	2624.1	379.4	263.2	164.1	-153.2	175.0	-154.6	148.3
27/03/2012	20	-109.8	199.4	-414.9	197.6	-548.6	172.2	300.4	181.0	2670.6	423.4	272.8	173.2	-140.0	187.5	-138.8	163.2
28/03/2012	21	-104.5	204.3	-410.4	201.9	-545.0	175.5	304.3	184.7	2675.0	427.6	273.3	173.6	-137.5	189.9	-136.7	165.2
29/03/2012	22	-123.9	186.0	-430.7	182.7	-566.3	155.4	281.3	162.9	2666.4	419.5	252.8	154.3	-155.5	172.9	-152.5	150.3
30/03/2012	23	-97.8	210.7	-401.3	210.6	-539.3	180.9	309.2	189.4	2706.6	457.6	280.0	180.0	-124.2	202.5	-123.7	177.5
31/03/2012	24	-70.8	236.3	-376.7	233.9	-514.5	204.5	332.9	211.8	2741.6	490.8	305.4	204.0	-97.9	227.4	-99.8	200.2
1/04/2012	25	-77.2	230.2	-382.0	228.9	-520.2	199.0	326.4	205.7	2747.3	496.1	299.8	198.7	-101.4	224.2	-101.7	198.4
2/04/2012	26	-117.2	192.3	-431.5	182.0	-563.8	157.7	282.6	164.1	2714.1	464.7	261.1	162.1	-138.8	188.7	-133.5	168.3
3/04/2012	27	-135.3	175.2	-443.4	170.7	-576.1	146.1	269.2	151.5	2710.3	461.1	247.8	149.5	-151.1	177.0	-147.6	154.8
4/04/2012	28	-112.0	197.2	-417.8	194.9	-553.8	167.2	289.1	170.3	2731.3	481.0	260.2	161.2	-136.1	191.2	-140.9	161.2
5/04/2012	29	-138.6	172.1	-446.8	167.4	-580.1	142.3	263.4	145.9	2715.6	466.1	238.2	140.4	-157.6	170.9	-159.5	143.6
6/04/2012	30	-155.1	156.4	-464.0	151.1	-596.3	126.9	248.2	131.6	2712.4	463.1	225.0	127.8	-168.7	160.3	-168.2	135.4
7/04/2012	31	-148.5	162.7	-457.6	157.2	-590.2	132.7	254.2	137.2	2717.5	467.9	230.4	133.0	-162.0	166.7	-162.7	140.6
8/04/2012	32	-150.8	160.5	-460.3	154.6	-593.4	129.7	250.3	133.6	2722.6	472.7	226.7	129.4	-164.2	164.6	-165.3	138.0
9/04/2012	33	-156.0	155.6	-466.9	148.4	-598.7	124.7	244.9	128.4	2728.9	478.7	221.8	124.9	-166.3	162.6	-168.4	135.2
10/04/2012	34	-124.5	185.4	-434.6	179.0	-569.4	152.4	274.0	156.0	2768.5	516.3	247.0	148.7	-138.6	188.9	-147.6	154.9
11/04/2012	35	-110.4	198.8	-422.7	190.3	-556.3	164.8	287.4	168.7	2788.5	535.2	259.8	160.8	-127.1	199.8	-136.4	165.5
12/04/2012	36	-104.1	204.8	-414.6	198.0	-549.9	170.9	293.4	174.4	2789.9	536.5	264.1	164.9	-121.8	204.8	-132.2	169.4
13/04/2012	37	-112.2	197.1	-421.9	191.0	-557.1	164.1	286.1	167.5	2789.1	535.7	257.0	158.2	-127.9	199.0	-138.6	163.3
16/04/2012	40	-95.6	212.8	-403.5	208.5	-540.3	180.0	302.8	183.3	2816.2	561.5	269.4	169.9	-111.7	214.3	-129.5	172.1
17/04/2012	41	-140.0	170.7	-450.6	163.9	-583.8	138.8	260.7	143.4	2777.0	524.3	238.1	140.3	-146.6	181.3	-156.6	146.3
18/04/2012	42	-143.0	167.9	-454.7	159.9	-586.5	136.2	257.7	140.6	2768.2	515.9	236.9	139.1	-148.8	179.2	-159.6	143.5
19/04/2012	43	-137.0	173.6	-449.6	164.8	-581.4	141.0	263.0	145.5	2764.1	512.1	242.8	144.7	-144.0	183.7	-156.2	146.7
20/04/2012	44	-144.9	166.1	-457.4	157.4	-588.5	134.3	255.5	138.5	2751.9	500.5	234.3	136.7	-149.9	178.2	-164.7	138.7
21/04/2012	45	-161.2	150.6	-474.5	141.2	-603.4	120.1	239.3	123.1	2738.5	487.8	219.3	122.5	-164.9	163.9	-177.1	126.9
22/04/2012	46	-168.8	143.5	-482.6	133.5	-611.4	112.6	230.7	114.9	2738.1	487.4	210.4	114.1	-172.4	156.8	-182.9	121.4
23/04/2012	47	-163.9	148.1	-477.3	138.5	-607.0	116.8	233.9	118.0	2746.3	495.2	214.3	117.7	-168.1	160.9	-178.8	125.3

24/04/2012	48	-142.9	168.0	-456.1	158.6	-588.2	134.6	252.1	135.3	2776.8	524.1	231.0	133.5	-150.6	177.5	-162.1	141.1
25/04/2012	49	-162.5	149.4	-474.7	141.0	-606.9	116.9	233.9	118.0	2789.2	535.9	213.4	116.9	-164.1	164.7	-176.6	127.4
26/04/2012	50	-161.2	150.7	-468.1	147.2	-601.3	122.1	241.2	125.0	2800.2	546.3	218.4	121.6	-155.6	172.8	-170.7	133.0
27/04/2012	51	-145.3	165.7	-456.1	158.6	-589.6	133.2	254.1	137.2	2810.1	555.6	231.0	133.6	-145.9	182.0	-163.3	140.0
28/04/2012	52	-146.6	164.4	-459.0	155.9	-591.9	131.1	252.3	135.4	2803.1	549.0	230.2	132.8	-147.6	180.3	-164.1	139.2
29/04/2012	53	-153.5	157.9	-466.1	149.1	-598.6	124.8	245.2	128.7	2798.1	544.3	223.6	126.5	-154.3	174.0	-171.5	132.2
30/04/2012	54	-147.8	163.4	-459.6	155.3	-593.7	129.4	248.0	131.4	2812.6	558.0	224.6	127.5	-150.3	177.8	-169.9	133.8
1/05/2012	55	-152.3	159.1	-463.8	151.3	-597.5	125.8	245.3	128.8	2810.2	555.8	222.7	125.6	-152.5	175.7	-172.3	131.4
2/05/2012	56	-148.7	162.5	-461.0	154.0	-595.1	128.1	248.2	131.5	2809.9	555.5	226.4	129.2	-149.4	178.6	-170.3	133.3
3/05/2012	57	-149.4	161.8	-461.4	153.6	-595.0	128.2	247.7	131.1	2808.2	553.9	226.9	129.6	-149.3	178.7	-170.4	133.2
4/05/2012	58	-151.0	160.3	-462.8	152.2	-596.6	126.6	245.1	128.6	2823.7	568.6	223.1	126.0	-150.7	177.4	-171.6	132.1
5/05/2012	59	-156.2	155.3	-469.3	146.1	-601.1	122.4	242.1	125.8	2831.2	575.7	221.1	124.1	-150.7	177.3	-170.3	133.4
6/05/2012	60	-155.4	156.2	-468.1	147.3	-599.4	124.0	243.8	127.4	2837.5	581.7	222.7	125.6	-148.6	179.4	-167.4	136.1
7/05/2012	61	-143.6	167.3	-455.2	159.4	-589.8	133.1	254.2	137.2	2849.9	593.4	230.2	132.8	-139.1	188.3	-160.1	143.0
8/05/2012	62	-133.8	176.6	-445.7	168.5	-581.0	141.4	262.5	145.1	2860.1	603.0	237.4	139.6	-132.2	194.9	-153.9	148.9
9/05/2012	63	-133.3	177.1	-445.5	168.7	-580.5	141.9	263.2	145.7	2861.7	604.6	239.1	141.2	-131.4	195.7	-153.0	149.7
10/05/2012	64	-138.0	172.7	-451.7	162.8	-586.0	136.7	257.9	140.8	2855.5	598.7	233.8	136.2	-136.4	190.9	-158.8	144.2
11/05/2012	65	-146.0	165.0	-460.2	154.7	-593.7	129.4	250.1	133.3	2847.9	591.5	226.2	129.0	-144.0	183.7	-166.6	136.9
12/05/2012	66	-136.3	174.2	-452.6	161.9	-585.6	137.1	257.0	139.9	2863.7	606.5	234.0	136.4	-135.3	191.9	-158.3	144.7
13/05/2012	67	-146.4	164.7	-460.4	154.6	-593.4	129.7	248.5	131.8	2866.4	609.1	226.5	129.3	-141.1	186.5	-165.9	137.5
14/05/2012	68	-129.4	180.8	-443.6	170.4	-576.5	145.7	265.4	147.9	2890.4	631.8	242.3	144.3	-124.3	202.4	-152.9	149.8
15/05/2012	69	-128.0	182.1	-442.5	171.5	-574.7	147.4	268.1	150.4	2897.6	638.6	244.3	146.1	-122.0	204.5	-152.1	150.6
16/05/2012	70	-129.6	180.5	-441.1	172.8	-574.5	147.6	270.8	153.0	2899.1	640.0	243.5	145.4	-119.1	207.3	-150.4	152.2
17/05/2012	71	-111.3	197.9	-427.2	186.0	-559.2	162.1	286.2	167.5	2914.5	654.6	260.6	161.6	-104.5	221.2	-135.7	166.1
18/05/2012	72	-119.1	190.5	-436.3	177.4	-569.2	152.6	276.8	158.7	2905.7	646.3	251.1	152.6	-114.0	212.2	-145.3	157.1
19/05/2012	73	-125.7	184.3	-439.6	174.2	-573.9	148.2	269.1	151.4	2902.0	642.8	244.2	146.0	-118.4	208.0	-149.5	153.0
20/05/2012	74	-122.0	187.7	-437.6	176.1	-571.3	150.6	272.1	154.2	2913.0	653.2	246.2	147.9	-115.5	210.8	-146.0	156.4
21/05/2012	75	-124.8	185.2	-438.8	175.0	-571.6	150.4	273.3	155.3	2903.6	644.2	244.1	145.9	-113.9	212.2	-148.8	153.8
22/05/2012	76	-124.5	185.4	-439.4	174.4	-571.6	150.4	271.3	153.5	2907.8	648.2	244.3	146.2	-114.8	211.4	-151.0	151.6
23/05/2012	77	-119.5	190.1	-431.4	182.0	-565.7	155.9	277.0	158.8	2928.7	668.1	248.0	149.6	-107.6	218.3	-144.2	158.1
24/05/2012	78	-125.2	184.7	-435.0	178.7	-569.9	152.0	273.8	155.9	2925.5	665.0	245.5	147.3	-110.3	215.6	-148.0	154.5
25/05/2012	79	-122.8	187.0	-432.7	180.8	-568.9	152.9	276.8	158.7	2915.8	655.9	247.1	148.8	-109.4	216.6	-150.2	152.4
26/05/2012	80	-116.5	193.0	-429.3	184.0	-565.5	156.1	278.6	160.3	2936.6	675.5	250.3	151.8	-104.4	221.3	-144.7	157.6
27/05/2012	81	-118.6	191.0	-432.4	181.1	-569.3	152.5	275.4	157.4	2935.7	674.7	247.7	149.4	-107.5	218.3	-147.6	154.9
28/05/2012	82	-107.8	201.3	-420.3	192.6	-559.3	162.0	287.1	168.4	2945.1	683.7	257.2	158.4	-97.4	227.9	-140.1	162.0
29/05/2012	83	-120.8	188.9	-431.8	181.7	-568.9	152.9	277.3	159.1	2928.6	668.0	249.2	150.8	-106.9	218.9	-150.0	152.5
30/05/2012	84	-106.6	202.4	-421.5	191.4	-557.9	163.3	287.3	168.6	2938.3	677.2	259.2	160.3	-98.3	227.1	-142.6	159.6

31/05/2012	85	-116.2	193.3	-429.5	183.8	-566.8	155.1	279.1	160.9	2933.1	672.3	250.2	151.7	-104.6	221.1	-149.3	153.3
1/06/2012	86	-108.5	200.5	-423.2	189.8	-556.8	164.3	287.7	169.0	2935.7	674.7	258.3	159.5	-95.8	229.4	-142.4	159.7
2/06/2012	87	-122.8	187.1	-441.5	172.5	-571.0	150.9	271.4	153.6	2912.9	653.1	244.9	146.7	-112.0	214.1	-157.2	145.7
3/06/2012	88	-116.4	193.1	-437.3	176.4	-567.5	154.2	274.0	156.0	2916.2	656.2	251.7	153.2	-109.1	216.8	-149.5	153.1
4/06/2012	89	-120.8	188.9	-440.7	173.2	-570.3	151.5	269.4	151.7	2913.5	653.7	247.7	149.4	-113.1	213.0	-153.9	148.9
5/06/2012	90	-108.2	200.9	-427.4	185.9	-557.7	163.5	279.9	161.6	2948.4	686.8	255.2	156.5	-100.3	225.1	-143.2	159.0
6/06/2012	91	-119.1	190.5	-436.1	177.5	-565.7	155.9	273.9	155.9	2940.0	678.8	245.5	147.3	-107.0	218.8	-151.4	151.3
7/06/2012	92	-103.8	205.1	-423.3	189.8	-553.6	167.4	285.7	167.1	2959.5	697.3	256.4	157.6	-95.8	229.4	-141.0	161.1
8/06/2012	93	-93.3	215.0	-415.7	196.9	-548.1	172.6	290.9	172.1	2977.1	713.9	266.1	166.8	-90.0	234.9	-130.3	171.3
9/06/2012	94	-94.2	214.2	-414.6	198.0	-549.3	171.5	290.9	172.0	2980.3	717.0	265.8	166.6	-89.0	235.8	-128.8	172.7
10/06/2012	95	-96.5	212.0	-414.8	197.7	-549.8	171.0	292.1	173.2	2976.4	713.3	264.8	165.6	-89.6	235.3	-131.4	170.2
11/06/2012	96	-105.1	203.8	-421.7	191.2	-557.0	164.2	288.8	170.0	2959.4	697.2	260.5	161.5	-94.6	230.5	-139.9	162.1
12/06/2012	97	-107.8	201.2	-424.6	188.4	-558.5	162.7	289.9	171.1	2952.3	690.5	258.2	159.3	-95.0	230.1	-144.0	158.3
13/06/2012	98	-102.6	206.2	-419.4	193.4	-553.6	167.4	293.7	174.6	2954.8	692.9	264.1	164.9	-92.7	232.3	-140.1	162.0
14/06/2012	99	-102.7	206.1	-420.0	192.9	-553.5	167.5	292.6	173.6	2948.9	687.3	264.3	165.1	-94.2	231.0	-141.8	160.3
15/06/2012	100	-110.5	198.7	-428.0	185.2	-559.8	161.5	285.5	166.9	2943.4	682.0	258.9	159.9	-99.5	225.9	-148.4	154.1
16/06/2012	101	-113.6	195.8	-432.7	180.8	-564.5	157.0	280.8	162.5	2941.1	679.9	253.3	154.7	-102.5	223.0	-148.9	153.6
17/06/2012	102	-115.9	193.6	-436.1	177.5	-566.8	154.9	277.1	159.0	2946.7	685.2	248.7	150.3	-104.8	220.9	-151.0	151.6
18/06/2012	103	-95.8	212.6	-414.1	198.4	-548.2	172.5	293.0	174.0	2984.5	721.0	264.3	165.1	-86.8	237.9	-132.5	169.2
19/06/2012	104	-94.9	213.5	-410.1	202.2	-546.7	173.9	293.8	174.8	2993.8	729.8	263.4	164.3	-86.1	238.6	-131.5	170.1
20/06/2012	105	-94.3	214.0	-408.0	204.2	-542.8	177.6	296.6	177.4	2997.2	733.0	265.1	165.8	-83.2	241.3	-129.5	172.0
21/06/2012	106	-85.2	222.7	-405.6	206.5	-538.0	182.2	302.2	182.7	3006.6	741.9	271.8	172.2	-78.3	246.0	-122.3	178.9
22/06/2012	107	-102.4	206.4	-415.2	197.4	-550.2	170.7	292.5	173.5	2994.6	730.5	259.8	160.8	-86.6	238.1	-131.4	170.2
23/06/2012	108	-90.9	217.3	-414.0	198.5	-541.8	178.6	300.2	180.9	3008.4	743.6	266.8	167.5	-79.8	244.6	-124.3	176.9
24/06/2012	109	-87.7	220.3	-436.9	176.8	-541.7	178.6	300.3	180.9	3013.0	748.0	268.5	169.1	-81.0	243.4	-124.2	177.0
25/06/2012	110	-85.9	222.0	-442.2	171.8	-541.5	178.8	301.7	182.3	3014.3	749.2	268.7	169.3	-80.1	244.3	-123.1	178.1
26/06/2012	111	-96.3	212.2	-450.9	163.5	-551.8	169.1	295.3	176.2	3000.4	736.1	261.5	162.5	-85.9	238.8	-129.7	171.8
27/06/2012	112	-96.3	212.2	-449.5	164.8	-550.7	170.2	295.3	176.2	2992.3	728.4	263.0	163.9	-86.6	238.2	-131.9	169.8
28/06/2012	113	-96.5	212.0	-450.5	163.9	-549.7	171.1	296.3	177.1	2994.2	730.1	264.1	164.9	-84.0	240.6	-130.7	170.9
29/06/2012	114	-108.1	200.9	-454.3	160.3	-560.2	161.2	288.7	169.9	2981.4	718.0	255.4	156.6	-90.6	234.3	-142.1	160.1
30/06/2012	115	-108.5	200.6	-452.4	162.1	-559.3	162.0	286.2	167.6	2978.8	715.6	252.8	154.2	-91.7	233.3	-144.2	158.1
1/07/2012	116	-106.4	202.6	-451.4	163.1	-555.9	165.2	287.1	168.5	2994.3	730.2	250.8	152.3	-88.5	236.3	-142.4	159.8
2/07/2012	117	-87.6	220.4	-438.9	174.9	-541.1	179.2	300.0	180.6	3023.8	758.3	264.4	165.2	-76.9	247.4	-127.6	173.8
3/07/2012	118	-82.8	224.9	-437.7	176.1	-537.4	182.8	305.5	185.9	3034.1	768.0	267.9	168.5	-71.1	252.8	-122.0	179.1
4/07/2012	119	-84.2	223.6	-442.2	171.8	-539.0	181.3	305.2	185.6	3037.0	770.7	267.4	168.0	-70.5	253.4	-122.8	178.4
5/07/2012	120	-86.0	221.9	-439.4	174.4	-542.1	178.3	306.5	186.8	3030.0	764.1	266.3	167.0	-69.7	254.1	-125.7	175.6
6/07/2012	121	-95.3	213.1	-444.2	169.9	-549.8	171.0	297.6	178.4	3015.0	749.9	259.3	160.3	-75.7	248.5	-134.1	167.6

7/07/2012	122	-93.5	214.8	-442.8	171.2	-548.8	171.9	297.7	178.4	3015.9	750.7	258.2	159.3	-74.6	249.5	-135.0	166.8
8/07/2012	123	-105.1	203.8	-449.5	164.9	-560.0	161.3	281.6	163.2	3000.0	735.7	247.2	148.9	-84.8	239.8	-149.7	152.9
9/07/2012	124	-86.6	221.3	-430.0	183.3	-544.0	176.5	296.7	177.5	3016.3	751.1	265.3	166.1	-70.8	253.1	-131.6	170.0
10/07/2012	125	-92.7	215.6	-435.3	178.4	-549.3	171.5	297.3	178.1	3008.9	744.1	262.4	163.3	-76.3	247.9	-134.2	167.5
11/07/2012	126	-104.1	204.7	-445.1	169.1	-557.0	164.2	292.0	173.1	2998.0	733.7	256.1	157.4	-82.0	242.5	-139.3	162.7
12/07/2012	127	-93.4	214.9	-427.9	185.3	-548.2	172.5	303.3	183.8	3009.5	744.7	263.7	164.6	-73.1	251.0	-133.7	168.1
13/07/2012	128	-99.2	209.4	-424.6	188.4	-553.1	167.9	307.4	187.6	3000.3	736.0	262.0	162.9	-75.1	249.0	-136.4	165.5
14/07/2012	129	-115.5	194.0	-453.3	161.3	-567.4	154.3	294.4	175.4	2983.3	719.8	241.2	143.2	-88.6	236.2	-149.4	153.2
15/07/2012	130	-114.4	195.0	-450.1	164.3	-564.9	156.7	294.3	175.3	3001.3	736.9	240.3	142.3	-86.5	238.2	-144.9	157.4
16/07/2012	131	-87.9	220.2	-432.6	180.8	-543.8	176.7	316.7	196.5	3039.7	773.3	260.3	161.3	-66.4	257.2	-123.4	177.8
17/07/2012	132	-91.0	217.2	-448.5	165.9	-549.4	171.3	312.6	192.6	3035.2	769.0	255.6	156.8	-69.7	254.1	-128.2	173.3
18/07/2012	133	-96.6	211.8	-453.0	161.6	-554.4	166.6	302.7	183.3	3035.0	768.9	249.1	150.7	-72.3	251.7	-133.3	168.5
19/07/2012	134	-93.7	214.6	-433.7	179.8	-550.0	170.8	292.6	173.6	3044.4	777.7	250.9	152.4	-69.4	254.4	-129.8	171.7
20/07/2012	135	-83.3	224.5	-417.7	195.0	-533.1	186.9	289.7	170.9	3056.1	788.9	260.2	161.3	-61.8	261.7	-119.1	181.9
21/07/2012	136	-95.4	213.0	-422.6	190.4	-545.4	175.2	284.9	166.3	3039.8	773.4	250.2	151.8	-69.2	254.6	-132.7	169.0
22/07/2012	137	-98.9	209.7	-425.9	187.2	-550.4	170.5	298.1	178.8	3033.1	767.1	246.9	148.7	-71.5	252.5	-138.0	164.0
23/07/2012	138	-101.5	207.2	-434.5	179.1	-555.9	165.2	300.1	180.8	3027.9	762.1	243.0	144.9	-73.9	250.1	-147.2	155.2
24/07/2012	139	-104.9	204.0	-440.2	173.7	-553.9	167.2	301.7	182.3	3018.5	753.2	245.4	147.2	-77.2	247.1	-146.4	156.0
25/07/2012	140	-103.1	205.8	-440.4	173.5	-552.9	168.1	302.7	183.2	3012.2	747.2	249.6	151.2	-77.8	246.4	-142.3	159.9
26/07/2012	141	-101.9	206.8	-441.0	173.0	-551.7	169.2	302.0	182.5	3020.9	755.5	247.4	149.1	-74.4	249.7	-137.1	164.8
27/07/2012	142	-101.0	207.7	-452.9	161.6	-550.9	169.9	298.8	179.5	3033.2	767.1	245.5	147.3	-75.1	249.0	-131.1	170.5
28/07/2012	143	-97.1	211.4	-454.7	160.0	-547.5	173.2	303.7	184.1	3048.8	782.0	248.6	150.3	-71.4	252.6	-122.6	178.6
29/07/2012	144	-95.2	213.2	-448.4	165.9	-546.9	173.7	308.0	188.2	3055.6	788.4	252.2	153.7	-67.7	256.1	-117.8	183.1
30/07/2012	145	-88.9	219.1	-445.8	168.4	-540.8	179.5	312.6	192.6	3064.3	796.7	261.8	162.7	-64.6	259.0	-108.5	192.0
31/07/2012	146	-83.5	224.3	-441.7	172.3	-536.4	183.7	317.7	197.4	3069.6	801.6	274.8	175.1	-59.6	263.8	-92.1	207.5
1/08/2012	147	-80.3	227.3	-440.8	173.1	-534.8	185.2	318.8	198.5	3072.4	804.3	281.0	181.0	-57.6	265.6	-70.7	227.7
2/08/2012	148	-80.7	226.9	-441.6	172.3	-535.5	184.6	324.9	204.3	3076.9	808.6	285.1	184.9	-56.8	266.4	-43.8	253.3
3/08/2012	149	-80.0	227.6	-441.7	172.3	-536.2	183.9	323.9	203.3	3077.7	809.3	286.8	186.5	-56.7	266.4	-36.7	260.0
4/08/2012	150	-87.7	220.3	-446.5	167.7	-542.1	178.3	315.2	195.1	3076.9	808.6	274.0	174.3	-63.0	260.5	-40.5	256.4
5/08/2012	151	-95.3	213.1	-448.5	165.9	-544.2	176.3	312.5	192.5	3076.5	808.2	262.0	163.0	-63.9	259.6	-39.2	257.6
6/08/2012	152	-96.6	211.9	-447.9	166.4	-541.8	178.6	314.6	194.5	3079.9	811.4	254.7	156.0	-62.3	261.1	-31.1	265.3
7/08/2012	153	-75.7	231.6	-434.9	178.7	-523.1	196.3	328.9	208.1	3099.5	830.0	265.0	165.7	-49.5	273.3	-13.0	282.5
8/08/2012	154	-77.3	230.2	-436.0	177.7	-525.4	194.1	326.3	205.6	3094.0	824.8	263.0	163.8	-51.5	271.4	20.8	314.5
9/08/2012	155	-88.4	219.7	-440.0	173.9	-530.2	189.5	321.5	201.0	3087.4	818.6	247.8	149.4	-56.0	267.2	33.8	326.8
10/08/2012	156	-78.9	228.6	-437.1	176.7	-525.4	194.1	327.1	206.4	3099.8	830.3	253.4	154.7	-51.9	271.0	43.7	336.2
11/08/2012	157	-97.2	211.3	-448.7	165.6	-539.2	181.1	315.9	195.8	3075.8	807.5	244.0	145.9	-62.0	261.5	29.0	322.3
12/08/2012	158	-108.8	200.3	-460.0	154.9	-547.0	173.6	307.2	187.5	3054.1	787.0	237.8	140.0	-68.9	254.9	5.0	299.5

13/08/2012	159	-98.8	209.8	-454.8	159.9	-544.1	176.4	309.0	189.2	3065.6	797.8	245.6	147.4	-67.6	256.1	6.8	301.2
14/08/2012	160	-88.3	219.7	-445.4	168.8	-535.4	184.6	319.0	198.7	3077.9	809.5	255.0	156.3	-59.3	264.0	-1.9	292.9
15/08/2012	161	-98.9	209.6	-449.3	165.1	-541.1	179.3	311.8	191.8	3078.5	810.1	238.6	140.8	-62.1	261.4	-35.3	261.3
16/08/2012	162	-95.8	212.6	-444.1	170.0	-538.7	181.6	315.9	195.7	3086.5	817.6	240.8	142.8	-59.2	264.1	-52.3	245.2
17/08/2012	163	-100.3	208.3	-449.9	164.5	-543.3	177.1	314.6	194.5	3087.1	818.2	234.7	137.1	-59.8	263.6	-55.9	241.7
18/08/2012	164	-102.4	206.4	-453.6	161.0	-546.2	174.4	312.6	192.6	3088.3	819.4	227.0	129.7	-61.7	261.7	-44.0	253.1
19/08/2012	165	-99.4	209.2	-450.7	163.7	-546.8	173.8	315.0	194.8	3092.9	823.7	232.3	134.7	-59.4	263.9	-10.6	284.7
20/08/2012	166	-85.4	222.5	-441.7	172.3	-539.9	180.4	321.3	200.9	3103.0	833.3	242.6	144.6	-54.7	268.4	36.2	329.1
21/08/2012	167	-95.8	212.6	-447.5	166.8	-547.9	172.8	314.8	194.7	3091.3	822.2	238.8	141.0	-60.3	263.1	56.0	347.8
22/08/2012	168	-104.5	204.4	-449.8	164.6	-552.6	168.3	311.7	191.7	3082.0	813.4	235.6	137.9	-60.7	262.7	65.9	357.2
23/08/2012	169	-93.9	214.5	-444.6	169.6	-548.2	172.5	315.0	194.8	3075.8	807.5	256.5	157.7	-56.7	266.5	108.1	397.3
24/08/2012	170	-101.3	207.4	-454.9	159.7	-556.6	164.5	304.0	184.4	3067.3	799.5	245.1	146.9	-65.7	257.9	133.6	421.4
25/08/2012	171	-108.4	200.7	-458.0	156.8	-561.7	159.7	297.9	178.6	3075.7	807.4	230.0	132.6	-70.1	253.8	130.2	418.2
26/08/2012	172	-106.1	202.9	-450.8	163.7	-555.7	165.5	305.0	185.4	3092.4	823.3	231.1	133.6	-61.8	261.6	141.7	429.1
27/08/2012	173	-91.7	216.5	-438.8	175.0	-545.1	175.5	316.4	196.2	3104.9	835.1	241.8	143.8	-53.8	269.3	159.7	446.1
28/08/2012	174	-100.3	208.3	-445.9	168.3	-551.6	169.3	311.2	191.3	3092.2	823.0	243.0	144.9	-58.9	264.4	172.4	458.2
29/08/2012	175	-102.6	206.2	-447.4	166.8	-552.7	168.2	313.6	193.5	3084.1	815.3	250.7	152.2	-59.1	264.2	190.4	475.2
30/08/2012	176	-98.0	210.5	-446.9	167.3	-553.1	167.8	315.4	195.3	3084.2	815.5	255.7	156.9	-57.6	265.6	238.0	520.3
31/08/2012	177	-98.2	210.3	-445.7	168.4	-548.9	171.8	312.3	192.3	3100.2	830.6	240.2	142.2	-59.9	263.4	245.3	527.3
1/09/2012	178	-81.9	225.8	-433.5	180.0	-538.3	181.9	327.5	206.7	3119.4	848.8	248.3	150.0	-50.1	272.7	257.4	538.7
2/09/2012	179	-91.0	217.2	-436.8	176.9	-542.8	177.6	325.7	205.0	3112.4	842.2	246.7	148.4	-52.1	270.8	250.3	532.0
3/09/2012	180	-81.0	226.7	-429.4	183.9	-537.4	182.8	332.3	211.3	3115.9	845.6	252.4	153.8	-47.1	275.6	241.8	524.0
4/09/2012	181	-86.2	221.7	-438.8	175.0	-546.3	174.3	326.8	206.0	3107.7	837.7	237.5	139.7	-55.0	268.1	233.3	515.9
5/09/2012	182	-91.1	217.1	-442.3	171.7	-551.0	169.9	325.7	205.1	3110.0	840.0	233.9	136.3	-60.6	262.7	214.5	498.0
6/09/2012	183	-79.6	228.0	-426.6	186.6	-537.9	182.3	343.4	221.7	3129.3	858.3	248.8	150.4	-47.9	274.8	231.8	514.4
7/09/2012	184	-74.5	232.8	-418.0	194.8	-529.7	190.0	362.1	239.5	3143.8	871.9	242.3	144.3	-39.5	282.8	243.6	525.7
8/09/2012	185	-75.3	232.0	-415.9	196.7	-528.7	191.0	371.5	248.4	3145.5	873.6	242.5	144.4	-35.5	286.6	246.7	528.6
9/09/2012	186	-89.3	218.8	-425.3	187.8	-538.4	181.8	366.3	243.5	3133.6	862.3	240.1	142.2	-42.5	280.0	235.5	518.0
10/09/2012	187	-90.6	217.6	-430.5	182.9	-542.8	177.6	364.9	242.1	3121.3	850.7	246.7	148.4	-45.7	276.9	227.4	510.4
11/09/2012	188	-84.3	223.6	-430.6	182.8	-542.0	178.4	368.0	245.1	3111.7	841.5	253.7	155.0	-44.3	278.2	230.8	513.5
12/09/2012	189	-84.1	223.7	-429.7	183.6	-540.1	180.2	372.9	249.8	3102.8	833.1	256.6	157.8	-42.1	280.3	232.9	515.5
13/09/2012	190	-95.1	213.3	-439.8	174.0	-548.5	172.3	364.8	242.1	3084.1	815.4	255.4	156.6	-50.5	272.3	225.4	508.4
14/09/2012	191	-80.9	226.8	-429.6	183.8	-538.6	181.6	374.2	251.0	3104.0	834.2	257.6	158.8	-43.9	278.6	240.1	522.3
15/09/2012	192	-96.9	211.5	-436.5	177.2	-545.7	174.9	366.0	243.3	3104.3	834.5	246.2	148.0	-49.4	273.4	232.0	514.6
16/09/2012	193	-106.4	202.6	-444.5	169.6	-552.8	168.2	361.2	238.7	3094.3	825.1	246.6	148.3	-44.5	278.1	225.0	508.1
17/09/2012	194	-102.2	206.5	-448.6	165.7	-552.6	168.3	363.0	240.3	3084.1	815.4	252.7	154.1	-36.3	285.8	224.2	507.2
18/09/2012	195	-99.7	208.9	-444.9	169.2	-554.0	167.1	365.0	242.3	3075.0	806.7	253.7	155.1	-30.4	291.4	229.2	512.0

19/09/2012	196	-97.4	211.1	-442.1	171.9	-554.4	166.6	364.1	241.4	3075.5	807.2	253.8	155.2	-24.1	297.4	229.9	512.7
20/09/2012	197	-97.2	211.3	-441.8	172.1	-556.2	164.9	365.0	242.3	3076.1	807.8	255.2	156.5	-17.4	303.8	229.0	511.8
21/09/2012	198	-84.4	223.4	-434.0	179.6	-547.5	173.2	371.8	248.7	3078.3	809.9	265.3	166.0	-12.7	308.2	239.2	521.5
22/09/2012	199	-89.4	218.7	-438.5	175.3	-550.5	170.3	366.2	243.4	3072.8	804.7	259.0	160.1	-31.9	290.0	236.2	518.7
23/09/2012	200	-94.5	213.9	-442.0	172.0	-553.9	167.1	363.8	241.1	3066.5	798.7	256.0	157.2	-52.6	270.4	234.9	517.4
24/09/2012	201	-81.2	226.5	-431.2	182.3	-541.9	178.4	372.5	249.4	3084.9	816.1	265.5	166.2	-41.2	281.1	255.2	536.7
25/09/2012	202	-78.6	228.9	-428.7	184.6	-541.1	179.3	373.0	249.8	3094.8	825.5	263.4	164.2	-44.1	278.4	261.9	543.0
26/09/2012	203	-79.6	228.0	-432.1	181.4	-546.1	174.5	369.8	246.8	3088.6	819.7	258.9	160.0	-47.0	275.6	256.2	537.6
27/09/2012	204	-77.7	229.8	-430.2	183.2	-543.5	177.0	371.5	248.4	3086.3	817.5	263.2	164.1	-45.1	277.5	256.7	538.1
28/09/2012	205	-85.2	222.7	-436.4	177.3	-549.4	171.4	366.9	244.1	3076.1	807.8	258.1	159.2	-50.2	272.7	250.9	532.6
29/09/2012	206	-91.8	216.4	-442.5	171.5	-553.2	167.8	361.3	238.8	3063.9	796.2	255.2	156.5	-55.8	267.3	245.8	527.8
30/09/2012	207	-87.4	220.6	-439.7	174.2	-549.6	171.2	361.8	239.2	3082.5	813.9	251.8	153.3	-53.2	269.8	247.7	529.5
1/10/2012	208	-80.3	227.3	-430.7	182.7	-542.7	177.7	369.2	246.3	3102.8	833.1	257.3	158.5	-43.7	278.8	257.4	538.7
2/10/2012	209	-92.9	215.4	-440.6	173.3	-553.7	167.3	360.1	237.6	3093.0	823.9	247.1	148.8	-52.2	270.7	247.1	529.0
3/10/2012	210	-85.0	222.8	-431.0	182.4	-545.4	175.2	370.2	247.2	3101.2	831.6	253.8	155.1	-42.5	279.9	253.5	535.0
4/10/2012	211	-80.3	227.3	-431.5	181.9	-547.8	172.9	370.5	247.5	3100.1	830.5	252.2	153.6	-42.3	280.2	253.2	534.7
5/10/2012	212	-77.6	229.9	-428.5	184.7	-545.7	174.9	370.2	247.2	3108.5	838.5	257.2	158.4	-41.7	280.7	255.9	537.3
6/10/2012	213	-80.3	227.3	-429.6	183.7	-545.5	175.0	372.3	249.2	3094.3	825.0	259.3	160.3	-43.5	279.0	253.8	535.4
7/10/2012	214	-82.6	225.1	-430.3	183.0	-543.0	177.5	372.8	249.6	3087.1	818.2	259.0	160.1	-42.3	280.1	253.1	534.7
8/10/2012	215	-80.9	226.7	-427.7	185.5	-542.2	178.2	373.3	250.2	3098.2	828.7	258.1	159.2	-40.4	282.0	252.5	534.1
9/10/2012	216	-72.4	234.8	-421.4	191.5	-539.3	181.0	381.0	257.4	3108.7	838.7	259.4	160.5	-33.1	288.9	258.6	539.9
10/10/2012	217	-68.3	238.7	-419.4	193.4	-538.2	182.0	382.0	258.4	3117.1	846.7	260.2	161.2	-31.2	290.7	258.1	539.4
11/10/2012	218	-77.8	229.6	-425.7	187.4	-543.5	177.0	376.1	252.8	3108.1	838.1	256.5	157.7	-35.9	286.2	253.2	534.8
12/10/2012	219	-41.6	264.0	-397.5	214.1	-515.4	203.6	399.9	275.3	3137.1	865.6	281.5	181.5	-15.4	305.6	277.3	557.6
13/10/2012	220	-52.6	253.6	-406.2	205.9	-526.8	192.8	390.0	266.0	3129.0	858.0	267.9	168.5	-24.0	297.5	266.7	547.6
14/10/2012	221	-69.4	237.6	-418.9	193.8	-538.0	182.2	381.0	257.4	3113.9	843.7	252.7	154.1	-32.1	289.8	252.8	534.4
15/10/2012	222	-72.5	234.7	-420.4	192.4	-539.1	181.2	383.5	259.8	3114.4	844.1	252.5	153.9	-31.5	290.4	252.4	534.0
16/10/2012	223	-73.4	233.8	-426.6	186.6	-544.5	176.0	378.0	254.6	3108.4	838.4	247.3	149.0	-38.1	284.1	250.6	532.3
17/10/2012	224	-86.5	221.5	-437.0	176.7	-554.7	166.4	367.1	244.2	3100.7	831.1	240.6	142.7	-48.7	274.1	244.5	526.5
18/10/2012	225	-85.4	222.5	-437.7	176.1	-554.3	166.7	368.4	245.4	3096.7	827.4	243.5	145.3	-47.7	275.0	241.9	524.0
19/10/2012	226	-68.9	238.1	-423.7	189.3	-538.3	181.9	381.0	257.4	3101.4	831.7	266.0	166.7	-36.3	285.8	257.1	538.4
20/10/2012	227	-76.3	231.1	-430.2	183.1	-541.7	178.7	375.0	251.7	3082.3	813.7	262.4	163.3	-45.1	277.4	247.2	529.1
21/10/2012	228	-87.2	220.8	-442.5	171.5	-552.8	168.2	363.6	241.0	3061.1	793.6	252.9	154.3	-57.3	265.9	236.4	518.8
22/10/2012	229	-86.5	221.4	-442.2	171.8	-552.1	168.8	362.4	239.8	3065.2	797.5	253.2	154.6	-56.9	266.3	240.8	523.0
23/10/2012	230	-73.5	233.8	-430.4	183.0	-543.2	177.3	368.6	245.7	3089.1	820.1	257.2	158.4	-48.6	274.2	250.8	532.5
24/10/2012	231	-68.3	238.7	-422.5	190.5	-534.2	185.8	378.9	255.5	3104.6	834.8	257.6	158.7	-38.2	284.0	258.2	539.5
25/10/2012	232	-87.2	220.8	-438.8	175.0	-550.6	170.3	363.9	241.2	3083.7	815.0	243.1	145.0	-52.7	270.3	241.7	523.8

26/10/2012	233	-89.5	218.6	-440.5	173.4	-552.1	168.8	363.1	240.4	3078.5	810.1	250.8	152.3	-53.5	269.5	241.3	523.5
27/10/2012	234	-76.8	230.6	-429.7	183.6	-542.4	178.0	371.8	248.7	3085.7	816.9	258.6	159.7	-44.8	277.8	250.1	531.8
28/10/2012	235	-75.5	231.9	-430.0	183.3	-543.4	177.1	369.6	246.6	3092.1	823.0	250.1	151.6	-45.7	276.9	248.4	530.2
29/10/2012	236	-81.3	226.4	-432.0	181.4	-545.6	175.0	367.7	244.9	3091.9	822.7	242.8	144.7	-47.1	275.6	244.6	526.6
30/10/2012	237	-87.8	220.2	-436.5	177.2	-550.1	170.7	364.8	242.1	3083.9	815.2	247.0	148.7	-51.3	271.6	240.1	522.4
31/10/2012	238	-82.4	225.3	-436.3	177.4	-548.2	172.6	366.5	243.7	3078.6	810.1	259.5	160.5	-51.0	271.9	246.3	528.2
1/11/2012	239	-58.6	247.9	-417.3	195.4	-530.4	189.4	384.1	260.4	3091.0	822.0	278.1	178.2	-36.4	285.7	263.2	544.2
2/11/2012	240	-68.0	239.0	-424.3	188.8	-537.5	182.7	374.3	251.1	3095.8	826.5	265.3	166.1	-41.8	280.6	258.8	540.1

Table E.11 Steel strain for slab D-SCC-a

Slab D-SCC-a		STEEL STRAIN BY SG															
		1		2		3		4		5		6		7		8	
Date	Age	Reading	Strain	Reading	Strain	Reading	Strain	Reading	Strain	Reading	Strain	Reading	Strain	Reading	Strain	Reading	Strain
4/04/2012	14	-1399.7		-953.7		-705.4		-1269.3		-923.6		-1542.3		-625.0		-1508.1	
5/04/2012	15	-1326.0	69.9	-911.8	39.7	-677.4	26.6	-1211.7	54.6	-849.5	70.3	-1532.0	9.8	-605.7	18.3	-1509.1	-0.9
6/04/2012	16	-1338.4	58.1	-927.0	25.3	-687.6	16.9	-1218.3	48.3	-855.1	65.0	-1539.7	2.5	-615.8	8.8	-1528.6	-19.4
7/04/2012	17	-1324.9	70.9	-922.2	29.8	-670.3	33.3	-1199.6	66.1	-837.1	82.1	-1523.5	17.9	-600.9	22.8	-1521.6	-12.8
8/04/2012	18	-1311.3	83.8	-910.8	40.6	-652.8	49.9	-1182.0	82.8	-817.5	100.6	-1504.6	35.8	-600.5	23.2	-1524.6	-15.7
9/04/2012	19	-1317.1	78.3	-910.6	40.8	-659.6	43.5	-1186.2	78.8	-821.0	97.3	-1501.9	38.3	-603.2	20.7	-1531.8	-22.4
10/04/2012	20	-1278.2	115.2	-867.4	81.8	-623.6	77.6	-1146.8	116.2	-785.5	130.9	-1466.4	72.0	-581.8	41.0	-1494.0	13.4
11/04/2012	21	-1265.9	126.8	-872.1	77.3	-610.6	89.9	-1134.4	127.9	-774.9	141.0	-1454.9	82.9	-580.8	41.9	-1478.9	27.7
12/04/2012	22	-1259.3	133.1	-882.3	67.6	-603.6	96.5	-1128.2	133.8	-767.2	148.3	-1444.7	92.6	-579.6	43.1	-1465.5	40.4
13/04/2012	23	-1256.3	135.9	-873.4	76.1	-595.2	104.5	-1112.8	148.4	-755.7	159.2	-1435.6	101.2	-554.4	67.0	-1475.8	30.6
16/04/2012	26	-1252.4	139.6	-872.1	77.3	-588.5	110.8	-1107.0	153.9	-752.3	162.5	-1428.2	108.2	-536.7	83.7	-1521.5	-12.7
17/04/2012	27	-1288.6	105.3	-896.6	54.1	-622.1	79.0	-1148.2	114.8	-793.5	123.4	-1468.1	70.4	-570.4	51.8	-1527.1	-18.0
18/04/2012	28	-1287.8	106.1	-889.7	60.6	-618.4	82.5	-1148.1	114.9	-789.8	126.9	-1459.0	79.0	-567.1	54.9	-1519.5	-10.8
19/04/2012	29	-1278.4	115.0	-869.3	80.0	-609.0	91.5	-1137.5	124.9	-788.2	128.4	-1451.2	86.3	-562.1	59.7	-1498.5	9.1
20/04/2012	30	-1278.0	115.4	-867.2	81.9	-609.8	90.7	-1136.6	125.8	-789.6	127.0	-1450.9	86.7	-562.8	59.0	-1498.2	9.4
21/04/2012	31	-1290.4	103.6	-876.4	73.2	-626.9	74.5	-1148.6	114.4	-803.4	114.0	-1463.4	74.9	-572.8	49.5	-1511.1	-2.9
22/04/2012	32	-1302.5	92.2	-876.9	72.8	-632.3	69.3	-1151.5	111.7	-808.4	109.2	-1466.6	71.8	-575.8	46.7	-1514.3	-5.9
23/04/2012	33	-1296.7	97.7	-868.4	80.9	-621.9	79.2	-1141.8	120.8	-801.5	115.8	-1462.0	76.1	-571.7	50.6	-1508.7	-0.6
24/04/2012	34	-1276.4	116.9	-853.5	95.0	-603.9	96.3	-1123.3	138.4	-777.7	138.4	-1448.3	89.1	-559.5	62.2	-1495.3	12.1
25/04/2012	35	-1301.3	93.3	-883.5	66.5	-632.6	69.0	-1146.5	116.4	-802.8	114.6	-1480.8	58.3	-587.7	35.4	-1529.9	-20.7
26/04/2012	36	-1299.3	95.2	-903.0	48.1	-622.0	79.1	-1143.5	119.3	-804.1	113.3	-1476.0	62.9	-586.4	36.7	-1519.7	-11.0
27/04/2012	37	-1284.6	109.1	-874.6	75.0	-606.4	93.9	-1123.2	138.5	-780.7	135.5	-1456.1	81.7	-566.5	55.5	-1502.8	5.1
28/04/2012	38	-1286.6	107.2	-869.6	79.7	-607.3	93.0	-1124.4	137.4	-780.9	135.3	-1457.2	80.7	-562.5	59.3	-1498.7	8.9
29/04/2012	39	-1294.7	99.5	-877.5	72.2	-618.5	82.5	-1134.4	127.9	-791.0	125.8	-1464.4	73.8	-579.7	42.9	-1513.9	-5.5
30/04/2012	40	-1286.4	107.4	-872.1	77.4	-610.8	89.8	-1129.8	132.2	-791.3	125.4	-1465.1	73.2	-582.9	39.9	-1515.4	-7.0
1/05/2012	41	-1291.2	102.8	-881.1	68.8	-613.5	87.1	-1132.2	130.0	-795.5	121.5	-1466.3	72.0	-585.0	37.9	-1514.1	-5.7
2/05/2012	42	-1286.8	107.1	-873.5	76.0	-608.8	91.6	-1121.9	139.7	-783.6	132.8	-1455.9	82.0	-575.2	47.2	-1502.9	4.9
3/05/2012	43	-1287.2	106.6	-874.1	75.4	-610.1	90.4	-1124.1	137.7	-785.1	131.3	-1457.3	80.6	-575.4	47.1	-1504.6	3.3
4/05/2012	44	-1290.1	103.9	-879.9	69.9	-613.6	87.1	-1122.9	138.8	-788.3	128.3	-1465.4	72.9	-582.2	40.7	-1515.2	-6.7
5/05/2012	45	-1306.7	88.2	-894.1	56.4	-626.7	74.6	-1138.7	123.8	-795.6	121.3	-1479.8	59.3	-592.0	31.3	-1530.7	-21.4
6/05/2012	46	-1311.3	83.8	-902.0	49.0	-631.2	70.3	-1138.8	123.7	-794.3	122.6	-1481.1	58.0	-593.3	30.1	-1529.8	-20.5
7/05/2012	47	-1296.2	98.2	-885.6	64.6	-614.7	86.0	-1121.6	140.0	-783.0	133.3	-1465.6	72.7	-583.4	39.5	-1512.0	-3.7

8/05/2012	48	-1278.4	115.0	-872.3	77.1	-596.9	102.9	-1104.3	156.4	-769.1	146.5	-1455.1	82.6	-574.2	48.2	-1500.3	7.4
9/05/2012	49	-1275.1	118.1	-873.0	76.5	-594.5	105.1	-1101.9	158.7	-766.8	148.7	-1453.8	83.9	-573.7	48.7	-1499.9	7.7
10/05/2012	50	-1279.0	114.5	-875.0	74.6	-598.7	101.1	-1104.9	155.8	-770.5	145.2	-1454.0	83.8	-577.8	44.8	-1502.6	5.2
11/05/2012	51	-1288.2	105.7	-881.9	68.0	-606.1	94.2	-1111.1	150.0	-778.8	137.3	-1456.3	81.6	-579.8	42.9	-1504.5	3.4
12/05/2012	52	-1283.3	110.4	-871.6	77.8	-601.8	98.3	-1103.6	157.1	-768.6	146.9	-1450.8	86.8	-574.2	48.2	-1501.7	6.0
13/05/2012	53	-1295.5	98.8	-888.0	62.3	-610.7	89.8	-1113.7	147.5	-783.9	132.5	-1468.8	69.7	-588.9	34.2	-1515.7	-7.2
14/05/2012	54	-1275.5	117.7	-875.7	74.0	-592.7	106.9	-1096.9	163.5	-768.8	146.8	-1450.4	87.1	-569.9	52.2	-1498.2	9.4
15/05/2012	55	-1275.8	117.5	-876.5	73.2	-594.1	105.6	-1095.5	164.7	-767.2	148.3	-1451.6	86.0	-572.2	50.1	-1497.9	9.7
16/05/2012	56	-1277.3	116.0	-889.4	61.0	-592.4	107.1	-1098.0	162.4	-769.1	146.4	-1450.6	86.9	-575.7	46.7	-1491.5	15.7
17/05/2012	57	-1262.8	129.8	-859.7	89.1	-585.1	114.1	-1080.7	178.8	-745.7	168.7	-1432.8	103.8	-559.2	62.4	-1475.3	31.1
18/05/2012	58	-1271.3	121.8	-869.0	80.3	-593.8	105.8	-1090.4	169.6	-755.4	159.5	-1440.5	96.5	-565.9	56.0	-1489.9	17.2
19/05/2012	59	-1278.9	114.5	-875.2	74.4	-596.5	103.3	-1097.9	162.5	-764.0	151.4	-1447.5	89.9	-571.0	51.2	-1490.9	16.3
20/05/2012	60	-1281.0	112.6	-877.2	72.5	-601.0	99.0	-1098.1	162.3	-761.9	153.3	-1449.1	88.4	-576.2	46.3	-1496.0	11.5
21/05/2012	61	-1282.7	110.9	-885.0	65.1	-602.5	97.6	-1101.4	159.2	-768.2	147.3	-1449.2	88.3	-575.3	47.2	-1491.9	15.4
22/05/2012	62	-1278.4	115.0	-873.7	75.8	-596.6	103.2	-1095.6	164.7	-762.5	152.7	-1446.4	90.9	-573.6	48.7	-1492.8	14.5
23/05/2012	63	-1275.7	117.6	-881.8	68.2	-592.2	107.4	-1087.4	172.5	-762.0	153.2	-1444.6	92.7	-575.0	47.4	-1492.2	15.0
24/05/2012	64	-1282.5	111.2	-895.3	55.4	-597.9	102.0	-1093.2	166.9	-770.3	145.4	-1447.9	89.6	-580.1	42.5	-1493.8	13.6
25/05/2012	65	-1278.3	115.1	-885.7	64.4	-592.1	107.4	-1092.2	167.9	-765.0	150.4	-1440.5	96.5	-574.0	48.4	-1486.5	20.5
26/05/2012	66	-1279.3	114.2	-882.4	67.6	-593.9	105.7	-1091.4	168.6	-766.3	149.1	-1444.9	92.4	-576.6	45.9	-1491.2	16.0
27/05/2012	67	-1284.3	109.4	-893.5	57.1	-597.0	102.8	-1096.7	163.7	-771.3	144.4	-1452.0	85.7	-582.7	40.1	-1495.1	12.3
28/05/2012	68	-1270.4	122.6	-870.4	78.9	-584.3	114.8	-1084.0	175.6	-755.3	159.6	-1435.1	101.7	-570.4	51.8	-1480.6	26.0
29/05/2012	69	-1286.3	107.5	-883.7	66.4	-597.3	102.5	-1096.7	163.6	-766.0	149.4	-1448.4	89.1	-579.9	42.8	-1492.1	15.1
30/05/2012	70	-1273.4	119.7	-870.0	79.4	-583.0	116.1	-1083.8	175.9	-751.9	162.8	-1435.6	101.2	-568.1	54.0	-1479.6	27.0
31/05/2012	71	-1284.2	109.5	-881.1	68.8	-593.7	105.9	-1093.8	166.4	-764.0	151.3	-1445.4	91.9	-579.2	43.4	-1489.0	18.1
1/06/2012	72	-1274.3	118.9	-876.6	73.0	-581.3	117.7	-1084.2	175.5	-753.1	161.7	-1434.3	102.4	-567.6	54.4	-1477.5	29.0
2/06/2012	73	-1289.9	104.1	-884.2	65.8	-599.1	100.8	-1098.3	162.1	-767.8	147.7	-1447.7	89.7	-581.3	41.4	-1492.6	14.7
3/06/2012	74	-1285.5	108.2	-877.2	72.5	-592.3	107.2	-1091.5	168.6	-761.5	153.7	-1442.6	94.5	-573.6	48.8	-1488.0	19.0
4/06/2012	75	-1288.4	105.5	-877.9	71.8	-595.1	104.5	-1094.2	166.0	-762.8	152.5	-1444.2	93.1	-577.5	45.0	-1492.1	15.2
5/06/2012	76	-1275.5	117.8	-872.8	76.7	-585.7	113.5	-1080.8	178.7	-749.3	165.3	-1434.8	101.9	-568.8	53.3	-1483.6	23.2
6/06/2012	77	-1288.6	105.4	-886.8	63.4	-597.2	102.6	-1093.3	166.9	-762.3	153.0	-1445.7	91.6	-583.0	39.9	-1494.6	12.8
7/06/2012	78	-1272.5	120.6	-869.0	80.3	-582.9	116.2	-1074.5	184.6	-745.4	168.9	-1429.3	107.2	-568.1	54.0	-1478.9	27.6
8/06/2012	79	-1269.1	123.8	-870.5	78.9	-581.9	117.1	-1067.6	191.2	-736.2	177.6	-1429.7	106.8	-562.5	59.3	-1477.5	29.0
9/06/2012	80	-1269.4	123.5	-876.4	73.2	-581.3	117.7	-1069.3	189.6	-738.9	175.1	-1428.5	107.9	-564.2	57.7	-1477.3	29.2
10/06/2012	81	-1267.9	124.9	-875.1	74.5	-579.0	119.8	-1070.2	188.7	-741.9	172.2	-1429.4	107.1	-564.4	57.5	-1474.5	31.8
11/06/2012	82	-1274.3	118.9	-880.6	69.3	-584.6	114.6	-1078.5	180.9	-752.2	162.5	-1436.3	100.5	-572.1	50.2	-1477.9	28.7
12/06/2012	83	-1276.3	117.0	-888.1	62.2	-584.5	114.6	-1079.8	179.6	-751.7	163.0	-1436.5	100.3	-570.9	51.4	-1476.3	30.1
13/06/2012	84	-1271.5	121.6	-873.3	76.2	-580.7	118.2	-1074.5	184.6	-743.3	171.0	-1430.7	105.8	-562.9	58.9	-1470.6	35.6

14/06/2012	85	-1271.3	121.7	-868.4	80.9	-577.0	121.7	-1071.9	187.1	-740.5	173.6	-1427.0	109.4	-560.5	61.2	-1467.2	38.8
15/06/2012	86	-1275.6	117.6	-860.6	88.2	-580.4	118.5	-1074.7	184.4	-743.8	170.5	-1431.2	105.4	-566.8	55.2	-1471.7	34.5
16/06/2012	87	-1281.5	112.1	-866.2	83.0	-587.2	112.1	-1082.0	177.5	-749.2	165.3	-1438.7	98.2	-573.9	48.5	-1477.7	28.8
17/06/2012	88	-1289.7	104.3	-881.2	68.7	-598.6	101.3	-1088.6	171.3	-754.8	160.0	-1448.6	88.9	-580.3	42.4	-1488.9	18.2
18/06/2012	89	-1268.2	124.7	-871.4	78.0	-576.4	122.3	-1066.1	192.6	-734.1	179.7	-1430.0	106.5	-564.7	57.2	-1472.7	33.5
19/06/2012	90	-1270.8	122.2	-884.1	66.0	-578.3	120.5	-1065.1	193.6	-736.0	177.8	-1432.0	104.6	-568.0	54.1	-1476.5	30.0
20/06/2012	91	-1270.9	122.1	-897.3	53.5	-579.7	119.2	-1067.6	191.2	-737.3	176.6	-1435.8	100.9	-569.1	53.0	-1476.4	30.1
21/06/2012	92	-1266.8	126.0	-888.5	61.8	-580.1	118.8	-1063.1	195.5	-731.6	182.0	-1432.3	104.4	-565.7	56.3	-1475.7	30.7
22/06/2012	93	-1279.5	114.0	-904.6	46.5	-589.8	109.6	-1079.5	179.9	-749.2	165.4	-1444.3	92.9	-581.6	41.2	-1486.5	20.4
23/06/2012	94	-1273.0	120.2	-899.5	51.4	-588.5	110.8	-1070.8	188.2	-739.2	174.8	-1441.4	95.6	-571.0	51.3	-1480.2	26.5
24/06/2012	95	-1276.2	117.1	-899.1	51.7	-590.3	109.2	-1069.1	189.8	-739.8	174.3	-1444.9	92.3	-570.5	51.7	-1482.9	23.9
25/06/2012	96	-1272.6	120.5	-902.5	48.5	-585.1	114.1	-1068.4	190.4	-738.4	175.6	-1443.3	93.9	-572.2	50.1	-1480.1	26.5
26/06/2012	97	-1278.9	114.5	-907.0	44.3	-592.3	107.3	-1079.7	179.7	-749.3	165.2	-1446.9	90.5	-578.4	44.2	-1483.2	23.6
27/06/2012	98	-1277.8	115.6	-893.3	57.2	-590.3	109.1	-1076.5	182.7	-743.7	170.6	-1444.5	92.8	-571.8	50.5	-1479.9	26.7
28/06/2012	99	-1278.2	115.2	-887.8	62.4	-590.6	108.9	-1075.3	183.9	-741.5	172.6	-1442.2	95.0	-572.2	50.1	-1479.3	27.3
29/06/2012	100	-1285.6	108.2	-910.1	41.3	-593.4	106.2	-1082.3	177.3	-749.5	165.1	-1447.5	89.9	-579.2	43.5	-1483.5	23.3
30/06/2012	101	-1287.8	106.1	-909.7	41.7	-594.3	105.4	-1084.2	175.5	-751.0	163.7	-1448.1	89.3	-579.3	43.4	-1484.2	22.6
1/07/2012	102	-1286.8	107.0	-911.1	40.4	-594.2	105.5	-1080.3	179.2	-747.9	166.6	-1450.4	87.1	-579.2	43.5	-1487.2	19.8
2/07/2012	103	-1275.4	117.9	-900.5	50.5	-585.7	113.5	-1064.2	194.4	-732.0	181.7	-1439.4	97.6	-569.9	52.2	-1477.8	28.7
3/07/2012	104	-1271.9	121.1	-900.5	50.5	-582.2	116.8	-1060.6	197.9	-730.0	183.5	-1441.1	96.0	-568.3	53.8	-1473.2	33.0
4/07/2012	105	-1273.0	120.1	-896.4	54.3	-583.7	115.4	-1064.2	194.5	-735.1	178.7	-1441.3	95.8	-573.1	49.2	-1477.1	29.4
5/07/2012	106	-1275.3	117.9	-889.1	61.2	-588.0	111.3	-1067.0	191.8	-737.6	176.4	-1441.3	95.7	-570.8	51.4	-1474.9	31.5
6/07/2012	107	-1284.1	109.6	-896.4	54.3	-596.7	103.1	-1072.0	187.0	-743.6	170.7	-1450.2	87.3	-574.7	47.7	-1478.3	28.2
7/07/2012	108	-1280.9	112.7	-899.7	51.1	-595.2	104.5	-1070.2	188.7	-742.3	171.9	-1449.2	88.3	-572.4	49.9	-1476.3	30.1
8/07/2012	109	-1292.3	101.9	-912.5	39.0	-604.6	95.6	-1079.4	180.0	-754.0	160.8	-1457.2	80.7	-581.2	41.6	-1486.4	20.6
9/07/2012	110	-1275.7	117.6	-887.5	62.7	-587.6	111.7	-1063.1	195.5	-734.0	179.8	-1440.1	96.9	-566.0	55.9	-1470.4	35.8
10/07/2012	111	-1280.2	113.3	-894.5	56.1	-592.6	106.9	-1070.1	188.8	-740.2	173.8	-1442.9	94.3	-572.1	50.2	-1475.9	30.5
11/07/2012	112	-1300.3	94.3	-924.1	28.0	-611.2	89.3	-1091.0	169.0	-761.2	154.0	-1464.0	74.2	-586.8	36.2	-1495.0	12.4
12/07/2012	113	-1277.2	116.1	-905.3	45.9	-587.7	111.6	-1067.2	191.6	-741.0	173.1	-1440.7	96.3	-570.9	51.3	-1473.1	33.2
13/07/2012	114	-1281.4	112.2	-910.4	41.0	-592.6	107.0	-1072.6	186.5	-746.4	168.0	-1444.7	92.5	-573.1	49.3	-1473.7	32.6
14/07/2012	115	-1300.9	93.7	-922.7	29.4	-611.9	88.7	-1090.0	169.9	-765.6	149.8	-1462.4	75.8	-589.8	33.4	-1492.0	15.2
15/07/2012	116	-1302.8	91.8	-933.0	19.6	-609.9	90.5	-1087.4	172.4	-757.8	157.2	-1464.4	73.9	-592.3	31.0	-1497.7	9.8
16/07/2012	117	-1280.2	113.3	-912.1	39.4	-590.1	109.3	-1064.1	194.5	-734.6	179.2	-1443.2	94.0	-572.7	49.6	-1479.6	27.1
17/07/2012	118	-1284.4	109.4	-916.1	35.6	-593.9	105.8	-1069.9	189.0	-741.6	172.5	-1450.2	87.4	-579.0	43.6	-1484.8	22.0
18/07/2012	119	-1288.2	105.7	-935.1	17.7	-599.1	100.8	-1074.3	184.9	-748.6	166.0	-1453.1	84.6	-583.8	39.0	-1489.8	17.3
19/07/2012	120	-1285.8	108.0	-928.7	23.7	-596.9	102.9	-1071.2	187.8	-745.4	169.0	-1451.4	86.2	-581.4	41.3	-1487.1	19.9
20/07/2012	121	-1280.6	112.9	-922.1	29.9	-592.9	106.7	-1063.7	194.9	-735.5	178.3	-1449.5	88.0	-573.3	49.0	-1480.5	26.2

21/07/2012	122	-1288.5	105.4	-967.5	-13.0	-600.4	99.5	-1076.8	182.5	-748.2	166.3	-1458.8	79.2	-583.9	39.0	-1489.5	17.7
22/07/2012	123	-1290.6	103.4	-960.1	-6.1	-599.6	100.3	-1077.5	181.8	-750.8	163.8	-1460.2	77.9	-581.1	41.7	-1488.9	18.2
23/07/2012	124	-1290.8	103.2	-961.1	-7.0	-600.0	100.0	-1081.0	178.5	-753.1	161.6	-1461.8	76.4	-582.1	40.7	-1489.2	17.9
24/07/2012	125	-1296.6	97.8	-961.5	-7.4	-610.3	90.2	-1084.6	175.1	-755.6	159.2	-1466.0	72.4	-582.7	40.1	-1490.1	17.1
25/07/2012	126	-1296.1	98.3	-941.8	11.3	-608.5	91.9	-1081.8	177.7	-751.5	163.2	-1460.9	77.2	-581.1	41.6	-1487.1	19.9
26/07/2012	127	-1289.4	104.6	-947.3	6.0	-601.8	98.3	-1077.6	181.7	-750.6	164.0	-1455.8	82.0	-581.5	41.2	-1485.7	21.2
27/07/2012	128	-1294.0	100.2	-939.9	13.1	-605.4	94.8	-1078.7	180.7	-753.5	161.3	-1459.1	78.9	-585.8	37.2	-1491.0	16.2
28/07/2012	129	-1292.0	102.1	-945.7	7.5	-603.6	96.6	-1079.1	180.3	-752.1	162.6	-1461.1	77.0	-586.7	36.3	-1493.3	14.1
29/07/2012	130	-1291.5	102.6	-947.0	6.3	-600.3	99.7	-1077.6	181.8	-750.5	164.1	-1460.6	77.5	-585.5	37.5	-1493.2	14.1
30/07/2012	131	-1289.5	104.5	-943.2	10.0	-602.4	97.7	-1072.7	186.4	-746.1	168.3	-1461.2	76.9	-580.6	42.2	-1488.7	18.4
31/07/2012	132	-1286.9	106.9	-933.1	19.5	-603.3	96.8	-1069.9	189.0	-744.1	170.2	-1459.6	78.5	-578.5	44.1	-1484.1	22.8
1/08/2012	133	-1282.9	110.8	-925.0	27.2	-596.4	103.4	-1065.9	192.9	-740.4	173.7	-1456.8	81.1	-576.9	45.7	-1480.2	26.5
2/08/2012	134	-1284.3	109.4	-930.2	22.2	-599.0	100.9	-1068.4	190.5	-741.8	172.4	-1458.7	79.3	-579.3	43.3	-1481.9	24.8
3/08/2012	135	-1283.3	110.4	-919.6	32.3	-597.0	102.8	-1068.7	190.2	-740.7	173.4	-1461.2	76.9	-578.1	44.5	-1482.7	24.1
4/08/2012	136	-1289.7	104.3	-925.7	26.6	-598.3	101.6	-1074.7	184.5	-749.2	165.4	-1465.0	73.3	-586.8	36.2	-1491.1	16.1
5/08/2012	137	-1292.4	101.7	-940.6	12.4	-593.6	106.0	-1078.9	180.5	-755.2	159.6	-1466.5	71.9	-589.1	34.0	-1494.0	13.3
6/08/2012	138	-1292.7	101.4	-940.8	12.2	-593.3	106.3	-1082.5	177.1	-758.4	156.6	-1466.3	72.1	-589.0	34.1	-1494.7	12.7
7/08/2012	139	-1280.6	112.9	-934.7	18.0	-584.0	115.2	-1064.2	194.5	-741.4	172.7	-1463.4	74.8	-574.2	48.2	-1480.2	26.4
8/08/2012	140	-1282.1	111.5	-935.7	17.0	-585.9	113.3	-1066.8	192.0	-748.6	165.9	-1466.8	71.6	-575.9	46.6	-1479.9	26.7
9/08/2012	141	-1284.5	109.2	-941.4	11.6	-587.7	111.6	-1072.6	186.5	-757.6	157.4	-1473.1	65.6	-580.8	42.0	-1485.7	21.3
10/08/2012	142	-1284.1	109.6	-939.9	13.1	-600.0	100.0	-1068.8	190.1	-750.2	164.4	-1473.5	65.3	-576.7	45.8	-1483.1	23.7
11/08/2012	143	-1294.0	100.2	-935.8	17.0	-607.5	92.8	-1087.0	172.8	-769.0	146.6	-1489.6	50.0	-588.6	34.6	-1494.2	13.2
12/08/2012	144	-1298.3	96.1	-931.8	20.7	-613.4	87.2	-1092.4	167.7	-769.7	145.9	-1476.5	62.4	-591.1	32.2	-1494.6	12.8
13/08/2012	145	-1290.5	103.5	-926.7	25.6	-609.7	90.8	-1080.1	179.3	-756.6	158.3	-1467.6	70.8	-584.3	38.7	-1488.3	18.8
14/08/2012	146	-1282.0	111.6	-920.6	31.4	-602.1	97.9	-1069.0	189.9	-746.0	168.4	-1460.1	77.9	-576.2	46.3	-1478.6	28.0
15/08/2012	147	-1286.2	107.6	-953.1	0.5	-600.0	100.0	-1074.4	184.8	-757.9	157.1	-1465.8	72.5	-584.0	38.9	-1484.8	22.1
16/08/2012	148	-1282.1	111.5	-946.6	6.7	-592.2	107.3	-1071.6	187.4	-752.6	162.2	-1476.6	62.3	-582.8	40.1	-1483.8	23.1
17/08/2012	149	-1283.6	110.1	-959.7	-5.7	-594.3	105.3	-1072.8	186.3	-756.1	158.8	-1478.0	61.0	-584.4	38.5	-1484.5	22.4
18/08/2012	150	-1285.8	108.0	-970.6	-16.0	-597.1	102.7	-1074.1	185.0	-756.4	158.5	-1490.3	49.3	-588.2	34.9	-1486.5	20.5
19/08/2012	151	-1284.2	109.5	-971.3	-16.7	-590.4	109.1	-1069.5	189.4	-756.1	158.8	-1488.2	51.3	-584.1	38.8	-1483.9	22.9
20/08/2012	152	-1277.0	116.4	-953.9	-0.2	-586.1	113.1	-1062.0	196.5	-744.3	170.0	-1474.5	64.3	-580.2	42.5	-1477.1	29.4
21/08/2012	153	-1283.4	110.3	-960.3	-6.3	-594.4	105.3	-1068.1	190.7	-749.5	165.1	-1477.0	62.0	-584.5	38.4	-1480.1	26.5
22/08/2012	154	-1285.7	108.1	-964.3	-10.1	-595.4	104.3	-1073.4	185.7	-753.2	161.5	-1481.5	57.7	-584.5	38.4	-1481.6	25.1
23/08/2012	155	-1281.2	112.3	-945.1	8.1	-599.1	100.8	-1071.2	187.8	-751.9	162.8	-1459.6	78.4	-581.6	41.2	-1476.1	30.3
24/08/2012	156	-1290.5	103.5	-935.2	17.5	-606.4	93.9	-1077.4	181.9	-757.2	157.8	-1463.6	74.6	-590.6	32.7	-1484.0	22.8
25/08/2012	157	-1294.5	99.8	-938.8	14.1	-603.0	97.1	-1075.5	183.7	-756.8	158.2	-1472.4	66.3	-593.3	30.1	-1487.0	20.0
26/08/2012	158	-1289.6	104.4	-949.8	3.7	-597.4	102.4	-1070.1	188.9	-755.7	159.2	-1471.3	67.3	-590.8	32.5	-1484.9	22.0

27/08/2012	159	-1279.9	113.6	-942.7	10.5	-587.4	111.9	-1060.8	197.6	-745.8	168.6	-1467.0	71.4	-582.1	40.7	-1476.3	30.1
28/08/2012	160	-1285.0	108.7	-953.3	0.4	-596.8	103.0	-1068.7	190.2	-753.5	161.3	-1462.2	76.0	-588.9	34.3	-1482.2	24.6
29/08/2012	161	-1283.8	109.9	-943.1	10.1	-597.5	102.3	-1068.7	190.2	-753.8	161.0	-1463.1	75.1	-584.6	38.4	-1479.1	27.5
30/08/2012	162	-1282.2	111.4	-948.2	5.2	-594.3	105.3	-1067.3	191.5	-751.3	163.3	-1459.1	78.9	-583.0	39.8	-1477.7	28.8
31/08/2012	163	-1283.1	110.5	-962.4	-8.2	-589.0	110.4	-1066.2	192.6	-747.5	167.0	-1460.5	77.5	-585.4	37.6	-1482.2	24.6
1/09/2012	164	-1280.2	113.3	-941.8	11.3	-591.4	108.1	-1060.5	198.0	-743.6	170.7	-1460.2	77.9	-582.2	40.6	-1479.3	27.3
2/09/2012	165	-1283.3	110.4	-940.4	12.6	-598.6	101.3	-1063.9	194.7	-748.4	166.1	-1459.6	78.4	-582.6	40.2	-1478.8	27.7
3/09/2012	166	-1273.8	119.4	-930.8	21.7	-586.7	112.5	-1055.8	202.4	-738.5	175.5	-1454.5	83.3	-574.8	47.6	-1468.7	37.4
4/09/2012	167	-1281.1	112.4	-951.1	2.5	-593.6	106.0	-1065.8	192.9	-748.0	166.5	-1460.9	77.2	-582.4	40.4	-1476.0	30.4
5/09/2012	168	-1288.4	105.5	-956.0	-2.2	-601.6	98.4	-1074.6	184.6	-754.0	160.8	-1480.2	58.9	-591.3	32.0	-1490.9	16.3
6/09/2012	169	-1276.5	116.8	-935.0	17.7	-587.8	111.5	-1064.3	194.3	-740.9	173.2	-1472.6	66.1	-583.9	39.0	-1482.8	24.0
7/09/2012	170	-1271.7	121.4	-943.2	9.9	-581.8	117.2	-1062.5	196.0	-739.4	174.6	-1469.5	69.0	-582.1	40.7	-1479.9	26.8
8/09/2012	171	-1273.8	119.3	-953.9	-0.2	-584.3	114.8	-1060.6	197.8	-740.2	173.9	-1472.7	66.0	-580.4	42.3	-1478.8	27.8
9/09/2012	172	-1280.5	113.0	-956.5	-2.7	-595.8	103.9	-1070.1	188.8	-750.5	164.1	-1478.9	60.2	-585.8	37.2	-1482.9	23.9
10/09/2012	173	-1276.9	116.4	-953.1	0.5	-596.0	103.7	-1067.5	191.3	-748.6	165.9	-1477.5	61.5	-583.4	39.4	-1480.1	26.5
11/09/2012	174	-1276.4	116.9	-930.1	22.4	-596.3	103.5	-1065.8	192.9	-746.9	167.5	-1459.9	78.1	-580.9	41.8	-1474.6	31.7
12/09/2012	175	-1275.2	118.0	-939.6	13.3	-595.3	104.4	-1062.3	196.3	-745.8	168.5	-1452.9	84.8	-575.4	47.1	-1469.8	36.3
13/09/2012	176	-1279.8	113.7	-936.5	16.3	-604.1	96.1	-1066.3	192.4	-751.7	163.0	-1456.9	81.0	-579.8	42.9	-1472.2	34.0
14/09/2012	177	-1269.7	123.3	-916.1	35.6	-590.1	109.3	-1054.2	203.9	-736.7	177.2	-1445.7	91.6	-570.9	51.3	-1463.8	42.0
15/09/2012	178	-1276.9	116.4	-937.5	15.4	-599.9	100.1	-1062.8	195.8	-747.2	167.2	-1451.9	85.8	-581.5	41.2	-1472.6	33.6
16/09/2012	179	-1277.8	115.6	-946.0	7.3	-610.3	90.2	-1067.6	191.2	-749.7	164.9	-1453.1	84.6	-584.4	38.5	-1473.2	33.1
17/09/2012	180	-1277.2	116.2	-941.9	11.2	-612.0	88.6	-1067.6	191.2	-752.6	162.1	-1453.3	84.4	-581.9	40.9	-1470.9	35.2
18/09/2012	181	-1277.6	115.8	-944.0	9.2	-614.6	86.1	-1066.8	192.0	-750.5	164.2	-1449.1	88.4	-580.0	42.7	-1467.8	38.2
19/09/2012	182	-1277.2	116.2	-935.2	17.6	-611.9	88.7	-1067.1	191.7	-746.4	168.0	-1444.8	92.5	-581.6	41.2	-1468.1	38.0
20/09/2012	183	-1276.2	117.1	-931.7	20.9	-604.9	95.3	-1065.1	193.6	-744.5	169.8	-1445.8	91.5	-579.0	43.6	-1466.4	39.6
21/09/2012	184	-1270.9	122.1	-923.4	28.7	-598.2	101.6	-1061.4	197.1	-738.1	175.8	-1438.9	98.0	-571.7	50.6	-1460.7	44.9
22/09/2012	185	-1277.0	116.3	-918.9	33.0	-603.9	96.3	-1065.1	193.6	-740.3	173.8	-1443.0	94.1	-578.6	44.0	-1464.4	41.4
23/09/2012	186	-1279.1	114.3	-919.9	32.0	-607.0	93.3	-1068.0	190.9	-743.4	170.8	-1447.2	90.2	-581.6	41.2	-1466.6	39.3
24/09/2012	187	-1264.4	128.2	-898.0	52.8	-589.7	109.7	-1052.2	205.8	-728.3	185.1	-1431.4	105.2	-568.8	53.4	-1456.9	48.6
25/09/2012	188	-1264.4	128.3	-904.3	46.8	-594.8	104.9	-1050.2	207.7	-726.8	186.6	-1428.5	107.9	-571.7	50.5	-1459.4	46.1
26/09/2012	189	-1269.7	123.3	-923.2	28.9	-602.0	98.0	-1059.1	199.3	-734.1	179.7	-1437.1	99.7	-577.1	45.4	-1463.1	42.6
27/09/2012	190	-1266.8	126.0	-912.7	38.8	-597.2	102.6	-1059.6	198.8	-731.8	181.9	-1433.7	103.0	-574.1	48.3	-1458.7	46.8
28/09/2012	191	-1272.2	120.9	-917.3	34.5	-597.5	102.3	-1066.1	192.6	-737.0	176.9	-1443.8	93.5	-576.1	46.4	-1462.8	43.0
29/09/2012	192	-1279.3	114.1	-919.7	32.2	-603.9	96.2	-1070.2	188.8	-742.3	171.9	-1447.8	89.6	-581.3	41.5	-1467.9	38.1
30/09/2012	193	-1277.3	116.0	-925.2	27.0	-599.6	100.3	-1061.1	197.4	-737.0	176.9	-1442.9	94.3	-582.3	40.5	-1471.0	35.2
1/10/2012	194	-1269.0	124.0	-930.5	22.0	-597.4	102.4	-1051.2	206.7	-729.3	184.2	-1432.4	104.2	-576.2	46.3	-1469.3	36.8
2/10/2012	195	-1278.2	115.2	-932.9	19.7	-607.7	92.6	-1062.9	195.6	-740.3	173.8	-1444.2	93.0	-588.3	34.8	-1477.7	28.8

3/10/2012	196	-1266.5	126.3	-923.5	28.7	-594.6	105.0	-1049.9	208.0	-728.3	185.1	-1433.6	103.1	-575.2	47.2	-1464.0	41.8
4/10/2012	197	-1266.4	126.4	-920.2	31.8	-596.1	103.6	-1054.3	203.8	-734.7	179.1	-1437.0	99.9	-575.9	46.6	-1465.3	40.5
5/10/2012	198	-1268.0	124.8	-919.6	32.3	-596.8	103.0	-1051.5	206.5	-728.5	184.9	-1435.1	101.7	-577.0	45.5	-1468.5	37.6
6/10/2012	199	-1269.1	123.8	-919.0	32.9	-598.6	101.3	-1056.2	202.0	-730.3	183.2	-1441.2	95.9	-574.8	47.6	-1465.1	40.7
7/10/2012	200	-1268.4	124.5	-913.5	38.1	-602.8	97.2	-1056.2	202.0	-730.7	182.9	-1441.5	95.6	-573.8	48.6	-1460.6	45.0
8/10/2012	201	-1263.6	129.0	-910.1	41.3	-591.4	108.1	-1045.3	212.3	-721.8	191.4	-1428.2	108.2	-569.3	52.8	-1456.8	48.6
9/10/2012	202	-1258.7	133.7	-904.1	47.0	-585.1	114.1	-1040.4	217.0	-718.8	194.2	-1421.9	114.1	-565.8	56.1	-1451.4	53.7
10/10/2012	203	-1253.5	138.6	-906.0	45.2	-577.0	121.7	-1037.1	220.1	-712.2	200.5	-1417.5	118.3	-562.4	59.4	-1448.9	56.1
11/10/2012	204	-1261.8	130.8	-911.8	39.7	-587.5	111.8	-1046.2	211.5	-719.5	193.5	-1426.4	109.9	-571.1	51.1	-1456.1	49.3
12/10/2012	205	-1233.0	158.0	-877.7	72.0	-562.3	135.7	-1016.8	239.4	-687.8	223.6	-1403.1	132.0	-540.5	80.1	-1426.7	77.1
13/10/2012	206	-1245.0	146.7	-903.5	47.6	-580.0	118.9	-1027.4	229.3	-704.6	207.6	-1410.4	125.1	-555.7	65.7	-1441.5	63.2
14/10/2012	207	-1251.1	140.9	-909.7	41.7	-582.6	116.5	-1035.2	221.9	-713.6	199.1	-1416.7	119.1	-562.9	58.9	-1447.5	57.4
15/10/2012	208	-1248.0	143.8	-902.7	48.4	-573.9	124.7	-1032.0	225.0	-712.2	200.4	-1414.1	121.6	-557.1	64.4	-1441.6	63.0
16/10/2012	209	-1255.4	136.8	-909.7	41.7	-580.3	118.6	-1040.6	216.8	-716.8	196.1	-1416.7	119.1	-565.0	56.9	-1448.7	56.3
17/10/2012	210	-1271.2	121.8	-925.1	27.1	-591.3	108.2	-1053.6	204.5	-732.3	181.4	-1430.2	106.3	-577.7	44.9	-1463.5	42.3
18/10/2012	211	-1266.6	126.2	-925.4	26.8	-587.1	112.2	-1050.7	207.3	-730.3	183.2	-1425.8	110.5	-575.4	47.0	-1458.5	47.1
19/10/2012	212	-1257.2	135.1	-906.6	44.6	-580.3	118.6	-1046.7	211.0	-724.4	188.8	-1420.6	115.4	-562.0	59.7	-1446.8	58.1
20/10/2012	213	-1267.1	125.8	-895.0	55.6	-589.5	109.9	-1054.5	203.6	-725.7	187.6	-1428.1	108.2	-568.1	54.0	-1453.8	51.5
21/10/2012	214	-1280.5	113.0	-912.8	38.8	-602.4	97.7	-1067.9	191.0	-738.7	175.3	-1442.7	94.4	-581.6	41.2	-1465.4	40.5
22/10/2012	215	-1278.1	115.3	-898.4	52.4	-596.2	103.6	-1064.0	194.6	-736.4	177.4	-1440.7	96.3	-579.9	42.8	-1464.3	41.5
23/10/2012	216	-1267.2	125.6	-887.7	62.5	-586.3	112.9	-1050.2	207.7	-723.8	189.4	-1427.8	108.6	-573.5	48.8	-1456.8	48.6
24/10/2012	217	-1262.1	130.5	-890.5	59.9	-585.0	114.2	-1042.8	214.7	-717.7	195.2	-1423.0	113.1	-570.7	51.5	-1450.9	54.3
25/10/2012	218	-1270.5	122.5	-900.2	50.7	-597.1	102.7	-1055.1	203.1	-730.9	182.7	-1433.6	103.1	-579.6	43.1	-1458.9	46.6
26/10/2012	219	-1272.2	120.8	-897.6	53.1	-599.6	100.4	-1058.9	199.5	-733.2	180.5	-1437.4	99.4	-578.9	43.8	-1460.2	45.4
27/10/2012	220	-1266.4	126.4	-890.8	59.6	-594.4	105.2	-1050.4	207.5	-724.4	188.8	-1432.2	104.4	-574.3	48.1	-1454.4	50.9
28/10/2012	221	-1270.1	122.8	-893.0	57.5	-594.1	105.5	-1050.4	207.5	-726.8	186.6	-1433.0	103.6	-578.3	44.3	-1456.4	49.0
29/10/2012	222	-1268.5	124.4	-888.9	61.4	-587.8	111.5	-1049.4	208.5	-726.5	186.8	-1430.7	105.8	-578.3	44.3	-1457.9	47.5
30/10/2012	223	-1262.6	130.0	-887.5	62.7	-585.6	113.6	-1048.8	209.1	-724.8	188.5	-1423.6	112.5	-575.4	47.1	-1452.1	53.1
31/10/2012	224	-1267.6	125.2	-886.6	63.6	-588.9	110.5	-1056.6	201.7	-731.9	181.8	-1429.2	107.3	-575.2	47.3	-1455.7	49.6
1/11/2012	225	-1249.6	142.3	-860.8	88.1	-567.3	130.9	-1035.8	221.4	-709.5	203.0	-1409.1	126.3	-555.3	66.1	-1437.5	66.9
2/11/2012	226	-1262.2	130.4	-868.3	81.0	-580.3	118.6	-1046.1	211.6	-722.2	191.0	-1422.6	113.5	-569.1	53.0	-1452.2	53.0
3/11/2012	227	-1265.3	127.4	-872.7	76.7	-585.7	113.5	-1046.8	210.9	-721.6	191.5	-1423.5	112.6	-570.7	51.5	-1452.4	52.8
4/11/2012	228	-1263.4	129.3	-871.3	78.1	-586.6	112.7	-1047.2	210.5	-723.0	190.2	-1424.4	111.8	-571.3	51.0	-1450.5	54.6
5/11/2012	229	-1262.6	130.0	-866.1	83.0	-582.5	116.5	-1050.1	207.8	-724.9	188.4	-1423.4	112.8	-569.6	52.5	-1451.6	53.6
6/11/2012	230	-1265.2	127.5	-863.6	85.3	-579.8	119.1	-1052.1	205.9	-728.6	184.9	-1422.7	113.4	-569.6	52.5	-1449.5	55.5
7/11/2012	231	-1274.6	118.6	-864.7	84.3	-586.3	112.9	-1061.5	197.0	-736.4	177.5	-1428.2	108.2	-576.8	45.7	-1456.7	48.7
8/11/2012	232	-1265.3	127.4	-852.3	96.1	-574.4	124.2	-1052.9	205.1	-727.7	185.8	-1416.3	119.5	-568.5	53.6	-1446.8	58.1

9/11/2012	233	-1274.4	118.8	-855.3	93.3	-583.3	115.8	-1061.8	196.7	-734.5	179.3	-1425.9	110.4	-576.0	46.5	-1453.8	51.4
10/11/2012	234	-1267.7	125.2	-849.2	99.1	-579.2	119.6	-1053.5	204.6	-725.8	187.5	-1420.0	116.0	-568.2	53.9	-1446.5	58.3
11/11/2012	235	-1266.8	126.0	-851.1	97.2	-579.3	119.5	-1050.9	207.0	-723.4	189.8	-1421.0	115.0	-569.1	53.1	-1449.1	55.9
12/11/2012	236	-1256.4	135.8	-847.2	100.9	-564.4	133.7	-1040.8	216.6	-714.9	197.8	-1410.0	125.4	-561.9	59.8	-1443.3	61.4
13/11/2012	237	-1256.4	135.9	-854.1	94.4	-565.6	132.5	-1041.8	215.6	-717.1	195.7	-1411.1	124.4	-564.0	57.8	-1443.7	61.1
14/11/2012	238	-1264.1	128.5	-860.1	88.7	-573.9	124.7	-1050.2	207.7	-724.3	189.0	-1419.3	116.6	-571.6	50.7	-1451.1	54.0
15/11/2012	239	-1243.4	148.1	-840.4	107.4	-553.5	144.1	-1031.9	225.0	-705.4	206.9	-1399.0	135.8	-554.3	67.1	-1430.9	73.2
16/11/2012	240	-1263.7	128.9	-857.6	91.1	-572.9	125.7	-1052.0	206.0	-727.8	185.6	-1419.0	116.9	-572.6	49.7	-1449.0	56.0

Table E.12 Steel strain for slab D-SCC-b

Slab D-SCC-b		STEEL STRAIN BY SG															
		1		2		3		4		5		6		7		8	
Date	Age	Reading	Strain	Reading	Strain	Reading	Strain	Reading	Strain	Reading	Strain	Reading	Strain	Reading	Strain	Reading	Strain
4/04/2012	14	-875.8		-356.7		-1173.0		-1584.7		-841.1		-880.9		-348.5		-1191.5	
5/04/2012	15	-785.6	85.5	-304.1	49.9	-978.3	184.6	-1267.8	300.4	-502.7	320.7	-825.6	52.4	-153.7	184.7	-1093.6	92.8
6/04/2012	16	-793.1	78.5	-311.2	43.1	-984.4	178.8	-1283.3	285.7	-515.8	308.3	-831.8	46.5	-176.0	163.5	-1096.4	90.2
7/04/2012	17	-785.0	86.1	-299.1	54.6	-959.5	202.4	-1247.7	319.4	-480.7	341.6	-818.8	58.8	-136.8	200.7	-1075.7	109.8
8/04/2012	18	-776.8	93.9	-286.8	66.2	-946.6	214.6	-1230.4	335.8	-461.9	359.4	-803.7	73.2	-117.9	218.5	-1059.7	124.9
9/04/2012	19	-780.3	90.6	-291.6	61.7	-937.0	223.8	-1217.3	348.2	-449.2	371.5	-801.5	75.2	-105.6	230.2	-1050.4	133.7
10/04/2012	20	-756.9	112.7	-266.4	85.6	-919.2	240.5	-1191.7	372.5	-424.7	394.6	-773.1	102.1	-80.1	254.4	-1027.4	155.5
11/04/2012	21	-749.6	119.7	-257.3	94.2	-919.8	240.1	-1189.8	374.3	-423.0	396.3	-763.9	110.8	-79.8	254.7	-1025.1	157.8
12/04/2012	22	-745.6	123.4	-252.4	98.8	-916.6	243.0	-1186.0	377.9	-417.6	401.5	-755.8	118.6	-74.2	260.0	-1015.6	166.7
13/04/2012	23	-743.8	125.2	-246.5	104.5	-909.1	250.2	-1170.8	392.4	-405.0	413.4	-748.5	125.5	-62.4	271.2	-1005.0	176.8
16/04/2012	26	-741.5	127.4	-241.9	108.9	-915.2	244.4	-1168.5	394.6	-400.1	418.0	-742.5	131.1	-71.2	262.8	-1001.7	179.9
17/04/2012	27	-763.2	106.8	-265.3	86.6	-916.9	242.8	-1182.4	381.3	-414.5	404.4	-774.5	100.9	-81.5	253.1	-1012.0	170.2
18/04/2012	28	-762.7	107.3	-262.8	89.0	-907.8	251.4	-1179.4	384.2	-411.3	407.4	-767.2	107.7	-75.9	258.4	-1003.0	178.7
19/04/2012	29	-757.0	112.6	-256.2	95.3	-885.9	272.1	-1165.1	397.8	-397.4	420.6	-761.0	113.6	-50.9	282.1	-976.6	203.7
20/04/2012	30	-756.8	112.8	-256.7	94.8	-889.6	268.6	-1170.5	392.6	-407.5	411.0	-760.7	113.9	-58.4	274.9	-984.9	195.9
21/04/2012	31	-764.3	105.8	-268.7	83.4	-911.6	247.8	-1185.7	378.2	-427.6	391.9	-770.7	104.4	-80.1	254.3	-1010.2	171.9
22/04/2012	32	-771.5	98.9	-272.5	79.8	-924.4	235.7	-1191.1	373.1	-433.4	386.5	-773.3	102.0	-87.5	247.3	-1021.8	160.9
23/04/2012	33	-768.0	102.2	-265.2	86.7	-904.7	254.3	-1175.8	387.6	-415.1	403.8	-769.6	105.5	-72.3	261.8	-1008.3	173.6
24/04/2012	34	-755.8	113.8	-252.6	98.7	-886.1	272.0	-1159.2	403.4	-395.6	422.3	-758.6	115.9	-52.4	280.7	-1000.3	181.2
25/04/2012	35	-770.8	99.6	-272.7	79.6	-909.3	250.0	-1166.1	396.8	-403.9	414.4	-784.7	91.2	-71.3	262.8	-1035.6	147.8
26/04/2012	36	-769.6	100.7	-265.3	86.6	-955.7	206.0	-1192.8	371.4	-442.3	378.0	-780.8	94.8	-128.1	208.9	-1072.1	113.2
27/04/2012	37	-760.8	109.1	-254.4	97.0	-948.9	212.5	-1190.5	373.7	-443.8	376.6	-764.9	109.9	-114.8	221.5	-1063.0	121.8
28/04/2012	38	-762.0	107.9	-255.0	96.4	-957.5	204.3	-1197.2	367.3	-452.2	368.6	-765.7	109.1	-122.8	213.9	-1068.1	117.0
29/04/2012	39	-766.8	103.3	-262.8	89.0	-957.0	204.7	-1194.5	369.8	-449.5	371.2	-771.6	103.6	-128.4	208.6	-1063.8	121.0
30/04/2012	40	-761.8	108.1	-257.4	94.1	-956.0	205.7	-1190.8	373.4	-445.5	375.0	-772.1	103.1	-132.7	204.5	-1062.0	122.7
1/05/2012	41	-764.7	105.3	-259.4	92.3	-961.9	200.2	-1197.2	367.3	-453.0	367.9	-773.1	102.2	-140.4	197.2	-1066.9	118.1
2/05/2012	42	-762.1	107.8	-256.1	95.4	-948.1	213.2	-1186.6	377.3	-442.6	377.7	-764.7	110.1	-122.4	214.3	-1058.0	126.5
3/05/2012	43	-762.3	107.6	-257.0	94.5	-945.2	216.0	-1185.1	378.7	-440.4	379.8	-765.8	109.1	-119.0	217.5	-1056.0	128.5
4/05/2012	44	-764.1	105.9	-259.4	92.2	-952.2	209.3	-1187.8	376.2	-443.9	376.5	-772.3	102.9	-118.6	217.9	-1060.3	124.3
5/05/2012	45	-774.0	96.5	-268.6	83.5	-969.8	192.6	-1204.0	360.8	-463.9	357.5	-783.8	92.0	-140.9	196.8	-1088.8	97.3
6/05/2012	46	-776.8	93.9	-271.8	80.5	-978.3	184.6	-1208.1	356.9	-470.3	351.5	-784.9	91.0	-145.4	192.5	-1097.0	89.6
7/05/2012	47	-767.7	102.5	-260.2	91.5	-960.7	201.2	-1193.4	370.9	-456.8	364.3	-772.5	102.7	-137.8	199.7	-1081.4	104.4

8/05/2012	48	-757.1	112.6	-247.7	103.3	-949.6	211.7	-1183.4	380.4	-450.0	370.7	-764.1	110.7	-120.6	216.0	-1059.8	124.9
9/05/2012	49	-755.1	114.5	-246.1	104.9	-946.5	214.7	-1183.7	380.1	-449.9	370.8	-763.1	111.7	-119.4	217.1	-1057.7	126.8
10/05/2012	50	-757.4	112.3	-249.0	102.1	-945.5	215.7	-1183.5	380.3	-450.1	370.6	-763.2	111.6	-120.1	216.5	-1055.7	128.8
11/05/2012	51	-762.9	107.0	-254.2	97.2	-936.4	224.3	-1184.6	379.3	-437.6	382.4	-765.0	109.8	-121.3	215.3	-1056.0	128.4
12/05/2012	52	-760.0	109.8	-251.1	100.1	-940.2	220.7	-1187.6	376.5	-436.7	383.4	-760.6	114.0	-116.9	219.5	-1060.5	124.2
13/05/2012	53	-767.3	102.9	-257.4	94.2	-948.5	212.8	-1188.1	375.9	-435.8	384.1	-775.0	100.3	-126.5	210.4	-1064.8	120.1
14/05/2012	54	-755.3	114.2	-244.8	106.1	-949.2	212.1	-1180.6	383.0	-429.2	390.4	-760.3	114.3	-134.9	202.4	-1065.7	119.3
15/05/2012	55	-755.5	114.1	-245.7	105.2	-952.4	209.1	-1181.6	382.1	-432.9	386.9	-761.2	113.4	-134.2	203.1	-1069.7	115.4
16/05/2012	56	-756.4	113.2	-244.6	106.3	-951.8	209.7	-1171.6	391.6	-423.8	395.5	-760.5	114.1	-150.5	187.7	-1062.1	122.7
17/05/2012	57	-747.7	121.5	-239.5	111.1	-965.3	196.9	-1184.7	379.2	-434.7	385.2	-746.2	127.6	-143.8	194.0	-1070.7	114.5
18/05/2012	58	-752.8	116.7	-245.6	105.3	-955.1	206.6	-1182.9	380.9	-435.5	384.5	-752.4	121.8	-140.1	197.5	-1065.4	119.6
19/05/2012	59	-757.4	112.3	-247.4	103.6	-958.0	203.8	-1184.0	379.8	-438.1	382.0	-758.0	116.4	-142.6	195.1	-1067.9	117.1
20/05/2012	60	-758.6	111.1	-250.6	100.6	-955.0	206.6	-1182.9	380.9	-436.7	383.4	-759.3	115.3	-147.2	190.7	-1070.4	114.8
21/05/2012	61	-759.6	110.1	-251.6	99.6	-955.8	205.9	-1185.0	378.9	-435.5	384.5	-759.3	115.2	-160.2	178.5	-1064.6	120.3
22/05/2012	62	-757.1	112.6	-247.5	103.5	-953.0	208.6	-1186.5	377.5	-438.2	381.9	-757.1	117.3	-153.9	184.4	-1067.6	117.4
23/05/2012	63	-755.4	114.2	-244.4	106.4	-953.8	207.8	-1181.3	382.4	-435.7	384.2	-755.6	118.7	-156.3	182.2	-1069.1	116.1
24/05/2012	64	-759.5	110.3	-248.4	102.6	-963.7	198.4	-1188.8	375.3	-444.9	375.6	-758.3	116.2	-164.1	174.8	-1076.0	109.5
25/05/2012	65	-757.0	112.7	-244.4	106.5	-960.1	201.8	-1188.1	376.0	-446.3	374.2	-752.4	121.8	-161.8	177.0	-1067.5	117.6
26/05/2012	66	-757.6	112.1	-245.6	105.3	-968.7	193.6	-1193.1	371.2	-450.7	370.1	-755.9	118.5	-169.5	169.6	-1082.5	103.4
27/05/2012	67	-760.6	109.3	-247.8	103.2	-971.3	191.2	-1192.4	371.9	-449.3	371.4	-761.6	113.1	-170.2	169.0	-1079.4	106.2
28/05/2012	68	-752.3	117.1	-238.9	111.7	-955.4	206.3	-1182.9	380.8	-436.7	383.3	-748.1	125.9	-154.9	183.4	-1065.6	119.4
29/05/2012	69	-761.8	108.1	-248.0	103.0	-955.3	206.3	-1190.7	373.4	-448.4	372.2	-758.7	115.8	-160.8	177.9	-1068.5	116.6
30/05/2012	70	-754.1	115.4	-238.0	112.6	-953.9	207.7	-1190.9	373.3	-444.5	375.9	-748.5	125.5	-161.9	176.8	-1068.1	117.0
31/05/2012	71	-760.5	109.3	-245.5	105.4	-961.1	200.9	-1195.9	368.5	-447.6	373.0	-756.3	118.1	-174.1	165.3	-1072.9	112.4
1/06/2012	72	-754.6	115.0	-236.8	113.7	-962.9	199.2	-1198.4	366.2	-449.6	371.1	-747.4	126.5	-167.0	172.0	-1073.1	112.3
2/06/2012	73	-763.9	106.1	-249.2	101.9	-959.8	202.1	-1200.2	364.5	-450.3	370.4	-758.1	116.3	-168.3	170.8	-1070.0	115.2
3/06/2012	74	-761.3	108.5	-244.5	106.3	-955.2	206.4	-1199.8	364.8	-452.5	368.3	-754.1	120.2	-158.8	179.8	-1069.5	115.6
4/06/2012	75	-763.0	106.9	-246.5	104.5	-959.3	202.6	-1202.4	362.4	-457.1	364.0	-755.3	119.0	-165.3	173.6	-1075.8	109.7
5/06/2012	76	-755.3	114.3	-239.9	110.8	-957.3	204.5	-1191.0	373.2	-446.0	374.5	-747.8	126.1	-155.7	182.7	-1079.9	105.8
6/06/2012	77	-763.1	106.8	-247.9	103.1	-974.6	188.1	-1205.9	359.1	-459.1	362.0	-756.6	117.8	-183.4	156.5	-1093.5	92.9
7/06/2012	78	-753.5	116.0	-237.9	112.6	-966.4	195.8	-1200.8	363.9	-454.9	366.0	-743.4	130.3	-170.6	168.6	-1085.7	100.3
8/06/2012	79	-751.5	117.9	-237.2	113.3	-955.2	206.5	-1187.4	376.6	-442.1	378.2	-743.8	130.0	-147.8	190.2	-1080.5	105.2
9/06/2012	80	-751.7	117.7	-236.8	113.7	-951.9	209.6	-1186.2	377.7	-439.2	380.9	-742.8	130.9	-152.5	185.7	-1081.1	104.7
10/06/2012	81	-750.8	118.6	-235.2	115.2	-946.0	215.2	-1181.2	382.5	-434.2	385.7	-743.5	130.2	-166.4	172.6	-1072.9	112.5
11/06/2012	82	-754.6	114.9	-239.1	111.5	-951.6	209.9	-1191.1	373.1	-444.8	375.7	-749.0	125.0	-177.6	162.0	-1073.7	111.7
12/06/2012	83	-755.8	113.8	-239.1	111.5	-950.4	211.0	-1195.4	369.0	-448.5	372.2	-749.2	124.8	-192.7	147.7	-1077.5	108.1
13/06/2012	84	-752.9	116.5	-236.4	114.0	-939.6	221.3	-1189.7	374.5	-444.0	376.4	-744.5	129.2	-171.1	168.1	-1072.2	113.1

14/06/2012	85	-752.8	116.7	-233.8	116.5	-939.3	221.6	-1191.5	372.7	-443.2	377.2	-741.6	132.0	-174.8	164.6	-1067.1	117.9
15/06/2012	86	-755.4	114.2	-236.2	114.2	-951.0	210.4	-1201.2	363.6	-454.9	366.1	-744.9	128.9	-177.7	161.9	-1070.2	115.0
16/06/2012	87	-758.9	110.9	-240.9	109.7	-948.6	212.7	-1197.5	367.0	-450.3	370.4	-751.0	123.1	-171.1	168.2	-1071.3	113.9
17/06/2012	88	-763.8	106.2	-248.9	102.2	-960.3	201.6	-1203.2	361.6	-462.6	358.8	-758.8	115.7	-183.4	156.5	-1088.2	97.9
18/06/2012	89	-750.9	118.4	-233.4	116.9	-960.2	201.7	-1196.9	367.6	-451.8	369.0	-744.0	129.7	-175.3	164.2	-1087.2	98.9
19/06/2012	90	-752.5	116.9	-234.7	115.6	-961.8	200.2	-1193.7	370.7	-445.3	375.2	-745.6	128.2	-172.6	166.7	-1083.4	102.5
20/06/2012	91	-752.6	116.8	-235.7	114.7	-965.8	196.4	-1194.3	370.1	-445.5	375.0	-748.7	125.3	-182.5	157.3	-1083.8	102.1
21/06/2012	92	-750.1	119.2	-236.0	114.4	-958.3	203.6	-1189.5	374.6	-443.7	376.6	-745.8	128.0	-171.0	168.2	-1080.4	105.3
22/06/2012	93	-757.7	112.0	-242.7	108.0	-970.4	192.1	-1196.9	367.6	-449.8	370.9	-755.5	118.9	-184.8	155.1	-1086.4	99.6
23/06/2012	94	-753.8	115.7	-241.9	108.8	-967.5	194.9	-1190.8	373.4	-448.5	372.2	-753.2	121.1	-186.9	153.1	-1086.0	100.0
24/06/2012	95	-755.7	113.8	-243.1	107.7	-966.6	195.7	-1188.3	375.8	-450.6	370.1	-756.0	118.4	-176.7	162.8	-1085.8	100.2
25/06/2012	96	-753.6	115.9	-239.5	111.1	-964.5	197.7	-1187.0	377.0	-448.0	372.6	-754.7	119.6	-178.0	161.6	-1082.5	103.4
26/06/2012	97	-757.4	112.3	-244.5	106.4	-968.9	193.5	-1196.1	368.4	-454.6	366.3	-757.5	116.9	-200.3	140.4	-1087.5	98.6
27/06/2012	98	-756.7	112.9	-243.1	107.7	-962.9	199.2	-1198.0	366.5	-452.5	368.3	-755.6	118.8	-188.6	151.6	-1080.9	104.8
28/06/2012	99	-756.9	112.7	-243.3	107.5	-966.3	195.9	-1200.9	363.8	-453.9	367.0	-753.7	120.5	-202.9	138.0	-1080.9	104.9
29/06/2012	100	-761.4	108.5	-245.3	105.6	-968.3	194.0	-1198.9	365.7	-455.4	365.6	-758.0	116.5	-191.9	148.4	-1079.0	106.6
30/06/2012	101	-762.7	107.3	-245.9	105.0	-971.5	191.0	-1202.9	361.9	-459.7	361.5	-758.5	116.0	-193.5	146.9	-1084.7	101.2
1/07/2012	102	-762.1	107.8	-245.8	105.1	-979.0	183.9	-1201.9	362.8	-459.5	361.7	-760.3	114.3	-191.0	149.2	-1090.9	95.4
2/07/2012	103	-755.2	114.3	-239.9	110.8	-972.0	190.5	-1187.6	376.4	-444.0	376.4	-751.5	122.6	-171.6	167.7	-1085.0	101.0
3/07/2012	104	-753.2	116.3	-237.4	113.0	-973.5	189.1	-1188.8	375.2	-445.0	375.5	-752.9	121.3	-180.8	159.0	-1088.2	97.9
4/07/2012	105	-753.8	115.7	-238.5	112.1	-971.0	191.5	-1187.4	376.6	-443.8	376.6	-753.1	121.2	-185.1	154.9	-1087.6	98.5
5/07/2012	106	-755.2	114.4	-241.5	109.2	-978.2	184.6	-1192.5	371.8	-451.3	369.5	-753.1	121.1	-200.1	140.6	-1091.5	94.8
6/07/2012	107	-760.5	109.3	-247.6	103.5	-980.6	182.4	-1197.6	366.9	-456.6	364.5	-760.2	114.4	-204.4	136.6	-1092.1	94.2
7/07/2012	108	-758.5	111.2	-246.5	104.5	-972.8	189.8	-1192.5	371.7	-452.3	368.5	-759.4	115.2	-201.3	139.5	-1087.9	98.2
8/07/2012	109	-765.4	104.7	-253.1	98.2	-977.9	184.9	-1199.5	365.1	-461.0	360.3	-765.8	109.1	-201.9	139.0	-1092.0	94.3
9/07/2012	110	-755.4	114.2	-241.2	109.5	-962.3	199.8	-1186.2	377.7	-450.8	370.0	-752.1	122.1	-176.7	162.8	-1082.1	103.7
10/07/2012	111	-758.1	111.6	-244.8	106.1	-961.0	201.0	-1186.2	377.7	-452.3	368.5	-754.3	120.0	-174.6	164.8	-1081.8	104.0
11/07/2012	112	-770.2	100.2	-257.7	93.8	-984.4	178.8	-1205.9	359.1	-476.3	345.7	-771.2	103.9	-192.9	147.5	-1103.4	83.5
12/07/2012	113	-756.3	113.3	-241.3	109.4	-969.6	192.8	-1192.7	371.6	-458.1	363.1	-752.6	121.6	-177.3	162.2	-1087.4	98.7
13/07/2012	114	-758.8	110.9	-244.7	106.2	-970.1	192.4	-1196.1	368.4	-463.7	357.7	-755.8	118.6	-180.9	158.8	-1089.7	96.5
14/07/2012	115	-770.5	99.8	-258.2	93.4	-973.0	189.6	-1200.6	364.0	-468.2	353.4	-769.9	105.2	-187.6	152.5	-1093.4	93.0
15/07/2012	116	-771.7	98.7	-256.9	94.7	-980.0	183.0	-1200.3	364.3	-465.9	355.6	-771.5	103.7	-186.0	154.0	-1101.5	85.3
16/07/2012	117	-758.1	111.6	-243.0	107.8	-966.7	195.6	-1182.3	381.4	-446.3	374.2	-754.5	119.8	-165.4	173.5	-1089.1	97.1
17/07/2012	118	-760.6	109.2	-245.6	105.3	-957.1	204.6	-1173.9	389.4	-436.2	383.8	-760.1	114.4	-161.6	177.2	-1078.3	107.3
18/07/2012	119	-762.9	107.0	-249.2	101.9	-938.6	222.2	-1151.7	410.4	-415.3	403.6	-762.5	112.2	-140.3	197.3	-1058.8	125.8
19/07/2012	120	-761.5	108.4	-247.7	103.3	-933.6	226.9	-1147.3	414.6	-411.4	407.3	-761.1	113.5	-138.9	198.7	-1056.8	127.7
20/07/2012	121	-758.3	111.4	-244.9	106.0	-929.1	231.2	-1138.1	423.3	-404.0	414.3	-759.6	115.0	-137.5	199.9	-1052.4	131.8

21/07/2012	122	-763.1	106.9	-250.2	101.0	-941.8	219.2	-1144.7	417.1	-411.3	407.4	-767.0	107.9	-155.3	183.2	-1054.2	130.2
22/07/2012	123	-764.4	105.7	-249.6	101.5	-945.3	215.9	-1148.9	413.1	-415.9	403.0	-768.1	106.9	-152.2	186.0	-1055.1	129.3
23/07/2012	124	-764.5	105.5	-249.9	101.3	-963.2	198.9	-1169.6	393.5	-436.5	383.5	-769.4	105.6	-168.0	171.1	-1073.6	111.8
24/07/2012	125	-768.0	102.3	-257.1	94.4	-991.5	172.1	-1197.3	367.2	-468.0	353.7	-772.8	102.5	-197.3	143.3	-1100.8	86.0
25/07/2012	126	-767.6	102.6	-255.8	95.6	-980.9	182.1	-1192.0	372.2	-459.6	361.6	-768.8	106.3	-182.9	156.9	-1091.2	95.1
26/07/2012	127	-763.6	106.4	-251.1	100.1	-982.0	181.1	-1196.8	367.7	-462.8	358.5	-764.6	110.2	-188.5	151.7	-1097.3	89.3
27/07/2012	128	-766.4	103.8	-253.7	97.6	-961.5	200.5	-1170.7	392.5	-436.9	383.1	-767.3	107.7	-161.6	177.1	-1077.5	108.0
28/07/2012	129	-765.2	104.9	-252.4	98.9	-941.7	219.3	-1140.9	420.7	-407.7	410.8	-768.9	106.2	-141.8	195.9	-1054.3	130.0
29/07/2012	130	-764.9	105.2	-250.1	101.1	-953.1	208.5	-1145.2	416.6	-410.3	408.3	-768.4	106.6	-157.6	181.0	-1059.6	125.1
30/07/2012	131	-763.7	106.3	-251.6	99.6	-944.2	216.9	-1138.3	423.2	-405.8	412.6	-768.9	106.1	-150.7	187.4	-1057.7	126.8
31/07/2012	132	-762.2	107.8	-252.2	99.0	-943.6	217.4	-1139.5	422.0	-408.2	410.3	-767.6	107.3	-160.3	178.3	-1058.9	125.7
1/08/2012	133	-759.7	110.1	-247.4	103.6	-933.3	227.2	-1133.8	427.4	-401.1	417.0	-765.4	109.4	-150.7	187.5	-1052.7	131.5
2/08/2012	134	-760.6	109.2	-249.2	101.9	-932.3	228.2	-1131.5	429.6	-398.9	419.1	-767.0	108.0	-161.7	177.1	-1052.4	131.9
3/08/2012	135	-760.0	109.8	-247.8	103.2	-931.5	229.0	-1132.2	428.9	-399.5	418.6	-769.0	106.1	-149.1	189.0	-1052.5	131.8
4/08/2012	136	-763.8	106.2	-248.7	102.4	-933.3	227.3	-1131.7	429.4	-397.6	420.4	-772.0	103.2	-151.0	187.1	-1051.6	132.6
5/08/2012	137	-765.5	104.6	-245.4	105.5	-948.2	213.1	-1134.7	426.6	-399.8	418.3	-773.2	102.0	-146.3	191.6	-1053.6	130.7
6/08/2012	138	-765.6	104.5	-245.2	105.7	-953.8	207.8	-1132.6	428.6	-398.3	419.8	-773.0	102.2	-146.7	191.3	-1053.3	131.0
7/08/2012	139	-758.4	111.4	-238.7	111.9	-933.8	226.8	-1122.6	438.0	-390.6	427.0	-770.7	104.4	-150.3	187.8	-1044.4	139.4
8/08/2012	140	-759.3	110.5	-240.0	110.6	-938.7	222.1	-1125.2	435.5	-392.7	425.0	-773.5	101.8	-150.6	187.5	-1043.8	140.0
9/08/2012	141	-760.7	109.1	-241.3	109.4	-949.1	212.2	-1127.2	433.7	-393.4	424.4	-778.5	97.0	-149.3	188.8	-1045.6	138.3
10/08/2012	142	-760.5	109.3	-249.9	101.3	-948.4	212.9	-1129.2	431.7	-398.3	419.7	-778.8	96.8	-151.3	186.9	-1052.2	132.1
11/08/2012	143	-766.4	103.7	-255.2	96.3	-960.4	201.5	-1135.4	425.9	-404.5	413.9	-791.7	84.6	-164.9	174.0	-1054.0	130.4
12/08/2012	144	-769.0	101.3	-259.3	92.3	-964.7	197.5	-1139.1	422.4	-408.8	409.7	-781.2	94.5	-168.8	170.3	-1055.2	129.2
13/08/2012	145	-764.3	105.7	-256.7	94.8	-942.6	218.4	-1133.3	427.9	-399.8	418.3	-774.1	101.2	-146.5	191.5	-1045.0	138.9
14/08/2012	146	-759.2	110.5	-251.4	99.8	-932.1	228.4	-1132.5	428.7	-398.6	419.4	-768.1	106.9	-143.7	194.1	-1043.9	139.9
15/08/2012	147	-761.7	108.2	-249.9	101.3	-951.8	209.7	-1137.3	424.1	-401.3	416.9	-772.7	102.6	-162.0	176.8	-1048.5	135.5
16/08/2012	148	-759.3	110.5	-244.5	106.4	-956.7	205.1	-1137.3	424.0	-400.6	417.5	-781.3	94.4	-145.0	192.9	-1048.0	136.0
17/08/2012	149	-760.1	109.7	-245.9	105.0	-966.1	196.1	-1142.1	419.6	-407.5	411.0	-782.4	93.4	-149.4	188.7	-1056.5	127.9
18/08/2012	150	-761.5	108.4	-247.9	103.2	-960.6	201.3	-1131.8	429.3	-401.1	417.1	-792.3	84.0	-158.8	179.8	-1050.6	133.5
19/08/2012	151	-760.5	109.3	-243.2	107.6	-954.7	207.0	-1133.3	427.9	-401.2	416.9	-790.6	85.6	-160.8	177.9	-1051.6	132.7
20/08/2012	152	-756.2	113.4	-240.2	110.4	-945.4	215.7	-1134.5	426.7	-402.0	416.2	-779.6	96.0	-147.0	191.0	-1052.8	131.5
21/08/2012	153	-760.1	109.8	-246.0	105.0	-973.7	188.9	-1155.7	406.7	-421.5	397.7	-781.6	94.1	-166.0	173.0	-1070.6	114.6
22/08/2012	154	-761.4	108.4	-246.7	104.3	-1002.1	162.1	-1156.5	405.9	-423.6	395.7	-785.2	90.7	-172.3	167.0	-1071.2	114.1
23/08/2012	155	-758.7	111.0	-249.2	101.9	-980.6	182.4	-1156.5	405.9	-424.8	394.6	-767.7	107.3	-170.5	168.7	-1064.1	120.8
24/08/2012	156	-764.3	105.7	-254.4	97.0	-978.0	184.8	-1164.0	398.8	-431.7	388.0	-770.9	104.2	-175.8	163.7	-1071.6	113.7
25/08/2012	157	-766.7	103.5	-252.0	99.3	-991.5	172.1	-1163.4	399.4	-428.5	391.1	-777.9	97.6	-191.1	149.2	-1078.8	106.8
26/08/2012	158	-763.8	106.2	-248.1	103.0	-991.6	172.0	-1165.0	397.8	-431.2	388.5	-777.1	98.4	-198.5	142.2	-1082.6	103.2

27/08/2012	159	-757.9	111.7	-241.1	109.6	-974.8	187.9	-1154.8	407.5	-418.8	400.3	-773.6	101.7	-177.4	162.1	-1073.6	111.7
28/08/2012	160	-761.0	108.8	-247.7	103.4	-989.4	174.1	-1156.3	406.1	-421.7	397.6	-769.8	105.3	-183.5	156.4	-1072.8	112.6
29/08/2012	161	-760.3	109.5	-248.2	102.9	-1014.8	150.0	-1158.5	404.0	-424.5	394.9	-770.5	104.6	-184.0	155.9	-1072.4	112.9
30/08/2012	162	-759.3	110.4	-245.9	105.0	-1003.8	160.4	-1154.0	408.3	-421.3	397.9	-767.3	107.7	-177.8	161.8	-1067.1	118.0
31/08/2012	163	-759.9	109.9	-242.2	108.5	-995.2	168.5	-1155.6	406.7	-420.9	398.3	-768.4	106.6	-174.9	164.5	-1071.4	113.8
1/09/2012	164	-758.1	111.6	-243.8	107.0	-982.6	180.5	-1145.3	416.5	-413.5	405.3	-768.1	106.9	-173.3	166.0	-1068.7	116.4
2/09/2012	165	-760.0	109.8	-248.9	102.2	-1015.2	149.6	-1154.3	408.0	-421.9	397.4	-767.7	107.3	-188.0	152.1	-1078.7	106.9
3/09/2012	166	-754.3	115.2	-240.6	110.1	-989.2	174.2	-1146.8	415.1	-411.3	407.4	-763.6	111.2	-152.3	185.9	-1068.5	116.6
4/09/2012	167	-758.7	111.1	-245.4	105.5	-1010.0	154.5	-1152.5	409.7	-418.2	400.9	-768.7	106.3	-159.3	179.3	-1075.9	109.6
5/09/2012	168	-763.1	106.9	-251.0	100.2	-994.3	169.4	-1158.0	404.5	-419.6	399.5	-784.2	91.7	-155.5	182.9	-1076.5	109.0
6/09/2012	169	-755.9	113.7	-241.4	109.3	-983.7	179.4	-1152.0	410.2	-411.7	407.0	-778.1	97.5	-141.1	196.6	-1071.2	114.0
7/09/2012	170	-753.0	116.4	-237.2	113.3	-995.8	168.0	-1151.1	411.0	-409.3	409.3	-775.6	99.8	-151.8	186.5	-1069.6	115.5
8/09/2012	171	-754.3	115.2	-238.9	111.7	-1011.4	153.2	-1156.8	405.6	-413.7	405.1	-778.1	97.4	-180.1	159.6	-1072.4	112.9
9/09/2012	172	-758.3	111.4	-247.0	104.0	-1005.6	158.7	-1164.4	398.4	-421.2	398.0	-783.1	92.7	-179.2	160.5	-1076.9	108.7
10/09/2012	173	-756.2	113.4	-247.1	103.9	-987.1	176.2	-1156.9	405.6	-418.0	401.1	-782.0	93.7	-161.7	177.0	-1070.5	114.7
11/09/2012	174	-755.8	113.8	-247.3	103.7	-977.1	185.7	-1155.6	406.8	-420.3	398.8	-767.9	107.0	-155.6	182.8	-1066.7	118.3
12/09/2012	175	-755.1	114.4	-246.6	104.4	-1031.0	134.6	-1169.7	393.3	-435.5	384.5	-762.3	112.4	-173.4	166.0	-1079.8	105.8
13/09/2012	176	-757.9	111.8	-252.8	98.5	-1032.9	132.8	-1167.6	395.4	-432.6	387.2	-765.5	109.3	-160.6	178.1	-1070.1	115.1
14/09/2012	177	-751.8	117.6	-243.0	107.8	-1003.1	161.1	-1164.2	398.6	-426.9	392.6	-756.5	117.9	-148.2	189.9	-1069.2	115.9
15/09/2012	178	-756.1	113.5	-249.8	101.3	-1058.7	108.4	-1173.7	389.6	-432.6	387.2	-761.5	113.2	-175.2	164.2	-1081.4	104.4
16/09/2012	179	-756.7	112.9	-257.1	94.4	-1074.0	93.9	-1174.9	388.4	-436.4	383.6	-762.5	112.2	-175.2	164.3	-1080.9	104.9
17/09/2012	180	-756.3	113.3	-258.3	93.3	-1029.5	136.0	-1173.2	390.1	-433.4	386.4	-762.6	112.1	-162.5	176.2	-1070.5	114.7
18/09/2012	181	-756.6	113.1	-260.1	91.6	-1015.5	149.4	-1172.2	391.0	-433.9	386.0	-759.3	115.2	-157.6	180.9	-1065.2	119.7
19/09/2012	182	-756.3	113.3	-258.2	93.4	-1016.5	148.4	-1174.5	388.8	-435.0	385.0	-755.8	118.5	-151.0	187.2	-1065.8	119.2
20/09/2012	183	-755.7	113.8	-253.3	98.0	-1012.4	152.2	-1174.9	388.4	-433.1	386.7	-756.6	117.8	-158.2	180.4	-1064.8	120.1
21/09/2012	184	-752.6	116.9	-248.7	102.4	-976.4	186.3	-1172.8	390.4	-432.4	387.3	-751.1	123.0	-152.2	186.1	-1061.4	123.3
22/09/2012	185	-756.2	113.4	-252.6	98.7	-969.5	192.9	-1172.9	390.4	-431.1	388.7	-754.4	119.8	-148.8	189.3	-1061.4	123.3
23/09/2012	186	-757.5	112.2	-254.8	96.6	-972.8	189.8	-1177.4	386.1	-434.8	385.1	-757.7	116.7	-152.9	185.4	-1064.1	120.8
24/09/2012	187	-748.7	120.5	-242.7	108.1	-961.8	200.2	-1175.5	387.9	-431.5	388.3	-745.1	128.7	-143.1	194.7	-1064.7	120.2
25/09/2012	188	-748.6	120.6	-246.2	104.7	-971.8	190.7	-1174.7	388.6	-428.4	391.2	-742.8	130.9	-146.2	191.8	-1066.7	118.3
26/09/2012	189	-751.8	117.6	-251.3	99.9	-995.1	168.7	-1176.9	386.6	-431.9	387.8	-749.7	124.3	-149.0	189.1	-1068.9	116.2
27/09/2012	190	-750.1	119.2	-247.9	103.1	-977.5	185.3	-1177.2	386.3	-432.2	387.6	-747.0	126.9	-146.9	191.0	-1065.5	119.4
28/09/2012	191	-753.3	116.1	-248.2	102.9	-959.4	202.5	-1178.9	384.7	-434.8	385.1	-755.0	119.3	-147.5	190.5	-1065.5	119.4
29/09/2012	192	-757.6	112.1	-252.6	98.6	-954.2	207.4	-1185.4	378.5	-437.6	382.4	-758.3	116.2	-148.9	189.1	-1066.6	118.4
30/09/2012	193	-756.4	113.2	-249.6	101.5	-982.3	180.8	-1185.1	378.8	-434.0	385.9	-754.3	120.0	-149.6	188.5	-1073.6	111.8
1/10/2012	194	-751.4	118.0	-248.1	103.0	-1009.3	155.2	-1186.2	377.7	-432.3	387.5	-745.9	127.9	-149.0	189.1	-1077.4	108.2
2/10/2012	195	-756.9	112.7	-255.3	96.1	-1024.7	140.6	-1193.7	370.6	-440.4	379.8	-755.4	118.9	-159.9	178.8	-1084.2	101.7

3/10/2012	196	-749.9	119.4	-246.1	104.8	-1017.2	147.7	-1190.3	373.8	-437.2	382.8	-746.9	127.0	-151.9	186.4	-1077.5	108.1
4/10/2012	197	-749.9	119.4	-247.2	103.8	-1014.7	150.0	-1188.8	375.2	-436.7	383.3	-749.6	124.4	-148.0	190.0	-1074.5	111.0
5/10/2012	198	-750.8	118.5	-247.7	103.4	-1000.4	163.6	-1189.7	374.4	-432.8	387.0	-748.1	125.9	-145.0	192.9	-1076.8	108.8
6/10/2012	199	-751.5	117.9	-248.9	102.2	-1002.9	161.2	-1192.5	371.7	-438.8	381.3	-753.0	121.2	-146.4	191.5	-1076.4	109.1
7/10/2012	200	-751.0	118.3	-251.9	99.4	-1019.5	145.5	-1199.0	365.6	-447.3	373.3	-753.2	121.0	-158.8	179.8	-1081.3	104.5
8/10/2012	201	-748.2	121.0	-243.9	106.9	-1025.7	139.6	-1193.7	370.6	-441.2	379.0	-742.6	131.1	-159.7	179.0	-1078.0	107.6
9/10/2012	202	-745.2	123.8	-239.5	111.1	-1036.5	129.4	-1194.9	369.5	-441.5	378.8	-737.6	135.8	-160.4	178.2	-1078.6	107.0
10/10/2012	203	-742.1	126.8	-233.8	116.5	-1022.5	142.7	-1187.7	376.3	-432.1	387.7	-734.0	139.2	-147.9	190.1	-1072.4	113.0
11/10/2012	204	-747.1	122.1	-241.2	109.5	-1059.8	107.3	-1195.1	369.3	-441.0	379.3	-741.1	132.5	-152.5	185.7	-1080.8	104.9
12/10/2012	205	-729.8	138.4	-223.5	126.3	-995.0	168.8	-1166.9	396.1	-416.6	402.3	-722.5	150.1	-117.7	218.8	-1058.8	125.8
13/10/2012	206	-737.0	131.6	-235.9	114.5	-1036.2	129.7	-1171.2	392.0	-421.0	398.2	-728.3	144.6	-133.9	203.4	-1061.9	122.8
14/10/2012	207	-740.6	128.2	-237.7	112.8	-1081.2	87.0	-1180.1	383.5	-429.2	390.4	-733.3	139.9	-153.7	184.6	-1068.8	116.3
15/10/2012	208	-738.8	129.9	-231.6	118.6	-1050.0	116.6	-1179.3	384.2	-428.5	391.1	-731.3	141.8	-150.4	187.7	-1067.4	117.6
16/10/2012	209	-743.2	125.7	-236.1	114.3	-1023.0	142.2	-1184.4	379.4	-431.6	388.1	-733.3	139.9	-150.8	187.4	-1069.7	115.5
17/10/2012	210	-752.7	116.7	-243.8	107.0	-1038.8	127.2	-1194.4	369.9	-442.0	378.2	-744.1	129.6	-152.9	185.4	-1081.1	104.7
18/10/2012	211	-750.0	119.3	-240.9	109.8	-1014.0	150.8	-1188.2	375.8	-435.5	384.5	-740.6	132.9	-138.3	199.2	-1070.5	114.7
19/10/2012	212	-744.3	124.6	-236.1	114.3	-991.9	171.7	-1203.6	361.2	-437.9	382.1	-736.5	136.9	-129.0	208.1	-1070.2	115.0
20/10/2012	213	-750.2	119.1	-242.6	108.2	-988.8	174.6	-1211.1	354.1	-436.0	384.0	-742.5	131.1	-133.6	203.7	-1067.6	117.5
21/10/2012	214	-758.3	111.4	-251.5	99.7	-994.5	169.2	-1220.1	345.6	-444.4	376.0	-754.2	120.1	-143.3	194.5	-1074.2	111.2
22/10/2012	215	-756.9	112.8	-247.2	103.8	-985.3	178.0	-1227.0	339.0	-448.8	371.8	-752.6	121.6	-140.5	197.1	-1079.7	106.0
23/10/2012	216	-750.3	119.0	-240.3	110.3	-983.5	179.7	-1216.7	348.9	-435.5	384.5	-742.2	131.4	-125.7	211.2	-1073.0	112.4
24/10/2012	217	-747.2	121.9	-239.4	111.2	-1010.5	154.0	-1217.9	347.7	-436.7	383.3	-738.4	135.0	-134.9	202.4	-1077.3	108.3
25/10/2012	218	-752.3	117.1	-247.9	103.2	-997.1	166.8	-1219.9	345.8	-438.8	381.3	-746.9	127.0	-138.7	198.8	-1076.9	108.6
26/10/2012	219	-753.3	116.1	-249.6	101.5	-978.9	184.0	-1227.6	338.5	-442.4	377.9	-750.0	124.1	-140.7	196.9	-1077.0	108.5
27/10/2012	220	-749.8	119.4	-246.0	105.0	-998.3	165.6	-1224.7	341.3	-439.4	380.8	-745.7	128.1	-144.1	193.7	-1075.9	109.6
28/10/2012	221	-752.1	117.3	-245.8	105.2	-1014.8	150.0	-1228.8	337.4	-443.1	377.3	-746.4	127.4	-143.5	194.3	-1083.0	102.9
29/10/2012	222	-751.1	118.2	-241.4	109.3	-1005.9	158.4	-1226.3	339.7	-439.4	380.7	-744.6	129.2	-142.0	195.7	-1078.9	106.7
30/10/2012	223	-747.5	121.6	-239.9	110.8	-983.1	180.0	-1223.5	342.4	-436.4	383.6	-738.9	134.6	-137.9	199.6	-1073.4	112.0
31/10/2012	224	-750.6	118.7	-242.1	108.6	-954.5	207.2	-1237.4	329.2	-440.3	379.9	-743.3	130.4	-128.1	208.9	-1072.0	113.3
1/11/2012	225	-739.8	129.0	-227.0	122.9	-936.0	224.7	-1240.7	326.1	-430.0	389.7	-727.3	145.6	-113.9	222.3	-1061.4	123.4
2/11/2012	226	-747.3	121.8	-236.1	114.3	-959.7	202.2	-1247.9	319.3	-438.2	381.9	-738.1	135.4	-121.2	215.4	-1077.5	108.1
3/11/2012	227	-749.2	120.0	-239.9	110.8	-978.0	184.8	-1253.7	313.8	-443.1	377.2	-738.8	134.6	-127.9	209.0	-1084.0	101.9
4/11/2012	228	-748.0	121.2	-240.5	110.2	-988.0	175.3	-1255.5	312.1	-444.7	375.7	-739.5	134.0	-132.2	205.0	-1081.9	103.9
5/11/2012	229	-747.6	121.6	-237.6	112.9	-956.7	205.1	-1246.8	320.3	-437.3	382.7	-738.7	134.8	-120.0	216.5	-1067.3	117.7
6/11/2012	230	-749.1	120.1	-235.7	114.7	-940.4	220.5	-1251.3	316.0	-443.2	377.1	-738.2	135.2	-120.4	216.2	-1069.1	116.0
7/11/2012	231	-754.8	114.8	-240.3	110.3	-940.8	220.1	-1249.8	317.4	-445.0	375.5	-742.5	131.1	-117.0	219.4	-1069.1	116.0
8/11/2012	232	-749.2	120.0	-232.0	118.2	-929.9	230.5	-1244.6	322.4	-441.0	379.2	-733.0	140.1	-113.6	222.6	-1062.8	122.0

9/11/2012	233	-754.7	114.9	-238.2	112.3	-932.1	228.3	-1245.2	321.8	-447.1	373.4	-740.7	132.8	-115.9	220.4	-1067.3	117.7
10/11/2012	234	-750.6	118.7	-235.4	115.0	-931.1	229.3	-1244.3	322.7	-446.0	374.5	-736.0	137.3	-110.2	225.9	-1069.2	116.0
11/11/2012	235	-750.1	119.2	-235.4	115.0	-935.2	225.4	-1241.3	325.5	-442.6	377.7	-736.8	136.5	-109.8	226.3	-1070.4	114.8
12/11/2012	236	-743.9	125.1	-225.0	124.9	-935.6	225.1	-1237.8	328.8	-435.8	384.1	-728.0	144.9	-107.1	228.8	-1068.7	116.4
13/11/2012	237	-743.8	125.1	-225.8	124.1	-938.8	222.0	-1240.3	326.5	-438.0	382.1	-728.9	144.1	-113.5	222.8	-1071.0	114.2
14/11/2012	238	-748.5	120.7	-231.6	118.6	-940.4	220.4	-1241.4	325.4	-439.3	380.8	-735.4	137.9	-118.4	218.1	-1071.3	114.0
15/11/2012	239	-736.1	132.5	-217.3	132.1	-931.9	228.6	-1234.1	332.4	-431.7	388.1	-719.2	153.2	-112.8	223.4	-1061.5	123.3
16/11/2012	240	-748.2	121.0	-230.9	119.2	-939.3	221.5	-1244.7	322.3	-444.9	375.6	-735.2	138.1	-121.5	215.1	-1071.6	113.7

Table E.13 Steel strain for slab S-SCC-a

Slab S-SCC-a		STEEL STRAIN BY SG															
		1		2		3		4		5		6		7		8	
Date	Age	Reading	Strain	Reading	Strain	Reading	Strain	Reading	Strain	Reading	Strain	Reading	Strain	Reading	Strain	Reading	Strain
26/04/2012	14	-1029.3		-1170.0		-1050.0		-637.3		-1248.6		-1601.3		-810.8		-1255.5	
27/04/2012	15	-924.4	99.4	-1091.1	74.8	-924.1	119.4	-471.3	157.4	-1087.2	153.1	-1452.4	141.1	-756.2	51.8	-1179.0	72.5
28/04/2012	16	-915.2	108.1	-1072.0	92.8	-917.1	126.0	-458.0	169.9	-1066.2	172.9	-1434.2	158.4	-749.9	57.7	-1164.5	86.3
29/04/2012	17	-901.7	120.9	-1052.5	111.3	-907.9	134.7	-442.7	184.5	-1049.1	189.1	-1420.6	171.2	-746.9	60.5	-1148.5	101.4
30/04/2012	18	-885.1	136.7	-1025.4	137.1	-889.9	151.7	-422.6	203.6	-1030.0	207.3	-1400.2	190.6	-730.4	76.1	-1131.9	117.1
1/05/2012	19	-883.7	138.0	-1017.9	144.1	-892.4	149.4	-424.0	202.2	-1029.8	207.4	-1402.2	188.8	-731.7	74.9	-1132.4	116.7
2/05/2012	20	-871.1	150.0	-1008.1	153.4	-880.0	161.2	-412.2	213.4	-1016.6	220.0	-1391.5	198.9	-720.8	85.2	-1119.6	128.8
3/05/2012	21	-865.7	155.1	-1002.2	159.0	-870.4	170.2	-403.9	221.2	-1009.9	226.3	-1384.0	206.0	-712.8	92.8	-1111.6	136.4
4/05/2012	22	-861.4	159.1	-991.1	169.5	-866.9	173.6	-392.9	231.7	-1002.5	233.3	-1374.9	214.6	-700.7	104.3	-1104.0	143.6
5/05/2012	23	-870.8	150.3	-998.3	162.7	-880.6	160.6	-401.5	223.6	-1008.6	227.5	-1386.6	203.6	-711.0	94.6	-1113.7	134.4
6/05/2012	24	-873.3	147.9	-1000.9	160.2	-885.7	155.7	-402.4	222.6	-1009.0	227.2	-1387.5	202.7	-712.3	93.4	-1111.7	136.2
7/05/2012	25	-860.4	160.1	-991.5	169.1	-869.7	170.9	-385.7	238.5	-992.4	242.8	-1369.6	219.7	-695.6	109.2	-1094.4	152.6
8/05/2012	26	-844.8	174.9	-974.4	185.3	-851.3	188.4	-367.1	256.1	-981.5	253.2	-1353.1	235.3	-676.3	127.5	-1074.4	171.6
9/05/2012	27	-836.5	182.8	-967.6	191.8	-843.3	196.0	-357.6	265.2	-974.5	259.8	-1345.7	242.3	-660.6	142.4	-1067.4	178.3
10/05/2012	28	-825.6	193.1	-959.9	199.1	-836.3	202.6	-352.0	270.4	-971.0	263.2	-1341.2	246.5	-653.3	149.2	-1062.5	182.9
11/05/2012	29	-823.2	195.3	-956.5	202.3	-835.0	203.8	-351.0	271.4	-966.7	267.2	-1340.1	247.6	-652.6	149.9	-1062.6	182.8
12/05/2012	30	-824.5	194.1	-955.5	203.3	-837.6	201.3	-349.1	273.2	-965.6	268.2	-1339.4	248.3	-653.2	149.3	-1061.7	183.7
13/05/2012	31	-825.9	192.8	-954.1	204.6	-836.3	202.6	-344.4	277.7	-968.9	265.2	-1340.0	247.6	-651.1	151.3	-1057.8	187.4
14/05/2012	32	-814.8	203.3	-946.1	212.2	-818.1	219.9	-331.7	289.6	-954.7	278.7	-1325.4	261.5	-639.7	162.2	-1037.6	206.6
15/05/2012	33	-817.3	201.0	-948.6	209.8	-818.6	219.4	-330.4	290.9	-942.1	290.5	-1319.0	267.6	-631.2	170.2	-1029.9	213.8
16/05/2012	34	-812.9	205.1	-943.2	215.0	-814.8	222.9	-320.8	300.0	-937.8	294.6	-1318.5	268.1	-633.4	168.1	-1028.0	215.6
17/05/2012	35	-821.9	196.6	-947.5	210.9	-826.4	211.9	-330.3	291.0	-944.3	288.5	-1318.2	268.3	-633.7	167.8	-1030.9	212.9
18/05/2012	36	-814.6	203.5	-944.1	214.1	-817.9	220.0	-323.7	297.2	-936.9	295.5	-1300.6	285.1	-623.8	177.2	-1025.8	217.7
19/05/2012	37	-815.1	203.0	-946.8	211.5	-819.6	218.4	-322.3	298.6	-937.7	294.8	-1311.7	274.5	-627.2	174.0	-1030.0	213.8
20/05/2012	38	-814.0	204.1	-947.5	210.8	-822.3	215.8	-319.3	301.4	-939.3	293.2	-1310.7	275.5	-617.5	183.2	-1024.4	219.0
21/05/2012	39	-817.3	200.9	-951.1	207.4	-823.7	214.5	-321.7	299.2	-941.7	291.0	-1311.8	274.4	-621.8	179.2	-1026.0	217.5
22/05/2012	40	-811.1	206.8	-943.9	214.3	-820.2	217.8	-316.1	304.5	-938.9	293.6	-1306.1	279.9	-619.1	181.6	-1022.2	221.1
23/05/2012	41	-804.4	213.2	-943.1	215.0	-816.9	221.0	-308.8	311.4	-937.0	295.4	-1300.7	285.0	-614.3	186.2	-1016.3	226.7
24/05/2012	42	-815.3	202.8	-953.4	205.3	-828.6	209.9	-316.6	304.0	-942.2	290.4	-1305.0	280.8	-612.3	188.1	-1019.7	223.4
25/05/2012	43	-813.2	204.9	-949.1	209.4	-824.8	213.5	-315.0	305.5	-942.8	289.9	-1301.3	284.3	-606.7	193.5	-1020.5	222.7
26/05/2012	44	-819.8	198.6	-955.3	203.5	-830.1	208.4	-315.8	304.8	-944.9	287.9	-1303.5	282.2	-606.0	194.1	-1022.9	220.5
27/05/2012	45	-818.5	199.8	-956.3	202.5	-828.0	210.5	-310.5	309.8	-940.2	292.3	-1300.8	284.8	-601.5	198.4	-1019.1	224.0

28/05/2012	46	-805.2	212.4	-942.0	216.1	-814.9	222.9	-297.7	321.9	-924.7	307.0	-1286.9	298.0	-582.5	216.4	-1004.1	238.3
29/05/2012	47	-809.8	208.0	-947.9	210.5	-821.7	216.4	-305.4	314.6	-933.5	298.7	-1295.3	290.1	-592.7	206.7	-1013.8	229.1
30/05/2012	48	-805.2	212.5	-942.7	215.4	-813.6	224.2	-297.4	322.1	-923.6	308.0	-1287.8	297.2	-587.1	212.0	-1008.0	234.6
31/05/2012	49	-810.2	207.7	-949.2	209.2	-816.2	221.7	-302.4	317.4	-926.9	305.0	-1289.8	295.2	-587.9	211.2	-1009.0	233.7
1/06/2012	50	-812.0	206.0	-947.6	210.8	-821.2	216.9	-305.9	314.1	-928.7	303.2	-1289.5	295.5	-589.7	209.5	-1008.6	234.0
2/06/2012	51	-812.1	205.9	-944.1	214.1	-817.7	220.2	-305.9	314.2	-932.0	300.1	-1292.7	292.5	-595.8	203.8	-1008.4	234.2
3/06/2012	52	-809.6	208.3	-940.4	217.5	-815.8	222.1	-304.6	315.4	-929.9	302.1	-1292.6	292.6	-590.9	208.4	-1009.2	233.5
4/06/2012	53	-813.1	204.9	-944.8	213.4	-818.2	219.7	-306.5	313.6	-933.7	298.5	-1291.4	293.7	-591.0	208.3	-1010.4	232.3
5/06/2012	54	-807.6	210.1	-941.4	216.6	-815.0	222.7	-296.2	323.3	-934.1	298.1	-1285.5	299.3	-595.6	204.0	-1006.4	236.1
6/06/2012	55	-819.0	199.4	-957.2	201.7	-830.6	208.0	-311.1	309.2	-942.7	290.0	-1293.9	291.4	-600.1	199.6	-1010.9	231.8
7/06/2012	56	-808.1	209.7	-950.3	208.2	-823.0	215.2	-301.6	318.2	-932.2	299.9	-1284.8	300.0	-591.5	207.9	-1004.3	238.1
8/06/2012	57	-799.9	217.5	-937.5	220.4	-817.9	220.0	-290.8	328.5	-916.2	315.1	-1276.9	307.5	-585.6	213.5	-999.5	242.6
9/06/2012	58	-803.3	214.2	-940.4	217.6	-817.6	220.3	-288.7	330.5	-912.8	318.3	-1276.4	308.0	-581.9	217.0	-996.4	245.6
10/06/2012	59	-802.7	214.8	-938.5	219.4	-812.5	225.2	-286.1	332.9	-906.2	324.6	-1272.1	312.0	-572.0	226.3	-992.7	249.0
11/06/2012	60	-807.7	210.0	-941.3	216.7	-813.8	224.0	-291.9	327.4	-916.5	314.9	-1277.3	307.1	-581.5	217.4	-995.5	246.5
12/06/2012	61	-807.1	210.6	-947.0	211.3	-816.0	221.8	-295.6	323.9	-927.1	304.8	-1283.3	301.4	-591.0	208.3	-999.4	242.7
13/06/2012	62	-800.0	217.4	-935.4	222.4	-807.4	230.0	-287.1	331.9	-913.1	318.0	-1274.2	310.1	-580.8	218.0	-992.7	249.1
14/06/2012	63	-798.9	218.4	-933.8	223.8	-803.7	233.5	-286.2	332.8	-911.7	319.4	-1273.2	311.0	-576.4	222.1	-991.7	250.0
15/06/2012	64	-805.6	212.1	-939.7	218.2	-811.2	226.4	-291.5	327.8	-919.3	312.1	-1279.3	305.2	-582.5	216.4	-997.6	244.4
16/06/2012	65	-802.6	214.9	-937.8	220.1	-810.3	227.3	-289.4	329.8	-918.0	313.4	-1280.0	304.6	-582.8	216.1	-995.8	246.1
17/06/2012	66	-810.7	207.2	-946.3	212.0	-823.1	215.1	-298.8	320.8	-921.6	309.9	-1286.1	298.8	-593.6	205.8	-1006.0	236.5
18/06/2012	67	-810.4	207.5	-945.8	212.5	-820.2	217.8	-290.1	329.1	-920.1	311.4	-1281.4	303.2	-589.8	209.4	-1001.7	240.5
19/06/2012	68	-804.0	213.6	-941.9	216.2	-818.7	219.3	-283.7	335.2	-916.8	314.5	-1276.6	307.8	-583.9	215.0	-997.3	244.8
20/06/2012	69	-809.4	208.5	-948.5	209.9	-822.5	215.7	-287.3	331.8	-912.4	318.7	-1277.8	306.7	-581.3	217.5	-997.1	244.9
21/06/2012	70	-800.8	216.6	-939.4	218.6	-816.1	221.7	-278.9	339.7	-901.4	329.2	-1271.4	312.7	-569.1	229.1	-992.0	249.8
22/06/2012	71	-812.7	205.4	-956.2	202.6	-825.9	212.5	-288.2	330.9	-906.3	324.4	-1280.8	303.8	-572.4	226.0	-997.9	244.1
23/06/2012	72	-809.7	208.2	-948.3	210.1	-824.8	213.5	-284.4	334.6	-907.5	323.3	-1276.0	308.3	-567.3	230.7	-994.2	247.7
24/06/2012	73	-809.2	208.6	-943.4	214.8	-823.4	214.8	-282.3	336.5	-903.3	327.3	-1275.1	309.2	-567.1	231.0	-994.8	247.0
25/06/2012	74	-807.7	210.0	-940.4	217.6	-818.6	219.4	-277.0	341.5	-900.4	330.1	-1269.5	314.5	-563.4	234.5	-988.3	253.2
26/06/2012	75	-818.8	199.5	-949.7	208.8	-822.3	215.9	-286.2	332.8	-910.3	320.7	-1277.7	306.8	-576.3	222.2	-995.2	246.7
27/06/2012	76	-812.9	205.2	-950.3	208.2	-816.7	221.2	-281.7	337.1	-910.6	320.4	-1277.1	307.3	-568.8	229.3	-996.1	245.8
28/06/2012	77	-816.7	201.5	-950.8	207.8	-817.3	220.6	-282.5	336.3	-909.0	321.9	-1276.1	308.2	-566.4	231.6	-995.7	246.3
29/06/2012	78	-812.9	205.2	-949.5	208.9	-814.6	223.1	-282.2	336.6	-908.0	322.8	-1278.5	306.0	-566.6	231.5	-996.6	245.4
30/06/2012	79	-814.9	203.3	-953.6	205.1	-818.6	219.3	-285.7	333.3	-914.6	316.6	-1282.8	301.9	-570.8	227.4	-1001.8	240.5
1/07/2012	80	-818.8	199.5	-955.2	203.5	-822.1	216.1	-286.1	332.9	-919.3	312.2	-1287.5	297.5	-580.8	218.0	-1008.4	234.2
2/07/2012	81	-809.5	208.3	-939.9	218.0	-814.8	223.0	-273.2	345.1	-904.2	326.5	-1271.8	312.3	-566.3	231.7	-998.8	243.3
3/07/2012	82	-816.3	201.9	-941.4	216.7	-820.8	217.3	-275.7	342.7	-907.2	323.7	-1274.5	309.8	-567.9	230.2	-1000.6	241.6

4/07/2012	83	-816.7	201.5	-944.6	213.6	-821.4	216.8	-275.3	343.2	-902.4	328.2	-1271.2	312.9	-562.7	235.2	-997.5	244.6
5/07/2012	84	-825.8	192.9	-953.6	205.1	-826.1	212.3	-281.9	336.9	-909.1	321.9	-1274.3	309.9	-567.2	230.9	-999.2	242.9
6/07/2012	85	-828.7	190.2	-956.0	202.8	-828.2	210.3	-284.2	334.7	-918.9	312.5	-1278.5	306.0	-571.9	226.4	-1000.4	241.8
7/07/2012	86	-819.4	199.0	-950.2	208.3	-823.4	214.8	-278.6	340.0	-916.0	315.3	-1275.0	309.3	-566.7	231.4	-997.3	244.7
8/07/2012	87	-825.6	193.1	-959.3	199.6	-827.3	211.1	-285.0	334.0	-922.9	308.8	-1282.8	301.9	-572.5	225.8	-1003.3	239.0
9/07/2012	88	-811.8	206.2	-950.7	207.8	-816.0	221.9	-273.8	344.6	-906.5	324.3	-1272.2	311.9	-560.2	237.5	-992.0	249.7
10/07/2012	89	-810.7	207.2	-951.2	207.3	-813.8	223.9	-275.3	343.2	-906.4	324.4	-1272.8	311.4	-558.2	239.4	-994.0	247.9
11/07/2012	90	-822.7	195.9	-970.3	189.2	-830.0	208.5	-293.3	326.0	-921.8	309.8	-1289.4	295.6	-574.2	224.2	-1010.3	232.4
12/07/2012	91	-810.2	207.7	-959.8	199.2	-816.9	220.9	-281.3	337.4	-914.6	316.7	-1276.6	307.8	-564.0	233.9	-996.3	245.7
13/07/2012	92	-811.9	206.1	-960.5	198.6	-817.6	220.3	-285.9	333.1	-916.1	315.2	-1283.0	301.7	-569.4	228.8	-1000.9	241.3
14/07/2012	93	-814.9	203.3	-963.5	195.7	-822.6	215.5	-291.5	327.8	-919.8	311.7	-1287.5	297.5	-573.0	225.3	-1002.9	239.4
15/07/2012	94	-817.1	201.1	-971.0	188.6	-828.2	210.2	-290.7	328.5	-920.5	311.0	-1288.0	296.9	-579.7	219.0	-1005.5	236.9
16/07/2012	95	-804.0	213.6	-957.1	201.8	-815.2	222.6	-272.1	346.1	-906.3	324.5	-1270.0	314.0	-563.7	234.2	-991.8	249.9
17/07/2012	96	-800.3	217.0	-949.8	208.7	-806.9	230.4	-262.8	355.0	-909.6	321.4	-1269.8	314.3	-562.3	235.6	-991.9	249.8
18/07/2012	97	-783.1	233.4	-930.2	227.2	-786.3	250.0	-242.7	374.0	-910.4	320.6	-1274.4	309.9	-564.9	233.0	-992.9	248.9
19/07/2012	98	-778.2	238.1	-918.6	238.3	-780.6	255.4	-236.6	379.9	-902.2	328.3	-1269.4	314.6	-560.2	237.5	-988.4	253.1
20/07/2012	99	-774.1	241.9	-912.1	244.4	-778.1	257.7	-230.7	385.4	-898.9	331.5	-1260.0	323.5	-550.1	247.1	-983.0	258.2
21/07/2012	100	-781.5	234.9	-926.6	230.7	-781.7	254.3	-238.8	377.8	-921.4	310.1	-1268.2	315.7	-554.6	242.9	-990.6	251.0
22/07/2012	101	-781.4	235.0	-928.0	229.3	-784.6	251.6	-241.8	374.9	-918.9	312.5	-1273.8	310.4	-557.9	239.7	-990.5	251.2
23/07/2012	102	-803.6	214.0	-949.1	209.4	-804.0	233.2	-261.6	356.1	-920.3	311.2	-1278.6	305.9	-561.7	236.1	-995.1	246.8
24/07/2012	103	-827.7	191.2	-974.7	185.1	-830.2	208.3	-288.1	331.0	-919.0	312.5	-1276.2	308.1	-563.8	234.1	-994.8	247.1
25/07/2012	104	-818.0	200.3	-966.4	193.0	-820.7	217.4	-280.6	338.2	-912.3	318.8	-1269.7	314.3	-554.4	243.0	-986.6	254.9
26/07/2012	105	-821.7	196.8	-970.5	189.1	-824.0	214.2	-285.7	333.3	-916.4	314.9	-1274.3	310.0	-558.7	239.0	-990.9	250.8
27/07/2012	106	-801.4	216.0	-946.1	212.2	-801.7	235.3	-259.1	358.5	-904.1	326.5	-1268.9	315.1	-556.3	241.2	-988.0	253.5
28/07/2012	107	-776.4	239.7	-914.8	241.8	-776.8	259.0	-231.0	385.1	-906.6	324.2	-1268.0	315.9	-560.6	237.2	-989.1	252.5
29/07/2012	108	-787.8	228.9	-922.3	234.8	-782.9	253.2	-236.1	380.3	-908.5	322.4	-1272.5	311.6	-563.8	234.1	-991.1	250.5
30/07/2012	109	-783.8	232.8	-914.3	242.3	-782.1	254.0	-230.4	385.7	-901.1	329.4	-1267.2	316.6	-557.8	239.8	-987.8	253.7
31/07/2012	110	-789.3	227.5	-916.8	239.9	-784.1	252.1	-231.3	384.9	-901.8	328.8	-1265.6	318.3	-552.7	244.6	-987.2	254.3
1/08/2012	111	-785.4	231.2	-911.6	244.9	-777.6	258.2	-224.0	391.8	-890.3	339.6	-1255.8	327.5	-544.8	252.1	-978.1	262.9
2/08/2012	112	-790.8	226.1	-912.5	244.0	-777.1	258.7	-223.7	392.1	-889.0	340.8	-1256.3	327.0	-547.7	249.4	-981.8	259.4
3/08/2012	113	-790.6	226.3	-915.4	241.3	-776.3	259.5	-222.9	392.8	-889.3	340.6	-1256.5	326.8	-548.5	248.6	-979.9	261.2
4/08/2012	114	-785.6	231.1	-920.1	236.8	-771.6	263.9	-221.0	394.6	-894.2	336.0	-1258.0	325.4	-547.8	249.3	-978.3	262.8
5/08/2012	115	-789.0	227.8	-934.4	223.3	-773.6	262.0	-223.7	392.0	-906.4	324.4	-1263.4	320.3	-550.6	246.6	-978.1	262.9
6/08/2012	116	-785.4	231.2	-939.6	218.3	-773.4	262.2	-221.4	394.2	-904.1	326.6	-1262.5	321.1	-555.4	242.0	-972.2	268.5
7/08/2012	117	-778.8	237.5	-925.5	231.7	-770.1	265.3	-212.3	402.9	-893.1	337.0	-1250.6	332.4	-543.4	253.4	-964.0	276.3
8/08/2012	118	-781.3	235.1	-926.9	230.3	-773.5	262.1	-212.3	402.8	-896.6	333.6	-1250.7	332.3	-546.9	250.2	-965.6	274.7
9/08/2012	119	-779.0	237.3	-934.2	223.4	-773.2	262.4	-215.3	400.0	-900.8	329.7	-1257.5	325.9	-555.8	241.7	-965.3	275.1

10/08/2012	120	-785.0	231.6	-936.5	221.3	-782.0	254.1	-220.4	395.2	-902.1	328.4	-1259.9	323.6	-554.9	242.5	-970.8	269.8
11/08/2012	121	-785.5	231.1	-940.6	217.4	-781.6	254.4	-228.2	387.8	-910.4	320.6	-1265.5	318.3	-568.4	229.7	-979.0	262.1
12/08/2012	122	-782.8	233.7	-934.9	222.8	-782.8	253.3	-232.6	383.6	-919.4	312.1	-1269.8	314.3	-561.9	235.9	-982.9	258.3
13/08/2012	123	-769.8	246.0	-925.0	232.2	-774.3	261.3	-220.2	395.3	-902.3	328.3	-1257.3	326.0	-547.2	249.8	-969.1	271.4
14/08/2012	124	-768.6	247.1	-920.5	236.5	-772.1	263.5	-216.8	398.6	-892.9	337.1	-1252.3	330.8	-537.1	259.4	-963.3	276.9
15/08/2012	125	-775.6	240.5	-936.4	221.4	-775.4	260.4	-222.0	393.7	-896.9	333.4	-1257.7	325.7	-545.0	251.9	-965.2	275.2
16/08/2012	126	-772.2	243.7	-941.1	216.9	-774.5	261.2	-221.9	393.8	-901.3	329.2	-1256.1	327.2	-546.0	250.9	-964.7	275.6
17/08/2012	127	-775.5	240.6	-946.4	211.9	-780.3	255.7	-228.6	387.4	-906.6	324.2	-1261.6	322.0	-548.3	248.8	-970.2	270.4
18/08/2012	128	-771.7	244.2	-940.4	217.6	-775.8	260.0	-223.4	392.4	-903.0	327.6	-1256.7	326.6	-556.7	240.9	-965.2	275.1
19/08/2012	129	-767.3	248.4	-939.4	218.5	-774.4	261.3	-221.4	394.2	-901.6	328.9	-1255.1	328.2	-555.6	241.8	-962.9	277.4
20/08/2012	130	-769.0	246.8	-937.9	219.9	-777.9	257.9	-218.7	396.8	-898.0	332.4	-1251.1	331.9	-544.4	252.4	-959.5	280.5
21/08/2012	131	-787.8	228.9	-963.0	196.2	-796.1	240.7	-238.6	377.9	-913.4	317.8	-1261.2	322.4	-554.7	242.8	-968.4	272.1
22/08/2012	132	-784.0	232.5	-951.2	207.4	-793.0	243.7	-239.8	376.8	-915.3	315.9	-1265.0	318.8	-555.1	242.3	-969.9	270.7
23/08/2012	133	-778.8	237.5	-943.9	214.3	-785.6	250.7	-237.2	379.2	-921.0	310.6	-1264.1	319.6	-543.2	253.7	-970.9	269.8
24/08/2012	134	-786.4	230.3	-947.2	211.1	-792.9	243.8	-242.5	374.2	-925.8	306.0	-1267.9	316.0	-546.5	250.5	-974.1	266.7
25/08/2012	135	-795.3	221.8	-960.3	198.7	-798.0	238.9	-244.1	372.8	-922.6	309.0	-1266.9	317.0	-549.8	247.3	-969.9	270.7
26/08/2012	136	-800.5	216.9	-965.2	194.1	-803.1	234.1	-244.8	372.1	-918.0	313.3	-1267.5	316.4	-556.7	240.8	-974.1	266.7
27/08/2012	137	-792.3	224.6	-955.0	203.7	-795.4	241.3	-233.8	382.5	-909.7	321.3	-1255.8	327.5	-543.8	253.0	-964.2	276.1
28/08/2012	138	-791.8	225.1	-953.7	205.0	-795.9	240.9	-235.9	380.5	-918.9	312.5	-1259.6	323.9	-544.4	252.5	-966.4	274.0
29/08/2012	139	-790.7	226.1	-947.4	210.9	-796.0	240.8	-238.5	378.1	-921.3	310.3	-1263.8	319.9	-546.0	250.9	-968.1	272.4
30/08/2012	140	-785.9	230.7	-947.2	211.1	-788.2	248.2	-232.4	383.8	-915.6	315.7	-1258.5	324.9	-536.3	260.1	-962.6	277.6
31/08/2012	141	-791.0	225.9	-960.2	198.8	-795.9	240.9	-233.1	383.2	-907.5	323.4	-1258.8	324.7	-544.6	252.3	-964.5	275.8
1/09/2012	142	-786.6	230.1	-959.0	200.0	-793.2	243.4	-223.7	392.0	-892.2	337.8	-1244.4	338.3	-530.8	265.4	-955.8	284.0
2/09/2012	143	-799.8	217.6	-963.9	195.3	-803.6	233.6	-232.3	383.9	-908.3	322.6	-1254.7	328.5	-543.1	253.8	-963.8	276.5
3/09/2012	144	-788.7	228.1	-946.0	212.2	-791.0	245.5	-221.2	394.4	-898.4	332.0	-1245.8	336.9	-531.8	264.4	-953.4	286.3
4/09/2012	145	-792.2	224.7	-953.8	204.9	-795.6	241.1	-227.5	388.5	-905.2	325.5	-1248.9	334.1	-540.2	256.4	-957.1	282.8
5/09/2012	146	-797.4	219.9	-957.8	201.1	-796.7	240.2	-230.1	385.9	-898.5	331.9	-1249.4	333.6	-533.2	263.1	-955.1	284.7
6/09/2012	147	-791.3	225.6	-949.8	208.7	-789.7	246.8	-224.6	391.2	-893.1	337.0	-1244.3	338.3	-523.0	272.8	-948.0	291.5
7/09/2012	148	-792.4	224.6	-953.6	205.1	-788.9	247.5	-223.5	392.2	-895.4	334.9	-1245.0	337.7	-524.7	271.1	-946.2	293.2
8/09/2012	149	-801.5	215.9	-964.0	195.2	-796.1	240.7	-231.7	384.5	-901.7	328.9	-1246.9	335.9	-530.1	266.0	-947.2	292.2
9/09/2012	150	-801.6	215.9	-965.8	193.5	-799.4	237.5	-233.8	382.4	-906.4	324.4	-1252.1	331.0	-533.3	263.0	-953.0	286.7
10/09/2012	151	-787.9	228.8	-960.4	198.6	-793.8	242.9	-227.3	388.6	-903.7	327.0	-1248.4	334.5	-526.7	269.3	-951.3	288.4
11/09/2012	152	-785.5	231.1	-943.0	215.1	-789.0	247.4	-224.8	391.0	-907.2	323.7	-1245.3	337.5	-523.5	272.3	-952.4	287.3
12/09/2012	153	-791.6	225.3	-954.6	204.1	-799.7	237.3	-235.8	380.6	-911.0	320.0	-1255.7	327.6	-536.4	260.1	-965.3	275.1
13/09/2012	154	-784.5	232.1	-942.8	215.3	-791.1	245.4	-230.8	385.4	-906.5	324.3	-1254.5	328.7	-527.8	268.2	-961.5	278.6
14/09/2012	155	-782.9	233.6	-938.9	219.0	-790.1	246.4	-222.0	393.7	-899.5	330.9	-1244.7	338.0	-520.5	275.1	-953.5	286.2
15/09/2012	156	-793.8	223.2	-952.0	206.6	-800.1	236.9	-230.1	386.0	-915.7	315.6	-1251.1	332.0	-531.5	264.7	-955.0	284.8

16/09/2012	157	-795.3	221.8	-953.5	205.2	-800.6	236.4	-233.6	382.7	-918.5	312.9	-1255.4	327.8	-537.4	259.1	-957.6	282.4
17/09/2012	158	-784.3	232.2	-940.2	217.8	-793.3	243.3	-225.2	390.6	-907.0	323.8	-1252.2	330.9	-531.3	264.9	-958.9	281.2
18/09/2012	159	-780.4	236.0	-931.2	226.3	-786.4	249.9	-219.1	396.4	-904.0	326.7	-1249.9	333.1	-529.1	267.0	-959.0	281.0
19/09/2012	160	-785.8	230.8	-930.9	226.6	-787.2	249.1	-215.6	399.7	-901.0	329.5	-1249.1	333.8	-525.6	270.3	-953.8	285.9
20/09/2012	161	-786.5	230.2	-934.8	222.9	-786.3	250.0	-212.4	402.8	-889.6	340.3	-1243.1	339.5	-516.0	279.4	-947.9	291.5
21/09/2012	162	-782.8	233.7	-931.2	226.3	-783.2	252.9	-209.7	405.3	-889.1	340.8	-1241.7	340.8	-512.3	282.9	-946.1	293.2
22/09/2012	163	-785.1	231.5	-928.7	228.7	-781.5	254.5	-208.2	406.7	-885.1	344.6	-1242.5	340.1	-513.5	281.7	-944.2	295.1
23/09/2012	164	-787.8	229.0	-933.8	223.9	-783.8	252.4	-211.2	403.9	-884.2	345.4	-1246.0	336.8	-518.8	276.7	-950.1	289.4
24/09/2012	165	-782.5	234.0	-934.7	223.0	-784.5	251.7	-206.1	408.7	-887.0	342.7	-1249.1	333.8	-521.4	274.3	-952.6	287.1
25/09/2012	166	-787.6	229.2	-933.6	224.0	-787.2	249.1	-204.0	410.7	-892.3	337.8	-1251.4	331.6	-522.9	272.9	-953.5	286.2
26/09/2012	167	-793.5	223.5	-940.2	217.7	-790.8	245.8	-209.2	405.8	-892.3	337.8	-1253.8	329.4	-528.1	268.0	-956.1	283.7
27/09/2012	168	-790.6	226.3	-936.6	221.2	-785.8	250.4	-208.6	406.4	-896.3	333.9	-1253.1	330.1	-526.1	269.8	-955.0	284.8
28/09/2012	169	-790.1	226.7	-937.8	220.1	-784.3	251.9	-210.1	404.9	-899.4	331.0	-1254.1	329.1	-530.6	265.5	-959.7	280.3
29/09/2012	170	-788.1	228.7	-937.2	220.6	-786.5	249.8	-211.9	403.2	-898.4	332.0	-1254.6	328.7	-527.5	268.5	-957.8	282.1
30/09/2012	171	-792.3	224.7	-941.5	216.5	-792.0	244.6	-208.9	406.1	-900.9	329.6	-1259.2	324.3	-536.0	260.4	-961.9	278.3
1/10/2012	172	-795.2	221.9	-947.9	210.5	-797.5	239.3	-211.4	403.7	-894.7	335.5	-1257.8	325.6	-534.0	262.3	-961.8	278.4
2/10/2012	173	-800.4	217.0	-952.4	206.2	-805.8	231.5	-221.4	394.2	-901.7	328.8	-1262.9	320.8	-537.5	259.0	-963.8	276.5
3/10/2012	174	-795.6	221.5	-947.7	210.7	-800.4	236.6	-217.6	397.8	-896.7	333.6	-1255.4	327.8	-532.4	263.9	-957.0	282.9
4/10/2012	175	-794.9	222.2	-943.0	215.2	-797.8	239.1	-214.8	400.4	-896.3	333.9	-1257.0	326.3	-532.4	263.9	-957.8	282.1
5/10/2012	176	-794.6	222.5	-941.6	216.4	-798.7	238.2	-214.0	401.2	-888.4	341.4	-1251.5	331.6	-524.2	271.7	-952.9	286.8
6/10/2012	177	-797.3	219.9	-943.9	214.3	-798.2	238.7	-219.5	396.0	-899.7	330.8	-1253.5	329.7	-529.2	266.9	-957.0	282.9
7/10/2012	178	-805.0	212.7	-950.9	207.7	-802.5	234.7	-227.1	388.8	-908.4	322.5	-1259.8	323.7	-538.9	257.7	-962.2	278.0
8/10/2012	179	-796.4	220.8	-949.1	209.4	-799.0	238.0	-219.0	396.5	-896.3	334.0	-1253.9	329.3	-529.6	266.5	-954.5	285.2
9/10/2012	180	-798.9	218.4	-948.9	209.6	-802.7	234.4	-220.0	395.5	-889.0	340.8	-1256.3	327.1	-530.1	266.1	-953.2	286.5
10/10/2012	181	-790.7	226.2	-941.1	216.9	-794.0	242.7	-210.4	404.6	-886.2	343.6	-1248.6	334.3	-522.2	273.6	-949.8	289.7
11/10/2012	182	-798.5	218.8	-951.4	207.2	-803.3	233.8	-221.9	393.7	-894.0	336.2	-1256.3	327.0	-528.7	267.4	-958.6	281.4
12/10/2012	183	-781.7	234.7	-922.2	234.8	-780.6	255.4	-192.0	422.1	-867.6	361.1	-1227.5	354.3	-505.8	289.0	-934.4	304.3
13/10/2012	184	-787.3	229.4	-934.6	223.1	-788.4	248.0	-200.1	414.4	-879.0	350.3	-1228.5	353.3	-511.0	284.2	-938.9	300.1
14/10/2012	185	-790.6	226.2	-943.5	214.7	-795.0	241.7	-209.6	405.4	-886.4	343.3	-1241.0	341.6	-521.7	274.0	-950.1	289.4
15/10/2012	186	-785.5	231.1	-943.3	214.8	-791.0	245.6	-206.1	408.7	-881.1	348.4	-1238.3	344.0	-516.6	278.8	-946.2	293.1
16/10/2012	187	-787.9	228.8	-947.2	211.1	-793.3	243.3	-207.4	407.5	-886.7	343.0	-1245.6	337.2	-520.7	275.0	-950.7	288.9
17/10/2012	188	-796.8	220.4	-955.9	202.9	-805.1	232.1	-217.0	398.4	-889.8	340.1	-1255.0	328.3	-527.6	268.4	-957.3	282.6
18/10/2012	189	-787.0	229.7	-951.9	206.7	-794.5	242.2	-208.0	406.9	-884.8	344.9	-1248.4	334.5	-519.2	276.4	-950.0	289.5
19/10/2012	190	-787.2	229.5	-949.6	208.9	-792.6	244.0	-207.0	407.9	-889.7	340.2	-1247.3	335.6	-520.7	274.9	-952.0	287.6
20/10/2012	191	-788.5	228.3	-946.1	212.2	-789.9	246.5	-203.9	410.8	-883.3	346.3	-1243.3	339.4	-514.9	280.4	-947.1	292.3
21/10/2012	192	-793.7	223.3	-949.6	208.8	-795.7	241.1	-210.4	404.6	-889.8	340.1	-1251.5	331.6	-515.5	279.9	-954.3	285.5
22/10/2012	193	-796.1	221.1	-952.6	206.1	-800.8	236.2	-211.2	403.9	-892.4	337.7	-1257.0	326.4	-519.6	276.0	-958.2	281.8

23/10/2012	194	-788.4	228.3	-950.3	208.2	-793.6	243.1	-199.2	415.3	-880.1	349.3	-1243.6	339.1	-512.5	282.7	-944.5	294.7
24/10/2012	195	-795.6	221.6	-960.3	198.8	-800.3	236.7	-204.9	409.8	-884.9	344.7	-1249.2	333.7	-524.0	271.8	-950.9	288.7
25/10/2012	196	-793.5	223.6	-959.1	199.9	-800.0	237.0	-205.7	409.1	-885.7	344.0	-1250.3	332.7	-522.6	273.2	-952.3	287.4
26/10/2012	197	-795.9	221.2	-958.8	200.2	-798.1	238.8	-205.4	409.4	-886.2	343.5	-1251.2	331.9	-516.8	278.6	-952.0	287.7
27/10/2012	198	-794.7	222.4	-951.6	206.9	-795.8	241.0	-201.7	412.9	-885.8	343.9	-1249.9	333.1	-514.6	280.8	-951.5	288.2
28/10/2012	199	-804.1	213.5	-960.4	198.7	-803.3	233.8	-209.1	405.8	-889.3	340.6	-1255.7	327.6	-522.2	273.5	-955.4	284.4
29/10/2012	200	-800.4	217.0	-960.8	198.2	-798.8	238.2	-204.8	409.9	-880.7	348.7	-1252.9	330.2	-524.1	271.7	-950.4	289.2
30/10/2012	201	-794.5	222.6	-957.4	201.5	-792.6	244.0	-199.3	415.1	-876.7	352.5	-1248.2	334.7	-513.3	282.0	-946.3	293.1
31/10/2012	202	-787.8	229.0	-949.4	209.0	-791.5	245.1	-197.5	416.9	-877.4	351.9	-1249.2	333.8	-508.1	286.9	-946.2	293.2
1/11/2012	203	-776.2	239.9	-935.5	222.2	-781.7	254.4	-185.9	427.8	-867.7	361.0	-1240.9	341.6	-499.7	294.9	-937.0	301.9
2/11/2012	204	-790.3	226.6	-951.8	206.8	-795.4	241.4	-195.9	418.4	-879.9	349.5	-1250.2	332.8	-511.5	283.7	-947.5	291.9
3/11/2012	205	-799.9	217.5	-960.3	198.7	-802.5	234.6	-204.6	410.2	-883.4	346.2	-1254.9	328.3	-517.0	278.4	-949.8	289.7
4/11/2012	206	-801.5	216.0	-957.1	201.8	-803.1	234.0	-207.4	407.5	-887.7	342.1	-1258.2	325.2	-521.7	274.0	-954.0	285.8
5/11/2012	207	-785.8	230.8	-941.1	216.9	-787.6	248.7	-195.5	418.8	-878.7	350.6	-1250.2	332.8	-517.0	278.4	-946.6	292.7
6/11/2012	208	-783.2	233.3	-939.4	218.5	-785.0	251.2	-194.8	419.5	-879.5	349.9	-1249.3	333.7	-514.0	281.3	-947.3	292.1
7/11/2012	209	-780.8	235.6	-939.8	218.2	-784.7	251.5	-196.6	417.7	-878.0	351.3	-1248.8	334.1	-510.8	284.4	-945.7	293.6
8/11/2012	210	-773.4	242.6	-934.3	223.4	-778.6	257.2	-192.4	421.7	-875.4	353.8	-1244.9	337.8	-504.8	290.0	-942.0	297.1
9/11/2012	211	-773.7	242.3	-932.9	224.7	-783.0	253.2	-197.4	417.0	-878.8	350.6	-1249.5	333.5	-502.0	292.7	-945.3	294.0
10/11/2012	212	-774.0	242.0	-928.1	229.3	-784.5	251.7	-196.9	417.5	-876.3	352.9	-1248.5	334.4	-503.2	291.5	-946.1	293.2
11/11/2012	213	-776.6	239.6	-930.9	226.6	-785.5	250.8	-195.1	419.2	-879.1	350.3	-1248.9	334.0	-505.1	289.8	-947.5	292.0
12/11/2012	214	-776.2	239.9	-933.2	224.4	-782.7	253.4	-189.9	424.1	-867.9	360.9	-1242.7	339.9	-500.4	294.1	-939.5	299.5
13/11/2012	215	-778.7	237.6	-939.8	218.2	-786.0	250.3	-194.6	419.6	-874.3	354.8	-1248.6	334.3	-509.8	285.3	-943.8	295.4
14/11/2012	216	-779.4	236.9	-939.4	218.5	-788.2	248.2	-197.5	416.8	-875.6	353.6	-1249.1	333.8	-510.7	284.4	-945.2	294.1
15/11/2012	217	-771.9	244.0	-934.2	223.5	-779.8	256.2	-190.0	424.0	-867.7	361.1	-1238.3	344.1	-500.5	294.1	-938.1	300.9
16/11/2012	218	-781.7	234.7	-937.9	220.0	-788.9	247.5	-200.5	414.1	-878.1	351.2	-1248.9	334.0	-506.3	288.6	-948.8	290.7
17/11/2012	219	-779.4	236.9	-936.8	221.0	-789.6	246.8	-198.7	415.8	-874.8	354.4	-1249.1	333.9	-505.3	289.5	-947.0	292.4
18/11/2012	220	-787.8	228.9	-940.8	217.3	-794.6	242.1	-204.1	410.6	-885.8	343.9	-1254.0	329.2	-511.6	283.6	-952.6	287.0
19/11/2012	221	-788.3	228.4	-943.4	214.7	-795.7	241.1	-202.3	412.3	-878.8	350.6	-1253.1	330.1	-511.8	283.4	-951.7	287.9
20/11/2012	222	-783.7	232.8	-938.5	219.3	-788.0	248.4	-193.0	421.1	-869.6	359.3	-1242.7	339.9	-502.8	291.9	-939.6	299.4
21/11/2012	223	-780.4	236.0	-934.4	223.3	-784.5	251.6	-187.8	426.1	-861.4	367.0	-1233.6	348.5	-496.6	297.8	-930.3	308.2
22/11/2012	224	-802.9	214.7	-958.5	200.4	-809.0	228.4	-213.5	401.8	-878.2	351.1	-1247.7	335.2	-511.5	283.7	-943.0	296.2
23/11/2012	225	-819.0	199.4	-975.8	184.1	-826.9	211.5	-229.9	386.1	-879.1	350.3	-1251.3	331.8	-514.5	280.8	-946.0	293.3
24/11/2012	226	-806.8	211.0	-958.5	200.4	-811.1	226.5	-215.6	399.7	-858.7	369.6	-1227.6	354.2	-485.8	308.1	-921.2	316.9
25/11/2012	227	-784.9	231.7	-934.6	223.1	-784.8	251.4	-191.7	422.4	-836.5	390.6	-1202.8	377.7	-458.5	333.9	-897.3	339.5
26/11/2012	228	-810.1	207.8	-961.4	197.7	-809.1	228.4	-219.8	395.7	-864.3	364.3	-1234.1	348.1	-485.2	308.6	-930.3	308.2
27/11/2012	229	-792.3	224.6	-941.8	216.3	-793.7	243.0	-205.3	409.4	-844.6	382.9	-1216.6	364.7	-466.8	326.1	-914.3	323.4
28/11/2012	230	-787.9	228.8	-935.7	222.0	-791.3	245.2	-201.2	413.3	-839.3	388.0	-1212.9	368.2	-463.6	329.1	-909.3	328.1

29/11/2012	231	-798.7	218.6	-949.7	208.8	-805.1	232.1	-216.2	399.1	-839.9	387.5	-1226.3	355.5	-478.5	314.9	-922.7	315.5
30/11/2012	232	-796.7	220.5	-950.0	208.5	-806.1	231.3	-217.1	398.3	-846.4	381.2	-1229.4	352.5	-478.5	315.0	-924.0	314.2
1/12/2012	233	-771.1	244.7	-918.4	238.5	-778.5	257.4	-190.8	423.3	-821.6	404.7	-1201.7	378.7	-449.4	342.5	-896.2	340.6
2/12/2012	234	-773.6	242.4	-918.7	238.1	-779.7	256.3	-192.4	421.7	-819.2	407.0	-1203.4	377.1	-449.7	342.3	-898.4	338.5
3/12/2012	235	-805.1	212.5	-948.6	209.8	-813.9	223.8	-225.9	390.0	-850.9	377.0	-1238.5	343.8	-484.7	309.1	-931.4	307.2
4/12/2012	236	-833.8	185.4	-976.6	183.3	-843.8	195.5	-252.8	364.4	-878.5	350.8	-1268.8	315.1	-516.9	278.6	-964.0	276.2
5/12/2012	237	-838.1	181.3	-979.8	180.3	-848.0	191.5	-250.4	366.7	-870.9	358.0	-1264.1	319.6	-518.4	277.1	-961.1	279.1
6/12/2012	238	-838.9	180.5	-982.9	177.3	-846.2	193.2	-247.7	369.3	-854.6	373.5	-1260.5	323.0	-516.9	278.5	-955.6	284.3
7/12/2012	239	-773.6	242.4	-921.9	235.1	-779.1	256.8	-181.3	432.2	-840.4	387.0	-1265.3	318.5	-521.0	274.7	-960.3	279.8
8/12/2012	240	-726.0	287.5	-873.4	281.1	-734.4	299.2	-138.6	472.7	-814.1	411.9	-1256.6	326.7	-511.0	284.1	-951.3	288.3

Table E.14 Steel strain for slab S-SCC-b

Slab S-SCC-b		STEEL STRAIN BY SG															
		1		2		3		4		5		6		7		8	
Date	Age	Reading	Strain	Reading	Strain	Reading	Strain	Reading	Strain	Reading	Strain	Reading	Strain	Reading	Strain	Reading	Strain
26/04/2012	14	-839.6		-317.0		-543.9		-405.8		-1420.7		-770.7		-1134.5		-900.6	
27/04/2012	15	-786.7	50.2	-266.7	47.7	-470.8	69.3	-352.4	50.6	-1371.7	46.5	-732.3	36.4	-1090.5	41.7	-816.4	79.8
28/04/2012	16	-766.7	69.1	-250.6	62.9	-440.5	98.0	-330.3	71.5	-1351.6	65.5	-718.2	49.8	-1072.6	58.7	-802.1	93.4
29/04/2012	17	-752.7	82.4	-237.8	75.0	-420.2	117.3	-315.4	85.6	-1334.3	81.9	-708.6	58.8	-1059.7	70.9	-791.8	103.2
30/04/2012	18	-732.9	101.1	-219.7	92.2	-390.7	145.2	-293.9	106.0	-1313.9	101.2	-692.4	74.2	-1039.0	90.5	-775.2	118.8
1/05/2012	19	-735.1	99.0	-222.6	89.4	-391.6	144.4	-294.6	105.4	-1311.3	103.7	-694.5	72.2	-1040.8	88.9	-776.6	117.6
2/05/2012	20	-724.3	109.3	-210.3	101.1	-375.8	159.4	-283.0	116.3	-1299.2	115.1	-684.7	81.5	-1029.9	99.2	-767.9	125.8
3/05/2012	21	-717.2	116.1	-202.8	108.2	-364.1	170.4	-274.5	124.4	-1287.6	126.2	-678.2	87.6	-1022.7	106.0	-762.2	131.2
4/05/2012	22	-710.2	122.7	-194.8	115.8	-351.8	182.1	-265.6	132.9	-1276.3	136.9	-673.7	91.9	-1016.0	112.4	-756.8	136.4
5/05/2012	23	-723.3	110.3	-208.5	102.8	-366.9	167.8	-276.6	122.5	-1286.1	127.6	-686.7	79.6	-1028.6	100.4	-766.9	126.7
6/05/2012	24	-726.5	107.3	-212.0	99.4	-370.2	164.6	-279.0	120.2	-1290.6	123.3	-691.3	75.2	-1032.0	97.2	-769.6	124.2
7/05/2012	25	-705.0	127.6	-191.6	118.8	-340.0	193.3	-256.9	141.1	-1279.4	133.9	-671.1	94.4	-1010.0	118.0	-752.0	140.9
8/05/2012	26	-685.2	146.4	-175.0	134.6	-309.5	222.2	-234.7	162.2	-1252.7	159.2	-651.9	112.6	-989.4	137.6	-735.5	156.5
9/05/2012	27	-680.8	150.6	-170.4	138.9	-301.2	230.0	-228.6	167.9	-1236.5	174.6	-646.4	117.8	-984.2	142.5	-731.4	160.4
10/05/2012	28	-677.8	153.4	-166.0	143.1	-295.2	235.8	-224.2	172.1	-1236.7	174.4	-641.7	122.2	-980.8	145.7	-728.6	163.0
11/05/2012	29	-676.2	154.9	-162.7	146.2	-290.6	240.1	-220.9	175.3	-1234.5	176.5	-640.0	123.9	-978.0	148.3	-726.4	165.1
12/05/2012	30	-676.4	154.7	-162.7	146.2	-288.9	241.8	-219.6	176.5	-1231.3	179.5	-641.9	122.0	-977.4	149.0	-725.9	165.6
13/05/2012	31	-675.7	155.4	-164.5	144.5	-285.3	245.1	-217.0	178.9	-1225.8	184.7	-642.4	121.5	-976.6	149.7	-725.3	166.2
14/05/2012	32	-662.4	168.0	-152.8	155.6	-267.1	262.4	-203.7	191.5	-1219.8	190.4	-629.7	133.6	-962.6	163.0	-714.1	176.8
15/05/2012	33	-656.9	173.2	-146.2	161.9	-258.0	271.0	-197.1	197.8	-1208.0	201.6	-625.2	137.8	-957.9	167.4	-710.3	180.4
16/05/2012	34	-654.7	175.3	-140.1	167.6	-249.7	278.9	-191.0	203.6	-1193.1	215.7	-618.8	143.9	-949.7	175.2	-703.7	186.6
17/05/2012	35	-659.7	170.5	-144.9	163.1	-258.2	270.8	-197.2	197.7	-1199.5	209.7	-621.9	141.0	-959.1	166.3	-711.3	179.5
18/05/2012	36	-653.0	176.9	-137.7	169.9	-246.6	281.8	-188.8	205.7	-1190.2	218.4	-611.5	150.9	-952.1	172.9	-705.7	184.8
19/05/2012	37	-655.6	174.4	-140.7	167.1	-248.7	279.9	-190.3	204.3	-1191.7	217.1	-617.5	145.2	-952.3	172.7	-705.8	184.6
20/05/2012	38	-655.3	174.8	-139.9	167.8	-244.9	283.4	-187.5	206.9	-1186.8	221.7	-616.0	146.6	-954.0	171.1	-707.2	183.3
21/05/2012	39	-656.8	173.3	-140.6	167.1	-246.0	282.4	-188.3	206.1	-1192.9	215.9	-615.6	147.0	-955.1	170.1	-708.1	182.5
22/05/2012	40	-653.6	176.3	-136.0	171.6	-238.1	289.9	-182.6	211.6	-1184.6	223.8	-613.1	149.3	-951.3	173.7	-705.0	185.4
23/05/2012	41	-647.9	181.7	-133.3	174.1	-227.2	300.2	-174.6	219.1	-1179.5	228.6	-610.9	151.4	-945.0	179.7	-700.0	190.2
24/05/2012	42	-651.7	178.1	-138.6	169.1	-230.1	297.4	-176.7	217.1	-1180.0	228.1	-613.3	149.2	-948.9	176.0	-703.1	187.2
25/05/2012	43	-651.6	178.2	-137.9	169.7	-233.1	294.6	-178.9	215.0	-1190.6	218.0	-609.9	152.3	-950.8	174.1	-704.6	185.8
26/05/2012	44	-652.8	177.1	-141.0	166.8	-232.3	295.4	-178.3	215.6	-1184.0	224.4	-614.9	147.6	-949.0	175.9	-703.2	187.1
27/05/2012	45	-648.9	180.8	-136.2	171.3	-227.1	300.3	-174.6	219.2	-1188.7	219.9	-611.7	150.6	-947.5	177.3	-702.0	188.3

28/05/2012	46	-634.4	194.5	-122.4	184.4	-204.7	321.5	-158.2	234.7	-1185.6	222.8	-594.9	166.6	-932.4	191.6	-689.9	199.7
29/05/2012	47	-645.4	184.2	-133.6	173.8	-218.1	308.8	-168.0	225.4	-1174.6	233.2	-602.0	159.9	-943.7	180.8	-699.0	191.1
30/05/2012	48	-640.0	189.3	-124.1	182.8	-206.9	319.5	-159.8	233.2	-1165.1	242.2	-595.0	166.5	-935.3	188.8	-692.3	197.5
31/05/2012	49	-641.5	187.8	-126.7	180.3	-205.3	320.9	-158.6	234.3	-1168.7	238.9	-596.6	164.9	-937.0	187.2	-693.6	196.2
1/06/2012	50	-641.3	188.0	-126.9	180.2	-207.8	318.6	-160.5	232.5	-1176.8	231.1	-595.3	166.2	-939.7	184.7	-695.8	194.2
2/06/2012	51	-644.2	185.3	-127.6	179.5	-214.1	312.6	-165.0	228.2	-1180.3	227.9	-597.0	164.6	-941.0	183.4	-696.8	193.2
3/06/2012	52	-644.7	184.8	-126.1	180.9	-212.1	314.5	-163.6	229.6	-1164.0	243.3	-596.9	164.7	-943.7	180.9	-698.9	191.2
4/06/2012	53	-644.6	184.9	-125.9	181.1	-209.6	316.9	-161.7	231.3	-1162.3	244.9	-596.5	165.1	-942.6	181.9	-698.1	192.0
5/06/2012	54	-639.3	189.9	-122.4	184.4	-201.5	324.6	-155.8	236.9	-1160.0	247.1	-595.0	166.5	-935.5	188.7	-692.4	197.4
6/06/2012	55	-644.8	184.7	-128.6	178.5	-206.9	319.4	-159.8	233.1	-1169.2	238.4	-599.5	162.2	-940.3	184.1	-696.3	193.7
7/06/2012	56	-636.4	192.6	-119.8	186.9	-196.8	329.0	-152.4	240.2	-1154.7	252.1	-592.3	169.1	-932.8	191.2	-690.3	199.4
8/06/2012	57	-631.1	197.7	-113.5	192.8	-186.4	338.8	-144.8	247.3	-1151.7	255.0	-588.0	173.1	-926.9	196.8	-685.6	203.9
9/06/2012	58	-628.7	199.9	-112.4	193.9	-182.5	342.6	-141.9	250.1	-1155.3	251.5	-586.0	175.1	-925.1	198.5	-684.1	205.3
10/06/2012	59	-623.1	205.2	-107.7	198.3	-174.9	349.7	-136.4	255.3	-1147.2	259.2	-581.0	179.7	-921.1	202.3	-680.9	208.3
11/06/2012	60	-628.4	200.3	-112.7	193.6	-184.2	341.0	-143.2	248.9	-1153.0	253.7	-583.9	177.0	-928.2	195.5	-686.6	202.9
12/06/2012	61	-633.5	195.4	-119.0	187.7	-191.9	333.6	-148.9	243.5	-1154.8	252.0	-585.6	175.4	-931.1	192.8	-688.9	200.7
13/06/2012	62	-627.9	200.7	-108.7	197.4	-183.2	341.9	-142.5	249.5	-1139.6	266.5	-579.0	181.7	-924.6	199.0	-683.7	205.6
14/06/2012	63	-627.5	201.1	-106.9	199.1	-180.2	344.7	-140.3	251.6	-1140.6	265.4	-577.8	182.8	-924.2	199.3	-683.4	205.9
15/06/2012	64	-631.6	197.2	-112.2	194.0	-183.0	342.1	-142.3	249.7	-1144.9	261.4	-582.3	178.6	-927.0	196.7	-685.6	203.8
16/06/2012	65	-631.4	197.4	-111.9	194.4	-179.7	345.2	-139.9	252.0	-1145.0	261.3	-582.7	178.2	-925.7	197.9	-684.6	204.8
17/06/2012	66	-642.1	187.2	-121.1	185.7	-193.7	332.0	-150.1	242.3	-1164.9	242.5	-594.4	167.0	-936.5	187.7	-693.2	196.6
18/06/2012	67	-635.3	193.7	-115.7	190.8	-183.0	342.1	-142.3	249.7	-1147.0	259.4	-589.6	171.6	-929.1	194.7	-687.3	202.2
19/06/2012	68	-629.7	199.0	-110.9	195.3	-173.8	350.9	-135.6	256.1	-1145.4	260.9	-586.1	174.9	-924.1	199.4	-683.3	206.0
20/06/2012	69	-629.5	199.2	-112.6	193.7	-174.4	350.3	-136.0	255.7	-1148.8	257.7	-586.4	174.6	-924.5	199.1	-683.6	205.7
21/06/2012	70	-625.1	203.4	-107.3	198.8	-167.2	357.1	-130.8	260.6	-1143.1	263.1	-582.0	178.8	-919.4	203.9	-679.5	209.6
22/06/2012	71	-629.5	199.2	-113.1	193.2	-171.1	353.4	-133.6	257.9	-1141.5	264.6	-586.4	174.6	-923.7	199.8	-683.0	206.3
23/06/2012	72	-627.8	200.8	-110.0	196.1	-171.0	353.5	-133.6	258.0	-1138.3	267.7	-585.9	175.1	-922.4	201.0	-681.9	207.3
24/06/2012	73	-628.7	199.9	-111.0	195.2	-170.1	354.3	-132.9	258.6	-1145.1	261.2	-588.2	172.9	-926.9	196.8	-685.5	203.9
25/06/2012	74	-623.6	204.8	-106.1	199.8	-161.6	362.4	-126.7	264.5	-1140.9	265.2	-584.0	176.9	-923.0	200.5	-682.4	206.8
26/06/2012	75	-628.5	200.2	-112.6	193.7	-170.9	353.5	-133.5	258.1	-1153.0	253.8	-588.3	172.9	-931.7	192.3	-689.4	200.2
27/06/2012	76	-629.2	199.5	-110.3	195.8	-172.0	352.6	-134.3	257.3	-1144.4	261.9	-586.6	174.4	-929.8	194.1	-687.8	201.7
28/06/2012	77	-628.9	199.8	-112.3	194.0	-170.5	353.9	-133.2	258.3	-1140.1	266.0	-586.0	175.0	-928.7	195.1	-686.9	202.6
29/06/2012	78	-629.4	199.3	-112.1	194.2	-172.3	352.2	-134.5	257.1	-1140.6	265.5	-583.5	177.4	-929.1	194.7	-687.3	202.2
30/06/2012	79	-634.6	194.3	-115.6	190.8	-177.9	346.9	-138.6	253.2	-1137.1	268.8	-587.6	173.5	-933.3	190.7	-690.6	199.0
1/07/2012	80	-640.2	189.1	-122.2	184.6	-182.5	342.6	-142.0	250.0	-1145.5	260.8	-596.3	165.3	-937.2	187.0	-693.8	196.0
2/07/2012	81	-628.1	200.5	-110.3	195.9	-163.8	360.3	-128.3	263.0	-1142.8	263.4	-586.0	175.1	-921.8	201.6	-681.4	207.8
3/07/2012	82	-630.6	198.2	-113.1	193.2	-162.9	361.1	-127.7	263.6	-1144.0	262.2	-589.5	171.7	-928.5	195.3	-686.8	202.7

4/07/2012	83	-626.6	201.9	-112.3	194.0	-159.6	364.2	-125.3	265.9	-1147.9	258.6	-585.4	175.6	-925.4	198.2	-684.3	205.0
5/07/2012	84	-629.5	199.2	-115.0	191.5	-163.7	360.4	-128.2	263.1	-1157.4	249.5	-587.2	173.9	-929.7	194.2	-687.8	201.8
6/07/2012	85	-633.6	195.3	-116.7	189.8	-171.1	353.3	-133.7	257.9	-1157.9	249.1	-589.3	171.9	-933.8	190.3	-691.0	198.7
7/07/2012	86	-629.0	199.7	-112.5	193.8	-167.7	356.6	-131.1	260.3	-1145.0	261.3	-585.2	175.8	-930.1	193.8	-688.1	201.5
8/07/2012	87	-636.0	193.0	-119.4	187.3	-179.8	345.2	-140.0	251.9	-1148.2	258.3	-591.2	170.1	-937.0	187.2	-693.6	196.2
9/07/2012	88	-627.0	201.6	-107.0	199.0	-165.0	359.1	-129.2	262.1	-1137.0	268.9	-581.3	179.5	-927.1	196.6	-685.7	203.7
10/07/2012	89	-626.8	201.8	-106.8	199.2	-163.3	360.8	-128.0	263.3	-1137.4	268.5	-580.4	180.4	-926.6	197.1	-685.3	204.1
11/07/2012	90	-646.0	183.5	-125.8	181.2	-188.7	336.7	-146.5	245.8	-1148.6	257.9	-598.1	163.6	-945.4	179.3	-700.3	189.9
12/07/2012	91	-630.0	198.7	-112.0	194.3	-166.9	357.4	-130.6	260.8	-1128.3	277.1	-583.0	177.9	-927.1	196.7	-685.6	203.8
13/07/2012	92	-636.1	192.9	-117.8	188.8	-176.9	347.9	-137.9	253.9	-1140.5	265.6	-585.2	175.8	-932.0	192.0	-689.6	200.0
14/07/2012	93	-640.9	188.4	-124.1	182.8	-182.0	343.1	-141.6	250.4	-1150.8	255.9	-589.1	172.1	-939.0	185.3	-695.2	194.7
15/07/2012	94	-643.4	186.0	-124.1	182.8	-180.8	344.2	-140.7	251.2	-1146.4	260.0	-595.3	166.3	-938.8	185.5	-695.0	194.9
16/07/2012	95	-627.2	201.4	-107.4	198.6	-155.3	368.3	-122.1	268.9	-1130.8	274.8	-580.1	180.7	-920.2	203.1	-680.2	208.9
17/07/2012	96	-625.8	202.7	-106.5	199.5	-154.4	369.2	-121.5	269.5	-1139.5	266.5	-578.8	181.9	-921.5	201.9	-681.2	208.0
18/07/2012	97	-626.9	201.7	-110.3	195.9	-155.1	368.5	-122.0	269.0	-1147.4	259.0	-579.5	181.2	-923.6	199.9	-682.9	206.4
19/07/2012	98	-623.2	205.1	-107.6	198.4	-149.4	374.0	-117.8	273.0	-1141.7	264.4	-576.0	184.5	-919.8	203.5	-679.8	209.3
20/07/2012	99	-617.5	210.6	-100.1	205.5	-140.5	382.4	-111.3	279.1	-1132.8	272.9	-572.0	188.3	-914.3	208.7	-675.5	213.4
21/07/2012	100	-621.0	207.2	-106.9	199.1	-147.2	376.1	-116.2	274.5	-1147.0	259.4	-574.8	185.6	-919.7	203.6	-679.8	209.3
22/07/2012	101	-623.8	204.6	-110.3	195.9	-154.3	369.3	-121.4	269.6	-1147.7	258.7	-577.3	183.2	-922.6	200.9	-682.1	207.1
23/07/2012	102	-628.2	200.4	-113.9	192.5	-163.2	360.9	-127.9	263.4	-1146.2	260.2	-580.8	179.9	-926.4	197.3	-685.1	204.3
24/07/2012	103	-631.7	197.1	-112.4	193.9	-168.8	355.5	-132.0	259.5	-1142.7	263.5	-581.5	179.3	-930.6	193.3	-688.5	201.1
25/07/2012	104	-626.5	202.1	-103.6	202.2	-159.5	364.4	-125.2	266.0	-1131.9	273.7	-574.4	186.0	-924.2	199.4	-683.4	205.9
26/07/2012	105	-626.1	202.4	-104.6	201.3	-157.9	365.9	-124.0	267.1	-1128.5	276.9	-576.7	183.8	-925.2	198.4	-684.1	205.2
27/07/2012	106	-623.3	205.0	-101.7	204.1	-150.5	372.9	-118.6	272.2	-1127.1	278.3	-573.8	186.6	-919.5	203.8	-679.6	209.5
28/07/2012	107	-621.9	206.4	-101.2	204.5	-144.9	378.2	-114.5	276.1	-1124.3	280.9	-572.3	188.0	-919.1	204.2	-679.3	209.8
29/07/2012	108	-624.5	203.9	-104.2	201.7	-145.7	377.4	-115.1	275.5	-1131.2	274.4	-574.7	185.7	-919.1	204.2	-679.3	209.8
30/07/2012	109	-622.1	206.2	-102.6	203.1	-142.1	380.9	-112.5	278.0	-1123.9	281.3	-575.3	185.2	-918.9	204.4	-679.1	209.9
31/07/2012	110	-620.9	207.3	-102.3	203.5	-139.7	383.1	-110.8	279.6	-1136.6	269.3	-575.6	184.9	-919.0	204.3	-679.2	209.9
1/08/2012	111	-610.8	216.9	-93.1	212.2	-125.7	396.4	-100.5	289.3	-1135.8	270.1	-567.2	192.9	-909.9	212.9	-671.9	216.8
2/08/2012	112	-611.9	215.9	-93.2	212.1	-124.4	397.6	-99.6	290.2	-1136.1	269.8	-569.4	190.7	-910.4	212.5	-672.3	216.4
3/08/2012	113	-611.6	216.2	-91.7	213.5	-124.2	397.8	-99.4	290.4	-1126.0	279.3	-570.0	190.2	-908.8	214.0	-671.0	217.6
4/08/2012	114	-611.1	216.6	-92.6	212.6	-122.4	399.6	-98.1	291.6	-1108.4	296.0	-572.1	188.3	-907.1	215.5	-669.7	218.9
5/08/2012	115	-614.9	213.0	-97.4	208.1	-126.1	396.0	-100.8	289.0	-1102.7	301.4	-575.2	185.3	-909.9	212.9	-671.9	216.8
6/08/2012	116	-612.9	214.9	-94.9	210.5	-122.2	399.7	-98.0	291.8	-1101.6	302.5	-573.1	187.3	-907.6	215.1	-670.1	218.5
7/08/2012	117	-606.6	220.9	-88.9	216.2	-113.7	407.8	-91.7	297.7	-1093.5	310.2	-568.6	191.5	-902.8	219.6	-666.3	222.1
8/08/2012	118	-605.7	221.7	-89.0	216.1	-115.7	405.8	-93.2	296.2	-1105.4	298.9	-567.5	192.6	-903.1	219.4	-666.4	222.0
9/08/2012	119	-607.3	220.3	-93.0	212.2	-116.2	405.4	-93.6	295.9	-1107.6	296.7	-566.1	193.9	-902.8	219.6	-666.2	222.2

10/08/2012	120	-613.0	214.8	-96.6	208.9	-126.3	395.8	-101.0	288.9	-1110.2	294.3	-575.2	185.2	-909.2	213.5	-671.4	217.3
11/08/2012	121	-615.3	212.7	-102.5	203.3	-129.3	393.0	-103.1	286.9	-1117.4	287.5	-575.3	185.2	-912.2	210.7	-673.8	215.0
12/08/2012	122	-620.4	207.8	-105.1	200.9	-139.4	383.4	-110.5	279.9	-1109.2	295.2	-576.8	183.8	-918.9	204.3	-679.2	209.9
13/08/2012	123	-609.7	218.0	-89.1	216.0	-125.5	396.6	-100.4	289.5	-1095.2	308.5	-566.8	193.2	-906.0	216.6	-668.8	219.8
14/08/2012	124	-605.2	222.2	-83.7	221.1	-121.3	400.6	-97.3	292.4	-1097.8	306.1	-562.9	196.9	-899.5	222.8	-663.6	224.7
15/08/2012	125	-604.8	222.6	-89.6	215.5	-118.1	403.6	-95.0	294.6	-1098.7	305.2	-561.6	198.2	-896.5	225.6	-661.2	226.9
16/08/2012	126	-606.6	220.9	-94.5	210.9	-117.8	403.9	-94.8	294.8	-1101.6	302.5	-564.9	195.0	-899.6	222.7	-663.7	224.6
17/08/2012	127	-611.4	216.3	-97.8	207.8	-124.8	397.3	-99.8	290.0	-1102.7	301.4	-567.7	192.4	-904.0	218.5	-667.2	221.3
18/08/2012	128	-607.3	220.2	-94.9	210.5	-118.7	403.0	-95.4	294.2	-1096.1	307.6	-564.9	195.0	-897.1	225.1	-661.7	226.5
19/08/2012	129	-605.7	221.7	-91.7	213.5	-119.0	402.7	-95.7	294.0	-1101.9	302.2	-561.9	197.9	-896.7	225.4	-661.4	226.8
20/08/2012	130	-604.4	222.9	-88.4	216.7	-115.8	405.8	-93.2	296.2	-1092.6	311.0	-561.1	198.6	-897.8	224.4	-662.3	225.9
21/08/2012	131	-610.8	216.9	-97.2	208.3	-126.8	395.3	-101.3	288.6	-1107.3	297.0	-566.4	193.6	-906.1	216.5	-668.9	219.6
22/08/2012	132	-612.9	214.9	-101.2	204.5	-132.6	389.9	-105.6	284.6	-1105.9	298.3	-565.1	194.9	-906.3	216.4	-669.0	219.5
23/08/2012	133	-612.0	215.7	-94.9	210.5	-132.6	389.9	-105.5	284.6	-1093.3	310.3	-563.4	196.5	-909.5	213.3	-671.6	217.1
24/08/2012	134	-617.9	210.2	-101.2	204.5	-135.9	386.7	-108.0	282.3	-1102.8	301.3	-571.2	189.0	-916.7	206.5	-677.3	211.6
25/08/2012	135	-616.9	211.1	-103.5	202.4	-127.7	394.5	-102.0	288.0	-1101.7	302.3	-572.5	187.8	-908.6	214.1	-670.9	217.7
26/08/2012	136	-620.9	207.4	-106.4	199.6	-132.4	390.1	-105.4	284.7	-1101.1	303.0	-574.1	186.3	-911.6	211.3	-673.3	215.5
27/08/2012	137	-608.8	218.8	-93.3	212.0	-116.8	404.9	-94.0	295.5	-1093.4	310.2	-562.5	197.3	-899.1	223.1	-663.3	224.9
28/08/2012	138	-611.3	216.4	-92.6	212.6	-121.5	400.4	-97.5	292.2	-1088.7	314.7	-562.1	197.6	-905.0	217.5	-668.0	220.5
29/08/2012	139	-614.5	213.4	-97.7	207.8	-132.2	390.2	-105.3	284.8	-1088.5	314.8	-563.5	196.4	-909.0	213.8	-671.2	217.5
30/08/2012	140	-607.7	219.8	-92.4	212.8	-121.4	400.5	-97.4	292.3	-1084.8	318.4	-558.6	201.0	-906.0	216.6	-668.8	219.7
31/08/2012	141	-613.4	214.5	-96.2	209.3	-120.0	401.8	-96.3	293.3	-1086.5	316.8	-564.9	195.1	-904.6	217.9	-667.7	220.8
1/09/2012	142	-600.3	226.9	-83.1	221.7	-105.0	416.1	-85.4	303.7	-1078.5	324.3	-556.9	202.6	-892.3	229.6	-657.8	230.1
2/09/2012	143	-607.7	219.9	-96.3	209.1	-116.8	404.8	-94.0	295.5	-1091.2	312.3	-564.7	195.3	-902.9	219.6	-666.3	222.1
3/09/2012	144	-597.6	229.4	-82.4	222.4	-99.2	421.5	-81.1	307.7	-1078.7	324.2	-552.1	207.1	-891.0	230.9	-656.8	231.1
4/09/2012	145	-599.7	227.5	-86.0	218.9	-99.6	421.2	-81.5	307.4	-1089.1	314.3	-553.3	206.0	-894.2	227.8	-659.3	228.7
5/09/2012	146	-601.4	225.9	-85.4	219.5	-101.1	419.7	-82.5	306.4	-1094.7	309.0	-555.5	203.9	-894.2	227.8	-659.4	228.7
6/09/2012	147	-594.3	232.6	-77.5	227.0	-87.5	432.7	-72.6	315.8	-1072.7	329.8	-548.4	210.7	-885.6	236.0	-652.5	235.2
7/09/2012	148	-592.9	233.9	-79.0	225.6	-87.8	432.3	-72.9	315.6	-1067.4	334.8	-547.4	211.6	-884.4	237.1	-651.5	236.1
8/09/2012	149	-595.5	231.4	-83.4	221.4	-93.2	427.2	-76.8	311.8	-1072.5	330.0	-549.2	209.9	-888.2	233.5	-654.6	233.2
9/09/2012	150	-599.5	227.6	-92.2	213.0	-103.4	417.6	-84.2	304.8	-1080.9	322.0	-550.3	208.9	-892.0	229.9	-657.6	230.3
10/09/2012	151	-598.0	229.0	-88.4	216.7	-103.5	417.5	-84.3	304.7	-1072.3	330.2	-548.8	210.3	-891.6	230.3	-657.3	230.6
11/09/2012	152	-596.4	230.5	-79.7	224.9	-102.8	418.1	-83.8	305.2	-1071.3	331.2	-545.2	213.7	-895.5	226.5	-660.4	227.7
12/09/2012	153	-605.5	222.0	-88.5	216.6	-119.5	402.3	-96.0	293.6	-1077.7	325.1	-551.1	208.1	-904.8	217.7	-667.8	220.6
13/09/2012	154	-602.7	224.5	-84.8	220.0	-113.5	407.9	-91.6	297.8	-1073.5	329.0	-547.9	211.1	-905.1	217.4	-668.1	220.4
14/09/2012	155	-597.1	229.9	-77.7	226.8	-103.9	417.1	-84.6	304.4	-1049.4	351.9	-546.4	212.6	-899.1	223.2	-663.3	225.0
15/09/2012	156	-599.5	227.6	-87.4	217.6	-106.3	414.8	-86.3	302.8	-1060.0	341.9	-551.9	207.3	-899.0	223.2	-663.2	225.0

16/09/2012	157	-605.4	222.0	-89.9	215.2	-118.4	403.4	-95.2	294.4	-1058.3	343.5	-554.1	205.2	-904.3	218.2	-667.4	221.0
17/09/2012	158	-602.2	225.1	-82.5	222.3	-114.9	406.6	-92.6	296.8	-1049.4	351.9	-546.1	212.9	-901.3	221.0	-665.1	223.3
18/09/2012	159	-601.1	226.1	-81.7	223.0	-110.2	411.1	-89.2	300.1	-1079.1	323.8	-543.2	215.6	-901.7	220.7	-665.3	223.0
19/09/2012	160	-599.2	227.9	-78.9	225.7	-105.5	415.6	-85.8	303.3	-1076.7	326.0	-541.4	217.3	-901.8	220.6	-665.4	223.0
20/09/2012	161	-594.1	232.8	-73.9	230.4	-99.3	421.5	-81.2	307.6	-1064.8	337.4	-534.8	223.6	-895.3	226.7	-660.3	227.8
21/09/2012	162	-595.8	231.2	-73.6	230.7	-99.8	421.0	-81.6	307.3	-1057.2	344.5	-533.7	224.6	-898.4	223.9	-662.7	225.5
22/09/2012	163	-595.5	231.4	-72.7	231.5	-97.0	423.6	-79.6	309.2	-1049.5	351.8	-534.5	223.8	-896.8	225.3	-661.4	226.7
23/09/2012	164	-598.1	229.0	-74.6	229.7	-102.8	418.1	-83.8	305.2	-1049.8	351.6	-537.9	220.6	-897.2	225.0	-661.8	226.4
24/09/2012	165	-600.1	227.0	-75.8	228.6	-101.8	419.0	-83.1	305.9	-1045.5	355.7	-542.7	216.1	-896.9	225.3	-661.5	226.7
25/09/2012	166	-603.2	224.1	-79.5	225.1	-104.5	416.5	-85.0	304.0	-1055.0	346.6	-548.0	211.1	-899.6	222.7	-663.6	224.6
26/09/2012	167	-605.5	221.9	-85.0	219.8	-110.0	411.3	-89.0	300.2	-1060.8	341.1	-546.6	212.3	-901.9	220.5	-665.5	222.9
27/09/2012	168	-607.3	220.2	-87.1	217.9	-113.7	407.8	-91.7	297.7	-1064.4	337.7	-546.1	212.8	-903.1	219.4	-666.5	222.0
28/09/2012	169	-610.5	217.2	-88.8	216.3	-117.0	404.7	-94.1	295.4	-1060.4	341.5	-547.7	211.3	-907.3	215.3	-669.9	218.7
29/09/2012	170	-612.3	215.5	-88.1	217.0	-117.0	404.7	-94.2	295.4	-1065.0	337.1	-547.5	211.5	-909.4	213.4	-671.5	217.1
30/09/2012	171	-612.7	215.1	-91.7	213.5	-116.6	405.0	-93.9	295.6	-1067.8	334.5	-554.2	205.2	-907.1	215.6	-669.7	218.9
1/10/2012	172	-609.9	217.7	-91.1	214.1	-112.6	408.8	-91.0	298.4	-1076.5	326.2	-555.0	204.4	-903.5	219.0	-666.8	221.6
2/10/2012	173	-615.4	212.6	-99.0	206.6	-121.6	400.3	-97.5	292.2	-1081.8	321.2	-558.6	201.0	-909.6	213.2	-671.7	217.0
3/10/2012	174	-608.8	218.8	-92.1	213.1	-113.0	408.5	-91.2	298.2	-1074.9	327.7	-551.7	207.6	-903.3	219.2	-666.6	221.8
4/10/2012	175	-610.4	217.2	-95.3	210.1	-115.4	406.2	-93.0	296.5	-1074.4	328.2	-553.7	205.7	-907.2	215.5	-669.8	218.8
5/10/2012	176	-604.1	223.3	-84.9	219.9	-102.7	418.2	-83.7	305.2	-1061.1	340.8	-546.3	212.6	-898.6	223.6	-662.9	225.3
6/10/2012	177	-608.0	219.6	-87.9	217.1	-110.4	410.9	-89.4	299.9	-1071.2	331.3	-549.3	209.9	-905.8	216.8	-668.6	219.9
7/10/2012	178	-615.0	212.9	-93.4	211.9	-121.6	400.3	-97.5	292.2	-1073.7	328.9	-555.1	204.3	-914.6	208.4	-675.7	213.2
8/10/2012	179	-606.6	220.9	-87.4	217.5	-110.2	411.1	-89.2	300.1	-1067.7	334.6	-548.3	210.8	-903.5	219.0	-666.8	221.6
9/10/2012	180	-607.4	220.1	-90.5	214.6	-110.8	410.5	-89.6	299.7	-1071.0	331.5	-550.9	208.3	-901.8	220.6	-665.4	223.0
10/10/2012	181	-601.1	226.1	-80.9	223.7	-100.9	419.9	-82.4	306.5	-1059.8	342.1	-546.7	212.3	-894.7	227.4	-659.7	228.3
11/10/2012	182	-607.5	220.0	-89.1	215.9	-109.2	412.0	-88.5	300.8	-1072.5	330.1	-554.0	205.3	-902.9	219.6	-666.3	222.1
12/10/2012	183	-586.2	240.2	-63.4	240.3	-75.9	443.6	-64.2	323.8	-1041.1	359.8	-533.2	225.1	-882.0	239.3	-649.6	237.9
13/10/2012	184	-585.3	241.1	-68.2	235.8	-76.5	443.0	-64.6	323.4	-1061.8	340.2	-535.0	223.4	-884.5	237.0	-651.6	236.0
14/10/2012	185	-594.8	232.1	-80.9	223.7	-94.0	426.4	-77.4	311.3	-1070.2	332.2	-544.1	214.8	-896.0	226.1	-660.8	227.3
15/10/2012	186	-592.9	233.9	-76.7	227.8	-90.7	429.6	-75.0	313.6	-1060.8	341.1	-540.2	218.5	-892.9	229.0	-658.3	229.7
16/10/2012	187	-597.6	229.4	-80.0	224.6	-94.4	426.1	-77.6	311.0	-1065.3	336.8	-541.7	217.0	-898.1	224.1	-662.5	225.7
17/10/2012	188	-604.6	222.8	-86.2	218.7	-104.3	416.7	-84.9	304.2	-1071.8	330.7	-548.3	210.7	-903.3	219.1	-666.7	221.8
18/10/2012	189	-598.0	229.1	-79.8	224.8	-98.2	422.5	-80.4	308.4	-1066.9	335.3	-539.2	219.4	-896.3	225.8	-661.0	227.1
19/10/2012	190	-602.1	225.1	-79.7	224.9	-101.3	419.5	-82.7	306.2	-1060.2	341.7	-541.5	217.2	-901.9	220.5	-665.5	222.9
20/10/2012	191	-599.3	227.8	-75.1	229.2	-96.4	424.2	-79.1	309.6	-1054.1	347.4	-537.8	220.7	-900.3	222.0	-664.2	224.1
21/10/2012	192	-607.2	220.3	-83.0	221.8	-107.2	413.9	-87.0	302.2	-1070.3	332.2	-544.0	214.9	-909.2	213.6	-671.4	217.3
22/10/2012	193	-610.9	216.8	-86.7	218.3	-110.4	410.9	-89.3	300.0	-1070.0	332.4	-548.4	210.7	-910.1	212.7	-672.1	216.6

23/10/2012	194	-597.5	229.5	-74.1	230.2	-90.0	430.3	-74.4	314.1	-1048.5	352.8	-538.5	220.1	-894.7	227.3	-659.8	228.3
24/10/2012	195	-601.9	225.4	-84.2	220.6	-96.6	424.0	-79.3	309.5	-1054.4	347.2	-543.1	215.7	-898.7	223.5	-663.0	225.3
25/10/2012	196	-603.4	223.9	-85.9	219.0	-102.5	418.4	-83.6	305.4	-1057.5	344.2	-543.4	215.4	-901.7	220.7	-665.4	223.0
26/10/2012	197	-604.6	222.8	-82.7	222.0	-101.1	419.7	-82.6	306.3	-1058.6	343.2	-542.5	216.2	-903.5	219.0	-666.8	221.6
27/10/2012	198	-603.1	224.2	-81.7	223.0	-100.0	420.8	-81.7	307.1	-1060.9	341.0	-544.4	214.4	-900.9	221.5	-664.7	223.6
28/10/2012	199	-606.8	220.7	-85.3	219.5	-103.9	417.1	-84.6	304.4	-1065.1	337.1	-549.8	209.4	-902.9	219.5	-666.3	222.1
29/10/2012	200	-602.0	225.2	-82.2	222.5	-97.1	423.5	-79.6	309.1	-1067.7	334.6	-544.5	214.4	-897.3	224.8	-661.9	226.3
30/10/2012	201	-597.0	230.0	-75.0	229.4	-90.8	429.5	-75.1	313.5	-1066.7	335.5	-539.5	219.2	-894.9	227.1	-659.9	228.2
31/10/2012	202	-599.5	227.6	-72.2	232.0	-92.3	428.1	-76.1	312.5	-1062.3	339.7	-538.5	220.1	-897.9	224.3	-662.4	225.8
1/11/2012	203	-591.6	235.1	-61.3	242.3	-80.2	439.5	-67.3	320.8	-1055.1	346.5	-529.8	228.3	-889.7	232.1	-655.7	232.1
2/11/2012	204	-601.4	225.8	-74.4	230.0	-93.4	427.0	-76.9	311.7	-1069.2	333.1	-543.4	215.4	-897.7	224.5	-662.2	226.0
3/11/2012	205	-604.1	223.2	-79.8	224.8	-98.8	421.9	-80.9	308.0	-1076.0	326.7	-548.2	210.9	-901.2	221.2	-665.0	223.4
4/11/2012	206	-606.9	220.6	-81.7	223.0	-102.6	418.3	-83.7	305.3	-1086.4	316.9	-549.1	210.0	-905.1	217.5	-668.1	220.4
5/11/2012	207	-597.9	229.1	-70.2	233.9	-90.2	430.1	-74.6	313.9	-1074.6	328.1	-538.7	219.9	-898.0	224.2	-662.4	225.8
6/11/2012	208	-600.6	226.6	-71.1	233.0	-94.9	425.6	-78.0	310.7	-1071.4	331.1	-537.7	220.8	-903.9	218.6	-667.1	221.3
7/11/2012	209	-599.9	227.2	-68.8	235.3	-94.5	426.0	-77.7	311.0	-1065.7	336.5	-535.9	222.6	-902.8	219.6	-666.3	222.1
8/11/2012	210	-594.8	232.1	-62.3	241.4	-88.7	431.5	-73.5	315.0	-1055.6	346.1	-531.2	227.0	-899.4	222.8	-663.5	224.7
9/11/2012	211	-601.6	225.7	-67.3	236.6	-100.4	420.4	-82.0	306.8	-1059.9	342.0	-535.7	222.7	-908.7	214.1	-670.9	217.7
10/11/2012	212	-602.7	224.6	-68.0	236.0	-101.5	419.4	-82.8	306.1	-1065.6	336.6	-538.8	219.8	-909.1	213.6	-671.3	217.4
11/11/2012	213	-602.3	224.9	-68.1	235.8	-99.3	421.4	-81.2	307.6	-1069.9	332.4	-543.7	215.2	-907.9	214.8	-670.4	218.3
12/11/2012	214	-594.6	232.3	-63.2	240.5	-86.0	434.0	-71.5	316.8	-1055.7	345.9	-534.9	223.5	-896.7	225.4	-661.3	226.8
13/11/2012	215	-599.5	227.6	-67.7	236.3	-92.2	428.2	-76.1	312.5	-1069.5	332.9	-541.2	217.5	-900.8	221.5	-664.7	223.7
14/11/2012	216	-600.6	226.5	-69.0	235.0	-94.8	425.7	-77.9	310.7	-1071.2	331.3	-544.7	214.2	-901.8	220.6	-665.5	222.9
15/11/2012	217	-590.6	236.0	-59.2	244.3	-80.9	438.8	-67.8	320.3	-1057.6	344.2	-533.3	225.0	-892.2	229.7	-657.8	230.2
16/11/2012	218	-602.1	225.2	-68.0	235.9	-98.9	421.8	-80.9	307.9	-1060.9	341.0	-541.7	217.0	-906.2	216.4	-669.0	219.6
17/11/2012	219	-602.5	224.8	-60.3	243.3	-99.6	421.2	-81.5	307.4	-1062.1	339.9	-540.5	218.2	-905.5	217.1	-668.4	220.1
18/11/2012	220	-606.9	220.6	-64.7	239.1	-104.8	416.2	-85.3	303.8	-1071.6	330.9	-550.0	209.2	-910.9	212.0	-672.7	216.0
19/11/2012	221	-605.9	221.5	-64.7	239.1	-102.1	418.8	-83.3	305.7	-1070.1	332.3	-546.2	212.7	-907.2	215.5	-669.7	218.9
20/11/2012	222	-592.8	234.0	-51.0	252.1	-82.4	437.5	-68.9	319.3	-1062.0	340.0	-532.5	225.7	-891.6	230.2	-657.3	230.6
21/11/2012	223	-583.3	243.0	-40.3	262.2	-69.3	449.9	-59.3	328.4	-1047.5	353.7	-523.0	234.7	-880.8	240.5	-648.6	238.9
22/11/2012	224	-598.7	228.4	-55.3	248.0	-89.1	431.1	-73.8	314.7	-1065.7	336.5	-537.8	220.7	-896.9	225.3	-661.5	226.7
23/11/2012	225	-602.1	225.2	-59.1	244.4	-94.0	426.5	-77.4	311.3	-1070.3	332.1	-540.7	218.0	-899.5	222.7	-663.6	224.6
24/11/2012	226	-576.9	249.0	-35.4	266.9	-62.6	456.3	-54.4	333.0	-1045.9	355.2	-520.6	237.0	-876.3	244.8	-645.0	242.3
25/11/2012	227	-555.0	269.8	-12.7	288.4	-31.7	485.5	-31.9	354.4	-1026.0	374.1	-498.6	257.9	-856.4	263.6	-629.1	257.4
26/11/2012	228	-585.3	241.0	-41.7	260.9	-73.3	446.1	-62.3	325.6	-1045.4	355.7	-521.1	236.6	-888.4	233.3	-654.7	233.1
27/11/2012	229	-569.6	256.0	-23.0	278.7	-51.7	466.6	-46.5	340.6	-1030.3	370.0	-505.1	251.7	-873.7	247.2	-643.0	244.2
28/11/2012	230	-564.3	261.0	-19.4	282.1	-46.6	471.3	-42.8	344.1	-1033.3	367.2	-500.4	256.1	-869.9	250.9	-639.9	247.1

29/11/2012	231	-577.1	248.9	-24.9	276.8	-65.9	453.1	-56.9	330.7	-1042.1	358.8	-512.5	244.7	-883.5	237.9	-650.8	236.8
30/11/2012	232	-580.6	245.5	-34.6	267.6	-71.9	447.4	-61.3	326.6	-1038.4	362.4	-513.5	243.8	-887.7	234.0	-654.1	233.7
1/12/2012	233	-554.3	270.5	-7.9	292.9	-32.6	484.7	-32.5	353.8	-1014.3	385.2	-485.8	270.0	-861.3	259.0	-633.0	253.7
2/12/2012	234	-556.0	268.9	-11.3	289.7	-35.5	481.9	-34.7	351.8	-1017.3	382.4	-489.0	266.9	-864.1	256.3	-635.3	251.5
3/12/2012	235	-587.6	238.9	-44.6	258.2	-80.9	438.9	-67.8	320.4	-1045.1	356.0	-519.8	237.8	-895.7	226.4	-660.5	227.6
4/12/2012	236	-618.5	209.7	-74.4	229.9	-120.9	400.9	-97.0	292.6	-1070.8	331.6	-550.1	209.0	-924.4	199.2	-683.5	205.8
5/12/2012	237	-619.0	209.1	-71.1	233.0	-115.5	406.1	-93.0	296.4	-1070.1	332.3	-554.7	204.7	-920.2	203.1	-680.2	209.0
6/12/2012	238	-613.4	214.4	-67.6	236.3	-105.4	415.6	-85.7	303.4	-1064.6	337.5	-551.9	207.3	-911.6	211.4	-673.2	215.5
7/12/2012	239	-616.1	211.9	-72.6	231.6	-109.4	411.9	-88.6	300.6	-1074.3	328.3	-558.5	201.1	-914.3	208.7	-675.5	213.4
8/12/2012	240	-609.3	218.3	-66.5	237.4	-102.0	418.9	-83.2	305.8	-1069.4	332.9	-553.2	206.1	-909.9	213.0	-671.9	216.8

Table E.15 Steel strain for slab DS-SCC-a

Slab DS-SCC-a		STEEL STRAIN BY SG															
		1		2		3		4		5		6		7		8	
Date	Age	Reading	Strain	Reading	Strain	Reading	Strain	Reading	Strain	Reading	Strain	Reading	Strain	Reading	Strain	Reading	Strain
16/05/2012	14	-1043.0		-695.6		-370.5		-211.9		-1279.8		-608.7		-350.6		-477.8	
17/05/2012	15	-785.2	244.4	-444.5	238.0	-126.8	231.0	41.1	239.8	-1054.6	213.4	-398.2	199.5	-170.4	170.7	-304.5	164.2
18/05/2012	16	-773.9	255.0	-419.6	261.6	-97.3	258.9	67.4	264.7	-1029.5	237.2	-368.6	227.6	-136.6	202.9	-287.6	180.3
19/05/2012	17	-760.9	267.4	-406.6	274.0	-84.5	271.1	85.5	281.8	-1024.4	242.1	-353.2	242.2	-127.4	211.5	-280.9	186.6
20/05/2012	18	-746.2	281.3	-397.8	282.3	-79.9	275.4	96.7	292.5	-1016.1	250.0	-335.9	258.6	-116.0	222.3	-275.0	192.2
21/05/2012	19	-737.3	289.8	-391.4	288.4	-70.9	284.0	102.2	297.7	-1011.0	254.8	-325.3	268.6	-107.3	230.6	-276.0	191.2
22/05/2012	20	-724.4	302.0	-378.7	300.4	-61.1	293.3	119.5	314.1	-1002.0	263.4	-310.4	282.7	-93.3	243.8	-266.9	199.9
23/05/2012	21	-718.1	308.0	-361.3	316.9	-46.5	307.1	131.8	325.8	-989.7	274.9	-291.3	300.9	-82.5	254.1	-255.5	210.7
24/05/2012	22	-710.9	314.8	-359.9	318.3	-42.9	310.5	134.0	327.9	-990.0	274.7	-286.4	305.5	-80.3	256.1	-257.7	208.6
25/05/2012	23	-699.2	325.9	-355.6	322.3	-37.3	315.9	161.0	353.5	-984.4	280.0	-276.4	315.0	-72.6	263.4	-253.7	212.4
26/05/2012	24	-694.2	330.6	-349.9	327.7	-37.6	315.5	141.1	334.6	-984.6	279.8	-271.4	319.8	-73.5	262.6	-247.8	218.0
27/05/2012	25	-683.8	340.5	-342.9	334.4	-33.5	319.4	153.2	346.1	-978.8	285.3	-259.9	330.6	-67.7	268.1	-245.2	220.4
28/05/2012	26	-673.6	350.1	-327.9	348.5	-18.4	333.7	171.1	363.0	-962.7	300.5	-240.3	349.2	-50.3	284.7	-236.5	228.7
29/05/2012	27	-672.4	351.2	-336.1	340.8	-21.5	330.8	161.3	353.7	-969.3	294.3	-244.1	345.6	-51.1	283.8	-245.8	219.9
30/05/2012	28	-664.3	359.0	-327.7	348.8	-11.4	340.4	176.0	367.6	-959.4	303.7	-232.9	356.2	-40.6	293.9	-234.4	230.6
31/05/2012	29	-660.1	362.9	-328.3	348.2	-13.7	338.2	173.7	365.5	-959.7	303.4	-230.7	358.3	-42.3	292.2	-236.2	229.0
1/06/2012	30	-652.2	370.5	-328.6	347.9	-11.2	340.6	170.9	362.9	-957.6	305.4	-227.0	361.8	-40.0	294.4	-232.6	232.4
2/06/2012	31	-651.6	371.0	-329.4	347.2	-10.3	341.4	173.5	365.3	-956.8	306.2	-226.0	362.8	-37.6	296.6	-228.0	236.8
3/06/2012	32	-656.6	366.3	-329.5	347.0	-4.2	347.3	179.1	370.6	-955.0	307.8	-222.5	366.0	-35.9	298.3	-224.6	239.9
4/06/2012	33	-659.9	363.1	-327.6	348.8	-0.2	351.0	176.2	367.8	-954.8	308.1	-219.9	368.5	-35.5	298.7	-225.8	238.8
5/06/2012	34	-644.9	377.3	-314.1	361.7	9.6	360.3	186.0	377.1	-947.0	315.4	-209.7	378.2	-27.5	306.2	-218.6	245.7
6/06/2012	35	-647.6	374.8	-322.2	354.0	0.9	352.0	179.8	371.3	-951.3	311.4	-212.7	375.3	-36.2	298.0	-219.6	244.7
7/06/2012	36	-642.9	379.3	-311.7	363.9	8.6	359.4	189.9	380.8	-945.3	317.0	-202.8	384.8	-25.3	308.3	-215.7	248.4
8/06/2012	37	-639.2	382.7	-300.4	374.7	21.3	371.4	203.3	393.6	-938.0	323.9	-191.0	395.9	-15.2	317.9	-211.0	252.9
9/06/2012	38	-635.7	386.0	-299.0	376.0	22.8	372.8	205.6	395.7	-934.9	327.0	-187.0	399.7	-12.7	320.2	-218.2	246.0
10/06/2012	39	-629.9	391.6	-296.0	378.8	27.2	377.0	207.4	397.4	-929.2	332.3	-180.1	406.2	-7.5	325.2	-211.4	252.5
11/06/2012	40	-636.9	384.9	-307.4	368.0	20.0	370.1	194.3	385.0	-935.1	326.7	-185.0	401.6	-13.9	319.1	-214.5	249.5
12/06/2012	41	-644.2	378.0	-311.9	363.7	15.2	365.6	187.5	378.6	-939.4	322.6	-188.1	398.7	-16.2	317.0	-213.6	250.4
13/06/2012	42	-636.2	385.6	-302.4	372.7	27.6	377.3	202.1	392.4	-929.4	332.2	-177.6	408.6	-2.3	330.1	-202.2	261.2
14/06/2012	43	-640.5	381.5	-303.6	371.6	29.6	379.3	200.9	391.2	-930.1	331.5	-176.7	409.5	-0.3	332.0	-198.6	264.6
15/06/2012	44	-642.9	379.2	-309.9	365.6	27.0	376.8	196.4	387.0	-935.9	326.0	-181.5	404.9	-5.9	326.7	-205.5	258.1
16/06/2012	45	-642.1	380.0	-306.9	368.5	30.7	380.3	199.9	390.3	-934.1	327.7	-179.3	407.0	-3.9	328.6	-203.3	260.2

17/06/2012	46	-648.1	374.4	-313.6	362.1	23.3	373.3	192.1	383.0	-943.4	318.8	-186.3	400.4	-13.3	319.7	-211.6	252.3
18/06/2012	47	-642.7	379.4	-305.9	369.4	26.1	375.9	200.4	390.8	-937.9	324.1	-179.7	406.6	-9.5	323.3	-207.8	255.9
19/06/2012	48	-634.5	387.2	-299.5	375.4	30.8	380.4	208.8	398.7	-932.3	329.4	-172.5	413.4	-5.0	327.5	-201.9	261.5
20/06/2012	49	-633.1	388.5	-298.6	376.3	30.2	379.8	205.6	395.7	-931.9	329.8	-169.7	416.1	-3.2	329.2	-204.0	259.5
21/06/2012	50	-629.7	391.8	-291.8	382.8	36.9	386.2	212.8	402.5	-927.6	333.8	-162.5	422.9	3.7	335.8	-202.9	260.5
22/06/2012	51	-631.2	390.4	-299.3	375.7	33.7	383.1	198.0	388.5	-932.7	329.0	-168.0	417.7	-2.6	329.8	-209.9	253.9
23/06/2012	52	-642.6	379.5	-295.6	379.2	34.3	383.7	205.3	395.4	-932.2	329.4	-165.3	420.3	-1.7	330.7	-210.4	253.5
24/06/2012	53	-641.0	381.0	-293.5	381.2	35.8	385.1	207.7	397.7	-933.2	328.5	-162.2	423.3	-1.2	331.2	-211.9	252.1
25/06/2012	54	-638.0	383.9	-288.5	385.9	42.1	391.1	212.7	402.4	-926.6	334.8	-155.5	429.5	5.4	337.4	-211.6	252.3
26/06/2012	55	-646.3	376.0	-296.5	378.3	35.2	384.5	198.1	388.7	-928.6	332.9	-155.4	429.6	-0.1	332.2	-217.3	246.9
27/06/2012	56	-641.2	380.8	-299.0	376.0	33.9	383.4	200.6	391.0	-929.4	332.2	-159.2	426.0	4.4	336.5	-214.6	249.4
28/06/2012	57	-644.5	377.7	-301.3	373.8	34.0	383.4	194.7	385.4	-930.7	330.9	-159.9	425.4	1.4	333.7	-213.7	250.3
29/06/2012	58	-637.2	384.7	-304.4	370.8	35.7	385.0	194.3	385.0	-929.3	332.2	-157.6	427.6	2.4	334.6	-204.5	259.1
30/06/2012	59	-642.4	379.7	-308.5	367.0	29.5	379.2	190.7	381.6	-934.8	327.0	-162.5	422.9	-1.5	330.8	-211.0	252.9
1/07/2012	60	-643.9	378.3	-308.2	367.3	31.8	381.4	184.8	376.0	-940.3	321.8	-166.3	419.3	-7.0	325.7	-218.4	245.8
2/07/2012	61	-630.8	390.7	-292.4	382.3	43.2	392.1	202.1	392.4	-920.9	340.2	-152.9	432.1	5.4	337.4	-208.3	255.4
3/07/2012	62	-637.3	384.6	-294.2	380.5	43.3	392.3	189.9	380.8	-931.3	330.3	-155.3	429.8	2.9	335.1	-213.7	250.3
4/07/2012	63	-628.2	393.2	-290.9	383.6	47.3	396.0	195.7	386.4	-927.5	333.9	-151.2	433.6	6.5	338.5	-211.7	252.2
5/07/2012	64	-639.4	382.5	-295.2	379.6	42.2	391.2	186.0	377.1	-930.0	331.5	-152.9	432.0	5.2	337.2	-211.0	252.9
6/07/2012	65	-642.2	379.9	-301.5	373.6	36.8	386.1	177.6	369.1	-933.9	327.8	-155.6	429.4	1.2	333.4	-209.9	253.9
7/07/2012	66	-641.6	380.4	-296.3	378.5	42.1	391.2	181.9	373.3	-929.7	331.8	-150.6	434.3	6.2	338.2	-209.1	254.6
8/07/2012	67	-651.1	371.5	-304.8	370.4	33.9	383.4	174.9	366.7	-937.3	324.7	-158.3	426.9	-0.5	331.8	-214.6	249.4
9/07/2012	68	-638.3	383.6	-296.7	378.1	42.9	391.8	196.3	386.9	-928.3	333.2	-148.4	436.3	11.5	343.2	-200.5	262.8
10/07/2012	69	-636.4	385.4	-299.8	375.2	44.1	393.0	201.9	392.2	-928.0	333.5	-149.1	435.6	12.6	344.3	-198.5	264.7
11/07/2012	70	-648.2	374.2	-319.0	357.0	27.0	376.8	180.8	372.2	-944.4	317.9	-166.0	419.7	-3.8	328.7	-214.6	249.4
12/07/2012	71	-639.5	382.5	-306.6	368.8	39.4	388.5	194.3	385.0	-932.2	329.4	-153.1	431.8	7.4	339.3	-205.1	258.5
13/07/2012	72	-645.5	376.8	-311.7	363.9	36.0	385.3	190.0	381.0	-934.7	327.1	-155.7	429.4	5.3	337.3	-203.7	259.8
14/07/2012	73	-652.1	370.5	-317.1	358.8	33.3	382.8	180.0	371.5	-942.3	319.9	-161.1	424.2	-2.4	330.0	-207.8	255.9
15/07/2012	74	-650.6	372.0	-314.2	361.5	34.6	384.0	186.4	377.5	-945.3	317.0	-163.4	422.1	-2.7	329.7	-216.1	248.0
16/07/2012	75	-630.0	391.5	-294.6	380.2	51.1	399.6	209.0	398.9	-929.4	332.2	-144.9	439.6	13.7	345.3	-202.7	260.8
17/07/2012	76	-639.2	382.7	-298.6	376.4	47.5	396.3	199.4	389.9	-930.7	330.9	-147.0	437.6	12.2	343.9	-206.5	257.2
18/07/2012	77	-638.6	383.4	-303.8	371.4	44.8	393.7	186.7	377.8	-936.2	325.7	-152.7	432.2	6.8	338.7	-216.2	247.9
19/07/2012	78	-637.7	384.1	-298.2	376.7	48.5	397.2	189.9	380.8	-933.0	328.7	-148.9	435.9	10.1	341.9	-215.4	248.7
20/07/2012	79	-628.8	392.6	-292.0	382.6	54.1	402.5	201.9	392.3	-928.8	332.7	-141.2	443.1	16.0	347.4	-211.3	252.6
21/07/2012	80	-642.5	379.6	-298.4	376.5	50.7	399.2	186.2	377.3	-929.6	331.9	-144.7	439.8	12.6	344.3	-218.1	246.2
22/07/2012	81	-645.5	376.7	-302.0	373.1	48.3	397.0	186.3	377.4	-932.2	329.5	-145.9	438.6	12.0	343.7	-216.6	247.5
23/07/2012	82	-646.4	375.9	-305.4	369.9	45.8	394.6	184.0	375.2	-935.2	326.6	-148.5	436.2	10.1	341.9	-214.1	249.9

24/07/2012	83	-650.3	372.2	-309.7	365.8	33.3	382.8	173.2	365.0	-939.8	322.3	-151.7	433.2	6.5	338.4	-215.8	248.3
25/07/2012	84	-645.3	376.9	-306.6	368.8	39.6	388.7	184.8	376.0	-935.5	326.3	-147.6	437.0	11.9	343.6	-207.0	256.6
26/07/2012	85	-651.2	371.4	-309.2	366.3	42.7	391.7	186.8	377.9	-935.9	326.0	-149.2	435.5	9.1	340.9	-208.2	255.5
27/07/2012	86	-637.8	384.1	-300.8	374.3	49.0	397.6	197.1	387.7	-932.3	329.4	-142.2	442.2	16.1	347.5	-206.9	256.8
28/07/2012	87	-630.3	391.1	-295.6	379.2	53.7	402.1	201.1	391.5	-930.3	331.3	-139.0	445.2	17.1	348.5	-209.4	254.4
29/07/2012	88	-632.3	389.3	-300.0	375.0	51.4	399.9	190.0	381.0	-933.2	328.5	-142.9	441.6	11.3	343.0	-213.9	250.1
30/07/2012	89	-626.4	394.8	-294.4	380.3	52.9	401.3	199.7	390.1	-932.4	329.3	-138.3	445.9	13.9	345.5	-215.1	249.0
31/07/2012	90	-633.4	388.3	-296.3	378.5	49.9	398.5	192.0	382.9	-934.6	327.2	-136.6	447.5	9.9	341.7	-221.6	242.9
1/08/2012	91	-629.7	391.7	-291.2	383.4	55.4	403.7	198.2	388.7	-929.6	331.9	-128.9	454.8	14.6	346.1	-214.3	249.7
2/08/2012	92	-627.0	394.3	-290.2	384.3	54.4	402.7	200.4	390.8	-929.2	332.3	-128.9	454.8	15.5	347.0	-211.6	252.3
3/08/2012	93	-621.9	399.1	-289.0	385.5	57.1	405.3	203.6	393.9	-928.0	333.5	-129.0	454.7	17.6	349.0	-207.3	256.4
4/08/2012	94	-620.0	400.9	-290.2	384.3	59.1	407.2	210.6	400.4	-926.5	334.9	-130.4	453.4	19.5	350.7	-204.9	258.7
5/08/2012	95	-618.1	402.7	-295.6	379.1	56.8	405.1	215.2	404.8	-930.6	331.0	-134.6	449.4	11.6	343.3	-207.1	256.5
6/08/2012	96	-617.0	403.8	-293.5	381.2	58.4	406.5	221.9	411.2	-929.7	331.9	-131.7	452.1	13.9	345.5	-210.1	253.7
7/08/2012	97	-613.1	407.5	-282.9	391.2	64.0	411.9	229.6	418.4	-925.1	336.2	-124.4	459.1	22.8	353.9	-214.6	249.5
8/08/2012	98	-619.8	401.1	-286.0	388.3	62.3	410.2	222.6	411.8	-925.3	336.0	-125.6	457.9	19.6	350.8	-217.2	247.0
9/08/2012	99	-613.7	406.9	-288.8	385.7	62.1	410.1	218.6	408.1	-924.7	336.5	-125.4	458.1	19.3	350.6	-213.7	250.3
10/08/2012	100	-633.7	388.0	-294.8	379.9	53.7	402.1	213.8	403.5	-936.1	325.8	-133.9	450.0	9.8	341.6	-236.1	229.0
11/08/2012	101	-625.7	395.5	-300.1	374.9	53.5	401.9	208.1	398.1	-936.1	325.8	-138.2	446.0	7.9	339.8	-227.1	237.6
12/08/2012	102	-630.4	391.1	-300.8	374.3	47.4	396.1	201.1	391.4	-937.6	324.4	-139.6	444.6	9.3	341.1	-227.0	237.7
13/08/2012	103	-621.7	399.4	-289.9	384.6	56.2	404.5	211.2	401.0	-930.4	331.2	-130.2	453.6	17.6	349.0	-218.7	245.6
14/08/2012	104	-610.0	410.5	-282.3	391.8	63.1	411.1	220.3	409.6	-926.3	335.1	-125.0	458.5	22.4	353.6	-211.9	252.0
15/08/2012	105	-594.8	424.9	-281.9	392.1	65.8	413.5	224.6	413.8	-925.0	336.3	-125.6	458.0	24.1	355.1	-208.1	255.6
16/08/2012	106	-587.4	431.9	-280.3	393.7	66.3	414.0	227.3	416.3	-926.0	335.4	-125.7	457.9	27.3	358.1	-202.0	261.4
17/08/2012	107	-588.4	430.9	-284.2	390.0	63.6	411.5	219.5	408.9	-931.5	330.1	-129.4	454.3	26.0	356.9	-207.9	255.8
18/08/2012	108	-582.8	436.2	-280.3	393.6	63.7	411.6	215.8	405.4	-929.3	332.2	-128.6	455.1	23.2	354.3	-212.5	251.4
19/08/2012	109	-581.5	437.5	-281.2	392.8	62.5	410.4	212.8	402.5	-930.7	330.9	-129.2	454.5	25.1	356.1	-214.0	250.1
20/08/2012	110	-577.1	441.6	-274.4	399.3	67.8	415.4	218.1	407.6	-926.8	334.6	-123.2	460.1	31.1	361.8	-212.6	251.3
21/08/2012	111	-585.7	433.5	-281.9	392.2	61.2	409.2	207.7	397.7	-931.5	330.1	-129.8	453.9	27.6	358.5	-217.6	246.6
22/08/2012	112	-582.8	436.2	-282.1	392.0	64.2	412.1	204.9	395.1	-928.1	333.3	-126.2	457.4	35.3	365.7	-210.3	253.6
23/08/2012	113	-581.1	437.8	-280.8	393.2	66.4	414.1	212.2	402.0	-923.4	337.8	-124.0	459.4	39.2	369.5	-205.4	258.2
24/08/2012	114	-590.8	428.6	-269.6	403.8	60.1	408.2	201.4	391.7	-931.2	330.4	-131.1	452.7	31.9	362.5	-215.7	248.4
25/08/2012	115	-582.4	436.6	-252.7	419.9	59.9	408.0	186.6	377.7	-934.4	327.4	-130.4	453.4	28.8	359.6	-218.6	245.6
26/08/2012	116	-580.6	438.3	-245.3	426.9	60.8	408.8	191.8	382.6	-935.7	326.1	-130.2	453.5	27.9	358.7	-224.0	240.6
27/08/2012	117	-568.8	449.5	-233.2	438.3	70.3	417.9	205.5	395.6	-925.8	335.5	-120.2	463.1	36.3	366.7	-219.4	244.9
28/08/2012	118	-575.4	443.2	-235.0	436.6	66.5	414.2	204.3	394.5	-926.2	335.2	-120.4	462.8	37.8	368.2	-217.4	246.8
29/08/2012	119	-578.8	440.0	-237.3	434.5	64.1	412.0	193.9	384.6	-928.6	332.9	-122.1	461.2	39.2	369.4	-212.4	251.6

30/08/2012	120	-575.8	442.8	-233.4	438.2	68.6	416.2	203.9	394.2	-924.9	336.4	-119.6	463.6	42.0	372.1	-206.0	257.6
31/08/2012	121	-572.9	445.6	-229.3	442.1	68.7	416.3	202.9	393.2	-930.8	330.8	-122.5	460.8	34.9	365.3	-213.8	250.3
1/09/2012	122	-561.2	456.7	-215.4	455.2	76.0	423.2	221.2	410.5	-922.1	339.0	-110.6	472.1	42.7	372.7	-215.3	248.8
2/09/2012	123	-574.6	444.0	-230.4	441.0	64.8	412.6	203.7	393.9	-930.0	331.6	-120.3	462.9	32.8	363.4	-233.0	232.0
3/09/2012	124	-562.4	455.5	-218.9	451.9	76.8	424.0	215.5	405.1	-919.0	342.0	-109.7	473.0	46.1	376.0	-215.6	248.5
4/09/2012	125	-569.3	449.0	-222.6	448.3	73.2	420.6	210.8	400.6	-921.0	340.1	-113.5	469.4	44.5	374.5	-211.7	252.2
5/09/2012	126	-570.3	448.1	-220.4	450.4	73.2	420.6	220.8	410.1	-923.0	338.2	-115.3	467.6	44.1	374.1	-209.4	254.4
6/09/2012	127	-555.2	462.4	-215.5	455.1	78.4	425.5	231.6	420.3	-918.7	342.3	-112.2	470.6	48.5	378.3	-202.8	260.6
7/09/2012	128	-558.8	459.0	-213.4	457.1	75.6	422.8	230.9	419.7	-921.3	339.8	-114.5	468.4	45.3	375.2	-209.2	254.5
8/09/2012	129	-560.4	457.4	-218.0	452.7	68.6	416.2	223.3	412.5	-925.5	335.8	-118.8	464.4	40.1	370.3	-220.5	243.9
9/09/2012	130	-564.3	453.7	-225.2	445.9	65.7	413.5	215.4	405.0	-929.4	332.2	-122.1	461.3	36.8	367.2	-224.4	240.1
10/09/2012	131	-564.0	454.1	-220.3	450.5	71.9	419.3	215.7	405.3	-923.7	337.5	-118.0	465.1	44.8	374.8	-214.9	249.2
11/09/2012	132	-559.5	458.3	-215.9	454.7	78.0	425.1	218.8	408.3	-915.2	345.6	-111.0	471.8	53.2	382.7	-200.7	262.6
12/09/2012	133	-572.6	445.9	-224.8	446.3	65.5	413.3	192.8	383.6	-923.7	337.5	-119.3	463.8	47.5	377.3	-201.8	261.6
13/09/2012	134	-562.2	455.7	-221.0	449.9	72.7	420.1	201.8	392.1	-917.6	343.3	-112.2	470.6	57.3	386.6	-189.9	272.9
14/09/2012	135	-556.6	461.0	-212.9	457.6	81.4	428.3	219.9	409.3	-915.2	345.6	-109.3	473.4	60.6	389.7	-191.7	271.2
15/09/2012	136	-540.0	476.7	-222.2	448.8	68.5	416.1	206.0	396.1	-920.9	340.2	-116.1	466.9	57.7	387.0	-200.3	263.1
16/09/2012	137	-541.1	475.8	-231.7	439.7	68.4	416.0	201.2	391.6	-927.6	333.8	-121.6	461.7	52.1	381.7	-200.5	262.8
17/09/2012	138	-536.2	480.4	-224.6	446.5	79.0	426.1	209.6	399.5	-921.4	339.8	-115.2	467.8	54.6	384.1	-193.9	269.1
18/09/2012	139	-532.3	484.0	-222.9	448.1	79.0	426.1	205.1	395.2	-918.6	342.3	-114.5	468.5	54.0	383.4	-187.4	275.2
19/09/2012	140	-528.0	488.2	-225.2	445.9	75.5	422.8	212.2	401.9	-918.3	342.7	-108.0	474.6	53.2	382.7	-183.8	278.6
20/09/2012	141	-528.5	487.7	-221.3	449.6	74.5	421.8	213.6	403.3	-914.9	345.9	-101.0	481.3	57.6	386.9	-181.6	280.7
21/09/2012	142	-524.4	491.6	-217.6	453.1	80.1	427.1	225.1	414.2	-910.8	349.7	-95.5	486.4	62.1	391.1	-177.5	284.7
22/09/2012	143	-526.4	489.6	-218.3	452.5	82.6	429.5	220.8	410.1	-910.3	350.3	-94.4	487.5	63.8	392.8	-176.9	285.2
23/09/2012	144	-528.2	488.0	-220.6	450.3	78.0	425.1	210.8	400.7	-912.3	348.3	-99.8	482.4	62.0	391.0	-179.2	283.0
24/09/2012	145	-520.9	494.8	-217.4	453.3	82.0	428.9	216.1	405.6	-914.5	346.3	-101.5	480.8	60.3	389.5	-179.6	282.6
25/09/2012	146	-526.8	489.2	-218.4	452.4	80.3	427.3	222.0	411.3	-916.1	344.7	-103.1	479.3	57.4	386.7	-182.2	280.1
26/09/2012	147	-536.6	480.0	-221.9	449.0	76.4	423.6	212.9	402.6	-916.7	344.2	-104.7	477.7	61.6	390.7	-180.9	281.4
27/09/2012	148	-538.9	477.8	-222.0	448.9	78.0	425.2	211.7	401.5	-915.3	345.5	-103.7	478.7	64.6	393.5	-175.5	286.5
28/09/2012	149	-537.1	479.6	-223.8	447.2	79.1	426.2	204.6	394.8	-916.8	344.1	-104.4	478.0	68.5	397.2	-175.3	286.7
29/09/2012	150	-535.2	481.3	-224.4	446.7	79.7	426.7	209.3	399.3	-918.3	342.7	-107.6	475.0	72.3	400.8	-176.7	285.4
30/09/2012	151	-531.6	484.8	-223.2	447.8	75.1	422.4	203.5	393.7	-922.9	338.3	-111.0	471.8	72.6	401.1	-185.0	277.5
1/10/2012	152	-525.9	490.2	-219.3	451.5	84.1	430.9	204.9	395.0	-921.6	339.6	-108.7	474.0	73.7	402.1	-188.6	274.1
2/10/2012	153	-537.0	479.6	-227.5	443.7	76.7	423.9	188.2	379.2	-928.2	333.2	-113.9	469.0	69.9	398.5	-195.9	267.2
3/10/2012	154	-530.3	485.9	-220.9	450.0	80.8	427.8	197.2	387.7	-921.2	339.9	-105.7	476.8	78.7	406.9	-189.3	273.4
4/10/2012	155	-527.3	488.8	-219.7	451.1	81.6	428.6	199.8	390.2	-918.4	342.5	-104.4	478.0	80.8	408.9	-189.8	272.9
5/10/2012	156	-517.6	498.0	-213.5	457.0	88.8	435.4	214.9	404.5	-913.0	347.7	-98.1	483.9	87.6	415.3	-183.1	279.3

6/10/2012	157	-526.6	489.4	-219.0	451.8	81.3	428.2	212.4	402.1	-914.2	346.5	-101.6	480.7	85.7	413.5	-183.2	279.2
7/10/2012	158	-534.9	481.6	-226.5	444.6	71.3	418.8	189.6	380.5	-921.8	339.4	-108.0	474.6	79.4	407.5	-184.7	277.8
8/10/2012	159	-525.4	490.6	-219.5	451.3	77.6	424.8	195.9	386.5	-917.5	343.4	-101.7	480.6	85.8	413.6	-185.0	277.6
9/10/2012	160	-522.9	493.0	-220.2	450.7	77.9	425.0	195.6	386.2	-918.5	342.4	-101.9	480.4	86.3	414.1	-186.8	275.8
10/10/2012	161	-513.2	502.1	-210.7	459.6	88.2	434.8	208.8	398.7	-911.4	349.2	-94.1	487.8	94.1	421.4	-181.6	280.8
11/10/2012	162	-521.5	494.3	-220.8	450.1	81.5	428.5	194.4	385.1	-917.2	343.7	-102.3	480.0	86.5	414.3	-186.9	275.7
12/10/2012	163	-497.8	516.8	-195.5	474.0	99.8	445.8	240.4	428.7	-898.6	361.3	-79.2	501.9	103.8	430.7	-169.1	292.6
13/10/2012	164	-500.0	514.7	-198.4	471.3	99.0	445.1	229.7	418.6	-897.8	362.0	-79.4	501.7	99.9	427.0	-173.4	288.5
14/10/2012	165	-510.5	504.7	-208.8	461.4	90.1	436.6	201.4	391.8	-907.7	352.7	-87.6	493.9	94.2	421.6	-182.3	280.1
15/10/2012	166	-506.6	508.4	-205.5	464.6	92.2	438.6	207.8	397.8	-904.7	355.5	-84.3	497.1	98.3	425.5	-175.4	286.7
16/10/2012	167	-508.3	506.8	-209.9	460.4	89.9	436.4	210.4	400.3	-906.3	354.0	-88.4	493.2	94.8	422.2	-174.7	287.3
17/10/2012	168	-518.8	496.9	-219.4	451.5	83.9	430.7	201.1	391.5	-915.2	345.5	-98.2	483.9	85.5	413.4	-186.9	275.7
18/10/2012	169	-512.8	502.6	-214.6	456.0	87.5	434.1	199.1	389.6	-909.7	350.8	-93.0	488.8	91.3	418.8	-179.7	282.6
19/10/2012	170	-516.9	498.7	-217.0	453.7	85.5	432.3	212.0	401.8	-910.1	350.4	-94.8	487.1	90.3	417.9	-178.3	283.9
20/10/2012	171	-519.5	496.2	-216.0	454.7	91.4	437.9	207.8	397.8	-909.2	351.3	-94.3	487.6	91.7	419.3	-173.8	288.2
21/10/2012	172	-525.0	491.0	-222.8	448.2	87.3	433.9	197.8	388.3	-915.8	345.0	-99.8	482.3	86.0	413.8	-179.0	283.2
22/10/2012	173	-525.2	490.8	-225.2	445.9	84.4	431.2	199.8	390.2	-918.6	342.4	-103.6	478.8	81.5	409.5	-183.5	279.0
23/10/2012	174	-510.8	504.5	-213.1	457.4	88.5	435.1	222.1	411.4	-909.0	351.5	-92.9	488.9	89.9	417.5	-174.0	288.0
24/10/2012	175	-518.6	497.0	-219.3	451.5	80.1	427.2	206.9	397.0	-915.1	345.6	-98.3	483.8	85.0	412.9	-185.3	277.2
25/10/2012	176	-520.4	495.3	-222.4	448.6	83.1	430.0	205.4	395.5	-915.2	345.6	-98.6	483.5	84.6	412.5	-184.0	278.4
26/10/2012	177	-521.0	494.8	-222.5	448.4	86.0	432.7	214.2	403.9	-913.9	346.8	-98.2	483.9	87.1	414.8	-180.5	281.8
27/10/2012	178	-519.5	496.2	-218.9	451.9	85.8	432.5	210.7	400.6	-913.8	346.9	-96.5	485.5	89.1	416.8	-180.0	282.3
28/10/2012	179	-522.4	493.5	-220.7	450.2	85.7	432.5	202.1	392.4	-919.0	342.0	-101.4	480.9	84.3	412.2	-186.0	276.5
29/10/2012	180	-513.2	502.2	-216.0	454.6	88.3	434.9	210.6	400.5	-914.2	346.5	-95.6	486.4	89.8	417.4	-182.4	280.0
30/10/2012	181	-514.6	500.9	-214.2	456.3	93.9	440.2	217.0	406.5	-908.3	352.2	-91.2	490.5	94.8	422.2	-173.3	288.6
31/10/2012	182	-513.3	502.1	-216.7	453.9	93.6	439.9	231.6	420.4	-905.9	354.4	-91.1	490.6	95.6	422.9	-167.5	294.1
1/11/2012	183	-505.4	509.6	-207.7	462.5	104.7	450.4	243.8	431.9	-897.6	362.3	-81.9	499.3	104.0	430.9	-157.3	303.8
2/11/2012	184	-519.1	496.6	-216.6	454.1	89.0	435.5	220.9	410.2	-909.7	350.8	-94.2	487.7	88.7	416.4	-173.9	288.1
3/11/2012	185	-526.3	489.8	-222.8	448.2	82.6	429.5	213.4	403.1	-917.2	343.7	-100.0	482.2	82.3	410.3	-182.3	280.1
4/11/2012	186	-529.4	486.8	-224.8	446.2	86.4	433.1	206.6	396.7	-917.4	343.5	-101.4	480.9	81.7	409.8	-183.9	278.6
5/11/2012	187	-516.1	499.4	-216.1	454.6	99.6	445.6	219.6	409.0	-905.0	355.3	-91.2	490.5	94.3	421.7	-167.9	293.7
6/11/2012	188	-518.8	496.9	-220.9	450.0	92.9	439.3	215.4	405.0	-907.0	353.3	-95.8	486.2	91.1	418.6	-167.3	294.2
7/11/2012	189	-514.5	501.0	-220.6	450.2	91.4	437.8	219.5	408.9	-905.1	355.2	-94.6	487.3	94.9	422.3	-163.5	297.9
8/11/2012	190	-514.2	501.3	-216.5	454.2	94.3	440.6	224.2	413.3	-900.1	359.9	-89.0	492.7	100.6	427.7	-158.7	302.4
9/11/2012	191	-518.6	497.1	-222.3	448.7	87.9	434.5	223.8	413.0	-906.3	354.0	-94.5	487.4	95.6	422.9	-162.1	299.2
10/11/2012	192	-522.4	493.5	-222.1	448.9	84.1	431.0	225.5	414.6	-909.2	351.3	-95.4	486.5	93.6	421.0	-164.2	297.3
11/11/2012	193	-524.6	491.4	-219.5	451.3	86.4	433.1	215.7	405.3	-910.4	350.2	-94.2	487.7	92.9	420.4	-167.7	293.9

12/11/2012	194	-515.1	500.4	-213.7	456.8	100.5	446.4	212.5	402.3	-905.5	354.7	-89.9	491.7	96.7	424.0	-162.3	299.1
13/11/2012	195	-519.5	496.2	-219.0	451.8	96.6	442.8	211.2	401.0	-909.2	351.3	-93.2	488.7	93.2	420.6	-165.7	295.8
14/11/2012	196	-518.5	497.2	-218.6	452.2	94.7	440.9	214.0	403.7	-908.6	351.8	-91.9	489.8	93.9	421.3	-164.8	296.7
15/11/2012	197	-510.6	504.6	-209.6	460.7	103.0	448.8	220.6	410.0	-898.7	361.2	-82.5	498.8	103.5	430.4	-154.2	306.7
16/11/2012	198	-519.5	496.2	-222.0	449.0	88.1	434.7	213.1	402.8	-909.2	351.3	-94.5	487.4	93.8	421.2	-162.3	299.1
17/11/2012	199	-519.4	496.3	-221.1	449.8	87.3	433.9	227.4	416.3	-909.9	350.6	-94.4	487.5	93.5	420.9	-162.2	299.1
18/11/2012	200	-531.8	484.5	-225.0	446.1	79.5	426.6	209.6	399.5	-915.5	345.3	-99.0	483.1	86.1	413.9	-173.1	288.8
19/11/2012	201	-525.1	490.9	-222.3	448.7	88.5	435.1	203.7	393.9	-914.3	346.4	-98.7	483.5	88.3	416.0	-172.2	289.6
20/11/2012	202	-512.3	503.0	-212.9	457.5	102.3	448.2	214.5	404.2	-904.4	355.8	-89.4	492.3	97.7	424.9	-160.4	300.8
21/11/2012	203	-502.6	512.2	-205.0	465.0	109.1	454.7	238.6	427.0	-894.5	365.2	-79.7	501.4	107.3	434.0	-150.7	310.0
22/11/2012	204	-514.7	500.8	-216.9	453.8	99.8	445.8	223.0	412.2	-905.3	355.0	-90.6	491.1	96.9	424.1	-161.6	299.7
23/11/2012	205	-519.7	496.0	-221.6	449.3	93.3	439.6	218.7	408.2	-910.3	350.2	-94.6	487.3	92.4	419.9	-169.6	292.1
24/11/2012	206	-498.7	516.0	-197.7	471.9	114.7	459.9	237.7	426.1	-888.3	371.0	-71.5	509.2	114.4	440.7	-148.2	312.4
25/11/2012	207	-479.6	534.0	-172.6	495.8	133.4	477.6	265.9	452.8	-865.2	393.0	-48.1	531.4	137.1	462.3	-124.0	335.3
26/11/2012	208	-503.6	511.3	-203.6	466.4	107.0	452.6	239.0	427.4	-887.8	371.6	-74.7	506.1	112.8	439.2	-143.8	316.5
27/11/2012	209	-489.3	524.8	-192.1	477.3	121.0	465.8	259.4	446.8	-875.1	383.6	-62.6	517.6	125.3	451.1	-124.6	334.7
28/11/2012	210	-486.5	527.5	-188.3	480.9	123.0	467.8	262.7	449.8	-870.9	387.6	-59.7	520.3	127.8	453.4	-123.1	336.2
29/11/2012	211	-499.2	515.4	-200.2	469.6	109.7	455.2	248.9	436.8	-882.7	376.4	-73.0	507.8	116.7	442.9	-135.3	324.7
30/11/2012	212	-499.4	515.3	-203.2	466.7	109.6	455.1	248.3	436.2	-886.3	373.0	-76.3	504.6	114.3	440.6	-134.6	325.3
1/12/2012	213	-475.1	538.3	-175.4	493.2	134.1	478.3	269.0	455.8	-862.2	395.8	-50.5	529.1	140.2	465.2	-110.5	348.1
2/12/2012	214	-476.9	536.6	-175.7	492.8	133.0	477.3	258.8	446.2	-861.7	396.2	-51.5	528.1	137.8	462.9	-113.6	345.2
3/12/2012	215	-506.8	508.2	-208.1	462.1	103.4	449.2	218.7	408.1	-893.4	366.3	-82.1	499.2	107.5	434.2	-143.6	316.8
4/12/2012	216	-531.4	485.0	-234.9	436.8	76.3	423.5	195.2	385.9	-921.4	339.7	-110.2	472.5	79.6	407.7	-171.6	290.2
5/12/2012	217	-526.5	489.6	-232.5	438.9	81.8	428.7	212.0	401.7	-922.9	338.3	-110.5	472.2	78.8	407.0	-170.9	290.9
6/12/2012	218	-527.0	489.1	-227.0	444.2	89.4	436.0	213.5	403.2	-919.3	341.7	-104.0	478.4	82.8	410.7	-172.5	289.3
7/12/2012	219	-533.1	483.3	-231.0	440.5	86.7	433.3	200.0	390.4	-921.7	339.4	-105.7	476.8	79.9	408.0	-181.2	281.1
8/12/2012	220	-524.0	492.0	-224.9	446.2	92.4	438.7	213.5	403.2	-913.9	346.8	-97.5	484.5	86.5	414.2	-173.6	288.3
9/12/2012	221	-508.7	506.4	-207.6	462.6	105.7	451.4	228.1	417.0	-895.4	364.3	-79.9	501.3	104.4	431.2	-153.6	307.3
10/12/2012	222	-536.4	480.2	-230.3	441.1	87.1	433.7	203.6	393.9	-915.9	344.9	-101.7	480.6	83.3	411.3	-175.8	286.2
11/12/2012	223	-534.0	482.4	-227.9	443.4	89.5	436.1	198.9	389.4	-913.7	347.0	-98.4	483.7	85.7	413.5	-175.5	286.5
12/12/2012	224	-514.9	500.5	-214.8	455.7	101.5	447.4	219.8	409.2	-899.8	360.2	-85.6	495.8	100.9	427.9	-159.5	301.7
13/12/2012	225	-532.5	483.9	-228.9	442.4	88.5	435.1	202.2	392.5	-912.8	347.9	-99.3	482.9	87.1	414.8	-173.1	288.8
14/12/2012	226	-534.7	481.8	-235.1	436.6	81.9	428.8	200.8	391.2	-918.6	342.4	-105.8	476.7	82.7	410.6	-175.2	286.8
15/12/2012	227	-532.9	483.5	-235.9	435.8	76.2	423.5	196.2	386.8	-921.4	339.7	-107.2	475.4	79.6	407.8	-175.6	286.4
28/12/2012	240	-534.4	482.1	-234.2	437.4	72.5	420.0	190.7	381.6	-919.7	341.3	-106.7	475.8	81.2	409.2	-175.6	286.5

Table E.16 Steel strain for slab DS-SCC-b

Slab DS-SCC-b		STEEL STRAIN BY SG															
		1		2		3		4		5		6		7		8	
Date	Age	Reading	Strain	Reading	Strain	Reading	Strain	Reading	Strain	Reading	Strain	Reading	Strain	Reading	Strain	Reading	Strain
16/05/2012	14	-1684.6		-1294.4		-875.7		-159.8		-926.5		-766.1		-1137.3		-550.2	
17/05/2012	15	-1541.7	135.4	-1032.4	248.4	-655.8	208.4	-39.9	113.7	-791.7	127.8	-500.4	251.9	-1005.7	124.7	-451.1	94.0
18/05/2012	16	-1528.4	148.0	-1015.0	264.9	-633.2	229.8	-22.9	129.7	-775.3	143.3	-312.6	429.8	-989.4	140.2	-435.1	109.1
19/05/2012	17	-1523.4	152.8	-1009.6	270.0	-629.0	233.8	-11.6	140.5	-766.4	151.8	-314.2	428.3	-984.7	144.6	-430.5	113.5
20/05/2012	18	-1512.4	163.1	-1002.6	276.6	-619.3	243.0	-2.5	149.1	-754.4	163.1	-322.5	420.4	-973.9	154.9	-423.0	120.6
21/05/2012	19	-1512.3	163.2	-1000.7	278.5	-618.8	243.5	3.7	155.0	-745.4	171.7	-323.1	419.9	-970.3	158.3	-422.8	120.8
22/05/2012	20	-1500.4	174.6	-991.7	287.0	-606.7	254.9	20.5	170.9	-735.5	181.1	-331.2	412.2	-961.9	166.2	-411.5	131.4
23/05/2012	21	-1486.0	188.2	-980.7	297.4	-590.5	270.3	29.0	179.0	-718.4	197.2	-344.6	399.5	-948.5	179.0	-399.0	143.3
24/05/2012	22	-1489.1	185.3	-985.6	292.8	-589.5	271.3	31.9	181.7	-715.8	199.7	-343.1	400.9	-948.0	179.5	-399.0	143.3
25/05/2012	23	-1487.7	186.6	-980.8	297.2	-588.9	271.8	42.9	192.1	-704.2	210.7	-348.5	395.8	-943.9	183.4	-393.1	148.9
26/05/2012	24	-1482.8	191.2	-982.6	295.6	-575.8	284.3	39.5	188.9	-703.3	211.6	-348.5	395.8	-943.3	183.9	-394.8	147.3
27/05/2012	25	-1470.6	202.8	-978.9	299.1	-568.6	291.0	49.0	197.9	-694.3	220.1	-356.9	387.8	-935.6	191.2	-384.8	156.8
28/05/2012	26	-1456.2	216.4	-965.7	311.6	-556.7	302.4	68.1	216.0	-676.4	237.1	-371.5	374.0	-921.7	204.4	-365.8	174.8
29/05/2012	27	-1458.6	214.2	-966.5	310.8	-569.4	290.3	69.0	216.9	-673.8	239.5	-369.6	375.8	-925.3	201.0	-366.1	174.5
30/05/2012	28	-1449.4	222.9	-959.3	317.7	-554.0	304.9	79.4	226.8	-665.5	247.4	-374.1	371.5	-919.3	206.7	-358.7	181.5
31/05/2012	29	-1453.3	219.2	-962.8	314.3	-562.4	297.0	76.1	223.6	-665.7	247.3	-371.5	374.0	-919.4	206.5	-359.7	180.6
1/06/2012	30	-1448.2	224.1	-960.5	316.5	-558.5	300.6	82.1	229.3	-662.3	250.4	-375.2	370.5	-920.0	206.0	-359.7	180.6
2/06/2012	31	-1456.4	216.2	-962.1	315.0	-554.0	304.9	84.7	231.7	-659.5	253.1	-375.7	370.1	-920.0	206.0	-358.6	181.6
3/06/2012	32	-1451.6	220.9	-959.0	317.9	-551.9	306.9	88.2	235.0	-656.6	255.9	-380.1	365.9	-915.2	210.6	-355.4	184.6
4/06/2012	33	-1453.8	218.7	-960.7	316.3	-556.9	302.1	88.2	235.1	-656.3	256.1	-378.9	367.0	-916.2	209.6	-357.4	182.7
5/06/2012	34	-1440.3	231.5	-949.9	326.6	-535.4	322.5	95.1	241.6	-647.6	264.4	-383.7	362.5	-907.7	217.6	-350.5	189.2
6/06/2012	35	-1445.8	226.3	-959.7	317.2	-548.0	310.6	89.0	235.8	-646.8	265.1	-380.1	365.9	-910.7	214.8	-352.7	187.2
7/06/2012	36	-1433.3	238.1	-950.5	326.0	-533.3	324.5	100.4	246.6	-641.7	270.0	-388.4	358.0	-902.4	222.7	-345.2	194.3
8/06/2012	37	-1414.5	255.9	-939.7	336.2	-515.7	341.2	108.6	254.4	-631.7	279.4	-397.6	349.3	-895.1	229.6	-332.4	206.5
9/06/2012	38	-1411.9	258.5	-939.4	336.6	-517.4	339.6	110.0	255.8	-627.4	283.5	-399.6	347.4	-892.8	231.8	-328.3	210.3
10/06/2012	39	-1410.9	259.4	-936.6	339.2	-515.7	341.2	115.9	261.3	-622.5	288.1	-404.3	342.9	-887.5	236.7	-323.3	215.1
11/06/2012	40	-1425.5	245.6	-946.6	329.7	-529.5	328.1	111.6	257.2	-625.7	285.1	-399.1	347.9	-892.3	232.2	-328.9	209.8
12/06/2012	41	-1430.5	240.8	-955.3	321.4	-534.1	323.8	107.5	253.4	-630.8	280.3	-392.1	354.4	-900.9	224.1	-337.4	201.7
13/06/2012	42	-1417.2	253.4	-943.0	333.1	-523.9	333.4	122.0	267.1	-621.4	289.2	-403.8	343.4	-890.3	234.1	-329.7	209.0
14/06/2012	43	-1423.7	247.2	-943.6	332.5	-526.1	331.3	125.0	269.9	-618.9	291.5	-403.2	344.0	-890.9	233.6	-328.8	209.8
15/06/2012	44	-1430.4	240.9	-951.3	325.2	-533.2	324.6	116.4	261.8	-624.8	286.0	-396.9	349.9	-898.4	226.4	-333.0	205.9
16/06/2012	45	-1429.1	242.2	-951.0	325.6	-532.8	325.0	115.7	261.1	-623.5	287.2	-396.4	350.4	-898.0	226.8	-332.3	206.6

17/06/2012	46	-1425.9	245.2	-951.6	324.9	-527.6	329.9	113.7	259.2	-627.8	283.2	-390.9	355.6	-900.7	224.3	-340.3	199.0
18/06/2012	47	-1420.9	249.9	-946.4	329.9	-524.0	333.3	118.7	263.9	-623.5	287.2	-393.9	352.7	-895.7	229.0	-336.2	202.9
19/06/2012	48	-1413.7	256.8	-942.5	333.6	-516.8	340.1	121.9	267.1	-619.0	291.4	-397.5	349.4	-890.9	233.6	-332.9	205.9
20/06/2012	49	-1414.0	256.4	-941.6	334.5	-512.0	344.7	120.5	265.7	-618.4	292.1	-399.1	347.9	-888.4	235.9	-341.0	198.3
21/06/2012	50	-1404.1	265.9	-937.6	338.3	-503.1	353.1	128.9	273.7	-612.1	298.0	-405.1	342.1	-883.7	240.4	-327.6	211.0
22/06/2012	51	-1413.5	257.0	-947.1	329.2	-514.5	342.4	123.5	268.5	-615.0	295.2	-399.5	347.5	-888.8	235.6	-336.1	203.0
23/06/2012	52	-1410.4	259.8	-940.4	335.6	-505.3	351.0	126.5	271.4	-613.1	297.1	-402.6	344.5	-886.7	237.6	-332.5	206.3
24/06/2012	53	-1404.7	265.3	-938.7	337.2	-500.1	356.0	128.5	273.3	-611.7	298.4	-404.2	343.0	-886.0	238.2	-331.1	207.6
25/06/2012	54	-1399.8	269.9	-934.3	341.3	-495.8	360.0	136.2	280.5	-605.6	304.1	-409.6	337.9	-880.8	243.1	-325.3	213.2
26/06/2012	55	-1405.5	264.5	-941.7	334.3	-504.9	351.4	133.1	277.6	-610.5	299.6	-406.4	340.9	-883.7	240.4	-327.2	211.4
27/06/2012	56	-1407.1	263.0	-941.8	334.2	-509.3	347.2	136.9	281.2	-608.8	301.1	-407.6	339.8	-883.1	241.0	-327.5	211.1
28/06/2012	57	-1408.8	261.4	-942.4	333.7	-510.2	346.4	137.0	281.4	-607.9	302.0	-407.1	340.2	-883.5	240.5	-327.8	210.8
29/06/2012	58	-1409.5	260.8	-944.3	331.9	-514.8	342.0	138.8	283.1	-610.4	299.6	-405.2	342.1	-883.2	240.8	-325.1	213.4
30/06/2012	59	-1415.2	255.3	-948.3	328.1	-514.9	342.0	136.5	280.8	-614.4	295.8	-399.2	347.8	-888.9	235.5	-331.7	207.1
1/07/2012	60	-1418.3	252.4	-950.2	326.3	-512.7	344.1	128.7	273.4	-619.7	290.8	-394.1	352.6	-893.9	230.7	-336.8	202.2
2/07/2012	61	-1403.9	266.0	-937.4	338.5	-498.0	358.0	137.9	282.2	-606.9	303.0	-409.0	338.5	-884.0	240.1	-327.9	210.7
3/07/2012	62	-1401.7	268.1	-940.2	335.7	-496.3	359.6	140.7	284.8	-605.7	304.0	-404.8	342.5	-884.8	239.4	-328.4	210.2
4/07/2012	63	-1398.2	271.5	-940.7	335.3	-492.1	363.5	144.3	288.2	-602.9	306.7	-407.5	339.9	-881.5	242.5	-323.1	215.3
5/07/2012	64	-1401.7	268.1	-944.1	332.1	-498.1	357.9	142.4	286.4	-607.1	302.8	-406.8	340.5	-883.0	241.0	-324.7	213.8
6/07/2012	65	-1405.9	264.2	-949.7	326.8	-507.1	349.3	142.7	286.7	-610.5	299.6	-401.9	345.2	-888.0	236.3	-329.7	209.0
7/07/2012	66	-1404.1	265.9	-946.5	329.8	-504.7	351.7	146.2	290.0	-607.2	302.6	-406.8	340.5	-885.5	238.7	-326.1	212.4
8/07/2012	67	-1410.2	260.0	-952.7	324.0	-510.3	346.3	140.0	284.2	-612.2	298.0	-402.0	345.1	-891.9	232.6	-331.3	207.5
9/07/2012	68	-1401.7	268.1	-941.7	334.4	-500.4	355.7	149.4	293.1	-603.4	306.3	-409.0	338.4	-883.2	240.9	-321.5	216.7
10/07/2012	69	-1404.9	265.1	-942.3	333.8	-504.0	352.2	149.2	292.9	-602.4	307.3	-407.7	339.7	-883.6	240.5	-321.5	216.8
11/07/2012	70	-1418.3	252.4	-954.5	322.2	-520.0	337.1	138.0	282.2	-613.1	297.1	-395.0	351.7	-894.0	230.6	-332.8	206.1
12/07/2012	71	-1414.6	255.9	-949.9	326.6	-516.2	340.7	146.7	290.5	-606.4	303.4	-399.7	347.3	-888.2	236.1	-325.4	213.1
13/07/2012	72	-1422.3	248.6	-958.0	318.9	-519.8	337.3	140.5	284.6	-612.1	298.0	-399.6	347.4	-892.3	232.3	-328.3	210.3
14/07/2012	73	-1423.5	247.5	-963.2	314.0	-525.6	331.8	131.9	276.5	-617.3	293.1	-394.0	352.7	-898.1	226.8	-334.3	204.7
15/07/2012	74	-1422.6	248.3	-959.2	317.7	-519.9	337.2	133.9	278.4	-618.3	292.1	-388.1	358.3	-900.8	224.2	-336.2	202.9
16/07/2012	75	-1410.5	259.8	-942.8	333.3	-503.9	352.4	147.0	290.8	-604.9	304.9	-402.8	344.4	-886.5	237.7	-323.6	214.8
17/07/2012	76	-1408.1	262.1	-946.8	329.6	-508.4	348.1	146.7	290.5	-606.5	303.3	-401.7	345.4	-886.2	238.0	-324.1	214.3
18/07/2012	77	-1409.8	260.4	-953.5	323.2	-511.5	345.1	142.8	286.8	-611.1	299.0	-396.4	350.4	-891.1	233.4	-332.6	206.3
19/07/2012	78	-1404.7	265.2	-951.6	324.9	-505.4	351.0	144.3	288.2	-611.0	299.1	-399.3	347.6	-889.5	234.9	-336.9	202.2
20/07/2012	79	-1399.3	270.4	-943.9	332.3	-497.4	358.5	147.8	291.6	-603.5	306.1	-404.5	342.7	-883.9	240.2	-328.9	209.8
21/07/2012	80	-1399.9	269.8	-953.4	323.2	-506.4	350.0	144.4	288.3	-607.3	302.6	-400.4	346.6	-887.5	236.8	-329.8	208.9
22/07/2012	81	-1402.9	267.0	-954.8	322.0	-512.7	344.1	143.8	287.8	-610.3	299.7	-399.1	347.8	-889.3	235.1	-334.3	204.7
23/07/2012	82	-1409.9	260.4	-959.1	317.9	-519.4	337.7	142.2	286.2	-614.8	295.5	-396.0	350.8	-893.7	230.9	-337.4	201.7

24/07/2012	83	-1415.2	255.3	-955.3	321.4	-523.9	333.4	141.6	285.7	-613.8	296.4	-396.0	350.7	-895.2	229.5	-339.6	199.6
25/07/2012	84	-1412.3	258.0	-951.3	325.3	-516.6	340.4	146.7	290.5	-606.6	303.2	-400.5	346.5	-892.6	232.0	-334.8	204.2
26/07/2012	85	-1422.6	248.3	-956.2	320.6	-522.7	334.5	143.1	287.2	-608.7	301.2	-397.1	349.7	-896.0	228.7	-337.7	201.4
27/07/2012	86	-1412.4	258.0	-949.1	327.4	-507.8	348.7	146.1	290.0	-604.4	305.3	-401.4	345.7	-891.1	233.4	-333.9	205.0
28/07/2012	87	-1404.1	265.8	-945.0	331.2	-502.8	353.4	147.7	291.5	-601.1	308.5	-402.9	344.3	-888.4	236.0	-332.9	205.9
29/07/2012	88	-1414.7	255.8	-951.4	325.1	-503.3	352.9	144.8	288.7	-604.6	305.1	-401.0	346.1	-890.4	234.1	-336.4	202.7
30/07/2012	89	-1411.5	258.8	-945.6	330.7	-497.8	358.2	145.4	289.3	-602.2	307.4	-403.4	343.8	-886.6	237.6	-332.9	206.0
31/07/2012	90	-1412.3	258.0	-944.8	331.4	-498.6	357.4	144.3	288.2	-599.6	309.9	-404.8	342.5	-885.8	238.4	-331.5	207.3
1/08/2012	91	-1405.1	264.9	-940.9	335.1	-491.3	364.3	150.6	294.3	-593.4	315.8	-410.6	336.9	-881.5	242.4	-326.0	212.5
2/08/2012	92	-1392.8	276.5	-940.3	335.7	-489.4	366.2	151.8	295.4	-595.3	313.9	-409.7	337.8	-881.7	242.3	-324.5	213.9
3/08/2012	93	-1382.3	286.5	-939.7	336.2	-488.9	366.6	153.5	297.0	-595.2	314.0	-411.0	336.5	-881.2	242.8	-324.5	213.9
4/08/2012	94	-1364.7	303.2	-941.0	335.0	-488.6	366.9	155.9	299.2	-596.0	313.3	-410.9	336.7	-881.4	242.6	-323.2	215.2
5/08/2012	95	-1372.6	295.7	-947.9	328.5	-493.9	361.8	154.2	297.7	-601.2	308.3	-406.3	341.0	-884.9	239.3	-325.3	213.2
6/08/2012	96	-1371.3	296.9	-950.2	326.3	-494.0	361.8	156.8	300.1	-602.4	307.2	-402.6	344.6	-885.2	239.0	-323.1	215.3
7/08/2012	97	-1363.8	304.0	-938.1	337.8	-482.0	373.1	161.0	304.1	-597.0	312.3	-410.4	337.2	-878.2	245.6	-318.6	219.6
8/08/2012	98	-1354.0	313.3	-937.6	338.2	-483.5	371.7	162.1	305.1	-597.0	312.4	-409.2	338.2	-876.8	246.9	-318.0	220.1
9/08/2012	99	-1353.4	313.9	-943.7	332.5	-487.5	368.0	161.1	304.2	-598.7	310.8	-404.3	342.9	-879.1	244.8	-316.9	221.1
10/08/2012	100	-1358.1	309.4	-944.4	331.8	-491.3	364.3	153.2	296.7	-603.5	306.2	-399.9	347.1	-884.4	239.7	-324.6	213.8
11/08/2012	101	-1357.2	310.3	-952.5	324.1	-496.6	359.3	152.7	296.2	-608.3	301.7	-392.6	354.0	-890.6	233.9	-324.7	213.8
12/08/2012	102	-1353.4	313.9	-956.1	320.7	-502.2	354.0	149.4	293.1	-613.8	296.4	-386.4	359.8	-897.4	227.4	-328.2	210.4
13/08/2012	103	-1390.5	278.7	-945.0	331.2	-494.2	361.5	157.5	300.8	-604.9	304.8	-399.0	347.9	-885.6	238.5	-320.2	218.0
14/08/2012	104	-1396.2	273.4	-941.7	334.3	-490.3	365.3	159.9	303.1	-598.6	310.8	-405.7	341.6	-879.3	244.6	-317.1	220.9
15/08/2012	105	-1386.7	282.3	-946.0	330.3	-488.2	367.3	162.7	305.7	-597.2	312.2	-400.8	346.3	-877.8	246.0	-314.7	223.2
16/08/2012	106	-1373.0	295.3	-950.9	325.7	-489.9	365.7	160.5	303.6	-598.0	311.4	-396.5	350.3	-881.5	242.5	-315.7	222.3
17/08/2012	107	-1371.1	297.2	-957.3	319.6	-492.9	362.8	153.5	297.0	-602.5	307.1	-385.9	360.3	-889.7	234.7	-320.4	217.8
18/08/2012	108	-1330.0	336.1	-950.2	326.3	-485.1	370.2	157.2	300.5	-598.7	310.7	-390.8	355.7	-881.7	242.3	-315.7	222.3
19/08/2012	109	-1312.7	352.5	-949.7	326.8	-485.9	369.5	157.4	300.7	-595.6	313.6	-392.9	353.7	-879.6	244.3	-314.3	223.6
20/08/2012	110	-1299.9	364.6	-945.8	330.5	-485.9	369.5	158.9	302.1	-595.8	313.5	-396.5	350.3	-878.5	245.3	-314.0	223.9
21/08/2012	111	-1270.6	392.3	-950.2	326.3	-492.8	362.9	158.8	302.0	-601.1	308.4	-388.5	357.8	-883.3	240.8	-317.1	220.9
22/08/2012	112	-1242.1	419.4	-952.3	324.3	-491.5	364.1	156.4	299.7	-601.0	308.5	-391.7	354.8	-882.3	241.7	-316.8	221.2
23/08/2012	113	-1234.2	426.9	-949.4	327.0	-492.9	362.8	155.4	298.8	-602.8	306.8	-407.6	339.8	-880.2	243.7	-316.8	221.2
24/08/2012	114	-1234.6	426.5	-953.0	323.6	-500.0	356.1	151.7	295.3	-606.3	303.5	-402.0	345.1	-886.5	237.8	-321.7	216.6
25/08/2012	115	-1240.1	421.3	-958.5	318.5	-496.4	359.5	151.7	295.3	-603.4	306.2	-399.5	347.4	-888.3	236.0	-321.3	217.0
26/08/2012	116	-1237.2	424.0	-960.5	316.5	-496.2	359.6	148.1	291.8	-609.0	300.9	-388.8	357.6	-889.8	234.6	-324.6	213.8
27/08/2012	117	-1231.6	429.3	-952.9	323.7	-487.9	367.5	156.9	300.2	-601.5	308.0	-397.0	349.8	-881.9	242.1	-315.7	222.3
28/08/2012	118	-1243.4	418.2	-952.3	324.3	-490.8	364.8	154.1	297.5	-604.4	305.3	-399.8	347.2	-881.2	242.8	-316.0	222.0
29/08/2012	119	-1242.9	418.6	-952.7	323.9	-493.7	362.1	153.2	296.7	-607.6	302.2	-402.0	345.1	-882.4	241.7	-319.3	218.9

30/08/2012	120	-1231.0	429.9	-951.1	325.5	-489.6	365.9	157.3	300.6	-604.2	305.5	-407.6	339.8	-879.4	244.5	-316.3	221.7
31/08/2012	121	-1236.9	424.3	-952.3	324.3	-488.4	367.1	155.9	299.2	-604.4	305.3	-400.3	346.7	-884.6	239.6	-319.0	219.1
1/09/2012	122	-1229.5	431.3	-939.5	336.5	-479.1	375.9	160.5	303.6	-599.4	310.0	-405.7	341.6	-875.6	248.1	-311.4	226.4
2/09/2012	123	-1236.5	424.7	-950.1	326.4	-487.5	367.9	153.9	297.4	-602.8	306.9	-397.3	349.5	-880.6	243.3	-316.6	221.4
3/09/2012	124	-1222.4	438.1	-941.5	334.5	-479.8	375.2	165.1	307.9	-595.7	313.6	-406.2	341.1	-873.7	249.9	-307.9	229.7
4/09/2012	125	-1222.6	437.8	-947.6	328.8	-483.0	372.1	160.0	303.1	-596.3	312.9	-400.6	346.4	-877.8	246.0	-310.5	227.2
5/09/2012	126	-1221.3	439.1	-945.9	330.4	-483.0	372.2	162.2	305.2	-596.7	312.6	-399.9	347.0	-879.6	244.3	-309.5	228.2
6/09/2012	127	-1217.1	443.1	-940.6	335.4	-480.1	374.9	168.9	311.5	-590.5	318.4	-404.3	342.9	-876.8	247.0	-304.7	232.7
7/09/2012	128	-1213.5	446.5	-939.0	336.9	-479.1	375.9	169.9	312.6	-591.6	317.5	-404.4	342.8	-876.9	246.8	-304.1	233.3
8/09/2012	129	-1216.8	443.4	-946.0	330.3	-483.7	371.5	166.5	309.3	-594.0	315.2	-399.7	347.3	-878.4	245.4	-304.4	233.0
9/09/2012	130	-1220.8	439.6	-946.2	330.1	-485.6	369.7	162.2	305.3	-598.0	311.4	-392.0	354.6	-880.8	243.1	-306.7	230.8
10/09/2012	131	-1222.8	437.7	-939.8	336.1	-483.6	371.6	162.6	305.6	-597.8	311.6	-390.7	355.8	-879.2	244.6	-303.1	234.3
11/09/2012	132	-1224.0	436.6	-936.0	339.7	-480.9	374.2	163.0	305.9	-593.9	315.3	-401.5	345.5	-874.3	249.3	-298.8	238.3
12/09/2012	133	-1235.2	426.0	-939.1	336.8	-493.6	362.2	152.1	295.6	-604.1	305.6	-402.1	345.0	-882.0	242.0	-307.9	229.6
13/09/2012	134	-1228.2	432.6	-934.6	341.1	-489.8	365.8	160.4	303.5	-601.6	308.0	-416.2	331.6	-879.6	244.3	-308.0	229.6
14/09/2012	135	-1221.1	439.3	-933.0	342.6	-484.5	370.8	167.6	310.4	-597.1	312.2	-417.3	330.6	-876.0	247.7	-303.9	233.4
15/09/2012	136	-1227.7	433.1	-943.6	332.6	-489.7	365.9	160.6	303.7	-598.9	310.5	-411.6	336.0	-886.2	238.1	-307.7	229.9
16/09/2012	137	-1232.5	428.4	-952.8	323.8	-494.6	361.2	146.6	290.4	-612.9	297.3	-409.1	338.4	-892.1	232.4	-313.2	224.6
17/09/2012	138	-1234.3	426.8	-945.1	331.1	-494.9	360.9	153.6	297.1	-606.4	303.4	-412.9	334.8	-883.7	240.3	-307.1	230.4
18/09/2012	139	-1228.1	432.7	-937.5	338.4	-497.7	358.3	155.7	299.0	-604.4	305.3	-415.3	332.4	-880.8	243.2	-308.0	229.5
19/09/2012	140	-1230.9	430.0	-937.3	338.5	-502.2	354.0	156.2	299.5	-600.5	309.0	-414.3	333.4	-884.8	239.3	-305.7	231.7
20/09/2012	141	-1228.1	432.7	-933.0	342.6	-503.4	352.9	161.4	304.4	-598.5	310.9	-413.2	334.5	-881.4	242.5	-302.6	234.7
21/09/2012	142	-1225.3	435.3	-928.9	346.5	-493.9	361.8	161.0	304.1	-593.1	316.0	-417.1	330.7	-874.2	249.4	-297.2	239.8
22/09/2012	143	-1222.8	437.6	-927.4	347.9	-495.3	360.6	159.2	302.3	-589.6	319.3	-419.2	328.8	-873.9	249.7	-296.9	240.1
23/09/2012	144	-1227.4	433.3	-930.9	344.6	-495.7	360.2	151.1	294.7	-593.9	315.2	-419.1	328.8	-874.4	249.2	-297.9	239.2
24/09/2012	145	-1226.2	434.4	-933.1	342.5	-496.3	359.6	155.3	298.7	-592.4	316.6	-414.5	333.2	-876.6	247.1	-300.9	236.3
25/09/2012	146	-1223.1	437.4	-934.1	341.5	-497.1	358.8	158.7	301.9	-590.2	318.8	-409.9	337.6	-876.5	247.2	-300.6	236.6
26/09/2012	147	-1225.9	434.7	-934.7	341.0	-499.4	356.6	155.3	298.7	-594.4	314.8	-408.8	338.6	-877.9	245.9	-304.5	232.9
27/09/2012	148	-1227.0	433.7	-936.1	339.6	-499.3	356.7	156.8	300.1	-597.3	312.0	-409.8	337.7	-875.7	248.0	-304.4	233.0
28/09/2012	149	-1227.7	433.0	-936.2	339.6	-496.4	359.5	156.0	299.4	-598.5	311.0	-408.3	339.1	-874.3	249.3	-305.8	231.6
29/09/2012	150	-1227.5	433.3	-935.5	340.2	-496.3	359.6	149.2	292.9	-597.6	311.8	-408.9	338.6	-852.4	270.1	-307.5	230.0
30/09/2012	151	-1230.1	430.8	-941.1	335.0	-498.3	357.6	152.4	296.0	-599.4	310.0	-402.5	344.7	-812.4	308.0	-308.4	229.2
1/10/2012	152	-1224.8	435.8	-939.6	336.3	-494.2	361.6	156.4	299.7	-595.6	313.7	-402.7	344.4	-766.1	351.8	-305.0	232.5
2/10/2012	153	-1233.5	427.6	-951.3	325.3	-507.7	348.8	146.5	290.4	-602.8	306.8	-394.9	351.8	-749.7	367.4	-311.6	226.2
3/10/2012	154	-1227.9	432.9	-947.9	328.4	-503.4	352.8	147.7	291.5	-600.9	308.6	-394.3	352.4	-736.6	379.8	-307.1	230.4
4/10/2012	155	-1226.3	434.4	-944.3	331.9	-500.0	356.0	144.6	288.5	-601.2	308.3	-397.4	349.5	-730.3	385.8	-306.0	231.5
5/10/2012	156	-1215.3	444.8	-935.7	340.0	-491.8	363.9	166.6	309.4	-587.6	321.2	-408.9	338.6	-719.0	396.5	-297.6	239.4

6/10/2012	157	-1221.7	438.7	-936.8	339.0	-498.5	357.5	159.0	302.1	-593.5	315.7	-406.7	340.6	-716.3	399.1	-303.9	233.4
7/10/2012	158	-1228.7	432.1	-942.6	333.5	-507.2	349.3	144.7	288.6	-603.3	306.3	-397.8	349.0	-720.4	395.2	-309.7	228.0
8/10/2012	159	-1221.8	438.7	-935.5	340.2	-502.8	353.4	149.0	292.7	-596.6	312.7	-401.2	345.9	-711.8	403.3	-304.6	232.7
9/10/2012	160	-1221.0	439.4	-940.9	335.1	-499.5	356.6	149.4	293.1	-596.0	313.2	-396.4	350.4	-709.1	405.9	-305.2	232.2
10/10/2012	161	-1215.8	444.4	-932.4	343.2	-489.2	366.3	160.2	303.3	-593.2	316.0	-403.7	343.5	-702.5	412.2	-299.5	237.6
11/10/2012	162	-1221.6	438.8	-942.3	333.8	-504.8	351.6	148.4	292.1	-596.6	312.7	-395.6	351.2	-705.2	409.6	-304.1	233.3
12/10/2012	163	-1205.8	453.8	-915.9	358.8	-479.4	375.6	176.9	319.1	-578.9	329.5	-420.7	327.3	-685.8	428.0	-288.8	247.8
13/10/2012	164	-1209.3	450.5	-923.4	351.7	-485.8	369.5	171.7	314.2	-578.6	329.8	-421.5	326.6	-684.7	429.0	-289.5	247.1
14/10/2012	165	-1219.5	440.8	-938.3	337.6	-499.4	356.6	156.7	300.0	-588.9	320.0	-406.9	340.4	-695.6	418.7	-297.5	239.5
15/10/2012	166	-1216.9	443.3	-933.8	341.9	-495.4	360.4	156.6	299.9	-588.1	320.7	-404.3	342.9	-694.1	420.1	-297.1	239.9
16/10/2012	167	-1217.0	443.2	-931.3	344.2	-497.0	358.9	155.1	298.5	-590.5	318.5	-407.3	340.1	-697.5	416.9	-299.5	237.7
17/10/2012	168	-1221.7	438.8	-936.2	339.6	-509.1	347.4	151.7	295.2	-590.2	318.8	-398.1	348.8	-700.4	414.2	-303.8	233.5
18/10/2012	169	-1219.0	441.3	-930.9	344.6	-499.5	356.5	153.9	297.3	-588.8	320.1	-404.8	342.4	-697.5	416.9	-301.8	235.4
19/10/2012	170	-1220.3	440.0	-927.5	347.8	-498.0	358.0	157.6	300.9	-589.5	319.4	-409.3	338.1	-694.8	419.4	-299.9	237.3
20/10/2012	171	-1215.7	444.4	-926.3	349.0	-497.3	358.6	160.4	303.5	-583.4	325.2	-414.1	333.6	-692.3	421.8	-300.1	237.1
21/10/2012	172	-1220.8	439.5	-931.7	343.8	-498.6	357.4	159.8	302.9	-584.6	324.1	-409.8	337.7	-701.2	413.4	-306.1	231.4
22/10/2012	173	-1221.9	438.5	-932.1	343.5	-501.1	355.0	157.1	300.4	-586.6	322.2	-403.7	343.4	-704.7	410.0	-307.9	229.7
23/10/2012	174	-1214.7	445.4	-927.5	347.8	-493.5	362.3	163.4	306.3	-580.1	328.3	-410.4	337.1	-698.5	415.9	-300.0	237.2
24/10/2012	175	-1217.4	442.8	-933.1	342.5	-494.4	361.4	157.2	300.5	-585.4	323.3	-401.9	345.2	-701.9	412.7	-304.6	232.8
25/10/2012	176	-1218.1	442.1	-933.5	342.2	-493.6	362.1	146.0	289.9	-587.4	321.4	-404.9	342.4	-700.6	414.0	-306.3	231.2
26/10/2012	177	-1218.8	441.5	-932.4	343.2	-492.4	363.3	149.7	293.4	-585.9	322.9	-413.2	334.5	-695.4	418.9	-308.4	229.2
27/10/2012	178	-1217.4	442.9	-931.3	344.2	-487.1	368.3	145.8	289.6	-586.8	322.0	-411.1	336.4	-696.9	417.4	-305.4	232.1
28/10/2012	179	-1219.7	440.7	-938.2	337.7	-490.0	365.5	143.8	287.7	-589.9	319.1	-401.9	345.2	-701.7	412.9	-308.1	229.5
29/10/2012	180	-1214.3	445.8	-935.2	340.5	-489.2	366.3	150.4	294.1	-583.9	324.8	-404.8	342.4	-699.7	414.8	-307.2	230.3
30/10/2012	181	-1213.6	446.4	-930.9	344.6	-488.5	367.0	157.2	300.4	-583.4	325.2	-412.1	335.5	-693.8	420.4	-302.5	234.8
31/10/2012	182	-1213.1	446.9	-927.1	348.2	-486.1	369.2	164.1	307.1	-581.2	327.3	-417.2	330.7	-690.1	423.9	-296.8	240.2
1/11/2012	183	-1205.4	454.2	-919.0	355.8	-480.7	374.4	172.6	315.0	-573.1	335.0	-427.3	321.1	-681.9	431.7	-289.0	247.6
2/11/2012	184	-1212.7	447.3	-931.2	344.3	-487.1	368.3	159.4	302.5	-581.6	326.9	-415.9	331.9	-692.4	421.7	-299.6	237.6
3/11/2012	185	-1218.0	442.3	-936.8	339.0	-495.9	360.0	156.5	299.8	-585.7	323.1	-408.6	338.8	-698.1	416.3	-307.5	230.0
4/11/2012	186	-1222.9	437.6	-938.9	337.0	-499.4	356.6	151.4	295.0	-586.8	322.0	-403.2	343.9	-700.4	414.1	-310.5	227.2
5/11/2012	187	-1216.4	443.7	-928.2	347.2	-489.2	366.3	169.0	311.7	-579.1	329.3	-414.4	333.3	-689.7	424.3	-298.0	239.0
6/11/2012	188	-1218.0	442.2	-928.8	346.5	-493.0	362.7	164.4	307.3	-585.6	323.2	-415.9	331.9	-691.2	422.9	-299.2	237.9
7/11/2012	189	-1215.6	444.5	-926.7	348.6	-492.8	362.9	162.7	305.6	-584.9	323.8	-419.5	328.5	-690.0	424.0	-294.8	242.1
8/11/2012	190	-1211.7	448.2	-920.7	354.3	-487.7	367.7	168.9	311.6	-578.8	329.5	-421.1	326.9	-684.7	429.0	-288.7	247.8
9/11/2012	191	-1216.3	443.8	-923.6	351.5	-491.9	363.7	161.0	304.1	-579.8	328.6	-419.6	328.4	-688.1	425.8	-292.2	244.6
10/11/2012	192	-1216.6	443.6	-923.5	351.6	-491.1	364.6	159.1	302.3	-582.5	326.1	-418.4	329.6	-689.9	424.1	-295.7	241.2
11/11/2012	193	-1215.1	444.9	-923.4	351.7	-489.5	366.1	159.3	302.5	-582.5	326.0	-414.6	333.2	-691.2	422.9	-298.0	239.1

12/11/2012	194	-1210.3	449.6	-920.6	354.4	-485.9	369.5	165.6	308.4	-578.4	330.0	-419.0	328.9	-688.0	425.9	-294.3	242.5
13/11/2012	195	-1214.4	445.6	-926.5	348.7	-491.7	363.9	157.4	300.6	-582.9	325.6	-413.9	333.8	-691.5	422.6	-298.8	238.3
14/11/2012	196	-1213.4	446.6	-924.0	351.1	-489.6	366.0	159.6	302.8	-583.1	325.5	-414.0	333.7	-689.8	424.2	-298.0	239.1
15/11/2012	197	-1207.0	452.7	-917.6	357.2	-481.2	373.9	171.2	313.8	-578.0	330.4	-419.3	328.7	-682.6	431.0	-288.9	247.7
16/11/2012	198	-1217.7	442.5	-925.2	350.0	-490.2	365.4	160.4	303.5	-587.3	321.5	-410.5	337.0	-691.2	422.9	-296.6	240.4
17/11/2012	199	-1216.1	444.0	-925.1	350.1	-492.4	363.3	161.7	304.8	-584.9	323.8	-414.4	333.3	-692.0	422.1	-299.5	237.6
18/11/2012	200	-1226.3	434.4	-932.0	343.5	-494.7	361.1	149.7	293.4	-591.1	317.9	-401.1	346.0	-696.5	417.8	-305.6	231.9
19/11/2012	201	-1222.8	437.6	-931.3	344.2	-493.6	362.1	154.8	298.2	-589.7	319.3	-403.5	343.7	-697.9	416.6	-303.4	234.0
20/11/2012	202	-1213.5	446.5	-922.4	352.7	-488.5	366.9	166.3	309.1	-579.0	329.4	-414.1	333.6	-688.8	425.2	-295.2	241.7
21/11/2012	203	-1203.4	456.1	-915.0	359.7	-480.2	374.8	177.5	319.7	-571.7	336.3	-422.5	325.7	-680.1	433.4	-286.3	250.1
22/11/2012	204	-1213.1	446.9	-925.8	349.4	-490.1	365.4	165.3	308.2	-584.3	324.4	-409.5	338.0	-688.7	425.2	-296.5	240.5
23/11/2012	205	-1214.4	445.7	-928.5	346.8	-493.4	362.4	163.4	306.3	-587.6	321.2	-403.6	343.6	-692.9	421.3	-300.7	236.5
24/11/2012	206	-1197.6	461.6	-907.6	366.6	-474.7	380.1	187.5	329.2	-566.3	341.5	-426.7	321.7	-673.0	440.1	-279.6	256.5
25/11/2012	207	-1185.0	473.5	-890.7	382.7	-459.4	394.6	207.5	348.1	-551.4	355.5	-444.3	305.0	-656.7	455.5	-261.8	273.3
26/11/2012	208	-1207.1	452.6	-910.7	363.7	-479.1	375.9	183.3	325.2	-572.7	335.3	-425.2	323.1	-675.6	437.7	-281.4	254.8
27/11/2012	209	-1195.6	463.5	-900.1	373.8	-470.4	384.2	195.1	336.4	-561.6	345.8	-442.3	306.9	-664.7	447.9	-270.3	265.3
28/11/2012	210	-1193.6	465.4	-897.1	376.6	-467.5	386.9	196.1	337.3	-558.2	349.1	-444.6	304.7	-660.5	452.0	-266.6	268.8
29/11/2012	211	-1202.2	457.2	-906.1	368.1	-474.9	379.9	183.9	325.8	-566.4	341.3	-437.1	311.8	-668.4	444.4	-274.7	261.1
30/11/2012	212	-1202.7	456.7	-909.2	365.1	-478.0	377.0	185.2	327.0	-569.9	338.0	-436.1	312.7	-671.8	441.3	-276.6	259.3
1/12/2012	213	-1184.2	474.2	-891.0	382.4	-459.1	394.8	203.1	343.9	-553.8	353.3	-456.2	293.7	-653.6	458.5	-258.9	276.1
2/12/2012	214	-1186.3	472.3	-892.5	381.0	-460.9	393.1	198.6	339.7	-555.4	351.8	-453.8	296.0	-654.6	457.5	-260.7	274.4
3/12/2012	215	-1206.1	453.5	-914.8	359.9	-482.1	373.1	170.0	312.6	-574.7	333.4	-430.5	318.0	-676.9	436.4	-284.6	251.7
4/12/2012	216	-1227.8	432.9	-935.8	340.0	-502.0	354.2	142.5	286.5	-594.7	314.5	-406.0	341.3	-700.4	414.1	-311.7	226.1
5/12/2012	217	-1225.8	434.8	-934.4	341.3	-503.9	352.4	157.9	301.1	-593.2	316.0	-403.6	343.6	-702.7	411.9	-312.0	225.7
6/12/2012	218	-1218.7	441.6	-928.2	347.1	-498.1	357.9	163.2	306.1	-588.0	320.9	-408.3	339.1	-697.3	417.0	-307.5	230.0
7/12/2012	219	-1221.1	439.3	-931.7	343.8	-501.1	355.1	158.0	301.2	-591.7	317.3	-403.8	343.3	-700.9	413.7	-309.1	228.6
8/12/2012	220	-1215.1	445.0	-923.4	351.7	-495.7	360.1	164.9	307.8	-585.2	323.5	-410.7	336.8	-693.2	421.0	-303.4	234.0
9/12/2012	221	-1205.3	454.3	-911.5	363.0	-483.4	371.8	175.5	317.8	-573.2	334.9	-422.4	325.8	-679.5	434.0	-288.0	248.5
10/12/2012	222	-1222.2	438.3	-929.8	345.7	-499.0	357.1	153.7	297.1	-588.4	320.5	-401.6	345.5	-696.2	418.1	-307.6	230.0
11/12/2012	223	-1222.0	438.4	-932.9	342.7	-496.8	359.1	155.8	299.2	-588.0	320.8	-391.7	354.8	-698.0	416.4	-307.3	230.2
12/12/2012	224	-1212.7	447.2	-922.3	352.8	-487.7	367.7	162.7	305.7	-583.2	325.4	-410.6	336.9	-687.5	426.4	-297.4	239.6
13/12/2012	225	-1221.1	439.3	-933.0	342.6	-496.0	359.9	148.6	292.3	-593.2	316.0	-388.1	358.3	-699.4	415.1	-309.4	228.3
14/12/2012	226	-1222.7	437.8	-936.5	339.3	-499.8	356.3	146.9	290.8	-593.7	315.5	-394.3	352.3	-700.5	414.1	-310.8	226.9
15/12/2012	227	-1224.2	436.4	-936.6	339.2	-502.7	353.6	147.5	291.3	-596.9	312.5	-399.1	347.8	-701.0	413.6	-311.6	226.1
28/12/2012	240	-1223.5	437.0	-936.1	339.7	-502.3	353.9	147.3	291.1	-595.4	313.8	-399.5	347.5	-699.9	414.6	-309.9	227.8

Figure E.1 Long-term typical experimental test view-1

Figure E.2 Long-term typical experimental test view-2

Figure E.3 Long-term typical experimental test view-3

APPENDIX F

CREEP AND SHRINKAGE TESTS

Table F.1 Creep and shrinkage results for N-SCC mix

Time	Mix 1			
	Total (μm)	shrinkage (μm)	creep (μm)	creep coefficient
0hr	869	0	0	0.00
2hr	1180	0	311	0.36
6hr	1263	1	393	0.45
1d	1360	12	479	0.55
2d	*	*	*	*
3d	1522	52	601	0.70
4d	1605	64	672	0.78
5d	1702	91	742	0.86
6d	1817	121	827	0.96
7d	1891	150	872	1.01
14d	2102	242	991	1.15
21d	2303	329	1105	1.28
28d	2444	403	1172	1.36
56d	2780	567	1344	1.55
84d	3031	693	1469	1.70
112d	3149	756	1525	1.76
140d	3232	793	1570	1.82
168d	3299	827	1603	1.85
196d	3364	848	1647	1.91
224d	3435	870	1696	1.96
252d	3485	896	1720	1.99

Table F.2 Creep and shrinkage results for D-SCC mix

Time	Mix 2			
	Total (μm)	shrinkage (μm)	creep (μm)	creep coefficient
0hr	999	0	0	0.00
2hr	1114	11	104	0.10
6hr	1218	17	202	0.20
1d	1430	42	389	0.39
2d	1537	79	459	0.46
3d	1622	105	518	0.52
4d	1702	134	569	0.57
5d	*	*	*	*
6d	1836	166	671	0.67
7d	1933	204	730	0.73
14d	2362	339	1024	1.02
21d	2534	419	1116	1.12
28d	2680	479	1202	1.20
56d	3062	631	1432	1.43
84d	3307	713	1595	1.60
112d	3428	757	1671	1.67
140d	3520	803	1718	1.72
168d	3574	816	1759	1.76
196d	3644	830	1815	1.82
224d	3701	844	1858	1.86
252d	3746	853	1894	1.89

Table F.3 Creep and shrinkage results for S-SCC mix

Time	Mix			
	Total (μm)	shrinkage (μm)	creep (μm)	creep coefficient
0hr	870	0	0	0.00
2hr	990	3	117	0.13
6hr	1060	8	182	0.21
1d	1201	22	309	0.36
2d	1324	42	412	0.47
3d	1466	81	515	0.59
4d	1539	98	571	0.66
5d	*	*	*	*
6d	1643	119	654	0.75
7d	1700	150	680	0.78
14d	1956	251	835	0.96
21d	2192	348	974	1.12
28d	2309	404	1035	1.19
56d	2657	565	1222	1.41
84d	2825	650	1305	1.50
112d	2947	709	1368	1.58
140d	3047	749	1428	1.64
168d	3143	780	1493	1.72
196d	3219	811	1538	1.77
224d	3274	823	1581	1.82
252d	3320	833	1617	1.86

Table F.4 Creep and shrinkage results for DS-SCC mix

Time	Mix 4			
	Total (μm)	shrinkage (μm)	creep (μm)	creep coefficient
0hr	1110	0	0	0.00
2hr	1236	10	116	0.10
6hr	1268	10	148	0.13
1d	1366	36	220	0.20
2d	1490	64	316	0.28
3d	1590	95	385	0.35
4d	*	*	*	*
5d	1797	142	545	0.49
6d	1892	172	610	0.55
7d	1990	210	670	0.60
14d	2239	310	819	0.74
21d	2455	394	951	0.85
28d	2606	436	1060	0.95
56d	2932	596	1226	1.10
84d	3139	688	1341	1.21
112d	3282	758	1414	1.27
140d	3409	830	1469	1.32
168d	3489	849	1530	1.38
196d	3548	869	1569	1.41
224d	3604	882	1612	1.45
252d	3654	898	1646	1.48

Figure F.1 General view of creep tests-1

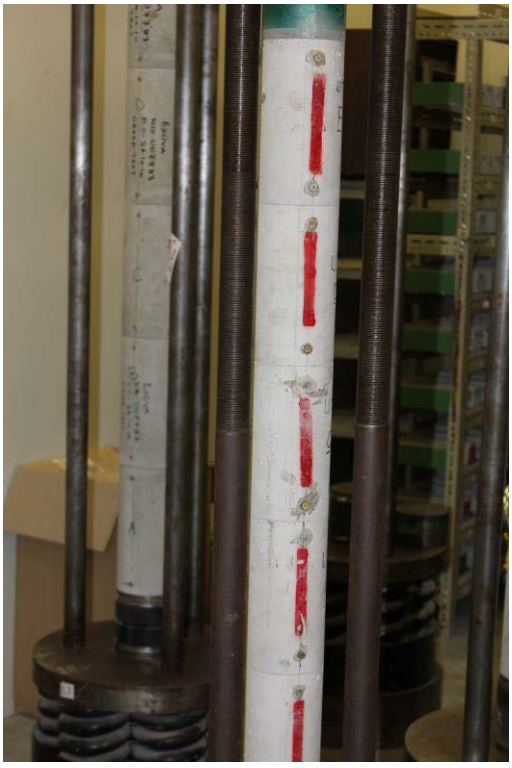

Figure F.2 General view of creep tests-2

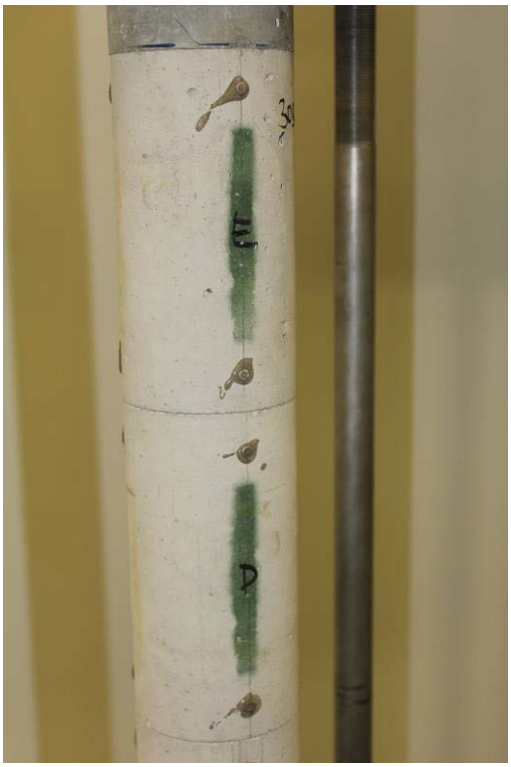

Figure F.3 General view of creep tests-3

Figure F.4 General view of creep tests-4

Figure F.5 General view of creep tests-5

Figure F.6 General view of shrinkage tests of monitor specimens-1

Figure F.7 General view of shrinkage tests of monitor specimens-2

Figure F.8 General view of shrinkage tests of monitor specimens-3

Figure F.9 General view of standard shrinkage tests-1

Figure F.10 General view of standard shrinkage tests-2

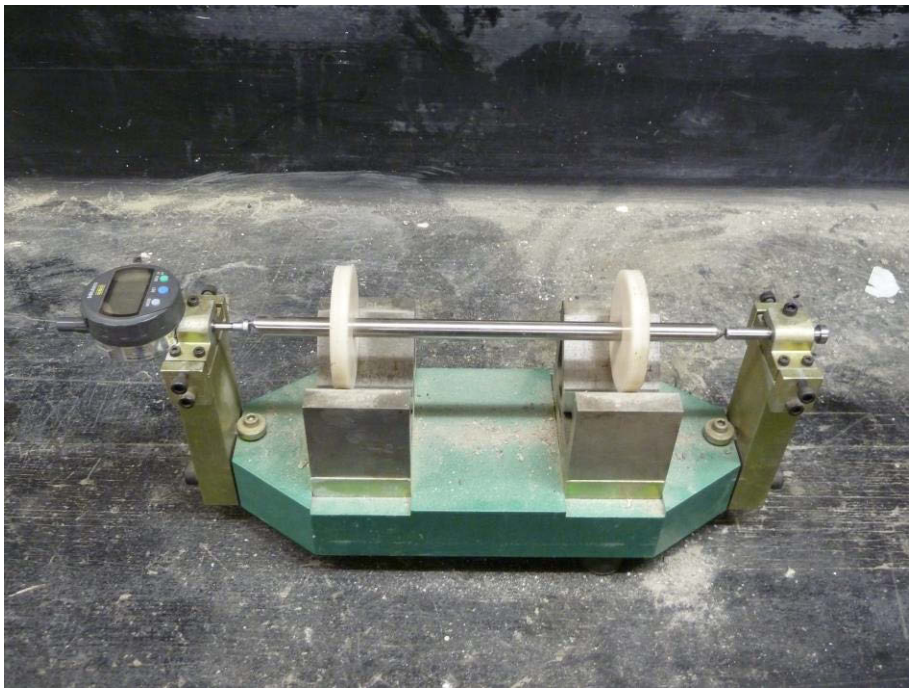

Figure F.11 General view of standard shrinkage tests-3

APPENDIX G

TYPICAL FEM PARAMETRIC STUDY RESULTS

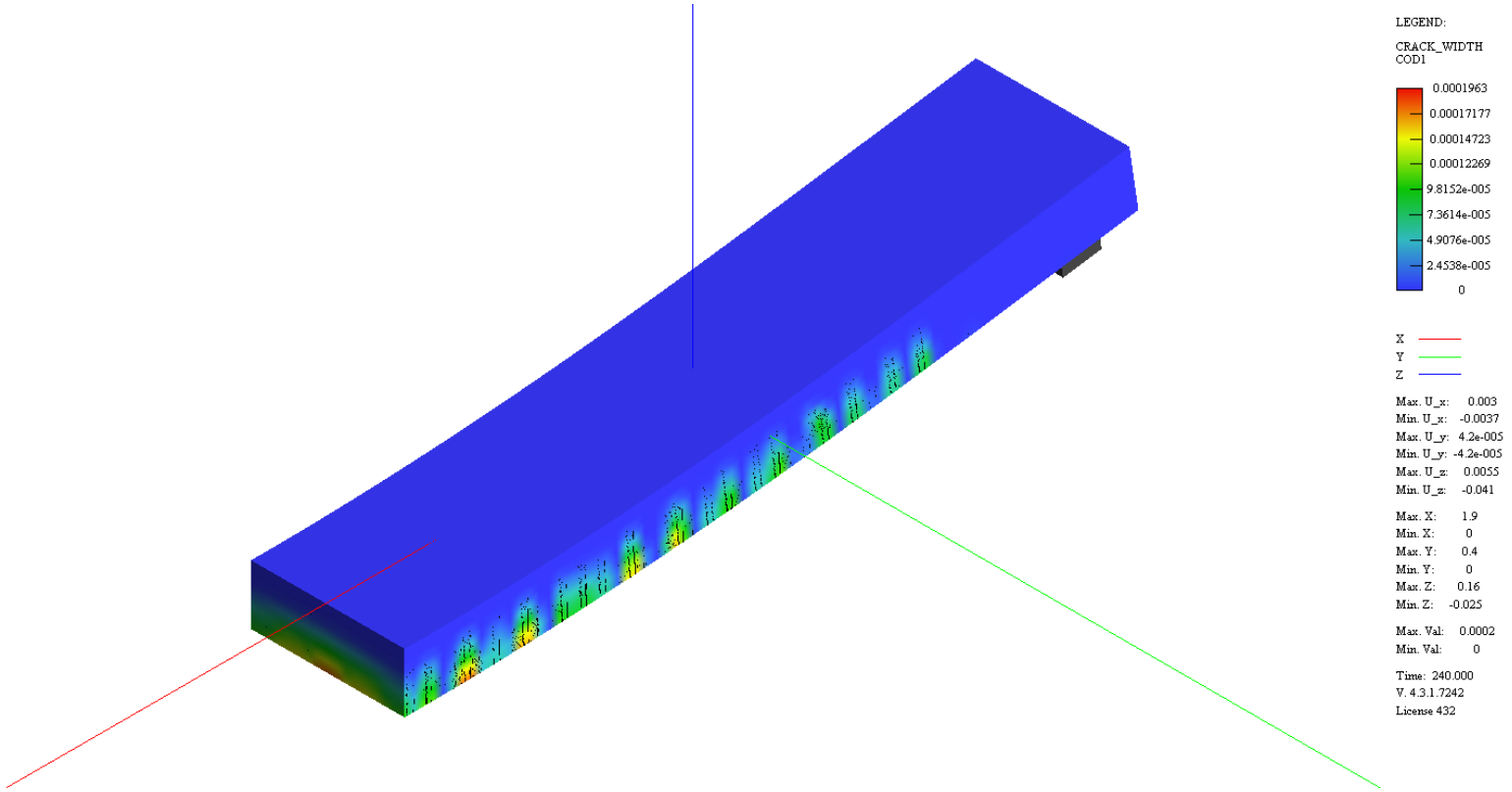

Figure G.1 Typical FEM time-dependent crack width result for N-SCC-a slab

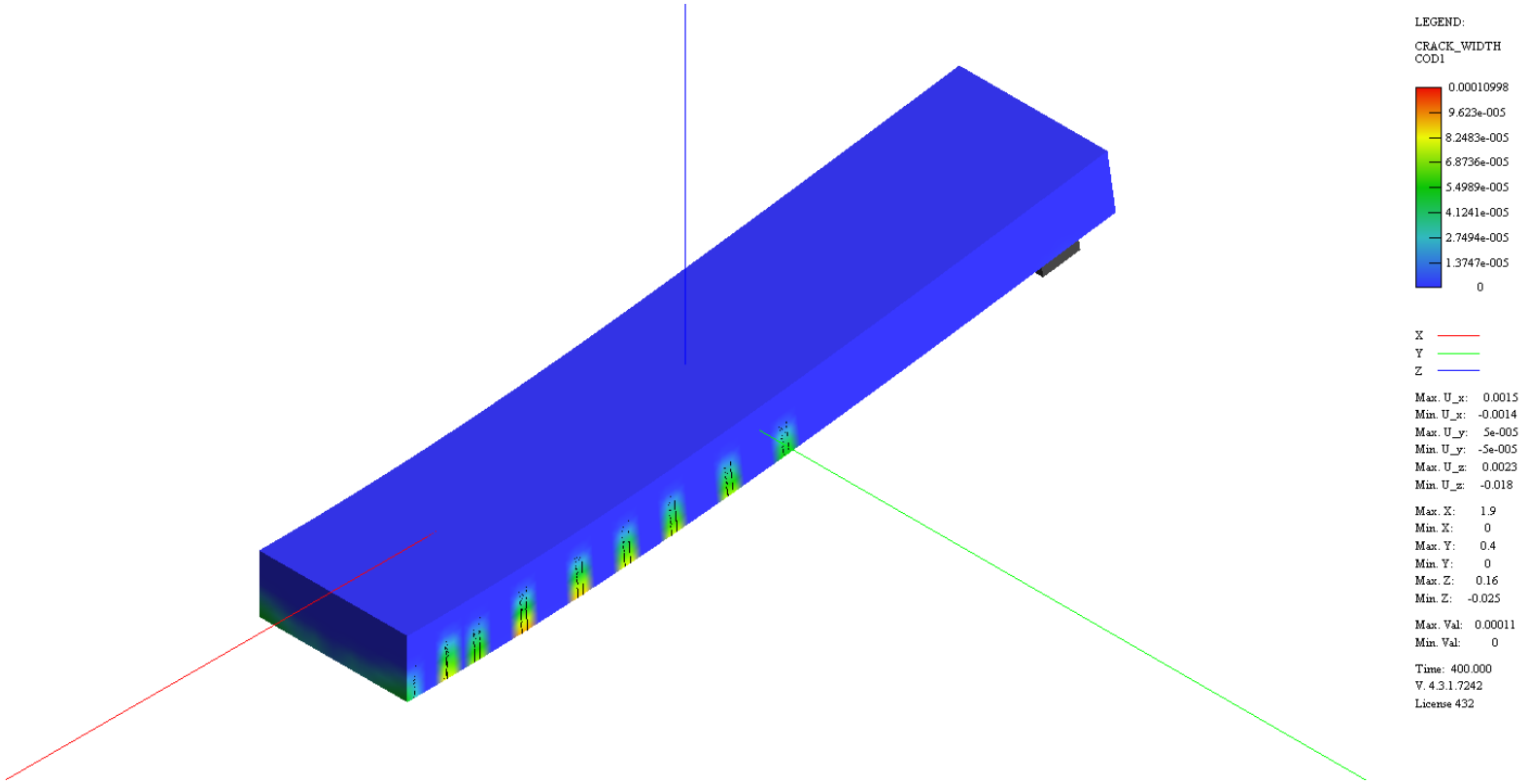

Figure G.2 Typical FEM time-dependent crack width result for N-SCC-b slab

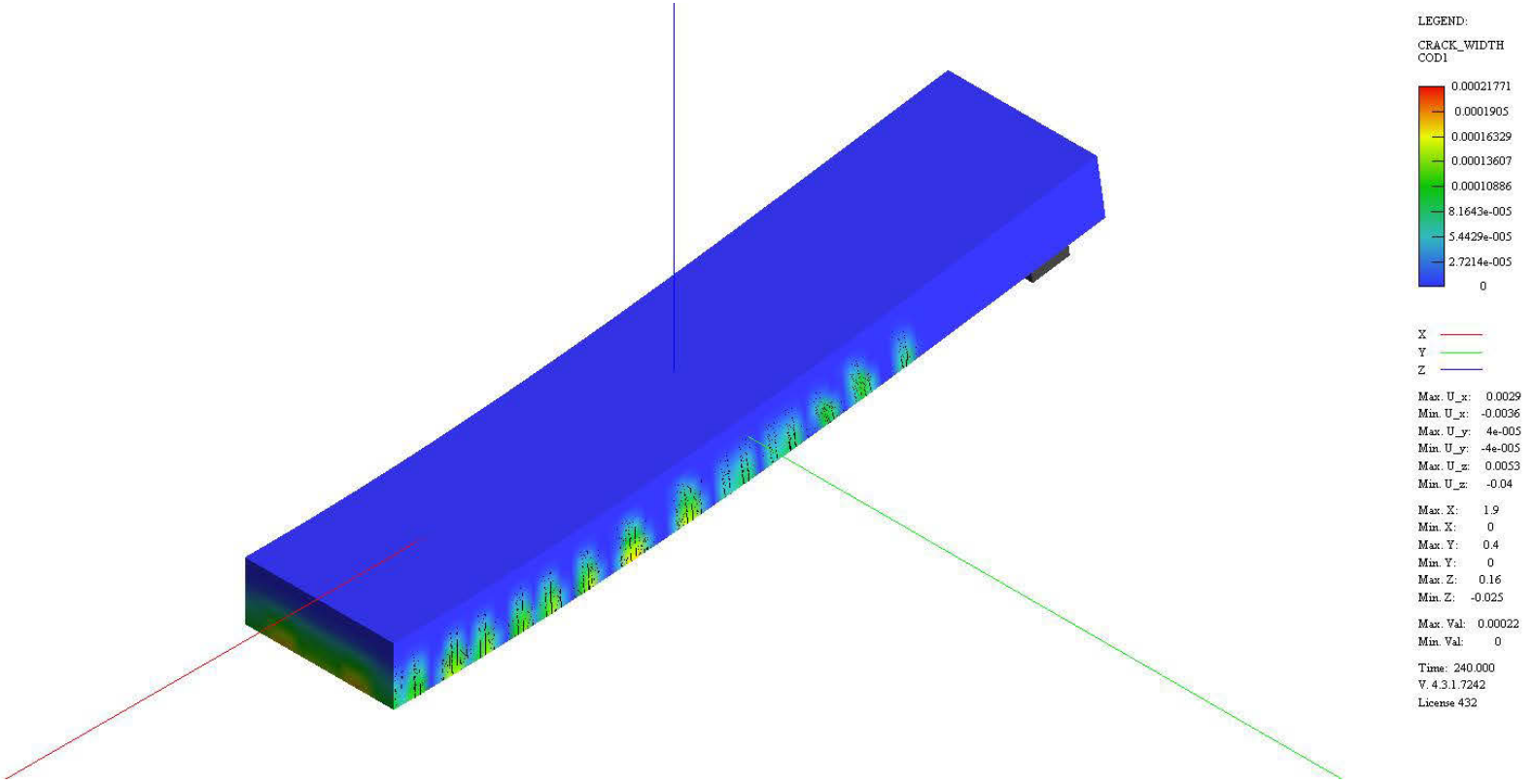

Figure G.3 Typical FEM time-dependent crack width result for D-SCC-a slab

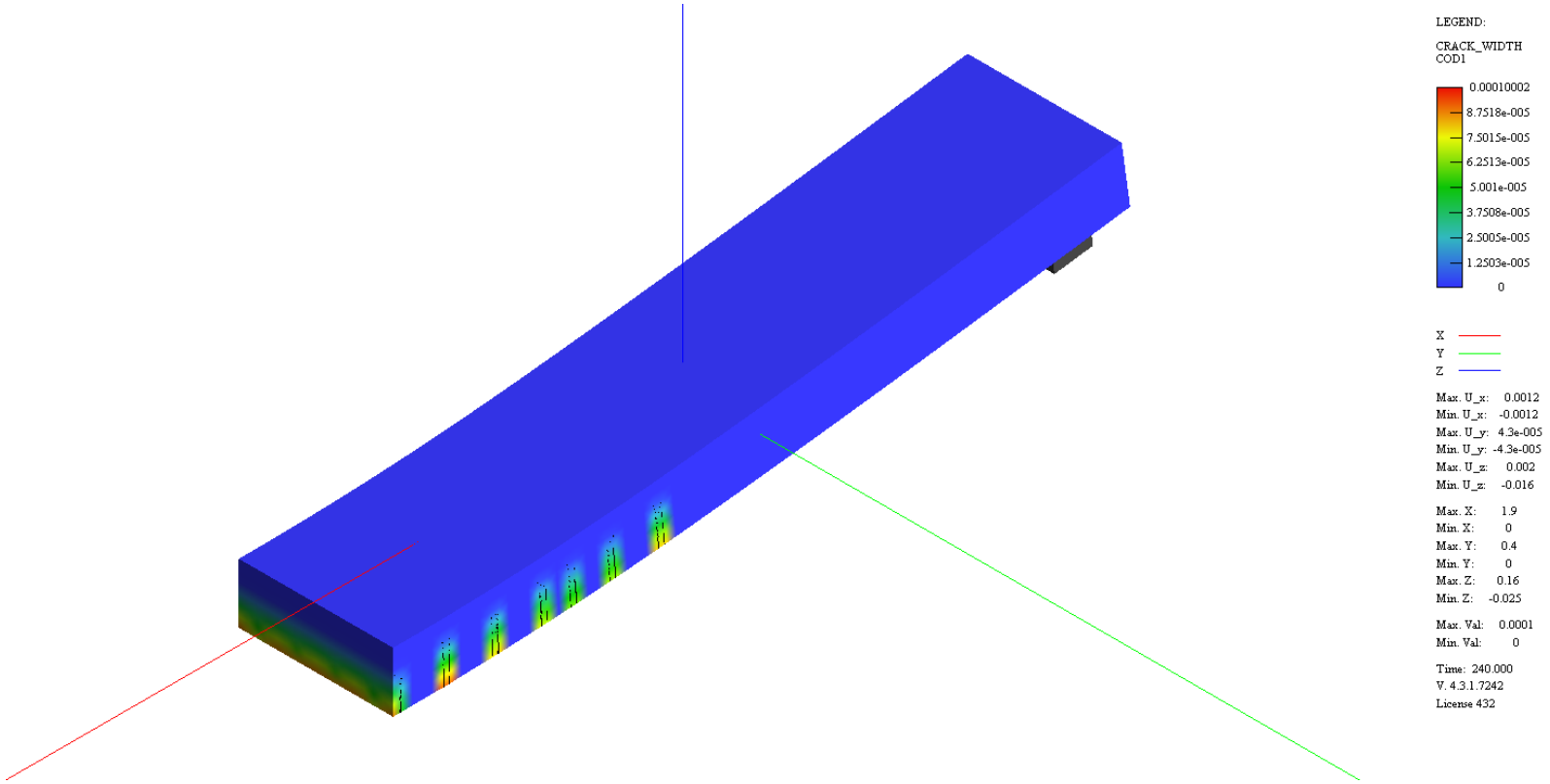

Figure G.4 Typical FEM time-dependent crack width result for D-SCC-b slab

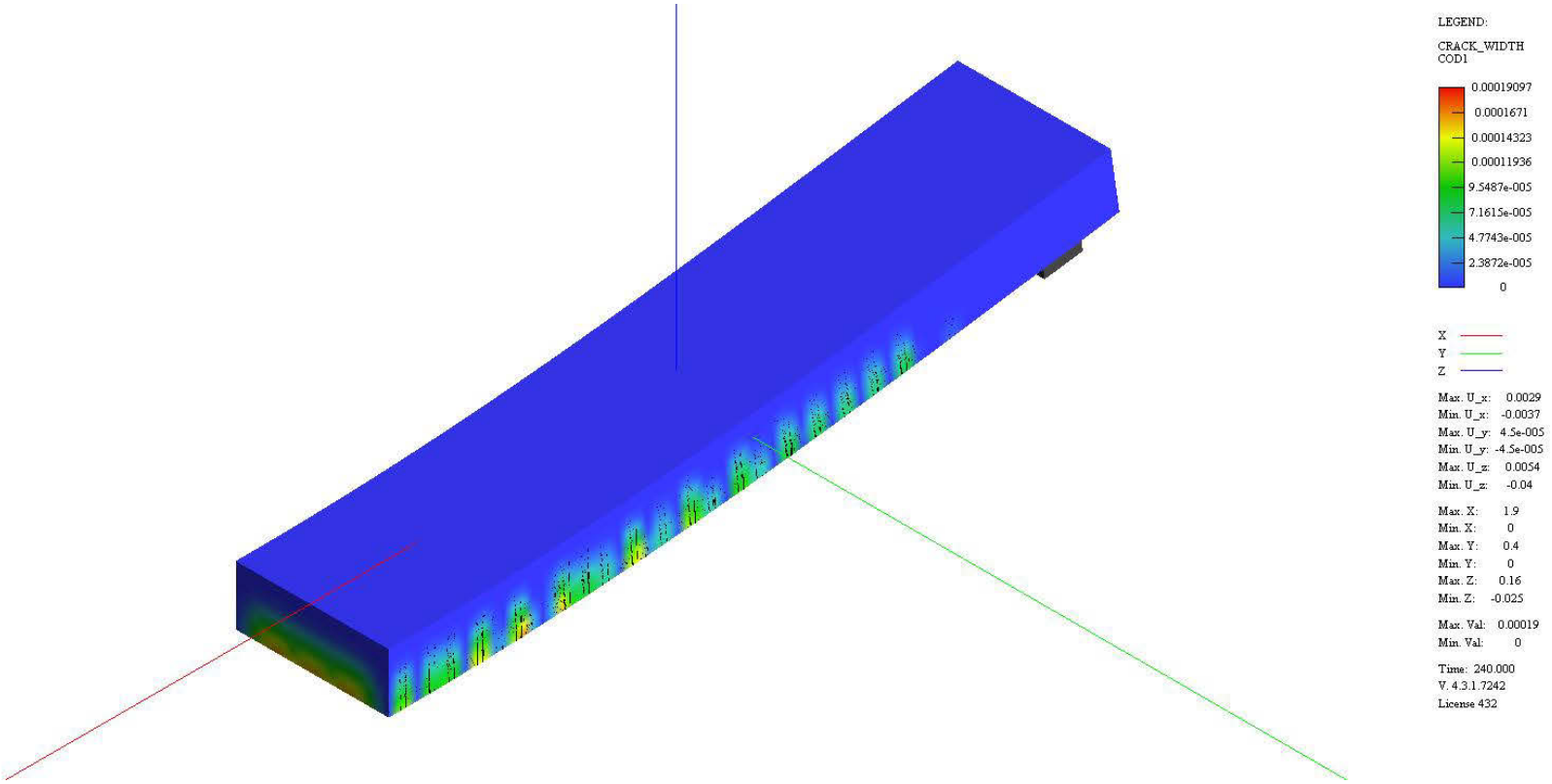

Figure G.5 Typical FEM time-dependent crack width result for S-SCC-a slab

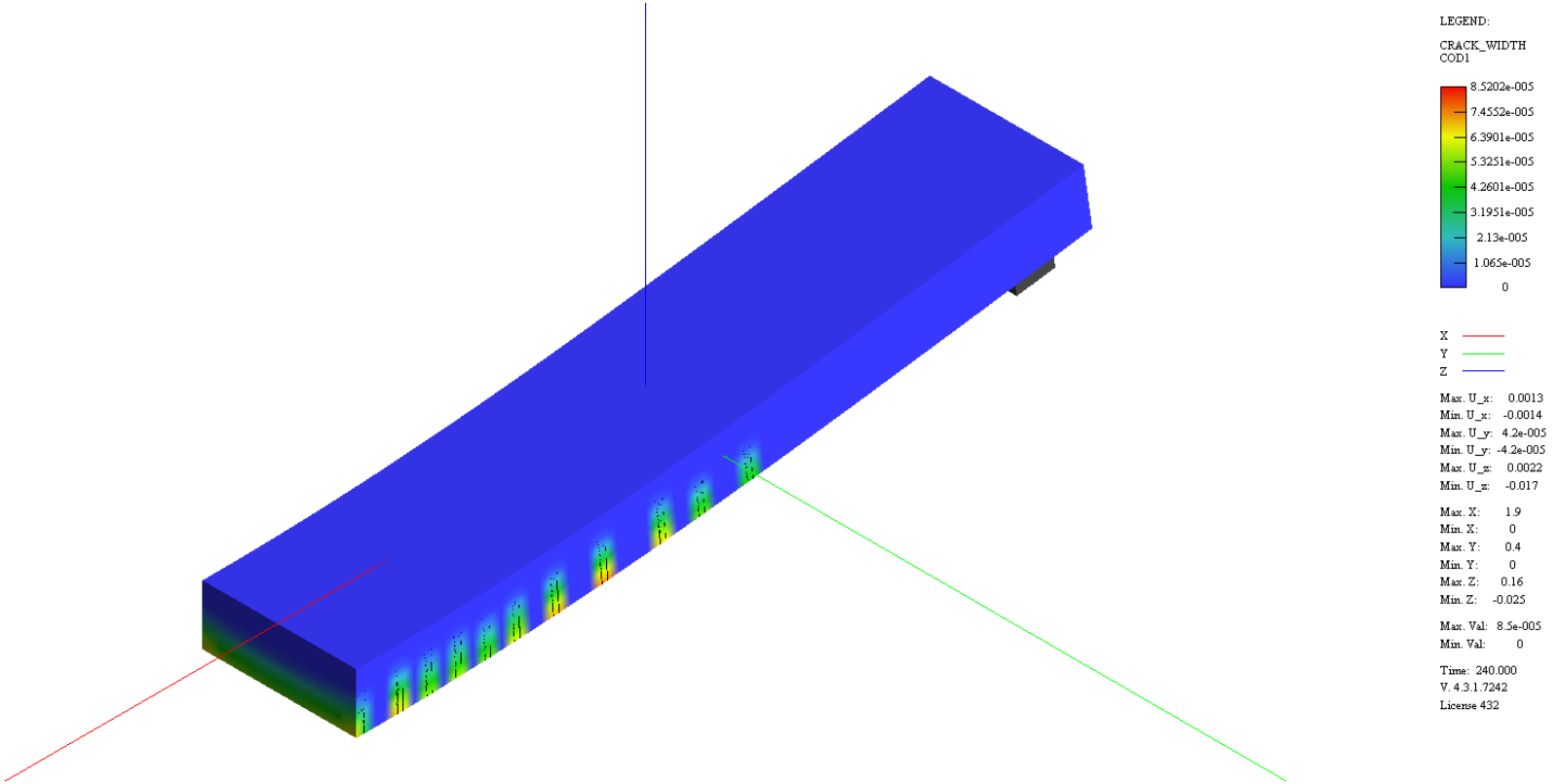

Figure G.6 Typical FEM time-dependent crack width result for S-SCC-b slab

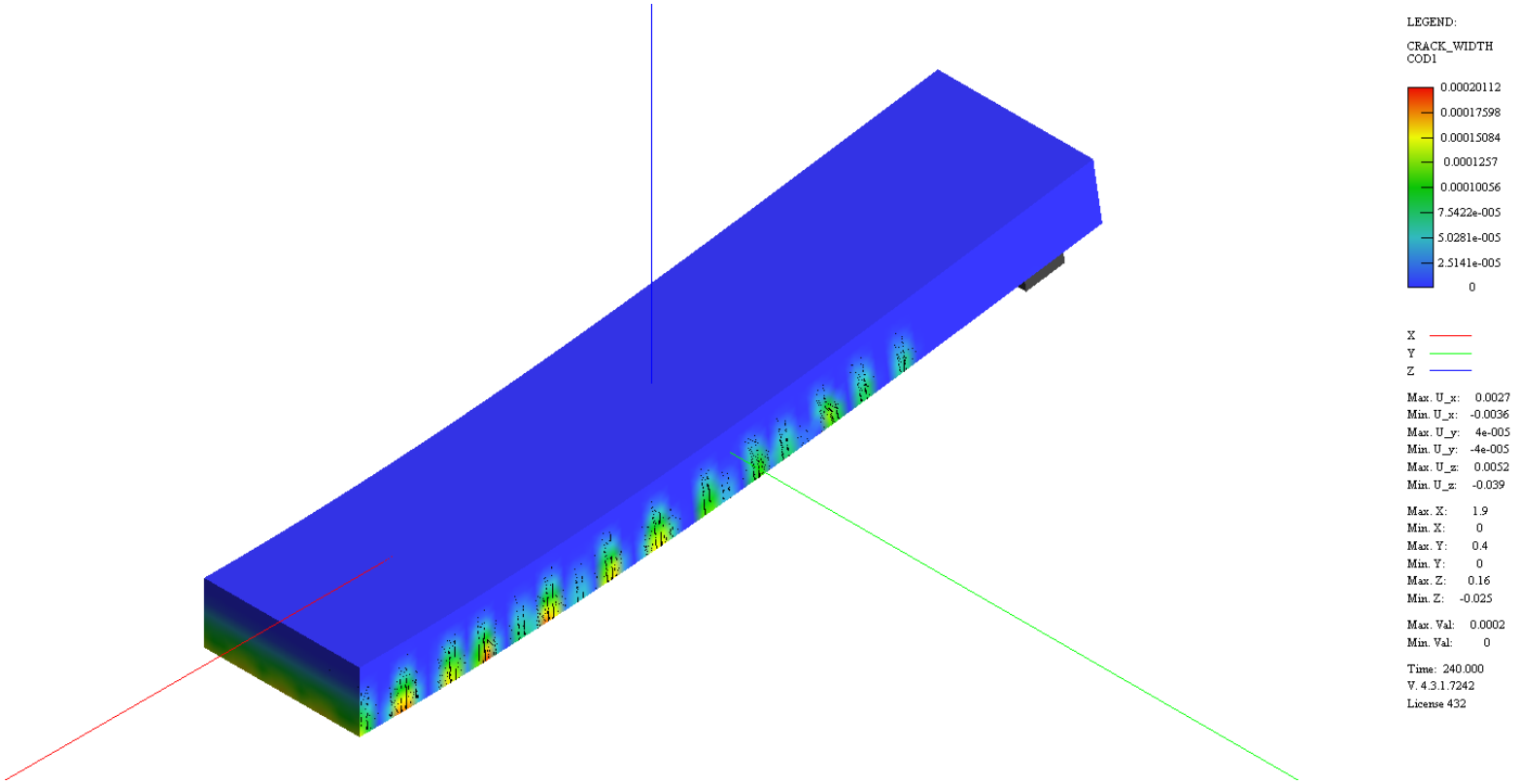

Figure G.7 Typical FEM time-dependent crack width result for DS-SCC-a slab

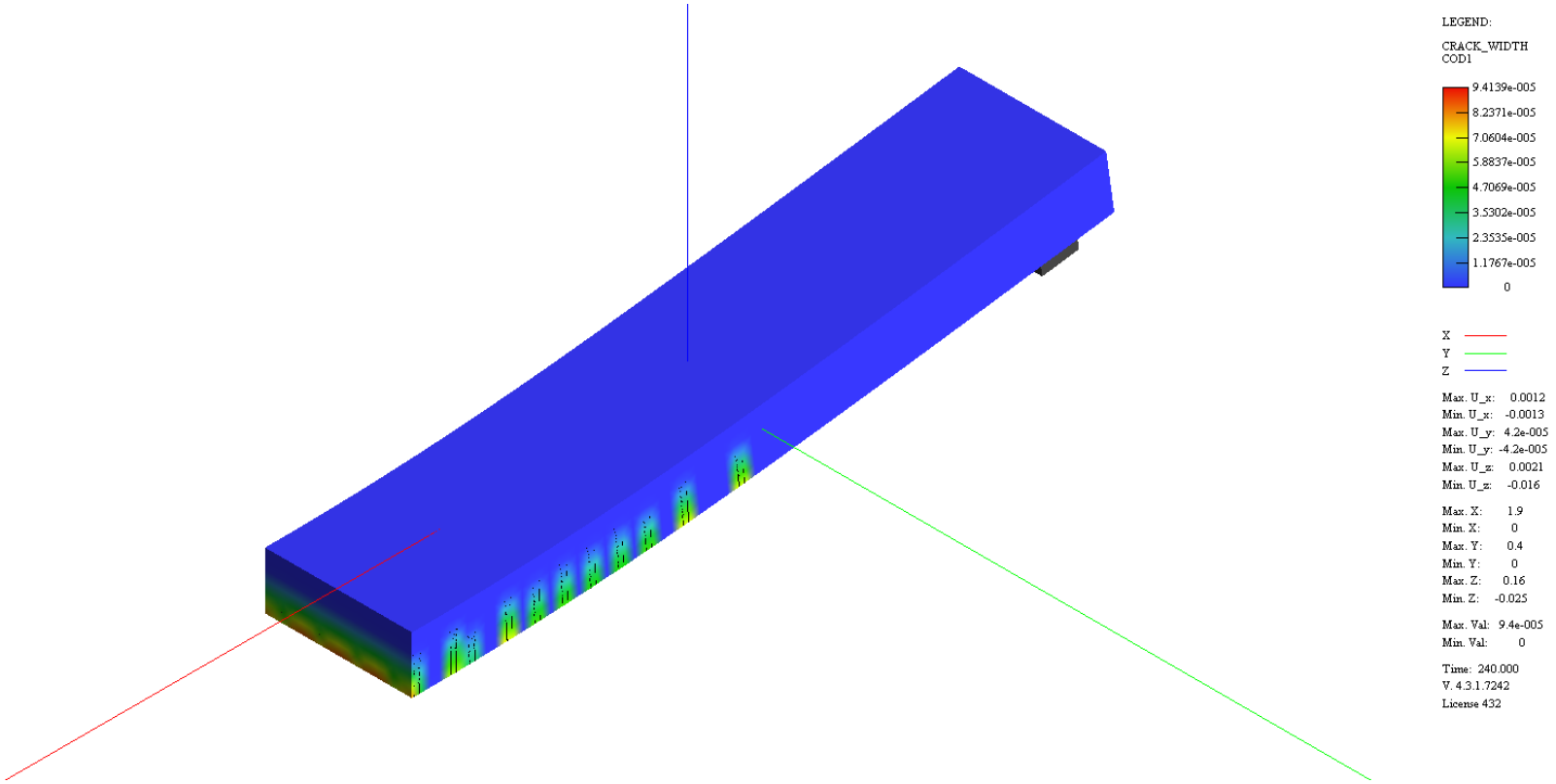

Figure G.8 Typical FEM time-dependent crack width result for DS-SCC-b slab

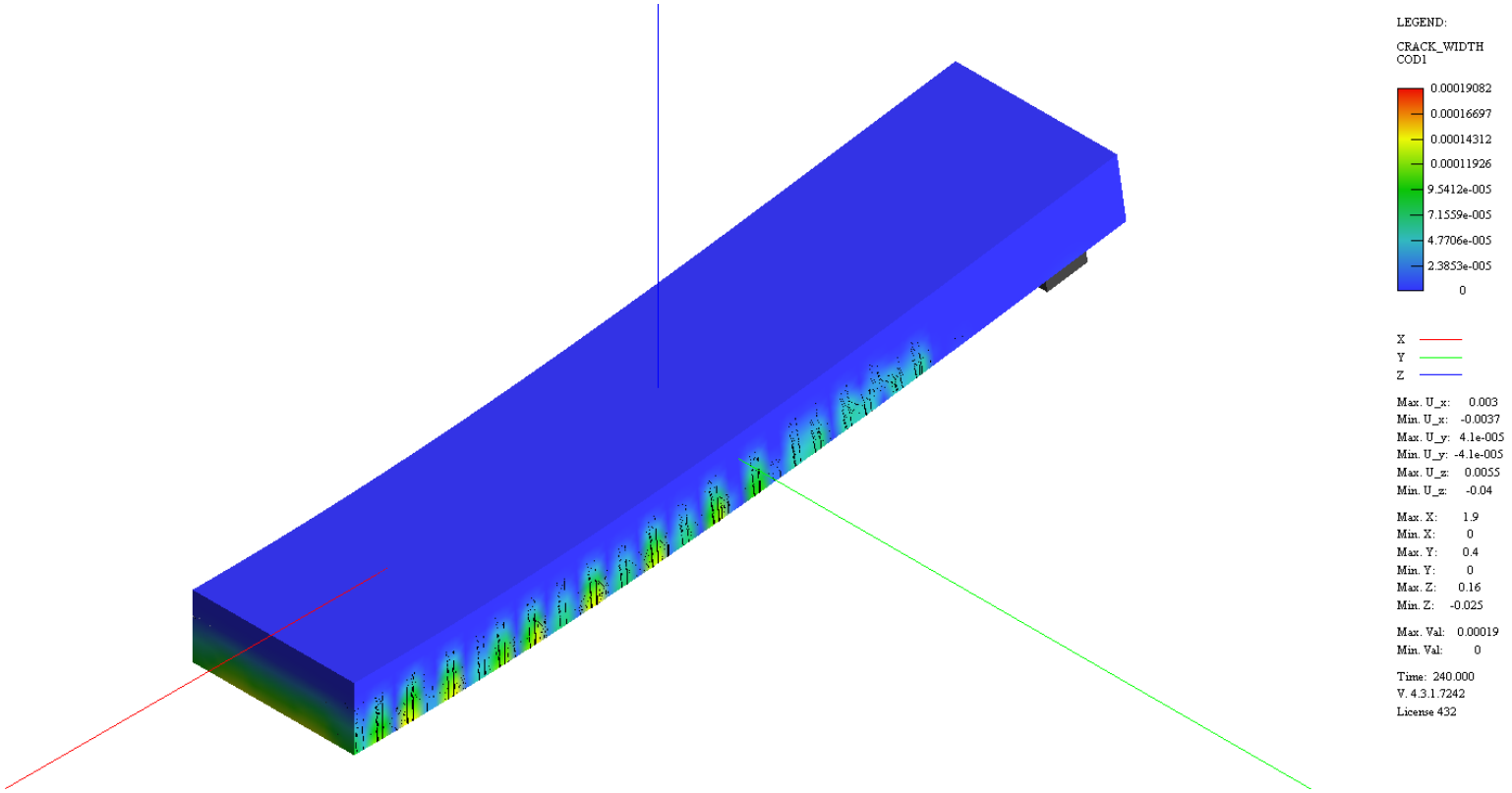

Figure G.9 Typical FEM time-dependent crack width result for N-CC-a slab

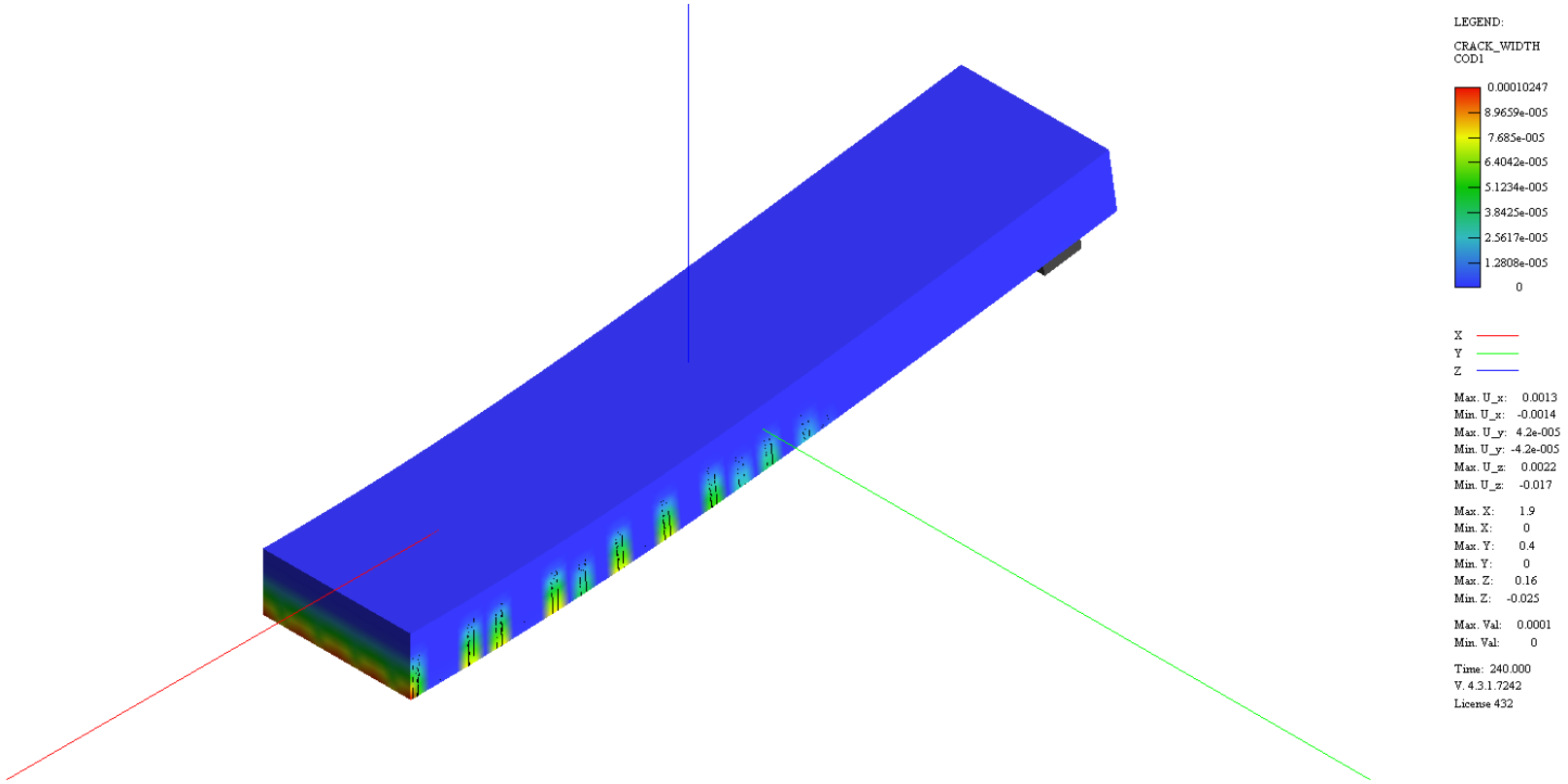

Figure G.10 Typical FEM time-dependent crack width result for N-CC-b slab

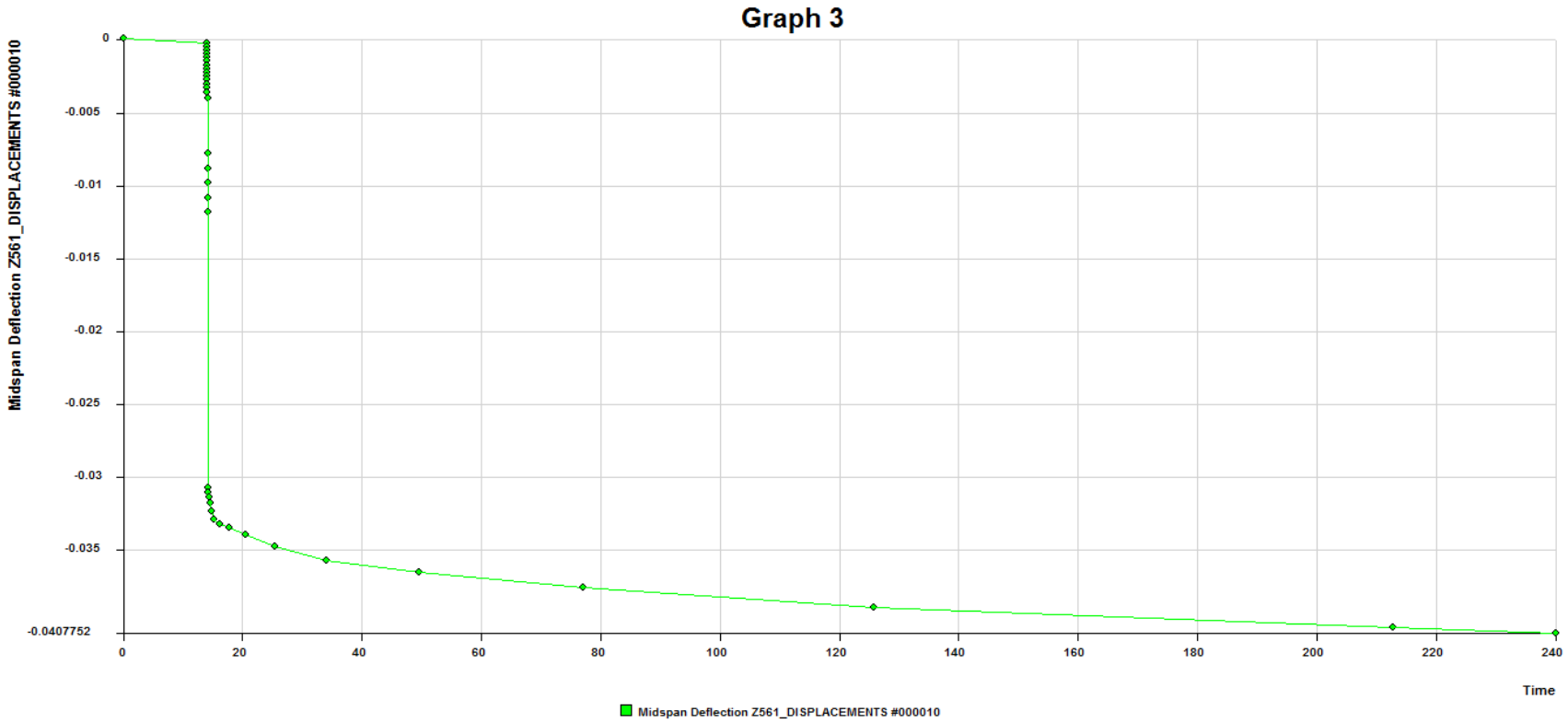

Figure G.11 Typical FEM time-dependent deflection result for N-SCC-a slab

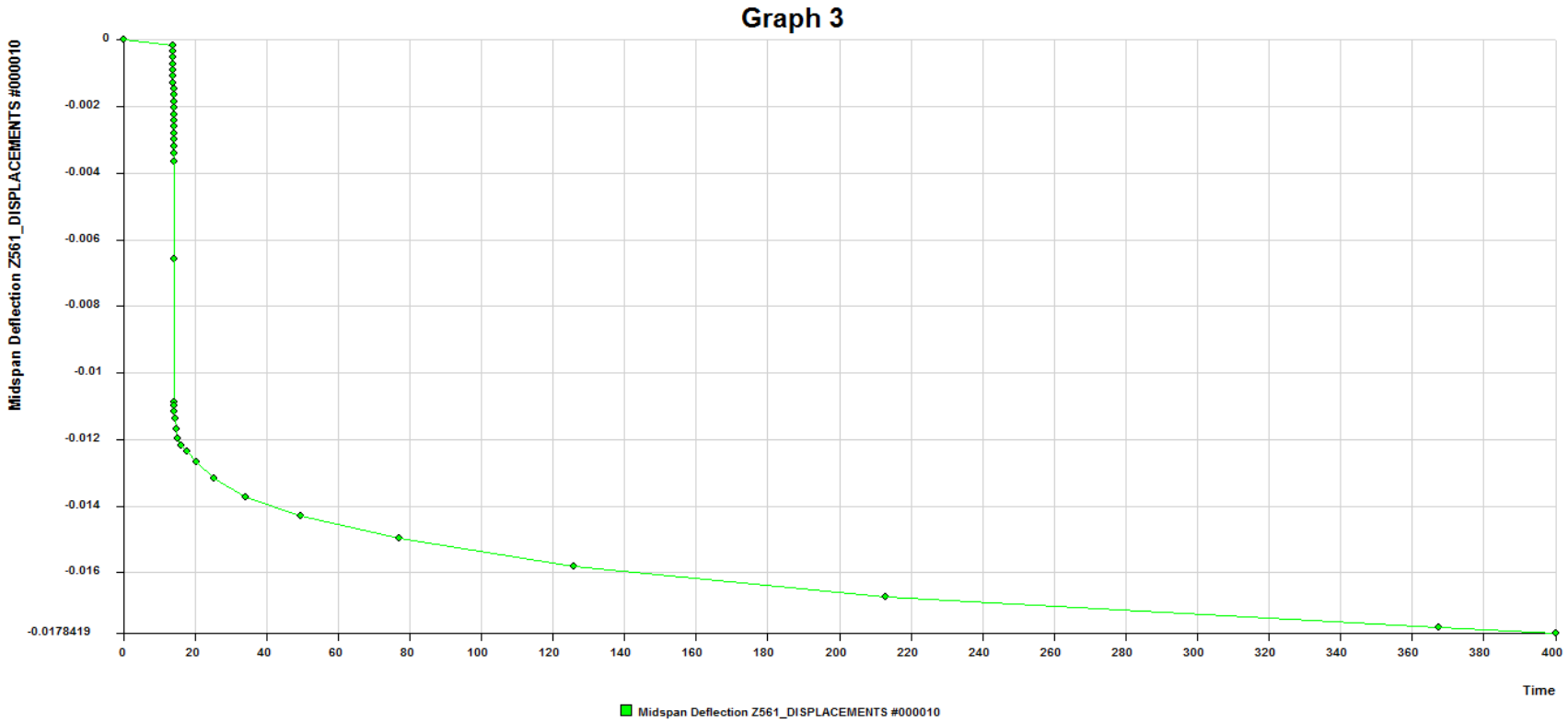

Figure G.12 Typical FEM time-dependent deflection result for N-SCC-b slab

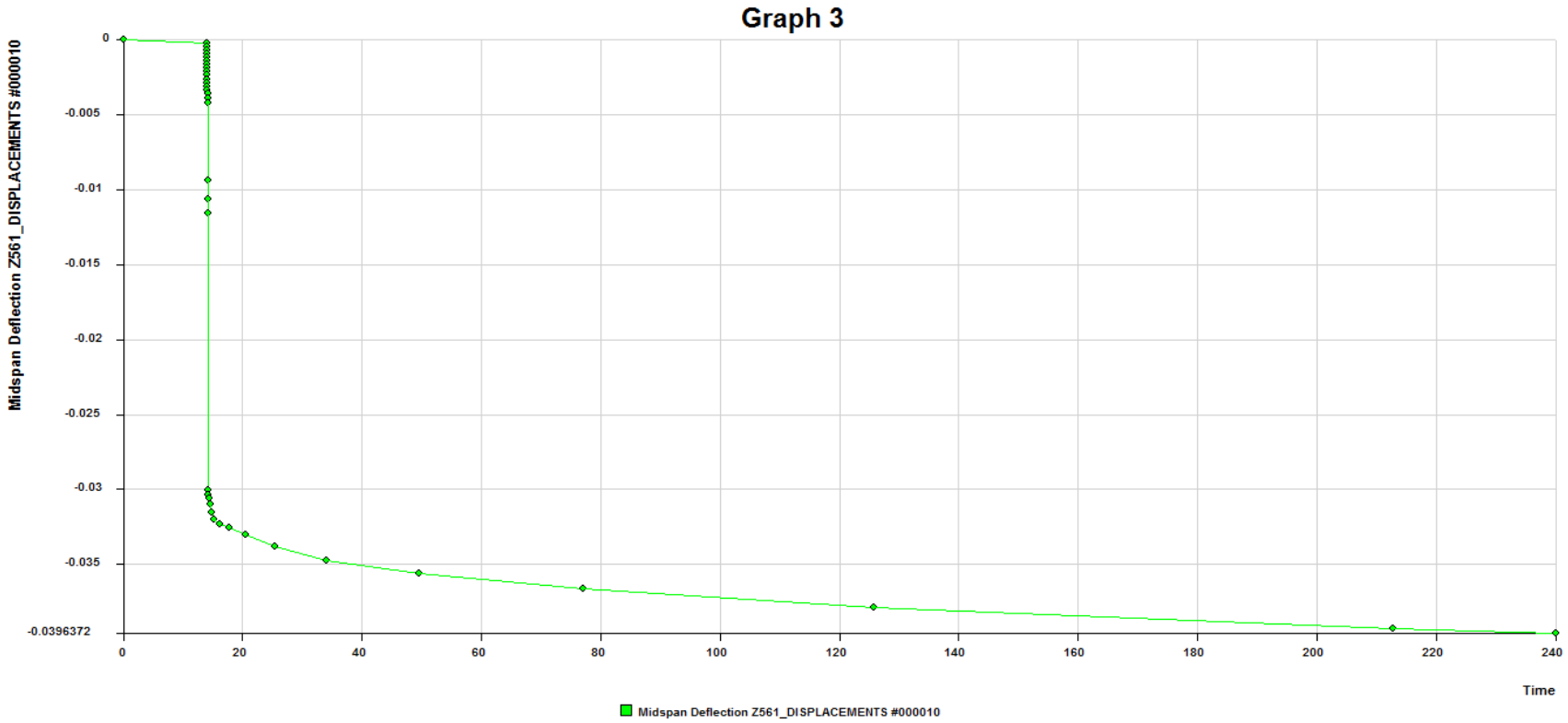

Figure G.13 Typical FEM time-dependent deflection result for D-SCC-a slab

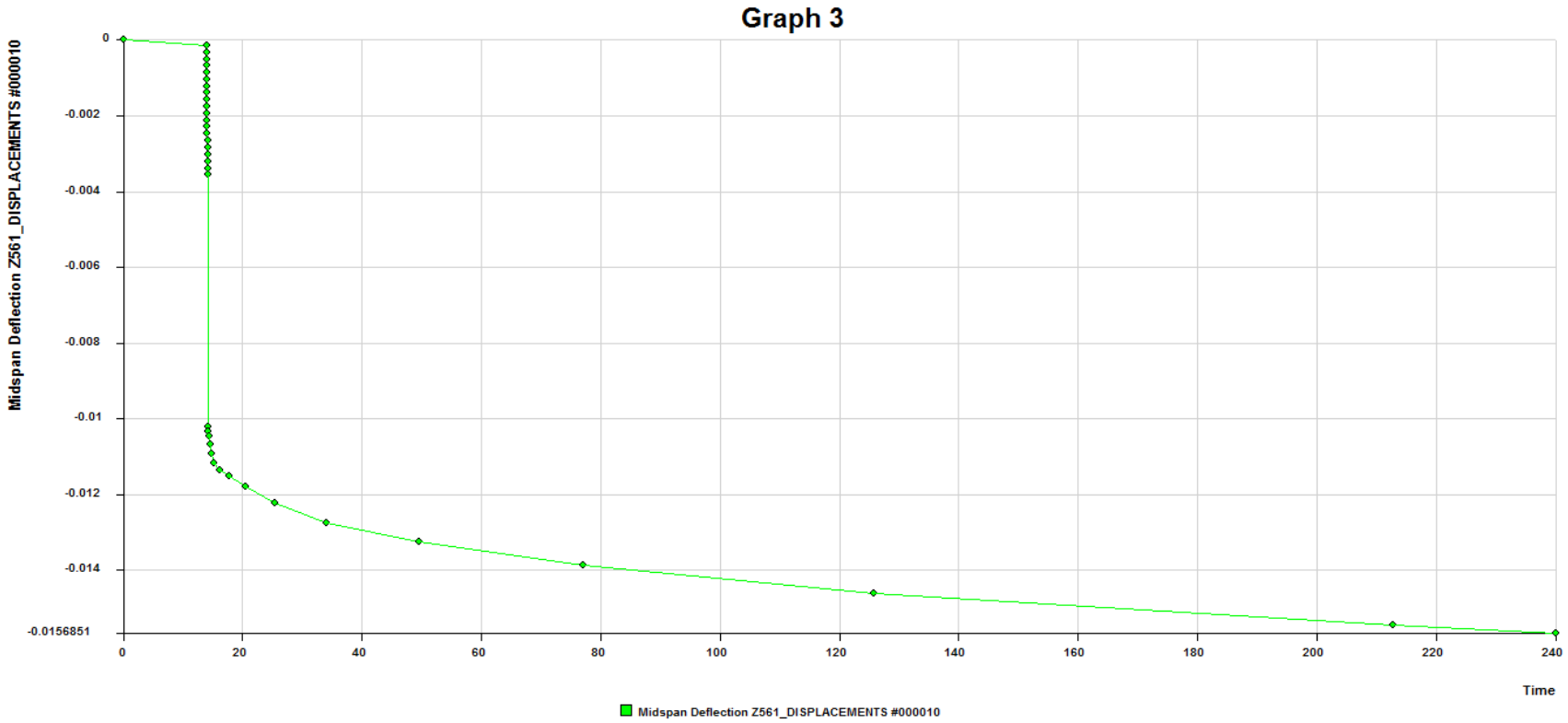

Figure G.14 Typical FEM time-dependent deflection result for D-SCC-b slab

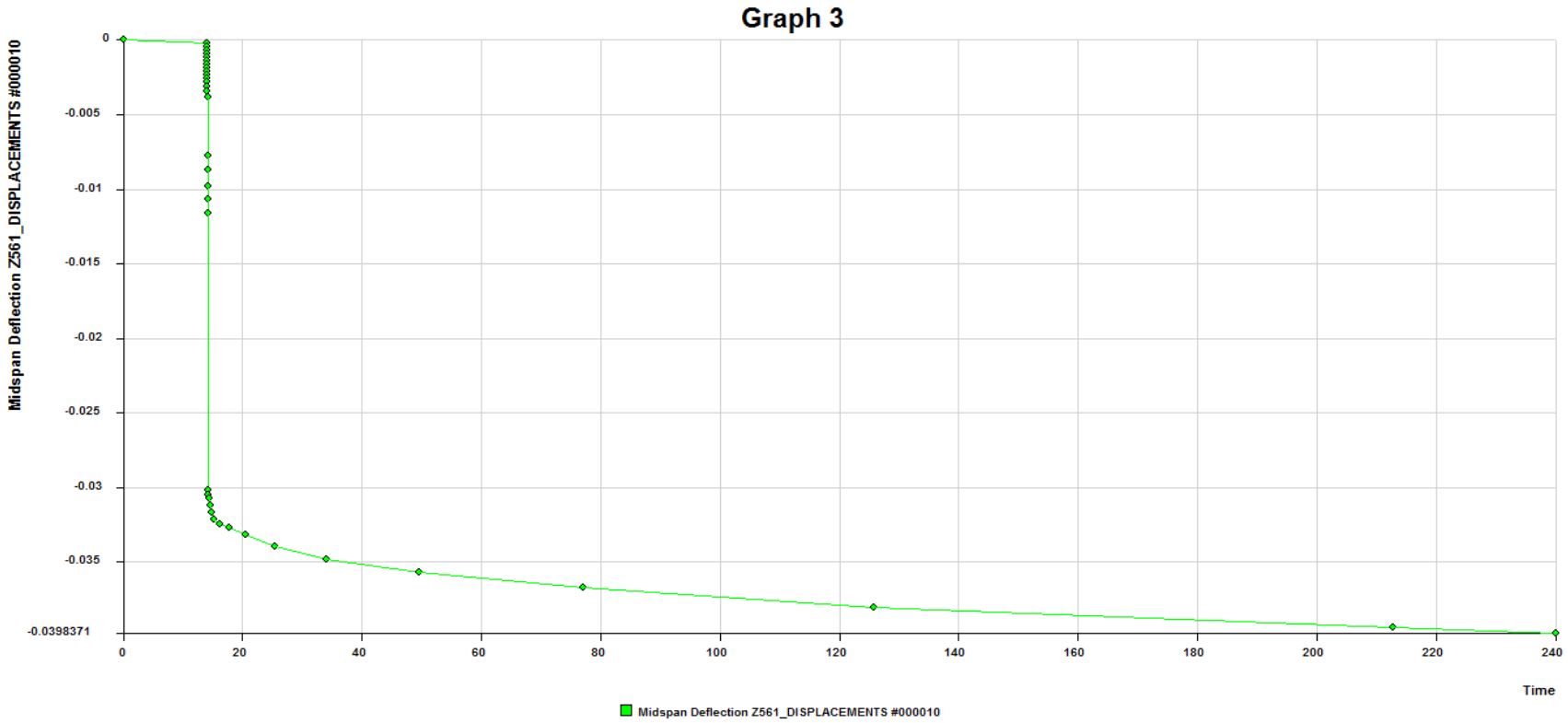

Figure G.15 Typical FEM time-dependent deflection result for S-SCC-a slab

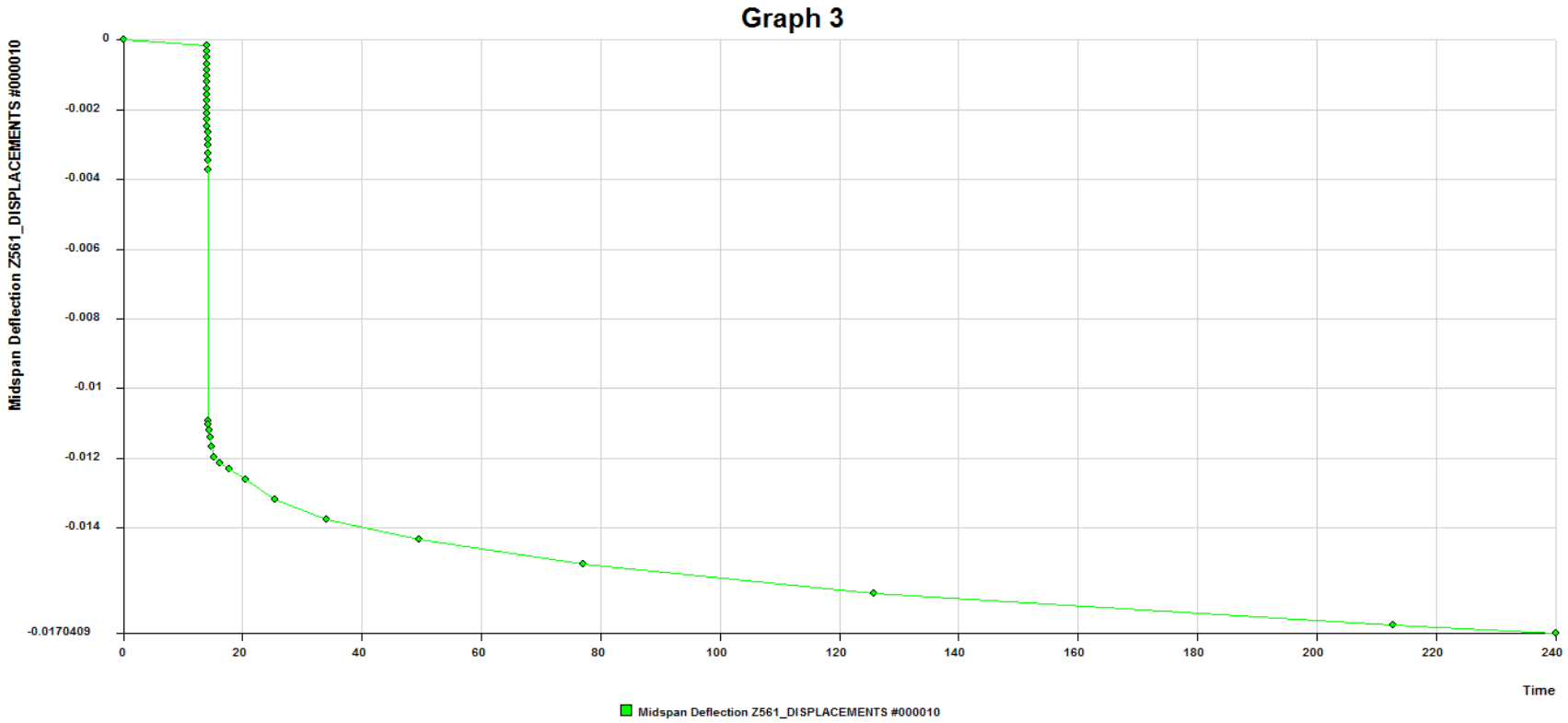

Figure G.16 Typical FEM time-dependent deflection result for S-SCC-b slab

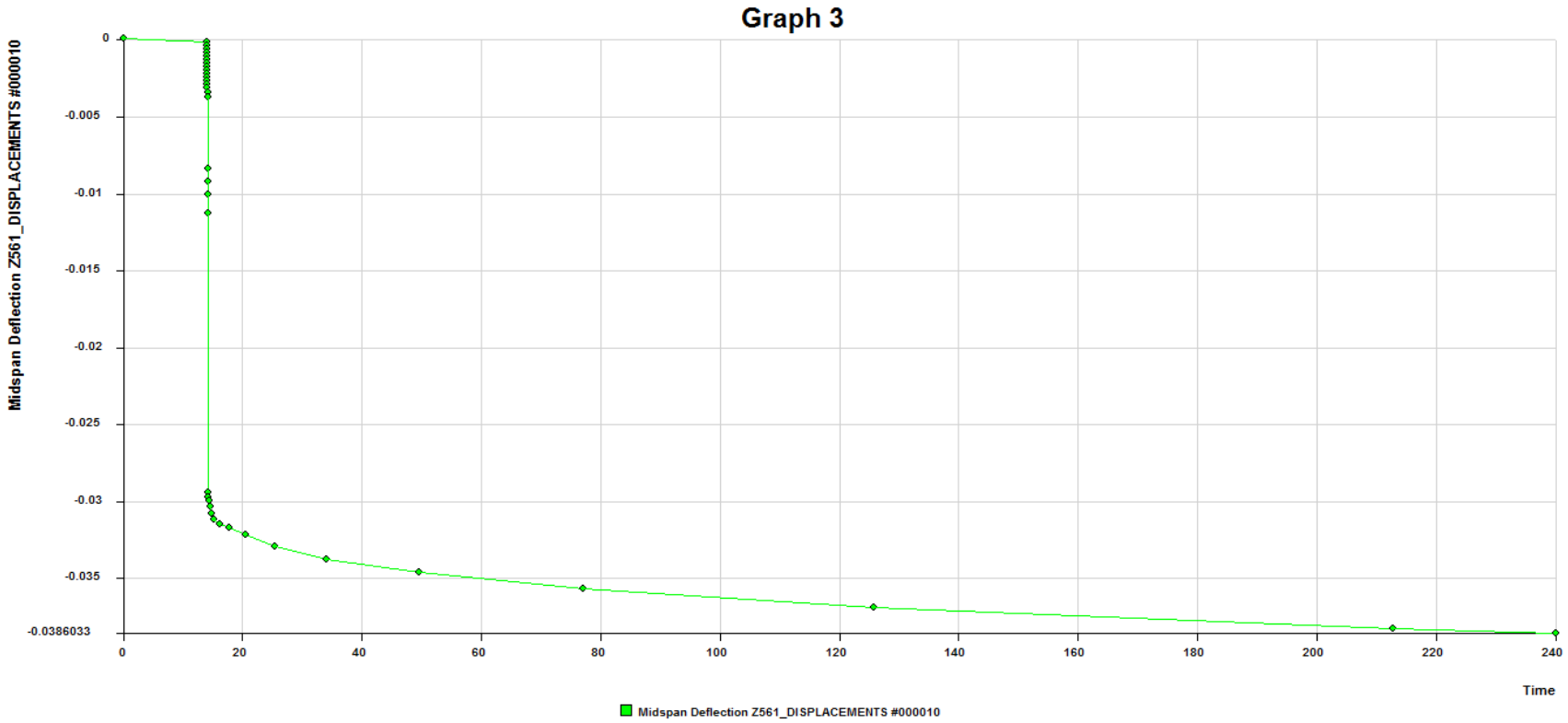

Figure G.17 Typical FEM time-dependent deflection result for DS-SCC-a slab

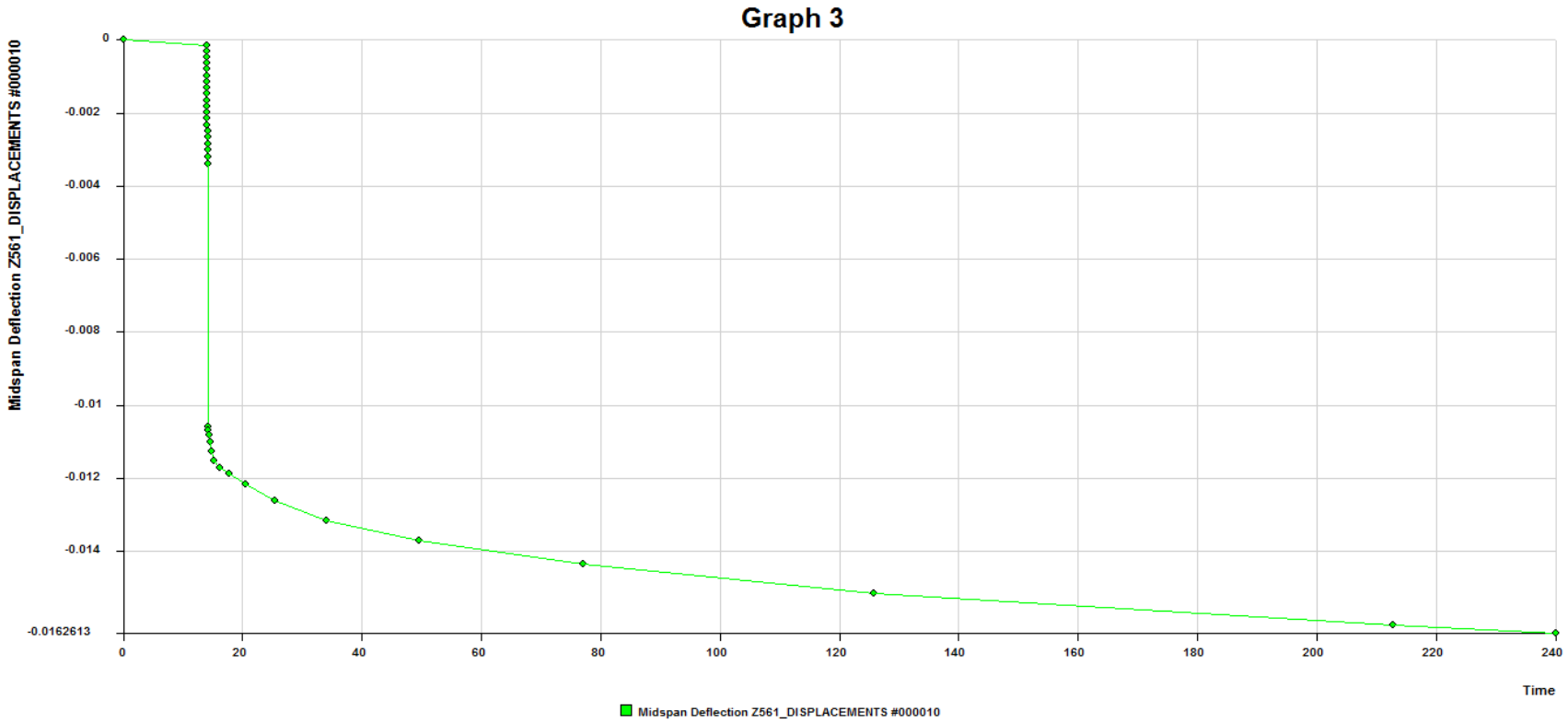

Figure G.18 Typical FEM time-dependent deflection result for DS-SCC-b slab

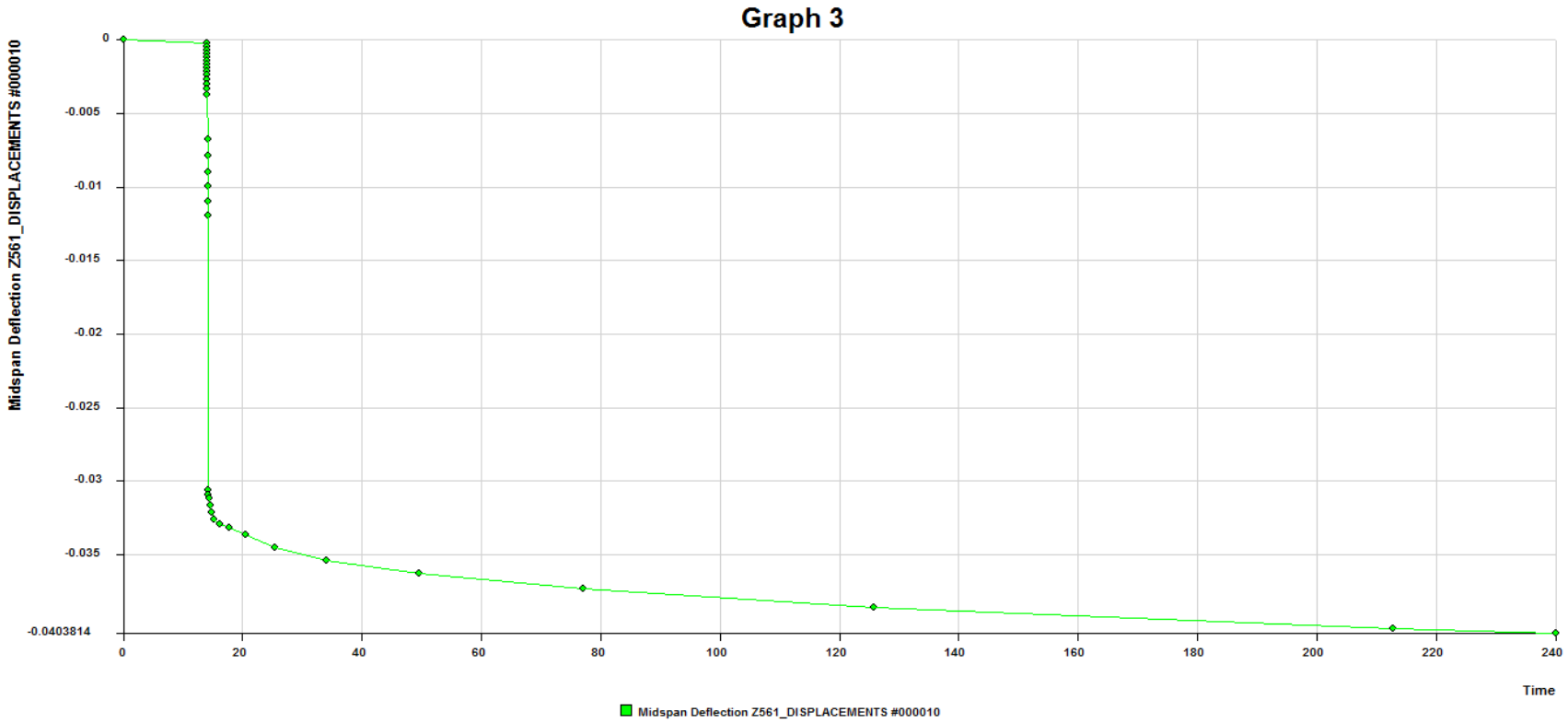

Figure G.19 Typical FEM time-dependent deflection result for N-CC-a slab

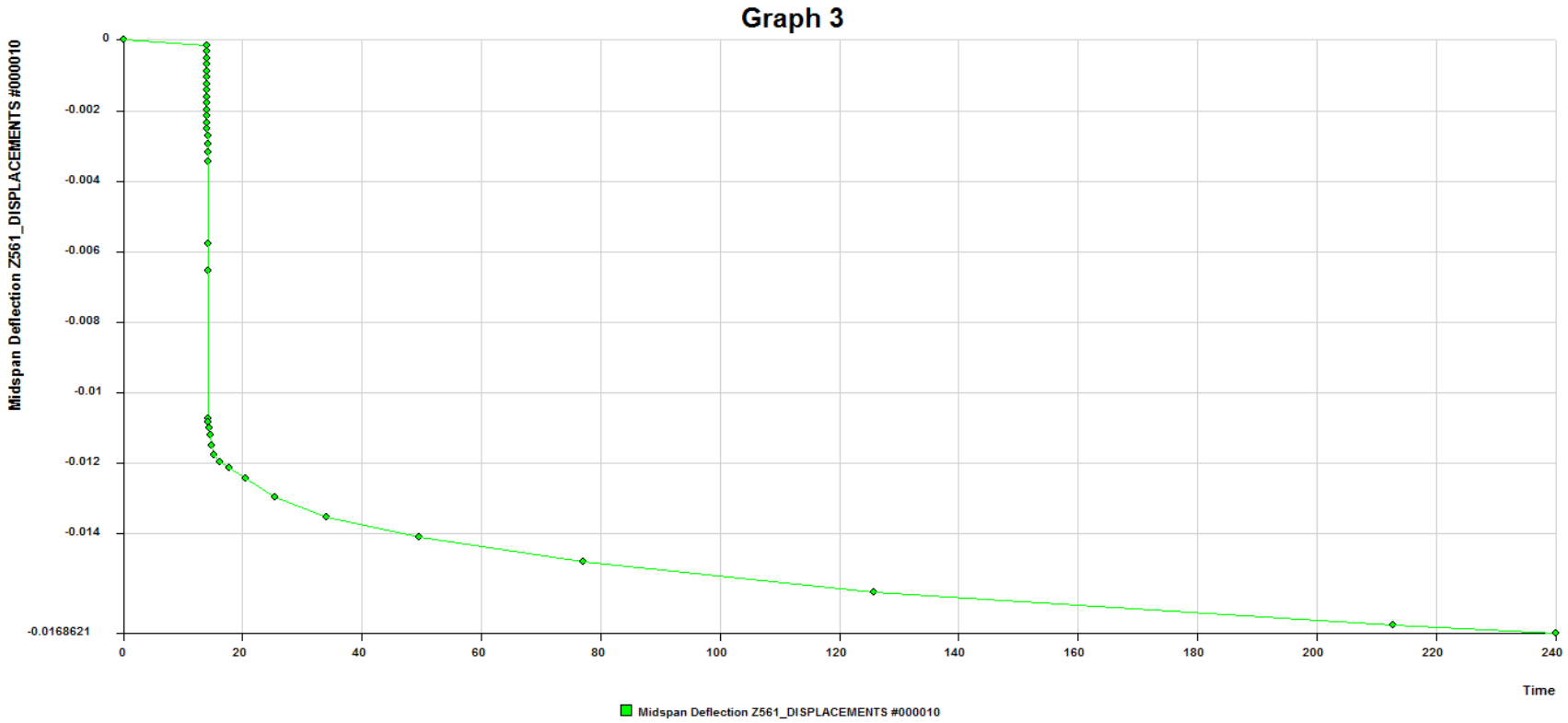

Figure G.20 Typical FEM time-dependent deflection result for N-CC-a slab

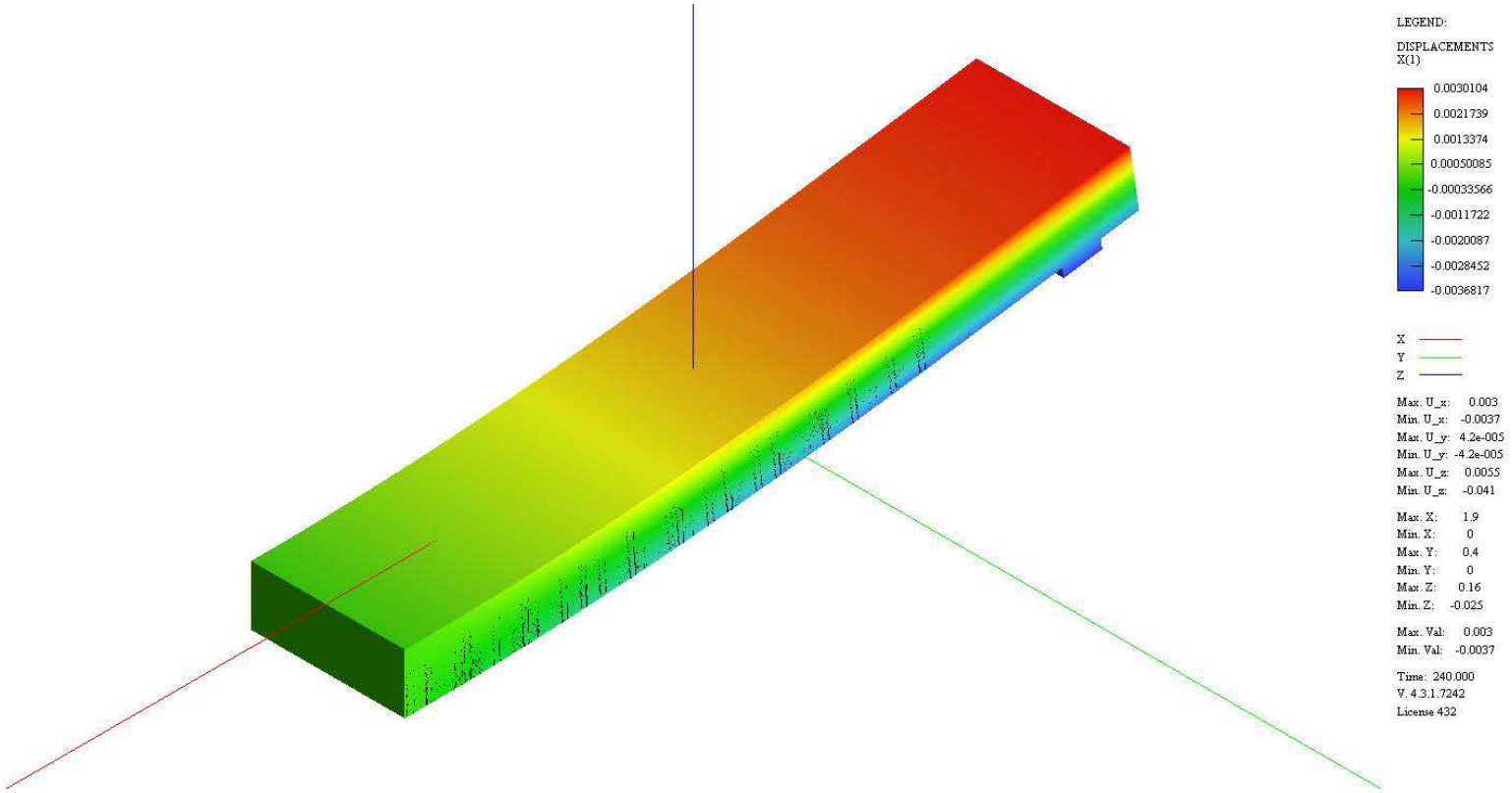

Figure G.21 Typical FEM time-dependent displacement result for N-SCC-a slab

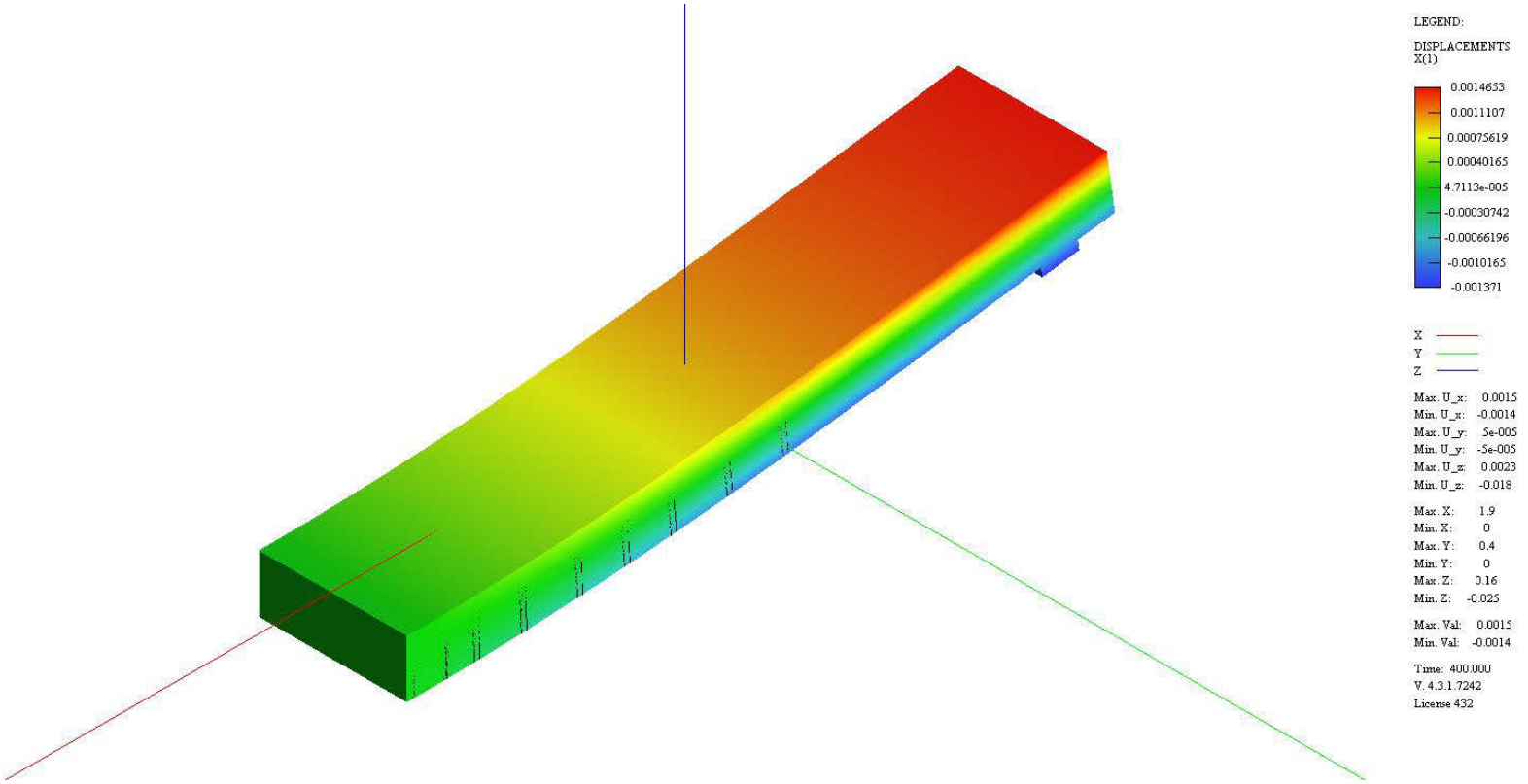

Figure G.22 Typical FEM time-dependent displacement result for N-SCC-b slab

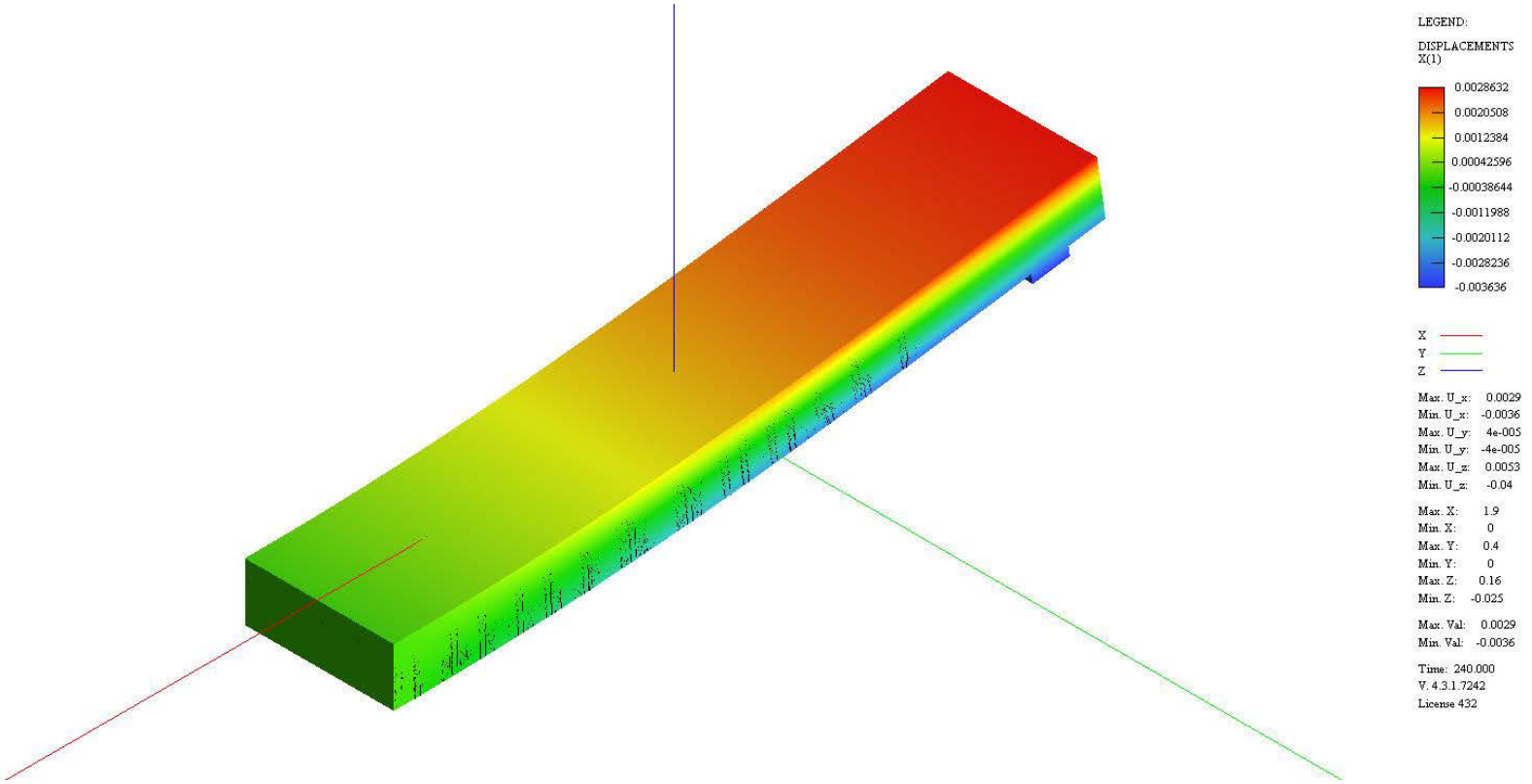

Figure G.23 Typical FEM time-dependent displacement result for D-SCC-a slab

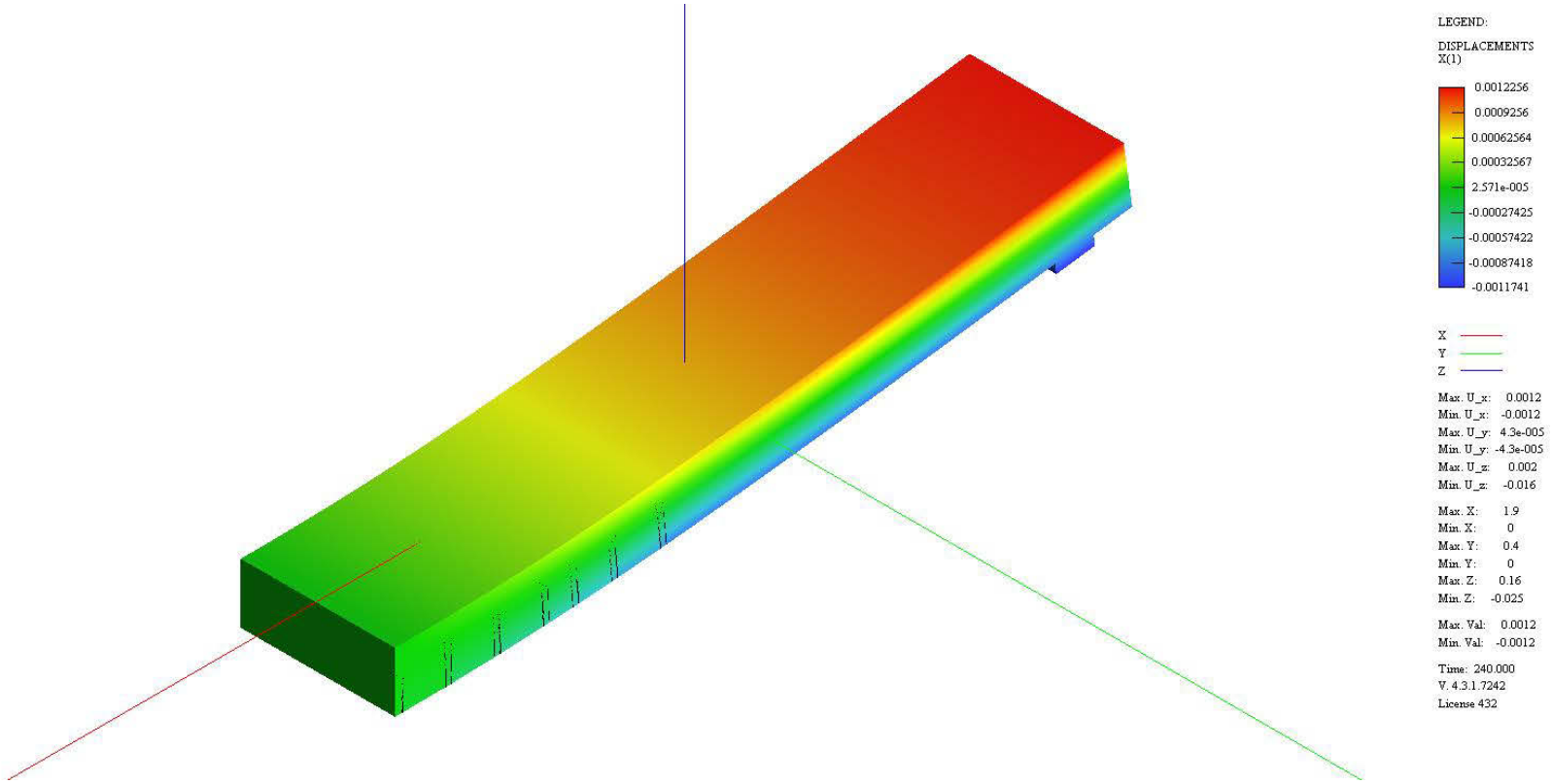

Figure G.24 Typical FEM time-dependent displacement result for D-SCC-b slab

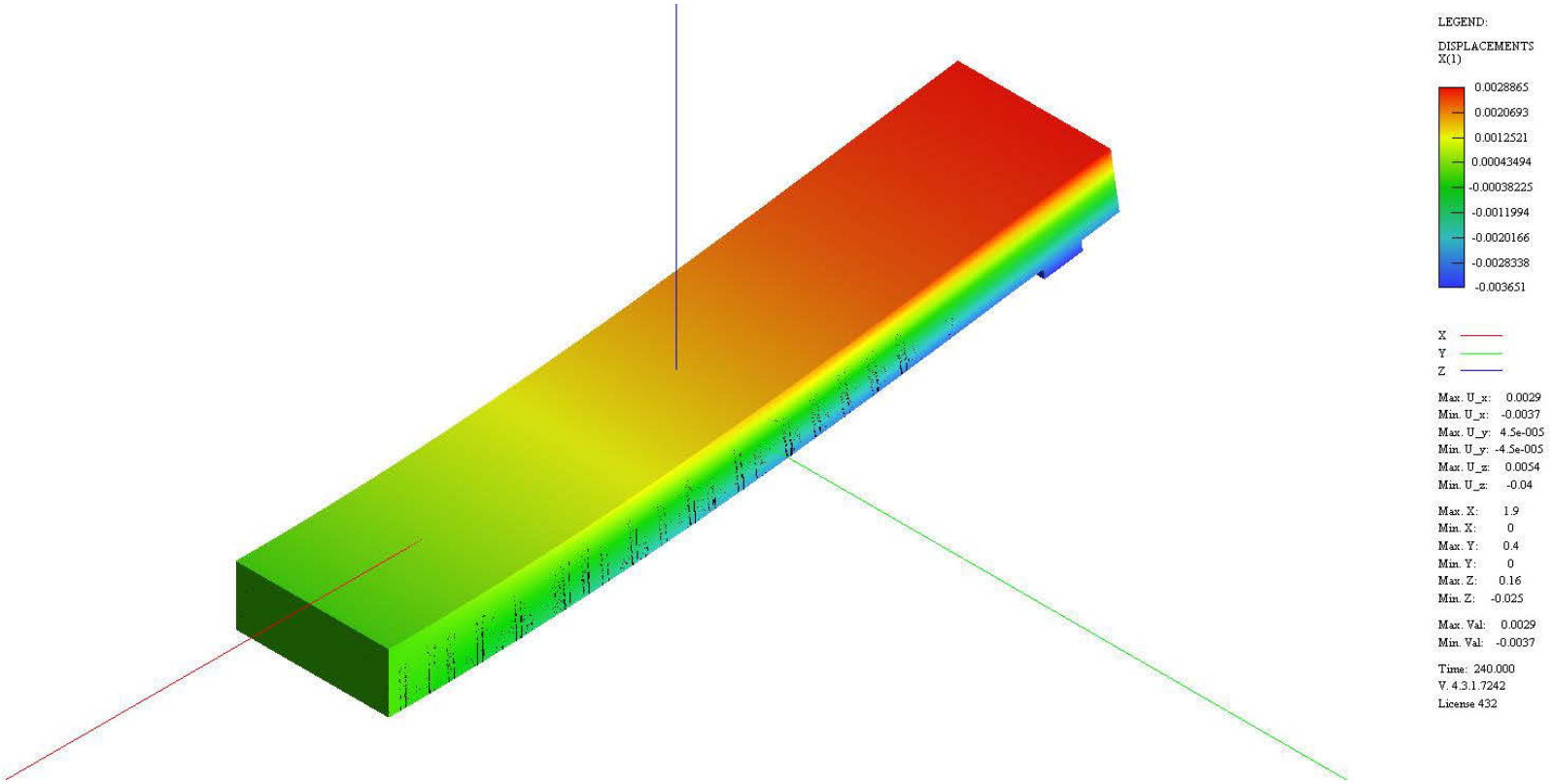

Figure G.25 Typical FEM time-dependent displacement result for S-SCC-a slab

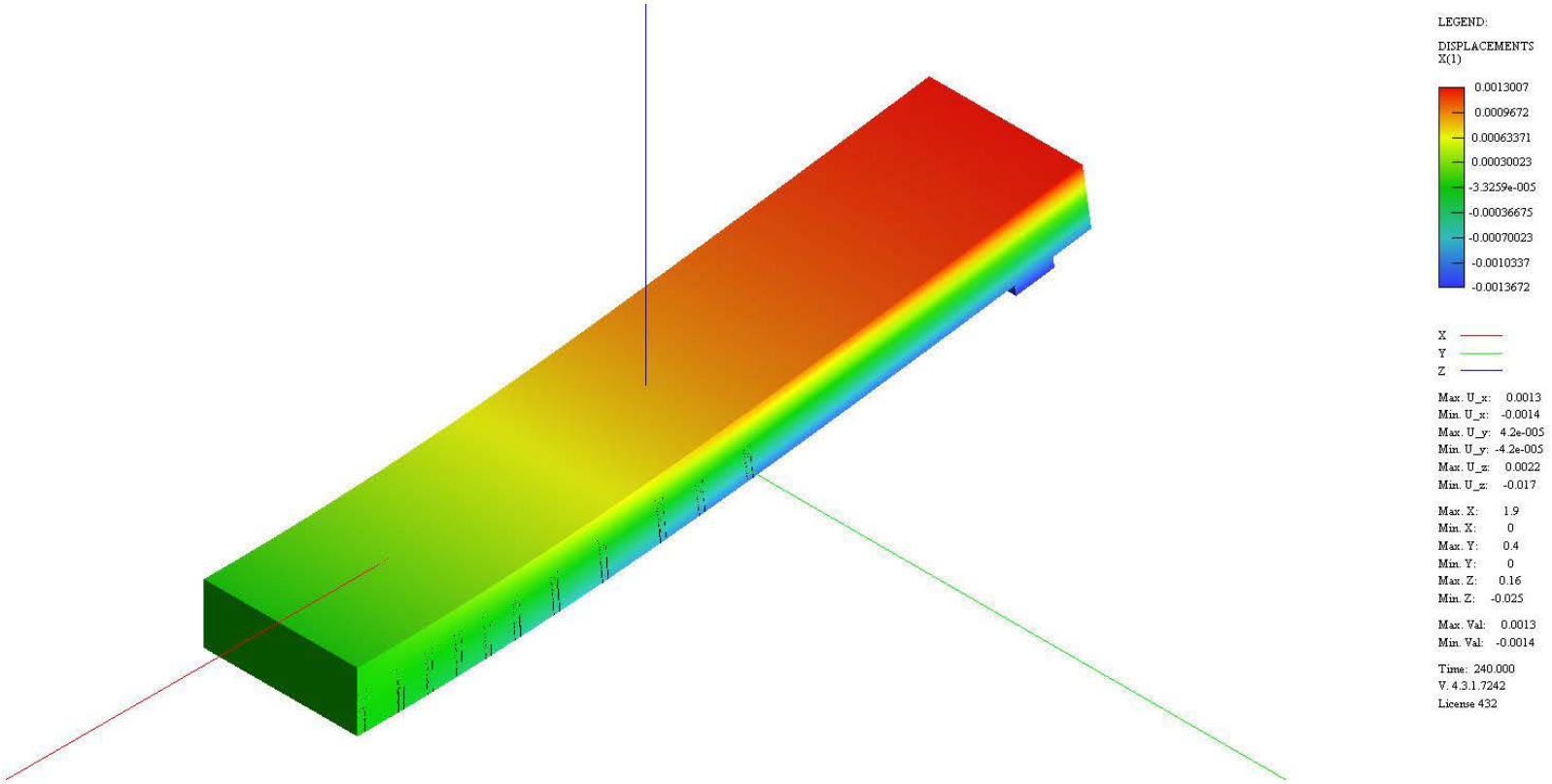

Figure G.26 Typical FEM time-dependent displacement result for S-SCC-b slab

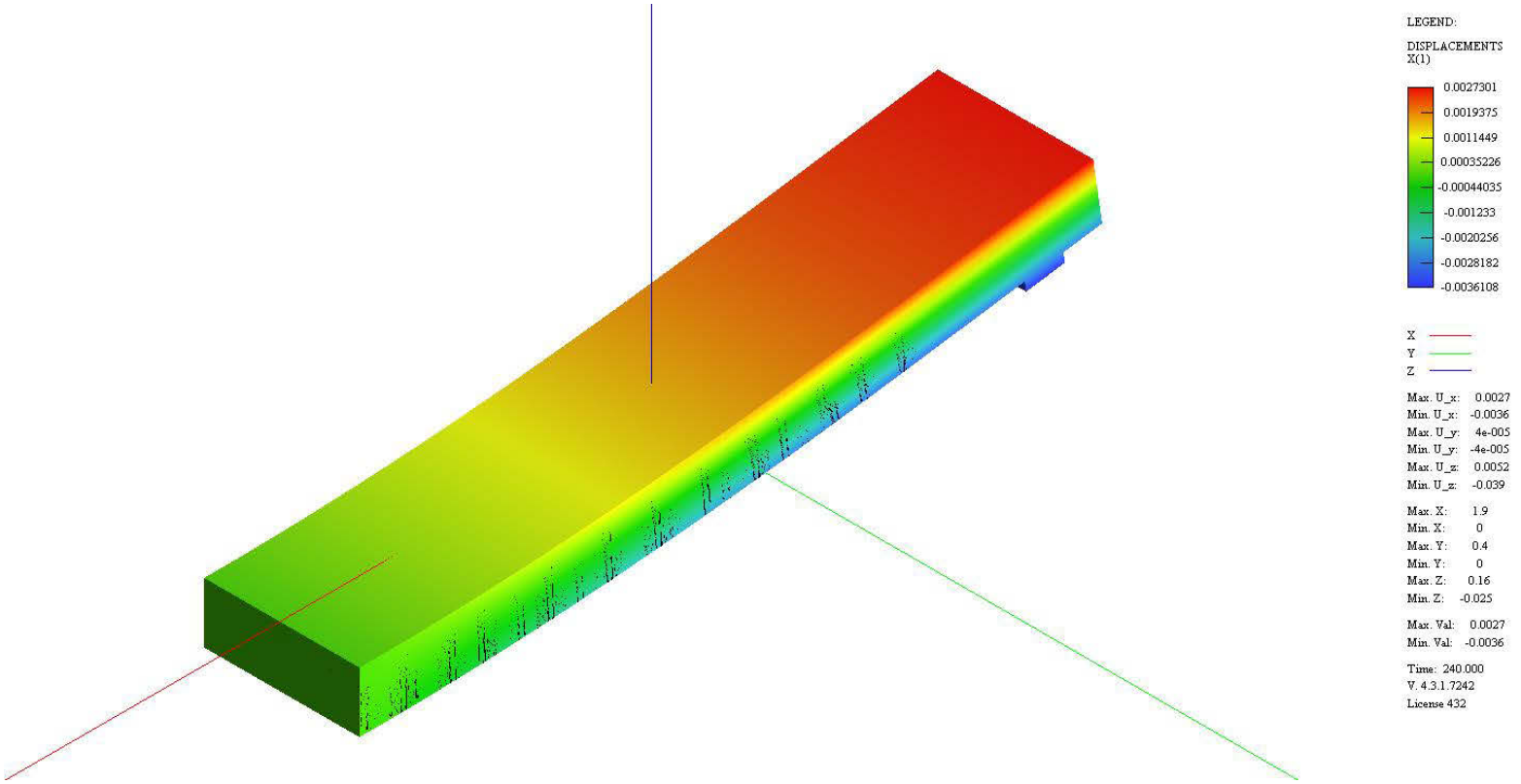

Figure G.27 Typical FEM time-dependent displacement result for DS-SCC-a slab

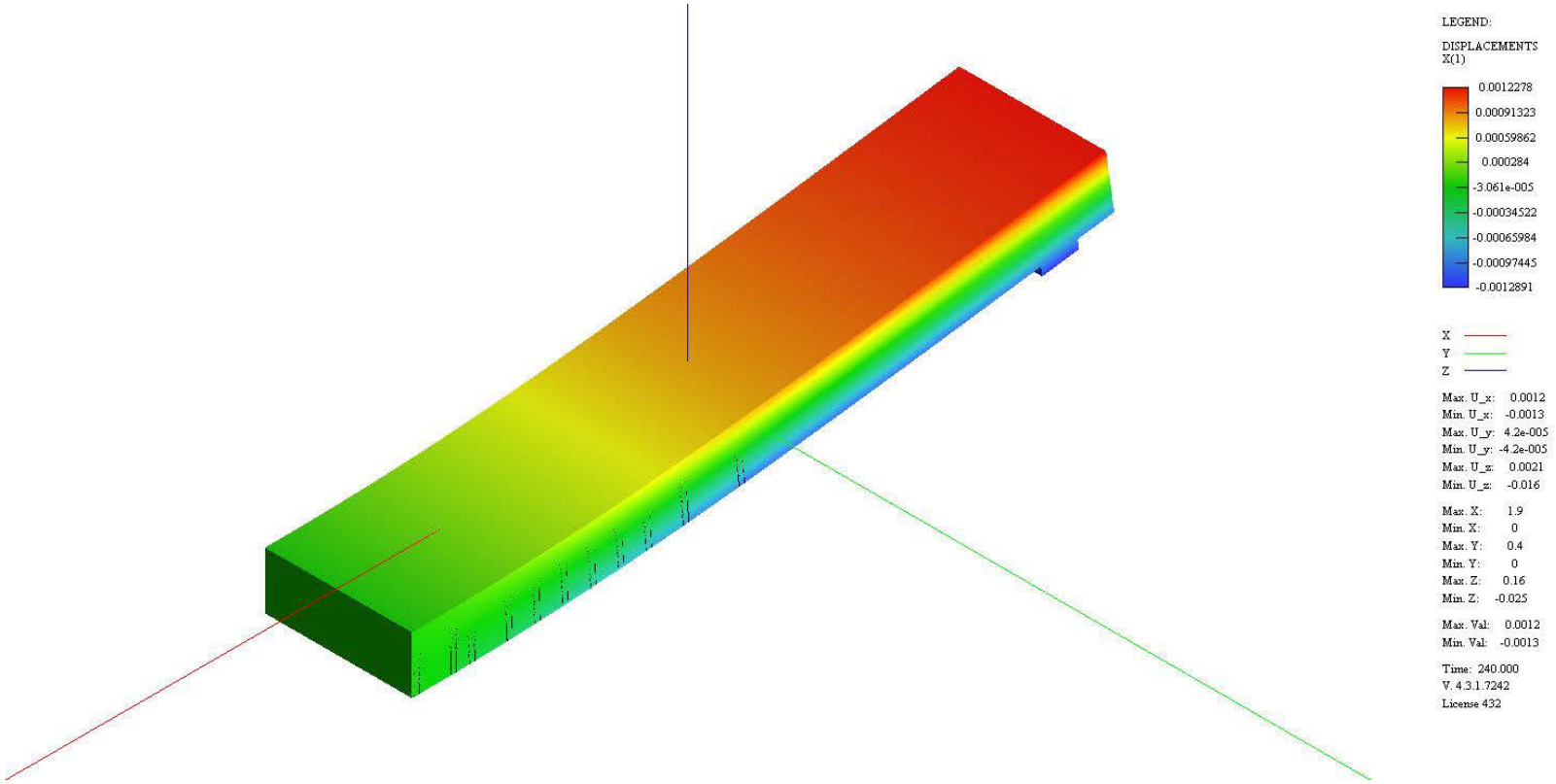

Figure G.28 Typical FEM time-dependent displacement result for DS-SCC-b slab

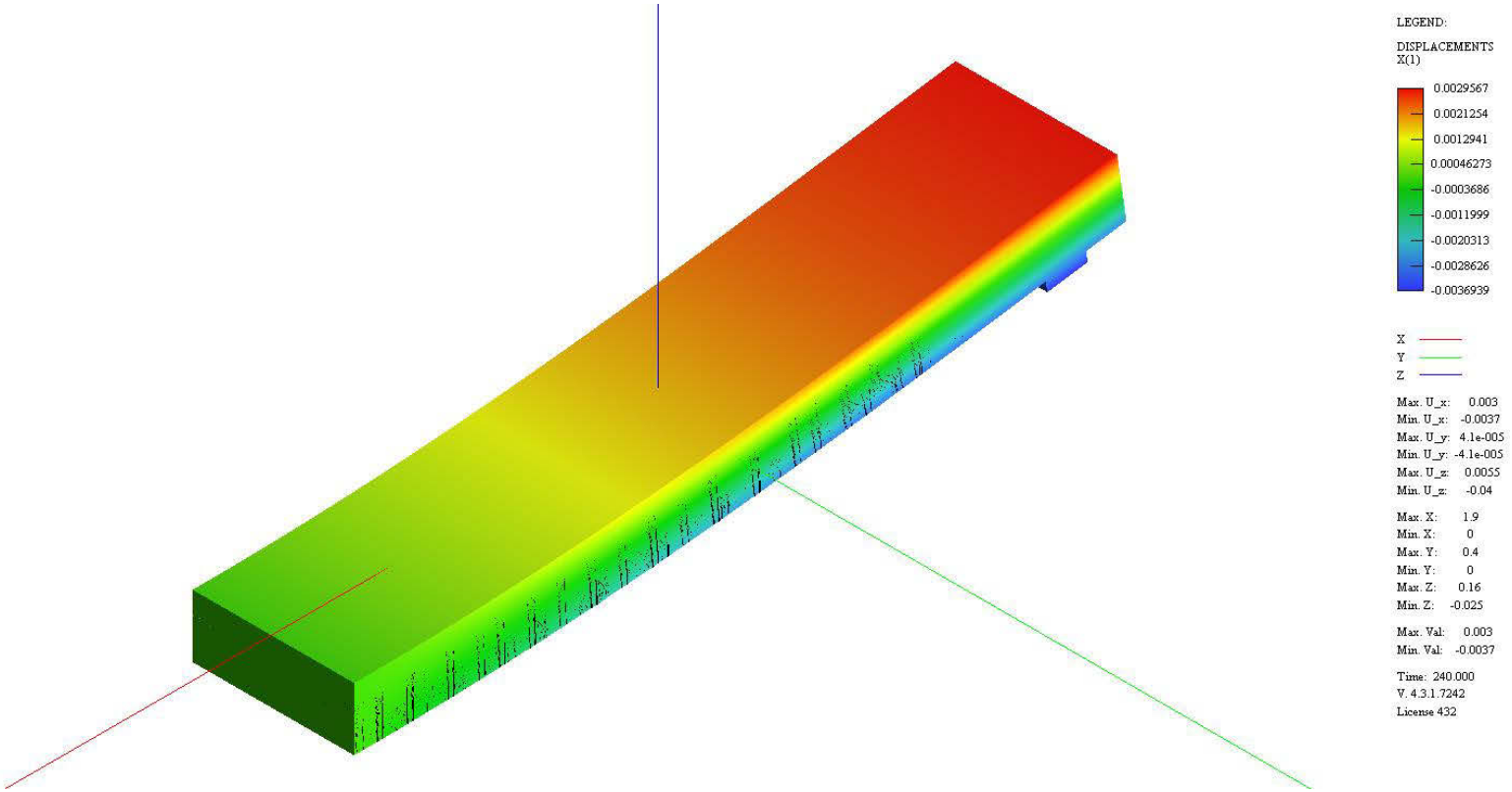

Figure G.29 Typical FEM time-dependent displacement result for N-CC-a slab

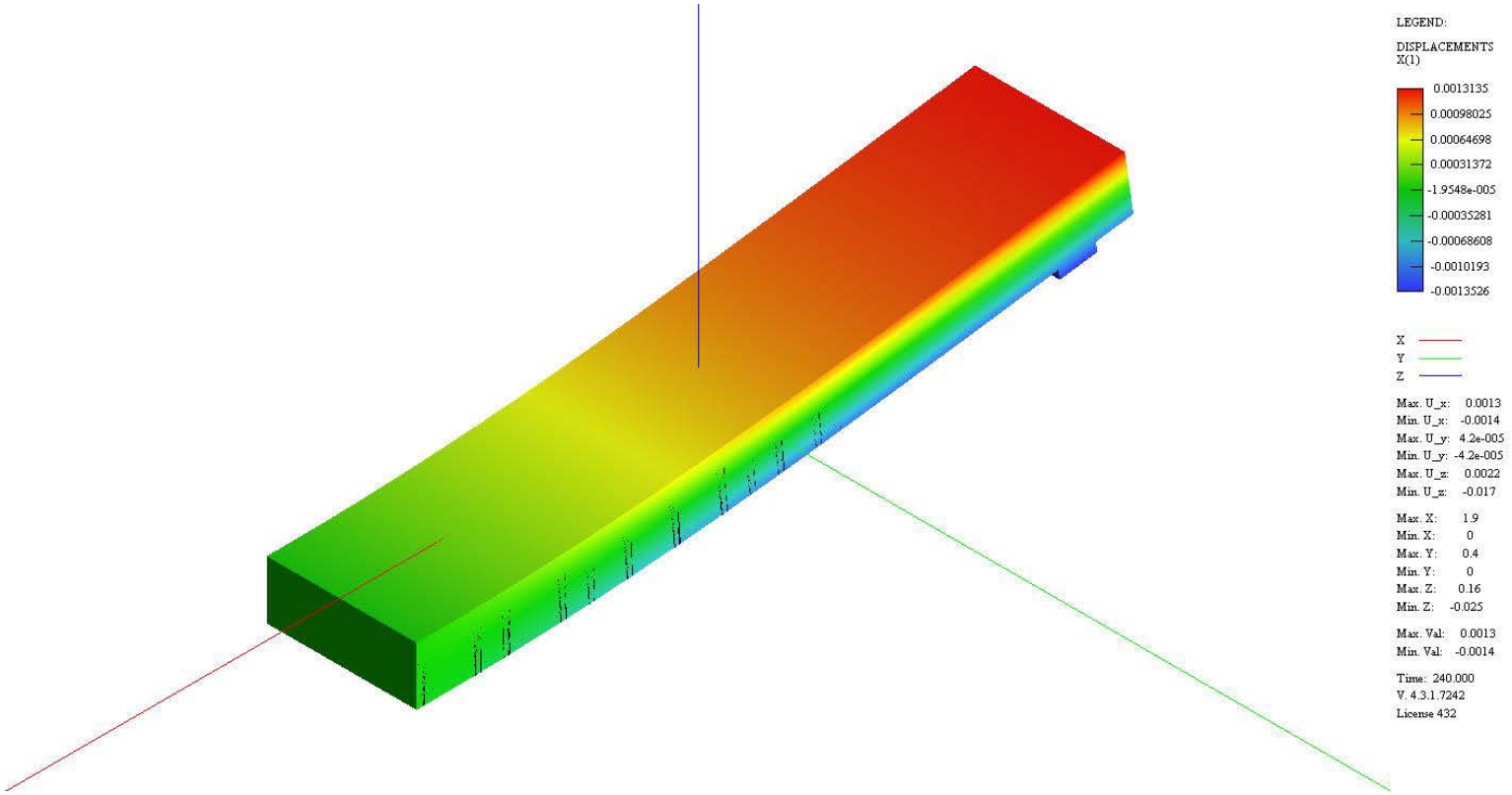

Figure G.30 Typical FEM time-dependent displacement result for N-CC-a slab